

Blast Furnace Ironmaking

Analysis, Control, and Optimization



Ian Cameron

Mitren Sukhram

Kyle Lefebvre

William Davenport



BLAST FURNACE IRONMAKING

BLAST FURNACE IRONMAKING

Analysis, Control, and Optimization

IAN CAMERON

Hatch Ltd., Sheridan Science and Technology Park, Mississauga, ON, Canada

MITREN SUKHRAM

Hatch Ltd., Sheridan Science and Technology Park, Mississauga, ON, Canada

KYLE LEFEBVRE

Hatch Ltd., Sheridan Science and Technology Park, Mississauga, ON, Canada

WILLIAM DAVENPORT

Department of Materials Science and Engineering, University of Arizona, Tucson, AZ, United States



Elsevier
Radarweg 29, PO Box 211, 1000 AE Amsterdam, Netherlands
The Boulevard, Langford Lane, Kidlington, Oxford OX5 1GB, United Kingdom
50 Hampshire Street, 5th Floor, Cambridge, MA 02139, United States

Copyright © 2020 Elsevier Inc. All rights reserved.

No part of this publication may be reproduced or transmitted in any form or by any means, electronic or mechanical, including photocopying, recording, or any information storage and retrieval system, without permission in writing from the publisher. Details on how to seek permission, further information about the Publisher's permissions policies and our arrangements with organizations such as the Copyright Clearance Center and the Copyright Licensing Agency, can be found at our website: www.elsevier.com/permissions.

This book and the individual contributions contained in it are protected under copyright by the Publisher (other than as may be noted herein).

Notices

Knowledge and best practice in this field are constantly changing. As new research and experience broaden our understanding, changes in research methods, professional practices, or medical treatment may become necessary.

Practitioners and researchers must always rely on their own experience and knowledge in evaluating and using any information, methods, compounds, or experiments described herein. In using such information or methods they should be mindful of their own safety and the safety of others, including parties for whom they have a professional responsibility.

To the fullest extent of the law, neither the Publisher nor the authors, contributors, or editors, assume any liability for any injury and/or damage to persons or property as a matter of products liability, negligence or otherwise, or from any use or operation of any methods, products, instructions, or ideas contained in the material herein.

British Library Cataloguing-in-Publication Data

A catalogue record for this book is available from the British Library

Library of Congress Cataloging-in-Publication Data

A catalog record for this book is available from the Library of Congress

ISBN: 978-0-12-814227-1

For Information on all Elsevier publications
visit our website at <https://www.elsevier.com/books-and-journals>

Publisher: Susan Dennis
Acquisition Editor: Kostas Marinakis
Editorial Project Manager: Michelle Fisher
Production Project Manager: Prem Kumar Kaliamoorthi
Cover Designer: Victoria Pearson

Typeset by MPS Limited, Chennai, India



Working together
to grow libraries in
developing countries

www.elsevier.com • www.bookaid.org

Author Biography

Ian Cameron is the principal metallurgist, ferrous in the Pyrometallurgy sector practice at Hatch Ltd., Ontario, Canada. He develops client-focused solutions to produce iron and steel starting from the basic raw materials. Ian has extensive international experience in process technology, plant operations, technology transfer, commissioning and training with iron and steel clients and resource companies. His experience includes coke plant, pellet plant and blast furnace design and operations, assessing steel works energy balances, and the implementation/impact of future iron and coke-making technologies. Ian holds bachelor and master's degrees in metallurgical engineering from McGill University, Montréal, Quebec, Canada and is a licensed professional engineer in Ontario, Canada. He has 38+ years of experience including 23+ years as a consulting engineer for Hatch and previously Corus Consulting and Hoogovens Technical Services. Cameron is a life member of the Association for Iron and Steel Technology (AIST) and two time winner of AIST's Joseph S. Kapitan award for best technical paper in the ironmaking division.

Mitren Sukhram is a senior process engineer in the Pyrometallurgy sector practice at Hatch Ltd., Ontario, Canada. He works on all aspects of blast furnace ironmaking including reline planning, techno-economic assessments, campaign life assessment/extension, and operational support for blast furnaces located around the world.

More recently, Mitren has focused on developing innovative technologies to improve blast furnace productivity and reduce greenhouse gas emissions. Mitren is a graduate of the University of Toronto, Toronto, Canada where he completed bachelor, master's, and PhD degrees in materials science and engineering. His areas of expertise include thermodynamics, heat, mass, and momentum transfer in pyrometallurgical processes. Mitren is a licensed professional engineer in Ontario, Canada with 5+ years experience as a consulting process metallurgist.

Kyle Lefebvre is a process engineer in the Pyrometallurgy sector practice at Hatch Ltd., Ontario, Canada. He has worked extensively on mass, energy, and logistics models to design and improve the performance of numerous iron and steel production facilities. Kyle has worked across the globe in the iron and steel industry with experience in the design and optimization of both integrated and electric arc furnace based steel plants. Kyle holds a bachelor's degree in chemical engineering and biosciences, and a master's degree in applied science from McMaster University in Hamilton, Ontario, Canada. Kyle is a licensed professional engineer in Ontario, Canada with 4+ years of experience in the field of process engineering.

Emeritus Professor William George Davenport is a graduate of the University of British Columbia, Canada and Imperial College, University of London, UK. Prior to his

academic career, he worked on iron- and steel-making technologies with the Linde Division of Union Carbide in Tonawanda, New York, USA. He spent a combined 43 years of teaching at McGill University, Montréal, Quebec, Canada and the University of Arizona, USA. He was also a visiting professor at Tohoku University, Sendai, Japan and visitor at Cambridge University, UK.

Professor Davenport spent much of his career visiting industrial plants around the world. This has resulted in his co-authoring of the following books:

Extractive Metallurgy of Copper
Iron Blast Furnace
Flash Smelting

Extractive Metallurgy of Nickel, Cobalt and Platinum Group Metals
Sulfuric Acid Manufacture and:
Rare Earths, Science, Technology, Production and Use.

Professor Davenport is a fellow and life member of the Canadian Institute of Mining, Metallurgy and Petroleum and a 25-year member of the (U.S.) Society of Mining, Metallurgy, and Exploration. He is a recipient of the CIM Alcan Award, the TMS Extractive Metallurgy Lecture Award, the Aus. IMM Sir George Fisher Award, the AIME Mineral Industry Education Award, the American Mining Hall of Fame Medal of Merit, and the SME Milton E. Wadsworth award.

Preface

The idea for this book arose following an iron-making lecture by Ian Cameron at the 2014 Conference of Metallurgists, Vancouver, Canada. His lecture entitled, *The Iron Blast Furnace; Theory and Practice-35 Years Later*, discussed how the fundamental approach provided in the 1979 book by John Peacey and Bill Davenport had applied to ensuing industry improvements. Bill Davenport attended the lecture and afterward asked Ian if he would like to write a new book on the iron blast furnace. In 1979, Ian had been a student in Bill's ironmaking/steelmaking class at McGill University, Montréal, Quebec, Canada. Later, Ian was fortunate to work with John Peacey as part of the Noranda group and at Hatch.

Ian agreed, and writing began. These authors were soon joined by Mitren Sukhram and Kyle Lefebvre, co-authors, who work with Ian at Hatch Ltd., Mississauga, Canada. Anqi Cai joined in 2018 and made a strong contribution during the last 8 months when the book was finalized.

We were very fortunate to work with five young university interns, all from McGill University, during our writing, namely;

- Anqi Cai,
- Sabrina Lao,
- Denzel Guye,
- Max (Shuhong) Shen, and
- William Dixon.

They proofread our manuscripts, did the end-of-chapter exercises, and showed us older folks what engineering students in 2015–18 already knew and didn't know. They were all

proficient in matrix algebra, Excel Goal Seek, Excel Solver, and Optimization. We thank them profusely for their help and wish them the best of luck with their studies and future careers.

The objectives of our book are to describe blast furnace ironmaking as it is today and to suggest how it will be in the near and distant future. To achieve these objectives, we visited and worked at many blast furnaces around the world while we were writing. The principle visits were to:

- AK Steel, Dearborn, Blast Furnace C, United States
- Algoma Steel, Blast Furnace 7, Canada
- ArcelorMittal Dofasco Blast Furnaces 2 and 4, Canada
- ArcelorMittal, Fos-sur-Mer, Blast Furnaces 1 and 2, France
- ArcelorMittal Monlevade Blast Furnace A, Brazil
- ArcelorMittal Indiana Harbor, Blast Furnace 7, United States
- ArcelorMittal, Tubarão Blast Furnace 1 and 3, Brazil
- BlueScope Steel, Port Kembla, Blast Furnace 5, Australia
- EVRAZ NTMK Blast Furnace 5 and 6, Russian Federation
- JFE Fukuyama Works, Blast Furnace 5, Japan
- Hebei Iron & Steel, Handan Works, P. R. China
- NLMK, Blast Furnaces 3–7, Russian Federation
- Nippon Steel, Nagoya Works, Blast Furnace 1, Japan

- Nippon Steel, Oita Works, Blast Furnace 2, Japan
- Gerdau, Acominas, Blast Furnaces 1 and 2, Brazil
- Stelco Lake Erie Works, Blast Furnace 1, Canada
- Tata Steel Europe, Blast Furnaces 6 and 7, The Netherlands
- Ternium CSA, Blast Furnaces 1 and 2, Brazil
- Ternium Siderar, Blast Furnace 2, Argentina
- U. S. Steel Great Lakes Works, Blast Furnaces B2 and D4, United States
- U. S. Steel Gary Works, Blast Furnaces 4 and 14, United States

We thank the personnel at these facilities for their kindness in showing us around their plants and for answering all our questions.

Our book consists of three main sections:

1. Three introductory chapters describing the blast furnace from the outside and then the inside. This is followed by a brief description of how the blast furnace's molten iron product is used for making steel.
2. An arithmetical section that develops a thermochemical model of the blast furnace process from first principles and culminating with several chapters on control and optimization.

3. A thorough examination of modern industrial blast furnace practice around the world based on prior knowledge and our plant visits.

A brief note about units. We have used SI units throughout except °C for temperature and pascals and bar (1×10^5 Pa) for pressure. We also use the unit normal cubic meter (Nm³) which is a m³ of gas at 0°C and 1 bar pressure. A Nm³ contains 0.0440 kg mol of ideal gas.

One of the authors would like to thank his wife Margaret Davenport for reading portions of the manuscript and his son George Davenport for his assistance with many calculations. The authors thank Hatch Ltd., especially Mr. Ted Lyon, Managing Director, Bulk Metals, for the continuing support we received as we completed the book over a 5-year period.

Preparing the book provided a great education as we discussed and debated the best way to present blast furnace practice to you, that is, our readers. Our approach will help you build knowledge/tools to understand and control the complex blast furnace operation—one of mankind's most important industrial furnaces.

**Ian Cameron, Mitren Sukhram,
Kyle Lefebvre and William Davenport**
September 2019.

Acknowledgments

ANQI CAI, MCGILL UNIVERSITY

Ms. Anqi Cai played a key role in writing this book. She was especially helpful to Professor Davenport. They spoke every day for about 3 months even though she was in Mississauga, Ontario and he was in Tucson, Arizona. She was especially helpful in the thermodynamic aspects of the book, writing equations, challenging others and providing documentation to prove every point. Vigorous arguments often ensued.

Anqi also made critical contributions to the book's matrices, making sure that the variables were properly identified and unchanged throughout the book, that the equations were properly numbered and that every cell had its proper value. Her consistent equation numbering was especially critical.

Finally, Anqi completed all the book's after-chapter exercises and made sure that the exercises were appropriate and clearly worded. Students completing the exercises will have her to thank for their clarity.

TED LYON, MANAGING DIRECTOR—BULK METALS, HATCH LTD.

Mr. Ted Lyon provided important sponsorship of the Hatch team during the authoring of the book. He was always encouraging and supported the completion of the book, understanding its importance to the ironmaking

community and as a tool to train process engineers.

CONTRIBUTING AUTHORS

Dr. Afshin Sadri, Mr. Manuel Huerta, and Mr. Luke Boivin all of Hatch Ltd. took on the challenge of providing important content to several chapters in the book. Their dedication to provide high-quality materials is appreciated by the authors.

SUSANNE CRAGO, CHAMELEON GRAPHICS

Susanne created the excellent graphics in the book. She persevered through the many changes requested by the authors. We appreciate her skills as a graphics artist and patience to get the best possible images.

WILLIAM DIXON, DENZEL GUYE, SABRINA LAO, AND MAX (SHUHONG) SHEN, ALL FROM MCGILL UNIVERSITY

In addition to Ms. Anqi Cai, these students reviewed parts of the book as the authors were preparing the manuscript. Their input on the content and approach are greatly appreciated by the authors. Knowing that the books' content appealed to each of these students reinforced our approach and direction.

The students also helped with more routine aspects that every author appreciates when preparing a manuscript.

OTHER CONTRIBUTORS

The authors would like to thank and acknowledge many others who contributed to the book. Our supporters are listed below and reflect the global nature of the ironmaking community.

Michael Grant	Air Liquide, Germany	KC Woody	Midrex Corporation, United States
Peter Hamerlinck	ArcelorMittal Dofasco, Canada	Professor Ivan Kurunov	NLMK Lipetsk, Russia
Adelmo Monaco	ArcelorMittal Dofasco, Canada	Tadashi Imai	Nippon Steel, Nagoya, Japan
Douglas Ruy	ArcelorMittal Tubarão, Brazil	Takayuki Nishi	Nippon Steel, Nagoya, Japan
Ken Landau	Association of Iron and Steel Technology (AIST), United States	Jumpei Konishi	Nippon Steel, Oita, Japan
Darryle Lathlean	BlueScope Steel, Australia	Laurence Kayl	Paul Wurth S.A., Luxembourg
Fang Yuan Qing (Tracy)	CISDI International Engineering & Consulting, P.R. China	Robert Neuhold	Primetals Technologies, Austria
Li Zhiyou (William)	CISDI International Engineering & Consulting, P.R. China	Professor Chenn Qui Zhou	Purdue University, United States
Peter McCallum	CRH, Canada	Dr. Jens Kempken	SMS Group, Germany
John Busser	Hatch Ltd., Canada	John D'Alessio	Stelco Holdings Inc., Canada
Anneliese Dalmoro	Hatch Ltd., Canada	Scott Dedrick	Stelco Holdings Inc., Canada
Barry Hyde	Hatch Ltd., Canada	Dr. John Quanci	SunCoke Energy, United States
Anne Kirkpatrick	Hatch Ltd., Canada	Gerard Tijhuis	Tata Steel Europe, The Netherlands
Kiyoshi Fukuda	JFE, Fukushima, Japan	Gerald Toop	Teck Resources, Trail, Canada
Hedetoshi Matsuno	JFE, Fukushima, Japan	Frederico Godinho Cunha	Ternium CSA, Brazil
Kentaro Nozawa	Kobe Steel, Kakogawa, Japan	Oscar Lingiardi	Ternium Siderar, Argentina
Professor Hiro Fukunaka	Kyoto University, Japan	Matt Kraeuter	Thyssenkrupp Industrial Solutions, United States
Chris Ravenscroft	Midrex Corporation, United States	Claude, Bodeving	TMT – Tapping Measuring Technology, Luxembourg
		Professor Toru Okabe	Tokyo University, Japan
		Ralph Albanese	United States Steel Corporation, United States
		Devbrat Dutta	United States Steel Corporation, United States
		Jason Entwistle	United States Steel Corporation, United States
		Michael J. McCoy	United States Steel Corporation, United States
		Professor Evgueni Jak	University of Queensland, Australia

The Iron Blast Furnace Process

O U T L I N E

1.1 Introduction to the Blast Furnace Process		<i>1.4.5 Production Statistics</i>	11
	1	<i>1.4.6 Campaign Life</i>	11
1.2 Blast Furnace Raw Materials	2	1.5 Costs	15
1.2.1 Top-Charged Materials	4	<i>1.5.1 Investment (Capital) Costs</i>	15
1.2.2 Charging Methods	6	<i>1.5.2 Operating Costs</i>	15
1.2.3 Tuyere-Injected Materials	7	<i>1.5.3 Maintenance and Relining Costs</i>	16
1.3 Products From the Blast Furnace	7	1.6 Safety	16
1.3.1 Molten Iron	7	1.7 Environment	16
1.3.2 Molten Slag	8		
1.3.3 Top Gas	9	1.8 Summary	17
1.4 Blast Furnace Operations	10	Exercises	18
1.4.1 Pressure	10	References	18
1.4.2 Principle Chemical Reactions	11	Suggested Reading	18
1.4.3 Main Thermal Processes	11		
1.4.4 Blast Furnace Information	11		

1.1 INTRODUCTION TO THE BLAST FURNACE PROCESS

The iron blast furnace is a tall vertical shaft furnace, Fig. 1.1. Its principle objective is to produce molten iron from iron ores for subsequent and immediate production of molten/

liquid steel. A photograph of a blast furnace plant is shown in Fig. 1.2.

Solid Fe oxide ore (hematite, Fe_2O_3), coke (87–91% carbon), and fluxes are charged to the top of the blast furnace. A molten iron alloy, 1500°C, 94.5% Fe, 4.5% C, and 1% [Si + Mn], is cast from the hearth along with molten and

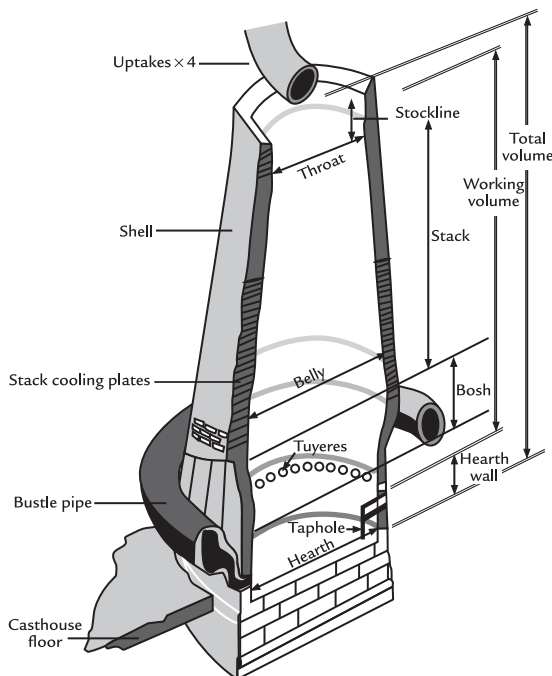


FIGURE 1.1 Cutaway drawing of an iron blast furnace. It is a tall cylindrical furnace ~40 m high and 10–15 m in diameter.

impurity-rich oxide slag. Hot, high pressure air is blown into the blast furnace through the tuyeres, burning coke, and injected fuel to create the heat needed to smelt the iron ores and fluxes. The resulting gas rises quickly up through the furnace charge materials also known as burden. The burden is heated, Fe oxides are reduced to Fe, and solid materials are melted and collected in the hearth. Molten iron production is typically 4,000–12,000 tonne per blast furnace per day. The process is continuous and operates with very high availability, typically over 95% of the available time.

In 2016, 94% of the world's iron ore reduction was done in blast furnaces. The remainder was done by solid state reduction known as Direct Reduction Ironmaking. The blast furnace employs carbon in coke to reduce Fe oxide pellets, sinter, and crushed ore to

metallic iron. In this book, reduction means removal of oxygen (O) from iron oxides. The blast furnace produces a molten iron alloy at 1500°C:

- 94.5 mass% Fe;
- 4.5 mass% C;
- 0.6 mass% Si;
- 0.4 mass% Mn; and
- minor amounts of S, P, and Ti.

Virtually all the molten iron alloy, commonly referred to as hot metal or raw iron, is immediately refined into lower carbon molten steel at other furnaces within the steel plant.

The Fe oxides and coke are charged to the top of the blast furnace at furnace pressure and in separate layers. The molten iron is tapped from the bottom of the furnace into ladles known as torpedo ladles. It is immediately sent molten to the steelmaking shop. By-product molten and impurity-rich oxide slag is tapped with the molten iron, separated immediately outside of the blast furnace, solidified, and sold as road aggregate or for use in cement production. The slag is made up of;

1. impurity oxides, mostly SiO_2 and Al_2O_3 present in ore gangue and coke ash, plus
2. flux oxides, mostly CaO and MgO .

Iron ore pellets and metallurgical coke can be seen in [Figs. 1.3 and 1.4](#).

Heat for the process is created by burning the coke with hot ~1200°C high pressure air injected through tuyeres located near the bottom of the furnace. The air is blown through as few as 15 to as many as 45 water-cooled copper tuyeres located around the furnace circumference at the top of the hearth, [Figs. 1.1 and 1.5](#).

1.2 BLAST FURNACE RAW MATERIALS

The blast furnace's principle raw materials are:



Blast furnace in formosa Ha Tinh, Vietnam, supplied by CISDI



Blast furnace in formosa Ha Tinh, Vietnam, supplied by CISDI

FIGURE 1.2 Two iron blast furnaces and supporting equipment at Formosa Ha Tinh in Vietnam supplied by China's CISDI. Conveyor belts (from right to left in the upper picture) transport iron oxide ores/sinter/pellets, coke, and flux up to the top of each furnace. Four vertical blast heaters or stoves (lower picture) heat the blast air to $\sim 1200^{\circ}\text{C}$. A large flue, known as the downcomer, descends from the furnace top and removes top gas from the blast furnace. The blast furnace gas is cleaned and the stoves use this as a fuel. *Source: Photographs courtesy of CISDI International Engineering & Consulting Co.*



FIGURE 1.3 Fired hematite (Fe_2O_3) pellets ready for charging to an iron blast furnace. They are 8–16 mm in diameter and contain ~64 mass% Fe as compared to 70 mass% Fe in pure Fe_2O_3 . *Source: Photograph courtesy of Midrex Technologies Inc.*



FIGURE 1.4 Metallurgical coke, about 70–100 mm long. Coke is made by high-temperature vaporization of volatiles, (e.g., CH_4) from coal heated in the absence of air, Chapter 55, Metallurgical Coke—A Key to Blast Furnace Operations. “Met” coke contains 87–91% carbon and 9–13% oxide ash; mostly silica and alumina from the original coal. The coke burns with blast air near the bottom of the blast furnace and in front of the tuyeres to (1) provide heat for the ironmaking process, and (2) carbon monoxide for iron oxide reduction. *Source: Photograph courtesy of SunCoke Energy Inc.*

1. top-charge solids (Fe oxide, coke, and flux), and
2. hot blast air $\sim 1200^\circ\text{C}$, which is forcefully blown into the furnace through tuyeres near the bottom of the furnace, *Figs. 1.1 and 1.5*.



FIGURE 1.5 New tuyeres in a rebuilt blast furnace. They are water-cooled copper with a protective metal coating near the tip. Tuyeres are about 0.15 m inside diameter and penetrate about 0.4 m into the furnace. They are situated about 3 m above the blast furnace taphole and are about 1.2 m apart around the blast furnace circumference. 1200°C blast air enters the tuyeres at 180–240 m/s and a pressure of 3.5–4.5 bar (gauge). *Source: Photograph courtesy of Stelco Holdings Inc.*

Pulverized coal, natural gas, and other hydrocarbons are injected in through the tuyeres to replace coke. Oxygen and steam are also added to the blast air.

1.2.1 Top-Charged Materials

The top-charged raw materials are typically:

1. **iron oxides:** Overwhelmingly hematite, Fe_2O_3 . This oxide is added as;
 - a. 8–16 mm diameter pellets (~64 mass% Fe) produced by heating finely ground and beneficiated ore, *Fig. 1.6*;
 - b. 10–45 mm sinter pieces (57 mass% Fe) produced by heating nonbeneficiated ore fines and other solids; and
 - c. natural ore, crushed to 50 mm pieces (62–67 mass% Fe).

All iron oxides contain silica (SiO_2) and other oxide impurities.

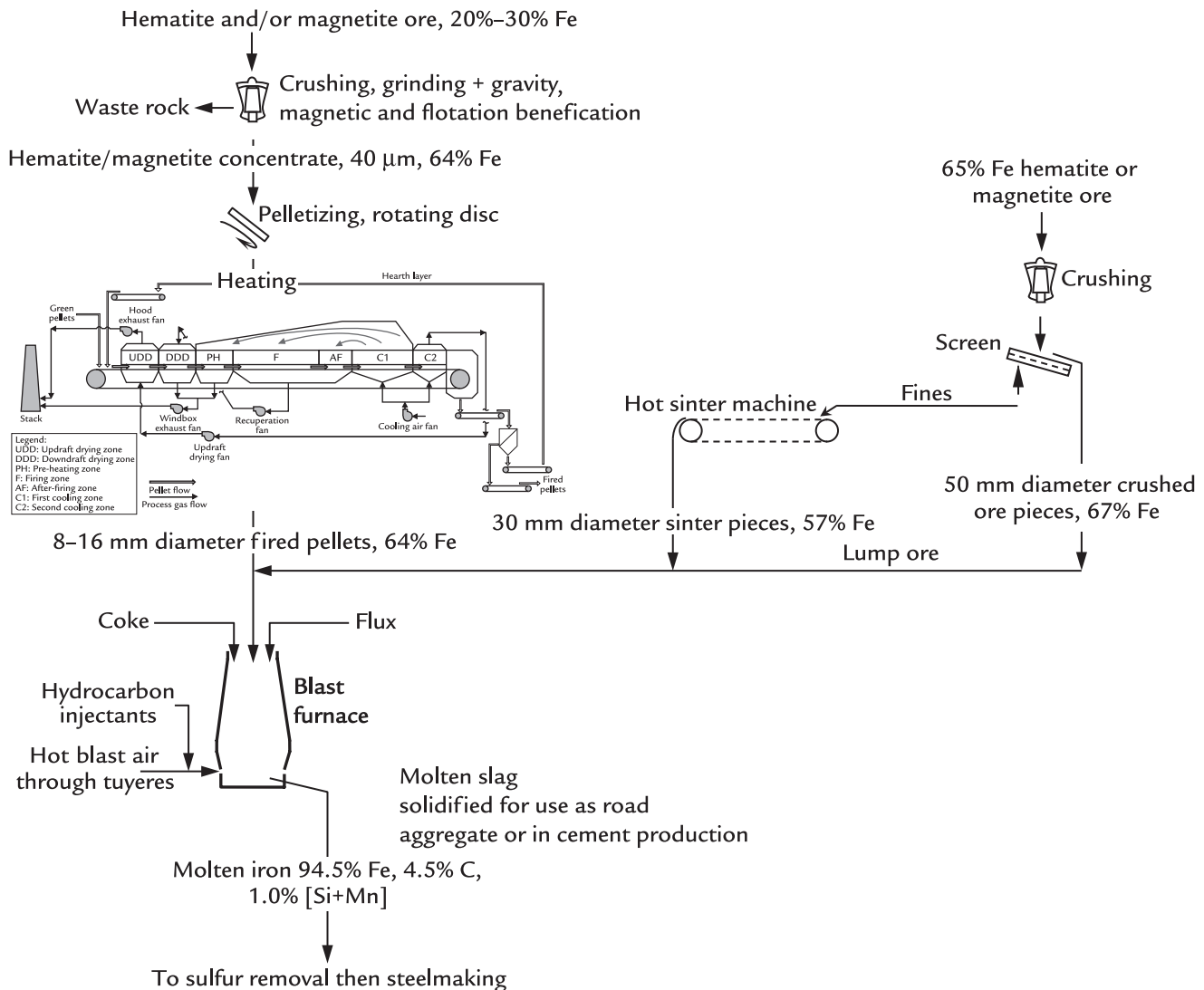


FIGURE 1.6 Blast furnace input and output material flows. All % are mass%. Three iron oxide feeds; pellets, sinter, and crushed ore are charged with coke. Products are molten iron and slag. The molten iron goes directly to steelmaking, and molten slag is solidified and used for road aggregate or in cement production. Reductants for ironmaking are (1) charged to the top of the furnace as metallurgical coke, and (2) injected with hot blast air as pulverized coal and other hydrocarbon fuels. The top-charged coke and iron oxides are added in layers; a ~0.7 m thick Fe oxide ore layer then a 0.4 m thick coke layer, then a 0.7 m thick ore layer, and so on. Not shown is top gas leaving the furnace; it leaves at 100–200°C and is sent to dedusting and demisting before it is used as fuel for heating blast air and for other in-plant duties.

2. **coke:** 87–91 mass% C, 9%–13% ash, both on a dry basis, and 1–5 mass% H₂O—added as 50–60 mm diameter pieces. This material must be:
 - a. reactive enough to combust rapidly at elevated temperature, and
 - b. strong enough to avoid being crushed in the blast furnace.
 Coke ash consists of alumina (Al₂O₃) and silica (SiO₂) and often alkali impurities (K₂O and Na₂O). Large and strong coke is essential in the blast furnace to:
 - a. prevent the charge from collapsing into the bottom of the furnace;
 - b. permit upward gas flow between the coke pieces where ore and flux are reduced and melted; and
 - c. allow downward dripping of newly formed molten iron and slag.
3. **fluxes:** Mostly CaO and MgO. These oxides flux the silica and alumina impurities in ore and coke to make a fluid molten slag which is cast or tapped from the furnace together with the product molten iron. Fluxes are added as 50 mm diameter limestone (CaCO₃) and dolomite (CaCO₃:MgCO₃) pieces or as CaO and MgO contained in pellets and sinter. These fluxes cause sulfur, and alkali impurities to be absorbed in molten slag rather than in the molten iron.

1.2.2 Charging Methods

Continuous blast furnace operation demands that top charging does not interfere with gas flow out of the furnace, while the charge burden must be added at 1–3 bar furnace pressure (gauge). This is achieved using:

1. gas uptake flues located *away from the central solids charging equipment*, and
2. two central sealed charge hoppers, one loading at ambient pressure, while the other

is discharging into the furnace at furnace pressure, Fig. 1.7.

This system allows top gas to flow continuously out of the furnace while the furnace is being charged with solids.

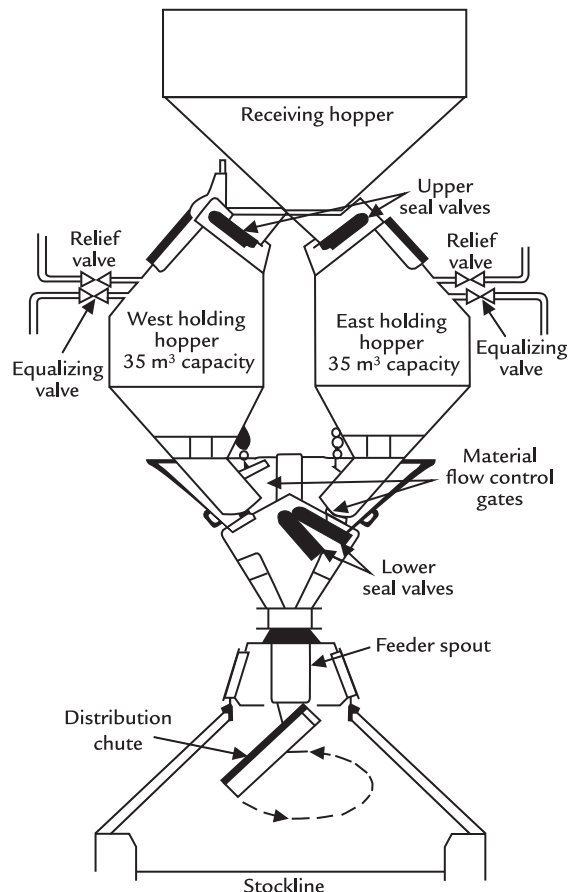


FIGURE 1.7 Bell-less charging system developed by Paul Wurth for charging a blast furnace under pressure. The two holding hoppers are notable. They are filled cyclically where one hopper is filling at ambient pressure, while the other is emptying at furnace pressure. The charge is distributed across the blast furnace throat area by a rotating distribution chute. The furnace's top gas leaves the blast furnace continuously through four gas uptakes located below the charging system in the furnace top cone (between stockline and feeder spout)—see Fig. 1.8.



Blast Furnace in Baosteel Zhanjiang, China, Supplied by CISDI

FIGURE 1.8 Three of four gas uptakes and the downcomer pipe used to capture and remove top gas from a blast furnace. *Source: Photograph courtesy of CISDI International Engineering & Consulting Co.*

1.2.3 Tuyere-Injected Materials

Raw materials introduced through the tuyeres (Fig. 1.5) are:

1. *hot blast air*: Heated to $\sim 1200^{\circ}\text{C}$ and often enriched with pure oxygen. The blast air burns descending incandescent coke $>1500^{\circ}\text{C}$ in front of the tuyeres to provide a $2000\text{--}2200^{\circ}\text{C}$ flame that is hot enough to:
 - a. heat and reduce iron oxides throughout the blast furnace, and
 - b. melt iron and slag.
2. *injectants*: Most often pulverized coal but also other hydrocarbons (e.g. natural gas) are injected and combusted in front of the tuyeres to provide heat plus extra CO(g) and $\text{H}_2\text{(g)}$ reducing gases.

Pulverized coal is cheaper than coke per kg of contained C. Pulverized coal injection lowers the blast furnace coke requirement and total operating cost.

1.3 PRODUCTS FROM THE BLAST FURNACE

The iron blast furnace makes three products:

1. molten blast furnace iron, also known as hot metal or raw iron;
2. molten oxide slag, known as blast furnace slag; and
3. blast furnace top gas, known as BFG.

1.3.1 Molten Iron

The main product of the blast furnace is molten iron, cast at 1500°C . It is cast through a pluggable taphole in the furnace hearth wall near the bottom of the furnace. A small blast furnace is equipped with one taphole; a large furnace will need three or four tapholes to continuously drain the furnace. Larger furnaces

alternately use two tapholes with the others being refurbished or on standby.

The molten iron exits the blast furnace saturated with carbon. The iron typically contains the following:

Element	Mass%
Fe	94.4
C	4.5
Si	0.6
Mn	0.4
P	0.06
S	0.03
Ti	0.01

The hot metal is immediately sent molten $\sim 1500^{\circ}\text{C}$ to the steelmaking plant where it is sequentially:

- desulfurized in a large ladle by injecting a [CaO, CaC₂, and/or Mg]-based powder into the iron, thereby removing the sulfur contained as a molten CaO-, MgO-, S-rich slag¹;
- oxidized with virtually pure oxygen and fluxed with CaO and MgO in a basic oxygen furnace to remove most of the impurities, that is, Si, C, S, and P;
- alloyed with other metals; for example, Mn, Cr, Ni, V, and Mo;
- degassed to remove H₂(g), N₂(g) and lower carbon to very low levels [removing C as CO(g)];
- continuously cast into steel slabs, billets, and/or blooms; and
- finished by hot and cold rolling, occasionally coated, and then sold

as described in Chapter 3, Making Steel From Molten Blast Furnace Iron.

1.3.2 Molten Slag

As shown in Fig. 1.9, molten blast furnace slag is tapped from the blast furnace together with the molten iron. Slag is separated from iron by gravity then solidified and sold.

Blast furnace slag is a molten oxide solution at 1500°C made up of the following:

Substance	Mass%
CaO	40
SiO ₂	38
Al ₂ O ₃	10
MgO	10
MnO	0.4
TiO ₂	0.5
P ₂ O ₅	<0.1
S	0.8
Fe (total in droplets and ions)	0.2

Chemically, the slag is a high temperature solution of cations (such as Ca⁺⁺ and Mg⁺⁺) and anions (such as O²⁻ and SiO₄⁴⁻).² Slag contains very little Fe - an indication of the blast furnace's excellent reduction efficiency.

Blast furnace slag composition is chosen to:

- guarantee that the slag is molten and fluid;
- remove the ore's gangue minerals and the coke's ash from the furnace burden as a fluid slag;
- absorb K₂O and Na₂O (alkalis), which will otherwise build up in the furnace; and
- absorb sulfur that will otherwise enter the product molten iron.

A slag "basicity" ratio, B4 is defined as:

$$\text{B4} = \frac{\text{Mass\% CaO} + \text{Mass\% MgO}}{\text{Mass\% SiO}_2 + \text{Mass\% Al}_2\text{O}_3}$$

A B4 value between 0.9 and 1.1 best meets these four slag composition objectives.



FIGURE 1.9 Molten iron and slag being tapped from a blast furnace. They are separated in the main trough by allowing dense molten iron (6.8 t/m^3) to flow under a refractory skimming block while forcing the less dense molten slag (2.7 t/m^3) to collect above the iron and flow into a slag runner. The molten iron flows continuously into a torpedo-shaped rail car ladle used to transport the hot metal to steelmaking. The molten slag flows to a granulation machine or is solidified in pits-then sold. Notice the huge bustle pipe that distributes blast air to individual tuyeres. *Source: Photograph courtesy of TMT—Tapping Measuring Technology S.à. r.l & G.m.b.H.*

1.3.2.1 Slag Uses

Solidified blast furnace slag is used for road aggregate and in cement production. For road aggregate, slag is air cooled in large pits then crushed. For cement, molten slag is water quenched then finely ground. This finely ground slag is added to Portland cement (30–70% blast furnace slag, remainder Portland cement). This mixture is stronger than Portland cement alone and more resistant to sulfate and chloride attack. Slag cement is also fire resistant.³

Successful slag granulation requires that the molten slag must always be hot,

1450–1500°C, so that it flows smoothly into the granulator.

1.3.3 Top Gas

BFG leaves the furnace through four widely spaced uptake flues located in the furnace top cone, [Figs. 1.1 and 1.8](#). The gas is dedusted, demisted, and burnt for:

1. heating blast air in regenerative stoves, [Fig. 1.2](#),
2. heating other furnaces around the steel plant,

3. producing low-pressure steam for the steel plant, and
4. making electricity.

BFG is typically composed of the following:

Gas	Volume %
CO	23
CO ₂	22
H ₂	3
H ₂ O	3
N ₂	49

BFG's fuel value is about 10% that of natural gas, that is, BFG is a "weak" fuel. Despite being a weak fuel, BFG has many valuable in-plant uses; it is by far the largest stream of waste energy in any steelworks. The moist dust from dedusting/demisting is agglomerated by sintering or briquetting then recycled to the blast furnace to recover its Fe and C. It accounts for about 5% of the blast furnace charge.

1.4 BLAST FURNACE OPERATIONS

The blast furnace operation entails:

1. nearly continuous charging of ore, coke, and flux through the top of the furnace;
2. continuous blowing of hot blast air and hydrocarbon injectants through the blast furnace tuyeres; and
3. continuous (on smaller furnaces intermittently) casting of molten iron and slag through a taphole near the bottom of the hearth.

Most of these operations are controlled by skilled operators using multiple sensors around the furnace. Continuously monitored process variables include the following:



FIGURE 1.10 Pt–Rh thermocouple in flowing-tapped molten iron stream. It is inside the vertical refractory probe (bottom end closed) to give a continuous measure of hot metal temperature. Source: Photo courtesy of Algoma Inc.

temperatures: Hot blast, cooling water, furnace wall, top gas;

pressures: Blast, furnace interior at several points, top;

flowrates: Blast air, tuyere injectants, cooling water; and

moisture: Of charge materials added to the furnace.

In addition, product iron and slag temperatures are measured continuously or intermittently with specialized high-temperature Pt–Rh thermocouples, Fig. 1.10.⁴

Powerful drilling machines are used to open the taphole. At the end of a cast, a mud gun is used to block the taphole and stop molten iron and slag flow.

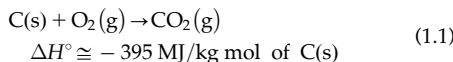
1.4.1 Pressure

Most blast furnaces are pressurized to 1–3 bar (gauge) at the top gas offtakes and 2.5–4.5 bar (gauge) at the tuyere tips. These pressures densify the gas ($n/V = P/RT$), giving it an extended residence/reaction time in the furnace.

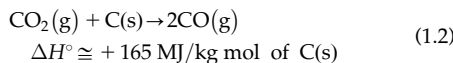
1.4.2 Principle Chemical Reactions

The main chemical reactions that occur inside the blast furnace are:

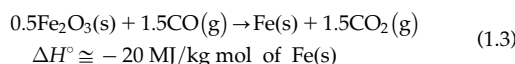
1. strongly exothermic oxidation of carbon by air/oxygen in front of the tuyeres to give $\text{CO}_2(\text{g})$ plus heat:



2. endothermic reaction of the $\text{CO}_2(\text{g})$ with carbon to produce $\text{CO}(\text{g})$, the principle reducing gas of the blast furnace process:



3. slightly exothermic reduction of hematite to solid Fe:



and

4. formation of molten iron from its solid components:



which is slightly exothermic.

1.4.3 Main Thermal Processes

The blast furnace is a countercurrent heat exchanger - tuyeres to furnace top - in which:

1. hot gas ($\sim 2100^\circ\text{C}$) is produced in front of the tuyeres by burning hot coke with hot blast air and added oxygen;
2. these hot gases ascend through the furnace, and sequentially:
 - a. heat and melt iron and slag,
 - b. provide heat to reduce iron oxides to iron,
 - c. heat the descending solid charge, and

- d. near the top of the blast furnace, remove moisture from the charge burden;
3. the ascending gas leaves the furnace at $100\text{--}200^\circ\text{C}$, above the gas $\text{H}_2\text{O}(\text{g})$ dew point.

This countercurrent flow aspect is discussed throughout this book. It is key to the blast furnace's outstanding chemical and thermal efficiency.

1.4.4 Blast Furnace Information

With its deep history and global footprint, blast furnace design and operation varies from region to region and company to company. Blast furnace operators work to obtain the lowest operating cost and longest campaign life to maximize the value that blast furnace iron-making provides. Specific basic design and important input and output information for selected industrial blast furnaces are provided in [Table 1.1](#).

1.4.5 Production Statistics

In 2016, about 1.2 billion tonnes of molten iron were produced from blast furnaces ranging in output from 0.2 to 5.0 M t/year.⁵ The exact number of blast furnaces operating is challenging to identify; annual production would suggest that 700–900 blast furnaces are in operation globally. Blast furnaces operate on every continent but Antarctica, [Table 1.2](#).

The global distribution of blast furnace capacity is illustrated further in [Fig. 1.11](#).

1.4.6 Campaign Life

Optimally, blast furnace ironmaking never stops except for safety concerns or to replace the furnace refractories and cooling system, known as a furnace reline. The blast furnace operates continuously for 12–15 years (occasionally 20+ years) before the furnace

TABLE 1.1 Statistics for Selected Blast Furnace Operations

Continent	Asia		Europe		Australia	South America		North America
Country	Japan	Kobe	Russia	Netherlands	Australia	Argentina	Brazil	Canada
Company	NSSMC	NLMIK	Tata Steel	BlueScope		Siderar	CSA	ArcelorMittal
Site/Location	Nagoya	Kakogawa	Lipetsk	IJmuiden	Port Kembla	San Nicolas	Santa Cruz	Dofasco
Furnace Identification	1	2	Rossiyanka	6	5	2	1 & 2	4
Operating Period	2015	2016 (May)	2015	05.2015 - 03.2016	2015	2015	2016	Q1 2016
Furnace Characteristics		Units						
Hearth Diameter	m	14.8	14.90	13.10	11.00	12.04	10.40	12.00
Working Volume - tuyeres to stockline	m ³	4583	4530	3361	2328	3000	2353	2775
Inner Volume - hearth bottom to stockline	m ³	5443	5400	4297	2678	3427	2610	3284
Number of tuyeres		42	40	36	28	28	27	32
Number of tapholes		4	4	4	3	3	2	2
Annual operating time	hours	8216	8784	8411	8474	8527	8520	8480
Inputs		per tonne HM						
Sinter	kg tonne ⁻¹	1259	754	1163	623	1361	467	970
Pellets	kg tonne ⁻¹	125	387	501	872	30	468	480
Lump Ore	kg tonne ⁻¹	237	466	17	27	232	629	150
Other (reverts, DRI, HBI, new Fe)	kg tonne ⁻¹	-	-	-	6.6	-	11	-
Fluxes	kg tonne ⁻¹	-	64	4	-	10	46	30
Total Dry Coke	kg tonne ⁻¹	337	302	405	282	391	388	390
Large coke		-	-	-	247	-	-	-
Small coke		-	-	-	35	-	-	-
Injected Coal	kg tonne ⁻¹	157	209	-	228	118	-	160
Injected Natural Gas	kg tonne ⁻¹	-	-	99	-	-	95	-
Blast Air*	Nm ³ tonne ⁻¹	935	1177	870	594	986	995	928
Oxygen Enrichment*	Nm ³ tonne ⁻¹	62	63	117	118	31	269	51
Total Blast Moisture*	grams Nm ³ Blast Air ⁻¹	15	14	6	8.3	30	17	30
Blast Temperature	°C	1206	1234	1222	1111	1157	1154	1250
Tuyere Pressure	bar, gauge	3.7	4.4	4.3	3.2	3.3	3.1	4.5
Flame Temperature	°C	2165	2329	2057	2279	2133	2002	2250
Outputs								
Production	tonne day ⁻¹	10371	11230	11888	7455	6925	5355	7500
Productivity - Working volume basis	tonne day ⁻¹ m ⁻³	2.3	2.5	3.5	3.2	2.3	2.4	2.7
Productivity - per m ² of hearth	tonne day ⁻¹ m ⁻²	60	64	88	79	61	63	66
Molten Iron								
Temperature	°C	1532	1504	1483	1507	1512	1474	1490
Silicon Content	mass %	0.59	0.45	0.42	0.45	0.60	0.45	0.40
Sulfur Content	mass %	0.022	0.016	0.019	0.032	0.017	0.024	0.06
Slag								
Mass	kg tonne ⁻¹	277	282	380	210	309	252	260
CaO/SiO ₂	mass ratio	1.2	1.3	1.0	1.1	1.2	1.1	1.1
CaO	%	-	43.2	-	38.7	41.8	37.6	39.0
MgO	%	-	6.5	-	9.6	5.7	9.9	8.0
Al ₂ O ₃	%	-	15.2	-	14.6	14.3	13.2	9.0
SiO ₂	%	-	34.1	-	34.1	36.2	35.8	37.0
Top Gas								
CO	% by volume	23.5	23.9	26.4	27.5	23.2	20.5	24.0
CO ₂	% by volume	23.1	22.6	22.0	27.3	21.9	20.6	23.0
H ₂	% by volume	3.7	4.7	10.0	6.0	4.1	10.6	4.0
Temperature	°C	125	122	96	109	102	120	175
Pressure	bar, gauge	2.2	2.6	2.3	1.6	1.8	1.6	2.5

*Nm³ = 1 m³ of gas at 1 bar pressure and 0 °C

TABLE 1.2 Blast Furnace Molten Iron Production by Country, 2016

Country	2016 Blast Furnace Iron Production, Megatonnes (Mt)
Argentina	2.1
Australia	3.6
Austria	5.6
Belgium	4.9
Brazil	26.0
Canada	6.2
Chile	0.7
China	701
Czech Republic	4.2
Finland	2.7
France	9.7
Germany	27.3
Hungary	0.9
India	63.0
Iran	2.3
Italy	6.0
Japan	80.2
Kazakhstan	3.3
Mexico	4.5
Morocco	0.8
The Netherlands	6.1
Poland	4.7
Romania	1.6
Russia	51.8
Slovakia	4.0
South Korea	46.3
Spain	4.1
South Africa	4.3
Sweden	3.1
Taiwan, China	14.9

(Continued)

TABLE 1.2 (Continued)

Country	2016 Blast Furnace Iron Production, Megatonnes (Mt)
Turkey	10.3
Ukraine	23.7
United Kingdom	6.1
United States	22.3
Other countries	4.6
Total	1160

China Dominates With India, Japan, Russia, and South Korea at a Second, Markedly Lower Levels⁵. worldsteel Association.

becomes unsafe and irreparable—whereupon it is relined or rebuilt. This is referred to as the blast furnace campaign life. The current record holder is ArcelorMittal, Blast Furnace #1, Tubarão, ES, Brazil. This blast furnace operated for over 28 years and produced more than 90 million tonnes of hot metal. Details of the Blast Furnace #1 campaign are provided in Fig. 1.12.

Long campaigns are obtained by good blast furnace design, stable operations, and quality burden materials to avoid refractory thermal shock, abrasion, and slag/chemical attack. Rebuilding halts iron production, which is expensive, so long campaigns are economically very advantageous.

Major improvements can be made outside the blast furnace while the furnace is operating. For example, the blast furnace's entire control system is often modernized during a long campaign. It is unlikely that the control system would have spare parts for 30 years! Other ancillary equipment may need to be replaced or upgraded.

Blast furnace utilization can be as high as 97% or 98% over extended periods, with only short 1- to 2-day long shutdowns for maintenance. World-class blast furnaces will only have four,

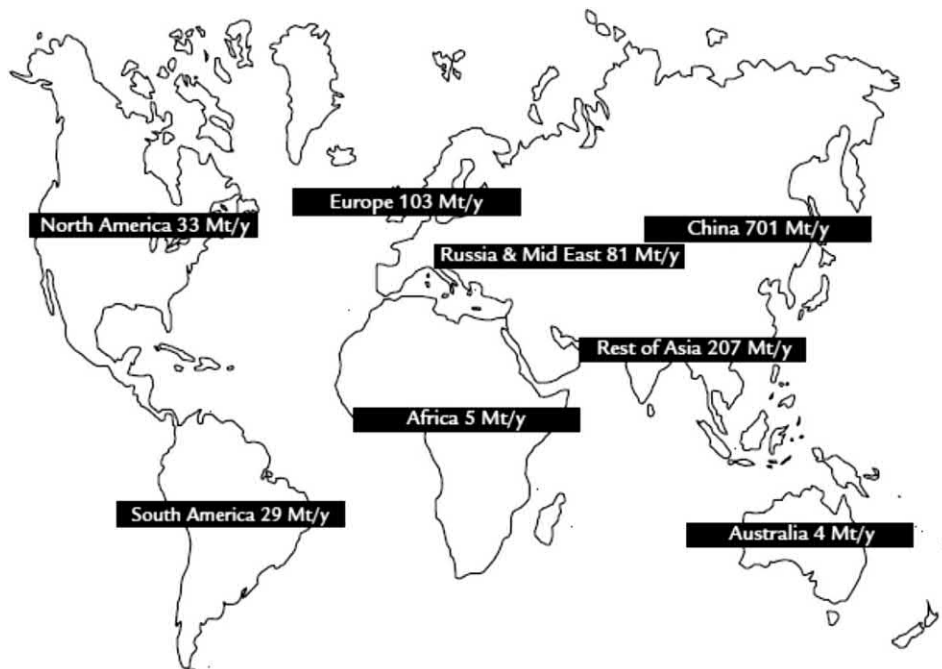


FIGURE 1.11 Capacity of the world's iron blast furnace plants. *Mt/y*, Megatonnes per year.

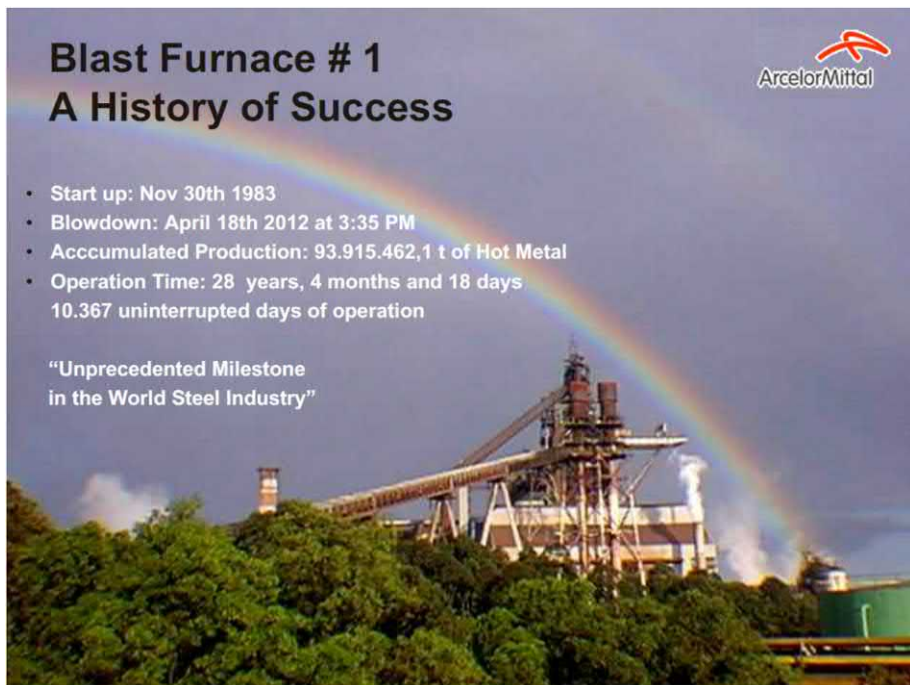


FIGURE 1.12 ArcelorMittal Tubarão Blast Furnace #1-Longest Campaign c.2012. Source: Photo courtesy of ArcelorMittal Brazil.

1–2 day maintenance stops per year. Longer stoppages (i.e., greater than 1 week) may be needed for interim refractory and cooling system repairs.

1.5 COSTS

Blast furnace ironmaking is the single most expensive operation in an integrated steelworks from an operating, maintenance, and capital cost perspective. The cost of producing molten pig iron is about 75% of the cast steel cost. Relines and rebuilds are among the most expensive maintenance activities that a steelworks must plan for. The initial investment for a new blast furnace is one of the cornerstone investments for a new steelworks.

1.5.1 Investment (Capital) Costs

At the time of writing, the cost to build a new blast furnace complex was estimated to

be 150 USD per annual tonne of product molten iron. Thus, the investment cost for a complex producing 4 million tonnes of molten iron per year is calculated by the equation:

Blast furnace complex cost

$$\begin{aligned} &= [\text{Investment cost per annual tonne of molten iron}] \\ &\quad * [\text{Plant capacity, tonnes of molten iron per year}] \\ &= [150 \text{ USD per annual tonne of molten iron}] \\ &\quad * [\text{Plant capacity, } 4 \times 10^6 \text{ tonnes of molten iron per year}] \\ &= 600 \text{ million USD} \end{aligned}$$

To this, we must add about 10% for working capital to cover the plant's start-up costs.

1.5.2 Operating Costs

Table 1.3 estimates the cash costs for producing molten blast furnace iron. The total 2017 cost is ~274 USD/t. About 95% of this cost is for iron ore and fuel inputs, so that total cost is controlled almost completely by the prices of iron

TABLE 1.3 Estimated Cash Cost (2017) of Producing Molten Iron From a 70% Sinter, 30% Pellet Blast Furnace Charge

Item	Unit Cost	Consumption	Cost of Producing 1 t of Molten Iron, USD
Fe oxide sinter	\$71/t	1.1 t	78.1
Fe oxide pellets	\$123/t	0.5 t	61.5
Coke	\$250/t	0.3 t	75.0
Injected pulverized coal	\$115/t	0.2 t	23.0
Flux: (CaCO ₃ –MgCO ₃)	\$10/t	0.03 t	0.3
Oxygen	\$0.03/Nm ³	50 Nm ³	1.5
Blower air	\$0.01/Nm ³	720 Nm ³	7.2
Electrical energy	\$0.1/kWh	150 kWh	15.0
Labor	\$25 per labor-hour	0.23 labor-hour	5.8
Repairs/Maintenance	\$6/t of product molten iron		6.0
Refractories	\$1/kg	1 kg	1.0
Total			274

The Largest Cost is Fe Sinter + Pellets Followed by Coke + Coal and Electrical Energy. Together These Account for 95% of Molten Iron Production Cost.

ore, metallurgical coal, and injected fuels, such as pulverized coal and natural gas.

1.5.3 Maintenance and Relining Costs

Blast furnaces must be completely relined and rebuilt at the end of the campaign life which is usually determined by the hearth life. Relines take about 2 years to plan and are an important opportunity to renew not only the blast furnace proper but many supporting systems that are at the end of their service life. A reline will last 60–90 days, and the cost will be between 150 and 300 M USD depending on the scope of the repair and size of the blast furnace.

Due to these high relining costs and related production losses, blast furnace operators work tirelessly to extend the campaign. This may include shorter stops from 5 to 20 days to replace worn cooling staves, spray refractory materials on the shaft walls, or rebuild the hearth wall and tapholes. In a very long campaign, two to three shorter repairs may be completed during the campaign. Very careful inspection and data analysis is completed in advance of these repairs to identify parts of the blast furnace that need to be replaced or remediated.

1.6 SAFETY

Of paramount concern around the blast furnace is worker safety. A safe working environment is fostered by:

1. setting safety as a primary goal;
2. close attention to safety by management;
3. thorough worker safety training;
4. thorough maintenance and hazard identification/elimination; and
5. special attention to unique blast furnace hazards:⁶
 - a. carbon monoxide poisoning,
 - b. molten iron/slag burns,
 - c. gaseous sulfur compound poisoning,

- d. water-molten iron/slag explosions,
- e. hydrogen or natural gas explosions,
- f. water leakage into the furnace, and
- g. worker heat stress.

CO poisoning is by far the greatest concern because:

1. enormous amounts of CO are present around the furnace, and
2. CO has a rapid, potentially fatal effect on the human body due to its rapid absorption into the blood stream and ability to block oxygen uptake by the human body.

Personal CO monitors must be worn in all areas, and a sign-in, sign-out system is rigorously enforced.

1.7 ENVIRONMENT

Blast furnace-based steel plants are very large, up to 3–10 km² of ground area. They typically have:

- ocean-going ship unloading facilities;
- marshaling yards for freight trains;
- ore and coal stock yards;
- coke plant and related facilities;
- sinter and/or pellet plants;
- blast furnaces; and
- slag solidification and crushing plants

which impact land, sea, and air.

It is imperative that close attention be paid to minimizing the environmental impact of the facility. This is being done in modern blast furnace plants by:

1. installing filters, precipitation tanks, and water treatment on all discharge water streams;
2. reusing water in critical systems;
3. biological treatment of coke plant waste water containing phenols and thiocyanates;
4. installing custom fitted hoods in the casthouse to collect fumes. Using bag filters

and electrostatic precipitators on all waste gas streams;

5. avoiding spillages and dust generation during ship unloading;
6. maximizing energy usage to minimize greenhouse gas [mostly CO₂(g)] emissions. Examples include top recovery turbines to generate electricity while depressurizing BFG and generating electrical power from blast furnace and coke oven gases; and
7. good housekeeping throughout, especially near the ore and coal yards.

Specific recent activities and ideas to improve blast furnace environmental performance include:

1. switching hot coke quenching from water to dry nitrogen quenching, thereby avoiding emission of clouds of steam and generating electrical energy;⁷
2. recovering H₂(g) and recycled CO(g) reductants from BFG and injecting these gases in blast furnaces shaft to minimize coke consumption and lower CO₂(g) greenhouse gas emissions;
3. using electrically plasma heated hot blast to minimize coke consumption and CO₂(g) greenhouse gas emissions⁸;
4. charging recycled steel scrap to the blast furnace, minimizing ferrous waste, coke consumption and CO₂(g) greenhouse gas emissions;
5. adding direct reduced iron produced from natural gas to the blast furnace to reduce CO₂(g) emissions;
6. reforming blast furnace gas into CO(g) and H₂ using a plasma-based reactor;
7. increasing use of self-fluxing sintered ore and pellets in the blast furnace, thereby lowering blast furnace CO₂(g) emission from carbonate fluxes; and
8. increasing the use of slag for cement and road aggregate rather than dumping—turning a waste product into a useful product.

1.8 SUMMARY

The iron blast furnace is an efficient process for continuously making enormous quantities of molten iron—ready for immediate pyrometallurgical refining into steel. The blast furnace's principle advantages are its:

1. exceptional process stability;
2. high chemical and thermal efficiency;
3. long campaign life between major repairs, and
4. high rate of iron production and with this economies of scale.

The blast furnace's disadvantages are its:

1. large unit size and consequentially high initial capital cost;
2. dependency on metallurgical coke, sinter, and iron ore pellets, all with their own challenges;
3. large CO₂ emission, a well-known greenhouse gas; and
4. high relining/rebuilding cost at the end of each campaign.

The blast furnace makes very efficient use of its carbon fuel/reductants. This high efficiency and the furnace's rapid rate of iron production are continually being improved by:

1. uniform charging with sized pellets, sinter, and crushed ore;
2. tuyere injection of coal and other hydrocarbons to partially replace expensive coke;
3. increased pressure and blast oxygen enrichment to speed up ironmaking without increasing gas velocities; and
4. continuous measurement and automatic control of blast furnace inputs.

Campaign lives of iron blast furnaces are 12–20+ years. Long campaigns are obtained by good initial furnace design, stable day-to-day operation, attentive maintenance, and practices that minimize refractory wear.

EXERCISES

- 1.1.** Nearly all a blast furnace's product molten iron is immediately sent (molten) to steelmaking. What is the difference between blast furnace iron and steel?
- 1.2.** Safety is a critical feature of industrial blast furnace ironmaking. Identify three important safety problems around a blast furnace and how they may be overcome.
- 1.3.** What is slag and what is its purpose and use? How is its composition adjusted?
- 1.4.** A common starting material for making molten iron is hematite, Fe_2O_3 . At 100% reduction efficiency, how much pure hematite will be required to make 1000 kg (1 t) of Fe in molten iron? Blast furnace stoichiometric data are given in Appendix A.
- 1.5.** Industrial hematite ore pellets contain 94 mass% hematite and 6 mass% SiO_2 (quartz). What is the Fe content of this ore, mass% Fe?
- 1.6.** Smelting of the Exercise 1.5 ore is producing molten iron: 95 mass% Fe, 4.5 mass% C, and 0.5 mass% Si. The blast furnace is producing 7000 t of Fe per day. How much molten iron is it producing per day?
- 1.7.** A blast furnace operator wishes to increase his hearth temperature by enriching his blast to 27 mass% $\text{O}_2(\text{g})$. What mass of $\text{O}_2(\text{g})$ must the operator add per 1000 kg of air to obtain this 27 mass% O_2 blast. Natural air contains 23.3 mass% $\text{O}_2(\text{g})$ and 76.7 mass% $\text{N}_2(\text{g})$, Appendix B.
- 1.8.** Why does O_2 enrichment of blast air increase hearth temperature?

References

1. Wolfe L, Olson L. *Yield improvements during iron desulfurization when utilizing "flow aided" compounds for modifying*

- slag characteristics.* Retrieved from: <<http://www.carmeusena.com/sites/default/files/brochures/steel/tp-iss-tech-20paper-yield-20improvements.pdf>>; [accessed 01.01.16].
2. Kumar V. *Ionic theory of slags.* Retrieved from: <<https://www.msm.cam.ac.uk/teaching/partIII/courseM3/M3H.pdf>>; 2015 [accessed 01.01.16].
 3. *Ground granulated blast furnace slag (architectural and engineering benefits).* Retrieved from: <https://en.wikipedia.org/wiki/Ground_granulated_blastfurnace_slag#Architectural_and_engineering_benefits>; 2016 [accessed 01.01.16].
 4. Van der Perre W. *Temperature measurement in liquid metal.* Retrieved from: <http://heraeus-electro-nite.com/media/webmedia_local/media/downloads/steel_2/temperature-control/temperature_wvdp_2000.pdf>; 2016 [accessed 01.01.16].
 5. worldsteel Association. *Blast furnace iron production 2016.* Recovered from: <<https://www.worldsteel.org/statistics/BFI-production.html>>; 2017 [accessed 10.01.18].
 6. Lucas D. *Incident and accident prevention in blast furnace ironmaking.* Lecture #4, 23rd blast furnace ironmaking course. Hamilton: McMaster University, School of Engineering; May 11–May 16, 2014. <www.google.com/?q=gws_rd=ssl#q=mcmaster+university+school+of+engineering>.
 7. Iipnetwork. *Coke dry quenching/industrial efficiency technology and measures.* Retrieved from: <ietd.iipnetwork.org/content/coke-dry-quenching>; 2018 [accessed 01.02.18].
 8. Sukhram M, Lao S, Cameron I, Hyde B, Busser J, Gorodetsky A. Hot blast superheating – a scalable technology to reduce carbon consumption. In: *Presented at AISTech 2017*. Nashville; 2017.

Suggested Reading

- Geerdes M, Chaignau R, Kurunov I, Lingiardi O, Ricketts J. *Modern blast furnace ironmaking (an introduction).* 3rd ed. BV, Amsterdam: IOS Press; 2015.
- McMaster. *24rd Blast furnace ironmaking course (two volumes).* Hamilton: McMaster University, Materials Science and Engineering; 2016.
- Babich A, Senk D, Gudenu HW, Mavrommatis KT. *Ironmaking (textbook).* Aachen: Institut für Eisenhüttenkunde der RWTH Aachen; 2008.
- Ghosh A, Chatterjee A. *Ironmaking and steelmaking, theory and practice.* Delhi: PHI Learning Private Ltd.; 2013.

Inside the Blast Furnace

O U T L I N E

2.1 Blast Furnace Ironmaking—A Look Inside the Furnace	20	2.10 Reactions Above the 930°C Isotherm	25
2.2 Physical Behavior: Solids Descend	20	2.11 Reduction of Magnetite (Fe_3O_4) to Wustite ($\text{Fe}_{0.947}\text{O}$)	25
2.3 Physical Behavior: Blast Air and Gas Ascend	20	2.12 Steady-State Wustite ($\text{Fe}_{0.947}\text{O}$) Production and Consumption	25
2.4 Reactions in the Blast Furnace Hearth Zone	21	2.12.1 Thermal Reserve Zone—Evidence and Explanation	26
2.4.1 Hearth Reactions	21	2.13 Hematite (Fe_2O_3) Reduction Zone	27
2.5.1 The Raceway Zone	22	2.13.1 Industrial Top Gas Composition	27
2.5 Reactions in Front and Around the tuyeres	22	2.14 Chemical and Heat Transfer in the Blast Furnace	28
2.5.1 The Raceway Zone	22	2.15 Residence Times	28
2.6 Above the Raceway Zone	23	2.16 Summary	28
2.7 Fusion and Melting Zone	23	Exercises	29
2.7.1 Final Melting	23	References	30
2.8 Reactions Above the Fusion Zone	24	Suggested Reading	30
2.9 Kinetics of Coke Gasification	24		

2.1 BLAST FURNACE IRONMAKING—A LOOK INSIDE THE FURNACE

In Chapter 1, The Iron Blast Furnace Process, we examined the blast furnace looking from the outside, for example, its:

- size;
- structure;
- productivity;
- raw materials;
- reactions;
- products;
- operation;
- lifetime;
- safety;
- environment; and
- costs.

We learned that the blast furnace is a tall, durable, and high productivity unit that produces at 1500°C;

Molten iron – 94.5% Fe, 4.5% C, 1% [Si + Mn]

from solid Fe oxide, primarily hematite, ore charged as lump ore, sinter, and pellets.

2.2 PHYSICAL BEHAVIOR: SOLIDS DESCEND

Separate batches of Fe oxide ore and coke are charged to the top of the blast furnace while Fe as molten iron is tapped from the bottom, Fig. 2.1.

Large modern blast furnaces are tapped continuously using multiple tapholes. Smaller furnaces are tapped semicontinuously through a single taphole.

The top-charged coke's carbon is oxidized to CO(g) and/or CO₂(g) as the coke descends through the blast furnace and coke is combusted at the tuyeres. As a result, the top-charge solids, mainly ore and coke, continuously descend toward the tuyeres/taphole.

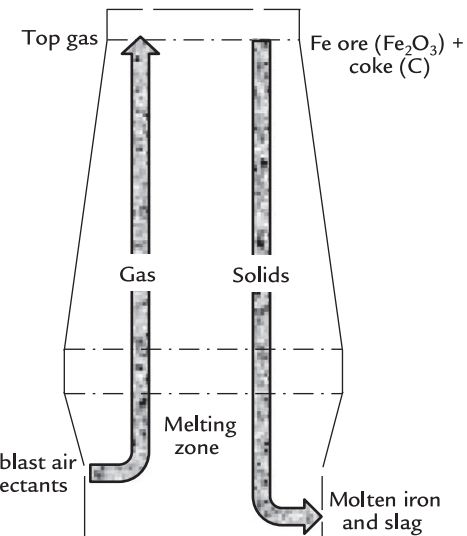


FIGURE 2.1 The blast furnace process with continuous upward gas flow and continuous downward solids flow.

The charge solids are pulled by gravity into space vacated as coke is combusted in front of the tuyeres and molten iron and slag are removed from the blast furnace.

The solids downward flow is due to:

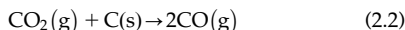
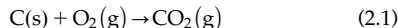
1. oxidation of C(s) to CO(g) and CO₂(g) and consequent shrinkage/consumption of coke pieces at the tuyeres and in the hearth;
2. removal of molten iron and oxide slag at the bottom; and
3. gravity.

The upward gas flow is due to the blowing of pressurized blast air through tuyeres into the furnace. Actual gas flows fill the entire blast furnace per Fig. 1.1. This view is a vertical slice down the center line of a blast furnace.

2.3 PHYSICAL BEHAVIOR: BLAST AIR AND GAS ASCEND

Simultaneously, lower in the blast furnace, pressurized hot blast air is continuously blown into the furnace, where its O₂ reacts

with descending hot coke and tuyere injected hydrocarbons to make hot CO(g), by the reactions:



This hot, $\sim 2100^\circ\text{C}$, CO(g) continuously ascends in the blast furnace - forced upward by the pressurized blast air injected through the tuyeres. As it ascends, the CO(g) reacts with descending Fe oxides to make Fe and CO₂:



As a result, we have continuous countercurrent flow of solid Fe oxides, coke pieces and eventually Fe downwards and CO, H₂, CO₂, H₂O, and N₂ gas upwards.

2.4 REACTIONS IN THE BLAST FURNACE HEARTH ZONE

We begin our analysis of blast furnace reactions by examining the furnace hearth, that is, below the tuyeres, Fig. 2.2.

All solid material below the tuyeres and extending down to the blast furnace floor consists only of pieces of hot coke. These pieces are smaller than charged because most of the top-charged C-in-coke has oxidized to CO(g) and CO₂(g) in front of and above the tuyeres.

Molten iron and slag, melted by the very high temperatures ($\sim 2100^\circ\text{C}$) in front of the tuyeres, drips through the coke percolator to form layers of heavier molten iron at the bottom followed by lighter molten slag between the coke pieces.

The blast furnace is operated to always keep the molten layers below the tuyeres. Molten

liquid depths are controlled by adjusting iron and slag outflow rates and duration of each cast - by changing the diameter of the drill bit that is used to open the tapholes and the casting schedule.

2.4.1 Hearth Reactions

The main chemical processes that occur during the dripping of iron and slag through the coke percolator are:

1. final reduction of the slag's Fe oxides to make molten iron;
2. partial reduction of the molten slag's SiO₂ and MnO to form dissolved Si and Mn in the molten iron;
3. final saturation of the molten iron with ~ 4.5 mass% carbon; and
4. formation of the final molten slag.

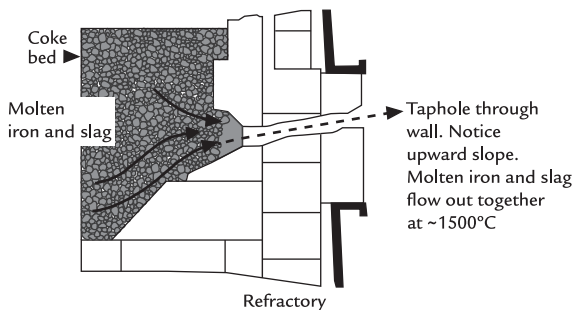


FIGURE 2.2 Blast furnace taphole (right) showing molten iron and molten slag being tapped from a blast furnace. The taphole is typically 3 m above the furnace floor. The molten iron and slag flow slightly upward because the furnace is under pressure (inside). Tapping is continuous with large furnaces, intermittent with small furnaces. Iron and slag flow are terminated by machine-plugging the hole with clay, which hardens and stops the flow. Typical molten iron tapping rates are 7 tonne/min with a flow velocity of 5 m/s through the taphole.

2.5 REACTIONS IN FRONT AND AROUND THE TUYERES

Hot blast air is injected into the blast furnace through 15–45 tuyeres positioned around the furnace circumference, Fig. 1.1. The hot blast enters at 180–240 m/s and at a pressure up to 420 kPa gauge. This pressure is necessary to:

1. push reducing gas rapidly up through the solid ore and coke particles, and
2. overcome the 200–250 kPa gauge pressure imposed at the top of the furnace.

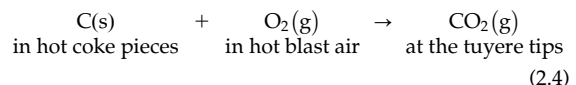
2.5.1 The Raceway Zone

Visual observations thorough peep sights located in each tuyere show that the blast

air forms a gas space called the raceway. Hot coke pieces fall into and race around the void formed by the pressurized blast air, Fig. 2.3.

O_2 in the hot blast air entering the raceway immediately forms hot $CO_2(g)$ at the tips of the tuyeres. This $CO_2(g)$ flows into the raceway and is completely reduced to $CO(g)$ by the time it leaves the raceway a few milliseconds later.

The reactions are:



and

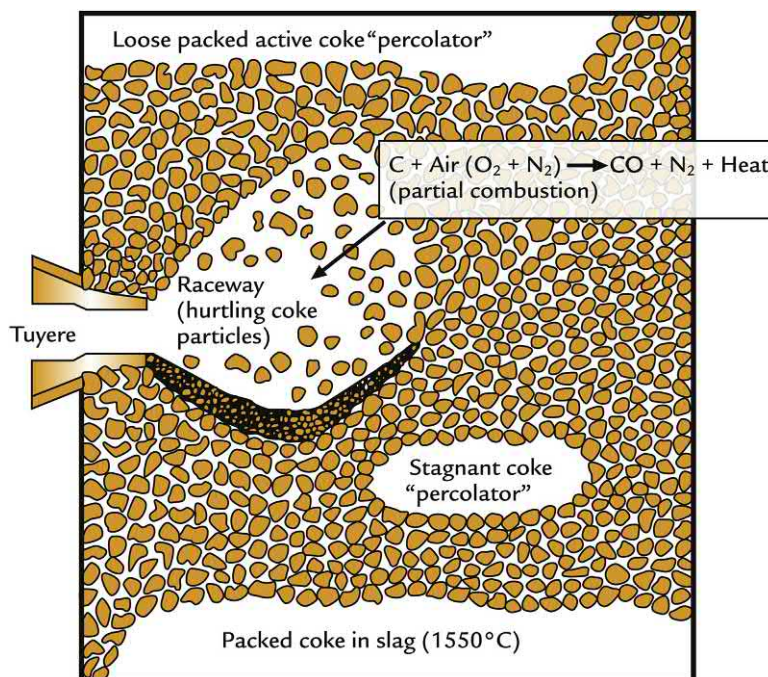
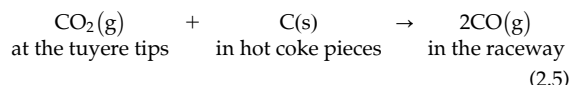
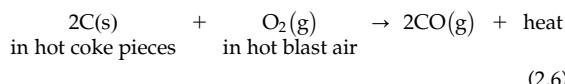


FIGURE 2.3 Sketch of tuyere raceway as interpreted from quenched blast furnaces. The sketch is a vertical slice through the center of a raceway. Visual observations through tuyere peep sights reveal pieces of coke descending into and tumbling around inside the raceway. Blast furnace tuyeres are typically 0.15 m inside diameter. They protrude some 0.4 m into the furnace. The carbonaceous portion of the exiting raceway gas is all $CO(g)$, Appendix D.

for a total of



The heat generated from this combined reaction is enough to heat the $[\text{CO(g)} + \text{N}_2\text{(g)}]$ raceway exit gas to $\sim 2100^\circ\text{C}$, as described in Chapter 14, Raceway Flame Temperature.

2.6 ABOVE THE RACEWAY ZONE

All the solid materials immediately above the raceway level are solid coke pieces, Fig. 2.3. These pieces are loosely packed immediately above the raceways and more tightly packed near the center of the blast furnace.

$\text{CO} + \text{N}_2$ raceway exit gas rapidly ascends through this coke reserve without reacting with the coke particles as the hot gases rise.

2.7 FUSION AND MELTING ZONE

Examinations of quenched blast furnaces indicated that the region of coke above the raceways is bounded above by a fusion zone that consists of alternate layers of:

1. solid coke pieces, and
2. softening and melting Fe , $\text{Fe}_{0.94}\text{O}$, and flux/gangue oxides.

This layered structure persists from the original top-charged ore and coke layers. The coke layers are particularly important because they provide a route for the ascending $\text{CO} + \text{N}_2$ gas to move horizontally across to ore that has not yet fused and up through the furnace charge, Fig. 2.4.

2.7.1 Final Melting

Fe and gangue oxides soften and fuse in the fusion zone shown in Fig. 2.4. As these fusion layers descend, their central tips encounter hotter gas and the fused layers melt and drip into the active coke zone.

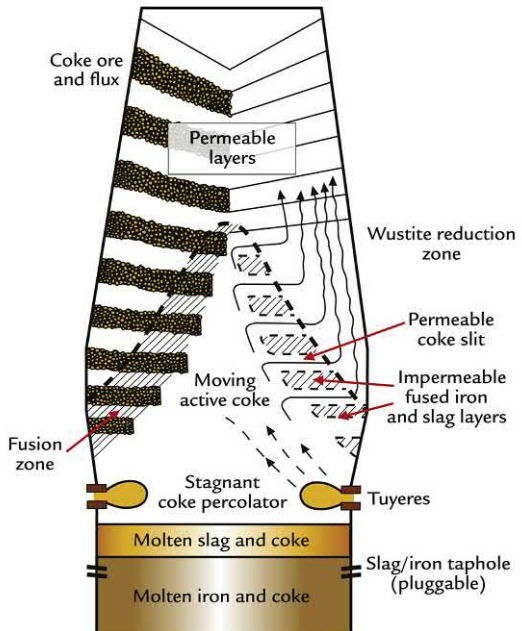


FIGURE 2.4 Central vertical slice of Fig. 1.1 blast furnace showing interior ore-coke-gas-slag-molten iron structure. Remember that:

- the furnace is batch charged in layers;
- the solids are continuously descending;
- the gases are continuously ascending; and
- molten iron and molten slag are being continuously collected and cast.

Note the inverted "V" (^)-shaped fusion zone and the coke slits through the sides of the fusion zone. The coke slits distribute the ascending gas to the furnace circumference and up to the top of the furnace. The ore layers are typically 0.7 m thick and the coke layers 0.4 m thick.¹

To summarize, low in the furnace, the descending ore layers are now:

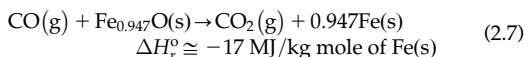
1. solid next to the furnace wall;
2. fusing further into the center; and
3. melting at the central tips.

2.8 REACTIONS ABOVE THE FUSION ZONE

When $\text{CO} + \text{N}_2$ gas flows horizontally into oxides particles that have not fused near the circumference, these gases encounter Fe oxide (mainly $\text{Fe}_{0.947}\text{O}$) pellets, sinter, and lump ore pieces. In the blast furnace, Fe oxide occurs as three discrete compounds: wustite, $\text{Fe}_{0.947}\text{O}$; magnetite, Fe_3O_4 ; and hematite, Fe_2O_3 .¹

The CO(g) immediately reduces these oxide particles to Fe . Two cyclic reactions occur:

- *Wustite reduction*



and

- *carbon-in-coke gasification*



The coke gasification shown in Eq. (2.8) is thermodynamically favored but highly endothermic. The gasification reaction absorbs considerable heat from the rising gas - causing rapid cooling of the gas.

These cyclical reactions may be visualized schematically in Fig. 2.5.

2.9 KINETICS OF COKE GASIFICATION

An important aspect of blast furnace ironmaking is the coke gasification reaction, Eq. (2.8). This reaction slows markedly as temperature decreases.^{2,3} The result is that CO(g) production

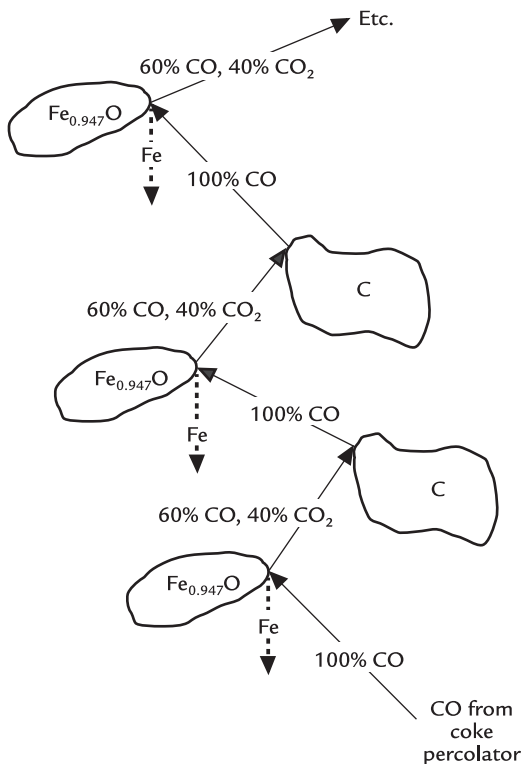


FIGURE 2.5 Sketch of $\text{Fe}_{0.947}\text{O}$ reduction and carbon gasification above the fusion zone. The gas compositions are mass %. CO(g) ascends from the coke percolator. It reacts with $\text{Fe}_{0.947}\text{O}$ to form Fe(s) and $\text{CO}_2\text{(g)}$. This $\text{CO}_2\text{(g)}$ ascends and contacts a coke piece where it reacts to form CO(g) by Eq. (2.8) and so on. A ratio of 60 mass % CO and 40 mass % CO_2 is the approximate equilibrium concentration of CO and CO_2 for Eq. (2.7) at $\sim 1000^\circ\text{C}$. A ratio of 100 mass % CO and 0 mass % CO_2 is the approximate equilibrium concentration of CO and CO_2 for Eq. (2.8) at around 1000°C . Gas temperature decreases rapidly as the reducing gases ascend through this region - because carbon gasification, Eq. (2.8), absorbs considerable heat.

comes to a virtual halt at temperatures less than $\sim 930^\circ\text{C}$, Fig. 2.6.

Thus, once the rising gas has cooled to $\sim 930^\circ\text{C}$, little more CO is regenerated. Two important consequences of this are:

1. *there is virtually no C-in-coke oxidation above the blast furnace's 930°C isotherm, and*

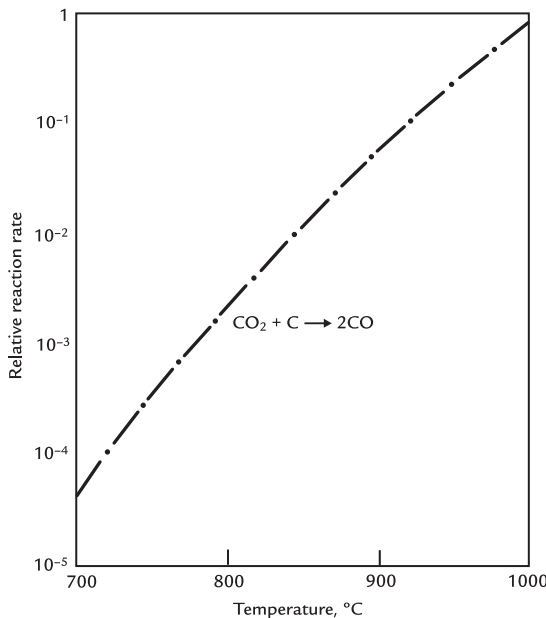


FIGURE 2.6 C-in-coke gasification slows markedly with decreasing temperature. The rate is taken as unity at 1100°C. Rates at other temperatures have been calculated using an activation energy of 360 MJ/kg mole of C(s), Von Bogdandy and Engell² and Nomura et al.³ show a similar curve.

2. hence, all reduction above the 930°C isotherm relies upon CO produced beneath the 930°C isotherm.

2.10 REACTIONS ABOVE THE 930°C ISOTHERM

From Fig. 2.5, gas rising from the cyclic reduction zone contains about:

60 mass% CO(g)

40 mass% CO₂(g).

It is the equilibrium gas from wustite reduction at 930°C [Eq. (2.7)].

Gas that is cooler than 930°C is too weak in CO(g) to reduce any more $\text{Fe}_{0.947}\text{O}$ (s). And for kinetic reasons, the available CO₂(g) no longer reacts with carbon to make more CO(g), see

Section 2.8. This CO-rich gas is strong enough to reduce Fe_3O_4 to $\text{Fe}_{0.947}\text{O}$ and further up in the furnace, Fe_2O_3 to Fe_3O_4 .

2.11 REDUCTION OF MAGNETITE (Fe_3O_4) TO WUSTITE ($\text{Fe}_{0.947}\text{O}$)

CO(g) reduction of magnetite to wustite is represented by the reaction:



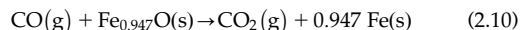
for which (1) the equilibrium constant at 930°C is 2.25, and (2) the equilibrium CO(g) and CO₂(g) concentrations are about 20 mass % CO and 80 mass % CO₂ in the carbonaceous portion of the ascending gas.

This shows that the gas rising out of the cyclic reduction zone (60 mass % CO, 40 mass % CO₂) is strong enough in CO(g) to reduce Fe_3O_4 to $\text{Fe}_{0.947}\text{O}$.

2.12 STEADY-STATE WUSTITE ($\text{Fe}_{0.947}\text{O}$) PRODUCTION AND CONSUMPTION

For the blast furnace to operate at steady state, the amount of wustite produced by Eq. (2.9) must be the same as the amount of wustite consumed by Eq. (2.7). In fact, there is more than enough CO rising from the cyclic reduction zone to accomplish this purpose. This is because:

1. each mole of CO oxidized to CO₂ by reaction with Fe_3O_4 produces ~3.8 mol of $\text{Fe}_{0.947}\text{O}$, Eq. (2.9), while
2. each mole of CO oxidized to CO₂ by reaction with $\text{Fe}_{0.947}\text{O}$ consumes only 1.0 mol of $\text{Fe}_{0.947}\text{O}$.



This excess $\text{Fe}_{0.947}\text{O}(\text{s})$ production by Eq. (2.9) results in:

1. creation of a vertical zone in the furnace, containing mostly $\text{Fe}_{0.947}\text{O}$ + coke, called the *chemical reserve zone*; and
2. restriction of unreduced Fe_3O_4 and Fe_2O_3 to a small zone near the top of the furnace, about the top 5 or 10% of the shaft. This zone is only of sufficient thickness/height for its $\text{Fe}_{0.947}\text{O}$ production rate to equal the rate of $\text{Fe}_{0.947}\text{O}$ reduction lower in the furnace, that is;

the top zone is shallow/short enough so that CO passes through the zone without making its equilibrium amount of CO_2 .

The region where the Fe-bearing material is virtually all $\text{Fe}_{0.947}\text{O}$ + coke is referred to as the *chemical reserve zone*. Because very few chemical reactions take place in this zone, it is also a region of roughly constant temperature and is called the *thermal reserve zone*. Vertical gas composition measurements in commercial blast furnaces show the presence of the chemical reserve zone, Fig. 2.7.

2.12.1 Thermal Reserve Zone—Evidence and Explanation

The gas rising into the chemical reserve zone is $\sim 930^\circ\text{C}$. Over time, this gas heats most of the chemical reserve's solids to this temperature because;

1. there are no endothermic reactions in the chemical reserve zone, and
2. heat losses through the blast furnace walls are relatively small.

At steady state, the gas temperature

1. falls markedly near the bottom of the furnace where $\text{CO}_2(\text{g})$ is endothermically reacting with $\text{C}(\text{s})$ to form $\text{CO}(\text{g})$, Eq. (2.8);
2. remains nearly constant as the gas rises through the chemical reserve, where no reactions are taking place; and
3. falls again above the chemical reserve where;
 - a. $\text{CO}(\text{g})$ endothermically reacts with $\text{Fe}_3\text{O}_4(\text{g})$ to form $\text{Fe}_{0.947}\text{O}(\text{s})$ and $\text{CO}_2(\text{g})$
 - b. carbonate fluxes are endothermically dissociating to $\text{CO}_2(\text{g})$ and oxides, and
 - c. $\text{H}_2\text{O}(\ell)$ in the top-charged solids is endothermically vaporized to $\text{H}_2\text{O}(\text{g})$.

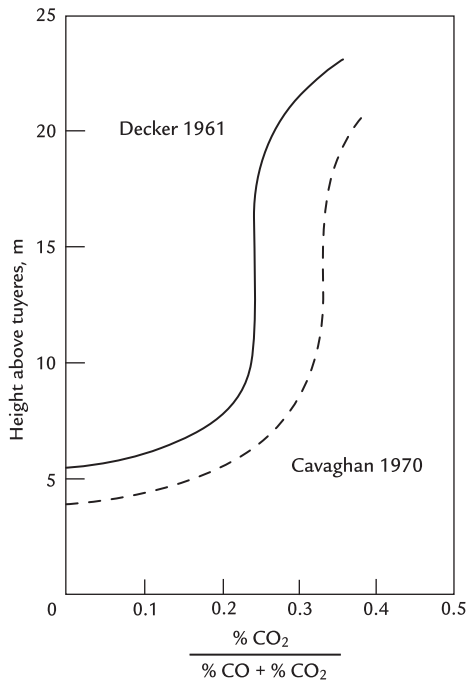


FIGURE 2.7 Vertical gas composition profiles in operating blast furnaces.^{4,5} Note the large vertical region where there is no change in ascending gas composition. It is known as the *chemical reserve zone* where no chemical reactions take place. Geerdes et al. (of Ref. [6], p 120) confirm the presence of this chemically inactive vertical zone. Lowing (1977) gives probe details.^{6,7}

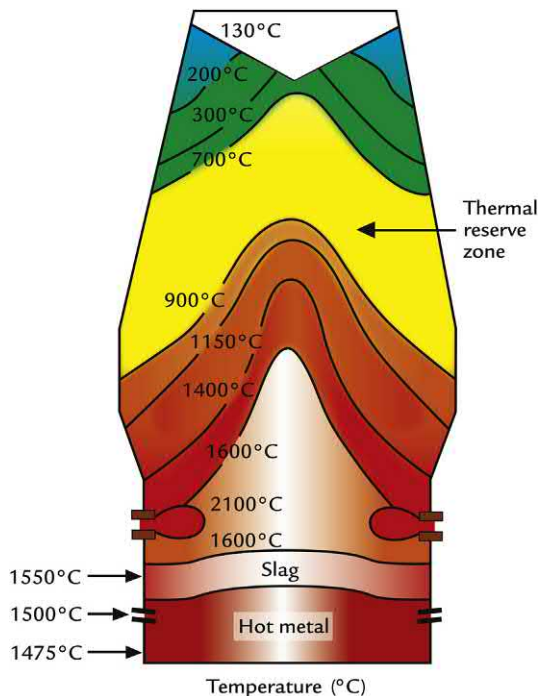


FIGURE 2.8 Gas temperatures in the blast furnace as interpreted from the quenched furnace data of Nakamura.⁸ The zone of near-constant temperature, that is, the thermal reserve zone, is shown.

The resulting gas temperature isotherms for an operating blast furnace are presented in Fig. 2.8.

In fact, the ascending gas temperature only begins to fall to the top gas temperature ($\sim 130^\circ\text{C}$) when it meets cool moist magnetite, hematite, coke, and flux near the top of the furnace, Fig. 2.9.⁶

2.13 HEMATITE (Fe_2O_3) REDUCTION ZONE

Hematite reduction in the upper blast furnace is completed by the following reaction:

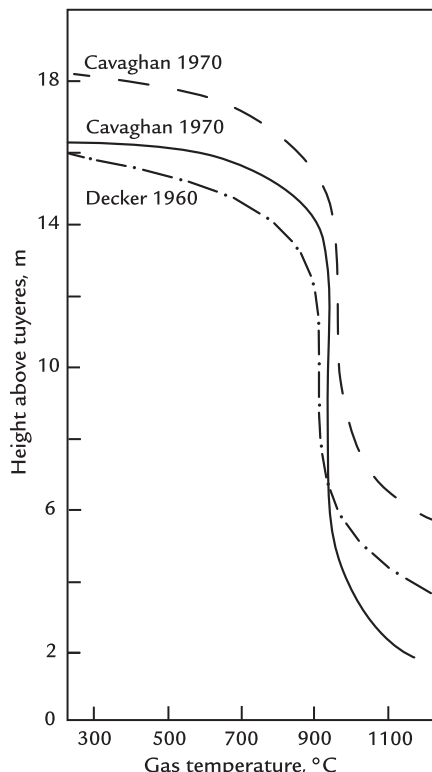


FIGURE 2.9 Vertical temperature profiles in operating blast furnaces as determined by thermocouple probes^{5,6} (see also Ref. [7]). The constant temperature *thermal reserve zone* is notable. This represents the region where the temperatures of ascending gas and descending solids are the same and change very little.

This takes place along with magnetite reduction near the top of the furnace. At equilibrium, the carbonaceous gas from this reaction would be nearly 100 vol.% CO_2 .

2.13.1 Industrial Top Gas Composition

The carbonaceous portion of industrial top gas contains about 50 vol.% CO and 50 vol.% CO_2 .¹

This is far less CO₂(g) than would be produced if Eq. (2.11) could come to equilibrium.

2.14 CHEMICAL AND HEAT TRANSFER IN THE BLAST FURNACE

The above discussion indicates the iron blast furnace is:

1. an equilibrium reactor at temperatures above ~930°C, that is, low in the furnace, and
2. a nonequilibrium reactor at temperatures below ~930°C, that is, high in the furnace.
3. These regions are separated by a wustite (Fe_{0.947}O) reserve zone in which the iron oxide is mostly Fe_{0.947}O and where no reactions are taking place.

This wustite reserve zone is equivalent to the chemical reserve zone where gas and solids compositions are not changing, Fig. 2.7, and where the temperature is roughly constant because nothing is reacting, Figs. 2.8 and 2.9.

2.15 RESIDENCE TIMES

The above discussions don't include blast furnace residence times. They are typically:

gas: ~1–5 s, tuyeres to charging level
solids/liquids: ~6–7 h, charging level to taphole.

The short gas residence time indicates that the solids must be very reactive to attain maximum carbon utilization, especially low in the furnace. The solids descent rate is about 30 m (charge height to taphole) in 300–500 minutes, that is, ~0.1 m/min. The overall process is described in Fig. 2.10.

2.16 SUMMARY

This chapter describes how the blast furnace arranges itself into seven major zones, bottom to top:

1. the 1500°C hearth zone where molten iron and slag drip down between coke pieces to attain their final highly reduced compositions just before being tapped from the furnace;
2. the tuyere-raceway zone in which incoming hot blast air reacts with descending hot carbon-in-coke and cool hydrocarbon tuyere injectants to produce hot CO(g);
3. a coke percolator where reducing conditions are strongest and where final reduction takes place;
4. the fusion zone, where (1) slag forms and (2) iron and slag fuse, then melt;
5. the cyclic reduction zone where CO(g) reacts with solid wustite (Fe_{0.947}O) to form solid Fe and where the resulting CO₂(g) reacts with carbon-in-coke to regenerate CO (g) for more reduction;
6. the wustite reserve zone where the gas is too cool to regenerate CO(g) from the reaction of C(s) + CO₂(g) and where the only oxide is wustite—which has been produced bountifully by Fe₃O₄ and Fe₂O₃ reduction near the top of the furnace; and
7. the furnace top where excess CO(g) produced low in the blast furnace reacts with layers of Fe₃O₄(s) and Fe₂O₃(s) to form just enough Fe_{0.947}O (wustite) to match the amount being reduced to Fe in the cyclic reduction zone.

The chapter has shown that the reducing gas ascends the furnace in ~5 seconds so that efficient CO(g) utilization requires rapid reaction rates and good gas/solid contact. Accurate sizing of charge materials and precise charging of separate coke and ore + flux layers provides these requirements.

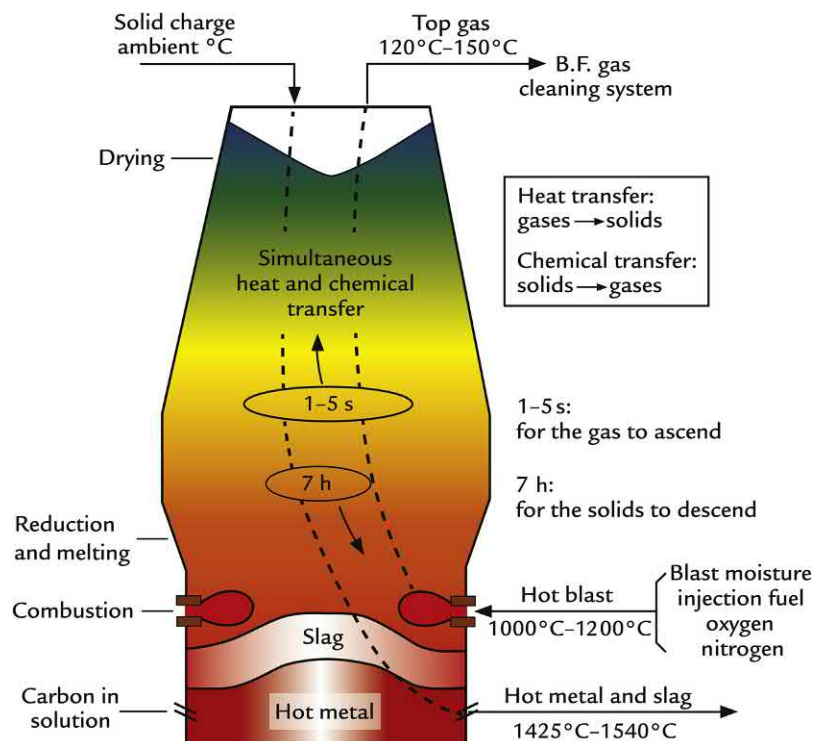


FIGURE 2.10 Overview of important heat and chemical transfer that occurs in the blast furnace.

We learned that blast furnace solids move down the furnace at $\sim 0.1 \text{ m/min}$. So, any sketch of a blast furnace interior is merely a snapshot, with all solids shifted noticeably downward 5 minutes later.

EXERCISES

- 2.1. What causes a blast furnace's top-charged solids to move rapidly down the furnace?
- 2.2. What happens to the blast furnace's blast air when it enters the furnace? Why does it rise so quickly up through the furnace? What will happen if a power failure stops the furnace's blast air blowers?
- 2.3. Fig. 2.1 indicates that the blast furnace is a countercurrent heat exchanger. What is so good about countercurrent heat exchange?

- 2.4. Blast furnace blast air is typically heated to 1200°C . What are the advantages of this heating?
- 2.5. What do you think would happen if you added 5 m to the top of the blast furnace of Fig. 2.4, that is, if you charged the furnace 5 m higher than is shown in Fig. 2.4?
- 2.6. What do you think would happen if less reactive hematite was added to the blast furnace of Fig. 2.4?
- 2.7. What are the main purposes of the blast furnace coke charge? Name at least three.
- 2.8. The temperature in the tuyere raceway reaches $\sim 2100^\circ\text{C}$, which is far above the melting points of Fe and Cu. Describe how you would prevent this elevated temperature from melting the tuyere tips and furnace walls.

- 2.9. If ore and coke layers of Fig. 2.4 are 0.6 m thick, how far down would the layers of Fig. 2.4 have moved in 6 minutes of descent? Sketch Fig. 2.4 at $t = 0$ minute and $t = 6$ minutes layer positions. Assume that the layers are descending at 0.1 m/min.

References

1. Peacey JG, Davenport WG. *The iron blast furnace – theory and practice*. New York: Elsevier; 1979.
2. Von Bogdandy L, Engell HJ. *The reduction of iron ores*. Berlin: Springer-Verlag; 1971. p. 289–96.
3. Nomura S, Naito M, Koizumi S, Kitaguchi H, Matsuzaki S, Ayukawa H, Abe T, Tahara T. Improvement in blast furnace reaction efficiency through the use of catalyst-doped highly reactive coke. In: *Nippon steel technical report no. 94*; July 2006.
4. Cavaghan NJ, Wilson AR. Use of probes in blast furnaces. *J Iron Steel Inst* 1970;208(3):231–46.
5. Decker A. Discussion of use of blast furnace probes. In: *Proceedings of blast furnace, coke oven and raw materials conference (AIME)*, vol. 20; 1961, p. 46.
6. Geerdes M, Chaigneau R, Kurunov I, Lingiardi O, Ricketts J. *Modern blast furnace ironmaking (an introduction)*. 3rd ed. BV, Amsterdam: IOS Press; 2015.
7. Lowing J. The diagnostic approach to overcoming blast furnace operational problems. In: *Ironmaking proceedings*, 36, Pittsburgh, AIME, New York; 1977, pp. 212–33.
8. Nakamura N, Togino Y, Tateoka M. Behavior of coke in large blast furnace. *Ironmaking Steelmaking* 1978;5 (1):5–7.

Suggested Reading

- Babich A, Senk D, Gudenau HW. *Ironmaking*. Aachen, Germany: RWTH Aachen, RWTH Aachen University; 2016.
- Ghosh A, Chatterjee A. *Ironmaking and steelmaking, theory and practice*. Delhi, India: PHI Learning Private Limited; 2013.
- McMaster University (Engineering). *25th blast furnace iron-making course*. Hamilton, Canada: McMaster University; 2018.

C H A P T E R

3

Making Steel From Molten Blast Furnace Iron

O U T L I N E

3.1 Blast Furnace Iron	32	3.9 Degassing	39
3.2 Steel	32	3.10 Continuous Casting	41
3.3 Steelmaking Steps	32	3.10.1 Start Casting	41
3.4 Sulfur Removal	32	3.10.2 The Copper Mold and Its Oscillation	41
3.5 Oxygen Steelmaking	34	3.10.3 Mold Powder	42
3.5.1 Nitrogen Avoidance	35	3.11 The Cast Product	42
3.5.2 Molten Slag	35	3.12 Summary	43
3.5.3 Process Steps	35		
3.6 Additions to the Final Liquid Steel	37	Exercises	44
3.7 Ultralow Phosphorus Steel	38	References	44
3.8 Ladle Metallurgy Furnace	39		

3.1 BLAST FURNACE IRON

The iron blast furnace takes Fe oxide pellets, sinter, and crushed ore plus coke at ambient temperature and from them produces molten high-carbon blast furnace iron at 1500°C, containing the following:

Element	Mass (%)
Fe	94.4
C	4.5
Si	0.6
Mn	0.4
P	0.05
S	0.04
Ti	0.01

Blast furnace iron has few final uses as it is relatively brittle and not formable. Converting the molten iron into steel provides a metal with many engineering applications. Virtually all molten iron produced by blast furnaces is immediately made into molten steel at 1630°C, Fig. 3.1. A small amount is used in the form of high carbon iron alloys for castings such as motor engine blocks.

The objectives of this chapter are to describe the steelmaking process - from molten blast furnace iron to continuously cast solid steel.

3.2 STEEL

Most steel (~90%) is a low carbon Fe–C–Mn alloy, containing the following:

Element	Mass (%)
Fe	98–99
C	0.05–0.1
Si	0.4 max
Mn	0.3–3.0
P	0.01–0.05
S	0.03 max
Ti	0.01

This steel is called carbon steel. It is strong, tough, and easily made into many industrial products, for example, buildings, machinery, and automobiles.

The steelmaking process converts or refines the molten blast furnace iron into steel, as described in Fig. 3.1.

3.3 STEELMAKING STEPS

Steelmaking takes place in four discrete sequential steps - all starting with molten blast furnace iron:

1. sulfur removal;
2. carbon, phosphorus, silicon, and titanium removal via oxygen steelmaking;
3. deoxidation; and
4. ladle refining, temperature control, and alloying such as vacuum degassing (H₂, N₂, and C removal).

All are batch processes. All are done under decidedly different chemical and physical conditions.

These steps and continuous casting are shown in Fig. 3.1.

3.4 SULFUR REMOVAL

Sulfur-in-steel causes the steel to crack and tear during hot rolling. This is due to the presence of low melting point FeS–Fe eutectic crystals at the steel's grain boundaries. To avoid this, most steels must contain below 0.01 mass% S. Today's most advanced steel must have <0.003 mass% S.

Sulfur at low concentration can't be removed from blast furnace iron by simple oxidation. This is because, thermodynamically, iron more easily oxidized than very dilute dissolved sulfur.

The sulfur is most often removed using nitrogen to inject reagents such as CaO and/or magnesium metal or CaC₂ rich powder

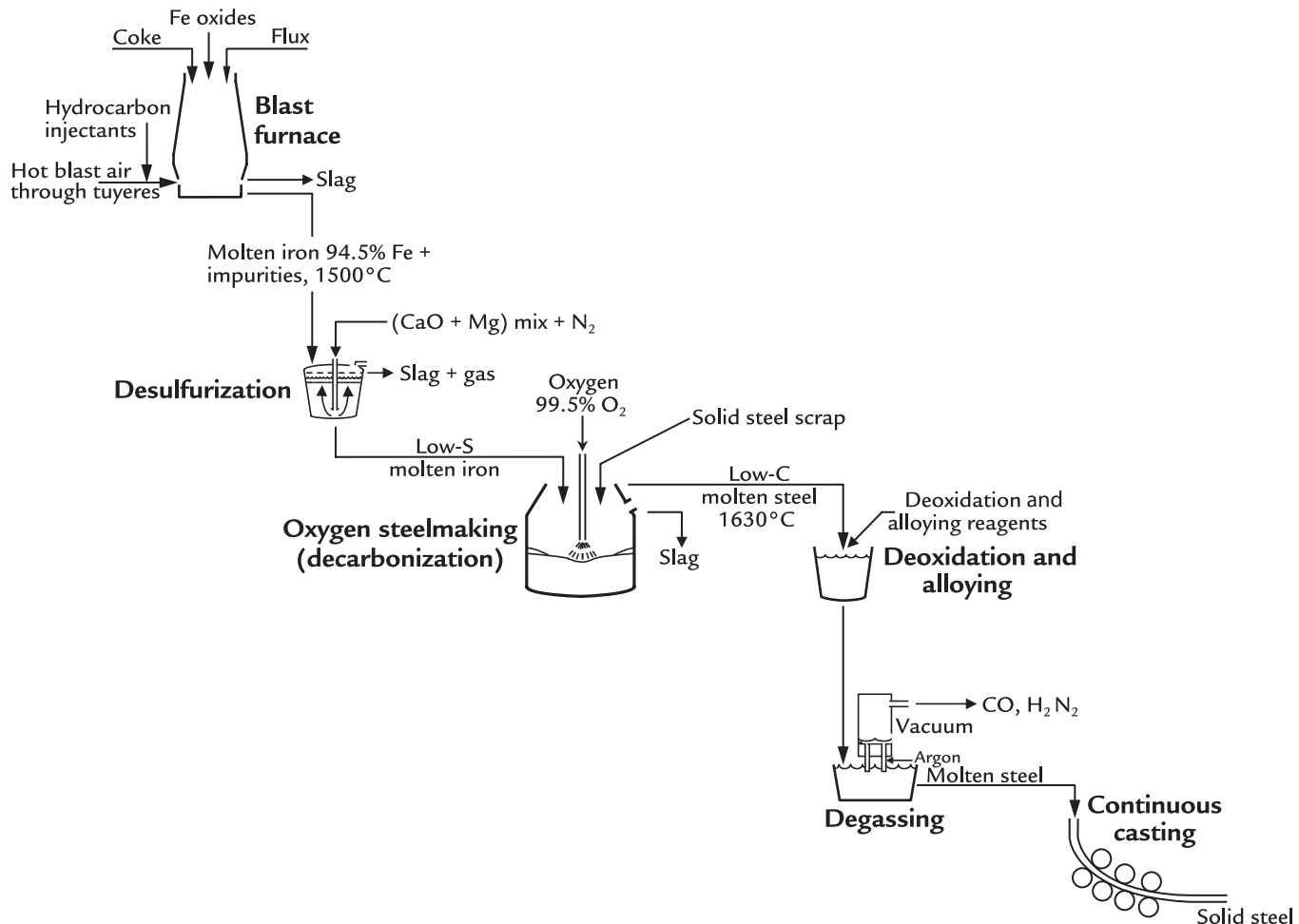
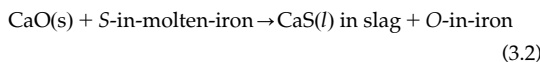
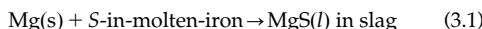


FIGURE 3.1 Flow sheet for making continuously cast low-carbon steel, 0.05 mass% C from molten blast furnace iron, 4.5 mass% C. The main chemical process is carbon oxidation, that is, $C_{\text{dissolved}} + 0.5\text{O}_2(\text{g}) \rightarrow \text{CO}(\text{g})$. H, N, P, S, Si, and Ti are also removed. Blast furnace ironmaking and continuous casting are continuous. Desulfurization, oxygen steelmaking, deoxidation, and degassing are batch, that is, discontinuous.

through a lance - deep into a ladle of freshly produced blast furnace iron, Fig. 3.2.

Typical desulfurization reactions are:



The products are:

1. desulfurized molten iron containing <0.01% S³, and
2. high sulfur CaO–MgS–CaS slag.

The high sulfur slag is usually removed by raking the lighter slag off the heavier molten iron. The slag is then discarded. The remaining desulfurized molten iron is charged to the basic oxygen furnaces (BOFs).

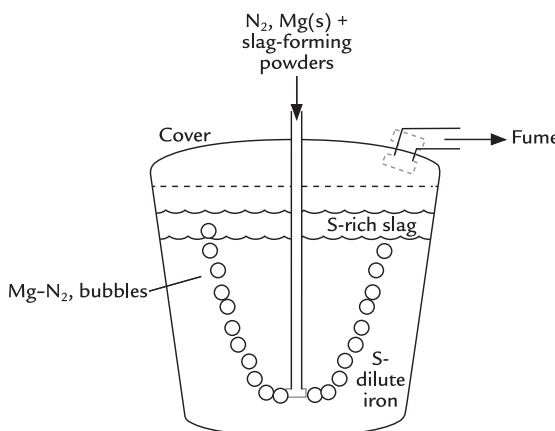


FIGURE 3.2 Sketch of magnesium powder injection desulfurization, 1350°C.^{1,2} A ladle is typically 4 m high and 3 m diameter inside its steel shell and refractory lining. The ascending Mg(g)–N₂(g) bubbles are notable. The slag-forming powder also ascends due to its low density. The process is batch, that is, the ladle is filled with molten blast furnace iron, the iron is desulfurized, the slag is skimmed, and the desulfurized molten iron is railed or carried to oxygen steelmaking. The process then begins again with a new batch of molten blast furnace iron in a different ladle. A typical batch is 100–300 t. Its desulfurization takes 5–15 min.

Factors for maximizing sulfur removal are;

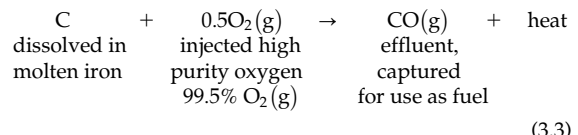
1. nonoxidizing (reducing) conditions in the molten iron - to (1) avoid oxidizing the magnesium and (2) promote Reaction (3.1);
2. deep injection;
3. good mixing; and
4. clean slag–metal separation.

3.5 OXYGEN STEELMAKING

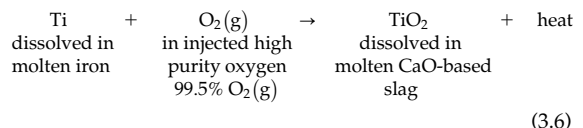
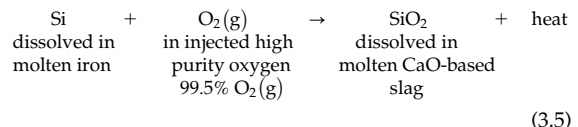
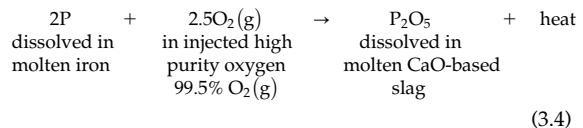
Section 3.4 described sulfur removal from blast furnace iron. This section describes C, P, Si, and Ti removal from desulfurized molten iron by oxygen steelmaking, which;

1. oxidizes dissolved C to CO(g) with high purity oxygen, and
2. oxidizes dissolved P, Si, and Ti to their oxides and disposes of them in basic, high CaO, MgO molten slags.

The reaction for carbon removal is:



The reactions for phosphorus, silicon, and titanium are represented by:



In addition, some of the blast furnace iron's manganese is inadvertently oxidized. It is restored by adding ferromanganese to the product steel, [Section 3.6](#).

All these oxidation reactions generate heat. This heat:

1. keeps the molten metal and slag hot and molten
2. economically melts steel scrap added as a coolant to the steelmaking furnace, and
3. raises the product steel's temperature to ~1630°C.

This elevated temperature is required because (1) the melting point of low carbon steel is higher than that of high carbon iron and (2) downstream processes and handling (e.g., alloying and vacuum degassing) cools the steel.

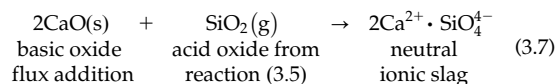
3.5.1 Nitrogen Avoidance

Notice that the O₂(g) for oxygen steelmaking is supplied as high purity industrial oxygen, 99.5% O₂(g), with the remainder being mostly argon. This is to prevent nitrogen absorption during steelmaking.

Nitrogen embrittles solid steel by precipitating iron nitride crystals at the steel's grain boundaries. It must be avoided.

3.5.2 Molten Slag

Oxygen steelmaking is always done with basic (i.e., high CaO, MgO) slag and a basic (i.e., MgO) refractory furnace lining. The slag has a high concentration of these basic oxides so that it can absorb the products of Reactions [\(3.4\)](#), [\(3.5\)](#) and [\(3.6\)](#) that are acidic slag components; SiO₂, P₂O₅, and TiO₂ by reactions such as:



which form moderately low melting point slags. CaO and MgO flux additions increase

the slag basicity which ensures that the MgO steelmaking furnace refractory lining is not attacked by reacting with the SiO₂, P₂O₅, and TiO₂ reaction products from the steelmaking process.

Typical basic oxygen steelmaking slag contains⁵ the following:

Substance	Mass (%)
CaO	46.0
Total iron oxide	17.0
SiO ₂	11.0
MgO	7.0
MnO	5.0
Al ₂ O ₃	2.0
P ₂ O ₅	1.7
S	0.01

3.5.3 Process Steps

[Fig. 3.3](#) depicts the basic oxygen steelmaking furnace. The process steps to make a heat of steel are:

1. with the top oxygen lance removed, tilting the furnace about 45 degrees and adding solid steel scrap from above;
2. pouring desulfurized molten blast furnace iron from its transfer ladle into the BOF ([Figs. 3.4](#) and [3.5](#));
3. tilting the BOF back into its vertical position, lowering the oxygen lance, and begin oxygen blowing;
4. blowing until the end point temperature and desired carbon is near. Blowing time can be determined three ways:
 - a. by calculation and then interrupting the blowing period after 90% of the total blow time (called a turn down) to sample/measure temperature, recalculate, and then continue blowing to the endpoint temperature and carbon content;

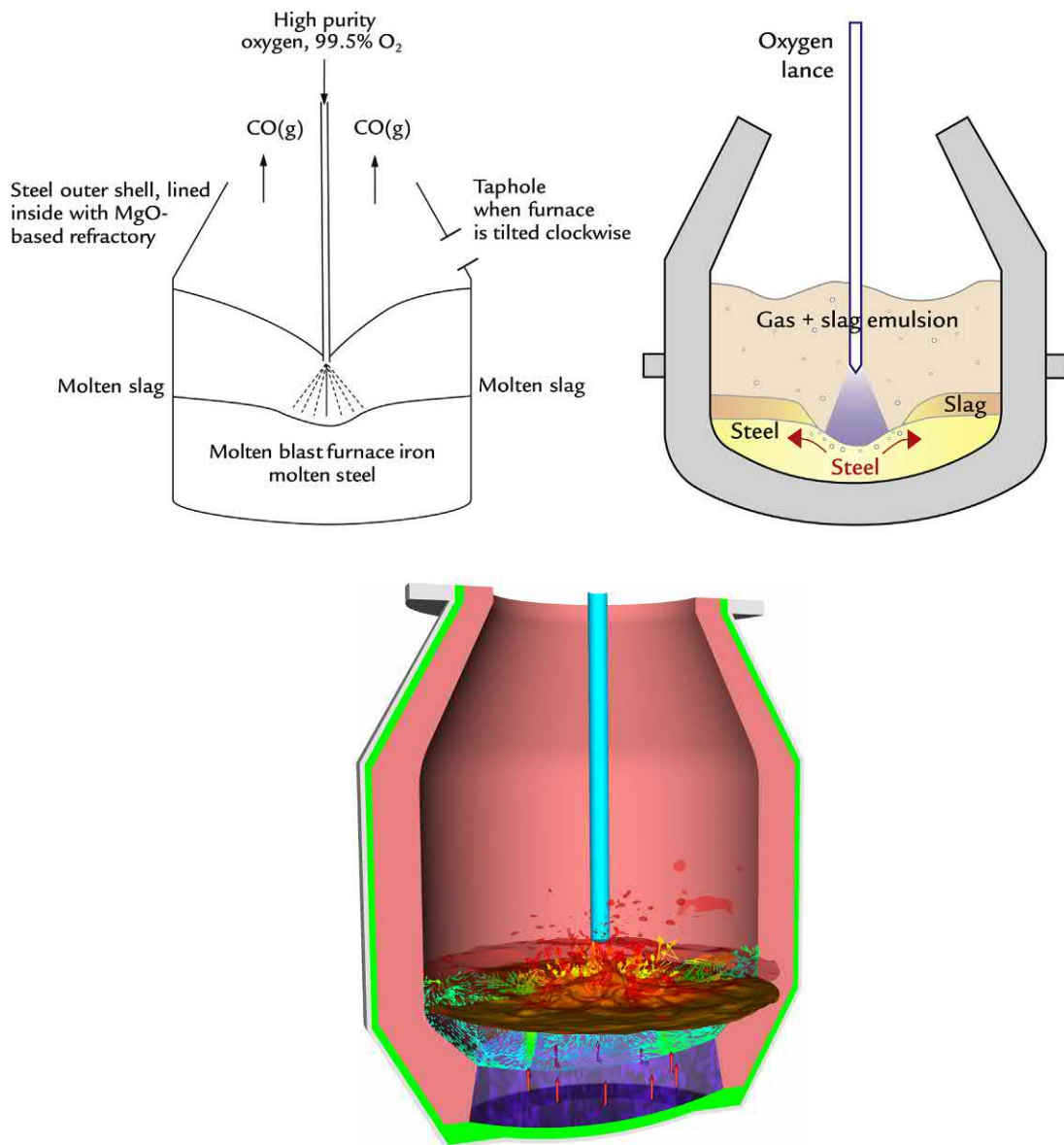


FIGURE 3.3 Sketches of BOF for removing dissolved C, P, Si, and Ti from molten desulfurized blast furnace iron. A typical furnace is 10 m high and 6 m inside diameter. The steel shell is typically 0.03 m thick, the MgO-based refractory lining 1 m thick. A typical batch of product molten steel is 200–300 t. Including all process steps plus cleanup and refractory maintenance, production of a batch of steel takes about 40–45 min. Other steelmaking furnaces (1) blow oxygen and other gases from below (KOBM) while (2) others blow top and bottom.⁴ BOF, Basic oxygen furnace. Source: Sketch courtesy of SMS Group.



FIGURE 3.4 Charging hot metal to a BOF converter. About 80–90% of the ferrous charge to make a heat of steel is hot metal produced by adjacent blast furnaces. The balance is scrap used as a coolant to mitigate the exothermic oxidation of silicon and carbon in the hot metal. Iron ore pellets can also be used as a coolant. *BOF*, Basic oxygen furnace. *Source: Photograph courtesy of SMS Group.*

- b. by using the waste gas analysis to estimate C removed. Once the CO content drops rapidly, the time to the final carbon content can be estimated. This approach only works with a closed off-gas system that minimizes air infiltration into the off-gases produced by the BOF; and
- c. by measuring the molten metal temperature and carbon content with a sublance while continuing to blow oxygen into the BOF^{6,7}. The sublance is lowered adjacent to the main oxygen lance during blowing, sample/temperature is taken, and the sublance is removed. Using the sublance results, the additional blowing time is calculated to

reach the target temperature and carbon content. This amount of oxygen is blown, and the heat is stopped.

5. raising the oxygen lance, tilting the furnace and pouring the steel into a large teeming ladle while preventing low density slag from flowing through the taphole;
6. adding deoxidizing and alloying reagents (e.g., aluminum and ferrosilicon) into the molten steel stream as the liquid steel is poured into the teeming ladle; and
7. turning the vessel vertically and then to the side opposite the taphole to pour out the slag over the BOF lip.

3.6 ADDITIONS TO THE FINAL LIQUID STEEL

Two types of reagents are added to the steel teeming ladle along with the molten steel, Fig. 3.1. They are:

1. deoxidizers⁸, and
2. steel property enhancers.

The steel produced during oxygen steel-making is saturated with oxygen. This oxygen must be removed before casting to avoid CO(g) evolution and consequential casting defects. The usual deoxidizers are aluminum and ferrosilicon. They react strongly with the oxygen to form Al₂O₃–SiO₂–FeO slag which may be removed before further processing. Deoxidizing steel is often referred to as *killing* steel as foaming is eliminated. Aluminum will provide a finer grain structure than ferrosilicon killed steel. The resulting mechanical properties are preferred for certain applications.

Ferromanganese is also used to deoxidize steel. However, its main purpose is to restore the steel's manganese content and ultimately



FIGURE 3.5 The charging of a ladle of molten iron into a BOF. The BOF converts molten blast furnace iron into low carbon liquid steel. Its position in the steelmaking flow sheet is shown in Fig. 3.1. The main chemical process is carbon oxidation. P, Si, and Ti are also oxidized as is Mn (undesirably). A typical BOF is 6 m diameter inside by 10 m high. A 200–300 t batch (“heat”) of steel is produced by about 20 min of oxygen blowing. *BOF*, Basic oxygen furnace. *Source: Photograph courtesy of SMS Group.*

deliver needed mechanical properties. Modern advanced formable steels used for automotive sheet applications require increasingly greater amounts of Mn in the final cast steel, typically 1.5–2.5% Mn. Future grades will require even more Mn to be added.

3.7 ULTRALOW PHOSPHORUS STEEL

Phosphorus embrittles steel. For this reason, it is always removed from molten blast furnace iron to the greatest extent possible.

As described in Section 3.5, phosphorus is removed into the slag during oxygen steelmaking by Reaction (3.4).

Phosphorus removal is favored by low temperature, strongly oxidizing conditions, and CaO-rich slag.

Ultralow phosphorus (<0.01% P) steel is required for many applications including highly formable sheet steel for automobiles and trucks. Such ultralow P product can be obtained by using two sequential BOFs with slag removal between (Fig. 3.6) and by other similar processes.⁹

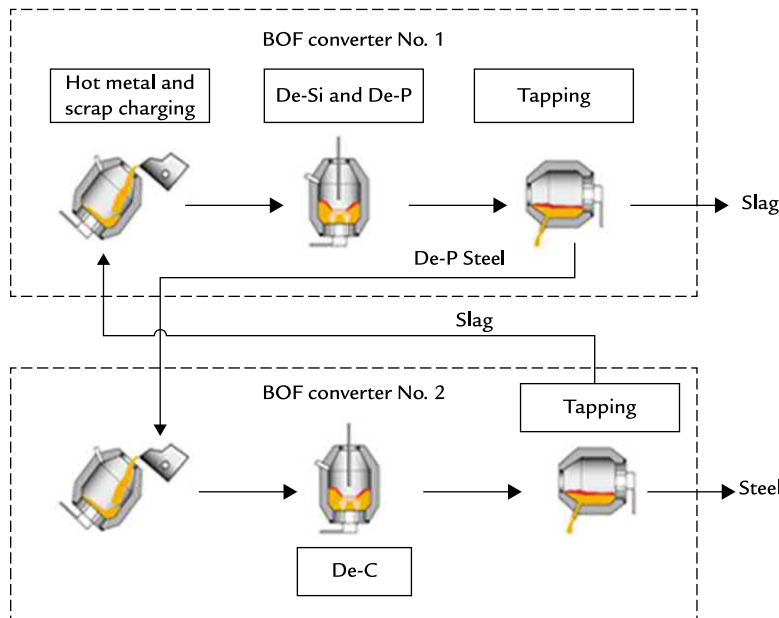


FIGURE 3.6 SRP developed by Nippon Steel, circa 1987.⁹ SRP, Single refining process.

3.8 LADLE METALLURGY FURNACE

Post BOF steelmaking, a ladle metallurgy furnace (LMF), is used to reheat steel to temperatures suitable for continuous casting. The LMF is used to complete final deoxidation, desulfurization, and alloying, as well as serves as a buffer between the batch BOF process and the continuous casting process. Three graphite electrodes are used to heat the liquid steel from the top like a small electric arc furnace. Argon stirring can be done by lance but is more commonly done through a porous refractory plug located in the bottom of the ladle. Stirring homogenizes the steel temperature and encourages flotation of fine solids that are deoxidation reaction products.

A synthetic slag is added to capture impurities that contain reaction products from the deoxidation and desulfurization reactions. This slag is often removed at the end of the LMF treatment using a slag raking machine.

Alloying will include a variety of elements, Mn, V, Nb, Ca, and other alloys for mechanical property control. The alloys can be added;

- in bulk and stirred into the steel;
- injected as a powder, or
- fed as a cored wire added at high speed.

An LMF reheating steel can be seen in Fig. 3.7.

3.9 DEGASSING

Despite all precautions, the product molten steel contains dissolved hydrogen and nitrogen. These elements both tend to embrittle steel. They are readily removed by vacuum degassing where the liquid steel is exposed to very low pressure. One of the most common industrial



FIGURE 3.7 Ladle metallurgy furnace reheating liquid steel in preparation for continuous casting. Graphite electrodes heat the steel from the top, while the liquid steel is argon stirred from the bottom. Alloys are added by gravity through drop chutes and using solid metal and powder-filled wires added at high speed. *Source: Photograph courtesy of SMS Group.*

degassing processes is the Ruhrstahl Heraeus (RH) vacuum degasser, Fig. 3.8.¹⁰ Tank degassers are also popular.

The RH steel degassing process entails:

1. lowering the vacuum unit into a large ladle of steel;
2. bubbling argon gas into the right leg, lowering the average density of its contents, while simultaneously applying a vacuum at the top of the unit;
3. drawing gas from the unit including Ar, H₂, N₂, and CO (top);
4. stopping the vacuum and argon flow;

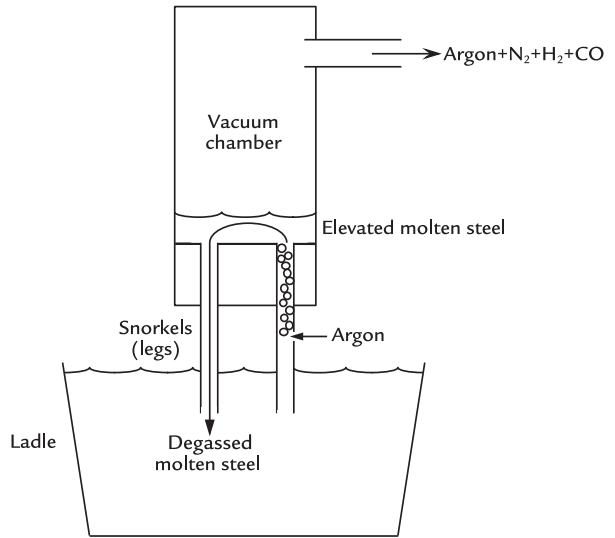


FIGURE 3.8 An RH vacuum degasser for removing N₂, H₂, and CO from *killed* steel. It is about 3 m in diameter. Molten steel is drawn up into the vacuum chamber by bubbling argon into one of the legs or submerged snorkels. N₂, H₂, and CO are desorbed into the rising argon bubbles and across the steel surface. They are pumped out of the system (top) and evacuated into a gas-cleaning system. The degassed steel falls back down the second leg into the ladle (left). The steel circulation and degassing continues until the steel has attained its prescribed N, H, and C levels. Typical degassed element-in-steel concentrations are H: 1 ppm, N: 50 ppm, and C: 5 ppm. Molten steel temperature cools 20°C–50°C during this process unless chemical heating is employed.

5. lifting the degassing unit from the steel; and
6. sending the ladle of degassed steel to continuous casting.

Step (2) causes molten steel to be drawn up the right leg of the apparatus into the vacuum chamber where it is degassed. The degassed steel then falls down the left leg due to its higher average density without argon bubbles. The process removes hydrogen and nitrogen to low levels and removes carbon as CO(g). They desorb into the rising argon bubbles and through the molten steel-vacuum surface.

The ladle of degassed steel is then sent to continuous casting, which is further described in the next section.

3.10 CONTINUOUS CASTING

Most liquid steel is continuously cast, which entails the following:

1. Pouring the *killed* steel at a controlled rate and temperature into a vertical water-cooled copper mold, thereby forming a solid steel shell that contains the remaining liquid steel.
2. Allowing this partially solidified steel to descend through the copper mold into strong water sprays, where solidification finishes, Fig. 3.9.
3. Curving the partially solidified steel in the horizontal direction through a series of rolls, while solidification is completed using the water sprays.
4. Cutting and sending the newly solidified steel to a reheat furnace and rolling mill.



FIGURE 3.9 Steel being cast via a submerged nozzle located into a thin slab caster copper mold. The molds are made of high purity copper—due to its very high thermal conductivity. Cooling and solidification is obtained by rapid extraction of heat from the molten steel through copper and into sprays of cooling water. *Source: Photograph courtesy of SMS Group.*

Many continuous casting systems have multiple casting streams or strands, all fed from the same steel holding vessel known as a tundish, Fig. 3.10.

Not shown are (1) cooling water sprays, and (2) a hot rolling mill at the end. Steel descent rates are 0.5–8 m/min, depending on the cross section of the casting and design of the casting machine.^{11,12}

3.10.1 Start Casting

The continuous casting starting procedure is as follows:

1. place a tight-fitting steel *dummy bar* inside the water-cooled copper mold. This can be fed from the top or bottom of the strand;
2. start pouring molten steel into the copper mold onto the *dummy bar* while commensurately pulling the *dummy bar* downwards;
3. continue until the *dummy bar* is at the cutoff station at the end of the strand; and
4. cut the newly cast steel attached to the *dummy bar*, remove and continue with casting.

This starting procedure is designed to ensure that the steel has a solid shell by the time it leaves the copper mold. Repeating the startup may be postponed indefinitely by having a molten steel handling system that has an always replenished holding vessel above the caster, hence continuous casting, Fig. 3.10.

3.10.2 The Copper Mold and Its Oscillation

The horizontal copper mold dimensions are 0.1–2.0 m wide, rectangular, square, round, or dog-bone shaped (for I beams). Mold heights are typically 0.5–2.0 m.

The molds are oscillating vertically to prevent sticking of the newly cast steel to the



FIGURE 3.10 Continuous steel casting arrangement. Notice:

- the top ladle of killed molten steel, $\sim 1560^{\circ}\text{C}$;
- the continuously replenished molten steel holding vessel, known as a tundish;
- the copper molds;
- bending of the hot solid steel for feeding to a reheat furnace or hot rolling mill.

Source: Photograph courtesy of SMS Group.

copper. The oscillation is about 150 cycles/min, amplitude about 7 mm.

surface and promotes heat transfer to the mold.

3.10.3 Mold Powder

A CaO–SiO₂ flux powder is continuously added to the steel-in-mold top surface. It infiltrates the copper–steel interface and prevents sticking between the mold and newly cast steel. The powder also reduces heat loss through the molten metal

3.11 THE CAST PRODUCT

Fig. 3.11 is a photograph of a continuous cast slab being cut from the continuous strand of steel. This steel slab is of high quality; ready for hot rolling, cold rolling, coating, and manufacture. It may well appear in your



FIGURE 3.11 A continuously cast solid steel slab being cut for hot rolling and subsequent manufacturing processes. The slabs are about 2 m wide and 0.8 m thick. They are being cut into 10 m lengths for rolling by *flying* gas torches that clamp onto and move forward at the same speed as the steel, ~1–2 m/min. *Source: Photograph courtesy of SMS Group.*

next car as the frame (chassis), roof, hood, doors, etc.

3.12 SUMMARY

Molten low-carbon steel is made from molten blast furnace iron by;

1. removing the iron's sulfur and transferring it to molten slag by reacting it with magnesium and/or CaO, MgO, CaC₂, etc. powder;
2. oxidizing the iron's carbon to CO(g) with high purity oxygen in a BOF;
3. simultaneously oxidizing the iron's phosphorus, silicon, and titanium while adding CaO and MgO flux to form basic molten CaO–FeO–MgO–P₂O₅–SiO₂–TiO₂ slag;
4. pouring the resulting steel into a large teeming ladle while;
 - a. adding deoxidizing agents, for example, aluminum and ferrosilicon, to remove the steel's excess oxygen—thereby *killing* the steel;
 - b. adding alloy ingredients to the steel, for example, Mn in ferromanganese, Ni in ferronickel, V as ferrovanadium, and Cr in ferrochrome;
5. degassing the *killed* molten steel under vacuum to remove N₂(g), H₂(g), and C as CO(g); and
6. continuously casting the degassed steel and directing the solidified steel into rolling mills for solid state fabrication.

Two vital details of oxygen steelmaking are:

1. Nitrogen embrittlement is avoided during oxygen steelmaking by using high purity oxygen, 99.5% O₂ remainder argon, rather than air.
2. Ultralow phosphorus steels can be made by using two sequential oxygen steelmaking furnaces with slag removal in between.

EXERCISES

- 3.1. Your steelmaking company's purchasing department has located a cheap supplier of industrial oxygen for your basic oxygen steelmaking's furnace. They want to sign a contract for it but ask your advice. What will you tell them?
- 3.2. Find a phase diagram online that shows the molten steel must be processed at a higher temperature than molten blast furnace iron. Can you come up with a general statement based on this without becoming depressed?
- 3.3. Oxygen steelmaking's molten product contains considerable dissolved oxygen. This oxygen is removed by adding aluminum metal and ferrochrome alloy. What chemical reactions are involved?
- 3.4. Will you need to supply heat for these O-removal reactions?
- 3.5. What is the key step for making continuous-casting process of Fig. 3.10 truly continuous?
- 3.6. Write chemical reactions for H and N removal by vacuum degassing. What does Le Chatelier's principle say about these reactions?
- 3.7. The biggest difference between blast furnace iron and oxygen steelmaking's steel is their carbon content. What is the biggest difference between ironmaking

and steelmaking slag? What causes this difference?

- 3.8. Why isn't molten steel made directly from iron ore in one step, that is, in one furnace? Perhaps the difference between blast furnace slag composition of Section 1.3 and oxygen steelmaking slag composition of Section 3.5.2 will help you.
- 3.9. The molten steel cools during degassing, Section 3.8. Where does the heat go? Why doesn't the steel cool during oxygen steelmaking?

References

1. International Magnesium Association. *Desulfurizing steel: magnesium is the reagent of choice*; 2012. Recovered by Googling title, 20.05.16.
2. Wolfe L, Olson L. *Yield improvements during iron desulfurization when utilizing "flow aided" compounds for modifying slag characteristics*; 2016. Recovered by Googling title on 20.05.16.
3. Kopeliovich D. *Desulfurization of steel [Subs Tech]*; 2016. Recovered by Googling title on 20.05.16.
4. JFE Steel Corporation. *BOF (basic oxygen furnace)*; 2003. Recovered by Googling Kawasaki Steel 21st Continuing Foundation/Index then tapping Chapter 2 then tapping BOF Facilities then tapping BOF Operation on 20.05.16.
5. Nippon Slag Association. *Chemical characteristics iron and steel slag*; 2003. Recovered by Googling title on 20.05.16.
6. Danieli Corus. *Sublance systems and static-dynamic process model*; 2016. Recovered by Googling Sublance & SDM – Danieli Corus, 20.05.16.
7. Spanjers M, Glitscher W. *Sublance-based on-line slag control in BOF steelmaking*; 2016. Recovered by Googling title, 20.05.16.
8. Satyendra. *Deoxidation of steel*; 2014. Recovered by Googling title on 20.05.16.
9. Ghobara Y, Cameron I. Removal of phosphorus – technology alternatives. In: *Iron & steel technology, association of iron & steel technology (AIST) 7*; pp. 80–89, April 2017.
10. JFE Steel Corporation. *Secondary refining*; 2003. Recovered by Googling: Kawasaki Steel 21st Continuing

- Foundation/Index and *tapping* Chapter 2 then *tapping* Secondary Refining on 20.05.16.
11. JFE Steel Corporation. *Continuous casting*; 2003. Recovered by Googling: Kawasaki Steel 21st Continuing Foundation/Index and *tapping* Chapter 2 then *tapping* Basics of Continuous Casting, Continuous Caster and Continuous Caster Operation on 20.05.16.
12. Kozak B, Dzierzawski J. *Continuous casting of steel: basic principles*; 2016. Recovered by Googling Continuous Casting of Steel: Basic Principles – American Iron and Steel Institute, 20.05.16.

Introduction to the Blast Furnace Mass Balance

OUTLINE

4.1 Developing Steady-State Mass Balances for the Blast Furnace	47	4.5 Equation Shortage	51
4.2 Mathematical Development	48	4.6 A Useful Calculation	51
4.3 Steady-State Mass Balance Equations	48	4.7 Top Gas Composition	51
4.3.1 Fe Mass Balance Equation	49	4.8 Magnetite (Fe_3O_4) Ore Charge	51
4.3.2 Oxygen Balance Equation	49	4.9 Addition of a New Variable: Carbon in Product Molten Iron	53
4.3.3 Carbon Balance Equation	50		
4.3.4 Nitrogen Balance Equation	50	4.10 Summary	55
4.4 Additional Specifications	50	Exercises	55
4.4.1 Blast Air Composition Specification	50		
4.4.2 1000 kg of Fe in Product Molten Iron Specification	50		

4.1 DEVELOPING STEADY-STATE MASS BALANCES FOR THE BLAST FURNACE

Chapter 1, The Iron Blast Furnace Process, and Chapter 2, Inside the Blast Furnace, showed that blast furnace ironmaking entails;

1. combusting hot coke with hot blast air near the bottom of the furnace - producing hot carbon monoxide (which rises), and
2. transferring oxygen from descending iron oxide ore to this ascending CO(g) - producing CO₂(g) (which rises), and Fe (which descends and melts).

The result is production of molten iron ~95.5 mass% Fe, 4.5 mass% C - which is tapped from the furnace hearth. The shaft of the blast furnace is a countercurrent gas - solid oxygen exchanger. It is also a countercurrent gas - solid heat exchanger.

Development of our mathematical description is begun in this chapter by developing *steady-state* mass balance equations for a greatly simplified blast furnace, Fig. 4.1.

Chapter 5, Introduction to the Blast Furnace Enthalpy Balance, develops a steady-state enthalpy balance equation. Finally, Chapter 6, Combining Mass and Enthalpy Balance Equations, combines the mass and

enthalpy equations to provide a framework for our blast furnace model.

This framework is instructive as to how the blast furnace works. But it doesn't provide an *a priori* mathematical description of how a blast furnace must be operated to achieve any given goal, for example, minimum coke consumption.

The final goal of a fully predictive model is attained by:

1. conceptually dividing the furnace, top from bottom, through its chemical reserve zone (Section 2.11);
2. preparing mass and enthalpy balance equations for the bottom segment;
3. preparing mass and enthalpy balance equations for the top segment; and
4. adding details such as (1) tuyere injectants; (2) ore gangue and coke ash; and (3) slag.

4.2 MATHEMATICAL DEVELOPMENT

Inspection of Fig. 4.1 blast furnace indicates that it has eight input and output variables. They are:

- mass Fe_2O_3 in ore charge,
- mass C in coke charge,
- mass O_2 in blast air,
- mass N_2 in blast air,
- mass Fe out in molten iron,
- mass CO out in top gas,
- mass CO_2 out in top gas, and
- mass N_2 out in top gas.

We must, therefore, develop eight equations to fully define the Fig. 4.1 furnace.

4.3 STEADY-STATE MASS BALANCE EQUATIONS

Steady-state mass balances provide four of these eight equations. They are:

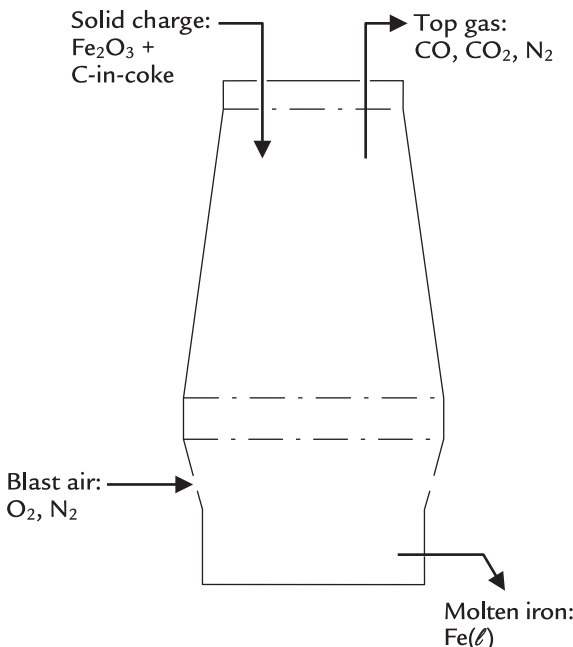


FIGURE 4.1 Blast furnace vertical slice showing major inputs and outputs. For simplicity, input tuyere injectants (e.g., pulverized coal), input impurity oxides and output oxide slag are ignored until later chapters. Likewise, carbon in the blast furnace's product molten iron is postponed until Section 4.9. All gas flows are continuous. Molten iron tapping is continuous or very nearly continuous. Solids charging is very nearly continuous.

$$\text{mass Fe in} = \text{mass Fe out} \quad (4a)$$

$$\text{mass O in} = \text{mass O out} \quad (4b)$$

$$\text{mass C in} = \text{mass C out} \quad (4c)$$

$$\text{mass N in} = \text{mass N out} \quad (4d)$$

where *mass in* is kg of each element entering the furnace and *mass out* is kg of each element leaving the furnace, all expressed per 1000 kg (1 t) of Fe leaving the furnace in its product molten iron.

In terms of Section 4.2's blast furnace variables, these mass balance equations expand to the following:

4.3.1 Fe Mass Balance Equation

Fe enters Fig. 4.1 blast furnace as hematite, Fe_2O_3 (Fig. 4.2).

Fe leaves in the blast furnace's product molten iron also known as hot metal. These specifications and Eq. (4a) give:

$$\begin{aligned} \left[\frac{\text{mass Fe}_2\text{O}_3 \text{ in}}{\text{ore charge}} \right] * \frac{\left[\frac{69.9 \text{ mass\% Fe}}{\text{in Fe}_2\text{O}_3} \right]}{100\%} \\ = \left[\frac{\text{mass Fe out}}{\text{in molten iron}} \right] * \frac{\left[\frac{100\% \text{ Fe in Fig. 4.1}}{\text{molten iron}} \right]}{100\%} \end{aligned}$$



FIGURE 4.2 Hematite (Fe_2O_3) iron ore pellets ready for charging to an iron blast furnace. They are approximately 8–16 mm diameter. *Source: Photo courtesy: Midrex Technologies Inc.*

or

$$\left[\frac{\text{mass Fe}_2\text{O}_3 \text{ in}}{\text{ore charge}} \right] * 0.699 = \left[\frac{\text{mass Fe out}}{\text{in molten iron}} \right] * 1$$

or, subtracting $\left\{ \left[\frac{\text{mass Fe}_2\text{O}_3 \text{ in}}{\text{ore charge}} \right] * 0.699 \right\}$ from both sides to put the equation in matrix form:

$$0 = - \left[\frac{\text{mass Fe}_2\text{O}_3 \text{ in}}{\text{ore charge}} \right] * 0.699 + \left[\frac{\text{mass Fe out}}{\text{in molten iron}} \right] * 1 \quad (4.1)$$

4.3.2 Oxygen Balance Equation

Oxygen enters Fig. 4.1 blast furnace in input Fe_2O_3 and input blast air. It leaves in top gas as CO and CO_2 .

These specifications and Eq. (4b) give:

$$\begin{aligned} \left[\frac{\text{mass Fe}_2\text{O}_3 \text{ in}}{\text{ore charge}} \right] * \left[\frac{\begin{array}{l} 30.1 \text{ mass\% O} \\ \text{in Fe}_2\text{O}_3 \end{array}}{100\%} \right] + \left[\frac{\text{mass O}_2 \text{ in}}{\text{blast air}} \right] \\ * \left[\frac{100\% \text{ O}}{\text{in O}_2} \right] = \left[\frac{\text{mass CO out}}{\text{in top gas}} \right] * \left[\frac{\begin{array}{l} 57.1 \text{ mass\% O} \\ \text{in CO} \end{array}}{100\%} \right] \\ + \left[\frac{\text{mass CO}_2 \text{ out}}{\text{in top gas}} \right] * \left[\frac{\begin{array}{l} 72.7 \text{ mass\% O} \\ \text{in CO}_2 \end{array}}{100\%} \right] \end{aligned}$$

or

$$\begin{aligned} \left[\frac{\text{mass Fe}_2\text{O}_3 \text{ in}}{\text{ore charge}} \right] * 0.301 + \left[\frac{\text{mass O}_2 \text{ in}}{\text{blast air}} \right] * 1 \\ = \left[\frac{\text{mass CO out}}{\text{in top gas}} \right] * 0.571 + \left[\frac{\text{mass CO}_2 \text{ out}}{\text{in top gas}} \right] * 0.727 \end{aligned}$$

or subtracting $\left\{ \left[\frac{\text{mass Fe}_2\text{O}_3 \text{ in}}{\text{ore charge}} \right] * 0.301 + \left[\frac{\text{mass O}_2 \text{ in}}{\text{blast air}} \right] * 1 \right\}$ from both sides to put the equation in matrix form:

$$0 = - \left[\frac{\text{mass Fe}_2\text{O}_3 \text{ in}}{\text{ore charge}} \right] * 0.301 - \left[\frac{\text{mass O}_2 \text{ in}}{\text{blast air}} \right] * 1 + \left[\frac{\text{mass CO out}}{\text{in top gas}} \right] * 0.571 + \left[\frac{\text{mass CO}_2 \text{ out}}{\text{in top gas}} \right] * 0.727 \quad (4.2)$$

4.3.3 Carbon Balance Equation

Carbon enters Fig. 4.1 blast furnace in the top charged coke. It leaves the furnace in top gas as CO and CO₂.

These specifications and Eq. (4c) give:

$$\left[\frac{\text{mass C in coke charge}}{100\%} * \frac{100\% \text{ C}}{100\%} \right] = \left[\frac{\text{mass CO out in top gas}}{100\%} \right] + \left[\frac{42.9 \text{ mass\% C in CO}}{100\%} \right] + \left[\frac{\text{mass CO}_2 \text{ out in top gas}}{100\%} \right] * \left[\frac{27.3 \text{ mass\% C in CO}_2}{100\%} \right]$$

or

$$\left[\frac{\text{mass C in coke charge}}{100\%} * 1 \right] = \left[\frac{\text{mass CO out in top gas}}{100\%} \right] * 0.429 + \left[\frac{\text{mass CO}_2 \text{ out in top gas}}{100\%} \right] * 0.273$$

or subtracting $\left\{ \left[\frac{\text{mass C in coke charge}}{100\%} * 1 \right] \right\}$ from both sides:

$$0 = - \left[\frac{\text{mass C in coke charge}}{100\%} * 1 \right] + \left[\frac{\text{mass CO out in top gas}}{100\%} \right] * 0.429 + \left[\frac{\text{mass CO}_2 \text{ out in top gas}}{100\%} \right] * 0.273 \quad (4.3)$$

4.3.4 Nitrogen Balance Equation

Nitrogen enters Fig. 4.1 blast furnace in input blast air. It leaves in top gas.

These specifications and nitrogen balance Eq. (4d) give the equation:

$$\begin{aligned} & \left[\frac{\text{mass N}_2 \text{ in blast air}}{100\%} * \frac{100\% \text{ N in N}_2}{100\%} \right] \\ &= \left[\frac{\text{mass N}_2 \text{ out in top gas}}{100\%} * \frac{100\% \text{ N in N}_2}{100\%} \right] \end{aligned}$$

or

$$\left[\frac{\text{mass N}_2 \text{ in blast air}}{100\%} * 1 \right] = \left[\frac{\text{mass N}_2 \text{ out in top gas}}{100\%} * 1 \right]$$

or subtracting $\left\{ \left[\frac{\text{mass N}_2 \text{ in blast air}}{100\%} * 1 \right] \right\}$ from both sides:

$$0 = - \left[\frac{\text{mass N}_2 \text{ in blast air}}{100\%} * 1 \right] + \left[\frac{\text{mass N}_2 \text{ out in top gas}}{100\%} * 1 \right] \quad (4.4)$$

4.4 ADDITIONAL SPECIFICATIONS

Fig. 4.1 blast furnace provides two additional specifications:

1. its blast air composition, and
2. its mass Fe in output molten iron = 1000 kg specification,

both of which are readily described in equation form.

4.4.1 Blast Air Composition Specification

Air contains 76.7 mass% N₂ and 23.3 mass% O₂ (Appendix B). This composition is described in equation form by:

$$\left[\frac{\text{mass N}_2 \text{ in blast air}}{\text{mass O}_2 \text{ in blast air}} \right] = \frac{76.7 \text{ mass\% N}_2 \text{ in air}}{23.3 \text{ mass\% O}_2 \text{ in air}} = 3.3$$

or multiplying both sides by $\left\{ \left[\frac{\text{mass O}_2 \text{ in blast air}}{100\%} \right] \right\}$:

$$\left[\frac{\text{mass N}_2 \text{ in blast air}}{100\%} * 1 \right] = \left[\frac{\text{mass O}_2 \text{ in blast air}}{100\%} \right] * 3.3$$

or subtracting $\left\{ \left[\frac{\text{mass N}_2 \text{ in blast air}}{100\%} * 1 \right] \right\}$ from both sides:

$$0 = - \left[\frac{\text{mass N}_2 \text{ in blast air}}{100\%} * 1 \right] + \left[\frac{\text{mass O}_2 \text{ in blast air}}{100\%} * 3.3 \right] \quad (4.5)$$

4.4.2 1000 kg of Fe in Product Molten Iron Specification

All the calculations of this book are based on 1000 kg of Fe in a blast furnace's molten iron product. This is described by the equation:

$$\left[\frac{\text{mass Fe out in molten iron}}{100\%} * 1 \right] = 1000$$

or

$$1000 = \left[\frac{\text{mass Fe out}}{\text{in molten iron}} \right] * 1 \quad (4.6)$$

4.5 EQUATION SHORTAGE

The above sections show that we have eight variables but only six equations.

So, we are still a long way from defining Fig. 4.1 blast furnace operation.

4.6 A USEFUL CALCULATION

The above equations are not without value. We can, for example, check our top gas measurement devices by calculating top gas composition for any given carbon input and blast oxygen input combination; for example, 400 kg of C in coke charge, per 1000 kg of Fe in product molten iron and 370 kg of O_2 in input blast air per 1000 kg of Fe in product molten iron.

In equation form, these specifications are

$$400 = \left[\frac{\text{mass C in}}{\text{in coke charge}} \right] * 1 \quad (4.7)$$

$$370 = \left[\frac{\text{mass O}_2 \text{ in}}{\text{blast air}} \right] * 1 \quad (4.8)$$

With these we now have eight equations, (4.1)–(4.8) so that that we can determine numerical values for all eight of our variables.

Eqs. (4.1)–(4.8) are now arranged in matrix form and solved. Try it! Matrix Table 4.1 and Appendix I provide details.

Solving the matrix is straight forward (described in Appendix I). Try it! It calculates values for all the variables. Each value is unique because the matrix has eight variables and eight linear equations.

4.7 TOP GAS COMPOSITION

Top gas CO, CO_2 , and N_2 masses are shown in the *calculated value* cells at the bottom left of the Table 4.1 matrix. Per 1000 kg of Fe in product molten iron they are:

$$\text{mass CO} = 463 \text{ kg}$$

$$\text{mass CO}_2 = 738 \text{ kg}$$

$$\text{mass N}_2 = 1221 \text{ kg}$$

They are equivalent to

$$\text{mass\% CO} = \frac{463 \text{ kg CO}}{463 \text{ kg} + 738 \text{ kg} + 1221 \text{ kg}} * 100\% = 19.1$$

$$\text{mass\% CO}_2 = \frac{738 \text{ kg CO}_2}{463 \text{ kg} + 738 \text{ kg} + 1221 \text{ kg}} * 100\% = 30.5$$

$$\text{mass\% N}_2 = \frac{1221 \text{ kg N}_2}{463 \text{ kg} + 738 \text{ kg} + 1221 \text{ kg}} * 100\% = 50.4$$

for a total of 100%.

4.8 MAGNETITE (Fe_3O_4) ORE CHARGE

Suppose now that the blast furnace plant changes its ore charge to magnetite lump ore (which is quite rare) without changing:

$$\left[\frac{\text{mass C in}}{\text{coke charge}} \right]$$

or

$$\left[\frac{\text{mass O}_2 \text{ in}}{\text{blast air}} \right]$$

What effect will this have on the blast furnace operation?

Only Eqs. (4.1) and (4.2) change. Because magnetite contains 72.4 mass% Fe and 27.6 mass% O (Appendix A), the Fe mass balance in Eq. (4.1) becomes:

$$0 = -\left[\frac{\text{mass Fe}_3\text{O}_4 \text{ in}}{\text{ore charge}} \right] * 0.724 + \left[\frac{\text{mass Fe out}}{\text{in molten iron}} \right] * 1 \quad (4.9)$$

TABLE 4.1 Matrix for Solving Eqs. (4.1)–(4.8)

	A	B	C	D	E	F	G	H	I	J	K
	Equation	Description	Numerical term	mass Fe ₂ O ₃ in ore charge	mass C in coke charge	mass O ₂ in blast air	mass N ₂ in blast air	mass Fe out in molten iron	mass CO out in top gas	mass CO ₂ out in top gas	mass N ₂ out in top gas
1											
2	4.6	Fe out in molten iron specification	1000	0	0	0	0	1	0	0	0
3	4.1	Fe mass balance	0	-0.699	0	0	0	1	0	0	0
4	4.2	O mass balance	0	-0.301	0	-1	0	0	0.571	0.727	0
5	4.3	C mass balance	0	0	-1	0	0	0	0.429	0.273	0
6	4.4	N mass balance	0	0	0	0	-1	0	0	0	1
7	4.5	N ₂ in air specification	0	0	0	3.3	-1	0	0	0	0
8	4.7	C in coke charge specification	400	0	1	0	0	0	0	0	0
9	4.8	O ₂ in blast air specification	370	0	0	1	0	0	0	0	0
10											
11		Calculated values	kg per 1000 kg of Fe in product molten iron								
12		mass Fe ₂ O ₃ in ore charge	1431								
13		mass C in coke charge	400								
14		mass O ₂ in blast air	370								
15		mass N ₂ in blast air	1221								
16		mass Fe out in molten iron	1000								
17		mass CO out in top gas	463								
18		mass CO ₂ out in top gas	738								
19		mass N ₂ out in top gas	1221								

Cells C17–C19 are now used to calculate top gas composition for checking our top gas analyzer. Note that the calculated values (cells C12–C19) are in the same order as the specifications (cells D1–K1).

and the O mass balance in Eq. (4.2) becomes;

$$0 = - \left[\begin{array}{l} \text{mass Fe}_3\text{O}_4 \text{ in} \\ \text{ore charge} \end{array} \right] * 0.276 - \left[\begin{array}{l} \text{mass O}_2 \text{ in} \\ \text{blast air} \end{array} \right] * 1 + \left[\begin{array}{l} \text{mass CO out} \\ \text{in top gas} \end{array} \right] * 0.571 + \left[\begin{array}{l} \text{mass CO}_2 \text{ out} \\ \text{in top gas} \end{array} \right] * 0.727 \quad (4.10)$$

as shown in Table 4.2.

We don't need to prepare a new matrix for this exercise. All we do is put -0.724 in cell D3 and -0.276 in cell D4 to represent magnetite, Eqs. (4.9) and (4.10). Try it!

The matrix automatically determines new values for the output variables.

We now repeat the above calculation with various mass% Fe and mass% O in the input ore charge. The results are shown in Fig. 4.3.

As expected, mass ore charge per 1000 kg of Fe in product molten iron decreases with increasing mass% Fe in the input iron oxide. This is because of the ore charge's decreasing mass O/mass Fe ratio with increasing mass% Fe in ore charge. Mass output $\text{CO}_2(\text{g})$ also decreases. This is because high mass% Fe/low mass% O ore supplies less O to the furnace, while the carbon input remains the same, Eq. (4.7).

4.9 ADDITION OF A NEW VARIABLE: CARBON IN PRODUCT MOLTEN IRON

For simplicity, Fig. 4.1 blast furnace doesn't include carbon in its molten iron product. This section shows how this variable is added to our Table 4.1 matrix. Of course, addition of a new variable requires addition of a new equation.

Without impurities, molten blast furnace iron may be represented as containing 4.5 mass% C and 95.5 mass% Fe (Fig. 4.4). This composition is described in equation form by

$$\frac{\left[\begin{array}{l} \text{mass C out} \\ \text{in molten iron} \end{array} \right]}{\left[\begin{array}{l} \text{mass Fe out} \\ \text{in molten iron} \end{array} \right]} = \frac{[4.5 \text{ mass \%C in molten iron}]}{[95.5 \text{ mass \%Fe in molten iron}]} = 0.047$$

or, multiplying both sides by $\left[\begin{array}{l} \text{mass Fe out} \\ \text{in molten iron} \end{array} \right]$

$$\left[\begin{array}{l} \text{mass C out} \\ \text{in molten iron} \end{array} \right] * 1 = \left[\begin{array}{l} \text{mass Fe out} \\ \text{in molten iron} \end{array} \right] * 0.047$$

or, subtracting $\left\{ \left[\begin{array}{l} \text{mass C out} \\ \text{in molten iron} \end{array} \right] * 1 \right\}$ from both sides:

$$0 = - \left[\begin{array}{l} \text{mass C out} \\ \text{in molten iron} \end{array} \right] * 1 + \left[\begin{array}{l} \text{mass Fe out} \\ \text{in molten iron} \end{array} \right] * 0.047 \quad (4.11)$$

Table 4.3 shows our matrix with the above-described new variable $\left[\begin{array}{l} \text{mass C out} \\ \text{in molten iron} \end{array} \right]$ column and new Eq. (4.11) row.

Of course, carbon balance Eq. (4.3) is enlarged to:

$$\begin{aligned} \left[\begin{array}{l} \text{mass C in} \\ \text{coke charge} \end{array} \right] * 1 &= \left[\begin{array}{l} \text{mass CO out} \\ \text{in top gas} \end{array} \right] * 0.429 \\ &+ \left[\begin{array}{l} \text{mass CO}_2 \text{ out} \\ \text{in top gas} \end{array} \right] * 0.273 + \left[\begin{array}{l} \text{mass C out} \\ \text{in molten iron} \end{array} \right] * 1 \end{aligned} \quad (4.12a)$$

or subtracting $\left[\begin{array}{l} \text{mass C in} \\ \text{coke charge} \end{array} \right]$ from both sides:

$$\begin{aligned} 0 &= - \left[\begin{array}{l} \text{mass C in} \\ \text{coke charge} \end{array} \right] * 1 + \left[\begin{array}{l} \text{mass CO out} \\ \text{in top gas} \end{array} \right] * 0.429 \\ &+ \left[\begin{array}{l} \text{mass CO}_2 \text{ out} \\ \text{in top gas} \end{array} \right] * 0.273 + \left[\begin{array}{l} \text{mass C out} \\ \text{in molten iron} \end{array} \right] * 1 \end{aligned} \quad (4.12b)$$

as shown in Table 4.3.

Solution of the matrix in Table 4.3 shows 47 kg of C leaving the furnace in molten iron per 1000 kg of Fe in molten iron. It also shows more CO_2 -in-top gas than Table 4.1 and less CO. This is because:

1. mass C in top gas decreases because some C goes to product molten iron, and
2. mass input O is unchanged.

TABLE 4.2 Matrix Describing Fig. 4.1 Blast Furnace Operation With Magnetite Ore Rather Than Hematite Ore

	A	B	C	D	E	F	G	H	I	J	K
	Equation	Description	Numerical term	mass Fe ₃ O ₄ in ore charge	mass C in coke charge	mass O ₂ in blast air	mass N ₂ in blast air	mass Fe out in molten iron	mass CO out in top gas	mass CO ₂ out in top gas	mass N ₂ out in top gas
1											
2	4.6	Fe out in molten iron specification	1000	0	0	0	0	1	0	0	0
3	4.9	Fe mass balance	0	-0.724	0	0	0	1	0	0	0
4	4.10	O mass balance	0	-0.276	0	-1	0	0	0.571	0.727	0
5	4.3	C mass balance	0	0	-1	0	0	0	0.429	0.273	0
6	4.4	N mass balance	0	0	0	0	-1	0	0	0	1
7	4.5	N ₂ in air specification	0	0	0	3.3	-1	0	0	0	0
8	4.7	C in coke charge specification	400	0	1	0	0	0	0	0	0
9	4.8	O ₂ in blast air specification	370	0	0	1	0	0	0	0	0
10											
11		Calculated values	kg per 1000 kg of Fe in product molten iron								
12		mass Fe ₃ O ₄ in ore charge	1381								
13		mass C in coke charge	400								
14		mass O ₂ in blast air	370								
15		mass N ₂ in blast air	1221								
16		mass Fe out in molten iron	1000								
17		mass CO out in top gas	549								
18		mass CO ₂ out in top gas	602								
19		mass N ₂ out in top gas	1221								

Cells D3 and D4 in Table 4.1 are changed. Notice that the only *calculated value* changes are to iron oxide input mass (which decreases), CO₂ mass (which decreases), and CO mass (which increases). These changes are all due to magnetite's smaller O/Fe ratio and the unchanged C in coke and blast air O₂ inputs.

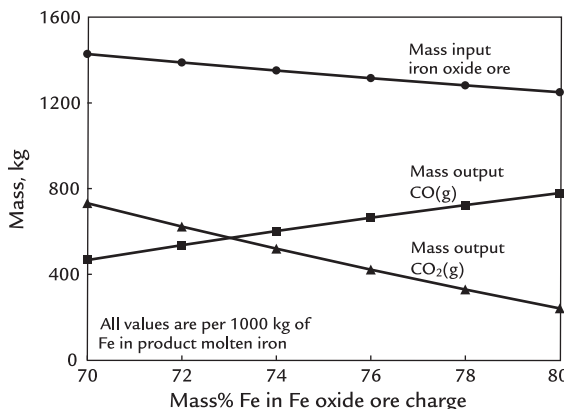


FIGURE 4.3 Graph showing iron oxide ore input mass and CO and CO₂ output masses as a function of mass% Fe in iron oxide feed. The points are calculated by varying the values in matrix as shown in D3 and D4 cells of Table 4.2. Values above 72.4 mass% Fe (i.e., magnetite) are obtained by including scrap steel (Fe) in the charge.



FIGURE 4.4 Molten iron 1500°C flowing out of an iron blast furnace. Excluding other impurities, for example, Si, it contains ~95.5 mass% Fe and 4.5 mass% C. In practice, molten iron and molten slag are tapped together. Source: Photograph courtesy: TMT—Tapping Measuring Technology S.à. r.l & G.m.b.H.

4.10 SUMMARY

This chapter provides the first step in developing our mathematical model of the iron blast furnace. It does so by preparing:

1. four steady-state mass balance equations for a simplified blast furnace (Fig. 4.1), and
2. four quantity specification equations (e.g., air composition equation)

to provide as many equations as operating variables. The equations are arranged in matrix form and solved with an Excel matrix technique (Appendix I).

The numerical results of this chapter are informative. They can, for example, be used to check top gas composition measurement equipment. They don't, however, *a priori* predict blast furnace input carbon and blast air requirements.

The next two chapters take a second step toward our *a priori* model by:

1. developing a steady-state enthalpy equation for Fig. 4.1 blast furnace (Chapter 5: Introduction to the Blast Furnace Enthalpy Balance), and
2. combining this enthalpy equation with the equations of this chapter (Chapter 6: Combining Mass and Enthalpy Balance Equations).

EXERCISES

- 4.1. Calculate the top gas composition, mass% CO, CO₂, and N₂ and volume% CO, CO₂, and N₂, for a blast furnace that is charging:
 - a 50 mass% hematite, 50 mass% magnetite ore mixture;
 - 400 kg of C in top charged coke per 1000 kg of Fe in product molten iron; and
 - 370 kg of O₂ in input blast air per 1000 kg of Fe in product molten iron. Assume for now that the product molten iron is pure Fe.
- 4.2. The blast air in Exercise 4.1 is enriched with pure O₂. After this enrichment, the blast contains 27 mass% O₂ and 73 mass% N₂.

TABLE 4.3 Table 4.1 Matrix With Addition of (1) New Mass C Out in Molten Iron Variable, (2) New Iron Composition Specification Eq. (4.11), and (3) Altered Carbon Mass Balance Eq. (4.12b)

What is the blast furnace's top gas composition (mass%) with this O₂ enrichment?

- 4.3.** An advantage of blast air O₂ enrichment is that it decreases the mass of gas rising through the blast furnace, per 1000 kg of Fe in product molten iron.

- a. Compare the Exercises 4.1 and 4.2 top gas masses, that is, with and without O₂ enrichment.
- b. Calculate molten iron production rate (tonnes per hour) before and after blast air O₂ enrichment.

To answer (b), assume that Fe production is limited by a 400,000 kg/hour top gas production rate. Above this rate, the ascending gas opens channels through the charge, decreasing thermal and chemical reaction efficiencies.

- 4.4.** Industrial iron blast furnaces are sometimes partially charged with reduced iron pellets from direct iron ore reduction plants. An important objective is to increase the furnaces' Fe production rate.

Consider now that the Exercise 4.1 blast furnace is being charged with a mixture of hematite (Fe₂O₃) pellets and solid-reduced iron pellets (assume for simplicity, 100% Fe).

The mixture contains 80 mass% hematite pellets, 20 mass% reduced iron pellets.

How much faster can the 80% Fe₂O₃–20% reduced iron pellet blast furnace produce Fe (in molten iron) compared to the Exercise 4.1 Fe (in molten iron) production rate. Assume that the 400,000 kg of top gas per hour maximum still applies. The blast is air.

- 4.5.** Redo Exercise 4.1 with 5 mass% C in the product molten iron. Predict beforehand what you expect to happen to

$$\left[\frac{\text{mass CO out in top gas}}{\text{mass CO}_2 \text{ out in top gas}} \right] \text{ ratio of Exercise 4.1, then calculate it.}$$

Perhaps start with matrix [Table 4.3](#).

- 4.6.** You may have noticed that

$$\left[\frac{\text{mass N}_2 \text{ out}}{\text{in top gas}} \right]$$

has the same value in [Tables 4.1–4.3](#). Why?

- 4.7.** Exercise 4.3 considers enriching blast air with pure oxygen to decrease gas flow (per kg of Fe in product molten iron) up through the blast furnace.

- a. How is pure oxygen made in large industrial operations?
- b. What cost must be considered when using pure oxygen in the blast furnace?
- c. Can you think of any use for the byproduct nitrogen in iron and steel industry, perhaps from Chapter 3, [Making Steel from Molten Blast Furnace Iron?](#)

Introduction to the Blast Furnace Enthalpy Balance

O U T L I N E

5.1 The Enthalpy Balance	59	5.5 Numerical Values and Final Enthalpy Equations	61
5.2 Input and Output Enthalpies	60		
5.3 Enthalpy of Mixing Fe (ℓ) + C(s)	61	5.6 Summary Exercises	62
5.4 Conductive, Convective, and Radiative Heat Losses	61	References	63

5.1 THE ENTHALPY BALANCE

Blast furnace inputs and outputs for developing the enthalpy balance are provided in Fig. 5.1.

The steady-state enthalpy balance equation for the blast furnace in Fig. 5.1 is:

$$\text{Total enthalpy } in = \text{total enthalpy } out + \left[\begin{array}{l} \text{conductive, convective} \\ \text{and radiative heat loss} \\ \text{from the furnace} \end{array} \right] \quad (5.1)$$

or

$$\sum_{i=1}^n m_i H_{i\text{inputs}} = \sum_{j=1}^m m_j H_{j\text{Outputs}} + \left[\begin{array}{l} \text{conductive, convective} \\ \text{and radiative heat loss} \\ \text{from the furnace} \end{array} \right] \quad (5.2)$$

where

1. m_i and m_j are the masses of the furnace's input and output substances, with units of kg per 1000 kg of Fe in product molten iron.

2. H_i and H_j are the enthalpies of the input and output substances, with units of megajoules (MJ) per kg of substance.
3. Conductive, convective, and radiative heat loss is the total heat loss by these mechanisms, with units of MJ per 1000 kg of Fe in product molten iron.

5.2 INPUT AND OUTPUT ENTHALPIES

Fig. 5.1's input enthalpy is:

$$\sum_{i=1}^n m_i H_{i\text{Inputs}} = \left[\begin{array}{l} \text{mass Fe}_2\text{O}_3 \text{ in} \\ \text{ore charge} \end{array} \right] * \frac{H_{25^\circ\text{C}}^{\circ}}{\text{Fe}_2\text{O}_3(\text{s})} + \left[\begin{array}{l} \text{mass C in} \\ \text{coke charge} \end{array} \right] * \frac{H_{25^\circ\text{C}}^{\circ}}{\text{C(s)}} + \left[\begin{array}{l} \text{mass O}_2 \text{ in} \\ \text{blast air} \end{array} \right] * \frac{H_{1200^\circ\text{C}}^{\circ}}{\text{O}_2(\text{g})} + \left[\begin{array}{l} \text{mass N}_2 \text{ in} \\ \text{blast air} \end{array} \right] * \frac{H_{1200^\circ\text{C}}^{\circ}}{\text{N}_2(\text{g})} \quad (5.3)$$

The H°/MW terms are the enthalpies (MJ) of a substance *per kg* (H° = enthalpy, MJ per kg mol of pure substance; MW = molecular mass, kg per kg mol of the substance). This book's enthalpy values are obtained from NIST-JANAF.¹² Appendix J describes their calculation. Appendix J gives practical enthalpy versus temperature equations.

The enthalpy values may be calculated from H° and MW or by the enthalpy versus temperature equations in Appendix J. They are strongly dependent on temperature but virtually independent of pressure.³

H° is the enthalpy of a pure substance or a substance in an ideal solution, for example, O_2

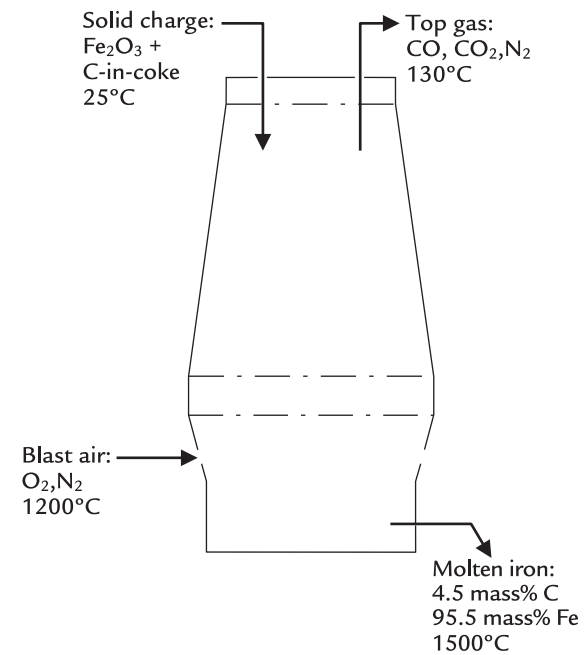


FIGURE 5.1 Blast furnace vertical slice showing inputs and outputs for this chapter's simplified enthalpy balance equation.

in air, or CO in top gas. Section 5.3 describes a case where H° can not be used.

Fig. 5.1's output enthalpy is:

$$\sum_{j=1}^m m_j H_{j\text{Outputs}} = \left[\begin{array}{l} \text{mass Fe out} \\ \text{in molten iron} \end{array} \right] * \frac{H_{1500^\circ\text{C}}^{\circ}}{\text{Fe(f)}} + \left[\begin{array}{l} \text{mass C out} \\ \text{in molten iron} \end{array} \right] * \frac{H_{1500^\circ\text{C}}^{\circ}}{\text{C(dissolved)}} + \left[\begin{array}{l} \text{mass CO out} \\ \text{in top gas} \end{array} \right] * \frac{H_{130^\circ\text{C}}^{\circ}}{\text{CO(g)}} + \left[\begin{array}{l} \text{mass CO}_2 \text{ out} \\ \text{in top gas} \end{array} \right] * \frac{H_{130^\circ\text{C}}^{\circ}}{\text{CO}_2(\text{g})} + \left[\begin{array}{l} \text{mass N}_2 \text{ out} \\ \text{in top gas} \end{array} \right] * \frac{H_{130^\circ\text{C}}^{\circ}}{\text{N}_2(\text{g})} \quad (5.4)$$

5.3 ENTHALPY OF MIXING $\text{Fe}(\ell) + \text{C(s)}$

Eq. (5.4)'s output carbon enthalpy is represented by $H_{\text{C(dissolved)}}$ rather than $H^{\circ}_{\text{C(s)}}$. This is because the carbon is present in a thermodynamically nonideal molten Fe–C alloy.

The enthalpy of mixing $\text{Fe}(\ell)_{1600^{\circ}\text{C}} + \text{C(s)}_{1600^{\circ}\text{C}}$ to make 95.5 mass% Fe 4.5 mass% C molten blast furnace iron alloy (1600°C) is $+5.4 \text{ MJ/kg mol}$ of alloy,⁴ which we assume to also be the enthalpy of mixing at 1500°C .

Ascribing, for convenience, all this enthalpy of mixing to the alloy's carbon, this value is equivalent to $+2.5 \text{ MJ/kg}$ of dissolved carbon, as described in Appendix J.

With this term, the output carbon enthalpy equation is:

$$\frac{H_{1500^{\circ}\text{C}}}{\text{C(dissolved)}} = \left\{ \frac{H^{\circ}_{1500^{\circ}\text{C}}}{\text{MW}_\text{C}} + 2.5 \right\}$$

MJ per kg of C in product molten iron (5.5a)

$$= \{2.488 + 2.5\} = 5 \text{ MJ/kg of C in product molten iron}$$

(5.5b)

This equation is used through the remainder of our book. Note that it leaves

$$\frac{H^{\circ}_{1500^{\circ}\text{C}}}{\text{MW}_\text{Fe}} \text{ unaltered.}$$

5.4 CONDUCTIVE, CONVECTIVE, AND RADIATIVE HEAT LOSSES

Most of a blast furnace's *conductive, convective, and radiative heat losses* go to the furnace's cooling water, Fig. 5.2.

Measurements of cooling water flows and temperatures indicate that this whole-furnace heat loss rate is $\sim 400 \text{ MJ per } 1000 \text{ kg of Fe in product molten iron}$.⁵



FIGURE 5.2 Water-cooled blast furnace cooling element - called a stave. These staves are attached to the inside of the blast furnace walls. Cooling staves can made from copper or cast iron. Their job is to maintain the structural integrity of the furnace by cooling the walls. Cool water is pumped into, around, and out of a hollow flow pattern or pipe inside the stave - removing heat from the furnace wall. In service, the grooved interior face (left) is packed with refractory bricks. Many other water cooling shapes are used as needed.⁶

5.5 NUMERICAL VALUES AND FINAL ENTHALPY EQUATIONS

Table 5.1 gives our input and output enthalpy values. With them, Eq. (5.2) becomes:

$$\begin{aligned}
 & [\text{mass Fe}_2\text{O}_3 \text{ in ore charge}] * (-5.169) \\
 & + [\text{mass C in coke charge}] * 0 \\
 & + [\text{mass O}_2 \text{ in blast air}] * 1.239 \\
 & + [\text{mass N}_2 \text{ in blast air}] * 1.339 \\
 & = [\text{mass Fe out in molten iron}] * 1.269 \\
 & + [\text{mass C out in molten iron}] * 5 \\
 & + [\text{mass CO out in top gas}] * (-3.836) \\
 & + [\text{mass CO}_2 \text{ out in top gas}] * (-8.844) \\
 & + [\text{mass N}_2 \text{ out in top gas}] * 0.1099 \\
 & + \left[\begin{array}{l} 400 \text{ MJ conductive, convective} \\ \text{and radiative heat loss per 1000} \\ \text{kg of Fe in product molten iron} \end{array} \right] \quad (5.6)
 \end{aligned}$$

or subtracting the left side of Eq. (5.6) and the last term of the right side from both sides and rearranging;

$$\begin{aligned}
 -400 = & -[\text{mass Fe}_2\text{O}_3 \text{ in ore charge}] * (-5.169) \\
 & - [\text{mass C in coke charge}] * 0 \\
 & - [\text{mass O}_2 \text{ in blast air}] * 1.239 \\
 & - [\text{mass N}_2 \text{ in blast air}] * 1.339 \\
 & + [\text{mass Fe out in molten iron}] * 1.269 \quad (5.7) \\
 & + [\text{mass C out in molten iron}] * 5 \\
 & + [\text{mass CO out in top gas}] * (-3.836) \\
 & + [\text{mass CO}_2 \text{ out in top gas}] * (-8.844) \\
 & + [\text{mass N}_2 \text{ out in top gas}] * 0.1099
 \end{aligned}$$

where the enthalpy values are at the temperatures specified in Fig. 5.1.

5.6 SUMMARY

Chapter 4, Introduction to the Blast Furnace Mass Balance, developed mass balance equations for the blast furnace in Fig. 5.1. This chapter has developed the equivalent enthalpy balance equation. Chapter 6, Combining Mass and Enthalpy Balance Equations, combines these equations and takes us further toward our fully predictive blast furnace model. Other enthalpies, for example, flux, pulverized coal, and slag enthalpies, are added in later chapters.

TABLE 5.1 Enthalpies of Fig. 5.1's Inputs and Outputs. They are Calculated From the Enthalpy versus Temperature Equations in Appendix J

Description	Value, MJ per kg of Substance
$H_{25^\circ\text{C}}^{\circ}/\text{MW}_{\text{Fe}_2\text{O}_3}$ $\text{Fe}_2\text{O}_3(\text{s})$	-5.169
$H_{25^\circ\text{C}}^{\circ}/\text{MW}_\text{C}$ $\text{C}(\text{s})$	0
$H_{1200^\circ\text{C}}^{\circ}/\text{MW}_{\text{O}_2}$ $\text{O}_2(\text{g})$	1.239
$H_{1200^\circ\text{C}}^{\circ}/\text{MW}_{\text{N}_2}$ $\text{N}_2(\text{g})$	1.339
$H_{1500^\circ\text{C}}^{\circ}/\text{MW}_\text{Fe}$ $\text{Fe}(\ell)$	1.269 (Ref. [7])
$H_{1500^\circ\text{C}}^{\circ}/\text{MW}_\text{C}$ $\text{C}(\text{dissolved})$	5 (Section 5.3)
$H_{130^\circ\text{C}}^{\circ}/\text{MW}_{\text{CO}}$ $\text{CO}(\text{g})$	-3.836
$H_{130^\circ\text{C}}^{\circ}/\text{MW}_{\text{CO}_2}$ $\text{CO}_2(\text{g})$	-8.844
$H_{130^\circ\text{C}}^{\circ}/\text{MW}_{\text{N}_2}$ $\text{N}_2(\text{g})$	0.1099

EXERCISES

- 5.1. A blast furnace plant increases its blast air temperature from 1200 to 1300°C. How can this change be represented in Eq. (5.7)? Refer to Table J.3 for the applicable enthalpy versus temperature equations.
- 5.2. Blast furnace management wants to increase its product molten iron temperature to 1550°C. How can this change be represented in Eq. (5.7)? Refer to Table J.6 for an Fe-in-molten iron enthalpy versus temperature equation.
- 5.3. Heating of blast air was first practiced in 1828.⁸ Blast air is now commonly heated to 1200, even 1300°C. Suggest several important advantages of higher hot blast temperature.

- 5.4. This chapter uses the term enthalpy balance rather than heat balance. What are the advantages of using enthalpy in our blast furnace calculations?
- 5.5. Air is an ideal solution. What is the enthalpy of a kg mol of air at 25°C and 1 bar (100 kPa) pressure? What is the enthalpy at 25°C at 4 bar (400 kPa) pressure?

References

1. NIST-JANAF. *NIST-JANAF [Thermochemical] tables PDF*. Gaithersburg, MD: U. S. Institute of Standards and Technology; 2017. [recovered on 17.01.27]. By Googling the title.
2. NIST-JANAF. Retrieved by Googling <kinetics.nist.gov/janaf/janaf4pdf.html>. Then tapping NIST-JANAF tables PDF-NIST chemical kinetics database then tapping Al for Al_2O_3 or O for O_2 , Si, etc.; 2017.
3. Gaskell DR. *Introduction to metallurgical thermodynamics*. New York: McGraw Hill; 1981.
4. Hultgren R, Desai PD, Hawkins DT, Gleiser M, Kelley KK. *Selected values of the thermodynamic properties of binary alloys*. Metals Park, OH: American Society for Metals; 1973. p. 484.
5. Flierman, GA, Homminga, F. A comparison of BF-operating results obtained with sinter or pellet burden. In: Sastry KVS, editors. *Agglomeration 77*. AIM: New York; 1977. p. 829.
6. Shaw A, Sadri A, Cameron I, Jastrzebski M, Brown R, Hyde JB. *Preserving copper staves and extending blast furnace campaign life*. Indianapolis, IN: AISTech; p. 715–22. May 2014.
7. Desai PD. Thermodynamic properties of iron and silicon. *J Phys Chem Ref Data* 1986;15(3):967–83 Retrieved on February 18, 2015 by Googling title.
8. Hot Blast. *Hot Blast-Wikipedia*; 2018. Retrieved by Googling [Hot Blast-Wikipedia on 19.11.18].

Combining Mass and Enthalpy Balance Equations

O U T L I N E

6.1 Developing a Predictive Blast Furnace Model - Initial Steps	65	6.5 Altered O ₂ (g) and N ₂ (g) Enthalpy Values	68
6.2 Benefit of Including Enthalpy	66	6.6 Discussion	68
6.3 Effect of Blast Temperature on Blast Air Requirement	66	6.7 Summary	68
6.4 Altered Enthalpy Equation	66	Exercises	70

6.1 DEVELOPING A PREDICTIVE BLAST FURNACE MODEL - INITIAL STEPS

This chapter:

1. combines enthalpy balance equations of Chapter 5, Introduction to the Blast Furnace Enthalpy Balance, with,
2. mass balance and quantity specification equations of Chapter 4, Introduction to the Blast Furnace Mass Balance.

In doing so, our objective is to move further toward a fully predictive blast furnace model. The basis for these initial steps is shown in Fig. 6.1.

We begin the process (Table 6.1) by:

1. adding enthalpy balance Eq. (5.7) to the Table 4.3 matrix, and
2. removing O₂-in-blast air specification Eq. (4.8) from the Table 4.3 matrix.

Step (2) is required to avoid having more equations than variables.

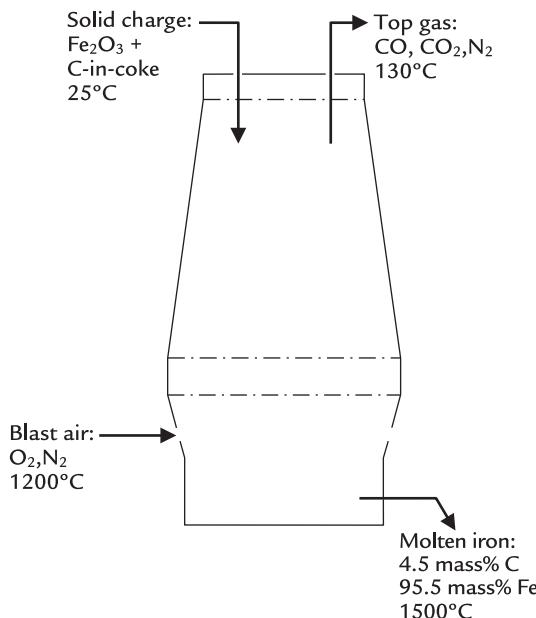


FIGURE 6.1 Simplified inputs, outputs, and temperatures for calculating the amounts of C-in-coke and O₂-in-blast air that will give steady production of molten iron 1500°C.

Notice how Eq. (5.7)

$$\begin{aligned}
 -400 = & -[\text{mass Fe}_2\text{O}_3 \text{ in ore charge}] * (-5.169) \\
 & -[\text{mass C in coke charge}] * 0 \\
 & -[\text{mass O}_2 \text{ in blast air}] * 1.239 \\
 & -[\text{mass N}_2 \text{ in blast air}] * 1.339 \\
 & +[\text{mass Fe out in molten iron}] * 1.269 \quad (5.7) \\
 & +[\text{mass C out in molten iron}] * 5 \\
 & +[\text{mass CO out in top gas}] * (-3.836) \\
 & +[\text{mass CO}_2 \text{ out in top gas}] * (-8.844) \\
 & +[\text{mass N}_2 \text{ out in top gas}] * 0.1099
 \end{aligned}$$

is included in matrix Table 6.1, especially the minus signs.

6.2 BENEFIT OF INCLUDING ENTHALPY

The benefit of including enthalpy Eq. (5.7) in the matrix is that the O₂-in-blast air requirement is now calculated rather than specified. So, we are half way toward our fully predictive model.

The matrix solution shows that:

1. 298 kg of O₂-in-blast air per 1000 kg of Fe in product molten iron, and,
2. 1283 kg of air (mass O₂ + mass N₂) per 1000 kg of Fe in product molten iron

are required to keep Table 6.1 blast furnace operating at steady state.

6.3 EFFECT OF BLAST TEMPERATURE ON BLAST AIR REQUIREMENT

An instructive use of the matrix as shown in Table 6.1 is to demonstrate the effect of blast temperature on Fig. 6.1's steady-state O₂-blast air and total blast air requirements.

A specific example problem is that the temperature of the blast air, as shown in Fig. 6.1, is to be increased to 1300°C. Predict how this change will affect the blast furnace's steady-state O₂-in-blast air and total blast air requirements.

All other temperatures and the 400 kg C-in-coke charge specification are unchanged.

6.4 ALTERED ENTHALPY EQUATION

The above blast air temperature change alters Fig. 6.1's input enthalpy Eq. (5.3) to:

$$\sum_{i=1}^n m_i H_{i,\text{inputs}} = \left[\text{mass Fe}_2\text{O}_3 \text{ in ore charge} \right] * \frac{H_{25^\circ\text{C}}^{\circ}}{\text{MW}_{\text{Fe}_2\text{O}_3}} + \left[\text{mass C in coke charge} \right] * \frac{H_{25^\circ\text{C}}^{\circ}}{\text{MW}_C} + \left[\text{mass O}_2 \text{ in blast air} \right] * \frac{H_{1300^\circ\text{C}}^{\circ}}{\text{MW}_{\text{O}_2}} + \left[\text{mass N}_2 \text{ in blast air} \right] * \frac{H_{1300^\circ\text{C}}^{\circ}}{\text{MW}_{\text{N}_2}} \quad (6.1)$$

TABLE 6.1 Matrix for calculating Blast Furnace O₂-in-Blast air requirement for any specified Carbon-in-Coke charge

	A	B	C	D	E	F	G	H	I	J	K	L
1	Equation	Description	Numerical term	mass Fe ₂ O ₃ in ore charge	mass C in coke charge	mass O ₂ in blast air	mass N ₂ in blast air	mass Fe out in molten iron	mass C out in molten iron	mass CO out in top gas	mass CO ₂ out in top gas	mass N ₂ out in top gas
2	4.6	Fe out in molten iron specification	1000	0	0	0	0	1	0	0	0	0
3	4.1	Fe mass balance	0	-0.699	0	0	0	1	0	0	0	0
4	4.2	O mass balance	0	-0.301	0	-1	0	0	0	0.571	0.727	0
5	4.12b	C mass balance	0	0	-1	0	0	0	1	0.429	0.273	0
6	4.4	N mass balance	0	0	0	0	-1	0	0	0	0	1
7	4.5	N ₂ in blast air specification	0	0	0	3.3	-1	0	0	0	0	0
8	4.7	C in coke charge specification	400	0	1	0	0	0	0	0	0	0
9	4.11	C out in molten iron specification	0	0	0	0	0	0.047	-1	0	0	0
10	5.7	Enthalpy balance	-400	5.169	0	-1.239	-1.339	1.269	5	-3.836	-8.844	0.1099
11		Calculated values	kg per 1000 kg of Fe in product molten iron									
12		mass Fe ₂ O ₃ in ore charge	1431									
13		mass C in coke charge	400									
14		mass O ₂ in blast air	298									
15		mass N ₂ in blast air	985									
16		mass Fe out in molten iron	1000									
17		mass C out in molten iron	47									
18		mass CO out in top gas	369									
19		mass CO ₂ out in top gas	713									
20		mass N ₂ out in top gas	985									
21				25°C	25°C	1200°C	1200°C	1500°C	1500°C	130°C	130°C	130°C
22												

Note: enthalpy balance Eq. (5.7) in row 10; absent O₂-in-blast air quantity specification Eq. (4.8); C-in-coke charge specification of 400 kg C per 1000 kg of Fe product molten iron, row 8. The matrix solution shows that steady-state operation with 400 kg of C-in-coke charge requires 298 kg of O₂-in-blast air. This matrix was prepared by altering matrix Table 4.3 as described in assigned Problem 4.6. It can also be prepared from scratch. Appendix J shows how to solve it. Try it!

where the last two lines are different from those in Eq. (5.7).

6.5 ALTERED O₂(g) AND N₂(g) ENTHALPY VALUES

$$\frac{H^\circ_{T[^\circ\text{C}]} - H^\circ_{1300^\circ\text{C}}}{\text{MW}_{\text{O}_2}} = \frac{O_2(\text{g})}{\text{MW}_{\text{O}_2}}$$

$$\frac{H^\circ_{T[^\circ\text{C}]} - H^\circ_{1300^\circ\text{C}}}{\text{MW}_{\text{N}_2}} = \frac{N_2(\text{g})}{\text{MW}_{\text{N}_2}}$$

The values of $\frac{O_2(\text{g})}{\text{MW}_{\text{O}_2}}$ and $\frac{N_2(\text{g})}{\text{MW}_{\text{N}_2}}$ are calculated from Appendix J's O₂(g) and N₂(g) enthalpy versus temperature equations. They are:

$$\frac{H^\circ_{T[^\circ\text{C}]} - H^\circ_{1300^\circ\text{C}}}{\text{MW}_{\text{O}_2}} = 0.001137 * T [^\circ\text{C}] - 0.1257$$

$$\frac{H^\circ_{T[^\circ\text{C}]} - H^\circ_{1300^\circ\text{C}}}{\text{MW}_{\text{N}_2}} = 0.001237 * T [^\circ\text{C}] - 0.1450$$

from which:

$$\frac{H^\circ_{T[^\circ\text{C}]} - H^\circ_{1300^\circ\text{C}}}{\text{MW}_{\text{O}_2}} = 1.352$$

$$\frac{H^\circ_{T[^\circ\text{C}]} - H^\circ_{1300^\circ\text{C}}}{\text{MW}_{\text{N}_2}} = 1.463$$

where the units are all MJ per kg of substance.

These values are now inserted into Eq. (5.7), which becomes

$$\begin{aligned} -400 = & -[\text{mass Fe}_2\text{O}_3 \text{ in ore charge}] * (-5.169) \\ & -[\text{mass C in coke charge}] * 0 \\ & -[\text{mass O}_2 \text{ in blast air}] * 1.352 \\ & -[\text{mass N}_2 \text{ in blast air}] * 1.463 \\ & +[\text{mass Fe out in molten iron}] * 1.269 \quad (6.2) \\ & +[\text{mass C out in molten iron}] * 5 \\ & +[\text{mass CO out in top gas}] * (-3.836) \\ & +[\text{mass CO}_2 \text{ out in top gas}] * (-8.844) \\ & +[\text{mass N}_2 \text{ out in top gas}] * 0.1099 \end{aligned}$$

as shown in matrix Table 6.2.

The matrix solution shows that;

1. 292 kg of O₂-in-blast air per 1000 kg of Fe in product molten iron, and,
2. 1255 kg of air (mass O₂ + mass N₂) per 1000 kg of Fe in product molten iron

are required to keep Table 6.2 blast furnace operating at steady state.

These are noticeably lower than with 1200°C blast, Section 6.1. Figs. 6.2 and 6.3 confirm these results.

6.6 DISCUSSION

Section 6.1 suggests that we are now half way to a fully predictive blast furnace model. Unfortunately, this is not quite true because Fig. 6.1 specifies that the top gas temperature is 130°C.

In reality, top gas temperature is a dependent variable. So, we are only a third of the way toward our fully predictive objective. Chapters 7–10 will show how this objective is attained.

6.7 SUMMARY

This chapter shows how to combine the enthalpy balance of Chapter 5, Introduction to the Blast Furnace Enthalpy Balance, with the mass balance and quantity specification equations of Chapter 4, Introduction to the Blast Furnace Mass Balance.

The variables are the same - so, the equations are easily combined into an Excel matrix.

The combined equations indicate that raising blast temperature *decreases* the steady-state blast furnace O₂-in-blast air and air requirements, all else being constant.

TABLE 6.2 Matrix Table 6.1 but with 1300°C blast. Only Cells F10 and G10 are altered. The steady state O₂-in-blast air requirement is lowered from 298 to 292 kg by increasing blast temperature from 1200 to 1300°C

A	B	C	D	E	F	G	H	I	J	K	L
1	Equation	Description	Numerical term	mass Fe ₂ O ₃ in ore charge	mass C in coke charge	mass O ₂ in blast air	mass N ₂ in blast air	mass Fe out in molten iron	mass C out in molten iron	mass CO out in top gas	mass CO ₂ out in top gas
2	4.6	Fe out in molten iron specification	1000	0	0	0	0	1	0	0	0
3	4.1	Fe mass balance	0	-0.699	0	0	0	1	0	0	0
4	4.2	O mass balance	0	-0.301	0	-1	0	0	0	0.571	0.727
5	4.12b	C mass balance	0	0	-1	0	0	0	1	0.429	0.273
6	4.4	N mass balance	0	0	0	0	-1	0	0	0	0
7	4.5	N ₂ in air specification	0	0	0	3.3	-1	0	0	0	0
8	4.7	C in coke charge specification	400	0	1	0	0	0	0	0	0
9	4.11	C out in molten iron specification	0	0	0	0	0	0.047	-1	0	0
10	6.2	Enthalpy balance	-400	5.169	0	-1.352	-1.463	1.269	5	-3.836	8.844
11											
12		Calculated values	kg per 1000 kg of Fe in product molten iron								
13		mass Fe ₂ O ₃ in ore charge	1431								
14		mass C in coke charge	400								
15		mass O ₂ in blast air	292								
16		mass N ₂ in blast air	963								
17		mass Fe out in molten iron	1000								
18		mass C out in molten iron	47								
19		mass CO out in top gas	381								
20		mass CO ₂ out in top gas	694								
21		mass N ₂ out in top gas	963								
22				25°C	25°C	1300°C	1300°C	1500°C	1500°C	130°C	130°C

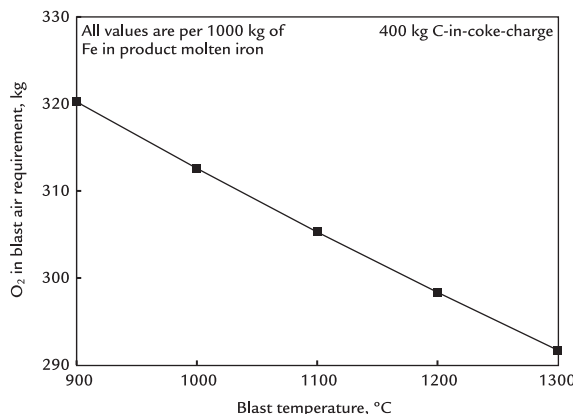


FIGURE 6.2 Effect of blast temperature on steady-state O₂-in-blast air requirement. The requirement decreases appreciably with increasing blast temperature. This is because hotter air brings more enthalpy into the furnace—decreasing the amount of C that must be exothermically oxidized to CO₂(g).

EXERCISES

All masses are kg per 1000 kg of Fe in product molten iron.

- 6.1. Matrix Table 6.1's carbon charge is lowered to 380 kg per 1000 kg of Fe in product molten iron. Predict what this operation's steady-state O₂-in-blast and

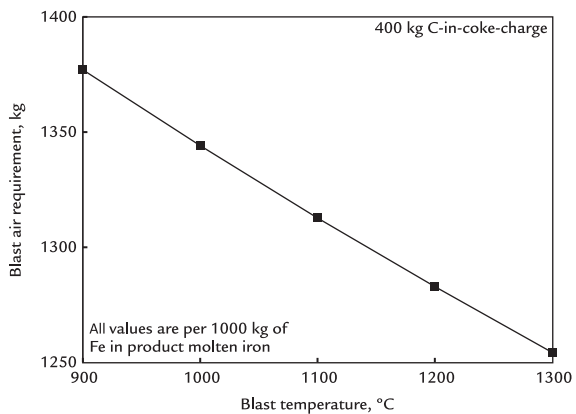


FIGURE 6.3 Effect of blast temperature on steady-state blast air requirement. The requirement decreases appreciably with increasing blast temperature.

total blast air requirements will be with this decreased carbon charge. Assume that the top gas temperature remains at 130°C.

- 6.2. Matrix Table 6.1's stoves are under repair so that they can only attain 1100°C blast. What is the blast furnace's steady-state O₂-in-blast air requirement with this cooler blast? The C-in-coke charge is 400 kg per 1000 kg of Fe in product molten iron.

Conceptual Division of the Blast Furnace - Bottom Segment Calculations

O U T L I N E

7.1 Dividing the Blast Furnace Into Two Segments	72	7.10 Bottom Segment Matrix and Results	78
7.2 Conditions in the Chemical Reserve	72	7.11 Analysis of Results	78
7.11.1 Fe		7.11.1 Fe	78
7.11.2 C		7.11.2 C	78
7.11.3 O		7.11.3 O	78
7.11.4 N		7.11.4 N	80
7.11.5 CO ₂ /CO Mass Ratio		7.11.5 CO ₂ /CO Mass Ratio	80
7.3 Bottom Segment Inputs and Outputs	73	7.12 C-in-Coke Entering Bottom Segment = C-in-Blast Furnace's Coke Charge	80
7.4 Bottom Segment Calculations	73	7.13 Effect of Blast Temperature on Carbon and Oxygen Requirements	80
7.5 Steady-State Mass Balance Equations	74	7.13.1 Results	80
7.5.1 Fe Mass Balance Equation	74	7.14 Discussion	80
7.5.2 Oxygen Mass Balance Equation	74	7.15 Summary	82
7.5.3 Carbon Mass Balance Equation	75	Exercises	83
7.5.4 Nitrogen Mass Balance Equation	75	References	83
7.6 Additional Specifications from Chapter 4	75		
7.7 Additional Chemical Reserve Gas Composition Specification	76		
7.8 Bottom Segment Enthalpy Balance	76		
7.9 Numerical Values and Final Enthalpy Equation	77		

7.1 DIVIDING THE BLAST FURNACE INTO TWO SEGMENTS

This chapter:

1. conceptually divides the blast furnace horizontally through its chemical reserve (Figs. 7.1–7.3),
2. describes chemical and thermal conditions at the division, and
3. repeats Chapters 4–6 calculations for the bottom segment.

This completes our basic predictive blast furnace model. Its principle objective is to show how the division enables us to;

- *a priori* calculate a blast furnace's steady-state C-in-coke and O₂-in-blast air requirements.

for steady-state production of molten iron, 95.5 mass% Fe, 4.5 mass% C, 1500°C.

A second objective is to show how these requirements are affected by blast temperature.

7.2 CONDITIONS IN THE CHEMICAL RESERVE

Chapter 2, Inside the Blast Furnace, described the chemical reserve zone in well-operated blast furnaces. It is a vertical region where;

1. no reactions take place;
2. the only Fe-bearing material is wüstite, Fe_{0.947}O; and
3. the CO₂/CO mass ratio in the gas rising into the chemical reserve is 0.694, which is

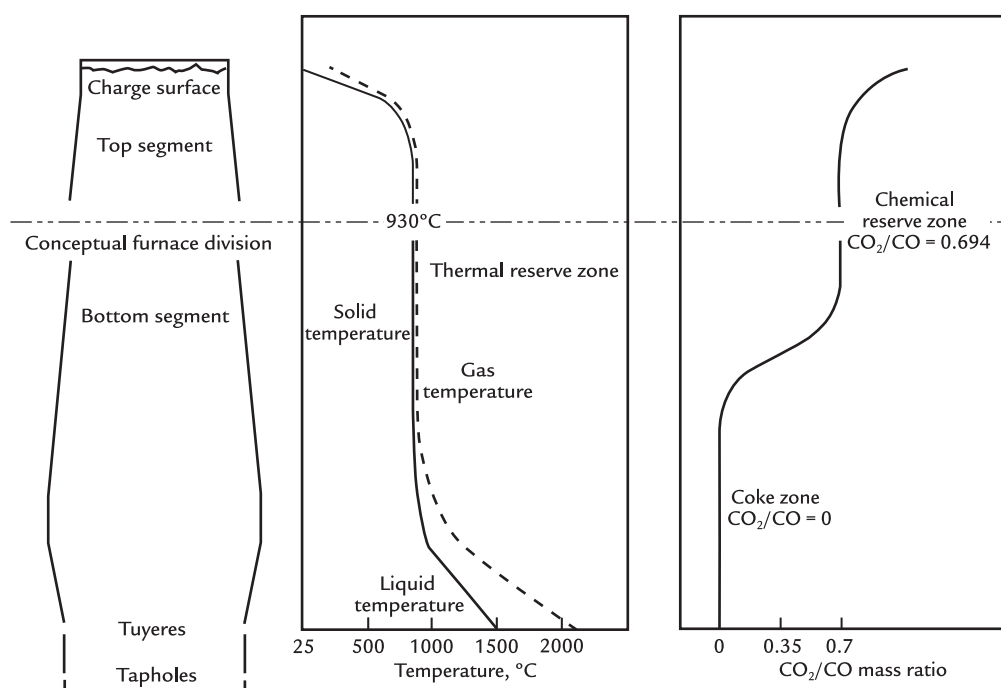


FIGURE 7.1 Blast furnace central slice, showing conceptual division of the furnace through its chemical reserve. This division provides two additional equations for our blast furnace model - making it fully predictive. The chemical reserve zone is a consequence of stoichiometric, equilibrium, and kinetic conditions in the blast furnace (Chapter 2: Inside the Blast Furnace).¹ From this point on, all our calculations specify the presence of this zone.

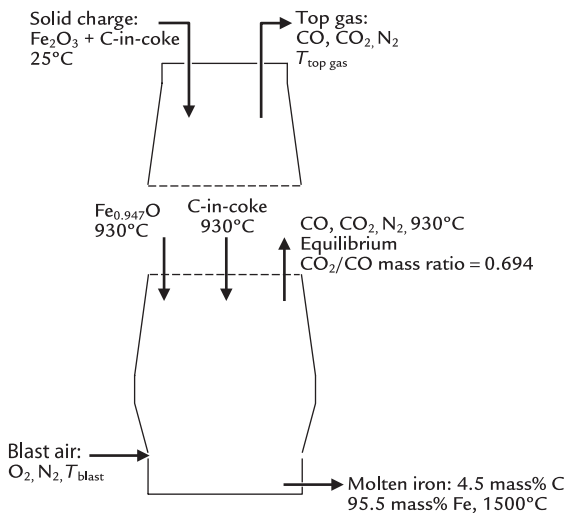


FIGURE 7.2 Central slice of the blast furnace showing details of our conceptual division. Blast temperature T_{blast} is an adjustable variable. Top-gas temperature $T_{top\ gas}$ is a dependent variable.

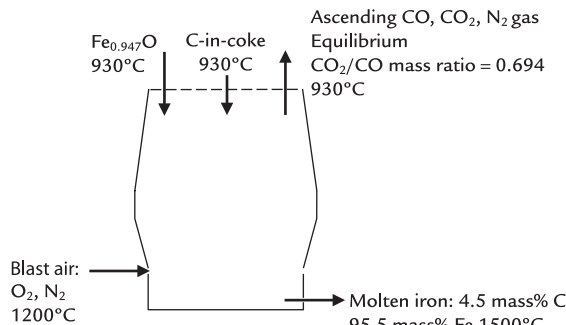
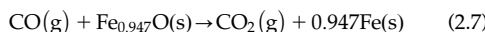


FIGURE 7.3 Bottom segment of the conceptually divided blast furnace. Solids continuously descend. Gases continuously ascend. Molten iron is tapped continuously or nearly continuously. Notice that many industrial details are missing, for example, hydrocarbon tuyere injectants, limestone flux, etc. These are added in later chapters.

the equilibrium CO_2/CO mass ratio for the reaction:



at 930°C , Appendices K and L. It is the gas composition throughout the *chemical reserve zone*.

We now conceptually divide the blast furnace top from bottom and then calculate *a priori*, the bottom segment's steady-state C and O_2 requirements.

7.3 BOTTOM SEGMENT INPUTS AND OUTPUTS

Fig. 7.3 shows the bottom segment of our divided blast furnace. Its steady-state inputs and outputs are:

Inputs

blast air, $\text{N}_2(\text{g}) + \text{O}_2(\text{g})$, 1200°C .
descending wüstite, $\text{Fe}_{0.947}(\text{s})$, 930°C .
descending C(s)-in-coke, 930°C .

Outputs

molten iron, 4.5 mass% C, 95.5 mass% Fe, 1500°C , being tapped from the blast furnace.
 $\text{CO}, \text{CO}_2, \text{N}_2$ gas, 930°C , CO_2/CO mass ratio = 0.694 ascending through the chemical reserve.

7.4 BOTTOM SEGMENT CALCULATIONS

We now develop equations that enable *a priori* calculation of the steady-state C and O_2 requirements of **Fig. 7.3**.

The calculations use the concepts that:

1. the only Fe-bearing material in the chemical reserve is wüstite, $\text{Fe}_{0.947}\text{O}$, and
 2. the CO_2/CO mass ratio in the chemical reserve gas is 0.694.
- They then,
3. develop steady-state mass balance equations and a steady-state enthalpy balance equation for the bottom segment of **Fig. 7.3**;

4. use the air composition and 1000 kg of Fe in product molten iron specifications in Chapter 4, Introduction to the Blast Furnace Mass Balance;
5. arrange these equations in matrix form; and
6. calculate *a priori* all Fig. 7.3 bottom segment inputs and outputs.

7.5 STEADY-STATE MASS BALANCE EQUATIONS

By analogy with the whole furnace calculations in Chapter 4, Introduction to the Blast Furnace Mass Balance, our basic steady-state bottom segment mass balances are;

$$[\text{mass Fe in}] = [\text{mass Fe out}] \quad (7.1a)$$

$$[\text{mass O in}] = [\text{mass O out}] \quad (7.1b)$$

$$[\text{mass C in}] = [\text{mass C out}] \quad (7.1c)$$

$$[\text{mass N in}] = [\text{mass N out}] \quad (7.1d)$$

where *mass in* is kg of each element entering the bottom segment and *mass out* is kg of each element leaving the bottom segment, *all per 1000 kg of Fe leaving the furnace in its product molten iron*.

The expanded mass balance equations are derived in the following sections.

7.5.1 Fe Mass Balance Equation

Fe enters Fig. 7.3 bottom segment as wüstite, $\text{Fe}_{0.947}\text{O}$. It leaves in product molten iron, 4.5 mass% C, 95.5 mass % Fe. These specifications and Eq. (7.1a) give:

$$\begin{aligned} & [\text{mass } \text{Fe}_{0.947}\text{O into}] * \frac{76.8 \text{ mass\% Fe in } \text{Fe}_{0.947}\text{O}}{100\%} \\ &= [\text{mass Fe out}] * 1 \end{aligned}$$

or

$$[\text{mass } \text{Fe}_{0.947}\text{O into}] * 0.768 = [\text{mass Fe out}] * 1$$

or subtracting $\left\{ [\text{mass } \text{Fe}_{0.947}\text{O into}] * 0.768 \right\}$ from both sides:

$$0 = -[\text{mass } \text{Fe}_{0.947}\text{O into}] * 0.768 + [\text{mass Fe out}] * 1 \quad (7.2)$$

7.5.2 Oxygen Mass Balance Equation

Oxygen enters the bottom segment of Fig. 7.3 in descending $\text{Fe}_{0.947}\text{O}$ and input blast air. It leaves as CO and CO_2 in ascending bottom segment exit gas.

These specifications and Eq. (7.1b) give:

$$\begin{aligned} & [\text{mass } \text{Fe}_{0.947}\text{O into}] * \frac{23.2 \text{ mass\% O in } \text{Fe}_{0.947}\text{O}}{100\%} \\ &+ [\text{mass O}_2 \text{ in}] * \frac{100 \text{ mass\% O in O}_2}{100\%} \\ &= [\text{mass CO out}] * \frac{57.1 \text{ mass\% O in CO}}{100\%} \\ &+ [\text{mass CO}_2 \text{ out}] * \frac{72.7 \text{ mass\% O in CO}_2}{100\%} \end{aligned}$$

or

$$\begin{aligned} & [\text{mass } \text{Fe}_{0.947}\text{O into}] * 0.232 + [\text{mass O}_2 \text{ in}] * 1 \\ &= [\text{mass CO out}] * 0.571 \\ &+ [\text{mass CO}_2 \text{ out}] * 0.727 \end{aligned}$$

or subtracting $\left\{ [\text{mass } \text{Fe}_{0.947}\text{O into}] * 0.232 + [\text{mass O}_2 \text{ in}] * 1 \right\}$ from both sides:

$$\begin{aligned} 0 = & -[\text{mass } \text{Fe}_{0.947}\text{O into}] * 0.232 - [\text{mass O}_2 \text{ in}] * 1 \\ &+ [\text{mass CO out}] * 0.571 \\ &+ [\text{mass CO}_2 \text{ out}] * 0.727 \end{aligned} \quad (7.3)$$

7.5.3 Carbon Mass Balance Equation

Carbon enters the bottom segment of Fig. 7.3 in descending coke. It leaves:

1. as CO and CO₂ in ascending bottom segment exit gas, and
2. in the blast furnace's product molten iron, 4.5 mass% C.

These specifications and Eq. (7.1c) give:

$$\begin{aligned} & \left[\frac{\text{mass C in}}{\text{descending coke}} \right] * \frac{100\% \text{ C}}{100\%} \\ &= \left[\frac{\text{mass CO out}}{\text{in ascending gas}} \right] * \frac{42.9 \text{ mass\% C in CO}}{100\%} \\ &+ \left[\frac{\text{mass CO}_2 \text{ out}}{\text{in ascending gas}} \right] * \frac{27.3 \text{ mass\% C in CO}_2}{100\%} \\ &+ \left[\frac{\text{mass C out}}{\text{in molten iron}} \right] * 1 \end{aligned}$$

or

$$\begin{aligned} & \left[\frac{\text{mass C in}}{\text{descending coke}} \right] * 1 = \left[\frac{\text{mass CO out}}{\text{in ascending gas}} \right] \\ & * 0.429 + \left[\frac{\text{mass CO}_2 \text{ out}}{\text{in ascending gas}} \right] * 0.273 \\ &+ \left[\frac{\text{mass C out}}{\text{in molten iron}} \right] * 1 \end{aligned}$$

or, subtracting $\left\{ \left[\frac{\text{mass C in}}{\text{descending coke}} \right] * 1 \right\}$ from both sides:

$$\begin{aligned} 0 &= - \left[\frac{\text{mass C in}}{\text{descending coke}} \right] * 1 + \left[\frac{\text{mass CO out}}{\text{in ascending gas}} \right] \\ & * 0.429 + \left[\frac{\text{mass CO}_2 \text{ out}}{\text{in ascending gas}} \right] * 0.273 \\ &+ \left[\frac{\text{mass C out}}{\text{in molten iron}} \right] * 1 \end{aligned} \quad (7.4)$$

7.5.4 Nitrogen Mass Balance Equation

Nitrogen enters the bottom segment of Fig. 7.3 in input blast air. It leaves in ascending bottom segment exit gas.

These specifications and nitrogen balance Eq. (7.1d) give the equation:

$$\begin{aligned} & \left[\frac{\text{mass N}_2 \text{ in}}{\text{blast air}} \right] * \frac{100\% \text{ N in N}_2}{100\%} \\ &= \left[\frac{\text{mass N}_2 \text{ out}}{\text{in ascending gas}} \right] * \frac{100\% \text{ N in N}_2}{100\%} \end{aligned}$$

or $\left[\frac{\text{mass N}_2 \text{ in}}{\text{blast air}} \right] * 1 = \left[\frac{\text{mass N}_2 \text{ out}}{\text{in ascending gas}} \right] * 1$
or, subtracting $\left\{ \left[\frac{\text{mass N}_2 \text{ in}}{\text{blast air}} \right] * 1 \right\}$ from both sides:

$$0 = - \left[\frac{\text{mass N}_2 \text{ in}}{\text{blast air}} \right] * 1 + \left[\frac{\text{mass N}_2 \text{ out}}{\text{in ascending gas}} \right] * 1 \quad (7.5)$$

7.6 ADDITIONAL SPECIFICATIONS FROM CHAPTER 4

Chapter 4, Introduction to the Blast Furnace Mass Balance, provides three additional specifications:

1. blast air composition (Eq. (4.5)),
2. the mass Fe in output molten iron = 1000 kg specification (Eq. (4.6)), and
3. Carbon out in molten iron equation (Eq. (4.11)).

These also apply to the bottom segment, Fig. 7.3.

The blast air composition equation is:

$$0 = - \left[\frac{\text{mass N}_2 \text{ in}}{\text{blast air}} \right] * 1 + \left[\frac{\text{mass O}_2 \text{ in}}{\text{blast air}} \right] * 3.3 \quad (7.6)$$

The 1000 kg of Fe in product molten iron equation is:

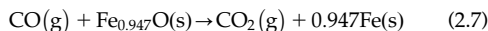
$$1000 = \left[\frac{\text{mass Fe out}}{\text{in molten iron}} \right] * 1 \quad (7.7)$$

The carbon in output molten iron is:

$$0 = - \left[\frac{\text{mass C out}}{\text{in molten iron}} \right] * 1 + \left[\frac{\text{mass Fe out}}{\text{in molten iron}} \right] * 0.047 \quad (7.8)$$

7.7 ADDITIONAL CHEMICAL RESERVE GAS COMPOSITION SPECIFICATION

The chemical reserve zone is a region where the reaction:



has approached equilibrium at 930°C.

Appendices K and L show that this reaction's equilibrium CO₂/CO mass ratio at 930°C is 0.694 - or in equation form:

$$\frac{[\text{mass CO}_2]}{[\text{mass CO}]} = 0.694$$

or multiplying both sides by mass CO:

$$\text{mass CO}_2 * 1 = \text{mass CO} * 0.694$$

This is the composition of the chemical reserve gas, that is the gas ascending across the conceptual division of Fig. 7.2. In this application, it may be written:

$$\left[\begin{array}{l} \text{mass CO}_2 \text{ out} \\ \text{in ascending gas} \end{array} \right] * 1 = \left[\begin{array}{l} \text{mass CO out} \\ \text{in ascending gas} \end{array} \right] * 0.694$$

or subtracting $\left[\begin{array}{l} \text{mass CO}_2 \text{ out} \\ \text{in ascending gas} \end{array} \right] * 1$ from both sides:

$$0 = - \left[\begin{array}{l} \text{mass CO}_2 \text{ out} \\ \text{in ascending gas} \end{array} \right] * 1 + \left[\begin{array}{l} \text{mass CO out} \\ \text{in ascending gas} \end{array} \right] * 0.694 \quad (7.9)$$

7.8 BOTTOM SEGMENT ENTHALPY BALANCE

By analogy with Section 5.1, the steady-state enthalpy balance equation for Fig. 7.3 bottom segment is:

$$\begin{aligned} \text{total enthalpy in} &= \text{total enthalpy out} \\ &+ \left[\begin{array}{l} \text{bottom segment} \\ \text{conductive, convective} \\ \text{and radiative heat loss} \end{array} \right] \end{aligned} \quad (7.10)$$

or

$$\sum_{i=1}^n m_i H_{i,\text{Inputs}} = \sum_{j=1}^m m_j H_{j,\text{Outputs}} + \left[\begin{array}{l} \text{bottom segment} \\ \text{conductive, convective} \\ \text{and radiative heat loss} \end{array} \right] \quad (7.11)$$

where:

1. m_i and m_j are the masses of the bottom segment input and output substances, kg per 1000 kg of Fe in product molten iron.
2. H_i and H_j are the enthalpies of the input and output substances, megajoules (MJ) per kg of substance.
3. The last term is bottom segment conductive, convective and radiative heat loss, megajoules per 1000 kg of Fe in product molten iron. Water flow and temperature measurements indicate that it accounts for about 80% of total furnace conductive, convective and radiative heat loss.

Bottom segment *input* enthalpy of Fig. 7.3 is:

$$\begin{aligned} \sum_{i=1}^n m_i H_{i,\text{Inputs}} &= \left[\begin{array}{l} \text{mass Fe}_{0.947}\text{O into} \\ \text{bottom segment} \end{array} \right] * \frac{H^\circ_{930^\circ\text{C}} \text{ Fe}_{0.947}\text{O(s)}}{\text{MW}_{\text{Fe}_{0.947}\text{O}}} \\ &+ \left[\begin{array}{l} \text{mass C in} \\ \text{descending coke} \end{array} \right] * \frac{H^\circ_{930^\circ\text{C}} \text{ C(s)}}{\text{MW}_\text{C}} \\ &+ \left[\begin{array}{l} \text{mass O}_2 \text{ in} \\ \text{blast air} \end{array} \right] * \frac{H^\circ_{1200^\circ\text{C}} \text{ O}_2\text{(g)}}{\text{MW}_{\text{O}_2}} \\ &+ \left[\begin{array}{l} \text{mass N}_2 \text{ in} \\ \text{blast air} \end{array} \right] * \frac{H^\circ_{1200^\circ\text{C}} \text{ N}_2\text{(g)}}{\text{MW}_{\text{N}_2}} \end{aligned} \quad (7.12)$$

where the H°/MW terms are the enthalpies megajoules MJ of each substance *per kg*. The values may be calculated from H° and MW or from the enthalpy-temperature equations in Appendix J.

The bottom segment *output enthalpy* of Fig. 7.3 is:

$$\sum_{j=1}^m m_j H_{j\text{Outputs}} = \left[\begin{array}{l} \text{mass Fe out} \\ \text{in molten iron} \end{array} \right] * \frac{H_{1500^\circ\text{C}}}{\text{MW}_{\text{Fe}}} + \left[\begin{array}{l} \text{mass C out} \\ \text{in molten iron} \end{array} \right] * \frac{H_{1500^\circ\text{C}}}{\text{MW}_\text{C}} + \left[\begin{array}{l} \text{mass CO out} \\ \text{in ascending gas} \end{array} \right] * \frac{H_{930^\circ\text{C}}}{\text{MW}_{\text{CO}}} + \left[\begin{array}{l} \text{mass CO}_2 \text{ out} \\ \text{in ascending gas} \end{array} \right] * \frac{H_{930^\circ\text{C}}}{\text{MW}_{\text{CO}_2}} + \left[\begin{array}{l} \text{mass N}_2 \text{ out} \\ \text{in ascending gas} \end{array} \right] * \frac{H_{930^\circ\text{C}}}{\text{MW}_{\text{N}_2}} \quad (7.13)$$

Lastly, bottom segment conductive, convective and radiative heat loss in Fig. 7.3 is $\sim 80\%$ of that from the whole blast furnace (Section 5.4), that is $400 \text{ MJ} * (80\% / 100\%) = 320 \text{ MJ}$ per 1000 kg of Fe in product molten iron.

7.9 NUMERICAL VALUES AND FINAL ENTHALPY EQUATION

Table 7.1 gives bottom segment enthalpy values represented in Fig. 7.3.

Conductive, convective and radiative heat loss value in Eqs. (7.10)–(7.13) and Section 7.7

TABLE 7.1 Enthalpies of Inputs and Outputs of Fig. 7.3

Description	Value, MJ per kg of substance
$H_{930^\circ\text{C}} / \text{MW}_{\text{Fe}_{0.947}\text{O(s)}}$	-3.152
$H_{930^\circ\text{C}} / \text{MW}_\text{C}$	1.359
$H_{1200^\circ\text{C}} / \text{MW}_{\text{O}_2}$	1.239
$H_{1200^\circ\text{C}} / \text{MW}_{\text{N}_2}$	1.339
$H_{1500^\circ\text{C}} / \text{MW}_{\text{Fe}}$	1.269 ²
$H_{1500^\circ\text{C}} / \text{MW}_\text{C}$ C(dissolved)	5 (Section 5.3) ^a
$= \left\{ \left(\begin{array}{l} H_{1500^\circ\text{C}} / \text{MW}_\text{C} \\ \text{C(s)} \end{array} \right) + 2.5 \right\}$	
$H_{930^\circ\text{C}} / \text{MW}_{\text{CO}}$ CO(g)	-2.926
$H_{930^\circ\text{C}} / \text{MW}_{\text{CO}_2}$ CO ₂ (g)	-7.926
$H_{930^\circ\text{C}} / \text{MW}_{\text{N}_2}$ N ₂ (g)	1.008

^a2.5 is the enthalpy of mixing Fe (ℓ)_{1500°C} + C(s)_{1500°C} to make 95.5 mass% Fe 4.5 mass% C molten iron alloy (1500°C) MJ per kg of C (Section 5.3).

gives the following overall enthalpy balance equation:

$$\begin{aligned}
 & [\text{mass Fe}_{0.947}\text{O into bottom segment}] * (-3.152) \\
 & + [\text{mass C in descending coke}] * 1.359 \\
 & + [\text{mass O}_2 \text{ in blast air}] * 1.239 \\
 & + [\text{mass N}_2 \text{ in blast air}] * 1.339 \\
 & = [\text{mass Fe out in molten iron}] * 1.269 \\
 & + [\text{mass C out in molten iron}] * 5 \\
 & + [\text{mass CO out in ascending gas}] * (-2.926) \\
 & + [\text{mass CO}_2 \text{ out in ascending gas}] * (-7.926) \\
 & + [\text{mass N}_2 \text{ out in ascending gas}] * 1.008 \\
 & + \left[\begin{array}{l} 320 \text{ MJ bottom segment conductive,} \\ \text{convective and radiative heat loss per 1000} \\ 1000 \text{ kg of Fe in product molten iron} \end{array} \right] \\
 & \quad (7.14)
 \end{aligned}$$

or subtracting the left side of Eq. (7.14) and the last term of the right side of Eq. (7.14) from both sides and rearranging:

$$\begin{aligned}
 -320 &= -[\text{mass Fe}_{0.947}\text{O into bottom segment}] * (-3.152) \\
 &- [\text{mass C in descending coke}] * 1.359 \\
 &- [\text{mass O}_2 \text{ in blast air}] * 1.239 \\
 &- [\text{mass N}_2 \text{ in blast air}] * 1.339 \\
 &+ [\text{mass Fe out in molten iron}] * 1.269 \\
 &+ [\text{mass C out in molten iron}] * 5 \\
 &+ [\text{mass CO gas out in ascending gas}] * (-2.926) \\
 &+ [\text{mass CO}_2 \text{ out in ascending gas}] * (-7.926) \\
 &+ [\text{mass N}_2 \text{ out in ascending gas}] * 1.008
 \end{aligned}
 \quad (7.15)$$

where the enthalpy values are for temperatures as specified in Fig. 7.3.

7.10 BOTTOM SEGMENT MATRIX AND RESULTS

Table 7.2 is bottom segment matrix of Fig. 7.3. It is made up of nine equations [Eqs. (7.2)–(7.9) and (7.16)] and nine variables. It is solved as described in Appendix I. Try it!

7.11 ANALYSIS OF RESULTS

This section examines the matrix Table 7.2 results.

7.11.1 Fe

As defined, 1000 kg of Fe departs the furnace in the product molten iron, 4.5 mass% C, 95.5 mass% Fe.

The Fe all comes from the input of 1302 kg of Fe_{0.947}O, which at 76.8 mass% Fe, contains 1000 kg of Fe and 302 kg of O.

7.11.2 C

392 kg of C-in-coke descends into the bottom segment. 47 kg departs in the product molten iron:

$$\begin{aligned}
 & 239 \text{ kg C leaves in ascending CO} \\
 & = \left(558 \text{ kg CO} * \frac{42.9 \text{ mass\% C in CO}}{100\%} \right) \\
 & 106 \text{ kg C leaves in ascending CO}_2 \\
 & = \left(387 \text{ kg CO}_2 * \frac{27.3 \text{ mass\% C in CO}_2}{100\%} \right)
 \end{aligned}$$

These outputs plus the 47 kg departing as dissolved C in molten iron account for the 392 kg input, as expected.

7.11.3 O

302 kg of O enters the bottom segment in Fe_{0.947}O and 298 kg of O enters as O₂-in-blast air, total 600 kg;

$$\begin{aligned}
 & 319 \text{ kg O leaves in ascending CO} \\
 & = \left(558 \text{ kg CO} * \frac{57.1 \text{ mass\% O in CO}}{100\%} \right) \\
 & 281 \text{ kg O leaves in ascending CO}_2 \\
 & = \left(387 \text{ kg CO}_2 * \frac{72.7 \text{ mass\% O in CO}_2}{100\%} \right)
 \end{aligned}$$

for an expected total of 600 kg out.

TABLE 7.2 Bottom Segment Matrix

	A	B	C	D	E	F	G	H	I	J	K	L
1 BOTTOM SEGMENT CALCULATIONS												
2	Equation	Description	Numerical term	mass Fe _{0.947} O into bottom segment	mass C in descending coke	mass O ₂ in blast air	mass N ₂ in blast air	mass Fe out in molten iron	mass C out in molten iron	mass CO out in ascending gas	mass CO ₂ out in ascending gas	mass N ₂ out in ascending gas
3	7.7	Fe out in molten iron specification	1000	0	0	0	0	1	0	0	0	0
4	7.2	Fe mass balance	0	-0.768	0	0	0	0	0	0	0	0
5	7.3	O mass balance	0	-0.232	0	-1	0	0	0	0.571	0.727	0
6	7.4	C mass balance	0	0	-1	0	0	1	0.429	0.273	0	
7	7.5	N mass balance	0	0	0	0	-1	0	0	0	0	1
8	7.6	N ₂ in air specification	0	0	0	3.3	-1	0	0	0	0	0
9	7.9	Equilibrium CO ₂ /CO mass ratio	0	0	0	0	0	0	0	0.694	-1	0
10	7.8	C out in molten iron specification	0	0	0	0	0	-1	0	0	0	0
11	7.15	Enthalpy balance	-320	3.152	-1.359	-1.239	-1.339	1.269	5	-2.926	-7.926	1.008
12				930°C	930°C	1200°C	1200°C	1500°C	1500°C	930°C	930°C	930°C
13												
14												
15												
16												
17	Bottom segment calculated values		kg per 1000 kg of Fe in product molten iron									
18	mass Fe _{0.947} O into bottom segment	1302										
19	mass C in descending coke	392	also = mass C in the furnace's coke charge, Eqn. (7.16)									
20	mass O ₂ in blast air	298										
21	mass N ₂ in blast air	983										
22	mass Fe out in molten iron	1000										
23	mass C out in molten iron	47										
24	mass CO out in ascending gas	558										
25	mass CO ₂ out in ascending gas	387										
26	mass N ₂ out in ascending gas	983										

Note the nine equations and nine variables. The temperatures at the bottom are just for guidance. Notice that the carbon and oxygen requirements are 392 and 298 kg per 1000 kg of Fe in product molten iron.

7.11.4 N

983 kg N enters the bottom segment in blast and 983 kg ascend out of the bottom segment in the ascending exit gas.

As prescribed, the nitrogen/oxygen mass ratio in the blast air is 983 kg nitrogen/298 kg oxygen = 3.3.

7.11.5 CO₂/CO Mass Ratio

The CO₂/CO ratio of the exiting gas is 387 kg CO₂/558 kg CO = 0.694, as prescribed by Eq. (7.9).

7.12 C-IN-COKE ENTERING BOTTOM SEGMENT = C-IN-BLAST FURNACE'S COKE CHARGE

Section 2.8 indicates that there is little or no C(s) oxidation at the cooler temperatures above the blast furnace's chemical reserve. This is represented by the equation:

$$\begin{bmatrix} \text{mass C in} \\ \text{furnace's} \\ \text{coke charge} \end{bmatrix} = \begin{bmatrix} \text{mass C in} \\ \text{bottom segment's} \\ \text{descending coke} \end{bmatrix} \quad (7.16)$$

The ramifications of Eq. 7.16 is that the whole furnace C-in-coke requirement of Fig. 7.2 is the same as matrix Table 7.2's calculated bottom segment's C in descending coke value.

Eq. (7.16) is used throughout this book.

7.13 EFFECT OF BLAST TEMPERATURE ON CARBON AND OXYGEN REQUIREMENTS

We now use matrix Table 7.2 to determine carbon and oxygen requirements as a function of blast temperature. Blast temperature is an adjustable variable. C-in-coke and O₂-in-blast air are dependent variables, calculated using

TABLE 7.3 Enthalpies of O₂(g) and N₂(g) at Various Blast Temperatures

T (°C)	O ₂ Enthalpy (MJ/kg)	N ₂ Enthalpy (MJ/kg)
900	0.898	0.968
1000	1.011	1.092
1100	1.125	1.216
1200	1.239	1.339
1300	1.352	1.463

These values are sequentially entered in the cells F11 and G11 of matrix Table 7.2. The matrix automatically calculates new input C and O₂ values as shown in matrix Table 7.4. The enthalpy values have been calculated using the equations in Appendix J.

the Table 7.2 bottom segment matrix and Eq. (7.16).

The calculations are done by changing the O₂ and N₂ enthalpies in the cells F11 and G11 of Table 7.2 using the enthalpy values in Table 7.3 (see Table 7.4).

7.13.1 Results

Fig. 7.4 shows the C-in-coke and O₂-in-blast air requirements over the industrial range of blast temperatures.

Neither line is straight. The slight curvatures are due to the slightly different heat capacities, dH°/dT of the bottom segment reactants and products, for example; $(dH^\circ_{C(s)}/dT + dH^\circ_{O_2(g)}/dT) \neq dH^\circ_{CO_2(g)}/dT$.

7.14 DISCUSSION

This chapter:

1. divides the blast furnace horizontally through its chemical reserve, forming top, and bottom segments, and

TABLE 7.4 Matrix Table 7.4 is the same as Matrix Table 7.2 except for Cells F11 and G11, which now contain the enthalpies of O₂(g) and N₂(g) at 1300°C

A	B	C	D	E	F	G	H	I	J	K	L
1 BOTTOM SEGMENT CALCULATIONS											
2	Equation	Description	Numerical term	mass Fe _{0.94} O into bottom segment	mass C in descending coke	mass O ₂ in blast air	mass N ₂ in blast air	mass Fe out in molten iron	mass C out in molten iron	mass CO out in ascending gas	mass CO ₂ out in ascending gas
3	7.7	Fe out in molten iron specification	1000	0	0	0	0	1	0	0	0
4	7.2	Fe mass balance	0	-0.768	0	0	0	0	0	0	0
5	7.3	O mass balance	0	-0.232	0	-1	0	0	0	0.571	0.727
6	7.4	C mass balance	0	0	-1	0	0	0	1	0.429	0.273
7	7.5	N mass balance	0	0	0	0	-1	0	0	0	0
8	7.6	N ₂ in blast air specification	0	0	0	3.3	-1	0	0	0	0
9	7.9	Equilibrium CO ₂ /CO mass ratio	0	0	0	0	0	0	0	0.694	-1
10	7.8	C in out in molten iron specification	0	0	0	0	0	0.047	-1	0	0
11	7.15	Enthalpy balance	320	3.152	-1.359	-1.352	-1.463	1.269	5	-2.926	-7.926
12				930°C	930°C	1300°C	1300°C	1500°C	1500°C	930°C	930°C
13											
14											
15											
16											
17	Calculated values	kg per 1000 kg of Fe in product molten iron									
18	mass FeO _{1.05} into bottom segment	1302									
19	mass C in descending coke	384	also = mass C in the furnace's coke charge, Eqn. (7.16)								
20	mass O ₂ in blast air	284									
21	mass N ₂ in blast air	938									
22	mass Fe out in molten iron	1000									
23	mass C out in molten iron	47									
24	mass CO out in ascending gas	545									
25	mass CO ₂ out in ascending gas	378									
26	mass N ₂ out in ascending gas	938									

The resulting new steady-state inputs and outputs are shown in cells C18–C26. These results are generated automatically when the new cell F11 and G11 values are entered. Notice that increasing blast temperature from 1200 to 1300°C lowers the carbon requirement from 392 to 384 kg and the O₂-in-blast requirement from 298 to 284 kg, all per 1000 kg of Fe in product molten iron. Notice the negative values in cells F11 and G11. This is the result of Eq. (7.15).

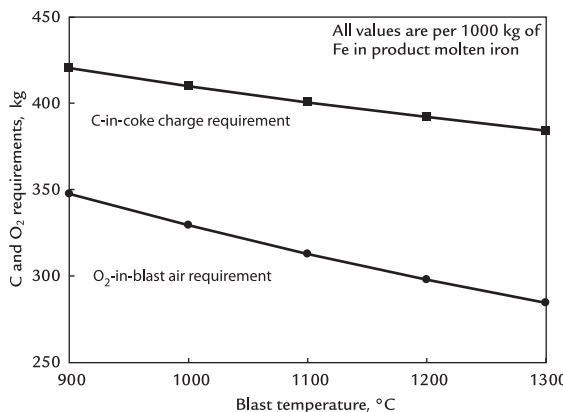
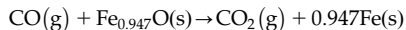


FIGURE 7.4 Steady-state C-in-coke charge and O₂-in-blast air requirements of Fig. 7.3 as a function of blast temperature. The blast is air, 76.9 mass% nitrogen, 23.1 mass% oxygen. Carbon does not react in and above the chemical reserve zone so that kg of C descending into the bottom segment is the same as kg of C in the furnace charge, Eq. (7.16). C and O₂ requirements both decrease with increasing blast temperature. This is a consequence of all our matrix equations. We may postulate, however, that it is because steady-state bottom segment operation requires less carbon combustion (per 1000 kg of product molten iron) with *increasing enthalpy in blast MJ per kg of O₂ and N₂*.

2. uses conditions at the division to provide an additional specification for our blast furnace calculations.

The new specification is that the gas rising through the chemical reserve is the equilibrium product of the reaction;



at the chemical reserve temperature, 930°C, is written as:

$$0 = - \left[\begin{array}{l} \text{mass CO}_2 \text{ out} \\ \text{in ascending gas} \end{array} \right] * 1 + \left[\begin{array}{l} \text{mass CO out} \\ \text{in ascending gas} \end{array} \right] * 0.694 \quad (7.9)$$

The chapter also specifies that there is no C(s) oxidation at the cooler temperatures in

and above the chemical reserve zone of Fig. 7.1. This specification may be written as:

$$\left[\begin{array}{l} \text{whole furnace} \\ \text{C-in-coke charge} \end{array} \right] = \left[\begin{array}{l} \text{C-in-coke} \\ \text{descending into} \\ \text{the bottom segment} \end{array} \right] \quad (7.17)$$

Chapter 8, Tuyere Injection of Pulverized Carbon, and subsequent chapters takes the calculations of this chapter to actual blast furnace operating conditions. Some added features are:

- a. tuyere-injection of pulverized coal, natural gas, and other hydrocarbons,
- b. oxygen injection into the blast air,
- c. H₂O(g) in the blast, natural (humidity), and in injected steam, and
- d. inclusion of prereduced iron ore pellets in the furnace charge

as shown in our table of contents.

Other industrial features of blast furnace operation are also added, for example:

1. Flux addition and slag production.
2. Silica reduction and dissolved Si in product molten iron.
3. Other molten iron and slag impurities, for example, K, Mn, Na, Ti, and Zn.

Also, we do not ignore the top segment of the furnace. We look at:

1. top-gas composition, enthalpy, and temperature;
2. charge drying; and
3. carbonate flux decomposition,

to name a few.

7.15 SUMMARY

This chapter divided the blast furnace in Fig. 7.1 horizontally through its chemical reserve. Two additional equations (7.9) and (7.17) are provided, and this enables *a priori* calculation of the steady-state of the blast furnace in Fig. 7.2;

1. oxygen-in-blast requirement,
2. carbon-in-coke charge requirement,
3. ore-in-charge requirement, and
4. molten iron production

all kg per 1000 kg of Fe in product molten iron.

We also calculated and showed the effects of blast temperature on the amounts of O₂(g)-in-blast air and C(s)-in-coke charge that are required for steady production of molten iron at 1500°C. Both are decreased by raising blast temperature.

The decreased O₂(g)-in-blast air and C(s)-in-coke charge result from all of our matrix equations. We may speculate that the decreases are mainly due to the increased enthalpy of the hotter blast, which lowers the requirement for C(s) + O₂(g) combustion in front of the tuyeres.

Subsequent chapters add other industrial details to our calculations. They also evaluate the suitability of our calculation technique.

EXERCISES

- 7.1. Blast heating stoves of Fig. 7.3 need repairs. The plant's engineering department expects that their output blast temperature will drop to 1100°C, while the repairs are being made. Please determine for them how much extra C-in-coke will be required to steadily produce 1500°C molten iron during the repairs.

Also determine how much;

- a. O₂-in-blast air,
- b. N₂-in-blast air, and
- c. blast air

will be required during the repairs.

Use the enthalpy values in Table 7.3 or the enthalpy equations in Appendix J.

Please give your answers in kg per 1000 kg of Fe in product molten iron.

- 7.2. By how much will the 1100°C blast air requirement of Exercise 7.1 increase the mass of nitrogen rising out of;
- a. the conceptual bottom segment of the blast furnace of Fig. 7.2, and
 - b. the top of the blast furnace of Fig. 7.1.
- 7.3. The blast furnace operating company of Table 7.2 is running short of coke. It needs to cut coke consumption by 1%. Suggest (quantitatively) what it can do to achieve this saving, perhaps by employing its newly repaired blast heating stoves.

Of course, this decrease in C-in-coke consumption will lower operating cost.

Will any other cost be increased?

How else other could you decrease coke consumption?

- 7.4. The blast furnace's top gas of Fig. 7.2,
- a. contains CO(g), and
 - b. leaves the furnace at 2 bar (200 kPa) pressure (gauge).

How can the blast furnace operator make use of these two items?

Unfortunately, CO(g) has a disadvantage. What is it and how can it be overcome?

References

1. Geerdes M, Chaigneau R, Kurunov I, Lingiardi O, Ricketts J. *Modern blast furnace ironmaking (an introduction)*. 3rd ed. Amsterdam: IOS Press B.V.; 2015. p. 120.
2. Desai PD. Thermodynamic properties of iron and silicon. *J Phys Chem Ref Data* 1986;15(3):967–83. Retrieved on February 18, 2015 by Googling title.

Bottom Segment with Pulverized Carbon Injection

O U T L I N E

8.1 The Importance of Injecting Hydrocarbon Fuel Through Blast Furnace Tuyeres	85	8.5 Effect of Pulverized C Injection on Descending C-in-Coke Requirement	88
8.2 Pulverized Carbon C-in-Coal Injection	86	8.6 Discussion	88
8.3 Carbon Injection Calculations	86	8.7 Coke Replacement Ratio	88
8.3.1 <i>Injected Carbon Specification</i>	87	8.7.1 <i>Replacement Ratio Explanation</i>	90
8.3.2 <i>Bottom Segment Carbon Balance</i>	87	8.8 Total Carbon Requirement	90
8.3.3 <i>Bottom Segment Enthalpy Balance Equation</i>	88	8.9 Blast Air O₂ and N₂ Requirements	90
8.4 Matrix With C-in-Coal Through Tuyere Injection	88	8.10 Summary	91
		Exercises	91
		References	92

8.1 THE IMPORTANCE OF INJECTING HYDROCARBON FUEL THROUGH BLAST FURNACE TUYERES

All iron blast furnaces inject hydrocarbons through their tuyeres. The principle purpose is to replace expensive top-charged C-in-coke

(expensive because coke is extensively processed metallurgical coal, Chapter 56: Blast Furnace Fuel Injection) with cheaper tuyere-injected hydrocarbons.

Up to 40% of a blast furnace's reductant/fuel can be injected through its tuyeres. Far and away the most commonly used injectant is dried, ~75 µm diameter pulverized coal.

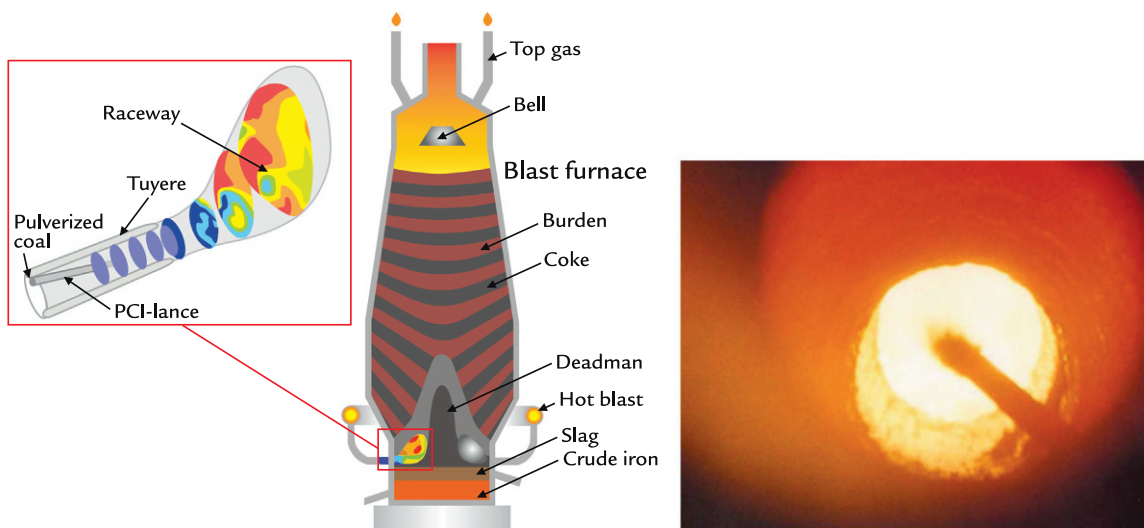


FIGURE 8.1 Sketch and photograph of pulverized coal being injected through a blast furnace tuyere.^{1,2} Coal is always injected equally through all the tuyeres. The sketch shows injection through one of the blast furnace tuyeres in Fig. 1.5.

Other injectants include natural gas, fuel oil, and recycled pulverized plastic (Fig. 8.1).

Two other substances are also added to the blast and blown through the tuyeres. They are purified oxygen, $O_2(g)$, and water vapor, $H_2O(g)$.

Their beneficial effects are described in Chapter 9, Bottom Segment with Oxygen Enrichment of Blast Air, and Chapter 14, Raceway Flame Temperature.

The objectives of this chapter are to:

1. show how tuyere injectants are included in our matrix calculations, and
2. indicate how C-in-coal injection affects a blast furnace's;
 - a. C-in-coke-charge requirement and
 - b. O_2 -in-blast air requirement

for steady production of molten iron, 1500°C.

The injectant in this chapter is pulverized PURE solid carbon, a simplified stand-in for pulverized coal.

All injectants except oxygen (e.g., coal, natural gas, and water vapor) contain hydrogen. This is described in Chapter 10, Bottom Segment with Low Purity Oxygen Enrichment.

8.2 PULVERIZED CARBON C-IN-COAL INJECTION

Bottom-segment Fig. 8.2 describes pulverized C injection into a simplified blast furnace.

8.3 CARBON INJECTION CALCULATIONS

This section describes our carbon injection calculations. It:

1. specifies C injectant quantity, kg per 1000 kg of Fe in product molten iron;
2. adds injected C into bottom segment carbon and enthalpy balance equations of Chapter 7, Conceptual Division of the Blast Furnace - Bottom Segment Calculations; and
3. calculates the bottom segment's;
 - a. C in descending coke requirement, and
 - b. O_2 in blast air requirement

for the steady-state operation of Fig. 8.2 bottom segment.

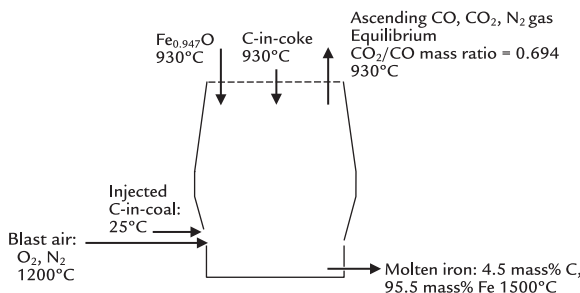


FIGURE 8.2 Bottom blast furnace segment showing C-in-coal injection through the furnace's tuyeres. This sketch is a vertical slice through the center of cylindrical blast furnace of Fig. 1.1.

The carbon injection calculation also calculates the steady state whole furnace C-in-coke-charge requirement, Eq. (7.16).

8.3.1 Injected Carbon Specification

A straight forward C in tuyere-injected carbon quantity specification is:

$$\left[\frac{\text{mass C in tuyere-}}{\text{injected carbon}} \right] = [100 \text{ kg C per } 1000 \text{ kg of Fe in product molten iron}]$$

or in matrix form:

$$100 = \left[\frac{\text{mass C in tuyere-}}{\text{injected carbon}} \right] * 1 \quad (8.1)$$

8.3.2 Bottom Segment Carbon Balance

In its most basic form, our steady-state bottom segment carbon balance is (Fig. 8.2):

$$\begin{aligned} & [\text{mass carbon into bottom segment}] \\ & = [\text{mass carbon out of bottom segment}] \end{aligned} \quad (8.2)$$

With pulverized C injection, this equation expands Eq. (7.4) to;

$$\begin{aligned} & \left[\frac{\text{mass C in tuyere-}}{\text{injected carbon}} \right] * \frac{100\% \text{ C}}{100\%} \\ & + \left[\frac{\text{mass C in}}{\text{descending coke}} \right] * \frac{100\% \text{ C}}{100\%} \\ & = \left[\frac{\text{mass CO out}}{\text{in ascending gas}} \right] * \frac{42.9 \text{ mass\% C in CO}}{100\%} \\ & + \left[\frac{\text{mass CO}_2 \text{ out}}{\text{in ascending gas}} \right] * \frac{27.3 \text{ mass\% C in CO}_2}{100\%} \\ & + \left[\frac{\text{mass C out}}{\text{in molten iron}} \right] * 1 \end{aligned}$$

or

$$\begin{aligned} & \left[\frac{\text{mass C in tuyere-}}{\text{injected carbon}} \right] * 1 + \left[\frac{\text{mass C in}}{\text{descending coke}} \right] * 1 \\ & = \left[\frac{\text{mass CO out}}{\text{in ascending gas}} \right] * 0.429 \\ & + \left[\frac{\text{mass CO}_2 \text{ out}}{\text{in ascending gas}} \right] * 0.273 \\ & + \left[\frac{\text{mass C out}}{\text{in molten iron}} \right] * 1 \\ & \text{or, subtracting } \left\{ \left[\frac{\text{mass C in tuyere-}}{\text{injected carbon}} \right] * 1 \right. \\ & \left. + \left[\frac{\text{mass C in}}{\text{descending coke}} \right] * 1 \right\} \text{ from both sides:} \end{aligned}$$

$$\begin{aligned} 0 &= - \left[\frac{\text{mass C in tuyere-}}{\text{injected carbon}} \right] * 1 \\ &- \left[\frac{\text{mass C in}}{\text{descending coke}} \right] * 1 \\ &+ \left[\frac{\text{mass CO out}}{\text{in ascending gas}} \right] * 0.429 \quad (8.3) \\ &+ \left[\frac{\text{mass CO}_2 \text{ out}}{\text{in ascending gas}} \right] * 0.273 \\ &+ \left[\frac{\text{mass C out}}{\text{in molten iron}} \right] * 1 \end{aligned}$$

The first right side term in Eq. (8.3) is new.

8.3.3 Bottom Segment Enthalpy Balance Equation

With carbon-through-tuyere injection, the bottom segment enthalpy balance Eq. (7.14) becomes;

$$\begin{aligned}
 & H^{\circ} 25^{\circ}\text{C} \\
 & + [\text{mass C in tuyere-injected carbon}] * \frac{C(s)}{MW_C} \\
 & + [\text{mass Fe}_{0.947}\text{O into bottom segment}] * (-3.152) \\
 & + [\text{mass C in descending coke}] * 1.359 \\
 & + [\text{mass O}_2 \text{ in blast air}] * 1.239 \\
 & + [\text{mass N}_2 \text{ in blast air}] * 1.339 \\
 & = [\text{mass Fe out in molten iron}] * 1.269 \\
 & + [\text{mass C out in molten iron}] * 5 \\
 & + [\text{mass CO out in ascending gas}] * (-2.926) \\
 & + [\text{mass CO}_2 \text{ out in ascending gas}] * (-7.926) \\
 & + [\text{mass N}_2 \text{ out in ascending gas}] * 1.008 \\
 & + \left[\begin{array}{l} 320 \text{ MJ bottom segment conductive,} \\ + \text{convective and radiative heat loss per} \\ 1000 \text{ kg of Fe in product molten iron} \end{array} \right] \\
 & \quad \quad \quad (8.4)
 \end{aligned}$$

where the first term in Eq. (8.4) is new.

We now:

$$H^{\circ} 25^{\circ}\text{C}$$

1. assign zero to $\frac{C(s)}{MW_C}$ (element in its most common state at 25°C),
2. subtract the left side of Eq. (8.4) from both sides, and
3. subtract the last term of the right side from both sides

to expand Eq. (7.15) to;

$$\begin{aligned}
 -320 = & -[\text{mass C in tuyere-injected carbon}] * 0.0 \\
 & -[\text{mass Fe}_{0.947}\text{O into bottom segment}] * (-3.152) \\
 & -[\text{mass C in descending coke}] * 1.359 \\
 & -[\text{mass O}_2 \text{ in blast air}] * 1.239 \\
 & -[\text{mass N}_2 \text{ in blast air}] * 1.339 \\
 & + [\text{mass Fe out in molten iron}] * 1.269 \\
 & + [\text{mass C out in molten iron}] * 5 \\
 & + [\text{mass CO out in ascending gas}] * (-2.926) \\
 & + [\text{mass CO}_2 \text{ out in ascending gas}] * (-7.926) \\
 & + [\text{mass N}_2 \text{ out in ascending gas}] * 1.008
 \end{aligned} \quad (8.5)$$

The right side of the top line is new.

8.4 MATRIX WITH C-IN-COAL THROUGH TUYERE INJECTION

We now add this chapter's new and modified equations to matrix Table 7.2 as shown in matrix Table 8.1.

8.5 EFFECT OF PULVERIZED C INJECTION ON DESCENDING C-IN-COKE REQUIREMENT

Fig. 8.3 shows the effect of injected carbon (25°C) on the bottom segment's descending C-in-coke requirement for steady production of molten iron, 1500°C . The points have been calculated by altering the amount of tuyere-injected carbon in cell C12.

8.6 DISCUSSION

Fig. 8.3 indicates that tuyere injection of 1 kg of pulverized carbon saves 0.93 kg of descending bottom segment C-in-coke; hence, 0.93 kg of top-charged C-in-coke all per 1000 kg of Fe in product molten iron.

8.7 COKE REPLACEMENT RATIO

The effectiveness of a tuyere injectant is often represented by the term *coke replacement ratio*, which is defined by the equation:

$$\text{Coke replacement ratio} = \frac{\text{mass coke saved}}{\text{mass substance injected}} \quad (8.6)$$

This chapter specifies that the coke and the injectant are both pure solid carbon, in which case:

Replacement ratio

$$= \frac{\text{mass top charged carbon saved}}{\text{mass pulverized carbon injected}} = 0.93$$

TABLE 8.1 Carbon Injection Bottom Segment Matrix

	A	B	C	D	E	F	G	H	I	J	K	L	M
1 BOTTOM SEGMENT CALCULATIONS													
2	Equation	Description	Numerical term	mass Fe _{0.98} O into bottom segment	mass C in descending coke	mass O ₂ in blast air	mass N ₂ in blast air	mass Fe out in molten iron	mass C out in molten iron	mass CO out in ascending gas	mass CO ₂ out in ascending gas	mass N ₂ out in ascending gas	mass C in tuyere-injected carbon
3	7.7	Fe in output iron specification	1000	0	0	0	0	1	0	0	0	0	0
4	7.2	Fe mass balance	0	-0.768	0	0	0	0	0	0	0	0	0
5	7.3	O mass balance	0	-0.232	0	-1	0	0	0	0.571	0.727	0	0
6	8.3	C mass balance	0	0	-1	0	0	0	1	0.429	0.273	0	-1
7	7.5	N mass balance	0	0	0	0	-1	0	0	0	0	1	0
8	7.6	N ₂ in air specification	0	0	0	3.3	-1	0	0	0	0	0	0
9	7.9	Equilibrium CO ₂ /CO mass ratio	0	0	0	0	0	0	0	0.694	-1	0	0
10	7.8	C out in molten iron specification	0	0	0	0	0	0.047	-1	0	0	0	0
11	8.5	Enthalpy balance	-320	3.152	-1.359	-1.239	-1.339	1.269	5	2.926	-7.926	1.008	0
12	8.1	C in tuyere-injected carbon	100	0	0	0	0	0	0	0	0	0	1
13													
14			930°C	930°C	1200°C	1200°C	1500°C	1500°C	930°C	930°C	930°C	930°C	25°C
15													
16													
17	Calculated values		kg per 1000 kg of Fe in product molten iron										
18	mass Fe _{0.98} O into bottom segment		1302										
19	mass C in descending coke		299	also = mass C in the furnace's coke charge, Eqn (7.16)									
20	mass O ₂ in blast air		310										
21	mass N ₂ in blast air		1024										
22	mass Fe out in molten iron		1000										
23	mass C out in molten iron		47										
24	mass CO out in ascending gas		569										
25	mass CO ₂ out in ascending gas		395										
26	mass N ₂ out in ascending gas		1024										
27	mass C in tuyere-injected carbon		100										
28													

Eq. (8.1) shows that 100 kg of carbon are being injected per 1000 kg of Fe in product molten iron. Note also modified carbon and enthalpy balance Eqs. (8.3) and (8.5). This matrix has one more variable, *mass C in tuyere-injected carbon*, and one more Eq. (8.1) than matrix Table 7.2.

8.7.1 Replacement Ratio Explanation

The 0.93 replacement ratio is the result of all the matrix [Table 8.1](#) equations. We may speculate that it is mostly due to the injectant's low temperature.

The injected C enters the furnace's bottom segment at 25°C, [Fig. 8.2](#). Descending C-in-coke enters the bottom segment at 930°C. So, the injected C brings less enthalpy into the bottom segment than the descending C(s), per kg. This must be offset by combusting more carbon in the bottom segment. Confirmation of this argument is obtained by specifying that the injected C temperature is the same as the descending C temperature, that is, 930°C. This is easily done by inserting the 930°C carbon enthalpy into cell M11 of [Table 8.1](#) [with a negative sign as shown by Eq. (8.5)]. The value is -1.359 , from cell E11.

As expected, the replacement ratio with 930°C carbon injection is 1.

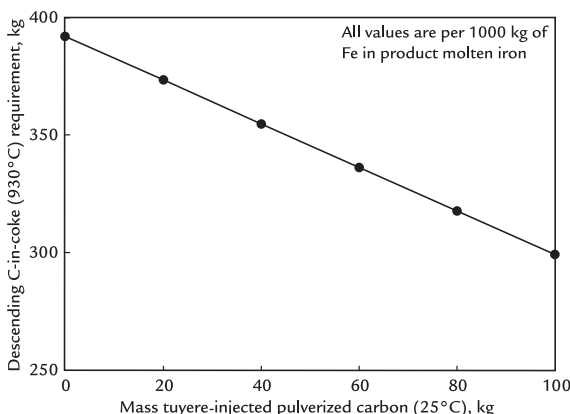


FIGURE 8.3 Effect of tuyere-injected carbon on steady-state bottom segment C-in-coke requirement. The line is straight. Injection of 1 kg of pulverized carbon lowers the bottom segment's C-in-coke requirement by 0.93 kg. By Eq. (7.16), it also lowers the whole furnace C-in-coke requirement by the same amount. For future reference, the C-in-coke requirement with 60 kg of C injection is 336 kg/1000 kg of Fe in product molten iron.

8.8 TOTAL CARBON REQUIREMENT

[Fig. 8.4](#) shows the total amount of carbon entering the blast furnace as a function tuyere-injected carbon quantity. It increases slightly with increasing injected carbon mass because it takes $(1/0.93) = 1.077$ kg of injected C to save 1 kg of top-charged carbon, [Section 8.7](#).

8.9 BLAST AIR O₂ AND N₂ REQUIREMENTS

[Figs. 8.5 and 8.6](#) show blast furnace O₂-in-blast air and N₂-in-blast air requirements as a function of mass of tuyere-injected carbon. Both increase slightly. This is because extra air must be supplied to combust extra carbon of [Fig. 8.4](#).

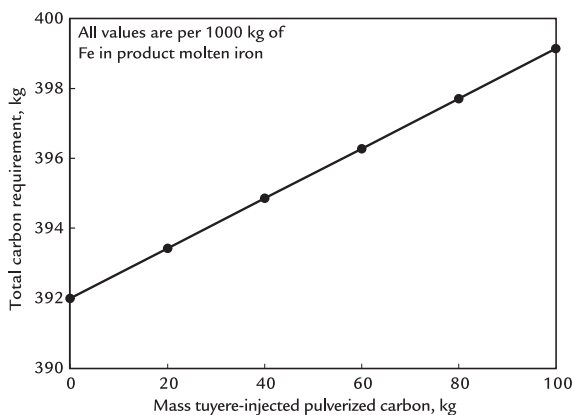


FIGURE 8.4 Total blast furnace carbon requirement as a function of tuyere-injected carbon quantity. This is obtained by adding cells C19 and C27, [Table 8.1](#). Total carbon increases slightly with increasing mass of injected carbon (25°C) because 1 kg of injected carbon saves only 0.93 kg of top-charged carbon-in-coke. The line is straight.

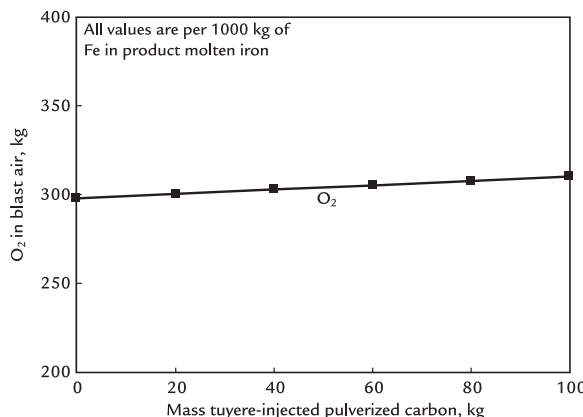


FIGURE 8.5 O₂-in-blast air requirement as a function of mass tuyere-injected carbon. O₂ requirement increases with increasing tuyere-injected carbon because combustion of extra carbon of Fig. 8.4 requires extra blast air. The line is straight. For future reference, the O₂ requirement with 60 kg of C-in-coal injection is 305 kg, both per 1000 kg of Fe in product molten iron.

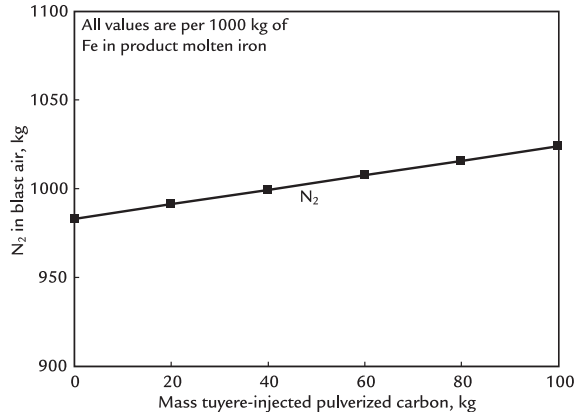


FIGURE 8.6 Effect of tuyere-injected carbon on steady-state mass N₂ in blast air. The slope is 3.3 × O₂ slope of Fig. 8.5. This is due to air's mass N₂/mass O₂ ratio = 3.3.

The calculations show that steady-state blast furnace operation is maintained by lowering the top-charged carbon input by 0.93 kg for each kg of tuyere-injected C. This would be profitable if, for example, pulverized carbon was half the price of carbon in coke.

There is a lower limit on the amount of coke that can be replaced. This is because coke is required to (1) support the blast furnace charge burden, and (2) provide space for gas to ascend and molten iron and slag to descend within the blast furnace reactor.

The current chapter speculates as to why the top-charged C saving is only 93% of the injected C quantity. However, there is no need to speculate - the answer is in the matrix!

8.10 SUMMARY

All iron blast furnaces inject hydrocarbons through their tuyeres. The principle objective is to replace expensive top-charged C-in-coke with inexpensive tuyere-injected hydrocarbons. This chapter examines hydrocarbon injection in its simplest form—pulverized pure carbon injection.

It uses the bottom segment matrix of Chapter 7, Conceptual Division of the Blast Furnace - Bottom Segment Calculations, modified to include;

1. an injected carbon quantity equation, and
2. modified carbon and enthalpy balance equations.

It also uses Eq. (7.16)

$$\begin{bmatrix} \text{whole furnace} \\ \text{C-in-coke charge} \end{bmatrix} = \begin{bmatrix} \text{C-in-coke} \\ \text{descending into} \\ \text{the bottom segment} \end{bmatrix} \quad (7.16)$$

from Section 7.12.

EXERCISES

Please remember that tuyere-injected pulverized carbon is a simplified stand-in for tuyere-injected pulverized coal. Please also remember that 100% C coke is a simplified stand-in for real coke, which contains many other elements, including hydrogen.

- 8.1. Why do blast furnace operators inject pulverized coal through their tuyeres?
- 8.2. Why don't these operators replace all their coke with tuyere-injected coal?
- 8.3. What would happen to replacement ratio of [Section 8.7](#) if a way could be found to safely heat the injected carbon to 1000°C before injection?
- 8.4. [Table 8.1](#) blast furnace company has purchased a large quantity of cheap coal. It would now like to inject 120 kg of coal (assume pure carbon) per 1000 kg of Fe in product molten iron.
What amount of coke (assume pure carbon) would be saved by making this change?
- 8.5. Carbon in pulverized coal is much cheaper than carbon in top-charged coke - because coke is extensively processed coal. Recognizing this, you want to maximize coal injection. However, you know that the [Table 8.1](#) blast furnace needs at least 250 kg of top-charged coke (assume pure

carbon) to provide support for the furnace charge and for even distribution of upward gas flow.

How much tuyere-injected coal (assume pure carbon) can be injected into the furnace before it decreases the steady-state coke (assume pure carbon) requirement below 250 kg, all per 1000 kg of Fe in product molten iron.

Answer any way you like. Perhaps by two different methods. Perhaps using Excel's Goal Seek tool.

References

1. Schott R. State-of-the-art PCI technology for blast furnace ensured by continuous technological and economical improvement. In: *AISTech 2012 Proceedings*. Atlanta, GA:589–604.
2. Paramanathan BK, Engel E. Pulverized coal injection optimizing the blast furnace process. In: *6th International Conference on the Science and Technology of Ironmaking (ICSTI)*. Rio de Janeiro, Brazil; 2012:2455–2463. ISSN 2176-3135.

Bottom Segment With Oxygen Enrichment of Blast Air

O U T L I N E

9.1 Benefits of Injecting Pure Oxygen With the Blast Air	93	9.3 Calculation Results	95
9.2 Oxygen Injection Calculations	94	9.4 Carbon Requirement	97
9.2.1 Injected Oxygen Quantity	94	9.5 Summary	98
9.2.2 Injected O ₂ in the Oxygen Mass Balance	94	Exercises	98
9.2.3 Enthalpy Balance With Injected Pure Oxygen	95		

9.1 BENEFITS OF INJECTING PURE OXYGEN WITH THE BLAST AIR

Many iron blast furnaces inject purified oxygen into their unheated blast air. The air–oxygen mixture is then;

- heated to $\sim 1200^{\circ}\text{C}$, and
- blown through the blast furnace tuyeres (Fig. 9.1).

Oxygen injection lowers the amount of nitrogen that is blown:

- through the tuyeres, and
- up the furnace shaft.

The principle objectives of oxygen injection are to:

1. increase molten iron production without increasing gas flow rate, and

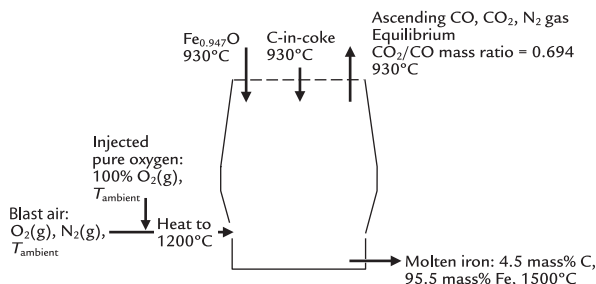


FIGURE 9.1 Bottom segment with heated (air + oxygen) blast, 1200°C . Pure oxygen is injected into unheated air. The mixture is then heated and blown into the blast furnace through its tuyeres. The drawing is a vertical slice through the center of the cylindrical furnace, Fig. 1.1. Modern blast furnaces inject up to 100 kg of purified oxygen per 1000 kg of Fe in product molten iron.

- offset the cooling effect of hydrocarbon injectants (Chapter 11: Bottom Segment with $\text{CH}_4(g)$ Injection) in the furnace bottom segment.

Objective (2) is a benefit that results from having to heat less nitrogen.

The objectives of this chapter are to:

- show how oxygen injection is included in our matrix calculations;
- indicate how oxygen injection affects the upward blast furnace gas flows;
- calculate steady-state bottom segment, and hence whole furnace, O_2 -in-blast air requirements with various amounts of injected oxygen;
- calculate steady-state bottom segment C-in-coke requirements with various amounts of injected oxygen; and
- calculate steady state whole-furnace C-in-coke charge requirements with various amounts of injected oxygen.

9.2 OXYGEN INJECTION CALCULATIONS

Oxygen injection calculations are like carbon injection calculations. They require:

- a new oxygen quantity specification,
- a modified steady-state oxygen balance, and
- a modified steady-state enthalpy balance.

9.2.1 Injected Oxygen Quantity

An example of oxygen quantity specification is:

$$\left[\frac{\text{mass } O_2 \text{ in injected}}{\text{pure oxygen}} \right] = \left[\frac{30 \text{ kg per 1000 kg of Fe}}{\text{in product molten iron}} \right]$$

or, in matrix form,

$$30 = \left[\frac{\text{mass } O_2 \text{ in injected}}{\text{pure oxygen}} \right] * 1 \quad (9.1)$$

9.2.2 Injected O_2 in the Oxygen Mass Balance

From Eq. (7.3), the bottom segment oxygen balance *including injected oxygen* is:

$$\begin{aligned} & \left[\frac{\text{mass } O_2 \text{ in injected}}{\text{pure oxygen}} \right] * \frac{100\% \text{ O in } O_2}{100\%} \\ & + \left[\frac{\text{mass } Fe_{0.947}O \text{ into}}{\text{bottom segment}} \right] * \frac{23.2 \text{ mass\% O in } Fe_{0.947}O}{100\%} \\ & + \left[\frac{\text{mass } O_2 \text{ in}}{\text{blast air}} \right] * \frac{100\% \text{ O in } O_2}{100\%} \\ & = \left[\frac{\text{mass } CO \text{ out}}{\text{in ascending gas}} \right] * \frac{57.1 \text{ mass\% O in } CO}{100\%} \\ & + \left[\frac{\text{mass } CO_2 \text{ out}}{\text{in ascending gas}} \right] * \frac{72.7 \text{ mass\% O in } CO_2}{100\%} \end{aligned}$$

or

$$\begin{aligned} & \left[\frac{\text{mass } O_2 \text{ in injected}}{\text{pure oxygen}} \right] * 1 + \left[\frac{\text{mass } Fe_{0.947}O \text{ into}}{\text{bottom segment}} \right] \\ & * 0.232 + \left[\frac{\text{mass } O_2 \text{ in}}{\text{blast air}} \right] * 1 = \left[\frac{\text{mass } CO \text{ out}}{\text{in ascending gas}} \right] \\ & * 0.571 + \left[\frac{\text{mass } CO_2 \text{ out}}{\text{in ascending gas}} \right] * 0.727 \end{aligned}$$

or subtracting $\left\{ \begin{array}{l} \text{mass O}_2 \text{ in injected} \\ \text{pure oxygen} \end{array} \right\} * 1 + \left[\begin{array}{l} \text{mass Fe}_{0.947}\text{O into} \\ \text{bottom segment} \end{array} \right] * 0.232 + \left[\begin{array}{l} \text{mass O}_2 \text{ in} \\ \text{blast air} \end{array} \right] * 1 \}$ from both sides:

$$0 = - \left[\begin{array}{l} \text{mass O}_2 \text{ in injected} \\ \text{pure oxygen} \end{array} \right] * 1 - \left[\begin{array}{l} \text{mass Fe}_{0.947}\text{O into} \\ \text{bottom segment} \end{array} \right] * 0.232 - \left[\begin{array}{l} \text{mass O}_2 \text{ in} \\ \text{blast air} \end{array} \right] * 1 + \left[\begin{array}{l} \text{mass CO out} \\ \text{in ascending gas} \end{array} \right] * 0.232 - \left[\begin{array}{l} \text{mass CO}_2 \text{ out} \\ \text{in ascending gas} \end{array} \right] * 0.571 + \left[\begin{array}{l} \text{mass N}_2 \text{ out} \\ \text{in ascending gas} \end{array} \right] * 0.727 \quad (9.2)$$

9.2.3 Enthalpy Balance With Injected Pure Oxygen

Including injected O_2 , the bottom segment enthalpy balance Eq. (7.14) becomes:

$$\begin{aligned} & [\text{mass O}_2 \text{ in injected pure oxygen}] * 1.239 \\ & + [\text{mass Fe}_{0.947}\text{O into bottom segment}] * (-3.152) \\ & + [\text{mass C in descending coke}] * 1.359 \\ & + [\text{mass O}_2 \text{ in blast air}] * 1.239 \\ & + [\text{mass N}_2 \text{ in blast air}] * 1.339 \\ & = [\text{mass Fe out in molten iron}] * 1.269 \\ & \quad + [\text{mass C out in molten iron}] * 5 \\ & \quad + [\text{mass CO out in ascending gas}] * (-2.926) \\ & \quad + [\text{mass CO}_2 \text{ out in ascending gas}] * (-7.926) \\ & \quad + [\text{mass N}_2 \text{ out in ascending gas}] * 1.008 \\ & \quad + \left[\begin{array}{l} 320 \text{ MJ bottom segment conductive,} \\ \text{convective and radiative heat loss per} \\ 1000 \text{ kg of Fe in product molten iron} \end{array} \right] \end{aligned} \quad (9.3)$$

where 1.239 is $H^\circ_{1200^\circ\text{C}} / \text{MW}_{\text{O}_2}$.

Subtracting the left side of Eq. (9.3) and the last term of the right side of Eq. (9.3) from both sides and rearranging:

$$\begin{aligned} & -320 = - [\text{mass O}_2 \text{ in injected pure oxygen}] * 1.239 \\ & - [\text{mass Fe}_{0.947}\text{O into bottom segment}] * (-3.152) \\ & - [\text{mass C in descending coke}] * 1.359 \\ & - [\text{mass O}_2 \text{ in blast air}] * 1.239 \\ & - [\text{mass N}_2 \text{ in blast air}] * 1.339 \\ & + [\text{mass Fe out in molten iron}] * 1.269 \\ & + [\text{mass C out in molten iron}] * 5 \\ & + [\text{mass CO gas out in ascending gas}] * (-2.926) \\ & + [\text{mass CO}_2 \text{ out in ascending gas}] * (-7.926) \\ & + [\text{mass N}_2 \text{ out in ascending gas}] * 1.008 \end{aligned} \quad (9.4)$$

The enthalpy values are for the temperatures in Fig. 9.1. Note that the injected oxygen is heated to 1200°C before it enters the furnace. It has the same enthalpy content (per kg) as the O_2 in blast air.

Eqs. (9.1), (9.2), and (9.4) plus our unchanged bottom segment equations are shown in matrix Table 9.1.

9.3 CALCULATION RESULTS

Fig. 9.2 shows the effect of pure oxygen injection on the,

- amount of blast air

that is required to produce molten iron, 1500°C .

As expected, the blast air requirement decreases appreciably with increasing pure oxygen injection. This decrease in input blast air also markedly decreases N_2 flow through the furnace (Fig. 9.3).

It is this decrease in N_2 flow that enables pure oxygen to;

- increase molten iron production rate without
- increasing the amount of gas that flows up the blast furnace shaft.

TABLE 9.1 Bottom Segment Pure Oxygen Injection Matrix

A	B	C	D	E	F	G	H	I	J	K	L	M	
1 BOTTOM SEGMENT CALCULATIONS													
Z	Equation	Description	Numerical term	mass Fe _{0.84} O into bottom segment	mass C in descending coke	mass O ₂ in blast air	mass N ₂ in blast air	mass Fe out in molten iron	mass C out in molten iron	mass CO out in ascending gas	mass CO ₂ out in ascending gas	mass N ₂ out in ascending gas	mass O ₂ in injected pure oxygen
3	7.7	Fe in output iron specification	1000	0	0	0	0	1	0	0	0	0	0
4	7.2	Fe mass balance	0	-0.768	0	0	0	1	0	0	0	0	0
5	9.2	O mass balance	0	-0.232	0	-1	0	0	0	0.571	0.727	0	-1
6	7.4	C mass balance	0	0	-1	0	0	1	0.429	0.273	0	0	0
7	7.5	N mass balance	0	0	0	0	-1	0	0	0	0	1	0
8	7.6	N ₂ in blast air specification	0	0	0	3.3	-1	0	0	0	0	0	0
9	7.9	Equilibrium CO ₂ /CO mass ratio	0	0	0	0	0	0	0	0.694	-1	0	0
10	7.8	C in output iron specification	0	0	0	0	0	0.047	-1	0	0	0	0
11	9.4	Enthalpy balance	-320	3.152	-1.359	-1.239	-1.339	1.269	5	2.926	-7.926	1.008	-1.239
12	9.1	Mass O ₂ in injected pure oxygen	30	0	0	0	0	0	0	0	0	0	1
13													
14				930°C	930°C	1200°C	1200°C	1500°C	1500°C	930°C	930°C	930°C	1200°C
15													
16													
17		Calculated values	kg per 1000 kg of Fe in product iron										
18		mass Fe _{0.84} O into bottom segment	1302										
19		mass C in descending coke	394	also = mass C in the furnace's coke charge; Eqn (7.16)									
20		mass O ₂ in blast air	271										
21		mass N ₂ in blast air	894										
22		mass Fe out in molten iron	1000										
23		mass C out in molten iron	47										
24		mass CO out in ascending gas	561										
25		mass CO ₂ out in ascending gas	389										
26		mass N ₂ out in ascending gas	894										
27		mass O ₂ in injected pure oxygen	30										
28													

The new O₂ injection quantity specification and altered oxygen balance/enthalpy balance equations are shown. Steady-state reactant and product quantities at other oxygen injection levels are determined by putting various values in cell C12. Try it!

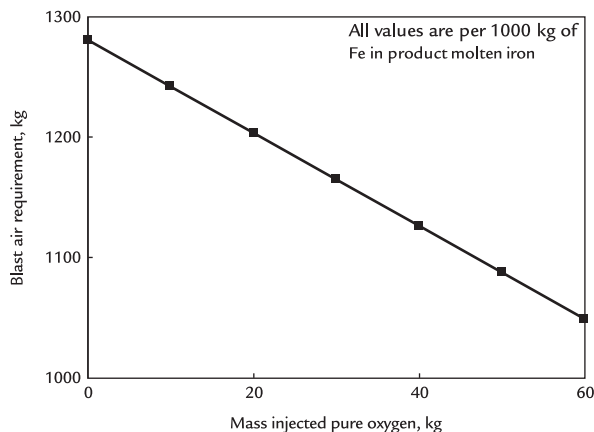


FIGURE 9.2 Effect of pure oxygen in blast on blast furnace blast air requirement. The line is straight. The points have been calculated by altering mass O_2 in injected oxygen, cell C12. Injected oxygen lowers blast air requirement by 3.9 kg of blast air per kg of injected pure oxygen.

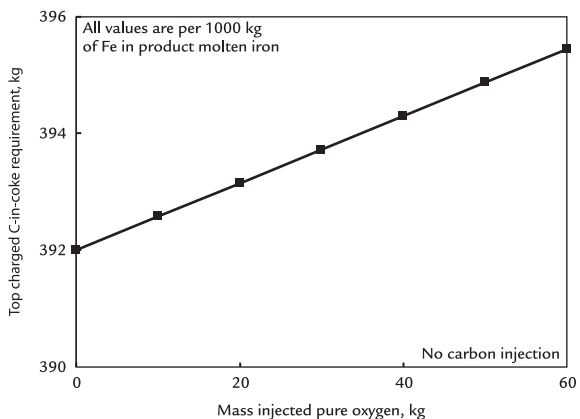


FIGURE 9.4 Effect of pure oxygen in blast on steady-state whole-furnace C-in-coke requirement. Whole-furnace C-in-coke requirement increases by about 0.06 kg C per kg of added pure oxygen.

9.4 CARBON REQUIREMENT

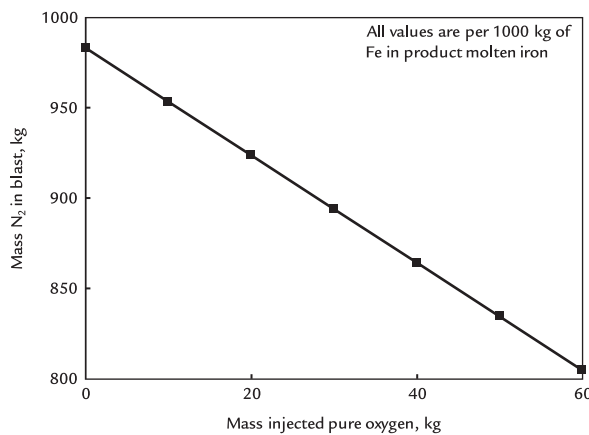


FIGURE 9.3 Effect of pure oxygen injection on the amount of N₂ entering the furnace in blast air. All N₂ flows up the blast furnace shaft and out in top-gas (i.e., it doesn't react in the furnace). Adding 1 kg of pure oxygen into the furnace reduces nitrogen flow by ~ 3 kg, both per 1000 kg of Fe in product molten iron. The line is straight.

Fig. 9.4 shows the effect of pure oxygen injection on the whole-furnace C-in-coke requirement. This is the same as matrix Table 9.1's bottom segment mass C in descending coke requirement (Eq. (7.16)).

Carbon requirements in top-charged coke increase slightly with increasing amount of pure oxygen injected. This is the result of all of Table 9.1's equations.

We may speculate, however, that the smaller amount of N₂ entering the blast furnace with oxygen injection;

1. brings less enthalpy into the bottom segment (per 1000 kg of Fe in product molten iron) which consequently,
2. requires more bottom segment carbon combustion to maintain the 930°C bottom segment exit gas temperature.

This is confirmed by an equivalent slight increase in total O₂-in-blast requirement (Fig. 9.5).

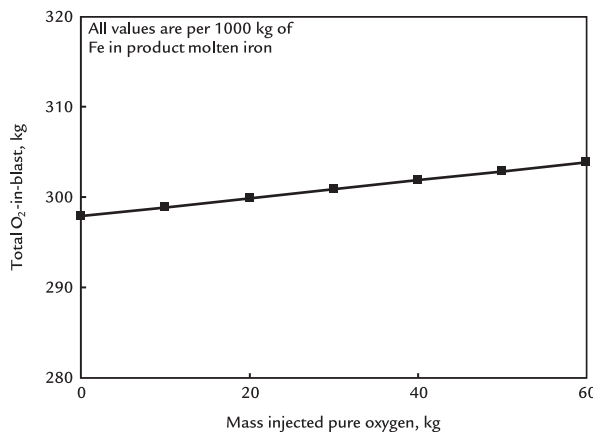


FIGURE 9.5 Effect of pure oxygen injection on steady-state total O₂-in-blast requirement. The total oxygen requirement increases by about 0.1 kg/kg of injected pure oxygen, both per 1000 kg of Fe in product molten iron. The line is straight.

9.5 SUMMARY

Purified oxygen is provided to the blast furnace by:

1. injecting pure oxygen into the blast air,
2. heating the air–oxygen mixture to about 1200°C in the stove shown in Fig. 1.2, and
3. blowing the heated mixture through all the blast furnace tuyeres.

Oxygen injection is readily represented in our blast furnace matrices. It requires a new mass O₂ in injected oxygen specification and modified steady-state oxygen and enthalpy balance equations.

Pure oxygen addition *decreases* nitrogen flows up the blast furnace, per 1000 kg of Fe in product molten iron. Purified oxygen injection can, therefore, give faster iron production without increasing the upward gas flow rate.

As Chapter 17, Raceway Flame Temperature with Oxygen Enrichment, shows, pure oxygen enrichment also increases tuyere raceway flame temperature and/or offsets the cooling effects of low enthalpy hydrocarbon tuyere injectants. These are both useful for steady production of 1500°C molten iron.

Chapter 8, Bottom Segment with Pulverized Carbon Injection, and this chapter have examined carbon and purified oxygen injection. Our next task is to examine injection of less purified oxygen, 90 mass% O₂(g) and 10 mass% N₂(g).

EXERCISES

- 9.1. What are the two (maybe three) advantages of injecting pure oxygen into a blast furnace's blast air ([Fig. 9.1](#))?
- 9.2. Are there any costs for this injection?
- 9.3. Are there any safety issues with handling of large amounts of pure oxygen?
- 9.4. The [Table 9.1](#) blast furnace operators increased their oxygen injection quantity specification to 65 kg per 1000 of Fe in product molten iron. By how much does this change its C-in-coke requirement and blast air requirement for steady production of 1500°C molten iron.
We suggest that you first predict the direction of these changes (increase, decrease) then calculate them. Please express your answers in kg per 1000 kg of Fe in product molten iron.
- 9.5. Blast furnace management believes that the amount of N₂ entering and leaving their blast furnace should be less than 700 kg per 1000 kg of Fe in product molten iron. More N₂ than this tends to cause

fluidization of the furnace's top-charged solids. Predict for them the minimum amount of injected pure oxygen (per 1000 kg of Fe in product molten iron) that will be needed to obtain this amount of N₂ input/output.

- 9.6.** What effect will blast temperature have on C-in-coke and blast air requirements

for steady-state production of 1500°C molten iron? Predict your answers (qualitatively) then calculate the results with 1150°C blast. Use Appendix J for the required enthalpy equations.

Please express your answers in kg per 1000 kg of Fe in product molten iron.

10

Bottom Segment With Low Purity Oxygen Enrichment

O U T L I N E

10.1 The Benefits of Using Impure Oxygen	101	10.6 Nitrogen Balance	104
10.2 Required Changes to Matrix	102	10.7 Enthalpy Balance	104
10.3 Specified Mass O ₂ in Injected Impure Oxygen	102	10.8 Results	104
10.4 Slightly Changed Oxygen Balance Equation	102	10.9 Summary	105
10.5 Mass N ₂ in Injected Impure Oxygen	104	Exercise	105

10.1 THE BENEFITS OF USING IMPURE OXYGEN

Some blast furnace operators buy less purified oxygen for their blast furnaces—because it is cheaper and the small amount of nitrogen is not detrimental to the ironmaking process. In steelmaking, nitrogen can dissolve in the liquid steel and cause steel quality problems.

The impure oxygen contains up to 10 mass% N₂, remainder O₂.

The objectives of this chapter are to:

1. show how impure oxygen is included in our bottom segment matrix (Fig. 10.1), and
2. indicate the effects of the nitrogen impurity on the furnace's C-in-coke and O₂-in-blast air requirements for steady production of 1500°C molten iron (Fig. 10.2).

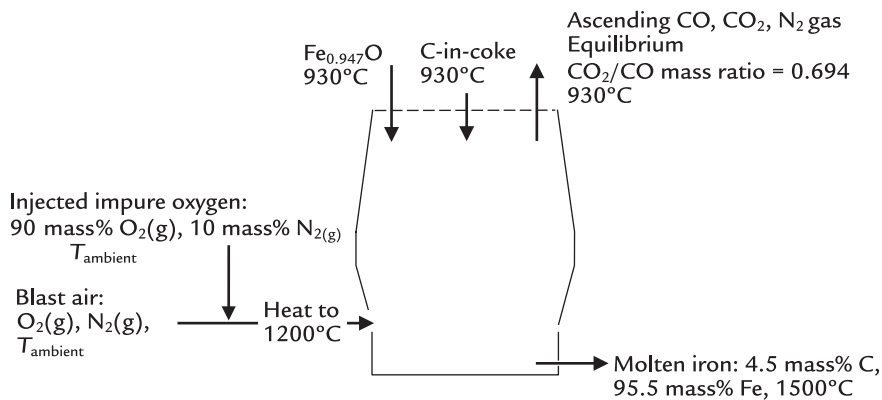


FIGURE 10.1 Conceptual blast furnace bottom segment with impure oxygen injection. The impure oxygen is injected into unheated air after the turbo blower. The mixture is then heated and blown into the furnace through all its tuyeres. The drawing is a vertical slice through the center of a cylindrical bottom segment (Fig. 1.1).

10.2 REQUIRED CHANGES TO MATRIX (TABLE 9.1)

Calculations with impure oxygen require:

1. a N_2 -in-impure-oxygen quantity specification,
2. inclusion of this N_2 in our bottom segment steady-state nitrogen mass balance, and
3. inclusion of this N_2 in our bottom segment steady-state enthalpy balance.

We also change the variable:

$$\left[\begin{array}{c} \text{mass O}_2 \text{ in injected} \\ \text{impure oxygen} \end{array} \right] \text{ to } \left[\begin{array}{c} \text{mass O}_2 \text{ in injected} \\ \text{impure oxygen} \end{array} \right]$$

as shown in matrix (Table 10.1).

10.3 SPECIFIED MASS O₂ IN INJECTED IMPURE OXYGEN

Mass O₂ in injected impure oxygen is specified by

$$\left[\begin{array}{c} \text{mass O}_2 \text{ in injected} \\ \text{impure oxygen} \end{array} \right] = [30 \text{ kg per 1000 kg of Fe in product molten iron}]$$

or, in matrix form:

$$30 = \left[\begin{array}{c} \text{mass O}_2 \text{ in injected} \\ \text{impure oxygen} \end{array} \right] * 1 \quad (10.1)$$

10.4 SLIGHTLY CHANGED OXYGEN BALANCE EQUATION

The new $\left[\begin{array}{c} \text{mass O}_2 \text{ in injected} \\ \text{impure oxygen} \end{array} \right]$ variable also slightly changes bottom segment oxygen balance Eq. (9.2) to:

$$0 = - \left[\begin{array}{c} \text{mass O}_2 \text{ in injected} \\ \text{impure oxygen} \end{array} \right] * 1 - \left[\begin{array}{c} \text{mass Fe}_{0.947}\text{O into} \\ \text{bottom segment} \end{array} \right] * 0.232 - \left[\begin{array}{c} \text{mass O}_2 \text{ in} \\ \text{blast air} \end{array} \right] * 1 + \left[\begin{array}{c} \text{mass CO out} \\ \text{in ascending gas} \end{array} \right] * 0.571 + \left[\begin{array}{c} \text{mass CO}_2 \text{ out} \\ \text{in ascending gas} \end{array} \right] * 0.727 \quad (10.2)$$

TABLE 10.1 Conceptual Bottom Segment Calculation Matrix With Injection of Impure Oxygen, 90 Mass% O₂(g) + 10 Mass% N₂(g)

	A	B	C	D	E	F	G	H	I	J	K	L	M	N
1 BOTTOM SEGMENT CALCULATIONS														
2	Equation	Description	Numerical term	mass Fe _{0.95} O into bottom segment	mass C in descending coke	mass O ₂ in blast air	mass N ₂ in blast air	mass Fe out in molten iron	mass C out in molten iron	mass CO out in ascending gas	mass CO ₂ out in ascending gas	mass N ₂ out in ascending gas	mass O ₂ in injected impure oxygen	mass N ₂ in injected impure oxygen
3	7.7	Fe in output iron specification	1000	0	0	0	0	1	0	0	0	0	0	0
4	7.2	Fe mass balance	0	-0.768	0	0	0	1	0	0	0	0	0	0
5	10.2	O mass balance	0	-0.232	0	-1	0	0	0	0.571	0.727	0	-1	0
6	7.4	C mass balance	0	0	-1	0	0	0	1	0.429	0.273	0	0	0
7	10.4	N mass balance	0	0	0	0	-1	0	0	0	0	1	0	-1
8	7.6	N ₂ in blast air specification	0	0	0	3.3	-1	0	0	0	0	0	0	0
9	7.9	Equilibrium CO ₂ /CO mass ratio	0	0	0	0	0	0	0	0.694	-1	0	0	0
10	7.8	C in output iron specification	0	0	0	0	0	0.047	-1	0	0	0	0	0
11	10.5	Enthalpy balance	-320	3.152	-1.359	-1.239	-1.339	1.269	5	-2.926	-7.926	1.008	-1.239	-1.339
12	10.1	Mass O ₂ in injected impure oxygen	30	0	0	0	0	0	0	0	0	0	1	0
13	10.3	Mass N ₂ in injected impure oxygen	0	0	0	0	0	0	0	0	0	0	0.111	-1
14														
15			930°C	930°C	1200°C	1200°C	1500°C	1500°C	930°C	930°C	930°C	930°C	1200°C	1200°C
16														
17		Calculated values	kg per 1000 kg of Fe in product iron											
18		mass Fe _{0.95} O into bottom segment	1302											
19		mass C in descending coke	394	also = mass C in the furnace's coke charge, Eqn (7.16)										
20		mass O ₂ in blast air	271											
21		mass N ₂ in blast air	894											
22		mass Fe out in molten iron	1000											
23		mass C out in molten iron	47											
24		mass CO out in ascending gas	561											
25		mass CO ₂ out in ascending gas	389											
26		mass N ₂ out in ascending gas	897											
27		mass O ₂ in injected impure oxygen	30											
28		mass N ₂ in injected impure oxygen	3.3											
29														

Eqs. (10.1)–(10.5) are new. The steady-state amount of N₂ entering the blast furnace in impure oxygen (3.3 kg, cell C28) is much smaller than the amount of N₂ entering in blast air (894 kg, cell C21). Note, these nitrogen inputs add to 897 kg (cell C26) in ascending bottom segment output gas.

10.5 MASS N₂ IN INJECTED IMPURE OXYGEN

For this discussion, we specify that the impure oxygen contains 90 mass% O₂ and 10 mass% N₂. 100 kg of this impure oxygen contains 90 kg of O₂ and 10 kg N₂. Its mass N₂/mass O₂ ratio is 10/90 = 0.111 stated as

$$\frac{\text{mass N}_2 \text{ in injected impure oxygen}}{\text{mass O}_2 \text{ in injected impure oxygen}} = 0.111$$

or

$$\begin{aligned} & \left[\frac{\text{mass N}_2 \text{ in injected}}{\text{impure oxygen}} \right] * 1 \\ &= \left[\frac{\text{mass O}_2 \text{ in injected}}{\text{impure oxygen}} \right] * 0.111 \end{aligned}$$

or subtracting $\left\{ \left[\frac{\text{mass N}_2 \text{ in injected}}{\text{impure oxygen}} \right] * 1 \right\}$ from both sides:

$$\begin{aligned} 0 &= - \left[\frac{\text{mass N}_2 \text{ in injected}}{\text{impure oxygen}} \right] * 1 \\ &+ \left[\frac{\text{mass O}_2 \text{ in injected}}{\text{impure oxygen}} \right] * 0.111 \end{aligned} \quad (10.3)$$

10.6 NITROGEN BALANCE

The addition of N₂ to the furnace in injected impure oxygen requires an additional variable in the nitrogen balance, Eq. (7.5):

$$\left[\frac{\text{mass N}_2 \text{ in injected}}{\text{impure oxygen}} \right] * 1$$

With this term, nitrogen balance Eq. (7.5) becomes:

$$\begin{aligned} 0 &= - \left[\frac{\text{mass N}_2 \text{ in injected}}{\text{impure oxygen}} \right] * 1 - \left[\frac{\text{mass N}_2 \text{ in}}{\text{blast air}} \right] * 1 \\ &+ \left[\frac{\text{mass N}_2 \text{ out}}{\text{in ascending gas}} \right] * 1 \end{aligned} \quad (10.4)$$

10.7 ENTHALPY BALANCE

N₂(g) in impure oxygen also requires inclusion of $\left[\frac{\text{mass N}_2 \text{ in injected}}{\text{impure oxygen}} \right]$ in the enthalpy, balance, Eq. (9.4). With this change enthalpy, Eq. (9.4) becomes:

$$\begin{aligned} -320 &= -[\text{mass O}_2 \text{ in injected impure oxygen}] * 1.239 \\ &- [\text{mass N}_2 \text{ in injected impure oxygen}] * 1.339 \\ &- [\text{mass FeO}_{0.947} \text{ O into bottom segment}] * (-3.152) \\ &- [\text{mass C in descending coke}] * 1.359 \\ &- [\text{mass O}_2 \text{ in blast air}] * 1.239 \\ &- [\text{mass N}_2 \text{ in blast air}] * 1.339 \\ &+ [\text{mass Fe out in molten iron}] * 1.269 \\ &+ [\text{mass C out in molten iron}] * 5 \\ &+ [\text{mass CO gas out in ascending gas}] * (-2.926) \\ &+ [\text{mass CO}_2 \text{ out in ascending gas}] * (-7.926) \\ &+ [\text{mass N}_2 \text{ out in ascending gas}] * 1.008 \end{aligned} \quad (10.5)$$

The enthalpy values are for the temperatures in Fig. 10.1. Note that the injected impure oxygen enters the furnace at 1200°C. This is indicated by the same O₂ and N₂ enthalpies (per kg) in injected impure oxygen and in blast air.

Eqs. (10.1)–(10.5) plus our unchanged bottom segment equations are shown in matrix Table 10.1.

10.8 RESULTS

Table 10.1 indicates that injection of 30 kg of O₂ in impure (90 mass% O₂, 10 mass% N₂) oxygen requires;

- 394 kg of C-in-coke, and
- 271 kg of O₂-in-blast air

for steady production of 1500°C molten iron.

These are virtually the same as with 30 kg of pure oxygen injection (Fig. 10.2).

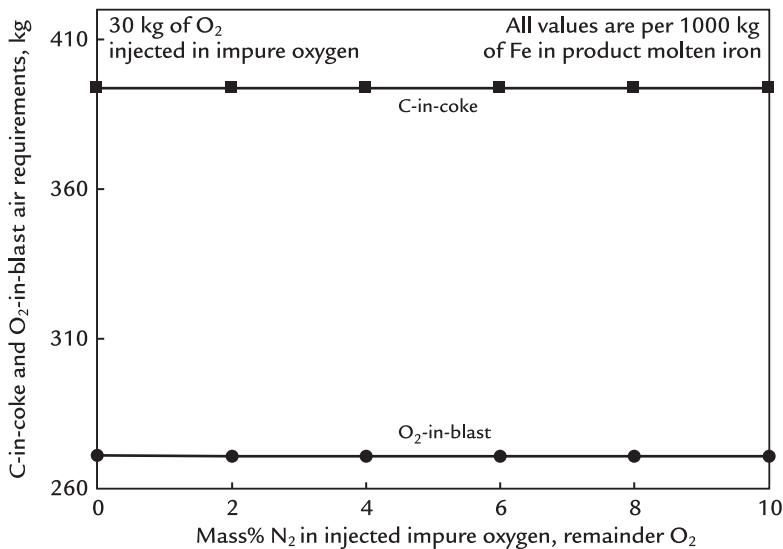


FIGURE 10.2 Steady-state C-in-coke and O₂-in-blast air requirements with injection of 30 kg of O₂ in impure oxygen. The N₂ impurity has virtually no effect. This is because the impure 90 mass% O₂–10% mass% N₂ supplies only 3.3 kg of N₂ as compared to 894 kg of N₂ in blast air (Table 10.1).

10.9 SUMMARY

N₂ in injected impure oxygen is readily incorporated into our matrix calculations. Nitrogen in impure oxygen has very little effect on the amount of C-in-coke and O₂-in-blast air that is needed for steady production of 1500°C molten iron. This is because the quantity of N₂ in impure oxygen injectant is tiny as compared to the quantity of N₂ in the accompanying blast air (Table 10.1).

EXERCISE

- 10.1 A blast furnace's accounting department has found a very cheap source of oxygen.

But the oxygen contains 20 mass% N₂, remainder O₂. Please predict the effect that this very low purity oxygen will have the amounts of;

- C-in-coke
- O₂-in-blast air
- N₂-in-blast air
- Blast air

that will be needed for steady production of 1500°C molten iron. Base your calculations on 30 kg of injected impure oxygen.

Calculate also the total amount of N₂ that will enter the furnace in blast and leave the furnace in top gas.

All masses in this problem are kg per 1000 kg of Fe in product molten iron.

11

Bottom Segment with CH₄(g) Injection

O U T L I N E

11.1 Natural Gas Injection	107	11.5 Effect of Injected CH ₄ (g) on Bottom-Segment C-in-Coke Requirement	111
11.2 CH ₄ (g) Injection Equations	108	11.6 Effect of Injected CH ₄ (g) on O ₂ -in-Blast Requirement	111
11.2.1 Injected CH ₄ (g) Quantity Equation	108	11.7 Effect of Injected CH ₄ (g) on N ₂ -in-Blast Air Requirement	111
11.2.2 Steady-State Hydrogen Balance	108		
11.2.3 Amended Carbon Balance	109		
11.2.4 Amended Steady-State Oxygen Balance	109		
11.2.5 Amended Enthalpy Balance	110	11.8 Comparison of C and CH ₄ (g) Injection	111
11.3 Equilibrium Mass (mass H ₂ O(g)/mass H ₂ (g)) Ratio	110	11.9 Summary	113
11.4 Matrix and Calculation Results	111	Exercises	113

11.1 NATURAL GAS INJECTION

Many blast furnace plants inject natural gas into their furnaces. The objective is to replace expensive C-in-coke reductant/fuel with inexpensive natural gas reductant/fuel.

Natural gas is mainly methane, CH₄(g), so we use CH₄(g) in this chapter's calculations.

Even with this simplification, our natural gas calculations require;

1. a CH₄(g) quantity specification;
2. a steady-state bottom-segment hydrogen mass balance;
3. introduction of three new compounds,
 - a. CH₄(g),
 - b. H₂(g), and
 - c. H₂O(g);

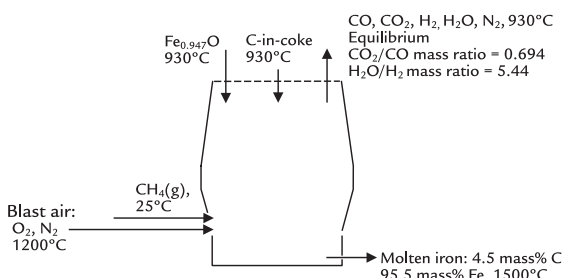
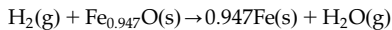


FIGURE 11.1 Conceptual blast furnace bottom segment with 25°C CH₄(g) injection through its tuyeres. The presence of input CH₄(g) and output H₂(g) and H₂O(g) is notable. The 5.44 H₂O/H₂ mass ratio is the equilibrium value for the reaction H₂(g) + Fe_{0.947}O(s) → 0.947Fe(s) + H₂O(g) at 930°C, [Section 11.3](#).

4. modified steady-state C, O and enthalpy balance equations; and
5. a new 930°C equilibrium [mass H₂O(g)]/[mass H₂(g)] ratio for the reaction:



at the top-segment/bottom-segment division, [Fig. 11.1](#).

The objectives of this chapter are to:

1. simulate natural gas injection by pure CH₄(g) injection, [Fig. 11.1](#),
2. show how CH₄(g) injection is included in our matrix calculations, and
3. indicate how CH₄(g) injection affects C-in-coke and blast air requirements for steady-state molten iron production.

11.2 CH₄(g) INJECTION EQUATIONS

11.2.1 Injected CH₄(g) Quantity Equation

A straightforward CH₄(g) quantity equation is:

$$\begin{aligned} & \left[\frac{\text{mass tuyere-}}{\text{injected CH}_4} \right] \\ &= [60 \text{ kg per 1000 kg of Fe in product molten iron}] \end{aligned}$$

or in matrix form

$$60 = \left[\frac{\text{mass tuyere-}}{\text{injected CH}_4} \right] * 1 \quad (11.1)$$

11.2.2 Steady-State Hydrogen Balance

In its most basic form, our steady-state bottom-segment hydrogen balance is:

$$\text{mass H in} = \text{mass H out} \quad (11.2)$$

In terms of CH₄(g) injectant and ascending H₂(g) and H₂O(g) gas, this expands to:

$$\begin{aligned} \left[\frac{\text{mass H in}}{\text{injected CH}_4} \right] &= \left[\frac{\text{mass H in}}{\text{ascending H}_2} \right] \\ &+ \left[\frac{\text{mass H in}}{\text{ascending H}_2\text{O}} \right] \end{aligned}$$

From Appendix A, this expands to:

$$\begin{aligned} & \left[\frac{\text{mass tuyere-}}{\text{injected CH}_4} \right] * \frac{25.1 \text{ mass\% H in CH}_4}{100\%} \\ &= \left[\frac{\text{mass H}_2 \text{ out}}{\text{in ascending gas}} \right] * \frac{100\% \text{ mass H in H}_2}{100\%} \\ &+ \left[\frac{\text{mass H}_2\text{O out}}{\text{in ascending gas}} \right] * \frac{11.2 \text{ mass\% H in H}_2\text{O}}{100\%} \end{aligned}$$

or

$$\begin{aligned} & \left[\frac{\text{mass tuyere-}}{\text{injected CH}_4} \right] * 0.251 = \left[\frac{\text{mass H}_2 \text{ out}}{\text{in ascending gas}} \right] * 1 \\ &+ \left[\frac{\text{mass H}_2\text{O out}}{\text{in ascending gas}} \right] * 0.112 \end{aligned}$$

or subtracting $\left\{ \left[\frac{\text{mass tuyere-}}{\text{injected CH}_4} \right] * 0.251 \right\}$ from both sides

$$0 = - \left[\begin{array}{l} \text{mass tuyere-} \\ \text{injected CH}_4 \end{array} \right] * 0.251 + \left[\begin{array}{l} \text{mass H}_2\text{ out} \\ \text{in ascending gas} \end{array} \right] * 1 \\ + \left[\begin{array}{l} \text{mass H}_2\text{O out} \\ \text{in ascending gas} \end{array} \right] * 0.112 \quad (11.3)$$

11.2.3 Amended Carbon Balance

Including C in tuyere-injected CH₄(g), the bottom segment's carbon balance is:

$$\left[\begin{array}{l} \text{mass tuyere-} \\ \text{injected CH}_4 \end{array} \right] * \frac{74.9 \text{ mass\% C in CH}_4}{100\%} \\ + \left[\begin{array}{l} \text{mass C in} \\ \text{descending coke} \end{array} \right] * \frac{100 \text{ mass\% C}}{100\%} \\ = \left[\begin{array}{l} \text{mass CO out} \\ \text{in ascending gas} \end{array} \right] * \frac{42.9 \text{ mass\% C in CO}}{100\%} \\ + \left[\begin{array}{l} \text{mass CO}_2 \text{ out} \\ \text{in ascending gas} \end{array} \right] * \frac{27.3 \text{ mass\% C in CO}_2}{100\%} \\ + \left[\begin{array}{l} \text{mass C out} \\ \text{in molten iron} \end{array} \right] * 1$$

or

$$\left[\begin{array}{l} \text{mass tuyere-} \\ \text{injected CH}_4 \end{array} \right] * 0.749 + \left[\begin{array}{l} \text{mass C in} \\ \text{descending coke} \end{array} \right] * 1 \\ = \left[\begin{array}{l} \text{mass CO out} \\ \text{in ascending gas} \end{array} \right] * 0.429 \\ + \left[\begin{array}{l} \text{mass CO}_2 \text{ out} \\ \text{in ascending gas} \end{array} \right] * 0.273 + \left[\begin{array}{l} \text{mass C out} \\ \text{in molten iron} \end{array} \right] * 1$$

$$\text{or subtracting } \left\{ \left[\begin{array}{l} \text{mass tuyere-} \\ \text{injected CH}_4 \end{array} \right] * 0.749 \right. \\ \left. + \left[\begin{array}{l} \text{mass C in} \\ \text{descending coke} \end{array} \right] * 1 \right\}$$

from both sides

$$0 = - \left[\begin{array}{l} \text{mass tuyere-} \\ \text{injected CH}_4 \end{array} \right] * 0.749 - \left[\begin{array}{l} \text{mass C in} \\ \text{descending coke} \end{array} \right] * 1 \\ + \left[\begin{array}{l} \text{mass CO out} \\ \text{in ascending gas} \end{array} \right] * 0.429 + \left[\begin{array}{l} \text{mass CO}_2 \text{ out} \\ \text{in ascending gas} \end{array} \right] * 0.273 \\ + \left[\begin{array}{l} \text{mass C out} \\ \text{in molten iron} \end{array} \right] * 1 \quad (11.4)$$

where the first right-hand side term is new.

11.2.4 Amended Steady-State Oxygen Balance

Including oxygen in ascending H₂O bottom-segment exit gas, the bottom-segment oxygen balance is:

$$\left[\begin{array}{l} \text{mass Fe}_{0.947}\text{O into} \\ \text{bottom segment} \end{array} \right] * \frac{23.2 \text{ mass\% O in Fe}_{0.947}\text{O}}{100\%} \\ + \left[\begin{array}{l} \text{mass O}_2 \text{ in} \\ \text{blast air} \end{array} \right] * \frac{100\% \text{ O in O}_2}{100\%} \\ = \left[\begin{array}{l} \text{mass CO out in} \\ \text{ascending gas} \end{array} \right] * \frac{57.1 \text{ mass\% O in CO}}{100\%} \\ + \left[\begin{array}{l} \text{mass CO}_2 \text{ out} \\ \text{in ascending gas} \end{array} \right] * \frac{72.7 \text{ mass\% O in CO}_2}{100\%} \\ + \left[\begin{array}{l} \text{mass H}_2\text{O out} \\ \text{in ascending gas} \end{array} \right] * \frac{88.8 \text{ mass\% O in H}_2\text{O}}{100\%}$$

or

$$\left[\begin{array}{l} \text{mass Fe}_{0.947}\text{O into} \\ \text{bottom segment} \end{array} \right] * 0.232 + \left[\begin{array}{l} \text{mass O}_2 \text{ in} \\ \text{blast air} \end{array} \right] * 1 \\ = \left[\begin{array}{l} \text{mass CO out in} \\ \text{ascending gas} \end{array} \right] * 0.571 + \left[\begin{array}{l} \text{mass CO}_2 \text{ out} \\ \text{in ascending gas} \end{array} \right] * 0.727 \\ + \left[\begin{array}{l} \text{mass H}_2\text{O out} \\ \text{in ascending gas} \end{array} \right] * 0.888$$

$$\text{or subtracting } \left\{ \left[\begin{array}{l} \text{mass Fe}_{0.947}\text{O into} \\ \text{bottom segment} \end{array} \right] * 0.232 \right. \\ \left. + \left[\begin{array}{l} \text{mass O}_2 \\ \text{in blast air} \end{array} \right] * 1 \right\}$$

from both sides:

$$0 = - \left[\begin{array}{l} \text{mass Fe}_{0.947}\text{O into} \\ \text{bottom segment} \end{array} \right] * 0.232 - \left[\begin{array}{l} \text{mass O}_2 \text{ in} \\ \text{blast air} \end{array} \right] * 1 \\ + \left[\begin{array}{l} \text{mass CO out in} \\ \text{ascending gas} \end{array} \right] * 0.571 + \left[\begin{array}{l} \text{mass CO}_2 \text{ out} \\ \text{in ascending gas} \end{array} \right] * 0.727 \\ + \left[\begin{array}{l} \text{mass H}_2\text{O out} \\ \text{in ascending gas} \end{array} \right] * 0.888 \quad (11.5)$$

11.2.5 Amended Enthalpy Balance

With CH₄(g)-through-tuyere injection, bottom-segment enthalpy [Eq. (7.14)] becomes;

$$\begin{aligned}
 & \text{H}^\circ \text{ } 25^\circ\text{C} \\
 & [\text{mass tuyere-injected CH}_4] * \frac{\text{CH}_4(\text{g})}{\text{MW}_{\text{CH}_4}} \\
 & + [\text{mass Fe}_{0.947}\text{O into bottom segment}] * (-3.152) \\
 & + [\text{mass C in descending coke}] * 1.359 \\
 & + [\text{mass O}_2 \text{ in blast air}] * 1.239 \\
 & + [\text{mass N}_2 \text{ in blast air}] * 1.339 \\
 & = [\text{mass Fe out in molten iron}] * 1.269 \\
 & + [\text{mass C out in molten iron}] * 5 \\
 & + [\text{mass CO out in ascending gas}] * (-2.926) \\
 & + [\text{mass CO}_2 \text{ out in ascending gas}] * (-7.926) \\
 & + [\text{mass N}_2 \text{ out in ascending gas}] * 1.008 \\
 & \text{H}^\circ \text{ } 930^\circ\text{C} \\
 & + [\text{mass H}_2 \text{ out in ascending gas}] * \frac{\text{H}_2(\text{g})}{\text{MW}_{\text{H}_2}} \\
 & \text{H}^\circ \text{ } 930^\circ\text{C} \\
 & + [\text{mass H}_2\text{O out in ascending gas}] * \frac{\text{H}_2\text{O}(\text{g})}{\text{MW}_{\text{H}_2\text{O}}} \\
 & + \left\{ \begin{array}{l} 320 \text{ MJ bottom segment conductive,} \\ \text{convective and radiative heat loss per} \\ 1000 \text{ kg of Fe in product molten iron} \end{array} \right\} \quad (11.6)
 \end{aligned}$$

where the additional terms are in bold.

The new enthalpy values are:

$$\frac{\text{H}^\circ \text{ } 25^\circ\text{C}}{\text{CH}_4(\text{g})} = -4.664$$

$$\frac{\text{H}^\circ \text{ } 930^\circ\text{C}}{\text{H}_2(\text{g})} = 13.35$$

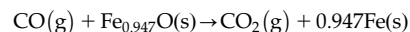
$$\frac{\text{H}^\circ \text{ } 930^\circ\text{C}}{\text{H}_2\text{O}(\text{g})} = -11.50$$

With these values and subtracting 320 and the left side of Eq. (11.6) from both sides of Eq. (11.6), the enthalpy equation becomes:

$$\begin{aligned}
 -320 &= -[\text{mass tuyere-injected CH}_4(\text{g})] * (-4.664) \\
 &- [\text{mass Fe}_{0.947}\text{O into bottom segment}] * (-3.152) \\
 &- [\text{mass C in descending coke}] * 1.359 \\
 &- [\text{mass O}_2 \text{ in blast air}] * 1.239 \\
 &- [\text{mass N}_2 \text{ in blast air}] * 1.339 \\
 &+ [\text{mass Fe out in molten iron}] * 1.269 \\
 &+ [\text{mass C out in molten iron}] * 5 \\
 &+ [\text{mass CO gas out in ascending gas}] * (-2.926) \\
 &+ [\text{mass CO}_2 \text{ gas out in ascending gas}] * (-7.926) \\
 &+ [\text{mass N}_2 \text{ out in ascending gas}] * 1.008 \\
 &+ [\text{mass H}_2 \text{ gas out in ascending gas}] * 13.35 \\
 &+ [\text{mass H}_2\text{O gas out in ascending gas}] * (-11.50) \quad (11.7)
 \end{aligned}$$

11.3 EQUILIBRIUM MASS (MASS H₂O(g)/MASS H₂(g)) RATIO

Section 7.7 indicates that the Chemical Reserve Zone is a region where the reaction;



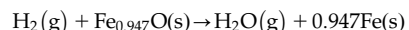
has approached equilibrium at 930°C.

Appendices K and L show that;

1. this reaction's equilibrium ([mass CO₂(g)]/[mass CO(g)]) mass ratio at 930°C is 0.694, and
2. this ratio is represented in our bottom-segment calculations by the following equation:

$$0 = - \left[\begin{array}{l} \text{mass CO}_2 \text{ out} \\ \text{in ascending gas} \end{array} \right] * 1 + \left[\begin{array}{l} \text{mass CO out} \\ \text{in ascending gas} \end{array} \right] * 0.694 \quad (7.9)$$

The reaction;



also approaches equilibrium in the chemical reserve zone, 930°C.

Appendices M and N show that this reaction's equilibrium ([mass H₂O(g)]/[mass H₂(g)]) mass ratio at 930°C = 5.44.

This ratio is applicable at the bottom-segment/top-segment division, so it may be written as;

$$\left[\frac{\text{mass H}_2\text{O out}}{\text{in ascending gas}} \right] * 1 = \left[\frac{\text{mass H}_2 \text{ out}}{\text{in ascending gas}} \right] * 5.44$$

or subtracting $\left\{ \left[\frac{\text{mass H}_2\text{O out}}{\text{in ascending gas}} \right] * 1 \right\}$ from both sides.

$$0 = - \left[\frac{\text{mass H}_2\text{O out}}{\text{in ascending gas}} \right] * 1 + \left[\frac{\text{mass H}_2 \text{ out}}{\text{in ascending gas}} \right] * 5.44 \quad (11.8)$$

These new and amended equations are now included in our bottom-segment matrix, [Table 11.1](#).

11.4 MATRIX AND CALCULATION RESULTS

[Table 11.1](#) shows our bottom-segment CH₄(g) injection matrix and one calculation result. It indicates that for steady production of 1500°C molten iron with injection of 60 kg CH₄(g) at 25°C requires;

- 323 kg of O₂-in-blast air, cell C21, and
- 335 kg of C-in-descending-coke, cell C20

per 1000 kg of Fe in product molten iron. Per Eq. (7.16), the whole furnace's C-in-coke requirement is also 335 kg/1000 kg of Fe in product molten iron.

11.5 EFFECT OF INJECTED CH₄(g) ON BOTTOM-SEGMENT C-IN-COKE REQUIREMENT

[Fig. 11.2](#) shows the effect of CH₄(g) injection on the bottom segment of [Fig. 11.1](#) and hence whole furnace C-in-coke requirement. The requirement *decreases* with increasing CH₄(g) injection because the CH₄(g) provides;

1. carbon reductant/fuel, and
2. hydrogen reductant/fuel.

11.6 EFFECT OF INJECTED CH₄(g) ON O₂-IN-BLAST REQUIREMENT

[Fig. 11.3](#) shows the effect of CH₄(g) injection on steady-state O₂-in-blast air requirement. This requirement increases slightly with increasing mass of tuyere-injected CH₄(g).

11.7 EFFECT OF INJECTED CH₄(g) ON N₂-IN-BLAST AIR REQUIREMENT

[Fig. 11.4](#) shows the effect of CH₄(g) injection on the amount of N₂-in-blast air entering the furnace.

The increase in N₂-in-blast air is notable. This is commensurate with the increasing amount of O₂-in-blast air provided in [Fig. 11.3](#). This increased amount of N₂ has a significant effect on tuyere raceway flame temperature and top gas temperature, more details in Chapter 18, Raceway Flame Temperature With CH₄(g) Tuyere Injection, and Chapter 27, Top Gas Temperature With CH₄(g) Injection.

11.8 COMPARISON OF C AND CH₄(g) INJECTION

Comparison of C and CH₄(g) injection shows that replacement of 1 kg of C-in-coke requires;

- 1.08 kg of injected pulverized carbon (Section 8.8), or
- 1.05 kg of injected CH₄(g) ([Section 11.5](#)).

The explanation for this difference lies in all the matrix equations for the two injectants. We may speculate that the hydrogen in CH₄(g) is

TABLE 11.1 Bottom-Segment CH₄(g) Injection Matrix With 60 kg of Injected 25°C CH₄(g) per 1000 kg of Fe in Product Molten Iron

	A	B	C	D	E	F	G	H	I	J	K	L	M	N	O
1 BOTTOM SEGMENT CALCULATIONS															
2	Equation	Description	Numerical term	mass tuyere-injected CH ₄	mass Fe _{0.94} O into bottom segment	mass C in descending coke	mass O ₂ in blast air	mass N ₂ in blast air	mass Fe out in molten iron	mass C out in molten iron	mass CO out in ascending gas	mass CO ₂ out in ascending gas	mass N ₂ out in ascending gas	mass H ₂ out in ascending gas	mass H ₂ O out in ascending gas
3	7.7	Fe out in molten iron specification	1000	0	0	0	0	0	1	0	0	0	0	0	0
4	7.2	Fe mass balance	0	0	0.768	0	0	0	0	0	0	0	0	0	0
5	11.5	O mass balance	0	0	0.232	0	1	0	0	0	0.371	0.277	0	0	0.688
6	11.4	O mass balance	0	0	0.745	0	0	0	0	1	0.429	0.375	0	0	0
7	7.6	N mass balance	0	0	0	0	0	1	0	0	0	0	1	0	0
8	7.6	N ₂ in blast air specification	0	0	0	0	2.3	-1	0	0	0	0	0	0	0
9	7.9	Equilibrium CO ₂ /CO mass ratio	0	0	0	0	0	0	0	0	0.694	-1	0	0	0
10	7.8	C out in molten iron specification	0	0	0	0	0	0	0.047	-1	0	0	0	0	0
11	11.7	Enthalpy balance	-320	4.664	3.152	-1.359	-1.239	-1.239	1.289	5	-2.926	-7.926	1.008	13.36	-11.50
12	11.3	H mass balance	0	-0.253	0	0	0	0	0	0	0	0	1	0.112	
13	11.8	Equilibrium H ₂ O/H ₂ mass ratio	0	0	0	0	0	0	0	0	0	0	5.44	-1	
14	11.3	CH ₄ injected through tuyeres	60	1	0	0	0	0	0	0	0	0	0	0	
15			25°C	930°C	930°C	1200°C	1200°C	1500°C	1500°C	930°C	930°C	930°C	930°C	930°C	930°C
16															
17	Bottom segment calculated values		kg per 1000 kg of Fe out in molten iron												
18	mass tuyere-injected CH ₄	60													
19	mass Fe _{0.94} O into bottom segment	1302													
20	mass C in descending coke	335	(also = mass C in the furnace's coke charge, Eqn. (7.16))												
21	mass O ₂ in blast air	323													
22	mass N ₂ in blast air	1064													
23	mass Fe out in molten iron	1000													
24	mass C out in molten iron	47													
25	mass CO out in ascending gas	536													
26	mass CO ₂ out in ascending gas	374													
27	mass N ₂ out in ascending gas	1064													
28	mass H ₂ out in ascending gas	9													
29	mass H ₂ O out in ascending gas	51													
30															

The effects of various input CH₄(g) quantities are determined by altering the quantity in Cell C14.

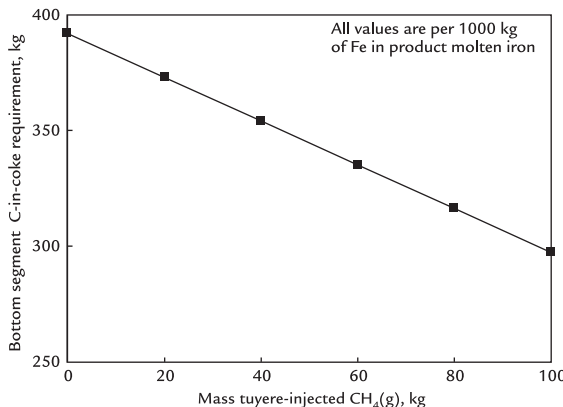


FIGURE 11.2 Mass-injected CH₄(g) versus bottom segment (hence whole furnace) C-in-coke requirement. The line is straight. It indicates that each kg of CH₄(g) saves 0.95 kg of C-in-coke.

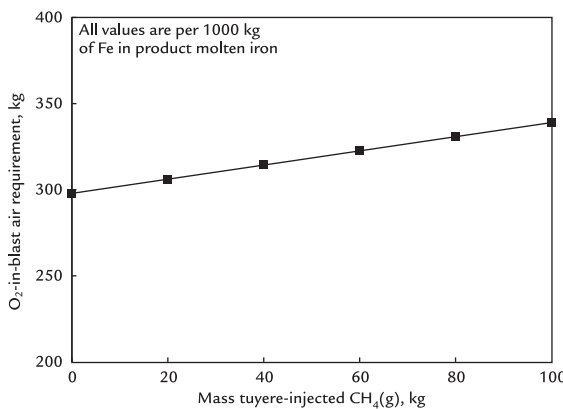


FIGURE 11.3 Effect of tuyere-injected CH₄(g) on blast furnace O₂-in-blast air requirement. The increase in O₂-in-blast requirement is due to all the equations in matrix Table 11.1. This is further discussed in Chapter 18, Raceway Flame Temperature With CH₄(g) Tuyere Injection.

at least partially responsible for its more efficient C-in-coke replacement ratio.

11.9 SUMMARY

Many blast furnaces inject natural gas through their tuyeres. The objective is to replace expensive C-in-top charged coke with inexpensive tuyere-injected natural gas.

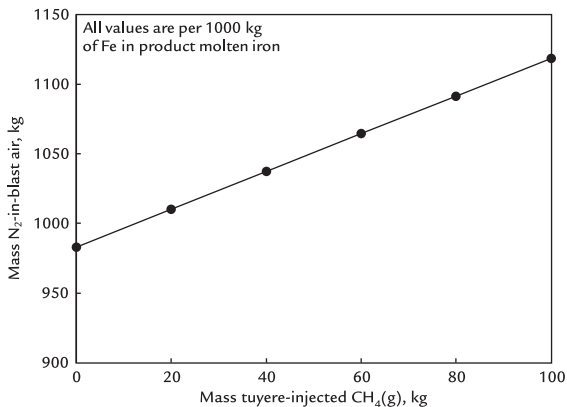


FIGURE 11.4 Effect of CH₄(g) injection on the amount of N₂(g) entering the blast furnace in blast air, per 1000 kg of Fe in product molten iron. The increase is notable. It is commensurate with increasing O₂(g), Fig. 11.3.

This chapter represents natural gas by pure CH₄(g), methane. Commercial natural gas is mainly CH₄(g).

Even with this CH₄(g) simplification, our natural gas calculations require;

1. a new steady-state hydrogen mass balance equation;
2. modified C, O, and enthalpy balance equations; and
3. an equilibrium [mass H₂O(g)]/[mass H₂(g)] equation at the bottom-segment/top-segment division.

Our calculations indicate that replacement of 1 kg of C-in-coke requires injection of 1.05 kg of CH₄(g).

This requirement is smaller than the 1.08 kg of injected pulverized carbon that is required to save 1 kg of C-in-coke, probably due to the hydrogen reductant/fuel in CH₄(g).

EXERCISES

Please express your answers in kg per 1000 kg of Fe in product molten iron.

- 11.1. Blast furnace team of Table 11.1 wishes to increase their CH₄(g) injection quantity

to 120 kg/1000 kg of Fe in product molten iron.

Please predict how much;

- a. C-in-coke,
- b. O₂-in-blast air,
- c. N₂-in-blast air, and
- d. blast air

will be required for steady production of 1500°C molten iron while injecting this 120 kg of CH₄(g).

- 11.2.** In North America, tuyere-injected CH₄(g) is often cheaper than C-in-top-charged coke. For this reason, a blast furnace team wishes to maximize CH₄(g) injection quantity. The team knows, however, that proper gas flow in the blast furnace requires at least 250 kg of

C-in-top-charged coke, per 1000 kg of Fe in product molten iron. Please determine how much CH₄(g) the team can inject into the furnace without lowering the blast furnace's steady-state C-in-coke requirement below this required minimum. Please use two different calculation methods.

- 11.3.** A blast furnace's research department suggests that heating CH₄(g) to 600°C before injection will be an inexpensive way of saving more C-in-coke. Please determine for them how much additional C-in-coke will be saved by this CH₄(g) heating. Use the example of 60 kg of injected CH₄(g) of [Table 11.1](#). The enthalpy of CH₄(g) at 600°C is -2.832 MJ/kg.

12

Bottom Segment With Moisture in Blast Air

O U T L I N E

12.1 The Importance of Steam Injection for Blast Furnace Control	116	12.8 Amended Steady-State Enthalpy Balance	120
12.2 $\text{H}_2\text{O(g)}$ Through-Tuyere Quantity Equation	116	12.9 Matrix and Calculations	120
12.3 $\text{H}_2\text{O(g)}$ Concentration, kg $\text{H}_2\text{O(g)}$ per kg of Dry Air in Blast	117	12.10 Effect of $\text{H}_2\text{O(g)}$ Concentration on Steady-State Through-Tuyere $\text{H}_2\text{O(g)}$ Input	121
12.4 Through-Tuyere $\text{H}_2\text{O(g)}$ Input Quantity Equation	117	12.11 Effect of $\text{H}_2\text{O(g)}$ Concentration on Steady-State Carbon Requirement	122
12.5 Steady-State Bottom-Segment Hydrogen Balance	117	12.12 Explanation	122
12.6 Amended Bottom-Segment Carbon Balance	119	12.13 Summary Exercises	122
12.7 Amended Steady-State Oxygen Balance	119		

12.1 THE IMPORTANCE OF STEAM INJECTION FOR BLAST FURNACE CONTROL

All blast furnace plants inject steam into their blast air, Fig. 12.1.

The primary objective of adding steam is to maintain a constant concentration of $\text{H}_2\text{O(g)}$ -in-blast while atmospheric $\text{H}_2\text{O(g)}$ -in-air (humidity) is varying due to changes in air temperature and relative humidity that occur between day and night and between seasons. Moisture in the blast air can impact the blast furnace performance; steam injection keeps the blast furnace operating steadily and smoothly. The moisture in blast is kept constant over a 24-hour period and can be modified for seasonal changes.

$\text{H}_2\text{O(g)}$ concentration in blast is measured with a *cooled mirror* dew point system or dew cell at point P in Fig. 12.1. The dew cell's output is calibrated to give a readout in grams of $\text{H}_2\text{O(g)}$ in blast per Nm^3 of dry blast (includes air plus added oxygen enrichment).

This chapter examines the effects of $\text{H}_2\text{O(g)}$ -in-blast. As compared to Chapter 11, Methane— $\text{CH}_4(\text{g})$ —Injection, it requires;

1. an $\text{H}_2\text{O(g)}$ input quantity specification (in place of $\text{CH}_4(\text{g})$ input quantity specification

of Chapter 11, Methane— $\text{CH}_4(\text{g})$ —Injection), and

2. modified steady-state C, O, H, and enthalpy balance equations.

The objectives of this chapter are to;

1. show how $\text{H}_2\text{O(g)}$ through-tuyere input is included in our matrix calculations, and
2. indicate how $\text{H}_2\text{O(g)}$ -in-blast affects blast furnace C-in-coke and O₂-in-blast air requirements for steady production of 1500°C molten iron.

12.2 $\text{H}_2\text{O(g)}$ THROUGH-TUYERE QUANTITY EQUATION

The amount of $\text{H}_2\text{O(g)}$ entering a blast furnace through its tuyeres is a function of;

1. its blast's measured $\text{H}_2\text{O(g)}$ concentration, usefully expressed as grams of $\text{H}_2\text{O(g)}$ in blast per Nm^3 of dry blast, and
2. the amount of dry air entering the blast furnace, kg per 1000 kg of Fe in product molten iron.

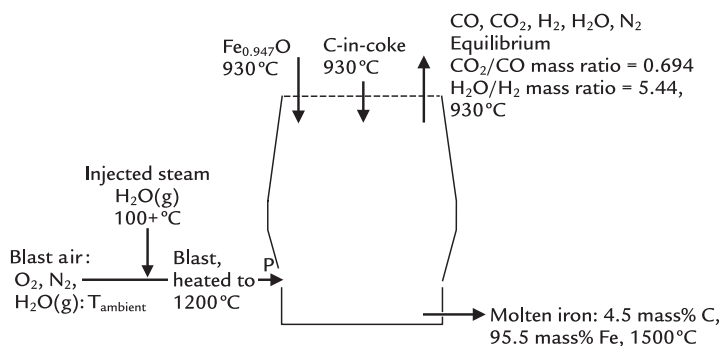


FIGURE 12.1 Conceptual blast furnace bottom segment with $\text{H}_2\text{O(g)}$ in blast air. $\text{H}_2\text{O(g)}$ is always present in ambient air. Its concentration is topped up to the blast furnace operator's prescribed level by injecting steam into this ambient air. The mixture is then heated to 1200°C, pressurized and blown into the blast furnace. The concentration of $\text{H}_2\text{O(g)}$ in blast is measured downstream of the stoves after the blast has been heated at 1200°C (point P).

12.3 H₂O(g) CONCENTRATION, kg H₂O(g) PER kg OF DRY AIR IN BLAST

Appendix O shows how to calculate H₂O(g) in dry air concentration expressed as kg H₂O(g)-in-blast per kg of dry-air-in-blast from measured H₂O(g) concentrations expressed as grams H₂O(g)-in-blast per Nm³ of dry-blast. It also shows that a typical industrial H₂O(g) concentration of 15 g H₂O(g)-in-blast per Nm³ of dry-blast is equivalent to 0.0118 kg H₂O(g)/kg of blast per kg of dry-air-in-blast.

We use this concentration throughout this chapter.

12.4 THROUGH-TUYERE H₂O(g) INPUT QUANTITY EQUATION

The basic blast furnace through-tuyere H₂O(g) input quantity equation is;

$$\left[\frac{\text{mass through-tuyere}}{\text{input H}_2\text{O(g)}} \right] = \left[\frac{\text{mass dry air}}{\text{in blast}} \right] * \left[\frac{\text{H}_2\text{O(g) concentration in}}{\text{blast, kg per kg of dry air}} \right] \quad (12.1)$$

where the input masses are kg per 1000 kg of product molten iron.

With an H₂O(g) concentration of 0.0118 kg of H₂O(g)-in-blast per kg of dry-air-in-blast, Eq. (12.1) becomes;

$$\left[\frac{\text{mass through-tuyere}}{\text{input H}_2\text{O(g)}} \right] * 1 = \left[\frac{\text{mass input}}{\text{dry air}} \right] * 0.0118$$

which is usefully expanded to;

$$\begin{aligned} & \left[\frac{\text{mass through-tuyere}}{\text{input H}_2\text{O(g)}} \right] * 1 \\ &= \left[\frac{\text{mass O}_2}{\text{in blast}} \right] * 0.0118 \\ &\quad + \left[\frac{\text{mass N}_2}{\text{in blast}} \right] * 0.0118 \end{aligned}$$

or, subtracting $\left\{ \left[\frac{\text{mass through-tuyere}}{\text{input H}_2\text{O(g)}} \right] * 1 \right\}$ from both sides;

$$\begin{aligned} 0 &= - \left[\frac{\text{mass through-tuyere}}{\text{input H}_2\text{O(g)}} \right] * 1 \\ &\quad + \left[\frac{\text{mass O}_2}{\text{in blast}} \right] * 0.0118 \\ &\quad + \left[\frac{\text{mass N}_2}{\text{in blast}} \right] * 0.0118 \end{aligned} \quad (12.2)$$

as shown in matrix Table 12.1.

12.5 STEADY-STATE BOTTOM-SEGMENT HYDROGEN BALANCE

In its most basic form, the bottom segment hydrogen balance is:

$$\text{mass H in} = \text{mass H out}$$

In terms of our input H₂O(g) and the H₂(g) and H₂O(g) ascending out of the bottom segment (Fig. 12.1), this expands to:

$$\begin{aligned} & \left[\frac{\text{mass H in through-}}{\text{tuyere input H}_2\text{O(g)}} \right] \\ &= \left[\frac{\text{mass H in}}{\text{ascending H}_2} \right] \\ &\quad + \left[\frac{\text{mass H in}}{\text{ascending H}_2\text{O}} \right] \end{aligned}$$

This expands further to:

$$\begin{aligned} & \left[\frac{\text{mass through-tuyere}}{\text{input H}_2\text{O(g)}} \right] * \frac{11.2 \text{ mass\% H in H}_2\text{O}}{100\%} \\ &= \left[\frac{\text{mass H}_2 \text{ out}}{\text{in ascending gas}} \right] * \frac{100 \text{ mass\% H in H}_2}{100\%} \\ &\quad + \left[\frac{\text{mass H}_2\text{O out}}{\text{in ascending gas}} \right] * \frac{11.2 \text{ mass\% H in H}_2\text{O}}{100\%} \end{aligned}$$

TABLE 12.1 Bottom-Segment H₂O(g) Injection Matrix

A	B	C	D	E	F	G	H	I	J	K	L	M	N	O
Equation	Description	Numerical term	mass Fe _{0.947} O into bottom segment	mass C in descending coke	mass O ₂ in blast air	mass N ₂ in blast air	mass Fe out in molten iron	mass C out in molten iron	mass CO out in ascending gas	mass CO ₂ out in ascending gas	mass N ₂ out in ascending gas	mass H ₂ out in ascending gas	mass H ₂ O out in ascending gas	mass through-tuyere input H ₂ O(g)
3	7.7 Fe out in molten iron specification	1000	0	0	0	0	1	0	0	0	0	0	0	0
4	7.2 Fe mass balance	0	-0.768	0	0	0	1	0	0	0	0	0	0	0
5	12.5 O mass balance	0	-0.232	0	-1	0	0	0	0.571	0.727	0	0	0.888	-0.888
6	7.4 C mass balance	0	0	-1	0	0	0	1	0.429	0.273	0	0	0	0
7	7.5 N mass balance	0	0	0	0	-1	0	0	0	0	1	0	0	0
8	12.3 H mass balance	0	0	0	0	0	0	0	0	0	0	1	0.112	-0.112
9	7.6 N ₂ in blast air specification	0	0	0	3.3	-1	0	0	0	0	0	0	0	0
10	7.9 Equilibrium CO ₂ /CO mass ratio	0	0	0	0	0	0	0	0.694	-1	0	0	0	0
11	11.8 Equilibrium H ₂ O/H ₂ mass ratio	0	0	0	0	0	0	0	0	0	0	5.44	-1	0
12	7.8 C out in molten iron specification	0	0	0	0	0	0.047	-1	0	0	0	0	0	0
13	12.7 Enthalpy balance	-320	3.152	-1.359	-1.239	-1.339	1.269	5	-2.926	-7.926	1.008	13.35	-11.50	10.81
14	12.2 Mass through-tuyere input H ₂ O(g)	0	0	0	0.0118	0.0118	0	0	0	0	0	0	0	-1
15			930°C	930°C	1200°C	1200°C	1500°C	1500°C	930°C	930°C	930°C	930°C	930°C	1200°C
16	Calculated values	kg per 1000 kg of Fe out in molten iron												
17	mass Fe _{0.947} O into bottom segment	1302												
18	mass C in descending coke	399	also = mass C in the furnace's coke charge, Eqn. (7.16)											
19	mass O ₂ in blast air	302												
20	mass N ₂ in blast air	995												
21	mass Fe out in molten iron	1000												
22	mass C out in molten iron	47												
23	mass CO out in ascending gas	569												
24	mass CO ₂ out in ascending gas	395												
25	mass N ₂ out in ascending gas	995												
26	mass H ₂ out in ascending gas	1.1												
27	mass H ₂ O out in ascending gas	5.8												
28	mass through-tuyere input H ₂ O(g)	15												
29														
30														

Eq. (12.2) shows that 0.0118 kg H₂O(g)/kg of dry air is being blown through the blast furnace tuyeres. It also shows altered C, H, O, and enthalpy balances. The effects of altering H₂O(g)-in-blast air are determined by changing the quantity in cells F14 and G14 as shown in Appendix O. Try it!

or

$$\begin{aligned} & \left[\frac{\text{mass through-tuyere}}{\text{input H}_2\text{O(g)}} \right] * 0.112 \\ &= \left[\frac{\text{mass H}_2 \text{ out}}{\text{in ascending gas}} \right] * 1 \\ &+ \left[\frac{\text{mass H}_2\text{O out}}{\text{in ascending gas}} \right] * 0.112 \end{aligned}$$

or subtracting $\left\{ \left[\frac{\text{mass through-tuyere}}{\text{input H}_2\text{O(g)}} \right] * 0.112 \right\}$ from both sides;

$$\begin{aligned} 0 = & - \left[\frac{\text{mass H in through-}}{\text{tuyere input H}_2\text{O(g)}} \right] * 0.112 \\ &+ \left[\frac{\text{mass H}_2 \text{ out}}{\text{in ascending gas}} \right] * 1 \\ &+ \left[\frac{\text{mass H}_2\text{O out}}{\text{in ascending gas}} \right] * 0.112 \end{aligned} \quad (12.3)$$

$$\begin{aligned} & \left[\frac{\text{mass through-tuyere}}{\text{input H}_2\text{O(g)}} \right] * \frac{88.8 \text{ mass\% O in H}_2\text{O}}{100\%} \\ &+ \left[\frac{\text{mass Fe}_{0.947}\text{O into}}{\text{bottom segment}} \right] * \frac{23.2 \text{ mass\% O in Fe}_{0.947}\text{O}}{100\%} \\ &+ \left[\frac{\text{mass O}_2}{\text{in blast}} \right] * \frac{100\% \text{ O in O}_2}{100\%} \\ &= \left[\frac{\text{mass CO out in}}{\text{ascending gas}} \right] * \frac{57.1 \text{ mass\% O in CO}}{100\%} \end{aligned}$$

$$\begin{aligned} &+ \left[\frac{\text{mass CO}_2 \text{ out}}{\text{in ascending gas}} \right] * \frac{72.7 \text{ mass\% O in CO}_2}{100\%} \\ &+ \left[\frac{\text{mass H}_2\text{O out}}{\text{in ascending gas}} \right] * \frac{88.8 \text{ mass\% O in H}_2\text{O}}{100\%} \end{aligned} \quad (12.4)$$

or

12.6 AMENDED BOTTOM-SEGMENT CARBON BALANCE

Without $\text{CH}_4(\text{g})$ injection, the steady-state bottom-segment carbon balance reverts to:

$$\begin{aligned} 0 = & - \left[\frac{\text{mass C in}}{\text{descending coke}} \right] * 1 \\ &+ \left[\frac{\text{mass CO out}}{\text{in ascending gas}} \right] * 0.429 \\ &+ \left[\frac{\text{mass CO}_2 \text{ out}}{\text{in ascending gas}} \right] * 0.273 \\ &+ \left[\frac{\text{mass C out}}{\text{in molten iron}} \right] * 1 \end{aligned} \quad (7.4)$$

$$\begin{aligned} & \left[\frac{\text{mass through-tuyere}}{\text{input H}_2\text{O(g)}} \right] * 0.888 \\ &+ \left[\frac{\text{mass Fe}_{0.947}\text{O into}}{\text{bottom segment}} \right] * 0.232 \\ &+ \left[\frac{\text{mass O}_2}{\text{in blast}} \right] * 1 \\ &= \left[\frac{\text{mass CO out in}}{\text{ascending gas}} \right] * 0.571 \\ &+ \left[\frac{\text{mass CO}_2 \text{ out}}{\text{in ascending gas}} \right] * 0.727 \\ &+ \left[\frac{\text{mass H}_2\text{O out}}{\text{in ascending gas}} \right] * 0.888 \end{aligned}$$

12.7 AMENDED STEADY-STATE OXYGEN BALANCE

Including the oxygen in through-tuyere $\text{H}_2\text{O(g)}$, this chapter's bottom-segment oxygen balance is;

or subtracting $\left\{ \left[\frac{\text{mass through-tuyere}}{\text{input H}_2\text{O(g)}} \right] * 0.888 + \left[\frac{\text{mass Fe}_{0.947}\text{O into}}{\text{bottom segment}} \right] * 0.232 + \left[\frac{\text{mass O}_2}{\text{in blast}} \right] * 1 \right\}$ from both sides:

$$\begin{aligned}
 0 = & - \left[\begin{array}{l} \text{mass through-tuyere} \\ \text{input } \text{H}_2\text{O(g)} \end{array} \right] * 0.888 \\
 & - \left[\begin{array}{l} \text{mass } \text{Fe}_{0.947}\text{O into} \\ \text{bottom segment} \end{array} \right] * 0.232 \\
 & - \left[\begin{array}{l} \text{mass } \text{O}_2 \\ \text{in blast} \end{array} \right] * 1 \\
 & + \left[\begin{array}{l} \text{mass CO out in} \\ \text{ascending gas} \end{array} \right] * 0.571 \\
 & + \left[\begin{array}{l} \text{mass } \text{CO}_2 \text{ out} \\ \text{in ascending gas} \end{array} \right] * 0.727 \\
 & + \left[\begin{array}{l} \text{mass } \text{H}_2\text{O out} \\ \text{in ascending gas} \end{array} \right] * 0.888
 \end{aligned} \tag{12.5}$$

12.8 AMENDED STEADY-STATE ENTHALPY BALANCE

With through-tuyere input $\text{H}_2\text{O(g)}$, enthalpy Eq. (11.6) becomes;

$$\begin{aligned}
 & \text{H}^\circ_{1200^\circ\text{C}} \\
 & [\text{mass through-tuyere input } \text{H}_2\text{O(g)}] * \frac{\text{H}_2\text{O(g)}}{\text{MW}_{\text{H}_2\text{O}}} \\
 & + [\text{mass } \text{Fe}_{0.947}\text{O into bottom segment}] * (-3.152) \\
 & + [\text{mass C in descending coke}] * 1.359 \\
 & + [\text{mass } \text{O}_2 \text{ in blast}] * 1.239 \\
 & + [\text{mass } \text{N}_2 \text{ in blast}] * 1.339 \\
 & = [\text{mass Fe out in molten iron}] * 1.269 \\
 & + [\text{mass C out in molten iron}] * 5 \\
 & + [\text{mass CO out in ascending gas}] * (-2.926) \\
 & + [\text{mass } \text{CO}_2 \text{ out in ascending gas}] * (-7.926) \\
 & + [\text{mass } \text{N}_2 \text{ out in ascending gas}] * 1.008 \\
 & + [\text{mass } \text{H}_2 \text{ out in ascending gas}] * 13.35 \\
 & + [\text{mass } \text{H}_2\text{O out in ascending gas}] * (-11.50) \\
 & + \left\{ \begin{array}{l} 320 \text{ MJ bottom segment conductive,} \\ \text{convective and radiative heat loss per} \end{array} \right\} \\
 & \quad 1000 \text{ kg of Fe in product molten iron}
 \end{aligned} \tag{12.6}$$

where the new term is italicized. It replaces the $\text{CH}_4\text{(g)}$ term in Eq. (11.6).

From Table J.1, the new enthalpy value is:

$$\frac{\text{H}^\circ_{1200^\circ\text{C}}}{\text{MW}_{\text{H}_2\text{O}}} = -10.81 \text{ MJ/kg of } \text{H}_2\text{O(g)}$$

With this new value and subtracting (1) 320 MJ per 1000 kg Fe, and (2) the left side of Eq. (12.6), from both sides of Eq. (12.6), the enthalpy equation becomes:

$$\begin{aligned}
 -320 = & -[\text{mass through-tuyere input } \text{H}_2\text{O(g)}] * (-10.81) \\
 & -[\text{mass } \text{Fe}_{0.947}\text{O into bottom segment}] * (-3.152) \\
 & -[\text{mass C in descending coke}] * 1.359 \\
 & -[\text{mass } \text{O}_2 \text{ in blast}] * 1.239 \\
 & -[\text{mass } \text{N}_2 \text{ in blast}] * 1.339 \\
 & + [\text{mass Fe out in molten iron}] * 1.269 \\
 & + [\text{mass C out in molten iron}] * 5 \\
 & + [\text{mass CO gas out in ascending gas}] * (-2.926) \\
 & + [\text{mass } \text{CO}_2 \text{ gas out in ascending gas}] * (-7.926) \\
 & + [\text{mass } \text{N}_2 \text{ out in ascending gas}] * 1.008 \\
 & + [\text{mass } \text{H}_2 \text{ gas out in ascending gas}] * 13.35 \\
 & + [\text{mass } \text{H}_2\text{O gas out in ascending gas}] * (-11.50)
 \end{aligned} \tag{12.7}$$

The remainder of the equations of this chapter remain unchanged.

12.9 MATRIX AND CALCULATIONS

Table 12.1 is our matrix with through-tuyere $\text{H}_2\text{O(g)}$ input. Notice that the $\text{H}_2\text{O(g)}$ enters the furnace at blast temperature, 1200°C in this case. Eqs. (12.2), (12.3), (12.5), and (12.7) are new.

Solving the matrix gives one calculated result. It indicates that steady-state operation of the Fig. 12.1 bottom segment with 0.0118 kg of $\text{H}_2\text{O(g)}$ per kg of dry air at 1200°C requires;

- 399 kg of C in descending coke, cell C19, and
- 302 kg of O_2 -in-blast, cell C20

both per 1000 kg of Fe in product molten iron. And by Eq. (7.16), the whole furnace C-in-coke requirement is also 399 kg/1000 kg of Fe in product molten iron.

Figs. 12.2–12.5 plot this and other calculated values.

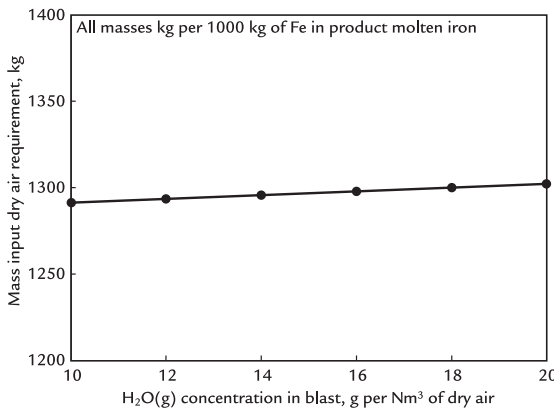


FIGURE 12.2 Steady-state dry air requirement as a function of H₂O(g) concentration in blast.

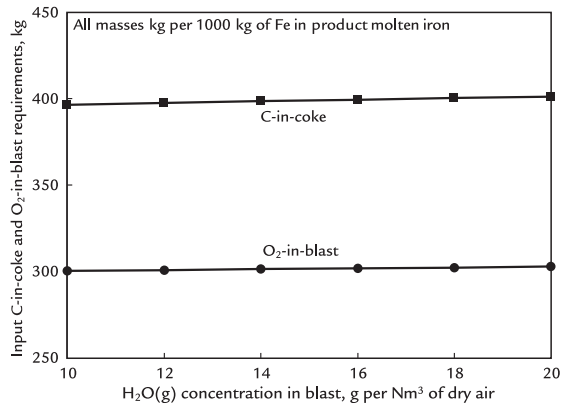


FIGURE 12.4 Effect of H₂O(g) concentration in blast air on blast furnace steady-state C-in-coke and O₂-in-blast requirement for steady production of 1500°C molten iron. Both increase slightly.

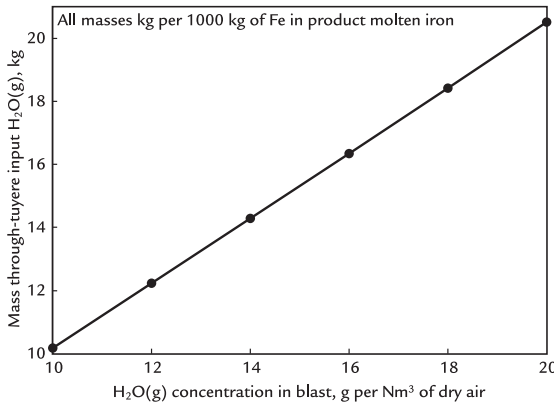


FIGURE 12.3 Effect of H₂O(g) concentration in blast air on steady-state through-tuyere H₂O(g) input mass. H₂O(g) input mass is obtained from Table 12.1, Cell C29.

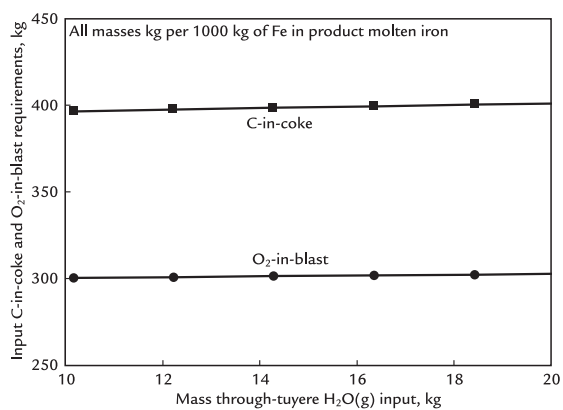


FIGURE 12.5 Steady-state blast furnace C-in-coke and O₂-in-blast requirements as a function of mass through-tuyere H₂O(g) input. H₂O(g) input mass is obtained from Table 12.1, Cell C29.

12.10 EFFECT OF H₂O(g) CONCENTRATION ON STEADY-STATE THROUGH-TUYERE H₂O(g) INPUT

Before discussing the effect of through-tuyere input H₂O(g) on C-in-coke and O₂-in-blast requirements, we examine the effect of H₂O(g) in blast concentration on;

1. the blast furnace's input air requirement, and
2. the equivalent mass input H₂O(g).

Fig. 12.2 plots the dry air requirement for steady production of molten 1500°C iron as a function of H₂O(g)-in-blast concentration. It increases slightly.

Fig. 12.3 plots the equivalent amount of $\text{H}_2\text{O(g)}$ that enters the blast furnace. This increases markedly with increasing $\text{H}_2\text{O(g)}$ concentration in blast. This is due to;

1. the increasing $\text{H}_2\text{O(g)}$ in blast concentration, and
2. the slight increase in air requirement,

Fig. 12.2.

12.11 EFFECT OF $\text{H}_2\text{O(g)}$ CONCENTRATION ON STEADY-STATE CARBON REQUIREMENT

Fig. 12.4 shows the effect of blast $\text{H}_2\text{O(g)}$ concentration on steady-state blast furnace C-in-coke and O_2 -in-blast requirements. Both increase slightly. **Section 12.12** explains these results.

12.12 EXPLANATION

Fig. 12.5 replots input C-in-coke and O_2 -in-blast requirements of **Fig. 12.4** as a function of through-tuyere $\text{H}_2\text{O(g)}$ input mass. Both increase.

The C-in-coke requirement increases by 0.46 kg for every kg of $\text{H}_2\text{O(g)}$ input. This increase is a consequence of all **Table 12.1** equations. We may, however, postulate that it is mostly due the large negative enthalpy that injected $\text{H}_2\text{O(g)}$ brings into the furnace, -10.81 MJ/kg , (Appendix J). This negative enthalpy must be offset by burning additional carbon in front of the tuyeres.

This also explains the increased O_2 -in-blast requirement of **Fig. 12.4**. It is the oxygen that is needed to burn the abovementioned additional carbon in front of the tuyeres. Its requirement increases by 0.24 kg for every additional kg of through-tuyere $\text{H}_2\text{O(g)}$ input.

12.13 SUMMARY

All blast furnaces blow $\text{H}_2\text{O(g)}$ through their tuyeres. The $\text{H}_2\text{O(g)}$ is from;

1. natural humidity in the blast's input air, and
2. steam that is injected into the humid air.

The effect of through-tuyere $\text{H}_2\text{O(g)}$ input is examined much like $\text{CH}_4\text{(g)}$ injection, Chapter 11, Methane— $\text{CH}_4\text{(g)$ —Injection. The input concentration of $\text{H}_2\text{O(g)}$ is specified in equation form and the C, H, O, and enthalpy balances are modified to represent $\text{H}_2\text{O(g)}$ at 1200°C in place of $\text{CH}_4\text{(g)$ at 25°C .

$\text{H}_2\text{O(g)}$ -in-blast increases the blast furnace's steady-state C-in-coke requirement per 1000 kg of Fe in product molten iron—thereby increasing product iron cost. The benefits of this extra cost are;

1. smooth, steady furnace operation, and burden descent;
2. quick blast furnace start-ups, especially when hanging occurs;
3. rapid flame temperature adjustment (Chapter 19: Raceway Flame Temperature with Moisture in Blast Air) by changing injected steam quantity (**Fig. 12.1**); and
4. ability to quickly control the hot metal thermal state and silicon content.

EXERCISES

- 12.1. For its furnace start-up, blast furnace team of **Table 12.1** wishes to increase their $\text{H}_2\text{O(g)}$ in blast concentration to 25 g/Nm^3 of dry air in blast. Please predict for them the amounts of C-in-coke and O_2 -in-blast that will be needed for steady production of 1500°C molten iron with this $\text{H}_2\text{O(g)}$ -in-blast concentration. You may wish to use Appendix O.

Please give your answers in kg per 1000 kg of Fe in product molten iron.

- 12.2. Will the requirements of Exercise 12.1 be affected by blast temperature? Determine this by changing blast temperature of Exercise 12.1 to 1300°C. Use Appendix J.3. Examine Fig. 12.1 before completing this exercise. The H₂O(g)-in-blast concentration remains at 25 g/Nm³ of dry air in blast.
- 12.3. Blast furnace plant of Table 12.1 is running out of coke. It can only afford to run the furnace with 395 kg (or less) of C-in-coke per 1000 kg of Fe in product molten iron. What is the maximum concentration of H₂O(g)-in-blast that can be used while meeting this 395 kg of C-in-coke limitation. Please express your answer in grams H₂O(g) in blast per Nm³

of dry air in blast. The blast temperature is 1200°C, as in Table 12.1.

- 12.4. Blast furnace of Table 12.1 is using 15 g H₂O(g)/Nm³ of dry air. Humid air of Fig. 12.1 contains 10 g H₂O(g)/Nm³ of dry air. How much steam must be added to this humid air to attain the prescribed 15 g H₂O(g)/Nm³ of dry air in blast? Please express your answer in;
1. g per Nm³ of dry air,
 2. kg per kg of dry air, and
 3. kg per 1000 kg (t) of Fe in product molten iron.
- 12.5. Blast furnace of Exercise 12.4 is producing molten iron at 400 t/h. At what rate must steam be injected into humid air of Fig. 12.1 to continuously meet the blast's specified 15 kg of H₂O (g)/Nm³ of dry air. Remember that the molten iron is not pure Fe.

13

Bottom Segment With Pulverized Hydrocarbon Injection

O U T L I N E

13.1 Understanding Coal Injection	125	13.6 Calculation Results and Comparison With Pulverized Pure Carbon Injection	127
13.2 Calculation Strategy	126	13.7 Summary	129
13.3 Coal Hydrocarbon Injected Quantity Specification	126	Exercises	129
13.4 Bottom Segment Steady-State Mass Balance	126	Reference	129
13.5 Bottom Segment Steady-State Enthalpy Balance	127		

13.1 UNDERSTANDING COAL INJECTION

Chapter 8, Tuyere Injection of Pulverized Carbon, represented tuyere injection of pulverized coal by tuyere injection of pure carbon.

This chapter gets closer to industrial reality by representing the injected coal by its hydrocarbon components, [Table 13.1](#).

Natural coal is made up of hydrocarbon molecules plus;

1. 5–10 mass% interstitial oxide particles, mainly aluminosilicates (e.g., granite);
2. ~1 mass% moisture, $H_2O(\ell)$;
3. ~5 mass% oxygen, O ;
4. ~1 mass% nitrogen, N ;
5. up to 0.7 mass% sulfur; and
6. small amounts of K, Na, and P, all detrimental to the blast furnace process.

The behavior of these components is discussed in Chapter 58, Blast Furnace Slag.

The objectives of this chapter are to;

TABLE 13.1 Elemental Composition of the Hydrocarbon Portion of a Coal (i.e., Ash-Free Coal)

Element	Mass%
C	88
H	6
O	5
N	1

This is used for all this chapter's calculations.

Table courtesy Wikipedia Commons.

1. show how coal hydrocarbons are represented in our blast furnace calculations, and
2. determine how pulverized coal hydrocarbon injection affects the amounts of C-in-top-charged coke and O₂-in-blast air that are needed for steady production of 1500°C molten iron.

13.2 CALCULATION STRATEGY

This chapter uses the same calculation strategy as Chapter 29, Bottom Segment Calculations with Natural Gas Injection.

In this chapter, we:

1. specify the amount of coal hydrocarbon being injected into the furnace per 1000 kg of Fe in product molten iron, [Fig. 13.1](#);
2. alter the blast furnace bottom segment C, H, N, and O steady-state mass balances to properly represent the coal hydrocarbon composition provided in [Table 13.1](#); and
3. alter the bottom segment enthalpy balance to properly represent 25°C coal hydrocarbon enthalpy.

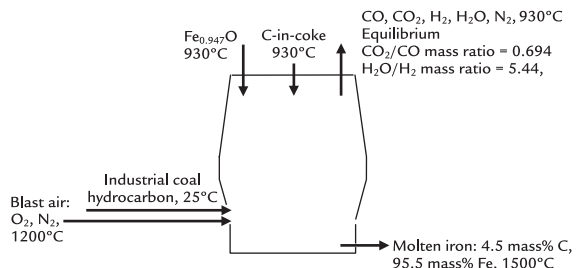


FIGURE 13.1 Conceptual blast furnace bottom segment with injection of pulverized coal hydrocarbon. The hydrocarbon is injected at 25°C.

13.3 COAL HYDROCARBON INJECTED QUANTITY SPECIFICATION

The quantity of injected coal hydrocarbon comes from Eq. (8.1). Adapted to this chapter's hydrocarbon injection, it is

$$60 = \left[\frac{\text{mass tuyere injected}}{\text{coal hydrocarbon}} \right] * 1 \quad (13.1)$$

13.4 BOTTOM SEGMENT STEADY-STATE MASS BALANCE

Adapted from the coal hydrocarbon composition of [Table 13.1](#), mass balance Eqs. (13.2)–(13.5) becomes;

Hydrogen balance

$$0 = - \left[\frac{\text{mass tuyere injected}}{\text{coal hydrocarbon}} \right] * 0.06 + \left[\frac{\text{mass H}_2 \text{ out}}{\text{in ascending gas}} \right] * 1 + \left[\frac{\text{mass H}_2\text{O out}}{\text{in ascending gas}} \right] * 0.112 \quad (13.2)$$

where 0.06 = (mass % H in the hydrocarbon)/100%, [Table 13.1](#)

Carbon balance

$$\begin{aligned}
 0 = & - \left[\frac{\text{mass tuyere injected}}{\text{coal hydrocarbon}} \right] * 0.88 \\
 & - \left[\frac{\text{mass C in}}{\text{descending coke}} \right] * 1 \\
 & + \left[\frac{\text{mass CO out}}{\text{in ascending gas}} \right] * 0.429 \\
 & + \left[\frac{\text{mass CO}_2 \text{ out}}{\text{in ascending gas}} \right] * 0.273 \\
 & + \left[\frac{\text{mass C out}}{\text{in molten iron}} \right] * 1
 \end{aligned} \tag{13.3}$$

where $0.88 = (\text{mass\% C in the hydrocarbon})/100\%$

Oxygen balance

$$\begin{aligned}
 0 = & - \left[\frac{\text{mass tuyere injected}}{\text{coal hydrocarbon}} \right] * 0.05 \\
 & - \left[\frac{\text{mass Fe}_{0.947}\text{O into}}{\text{bottom segment}} \right] * 0.232 \\
 & - \left[\frac{\text{mass O}_2}{\text{in blast air}} \right] * 1 \\
 & + \left[\frac{\text{mass CO out}}{\text{in ascending gas}} \right] * 0.571 \\
 & + \left[\frac{\text{mass CO}_2 \text{ out}}{\text{in ascending gas}} \right] * 0.727 \\
 & + \left[\frac{\text{mass H}_2\text{O out}}{\text{in ascending gas}} \right] * 0.888
 \end{aligned} \tag{13.4}$$

where $0.05 = (\text{mass\% O in the hydrocarbon})/100\%$.

Nitrogen balance

$$\begin{aligned}
 0 = & - \left[\frac{\text{mass tuyere injected}}{\text{coal hydrocarbon}} \right] * 0.01 \\
 & - \left[\frac{\text{mass N}_2}{\text{in blast air}} \right] * 1 + \left[\frac{\text{mass N}_2 \text{ out}}{\text{in ascending gas}} \right] * 1
 \end{aligned} \tag{13.5}$$

where $0.01 = (\text{mass\% N in the hydrocarbon})/100\%$

13.5 BOTTOM SEGMENT STEADY-STATE ENTHALPY BALANCE

The 25°C enthalpy of coal hydrocarbons is near 0. This is because most of its bonds are

C–C bonds, such as pure carbon itself. This may be written as:

$$H_{25^\circ\text{C}} = 0 \pm 0.3 \text{ MJ/kg of coal hydrocarbon}^1$$

We use the zero value in all our calculations. It alters bottom segment enthalpy Eq. (8.4) to

$$\begin{aligned}
 -320 = & -[\text{mass tuyere injected coal hydrocarbon}] * 0 \\
 & - [\text{mass Fe}_{0.947}\text{O into bottom segment}] * (-3.152) \\
 & - [\text{mass C in descending coke}] * 1.359 \\
 & - [\text{mass O}_2 \text{ in blast}] * 1.239 \\
 & - [\text{mass N}_2 \text{ in blast}] * 1.339 \\
 & + [\text{mass Fe out in molten iron}] * 1.269 \\
 & + [\text{mass C out in molten iron}] * 5 \\
 & + [\text{mass CO gas out in ascending gas}] * (-2.926) \\
 & + [\text{mass CO}_2 \text{ gas out in ascending gas}] * (-7.926) \\
 & + [\text{mass N}_2 \text{ out in ascending gas}] * 1.008 \\
 & + [\text{mass H}_2 \text{ gas out in ascending gas}] * 13.35 \\
 & + [\text{mass H}_2\text{O gas out in ascending gas}] * (-11.50)
 \end{aligned} \tag{13.6}$$

This change and the changes in Sections 13.3 and 13.4 are shown in [Table 13.2](#).

13.6 CALCULATION RESULTS AND COMPARISON WITH PULVERIZED PURE CARBON INJECTION

Matrix [Table 13.2](#) shows that steady blast furnace operation with 60 kg of injected coal hydrocarbon requires 336 kg of carbon-in-top-charged coke and 301 kg of O_2 -in-blast air as compared to 336 kg of carbon-in-top-charged coke (Fig. 8.3) and 306 kg of O_2 -in-blast air (Fig. 8.5) with 60 kg of injected pure carbon (all values per 1000 kg of Fe in product molten iron). So, coal hydrocarbon injection requires

TABLE 13.2 Blast Furnace Bottom Segment Matrix With Coal Hydrocarbon Injection

	A	B	C	D	E	F	G	H	I	J	K	L	M	N	O
1 BOTTOM SEGMENT CALCULATIONS															
1	Equation	Description	Numerical term	mass $\text{Fe}_{\text{bottom}}\text{O}$ into bottom segment	mass C in descending coke	mass O_2 in blast	mass N_2 in blast	mass Fe out in molten iron	mass C out in molten iron	mass CO out in ascending gas	mass CO_2 out in ascending gas	mass N_2 out in ascending gas	mass H_2 out in ascending gas	mass H_2O out in ascending gas	mass tuyere-injected coal hydrocarbon
2															
3	7.7	Fe out in molten iron specification	1000	0	0	0	0	5	0	0	0	0	0	0	0
4	7.2	Fe mass balance	0	-0.768	0	0	0	1	0	0	0	0	0	0	0
5	13.4	O mass balance	0	-0.232	0	-1	0	0	0	0.571	0.727	0	0	0.888	-0.05
6	13.3	C mass balance	0	0	-1	0	0	0	1	0.429	0.273	0	0	0	-0.88
7	13.5	N mass balance	0	0	0	0	-1	0	0	0	0	1	0	0	-0.01
8	7.6	N_2 in blast air specification	0	0	0	0	3.3	-1	0	0	0	0	0	0	0
9	7.9	Equilibrium CO_2/CO mass ratio	0	0	0	0	0	0	0	0.694	-1	0	0	0	0
10	7.8	C out in molten iron specification	0	0	0	0	0	0	0.047	-1	0	0	0	0	0
11	13.6	Enthalpy balance	-320	3.152	-1.359	-1.239	-1.339	1.269	5	-2.926	-7.926	1.008	13.35	-11.50	0
12	13.2	H mass balance	0	0	0	0	0	0	0	0	0	0	1	0.112	0.06
13	11.8	Equilibrium $\text{H}_2\text{O}/\text{H}_2$ mass ratio	0	0	0	0	0	0	0	0	0	0	5.44	-1	0
14	13.1	Coal hydrocarbon injected through tuyeres	60	0	0	0	0	0	0	0	0	0	0	0	1
15			930°C	930°C	1200°C	1200°C	1500°C	1500°C	980°C	990°C	930°C	930°C	930°C	930°C	25°C
16															
17	Bottom segment calculated values		kg per 1000 kg of Fe out in molten iron												
18	mass $\text{Fe}_{\text{bottom}}\text{O}$ into bottom segment	1302													
19	mass C in descending coke	336	also = mass C in the furnace's coke charge, Eqn. (7.16)												
20	mass O_2 in blast	301													
21	mass N_2 in blast	99.2													
22	mass Fe out in molten iron	1000													
23	mass C out in molten iron	47													
24	mass CO out in ascending gas	553													
25	mass CO_2 out in ascending gas	384													
26	mass N_2 out in ascending gas	993													
27	mass H_2 out in ascending gas	2.2													
28	mass H_2O out in ascending gas	12													
29	mass tuyere-injected coal hydrocarbon	60													
30															

Note new Eqs. (13.2)–(13.6).

about the same amount of C-in-coke as pure carbon injection but slightly less O₂-in-blast air for steady production of 1500°C molten iron.

The above values are the result of all our equations. We might postulate that oxygen in the coal hydrocarbon slightly lowers the steady-state need for O₂-in-blast air.

13.7 SUMMARY

Coal hydrocarbon tuyere injection is represented much like "real" natural gas injection, Chapter 29, Bottom Segment Calculations with Natural Gas Injection. The representative steps are;

1. the injectant quantity is specified;
2. bottom segment mass and enthalpy balances are developed and represented in an altered matrix, [Table 13.2](#); and
3. steady-state C-in-coke charge and O₂-in-blast air requirements for producing 1000 kg in product molten iron are calculated.

This chapter's coal hydrocarbon compounds contain 5 mass% oxygen. This slightly lowers the O₂-in-blast requirement for steady production of 1500°C molten iron. C-in-coke requirement is about the same as with pure carbon injection.

- 13.1.** [Table 13.1](#) blast furnace operators wish to increase their coal hydrocarbon injection to 200 kg/1000 kg of Fe in product molten iron.

Please predict for them the amounts of C-in-coke, O₂-in-blast, N₂-in-blast, and air that will be required for steady production of 1500°C molten iron while injecting this 200 kg of coal hydrocarbon.

- 13.2.** The Exercise 13.1 blast furnace operators have refurbished their blast-heating stoves. They hope to raise their blast temperature to 1300°C while continuing with 200 kg of 25°C coal hydrocarbon. How much C-in-coke will this higher blast temperature save?
- 13.3.** The Exercise 13.1 blast furnace plant is running low on coke. Their operators now wish to operate with 250 kg of C-in-coke per 1000 kg of Fe in product molten iron. They would like to know how much 25°C coal hydrocarbon needs to be injected to attain this lower coke requirement.

Please calculate this for them. Note that the blast temperature in this exercise is 1200°C.

Reference

1. Sciazko M. Rank-dependent formation enthalpy of coal. *Fuel* 2013;114:2–9.

EXERCISES

All of these problems refer to the coal hydrocarbon of [Table 13.1](#). All masses are per 1000 kg of Fe in product molten iron.

Raceway Flame Temperature

O U T L I N E

14.1 The Importance of Tuyere Raceway Flame Temperature	131	14.7.3 Raceway Carbon Balance Equation	135
14.2 Tuyere Raceways	132	14.8 Calculation of Raceway Masses	135
14.3 Raceway Flame Temperature	132	14.9 Raceway Input Enthalpy Calculation	135
14.4 Raceway Temperature Defined	132	14.10 Raceway Output Enthalpy	137
14.5 Calculation of Raceway Flame Temperature (No Tuyere Injectant)	133	14.11 Calculation of Raceway Flame Temperature From Total Output Enthalpy	137
14.6 Raceway Input Equations	133	14.12 Numerical Calculation	141
14.7 Raceway Mass Balances	133	14.13 Summary	141
14.7.1 Oxygen Mass Balance Equation	133	Exercises	141
14.7.2 Raceway Nitrogen Mass Balance Equation	135		

14.1 THE IMPORTANCE OF TUYERE RACEWAY FLAME TEMPERATURE

Previous chapters have shown how to calculate a blast furnace's mass O₂-in-blast air and mass C-in-coke requirements for steady production of 1500°C molten iron. They do so with;

- no tuyere injection,
- pulverized carbon and coal hydrocarbon injection,
- pure and impure oxygen injection,
- methane gas - CH₄(g) - injection,
- steam - H₂O(g) - injection, and
- humidity-in-blast air.

We also calculated the amount of N₂-in-blast air that accompanies the

above-mentioned O₂-in-blast air requirement. This, and the next five chapters use the above-calculated O₂ and N₂ masses to calculate raceway flame temperatures for these operating conditions.

This chapter's objectives are to;

1. describe tuyere raceways,
2. define raceway flame temperature and indicate its importance, and
3. show how raceway flame temperature is calculated *with no tuyere injectants*.

14.2 TUYERE RACEWAYS

Section 2.5.1 describes blast furnace raceway present in front of each tuyere. It also provides a sketch.

A raceway is a gas space that;

1. is formed by continuous rapid entry of high pressure blast air through the blast furnace's tuyeres, and
2. consists of hot gas and hot coke particles (~30 mm in diameter) that are continuously falling into and hurtling around the space, Fig. 2.3 and Fig. 14.1.

14.3 RACEWAY FLAME TEMPERATURE

A blast furnace's raceways are the hottest regions in the furnace. They are regions where oxygen in the hot blast reacts with carbon in falling hot coke particles to form even hotter (~2100°C) CO + N₂ gas.

This gas must be;

1. hot enough to ensure that the blast furnace's product iron and slag are completely molten, but
2. not so hot as to prematurely melt the ferrous raw materials before the Fe contained in ore is reduced to wüstite, Fe_{0.947}O.

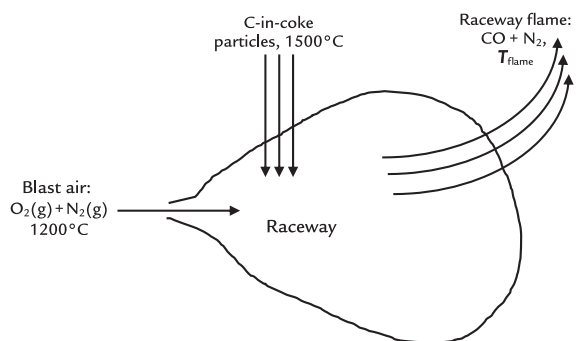


FIGURE 14.1 Sketch of blast furnace tuyere raceway with no tuyere injectants. The inputs are preheated blast air and falling hot C-in-coke particles. The output is hot CO + N₂ gas. All the furnace's blast enters through its raceways. The temperature of the falling C-in-coke particles is specified as 1500°C, the furnace's molten iron tapping temperature. In three dimensions, the raceway is shaped like a horizontal pear.

This chapter and Chapters 15–19 show how to;

1. calculate flame temperature, and
2. vary flame temperature by adjusting blast temperature and/or tuyere injectant quantities.

14.4 RACEWAY TEMPERATURE DEFINED

Raceway flame temperature is defined as the temperature of the raceway output gas;

1. with CO as the only carbonaceous gas product;
2. with H₂ (from hydrocarbon and steam tuyere injectants) as the only hydrogenous gas product; and
3. with no conductive, convective, and radiative heat loss from the raceway to its surroundings.

Definition (3) leads the raceway flame temperature to be called raceway adiabatic flame temperature; RAFT, the industrial acronym.

Product raceway output gas contains CO(g), H₂(g), and N₂(g). This is because;

- any CO₂ in the raceway immediately reacts with hot coke particles to form CO(g), that is,



- any H₂O(g) in the raceway immediately reacts with the hot coke particles to form H₂(g) + CO(g), that is,



- N₂(g) does not react in the raceway.

Reactions (14.1) and (14.2) go to near completion at 1500°C and above, Appendices D, E, G, and H.

14.5 CALCULATION OF RACEWAY FLAME TEMPERATURE (NO TUYERE INJECTANT)

We begin our flame temperature calculation by specifying that;

- calculated steady-state input of O₂-in-blast air, Cell C20 in [Table 14.1](#), and
- calculated steady-state input of N₂-in-blast air, Cell C21 in [Table 14.1](#)

are both blown into the [Fig. 14.1](#) raceway.

We then calculate the *raceway's* output masses, output enthalpy, and output gas (flame) temperature from;

- these O₂ and N₂ input masses and their temperatures, and
- steady-state raceway oxygen, nitrogen, carbon, and enthalpy balances.

14.6 RACEWAY INPUT EQUATIONS

From [Table 14.1](#), input mass equations of [Fig. 14.1](#) are:

$$\left[\begin{array}{l} \text{mass O}_2 \text{ entering} \\ \text{raceway in blast air} \end{array} \right] = \left[\begin{array}{l} 298 \text{ kg O}_2 \text{ per 1000 kg of Fe in product} \\ \text{molten iron (Cell C20)} \end{array} \right]$$

or

$$298 = \left[\begin{array}{l} \text{mass O}_2 \text{ entering} \\ \text{raceway in blast air} \end{array} \right] * 1 \quad (14.3)$$

and

$$\left[\begin{array}{l} \text{mass N}_2 \text{ entering} \\ \text{raceway in blast air} \end{array} \right] = \left[\begin{array}{l} 983 \text{ kg N}_2 \text{ per 1000 kg of Fe in product} \\ \text{molten iron (Cell C21)} \end{array} \right]$$

or

$$983 = \left[\begin{array}{l} \text{mass N}_2 \text{ entering} \\ \text{raceway in blast air} \end{array} \right] * 1 \quad (14.4)$$

14.7 RACEWAY MASS BALANCES

The raceway's basic steady-state mass balances are:

$$\text{mass O into raceway} = \text{mass O out of raceway} \quad (14.5)$$

$$\text{mass N into raceway} = \text{mass N out of raceway} \quad (14.6)$$

$$\text{mass C into raceway} = \text{mass C out of raceway} \quad (14.7)$$

The next three sections expand these equations into useful forms.

14.7.1 Oxygen Mass Balance Equation

Raceway oxygen mass balance [Eq. \(14.5\)](#) expands to;

$$\left[\begin{array}{l} \text{mass O}_2 \text{ entering} \\ \text{raceway in blast air} \end{array} \right] * \frac{100 \text{ mass\% O in O}_2}{100\%}$$

$$= \left[\begin{array}{l} \text{mass CO in} \\ \text{raceway output gas} \end{array} \right] * \frac{57.1 \text{ mass\% O in CO}}{100\%}$$

TABLE 14.1 Bottom-Segment Matrix Without Tuyere Injection

	A	B	C	D	E	F	G	H	I	J	K	L
1	BOTTOM SEGMENT CALCULATION											
2	Equation	Description	Numerical term	mass $\text{Fe}_{0.94}\text{O}$ into bottom segment	mass C in descending coke	mass O_2 in blast air	mass N_2 in blast air	mass Fe out in molten iron	mass C out in molten iron	mass CO out in ascending gas	mass CO_2 out in ascending gas	mass N_2 out in ascending gas
3	7.7	Fe out in molten iron specification	1000	0	0	0	0	1	0	0	0	0
4	7.2	Fe mass balance	0	-0.768	0	0	0	0	0	0	0	0
5	7.3	O mass balance	0	-0.232	0	-1	0	0	0	0.571	0.727	0
6	7.4	C mass balance	0	0	-1	0	0	0	1	0.429	0.273	0
7	7.5	N mass balance	0	0	0	0	-1	0	0	0	0	1
8	7.6	N_2 in air specification	0	0	0	3.3	-1	0	0	0	0	0
9	7.9	Equilibrium CO_2/CO mass ratio	0	0	0	0	0	0	0	0.694	-1	0
10	7.8	C in output molten iron specification	0	0	0	0	0	0.047	-1	0	0	0
11	7.15	Enthalpy balance	-320	3.152	-1.359	-1.239	-1.339	1.269	5	-2.926	-7.926	1.008
12				930°C	930°C	1200°C	1200°C	1500°C	1500°C	930°C	930°C	930°C
13												
14												
15												
16												
17	Bottom segment calculated values		kg per 1000 kg of Fe in product iron									
18	mass $\text{Fe}_{0.94}\text{O}$ into bottom segment		1302									
19	mass C in descending coke		392	also = mass C in the furnace's coke charge, Eqn. (7.16)								
20	mass O_2 in blast air		298									
21	mass N_2 in blast air		983									
22	mass Fe out in molten iron		1000									
23	mass C out in molten iron		47									
24	mass CO out in ascending gas		558									
25	mass CO_2 out in ascending gas		387									
26	mass N_2 out in ascending gas		983									
27												

It is copy of Table 7.2. This chapter uses Cell C20's mass O_2 -in-blast air and Cell C21's mass N_2 -in-blast air values in its raceway calculations. It also includes their enthalpies.

or

$$\left[\begin{array}{l} \text{mass O}_2 \text{ entering} \\ \text{raceway in} \\ \text{blast air} \end{array} \right] * 1 = \left[\begin{array}{l} \text{mass CO in} \\ \text{raceway output gas} \end{array} \right] * 0.571$$

or subtracting $\left\{ \left[\begin{array}{l} \text{mass O}_2 \text{ entering} \\ \text{raceway in blast air} \end{array} \right] * 1 \right\}$ from both sides

$$0 = - \left[\begin{array}{l} \text{mass O}_2 \text{ entering} \\ \text{raceway in blast air} \end{array} \right] * 1 + \left[\begin{array}{l} \text{mass CO in} \\ \text{raceway output gas} \end{array} \right] * 0.571 \quad (14.8)$$

14.7.2 Raceway Nitrogen Mass Balance Equation

Raceway nitrogen mass balance Eq. (14.6) expands to;

$$\left[\begin{array}{l} \text{mass N}_2 \text{ entering} \\ \text{raceway in blast air} \end{array} \right] * \frac{100 \text{ mass\% N in N}_2}{100\%} = \left[\begin{array}{l} \text{mass N}_2 \text{ in} \\ \text{raceway output gas} \end{array} \right] * \frac{100 \text{ mass\% N in N}_2}{100\%}$$

or

$$\left[\begin{array}{l} \text{mass N}_2 \text{ entering} \\ \text{raceway in blast air} \end{array} \right] * 1 = \left[\begin{array}{l} \text{mass N}_2 \text{ in} \\ \text{raceway output gas} \end{array} \right] * 1$$

or subtracting $\left\{ \left[\begin{array}{l} \text{mass N}_2 \text{ entering} \\ \text{raceway in blast air} \end{array} \right] * 1 \right\}$ from both sides

$$0 = - \left[\begin{array}{l} \text{mass N}_2 \text{ entering} \\ \text{raceway in blast air} \end{array} \right] * 1 + \left[\begin{array}{l} \text{mass N}_2 \text{ in} \\ \text{raceway output gas} \end{array} \right] * 1 \quad (14.9)$$

14.7.3 Raceway Carbon Balance Equation

Raceway carbon mass balance Eq. (14.7) expands to;

$$\left[\begin{array}{l} \text{mass C in} \\ \text{falling coke} \\ \text{particles} \end{array} \right] * \frac{100\% \text{ C}}{100\%} = \left[\begin{array}{l} \text{mass CO in} \\ \text{raceway output gas} \end{array} \right] * \frac{42.9 \text{ mass\% C in CO}}{100\%}$$

or

$$\left[\begin{array}{l} \text{mass C in} \\ \text{falling coke} \\ \text{particles} \end{array} \right] * 1 = \left[\begin{array}{l} \text{mass CO in} \\ \text{raceway output gas} \end{array} \right] * 0.429$$

or, subtracting $\left\{ \left[\begin{array}{l} \text{mass C in} \\ \text{falling coke} \\ \text{particles} \end{array} \right] * 1 \right\}$ from both sides

$$0 = - \left[\begin{array}{l} \text{mass C in} \\ \text{falling coke} \\ \text{particles} \end{array} \right] * 1 + \left[\begin{array}{l} \text{mass CO in} \\ \text{raceway output gas} \end{array} \right] * 0.429 \quad (14.10)$$

Table 14.2 shows these equations in matrix form.

14.8 CALCULATION OF RACEWAY MASSES

We use Table 14.1 to calculate raceway input C-in-coke mass and CO(g) and N₂(g) output masses. They are;

- 224 kg C(s) entering raceway in falling coke particles, Cell C45;
- 522 kg of CO(g) in raceway output gas, Cell C46; and
- 983 kg of N₂(g) in raceway output gas, Cell C47

all per 1000 kg of Fe in the furnace's product molten iron at 1500°C.

All are now used to calculate raceway input enthalpy, raceway output enthalpy, and raceway output (flame) temperature.

14.9 RACEWAY INPUT ENTHALPY CALCULATION

Raceway total input enthalpy is calculated from Table 14.1's;

TABLE 14.2 Raceway Matrix for Calculating Raceway Input and Output Masses

	A	B	C	D	E	F	G	H
31	RACEWAY INPUTS AND OUTPUTS CALCULATION							
32	Equation	Description	Numerical Term	mass O ₂ entering raceway in blast air	mass N ₂ entering raceway in blast air	mass C entering raceway in falling coke particles	mass CO in raceway output gas	mass N ₂ in raceway output gas
33	14.3	Mass O ₂ entering raceway in blast air	298	1	0	0	0	0
34	14.4	Mass N ₂ entering raceway in blast air	983	0	1	0	0	0
35	14.10	Raceway carbon balance	0	0	0	-1	0.429	0
36	14.8	Raceway oxygen balance	0	-1	0	0	0.571	0
37	14.9	Raceway nitrogen balance	0	0	-1	0	0	1
38				1200°C	1200°C	1500°C	T _{flame}	T _{flame}
39								
40								
41								
42	Raceway calculated values	kg per 1000 kg of Fe in product iron						
43	mass O ₂ entering raceway in blast air	298						
44	mass N ₂ entering raceway in blast air	983						
45	mass C entering raceway in falling coke particles	224						
46	mass CO in raceway output gas	522						
47	mass N ₂ in raceway output gas	983						
48								

The 298 in Cell C33 and the 983 in Cell C34 are manually carried forward from matrix Table 14.1. Note that mass C entering raceway in falling coke particles is not specified. It is calculated by the raceway matrix, which includes raceway carbon balance Eq. (14.8). Note also that this matrix is placed exactly below Table 14.1 matrix. This is convenient for automatically connecting the two matrices, next chapter.

mass O₂ entering raceway in air blast = 298 kg (Cell C43)
 mass N₂ entering raceway in air blast = 983 kg (Cell C44)

and

mass C entering raceway in falling coke particles
 = 224 kg (Cell C45).

The equation is:

$$\begin{aligned} \left[\begin{array}{l} \text{Total raceway} \\ \text{input enthalpy} \end{array} \right] &= \left[\begin{array}{l} \text{mass O}_2 \text{ entering} \\ \text{raceway in blast air} \end{array} \right] * \frac{H_{1200^\circ\text{C}}^{\circ}}{\text{MW}_{\text{O}_2}} \\ &\quad + \left[\begin{array}{l} \text{mass N}_2 \text{ entering} \\ \text{raceway in blast air} \end{array} \right] * \frac{H_{1200^\circ\text{C}}^{\circ}}{\text{MW}_{\text{N}_2}} \\ &\quad + \left[\begin{array}{l} \text{mass C in falling} \\ \text{coke particles} \end{array} \right] * \frac{H_{1500^\circ\text{C}}^{\circ}}{\text{MW}_{\text{C}}} \end{aligned} \quad (14.11)$$

total raceway input enthalpy in MJ/1000 kg of Fe in product molten iron.

Enthalpy values of Eq. (14.11) are;

$$\frac{H_{1200^\circ\text{C}}^{\circ}}{\text{MW}_{\text{O}_2}} = 1.239$$

$$\frac{H_{1200^\circ\text{C}}^{\circ}}{\text{MW}_{\text{N}_2}} = 1.339$$

$$\frac{H_{1500^\circ\text{C}}^{\circ}}{\text{MW}_{\text{C}}} = 2.488$$

all MJ per kg of substance, Table J.1.

From the above masses and enthalpies, the total raceway input enthalpy is:

$$\begin{aligned} \left[\begin{array}{l} \text{Total raceway} \\ \text{input enthalpy} \end{array} \right] &= 298 * 1.239 + 983 * 1.339 + 224 * 2.488 \\ &= 2243 \text{ MJ per 1000 kg of Fe in product molten iron.} \end{aligned} \quad (14.12)$$

This is included in matrix Table 14.3 by typing;

$$= 298 * 1.239 + 983 * 1.339 + 224 * 2.488$$

in Cell E52 of Table 14.3.

14.10 RACEWAY OUTPUT ENTHALPY

Our raceway temperature calculations specify that there is zero conductive, convective and radiative heat loss from the raceway to its surroundings. This is represented by the equation:

$$\text{Total raceway output enthalpy} + \text{zero} = \text{Total raceway input enthalpy} \quad (14.13a)$$

or from Eq. 14.12:

$$\begin{aligned} \text{total raceway output(flame) enthalpy} \\ = 2243 \text{ MJ/1000 kg of Fe in product molten iron} \end{aligned} \quad (14.13b)$$

This is included in matrix Table 14.3 by typing;

$$= 2243$$

in Cell E53.

14.11 CALCULATION OF RACEWAY FLAME TEMPERATURE FROM TOTAL OUTPUT ENTHALPY

Our raceway flame temperature calculations use;

1. raceway output (flame) enthalpy

2243 MJ per 1000 kg of Fe in product molten iron (Cell E53)

2. raceway output gas masses

$$\left[\begin{array}{l} \text{mass CO in raceway} \\ \text{output gas} \end{array} \right] = \left[\begin{array}{l} 522 \text{ kg per 1000 kg of Fe in} \\ \text{product molten iron (Cell C46)} \end{array} \right]$$

$$\left[\begin{array}{l} \text{mass N}_2 \text{ in raceway} \\ \text{output gas} \end{array} \right] = \left[\begin{array}{l} 983 \text{ kg per 1000 kg of Fe in} \\ \text{product molten iron (Cell C47)} \end{array} \right]$$

and

3. flame temperature enthalpy versus temperature equations of Table J.4:

TABLE 14.3 Matrix [Table 14.2](#) With Added Raceway Enthalpy Equations

	A	B	C	D	E	F	G	H
31	RACEWAY INPUTS AND OUTPUTS CALCULATION							
32	Equation	Description	Numerical Term	mass O ₂ entering raceway in blast air	mass N ₂ entering raceway in blast air	mass C entering raceway in falling coke particles	mass CO in raceway output gas	mass N ₂ in raceway output gas
33	14.3	Mass O ₂ entering raceway in blast air	298	1	0	0	0	0
34	14.4	Mass N ₂ entering raceway in blast air	983	0	1	0	0	0
35	14.10	Raceway carbon balance	0	0	0	-1	0.429	0
36	14.8	Raceway oxygen balance	0	-1	0	0	0.571	0
37	14.9	Raceway nitrogen balance	0	0	-1	0	0	1
38				1200°C	1200°C	1500°C	T _{flame}	T _{flame}
39								
40								
41								
42	Raceway calculated values		kg per 1000 kg of Fe in product iron					
43	mass O ₂ entering raceway in blast air		298					
44	mass N ₂ entering raceway in blast air		983					
45	mass C entering raceway in falling coke particles		224					
46	mass CO in raceway output gas		522					
47	mass N ₂ in raceway output gas		983					
48								
49								
50								
51	FLAME ENTHALPY AND FLAME TEMPERATURE CALCULATIONS							
52	14.12 Total Raceway input enthalpy =298*1.239+983*1.339+224*2.488 =				2243	MJ per 1000 kg of Fe in product molten iron		
53	14.13 Total Raceway output flame enthalpy =2243 =				2243	MJ per 1000 kg of Fe in product molten iron		
54								

Sections 14.11 and 14.12 use the output enthalpy value to calculate raceway flame temperature:

Cell E52 contains Eq. (14.12) = $298 * 1.239 + 983 * 1.339 + 224 * 2.488$

Cell E53 contains Eq. (14.13b) = 2243.

$$\frac{H^\circ T_{\text{flame}}}{\frac{\text{CO(g)}}{\text{MW}_{\text{CO}}}} = 0.001310 * T_{\text{flame}} - 4.183 \quad \text{in MJ per kg of CO(g)}$$

(14.14)

$$\frac{H^\circ T_{\text{flame}}}{\frac{\text{N}_2(\text{g})}{\text{MW}_{\text{N}_2}}} = 0.001301 * T_{\text{flame}} - 0.2448 \quad \text{in MJ per kg of N}_2(\text{g})$$

(14.15)

where T_{flame} is the raceway flame temperature (in °C) of matrix Table 14.3.

The equation that connects these values and equations is:

$$\begin{aligned} & \left[\begin{array}{l} \text{raceway output} \\ (\text{flame}) \text{ enthalpy} \end{array} \right] \\ &= \left[\begin{array}{l} \text{mass CO in raceway} \\ \text{output gas} \end{array} \right] * \frac{H^\circ T_{\text{flame}}}{\frac{\text{CO(g)}}{\text{MW}_{\text{CO}}}} \\ &+ \left[\begin{array}{l} \text{mass N}_2 \text{ in raceway} \\ \text{output gas} \end{array} \right] * \frac{H^\circ T_{\text{flame}}}{\frac{\text{N}_2(\text{g})}{\text{MW}_{\text{N}_2}}} \\ &= \left[\begin{array}{l} \text{mass CO in raceway} \\ \text{output gas} \end{array} \right] * (0.001310 * T_{\text{flame}} - 4.183) \\ &+ \left[\begin{array}{l} \text{mass N}_2 \text{ in raceway} \\ \text{output gas} \end{array} \right] * (0.001301 * T_{\text{flame}} - 0.2448) \end{aligned}$$

or

$$\begin{aligned} & \left[\begin{array}{l} \text{raceway output} \\ (\text{flame}) \text{ enthalpy} \end{array} \right] \\ &= \left[\begin{array}{l} \text{mass CO in raceway} \\ \text{output gas} \end{array} \right] * 0.001310 * T_{\text{flame}} \\ &+ \left[\begin{array}{l} \text{mass N}_2 \text{ in raceway} \\ \text{output gas} \end{array} \right] * 0.001301 * T_{\text{flame}} \\ &+ \left[\begin{array}{l} \text{mass CO in raceway} \\ \text{output gas} \end{array} \right] * (-4.183) \\ &+ \left[\begin{array}{l} \text{mass N}_2 \text{ in raceway} \\ \text{output gas} \end{array} \right] * (-0.2448) \end{aligned}$$

or

$$\begin{aligned} & \left[\begin{array}{l} \text{raceway output} \\ (\text{flame}) \text{ enthalpy} \end{array} \right] \\ &= \left\{ \begin{array}{l} \left[\begin{array}{l} \text{mass CO in raceway} \\ \text{output gas} \end{array} \right] * 0.001310 \\ + \left[\begin{array}{l} \text{mass N}_2 \text{ in raceway} \\ \text{output gas} \end{array} \right] * 0.001301 \end{array} \right\} * T_{\text{flame}} \\ &+ \left[\begin{array}{l} \text{mass CO in raceway} \\ \text{output gas} \end{array} \right] * (-4.183) \\ &+ \left[\begin{array}{l} \text{mass N}_2 \text{ in raceway} \\ \text{output gas} \end{array} \right] * (-0.2448) \end{aligned}$$

or subtracting $\left\{ \left[\begin{array}{l} \text{mass CO in raceway} \\ \text{output gas} \end{array} \right] * (-4.183) + \left[\begin{array}{l} \text{mass N}_2 \text{ in raceway} \\ \text{output gas} \end{array} \right] * (-0.2448) \right\}$ from both sides;

$$\begin{aligned} & \left[\begin{array}{l} \text{raceway output} \\ (\text{flame}) \text{ enthalpy} \end{array} \right] - \left[\begin{array}{l} \text{mass CO in raceway} \\ \text{output gas} \end{array} \right] * (-4.183) \\ &- \left[\begin{array}{l} \text{mass N}_2 \text{ in raceway} \\ \text{output gas} \end{array} \right] * (-0.2448) \\ &= \left\{ \begin{array}{l} \left[\begin{array}{l} \text{mass CO in raceway} \\ \text{output gas} \end{array} \right] * 0.001310 \\ + \left[\begin{array}{l} \text{mass N}_2 \text{ in raceway} \\ \text{output gas} \end{array} \right] * 0.001301 \end{array} \right\} * T_{\text{flame}} \end{aligned}$$

or dividing both sides by

$$\left\{ \begin{array}{l} \left[\begin{array}{l} \text{mass CO in raceway} \\ \text{output gas} \end{array} \right] * 0.001310 \\ + \left[\begin{array}{l} \text{mass N}_2 \text{ in raceway} \\ \text{output gas} \end{array} \right] * 0.001301 \end{array} \right\}$$

$$T_{\text{flame}}, ^\circ\text{C} = \frac{A}{B} \quad (14.16)$$

where

$$A = \left\{ \begin{array}{l} \left[\begin{array}{l} \text{raceway output} \\ (\text{flame}) \text{ enthalpy} \end{array} \right] - \left[\begin{array}{l} \text{mass CO in raceway} \\ \text{output gas} \end{array} \right] * (-4.183) \\ - \left[\begin{array}{l} \text{mass N}_2 \text{ in raceway} \\ \text{output gas} \end{array} \right] * (-0.2448) \end{array} \right\}$$

$$B = \left\{ \begin{array}{l} \left[\begin{array}{l} \text{mass CO in raceway} \\ \text{output gas} \end{array} \right] * 0.001310 \\ + \left[\begin{array}{l} \text{mass N}_2 \text{ in raceway} \\ \text{output gas} \end{array} \right] * 0.001301 \end{array} \right\}$$

TABLE 14.4 Spreadsheet for Calculating Steady State Raceway Flame Temperature of Fig. 14.1

A	B	C	D	E	F	G	H	
31 RACEWAY INPUTS AND OUTPUTS CALCULATION								
32	Equation	Description	Numerical Term	mass O ₂ entering raceway in blast air	mass N ₂ entering raceway in blast air	mass C entering raceway in falling coke particles	mass CO in raceway output gas	
33	14.3	Mass O ₂ entering raceway in blast air	298	1	0	0	0	
34	14.4	Mass N ₂ entering raceway in blast air	983	0	1	0	0	
35	14.10	Raceway carbon balance	0	0	0	-1	0.429	
36	14.8	Raceway oxygen balance	0	-1	0	0	0.571	
37	14.9	Raceway nitrogen balance	0	0	-1	0	1	
38				1200°C	1200°C	1500°C	T _{flame}	
39								
40								
41								
42	Raceway calculated values		kg per 1000 kg of Fe in product iron					
43	mass O ₂ entering raceway in blast air		298					
44	mass N ₂ entering raceway in blast air		983					
45	mass C entering raceway in falling coke particles		224					
46	mass CO in raceway output gas		522					
47	mass N ₂ in raceway output gas		983					
48								
49								
50								
51	FLAME ENTHALPY AND FLAME TEMPERATURE CALCULATIONS							
52	14.12	Total Raceway input enthalpy =	298*1.239+983*1.339+224*2.488 =		2243	MJ per 1000 kg of Fe in product molten iron		
53	14.13	Total Raceway output flame enthalpy =	2243 =		2243	MJ per 1000 kg of Fe in product molten iron		
54								
55	14.17	Flame temperature °C =	(2243-522*-4.183-983*-0.2448)/(522*0.001310+983*0.001301) =		2378	°C		
56								

An equation of Cell F55 is shown to the left of that Cell. The 298 and 983 input values are from bottom-segment matrix Table 14.1.

Cell E52 contains Eq. (14.12) = 298 * 1.239 + 983 * 1.339 + 224 * 2.488

Cell E53 contains Eq. (14.13b) = 2243

Cell F55 contains Eq. (14.17) = (2243 - 522 * -4.183 - 983 * -0.2448)/(522 * 0.001310 + 983 * 0.001301)

which is one linear equation with one unknown.

14.12 NUMERICAL CALCULATION

Including [Table 14.3](#)'s numerical values:

$$\begin{aligned} \left[\begin{array}{l} \text{raceway output} \\ (\text{flame}) \text{ enthalpy} \end{array} \right] &= \left[\begin{array}{l} 2243 \text{ MJ/1000 kg of Fe in product} \\ \text{molten iron, Cell E53} \end{array} \right] \\ \left[\begin{array}{l} \text{mass CO in raceway} \\ \text{output gas} \end{array} \right] &= 522 \text{ kg, Cell C46} \\ \left[\begin{array}{l} \text{mass N}_2 \text{ in raceway} \\ \text{output gas} \end{array} \right] &= 983 \text{ kg, Cell C47} \end{aligned}$$

[Eq. \(14.16\)](#) becomes:

$$\frac{2243 - 522 * (-4.183) - 983 * (-0.2448)}{522 * 0.001310 + 983 * 0.001301} = T_{\text{flame}} = 2378^\circ\text{C} \quad (14.17)$$

This equation is included in the matrix [Table 14.4](#) by typing;

$$= \frac{(2243 - 522 * -4.183 - 983 * -0.2448)}{(522 * 0.001310 + 983 * 0.001301)}$$

in Cell F55 of [Table 14.4](#).

14.13 SUMMARY

A blast furnace's steady-state tuyere raceway flame temperature must be;

1. hot enough to ensure that the furnace's iron and slag products are hot and fully molten, but
2. not so hot as to prematurely melt the ferrous raw materials before the Fe

contained in ore is reduced to wüstite, $\text{Fe}_{0.947}\text{O}$.

This chapter shows how to calculate steady-state tuyere raceway flame temperature. It sequentially calculates the raceway's;

1. input and output masses,
2. input and output enthalpies, and then
3. output gas (flame) temperature.

The next chapter automates these calculations and then describes the effect of blast temperature on raceway flame temperature.

EXERCISES

- 14.1. What must a flame temperature guarantee?
- 14.2. What must it not do?
- 14.3. Management of blast furnace of [Table 14.1](#) is planning to raise its blast temperature to 1250°C . Please predict for them the furnace's steady state:
 - a. total C-in-coke requirement (kg per 1000 kg of Fe in product molten iron)
 - b. air requirement (kg per 1000 kg of Fe in product molten iron)
 - c. raceway flame temperature, $^\circ\text{C}$ with this hotter blast.
 Use Appendix J.3 to determine your 1250°C enthalpies.
- 14.4. Can you draw a general conclusion from the flame temperatures of Exercise 14.3 and [Table 14.4](#)? Can you explain it?

Automating Matrix Calculations

O U T L I N E

15.1 Combining/Automating Blast Furnace Matrices	143	15.6 Forwarding to Our Flame Temperature Calculation	147
15.2 Equations in Cells	143	15.7 Blast Temperature's Effect on Raceway Flame Temperature	147
15.3 Carrying Numerical Values Forward	144	15.8 An Unexpected Benefit	147
15.4 Forwarding Raceway Matrix Masses to the Raceway Input Enthalpy Calculation	144	15.8.1 Explanation	150
15.4.1 Forwarding Blast O ₂ and N ₂ Enthalpies	147	15.9 Summary	150
15.5 Raceway Output Enthalpy	147	Exercises	150

15.1 COMBINING/AUTOMATING BLAST FURNACE MATRICES

This chapter shows how to automate our blast furnace calculations. Its objectives are to:

1. show how equations can be included in matrix cells using matrix Table 14.1 as an example, and
2. show how to automate connections between matrices and between matrices and equations using matrix Tables 14.1–14.4 as examples.

Finally, the chapter shows the effect of blast temperature on raceway flame temperature calculated using the above techniques.

15.2 EQUATIONS IN CELLS

Matrix Table 14.1 provides a perfect starting point for including equations in matrix cells. It manually inserts –1.239 into Cell F11 and –1.339 into Cell G11 where;

$$-1.239 = -\frac{H^\circ \text{ at } 1200^\circ\text{C}}{\text{MW}_{\text{O}_2}}$$

and

$$-1.339 = -\frac{H^\circ \text{ at } 1200^\circ\text{C}}{\text{MW}_{\text{N}_2}}$$

and where the negative signs are a consequence of Eq. (7.15).

These enthalpy values are calculated with Table J.3, enthalpy versus blast temperature equations, that is;

$$-\frac{H^\circ \text{ at } T^\circ\text{C}}{\text{MW}_{\text{O}_2}} = -(0.001137 * T^\circ\text{C} - 0.1257) \quad (15.1)$$

$$-\frac{H^\circ \text{ at } T^\circ\text{C}}{\text{MW}_{\text{N}_2}} = -(0.001237 * T^\circ\text{C} - 0.1450) \quad (15.2)$$

Both Eqs. (15.1) and (15.2) are in MJ per kg of substance.

We now automate these enthalpy calculations. We do so by;

1. typing a blast temperature into Cell D13 of matrix [Table 15.1](#),
2. typing $= -(0.001137 * \text{D13} - 0.1257)$ into Cell F11 of [Table 15.1](#), and
3. typing $= -(0.001237 * \text{D13} - 0.1450)$ into Cell G11 of [Table 15.1](#) so that;

$$\text{Cell F11} = -(0.001137 * \text{D13} - 0.1257) \quad (15.3)$$

and

$$\text{Cell G11} = -(0.001237 * \text{D13} - 0.1450) \quad (15.4)$$

as shown in matrix [Table 15.1](#).

15.3 CARRYING NUMERICAL VALUES FORWARD

Chapter 14, Raceway Flame Temperature, manually carries numerical values forward

from the *bottom segment* matrix calculated values of Table 14.1 to *raceway* matrix of Table 14.2.

Specifically,

1. the value 298 kg of O₂-in-blast air in Cell C20 of Table 14.1 is manually carried forward to Cell C33 of Table 14.2, and
2. the value 983 kg of N₂-in-blast air in Cell C21 of Table 14.1 is manually carried forward to Cell C34, Table 14.2.

We now automate these manual steps in [Table 15.2](#) by typing;

$$= \text{C20} \text{ into Cell C33}$$

and

$$= \text{C21} \text{ into Cell C34}$$

This causes the results from different blast temperatures in [Table 15.1](#) (Cell D13) to be automatically forwarded to the raceway matrix ([Table 15.2](#)).

15.4 FORWARDING RACEWAY MATRIX MASSES TO THE RACEWAY INPUT ENTHALPY CALCULATION

Section 14.9 manually forwards the raceway calculated values of Table 14.2, that is;

mass O₂ entering raceway in blast air = 298

mass N₂ entering raceway in blast air = 983

mass C entering raceway in falling coke particles = 224

to its input raceway enthalpy Eq. (14.12), Table 14.3.

[Table 15.3](#) now automates this step by;

replacing 298 in Eq. (14.12) by C43,
replacing 983 in Eq. (14.12) by C44, and
replacing 224 in Eq. (14.12) by C45

in Cell E52, which now contains:

TABLE 15.1 Matrix Table 14.1 With Enthalpy Versus Temperature Equations in Cells F11 and G11 and Blast Temperature in Cell D13

	A	B	C	D	E	F	G	H	I	J	K	L
1 BOTTOM SEGMENT CALCULATION												
2	Equation	Description	Numerical term	mass Fe _{0.94} O into bottom segment	mass C in descending coke	mass O ₂ in blast air	mass N ₂ in blast air	mass Fe out in molten iron	mass C out in molten iron	mass CO out in ascending gas	mass CO ₂ out in ascending gas	mass N ₂ out in ascending gas
3	7.7	Fe out in molten iron specification	1000	0	0	0	0	1	0	0	0	0
4	7.2	Fe mass balance	0	-0.768	0	0	0	1	0	0	0	0
5	7.3	O mass balance	0	-0.232	0	-1	0	0	0	0.571	0.727	0
6	7.4	C mass balance	0	0	-1	0	0	0	1	0.429	0.273	0
7	7.5	N mass balance	0	0	0	0	-1	0	0	0	0	1
8	7.6	N ₂ in air specification	0	0	0	3.3	-1	0	0	0	0	0
9	7.9	Equilibrium CO ₂ /CO mass ratio	0	0	0	0	0	0	0	0.694	-1	0
10	7.8	C in output molten iron specification	0	0	0	0	0	0.047	-1	0	0	0
11	7.15	Enthalpy balance	-320	3.152	-1.359	-1.239	-1.339	1.269	5	-2.926	-7.926	1.008
12				930°C	930°C	1200	1200	1500°C	1500°C	930°C	930°C	930°C
13		Blast temperature=	1200	°C								
14												
15					=-(0.001137*D13-0.1257)			=-(0.001237*D13-0.1450)				
16												
17		Bottom segment calculated values	kg per 1000 kg of Fe in product iron									
18		mass Fe _{0.94} O into bottom segment	1302									
19		mass C in descending coke	392	also = mass C in the furnace's coke charge, Eqn. (7.16)								
20		mass O ₂ in blast air	298									
21		mass N ₂ in blast air	983									
22		mass Fe out in molten iron	1000									
23		mass C out in molten iron	47									
24		mass CO out in ascending gas	558									
25		mass CO ₂ out in ascending gas	387									
26		mass N ₂ out in ascending gas	983									
27												

The effects of operating with different blast temperatures can now be determined by just altering blast temperature in Cell D13. This strategy can be followed wherever equations are available. For information, Cells F12 and G12 = D13, the blast temperature.

TABLE 15.2 Bottom Segment and Raceway Matrices With Values Automatically Carried Forward From the Bottom Segment Results to the Raceway Matrix. For Information, Cells F12, G12, D38, and E38 all Contain = D13, the Blast Temperature

$$= C43 * 1.239 + C44 * 1.329 + C45 * 2.488 \quad (15.5)$$

$$\left[\begin{array}{l} \text{mass CO in raceway} \\ \text{output gas} \end{array} \right]$$

$$= 522\text{kg}/1000\text{kg of Fe in product molten iron}$$

$$\left[\begin{array}{l} \text{mass N}_2 \text{ in raceway} \\ \text{output gas} \end{array} \right]$$

$$= 983 \text{ kg}/1000 \text{ kg of Fe in product molten iron}$$

to its Eq. (14.17), the raceway flame temperature calculation.

This is automated by replacing 2243 with E53, 522 with C46, and 983 with C47 in Eq. (14.17) so that;

$$T_{\text{flame}} = \frac{2243 - 522 * -4.183 - 983 * -0.2448}{522 * 0.001310 + 983 * 0.001301} \quad (15.8)$$

becomes

$$T_{\text{flame}} = \frac{E53 - C46 * -4.183 - C47 * -0.2448}{C46 * 0.001310 + C47 * 0.001301} \quad (15.9)$$

as shown in [Table 15.4](#).

[Table 15.5](#) now combines [Tables 15.1–15.4](#). It shows all the above-described instructions.

15.5 RACEWAY OUTPUT ENTHALPY

Finally, because we specify no conductive, convective and radiative heat loss from the raceway, Eq. (14.13) may be written as follows;

$$\begin{aligned} &\text{Total raceway output flame enthalpy} \\ &= \text{total raceway input enthalpy} = E52 \end{aligned} \quad (15.7)$$

as shown in [Table 15.3](#).

15.6 FORWARDING TO OUR FLAME TEMPERATURE CALCULATION

Section 14.11 manually forwards;

1. the calculated raceway output (flame) enthalpy = 2243 MJ/1000 kg of Fe in product molten iron, and
2. the calculated raceway output gas masses;

15.7 BLAST TEMPERATURE'S EFFECT ON RACEWAY FLAME TEMPERATURE

Now we can efficiently determine the effect of blast temperature on raceway flame temperature. We might speculate that hotter blast will give a hotter raceway flame. Let's see if this is true using matrix [Table 15.5](#). All we need do is sequentially type several blast temperatures in Cell D13 and record the equivalent Cell F55 raceway flame temperatures ([Fig. 15.1](#)).

15.8 AN UNEXPECTED BENEFIT

An unexpected benefit of this chapter's calculations is that they determine how much C-in-coke falls into a blast furnace's raceways as a function of blast temperature, that is blast enthalpy ([Fig. 15.2](#)).

TABLE 15.3 Calculation of Raceway Input and Output Enthalpies

A	B	C	D	E	F	G	H	I
FLAME ENTHALPY AND FLAME TEMPERATURE CALCULATIONS								
51	15.6	Total Raceway input enthalpy =C43*-F11+C44*-G11+C45*2.488 =		2243	MJ per 1000 kg of Fe in product molten iron			
53	15.7	Total Raceway output flame enthalpy = E52 =		2243	MJ per 1000 kg of Fe in product molten iron			
54								

Raceway masses and O₂-in-blast and N₂-in-blast enthalpies are automatically brought forward to these calculations by inserting their cell addresses as indicated:

Cell E52 = C43 * -F11 + C44 * -G11 + C45 * 2.488

Cell E53 = E52

TABLE 15.4 Calculation of Raceway Flame Temperature by Eq. (14.17) in Cell F55

A	B	C	D	E	F	G	H	I
FLAME ENTHALPY AND FLAME TEMPERATURE CALCULATIONS								
51	15.6	Total Raceway input enthalpy =C43*-F11+C44*-G11+C45*2.488 =		2243	MJ per 1000 kg of Fe in product molten iron			
53	15.7	Total Raceway output flame enthalpy = E52 =		2243	MJ per 1000 kg of Fe in product molten iron			
54								
55	15.9	Raceway flame temperature °C =(E53-C46*-4.183-C47*-0.2448)/(C46*0.00131+C47*0.001301) =		2377	°C			
56								

RAFT is calculated from raceway output enthalpy (Cell E53) and output CO(g) and N₂(g) masses, Cells C46 and C47, [Table 15.2](#).

Cell F55 = (E53 - C46 * -4.183 - C47 * -0.2448) / (C46 * 0.001310 + C47 * 0.001301).

TABLE 15.5 Matrix Showing All This Chapter's Forwarding Instructions

A	B	C	D	E	F	G	H	I	J	K	L
BOTTOM SEGMENT CALCULATION											
Equation	Description	Numerical term	mass Fe _{98%} O into bottom segment	mass C in descending coke	mass O ₂ in blast air	mass N ₂ in blast air	mass Fe out in molten iron	mass C out in molten iron	mass CO out in ascending gas	mass CO ₂ out in ascending gas	mass N ₂ out in ascending gas
7.1	Fe out in molten iron specification	1000	0	0	0	0	1	0	0	0	0
7.2	Fe mass balance	0	-0.768	0	0	0	1	0	0	0	0
7.3	O mass balance	0	-0.232	0	-1	0	0	0	0.571	0.727	0
7.4	C mass balance	0	0	-1	0	0	1	0.429	0.273	0	
7.5	N mass balance	0	0	0	0	-1	0	0	0	0	1
7.6	N ₂ in air specification	0	0	0	3.3	-1	0	0	0	0	0
7.9	Equilibrium CO ₂ /CO mass ratio	0	0	0	0	0	0	0	0.694	-1	0
7.8	C in output molten iron specification	0	0	0	0	0	0.047	-1	0	0	0
7.15	Enthalpy balance	-320	3.152	-1.359	-1.239	-1.339	1.269	5	-2.926	-7.926	1.008
7.2			930°C	930°C	1200	1200	1500°C	1500°C	930°C	930°C	930°C
13	Blast temperature=		1200	°C							
14											
15					=(-0.001137*D13*0.1257)			=(-0.001237*D13*0.1450)			
16											
17	Bottom segment calculated values	kg per 1000 kg of Fe in product iron									
18	mass Fe _{98%} O into bottom segment	1302									
19	mass C in descending coke	392	also = mass C in the furnace's coke charge, Eqn. (7.16)								
20	mass O ₂ in blast air	298									
21	mass N ₂ in blast air	983									
22	mass Fe out in molten iron	1000									
23	mass C out in molten iron	47									
24	mass CO out in ascending gas	558									
25	mass CO ₂ out in ascending gas	387									
26	mass N ₂ out in ascending gas	983									
27											
28											
29											
30					=C20	=C21					
31	RACEWAY INPUTS AND OUTPUTS CALCULATION										
32	Equation	Description	Numerical Term	mass O ₂ entering raceway in blast air	mass N ₂ entering raceway in blast air	mass C entering raceway in falling coke particles	mass CO in raceway output gas	mass N ₂ in raceway output gas			
33	14.3	Mass O ₂ entering raceway in blast air	298	1	0	0	0	0			
34	14.4	Mass N ₂ entering raceway in blast air	983	0	1	0	0	0			
35	14.10	Raceway carbon balance	0	0	0	-1	0.429	0			
36	14.8	Raceway oxygen balance	0	-1	0	0	0.571	0			
37	14.9	Raceway nitrogen balance	0	0	-1	0	0	1			
38				1200	1200	1500°C	T _{flame}	T _{flame}			
39											
40											
41											
42	Raceway calculated values	kg per 1000 kg of Fe in product iron									
43	mass O ₂ entering raceway in blast air	298									
44	mass N ₂ entering raceway in blast air	983									
45	mass C entering raceway in falling coke particles	224									
46	mass CO in raceway output gas	522									
47	mass N ₂ in raceway output gas	983									
48											
49											
50											
51	FLAME ENTHALPY AND FLAME TEMPERATURE CALCULATIONS										
52	15.6	Total Raceway input enthalpy =C43+F11+C44+G11+C45*2.488=			2243	MJ per 1000 kg of Fe in product molten iron					
53	15.7	Total Raceway output flame enthalpy = E52 =			2243	MJ per 1000 kg of Fe in product molten iron					
54											
55	15.9	Raceway flame temperature °C =(E53*C46*-4.183-C47*-0.2448)/(C46*0.00131+C47*0.001301) =			2377	°C					
56											

A change in blast furnace temperature (Cell D13) automatically calculates a new flame temperature, Cell F55.

Cell E52 = C43 * -F11 + C44 * -G11 + C45 * 2.488 and Cell E53 = E52

Cell F55 = (E53 - C46 * -4.183 - C47 * -0.2448)/(C46 * 0.00131 + C47 * 0.001301)

For information, Cells F12, G12, D38, and E38 all = D13.

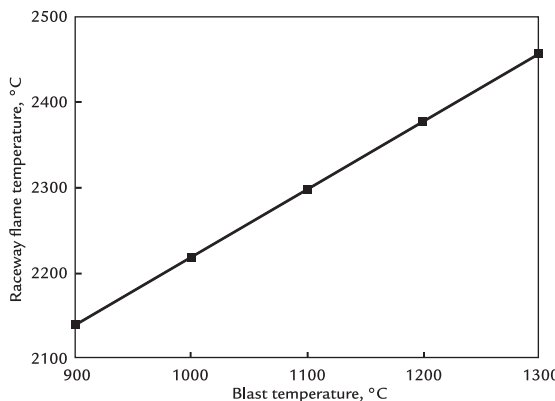


FIGURE 15.1 Graph showing that raceway flame temperature increases with increasing blast temperature. The line is straight. The slope is 0.79, indicating that a 100°C increase in blast temperature raises raceway flame temperature by 79°C. The reason for the difference lies in all the equations of Table 15.5. We may postulate that it is mainly because mass raceway output gas is always greater than mass blast (Table 15.5). The raceway output gas has more mass than the input blast air as the raceway output gas contains carbon while the blast air does not (Fig. 14.1).

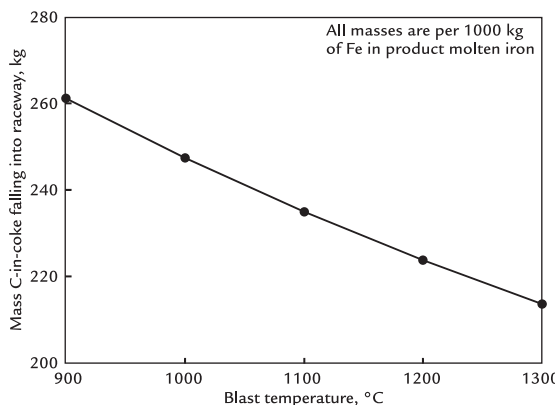


FIGURE 15.2 Effect of blast temperature on the amount of C-in-coke that is (1) falling into a blast furnace's raceways and (2) being burnt to CO(g) by blast air in the raceway. As shown, it decreases with increasing blast temperature as discussed below.

Fig. 15.2 shows that the amount of C-in-coke falling into the raceways decreases with increasing blast temperature.

15.8.1 Explanation

The result of Fig. 15.2 is a consequence of all the equations of Table 15.5. We may postulate that the main cause is the increase in blast enthalpy with increasing blast temperature.

The blast furnace's thermal balance is maintained with this increased blast enthalpy by reducing the amount of C-in-coke that is combusted by the blast air in the furnace's raceways, as shown in Fig. 15.2.

15.9 SUMMARY

This chapter shows how our matrices and equations can be connected so that the effect of blast temperature on raceway flame temperature can be determined by changing only one cell, Cell D13.

EXERCISES

- 15.1. The blast furnace engineering team of Table 15.5 has refurbished its blast-heating stoves and is now planning to raise its blast temperature to 1250°C. They wish to know what its raceway adiabatic flame temperature will be with this 1250°C blast. Please calculate it for them using Table 15.5 as a model matrix spreadsheet.
- 15.2. The engineering team of Table 15.5 wants its tuyere raceway flame temperature to be exactly 2400°C. Please calculate what their blast temperature must be to obtain this flame temperature. Use two methods.
- 15.3. Our flame temperature calculations specify adiabatic conditions. Flame temperatures calculated this way are useful for examining the effects of various tuyere inputs on raceway flame temperature. Your professor, however, states that raceway conditions are far from adiabatic. What do you think?

16

Raceway Flame Temperature With Pulverized Carbon Injection

O U T L I N E

16.1 Impact of Pulverized Carbon Injection on Raceway Flame Temperature	151	16.8 Raceway Matrix Results	155
16.2 Matrix Setup	152	16.9 Input Enthalpy Calculation	155
16.3 Raceway Injectant Quantity Specification	152	16.9.1 Automated Input Enthalpy Calculation	155
16.4 Raceway O ₂ -in-Blast Air Input Specification	152	16.10 Raceway Output Enthalpy	156
16.5 Raceway N ₂ -in-Blast Air Input Specification	154	16.11 Raceway Flame Temperature Calculation	156
16.6 Raceway Carbon Balance Equation With Pulverized C Injection	154	16.12 Effect of C Injection on Raceway Flame Temperature	156
16.7 Oxygen and Nitrogen Balances	154	16.13 Summary	157
		Exercise	157

16.1 IMPACT OF PULVERIZED CARBON INJECTION ON RACEWAY FLAME TEMPERATURE

Chapter 14, Raceway Flame Temperature, and Chapter 15, Automating Matrix Calculations, calculate raceway adiabatic flame

temperature (RAFT) without tuyere injectants (Fig. 14.1). This chapter calculates RAFT with *tuyere injection of pulverized carbon* (Fig. 16.1).

The objectives of this chapter are to;

1. show how injected pulverized carbon is included in our raceway flame temperature calculations,

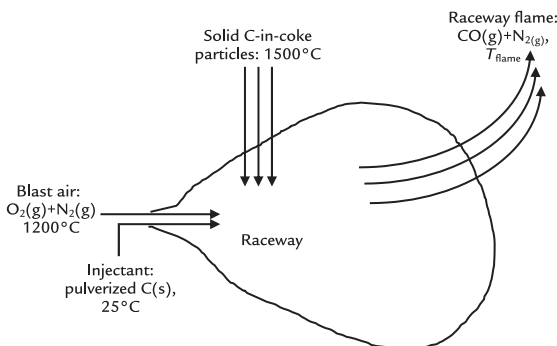


FIGURE 16.1 Sketch of blast furnace raceway with tuyere injection of pulverized C(s). The C(s) is a simplified stand-in for pulverized coal. All the blast furnace's blast air and injected C enter the furnace through its raceways. All the injectants are oxidized to CO(g) in the raceway. The sketch is a vertical slice through the center of a pear-shaped raceway.

2. indicate how injected pulverized carbon affects raceway flame temperature, and
3. explain this effect.

16.2 MATRIX SETUP

Our carbon injection raceway calculations start with the matrix of the *calculated results* of the bottom-segment carbon injection of Table 8.1 (**Table 16.1**).

We then prepare a tuyere *raceway calculation matrix* with these results by;

1. specifying that all the matrices of tuyere-injected carbon, O₂-in-blast air, and N₂-in-blast air, of Fig. 16.1, enter blast furnace through its raceways, and
2. developing raceway oxygen, nitrogen, and carbon balances.

The matrix's spreadsheet then calculates the raceway's;

1. mass input C-in-falling-coke particles;
2. mass output CO(g) and N₂(g);

3. input and output enthalpies from these input masses and their H°_T/MW
4. output gas (flame) temperature from the raceway's output masses, output enthalpy, and H°_{T_{flame}}/MW versus temperature equations of Table J.4.

The matrices and their results are shown in **Table 16.1**. Explanations follow.

16.3 RACEWAY INJECTANT QUANTITY SPECIFICATION

The raceway calculation begins by specifying that the raceway injectant C input mass is 100 kg, as shown in Cell C12 of matrix **Table 16.1**. It is;

$$\left[\begin{array}{l} \text{mass C in tuyere} \\ \text{injected carbon} \end{array} \right] = 100 \text{ (in this case)}$$

or in matrix form;

$$100 = \left[\begin{array}{l} \text{mass C in tuyere} \\ \text{injected carbon} \end{array} \right] * 1 \quad (16.1)$$

where 100 is the kg of injected pulverized carbon per 1000 kg of Fe in product molten iron.

For flexibility, this injection quantity is put into Cell C38 of matrix **Table 16.1** by the instruction =C12.

This instruction causes any prescribed amount of injected carbon to be automatically updated in the raceway matrix.

16.4 RACEWAY O₂-IN-BLAST AIR INPUT SPECIFICATION

The bottom-segment matrix results of matrix **Table 16.1** show that 310 kg of O₂-in-blast air per 1000 kg of Fe in product molten iron is required for steady-state bottom-segment operation, see Cell C21. This is also the amount of O₂ entering the blast furnace raceways per 1000 kg of Fe in product molten iron.

TABLE 16.1 Bottom Segment Matrix, Raceway Matrix, and Flame Temperature Calculation With C(s) Injection

A	B	C	D	E	F	G	H	I	J	K	L	M
1 BOTTOM SEGMENT CALCULATION												
Equation	Description	Numerical term	mass Fe _{0.94} O into bottom segment	mass C in descending coke	mass O ₂ in blast air	mass N ₂ in blast air	mass Fe out in molten iron	mass C out in molten iron	mass CO out in ascending gas	mass CO ₂ out in ascending gas	mass N ₂ out in ascending gas	mass C in tuyere-injected carbon
7.7	Fe out in molten iron specification	1000	0	0	0	0	1	0	0	0	0	0
7.2	Fe mass balance	0	-0.768	0	0	0	0	0	0	0	0	0
7.3	O mass balance	0	-0.232	0	-1	0	0	0	0.571	0.727	0	0
8.3	C mass balance	0	0	-1	0	0	1	0.429	0.273	0	-1	0
7.5	N mass balance	0	0	0	0	-1	0	0	0	0	1	0
7.6	N ₂ in air specification	0	0	0	3.3	-1	0	0	0	0	0	0
7.9	Equilibrium CO ₂ /CO mass ratio	0	0	0	0	0	0	0	0.694	-1	0	0
7.8	C in output molten iron specification	0	0	0	0	0	0.047	-1	0	0	0	0
8.5	Entropy balance	-320	3.152	-1.359	-1.239	-1.339	1.269	5	-2.926	-7.926	1.008	0
8.1	C injected through tuyeres	100	0	0	0	0	0	0	0	0	0	1
			930°C	930°C	1200	1200	1500°C	1500°C	930°C	930°C	930°C	25°C
14	Blast temperature=	1200	°C									
15			= (0.001137 * D13 - 0.1257)				= (0.001237 * D14 - 0.1450)					
16												
17	Bottom segment calculated values											
18	mass Fe _{0.94} O into bottom segment	1302										
19	mass C in descending coke	299	also = mass C in the furnace's coke charge, Eqn. (7.16)									
20	mass O ₂ in blast air	310										
21	mass N ₂ in blast air	1024										
22	mass Fe out in molten iron	1000										
23	mass C out in molten iron	47										
24	mass CO out in ascending gas	569										
25	mass CO ₂ out in ascending gas	395										
26	mass N ₂ out in ascending gas	1024										
27	mass C in tuyere-injected carbon	100										
28												
29												
30												
31	RACEWAY INPUTS AND OUTPUTS CALCULATION											
32	Equation	Description	Numerical Term	mass O ₂ entering raceway in blast air	mass N ₂ entering raceway in blast air	mass C entering raceway in falling coke particles	mass CO in raceway exit gas	mass N ₂ in raceway exit gas	mass C tuyere-injected pulverized carbon			
33	16.2	Mass O ₂ entering raceway in blast air	310	1	0	0	0	0	0			
34	16.3	Mass N ₂ entering raceway in blast air	1024	0	1	0	0	0	0			
35	14.8	Raceway oxygen balance	0	-1	0	0	0.571	0	0			
36	14.9	Raceway nitrogen balance	0	0	-1	0	0	1	0			
37	16.4	Raceway carbon balance	0	0	0	-1	0.429	0	1			
38	16.1	Mass C in tuyere-injected carbon	100	0	0	0	0	0	1			
39				1200	1200	1500°C	T _{flame}	T _{flame}	298°C			
40				=C12								
41												
42	Raceway calculated values											
43	mass O ₂ entering raceway in blast air	310										
44	mass N ₂ entering raceway in blast air	1024										
45	mass C entering raceway in falling coke particles	133										
46	mass CO in raceway output gas	543										
47	mass N ₂ in raceway output gas	1024										
48	mass C in tuyere-injected pulverized carbon	100										
49												
50												
51	FLAME ENTHALPY AND FLAME TEMPERATURE CALCULATIONS											
52	16.6b	Total Raceway input enthalpy = C48*0+C43*-F11+C44*-G11+C45*2.488 =	2087	MJ per 1000 kg of Fe in product molten iron								
53	16.7	Total Raceway output flame enthalpy = E52 =	2087	MJ per 1000 kg of Fe in product molten iron								
54												
55	16.8b	Raceway flame temperature °C = (E53-C46*4.183-C47*-0.2488)/(C46*0.001310+C47*0.001301) =	2258	°C								
56												

Cell E53 = E52

Cell E52 = C48 * 0 + C43 * - F11 + C44 * - G11 + C45 * 2.488

Cell F55 = (E53 - C46 * - 4.183 - C47 * - 0.2488)/(C46 * 0.001310 + C47 * 0.001301)

Oxygen is included in the raceway matrix by the O₂ specification equation;

$$\left[\frac{\text{mass O}_2 \text{ entering}}{\text{raceway in blast air}} \right] = 310$$

or in matrix terms

$$310 = \left[\frac{\text{mass O}_2 \text{ entering}}{\text{raceway in blast air}} \right] * 1 \quad (16.2a)$$

Of course, this numerical value will change with different amounts of injected C. This is automatically taken care of in [Table 16.1](#) by inserting the instruction

$$= C20 \quad (16.2b)$$

into raceway matrix Cell C33.

16.5 RACEWAY N₂-IN-BLAST AIR INPUT SPECIFICATION

The bottom-segment matrix of [Table 16.1](#) shows that 1024 kg of N₂ accompany 310 kg of O₂-in-blast air by [Eqs. \(16.2a\) and \(16.2b\)](#). This is also the amount of N₂ entering the blast furnace raceways per 1000 kg of Fe in product molten iron.

It is included in the raceway matrix by means of the specification equation;

$$\left[\frac{\text{mass N}_2 \text{ entering}}{\text{raceway in blast air}} \right] = 1024$$

or in matrix terms

$$1024 = \left[\frac{\text{mass N}_2 \text{ entering}}{\text{raceway in blast air}} \right] * 1 \quad (16.3a)$$

This numerical value will also change with different amounts of injected pulverized carbon. This is automatically taken care of in [Table 16.1](#) by inserting the instruction

$$= C21 \quad (16.3b)$$

into raceway matrix Cell C34.

16.6 RACEWAY CARBON BALANCE EQUATION WITH PULVERIZED C INJECTION

With pulverized C injection, the raceway carbon balance equation of Chapter 14, Raceway Flame Temperature, becomes;

$$\begin{aligned} & \left[\frac{\text{mass C in tuyere}}{\text{injected carbon}} \right] * \left[\frac{100 \text{ mass\% C}}{\text{in pulverized C}} \right] \\ & + \left[\frac{\text{mass C entering in}}{\text{falling coke particles}} \right] * \left[\frac{100 \text{ mass\% C}}{\text{in pulverized C}} \right] \\ & = \left[\frac{\text{mass CO in raceway}}{\text{output gas}} \right] * \frac{[42.9 \text{ mass\% C in CO}]}{100\%} \end{aligned}$$

or

$$\begin{aligned} & \left[\frac{\text{mass C in tuyere}}{\text{injected carbon}} \right] * 1 + \left[\frac{\text{mass C entering in}}{\text{falling coke particles}} \right] * 1 \\ & = \left[\frac{\text{mass CO in raceway}}{\text{output gas}} \right] * 0.429 \\ \text{or, subtracting } & \left\{ \left[\frac{\text{mass C in tuyere}}{\text{injected carbon}} \right] * 1 \right. \\ & \left. + \left[\frac{\text{mass C entering in}}{\text{falling coke particles}} \right] \right\} \text{ from both sides:} \\ 0 = & - \left[\frac{\text{mass C in tuyere}}{\text{injected carbon}} \right] * 1 - \left[\frac{\text{mass C entering in}}{\text{falling coke particles}} \right] * 1 \\ & + \left[\frac{\text{mass CO in raceway}}{\text{output gas}} \right] * 0.429 \end{aligned} \quad (16.4)$$

where the coal and coke are (for now) specified as pure carbon. The effects of real coal and real coke are described in the later chapters.

16.7 OXYGEN AND NITROGEN BALANCES

Oxygen and nitrogen balances of Chapter 14, Raceway Flame Temperature, are not altered by pulverized C injection. They are as shown in [Table 16.1](#).

16.8 RACEWAY MATRIX RESULTS

The raceway matrix results are shown in Cells C45–C47 of Table 16.1. The calculated masses are:

- 133 kg of C in falling coke particles,
- 543 kg CO in departing raceway gas, and
- 1024 kg N₂ in departing raceway gas.

16.9 INPUT ENTHALPY CALCULATION

The above-calculated 133 kg of C in falling coke particles now permits calculation of the raceway's input enthalpy. It is:

$$\begin{bmatrix} \text{raceway} \\ \text{input} \\ \text{enthalpy} \end{bmatrix} * 1 = \begin{bmatrix} \text{mass C in tuyere} \\ \text{injected carbon} \end{bmatrix} * \frac{H_{25^\circ\text{C}}}{\text{MW}_\text{C}}$$

$$+ \begin{bmatrix} \text{mass O}_2 \text{ entering} \\ \text{raceway in blast air} \end{bmatrix} * \frac{O_2(\text{g})}{\text{MW}_{O_2}}$$

$$+ \begin{bmatrix} \text{mass N}_2 \text{ entering} \\ \text{raceway in blast air} \end{bmatrix} * \frac{N_2(\text{g})}{\text{MW}_{N_2}}$$

$$+ \begin{bmatrix} \text{mass C entering} \\ \text{raceway in falling} \\ \text{coke particles} \end{bmatrix} * \frac{H_{1500^\circ\text{C}}}{\text{MW}_\text{C}}$$
(16.5)

or

$$\begin{bmatrix} \text{raceway} \\ \text{input} \\ \text{enthalpy} \end{bmatrix} = C48 * 0 + C43 * 1.239 + C44 * 1.339$$

$$+ C45 * 2.488 = 2087 \text{ MJ per 1000 kg of Fe in product molten iron}$$
(16.6a)

where Cell C48 and Cells C43–C45 refer to Table 16.1 and where;

$$0 = \frac{C(\text{s})}{\text{MW}_\text{C}}$$

$$1.239 = \frac{H_{1200^\circ\text{C}}}{\text{MW}_{O_2}}$$

$$1.339 = \frac{H_{1200^\circ\text{C}}}{\text{MW}_{N_2}}$$

$$2.488 = \frac{H_{1500^\circ\text{C}}}{\text{MW}_\text{C}}$$

all MJ per kg of substance, Table J.1.

16.9.1 Automated Input Enthalpy Calculation

Eq. (16.5) can be put in final automated form by replacing;

$$\frac{O_2(\text{g})}{\text{MW}_{O_2}} \text{ by } -F11$$

and

$$\frac{N_2(\text{g})}{\text{MW}_{N_2}} \text{ by } -G11$$

which changes Eq. (16.6a) to:

$$\begin{bmatrix} \text{raceway} \\ \text{input} \\ \text{enthalpy} \end{bmatrix} = C48 * 0 + C43 * -F11 + C44 * -G11$$

$$+ C45 * 2.488 = 2087 \text{ MJ per 1000 kg of Fe in product molten iron}$$
(16.6b)

This equation is now inserted into Cell E52 by the instruction:

$$= C48 * 0 + C43 * -F11 + C44 * -G11 + C45 * 2.488$$

16.10 RACEWAY OUTPUT ENTHALPY

Raceway output enthalpy is needed to calculate our raceway adiabatic flame temperature (RAFT).

RAFT is calculated by the following equation;

$$\begin{bmatrix} \text{Raceway} \\ \text{output} \\ \text{enthalpy} \end{bmatrix} + \text{zero} = \begin{bmatrix} \text{Raceway} \\ \text{input} \\ \text{enthalpy} \end{bmatrix}$$

assuming zero conductive, convective, and radiative heat loss from the raceway to its surroundings.

From [Section 16.9](#), the raceway input enthalpy is 2087 MJ so that:

$$\begin{bmatrix} \text{Raceway} \\ \text{output} \\ \text{enthalpy} \end{bmatrix} = \begin{bmatrix} \text{Raceway} \\ \text{input} \\ \text{enthalpy} \end{bmatrix} = E52$$

= 2087 MJ per 1000 kg of Fe in product molten iron. (16.7)

This equation is inserted into Cell E53 by the instruction;

= E52

16.11 RACEWAY FLAME TEMPERATURE CALCULATION

Our raceway flame temperature calculations use;

1. raceway CO and N₂ output masses, 543 and 1024 kg (from Cells C46 and C47), and
2. raceway output enthalpy, 2087 MJ from Cell E53

of matrix [Table 16.1](#) all per 1000 kg of Fe in product molten iron.

The flame temperature equation is the same as in [Section 14.11](#), that is;

$$\left\{ \begin{array}{l} \left[\begin{array}{l} \text{raceway output} \\ \text{(flame) enthalpy} \end{array} \right] \\ - \left[\begin{array}{l} \text{mass CO in raceway} \\ \text{output gas} \end{array} \right] * (-4.813) \\ - \left[\begin{array}{l} \text{mass N}_2 \text{ in raceway} \\ \text{output gas} \end{array} \right] * (-0.2488) \end{array} \right\} = T_{\text{flame}}, {}^{\circ}\text{C}$$

$$\left\{ \begin{array}{l} \left[\begin{array}{l} \text{mass CO in raceway} \\ \text{output gas} \end{array} \right] * 0.001310 \\ + \left[\begin{array}{l} \text{mass N}_2 \text{ in raceway} \\ \text{output gas} \end{array} \right] * 0.001301 \end{array} \right\}$$
(14.16)

where the numerical values are from our enthalpy versus flame temperature equations of [Table J.4](#), that is,

$$\frac{H^{\circ}_{T_{\text{flame}}}}{\text{CO(g)}} = 0.001310 * T_{\text{flame}} - 4.183 \text{ MJ per kg of CO(g)} \quad (14.14)$$

$$\frac{H^{\circ}_{T_{\text{flame}}}}{\text{N}_2(\text{g})} = 0.001301 * T_{\text{flame}} - 0.2488 \text{ MJ per kg of N}_2(\text{g}) \quad (14.15)$$

For the numerical example in [Table 16.1](#), the raceway flame temperature is:

$$T_{\text{flame}} = \frac{E53 - C46 * (-4.183) - C47 * (-0.2488)}{C46 * 0.001310 + C47 * 0.001301} = 2258^{\circ}\text{C} \quad (16.8a)$$

This is inserted into Cell F55 by the instruction:

$$= \frac{E53 - C46 * -4.183 - C47 * -0.2488}{C46 * 0.001310 + C47 * 0.001301} \quad (16.8b)$$

16.12 EFFECT OF C INJECTION ON RACEWAY FLAME TEMPERATURE

[Table 16.1](#) is now used to determine the effect of pulverized C injection on raceway flame temperature ([Fig. 16.2](#)).

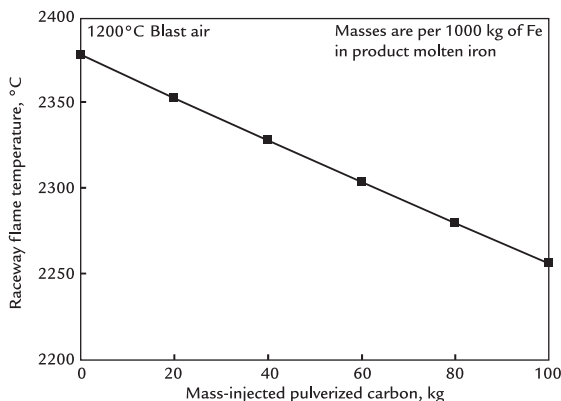


FIGURE 16.2 Effect of injected C on blast furnace raceway temperature. Raceway temperature decreases with increasing C injection. This is a consequence of all the equations of [Table 16.1](#). We may speculate that it is mainly due to replacing hot (high enthalpy) falling C-in-coke with cool (low enthalpy) tuyere-injected pulverized carbon. A quantity of 100 kg carbon injection per 1000 kg Fe in product molten iron lowers flame temperature by $\sim 120^{\circ}\text{C}$. The line segments are not quite straight. This is because [Eq. \(16.18a\)](#) is not linear.

16.13 SUMMARY

This chapter shows how to calculate raceway flame temperature with tuyere injection of pulverized carbon. The steps are to;

1. calculate the bottom-segment C-in-coke and O₂-in-blast air requirements for steady-state blast furnace operation with pulverized C injection;
2. calculate the corresponding amount of N₂-in-blast air;
3. preparation of a raceway matrix including pulverized carbon injection;
4. calculate the raceway's mass input C-in-falling-coke particles, mass output CO(g) and mass output N₂(g);
5. calculate raceway input and output enthalpies, using the enthalpy versus temperature equations of [Table J.4](#); and

6. calculate raceway output gas (flame) temperature, also using enthalpy versus flame temperature equations of [Table J.4](#).

These steps can all be automated as described in [Table 16.1](#).

Raceway flame temperature decreases with increasing C injection. This is mainly due to the replacement of hot (high enthalpy) falling C-in-coke particles with cool (low enthalpy) injected pulverized C-in-coal.

As it will be shown later, this decrease in flame temperature can be offset by;

1. simultaneous injection of pure oxygen into the furnace's blast air, and
2. higher temperature blast air.

EXERCISE

- 16.1. Please give your calculated masses in kg per 1000 kg of Fe in product molten iron.

The blast furnace management team of [Table 16.1](#) plans to increase its tuyere-injected pulverized carbon to 175 kg/1000 kg of Fe in product molten iron. They want to know how this increase will affect their raceway flame temperature. Please calculate this for them.

- 16.2. Please also calculate how much top-charge C-in-coke will be required with this injection of 175 kg pulverized carbon.

The blast furnace engineering team of [Table 16.1](#) believes that it shouldn't let its raceway flame temperature fall below 2200°C. What is the maximum amount of pulverized carbon that they can inject without cooling the flame below this

set-point? Please use two calculation methods.

Suggest several ways that pulverized carbon injection can be increased further without lowering the raceway flame temperature below 2200°C?

16.3. As we will see later, coal always contains $\text{Al}_2\text{O}_3 + \text{SiO}_2$ ash. So, tuyere-injected pulverized coal always brings these oxides into a blast furnace's raceways. What effect do you think will they have on flame temperature?

Raceway Flame Temperature With Oxygen Enrichment

O U T L I N E

17.1 Benefits of Oxygen Enrichment and Impact on Raceway Flame Temperature	160	17.9 Raceway Matrix Results	163
17.2 Matrix Setup	160	17.10 Raceway Input Enthalpy Calculation	164
17.3 Raceway Pure Oxygen Quantity Specification	160	17.10.1 Automated Input Enthalpy Calculation	164
17.4 Raceway O ₂ -in-Blast Air Input Specification	162	17.11 Automated Raceway Output Enthalpy	165
17.5 Raceway N ₂ -in-Blast Air Specification	162	17.12 Raceway Output Gas (Flame) Temperature	165
17.6 Raceway O Balance With Pure Oxygen Injection	162	17.13 Effect of Pure Oxygen Injection on Raceway Flame Temperature	166
17.7 Raceway Carbon Balance	163	17.14 Summary	166
17.8 Raceway Nitrogen Balance Equation	163	Exercise	166

17.1 BENEFITS OF OXYGEN ENRICHMENT AND IMPACT ON RACEWAY FLAME TEMPERATURE

Chapter 16, Raceway Flame Temperature With Pulverized Carbon Injection, calculated raceway flame temperature with pure carbon injection (Fig. 16.1). This chapter calculates it with tuyere injection of Pure Oxygen (Fig. 17.1). The objectives are to;

1. show how pure oxygen injection is included in our raceway flame temperature calculations,
2. indicate how pure oxygen injection affects raceway flame temperature, and
3. explain this flame temperature effect.

17.2 MATRIX SETUP

Our oxygen injection calculation uses bottom-segment oxygen injection results of Table 9.1 (as copied in Table 17.1). We then prepare a tuyere *raceway calculation matrix* with these results by;

1. specifying that all the injected pure oxygen of Fig. 17.1, O_2 -in-blast air, and N_2 -in-blast air enter the raceway at $1200^\circ C$, and
2. developing a new raceway oxygen balance.

The matrix then calculates the raceway's;

3. input and output masses;
4. input enthalpy from its input masses and their H_{T}° / MW values (remembering that the injected oxygen enters the raceway at the blast temperature);
5. output enthalpy from its input enthalpy; and
6. output gas (flame) temperature from the raceway's output enthalpy, output masses, and $H_{T_{\text{flame}}}^\circ / MW$ versus temperature equations of Table J.4.

The matrices and calculations are shown in Table 17.1. Explanations follow.

17.3 RACEWAY PURE OXYGEN QUANTITY SPECIFICATION

The raceway calculation is begun by specifying the raceway mass O_2 in injected pure oxygen, Cell C12 of matrix Table 17.1. It is;

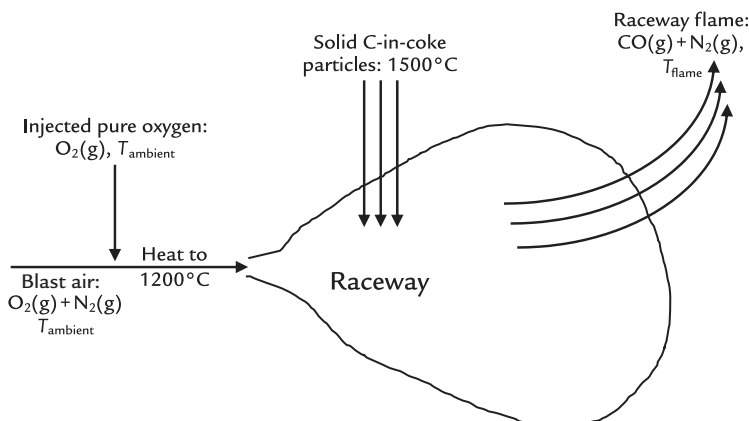


FIGURE 17.1 Sketch of blast furnace raceway with tuyere injection of pure oxygen. The pure oxygen is injected into the ambient blast air stream. It is then heated along with the blast air and blown into the blast furnace. All the blast furnace's blast air and injected pure oxygen enter the blast furnace through its raceways.

TABLE 17.1 Bottom-Segment Matrix, Raceway Matrix, and Flame Temperature Calculations With Pure Oxygen Injection

	A	B	C	D	E	F	G	H	I	J	K	L	M
1 BOTTOM SEGMENT CALCULATION													
2	Equation	Description	Numerical term	mass Fe ₉₀ O ₁₀ into bottom segment	mass C in descending coke	mass O ₂ in blast air	mass N ₂ in blast air	mass Fe out in molten iron	mass C out in molten iron	mass CO out in ascending gas	mass CO ₂ out in ascending gas	mass N ₂ out in ascending gas	mass O ₂ in injected pure oxygen
3	7.7	Fe out in molten iron specification	1000	0	0	0	1	0	0	0	0	0	0
4	7.2	Fe mass balance	0	-0.748	0	0	0	0	0	0	0	0	0
5	9.2	O mass balance	0	-0.232	0	-1	0	0	0	0.571	0.727	0	-1
6	7.4	C mass balance	0	0	-1	0	0	0	1	0.429	0.273	0	0
7	7.5	N mass balance	0	0	0	0	-1	0	0	0	0	1	0
8	7.6	N ₂ in air specification	0	0	0	3.3	-1	0	0	0	0	0	0
9	7.9	Equilibrium CO ₂ /CO mass ratio	0	0	0	0	0	0	0	0.694	-1	0	0
10	7.8	C in output molten iron specification	0	0	0	0	0	0.047	-1	0	0	0	0
11	9.4	Enthalpy balance	-320	3.152	-1.359	-1.239	-1.339	1.269	5	-2.926	-7.926	1.008	-1.239
12	9.1	O ₂ in injected pure oxygen	30	0	0	0	0	0	0	0	0	0	1
13				930°C	930°C	1200	1200	1500°C	1500°C	930°C	930°C	930°C	1200
14		Blast temperature=	1200	°C									
15					= (0.001137 * 0144-0.1257)								= (0.001137 * 0144-0.145)
16													= (0.001137 * 0144-0.1257)
17	Bottom segment calculated values												
18		kg per 1000 kg of Fe in product iron	mass Fe ₉₀ O ₁₀ into bottom segment	1302									
19			mass C in descending coke	394	also = mass C in the furnace's coke charge, Eqn. (7.16)								
20			mass O ₂ in blast air	271									
21			mass N ₂ in blast air	894									
22			mass Fe out in molten iron	1000									
23			mass C out in molten iron	47									
24			mass CO out in ascending gas	561									
25			mass CO ₂ out in ascending gas	389									
26			mass N ₂ out in ascending gas	894									
27			mass O ₂ in injected pure oxygen	30									
28													
29													
30													
31	RACEWAY INPUTS AND OUTPUTS CALCULATION												
32	Equation	Description	Numerical Term	mass O ₂ entering raceway in blast air	mass N ₂ entering raceway in blast air	mass C entering raceway in falling coke particles	mass CO in raceway output gas	mass N ₂ in raceway output gas	mass O ₂ in injected pure oxygen				
33	17.2	Mass O ₂ entering raceway in blast air	271	1	0	0	0	0	0				
34	17.3	Mass N ₂ entering raceway in blast air	894	0	1	0	0	0	0				
35	17.4	Raceway oxygen balance	0	-1	0	0	0.571	0	-1				
36	14.9	Raceway nitrogen balance	0	0	-1	0	0	1	0				
37	14.10	Raceway carbon balance	0	0	0	-1	0.429	0	0				
38	17.1	Mass O ₂ entering raceway in pure oxygen	30	0	0	0	0	0	0				
39				1200	1200	1500°C	T _{flame}	T _{flame}	1200				
40													
41	Raceway calculated values												
42		kg per 1000 kg of Fe in product iron	mass O ₂ entering raceway in blast air	271									
43			mass N ₂ entering raceway in blast air	894									
44			mass O ₂ entering raceway in falling coke particles	220									
45			mass CO in raceway output gas	527									
46			mass CO ₂ in raceway output gas	527									
47			mass N ₂ in raceway output gas	894									
48			mass O ₂ in injected pure oxygen	30									
49													
50													
51	FLAME ENTHALPY AND FLAME TEMPERATURE CALCULATIONS												
52	17.6c	Total Raceway input enthalpy = C48-M11+C43-F11+C44-G11+C45-2.488 =					2132	MJ per 1000 kg of Fe in product molten iron					
53	17.7	Total Raceway output flame enthalpy = E52 =					2132	MJ per 1000 kg of Fe in product molten iron					
54	17.9	Raceway flame temperature °C = (E53-C46 * -4.183-C47 * -0.2488)/(C46 * 0.001310+C47 * 0.001301) =					2460	°C					
55													
56													

Note how injectant quantity is fed from the bottom-segment matrix into the raceway matrix. Note also how the bottom-segment steady-state blast air O₂ and N₂ values are fed into the raceway matrix.

Cell E52 = C43 * -F11 + C44 * -G11 + C45 * 2.488 + C48 * -C11.

Cell E53 = E52.

Cell F55 = (E53 - C46 * -4.183 - C47 * -0.2488)/(C46 * 0.001310 + C47 * 0.001301)

$$\left[\begin{array}{l} \text{mass O}_2 \text{ in} \\ \text{injected} \\ \text{pure oxygen} \end{array} \right] = 30$$

or

$$30 = \left[\begin{array}{l} \text{mass O}_2 \text{ in} \\ \text{injected} \\ \text{pure oxygen} \end{array} \right] * 1 \quad (17.1)$$

where 30 kg of injected pure oxygen is added per 1000 kg of Fe in product molten iron.

For flexibility, this injection oxygen quantity is placed into Cell C38 of matrix [Table 17.1](#) by the instruction =C12.

17.4 RACEWAY O₂-IN-BLAST AIR INPUT SPECIFICATION

Cell C21 in the bottom-segment matrix results of [Table 17.1](#) shows that 271 kg of O₂-in-blast air is required for steady production of molten iron, 1500°C. This is also the amount of O₂ entering *the furnace's raceways* in blast air, per 1000 kg of Fe in product molten iron.

It is included in the raceway matrix by means of the O₂ specification equation;

$$\left[\begin{array}{l} \text{mass O}_2 \text{ entering} \\ \text{raceway in} \\ \text{blast air} \end{array} \right] = 271 \text{ kg/1000 kg of Fe in product molten iron}$$

or in matrix form

$$271 = \left[\begin{array}{l} \text{mass O}_2 \text{ entering} \\ \text{raceway in} \\ \text{blast air} \end{array} \right] * 1 \quad (17.2)$$

Of course, this numerical value will change with different amounts of injected pure oxygen.

This is automatically taken care of in [Table 17.1](#) by inserting the instruction, =C20, into raceway matrix Cell C33.

17.5 RACEWAY N₂-IN-BLAST AIR SPECIFICATION

The blast furnace steady-state N₂-in-blast air input also varies with the amount of injected pure oxygen. In this case, it is;

$$\left[\begin{array}{l} \text{mass N}_2 \text{ entering} \\ \text{raceway in} \\ \text{blast air} \end{array} \right] = 894 \text{ kg/1000 kg of Fe in product molten iron}$$

or in matrix form

$$894 = \left[\begin{array}{l} \text{mass N}_2 \text{ entering} \\ \text{raceway in} \\ \text{blast air} \end{array} \right] * 1 \quad (17.3)$$

This is automatically taken care of in [Table 17.1](#) by inserting the instruction, =C21, into Cell C34 of [Table 17.1](#).

17.6 RACEWAY O BALANCE WITH PURE OXYGEN INJECTION

The basic steady-state raceway O mass balance is:

$$\text{mass O into raceway} = \text{mass O out of raceway}$$

With inputs and outputs of [Fig. 17.1](#), this equation expands to;

$$\begin{aligned}
 & \left[\begin{array}{l} \text{mass O}_2 \text{ in} \\ \text{ injected} \\ \text{pure oxygen} \end{array} \right] * \frac{100 \text{ mass\% O in O}_2}{100\%} \\
 & + \left[\begin{array}{l} \text{mass O}_2 \text{ entering} \\ \text{ raceway in} \\ \text{blast air} \end{array} \right] * \frac{100 \text{ mass\% O in O}_2}{100\%} \\
 & = \left[\begin{array}{l} \text{mass CO in raceway} \\ \text{ output gas} \end{array} \right] * \frac{57.1 \text{ mass\% O in CO}}{100\%}
 \end{aligned}$$

or

$$\begin{aligned}
 & \left[\begin{array}{l} \text{mass O}_2 \text{ in} \\ \text{ injected} \\ \text{pure oxygen} \end{array} \right] * 1 + \left[\begin{array}{l} \text{mass O}_2 \text{ entering} \\ \text{ raceway in} \\ \text{blast air} \end{array} \right] * 1 \\
 & = \left[\begin{array}{l} \text{mass CO in raceway} \\ \text{ output gas} \end{array} \right] * 0.571
 \end{aligned}$$

$$\text{or subtracting } \left\{ \begin{array}{l} \left[\begin{array}{l} \text{mass O}_2 \text{ in} \\ \text{ injected} \\ \text{pure oxygen} \end{array} \right] * 1 \\ + \left[\begin{array}{l} \text{mass O}_2 \text{ entering} \\ \text{ raceway in} \\ \text{blast air} \end{array} \right] * 1 \end{array} \right\}$$

from both sides:

$$\begin{aligned}
 0 &= - \left[\begin{array}{l} \text{mass O}_2 \text{ in} \\ \text{ injected} \\ \text{pure oxygen} \end{array} \right] * 1 - \left[\begin{array}{l} \text{mass O}_2 \text{ entering} \\ \text{ raceway in} \\ \text{blast air} \end{array} \right] * 1 \\
 &+ \left[\begin{array}{l} \text{mass CO in raceway} \\ \text{ output gas} \end{array} \right] * 0.571 \quad (17.4)
 \end{aligned}$$

as is shown in Row 35 of the raceway matrix of [Table 17.1](#).

17.7 RACEWAY CARBON BALANCE

The carbon balance equation of this chapter reverts to that in Chapter 14, Raceway Flame Temperature. It is;

$$\begin{aligned}
 0 &= - \left[\begin{array}{l} \text{mass C in falling} \\ \text{ coke particles} \end{array} \right] * 1 \\
 &+ \left[\begin{array}{l} \text{mass CO in raceway} \\ \text{ output gas} \end{array} \right] * 0.429 \quad (14.10)
 \end{aligned}$$

as is shown in Row 37 of the raceway matrix of [Table 17.1](#).

17.8 RACEWAY NITROGEN BALANCE EQUATION

The nitrogen mass balance equation with pure oxygen injection is the same as in Chapter 14, Raceway Flame Temperature. It is;

$$\begin{aligned}
 0 &= - \left[\begin{array}{l} \text{mass N}_2 \text{ entering} \\ \text{ raceway in} \\ \text{blast air} \end{array} \right] * 1 \\
 &+ \left[\begin{array}{l} \text{mass N}_2 \text{ in raceway} \\ \text{ output gas} \end{array} \right] * 1 \quad (14.9)
 \end{aligned}$$

as shown in Row 36.

17.9 RACEWAY MATRIX RESULTS

The raceway matrix results are shown in Cells C43–C48. The calculated values with 30 kg of pure oxygen injection are;

- 527 kg of CO in raceway output gas,
- 894 kg of N₂ in raceway output gas, and
- 226 kg of C in falling coke particles

per 1000 kg of Fe in product molten iron.

We now calculate raceway input enthalpy, output enthalpy, and output gas (flame) temperature from these values.

17.10 RACEWAY INPUT ENTHALPY CALCULATION

With pure oxygen injection, the raceway input enthalpy of Table 17.1 is;

$$\begin{bmatrix} \text{raceway} \\ \text{input} \\ \text{enthalpy} \end{bmatrix} = \begin{bmatrix} \text{mass O}_2 \text{ in} \\ \text{injected} \\ \text{pure oxygen} \end{bmatrix} * \frac{H^\circ_{1200^\circ\text{C}}}{\text{MW}_{\text{O}_2}} + \begin{bmatrix} \text{mass O}_2 \text{ entering} \\ \text{raceway in} \\ \text{blast air} \end{bmatrix} * \frac{H^\circ_{1200^\circ\text{C}}}{\text{MW}_{\text{O}_2}} + \begin{bmatrix} \text{mass N}_2 \text{ entering} \\ \text{raceway in} \\ \text{blast air} \end{bmatrix} * \frac{H^\circ_{1200^\circ\text{C}}}{\text{MW}_{\text{N}_2}} + \begin{bmatrix} \text{mass C in} \\ \text{falling coke} \\ \text{particles} \end{bmatrix} * \frac{H^\circ_{1500^\circ\text{C}}}{\text{MW}_\text{C}}$$

or

$$\begin{bmatrix} \text{raceway} \\ \text{input} \\ \text{enthalpy} \end{bmatrix} = \begin{bmatrix} \text{mass O}_2 \text{ in} \\ \text{injected} \\ \text{pure oxygen} \end{bmatrix} * 1.239 + \begin{bmatrix} \text{mass O}_2 \text{ entering} \\ \text{raceway in} \\ \text{blast air} \end{bmatrix} * 1.239 + \begin{bmatrix} \text{mass N}_2 \text{ entering} \\ \text{raceway in} \\ \text{blast air} \end{bmatrix} * 1.339 + \begin{bmatrix} \text{mass C in} \\ \text{falling coke} \\ \text{particles} \end{bmatrix} * 2.488 \quad (17.5)$$

where, from Table J.1

$$1.239 = \frac{H^\circ_{1200^\circ\text{C}}}{\text{MW}_{\text{O}_2}}$$

$$1.339 = \frac{H^\circ_{1200^\circ\text{C}}}{\text{MW}_{\text{N}_2}}$$

$$2.488 = \frac{H^\circ_{1500^\circ\text{C}}}{\text{MW}_\text{C}}$$

all MJ per kg of substance.

Numerically, the input enthalpy is;

$$\begin{bmatrix} \text{raceway} \\ \text{input} \\ \text{enthalpy} \end{bmatrix} = \begin{bmatrix} \text{C48} \\ \text{C43} \\ \text{C44} \end{bmatrix} * 1.239 + \begin{bmatrix} \text{C43} \\ \text{C44} \\ \text{C45} \end{bmatrix} * 1.339 + \begin{bmatrix} \text{C48} \\ \text{C43} \\ \text{C45} \end{bmatrix} * 2.488 = 2132 \text{ MJ}/1000 \text{ kg of Fe in product molten iron} \quad (17.6a)$$

where the contents of Cells C43–C45 and C48 are shown in Table 17.1.

17.10.1 Automated Input Enthalpy Calculation

Eq. (17.6a) is further automated by replacing;

$$\frac{H^\circ_{1200^\circ\text{C}}}{\text{MW}_{\text{O}_2}} \text{ with } -\text{G11} \text{ and } -\text{M11}$$

and

$$\frac{H^\circ_{1200^\circ\text{C}}}{\text{MW}_{\text{N}_2}} \text{ with } -\text{H11}$$

which changes Eq. (17.6a) to

$$\begin{bmatrix} \text{raceway} \\ \text{input} \\ \text{enthalpy} \end{bmatrix} = \begin{bmatrix} \text{C48} \\ \text{C43} \\ \text{C44} \end{bmatrix} * -\text{M11} + \begin{bmatrix} \text{C43} \\ \text{C44} \\ \text{C45} \end{bmatrix} * -\text{F11} + \begin{bmatrix} \text{C43} \\ \text{C44} \\ \text{C45} \end{bmatrix} * 2.488 = 2132 \text{ MJ}/1000 \text{ kg of Fe in product molten iron} \quad (17.6b)$$

This equation is entered into spreadsheet of Table 17.1 typing the instruction;

$$= \text{C48} * -\text{M11} + \text{C43} * -\text{F11} + \text{C44} * -\text{G11} + \text{C45} * 2.488 \quad (17.6c)$$

in Cell E52, which causes it to automatically calculate raceway input enthalpy.

17.11 AUTOMATED RACEWAY OUTPUT ENTHALPY

Raceway output enthalpy is needed to calculate raceway output gas (flame) temperature.

It is calculated by the following equation;

$$\begin{bmatrix} \text{raceway output} \\ (\text{flame}) \text{ enthalpy} \end{bmatrix} + \text{zero} = \begin{bmatrix} \text{raceway} \\ \text{input} \\ \text{enthalpy} \end{bmatrix}$$

which continues our assumption that there is no conductive, convective, and radiative heat loss from the raceway (Section 14.10).

From [Section 17.10](#), the raceway input enthalpy is 2132 MJ/kg of Fe in product molten iron so that:

$$\begin{bmatrix} \text{raceway output} \\ (\text{flame}) \text{ enthalpy} \end{bmatrix} + \text{zero} = \begin{bmatrix} \text{raceway} \\ \text{input} \\ \text{enthalpy} \end{bmatrix} = \text{E52} \quad (17.7)$$

As shown in [Table 17.1](#), this calculation is automated by typing the instruction

= E52

into Cell E53.

17.12 RACEWAY OUTPUT GAS (FLAME) TEMPERATURE

Our raceway flame temperature calculations use matrix [Table 17.1](#)'s;

1. raceway CO and N₂ output masses, 527 and 894 kg, from Cells C46 and C47, and
2. raceway output gas (flame) enthalpy, 2132 MJ, from Cell E53

all per 1000 kg of Fe in product molten iron.

The following equation;

$$\left\{ \begin{array}{l} \begin{bmatrix} \text{raceway output} \\ (\text{flame}) \text{ enthalpy} \end{bmatrix} \\ - \begin{bmatrix} \text{mass CO in raceway} \\ \text{output gas} \end{bmatrix} * (-4.183) \\ - \begin{bmatrix} \text{mass N}_2 \text{ in raceway} \\ \text{output gas} \end{bmatrix} * (-0.2448) \end{array} \right\} = T_{\text{flame}}, {}^{\circ}\text{C}$$

$$\left\{ \begin{array}{l} \begin{bmatrix} \text{mass CO in raceway} \\ \text{output gas} \end{bmatrix} * 0.001310 \\ + \begin{bmatrix} \text{mass N}_2 \text{ in raceway} \\ \text{output gas} \end{bmatrix} * 0.001301 \end{array} \right\} \quad (14.16)$$

is used. The numerical values are from the flame temperature enthalpy versus temperature equations ([Table J.4](#)), that is:

$$\frac{H^{\circ} T_{\text{flame}}}{\text{CO(g)}} = 0.001310 * T_{\text{flame}} - 4.183 \text{ MJ/kg of CO(g)} \quad (14.14)$$

$$\frac{H^{\circ} T_{\text{flame}}}{\text{N}_2(\text{g})} = 0.001301 * T_{\text{flame}} - 0.2448 \text{ MJ/kg of N}_2(\text{g}) \quad (14.15)$$

For the numerical example in [Table 17.1](#), the raceway flame temperature is;

$$\frac{\text{E53} - \text{C46} * (-4.183) - \text{C47} * (-0.2448)}{\text{C46} * 0.001310 + \text{C47} * 0.001301} = T_{\text{flame}} = 2458 {}^{\circ}\text{C} \quad (17.8)$$

as shown in Row 55, [Table 17.1](#). Cells E53, C46, and C47 contain 2132, 527, and 894,

As in Section 16.11, this calculation is automated by typing the instruction;

$$= \frac{\text{E53} - \text{C46} * -4.183 - \text{C47} * -0.2448}{\text{C46} * 0.001310 + \text{C47} * 0.001301} \quad (17.9)$$

into Cell F55.

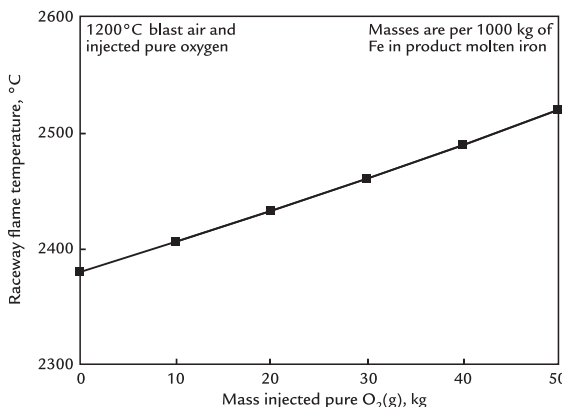


FIGURE 17.2 Effect of pure oxygen injection on tuyere raceway flame temperature. The increase in flame temperature is notable. 50 kg of O₂ increases flame temperature by 140°C. The line is not quite straight because Eq. (17.8) is not linear.

17.13 EFFECT OF PURE OXYGEN INJECTION ON RACEWAY FLAME TEMPERATURE

We now show the effect of pure oxygen injection on raceway flame temperature (Fig. 17.2). Flame temperature increases about 2.8°C for every kg of injected pure oxygen, per 1000 kg of Fe in product molten iron.

The reason for this increase in raceway adiabatic flame temperature (RAFT) is found in all our matrix equations. We speculate that it is mostly due to the decreased amount of N₂:

1. entering the raceway at 1200°C, and
2. leaving the raceway at T_{flame}

with increasing pure oxygen injection (Fig. 9.3).

This means that less of the carbon's heat of oxidation must be devoted to heating N₂ so that the raceway's CO (and depleted N₂) heats up to a higher (flame) temperature.

17.14 SUMMARY

This chapter shows how to calculate raceway flame temperature with tuyere injection of pure oxygen.

The RAFT calculation;

1. uses the results from bottom-segment matrix Table 9.1,
2. prepares a raceway matrix to calculate the raceway's input and output masses,
3. calculates the raceway's input and output enthalpies from these results, and
4. calculates raceway output gas (flame) temperature from;
 - a. the raceway's output masses and output enthalpy, and
 - b. $H_{T_{\text{flame}}}^{\circ}/\text{MW}$ versus temperature equations of CO(g) and N₂(g).

These steps are shown in Table 17.1.

Flame temperature increases with increasing pure oxygen injection. This is useful generally and for offsetting the cooling effects of other injectants, for example;

- pulverized coal (Chapter 16: Raceway Flame Temperature With Pulverized Carbon Injection),
- natural gas (Chapter 18: Raceway Flame Temperature With CH₄(g) Tuyere Injection), and
- H₂O(g) in natural humidity and steam (Chapter 19: Raceway Flame Temperature With Moisture in Blast Air).

EXERCISE

Please give your calculated masses in kg per 1000 kg of Fe in product molten iron.

- 17.1. The price of pure oxygen has decreased. The blast furnace management team of

- Table 17.1** wishes to take advantage of this by increasing its pure oxygen injection to 65 kg/1000 kg of Fe in product molten iron. They wish to know what effect this will have on their tuyere raceway flame temperature. Please calculate this for them.
- 17.2.** The Technology group of **Table 17.1** believes that the optimum raceway flame temperature in their blast furnace should be 2450°C. Please determine the amount

of pure oxygen injectant that will give this flame temperature. Use two calculation methods.

- 17.3.** The Purchasing department of **Table 17.1** has found a cheap supply of 90 mass% O₂, 10 mass% N₂ oxygen. What do you expect will happen to flame temperature of Problem 17.1 if its 65 kg of pure oxygen is replaced by 65 kg of the impure oxygen. A qualitative answer will do.

C H A P T E R

18

Raceway Flame Temperature With CH₄(g) Injection

O U T L I N E

18.1 Understanding The Impact of CH ₄ (g) Injection on Raceway Adiabatic Flame Temperature	170	18.9 Raceway Nitrogen Balance Equation	174
18.2 Matrix Setup	170	18.10 Raceway Matrix Results and Flame Temperature Calculation	174
18.3 Raceway Input CH ₄ (g) SPECIFICATION	170	18.11 Raceway Input Enthalpy Calculation	175
18.4 Raceway O ₂ -in-Blast Air Input Specification	170	18.12 Raceway Output Enthalpy	176
18.5 Raceway N ₂ -in-Blast Air Specification	173	18.13 Raceway Output Gas (Flame) Temperature	176
18.6 Modified Raceway Carbon Balance Equation	173	18.14 Effect of CH ₄ (g) Injection on Raceway Flame Temperature	177
18.7 Raceway Oxygen Balance Equation	173	18.15 Summary Exercises	177
18.8 New Hydrogen Balance Equation	174		178

18.1 UNDERSTANDING THE IMPACT OF CH₄(g) INJECTION ON RACEWAY ADIABATIC FLAME TEMPERATURE

In Chapter 17, Raceway Flame Temperature With Oxygen Enrichment, we calculated the raceway flame temperature with the injection of pure oxygen into the blast air. This chapter calculates the raceway adiabatic flame temperature (RAFT) with CH₄(g) injection. Our objectives are to;

1. show how CH₄(g) injection is included in our raceway flame temperature calculations,
2. indicate how CH₄(g) injection affects raceway flame temperature, and
3. explain this flame temperature effect.

CH₄(g) is the main component of natural gas. CH₄(g) injection adds a new variable to our flame temperature, the mass of H₂ in the raceway output gas. To compensate, it adds a new equation—the raceway H balance. We specify that the only hydrogenous gas in the raceway *output* gas is H₂ (Fig. 18.1). This is discussed in Appendices G and H. Fig. (18.1) is a sketch of the blast furnace raceway with CH₄(g) injection.

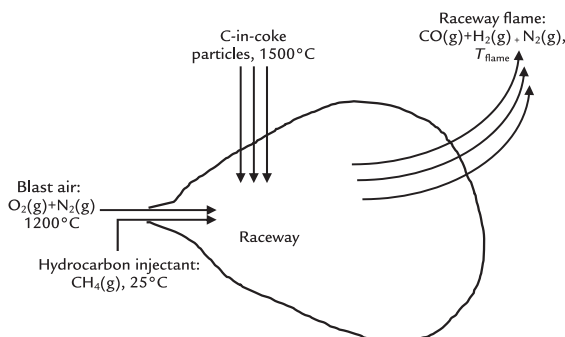


FIGURE 18.1 Sketch of blast furnace raceway with CH₄(g) injection. The drawing is a vertical slice through the center of a pear-shaped raceway. All blast furnaces' blast air and injected CH₄(g) enter the blast furnace through its raceways.

18.2 MATRIX SETUP

Our CH₄(g) injection flame temperature calculation starts with the bottom-segment matrix result of Table 11.1, copied into Table 18.1.

It then prepares *raceway* matrix Table 18.2 by;

1. setting up raceway C, H, N, and O mass balance equations, and
2. including bottom segment;
 - a. mass tuyere-injected CH₄(g),
 - b. mass O₂-in-blast air, and
 - c. mass N₂-in-blast air

of Table 18.1 in these raceway mass balance equations.

It then calculates the masses of the other raceway components, as shown in Table 18.2.

18.3 RACEWAY INPUT CH₄(g) SPECIFICATION

The CH₄(g) input mass equation is taken from Cell C14 of the bottom-segment matrix. It is;

$$\begin{bmatrix} \text{mass CH}_4 \text{ injected} \\ \text{into raceway} \end{bmatrix} = 60 \text{ kg injected per 1000 kg of Fe in product molten iron}$$

or in matrix form

$$60 = \begin{bmatrix} \text{mass CH}_4 \text{ injected} \\ \text{into raceway} \end{bmatrix} * 1 \quad (18.1)$$

For flexibility, this equation is put into Cell C39 of Table 18.2 by the instruction = C14

18.4 RACEWAY O₂-IN-BLAST AIR INPUT SPECIFICATION

The bottom-segment matrix results of Table 18.2 show that;

323 kg O₂ in blast air is required for steady production of molten iron 1500°C, Cell C20.

TABLE 18.1 Bottom-Segment Matrix With Injection of 60 kg of CH₄(g) per 1000 kg of Fe in Product Molten Iron

A	B	C	D	E	F	G	H	I	J	K	L	M	N	O	
1 BOTTOM SEGMENT CALCULATIONS															
	Description	Numerical term	mass Fe ₂ SiO ₄ into bottom segment	mass C in descending coke	mass O ₂ in blast air	mass N ₂ in blast air	mass Fe out in molten iron	mass C out in molten iron	mass CO out in ascending gas	mass CO ₂ out in ascending gas	mass N ₂ out in ascending gas	mass H ₂ out in ascending gas	mass H ₂ O out in ascending gas	mass tuyere-injected CH ₄	
2															
3	7.7 Fe out in molten iron specification	1000	0	0	0	0	1	0	0	0	0	0	0	0	
4	7.2 Fe mass balance	0	-0.768	0	0	0	0	0	0	0	0	0	0	0	
5	11.5 O mass balance	0	-0.232	0	-1	0	0	0	0.571	0.727	0	0	0.888	0	
6	11.4 C mass balance	0	0	-1	0	0	1	0.429	0.273	0	0	0	-0.749		
7	7.5 N mass balance	0	0	0	0	-1	0	0	0	0	1	0	0	0	
8	7.6 N ₂ in blast air specification	0	0	0	0	3.3	-1	0	0	0	0	0	0	0	
9	7.9 Equilibrium CO ₂ /CO mass ratio	0	0	0	0	0	0	0	0.694	-1	0	0	0	0	
10	7.8 C out in molten iron specification	0	0	0	0	0	0.047	-1	0	0	0	0	0	0	
11	11.7 Enthalpy balance	-320	3.152	-1.359	-1.239	-1.339	1.269	5	-2.926	-7.926	1.008	13.35	-11.50	4.064	
12	11.3 H mass balance	0	0	0	0	0	0	0	0	0	1	0.112	-0.251		
13	11.8 Equilibrium H ₂ O/H ₂ mass ratio	0	0	0	0	0	0	0	0	0	5.44	-1	0		
14	11.1 CH ₄ injected through tuyeres	60	0	0	0	0	0	0	0	0	0	0	0	1	
15		930°C	930°C	1200°C	1200°C	1500°C	1500°C	930°C	930°C	930°C	930°C	930°C	930°C	25°C	
16	Bottom segment calculated values														
17	kg per 1000 kg of Fe out in molten iron														
18	mass Fe ₂ SiO ₄ into bottom segment	1302													
19	mass C in descending coke	335	also = mass C in the furnace's coke charge; Eqn. (7.16)												
20	mass O ₂ in blast air	323													
21	mass N ₂ in blast air	1064													
22	mass Fe out in molten iron	1000													
23	mass C out in molten iron	47													
24	mass CO out in ascending gas	539													
25	mass CO ₂ out in ascending gas	374													
26	mass N ₂ out in ascending gas	1064													
27	mass H ₂ out in ascending gas	9.4													
28	mass H ₂ O out in ascending gas	51													
29	mass tuyere-injected CH ₄	60													
30															

This is a copy of matrix Table 11.1. The enthalpies in Row 11 are from Table J.1.

TABLE 18.2 Matrices and Equations for Calculating Raceway Flame Temperature With 60 kg of Injected CH₄(g)

A	B	C	D	E	F	G	H	I	J	K	L	M	N	O
1 BOTTOM SEGMENT CALCULATIONS														
Equation	Description	Numerical term	mass Fe _{0.947} O into bottom segment	mass C in descending coke	mass O ₂ in blast air	mass N ₂ in blast air	mass Fe out in molten iron	mass C out in molten iron	mass CO out in ascending gas	mass CO ₂ out in ascending gas	mass N ₂ out in ascending gas	mass H ₂ out in ascending gas	mass H ₂ O out in ascending gas	mass tuyere-injected CH ₄
7.7	Fe out in molten iron specification	1000	0	0	0	0	1	0	0	0	0	0	0	0
7.2	Fe mass balance	0	-0.768	0	0	0	1	0	0	0	0	0	0	0
11.5	O mass balance	0	-0.232	0	-1	0	0	0.571	0.727	0	0	0.888	0	0
11.4	C mass balance	0	0	-1	0	0	1	0.429	0.273	0	0	0	-0.749	0
7.5	N mass balance	0	0	0	0	-1	0	0	0	0	1	0	0	0
7.6	N ₂ in air specification	0	0	0	3.3	-1	0	0	0	0	0	0	0	0
7.9	Equilibrium CO ₂ /CO mass ratio	0	0	0	0	0	0	0	0.694	-1	0	0	0	0
7.8	C in output molten iron specification	0	0	0	0	0	0	0.047	-1	0	0	0	0	0
11.7	Enthalpy balance	-320	3.152	-1.359	-1.239	-1.339	1.269	5	-2.926	-7.926	1.008	13.34	-11.50	4.664
11.3	H mass balance	0	0	0	0	0	0	0	0	0	0	1	0.112	-0.251
11.8	Equilibrium H ₂ O/H ₂ mass ratio	0	0	0	0	0	0	0	0	0	0	5.44	-1	0
11.1	CH ₄ injected through tuyeres	60	0	0	0	0	0	0	0	0	0	0	0	1
		930°C	930°C	1200	1200	1500°C	1500°C	930°C	930°C	930°C	930°C	930°C	930°C	25°C
		Blast temperature =		1200	°C									
17 Bottom segment calculated values														
		kg per 1000 kg of Fe in product iron												
31 RACEWAY INPUTS AND OUTPUTS CALCULATION														
Equation	Description	Numerical Term	mass O ₂ entering raceway in blast air	mass N ₂ entering raceway in blast air	mass C entering raceway in falling coke particles	mass CO in raceway output gas	mass N ₂ in raceway output gas	mass H ₂ in raceway output gas	mass CH ₄ injected into raceway					
18.2	Mass O ₂ entering raceway in blast air	323	1	0	0	0	0	0	0					
18.3	Mass N ₂ entering raceway in blast air	1064	0	1	0	0	0	0	0					
18.4	Raceway carbon balance	0	0	0	-1	0	0.429	0	0	0.749				
14.8	Raceway oxygen balance	0	-1	0	0	0	0.571	0	0	0				
18.5	Raceway hydrogen balance	0	0	0	0	0	0	0	1	0.251				
14.9	Raceway nitrogen balance	0	0	-1	0	0	0	1	0	0				
18.1	Mass CH ₄ injected into raceway	60	0	0	0	0	0	0	0	1				
			1200	1200	1500°C	T _{flame}	T _{flame}	T _{flame}	25°C					
42 Raceway calculated values														
51 RACEWAY ENTHALPY AND FLAME TEMPERATURE CALCULATIONS														
18.7b	Total raceway input enthalpy = C49 * -4.664 + C43 * F11 + C44 * G11 + C45 * 2.488 =					2036	MJ per 1000 kg of Fe in product molten iron							
18.8	Total raceway output enthalpy = raceway input enthalpy = F52 =					2036	MJ per 1000 kg of Fe in product molten iron							
18.10b	Flame temperature = (F53 * C46 * -4.183 - C47 * -0.2448 - C48 * -4.13) / (C46 * 0.00131 + C47 * 0.001301 + C48 * 0.01756) =					1976	°C							

Note the raceway matrix and raceway enthalpy and flame temperature equations, Rows 52, 53, and 55. The matrix equations are developed in Sections 18.2–18.8.

Cell F52 = C49 * -4.667 + C43 * -F11 + C44 * -G11 + C45 * 2.488 Cell F53 = F52

Cell G55 = (F53 - C46 * -4.183 - C47 * -0.2448 - C48 * -4.130) / (C46 * 0.001310 + C47 * 0.001301 + C48 * 0.01756)

This is also the amount of O₂ entering the blast furnace raceways in blast air.

This oxygen is included in the raceway matrix by means of the O₂ specification;

$$\begin{bmatrix} \text{mass O}_2 \text{ entering} \\ \text{raceway in} \\ \text{blast air} \end{bmatrix} = 323 \text{ kg}/1000 \text{ kg of Fe in product molten iron}$$

or in matrix form:

$$323 = \begin{bmatrix} \text{mass O}_2 \text{ entering} \\ \text{raceway in} \\ \text{blast air} \end{bmatrix} * 1 \quad (18.2)$$

Of course, this numerical value changes with different amounts of injected CH₄(g).

This is automatically taken care of in **Table 18.2** by inserting the instruction;

$$= C20$$

into raceway matrix Cell C33.

18.5 RACEWAY N₂-IN-BLAST AIR SPECIFICATION

The blast furnace steady-state N₂-in-blast air input also varies with the amount of injected CH₄(g). In this case, it is;

$$\begin{bmatrix} \text{mass N}_2 \text{ entering} \\ \text{raceway in} \\ \text{blast air} \end{bmatrix} = 1064 \text{ kg}/1000 \text{ kg of Fe in product molten iron}$$

or in matrix form

$$1064 = \begin{bmatrix} \text{mass N}_2 \text{ entering} \\ \text{raceway in} \\ \text{blast air} \end{bmatrix} * 1 \quad (18.3)$$

This change is automatically taken care of in **Table 18.2** by inserting the instruction

$$= C21$$

into Cell C34.

18.6 MODIFIED RACEWAY CARBON BALANCE EQUATION

With CH₄(g) injection, the carbon balance equation of Chapter 14, Raceway Flame Temperature, becomes;

$$\begin{aligned} & \left[\text{mass CH}_4 \text{ (g) injected} \right] * \frac{\left[\text{74.9 mass\% C} \right]}{100\%} \\ & + \left[\text{mass C in falling} \right] * \frac{\left[\text{100 mass\% C} \right]}{100\%} \\ & = \left[\text{mass CO in raceway} \right] * \frac{\left[\text{42.9 mass\% C in CO} \right]}{100\%} \end{aligned}$$

or

$$\begin{aligned} & \left[\text{mass CH}_4 \text{ (g) injected} \right] * 0.749 \\ & + \left[\text{mass C in falling} \right] * 1 \\ & = \left[\text{mass CO in raceway} \right] * 0.429 \end{aligned}$$

or subtracting $\left\{ \left[\text{mass CH}_4 \text{ (g) injected} \right] * 0.749 + \left[\text{mass C in falling} \right] * 1 \right\}$ from both sides of the above equation and rearranging;

$$\begin{aligned} 0 = & - \left[\text{mass CH}_4 \text{ (g) injected} \right] * 0.749 \\ & - \left[\text{mass C in falling} \right] * 1 \\ & + \left[\text{mass CO in raceway} \right] * 0.429 \end{aligned} \quad (18.4)$$

as shown in Row 35 of raceway matrix of **Table 18.2**.

18.7 RACEWAY OXYGEN BALANCE EQUATION

The raceway oxygen balance equation is the same as in Chapter 14, Raceway Flame Temperature. It is;

$$0 = - \left[\begin{array}{l} \text{mass O}_2 \text{ entering} \\ \text{raceway in} \\ \text{blast air} \end{array} \right] * 1 + \left[\begin{array}{l} \text{mass CO in raceway} \\ \text{output gas} \end{array} \right] * 0.571 \quad (14.8)$$

or

$$0 = - \left[\begin{array}{l} \text{mass CH}_4(\text{g}) \text{ injected} \\ \text{into raceway} \end{array} \right] * 0.251 + \left[\begin{array}{l} \text{mass H}_2 \text{ in raceway} \\ \text{output gas} \end{array} \right] * 1 \quad (18.5)$$

as shown in Row 36.

18.8 NEW HYDROGEN BALANCE EQUATION

Injection of CH₄(g) into the raceway requires a hydrogen mass balance. It is;

$$\text{mass H into raceway} = \text{mass H out of raceway}$$

This expands to;

$$\text{mass H in injected CH}_4(\text{g}) = \text{mass H in raceway output gas}$$

or because the only hydrogenous gas in the raceway output gas is H₂(g);

$$\left[\begin{array}{l} \text{mass CH}_4(\text{g}) \text{ injected} \\ \text{into raceway} \end{array} \right] * \frac{\left[\begin{array}{l} 25.1 \text{ mass\% H} \\ \text{in injected CH}_4 \end{array} \right]}{100\%} = \left[\begin{array}{l} \text{mass H}_2 \text{ in raceway} \\ \text{output gas} \end{array} \right] * \frac{\left[\begin{array}{l} 100 \text{ mass\% H} \\ \text{in H}_2 \end{array} \right]}{100\%}$$

or

$$\left[\begin{array}{l} \text{mass CH}_4(\text{g}) \text{ injected} \\ \text{into raceway} \end{array} \right] * 0.251 = \left[\begin{array}{l} \text{mass H}_2 \text{ in raceway} \\ \text{output gas} \end{array} \right] * 1$$

or subtracting $\left\{ \left[\begin{array}{l} \text{mass CH}_4(\text{g}) \text{ injected} \\ \text{into raceway} \end{array} \right] * 0.251 \right\}$ from both sides;

as shown in Row 37.

18.9 RACEWAY NITROGEN BALANCE EQUATION

The nitrogen mass balance equation is the same as in Chapter 14, Raceway Flame Temperature. It is;

$$0 = - \left[\begin{array}{l} \text{mass N}_2 \text{ entering} \\ \text{raceway in} \\ \text{blast air} \end{array} \right] * 1 + \left[\begin{array}{l} \text{mass N}_2 \text{ in raceway} \\ \text{output gas} \end{array} \right] * 1 \quad (14.9)$$

as shown in Row 38.

18.10 RACEWAY MATRIX RESULTS AND FLAME TEMPERATURE CALCULATION

Our raceway matrix determines all the raceway's input and output masses, Cells C43–C49. We are now ready to calculate;

- raceway input enthalpy,
 - raceway output enthalpy, and
 - raceway output gas (flame) temperature
- as described in the next three sections.

18.11 RACEWAY INPUT ENTHALPY CALCULATION

With 25°C CH₄(g) injection, our raceway's input enthalpy is;

$$\begin{bmatrix} \text{raceway} \\ \text{input} \\ \text{enthalpy} \end{bmatrix} = \begin{bmatrix} \text{mass CH}_4(\text{g}) \\ \text{injected} \\ \text{into raceway} \end{bmatrix} * \frac{H^\circ_{25^\circ\text{C}}}{\text{MW}_{\text{CH}_4}} + \begin{bmatrix} \text{mass O}_2 \text{ entering} \\ \text{raceway in} \\ \text{blast air} \end{bmatrix} * \frac{H^\circ_{1200^\circ\text{C}}}{\text{MW}_{\text{O}_2}} + \begin{bmatrix} \text{mass N}_2 \text{ entering} \\ \text{raceway in} \\ \text{blast air} \end{bmatrix} * \frac{H^\circ_{1200^\circ\text{C}}}{\text{MW}_{\text{N}_2}} + \begin{bmatrix} \text{mass C in} \\ \text{falling coke} \\ \text{particles} \end{bmatrix} * \frac{H^\circ_{1500^\circ\text{C}}}{\text{MW}_\text{C}}$$

or

$$\begin{bmatrix} \text{raceway} \\ \text{input} \\ \text{enthalpy} \end{bmatrix} = \begin{bmatrix} \text{mass CH}_4(\text{g}) \\ \text{injected} \\ \text{into raceway} \end{bmatrix} * -4.664 + \begin{bmatrix} \text{mass O}_2 \text{ entering} \\ \text{raceway in} \\ \text{blast air} \end{bmatrix} * 1.239 + \begin{bmatrix} \text{mass N}_2 \text{ entering} \\ \text{raceway in} \\ \text{blast air} \end{bmatrix} * 1.339 + \begin{bmatrix} \text{mass C in} \\ \text{falling coke} \\ \text{particles} \end{bmatrix} * 2.488 \quad (18.6)$$

where from Table J.1

$$1.239 = \frac{H^\circ_{1200^\circ\text{C}}}{\text{MW}_{\text{O}_2}}$$

$$1.339 = \frac{H^\circ_{1200^\circ\text{C}}}{\text{MW}_{\text{N}_2}}$$

$$2.488 = \frac{H^\circ_{1500^\circ\text{C}}}{\text{MW}_\text{C}}$$

$$-4.664 = \frac{H^\circ_{25^\circ\text{C}}}{\text{MW}_{\text{CH}_4}}$$

all MJ/kg of substance.

Numerically, the input enthalpy is;

$$\begin{bmatrix} \text{raceway} \\ \text{input} \\ \text{enthalpy} \end{bmatrix} = 60 * -4.664 + 323 * 1.239 + 1064 * 1.339 + 197 * 2.488 = 2036 \text{ MJ/1000 kg of Fe in product molten iron.}$$

or

$$\begin{bmatrix} \text{raceway} \\ \text{input} \\ \text{enthalpy} \end{bmatrix} = \text{C49} * -4.664 + \text{C43} * 1.239 + \text{C44} * 1.339 + \text{C45} * 2.488 = 2036$$

and including blast temperature-dependent cells:

$$\begin{bmatrix} \text{raceway} \\ \text{input} \\ \text{enthalpy} \end{bmatrix} = \text{C49} * -4.664 + \text{C43} * -\text{F11} + \text{C44} * -\text{G11} + \text{C45} * 2.488 = 2036 \quad (18.7a)$$

This equation is included in Table 18.2 by inserting the instruction;

$$= \text{C49} * -4.664 + \text{C43} * -\text{F11} + \text{C44} * -\text{G11} + \text{C45} * 2.488 \quad (18.7b)$$

in Cell F52.

18.12 RACEWAY OUTPUT ENTHALPY

Raceway output enthalpy is needed to calculate raceway output gas (flame) temperature.

As described in Chapter 14, Raceway Flame Temperature, it is calculated by the equation;

$$\begin{bmatrix} \text{raceway output} \\ (\text{flame}) \text{ enthalpy} \end{bmatrix} + \text{zero} = \begin{bmatrix} \text{raceway} \\ \text{input} \\ \text{enthalpy} \end{bmatrix}$$

with zero conductive, convective and radiative heat loss from the raceway to its surroundings.

From [Section 18.11](#), the raceway input enthalpy is 2036 MJ/kg of Fe in product molten iron so that:

$$\begin{bmatrix} \text{raceway output} \\ (\text{flame}) \text{ enthalpy} \end{bmatrix} + \text{zero} = \begin{bmatrix} \text{raceway} \\ \text{input} \\ \text{enthalpy} \end{bmatrix} = F52$$

= 2036 MJ/1000 kg of Fe in product molten iron (18.8)

This included in [Table 18.2](#) by inserting the instruction;

$$= F52$$

in Cell F53.

18.13 RACEWAY OUTPUT GAS (FLAME) TEMPERATURE

Our raceway flame temperature calculations uses;

1. raceway CO, N₂, and H₂ output (flame) masses, 565, 1064, and 15 kg from Cells C46, C47, and C48,
2. raceway output gas (flame) enthalpy, 2036 MJ from Cell F53

of matrix [Table 18.2](#) all per 1000 kg of Fe in product molten iron.

We now;

1. modify flame temperature Eq. (14.16) of Chapter 14, Raceway Flame Temperature, to include H₂(g) in raceway output gas, and
2. calculate the raceway flame temperature.

The flame temperature equation (with two new H₂ terms) is;

$$\frac{\left\{ \begin{bmatrix} \text{raceway output} \\ (\text{flame}) \text{ enthalpy} \end{bmatrix} - \begin{bmatrix} \text{mass CO in raceway} \\ \text{output gas} \end{bmatrix} * (-4.183) - \begin{bmatrix} \text{mass N}_2 \text{ in raceway} \\ \text{output gas} \end{bmatrix} * (-0.2448) - \begin{bmatrix} \text{mass H}_2 \text{ in raceway} \\ \text{output gas} \end{bmatrix} * (-4.130) \right\}}{\left\{ \begin{bmatrix} \text{mass CO in raceway} \\ \text{output gas} \end{bmatrix} * 0.001310 + \begin{bmatrix} \text{mass N}_2 \text{ in raceway} \\ \text{output gas} \end{bmatrix} * 0.001301 + \begin{bmatrix} \text{mass H}_2 \text{ in raceway} \\ \text{output gas} \end{bmatrix} * 0.01756 \right\}} = T_{\text{flame}}, ^\circ\text{C} \quad (18.9)$$

is used. The numerical values are from the flame temperature range enthalpy versus temperature equations, Table J.4. They are;

$$\frac{H^\circ T_{\text{flame}}}{\text{MW}_{\text{CO}}} \text{CO(g)} = 0.001310 * T_{\text{flame}} - 4.183 \quad \text{MJ/kg of CO(g)}$$

$$\frac{H^\circ T_{\text{flame}}}{\text{MW}_{\text{N}_2}} \text{N}_2(\text{g}) = 0.001301 * T_{\text{flame}} - 0.2448 \quad \text{MJ/kg of N}_2(\text{g})$$

$$\frac{H^\circ T_{\text{flame}}}{\text{MW}_{\text{H}_2}} \text{H}_2(\text{g}) = 0.01756 * T_{\text{flame}} - 4.130 \quad \text{MJ/kg of H}_2(\text{g})$$

which are applicable in the T_{flame} temperature range of 1800–2400°C.

For the numerical example in [Table 18.2](#), the raceway flame temperature is;

$$\frac{2036 - 565 * (-4.183) - 1064 * (-0.2448) - 15 * (-4.130)}{565 * 0.001310 + 1064 * 0.001301 + 15 * 0.01756} = T_{\text{flame}} = 1976^{\circ}\text{C}$$

or in automatic calculation form:

$$\frac{(F53 - C46 * -4.183 - C47 * -0.2448 - C48 * -4.130)}{(C46 * 0.001310 + C47 * 0.001301 + C48 * 0.01756)} = T_{\text{flame}} = 1976^{\circ}\text{C} \quad (18.10a)$$

This is included in [Table 18.2](#) by inserting the instruction;

$$= \frac{(F53 - C46 * -4.183 - C47 * -0.2448 - C48 * -4.130)}{(C46 * 0.001310 + C47 * 0.001301 + C48 * 0.01756)} \quad (18.10b)$$

in Cell G55.

18.14 EFFECT OF CH₄(g) INJECTION ON RACEWAY FLAME TEMPERATURE

[Fig. 18.2](#) shows the effect of CH₄(g) injection on raceway flame temperature. The temperature drops significantly with increasing CH₄(g) injection.

This cooling effect is due to all the equations in the matrices. We can postulate that the cooling effect is mainly due the replacement of hot, highly positive enthalpy C-in-falling-coke-particles with 25°C negative enthalpy CH₄(g), [Fig. 18.3](#).

The line in [Fig. 18.2](#) is noticeably curved, because the raceway products' enthalpies are affected by raceway flame temperature.

18.15 SUMMARY

This chapter shows how to calculate raceway flame temperature with CH₄(g)

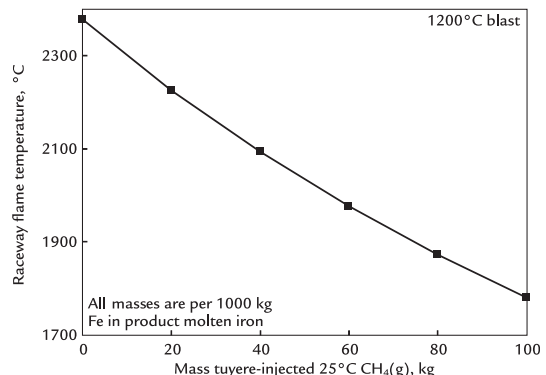


FIGURE 18.2 Influence of 25°C CH₄(g) injectant on raceway output gas (flame) temperature. The marked decrease is notable. Notice that the flame temperature decrease with CH₄(g) injectant is much greater (~600°C/100 kg of injectant) than with C injectant (~120°C/100 kg of injectant), [Fig. 16.2](#). This is a consequence of all the equations in our matrices, but we may speculate that it is mainly due to the large negative enthalpy (per kg of injectant) of the 25°C CH₄(g) as compared to the zero enthalpy of 25°C pulverized carbon. The line is strongly curved, because Eqs. [\(18.9\)](#) and [\(18.10b\)](#) are not linear.

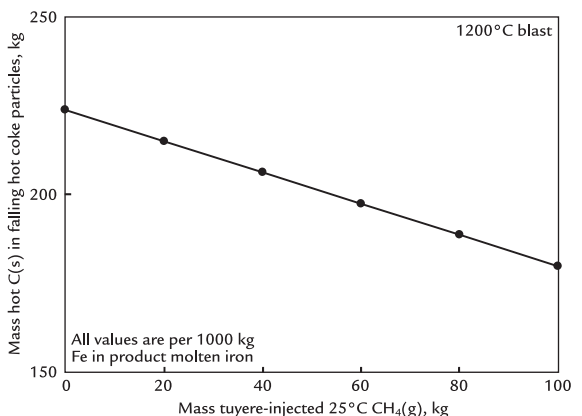


FIGURE 18.3 Effect of mass tuyere-injected CH₄(g) on mass of C-in-coke falling into blast furnace raceways, both per 1000 kg of Fe in product molten iron. Falling C-in-coke mass decreases with increasing CH₄(g) injection.

injection through a blast furnace's tuyeres. The calculations show that flame temperature decreases markedly with increasing CH₄(g) injection. This decrease is mainly due to 25°C CH₄(g)'s large negative enthalpy.

The decrease in flame temperature may be offset by;

1. injecting pure oxygen, and
2. raising blast temperature

while injecting the CH₄(g).

Please predict for them the flame temperature that will result from this amount of injection.

- 18.2.** Operators of Exercise 18.1 now wish to operate at 2050°C flame temperature. They wish to know how much CH₄(g) they will have to inject to obtain this temperature, kg per 1000 kg of Fe in product molten iron. Please calculate this for them. Use two methods of calculation.

- 18.3.** Blast furnace plant of [Table 18.2](#) has refurbished its blast heating stoves. It is now able to produce 1300°C blast. They still want to operate with a 2050°C flame temperature. Please calculate how much CH₄(g) injection they will now need to obtain this flame temperature.

EXERCISES

- 18.1.** Blast furnace operators of [Table 18.2](#) wish to raise their CH₄(g) injection to 120 kg/1000 kg of product molten iron.

Raceway Flame Temperature With Moisture in Blast Air

O U T L I N E

19.1 Moisture in the Blast Air and Its Impact on RAFT	180	19.9 Raceway Nitrogen Balance Equation	185
19.2 Modifying the Bottom Segment and Raceway Matrices	180	19.10 Raceway Matrix Results and Flame Temperature Calculation	185
19.3 Raceway $H_2O(g)$ Input Quantity Specification	182	19.11 Raceway Input Enthalpy Calculation	185
19.4 Raceway O_2 -in-Blast Air Input Specification	182	19.12 Raceway Output Enthalpy	186
19.5 Raceway Input N_2 -in-Blast Air Specification	182	19.13 Raceway Output Gas (Flame) Temperature	187
19.6 Modified Raceway Carbon Balance Equation	184	19.14 Calculation Results	187
19.7 Modified Raceway Oxygen Balance Equation	184	19.15 Discussion	187
19.8 Modified Raceway Hydrogen Balance Equation	184	19.16 Summary	188
		Exercises	189

19.1 MOISTURE IN THE BLAST AIR AND ITS IMPACT ON RAFT

Chapter 18, Raceway Flame Temperature With CH₄(g) Tuyere Injection, calculated raceway flame temperature with tuyere-injected CH₄(g). This chapter calculates the raceway adiabatic flame temperature (RAFT) with through-tuyere H₂O(g) input, Fig. 19.1. Our objectives are to;

1. show how H₂O(g) injection is included in our raceway flame temperature calculations,
2. indicate how H₂O(g) injection affects raceway flame temperature, and
3. explain this flame temperature effect.

Note that;

1. the H₂O(g) enters the blast furnace and raceway at blast temperature, and
2. the H₂O(g) enters blast furnace raceways in humid blast air plus injected steam, Chapter 12, Bottom Segment With Moisture in Blast Air.

19.2 MODIFYING THE BOTTOM SEGMENT AND RACEWAY MATRICES

Our flame temperature calculation begins with matrix bottom-segment input and output masses of Table 12.1 (copied here as Table 19.1).

It then prepares a tuyere raceway matrix from these results by;

1. specifying that all of H₂O(g), O₂, and N₂-in-blast air of matrix Table 12.1 enter the Fig. 19.1 raceway, and
 2. preparing new raceway hydrogen and oxygen mass balances.
- It then determines;
3. all raceway's input and output masses including mass input H₂O(g);
 4. the raceway input and output enthalpies from these masses and the raceway input temperatures; and

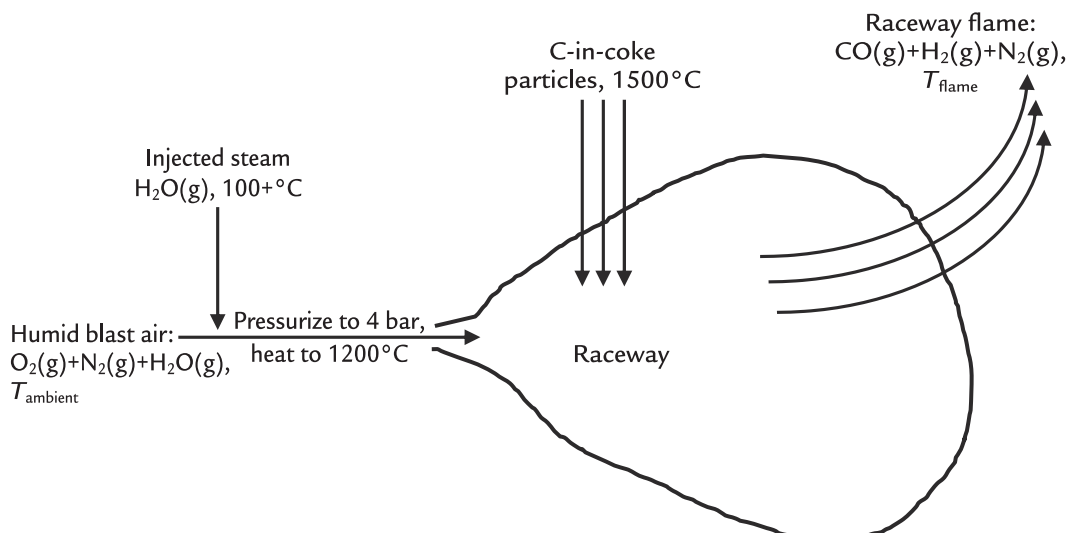


FIGURE 19.1 Sketch of blast furnace raceway with through-tuyere 1200°C H₂O(g) input in humid air and steam. All H₂O(g) enters the blast furnace through its raceways. In three dimensions, the raceway is a horizontal pear shape. It is full of gas and hurtling coke particles. This sketch is a vertical slice through the center of a raceway. The calculations in this chapter specify that the through-tuyere blast contains 15 g H₂O(g)/Nm³ of dry air (Eq. 12.2).

TABLE 19.1 Bottom-Segment Matrix With Through-Tuyere Input H₂O(g).

A	B	C	D	E	F	G	H	I	J	K	L	M	N	O	
BOTTOM SEGMENT CALCULATIONS															
Equation	Description	Numerical term	mass Fe _{0.94} O into bottom segment	mass C in descending coke	mass O ₂ in blast air	mass N ₂ in blast air	mass Fe out in molten iron	mass C out in molten iron	mass CO out in ascending gas	mass CO ₂ out in ascending gas	mass N ₂ out in ascending gas	mass H ₂ out in ascending gas	mass H ₂ O out in ascending gas	mass through-tuyere input H ₂ O(g)	
7.7	Fe out in molten iron specification	1000	0	0	0	0	1	0	0	0	0	0	0	0	
7.2	Fe mass balance	0	-0.768	0	0	0	1	0	0	0	0	0	0	0	
12.5	O mass balance	0	-0.232	0	-1	0	0	0	0.571	0.727	0	0	0.888	-0.888	
7.4	C mass balance	0	0	-1	0	0	0	1	0.429	0.273	0	0	0	0	
7.5	N mass balance	0	0	0	0	-1	0	0	0	0	1	0	0	0	
12.3	H mass balance	0	0	0	0	0	0	0	0	0	0	1	0.112	-0.112	
7.6	N ₂ in blast air specification	0	0	0	3.3	-1	0	0	0	0	0	0	0	0	
7.9	Equilibrium CO ₂ /CO mass ratio	0	0	0	0	0	0	0	0.694	-1	0	0	0	0	
11.8	Equilibrium H ₂ O/H ₂ mass ratio	0	0	0	0	0	0	0	0	0	0	5.44	-1	0	
7.8	C out in molten iron specification	0	0	0	0	0	0.047	-1	0	0	0	0	0	0	
12.7	Enthalpy balance	-320	3.152	-1.359	-1.239	-1.339	1.269	5	-2.926	-7.926	1.008	13.35	-11.50	10.81	
12.2	Mass through-tuyere input H ₂ O(g)	0	0	0	0.0118	0.0118	0	0	0	0	0	0	0	-1	
		930°C	930°C	1200°C	1200°C	1500°C	1500°C	930°C	930°C	930°C	930°C	930°C	930°C	1200°C	
16	Calculated values	kg per 1000 kg of Fe out in molten iron													
18	mass Fe _{0.94} O into bottom segment	1302													
19	mass C in descending coke	399	also = mass C in the furnace's coke charge, Eqn. (7.16)												
20	mass O ₂ in blast air	302													
21	mass N ₂ in blast air	995													
22	mass Fe out in molten iron	1000													
23	mass C out in molten iron	47													
24	mass CO out in ascending gas	569													
25	mass CO ₂ out in ascending gas	395													
26	mass N ₂ out in ascending gas	995													
27	mass H ₂ out in ascending gas	1.1													
28	mass H ₂ O out in ascending gas	5.8													
29	mass through-tuyere input H ₂ O(g)	15													
30															

It is a copy of Table 12.1. Row 14 describes the amount of H₂O(g) entering the raceways with 15 g of H₂O(g)/Nm³ of dry air in blast (Eq. 12.2). All mass is per 1000 kg of Fe in product molten iron.

5. the raceway output gas (flame) temperature from the raceway's output enthalpy and output masses.

The calculations are shown in Table 19.2. They are explained in Sections 19.3–19.13.

19.3 RACEWAY H₂O(g) INPUT QUANTITY SPECIFICATION

The raceway's H₂O(g) input mass specification is represented in Row 14 of the spreadsheet in Table 19.2. It is;

$$\left[\frac{\text{mass H}_2\text{O(g)}}{\text{entering raceway}} \right] * 1 = \left[\frac{\text{mass through-tuyere}}{\text{input H}_2\text{O(g)}} \right] * 1$$

or in the present case;

$$\begin{aligned} & \left[\frac{\text{mass H}_2\text{O(g)}}{\text{entering raceway}} \right] * 1 \\ & = 15 \text{ kg through-tuyere input H}_2\text{O, Cell C29} \end{aligned}$$

or in matrix form;

$$15 = \left[\frac{\text{mass H}_2\text{O(g)}}{\text{entering raceway}} \right] * 1 \quad (19.1)$$

as shown in Row 39, all masses per 1000 kg of Fe in product molten iron.

The numerical value is put into the raceway matrix by typing the instruction =C29 into raceway Cell C39. Note that it is for an H₂O(g) in blast concentration of 15 g of H₂O(g)/Nm³ of dry air.

19.4 RACEWAY O₂-IN-BLAST AIR INPUT SPECIFICATION

Bottom-segment matrix results of Table 19.2 show that 302 kg of O₂ in blast, Cell C20 is required for steady production of 1500°C molten iron with 15 kg of through-tuyere input

H₂O(g), Cell C29. This is also the amount of O₂ entering a furnace's raceways in blast.

This oxygen input value is included in our raceway matrix by means of the O₂ specification;

$$\begin{aligned} & \left[\frac{\text{mass O}_2 \text{ entering}}{\text{raceway in blast}} \right] \\ & = 302 \text{ kg/1000 kg of Fe in product molten iron (Cell C20)} \end{aligned}$$

or in matrix form;

$$302 = \left[\frac{\text{mass O}_2 \text{ entering}}{\text{raceway in blast}} \right] * 1 \quad (19.2)$$

Of course, this numerical value will change with different concentrations of H₂O(g)-in-blast. This is automatically taken care of by inserting the instruction;

$$=C20$$

into raceway matrix Cell C33.

19.5 RACEWAY INPUT N₂-IN-BLAST AIR SPECIFICATION

Blast furnace steady-state N₂ input varies with the amount of injected H₂O(g). This affects the amount of N₂-in-blast entering the raceway, hence raceway flame temperature. In this case, it is;

$$\begin{aligned} & \left[\frac{\text{mass N}_2 \text{ entering}}{\text{raceway in blast}} \right] \\ & = 995 \text{ kg/1000 kg of Fe in product molten iron (Cell C21)} \end{aligned}$$

or in matrix terms;

$$995 = \left[\frac{\text{mass N}_2 \text{ entering}}{\text{raceway in blast}} \right] * 1 \quad (19.3)$$

The nitrogen input is automatically inserted into raceway Cell C34 by the instruction;

$$=C21$$

TABLE 19.2 Bottom-Segment and Raceway Matrices/Equations With Through-Tuyere Input H₂O(g)

	A	B	C	D	E	F	G	H	I	J	K	L	M	N	O
1 BOTTOM SEGMENT CALCULATIONS															
3	Equation	Description	Numerical term	mass Fe _{0.94} O into bottom segment	mass C in descending coke	mass O ₂ in blast air	mass N ₂ in blast air	mass Fe out in molten iron	mass C out in molten iron	mass CO out in ascending gas	mass CO ₂ out in ascending gas	mass N ₂ out in ascending gas	mass H ₂ out in ascending gas	mass H ₂ O out in ascending gas	mass through-tuyere input H ₂ O(g)
3	7.7	Fe out in molten iron specification	1000	0	0	0	0	1	0	0	0	0	0	0	0
4	7.2	Fe mass balance	0	-0.768	0	0	0	1	0	0	0	0	0	0	0
5	12.5	O mass balance	0	-0.232	0	-1	0	0	0	0.571	0.727	0	0	0.888	-0.888
6	7.4	C mass balance	0	0	-1	0	0	0	1	0.429	0.273	0	0	0	0
7	7.5	N mass balance	0	0	0	0	-1	0	0	0	0	1	0	0	0
8	12.3	H mass balance	0	0	0	0	0	0	0	0	0	0	1	0.112	-0.112
9	7.6	N ₂ in blast air specification	0	0	0	3.3	-1	0	0	0	0	0	0	0	0
10	7.9	Equilibrium CO/CO mass ratio	0	0	0	0	0	0	0	0.694	-1	0	0	0	0
11	11.8	Equilibrium H ₂ /H ₂ mass ratio	0	0	0	0	0	0	0	0	0	5.44	-1	0	0
12	7.8	C out in molten iron specification	0	0	0	0	0	0.047	-1	0	0	0	0	0	0
13	12.7	Enthalpy balance	-320	3.152	1.359	-1.239	1.339	1.269	5	-2.926	7.926	1.008	13.34	-11.50	10.81
14	12.2	Mass through-tuyere input H ₂ O(g)	0	0	0	0.011811	0.011811	0	0	0	0	0	0	0	-1
15		Blast temperature	1200	°C											
16															
17		Calculated values	kg per 1000 kg of Fe out in molten iron												
18		mass Fe _{0.94} O into bottom segment	1302												=-(0.002582 * E15-13.9113)
19		mass C in descending coke	399												
20		mass O ₂ in blast air	302												
21		mass N ₂ in blast air	995												
22		mass Fe out in molten iron	1000												
23		mass C out in molten iron	47												
24		mass CO out in ascending gas	569												
25		mass CO ₂ out in ascending gas	395												
26		mass N ₂ out in ascending gas	995												
27		mass H ₂ out in ascending gas	1.1												
28		mass H ₂ O out in ascending gas	5.8												
29		mass through-tuyere input H ₂ O(g)	15												
30															
31		RACEWAY INPUTS AND OUTPUTS CALCULATION													
32	Equation	Description	Numerical Term	mass O ₂ entering raceway in blast air	mass N ₂ entering raceway in blast air	mass C entering raceway in falling coke particles	mass CO in raceway output gas	mass N ₂ in raceway output gas	mass H ₂ in raceway output gas	mass H ₂ O(g) entering raceway					
33	19.2	Mass O ₂ entering raceway in blast air	302	1	0	0	0	0	0	0	0				
34	19.3	Mass N ₂ entering raceway in blast air	995	0	1	0	0	0	0	0	0				
35	14.10	Raceway carbon balance	0	0	0	-1	0.429	0	0	0	0				
36	19.10	Raceway oxygen balance	0	-1	0	0	0.571	0	0	0	0				
37	19.5	Raceway hydrogen balance	0	0	0	0	0	0	0	0	0				
38	14.9	Raceway nitrogen balance	0	0	0	-1	0	0	1	0	0				
39	19.1	Mass H ₂ O(g) entering raceway	15	0	0	0	0	0	0	0	1				
40			1200°C	1200°C	1500°C	T _{flame}	T _{flame}	T _{flame}	T _{flame}	1200°C					
41															
42		Raceway calculated values	kg per 1000 kg of Fe out in molten iron												
43		mass O ₂ entering raceway in blast air	302												
44		mass N ₂ entering raceway in blast air	995												
45		mass C entering raceway in falling coke	237												
46		mass CO in raceway exit gas	552												
47		mass N ₂ in raceway exit gas	995												
48		mass H ₂ in raceway exit gas	1.7												
49		mass H ₂ O(g) entering raceway	15												
50															
51		FLAME ENTHALPY AND FLAME TEMPERATURE CALCULATIONS													
52	19.7c	Total Raceway input enthalpy =C49*-0.13+C43*-F13+C44*-G13+C45*-2.488 =					2130								
53	19.8	Total Raceway output flame enthalpy=total raceway input enthalpy *G52 =					2130								
54															
55	19.10b	Flame temperature °C =(053*C46*-4.183*C47*-0.2448*C48*-4.130)/(C46*0.001310+C47*0.001301+C48*0.01756) =					2290	°C							

Cell C33 = C20; Cell C34 = C21; and Cell C39 = C29. The blast contains 15 g of H₂O(g)/Nm³ of dry air. The flame temperature under these conditions is shown to be 2290°C.

19.6 MODIFIED RACEWAY CARBON BALANCE EQUATION

With $\text{H}_2\text{O(g)}$ injection, there is no C in the injectant so that the carbon balance reverts to;

$$\begin{aligned} & \left[\frac{\text{mass C in falling coke particles}}{\text{in solid carbon}} \right] * \frac{100 \text{ mass\% C}}{100\%} \\ & = \left[\frac{\text{mass CO in raceway output gas}}{\text{output gas}} \right] * \frac{[42.9 \text{ mass\% C in CO}]}{100\%} \end{aligned}$$

or

$$\left[\frac{\text{mass C in falling coke particles}}{\text{in solid carbon}} \right] * 1 = \left[\frac{\text{mass CO in raceway output gas}}{\text{output gas}} \right] * 0.429$$

or subtracting $\left\{ \left[\frac{\text{mass C in falling coke particles}}{\text{in solid carbon}} \right] * 1 \right\}$ from both sides;

$$\begin{aligned} 0 &= - \left[\frac{\text{mass C in falling coke particles}}{\text{in solid carbon}} \right] * 1 \\ &+ \left[\frac{\text{mass CO in raceway output gas}}{\text{output gas}} \right] * 0.429 \end{aligned} \quad (14.10)$$

as shown in Row 35.

19.7 MODIFIED RACEWAY OXYGEN BALANCE EQUATION

With $\text{H}_2\text{O(g)}$ input through the blast furnace tuyeres, the raceway oxygen balance becomes;

$$\begin{aligned} & [\text{mass O entering in injected } \text{H}_2\text{O}] \\ & + [\text{mass O entering in blast air}] = [\text{mass O leaving in CO}] \end{aligned}$$

With inputs and outputs of Fig. 19.1, this equation expands to;

$$\begin{aligned} & \left[\frac{\text{mass H}_2\text{O(g)}}{\text{entering raceways}} \right] * \frac{[88.8 \text{ mass\% O in H}_2\text{O}]}{100\%} \\ & + \left[\frac{\text{mass O}_2 \text{ entering}}{\text{raceway in blast}} \right] * \frac{[100 \text{ mass\% O in O}_2]}{100\%} \\ & = \left[\frac{\text{mass CO in raceway output gas}}{\text{output gas}} \right] * \frac{[57.1 \text{ mass\% O in CO}]}{100\%} \end{aligned}$$

or

$$\begin{aligned} & \left[\frac{\text{mass H}_2\text{O(g)}}{\text{entering raceways}} \right] * 0.888 + \left[\frac{\text{mass O}_2 \text{ entering}}{\text{raceway in blast}} \right] * 1 \\ & = \left[\frac{\text{mass CO in raceway output gas}}{\text{output gas}} \right] * 0.571 \end{aligned}$$

or subtracting $\left\{ \left[\frac{\text{mass H}_2\text{O(g)}}{\text{entering raceways}} \right] * 0.888 + \left[\frac{\text{mass O}_2 \text{ entering}}{\text{raceway in blast}} \right] * 1 \right\}$ from both sides;

$$\begin{aligned} 0 &= - \left[\frac{\text{mass H}_2\text{O(g)}}{\text{entering raceways}} \right] * 0.888 \\ &- \left[\frac{\text{mass O}_2 \text{ entering}}{\text{raceway in blast}} \right] * 1 \\ &+ \left[\frac{\text{mass CO in raceway output gas}}{\text{output gas}} \right] * 0.571 \end{aligned} \quad (19.4)$$

as shown in Row 36.

19.8 MODIFIED RACEWAY HYDROGEN BALANCE EQUATION

With through-tuyere input $\text{H}_2\text{O(g)}$, the raceway hydrogen balance becomes

$$\begin{aligned} & [\text{mass H entering raceway in H}_2\text{O(g)}] \\ & = [\text{mass H leaving raceway in H}_2\text{(g)}] \end{aligned}$$

It expands to;

$$\begin{aligned} & \left[\frac{\text{mass H}_2\text{O(g)}}{\text{entering raceway}} \right] * \frac{[11.2 \text{ mass\% H in injected H}_2\text{O}]}{100\%} \\ & = \left[\frac{\text{mass H}_2 \text{ in raceway}}{\text{output gas}} \right] * \frac{[100 \text{ mass\% H in ascending H}_2]}{100\%} \end{aligned}$$

or

$$\left[\frac{\text{mass H}_2\text{O(g)}}{\text{entering raceway}} \right] * 0.112 = \left[\frac{\text{mass H}_2 \text{ in raceway}}{\text{output gas}} \right] * 1$$

or subtracting $\left\{ \left[\frac{\text{mass H}_2\text{O(g)}}{\text{entering raceway}} \right] * 0.112 \right\}$ from both sides;

$$0 = - \left[\begin{array}{l} \text{mass H}_2\text{O(g)} \\ \text{entering raceways} \end{array} \right] * 0.112 + \left[\begin{array}{l} \text{mass H}_2 \text{ in raceway} \\ \text{output gas} \end{array} \right] * 1 \quad (19.5)$$

$$\left[\begin{array}{l} \text{raceway} \\ \text{input} \\ \text{enthalpy} \end{array} \right] = \left[\begin{array}{l} \text{mass H}_2\text{O(g)} \\ \text{entering raceway} \end{array} \right] * \frac{H^\circ_{1200^\circ\text{C}} \text{H}_2\text{O(g)}}{\text{MW}_{\text{H}_2\text{O}}} + \left[\begin{array}{l} \text{mass O}_2 \text{ entering} \\ \text{raceway in} \\ \text{blast} \end{array} \right] * \frac{H^\circ_{1200^\circ\text{C}} \text{O}_2(\text{g})}{\text{MW}_{\text{O}_2}} + \left[\begin{array}{l} \text{mass N}_2 \text{ entering} \\ \text{raceway in} \\ \text{blast} \end{array} \right] * \frac{H^\circ_{1200^\circ\text{C}} \text{N}_2(\text{g})}{\text{MW}_{\text{N}_2}} + \left[\begin{array}{l} \text{mass C in} \\ \text{falling coke} \\ \text{particles} \end{array} \right] * \frac{H^\circ_{1500^\circ\text{C}} \text{C(s)}}{\text{MW}_{\text{C}}}$$

as shown in Row 37.

19.9 RACEWAY NITROGEN BALANCE EQUATION

The raceway nitrogen balance remains the same as in all the previous flame temperature calculation chapters. It is;

$$0 = - \left[\begin{array}{l} \text{mass N}_2 \text{ entering} \\ \text{raceway in blast air} \end{array} \right] * 1 + \left[\begin{array}{l} \text{mass N}_2 \text{ in raceway} \\ \text{output gas} \end{array} \right] * 1 \quad (14.9)$$

or

$$\left[\begin{array}{l} \text{raceway} \\ \text{input} \\ \text{enthalpy} \end{array} \right] = \left[\begin{array}{l} \text{mass H}_2\text{O(g)} \\ \text{entering raceway} \end{array} \right] * (-10.81) + \left[\begin{array}{l} \text{mass O}_2 \text{ entering} \\ \text{raceway in} \\ \text{blast} \end{array} \right] * 1.239 + \left[\begin{array}{l} \text{mass N}_2 \text{ entering} \\ \text{raceway in} \\ \text{blast} \end{array} \right] * 1.339 + \left[\begin{array}{l} \text{mass C in} \\ \text{falling coke} \\ \text{particles} \end{array} \right] * 2.488 \quad (19.6)$$

as shown in Row 38.

19.10 RACEWAY MATRIX RESULTS AND FLAME TEMPERATURE CALCULATION

Our raceway matrix determines all raceway's input and output masses, Cells C43–C49. We are now ready to calculate;

- raceway input enthalpy,
- raceway output enthalpy, and
- raceway output gas (flame) temperature

as described in the next three sections.

where from Table J.1;

$$-10.81 = \frac{H^\circ_{1200^\circ\text{C}} \text{H}_2\text{O(g)}}{\text{MW}_{\text{H}_2\text{O}}}$$

$$1.239 = \frac{H^\circ_{1200^\circ\text{C}} \text{O}_2(\text{g})}{\text{MW}_{\text{O}_2}}$$

$$1.339 = \frac{H^\circ_{1200^\circ\text{C}} \text{N}_2(\text{g})}{\text{MW}_{\text{N}_2}}$$

19.11 RACEWAY INPUT ENTHALPY CALCULATION

With 1200°C $\text{H}_2\text{O(g)}$ injection, our raceway's input enthalpy is;

$$2.488 = \frac{H^\circ_{1500^\circ\text{C}}}{\text{MW}_\text{C}}$$

all MJ per kg of substance.

Numerically, the input enthalpy is;

$$\begin{bmatrix} \text{raceway} \\ \text{input} \\ \text{enthalpy} \end{bmatrix} = 15 * (-10.81) + 302 * 1.239 \\ + 995 * 1.339 + 237 * 2.488 = 2130 \text{ MJ}/1000\text{kg of Fe in product molten iron}$$
(19.7a)

where 15, 302, 995, and 237 are from Cells C49, C43, C44, and C45 of [Table 19.2](#).

Another form of this equation is;

$$\begin{bmatrix} \text{raceway} \\ \text{input} \\ \text{enthalpy} \end{bmatrix} = \text{C49} * (-10.81) + \text{C43} * 1.239 \\ + \text{C44} * 1.339 + \text{C45} * 2.488 = 2130 \text{ MJ}/1000\text{kg of Fe in product molten iron}$$
(19.7b)

and including blast temperature-dependent cells;

$$\begin{bmatrix} \text{raceway} \\ \text{input} \\ \text{enthalpy} \end{bmatrix} = \text{C49} * -\text{O13} + \text{C43} * -\text{F13} + \text{C44} * -\text{G13} \\ + \text{C45} * 2.488 = 2130 \text{ MJ}/1000\text{kg of Fe in product molten iron}$$
(19.7c)

where:

$$\text{Cell O13} = -\frac{H^\circ_{\text{blast}}}{\text{MW}_{\text{H}_2\text{O}}}$$

$$\text{Cell F13} = -\frac{H^\circ_{\text{blast}}}{\text{MW}_{\text{O}_2}}$$

and

$$\text{Cell G13} = -\frac{H^\circ_{\text{blast}}}{\text{MW}_{\text{N}_2}}$$

The left-hand side of Eq. (19.7c) are inserted into Cell G52, which calculates input enthalpy as a function of mass throughput, input $\text{H}_2\text{O(g)}$, Cell C29, and blast temperature, Cell E15.

19.12 RACEWAY OUTPUT ENTHALPY

Raceway output enthalpy is needed to calculate raceway output gas (flame) temperature.

As described in Chapter 14, Raceway Flame Temperature, it is calculated by the adiabatic equation;

$$\begin{bmatrix} \text{raceway output} \\ \text{(flame) enthalpy} \end{bmatrix} + \text{zero} = \begin{bmatrix} \text{raceway} \\ \text{input} \\ \text{enthalpy} \end{bmatrix}$$

with zero conductive, convective, and radiative heat loss from the raceway to its surroundings.

From [Section 19.11](#), the raceway input enthalpy is 2130 MJ/kg of Fe in product molten iron so that;

$$\begin{bmatrix} \text{raceway output} \\ \text{(flame) enthalpy} \end{bmatrix} = \begin{bmatrix} \text{raceway} \\ \text{input} \\ \text{enthalpy} \end{bmatrix} \\ = 2130 \text{ MJ}/1000\text{kg of Fe in product molten iron}$$
(19.8)

Matrix [Table 19.2](#) does this calculation with the instruction;

= G52

in Cell G53.

19.13 RACEWAY OUTPUT GAS (FLAME) TEMPERATURE

Our raceway flame temperature calculations use spreadsheet Table 19.2's;

1. raceway CO, N₂, and H₂ output masses, 552, 995, and 1.7 kg from Cells C46–C48, and
2. raceway output gas (flame) enthalpy, 2130 MJ from Cell G53

all per 1000 kg of Fe in product molten iron.

Flame temperature equation of Section 18.13, that is;

$$\left\{ \begin{bmatrix} \text{raceway} \\ \text{output} \\ (\text{flame}) \text{ enthalpy} \end{bmatrix} - \begin{bmatrix} \text{mass CO in} \\ \text{raceway} \\ \text{output gas} \end{bmatrix} * (-4.183) \right. \\ \left. - \begin{bmatrix} \text{mass N}_2 \text{ in raceway} \\ \text{output gas} \end{bmatrix} * (-0.2448) \right. \\ \left. - \begin{bmatrix} \text{mass H}_2 \text{ in raceway} \\ \text{output gas} \end{bmatrix} * (-4.130) \right\} \\ = T_{\text{flame}}, ^\circ \text{C} \quad (18.9)$$

is used. The numerical values are from the raceway output gas's enthalpy versus flame temperature equations, Table J.4. They are;

$$\frac{H^\circ T_{\text{flame}}}{\text{CO(g)}} = 0.001310 * T_{\text{flame}} - 4.183 \text{ MJ/kg of CO(g)}$$

$$\frac{H^\circ T_{\text{flame}}}{\text{N}_2(\text{g})} = 0.001301 * T_{\text{flame}} - 0.2448 \text{ MJ/kg of N}_2$$

and

$$\frac{H^\circ T_{\text{flame}}}{\text{H}_2(\text{g})} = 0.01756 * T_{\text{flame}} - 4.130 \text{ MJ/kg of H}_2(\text{g})$$

For the numerical example in Table 19.2, the raceway flame temperature is;

$$\frac{2130 - 552 * -4.183 - 995 * -0.2448 - 1.7 * -4.130}{552 * 0.001310 + 995 * 0.001301 + 1.7 * 0.01756} \\ = T_{\text{flame}} = 2290^\circ \text{C} \quad (19.9)$$

In cell terms, this is;

$$\frac{G53 - C46 * -4.183 - C47 * -0.2448 - C48 * -4.130}{C46 * 0.001310 + C47 * 0.001301 + C48 * 0.01756} \\ = T_{\text{flame}} = 2290^\circ \text{C} \quad (19.10a)$$

For automatic calculation, we insert;

$$= \frac{G53 - C46 * -4.183 - C47 * -0.2448 - C48 * -4.130}{C46 * 0.001310 + C47 * 0.001301 + C48 * 0.01756} \quad (19.10b)$$

in Cell G55.

19.14 CALCULATION RESULTS

Table 19.2 shows that flame temperature of Fig. 19.1 with 15 g of H₂O(g)/Nm³ of dry air blast is 2290°C.

19.15 DISCUSSION

Fig. 19.2 plots the above calculated raceway flame temperature point and others and shows that raceway flame temperature decreases with increasing H₂O(g) in blast. This is a consequence of all equations of matrix Table 19.2. We may speculate that it is mainly due to the input large negative enthalpy of H₂O(g) - which lowers the enthalpy and hence temperature of the raceway output gas Fig. 19.3 shows

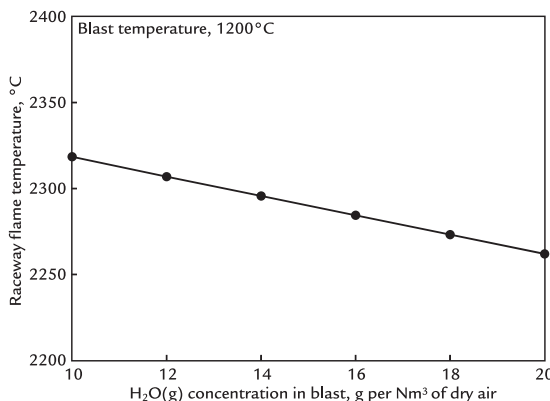


FIGURE 19.2 Steady-state raceway flame temperature with through-tuyere input H₂O(g). It has been plotted by varying the values in Cells F14 and G14 of [Table 19.2](#) (as described in Appendix O) and plotting Cell C49's H₂O(g) input quantity versus Cell G55's raceway flame temperature. As expected, flame temperature decreases with increasing through-tuyere H₂O(g) input. Each additional kg of H₂O(g) lowers the flame temperature by ~5.5°C, but the line isn't exactly straight.

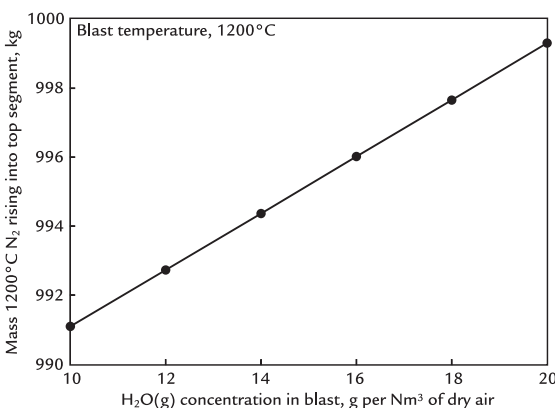


FIGURE 19.3 Graph showing that the mass of hot nitrogen rising into the top segment increases with increasing H₂O(g) concentration in blast. Our expectation is that this increase in hot nitrogen will result in hotter top gas, [Figs. 28.2 and 28.3](#). All masses are kg/1000 kg of Fe in product molten iron.

that increasing H₂O(g) concentration in the blast increases the mass of N₂ rising into the top segment. This is because more blast air

and carbon is required to satisfy the enthalpy balance of [Table 19.2](#).

19.16 SUMMARY

All iron blast furnace blast air contains H₂O(g), [Fig. 19.1](#). Moisture promotes smooth burden descent and rapid furnace start-ups. It also lowers the raceway flame temperature and hence Si content in product molten iron.

The H₂O(g)-in-blast is made up of the H₂O(g) in humid blast air topped up with steam to obtain a prescribed H₂O(g) concentration of about 15 g of H₂O(g)/Nm³ of dry air.

This moist blast enters the furnace through its tuyeres and into the tuyere raceways. There:

1. the O₂-in-blast reacts with falling coke particles to produce CO₂(g) plus heat,
2. the resulting CO₂(g) reacts further with the falling C-in-coke to produce CO(g), and
3. the input H₂O(g)-in-blast reacts with the C-in-coke to produce H₂(g).

The resulting CO(g) and H₂(g) then leave the raceway and begin the blast furnace iron oxide reduction process. Raceway flame temperature is the temperature at which CO(g) and H₂(g) plus N₂(g) from the blast air leave the raceway.

It is readily determined by our:

1. raceway matrix,
2. input enthalpy and output (flame) enthalpy calculations, and
3. output gas (flame) temperature calculation.

H₂O(g) is readily included in these calculations, in much the same way as described for injected CH₄(g), Chapter 18, Raceway Flame Temperature With CH₄(g) Tuyere Injection.

Raceway flame temperature decreases with increasing H₂O(g) concentration in blast,

Figs. 19.2. This is the result of all our equations, but we speculate that it is mainly due to the large negative enthalpy of the input H₂O (g) which lowers;

1. the enthalpy of the raceway inputs;
2. the enthalpy of the raceway outputs; and
3. the temperature of the outputs (i.e., the flame temperature).

EXERCISES

- 19.1.** To smooth their blast furnace's operation, blast furnace operators of [Table 19.2](#) plan

to increase the H₂O(g) concentration in their blast to 25 g of H₂O(g)/Nm³ of dry air in blast by injecting steam. Please predict for them the change in raceway flame temperature that will result from this change.

- 19.2.** Blast of Exercise 19.1 contains 25 g of H₂O (g)/Nm³ of dry air in blast. Its humid air portion contains 9 g of H₂O(g)/Nm³ of dry air. How much steam must be added to make the furnace's 25 g H₂O/Nm³ blast? Please express your answer in;
1. g/Nm³ of dry air,
2. kg/kg of dry air, and
3. kg/1000 kg of product molten iron.

Top Segment Mass Balance

O U T L I N E

20.1 Combining the Bottom and Top Segments of the Blast Furnace	191	20.5 No Carbon Oxidation in the Top Segment	196
20.2 Top-Segment Calculations	192	20.6 Top Gas Results	196
20.3 Mass Balance Equations	192	20.7 Coupling Top and Bottom-Segment Calculations	196
20.3.1 Fe Mass Balance Equation	192	20.8 Summary	198
20.3.2 Oxygen Mass Balance Equation	192	Exercises	198
20.3.3 Carbon Mass Balance Equation	194		
20.3.4 Nitrogen Mass Balance Equation	195		
20.4 Quantity Specification Equations	195		

20.1 COMBINING THE BOTTOM AND TOP SEGMENTS OF THE BLAST FURNACE

Chapter 7, Conceptual Division of the Blast Furnace, examined reactions in the bottom segment of the iron blast furnace, Fig. 20.1.

The principle outcome presented in Chapter 7, Conceptual Division of the Blast Furnace, was *a priori* calculation of carbon-in-coke and oxygen-in-blast requirements for steady production at 1500°C molten iron from iron oxide ore.

This chapter examines reactions in the top segment of the furnace (Fig. 20.2). Our objectives are to use bottom-segment results of Chapter 7, Conceptual Division of the Blast Furnace, Table 20.1, to determine;

1. blast furnace top gas composition, and
2. the effect of blast temperature on top gas composition.

Chapter 21, Top-Segment Enthalpy Balance, and Chapter 22, Top Gas Temperature Calculation, do the same for top gas enthalpy and temperature.

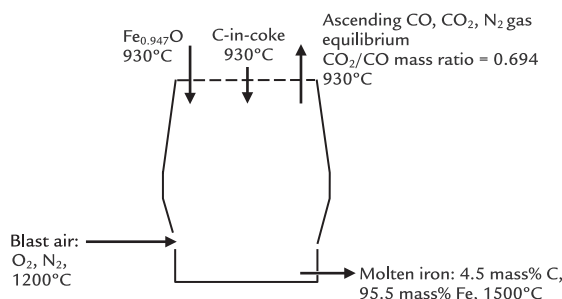


FIGURE 20.1 Bottom segment of conceptually divided blast furnace. This is a copy of Fig. 7.3.

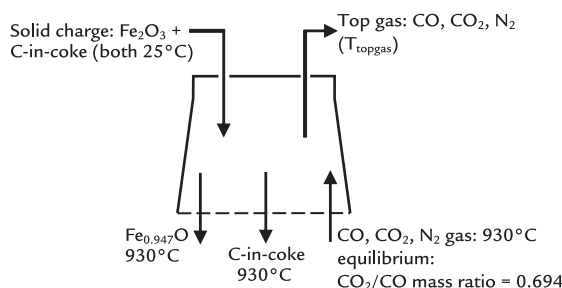


FIGURE 20.2 Top segment of conceptually divided blast furnace. Flows of $\text{Fe}_{0.947}\text{O}$, C-in-coke, CO, CO_2 , and N_2 across the division are the same as in Fig. 20.1.

This chapter's general conclusions are that;

1. blast furnace carbon and oxygen requirements are determined in the bottom segment of the furnace, but
2. reactions in the top segment determine top gas composition, top gas enthalpy, and top gas temperature.

20.2 TOP-SEGMENT CALCULATIONS

As with all our calculations, this chapter's calculations use steady-state mass balances and several quantity specifications.

The basic top-segment steady-state mass balances are;

$$\text{mass Fe in} = \text{mass Fe out} \quad (20.1\text{a})$$

$$\text{mass O in} = \text{mass O out} \quad (20.1\text{b})$$

$$\text{mass C in} = \text{mass C out} \quad (20.1\text{c})$$

$$\text{mass N in} = \text{mass N out} \quad (20.1\text{d})$$

all per 1000 kg of Fe in product molten iron.

The next four sections expand these equations to include top-segment variables of Fig. 20.2.

20.3 MASS BALANCE EQUATIONS

20.3.1 Fe Mass Balance Equation

Iron enters the top segment of Fig. 20.2 as hematite, Fe_2O_3 . It leaves in wustite, $\text{Fe}_{0.947}\text{O}$. There is no $\text{Fe}_{0.947}\text{O}$ to Fe reduction in the top segment (Section 7.1). These specifications and Eq. (20.1a) give;

$$\begin{aligned} & \left[\frac{\text{mass } \text{Fe}_2\text{O}_3 \text{ in}}{\text{furnace charge}} \right] * \frac{[69.9 \text{ mass\% Fe in } \text{Fe}_2\text{O}_3]}{100\%} \\ &= \left[\frac{\text{mass } \text{Fe}_{0.947}\text{O} \text{ descending}}{\text{into bottom segment}} \right] \\ & \quad * \frac{[76.8 \text{ mass\% Fe in } \text{Fe}_{0.947}\text{O}]}{100\%} \end{aligned}$$

or

$$\begin{aligned} & \left[\frac{\text{mass } \text{Fe}_2\text{O}_3 \text{ in}}{\text{furnace charge}} \right] * 0.699 \\ &= \left[\frac{\text{mass } \text{Fe}_{0.947}\text{O} \text{ descending}}{\text{into bottom segment}} \right] * 0.768 \end{aligned}$$

or subtracting $\left\{ \left[\frac{\text{mass } \text{Fe}_2\text{O}_3 \text{ in}}{\text{furnace charge}} \right] * 0.699 \right\}$ from both sides;

$$\begin{aligned} 0 &= - \left[\frac{\text{mass } \text{Fe}_2\text{O}_3 \text{ in}}{\text{furnace charge}} \right] * 0.699 \\ &+ \left[\frac{\text{mass } \text{Fe}_{0.947}\text{O} \text{ descending}}{\text{into bottom segment}} \right] * 0.768 \end{aligned} \quad (20.2)$$

20.3.2 Oxygen Mass Balance Equation

Oxygen enters the top segment in input Fe_2O_3 . It also enters in CO and CO_2 rising from the bottom segment, Fig. 20.2. Oxygen

TABLE 20.1 Fig. 20.1 Bottom-Segment Matrix

	A	B	C	D	E	F	G	H	I	J	K	L
1	BOTTOM SEGMENT CALCULATIONS											
2	Equation	Description	Numerical term	mass $Fe_{0.94}O$ into bottom segment	mass C in descending coke	mass O_2 in blast air	mass N_2 in blast air	mass Fe out in molten iron	mass C out in molten iron	mass CO out in ascending gas	mass CO ₂ out in ascending gas	mass N_2 out in ascending gas
3	7.7	Fe out in molten iron specification	1000	0	0	0	0	1	0	0	0	0
4	7.2	Fe mass balance	0	-0.768	0	0	0	1	0	0	0	0
5	7.3	O mass balance	0	0.232	0	-1	0	0	0.571	0.727	0	0
6	7.4	C mass balance	0	0	-1	0	0	0	1	0.429	0.273	0
7	7.5	N mass balance	0	0	0	0	-1	0	0	0	0	1
8	7.6	N_2 in blast air specification	0	0	0	3.3	-1	0	0	0	0	0
9	7.9	Equilibrium CO ₂ /CO mass ratio	0	0	0	0	0	0	0	0.694	-1	0
10	7.8	C out in molten iron specification	0	0	0	0	0	0.047	-1	0	0	0
11	7.15	Enthalpy balance	-320	3.152	-1.359	-1.239	-1.339	1.269	5	-2.926	-7.926	1.008
12				930°C	930°C	1200°C	1200°C	1500°C	1500°C	930°C	930°C	930°C
13		Blast temperature=		1200	"C							
14												
15					= (0.001137*D13-0.1257)			= (0.001237*D13-0.1450)				
16												
17	Bottom segment calculated values		kg per 1000 kg of Fe out in molten iron									
18	mass $Fe_{0.94}O$ into bottom segment		1302									
19	mass C in descending coke		392	also = mass C in the furnace's coke charge, Eqn. (7.16)								
20	mass O_2 in blast air		298									
21	mass N_2 in blast air		983									
22	mass Fe out in molten iron		1000									
23	mass C out in molten iron		47									
24	mass CO out in ascending gas		558									
25	mass CO ₂ out in ascending gas		387									
26	mass N ₂ out in ascending gas		983									
27												

This is the same as matrix Table 15.1. It is used here to determine (1) the masses of $Fe_{0.94}O$ and C descending from the top segment into the bottom segment, and (2) the masses of CO, CO₂, and N₂ ascending into the top segment from the bottom segment. All per 1000 kg of Fe in product molten iron.

leaves the top segment in descending $\text{Fe}_{0.947}\text{O}$ and departing top gas CO and CO_2 .

These specifications and Eq. (20.1b) give;

$$\begin{aligned} & \left[\frac{\text{mass Fe}_2\text{O}_3 \text{ in}}{\text{furnace charge}} \right] * \frac{[30.1 \text{ mass\% O in Fe}_2\text{O}_3]}{100\%} \\ & + \left[\frac{\text{mass CO ascending}}{\text{from bottom segment}} \right] * \frac{[57.1 \text{ mass\% O in CO}]}{100\%} \\ & + \left[\frac{\text{mass CO}_2 \text{ ascending}}{\text{from bottom segment}} \right] * \frac{[72.7 \text{ mass\% O in CO}_2]}{100\%} \\ & = \left[\frac{\text{mass Fe}_{0.947}\text{O descending}}{\text{into bottom segment}} \right] \\ & * \frac{[23.2 \text{ mass\% Fe in Fe}_{0.947}\text{O}]}{100\%} \\ & + \left[\frac{\text{mass CO out}}{\text{in top gas}} \right] * \frac{[57.1 \text{ mass\% O in CO}]}{100\%} \\ & + \left[\frac{\text{mass CO}_2 \text{ out}}{\text{in top gas}} \right] * \frac{[72.7 \text{ mass\% O in CO}_2]}{100\%} \end{aligned}$$

or

$$\begin{aligned} & \left[\frac{\text{mass Fe}_2\text{O}_3 \text{ in}}{\text{furnace charge}} \right] * 0.301 + \left[\frac{\text{mass CO ascending}}{\text{from bottom segment}} \right] * 0.571 \\ & + \left[\frac{\text{mass CO}_2 \text{ ascending}}{\text{from bottom segment}} \right] * 0.727 \\ & = \left[\frac{\text{mass Fe}_{0.947}\text{O descending}}{\text{into bottom segment}} \right] * 0.232 \\ & + \left[\frac{\text{mass CO out}}{\text{in top gas}} \right] * 0.571 + \left[\frac{\text{mass CO}_2 \text{ out}}{\text{in top gas}} \right] * 0.727 \end{aligned}$$

or subtracting $\left\{ \left[\frac{\text{mass Fe}_2\text{O}_3 \text{ in}}{\text{furnace charge}} \right] * 0.301 + \left[\frac{\text{mass CO ascending}}{\text{from bottom segment}} \right] * 0.571 + \left[\frac{\text{mass CO}_2 \text{ ascending}}{\text{from bottom segment}} \right] * 0.727 \right\}$ from both sides;

$$\begin{aligned} 0 &= - \left[\frac{\text{mass Fe}_2\text{O}_3 \text{ in}}{\text{furnace charge}} \right] * 0.301 \\ &- \left[\frac{\text{mass CO ascending}}{\text{from bottom segment}} \right] * 0.571 \\ &- \left[\frac{\text{mass CO}_2 \text{ ascending}}{\text{from bottom segment}} \right] * 0.727 \\ &+ \left[\frac{\text{mass Fe}_{0.947}\text{O descending}}{\text{into bottom segment}} \right] * 0.232 \\ &+ \left[\frac{\text{mass CO out}}{\text{in top gas}} \right] * 0.571 \\ &+ \left[\frac{\text{mass CO}_2 \text{ out}}{\text{in top gas}} \right] * 0.727 \end{aligned} \quad (20.3)$$

20.3.3 Carbon Mass Balance Equation

Carbon enters the top segment of Fig. 20.2 as C-in-coke charge and as CO and CO_2 in ascending bottom-segment output gas.

It leaves;

1. as unreacted C-in-coke descending into the bottom segment, and
2. as CO and CO_2 in departing top gas.

These specifications and Eq. (20.1c) give;

$$\begin{aligned} & \left[\frac{\text{mass C in}}{\text{coke charge}} \right] * \frac{100\% \text{ C}}{100\%} + \left[\frac{\text{mass CO ascending}}{\text{from bottom segment}} \right] \\ & * \frac{[42.9 \text{ mass\% C in CO}]}{100\%} + \left[\frac{\text{mass CO}_2 \text{ ascending}}{\text{from bottom segment}} \right] \\ & * \frac{[27.3 \text{ mass\% C in CO}_2]}{100\%} = \left[\frac{\text{mass C-in-coke}}{\text{descending}} \right] \\ & * \frac{100\% \text{ C}}{100\%} + \left[\frac{\text{mass CO out}}{\text{in top gas}} \right] * \frac{[42.9 \text{ mass\% C in CO}]}{100\%} \\ & + \left[\frac{\text{mass CO}_2 \text{ out}}{\text{in top gas}} \right] * \frac{[27.3 \text{ mass\% C in CO}_2]}{100\%} \end{aligned}$$

or

$$\begin{aligned} & \left[\begin{array}{l} \text{mass C in} \\ \text{coke charge} \end{array} \right] * 1 + \left[\begin{array}{l} \text{mass CO ascending} \\ \text{from bottom segment} \end{array} \right] * 0.429 \\ & + \left[\begin{array}{l} \text{mass CO}_2 \text{ ascending} \\ \text{from bottom segment} \end{array} \right] * 0.273 \\ & = \left[\begin{array}{l} \text{mass C-in-coke} \\ \text{descending} \\ \text{into bottom segment} \end{array} \right] * 1 \\ & + \left[\begin{array}{l} \text{mass CO out} \\ \text{in top gas} \end{array} \right] * 0.429 \\ & + \left[\begin{array}{l} \text{mass CO}_2 \text{ out} \\ \text{in top gas} \end{array} \right] * 0.273 \end{aligned}$$

or, subtracting

$$\left\{ \begin{array}{l} \left[\begin{array}{l} \text{mass C in} \\ \text{coke charge} \end{array} \right] * 1 \\ + \left[\begin{array}{l} \text{mass CO ascending} \\ \text{from bottom segment} \end{array} \right] * 0.429 \\ + \left[\begin{array}{l} \text{mass CO}_2 \text{ ascending} \\ \text{from bottom segment} \end{array} \right] * 0.273 \end{array} \right\} \text{ from both sides;}$$

$$0 = - \left[\begin{array}{l} \text{mass C in} \\ \text{coke charge} \end{array} \right] * 1 - \left[\begin{array}{l} \text{mass CO ascending} \\ \text{from bottom segment} \end{array} \right] * 0.429$$

$$- \left[\begin{array}{l} \text{mass CO}_2 \text{ ascending} \\ \text{from bottom segment} \end{array} \right] * 0.273$$

$$+ \left[\begin{array}{l} \text{mass C-in-coke} \\ \text{descending} \\ \text{into bottom segment} \end{array} \right] * 1 + \left[\begin{array}{l} \text{mass CO out} \\ \text{in top gas} \end{array} \right] * 0.429$$

$$+ \left[\begin{array}{l} \text{mass CO}_2 \text{ out} \\ \text{in top gas} \end{array} \right] * 0.273$$
(20.4)

or

$$\left[\begin{array}{l} \text{mass N}_2 \text{ ascending} \\ \text{from bottom segment} \end{array} \right] * 1 = \left[\begin{array}{l} \text{mass N}_2 \text{ out} \\ \text{in top gas} \end{array} \right] * 1$$

or subtracting $\left\{ \left[\begin{array}{l} \text{mass N}_2 \text{ ascending} \\ \text{from bottom segment} \end{array} \right] * 1 \right\}$ from both sides:

$$0 = - \left[\begin{array}{l} \text{mass N}_2 \text{ ascending} \\ \text{from bottom segment} \end{array} \right] * 1 + \left[\begin{array}{l} \text{mass N}_2 \text{ out} \\ \text{in top gas} \end{array} \right] * 1$$
(20.5)

20.4 QUANTITY SPECIFICATION EQUATIONS

Top-segment calculations of this chapter use the following bottom-segment calculation results, all from matrix [Table 20.1](#):

- $\left[\begin{array}{l} \text{mass Fe}_{0.947}\text{O descending} \\ \text{into bottom segment} \end{array} \right] = 1302 \text{ kg}/1000 \text{ kg of Fe in product molten iron (from Cell C18, Table 20.1).}$

For this chapter's matrix calculations, this is restated as;

$$1302 = \left[\begin{array}{l} \text{mass Fe}_{0.947}\text{O descending} \\ \text{into bottom segment} \end{array} \right] * 1$$
(20.6)

- $\left[\begin{array}{l} \text{mass C-in-coke descending} \\ \text{to bottom segment} \end{array} \right] = 392 \text{ kg (from Cell C19, Table 20.1)}$

or

$$392 = \left[\begin{array}{l} \text{mass C-in-coke descending} \\ \text{to bottom segment} \end{array} \right] * 1$$
(20.7)

- $\left[\begin{array}{l} \text{mass CO ascending} \\ \text{from bottom segment} \end{array} \right] = 558 \text{ kg (from Cell C24, Table 20.1)}$

or

$$558 = \left[\begin{array}{l} \text{mass CO ascending} \\ \text{from bottom segment} \end{array} \right] * 1$$
(20.8)

- $\left[\begin{array}{l} \text{mass CO}_2 \text{ ascending} \\ \text{from bottom segment} \end{array} \right] = 387 \text{ kg (from Cell C25, Table 20.1)}$

20.3.4 Nitrogen Mass Balance Equation

Nitrogen enters the top segment of [Fig. 20.2](#) in ascending bottom-segment output gas. It leaves unreacted in departing top gas.

These specifications and nitrogen balance Eq. [\(20.1d\)](#) give the equation;

$$\begin{aligned} & \left[\begin{array}{l} \text{mass N}_2 \text{ ascending} \\ \text{from bottom segment} \end{array} \right] * \frac{[100\% \text{ N in N}_2]}{100\%} \\ & = \left[\begin{array}{l} \text{mass N}_2 \text{ out} \\ \text{in top gas} \end{array} \right] * \frac{[100\% \text{ N in N}_2]}{100\%} \end{aligned}$$

or

$$387 = \left[\begin{array}{l} \text{mass CO}_2 \text{ ascending} \\ \text{from bottom segment} \end{array} \right] * 1 \quad (20.9)$$

5. $\left[\begin{array}{l} \text{mass N}_2 \text{ ascending} \\ \text{from bottom segment} \end{array} \right] = 983 \text{ (from Cell C26,}$

Table 20.1)

or

$$938 = \left[\begin{array}{l} \text{mass N}_2 \text{ ascending} \\ \text{from bottom segment} \end{array} \right] * 1 \quad (20.10)$$

all per 1000 kg of Fe in product molten iron.

20.5 NO CARBON OXIDATION IN THE TOP SEGMENT

Our final specification is that C(s)-in-coke doesn't react at the cool temperatures in the top segment for kinetic reasons, see Section 2.8 and Eq. (7.16).

This is expressed by the equation;

$$\begin{aligned} & \left[\begin{array}{l} \text{mass C in} \\ \text{coke charge} \end{array} \right] * \frac{100\% \text{ C}}{100\%} \\ &= \left[\begin{array}{l} \text{mass C-in-coke descending} \\ \text{into bottom segment} \end{array} \right] * \frac{100\% \text{ C}}{100\%} \end{aligned}$$

or

$$\left[\begin{array}{l} \text{mass C in} \\ \text{coke charge} \end{array} \right] * 1 = \left[\begin{array}{l} \text{mass C-in-coke descending} \\ \text{into bottom segment} \end{array} \right] * 1$$

or subtracting $\left\{ \left[\begin{array}{l} \text{mass C in} \\ \text{coke charge} \end{array} \right] * 1 \right\}$ from both sides:

$$0 = - \left[\begin{array}{l} \text{mass C in} \\ \text{coke charge} \end{array} \right] * 1 + \left[\begin{array}{l} \text{mass C-in-coke descending} \\ \text{into bottom segment} \end{array} \right] * 1 \quad (20.11)$$

We now enter Eqs. (20.2)–(20.11) into top-segment matrix **Table 20.2** and calculate mass CO, mass CO₂, and mass N₂ in top gas per 1000 kg of Fe in product molten iron.

20.6 TOP GAS RESULTS

Matrix **Table 20.2** indicates that the furnace top gas contains;

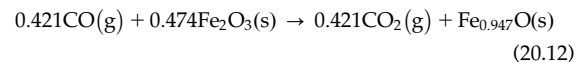
- 333 kg of CO,
- 741 kg of CO₂, and
- 983 kg of N₂.

all per 1000 kg of Fe in the furnace's product molten iron. This is the *top gas composition*.

In mass percentages, it is 16.2 mass% CO, 36.0 mass% CO₂, and 47.8 mass% N₂ (Appendix P).

In volume percentages, it is 18.6 volume% CO, 26.4 volume% CO₂, and 55.0 volume% N₂ (Appendix P). Top gas contains considerably more CO₂(g) and commensurately less CO(g) than the ascending bottom-segment exit gas.

This is the result of the overall top-segment reaction:



which produces CO₂(g) from CO(g).

20.7 COUPLING TOP AND BOTTOM-SEGMENT CALCULATIONS

Top-segment matrix **Table 20.2** is readily coupled to calculated values of bottom-segment matrix **Table 20.1**. The most convenient coupling is with both matrices on the same spreadsheet, 26 columns apart.

In the present case, the coupling instructions in matrix **Table 20.2** are;

Cell AC3 contains mass Fe_{0.947}O descending into the bottom segment, i.e., = C18

Cell AC8 contains mass CO ascending from bottom segment, i.e., = C24

Cell AC9 contains mass CO₂ ascending from bottom segment, i.e., = C25

Cell AC10 contains mass N₂ ascending from bottom segment, i.e., = C26

Cell AC11 contains mass C-in-coke descending into bottom segment = C19

Now, whenever a change is made to matrix **Table 20.1**, for example, blast temperature, the

TABLE 20.2 Top-Segment Matrix for Determining Top Gas Composition

	AA	AB	AC	AD	AE	AF	AG	AH	AI	AJ	AK	AL	AM
1	TOP SEGMENT CALCULATIONS												
Z	Equation	Description	Numerical term	mass $\text{Fe}_{0.94}\text{O}$ in furnace charge	mass C in coke charge	mass CO ascending from bottom segment	mass CO_2 ascending from bottom segment	mass N_2 ascending from bottom segment	mass $\text{Fe}_{0.94}\text{O}$ descending into bottom segment	mass C-in-coke descending into bottom segment	mass CO out in top-gas	mass CO_2 out in top-gas	mass N_2 out in top-gas
3	20.6	Mass $\text{Fe}_{0.94}\text{O}$ descending into bottom segment	1302	0	0	0	0	0	1	0	0	0	0
4	20.2	Fe mass balance	0	-0.699	0	0	0	0	0.768	0	0	0	0
5	20.3	O mass balance	0	-0.301	0	-0.571	-0.727	0	0.232	0	0.571	0.727	0
6	20.4	C mass balance	0	0	-1	-0.429	-0.273	0	0	1	0.429	0.273	0
7	20.5	N mass balance	0	0	0	0	0	-1	0	0	0	0	1
8	20.8	Mass CO ascending from bottom segment	558	0	0	1	0	0	0	0	0	0	0
9	20.9	Mass CO_2 ascending from bottom segment	387	0	0	0	1	0	0	0	0	0	0
10	20.10	Mass N_2 ascending from bottom segment	983	0	0	0	0	1	0	0	0	0	0
11	20.7	Mass C-in-coke descending into bottom segment	392	0	0	0	0	0	0	1	0	0	0
12	20.11	Unreacted C-in-coke specification	0	0	-1	0	0	0	0	1	0	0	0
13				25°C	25°C	930°C	930°C	930°C	930°C	930°C	$T_{\text{top gas}}$	$T_{\text{top gas}}$	$T_{\text{top gas}}$
14													
15													
16													
17	Top segment calculated values		kg per 1000 kg of Fe out in molten iron										
18	mass $\text{Fe}_{0.94}\text{O}$ in furnace charge												
19	mass C in coke charge												
20	mass CO ascending from bottom segment												
21	mass CO_2 ascending from bottom segment												
22	mass N_2 ascending from bottom segment												
23	mass $\text{Fe}_{0.94}\text{O}$ descending into bottom segment												
24	mass C-in-coke descending into bottom segment												
25	mass CO out in top-gas												
26	mass CO_2 out in top-gas												
27	mass N_2 out in top-gas												
28													

This matrix's solution gives a top gas composition of 333 kg CO, 741 kg CO_2 , and 983 kg N_2 (Cells AC25–AC27). The Row 13 temperatures are for information only. They are not used in this chapter's calculations. For convenience, this matrix is on the same spreadsheet as the matrix in Table 20.1—placed 26 columns to the right.

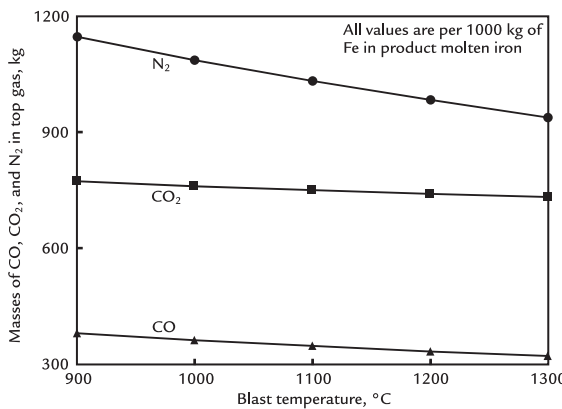


FIGURE 20.3 Effect of blast temperature on blast furnace top gas composition. CO, CO₂, and N₂ masses, per 1000 kg of Fe in product molten iron, all decrease with increasing blast temperature. This is consistent with decreasing steady-state bottom-segment C-in-coke of Fig. 7.4 and O₂-in-blast air requirements with increasing blast temperature. Mass N₂ in top gas also decreases because mass N₂-in-air/mass O₂-in-air is constant, Eq. (7.6). The lines are not exactly straight. This is the result of all our matrices' equations. We may speculate that it is because enthalpy balance Eq. (7.15) contains two nonlinear mass \times temperature terms, Cells F11 and G11.

top-segment matrix [Table 20.2](#) automatically recalculates the equivalent top-segment masses.

For example, this is done by changing blast temperature in Cell D13 of [Table 20.1](#)—generating the top gas compositions in [Fig. 20.3](#).

20.8 SUMMARY

Top gas composition is readily calculated by combining top-segment equations with

bottom-segment calculation results. Top gas enthalpy and top gas temperature are also calculated this way, Chapter 21, Top-Segment Enthalpy Balance and Chapter 22, Top Gas Temperature Calculation.

CO, CO₂, and N₂ top gas masses, per 1000 kg of Fe in product molten iron, all decrease with increasing blast temperature. This is a consequence of all the equations in our bottom and top-segment matrices. We postulate that it is mainly because the amounts of C-in-coke and O₂-in-blast air needed for steady production of 1500°C molten iron decrease with increasing blast temperature, [Fig. 7.4](#).

Practically, it means that gas flowrates in the blast furnace and in the top gas handling equipment can be decreased by raising blast temperature. This may be useful if, for example, top gas handling is a bottleneck in the blast furnace plant.

EXERCISES

- 20.1. Please calculate the top gas composition of [Fig. 20.2](#) when the blast temperature of [Table 20.1](#) is 1250°C. Use [Table 20.2](#).
- 20.2. Blast furnace operators of [Table 20.1](#) have learned of a cheap source of magnetite ore. They would like to know how this ore will affect the top gas composition of [Fig. 20.2](#), mass%. Please calculate this for them. The blast temperature is 1200°C.

Top-Segment Enthalpy Balance

O U T L I N E

21.1 Top-Segment Enthalpy Balance	199	21.5 Summary	203
21.2 Top-Segment Input Enthalpy	199	Exercises	204
21.3 Top-Segment Output Enthalpy	200	Reference	204
21.4 Calculated Values	203		

21.1 TOP-SEGMENT ENTHALPY BALANCE

This chapter calculates Fig. 21.1's;

1. top-segment *input* enthalpy, and
2. top-segment *output* enthalpy.

Our objective is to provide enthalpy information for calculating the top gas temperature of Fig. 21.1.

Top gas temperature is important because it strongly affects the rate and efficiency of (1) charge moisture evaporation, and (2) carbonate flux decomposition¹.

21.2 TOP-SEGMENT INPUT ENTHALPY

Fig. 21.1 shows that the top-segment inputs are;

- Fe₂O₃ in ore charge,
- C-in-coke charge,
- CO ascending from bottom segment,
- CO₂ ascending from bottom segment, and
- N₂ ascending from bottom segment.

Fig. 21.1 also shows their respective input temperatures.

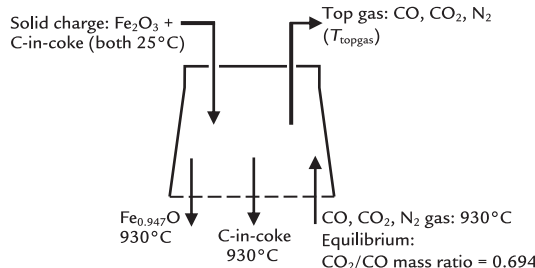


FIGURE 21.1 Sketch of conceptual blast furnace top segment with inputs and outputs. It is a copy of Fig. 20.2. This is a central vertical slice through the top of the blast furnace of Fig. 1.1.

The combined enthalpy of all these inputs is described by;

$$\begin{bmatrix} \text{top segment} \\ \text{input enthalpy} \end{bmatrix} = \begin{bmatrix} \text{mass Fe}_2\text{O}_3 \text{ in} \\ \text{furnace charge} \end{bmatrix} * \frac{H_{25^\circ\text{C}}^{\circ}}{\text{MW}_{\text{Fe}_2\text{O}_3}} + \begin{bmatrix} \text{mass C-in-} \\ \text{coke charge} \end{bmatrix} * \frac{H_{25^\circ\text{C}}^{\circ}}{\text{MW}_C} + \begin{bmatrix} \text{mass CO ascending} \\ \text{from bottom segment} \end{bmatrix} * \frac{H_{930^\circ\text{C}}^{\circ}}{\text{MW}_{\text{CO}}} + \begin{bmatrix} \text{mass CO}_2 \text{ ascending} \\ \text{from bottom segment} \end{bmatrix} * \frac{H_{930^\circ\text{C}}^{\circ}}{\text{MW}_{\text{CO}_2}} + \begin{bmatrix} \text{mass N}_2 \text{ ascending} \\ \text{from bottom segment} \end{bmatrix} * \frac{H_{930^\circ\text{C}}^{\circ}}{\text{MW}_{\text{N}_2}} \quad (21.1a)$$

Masses of Eq. (21.1a) are obtained from Table 21.2. The enthalpy values are obtained from Table J.1.

Together, they give;

$$\begin{aligned} & \left[\begin{array}{l} \text{top segment input enthalpy,} \\ \text{MJ per 1000 kg of Fe} \\ \text{in product molten iron} \end{array} \right] \\ &= \left[\begin{array}{l} 1431 \text{ kg Fe}_2\text{O}_3 \\ \text{in furnace charge} \end{array} \right] * (-5.169) \\ &+ \left[\begin{array}{l} 392 \text{ kg C-in-} \\ \text{coke charge} \end{array} \right] * 0 \\ &+ \left[\begin{array}{l} 558 \text{ kg CO ascending} \\ \text{from bottom segment} \end{array} \right] * (-2.926) \\ &+ \left[\begin{array}{l} 387 \text{ kg CO}_2 \text{ ascending} \\ \text{from bottom segment} \end{array} \right] * (-7.926) \\ &+ \left[\begin{array}{l} 983 \text{ kg N}_2 \text{ ascending} \\ \text{from bottom segment} \end{array} \right] * 1.008 \end{aligned} \quad (21.1b)$$

from which;

$$\begin{bmatrix} \text{top segment} \\ \text{input enthalpy} \end{bmatrix} = -11,105 \text{ MJ}/1000 \text{ kg of Fe in product molten iron}$$

Eq. (21.1b) may be expressed in spreadsheet form as;

$$\begin{bmatrix} \text{top segment} \\ \text{input enthalpy} \end{bmatrix} = \text{AC18} * -5.169 + \text{AC19} * 0 + \text{AC20} * -2.926 + \text{AC21} * -7.926 + \text{AC22} * 1.008 \quad (21.2)$$

where the cell addresses refer to Table 21.2. The equal sign and the right side of this equation are typed into Cell AG33 of Table 21.2.

21.3 TOP-SEGMENT OUTPUT ENTHALPY

Top-segment output enthalpy of Fig. 21.1 is given by the equation;

$$\begin{bmatrix} \text{top segment} \\ \text{output enthalpy} \end{bmatrix} = \begin{bmatrix} \text{top segment} \\ \text{input enthalpy} \end{bmatrix} - \begin{bmatrix} \text{conductive, convective} \\ \text{and radiative heat loss} \\ \text{from the top segment} \end{bmatrix} \quad (21.3)$$

TABLE 21.1 Fig. 20.1 Bottom-Segment Matrix

	A	B	C	D	E	F	G	H	I	J	K	L
1	BOTTOM SEGMENT CALCULATIONS		Numerical term	mass Fe _{0.947} O into bottom segment	mass C in descending coke	mass O ₂ in blast air	mass N ₂ in blast air	mass Fe out in molten iron	mass C out in molten iron	mass CO out in ascending gas	mass CO ₂ out in ascending gas	mass N ₂ out in ascending gas
2	Equation	Description										
3	7.7	Fe out in molten iron specification	1000	0	0	0	0	1	0	0	0	0
4	7.2	Fe mass balance	0	-0.768	0	0	0	1	0	0	0	0
5	7.3	O mass balance	0	-0.232	0	-1	0	0	0	0.571	0.727	0
6	7.4	C mass balance	0	0	-1	0	0	0	1	0.429	0.273	0
7	7.5	N mass balance	0	0	0	0	-1	0	0	0	0	1
8	7.6	N ₂ in blast air specification	0	0	0	3.3	-1	0	0	0	0	0
9	7.9	Equilibrium CO ₂ /CO mass ratio	0	0	0	0	0	0	0	0.694	-1	0
10	7.8	C out in molten iron specification	0	0	0	0	0	0.047	-1	0	0	0
11	7.15	Enthalpy balance	-320	3.152	-1.359	-1.239	-1.339	1.269	5	-2.926	-7.926	1.008
12		Blast temperature=	930°C	930°C	1200°C	1200°C	1500°C	1500°C	930°C	930°C	930°C	930°C
13			1200	°C								
14												
15					= (0.001137*D13-0.1257)			= (0.001237*D13-0.1450)				
16												
17		Bottom segment calculated values	kg per 1000 kg of Fe out in molten iron									
18		mass Fe _{0.947} O into bottom segment	1302									
19		mass C in descending coke	392	also = mass C in the furnace's coke charge, Eqn. (7.16)								
20		mass O ₂ in blast air	298									
21		mass N ₂ in blast air	983									
22		mass Fe out in molten iron	1000									
23		mass C out in molten iron	47									
24		mass CO out in ascending gas	558									
25		mass CO ₂ out in ascending gas	387									
26		mass N ₂ out in ascending gas	983									
27												

This is the same as matrix Table 20.1. This chapter uses it to calculate top-segment input and output enthalpies of Fig. 21.1.

TABLE 21.2 This is Matrix Table 20.2 Plus Eqs. (21.2), (21.5a) and (21.5b)

	AA	AB	AC	AD	AE	AF	AG	AH	AI	AJ	AK	AL	AM
1	TOP SEGMENT CALCULATIONS												
2	Equation	Description	Numerical term	mass Fe ₂ O ₃ in furnace charge	mass C in coke charge	mass CO ascending from bottom segment	mass CO ₂ ascending from bottom segment	mass N ₂ ascending from bottom segment	mass Fe ₂ O ₃ /O descending into bottom segment	mass C-in-coke descending into bottom segment	mass CO out in top-gas	mass CO ₂ out in top-gas	mass N ₂ out in top-gas
3	20.6	Mass Fe ₂ O ₃ /O descending into bottom segment	1302	0	0	0	0	0	1	0	0	0	0
4	20.2	Fe mass balance	0	-0.699	0	0	0	0	0.768	0	0	0	0
5	20.3	O mass balance	0	-0.301	0	-0.571	-0.727	0	0.232	0	0.571	0.727	0
6	20.4	C mass balance	0	0	-1	-0.429	-0.273	0	0	1	0.429	0.273	0
7	20.5	N mass balance	0	0	0	0	0	-1	0	0	0	0	1
8	20.8	Mass CO ascending from bottom segment	558	0	0	1	0	0	0	0	0	0	0
9	20.9	Mass CO ₂ ascending from bottom segment	387	0	0	0	1	0	0	0	0	0	0
10	20.10	Mass N ₂ ascending from bottom segment	983	0	0	0	0	1	0	0	0	0	0
11	20.7	Mass C-in-coke descending into bottom segment	392	0	0	0	0	0	0	1	0	0	0
12	20.11	Unreacted C-in-coke specification	0	0	-1	0	0	0	0	1	0	0	0
13				25°C	25°C	930°C	930°C	930°C	930°C	930°C	T _{top gas}	T _{top gas}	T _{top gas}
14													
15													
16													
17	Top segment calculated values		kg per 1000 kg of Fe out in molten iron										
18	mass Fe ₂ O ₃ in furnace charge		1431										
19	mass C in coke charge		392										
20	mass CO ascending from bottom segment		558										
21	mass CO ₂ ascending from bottom segment		387										
22	mass N ₂ ascending from bottom segment		983										
23	mass Fe ₂ O ₃ /O descending into bottom segment		1302										
24	mass C-in-coke descending into bottom segment		392										
25	mass CO out in top-gas		333										
26	mass CO ₂ out in top-gas		741										
27	mass N ₂ out in top-gas		983										
28													
29													
30													
31													
32	TOP SEGMENT INPUT AND OUTPUT ENTHALPY CALCULATIONS												
33	21.2	Top segment input enthalpy = AC18 * -5.169 + AC19 * 0 + AC20 * (-2.926) + AC21 * (-7.926) + AC22 * 1.008 =							-11105	MJ per 1000 kg of Fe in product molten iron			
34	21.5b	Top segment output enthalpy = AG33-80 =							-11185	MJ per 1000 kg of Fe in product molten iron			
35													

Cell AG33 = AC18 * (-5.169) + AC19 * 0 + AC20 * (-2.926) + AC21 * (-7.926) + AC22 * 1.008

Cell AG34 = AG33-80

In Section 5.4, the whole furnace conductive, convective and radiative heat losses are assumed to be 400 MJ/1000 kg of Fe in product molten iron based on actual measurements. Section 7.8 indicates that the bottom-segment conductive, convective plus radiative heat loss is 320 MJ/1000 kg of Fe in product molten iron. This means that the top-segment conductive, convective and radiative heat loss is 80 MJ/1000 kg of Fe in product molten iron. This small value is due to the low temperature of the top-segment's contents which leads to relatively slow heat transfer.

The top-segment conductive, convective and radiative heat loss gives;

$$\begin{bmatrix} \text{top segment} \\ \text{output enthalpy} \end{bmatrix} = \begin{bmatrix} \text{top segment} \\ \text{input enthalpy} \end{bmatrix} - \begin{bmatrix} 80 \text{ MJ conductive, convective} \\ \text{and radiative heat loss} \\ \text{from the top segment} \end{bmatrix} \quad (21.4)$$

where the terms are all MJ per 1000 kg of Fe in product molten iron.

Section 21.2 gives a top-segment *input* enthalpy of $-11,105 \text{ MJ}/1000 \text{ kg of Fe}$ in product molten iron. The top-segment *output* enthalpy is, therefore;

$$\begin{bmatrix} \text{top segment} \\ \text{output enthalpy} \end{bmatrix} = -11,105 - 80 \\ = -11,185 \quad \text{MJ per 1000 kg of Fe} \\ \text{in product molten iron} \quad (21.5a)$$

Eq. (21.5a) may be expressed in spreadsheet form as;

$$\begin{bmatrix} \text{top segment} \\ \text{output enthalpy} \end{bmatrix} = \text{AG33} - 80 \quad (21.5b)$$

Its equal sign and right side are typed in Cell AG34 of Table 21.2.

21.4 CALCULATED VALUES

The top-segment input and output enthalpy values with 1200°C blast air are shown in

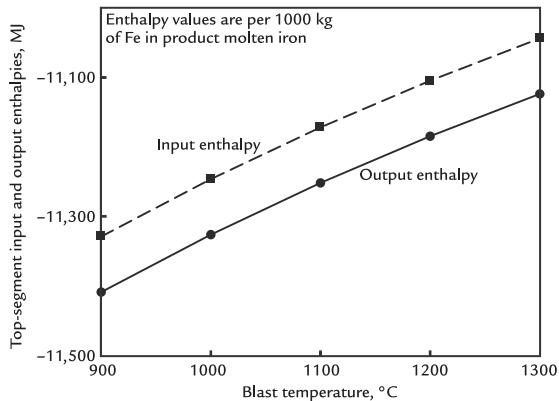


FIGURE 21.2 Top-segment input and output enthalpies as a function of blast temperature. Both become less negative with increasing blast temperature. This is the result of all the equations in our spreadsheets. We may postulate that they are due to the increasing enthalpy of the blast furnace's blast air with increasing blast temperature - the consequent increasing amount of enthalpy rising into the top segment. The enthalpy values have been obtained by varying blast temperature in Cell D13 of Table 21.1. All are per 1000 kg of Fe in product molten iron.

Table 21.2. Fig. 21.2 plots the latter as a function of blast temperature. It shows that top-segment output enthalpy becomes less negative with increasing blast temperature.

We can now calculate top gas enthalpy and top gas temperature from calculated values of;

1. top-segment output enthalpy,
2. top-segment output masses of Chapter 20, Top-Segment Mass Balance, and
3. $H^o_{T_{\text{top gas}}} / \text{MW}$ of Table J.5 versus top gas temperature equations,

as described in Chapter 22, Top Gas Temperature Calculation.

21.5 SUMMARY

Top gas temperature of Chapter 22, Top Gas Temperature Calculation, calculations start

with top-segment output enthalpy - which is readily calculated from;

1. top-segment input masses and temperatures, which we use to calculate top-segment *input* enthalpy, and
2. top-segment conductive, convective, and radiative heat loss.

The basic equation is:

$$\begin{bmatrix} \text{top segment} \\ \text{output enthalpy} \end{bmatrix} = \begin{bmatrix} \text{top segment} \\ \text{input enthalpy} \end{bmatrix} - \begin{bmatrix} \text{conductive, convective} \\ \text{and radiative heat loss} \\ \text{from the top segment} \end{bmatrix}$$

Top-segment output enthalpy increases with increasing blast temperature, that is,

with increasing blast enthalpy, MJ per kg of blast.

EXERCISES

- 21.1. Please calculate top-segment input and output enthalpies of Exercise 20.1.
- 21.2. Please calculate top-segment input and output enthalpies of Exercise 20.2. Remember that the enthalpies of Fe_2O_3 and Fe_3O_4 are different.

Reference

1. Geerdes M, Chaigneau R, Kurunov I, Lingiardi O, Ricketts J. *Modern blast furnace ironmaking, an introduction*. 2nd ed. BV, Amsterdam: IOS Press; 2015. p. 164.

Top Gas Temperature Calculation

O U T L I N E

22.1 Calculating Top Gas Temperature	205	22.5 Effect of Blast Temperature on Top Gas Temperature	210
22.2 Top Gas Enthalpy	205	22.6 Summary	211
22.3 Top Gas Temperature	206	Exercises	211
22.4 Calculation	210	Reference	211

22.1 CALCULATING TOP GAS TEMPERATURE

This chapter calculates top gas enthalpy and temperature from;

1. top-segment output enthalpy and output masses of Chapter 21, Top-Segment Enthalpy Balance, and
2. enthalpy versus top gas temperature equations of Table J.5.

for the Fig. 22.1 top segment. The input data from the bottom-segment are provided in Table 22.1.

22.2 TOP GAS ENTHALPY

Top gas enthalpy is a portion of the top-segment output enthalpy of Chapter 21, Top-Segment Enthalpy Balance.

The other portion is the enthalpy of the Fe_{0.947}O and C-in-coke that are descending into the bottom segment (Fig. 22.1). This is described by the equation;

$$\begin{aligned} \left[\begin{array}{l} \text{top gas} \\ \text{enthalpy} \end{array} \right] &= \left[\begin{array}{l} \text{top segment} \\ \text{output enthalpy} \end{array} \right] - \left[\begin{array}{l} \text{mass Fe}_{0.947}\text{O descending} \\ \text{into bottom segment} \end{array} \right] * \frac{H_{930^\circ\text{C}}^{\circ}}{\text{MW}_{\text{Fe}_{0.947}\text{O}}} \\ &\quad - \left[\begin{array}{l} \text{mass C-in-coke descending} \\ \text{into bottom segment} \end{array} \right] * \frac{H_{930^\circ\text{C}}^{\circ}}{\text{MW}_\text{C}} \end{aligned} \quad (22.1a)$$

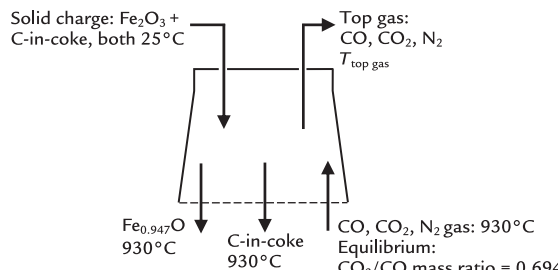


FIGURE 22.1 Conceptual iron blast furnace top segment showing its inputs, outputs, and temperatures. This is a copy of Fig. 20.2.

In the present case, the values for calculating top gas enthalpy, all per 1000 kg of Fe in product molten iron, are:

$$\begin{aligned} \left[\begin{array}{l} \text{top segment} \\ \text{output enthalpy} \end{array} \right] &= -11,185 \text{ MJ} \\ \left[\begin{array}{l} \text{mass Fe}_{0.947}\text{O descending} \\ \text{into bottom segment} \end{array} \right] &= 1302 \text{ kg} \\ \left[\begin{array}{l} \text{mass C-in-coke descending} \\ \text{into bottom segment} \end{array} \right] &= 392 \text{ kg} \end{aligned}$$

as shown in cells AG34, AC23, and AC24 of Table 21.2.

From Table J.1, ($H_{930^\circ\text{C}}^\circ/\text{MW}$) values of Eq. (22.1a) are;

$$\begin{aligned} \frac{H_{930^\circ\text{C}}^\circ}{\text{MW}_{\text{Fe}_{0.947}\text{O}}} &= -3.152 \text{ MJ/kg} \\ \frac{H_{930^\circ\text{C}}^\circ}{\text{MW}_\text{C}} &= 1.359 \text{ MJ/kg} \end{aligned}$$

so that Eq. (22.1a) becomes:

$$\begin{aligned} \left[\begin{array}{l} \text{top gas} \\ \text{enthalpy} \end{array} \right] &= -11,185 - 1302 * (-3.152) - 392 * 1.359 \\ &= -7613 \text{ MJ/1000 kg of Fe in product molten iron} \end{aligned} \quad (22.1b)$$

We calculate this in matrix Table 22.2 by typing the equal sign and right side of Eq. (22.2), that is,

$$\left[\begin{array}{l} \text{top gas} \\ \text{enthalpy} \end{array} \right] = \text{AG34} - \text{AC23} * -3.152 - \text{AC24} * 1.359 \quad (22.2)$$

into cell AG37 of Table 22.2.

22.3 TOP GAS TEMPERATURE

We now calculate top gas temperature from top gas enthalpy of Eq. (22.2). Blast furnace top gas temperature is important because the departing gas must be warm enough to rapidly remove moisture from the furnace charge burden. Otherwise, moisture tends to delay burden drying and subsequent preheating and reduction reactions. This can lead to a "short furnace" with uneven material descent and thermal control problems.¹

Top gas temperature is calculated as follows; top gas enthalpy equation of Fig. 22.1 is:

$$\begin{aligned} \left[\begin{array}{l} \text{top gas} \\ \text{enthalpy} \end{array} \right] &= \left[\begin{array}{l} \text{mass CO out} \\ \text{in top-gas} \end{array} \right] * \frac{H_{T_{\text{top gas}}}^\circ}{\text{MW}_\text{CO}} \\ &+ \left[\begin{array}{l} \text{mass CO}_2 \text{ out} \\ \text{in top-gas} \end{array} \right] * \frac{H_{T_{\text{top gas}}}^\circ}{\text{MW}_{\text{CO}_2}} \\ &+ \left[\begin{array}{l} \text{mass N}_2 \text{ out} \\ \text{in top-gas} \end{array} \right] * \frac{H_{T_{\text{top gas}}}^\circ}{\text{MW}_{\text{N}_2}} \end{aligned} \quad (22.3)$$

Eq. (22.3) is related to top gas temperature by the substitutions;

$$\begin{aligned} \frac{H_{T_{\text{top gas}}}^\circ}{\text{MW}_\text{CO}} &= 0.001049 * T_{\text{top gas}} - 3.972 \\ \frac{H_{T_{\text{top gas}}}^\circ}{\text{MW}_{\text{CO}_2}} &= 0.0009314 * T_{\text{top gas}} - 8.966 \\ \frac{H_{T_{\text{top gas}}}^\circ}{\text{MW}_{\text{N}_2}} &= 0.001044 * T_{\text{top gas}} - 0.02624 \end{aligned}$$

TABLE 22.1 Matrix for Fig. 20.1 Conceptual Blast Furnace Bottom-Segment

A	B	C	D	E	F	G	H	I	J	K	L
Equation	Description	Numerical term	mass $\text{Fe}_{0.94}\text{O}$ into bottom segment	mass C in descending coke	mass O_2 in blast air	mass N_2 in blast air	mass Fe out in molten iron	mass C out in molten iron	mass CO out in ascending gas	mass CO_2 out in ascending gas	mass N_2 out in ascending gas
3	7.7 Fe out in molten iron specification	1000	0	0	0	0	1	0	0	0	0
4	7.2 Fe mass balance	0	-0.768	0	0	0	1	0	0	0	0
5	7.3 O mass balance	0	-0.232	0	-1	0	0	0.571	0.727	0	0
6	7.4 C mass balance	0	0	-1	0	0	0	0.429	0.273	0	0
7	7.5 N mass balance	0	0	0	0	-1	0	0	0	0	1
8	7.6 N_2 in blast air specification	0	0	0	3.3	-1	0	0	0	0	0
9	7.9 Equilibrium CO_2/CO mass ratio	0	0	0	0	0	0	0.694	-1	0	0
10	7.8 C out in molten iron specification	0	0	0	0	0	0.047	-1	0	0	0
11	7.15 Enthalpy balance	-320	3.152	-1.359	-1.239	-1.339	1.269	5	-2.926	-7.926	1.008
12			930°C	930°C	1200°C	1200°C	1500°C	1500°C	930°C	930°C	930°C
13	Blast temperature=		1200	°C							
14											
15				=(-0.001137*D13-0.1257)			=(-0.001237*D13-0.1450)				
16											
17	Bottom segment calculated values	kg per 1000 kg of Fe out in molten iron									
18	mass $\text{Fe}_{0.94}\text{O}$ into bottom segment	1302									
19	mass C in descending coke	392	also = mass C in the furnace's coke charge, Eqn. (7.16)								
20	mass O_2 in blast air	298									
21	mass N_2 in blast air	983									
22	mass Fe out in molten iron	1000									
23	mass C out in molten iron	47									
24	mass CO out in ascending gas	558									
25	mass CO_2 out in ascending gas	387									
26	mass N_2 out in ascending gas	983									
27											

This is a copy of Table 20.1. It shows (1) the masses and temperatures of the $\text{Fe}_{0.94}\text{O}$ and C that are descending out of Fig. 22.1 top segment and (2) the masses and temperatures of CO, CO_2 , and N_2 that are ascending into Fig. 22.1 top segment. These masses and temperatures are all used in our calculation of top-segment input enthalpy, top-segment output enthalpy, top gas enthalpy, and top gas temperature. All masses are per 1000 kg of Fe in product molten iron.

TABLE 22.2 This is Table 21.2 Plus Equations for Calculating Top Gas Enthalpy [Eq. (22.2)] and Top Gas Temperature [Eq. (22.6)], Rows 37 and 40

AA	AB	AC	AD	AT	AF	AG	AH	AI	AJ	AK	AL	AM
TOP SEGMENT CALCULATIONS												
Equation	Description	Numerical term	mass Fe ₂ O ₃ in furnace charge	mass C in coke charge	mass CO ascending from bottom segment	mass CO ₂ ascending from bottom segment	mass N ₂ ascending from bottom segment	mass Fe ₂ O ₃ descending into bottom segment	mass C in coke descending into bottom segment	mass CO out in top-gas	mass CO ₂ out in top-gas	mass N ₂ out in top-gas
2												
3	20.6 Mass Fe ₂ O ₃ /O descending into bottom segment	1302	0	0	0	0	0	1	0	0	0	0
4	20.2 Fe mass balance	0	-0.699	0	0	0	0	0.768	0	0	0	0
5	20.3 O mass balance	0	-0.301	0	-0.571	-0.727	0	0.232	0	0.571	0.727	0
6	20.4 C mass balance	0	0	-1	0.429	0.273	0	0	1	0.429	0.273	0
7	20.5 N mass balance	0	0	0	0	0	-1	0	0	0	0	1
8	20.8 Mass CO descending from bottom segment	558	0	0	1	0	0	0	0	0	0	0
9	20.9 Mass CO ₂ ascending from bottom segment	387	0	0	0	1	0	0	0	0	0	0
10	20.10 Mass N ₂ ascending from bottom segment	983	0	0	0	0	1	0	0	0	0	0
11	20.7 Mass C in coke descending into bottom segment	392	0	0	0	0	0	0	1	0	0	0
12	20.11 Unreacted C in-coke specification	0	0	-1	0	0	0	0	1	0	0	0
13			25°C	25°C	930°C	930°C	930°C	930°C	930°C	T _{top-gas}	T _{top-gas}	T _{top-gas}
14												
15												
16												
17	Top segment calculated values	kg per 1000 kg of Fe out in molten iron										
18	mass Fe ₂ O ₃ in furnace charge	1431										
19	mass C in coke charge	392										
20	mass CO ascending from bottom segment	558										
21	mass CO ₂ ascending from bottom segment	387										
22	mass N ₂ ascending from bottom segment	983										
23	mass Fe ₂ O ₃ descending into bottom segment	1302										
24	mass C in coke descending into bottom segment	392										
25	mass CO out in top-gas	333										
26	mass CO ₂ out in top-gas	741										
27	mass N ₂ out in top-gas	983										
28												
29												
30												
31												
32	TOP SEGMENT INPUT AND OUTPUT ENTHALPY CALCULATIONS											
33	21.2 Top segment input enthalpy = AC18*-5.169+AC19*0+AC20*-2.926+AC21*-7.926+AC22*1.008 =						-11105	MJ per 1000 kg of Fe in product molten iron				
34	21.5b Top segment output enthalpy = AG33-80 =						-11185	MJ per 1000 kg of Fe in product molten iron				
35												
36	TOP-GAS ENTHALPY CALCULATION											
37	22.2 Top gas enthalpy = AG34-AC23*3.152-AC24*1.359 =						-7613	MJ per 1000 kg of Fe in product molten iron				
38												
39	TOP-GAS TEMPERATURE CALCULATION											
40	22.4 Top gas temperature =(AG37-AC25*3.972-AC26*-8.966-AC27*-0.02624)/(AC25*0.001049+AC26*0.0009314+AC27*0.001044) =						182	°C				
41												

Cell AG37 = AG34 - AC23 * -3.152 - AC24 * 1.359 [Eq. (22.2)]

Cell AG40: = (AG37 - AC25 * -3.972 - AC26 * -8.966 - AC27 * -0.02624) / (AC25 * 0.001049 + AC26 * 0.0009314 + AC27 * 0.001044) [Eq. (22.4)]

which give;

$$\begin{bmatrix} \text{top gas} \\ \text{enthalpy} \end{bmatrix} = \begin{bmatrix} \text{mass CO out} \\ \text{in top-gas} \end{bmatrix} * (0.001049 * T_{\text{top gas}} - 3.972) + \begin{bmatrix} \text{mass CO}_2 \text{ out} \\ \text{in top-gas} \end{bmatrix} * (0.0009314 * T_{\text{top gas}} - 8.966) + \begin{bmatrix} \text{mass N}_2 \text{ out} \\ \text{in top-gas} \end{bmatrix} * (0.001044 * T_{\text{top gas}} - 0.02624)$$

or

$$\begin{bmatrix} \text{top gas enthalpy} \end{bmatrix} = \begin{bmatrix} \text{mass CO out} \\ \text{in top-gas} \end{bmatrix} * 0.001049 * T_{\text{top gas}} + \begin{bmatrix} \text{mass CO}_2 \text{ out} \\ \text{in top-gas} \end{bmatrix} * 0.0009314 * T_{\text{top gas}} + \begin{bmatrix} \text{mass N}_2 \text{ out} \\ \text{in top-gas} \end{bmatrix} * 0.001044 * T_{\text{top gas}} + \begin{bmatrix} \text{mass CO out} \\ \text{in top-gas} \end{bmatrix} * -3.972 + \begin{bmatrix} \text{mass CO}_2 \text{ out} \\ \text{in top-gas} \end{bmatrix} * -8.966 + \begin{bmatrix} \text{mass N}_2 \text{ out} \\ \text{in top-gas} \end{bmatrix} * -0.02624$$

or

$$\begin{bmatrix} \text{top gas} \\ \text{enthalpy} \end{bmatrix} = \begin{bmatrix} \text{mass CO out} \\ \text{in top-gas} \end{bmatrix} * 0.001049 + \begin{bmatrix} \text{mass CO}_2 \text{ out} \\ \text{in top-gas} \end{bmatrix} * 0.0009314 + \begin{bmatrix} \text{mass N}_2 \text{ out} \\ \text{in top-gas} \end{bmatrix} * 0.001044 * T_{\text{top gas}} + \begin{bmatrix} \text{mass CO out} \\ \text{in top-gas} \end{bmatrix} * -3.972 + \begin{bmatrix} \text{mass CO}_2 \text{ out} \\ \text{in top-gas} \end{bmatrix} * -8.966 + \begin{bmatrix} \text{mass N}_2 \text{ out} \\ \text{in top-gas} \end{bmatrix} * -0.02624$$

or subtracting $\left\{ \begin{bmatrix} \text{mass CO out} \\ \text{in top-gas} \end{bmatrix} * -3.972 + \begin{bmatrix} \text{mass CO}_2 \text{ out} \\ \text{in top-gas} \end{bmatrix} * -8.966 + \begin{bmatrix} \text{mass N}_2 \text{ out} \\ \text{in top-gas} \end{bmatrix} * -0.02624 \right\}$ from both sides;

$$\begin{bmatrix} \text{top gas} \\ \text{enthalpy} \end{bmatrix} - \begin{bmatrix} \text{mass CO out} \\ \text{in top-gas} \end{bmatrix} * -3.972 - \begin{bmatrix} \text{mass CO}_2 \text{ out} \\ \text{in top-gas} \end{bmatrix} * -8.966 - \begin{bmatrix} \text{mass N}_2 \text{ out} \\ \text{in top-gas} \end{bmatrix} * -0.02624 = \left[\begin{bmatrix} \text{mass CO out} \\ \text{in top-gas} \end{bmatrix} * 0.001049 + \begin{bmatrix} \text{mass CO}_2 \text{ out} \\ \text{in top-gas} \end{bmatrix} * 0.0009314 + \begin{bmatrix} \text{mass N}_2 \text{ out} \\ \text{in top-gas} \end{bmatrix} * 0.001044 \right] * T_{\text{top gas}}$$

or dividing both sides by; $\left\{ \begin{bmatrix} \text{mass CO out} \\ \text{in top-gas} \end{bmatrix} * 0.001049 + \begin{bmatrix} \text{mass CO}_2 \text{ out} \\ \text{in top-gas} \end{bmatrix} * 0.0009314 + \begin{bmatrix} \text{mass N}_2 \text{ out} \\ \text{in top-gas} \end{bmatrix} * 0.001044 \right\}$

$$T_{\text{top gas}} = \frac{\left\{ \begin{bmatrix} \text{top gas} \\ \text{enthalpy} \end{bmatrix} - \begin{bmatrix} \text{mass CO out} \\ \text{in top-gas} \end{bmatrix} * -3.972 - \begin{bmatrix} \text{mass CO}_2 \text{ out} \\ \text{in top-gas} \end{bmatrix} * -8.966 - \begin{bmatrix} \text{mass N}_2 \text{ out} \\ \text{in top-gas} \end{bmatrix} * -0.02624 \right\}}{\left\{ \begin{bmatrix} \text{mass CO out} \\ \text{in top-gas} \end{bmatrix} * 0.001049 + \begin{bmatrix} \text{mass CO}_2 \text{ out} \\ \text{in top-gas} \end{bmatrix} * 0.0009314 + \begin{bmatrix} \text{mass N}_2 \text{ out} \\ \text{in top-gas} \end{bmatrix} * 0.001044 \right\}} \quad (22.4)$$

22.4 CALCULATION

The information required to calculate $T_{\text{top gas}}$ is in [Table 22.2](#). Top gas enthalpy is in cell AG40. Top gas CO, CO₂, and N₂ masses are in cells AC25–AC27. With these values, [Eq. \(22.4\)](#) becomes;

$$\begin{aligned} T_{\text{top gas}} &= \frac{-7613 - 333 * -3.972 - 741 * -8.966 - 983 * -0.02624}{333 * 0.001049 + 741 * 0.0009314 + 983 * 0.001044} \\ &= 182^\circ\text{C} \end{aligned} \quad (22.5)$$

In terms of cell locations of [Table 22.2](#), this is rewritten as;

$$T_{\text{top gas}} = \frac{\text{AG37} - \text{AC25} * -3.972 - \text{AC26} * -8.966 - \text{AC27} * -0.02624}{\text{AC25} * 0.001049 + \text{AC26} * 0.0009314 + \text{AC27} * 0.001044} \quad (22.6)$$

where the equal sign and right side are typed in cell AG40 of [Table 22.2](#).

22.5 EFFECT OF BLAST TEMPERATURE ON TOP GAS TEMPERATURE

[Section 20.7](#) determines the effect of blast temperature on top gas composition. It does so by;

- coupling the bottom-segment and top-segment calculations as described in [Section 20.4](#), and
- varying blast temperature in cell D13 of [Table 22.1](#).

This section does the same for top gas temperature ([Fig. 22.2](#)). We may speculate that this is due to a decrease in hot nitrogen from the bottom-segment when the blast temperature increases, [Fig. 22.3](#).

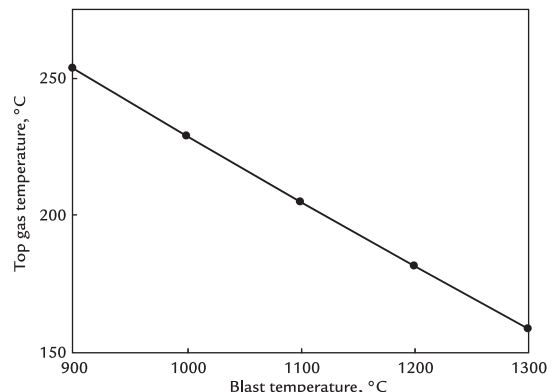


FIGURE 22.2 Graph showing that top gas temperature falls with increasing blast temperature as confirmed by industrial data.¹ The values are the result of this chapter's equations. We may speculate that at least some of the decrease may be due to the smaller amount of hot N₂ rising into the top segment ([Fig. 22.3](#)). The line is not exactly straight because $((d(H^\circ/\text{MW})_{\text{inputs}})/dT) \neq ((d(H^\circ/\text{MW})_{\text{outputs}})/dT)$ where T is temperature.

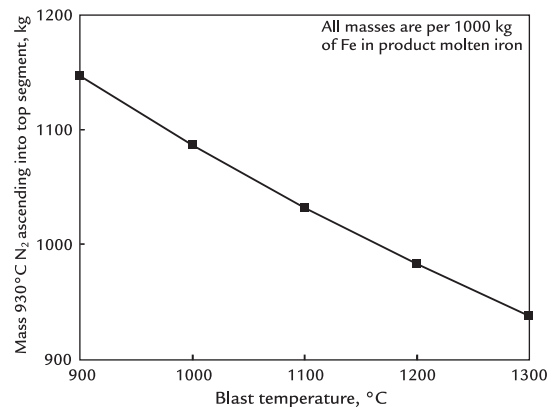


FIGURE 22.3 Mass hot nitrogen ascending into top segment of [Fig. 22.1](#) as a function of blast temperature. N₂(g) mass decreases with increasing blast temperature. The line is not straight because the bottom-segment enthalpy balance Eq. (7.15) is nonlinear, that is, cells F11 and G11 contain mass * temperature terms.

22.6 SUMMARY

This chapter calculates blast furnace top gas temperatures from;

1. top-segment input and output masses of Chapter 20, Top-Segment Mass Balance,
2. top-segment output enthalpy of Chapter 21, Top-Segment Enthalpy Balance, and
3. top gas enthalpy versus top gas temperature equations of Table J.5.

Top gas temperature decreases with increasing blast temperature-as shown here and by industrial data.¹

EXERCISES

- 22.1. Please calculate top gas temperature of Fig. 22.1 with top-charged hematite ore and 1250°C blast. Feel free to use your answers of Exercise 21.1. Use two calculation methods.
- 22.2. Please calculate top gas temperature of Fig. 22.1 with top-charged magnetite ore and 1200°C blast. Feel free to use your answers of Exercise 21.2.

Reference

1. Geerdes M, Chaignau R, Kurunov I, Lingiardi O, Ricketts J. *Modern blast furnace ironmaking, an introduction*. 2nd ed. Amsterdam: IOS Press BV; 2015. p. 164.

Top Segment Calculations With Pulverized Carbon Injection

O U T L I N E

23.1 Impact of Pulverized Carbon Injection on the Top Segment	213	23.4 Summary	218
23.2 Cross-Division Flows With Pulverized Carbon Injection	214	Exercises	218
23.3 Top-Segment Calculations	214	Reference	218

23.1 IMPACT OF PULVERIZED CARBON INJECTION ON THE TOP SEGMENT

Chapters 20–22 determined the top gas;

- composition,
- enthalpy, and
- temperature

without tuyere injectants.

This and many of the following chapters do the same with;

1. pulverized carbon injection (as a stand-in for pulverized coal), this chapter;

2. pure oxygen injection, Chapter 24, Top Segment Calculations with Oxygen Enrichment;
3. industrial (real) natural gas, Chapter 31, Top Segment Calculations with Natural Gas Injection; and
4. $\text{H}_2\text{O(g)}$ injection in steam and humid air, Chapter 28, Top Segment Calculations with Moisture in Blast Air.

Our primary objectives are to show how these injectants affect top gas temperature. Secondary objectives are to determine how each injectant affects top gas composition and enthalpy.

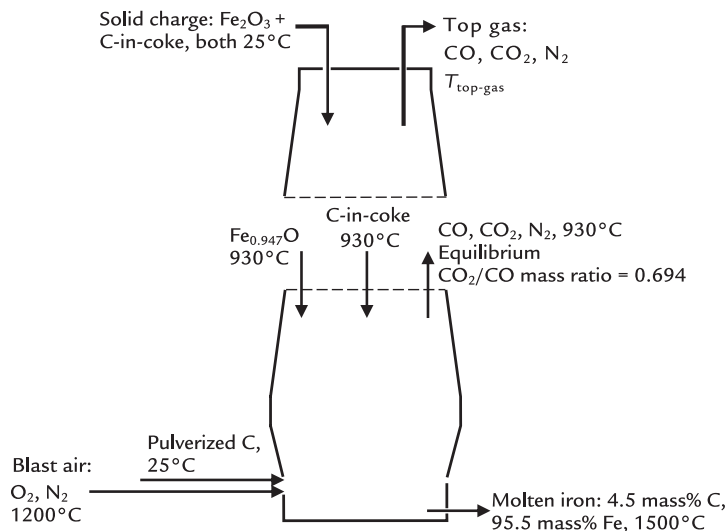


FIGURE 23.1 Conceptually divided blast furnace with tuyere injection of pulverized carbon, 25°C. Note the flows of $\text{Fe}_{0.947}\text{O}(\text{s})$, $\text{C}(\text{s})\text{-in-coke}$, $\text{CO}(\text{g})$, $\text{CO}_2(\text{g})$, and $\text{N}_2(\text{g})$ across the conceptual division.

23.2 CROSS-DIVISION FLOWS WITH PULVERIZED CARBON INJECTION

Fig. 23.1 shows steady-state mass flows across a blast furnace's conceptual division with C injection. The cross-division flows are;

- descending $\text{Fe}_{0.947}\text{O}(\text{s})$ and $\text{C}(\text{s})\text{-in-coke}$, and
- ascending $\text{CO}(\text{g})$, $\text{CO}_2(\text{g})$, and $\text{N}_2(\text{g})$.

We now calculate the steady-state mass flows of these substances per 1000 kg of Fe in product molten iron. Bottom-segment matrix of Chapter 8, Bottom Segment with Pulverized Carbon Injection, is used and shown here as Table 23.1.

With 100 kg of pulverized C injection, the cross-division mass flows are;

1. mass $\text{Fe}_{0.947}\text{O}$ into bottom segment = mass $\text{Fe}_{0.947}\text{O}$ out of top segment = 1302 kg,
2. mass C-in-coke into bottom segment = mass C-in-coke out of top segment = 299 kg,

3. mass CO out of bottom segment = mass CO into top segment = 569 kg,
4. mass CO_2 out of bottom segment = mass CO_2 into top segment = 395 kg, and
5. mass N_2 out of bottom segment = mass N_2 into top segment = 1024 kg

all per 1000 kg of Fe in product molten iron.

These are the only values that will keep the blast furnace of Fig. 23.1 steadily producing 1500°C molten iron while injecting 100 kg pulverized carbon per 1000 kg of Fe in product molten iron.

23.3 TOP SEGMENT CALCULATIONS

The above five values are now forwarded to the top-segment matrix, Table 23.2 as shown in Cells AC3 and AC8–AC11;

$$\text{Cell AC3} = \text{C18} \quad (23.1)$$

TABLE 23.1 Bottom-Segment Matrix for Calculating Bottom-Segment Inputs and Outputs of Fig. 23.1 With Injection of 100 kg of 25°C Pulverized Carbon

	A	B	C	D	E	F	G	H	I	J	K	L	M
1	BOTTOM SEGMENT CALCULATIONS												
2	Equation	Description	Numerical term	mass Fe _{0.947} O into bottom segment	mass C in descending coke	mass O ₂ in blast air	mass N ₂ in blast air	mass Fe out in molten iron	mass C out in molten iron	mass CO out in ascending gas	mass CO ₂ out in ascending gas	mass N ₂ out in ascending gas	mass C in tuyere-injected carbon
3	7.7	Fe out in molten iron specification	1000	0	0	0	0	1	0	0	0	0	0
4	7.2	Fe mass balance	0	-0.768	0	0	0	0	0	0	0	0	0
5	7.3	O mass balance	0	-0.232	0	-1	0	0	0	0.571	0.727	0	0
6	8.3	C mass balance	0	0	-1	0	0	0	0.429	0.273	0	-1	0
7	7.5	N mass balance	0	0	0	0	-1	0	0	0	0	1	0
8	7.6	N ₂ in blast air specification	0	0	0	3.3	-1	0	0	0	0	0	0
9	7.9	Equilibrium CO ₂ /CO mass ratio	0	0	0	0	0	0	0	0.694	-1	0	0
10	7.8	C out in molten iron specification	0	0	0	0	0	0.047	-1	0	0	0	0
11	8.5	Enthalpy balance	-320	3.152	-1.359	-1.239	-1.339	1.269	5	-2.926	-7.926	1.008	0
12	8.1	C injected through tuyeres	100	0	0	0	0	0	0	0	0	0	1
13													
14				930°C	1200°C	1200°C	1500°C	1500°C	930°C	930°C	930°C	930°C	25°C
15													
16	Bottom segment calculated values		kg per 1000 kg of Fe out in molten iron										
17	mass Fe _{0.947} O into bottom segment	1302											
18	mass C in descending coke	299	also = mass C in the furnace's coke charge, Eqn. (7.16)										
19	mass O ₂ in blast air	310											
20	mass N ₂ in blast air	1024											
21	mass Fe out in molten iron	1000											
22	mass C out in molten iron	47											
23	mass CO out in ascending gas	569											
24	mass CO ₂ out in ascending gas	395											
25	mass N ₂ out in ascending gas	1024											
26	mass C in tuyere-injected carbon	100											
27													
28													

This is a copy of Table 8.1. It calculates the O₂-in-blast air and C-in-coke requirements of blast furnace of Fig. 23.1 for steady production of molten iron, 1500°C. It also calculates the equivalent steady-state Fe_{0.947}O, C-in-coke, CO, CO₂, and N₂ mass flows across conceptual division of Fig. 23.1. All values are per 1000 kg of Fe in product molten iron.

TABLE 23.2 Spreadsheet for Top Segment of Fig. 23.1 With 100 kg of Pulverized Carbon Injection

	AA	AB	AC	AD	AE	AF	AG	AH	AI	AJ	AK	AL	AM	
TOP SEGMENT CALCULATIONS														
2	Equation	Description	Numerical term	mass Fe ₂ O ₃ in furnace charge	mass C in coke charge	mass CO ascending from bottom segment	mass CO ₂ ascending from bottom segment	mass N ₂ ascending from bottom segment	mass Fe ₂ O ₃ /O descending into bottom segment	mass C-in-coke descending into bottom segment	mass CO out in top-gas	mass CO ₂ out in top-gas	mass N ₂ out in top-gas	
3	20.6	Mass Fe ₂ O ₃ /O descending into bottom segment	1302	0	0	0	0	0	1	0	0	0	0	
4	20.2	Fe mass balance	0	-0.699	0	0	0	0	0.768	0	0	0	0	
5	20.3	O mass balance	0	-0.301	0	-0.571	-0.727	0	0.232	0	0.571	0.727	0	
6	20.4	C mass balance	0	0	-1	-0.429	-0.273	0	0	1	0.429	0.273	0	
7	20.5	N mass balance	0	0	0	0	0	-1	0	0	0	0	1	
8	20.8	Mass CO ascending from bottom segment	569	0	0	1	0	0	0	0	0	0	0	
9	20.9	Mass CO ₂ ascending from bottom segment	395	0	0	0	1	0	0	0	0	0	0	
10	20.10	Mass N ₂ ascending from bottom segment	1024	0	0	0	0	1	0	0	0	0	0	
11	20.7	Mass C-in-coke descending into bottom segment	299	0	0	0	0	0	0	1	0	0	0	
12	20.11	Unreacted C-in-coke specification	0	0	-1	0	0	0	0	1	0	0	0	
13			25°C	25°C	930°C	930°C	930°C	930°C	930°C	T _{top gas}	T _{top gas}	T _{top gas}	T _{top gas}	
14														
15														
16														
17	Top segment calculated values		kg per 1000 kg of Fe out in molten iron											
18	mass Fe ₂ O ₃ in furnace charge		1431											
19	mass C in coke charge		299											
20	mass CO ascending from bottom segment		569											
21	mass CO ₂ ascending from bottom segment		395											
22	mass N ₂ ascending from bottom segment		1024											
23	mass Fe ₂ O ₃ /O descending into bottom segment		1302											
24	mass C-in-coke descending into bottom segment		299											
25	mass CO out in top-gas		344											
26	mass CO ₂ out in top-gas		749											
27	mass N ₂ out in top-gas		1024											
28														
29														
30														
31														
32	TOP SEGMENT INPUT AND OUTPUT ENTHALPY CALCULATIONS													
33	21.2	Top segment input enthalpy = AC18*-5.169+AC19*0+AC20*(-2.926)+AC21*(-7.926)+AC22*1.008							-11161	MJ per 1000 kg of Fe in product molten iron				
34	21.5b	Top segment output enthalpy = AG33-80 =							-11241	MJ per 1000 kg of Fe in product molten iron				
35														
36	TOP-GAS ENTHALPY CALCULATION													
37	22.2	Top-gas enthalpy = AG34-AC23*-3.152-AC24*1.359 =							-7543	MJ per 1000 kg of Fe in product molten iron				
38														
39	TOP-GAS TEMPERATURE CALCULATION													
40	22.4	Top-gas temperature =(AG37-AC25*-3.972-AC26*-8.966-AC27*-0.02624)/(AC25*0.001049+AC26*0.0009314+AC27*0.001044) =							265	*C				
41														

This matrix calculates top gas composition, enthalpy, and temperature from cross-division mass flows of Table 23.1. All masses are per 1000 kg of Fe in product molten iron.

$$\text{Cell AG33} = \text{AC18} * (-5.169) + \text{AC19} * 0 + \text{AC20} * (-2.926) + \text{AC21} * (-7.926) + \text{AC22} * 1.008 \quad (21.2)$$

$$\text{Cell AG34} = \text{AG33} - 80 \quad (21.5b)$$

$$\text{Cell AG37} = \text{AG34} - \text{AC23} * (-3.152) - \text{AC24} * 1.359 \quad (22.2)$$

$$\text{Cell AH40} = \frac{(\text{AG37} - \text{AC25} * (-3.972) - \text{AC26} * (-8.966) - \text{AC27} * (-0.02624))}{(\text{AC25} * 0.001049 + \text{AC26} * 0.0009314 + \text{AC27} * 0.001044)} \quad (22.4)$$

$$\text{Cell AC8} = C24 \quad (23.2)$$

$$\text{Cell AC9} = C25 \quad (23.3)$$

$$\text{Cell AC10} = C26 \quad (23.4)$$

$$\text{Cell AC11} = C19 \quad (23.5)$$

where Column C cells refer to [Table 23.1](#).

Insertion of the above cross-division values into these cells automatically calculates the equivalent top gas;

- CO, CO₂, and N₂ masses, Cells AC25–27;
- enthalpy, Cell AG37; and
- temperature, Cell AH40.

[Fig. 23.2](#) plots the top gas temperature versus mass-injected pulverized carbon. This plot was made by varying the mass-injected pulverized carbon injection quantity in [Table 23.1](#) and recording the resultant top gas temperature in [Table 23.2](#). Top gas temperature increases with increasing pulverized carbon injection.

This is a consequence of the equations in [Tables 23.1](#) and [23.2](#). We may speculate that it is mainly due to;

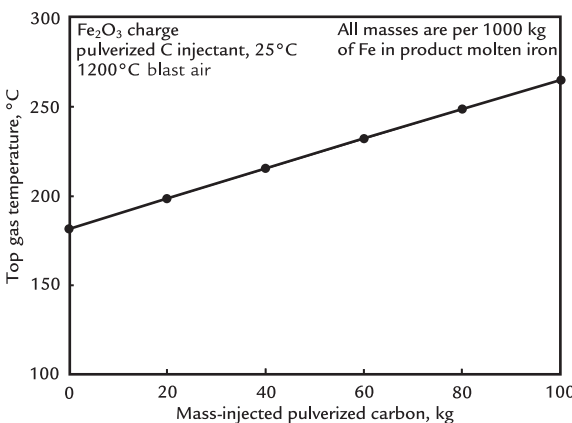


FIGURE 23.2 Trend showing that top gas temperature increases with increasing pulverized carbon tuyere injection. The temperature increases by $\sim 0.8^\circ\text{C}/\text{kg}$ of pulverized carbon injection, which is comparable to the industrial value in Geerdes et al. (p. 195).¹ The line is not quite straight because $dH^\circ_{\text{Inputs}}/dT \neq dH^\circ_{\text{Outputs}}/dT$. For future reference, the top gas temperature with 60 kg of pulverized carbon injection is 232°C.

1. the decreased amount of cool, low enthalpy, C-in-coke being fed to the top of the blast furnace ([Fig. 23.3](#)), and
2. the increased amount of hot, high enthalpy, N₂ rising into the top segment ([Fig. 23.4](#)).

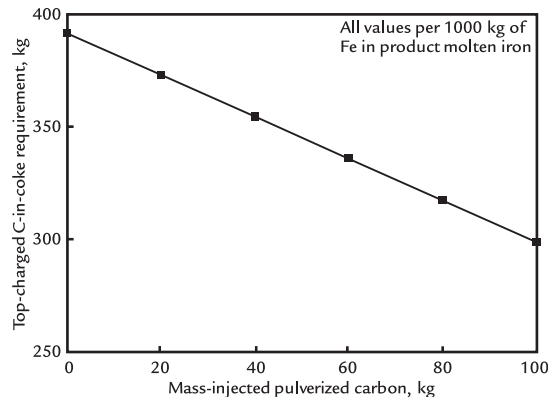


FIGURE 23.3 Effect of mass-injected carbon on top-charged C-in-coke requirement for steady production of 1500°C molten iron. As expected, the top-charged C-in-coke requirement decreases with increasing carbon injection. The line is straight.

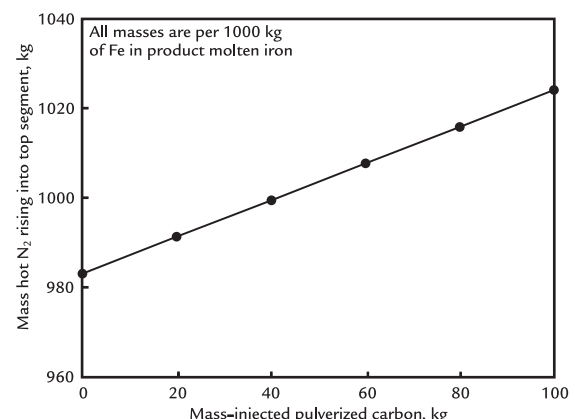


FIGURE 23.4 Trend showing that the mass of hot N₂ rising into the top segment of [Fig. 23.1](#) increases with increasing tuyere injection of pulverized carbon. This is because carbon injection requires more blast air.

It is important to note that the top gas temperatures (180–260°C) calculated in this chapter are higher than industrial top gas temperatures (110°C–140°C). This is because industrial blast furnace top segments must heat and decompose many other inputs, for example, CaCO₃ flux. This is detailed in later chapters.

23.4 SUMMARY

Tuyere injection of pulverized carbon into the blast furnace is readily included in our top gas;

- composition,
- enthalpy, and
- temperature calculations.

The calculations entail;

1. bottom-segment calculation of blast furnace C-in-coke and O₂-in-blast air requirements for steady-state 1500°C molten iron production - with pulverized C injection (Chapter 8: Bottom Segment with Pulverized Carbon Injection).
2. top-segment calculation of top gas composition, enthalpy, and temperature from the blast equivalent of furnace;
 - a. steady-state cross-division mass flows (Fig. 23.1 and Table 23.1), and
 - b. top-segment mass and enthalpy balances (Chapters 20–22).

The calculations show that top gas temperature increases with increasing pulverized carbon injection - confirming the industrial data in Geerdes et al. (p. 195).¹

We speculate that the increase is mainly due to;

1. the smaller requirement for cool top-charged C-in-coke with increasing carbon injection, and
2. the larger amount of hot nitrogen ascending into the top segment with increasing carbon injection.

EXERCISES

- 23.1. The Engineering department of Table 23.2 blast furnace plant thinks that its top gas temperature should be exactly 200°C. Please determine for them how much injected C-in-coal will produce this temperature. Use two calculation methods.
- 23.2. The Engineering department in Exercise 23.1 is unhappy with the small amount of pulverized carbon that can be injected while maintaining a 200°C top gas temperature. They wish to know how to increase the amount while obtaining this top gas temperature. Based on Fig. 22.2, one of the engineers suggests raising blast temperature. Test this out for them by raising blast temperature to 1300°C.
- 23.3. This chapter is rather simplistic with regard to its top-charged substances. What, do you think, also goes into industrial top charges that might lower top gas temperature?

Reference

1. Geerdes M, Chaigneau R, Kurunov I, Lingardi O, Ricketts J. *Modern blast furnace ironmaking, an introduction*. 2nd ed. Amsterdam: IOS Press, BV; 2015. p. 195.

24

Top Segment Calculations With Oxygen Enrichment

O U T L I N E

24.1 Impact of Blast Oxygen Enrichment on the Top Segment and Top Gas Conditions	219	24.4 Summary	223
24.2 Cross-Division Flows With Pure Oxygen Injection	219	Exercises	224
24.3 Top-Segment Calculations	220	Reference	224

24.1 IMPACT OF BLAST OXYGEN ENRICHMENT ON THE TOP SEGMENT AND TOP GAS CONDITIONS

Chapter 23, Top Gas Calculations With Pulverized Carbon Injection, determined top gas;

- composition,
- enthalpy, and
- temperature

with pulverized carbon injection.

This chapter does the same with pure oxygen injection, Fig. 24.1.

Our primary objective is to show how injection of pure oxygen affects top gas temperature. Secondary objectives are to determine top gas composition and enthalpy.

24.2 CROSS-DIVISION FLOWS WITH PURE OXYGEN INJECTION

Fig. 24.1 shows the steady-state flows across our oxygen-injected blast furnace's conceptual division.

The steady-state material flows, but not their rates, are the same as with carbon injection, that is;

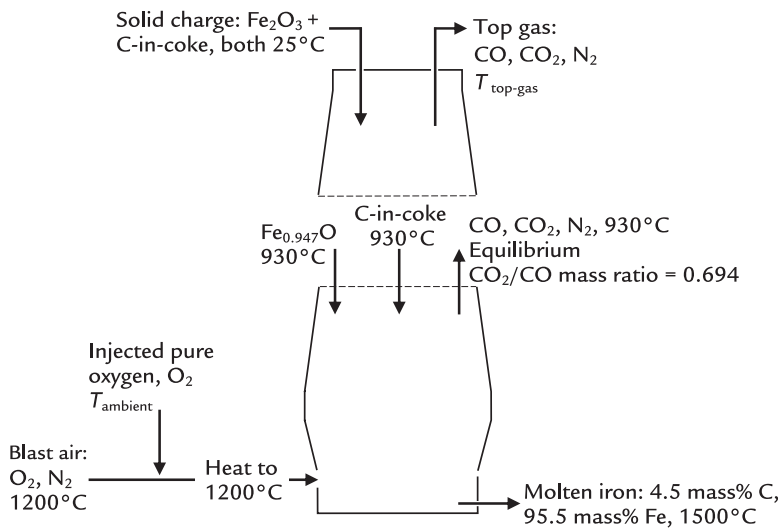


FIGURE 24.1 Conceptually divided blast furnace with pure oxygen injection. The oxygen is mixed with blast air, heated, and then blown into the blast furnace. Note the flows of $\text{Fe}_{0.947}\text{O}(\text{s})$, $\text{C}(\text{s})\text{-in-coke}$, CO(g) , $\text{CO}_2(\text{g})$, and $\text{N}_2(\text{g})$ across the conceptual division.

- $\text{Fe}_{0.947}\text{O}(\text{s})$ and $\text{C}(\text{s})\text{-in-coke}$ descending, and
- CO(g) , $\text{CO}_2(\text{g})$, and $\text{N}_2(\text{g})$ ascending.

We now calculate the steady-state mass flows of these substances, per 1000 kg of Fe in product molten iron using the bottom segment matrix of Chapter 9, Bottom Segment With Oxygen Enrichment of Blast Air, [Table 24.1](#).

With 30 kg of pure oxygen injection, the masses are;

- mass $\text{Fe}_{0.947}\text{O}$ into bottom segment = mass $\text{Fe}_{0.947}\text{O}$ out of top segment = 1302 kg,
- mass C -in-coke into bottom segment = mass C -in-coke out of top segment = 394 kg,
- mass CO out of bottom segment = mass CO into top segment = 561 kg,
- mass CO_2 out of bottom segment = mass CO_2 into top segment = 389 kg, and
- mass N_2 out of bottom segment = mass N_2 into top segment = 894 kg

all per 1000 kg of Fe in product molten iron.

These are the only values that will keep the blast furnace of [Fig. 24.1](#) steadily producing 1500°C molten iron with 30 kg of pure oxygen injectant.

24.3 TOP-SEGMENT CALCULATIONS

The above five values are now forwarded to the top segment matrix of [Fig. 24.1](#), [Table 24.2](#) as shown in Cells AC3 and AC8–AC11.

The forwarding instructions are;

$$\text{Cell AC3} = \text{C18}$$

$$\text{Cell AC8} = \text{C24}$$

$$\text{Cell AC9} = \text{C25}$$

$$\text{Cell AC10} = \text{C26}$$

$$\text{Cell AC11} = \text{C19}$$

where C Cells refer to [Table 24.1](#).

TABLE 24.1 Matrix for Calculating Bottom-Segment Inputs and Outputs of Fig. 24.1 With 30 kg of Pure Oxygen Injection

	A	B	C	D	E	F	G	H	I	J	K	L	M
1	BOTTOM SEGMENT CALCULATIONS												
2	Equation	Description	Numerical term	mass $\text{Fe}_{0.947}\text{O}$ into bottom segment	mass C in descending coke	mass O_2 in blast air	mass N_2 in blast air	mass Fe out in molten iron	mass C out in molten iron	mass CO out in ascending gas	mass CO_2 out in ascending gas	mass N_2 out in ascending gas	mass O_2 in injected pure oxygen
3	7.7	Fe out in molten iron specification	1000	0	0	0	0	1	0	0	0	0	0
4	7.2	Fe mass balance	0	-0.768	0	0	0	0	0	0	0	0	0
5	9.2	O mass balance	0	-0.232	0	-1	0	0	0	0.571	0.727	0	-1
6	7.4	C mass balance	0	0	-1	0	0	0	1	0.429	0.273	0	0
7	7.5	N mass balance	0	0	0	0	-1	0	0	0	0	1	0
8	7.6	N_2 in blast air specification	0	0	0	3.3	-1	0	0	0	0	0	0
9	7.9	Equilibrium CO_2/CO mass ratio	0	0	0	0	0	0	0	0.694	-1	0	0
10	7.8	C out in molten iron specification	0	0	0	0	0	0.047	-1	0	0	0	0
11	9.4	Enthalpy balance	-320	3.152	-1.359	-1.239	-1.339	1.269	5	-2.926	-7.926	1.008	-1.239
12	9.1	Mass O_2 injected into blast air	30	0	0	0	0	0	0	0	0	0	1
13													
14				930°C	930°C	1200°C	1500°C	1500°C	930°C	930°C	930°C	930°C	1200°C
15													
16													
17	Bottom segment calculated values		kg per 1000 kg of Fe out in molten iron										
18	mass $\text{Fe}_{0.947}\text{O}$ into bottom segment		1302										
19	mass C in descending coke		394	also = mass C in the furnace's coke charge, Eqn. (7.16)									
20	mass O_2 in blast air		271										
21	mass N_2 in blast air		894										
22	mass Fe out in molten iron		1000										
23	mass C out in molten iron		47										
24	mass CO out in ascending gas		561										
25	mass CO_2 out in ascending gas		389										
26	mass N_2 out in ascending gas		894										
27	mass O_2 in injected pure oxygen		30										
28													

This is a copy of Table 9.1. It calculates the amounts of O_2 -in-blast air and C-in-coke charge that will keep the blast furnace of Fig. 24.1 steadily producing molten iron, 1500°C. It also calculates the equivalent steady-state $\text{Fe}_{0.947}\text{O}$, C-in-coke, CO, CO_2 , and N_2 flows across conceptual division of Fig. 24.1. All masses are per 1000 kg of Fe in product molten iron.

TABLE 24.2 Spreadsheet for Blast Furnace Top-Segment of Fig. 24.1 With 30 kg of Pure Oxygen Injection

	AA	AB	AC	AD	AE	AF	AG	AH	AI	AJ	AK	AL	AM
1	TOP SEGMENT CALCULATIONS		Description	Numerical term	mass Fe ₂ O ₃ in furnace charge	mass C in coke charge	mass CO ascending from bottom segment	mass CO ₂ ascending from bottom segment	mass N ₂ ascending from bottom segment	mass Fe ₂ O ₃ O descending into bottom segment	mass C-in-coke descending into bottom segment	mass CO out in top-gas	mass CO ₂ out in top-gas
2													
3	20.6	Mass Fe ₂ O ₃ O descending into bottom segment	1302	0	0	0	0	0	1	0	0	0	0
4	20.2	Fe mass balance	0	-0.699	0	0	0	0	0.768	0	0	0	0
5	20.3	O mass balance	0	-0.301	0	-0.571	-0.727	0	0.232	0	0.571	0.727	0
6	20.4	C mass balance	0	0	-1	0.429	-0.273	0	0	1	0.429	0.273	0
7	20.5	N mass balance	0	0	0	0	0	-1	0	0	0	0	1
8	20.8	Mass CO ascending from bottom segment	561	0	0	1	0	0	0	0	0	0	0
9	20.9	Mass CO ₂ ascending from bottom segment	389	0	0	0	1	0	0	0	0	0	0
10	20.10	Mass N ₂ ascending from bottom segment	894	0	0	0	0	1	0	0	0	0	0
11	20.7	Mass C-in-coke descending into bottom segment	394	0	0	0	0	0	0	1	0	0	0
12	20.11	Unreacted C-in-coke specification	0	0	-1	0	0	0	0	1	0	0	0
13				25°C	25°C	930°C	930°C	930°C	930°C	930°C	T _{top gas}	T _{top gas}	T _{top gas}
14													
15													
16													
17	Top segment calculated values		kg per 1000 kg of Fe out in molten iron										
18	mass Fe ₂ O ₃ in furnace charge		1431										
19	mass C in coke charge		394										
20	mass CO ascending from bottom segment		561										
21	mass CO ₂ ascending from bottom segment		389										
22	mass N ₂ ascending from bottom segment		894										
23	mass Fe ₂ O ₃ O descending into bottom segment		1302										
24	mass C-in-coke descending into bottom segment		394										
25	mass CO out in top gas		336										
26	mass CO ₂ out in top gas		743										
27	mass N ₂ out in top gas		894										
28													
29													
30													
31													
32	TOP SEGMENT INPUT AND OUTPUT ENTHALPY CALCULATIONS												
33	21.2	Top segment input enthalpy = AC18 * -5.169 + AC19 * 0 + AC20 * (-2.926) + AC21 * (-7.926) + AC22 * 1.008 =							-11218	MJ per 1000 kg of Fe in product molten iron			
34	21.5b	Top segment output enthalpy = AG33 - 80 =							-11298	MJ per 1000 kg of Fe in product molten iron			
35													
36	TOP-GAS ENTHALPY CALCULATION												
37	22.2	Top-gas enthalpy = AG34 - AC23 * 3.152 - AC24 * 1.359 =							-7729	MJ per 1000 kg of Fe in product molten iron			
38													
39	TOP-GAS TEMPERATURE CALCULATION												
40	22.4	Top-gas temperature = (AG37 - AC25 * 3.972 - AC26 * 8.966 - AC27 * -0.02624) / (AC25 * 0.001049 + AC26 * 0.0009314 + AC27 * 0.001044) =							144	°C			
41													

The values in Cells AC3 and AC8–AC11 are from bottom segment calculated values of Table 24.1. Except for column AC, the matrix is the same as Fig. 23.2.

$$\text{Cell AG33} = \text{AC18} * (-5.169) + \text{AC19} * 0 + \text{AC20} * (-2.926) + \text{AC21} * (-7.926) + \text{AC22} * 1.008 \quad (21.2)$$

$$\text{Cell AG34} = \text{AG33} - 80 \quad (21.5b)$$

$$\text{Cell AG37} = \text{AG34} - \text{AC23} * (-3.152) - \text{AC24} * 1.359 \quad (22.2)$$

$$\text{Cell AH40} = \frac{(\text{AG37} - \text{AC25} * (-3.972) - \text{AC26} * (-8.966) - \text{AC27} * (-0.02624))}{(\text{AC25} * 0.001049 + \text{AC26} * 0.0009314 + \text{AC27} * 0.001044)} \quad (22.4)$$

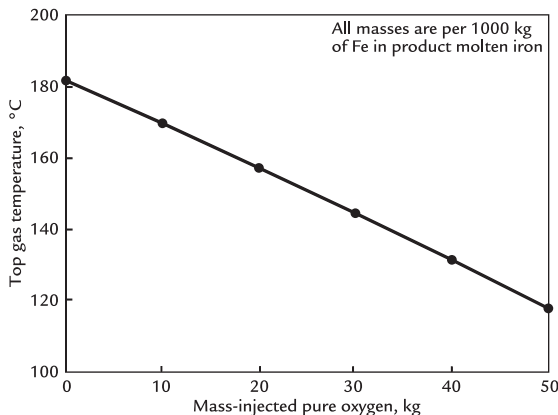


FIGURE 24.2 Top gas temperature falls with increasing pure oxygen injection - by about $1.3^{\circ}\text{C}/\text{kg}$ of oxygen. The line is not quite straight because Eq. (22.4) is not linear.

Insertion of the above oxygen-injection cross-division values into Table 24.2 automatically calculates the equivalent top gas;

- CO, CO₂, and N₂ masses, Cells AC25, 26, and 27;
- enthalpy, Cell AG37; and
- temperature, Cell AH40.

Top gas temperature of Table 24.2 is plotted in Fig. 24.2 - along with other oxygen injection results. Top gas temperature is seen to decrease with increasing pure oxygen injection.

This fall in temperature is a consequence of all equations of Tables 24.1 and 24.2. We may speculate that it is mainly due to;

- the decreased amount of hot, high enthalpy N₂ rising into the top segment, Fig. 24.3, and
- the increased amount of cool, low enthalpy top charged C-in-coke, Fig. 24.4,

with increasing pure oxygen injection.

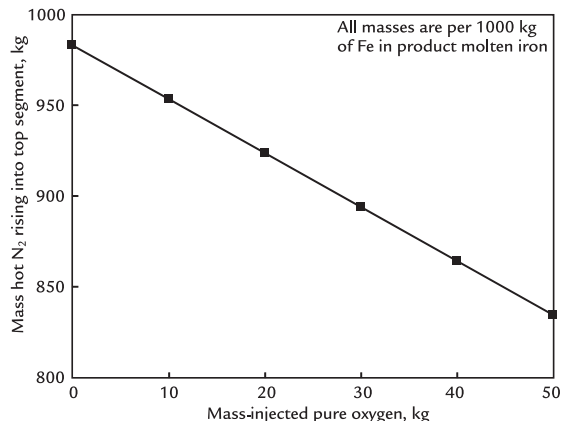


FIGURE 24.3 Mass of hot nitrogen rising into a blast furnace's top segment as a function of mass tuyere-injected pure oxygen. The decrease is notable. It is due to the replacement of air with pure oxygen in the bottom segment. The smaller amount of hot nitrogen brings less enthalpy into the top segment lowering top gas enthalpy and hence top gas temperature. The line is straight.

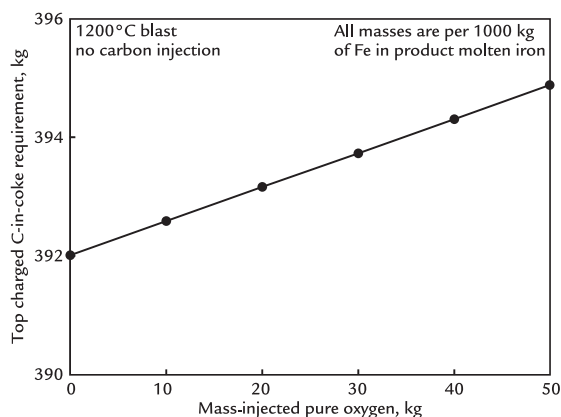


FIGURE 24.4 Effect of pure oxygen injection on the amount of top charge C-in-coke needed for steady production of 1500°C molten iron. Oxygen injection increases C-in-coke requirement but the effect is small. The line is straight. The cause of the increase is detailed in Section 9.4.

24.4 SUMMARY

Tuyere injection of pure oxygen into the blast furnace is readily included in our top gas;

- composition,
 - enthalpy, and
 - temperature
- calculations.

- The top gas calculations entail;
1. bottom segment calculation of blast furnace C-in-coke and O₂-in-blast air requirements for steady 1500°C molten iron production with pure oxygen injection, Chapter 9, Bottom Segment With Oxygen Enrichment of Blast Air, and
 2. top segment calculation of top gas composition, enthalpy, and temperature from the equivalent;
 - a. steady-state cross-division mass flows, [Fig. 24.1](#) and [Table 24.1](#), and
 - b. top segment mass and enthalpy balances, [Table 24.2](#).

The calculations show that top gas temperature falls with increasing pure oxygen injection—confirmed by the industrial data of Geerdes et al¹.

EXERCISES

All masses are per 1000 kg of Fe in product molten iron

- 24.1. What is the top gas temperature with 60 kg of injected pure oxygen?
- 24.2. What are the top gas masses with 30 kg and 60 kg of injected pure oxygen?
- 24.3. The top gas temperature must be greater than 160°C while simultaneously having the tuyere raceway flame temperature lower than 2400°C. Over what oxygen injection range are these requirements both met?

Reference

1. Geerdes M, Chaigneau R, Kurunov I, Lingiardi O, Ricketts J. *Modern blast furnace ironmaking, an introduction*. 2nd ed BV, Amsterdam: IOS Press; 2015. p. 195.

Top Segment Mass Balance With CH₄(g) Injection

O U T L I N E

25.1 Impact of Methane CH ₄ (g) Injection on Top Gas	225	25.5 With 60 kg of CH ₄ (g) Tuyere Injectant	231
25.2 Cross-Division Flows With CH ₄ (g) Injection	226	25.6 Top-Segment Matrix and Calculated Top Gas Values	231
25.3 Top-Segment Calculations	226	25.7 Full Spreadsheet Automation	232
25.3.1 Top-Segment Hydrogen Balance Equation	226	25.8 Calculation Results	233
25.3.2 Altered Top-Segment Oxygen Balance Equation	228	25.9 Summary	233
25.4 H ₂ /CO Reduction Ratio Equation	230	Exercises	233

25.1 IMPACT OF METHANE CH₄(g) INJECTION ON TOP GAS

Chapter 23, Top Segment Calculations With Pulverized Carbon Injection, and Chapter 24, Top Segment Calculations With Oxygen Enrichment, determined top gas composition with tuyere injection of pulverized carbon and pure oxygen.

This chapter determines top gas composition with tuyere injection of CH₄(g), as a stand-in for natural gas.

Our objectives are to;

1. show how hydrogen, from CH₄(g), is included in our top-segment calculations, and
2. calculate top gas composition with CH₄(g) injection, including H₂ and H₂O in top gas.

25.2 CROSS-DIVISION FLOWS WITH CH₄(g) INJECTION

Fig. 25.1 shows steady-state flows across our CH₄(g) injected blast furnace's conceptual division. They are;

- descending Fe_{0.947}O(s) and C(s)-in-coke, and
- ascending CO(g), CO₂(g), N₂(g), H₂(g), and H₂O(g).

The ascending H₂(g) and H₂O(g) are new. We now calculate these steady-state mass flows with 60 kg of tuyere-injected CH₄(g) per 1000 kg of Fe in product molten iron using matrix **Table 25.1**.

With 60 kg of CH₄(g) injection, the cross-division mass flows are;

- mass Fe_{0.947}O into bottom segment = mass Fe_{0.947}O out of top segment = 1302 kg (Cell C18),
- mass C-in-coke into bottom segment = mass C-in-coke out of top segment = 335 kg (Cell C19),
- mass CO out of bottom segment = mass CO into top segment = 539 kg (Cell C24),
- mass CO₂ out of bottom segment = mass CO₂ into top segment = 374 kg (Cell C25),

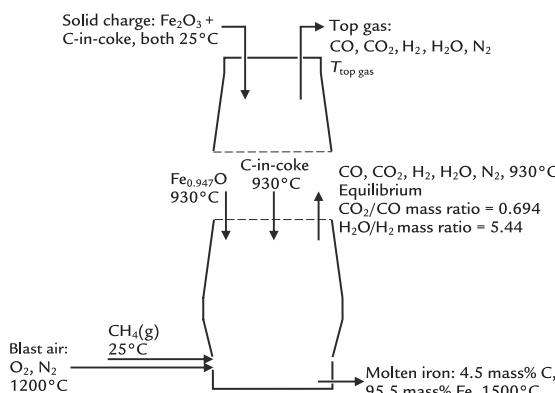


FIGURE 25.1 Conceptually divided blast furnace with tuyere injection of CH₄(g). Note the steady-state flows of Fe_{0.947}O(s), C(s)-in-coke, CO(g), CO₂(g), N₂(g), H₂(g), and H₂O(g) across the conceptual division.

- mass N₂ out of bottom segment = mass N₂ into top segment = 1064 kg (Cell C26),
- mass H₂ out of bottom segment = mass H₂ into top segment = 9.4 kg (Cell C27), and
- mass H₂O out of bottom segment = mass H₂O into top segment = 51 kg (Cell C28)

all per 1000 kg of Fe in product molten iron.

These are the only values that will keep the blast furnace of **Fig. 25.1** steadily producing 1500°C molten iron with 60 kg of CH₄(g) injection.

The last two equations in this list are used in our top-segment matrix as:

$$9.4 = \begin{bmatrix} \text{mass H}_2 \text{ ascending} \\ \text{from bottom segment} \end{bmatrix} \quad (25.1)$$

$$51 = \begin{bmatrix} \text{mass H}_2\text{O ascending} \\ \text{from bottom segment} \end{bmatrix} \quad (25.2)$$

25.3 TOP-SEGMENT CALCULATIONS

This section begins our top-segment calculations. It;

1. develops a top-segment hydrogen mass balance equation;
2. alters top-segment oxygen balance equation of Section 20.3.2 to include;
 - a. mass H₂O(g) ascending from the bottom segment,
 - b. mass H₂O(g) leaving the top segment in top gas; and
3. develops a (mass Fe₂O₃ reduced by H₂/mass Fe₂O₃ reduced by CO) ratio equation.

25.3.1 Top-Segment Hydrogen Balance Equation

Hydrocarbon injection adds a new steady state mass balance to our top-segment calculations. It is;

$$\text{mass H into top segment} = \text{mass H out of top segment} \quad (25.3)$$

TABLE 25.1 Bottom-Segment Matrix for Calculating Bottom-Segment Steady-State Inputs and Outputs of Fig. 25.1 With 60 kg of CH₄(g) Injection. This is a Copy of Table 11.1

A	B	C	D	E	F	G	H	I	J	K	L	M	N	O		
1	BOTTOM SEGMENT CALCULATIONS															
Equation	Description	Numerical term	mass Fe _{0.947} O into bottom segment	mass C in descending coke	mass O ₂ in blast air	mass N ₂ in blast air	mass Fe out in molten iron	mass C out in molten iron	mass CO out in ascending gas	mass CO ₂ out in ascending gas	mass N ₂ out in ascending gas	mass H ₂ out in ascending gas	mass H ₂ O out in ascending gas	mass tuyere-injected CH ₄		
2																
3	7.7 Fe out in molten iron specification	1000	0	0	0	1	0	0	0	0	0	0	0	0		
4	7.2 Fe mass balance	0	-0.763	0	0	1	0	0	0	0	0	0	0	0		
5	11.5 O mass balance	0	-0.232	0	-1	0	0	0.571	0.727	0	0	0	0.888	0		
6	11.4 C mass balance	0	0	-1	0	0	1	0.429	0.273	0	0	0	-0.749			
7	7.5 N mass balance	0	0	0	0	-1	0	0	0	0	1	0	0	0		
8	7.6 N in blast air specification	0	0	0	3.3	-1	0	0	0	0	0	0	0	0		
9	7.9 Equilibrium CO ₂ /CO mass ratio	0	0	0	0	0	0	0.694	-1	0	0	0	0	0		
10	7.8 C out in molten iron specification	0	0	0	0	0	0.047	-1	0	0	0	0	0	0		
11	11.7 Enthalpy balance	.320	3.152	-1.359	-1.239	-1.339	1.269	5	-2.926	-7.926	1.008	13.34	.11.5	4.667		
12	11.3 H mass balance	0	0	0	0	0	0	0	0	0	1	0.112	0.261			
13	11.8 Equilibrium H ₂ O/H ₂ mass ratio	0	0	0	0	0	0	0	0	0	0	5.44	-1	0		
14	Mass injected CH ₄	60	0	0	0	0	0	0	0	0	0	0	0	1		
15		1200		°C												
16																
17	Bottom segment calculated values	kg per 1000 kg of Fe out in molten iron														
18	mass Fe _{0.947} O into bottom segment	1302														
19	mass C in descending coke	335	also = mass C in the furnace's coke charge, Eqn. (7.16)													
20	mass O ₂ in blast air	323														
21	mass N ₂ in blast air	1064														
22	mass Fe out in molten iron	1000														
23	mass C out in molten iron	47														
24	mass CO out in ascending gas	539														
25	mass CO ₂ out in ascending gas	374														
26	mass N ₂ out in ascending gas	1064														
27	mass H ₂ out in ascending gas	9.4														
28	mass H ₂ O out in ascending gas	51														
29	mass tuyere injected CH ₄	60														

Table 25.1 calculates the amounts of O₂-in-blast-air and C-in-coke charge that will keep the blast furnace of Fig. 25.1 steadily producing 1500°C molten iron. It also calculates the equivalent steady-state Fe_{0.947}O, C-in-coke, CO, CO₂, N₂, H₂, and H₂O flows across the conceptual division of Fig. 25.1. Eqs. (7.9) and (11.8) are explained in Chapter 7, Conceptual Division of the Furnace - Bottom Segment Calculations and Chapter 11, Bottom Segment with CH₄(g) Injection

In terms of mass flows of Fig. 25.1, it expands to;

$$\begin{aligned} & \left[\begin{array}{l} \text{mass H}_2 \text{ ascending} \\ \text{from bottom segment} \end{array} \right] * \frac{100 \text{ mass\% H in H}_2}{100\%} \\ & + \left[\begin{array}{l} \text{mass H}_2\text{O ascending} \\ \text{from bottom segment} \end{array} \right] * \frac{11.2 \text{ mass\% H in H}_2\text{O}}{100\%} \\ & = \left[\begin{array}{l} \text{mass H}_2 \text{ out} \\ \text{in top gas} \end{array} \right] * \frac{100 \text{ mass\% H in H}_2}{100\%} \\ & + \left[\begin{array}{l} \text{mass H}_2\text{O out} \\ \text{in top gas} \end{array} \right] * \frac{11.2 \text{ mass\% H in H}_2\text{O}}{100\%} \end{aligned}$$

or

$$\begin{aligned} & \left[\begin{array}{l} \text{mass H}_2 \text{ ascending} \\ \text{from bottom segment} \end{array} \right] * 1 \\ & + \left[\begin{array}{l} \text{mass H}_2\text{O ascending} \\ \text{from bottom segment} \end{array} \right] * 0.112 \\ & = \left[\begin{array}{l} \text{mass H}_2 \text{ out} \\ \text{in top gas} \end{array} \right] * 1 + \left[\begin{array}{l} \text{mass H}_2\text{O out} \\ \text{in top gas} \end{array} \right] * 0.112 \end{aligned}$$

or subtracting $\left\{ \left[\begin{array}{l} \text{mass H}_2 \text{ ascending} \\ \text{from bottom segment} \end{array} \right] * 1 \right\}$

$$+ \left[\begin{array}{l} \text{mass H}_2\text{O ascending} \\ \text{from bottom segment} \end{array} \right] * 0.112 \Big\}$$

from both sides;

$$\begin{aligned} 0 &= - \left[\begin{array}{l} \text{mass H}_2 \text{ ascending} \\ \text{from bottom segment} \end{array} \right] * 1 \\ &- \left[\begin{array}{l} \text{mass H}_2\text{O ascending} \\ \text{from bottom segment} \end{array} \right] * 0.112 \\ &+ \left[\begin{array}{l} \text{mass H}_2 \text{ out} \\ \text{in top gas} \end{array} \right] * 1 + \left[\begin{array}{l} \text{mass H}_2\text{O out} \\ \text{in top gas} \end{array} \right] * 0.112 \end{aligned} \tag{25.4}$$

as shown in Row 13 of Table 25.2.

25.3.2 Altered Top-Segment Oxygen Balance Equation

Ascension of H₂O(g) into the top-segment and departure of H₂O(g) in top gas alters the top-segment oxygen balance;

$$\text{mass O into top segment} = \text{mass O out of top segment}$$

to

$$\begin{aligned} & \left[\begin{array}{l} \text{mass Fe}_2\text{O}_3 \text{ in} \\ \text{furnace charge} \end{array} \right] * \frac{30.1 \text{ mass\% O in Fe}_2\text{O}_3}{100\%} \\ & + \left[\begin{array}{l} \text{mass CO ascending} \\ \text{from bottom segment} \end{array} \right] * \frac{57.1 \text{ mass\% O in CO}}{100\%} \\ & + \left[\begin{array}{l} \text{mass CO}_2 \text{ ascending} \\ \text{from bottom segment} \end{array} \right] * \frac{72.7 \text{ mass\% O in CO}_2}{100\%} \\ & + \left[\begin{array}{l} \text{mass H}_2\text{O ascending} \\ \text{from bottom segment} \end{array} \right] * \frac{88.8 \text{ mass\% O in H}_2\text{O}}{100\%} \\ & = \left[\begin{array}{l} \text{mass Fe}_{0.947}\text{O descending} \\ \text{into bottom segment} \end{array} \right] * \frac{23.2 \text{ mass\% O in Fe}_{0.947}\text{O}}{100\%} \\ & + \left[\begin{array}{l} \text{mass CO out} \\ \text{in top gas} \end{array} \right] * \frac{57.1 \text{ mass\% O in CO}}{100\%} \\ & + \left[\begin{array}{l} \text{mass CO}_2 \text{ out} \\ \text{in top gas} \end{array} \right] * \frac{72.7 \text{ mass\% O in CO}_2}{100\%} \\ & + \left[\begin{array}{l} \text{mass H}_2\text{O out} \\ \text{in top gas} \end{array} \right] * \frac{88.8 \text{ mass\% O in H}_2\text{O}}{100\%} \end{aligned}$$

or

$$\begin{aligned} & \left[\begin{array}{l} \text{mass Fe}_2\text{O}_3 \text{ in} \\ \text{furnace charge} \end{array} \right] * 0.301 + \left[\begin{array}{l} \text{mass CO ascending} \\ \text{from bottom segment} \end{array} \right] * 0.571 \\ & + \left[\begin{array}{l} \text{mass CO}_2 \text{ ascending} \\ \text{from bottom segment} \end{array} \right] * 0.727 \\ & + \left[\begin{array}{l} \text{mass H}_2\text{O ascending} \\ \text{from bottom segment} \end{array} \right] * 0.888 \\ & = \left[\begin{array}{l} \text{mass Fe}_{0.947}\text{O descending} \\ \text{into bottom segment} \end{array} \right] * 0.232 \\ & + \left[\begin{array}{l} \text{mass CO out} \\ \text{in top gas} \end{array} \right] * 0.571 + \left[\begin{array}{l} \text{mass CO}_2 \text{ out} \\ \text{in top gas} \end{array} \right] * 0.727 \\ & + \left[\begin{array}{l} \text{mass H}_2\text{O out} \\ \text{in top gas} \end{array} \right] * 0.888 \end{aligned}$$

or subtracting;

$$\left\{ \begin{aligned} & \left[\begin{array}{l} \text{mass Fe}_2\text{O}_3 \text{ in} \\ \text{furnace charge} \end{array} \right] * 0.301 \\ & + \left[\begin{array}{l} \text{mass CO ascending} \\ \text{from bottom segment} \end{array} \right] * 0.571 \\ & + \left[\begin{array}{l} \text{mass CO}_2 \text{ ascending} \\ \text{from bottom segment} \end{array} \right] * 0.727 \\ & + \left[\begin{array}{l} \text{mass H}_2\text{O ascending} \\ \text{from bottom segment} \end{array} \right] * 0.888 \end{aligned} \right\}$$

TABLE 25.2 Top-Segment Matrix With Bottom-Segment Tuyere Injection of CH₄(g), Fig. 25.1

	A6	A8	AC	AD	AE	AF	AG	AH	AI	AJ	AK	AL	AM	AN	AO	AP	AQ
TOP SEGMENT CALCULATIONS																	
1	Equation:	Description	Numerical term	mass Fe ₂ O ₃ in furnace charge	mass C in coke charge	mass CO ascending from bottom segment	mass CO ₂ ascending from bottom segment	mass N ₂ ascending from bottom segment	mass Fe ₂ O ₃ descending into bottom segment	mass C in coke descending into bottom segment	mass CO out in top gas	mass CO ₂ out in top gas	mass N ₂ out in top gas	mass H ₂ ascending from bottom segment	mass H ₂ O ascending from bottom segment	mass H ₂ out in top gas	mass H ₂ O out in top gas
2																	
3	20.6	Mass Fe ₂ O ₃ descending into bottom segment	1302	0	0	0	0	1	0	0	0	0	0	0	0	0	0
4	20.2	Fe mass balance	0	0.699	0	0	0	0	0.768	0	0	0	0	0	0	0	0
5	25.5	D mass balance	0	0.301	0	0.571	0.727	0	0.232	0	0.571	0.727	0	0	0.888	0	0.888
6	20.4	C mass balance	0	0	1	-0.429	0.273	0	0	1	0.429	0.273	0	0	0	0	0
7	20.1	N mass balance	0	0	0	0	0	0	1	0	0	0	1	0	0	0	0
8	20.8	Mass CO descending from bottom segment	539	0	0	1	0	0	0	0	0	0	0	0	0	0	0
9	20.9	Mass CO ₂ ascending from bottom segment	374	0	0	0	0	1	0	0	0	0	0	0	0	0	0
10	20.10	Mass N ₂ descending from bottom segment	1064	0	0	0	0	0	1	0	0	0	0	0	0	0	0
11	20.7	Mass C in coke descending into bottom segment	335	0	0	0	0	0	0	0	1	0	0	0	0	0	0
12	20.11	Unrestricted C in coke specification	0	0	0	1	0	0	0	0	1	0	0	0	0	0	0
13	25.8	H mass balance	0	0	0	0	0	0	0	0	0	0	0	0	-0.112	0	0.112
14	25.1	Mass N ₂ ascending from bottom segment	0.4	0	0	0	0	0	0	0	0	0	0	1	0	0	0
15	25.2	Mass H ₂ O ascending from bottom segment	51	0	0	0	0	0	0	0	0	0	0	0	1	0	0
16	25.13	H ₂ /CO reaction ratio equation	0	0	0	0	0	-0.10	0	0	0	0.10	0	0	1	0	-1
17	Top segment calculated values		kg per 1000 kg of Fe out in molten iron														
18	mass Fe ₂ O ₃ in furnace charge		211														
19	mass C in coke charge		335														
20	mass CO ascending from bottom segment		539														
21	mass CO ₂ ascending from bottom segment		374														
22	mass N ₂ ascending from bottom segment		1064														
23	mass H ₂ ascending into bottom segment		335														
24	mass C in coke descending into bottom segment		335														
25	mass CO out in top gas		358														
26	mass CO ₂ out in top gas		658														
27	mass N ₂ out in top gas		1064														
28	mass H ₂ ascending from bottom segment		9.4														
29	mass H ₂ ascending into bottom segment		51														
30	mass H ₂ leaving in top gas		6.2														
31	mass H ₂ O leaving in top gas		79														

The values are for 60 kg of CH₄ injection. All values are per 1000 kg of Fe in product molten iron, 1500°C. Note that 9.4 kg of H₂(g) ascend into the top segment while 6.2 kg leave in top gas. This is a consequence of Eq. (25.7).

from both sides;

$$\begin{aligned}
 0 = & - \left[\frac{\text{mass Fe}_2\text{O}_3 \text{ in}}{\text{furnace charge}} \right] * 0.301 \\
 & - \left[\frac{\text{mass CO ascending}}{\text{from bottom segment}} \right] * 0.571 \\
 & - \left[\frac{\text{mass CO}_2 \text{ ascending}}{\text{from bottom segment}} \right] * 0.727 \\
 & - \left[\frac{\text{mass H}_2\text{O ascending}}{\text{from bottom segment}} \right] * 0.888 \\
 & + \left[\frac{\text{mass Fe}_{0.947}\text{O descending}}{\text{into bottom segment}} \right] * 0.232 \\
 & + \left[\frac{\text{mass CO out}}{\text{in top gas}} \right] * 0.571 + \left[\frac{\text{mass CO}_2 \text{ out}}{\text{in top gas}} \right] * 0.727 \\
 & + \left[\frac{\text{mass H}_2\text{O out}}{\text{in top gas}} \right] * 0.888
 \end{aligned} \tag{25.5}$$

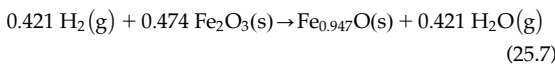
as shown in Row 5 of top-segment matrix Table 25.2.

25.4 H₂/CO REDUCTION RATIO EQUATION

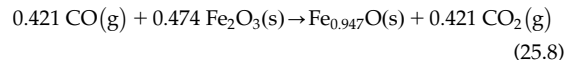
At this point, we still need one more equation to fully define steady-state operation of top segment [because we have introduced four new variables $\left[\frac{\text{mass H}_2 \text{ ascending}}{\text{from bottom segment}} \right]$, $\left[\frac{\text{mass H}_2\text{O ascending}}{\text{from bottom segment}} \right]$, $\left[\frac{\text{mass H}_2 \text{ out}}{\text{in top gas}} \right]$, and $\left[\frac{\text{mass H}_2\text{O out}}{\text{in top gas}} \right]$ but only three new Eqs. (25.1), (25.2), and (25.4)] of Fig. 25.1. We obtain this by specifying that;

$$\begin{aligned}
 & \frac{\text{H}_2 \text{ reduction of Fe}_2\text{O}_3 \text{ to Fe}_{0.947}\text{O, kg mol}}{\text{CO reduction of Fe}_2\text{O}_3 \text{ to Fe}_{0.947}\text{O, kg mol}} \\
 & = \frac{\text{kg mol H}_2(\text{g}) \text{ ascending into top segment}}{\text{kg mol CO(g) ascending into top segment}}
 \end{aligned} \tag{25.6}$$

This comes from the reduction reactions



and



which show that each kg mol of H₂ and CO;

- reduces the same molar quantity of Fe₂O₃ to Fe_{0.947}O, and
- produces the same molar quantity of H₂O or CO₂.

This allows us to expand Eq. (25.6) to:

$$\begin{aligned}
 & \frac{\{[\text{kg mol H}_2\text{O(g) out in top gas}] - [\text{kg mol H}_2\text{O(g) ascending from bottom segment}]\}}{\{[\text{kg mol CO}_2(\text{g}) \text{ out in top gas}] - [\text{kg mol CO}_2(\text{g}) \text{ ascending from bottom segment}]\}} \\
 & = \frac{\left[\frac{\text{kg mol H}_2 \text{ ascending}}{\text{from bottom segment}} \right]}{\left[\frac{\text{kg mol CO ascending}}{\text{from bottom segment}} \right]}
 \end{aligned} \tag{25.9}$$

We put this equation into mass form by substituting;

- kg mol H₂O = kg H₂O/18 (where 18 is the molecular mass of H₂O, kg per kg mol),
- kg mol CO₂ = kg CO₂/44,
- kg mol H₂ = kg H₂/2, and
- kg mol CO = kg CO/28

into Eq. (25.9), which gives

$$\begin{aligned}
 & \frac{\{(\text{mass H}_2\text{O(g) out in top gas}) - (\text{mass H}_2\text{O(g) ascending from bottom segment})\}/18}{\{(\text{mass CO}_2(\text{g}) \text{ out in top gas}) - (\text{mass CO}_2(\text{g}) \text{ ascending from bottom segment})\}/44} \\
 & = \frac{\{(\text{mass H}_2 \text{ ascending from bottom segment})/2\}}{\{(\text{mass CO ascending from bottom segment})/28\}}
 \end{aligned} \tag{25.10}$$

or

$$\begin{aligned}
 & \frac{\{(\text{mass H}_2\text{O(g) out in top gas}) - (\text{mass H}_2\text{O(g) ascending from bottom segment})\} * 0.056}{\{(\text{mass CO}_2(\text{g}) \text{ out in top gas}) - (\text{mass CO}_2(\text{g}) \text{ ascending from bottom segment})\} * 0.023} \\
 & = \frac{\{(\text{mass H}_2 \text{ ascending from bottom segment}) * 0.5\}}{\{(\text{mass CO ascending from bottom segment}) * 0.036\}}
 \end{aligned}$$

or

$$\begin{aligned} & \frac{(\text{mass H}_2\text{O(g)} \text{out in top gas}) - (\text{mass H}_2\text{O(g)} \text{ ascending from bottom segment})}{(\text{mass CO}_2\text{(g)} \text{out in top gas}) - (\text{mass CO}_2\text{(g)} \text{ ascending from bottom segment})} * 2.44 \\ & = \frac{(\text{mass H}_2 \text{ ascending from bottom segment})}{(\text{mass CO ascending from bottom segment})} * 13.9 \end{aligned}$$

or

$$\begin{aligned} & \frac{(\text{mass H}_2\text{O(g)} \text{out in top gas}) - (\text{mass H}_2\text{O(g)} \text{ ascending from bottom segment})}{(\text{mass CO}_2\text{(g)} \text{out in top gas}) - (\text{mass CO}_2\text{(g)} \text{ ascending from bottom segment})} \\ & = \frac{(\text{mass H}_2 \text{ ascending from bottom segment})}{(\text{mass CO ascending from bottom segment})} * 5.7 \end{aligned} \quad (25.11)$$

$$\begin{aligned} & \left[\begin{array}{l} \text{mass H}_2\text{O(g) out} \\ \text{in top gas} \end{array} \right] * 1 - \left[\begin{array}{l} \text{mass H}_2\text{O ascending} \\ \text{from bottom segment} \end{array} \right] * 1 \\ & = \left[\begin{array}{l} \text{mass CO}_2 \text{ out} \\ \text{in top gas} \end{array} \right] * 0.10 - \left[\begin{array}{l} \text{mass CO}_2 \text{ ascending} \\ \text{from bottom segment} \end{array} \right] * 0.10 \end{aligned}$$

$$\text{or subtracting } \left\{ \begin{array}{l} \left[\begin{array}{l} \text{mass H}_2\text{O(g) out} \\ \text{in top gas} \end{array} \right] * 1 \\ - \left[\begin{array}{l} \text{mass H}_2\text{O ascending} \\ \text{from bottom segment} \end{array} \right] * 1 \end{array} \right\}$$

from both sides and rearranging;

$$\begin{aligned} 0 &= - \left[\begin{array}{l} \text{mass H}_2\text{O(g) out} \\ \text{in top gas} \end{array} \right] * 1 \\ &+ \left[\begin{array}{l} \text{mass H}_2\text{O ascending} \\ \text{from bottom segment} \end{array} \right] * 1 \\ &+ \left[\begin{array}{l} \text{mass CO}_2\text{(g) out} \\ \text{in top gas} \end{array} \right] * 0.10 \\ &- \left[\begin{array}{l} \text{mass CO}_2 \text{ ascending} \\ \text{from bottom segment} \end{array} \right] * 0.10 \end{aligned}$$

(25.13)

as shown in Row 16 of **Table 25.2**.

Notice that this development is consistent with our specification that carbon-in-coke doesn't react at the cool temperatures of the top segment, Eq. (7.16).

25.5 WITH 60 kg OF CH₄(g) TUYERE INJECTANT

As shown in **Table 25.1**, tuyere injection of 60 kg CH₄(g)/1000 kg Fe in product molten iron sends;

- 9.4 kg of H₂ into the top segment, Cell C27, and
- 539 kg of CO into the top segment, Cell C24

With these quantities, Eq. (25.11) becomes;

$$\begin{aligned} & \frac{(\text{kg H}_2\text{O(g)} \text{out in top gas} - \text{kg H}_2\text{O(g)} \text{ ascending from bottom segment})}{(\text{kg CO}_2\text{(g)} \text{out in top gas} - \text{kg CO}_2\text{(g)} \text{ ascending from bottom segment})} \\ & = \frac{9.4 \text{ kg H}_2}{539 \text{ kg CO}} * 5.7 = 0.10 \end{aligned} \quad (25.12)$$

Further, multiplying both sides by ([kg CO₂(g) out in top gas] - [kg CO₂(g) ascending from bottom segment]) gives;

25.6 TOP-SEGMENT MATRIX AND CALCULATED TOP GAS VALUES

We now insert;

1. Eqs. (25.4), (25.5), and (25.13) into Rows 13, 5, and 16 of top-segment matrix of **Table 25.2**, and
2. matrix cross-division mass flow values **Table 25.1** into Cells AC3, AC8, AC9, AC10, AC11, AC14, and AC15 of top-segment matrix of **Table 25.2**

then solve.

The instructions in the Top-Segment Matrix Cells are;

Cell AC3 contains = C18

(25.14)

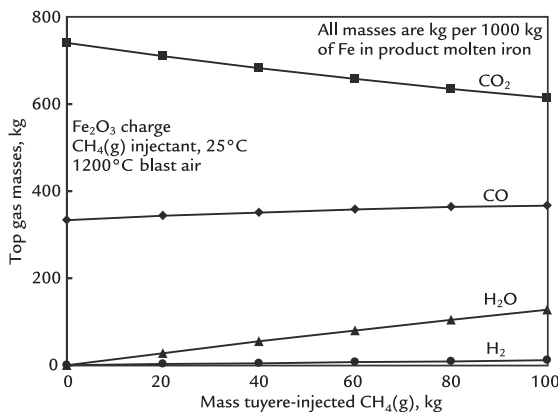


FIGURE 25.2 Top gas composition as a function of mass injected CH₄, H₂, H₂O, and CO masses all increase with increasing CH₄(g) injection. Mass CO₂ decreases. The lines are slightly curved because the values in Cells AG16 and AL16 of Table 25.3 vary with CH₄(g) injection quantity.

$$\text{Cell AC8 contains} = C24 \quad (25.15)$$

$$\text{Cell AC9 contains} = C25 \quad (25.16)$$

$$\text{Cell AC10 contains} = C26 \quad (25.17)$$

$$\text{Cell AC11 contains} = C19 \quad (25.18)$$

$$\text{Cell AC14 contains} = C27 \quad (25.19)$$

$$\text{Cell AC15 contains} = C28 \quad (25.20)$$

where C refers to the Column C in Table 25.1.

As shown, the top gas composition with 60 kg of CH₄(g) is;

- 358 kg CO,
- 658 kg CO₂,
- 1064 kg N₂,
- 6.2 kg H₂, and
- 79 kg H₂O

per 1000 kg of Fe in product molten iron.

This and top gas compositions at other CH₄(g) injection levels are plotted in Figs. 25.2 and 25.3.

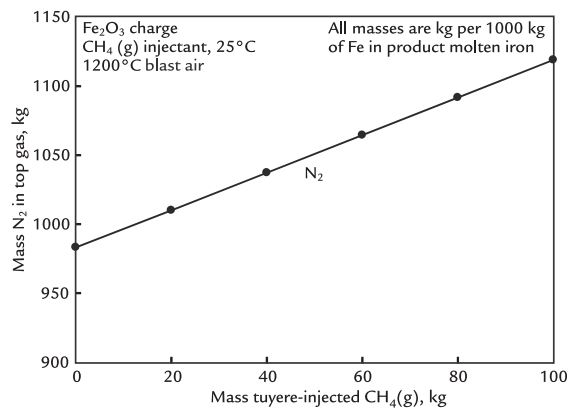


FIGURE 25.3 Mass N₂ in top gas increases with increasing amount of tuyere injected CH₄(g). The values are the same as in Fig. 11.4. This is because the amount of N₂(g) leaving the bottom segment, entering the top segment, and leaving in top gas are identical.

We developed a new equation from Eq. (25.12), that is;

$$\frac{(\text{mass H}_2\text{O(g) out in top gas} - \text{mass H}_2\text{O(g)} \text{ ascending from bottom segment})}{(\text{mass CO}_2\text{(g) out in top gas} - \text{mass CO}_2\text{(g)} \text{ ascending from bottom segment})} = \frac{9.4 \text{ kg H}_2}{539 \text{ kg CO}} * 5.7 \quad (25.21)$$

which we change to;

$$\frac{(\text{mass H}_2\text{O(g) out in top gas} - \text{mass H}_2\text{O(g)} \text{ ascending from bottom segment})}{(\text{mass CO}_2\text{(g) out in top gas} - \text{mass CO}_2\text{(g)} \text{ ascending from bottom segment})} = \frac{\text{AC14}}{\text{AC8}} * 5.7 \quad (25.21a)$$

where;

Cell AC14 always contains kg H₂ ascending from bottom segment

and;

Cell AC8 always contains kg CO ascending from bottom segment.

Further, multiplying both sides of Eq. (25.21a) by (kg CO₂(g) out in top

To fully automate our CH₄ calculations, we must generalize Eq. (25.13) of matrix Table 25.2.

gas – kg CO₂(g) ascending from bottom segment) gives;

$$\begin{aligned} & \left[\begin{array}{l} \text{mass H}_2\text{O out} \\ \text{in top gas} \end{array} \right] * 1 - \left[\begin{array}{l} \text{mass H}_2\text{O ascending} \\ \text{from bottom segment} \end{array} \right] * 1 \\ &= \left[\begin{array}{l} \text{mass CO}_2 \text{ out} \\ \text{in top gas} \end{array} \right] * \frac{\text{AC14}}{\text{AC8}} * 5.7 \\ & - \left[\begin{array}{l} \text{mass CO}_2 \text{ ascending} \\ \text{from bottom segment} \end{array} \right] * \frac{\text{AC14}}{\text{AC8}} * 5.7 \end{aligned}$$

or subtracting $\left\{ \left[\begin{array}{l} \text{mass H}_2\text{O out} \\ \text{in top gas} \end{array} \right] * 1 \right\}$

$$- \left[\begin{array}{l} \text{mass H}_2\text{O ascending} \\ \text{from bottom segment} \end{array} \right] * 1 \} \text{ from both sides;}$$

$$\begin{aligned} 0 = & - \left[\begin{array}{l} \text{mass H}_2\text{O out} \\ \text{in top gas} \end{array} \right] * 1 + \left[\begin{array}{l} \text{mass H}_2\text{O ascending} \\ \text{from bottom segment} \end{array} \right] * 1 \\ & + \left[\begin{array}{l} \text{mass CO}_2 \text{ out} \\ \text{in top gas} \end{array} \right] * \frac{\text{AC14}}{\text{AC8}} * 5.7 \\ & - \left[\begin{array}{l} \text{mass CO}_2 \text{ ascending} \\ \text{from bottom segment} \end{array} \right] * \frac{\text{AC14}}{\text{AC8}} * 5.7 \end{aligned} \quad (25.22)$$

as shown in Row 16 of **Table 25.3**.

Note that;

Cell AG16 = -(AC14/AC8)*5.7 which is -0.10 with 60 kg of CH₄(g) injection,

Cell AL16 = AC14/AC8*5.7 which is 0.10 with 60 kg of CH₄(g) in injection

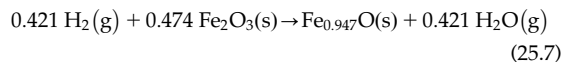
as shown in matrix **Tables 25.3**.

25.8 CALCULATION RESULTS

Figs. 25.2 and 25.3 show the major results of our CH₄(g) injection top gas composition calculations.

Fig. 25.2 shows that mass H₂ and mass H₂O in top gas both increase with increased CH₄(g) injection. This is totally predictable. The actual values depend on all the equations in matrix **Tables 25.1–25.3**.

Mass CO₂ in top gas decreases because Eq. 25.7;



consumes some of the O from top-segment Fe₂O₃ → Fe_{0.947}O reduction - letting more CO and hence less CO₂ depart in the top gas.

25.9 SUMMARY

This chapter shows how to determine the effect of tuyere-injected CH₄(g) on top gas composition. It;

1. develops a top-segment H mass balance,
2. modifies the top-segment O mass balance,
3. introduces a top segment H₂ reduction contribution/CO reduction contribution equation, and
4. constructs a matrix with these equations and solves as described in Chapter 20, Top-Segment Mass Balance.

Figs. 25.2 and 25.3 describe top gas composition with increasing CH₄(g) injection. Mass H₂, H₂O, CO, and N₂ increase. Mass CO₂ decreases.

Chapter 26, Top Enthalpy Balance With CH₄(g) Injection, and Chapter 27, Top Segment Enthalpy Balance with CH₄(g) Injection, now use top-segment mass flows and temperatures of this chapter to calculate;

- top gas enthalpy, and
- top gas temperature.

EXERCISES

All masses are kg per 1000 kg of Fe in product molten iron.

- 25.1.** The blast furnace management team of **Table 25.1** has located a cheap source of CH₄(g). They now wish to inject 120 kg

TABLE 25.3 Top-Segment Matrix Showing the Equations in Cells AG16 and AL16. They Complete the Connection Between our Bottom and Top-Segment Calculations

	AA	AB	AC	AD	AE	AF	AG	AH	AI	AJ	AK	AL	AM	AN	AO	AP	AQ
TOP SEGMENT CALCULATIONS																	
Equation	Description	Numerical term	mass Fe ₂ O ₃ in furnace charge	mass C in coke charge	mass CO ascending from bottom segment	mass CO ₂ ascending from bottom segment	mass N ₂ ascending from bottom segment	mass Fe _{0.947} O descending into bottom segment	mass C-in-coke descending into bottom segment	mass CO out in top gas	mass CO ₂ out in top gas	mass N ₂ out in top gas	mass H ₂ ascending from bottom segment	mass H ₂ O ascending from bottom segment	mass H ₂ out in top gas	mass H ₂ O out in top gas	
20.6	Mass Fe _{0.947} O descending into bottom segment	1302	0	0	0	0	0	1	0	0	0	0	0	0	0	0	
20.2	Fe mass balance	0	-0.699	0	0	0	0.768	0	0	0	0	0	0	0	0	0	
25.5	O mass balance	0	-0.301	0	-0.571	-0.727	0	0.232	0	0.571	0.727	0	0	-0.888	0	0.888	
20.4	C mass balance	0	0	-1	-0.429	-0.273	0	0	1	0.429	0.273	0	0	0	0	0	
20.5	N mass balance	0	0	0	0	0	-1	0	0	0	0	1	0	0	0	0	
20.8	Mass CO ascending from bottom segment	539	0	0	1	0	0	0	0	0	0	0	0	0	0	0	
20.9	Mass CO ₂ ascending from bottom segment	374	0	0	0	1	0	0	0	0	0	0	0	0	0	0	
20.10	Mass N ₂ ascending from bottom segment	1064	0	0	0	0	1	0	0	0	0	0	0	0	0	0	
20.7	Mass C-in-coke descending into bottom segment	335	0	0	0	0	0	0	0	1	0	0	0	0	0	0	
20.11	Unreacted C-in-coke specification	0	0	-1	0	0	0	0	0	1	0	0	0	0	0	0	
25.4	H mass balance	0	0	0	0	0	0	0	0	0	0	0	-1	-0.112	1	0.112	
25.1	Mass H ₂ ascending from bottom segment	9.4	0	0	0	0	0	0	0	0	0	1	0	0	0	0	
25.2	Mass H ₂ O ascending from bottom segment	51	0	0	0	0	0	0	0	0	0	0	0	1	0	0	
25.22	H ₂ /CO reaction ratio equation	0	0	0	0	-0.10	0	0	0	0	0.10	0	0	1	0	-1	
Top segment calculated values																	
	kg per 1000 kg of Fe in product iron																
18	mass Fe ₂ O ₃ in furnace charge	1431															
19	mass C in coke charge	335															
20	mass CO ascending from bottom segment	539															
21	mass CO ₂ ascending from bottom segment	374															
22	mass N ₂ ascending from bottom segment	1064															
23	mass Fe _{0.947} O descending into bottom segment	1302															
24	mass C-in-coke descending into bottom segment	335															
25	mass CO out in top gas	358															
26	mass CO ₂ out in top gas	659															
27	mass N ₂ out in top gas	1064															
28	mass H ₂ ascending from bottom segment	9.4															
29	mass H ₂ O ascending from bottom segment	51															
30	mass H ₂ leaving in top gas	6.2															
31	mass H ₂ O leaving in top gas	79															

=AC14/AC8*5.7

=AC14/AC8*5.7

of 25°C CH₄(g) through their tuyeres of blast furnace and would like to know what their top gas composition (mass% and vol. %) will be with this amount of injection. Please calculate it for them. Use Appendix P for your mass% and vol. % calculations.

- 25.2.** The research team of Exercise 25.1 believes that its mass H₂O(g) in top gas

is so large that it might cause excessive H₂O(g) → H₂O(ℓ) condensation near the top of the furnace charge. They wish to keep mass H₂O(g) in top gas at 55 kg or lower—and ask how much 25°C CH₄(g) they can inject without exceeding this limit. Please calculate this for them using any method you like.

26

Top Segment Enthalpy Balance with CH₄(g) Injection

O U T L I N E

26.1 Estimating Top Gas Enthalpy With H ₂ (g) and H ₂ O(g) Present	237	26.4 Top Gas Enthalpy	239
26.2 Top-Segment Input Enthalpy	238	26.5 Summary	241
26.3 Top-Segment Output Enthalpy	239	Exercises	241

26.1 ESTIMATING TOP GAS ENTHALPY WITH H₂(g) AND H₂O(g) PRESENT

In this chapter, we calculate;

1. top-segment input enthalpy,
2. top-segment output enthalpy, and
3. top gas enthalpy

with H₂(g) and H₂O(g) in the top segment.

Chapter 27, Top Gas Temperature With CH₄(g) Injection, then calculates top gas temperature from the calculated top gas enthalpy and top-segment input and output masses of

Chapter 25, Top Segment Mass Balance with CH₄(g) Injection.

The calculations are all for the specific case of 60 kg of tuyere-injected CH₄(g).

Top gas temperature is important because it strongly affects the rate and efficiency of a blast furnace's;

1. moisture-in-charge evaporation, and
2. carbonate flux decomposition (Chapter 42: Top Segment Calculations with Carbonate Fluxes).

26.2 TOP-SEGMENT INPUT ENTHALPY

Fig. 26.1 shows the top segment's inputs, that is;

- Fe₂O₃(s) in furnace charge,
- C(s)-in-coke charge,
- CO(g) ascending from bottom segment,
- CO₂(g) ascending from bottom segment,
- N₂(g) ascending from bottom segment,
- H₂(g) ascending from bottom segment, and
- H₂O(g) ascending from bottom segment

with 60 kg of tuyere-injected CH₄(g). It also shows their temperatures.

The combined enthalpy of these inputs with 60 kg of CH₄(g) injection is;

$$\begin{aligned}
 & \left[\begin{array}{l} \text{top segment} \\ \text{input enthalpy} \end{array} \right] \\
 & = \left[\begin{array}{l} \text{mass Fe}_2\text{O}_3 \text{ in} \\ \text{furnace charge} \end{array} \right] * \frac{H^\circ_{25^\circ\text{C}}}{\text{MW}_{\text{Fe}_2\text{O}_3}} \\
 & + \left[\begin{array}{l} \text{mass C-in-} \\ \text{coke charge} \end{array} \right] * \frac{H^\circ_{25^\circ\text{C}}}{\text{MW}_\text{C}} \\
 & + \left[\begin{array}{l} \text{mass CO ascending} \\ \text{from bottom segment} \end{array} \right] * \frac{H^\circ_{930^\circ\text{C}}}{\text{MW}_\text{CO}} \\
 & + \left[\begin{array}{l} \text{mass CO}_2 \text{ ascending} \\ \text{from bottom segment} \end{array} \right] * \frac{H^\circ_{930^\circ\text{C}}}{\text{MW}_{\text{CO}_2}} \\
 & + \left[\begin{array}{l} \text{mass N}_2 \text{ ascending} \\ \text{from bottom segment} \end{array} \right] * \frac{H^\circ_{930^\circ\text{C}}}{\text{MW}_{\text{N}_2}} \\
 & + \left[\begin{array}{l} \text{mass H}_2 \text{ ascending} \\ \text{from bottom segment} \end{array} \right] * \frac{H^\circ_{930^\circ\text{C}}}{\text{MW}_{\text{H}_2}} \\
 & + \left[\begin{array}{l} \text{mass H}_2\text{O ascending} \\ \text{from bottom segment} \end{array} \right] * \frac{H^\circ_{930^\circ\text{C}}}{\text{MW}_{\text{H}_2\text{O}}} \quad (26.1a)
 \end{aligned}$$

Masses of Eq. (26.1a) are obtained from Table 25.3. The enthalpy values are obtained from Table J.1.

Together, they give;

$$\begin{aligned}
 & \left[\begin{array}{l} \text{top segment input enthalpy,} \\ \text{MJ per 1000 kg of Fe} \\ \text{in product molten iron} \end{array} \right] \\
 & = \left[\begin{array}{l} 1431 \text{ kg Fe}_2\text{O}_3 \text{ in} \\ \text{ore charge} \end{array} \right] * (-5.169) \\
 & + \left[\begin{array}{l} 335 \text{ kg C-in-} \\ \text{coke charge} \end{array} \right] * 0 \\
 & + \left[\begin{array}{l} 539 \text{ kg CO ascending} \\ \text{from bottom segment} \end{array} \right] * (-2.926) \\
 & + \left[\begin{array}{l} 374 \text{ kg CO}_2 \text{ ascending} \\ \text{from bottom segment} \end{array} \right] * (-7.926) \\
 & + \left[\begin{array}{l} 1064 \text{ kg N}_2 \text{ ascending} \\ \text{from bottom segment} \end{array} \right] * 1.008 \\
 & + \left[\begin{array}{l} 9.4 \text{ kg H}_2 \text{ ascending} \\ \text{from bottom segment} \end{array} \right] * 13.35 \\
 & + \left[\begin{array}{l} 51 \text{ kg H}_2\text{O ascending} \\ \text{from bottom segment} \end{array} \right] * (-11.49) \quad (26.1b)
 \end{aligned}$$

from which;

$$\left[\begin{array}{l} \text{top segment} \\ \text{input enthalpy} \end{array} \right] = -11,322 \text{ MJ/1000 kg of} \\
 \text{Fe in product molten iron}$$

as is also calculated in cell AG33 of Table 26.1 by the equation:

$$\begin{aligned}
 & = \text{AC18} * (-5.169) + \text{AC19} * 0 + \text{AC20} * (-2.926) \\
 & + \text{AC21} * (-7.926) + \text{AC22} * 1.008 + \text{AC28} * 13.35 \\
 & + \text{AC29} * (-11.49) \quad (26.2)
 \end{aligned}$$

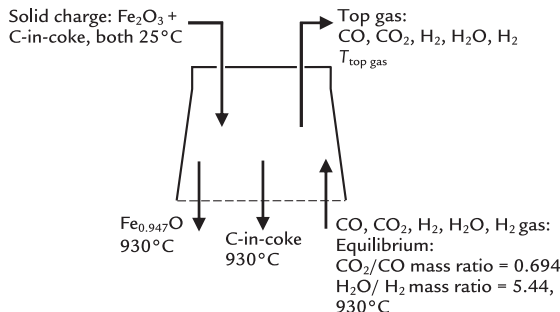


FIGURE 26.1 Conceptual top-segment inputs and outputs with hydrocarbon injection through blast furnace tuyeres. This drawing is the same as top segment of Fig. 25.1.

26.3 TOP-SEGMENT OUTPUT ENTHALPY

Top-segment output enthalpy of Fig. 26.1 is given by the equation:

$$\begin{bmatrix} \text{top segment} \\ \text{output enthalpy} \end{bmatrix} = \begin{bmatrix} \text{top segment} \\ \text{input enthalpy} \end{bmatrix} - \begin{bmatrix} \text{conductive, convective} \\ \text{and radiative heat loss} \\ \text{from the top segment} \end{bmatrix}$$

Section 21.3 showed that the top segment's $\begin{bmatrix} \text{conductive, convective} \\ \text{and radiative heat loss} \\ \text{from the top segment} \end{bmatrix}$ is 80 MJ/1000 kg of Fe in product molten iron. This value gives;

$$\begin{bmatrix} \text{top segment} \\ \text{output enthalpy} \end{bmatrix} = \begin{bmatrix} \text{top segment} \\ \text{input enthalpy} \end{bmatrix} - \begin{bmatrix} 80 \text{ MJ conductive, convective} \\ \text{and radiative heat loss} \\ \text{from the top segment} \end{bmatrix} \quad (21.4)$$

where all the terms are MJ per 1000 kg of Fe in product molten iron, 1500°C .

Eq. (26.2) gives a top-segment *input* enthalpy of $-11,322 \text{ MJ/1000 kg of Fe in product molten iron}$. With this value, the top-segment *output* enthalpy is;

$$\begin{bmatrix} \text{top segment} \\ \text{output enthalpy} \end{bmatrix} = -11,322 - 80 \quad (26.3)$$

$$= -11,402 \frac{\text{MJ}}{1000 \text{ kg of Fe in product molten iron}}$$

as shown in Cell AG34.

In matrix form, Eq. (26.3) is:

$$\begin{bmatrix} \text{top segment} \\ \text{output enthalpy} \end{bmatrix} = \text{AG33} - 80 \quad (26.4)$$

26.4 TOP GAS ENTHALPY

Top gas enthalpy is part of top-segment output enthalpy. The other part is enthalpy in descending $\text{Fe}_{0.947}\text{O}(s)$ and $\text{C}(s)$. This is described by the equation:

$$\begin{bmatrix} \text{top gas enthalpy} \end{bmatrix} = \begin{bmatrix} \text{top segment} \\ \text{output enthalpy} \end{bmatrix} - \begin{bmatrix} \text{mass } \text{Fe}_{0.947}\text{O descending} \\ \text{into bottom segment} \end{bmatrix} * \frac{H_{930^\circ\text{C}}^o}{\text{MW}_{\text{Fe}_{0.947}\text{O}}} - \begin{bmatrix} \text{mass C-in-coke descending} \\ \text{into bottom segment} \end{bmatrix} * \frac{H_{930^\circ\text{C}}^o}{\text{MW}_C} \quad (22.1)$$

The data for calculating top gas enthalpy with 60 kg of $\text{CH}_4(\text{g})$ injection are;

$$\begin{bmatrix} \text{top segment} \\ \text{output enthalpy} \end{bmatrix} = -11,402 \text{ MJ} \quad (\text{from cell AG34, Table 26.1})$$

$$\begin{bmatrix} \text{mass } \text{Fe}_{0.947}\text{O descending} \\ \text{into bottom segment} \end{bmatrix} = 1302 \text{ kg} \quad (\text{from cell AC23, Table 26.1})$$

$$\begin{bmatrix} \text{mass C-in-coke descending} \\ \text{into bottom segment} \end{bmatrix} = 335 \text{ kg} \quad (\text{from cell AC24, Table 26.1})$$

all per 1000 kg of Fe in product molten iron.

The enthalpy content values are (Table J.1);

TABLE 26.1 This is Matrix Table 25.3 Plus Eqs. (26.2), (26.4), and (26.5)

	AA	AB	AC	AD	AE	AF	AG	AH	AI	AJ	AK	AL	AM	AN	AO	AP	AQ	
TOP SEGMENT CALCULATIONS																		
Equation	Description	Numerical term	mass Fe _{0.94} O in furnace charge	mass C in coke charge	mass CO ascending from bottom segment	mass CO ₂ ascending from bottom segment	mass N ₂ ascending from bottom segment	mass Fe _{0.94} O descending into bottom segment	mass C-in-coke descending into bottom segment	mass CO out in top gas	mass CO ₂ out in top gas	mass N ₂ out in top gas	ascending from bottom segment	ascending from bottom segment	mass H ₂ out in top gas	mass H ₂ O out in top gas		
20.6	Mass Fe _{0.94} O descending into bottom segment	1302	0	0	0	0	1	0	0	0	0	0	0	0	0	0	0	
20.2	Fe mass balance	0	-0.699	0	0	0	0	0.768	0	0	0	0	0	0	0	0	0	
25.5	O mass balance	0	-0.301	0	-0.571	-0.727	0	0.232	0	0.571	0.727	0	0	-0.888	0	0.888	0	
20.4	C mass balance	0	0	-1	-0.429	-0.273	0	0	1	0.429	0.273	0	0	0	0	0	0	
20.5	N mass balance	0	0	0	0	0	-1	0	0	0	0	1	0	0	0	0	0	
20.8	Mass CO ascending from bottom segment	539	0	0	1	0	0	0	0	0	0	0	0	0	0	0	0	
20.9	Mass CO ₂ ascending from bottom segment	374	0	0	0	1	0	0	0	0	0	0	0	0	0	0	0	
20.10	Mass N ₂ ascending from bottom segment	1064	0	0	0	0	1	0	0	0	0	0	0	0	0	0	0	
20.7	Mass C-in-coke descending into bottom segment	335	0	0	0	0	0	0	1	0	0	0	0	0	0	0	0	
20.11	Unreacted C-in-coke specification	0	0	-1	0	0	0	0	1	0	0	0	0	0	0	0	0	
25.4	H mass balance	0	0	0	0	0	0	0	0	0	0	0	-1	-0.112	1	0.112	0	
25.1	Mass H ₂ ascending from bottom segment	9.4	0	0	0	0	0	0	0	0	0	0	1	0	0	0	0	
25.2	Mass H ₂ O ascending from bottom segment	51	0	0	0	0	0	0	0	0	0	0	0	1	0	0	0	
25.22	H ₂ /CO reaction ratio equation	0	0	0	0	-0.10	0	0	0	0	0.10	0	0	1	0	0	-1	
Top segment calculated values																		
	kg per 1000 kg of Fe in product iron																	
17	mass Fe _{0.94} O in furnace charge	1431																
18	mass C in coke charge	335																
19	mass CO ascending from bottom segment	539																
20	mass CO ₂ ascending from bottom segment	374																
21	mass N ₂ ascending from bottom segment	1064																
22	mass N ₂ out in top gas	1302																
23	mass Fe _{0.94} O descending into bottom segment	335																
24	mass C-in-coke descending into bottom segment	335																
25	mass CO out in top gas	358																
26	mass CO ₂ out in top gas	659																
27	mass N ₂ out in top gas	1064																
28	mass H ₂ ascending from bottom segment	9.4																
29	mass H ₂ O ascending from bottom segment	51																
30	mass H ₂ O leaving in top gas	6.2																
31	mass H ₂ O leaving in top gas	79																
TOP SEGMENT INPUT AND OUTPUT ENTHALPY CALCULATIONS																		
32	26.2 Top segment input enthalpy = AC18 * -5.169 + AC19 * 0 + AC20 * -2.926 + AC21 * -7.926 + AC22 * 1.008 + AC28 * 13.35 + AC29 * -11.49 =	-11322	MJ per 1000 kg of Fe in product molten iron															
33	26.4 Top segment output enthalpy = AG33 - 80 =	-11402	MJ per 1000 kg of Fe in product molten iron															
34																		
35																		
36																		
37	26.5 Top gas enthalpy = AG34 - AC23 * 3.152 - AC24 * 1.359 =	-7753	MJ per 1000 kg of Fe in product molten iron															
38																		

The values are for tuyere injection of 60 kg of CH₄(g) per 1000 kg of product molten iron (Table 25.1).

$$\text{Cell AG33} = \text{AC18} * (-5.169) + \text{AC19} * 0 + \text{AC20} * (-2.926) + \text{AC21} * (-7.926) + \text{AC22} * 1.008 + \text{AC28} * 13.35 + \text{AC29} * (-11.49) \quad (26.2)$$

$$\text{Cell AG34} = \text{AC33} - 80 \quad (26.4)$$

$$\text{Cell AG37} = \text{AG34} - \text{AC23} * (-3.152) - \text{AC24} * 1.359 \quad (26.5)$$

$$\frac{H^{\circ}_{\text{Fe}_{0.947}\text{O}(\text{s})}}{\text{MW}_{\text{Fe}_{0.947}\text{O}}} = -3.152 \text{ MJ/kg}$$

$$\frac{H^{\circ}_{\text{C}(\text{s})}}{\text{MW}_{\text{C}}} = 1.359 \text{ MJ/kg}$$

so that;

$$\begin{aligned} \text{top gas enthalpy} \\ &= -11,402 - 1302 * (-3.152) - 335 * 1.359 \\ &= \text{AG34} - \text{AC23} * (-3.152) - \text{AC24} * 1.359 \\ &= -7753 \text{ MJ/1000 kg of Fe in product molten iron} \end{aligned} \quad (26.5)$$

as shown in Cell AG37.

Chapter 27, Top Gas Temperature With CH₄ Injection, now uses this top gas enthalpy value to calculate top gas temperature of Fig. 26.1.

26.5 SUMMARY

Top gas enthalpy is required to calculate top gas temperature. It is readily determined from top-segment input enthalpy, top-segment conductive, convective and radiative heat loss, and the enthalpies of descending solids of Fig. 26.1, that is Fe_{0.947}O and C-in-coke.

EXERCISES

26.1 and 26.2 Please determine the Exercise 25.1 and 25.2 blast furnaces' top-segment input and output enthalpies and their top gas enthalpy, MJ per 1000 kg of Fe in product molten iron.

Top Gas Temperature with CH₄(g) Injection

OUTLINE

27.1 Top Gas Temperature	243	27.5 Summary	246
27.2 Calculation of Top Gas Temperature	243	Exercises	248
27.3 Calculation	246	Reference	248
27.4 Results	246		

27.1 TOP GAS TEMPERATURE

Chapter 25, Top Segment Mass Balance with CH₄(g) Injection, and Chapter 26, Top Segment Enthalpy Balance with CH₄(g) Injection, calculated;

1. top gas masses, for example, mass H₂O(g) in top gas, and
2. top gas enthalpy

with H₂(g) and H₂O(g) in top gas, Fig. 27.1.

The calculations are for the specific case of 60 kg of CH₄(g) tuyere injectant. All masses and enthalpies are per 1000 kg of Fe in product molten iron at 1500°C.

This chapter determines top gas temperature from these calculated enthalpy values.

27.2 CALCULATION OF TOP GAS TEMPERATURE

Section 22.3 showed how to calculate top gas temperature without H₂(g) and H₂O(g) in the top gas. This section shows how to calculate it *with* H₂(g) and H₂O(g) in the top gas. It is calculated from;

1. top gas masses of Chapter 25, Top Segment Mass Balance with CH₄(g) Injection,
2. top gas enthalpy of Chapter 26, Top Segment Enthalpy Balance with CH₄(g) Injection, and
3. enthalpy versus top gas temperature equations of Table J.5

using the equation;

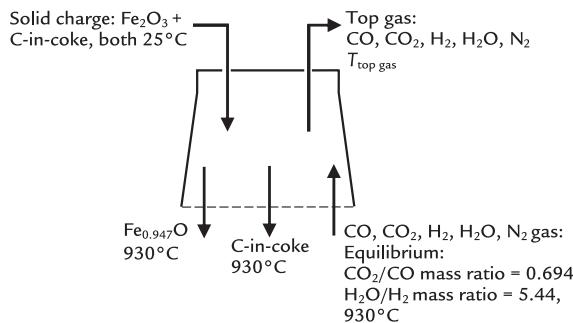


FIGURE 27.1 Top segment of blast furnace with H₂(g) and H₂O(g) in ascending cross-division gas and top gas. The sketch is the same as Fig. 26.1. The H in the gases comes from tuyere-injected CH₄(g).

$$\left[\begin{array}{l} \text{top gas} \\ \text{enthalpy} \end{array} \right] = \left[\begin{array}{l} \text{mass CO out} \\ \text{in top gas} \end{array} \right] * \frac{H_{T_{\text{top gas}}}^{\circ}}{\text{MW}_{\text{CO}}} + \left[\begin{array}{l} \text{mass CO}_2 \text{ out} \\ \text{in top gas} \end{array} \right] * \frac{H_{T_{\text{top gas}}}^{\circ}}{\text{MW}_{\text{CO}_2}} + \left[\begin{array}{l} \text{mass N}_2 \text{ out} \\ \text{in top gas} \end{array} \right] * \frac{H_{T_{\text{top gas}}}^{\circ}}{\text{MW}_{\text{N}_2}} + \left[\begin{array}{l} \text{mass H}_2 \text{ out} \\ \text{in top gas} \end{array} \right] * \frac{H_{T_{\text{top gas}}}^{\circ}}{\text{MW}_{\text{H}_2}} + \left[\begin{array}{l} \text{mass H}_2\text{O out} \\ \text{in top gas} \end{array} \right] * \frac{H_{T_{\text{top gas}}}^{\circ}}{\text{MW}_{\text{H}_2\text{O}}} \quad (27.1)$$

or, from Table J.5, the top gas enthalpy equals;

$$\left[\begin{array}{l} \text{top gas} \\ \text{enthalpy} \end{array} \right] = \left[\begin{array}{l} \text{mass CO out} \\ \text{in top gas} \end{array} \right] * (0.001049 * T_{\text{top gas}} - 3.972) + \left[\begin{array}{l} \text{mass CO}_2 \text{ out} \\ \text{in top gas} \end{array} \right] * (0.0009314 * T_{\text{top gas}} - 8.966) + \left[\begin{array}{l} \text{mass N}_2 \text{ out} \\ \text{in top gas} \end{array} \right] * (0.001044 * T_{\text{top gas}} - 0.02624) + \left[\begin{array}{l} \text{mass H}_2 \text{ out} \\ \text{in top gas} \end{array} \right] * (0.01442 * T_{\text{top gas}} - 0.3616) + \left[\begin{array}{l} \text{mass H}_2\text{O out} \\ \text{in top gas} \end{array} \right] * (0.001902 * T_{\text{top gas}} - 13.47)$$

Collecting terms, this becomes;

$$\left[\begin{array}{l} \text{top gas} \\ \text{enthalpy} \end{array} \right] = \left[\begin{array}{l} \text{mass CO out} \\ \text{in top gas} \end{array} \right] * 0.001049 * T_{\text{top gas}} + \left[\begin{array}{l} \text{mass CO}_2 \text{ out} \\ \text{in top gas} \end{array} \right] * 0.0009314 * T_{\text{top gas}} + \left[\begin{array}{l} \text{mass N}_2 \text{ out} \\ \text{in top gas} \end{array} \right] * 0.001044 * T_{\text{top gas}} + \left[\begin{array}{l} \text{mass H}_2 \text{ out} \\ \text{in top gas} \end{array} \right] * 0.01442 * T_{\text{top gas}} + \left[\begin{array}{l} \text{mass H}_2\text{O out} \\ \text{in top gas} \end{array} \right] * 0.001902 * T_{\text{top gas}} + \left[\begin{array}{l} \text{mass CO out} \\ \text{in top gas} \end{array} \right] * (-3.972) + \left[\begin{array}{l} \text{mass CO}_2 \text{ out} \\ \text{in top gas} \end{array} \right] * (-8.966) + \left[\begin{array}{l} \text{mass N}_2 \text{ out} \\ \text{in top gas} \end{array} \right] * (-0.02624) + \left[\begin{array}{l} \text{mass H}_2 \text{ out} \\ \text{in top gas} \end{array} \right] * (-0.3616) + \left[\begin{array}{l} \text{mass H}_2\text{O out} \\ \text{in top gas} \end{array} \right] * (-13.47)$$

or

$$\begin{aligned} \left[\frac{\text{top gas}}{\text{enthalpy}} \right] &= \left\{ \left[\frac{\text{mass CO out}}{\text{in top gas}} \right] * 0.001049 \right. \\ &\quad + \left[\frac{\text{mass CO}_2 \text{ out}}{\text{in top gas}} \right] * 0.0009314 \\ &\quad + \left[\frac{\text{mass N}_2 \text{ out}}{\text{in top gas}} \right] * 0.001044 \\ &\quad + \left[\frac{\text{mass H}_2 \text{ out}}{\text{in top gas}} \right] * 0.01442 \\ &\quad + \left[\frac{\text{mass H}_2\text{O out}}{\text{in top gas}} \right] * 0.001902 \Big\} * T_{\text{top gas}} \\ &\quad + \left[\frac{\text{mass CO out}}{\text{in top gas}} \right] * (-3.972) \\ &\quad + \left[\frac{\text{mass CO}_2 \text{ out}}{\text{in top gas}} \right] * (-8.966) \\ &\quad + \left[\frac{\text{mass N}_2 \text{ out}}{\text{in top gas}} \right] * (-0.02624) \\ &\quad + \left[\frac{\text{mass H}_2 \text{ out}}{\text{in top gas}} \right] * (-0.3616) \\ &\quad \left. + \left[\frac{\text{mass H}_2\text{O out}}{\text{in top gas}} \right] * (-13.47) \right\} \end{aligned}$$

or

$$\begin{aligned} \text{subtracting } &\left\{ \left[\frac{\text{mass CO out}}{\text{in top gas}} \right] * (-3.972) \right. \\ &+ \left[\frac{\text{mass CO}_2 \text{ out}}{\text{in top gas}} \right] * (-8.966) + \left[\frac{\text{mass N}_2 \text{ out}}{\text{in top gas}} \right] * (-0.02624) \\ &+ \left[\frac{\text{mass H}_2 \text{ out}}{\text{in top gas}} \right] * (-0.3616) \quad \left. + \left[\frac{\text{mass H}_2\text{O out}}{\text{in top gas}} \right] * (-13.47) \right\} \end{aligned}$$

from both sides;

$$\begin{aligned} \left[\frac{\text{top gas}}{\text{enthalpy}} \right] - \left\{ \left[\frac{\text{mass CO out}}{\text{in top gas}} \right] * (-3.972) \right. \\ + \left[\frac{\text{mass CO}_2 \text{ out}}{\text{in top gas}} \right] * (-8.966) \\ + \left[\frac{\text{mass N}_2 \text{ out}}{\text{in top gas}} \right] * (-0.02624) \\ + \left[\frac{\text{mass H}_2 \text{ out}}{\text{in top gas}} \right] * (-0.3616) \\ + \left[\frac{\text{mass H}_2\text{O out}}{\text{in top gas}} \right] * (-13.47) \Big\} \\ = \left\{ \left[\frac{\text{mass CO out}}{\text{in top gas}} \right] * 0.001049 \right. \\ + \left[\frac{\text{mass CO}_2 \text{ out}}{\text{in top gas}} \right] * 0.0009314 \\ + \left[\frac{\text{mass N}_2 \text{ out}}{\text{in top gas}} \right] * 0.001044 \\ + \left[\frac{\text{mass H}_2 \text{ out}}{\text{in top gas}} \right] * 0.01442 \\ \left. + \left[\frac{\text{mass H}_2\text{O out}}{\text{in top gas}} \right] * 0.001902 \right\} * T_{\text{top gas}} \end{aligned}$$

or dividing both sides by $\left\{ \left[\frac{\text{mass CO out}}{\text{in top gas}} \right] * 0.001049 \right. \\ + \left[\frac{\text{mass CO}_2 \text{ out}}{\text{in top gas}} \right] * 0.0009314 + \left[\frac{\text{mass N}_2 \text{ out}}{\text{in top gas}} \right] * 0.001044 \\ + \left[\frac{\text{mass H}_2 \text{ out}}{\text{in top gas}} \right] * 0.01442 + \left[\frac{\text{mass H}_2\text{O out}}{\text{in top gas}} \right] * 0.001902 \Big\}$ - and removing brackets of the numerator and switching sides;

$$\begin{aligned}
 & \left[\begin{array}{l} \text{top gas} \\ \text{enthalpy} \end{array} \right] - \left[\begin{array}{l} \text{mass CO out} \\ \text{in top gas} \end{array} \right] * (-3.972) \\
 & - \left[\begin{array}{l} \text{mass CO}_2 \text{ out} \\ \text{in top gas} \end{array} \right] * (-8.966) \\
 & - \left[\begin{array}{l} \text{mass N}_2 \text{ out} \\ \text{in top gas} \end{array} \right] * (-0.02624) \\
 & - \left[\begin{array}{l} \text{mass H}_2 \text{ out} \\ \text{in top gas} \end{array} \right] * (-0.3616) \\
 T_{\text{top gas}} = & \frac{- \left[\begin{array}{l} \text{mass H}_2\text{O out} \\ \text{in top gas} \end{array} \right] * (-13.47)}{\left\{ \begin{array}{l} \left[\begin{array}{l} \text{mass CO out} \\ \text{in top gas} \end{array} \right] * 0.001049 \end{array} \right\}} \quad (27.2) \\
 & + \left[\begin{array}{l} \text{mass CO}_2 \text{ out} \\ \text{in top gas} \end{array} \right] * 0.0009314 \\
 & + \left[\begin{array}{l} \text{mass N}_2 \text{ out} \\ \text{in top gas} \end{array} \right] * 0.001044 \\
 & + \left[\begin{array}{l} \text{mass H}_2 \text{ out} \\ \text{in top gas} \end{array} \right] * 0.01442 \\
 & + \left[\begin{array}{l} \text{mass H}_2\text{O out} \\ \text{in top gas} \end{array} \right] * 0.001902 \}
 \end{aligned}$$

27.3 CALCULATION

From Table 26.1 (60 kg of tuyere injected CH₄(g)), the masses in Eq. (27.2) are 358 kg CO, 659 kg CO₂, 1064 kg N₂, 6.2 kg H₂, and 79 kg H₂O all per 1000 kg of Fe in product molten iron.

Also from Table 26.1, the top gas enthalpy is -7753 MJ/1000 kg of Fe in product molten iron.

With these values, Eq. (27.2) becomes;

$$\begin{aligned}
 & -7753 - (358 * -3.972) - (659 * -8.966) \\
 & - (1064 * -0.02624) - (6.2 * -0.3616) \\
 & - (79 * -13.47) \\
 T_{\text{top gas}} = & \frac{358 * 0.001049 + 659 * 0.0009314}{358 * 0.001049 + 659 * 0.0009314} \\
 & + 1064 * 0.001044 + 6.2 * 0.01442 \\
 & + 79 * 0.001902 \\
 = & 285^\circ\text{C}
 \end{aligned} \quad (27.3)$$

In terms of cell addresses in Table 27.1, this equation is;

$$\begin{aligned}
 & (\text{AG37} - \text{AC25} * -3.972 - \text{AC26} \\
 & * -8.966 - \text{AC27} * -0.02624 - \text{AC30} \\
 & * -0.3616 - \text{AC31} * -13.47) \\
 T_{\text{top gas}} = & \frac{(\text{AC25} * 0.001049 + \text{AC26} \\
 & * 0.0009314 + \text{AC27} * 0.001044 + \text{AC30} \\
 & * 0.01442 + \text{AC31} * 0.001902)}{(\text{AC25} * 0.001049 + \text{AC26} \\
 & * 0.0009314 + \text{AC27} * 0.001044 + \text{AC30} \\
 & * 0.01442 + \text{AC31} * 0.001902)}
 \end{aligned} \quad (27.4)$$

Cell AK40 contains this equation as described in the caption of Table 27.1.

27.4 RESULTS

The above-calculated top gas temperature (285°C, Cell AK40) and others are plotted in Fig. 27.2. You can see that top gas temperature rises with increasing CH₄(g) injection.

27.5 SUMMARY

Blast furnace top gas temperature with H₂(g) and H₂O(g) in top gas is readily calculated from;

1. top gas masses of Chapter 25, Top Segment Mass Balance with CH₄(g) Injection,
2. top gas enthalpy of Chapter 26, Top Segment Enthalpy Balance with CH₄(g) Injection, and

TABLE 27.1 Matrix and Equation for Calculating Blast Furnace Top Gas Temperature

		AS	AC	AD	AE	AF	AG	AH	AI	AK	AL	AM	AN	AO	AP	AQ
TOP SEGMENT CALCULATIONS																
Equation	Description	Numerical term	mass Fe _{0.04} O ₂ in furnace charge	mass C in coke charge	mass CO ascending from bottom segment	mass CO ₂ ascending from bottom segment	mass N ₂ ascending from bottom segment	mass Fe ₃ Al ₂ O descending into bottom segment	mass C-in-coke descending into bottom segment	mass CO out in top gas	mass CO ₂ out in top gas	mass N ₂ out in top gas	mass H ₂ ascending from bottom segment	mass H ₂ O ascending from bottom segment	mass H ₂ out in top gas	mass H ₂ O out in top gas
20.6	Mass Fe _{0.04} O ₂ descending into bottom segment	1302	0	0	0	0	0	1	0	0	0	0	0	0	0	0
20.2	Fe mass balance	0	-0.699	0	0	0	0	0.768	0	0	0	0	0	0	0	0
20.25	O mass balance	0	-0.301	0	-0.571	-0.727	0	0.232	0	0.571	0.727	0	0	-0.888	0	0.888
20.4	O mass balance	0	0	0	-0.429	-0.773	0	0	0	0.429	0.273	0	0	0	0	0
20.5	N mass balance	0	0	0	0	0	-1	0	0	0	0	1	0	0	0	0
20.8	Mass CO ascending from bottom segment	539	0	0	1	0	0	0	0	0	0	0	0	0	0	0
20.9	Mass CO ₂ ascending from bottom segment	374	0	0	0	1	0	0	0	0	0	0	0	0	0	0
20.10	Mass N ₂ ascending from bottom segment	1064	0	0	0	0	1	0	0	0	0	0	0	0	0	0
20.7	Mass C-in-coke descending into bottom segment	335	0	0	0	0	0	0	1	0	0	0	0	0	0	0
20.11	Unreacted C-in-coke specification	0	0	-1	0	0	0	0	1	0	0	0	0	0	0	0
25.4	H mass balance	0	0	0	0	0	0	0	0	0	0	0	-1	-0.112	1	0.112
25.1	Mass H ₂ ascending from bottom segment	9.4	0	0	0	0	0	0	0	0	0	0	1	0	0	0
25.5	Mass H ₂ O ascending from bottom segment	51	0	0	0	0	0	0	0	0	0	0	1	0	0	0
25.22	H ₂ /CO reaction ratio equation	0	0	0	0	-0.10	0	0	0	0	0.10	0	0	1	0	-1
Top segment calculated values																
	kg per 1000 kg of Fe in product iron															
	mass Fe _{0.04} O ₂ in furnace charge	1431														
	mass C in coke charge	335														
	mass CO ascending from bottom segment	539														
	mass CO ₂ ascending from bottom segment	374														
	mass N ₂ ascending from bottom segment	1064														
	mass Fe _{0.04} O ₂ descending into bottom segment	1302														
	mass C-in-coke descending into bottom segment	335														
	mass CO out in top gas	358														
	mass CO ₂ out in top gas	659														
	mass N ₂ out in top gas	1064														
	mass H ₂ ascending from bottom segment	9.4														
	mass H ₂ O ascending from bottom segment	51														
	mass H ₂ leaving in top gas	6.2														
	mass H ₂ O leaving in top gas	79														
TOP SEGMENT INPUT AND OUTPUT ENTHALPY CALCULATIONS																
26.2	Top segment input enthalpy =AC18*-5.169+AC19*0+AC20*-2.926+AC21*-7.926+AC22*1.008+AC28*13.35+AC29*-11.49 =															
26.4	Top segment output enthalpy=AC33-80 =															
TOP GAS ENTHALPY CALCULATION																
26.5	Top gas enthalpy =AC34*AC23*-3.152*AC24+1.359 =															
TOP GAS TEMPERATURE CALCULATION																
27.4	Top gas temperature =(AG37*AC25*3.972*AC26*-8.966*AC27*-0.02624*AC30*-0.3616*AC31*-13.47)/(AC25*0.001049+AC26*0.0009314+AC27*0.001044+AC30*0.01442+AC31*0.001902) =													285	*C	

Table 27.1 is the same as Table 26.1 plus top gas temperature Row 40.

$$\text{Cell AK40} = \frac{(AG37 - AC25 * -3.972 - AC26 * -8.966 - AC27 * -0.02624 - AC30 * -0.3616 - AC31 * -13.47)}{(AC25 * 0.001049 + AC26 * 0.0009314 + AC27 * 0.001044 + AC30 * 0.01442 + AC31 * 0.001902)}$$

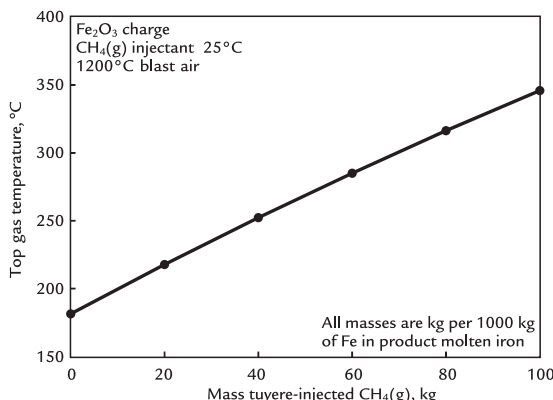


FIGURE 27.2 As tuyere injection of CH₄(g) increases, top gas temperature also increases as confirmed by Geerdes et al.¹ The effect is due to all the equations in our top and bottom-segment matrices. We may postulate that it is mainly due to;

1. the increasing mass of hot N₂ flowing into the top segment with increasing CH₄(g) injection, Fig. 25.3, and
2. the decreasing mass of cool C-in-coke being charged to the top segment with increasing CH₄(g) injection, Fig. 11.2. The line is not straight because the values in cells AG16 and AL16 of Table 27.1 vary with CH₄(g) injection quantity.

3. enthalpy versus top gas temperature equations of Table J.5.

Top gas temperature increases with increasing CH₄(g) injection. This is mainly due to;

1. an increasing upward mass flow of *hot* N₂ into the top segment, and
 2. a decreasing mass flow of *cool* C-in-coke being charged to the furnace
- with increasing CH₄(g) injection.

EXERCISES

All masses are in kg per 1000 kg of Fe in product molten iron.

- 27.1. The Management team of Exercise 25.1 would now like to know what their top gas temperature will be with 120 kg of 25°C CH₄(g) injection. Please calculate it for them - starting with matrix Tables 25.1 and 27.1.
- 27.2. The Research team of Exercise 25.2 would also like to know what *their* top gas temperature will be. Please calculate it for them using any information and method you wish.
- 27.3. The Management team of Exercise 25.1 and the Research team of Exercise 25.2 agree that their top gas temperatures are too high. They agree that the top gas temperature should be below 200°C. Suggest how they can do this by adjusting their 25°C CH₄(g) injection quantity. Use any information and method you wish.
- 27.4. Blast furnace ore charge of Exercise 27.1 has become moist sitting out in the rain. What do you think will happen to their top gas temperature when this moist ore is charged to the furnace?

Reference

1. Geerdes M, Chaignau R, Kurunov I, Lingiardi O, Ricketts J. *Modern blast furnace ironmaking (an introduction)*. 3rd ed BV, Amsterdam: IOS Press; 2015.

28

Top-Segment Calculations With Moisture in Blast Air

OUTLINE

28.1 Incorporating Blast Moisture Into Top-Segment Balances	249	28.5 Summary	253
28.2 Bottom-Segment Results	250	Exercises	254
28.3 Top-Segment Calculations	250	Reference	254
28.4 Top Gas Temperature Results	253		

28.1 INCORPORATING BLAST MOISTURE INTO TOP-SEGMENT BALANCES

Chapters 25–27 determined top gas composition, enthalpy, and temperature with tuyere-injected CH₄(g). This chapter does the same with through-tuyere input H₂O(g).

Our objectives are to;

1. show how to calculate top gas masses, enthalpies, and temperatures with H₂O(g) in blast, and
2. indicate the effect of this H₂O(g) on top gas temperature.

Fig. 28.1 shows steady-state flows across a blast furnace's conceptual division—with through-tuyere input H₂O(g). They are the same as with CH₄(g) injection, that is;

- descending Fe_{0.947}O(s) and C(s)-in-coke, and
- ascending CO(g), CO₂(g), N₂(g), H₂(g), and H₂O(g).

We now calculate the steady-state mass flows of these substances with:

- 15 g of H₂O(g) in blast per Nm³ of dry air in blast.

Matrix Table 28.1 is used. Note that the H₂O(g) always enters the furnace at blast temperature, which is 1200°C throughout this chapter.

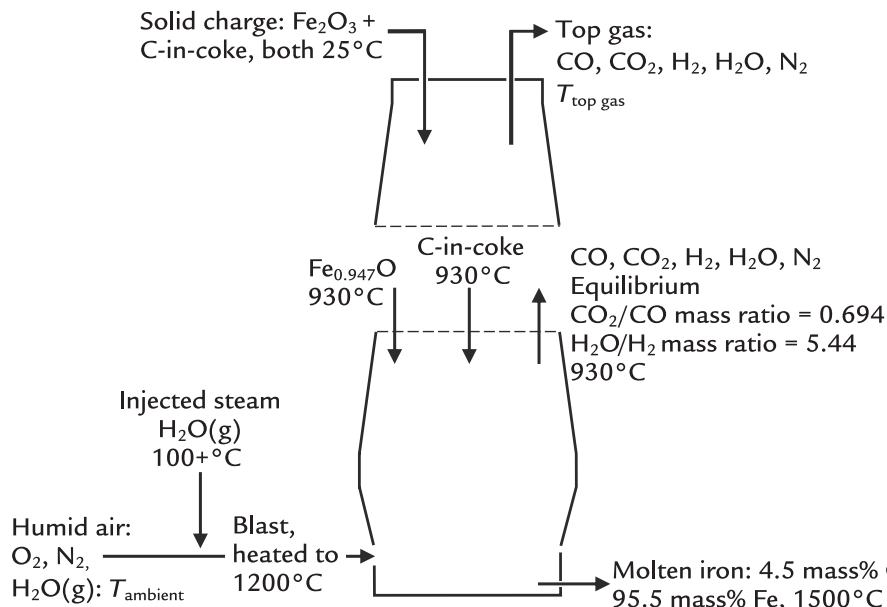


FIGURE 28.1 Conceptually divided blast furnace with $\text{H}_2\text{O}(\text{g})$ in blast. The blast's $\text{H}_2\text{O}(\text{g})$ is from humid air topped up with injected steam. Note the flows of $\text{Fe}_{0.947}\text{O}(\text{s})$, $\text{C}(\text{s})$ -in-coke, $\text{CO}(\text{g})$, $\text{CO}_2(\text{g})$, $\text{N}_2(\text{g})$, $\text{H}_2(\text{g})$, and $\text{H}_2\text{O}(\text{g})$ across the conceptual division.

28.2 BOTTOM-SEGMENT RESULTS

Table 28.1 shows that the steady-state cross-division mass flows with 15 g of $\text{H}_2\text{O}(\text{g})$ per Nm^3 of dry air in blast are;

- mass $\text{Fe}_{0.947}\text{O}$ into bottom segment = mass $\text{Fe}_{0.947}\text{O}$ out of top segment = 1302 kg; Cell C18
- mass C-in-coke into bottom segment = mass C-in-coke out of top segment = 399 kg; Cell C19
- mass CO out of bottom segment = mass CO into top segment = 569 kg; Cell C24
- mass CO_2 out of bottom segment = mass CO_2 into top segment = 395 kg; Cell C25
- mass N_2 out of bottom segment = mass N_2 into top segment = 995 kg; Cell C26
- mass H_2 out of bottom segment = mass H_2 into top segment = 1.1 kg; Cell C27
- mass H_2O out of bottom segment = mass H_2O into top segment = 5.8 kg; Cell C28

all per 1000 kg of Fe in product molten iron.

These are the only values that will keep Fig. 28.1 furnace steadily producing 1500°C molten iron with:

- 15 g of $\text{H}_2\text{O}(\text{g})$ in blast per Nm^3 of dry air in blast.

28.3 TOP-SEGMENT CALCULATIONS

Cross-division flows of Section 28.1 are now inserted into column AC of top-segment matrix Table 28.2.

The insertions can be manual, or more usefully by the instructions:

$$\text{Cell AC3} = \text{C18} \quad (28.1)$$

$$\text{Cell AC8} = \text{C24} \quad (28.2)$$

$$\text{Cell AC9} = \text{C25} \quad (28.3)$$

$$\text{Cell AC10} = \text{C26} \quad (28.4)$$

TABLE 28.1 Matrix for Calculating Bottom-Segment Steady-State Inputs and Outputs of Fig. 28.1 With 15 g of H₂O(g) per Nm³ of Dry Air in Blast

	A	B	C	D	E	F	G	H	I	J	K	L	M	N	O
1	BOTTOM SEGMENT CALCULATIONS														
2	Equation	Description	Numerical term	mass Fe _{0.947} O into bottom segment	mass C in descending coke	mass O ₂ in blast air	mass N ₂ in blast air	mass Fe out in molten iron	mass C out in molten iron	mass CO out in ascending gas	mass CO ₂ out in ascending gas	mass N ₂ out in ascending gas	mass H ₂ out in ascending gas	mass H ₂ O out in ascending gas	mass through-tuyere input H ₂ O(g)
3	7.7	Fe out in molten iron specification	1000	0	0	0	0	1	0	0	0	0	0	0	0
4	7.2	Fe mass balance	0	-0.768	0	0	0	1	0	0	0	0	0	0	0
5	12.5	O mass balance	0	-0.232	0	-1	0	0	0	0.571	0.727	0	0	0.888	0.888
6	7.4	C mass balance	0	0	-1	0	0	0	1	0.429	0.273	0	0	0	0
7	7.5	N mass balance	0	0	0	0	-1	0	0	0	0	1	0	0	0
8	12.3	H mass balance	0	0	0	0	0	0	0	0	0	0	1	0.112	-0.112
9	7.6	N ₂ in blast air specification	0	0	0	3.3	-1	0	0	0	0	0	0	0	0
10	7.9	Equilibrium CO _y /CO mass ratio	0	0	0	0	0	0	0.694	-1	0	0	0	0	0
11	11.8	Equilibrium H ₂ O/H ₂ mass ratio	0	0	0	0	0	0	0	0	0	0	5.44	-1	0
12	7.8	C out in molten iron specification	0	0	0	0	0	0.047	-1	0	0	0	0	0	0
13	12.7	Enthalpy balance	-320	3.152	-1.359	-1.239	-1.339	1.269	5	-2.926	-7.926	1.008	13.35	-11.50	10.81
14	12.2	Mass through-tuyere input H ₂ O(g)	0	0	0	0.0118	0.0118	0	0	0	0	0	0	0	-1
15			930°C	930°C	1200°C	1200°C	1500°C	1500°C	930°C	930°C	930°C	930°C	930°C	930°C	1200°C
16	Calculated values														
17		kg per 1000 kg of Fe out in molten iron													
18	mass Fe _{0.947} O into bottom segment	1302													
19	mass C in descending coke	399	also = mass C in the furnace's coke charge, Eqn. (7.16)												
20	mass O ₂ in blast air	302													
21	mass N ₂ in blast air	995													
22	mass Fe out in molten iron	1000													
23	mass C out in molten iron	47													
24	mass CO out in ascending gas	569													
25	mass CO ₂ out in ascending gas	395													
26	mass N ₂ out in ascending gas	995													
27	mass H ₂ out in ascending gas	1.1													
28	mass H ₂ O out in ascending gas	5.8													
29	mass through-tuyere input H ₂ O(g)	15													
30															

Table 28.1 is a copy of Table 12.1. It calculates the amounts of O₂-in-blast air and C-in-coke charge that will keep Fig. 28.1 blast furnace steadily producing 1500°C molten iron. It also calculates the equivalent steady-state Fe_{0.947}O, C-in-coke, CO, CO₂, N₂, H₂, and H₂O flows across conceptual division of Fig. 28.1. Eqs. (7.9), (11.8), and (12.2) are explained in Chapters 7, 11, and 12.

TABLE 28.2 Top-Segment Matrix With 15 g of H₂O(g) per Nm³ of Dry Air in Blast

	AA	AB	AC	AD	AE	AF	AG	AH	AI	AJ	AK	AL	AM	AN	AO	AP	AQ
TOP SEGMENT CALCULATIONS																	
Equation	Description	Numerical term	mass Fe ₂ O ₃ in furnace charge	mass C in coke charge	mass CO ascending from bottom segment	mass CO ₂ ascending from bottom segment	mass N ₂ ascending from bottom segment	mass Fe _{0.98} O descending into bottom segment	mass C-in-coke descending into bottom segment	mass CO out in top gas	mass N ₂ out in top gas	mass H ₂ ascending from bottom segment	mass H ₂ O ascending from bottom segment	mass H ₂ out in top gas	mass H ₂ O out in top gas		
20.6	Mass Fe ₂ O ₃ descending into bottom segment	1302	0	-0.699	0	0	0	0	0.768	0	0	0	0	0	0	0	
20.2	Fe mass balance	0	-0.699	0	-0.571	-0.727	0	0.232	0	0.571	0.727	0	0	-0.888	0	0.888	
20.4	C mass balance	0	0	-1	-0.429	-0.273	0	0	1	0.429	0.273	0	0	0	0	0	
20.5	N mass balance	0	0	0	0	-1	0	-1	0	0	0	1	0	0	0	0	
20.8	Mass CO ascending from bottom segment	569	0	0	1	0	0	0	0	0	0	0	0	0	0	0	
20.9	Mass CO ₂ ascending from bottom segment	395	0	0	0	0	1	0	0	0	0	0	0	0	0	0	
20.10	Mass N ₂ ascending from bottom segment	995	0	0	0	0	0	1	0	0	0	0	0	0	0	0	
20.7	Mass C-in-coke descending into bottom segment	369	0	0	0	0	0	0	0	1	0	0	0	0	0	0	
20.11	Unreacted C-in-coke specification	0	0	-1	0	0	0	0	0	1	0	0	0	0	0	0	
25.4	H mass balance	0	0	0	0	0	0	0	0	0	0	0	-1	0.112	1	0.112	
25.1	Mass H ₂ ascending from bottom segment	1.1	0	0	0	0	0	0	0	0	0	1	0	0	0	0	
25.5	Mass H ₂ O ascending from bottom segment	5.8	0	0	0	0	0	0	0	0	0	0	1	0	0	0	
25.22	H ₂ /CO reaction ratio equation	0	0	0	0	-0.011	0	0	0	0	0	0.011	0	0	1	0	-1
	Top segment calculated values	kg per 1000 kg of Fe out in molten iron															
	mass Fe ₂ O ₃ in furnace charge	1431															
	mass C in coke charge	399															
	mass CO ascending from bottom segment	369															
	mass CO ₂ ascending from bottom segment	305															
	mass N ₂ ascending from bottom segment	995															
	mass Fe _{0.98} O descending into bottom segment	1302															
	mass C-in-coke descending into bottom segment	399															
	mass CO out in top gas	350															
	mass CO ₂ out in top gas	739															
	mass N ₂ out in top gas	995															
	mass H ₂ ascending from bottom segment	1.1															
	mass H ₂ O ascending from bottom segment	5.8															
	mass H ₂ leaving in top gas	0.7															
	mass H ₂ O leaving in top gas	9.5															
TOP SEGMENT INPUT AND OUTPUT ENTHALPY CALCULATIONS																	
26.2	Top segment input enthalpy = AC18*-5.169+AC19*0+AC20*2.926+AC21*-7.926+AC22*1.008+AC28*13.35+AC29*-11.49 =								-11240	MJ per 1000 kg of Fe in product molten iron							
26.4	Top segment output enthalpy=AG33-80 =								-11320	MJ per 1000 kg of Fe in product molten iron							
TOP-GAS ENTHALPY CALCULATION																	
26.5	Top-gas enthalpy =AG34-AC23*-3.152-AC24*1.359 =								-7758	MJ per 1000 kg of Fe in product molten iron							
TOP-GAS TEMPERATURE CALCULATION																	
27.4	Top-gas temperature =(AG37-AC25*-3.972-AC26*-8.966-AC27*-0.02624-AC30*-0.3616-AC31*-3.347)/(AC25*0.001049+AC26*0.0009314+AC27*0.001044+AC30*0.01442+AC31*0.001902) =								196	°C							

All masses are per 1000 kg of Fe in product molten iron. The column AC matrix values have been forwarded from Table 28.1. The contents of Cells AG16 and AL16 are explained in Section 25.7.

Cell AC11 = C19	(28.5)
Cell AC14 = C27	(28.6)
Cell AC15 = C28	(28.7)

28.4 TOP GAS TEMPERATURE RESULTS

The top segment (column AC) of [Table 28.2](#) calculated masses show that steady-state top gas temperature of [Fig. 28.1](#) with;

- 15 g of $\text{H}_2\text{O(g)}$ in blast per Nm^3 of dry air in blast entering the furnace at 1200°C is 196°C .

This and other top gas temperatures are plotted in [Fig. 28.2](#), which shows that;

- top gas temperature increases by 0.95°C for each additional gram of $\text{H}_2\text{O(g)}$ per Nm^3 of dry air in blast.

This is comparable to the $+0.9^\circ\text{C}$ value suggested by Geerdes et al.¹

[Fig. 28.2](#) shows that top gas temperature increases with increasing concentration of $\text{H}_2\text{O(g)}$

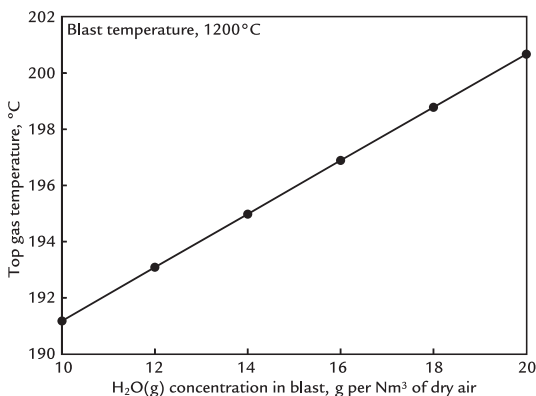


[FIGURE 28.2](#) Blast furnace top gas temperature with $\text{H}_2\text{O(g)}$ entering the furnace in blast ([Fig. 28.1](#)). Top gas temperature increases with increasing $\text{H}_2\text{O(g)}$ concentration in blast.

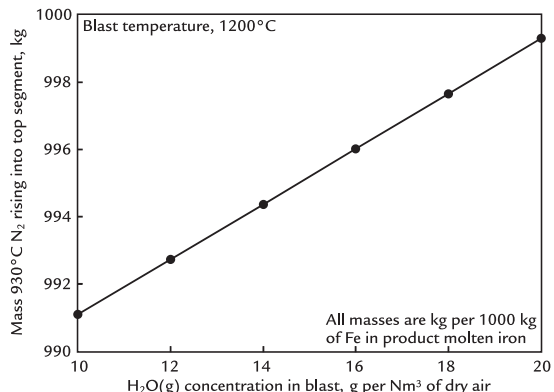


[FIGURE 28.3](#) Effect of $\text{H}_2\text{O(g)}$ concentration in blast on mass hot N_2 rising into top segment of [Fig. 28.1](#). The increase in mass N_2 with increasing $\text{H}_2\text{O(g)}$ -in-blast concentration is notable. We postulate that increasing top gas temperature of [Fig. 28.2](#) is at least partially due to this extra N_2 .

in blast. This is due to all our equations - but we may postulate that it is mainly due to;

- an increasing amount of hot (930°C) N_2 ascending from the bottom segment into the top segment

with an increasing $\text{H}_2\text{O(g)}$ concentration in blast ([Fig. 28.3](#)).

28.5 SUMMARY

The top-segment matrix with through-tuyere $\text{H}_2\text{O(g)}$ input is the same as with $\text{CH}_4\text{(g)}$ injection. Only the bottom-segment-top-segment cross-flow values (Column AC) vary - as calculated by their respective bottom-segment matrices.

Top gas temperature increases with increasing $\text{H}_2\text{O(g)}$ concentration in blast. This is due to all our equations—but we speculate that it is largely due to a greater amount of hot N_2 rising into the top segment with increasing $\text{H}_2\text{O(g)}$.

This increase may be offset by raising blast temperature and/or oxygen injection, Chapter 22, Top Gas Temperature Calculation,

and Chapter 24, Top Segment Calculations with Oxygen Enrichment.

EXERCISES

All masses are in kg per 1000 kg of Fe in product molten iron.

- 28.1.** Fig. 28.1 blast furnace's Engineering team plans to raise the moisture content of its blast to 25 g/Nm³ of dry air. They wish to know what its furnace's top gas temperature will be with this increased moisture content. Please calculate this for them.
- 28.2.** However, the blast furnace's Research department now believes that Exercise 28.1 furnace operators should restrict

their top gas temperature to 200°C or below. Please calculate the blast moisture level that will give 200°C top gas.

- 28.3.** Exercise 28.2 Research team also wants to know how much steam they will have to add to Fig. 28.1 humid air to obtain blast moisture level of Exercise 28.2.

Humid air of Fig. 28.1 contains 10 g of H₂O(g) per Nm³ of dry air.

Please express your answer in g per Nm³ of dry air and kg per kg of dry air.

Reference

1. Geerdes M, Chaigneau R, Kurunov I, Lingardi O, Ricketts J. *Modern blast furnace ironmaking, an introduction*. 2nd ed. Amsterdam: IOS Press BV; 2015. p. 195.

Bottom Segment Calculations With Natural Gas Injection

O U T L I N E

29.1 Replacing Tuyere Injection of CH₄(g) With Natural Gas Injection	255	29.3.4 Amended Oxygen Balance Equation	257
29.2 Comparison of CH₄(g) and Real Natural Gas	256	29.3.5 Amended Nitrogen Balance Equation	257
29.3 Natural Gas Injection Equations	256	29.3.6 Amended Enthalpy Balance Equation	257
29.3.1 Injected Natural Gas Quantity Equation	256	29.4 Results	257
29.3.2 Amended Hydrogen Balance Equation	256	29.5 C-in-Coke Replacement by Natural Gas of Appendix Q	258
29.3.3 Amended Carbon Balance Equation	256	29.6 Summary	258
		Exercises	258

29.1 REPLACING TUYERE INJECTION OF CH₄(g) WITH NATURAL GAS INJECTION

Chapter 11, Bottom Segment with CH₄(g) Injection, described tuyere injection of CH₄(g) with the CH₄(g) standing in for industrial natural gas. This chapter repeats calculations of

Chapter 11, Bottom Segment with CH₄(g) Injection, but using the composition of real natural gas (Fig. 29.1).

The objective of fuel injection is to replace expensive C-in-coke with inexpensive natural gas reductant/fuel.

In this chapter, we determine:

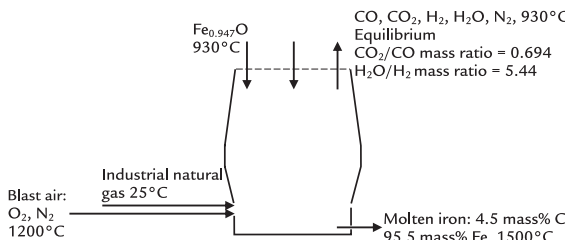


FIGURE 29.1 Conceptual blast furnace bottom segment with tuyere injection of 25°C real (industrial) natural gas. The composition and enthalpy of the natural gas are given in Table 29.1.

- the amount of C-in-coke (kg) that is saved by each kg of injected real natural gas.

29.2 COMPARISON OF CH₄(g) AND REAL NATURAL GAS

Table 29.1 compares the composition and 25°C enthalpy of CH₄(g) and real natural gas. They are quite similar.

29.3 NATURAL GAS INJECTION EQUATIONS

29.3.1 Injected Natural Gas Quantity Equation

As with CH₄(g), a straightforward natural gas quantity equation is;

$$\left[\frac{\text{mass tuyere injected}}{\text{natural gas}} \right] = 60 \text{ kg}/1000 \text{ kg of Fe in product}$$

molten iron

or, in matrix form

$$60 = \left[\frac{\text{mass tuyere injected}}{\text{natural gas}} \right] * 1 \quad (29.1)$$

TABLE 29.1 Composition of and 25°C Enthalpy of CH₄(g) and Real Natural Gas

Element (mass%)	CH ₄ (g)	Real Natural Gas(g)
C	74.9	73.4
H	25.1	24.0
N	0	1.7
O	0	1.0
25°C Enthalpy (MJ per kg)	- 4.66	- 4.52

Composition from Appendix Q. Enthalpy from Appendix R.

29.3.2 Amended Hydrogen Balance Equation

With 24.0 mass% H in our natural gas, hydrogen balance equation (11.3) of Chapter 11, Bottom Segment with CH₄ Injection, becomes;

$$0 = - \left[\frac{\text{mass tuyere injected}}{\text{natural gas}} \right] * 0.240 + \left[\frac{\text{mass H}_2\text{ out}}{\text{in ascending gas}} \right] * 1 + \left[\frac{\text{mass H}_2\text{O out}}{\text{in ascending gas}} \right] * 0.112 \quad (29.2)$$

where the first right-hand term is new and where 0.240 is 24.0 mass % H in natural gas/100%.

29.3.3 Amended Carbon Balance Equation

With 73.4 mass% C in our natural gas, carbon balance equation (11.4) of Chapter 11, Bottom Segment with CH₄ Injection, becomes;

$$0 = - \left[\frac{\text{mass tuyere injected}}{\text{natural gas}} \right] * 0.734 - \left[\frac{\text{mass C in}}{\text{descending coke}} \right] * 1 + \left[\frac{\text{mass CO out}}{\text{in ascending gas}} \right] * 0.429 + \left[\frac{\text{mass CO}_2 \text{ out}}{\text{in ascending gas}} \right] * 0.273 + \left[\frac{\text{mass C out}}{\text{in molten iron}} \right] * 1 \quad (29.3)$$

where the first right-hand term is new and $0.734 = 73.4$ mass % C in natural gas/100%.

29.3.4 Amended Oxygen Balance Equation

With 1.0 mass% O in our natural gas, oxygen balance equation (11.5) of Chapter 11, Bottom Segment with CH₄(g) Injection, becomes;

$$0 = - \left[\begin{array}{l} \text{mass tuyere injected} \\ \text{natural gas} \end{array} \right] * 0.01 - \left[\begin{array}{l} \text{mass Fe}_{0.947}\text{O into} \\ \text{bottom segment} \end{array} \right] * 0.232 - \left[\begin{array}{l} \text{mass O}_2 \\ \text{in blast air} \end{array} \right] * 1 + \left[\begin{array}{l} \text{mass CO out} \\ \text{in ascending gas} \end{array} \right] * 0.571 + \left[\begin{array}{l} \text{mass CO}_2 \text{ out} \\ \text{in ascending gas} \end{array} \right] * 0.727 + \left[\begin{array}{l} \text{mass H}_2\text{O out} \\ \text{in ascending gas} \end{array} \right] * 0.888 \quad (29.4)$$

where the first term is new and $0.01 = 1.0$ mass % O in natural gas/100%.

29.3.5 Amended Nitrogen Balance Equation

With 1.7 mass% N in our natural gas, nitrogen balance equation (7.5) of Chapter 7, Conceptual Division of the Blast Furnace - Bottom Segment Calculations, becomes;

$$0 = - \left[\begin{array}{l} \text{mass tuyere injected} \\ \text{natural gas} \end{array} \right] * 0.017 - \left[\begin{array}{l} \text{mass N}_2 \text{ in} \\ \text{blast air} \end{array} \right] * 1 + \left[\begin{array}{l} \text{mass N}_2 \text{ out} \\ \text{in ascending gas} \end{array} \right] * 1 \quad (29.5)$$

where the first right-hand term is new and $0.017 = 1.7$ mass % N in natural gas/100%.

29.3.6 Amended Enthalpy Balance Equation

Natural gas injection changes only one term in the enthalpy balance equation (11.7) of

Chapter 11, Bottom Segment with CH₄(g) Injection. The term;

$$-\text{mass tuyere-injected CH}_4(\text{g}) * (-4.667)$$

becomes;

$$-\text{mass tuyere-injected natural gas} * (-4.52)$$

and the steady-state enthalpy balance equation becomes;

$$\begin{aligned} -320 = & -[\text{mass tuyere-injected natural gas}] * (-4.52) \\ & -[\text{mass Fe}_{0.947}\text{O into bottom segment}] * (-3.152) \\ & -[\text{mass C in descending coke}] * 1.359 \\ & -[\text{mass O}_2 \text{ in blast}] * 1.239 \\ & -[\text{mass N}_2 \text{ in blast}] * 1.339 \\ & +[\text{mass Fe out in molten iron}] * 1.269 \\ & +[\text{mass C out in molten iron}] * 5 \\ & +[\text{mass CO gas out in ascending gas}] * (-2.926) \\ & +[\text{mass CO}_2 \text{ gas out in ascending gas}] * (-7.926) \\ & +[\text{mass N}_2 \text{ out in ascending gas}] * 1.008 \\ & +[\text{mass H}_2 \text{ gas out in ascending gas}] * 13.35 \\ & +[\text{mass H}_2\text{O gas out in ascending gas}] * (-11.49) \end{aligned} \quad (29.6)$$

The six amended equations are now introduced into matrix [Table 29.1](#) and the;

- C-in-coke, and
- O₂-in-blast

requirements for steady production of 1500°C molten iron are calculated.

29.4 RESULTS

Bottom segment calculated values of [Table 29.1](#) show that steady-state production of 1500°C molten iron with 60 kg of natural gas injection requires;

- 337 kg of C-in-coke, and
- 322 kg of O₂-in-blast air as compared to:
- 335 kg of C-in-coke, and
- 323 kg of O₂-in-blast air

with 60 kg of CH₄(g), Chapter 11.

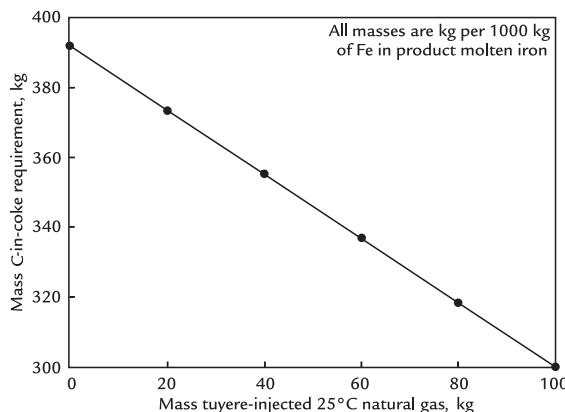


FIGURE 29.2 C-in-coke requirement for steady production of 1500°C molten iron as affected by injection of 25°C natural gas. As expected, the coke requirement decreases with increasing natural gas injection. The line is straight.

29.5 C-IN-COKE REPLACEMENT BY NATURAL GAS OF APPENDIX Q

Fig. 29.2 shows the effect of natural gas injection on steady-state C-in-coke requirement. Each kg of injected natural gas saves 0.92 kg of C-in-coke.

This is slightly less than the 0.95 kg of C-in-coke saved by injected CH₄(g) of Chapter 11, Bottom Segment with CH₄(g) Injection (Fig. 11.2). This difference is due to all the equations in matrix Tables 11.1 and 29.1 but we may postulate that is mainly due to;

1. the natural gas's smaller concentrations of C and H, Table 29.1, kg per kg of injectant, and
2. the natural gas's oxygen which is mainly in the form of CO₂(g) (Appendix Q), which is not a reductant/fuel.

29.6 SUMMARY

Industrial natural gas injection is readily represented in our matrix calculations. We do this for the remainder of the book.

This representation does require calculation of the gas's elemental composition and enthalpy as described in Appendices Q and R. These calculations can be automated in Excel if, for example, the steel company's gas supply varies in composition or if the company has some choice between natural gases of different composition.

Representation of industrial pulverized coal injectant is little more difficult. This is because it contains alumina-silicate ash. This task is tackled in Chapter 37, Bottom Segment Calculations With Pulverized Coal Injection.

EXERCISES

These exercises all refer to natural gas of Table 29.1, which contains 0.734 kg C, 0.24 kg H, 0.017 kg N, and 0.01 kg O, and an enthalpy content of -4.52 MJ (all per kg of gas).

All the masses in this set of exercises are in kg per 1000 kg in product molten iron.

- 29.1. Table 29.2 blast furnace team wishes to increase their natural gas injection quantity to 140 kg/1000 kg of Fe in product molten iron. They would like to know how much;
1. C-in-coke,
 2. O₂-in-blast,
 3. N₂-in-blast, and
 4. air

will be required for steady production of 1500°C molten iron while injecting this 140 kg of natural gas. Please calculate these for the team.

- 29.2. Tuyere-injected natural gas can sometimes be cheaper than C-in-top-charged coke and C-in-pulverized coal. For this reason, Exercise 29.1 team wishes to maximize natural gas injection quantity.

TABLE 29.2 Bottom-Segment Matrix With 60 kg of Injected 25°C Natural Gas

	A	B	C	D	E	F	G	H	I	J	K	L	M	N	O
	BOTTOM SEGMENT CALCULATIONS														
Equation	Description														
3	7.7	Fe out in molten iron specification	1000	0	0	0	0	1	0	0	0	0	0	0	0
4	7.2	Fe mass balance	0	-0.768	0	0	0	1	0	0	0	0	0	0	0
5	29.4	O mass balance	0	-0.232	0	-1	0	0	0	0.571	0.727	0	0	0.888	-0.010
6	29.3	C mass balance	0	0	-1	0	0	0	1	0.429	0.273	0	0	0	-0.734
7	29.1	N mass balance	0	0	0	0	-1	0	0	0	0	1	0	0	-0.017
8	7.6	N ₂ in blast air specification	0	0	0	3.3	-1	0	0	0	0	0	0	0	0
9	7.9	Equilibrium CO ₂ /CO mass ratio	0	0	0	0	0	0	0	0.694	-1	0	0	0	0
10	7.8	C out in molten iron specification	0	0	0	0	0	0.047	-1	0	0	0	0	0	0
11	29.6	Enthalpy balance	-320	3.152	-1.359	-1.239	-1.339	1.269	5	-2.926	-7.928	1.008	13.35	-11.49	4.52
12	29.2	H mass balance	0	0	0	0	0	0	0	0	0	1	0.112	0.240	
13	11.8	Equilibrium H ₂ O/H ₂ mass ratio	0	0	0	0	0	0	0	0	0	0	5.44	-1	0
14	29.1	Natural gas injected through tuyeres	60	0	0	0	0	0	0	0	0	0	0	0	1
15	Blast temperature														
16	1200 °C														
17	Bottom segment calculated values														
18	kg per 1000 kg of Fe out in molten iron														
19	mass Fe _{0.947} O into bottom segment														
20	1302														
21	mass C in descending coke														
22	337 also = mass C in the furnace's coke charge, Eqn. (7.16).														
23	mass O ₂ in blast air														
24	322														
25	mass N ₂ in blast air														
26	1061														
27	mass Fe out in molten iron														
28	1000														
29	mass C out in molten iron														
30	47														
31	mass CO out in ascending gas														
32	540														
33	mass CO ₂ out in ascending gas														
34	375														
35	mass N ₂ out in ascending gas														
36	1062														
37	mass H ₂ out in ascending gas														
38	8.9														
39	mass H ₂ O out in ascending gas														
40	49														
41	mass tuyere-injected natural gas														
42	60														

All masses are per 1000 kg of Fe in product molten iron.

The team knows, however, that proper gas flow in the blast furnace requires at least 250 kg of C-in-top-charged coke (per 1000 kg of Fe in product molten iron).

Please calculate the maximum amount of natural gas that they can inject into the furnace without lowering the furnace's steady-state C-in-coke input below this 250 kg minimum.

Use two calculation methods.

30

Raceway Flame Temperature With Natural Gas Injection

OUTLINE

30.1 The Impact of Natural Gas Injection on Raceway Flame Temperature	261	30.4 Results	264
30.2 Adapting the CH ₄ (g) Raceway Matrix to Natural Gas	261	30.5 Summary	264
30.3 Adapting the Raceway Enthalpy and Flame Temperature Calculations to Natural Gas	262	Exercises	264

30.1 THE IMPACT OF NATURAL GAS INJECTION ON RACEWAY FLAME TEMPERATURE

Chapter 18, Raceway Flame Temperature with CH₄(g) Injection, calculated the raceway flame temperature with CH₄(g) injection. This chapter expands calculations of Chapter 18, Raceway Flame Temperature with CH₄(g) Injection, to real natural gas injection, Fig. 30.1.

The objective is to bring our flame temperature calculations closer to industrial reality.

We start our natural gas calculations with bottom segment matrix (Table 29.2).

We then adapt CH₄(g) injection raceway matrix of Table 18.2 to natural gas injection, Table 30.1.

30.2 ADAPTING THE CH₄(g) RACEWAY MATRIX TO NATURAL GAS

The only differences between Tables 18.2 and 30.1 raceway matrices are in Column J,

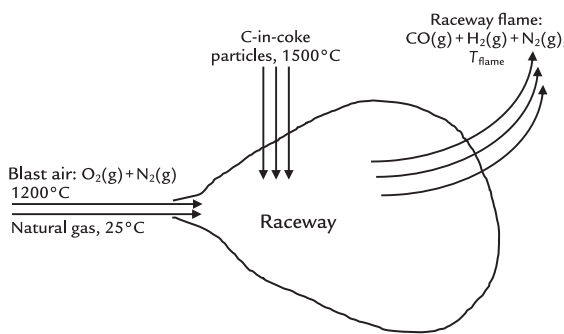


FIGURE 30.1 Blast furnace raceway with 25°C natural gas injection. All the blast and natural gas enter the raceway. The raceway is a horizontal pear-shaped space containing hot gas and hurtling coke particles, Fig. 2.3. This chapter uses carbon as a stand-in for the descending coke particles. Real coke is introduced in Chapter 34, Bottom Segment Calculations - Coke Ash.

which now represents our natural gas elemental composition, Table 29.1. It is 73.4 mass% C, 24.0 mass% H, 1.7 mass% N, and 1.0 mass% O.

Representing natural gas involves amending Chapter 18's raceway C, H, N, and O mass balance's equations as follows:

Raceway carbon balance Eq. (18.4) becomes;

$$0 = - \left[\frac{\text{mass natural gas}}{\text{injected into raceway}} \right] * 0.734 - \left[\frac{\text{mass C in falling coke particles}}{\text{in raceway}} \right] * 1 + \left[\frac{\text{mass CO in raceway output gas}}{\text{in raceway}} \right] * 0.429 \quad (30.1)$$

where $0.734 = 73.4 \text{ mass\% C in natural gas/100\%}$.

Raceway hydrogen balance Eq. (18.5) becomes;

$$0 = - \left[\frac{\text{mass natural gas}}{\text{injected into raceway}} \right] * 0.240 + \left[\frac{\text{mass H}_2 \text{ in raceway output gas}}{\text{in raceway}} \right] * 1 \quad (30.2)$$

where $0.240 = 24.0 \text{ mass\% H in natural gas/100\%}$.

Raceway nitrogen balance Eq. (14.9) becomes;

$$0 = - \left[\frac{\text{mass natural gas injected into raceway}}{\text{injected into raceway}} \right] * 0.017 - \left[\frac{\text{mass N}_2 \text{ entering raceway in blast air}}{\text{in blast air}} \right] * 1 + \left[\frac{\text{mass N}_2 \text{ in raceway output gas}}{\text{in raceway}} \right] * 1 \quad (30.3)$$

where $0.017 = 1.7 \text{ mass\% N in natural gas/100\%}$.

Raceway oxygen balance Eq. (14.8) becomes;

$$0 = - \left[\frac{\text{mass natural gas injected into raceway}}{\text{injected into raceway}} \right] * 0.010 - \left[\frac{\text{mass O}_2 \text{ entering raceway in blast air}}{\text{in blast air}} \right] * 1 + \left[\frac{\text{mass CO in raceway output gas}}{\text{in raceway}} \right] * 0.571 \quad (30.4)$$

where $0.010 = 1.0 \text{ mass\% O in natural gas/100\%}$.

Lastly, as a formality, $\text{CH}_4(\text{g})$ injection quantity Eq. (18.1) becomes:

$$60 = \left[\frac{\text{mass natural gas injected into raceway}}{\text{injected into raceway}} \right] * 1 \quad (30.5)$$

30.3 ADAPTING THE RACEWAY ENTHALPY AND FLAME TEMPERATURE CALCULATIONS TO NATURAL GAS

$\text{CH}_4(\text{g})$ injection input enthalpy equation of Chapter 18, was;

$$\begin{aligned} \left[\frac{\text{raceway input enthalpy}}{\text{into raceway}} \right] &= \left[\frac{\text{mass CH}_4(\text{g})}{\text{injected into raceway}} \right] * -4.667 \\ &+ \left[\frac{\text{mass O}_2 \text{ entering raceway in blast air}}{\text{in blast air}} \right] * 1.239 \\ &+ \left[\frac{\text{mass N}_2 \text{ entering raceway in blast air}}{\text{in blast air}} \right] * 1.339 \\ &+ \left[\frac{\text{mass C in falling coke particles}}{\text{in raceway}} \right] * 2.488 \end{aligned} \quad (18.6)$$

TABLE 30.1 Matrices and Equations for Calculating Raceway Flame Temperature With 60 kg of 25°C Natural Gas Injectant

A	B	C	D	E	F	G	H	I	J	K	L	M	N	O
Equation	Description	Numerical term	mass Fe _{0.94} O into bottom segment	mass C in descending coke	mass O ₂ in blast air	mass N ₂ in blast air	mass Fe out in molten iron	mass C out in molten iron	mass CO out in ascending gas	mass CO ₂ out in ascending gas	mass N ₂ out in ascending gas	mass H ₂ out in ascending gas	mass H ₂ O out in ascending gas	mass tuyere-injected natural gas
1	7.7 Fe out in molten iron specification	1000	0	0	0	0	1	0	0	0	0	0	0	0
4	7.2 Fe mass balance	0	-0.768	0	0	0	1	0	0	0	0	0	0	0
5	29.4 O mass balance	0	-0.232	0	-1	0	0	0	0.571	0.727	0	0	0.888	-0.010
6	29.3 C mass balance	0	0	-1	0	0	0	1	0.429	0.273	0	0	0	-0.734
7	29.5 N mass balance	0	0	0	0	-1	0	0	0	0	1	0	0	-0.017
8	7.6 N ₂ in air specification	0	0	0	0	3.3	-1	0	0	0	0	0	0	0
9	7.9 Equilibrium CO ₂ /CO mass ratio	0	0	0	0	0	0	0	0.694	-1	0	0	0	0
10	7.8 C in output molten iron specification	0	0	0	0	0	0	0.047	-1	0	0	0	0	0
11	29.6 Enthalpy balance	-320	3.152	-1.359	-1.239	-1.339	1.269	5	-2.926	-7.926	1.008	13.35	-11.49	4.52
12	29.2 H mass balance	0	0	0	0	0	0	0	0	0	0	1	0.112	0.240
13	11.8 Equilibrium H ₂ O/H ₂ mass ratio	0	0	0	0	0	0	0	0	0	0	5.44	-1	0
14	Natural gas injected through tuyeres	60	0	0	0	0	0	0	0	0	0	0	0	1
15			930°C	930°C	1200	1200	1500°C	1500°C	930°C	930°C	930°C	930°C	930°C	25°C
16			Blast temperature = 1200 °C											
17	Bottom segment calculated values	kg per 1000 kg of Fe in product iron	(=0.001137*E16-0.1257)											
18	mass Fe _{0.94} O into bottom segment	1302	(=0.001237*E16-0.145)											
19	mass C in descending coke	337	also = mass C in the furnace's coke charge, Eqn. (7.16)											
20	mass O ₂ in blast air	322												
21	mass N ₂ in blast air	1061												
22	mass Fe out in molten iron	1000												
23	mass C out in molten iron	47												
24	mass CO out in ascending gas	540												
25	mass CO ₂ out in ascending gas	375												
26	mass N ₂ out in ascending gas	1062												
27	mass H ₂ out in ascending gas	8.9												
28	mass H ₂ O out in ascending gas	49	=C20											
29	mass tuyere-injected natural gas	60	=C21											
30	RACEWAY INPUTS AND OUTPUTS CALCULATION													
32	Equation	Description	Numerical Term	mass O ₂ entering raceway in blast air	mass N ₂ entering raceway in blast air	mass C entering raceway in falling coke particles	mass CO in raceway exit gas	mass N ₂ in raceway exit gas	mass H ₂ in raceway exit gas	mass tuyere-injected natural gas				
33	18.2	Mass O ₂ entering raceway in blast air	322	1	0	0	0	0	0	0	0			
34	18.3	Mass N ₂ entering raceway in blast air	1061	0	1	0	0	0	0	0	0			
35	30.1	Raceway carbon balance	0	0	0	0	-1	0.429	0	0	-0.734			
36	30.4	Raceway oxygen balance	0	0	-1	0	0	0.571	0	0	-0.010			
37	30.2	Raceway hydrogen balance	0	0	0	0	0	0	1	0	-0.240			
38	30.3	Raceway nitrogen balance	0	0	-1	0	0	0	1	0	-0.017			
39	30.5	Mass tuyere-injected natural gas	60	0	0	0	0	0	0	0	1			
40				1200	1200	1500°C	T _{race}	T _{flame}	T _{flame}	25°C				
41	Raceway calculated values													
42							=C14							
43		mass O ₂ entering raceway in blast	322											
44		mass N ₂ entering raceway in blast	1061											
45		mass C into raceway in falling coke particles	198											
46		mass CO in raceway output gas	564											
47		mass N ₂ in raceway output gas	1062											
48		mass H ₂ in raceway output gas	14											
49		mass tuyere-injected natural gas	60											
50	RACEWAY ENTHALPY AND FLAME TEMPERATURE CALCULATIONS													
52	30.6	Total raceway input enthalpy = C49*4.52+C43*F11+C44*G11+C45*2.488 =					2041	MJ per 1000 kg of Fe in product molten iron						
53	18.8	Total raceway output enthalpy = raceway input enthalpy = F52					2041	MJ per 1000 kg of Fe in product molten iron						
54														
55	18.10b	Flame temperature=(F53-C46*4.183-C47*-0.2448-C48*-4.13)/(C46*0.00131+C47*0.001301+C48*0.01756)					1989	°C						
56														

The differences between this table and Table 18.2 are discussed in the following text. The equations in Cells F11 and G11 are explained in Section 15.1. The presence of – F11 and – G11 in Row 52 is explained in Section 15.3.1.

The only change needed to adapt this equation to natural gas injection is the first right side term which becomes;

$$\left[\begin{array}{l} \text{mass natural gas} \\ \text{injected into raceway} \end{array} \right] * (-4.52)$$

where -4.52 is the enthalpy of our 25°C natural gas, Table 29.1.

This is represented in the Table 30.1 matrix by the Cell F52 equation;

$$= \text{C49} * (-4.52) + \text{C43} * -\text{F11} + \text{C44} * -\text{G11} + \text{C45} * 2.488 \quad (30.6)$$

where the only change from Eq. (18.7) is that -4.664 is replaced by -4.52 , the enthalpy of our 25°C natural gas. The presence of $-\text{F11}$ and $-\text{G11}$ in the equation is explained in Section 15.3.

Cells F53 and G55 are unchanged by switching to natural gas.

30.4 RESULTS

Fig. 30.2 shows raceway temperatures for $\text{CH}_4(\text{g})$ and natural gas injection. Both decrease

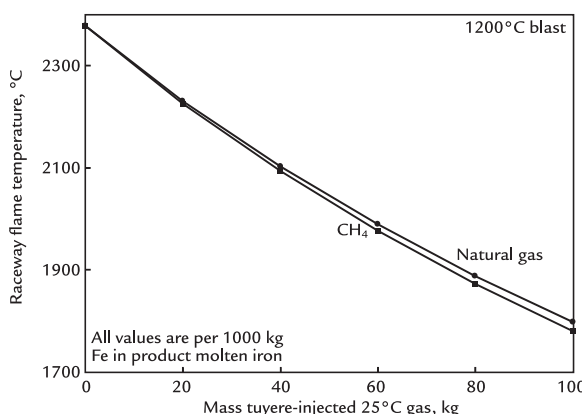


FIGURE 30.2 Effect of tuyere-injected $\text{CH}_4(\text{g})$ and natural gas on raceway flame temperature. Natural gas cools the flame slightly less than $\text{CH}_4(\text{g})$. Both lines are curved, because $d(H^\circ/\text{MW})_{\text{inputs}}/dT \neq d(H^\circ/\text{MW})_{\text{outputs}}/dT$ where T is the temperature.

flame temperature. Natural gas lowers flame temperature slightly less than $\text{CH}_4(\text{g})$. This is the result of all our equations. We may speculate that natural gas's smaller cooling effect is due at least partially to its enthalpy (-4.52 MJ), which is less negative than natural gas's enthalpy (-4.664 MJ) both per kg of substance.

30.5 SUMMARY

Our $\text{CH}_4(\text{g})$ injection raceway calculations are easily adapted to real natural gas injection calculations. $\text{CH}_4(\text{g})$ composition must be replaced with natural gas composition. Likewise, $\text{CH}_4(\text{g})$ enthalpy has to be replaced with natural gas enthalpy.

Raceway output enthalpy and flame temperature equations don't change.

$\text{CH}_4(\text{g})$ and natural gas both lower raceway flame temperature—natural gas slightly less than $\text{CH}_4(\text{g})$.

EXERCISES

- 30.1. The blast furnace team of Exercise 29.1 wishes to know what its tuyere raceway flame temperature will be while injecting 45 kg of Table 29.2 natural gas per 1000 kg of Fe in product molten iron. Please calculate this for them.
- 30.2. The blast furnace team of Exercise 30.1 now believes that it needs a flame temperature of at least 2200°C .

They want to know the maximum amount of Table 29.2 natural gas that can be injected while meeting this requirement. Please calculate this for them using any method of your choice.

- 30.3.** What can you simultaneously inject into a blast furnace's tuyeres that will allow you to increase natural gas injection without decreasing flame temperature?
- 30.4.** What do you see in Table 29.2 industrial natural gas that causes it to produce a slightly higher flame temperature than $\text{CH}_4(\text{g})$ alone, [Fig. 30.2](#)?

31

Top-Segment Calculations With Natural Gas Injection

O U T L I N E

31.1 Top Gas Temperature With Natural Gas	267	31.5 Results	268
31.2 Starting Our Top Gas Temperature Calculations	267	31.6 Discussion	268
31.3 Top-Segment Matrix	268	31.7 Summary	271
31.4 Top-Segment Enthalpy and Top Gas Equations	268	Exercises	271

31.1 TOP GAS TEMPERATURE WITH NATURAL GAS

Chapter 25, Top Segment Mass Balance with CH₄(g) Injection, calculated top gas temperature with tuyere-injected CH₄(g). This chapter repeats this calculation with tuyere-injected natural gas.

The objective is to bring our calculations closer to industrial reality, Fig. 31.1.

31.2 STARTING OUR TOP GAS TEMPERATURE CALCULATIONS

Our natural gas top gas temperature calculations start with natural gas bottom-segment matrix of Chapter 29, Bottom Segment Calculations With Natural Gas Injection (Table 31.1).

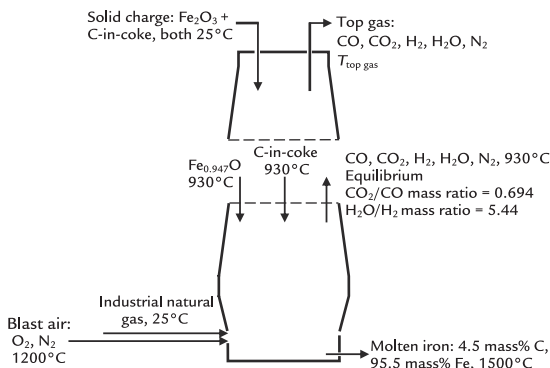


FIGURE 31.1 Sketch of the conceptually divided blast furnace with natural gas injection. It is a vertical slice through the center of the Fig. 1.1 blast furnace. The inputs, outputs, and cross-division flows are shown. They are the same as with CH₄(g) injection except that 25°C natural gas injection has replaced 25°C CH₄(g) injection.

31.3 TOP-SEGMENT MATRIX

We now prepare our top-segment matrix with 60 kg of natural gas injectant. It is the same as with 60 kg of CH₄(g) injection except for the values in Column AC.

Please note that;

$$\text{Cell AC3} = \text{C18} \quad (31.1)$$

$$\text{Cell AC8} = \text{C24} \quad (31.2)$$

$$\text{Cell AC9} = \text{C25} \quad (31.3)$$

$$\text{Cell AC10} = \text{C26} \quad (31.4)$$

$$\text{Cell AC11} = \text{C19} \quad (31.5)$$

$$\text{Cell AC14} = \text{C27} \quad (31.6)$$

$$\text{Cell AC15} = \text{C28} \quad (31.7)$$

which are the same as with CH₄(g) injection top-segment matrix of Chapter 25, Top Segment Mass Balance with CH₄(g) Injection, Table 25.2.

31.4 TOP-SEGMENT ENTHALPY AND TOP GAS EQUATIONS

The equations in Cells AG33, AG34, AG37, and AK 40 of [Table 31.2](#) are the same as the equations in CH₄(g) injection top-segment matrix Table 27.1. This is because the substances entering and leaving the top segment are the same in both, Figs. 27.1 and [31.1](#). They give [Fig. 31.2](#) results.

31.5 RESULTS

[Fig. 31.2](#) shows that CH₄(g) and natural gas injection both increase top gas temperature. We postulate that this mainly due to;

1. the increasing mass of hot N₂ ascending into the top segment heating the surrounding substances as it rises, and
2. the decreasing mass of cool top charged C-in-coke that must be heated

with increasing hydrocarbon injection.

Natural gas has a slightly smaller effect than CH₄(g) because its increase in hot N₂ flow and decrease in C-in-coke charge are slightly smaller with natural gas than with CH₄(g), [Tables 20.2, 27.1, and 31.2](#).

31.6 DISCUSSION

Our natural gas top gas calculations do not require any change to our top-segment input enthalpy, top-segment output enthalpy, top gas enthalpy, and top gas temperature Eqs. (26.2), (26.4), (26.5), and (27.4).

TABLE 31.1 Bottom-Segment Matrix With 60 kg of Natural Gas Injectant

	<i>a</i>	<i>b</i>	<i>c</i>	<i>d</i>	<i>e</i>	<i>f</i>	<i>g</i>	<i>h</i>	<i>i</i>	<i>j</i>	<i>k</i>	<i>l</i>	<i>m</i>	<i>n</i>	<i>o</i>
1 BOTTOM SEGMENT CALCULATIONS															
Equation	Description	Numerical term	mass Fe _{0.94} O into bottom segment	mass C in descending coke	mass O ₂ in blast air	mass N ₂ in blast air	mass Fe out in molten iron	mass C out in molten iron	mass CO out in ascending gas	mass CO ₂ out in ascending gas	mass N ₂ out in ascending gas	mass H ₂ out in ascending gas	mass H ₂ O out in ascending gas	mass tuyere-injected natural gas	
2															
3	7.7 Fe out in molten iron specification	1000	0	0	0	0	1	0	0	0	0	0	0	0	0
4	7.2 Fe mass balance	0	-0.768	0	0	0	1	0	0	0	0	0	0	0	0
5	29.4 O mass balance	0	-0.232	0	-1	0	0	0	0.571	0.727	0	0	0.888	-0.010	
6	29.3 C mass balance	0	0	-1	0	0	1	0.429	0.273	0	0	0	-0.734		
7	29.5 N mass balance	0	0	0	0	-1	0	0	0	0	1	0	0	-0.017	
8	7.6 N ₂ in blast air specification	0	0	0	3.3	-1	0	0	0	0	0	0	0	0	
9	7.9 Equilibrium CO ₂ /CO mass ratio	0	0	0	0	0	0	0.694	-1	0	0	0	0	0	
10	7.8 C out in molten iron specification	0	0	0	0	0	0.047	-1	0	0	0	0	0	0	
11	29.6 Enthalpy balance	-320	3.152	-1.359	-1.239	-1.339	1.269	5	-2.926	-7.926	1.008	13.35	-11.49	4.52	
12	29.2 H mass balance	0	0	0	0	0	0	0	0	0	0	1	0.112	-0.240	
13	11.8 Equilibrium H ₂ O/H ₂ mass ratio	0	0	0	0	0	0	0	0	0	0	5.44	-1	0	
14	29.1 Natural gas injected through tuyeres	60	0	0	0	0	0	0	0	0	0	0	0	0	1
15	Blast temperature	1200	°C												
16															
17	Bottom segment calculated values	kg per 1000 kg of Fe out in molten iron													
18	mass Fe _{0.94} O into bottom segment	1302													
19	mass C in descending coke	337	also = mass C in the furnace's coke charge, Eqn. (7.16)												
20	mass O ₂ in blast air	322													
21	mass N ₂ in blast air	1061													
22	mass Fe out in molten iron	1000													
23	mass C out in molten iron	47													
24	mass CO out in ascending gas	540													
25	mass CO ₂ out in ascending gas	375													
26	mass N ₂ out in ascending gas	1062													
27	mass H ₂ out in ascending gas	8.9													
28	mass H ₂ O out in ascending gas	49													
29	mass tuyere-injected natural gas	60													
30															

Table 31.1 is a copy of Table 29.2. It calculates the C-in-coke and O₂-in-blast air requirements for steady production of 1500°C molten iron. It also calculates the flows across conceptual bottom-segment–top-segment division of Fig. 31.1, in Cells C18, C19, and C24–C28. All masses are per 1000 kg of Fe in product molten iron.

TABLE 31.2 Top-Segment Matrix and Equations With 60 kg of Injected Natural Gas

	AC	AB	AC	AO	AE	AF	AG	AH	AI	AK	AL	AM	AN	AO	AP	AQ
TOP SEGMENT CALCULATIONS																
Equation	Description	Numerical term	mass $\text{Fe}_{0.04}\text{O}_3$ in furnace charge	mass C in coke charge	mass CO ascending from bottom segment	mass CO_2 ascending from bottom segment	mass N_2 ascending from bottom segment	mass $\text{Fe}_{0.04}\text{O}_3$ descending into bottom segment	mass C-in-coke descending into bottom segment	mass CO out in top gas	mass CO_2 out in top gas	mass N_2 out in top gas	mass H_2 ascending from bottom segment	mass H_2O ascending from bottom segment	mass H_2 out in top gas	mass H_2O out in top gas
20.6	Mass $\text{Fe}_{0.04}\text{O}_3$ descending into bottom segment	1302	0	0	0	0	0	1	0	0	0	0	0	0	0	0
20.2	Fe mass balance	0	-0.699	0	0	0	0	0.768	0	0	0	0	0	0	0	0
25.5	N mass balance	0	-0.301	0	-0.571	-0.727	0	0.232	0	0.571	0.727	0	0	-0.888	0	0.888
20.4	C mass balance	0	0	-1	-0.429	0.273	0	0	1	0.429	0.273	0	0	0	0	0
20.5	N mass balance	0	0	0	0	0	-1	0	0	0	0	1	0	0	0	0
20.8	Mass CO ascending from bottom segment	540	0	0	1	0	0	0	0	0	0	0	0	0	0	0
20.9	Mass CO_2 ascending from bottom segment	375	0	0	0	1	0	0	0	0	0	0	0	0	0	0
20.10	Mass N_2 ascending from bottom segment	1062	0	0	0	0	0	1	0	0	0	0	0	0	0	0
20.7	Mass C-in-coke descending into bottom segment	337	0	0	0	0	0	0	0	1	0	0	0	0	0	0
20.11	Unrelated C-in-coke specification	0	0	-1	0	0	0	0	0	1	0	0	0	0	0	0
25.4	Hydrogen mass balance	0	0	0	0	0	0	0	0	0	0	0	-1	-0.412	1	0.412
25.1	Mass H_2 ascending from bottom segment	8.9	0	0	0	0	0	0	0	0	0	0	1	0	0	0
25.2	Mass H_2O ascending from bottom segment	49	0	0	0	0	0	0	0	0	0	0	0	1	0	0
25.13	H_2/O_2 reaction ratio equation	0	0	0	0	-0.09	0	0	0	0	0.09	0	0	1	0	-1
17	Top segment calculated values	kg per 1000 kg of Fe out in molten iron														
18	mass $\text{Fe}_{0.04}\text{O}_3$ in furnace charge	1431														
19	mass C in coke charge	337														
20	mass CO ascending from bottom segment	540														
21	mass CO_2 ascending from bottom segment	375														
22	mass N_2 ascending from bottom segment	1062														
23	mass $\text{Fe}_{0.04}\text{O}_3$ descending into bottom segment	1302														
24	mass C-in-coke descending into bottom segment	337														
25	mass CO descending into bottom segment	351														
26	mass CO_2 out in top gas	662														
27	mass N_2 out in top gas	1062														
28	mass H_2 ascending from bottom segment	8.9														
29	mass H_2O ascending from bottom segment	49														
30	mass H_2 leaving in top gas	5.9														
31	mass H_2O leaving in top gas	76														
32	TOP SEGMENT INPUT AND OUTPUT ENTHALPY CALCULATIONS															
33	26.2 Top segment input enthalpy = $\text{AC18}^* - 5.169 + \text{AC19}^* 0 + \text{AC20}^* 2.926 + \text{AC21}^* - 7.926 + \text{AC22}^* 1.008 + \text{AC28}^* 13.35 + \text{AC29}^* 11.49 =$															
34	26.4 Top segment output enthalpy = $\text{AG33}^* - 80 =$															
35																
36	TOP GAS ENTHALPY CALCULATION															
37	26.5 Top gas enthalpy = $\text{AG34}^* - \text{AC23}^* 3.152 - \text{AC24}^* 1.359 =$															
38																
39	TOP GAS TEMPERATURE CALCULATION															
40	27.4 Top gas temperature = $(\text{AG37}^* - \text{AC25}^* 3.972 - \text{AC26}^* 8.966 - \text{AC27}^* 0.02624 - \text{AC30}^* 0.3613 - \text{AC31}^* 13.47) / (\text{AC25}^* 0.001049 + \text{AC26}^* 0.0009314 + \text{AC27}^* 0.001044 + \text{AC30}^* 0.01442 + \text{AC31}^* 0.001902) =$															
41															282	°C

Except for the values in Column AC, the matrix is the same as with $\text{CH}_4(\text{g})$ injection, Table 25.3. The calculations in Cells AG16 and AL16 are explained in Sections 25.3–25.4.

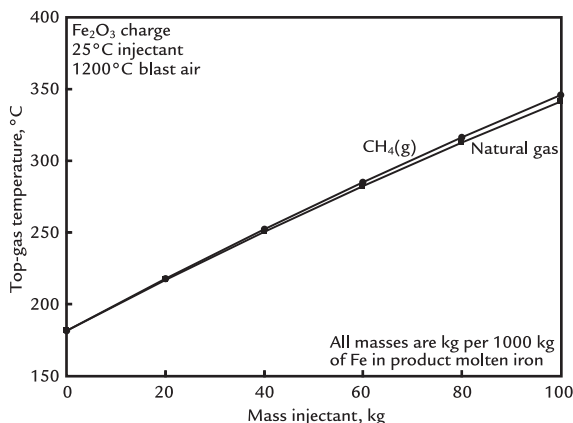


FIGURE 31.2 Comparison of top gas temperatures with CH₄(g) and natural gas injectants. Both raise top gas temperature, natural gas slightly less than CH₄(g). Both lines are curved because $d(H^\circ/\text{HW})_{\text{inputs}}/dT \neq d(H^\circ/\text{HW})_{\text{outputs}}/dT$ where T is temperature.

This is because our bottom segment, top segment, and whole furnace masses and enthalpies are consistent in every respect.

This is true when all the top charge masses can be related to the bottom segment's product masses.

It will not be true when the blast furnace top charge includes limestone (CaCO₃), etc., which decomposes to CaO(s) and CO₂(g) in the top segment.

31.7 SUMMARY

Top-segment calculations with tuyere-injected natural gas are almost the same as with tuyere-injected CH₄(g) injection.

Real natural gas and CH₄(g) tuyere injection both increase top gas temperature, Fig. 31.2. This is because they both increase upward hot N₂ mass flow and decrease downward (cool) C-in-coke mass flow (per 1000 kg of Fe in product molten iron).

EXERCISES

- 31.1. The blast furnace research team of Exercise 29.1 wishes to know what its top gas temperature will be while injecting 45 kg of Table 29.1 natural gas per 1000 kg of Fe in product molten iron.

Please calculate this for them. Please use two methods.

- 31.2. The blast furnace operating team specifies that its top gas temperature must be below 200°C. How much natural gas can they inject while meeting this specification?

Please calculate this for them using two methods of your choice.

C H A P T E R

32

Bottom-Segment Slag Calculations - Ore, Fluxes, and Slag

O U T L I N E

32.1 Molten Oxide Blast Furnace Slag	274	32.6 Masses of Al_2O_3 , CaO , and MgO in Molten Slag	277
32.1.1 Inadvertent Slag Production	274	32.7 Bottom-Segment Mass Balances and Input SiO_2 , Al_2O_3 , CaO , and MgO Masses	278
32.1.2 Other Slag Functions	274		
32.1.3 Chapter Objectives	274		
32.2 Inputs and Outputs	275	32.8 Bottom-Segment Enthalpy Balance Equation	278
32.3 1000 kg of Fe in Product Molten Iron Specification	276	32.9 Matrix and Calculations	279
32.4 A Mass SiO_2 Specification Equation	276	32.10 Results	279
32.5 SiO_2 Descending Into the Bottom Segment	276	32.11 Summary	279
32.5.1 Mass SiO_2 in Product Molten Slag	277	Exercises	282

32.1 MOLTEN OXIDE BLAST FURNACE SLAG

All iron blast furnaces produce 1500°C molten oxide slag as well as 1500°C molten iron. The slag typically contains;

- 10 mass% Al_2O_3 ,
- 41 mass% CaO ,
- 10 mass% MgO , and
- 39 mass% SiO_2

plus minor amounts of Mn, S, Ti, P, Na, K, and Fe.

32.1.1 Inadvertent Slag Production

Blast furnaces must produce molten slag to remove SiO_2 , Al_2O_3 , and other impurity oxides that are inevitably in their;

- ore charge (as gangue oxides),
- coke charge (as ash oxides), and
- injected coal (as ash oxides).

The blast furnace operator must ensure that the slag is molten at 1500°C by including fluxes in the blast furnace top charge. This is done by choosing slag compositions that are inside the slag's 1400°C melting point (liquidus) window (Fig. 32.1). This provides a 100°C safety factor where the slag's melting point is at least 100°C less than the product molten iron, 1500°C.

Fluxes are charged to the blast furnace as various oxides and/or carbonates (Chapter 59: Burden Distribution) but they all report to the slag as oxides, that is, Al_2O_3 , CaO , MgO , and SiO_2 .

32.1.2 Other Slag Functions

In addition to keeping the slag molten, the charged fluxes are chosen to produce a slag that will;

1. remove a prescribed amount of sulfur from the blast furnace rather than having it report to the product molten iron;

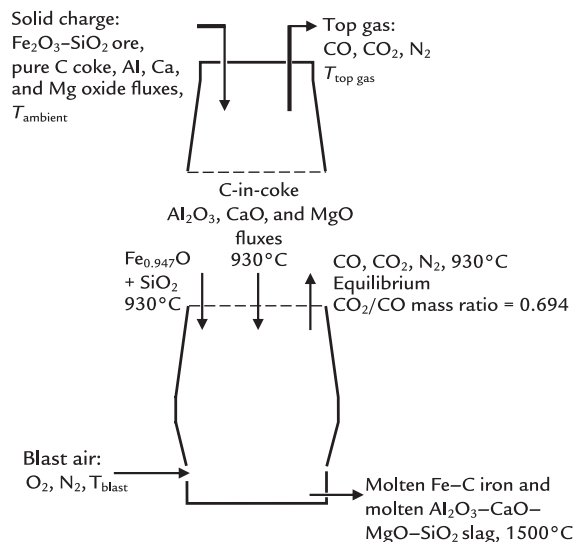


FIGURE 32.1 Central vertical slice through a blast furnace showing

1. conceptual division of the of the blast furnace through its chemical reserve zone and
2. the blast furnace's inputs, outputs, and cross-division flows with top-charged $\text{Fe}_2\text{O}_3\text{-SiO}_2$ ore and Al, Ca, and Mg oxide fluxes.
2. remove unwanted alkali elements, specifically Na and K that are present in the charge materials and that can accumulate in the blast furnace and form large accretions; and
3. give the slag a composition that is suitable for the solidified slag to be used in cement and road aggregate manufacturing.

These aspects are discussed in Chapter 58, Blast Furnace Slag.

32.1.3 Chapter Objectives

In this chapter, we will determine the effects of SiO_2 in ore on the quantities of;

1. Al_2O_3 , CaO , and MgO in flux;
2. C-in-coke; and
3. O₂-in-blast air

that are required to steadily produce;

1. 1500°C molten blast furnace iron, 95.5 mass % Fe, 4.5 mass% C, and
2. 1500°C molten blast furnace slag;
 - a. 10 mass% Al₂O₃,
 - b. 41 mass% CaO,
 - c. 10 mass% MgO, and
 - d. 39 mass% SiO₂.

The calculations are like those in previous chapters with the additional specification of;

1. ore composition, mass% Fe₂O₃ and SiO₂, and
2. slag composition, mass% Al₂O₃, CaO, MgO, and SiO₂.

We also specify that



remain as oxides in the blast furnace. This is a slight simplification, see Chapter 35—Bottom-Segment Calculations—Reduction of SiO₂.

For simplicity, we;

1. continue with our assumption that coke is pure carbon (i.e., we continue to ignore coke ash's Al₂O₃ and SiO₂), and
2. postpone pulverized coal injection and its ash component.

The effects of coke ash are described in Chapter 34, Bottom-Segment Slag Calculations - Coke Ash.

The effects of pulverized coal ash are described in Chapter 37, Bottom-Segment Calculations with Pulverized Coal Injection.

32.2 INPUTS AND OUTPUTS

This section begins our calculations. To start, Fig. 32.1 shows the blast furnace's inputs, outputs, and cross-division flows while Fig. 32.2 details its bottom-segment inputs and outputs.

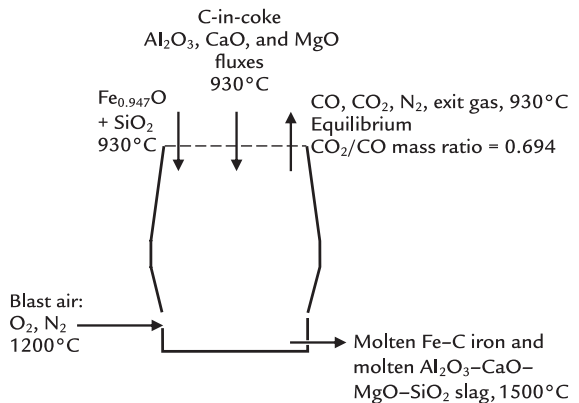


FIGURE 32.2 Central vertical slice through blast furnace bottom segment. Note the descending Al₂O₃, CaO, MgO, and SiO₂ and the molten Al₂O₃, CaO, MgO, and SiO₂ slag.

For simplicity, nothing is being injected through the tuyeres.

Together Figs. 32.1 and 32.2 show that;

1. all the top-charged Fe-in-ore descends into the bottom segment as Fe_{0.947}O(s) and ends up in the blast furnace's product molten iron;
2. all the top-charged SiO₂-in-ore descends into the bottom segment as SiO₂(s) and ends up in the blast furnace's product molten slag; and
3. all the top-charged Al, Ca, and Mg-bearing fluxes descend into the bottom segment as;
 - Al₂O₃(s),
 - CaO(s), and
 - MgO(s)

and end up in the blast furnace's product molten Al₂O₃, CaO, MgO, and SiO₂ slag.

The next five sections develop equations for calculating;

1. the steady-state masses of all these substances, and
2. the amounts of C-in-coke and O₂-in-blast air that will steadily produce molten iron and slag with these inputs and outputs.

32.3 1000 kg OF Fe IN PRODUCT MOLTEN IRON SPECIFICATION

Sections 4.4.2 and 7.6 specifies that all this book's calculations are based on 1000 kg of Fe in the blast furnace's product molten iron.

We continue with this specification here as described by the equation

$$1000 = \left[\frac{\text{mass Fe in product}}{\text{molten iron}} \right] * 1 \quad (7.7)$$

32.4 A MASS SiO₂ SPECIFICATION EQUATION

This section specifies that the blast furnace's top-charged ore contains;

- 95 mass% Fe₂O₃, and
- 5 mass% SiO₂

which, because Fe₂O₃ contains 69.9 mass% Fe and 30.1 mass% O, is equivalent to;

- 5.0 mass% SiO₂,
- 66.4 mass% Fe, and
- 28.6 mass% O (excluding the O in SiO₂).

[An amount of 100 kg of ore contains 5 kg of SiO₂ and 95 kg of Fe₂O₃. The 95 kg of Fe₂O₃ contains (69.9 mass% Fe in Fe₂O₃/100%) * 95 kg of Fe₂O₃ = 66.4 kg of Fe and (30.1 mass% O in Fe₂O₃/100%) * 95 kg of Fe₂O₃ = 28.6 kg of O.]

An equation that usefully describes this composition is;

$$\left[\frac{\text{mass SiO}_2 \text{ in}}{\text{top-charged ore}} \right] = \left[\frac{5 \text{ mass\% SiO}_2 \text{ in}}{66.4 \text{ mass\% Fe in}} \right] = 0.0753$$

or

$$\left[\frac{\text{mass SiO}_2 \text{ in}}{\text{top-charged ore}} \right] = 0.0753 * \left[\frac{\text{mass Fe in}}{\text{top-charged ore}} \right] \quad (32.1)$$

As always, all our masses are per 1000 kg of Fe in product molten iron.

32.5 SiO₂ DESCENDING INTO THE BOTTOM SEGMENT

Our conceptual bottom-segment matrix calculations need an equation that relates;

$$\left[\frac{\text{mass SiO}_2 \text{ in}}{\text{descending ore}} \right]$$

to

$$\left[\frac{\text{mass Fe in product}}{\text{molten iron}} \right]$$

This section develops that equation as follows;

1. because SiO₂ and Fe descend together into the bottom segment of Fig. 32.2, Eq. (32.1) may be extended to;

$$\left[\frac{\text{mass SiO}_2 \text{ in}}{\text{descending ore}} \right] = 0.0753 * \left[\frac{\text{mass Fe in}}{\text{descending ore}} \right]$$

2. and, because we specify that all the Fe descending into the bottom segment ends up in the blast furnace's product molten iron.

$$\left[\frac{\text{mass Fe in}}{\text{descending ore}} \right] = \left[\frac{\text{mass Fe in product}}{\text{molten iron}} \right]$$

These equations combine to give;

$$\begin{aligned} \left[\frac{\text{mass SiO}_2 \text{ in}}{\text{descending ore}} \right] &= 0.0753 * \left[\frac{\text{mass Fe in}}{\text{descending ore}} \right] \\ &= 0.0753 * \left[\frac{\text{mass Fe in product}}{\text{molten iron}} \right] \end{aligned}$$

or

$$\left[\frac{\text{mass SiO}_2 \text{ in}}{\text{descending ore}} \right] = 0.0753 * \left[\frac{\text{mass Fe in product}}{\text{molten iron}} \right]$$

or subtracting $\left\{ \left[\frac{\text{mass SiO}_2 \text{ in}}{\text{descending ore}} \right] \right\}$ from both sides;

$$\begin{aligned} 0 &= - \left[\frac{\text{mass SiO}_2 \text{ in}}{\text{descending ore}} \right] * 1 \\ &\quad + \left[\frac{\text{mass Fe in product}}{\text{molten iron}} \right] * 0.0753 \end{aligned} \quad (32.2)$$

this relationship is needed for our bottom-segment matrix calculations. Industrially, a

small amount of Fe in descending ore reports to slag rather than molten iron. So, Eq. (32.2) slightly underestimates the amount of SiO_2 that needs to be fluxed.

32.5.1 Mass SiO_2 in Product Molten Slag

We also need an equation that relates;

$$\left[\begin{array}{l} \text{mass } \text{SiO}_2 \text{ in} \\ \text{descending ore} \end{array} \right]$$

to

$$\left[\begin{array}{l} \text{mass } \text{SiO}_2 \text{ in} \\ \text{product molten slag} \end{array} \right]$$

This comes from the steady-state bottom-segment SiO_2 mass balance;

$$\left[\begin{array}{l} \text{mass } \text{SiO}_2 \text{ in} \\ \text{descending ore} \end{array} \right] = \left[\begin{array}{l} \text{mass } \text{SiO}_2 \text{ in} \\ \text{product molten slag} \end{array} \right] \quad (32.3)$$

or subtracting $\left\{ \left[\begin{array}{l} \text{mass } \text{SiO}_2 \text{ in} \\ \text{product molten slag} \end{array} \right] \right\}$ from both sides;

$$0 = - \left[\begin{array}{l} \text{mass } \text{SiO}_2 \text{ in} \\ \text{descending ore} \end{array} \right] * 1 + \left[\begin{array}{l} \text{mass } \text{SiO}_2 \text{ in} \\ \text{product molten slag} \end{array} \right] * 1 \quad (32.4)$$

This equation specifies (for now) that none of the descending SiO_2 is reduced to metallic Si. A more realistic specification is given in Chapter 35, Bottom-Segment Calculations - Reduction of SiO_2 .

32.6 MASSES OF Al_2O_3 , CaO , AND MgO IN MOLTEN SLAG

Remembering that our blast furnace slag is specified to contain:

- 10 mass% Al_2O_3 ,
- 41 mass% CaO ,
- 10 mass% MgO , and
- 39 mass% SiO_2 .

We now calculate the masses of Al_2O_3 , CaO , and MgO in slag per 1000 kg of Fe in product molten iron.

The amount of Al_2O_3 in the slag may be described by the ratio;

$$\frac{\left[\begin{array}{l} \text{mass } \text{Al}_2\text{O}_3 \text{ in} \\ \text{product molten slag} \end{array} \right]}{\left[\begin{array}{l} \text{mass } \text{SiO}_2 \text{ in} \\ \text{product molten slag} \end{array} \right]} = \frac{\left[\begin{array}{l} 10 \text{ mass\% } \text{Al}_2\text{O}_3 \text{ in} \\ \text{product molten slag} \end{array} \right]}{\left[\begin{array}{l} 39 \text{ mass\% } \text{SiO}_2 \text{ in} \\ \text{product molten slag} \end{array} \right]} = 0.256$$

or

$$\left[\begin{array}{l} \text{mass } \text{Al}_2\text{O}_3 \text{ in} \\ \text{product molten slag} \end{array} \right] * 1 = 0.256 * \left[\begin{array}{l} \text{mass } \text{SiO}_2 \text{ in} \\ \text{product molten slag} \end{array} \right]$$

or subtracting $\left\{ \left[\begin{array}{l} \text{mass } \text{Al}_2\text{O}_3 \text{ in} \\ \text{product molten slag} \end{array} \right] * 1 \right\}$ from both sides;

$$0 = - \left[\begin{array}{l} \text{mass } \text{Al}_2\text{O}_3 \text{ in} \\ \text{product molten slag} \end{array} \right] * 1 + \left[\begin{array}{l} \text{mass } \text{SiO}_2 \text{ in} \\ \text{product molten slag} \end{array} \right] * 0.256 \quad (32.5)$$

Likewise, the amount of CaO in the slag may be described by the ratio;

$$\frac{\left[\begin{array}{l} \text{mass } \text{CaO} \text{ in} \\ \text{product molten slag} \end{array} \right]}{\left[\begin{array}{l} \text{mass } \text{SiO}_2 \text{ in} \\ \text{product molten slag} \end{array} \right]} = \frac{\left[\begin{array}{l} 41 \text{ mass\% } \text{CaO} \text{ in} \\ \text{product molten slag} \end{array} \right]}{\left[\begin{array}{l} 39 \text{ mass\% } \text{SiO}_2 \text{ in} \\ \text{product molten slag} \end{array} \right]} = 1.05$$

or

$$\left[\begin{array}{l} \text{mass } \text{CaO} \text{ in} \\ \text{product molten slag} \end{array} \right] * 1 = 1.05 * \left[\begin{array}{l} \text{mass } \text{SiO}_2 \text{ in} \\ \text{product molten slag} \end{array} \right]$$

or subtracting $\left\{ \left[\begin{array}{l} \text{mass } \text{CaO} \text{ in} \\ \text{product molten slag} \end{array} \right] * 1 \right\}$ from both sides;

$$0 = - \left[\begin{array}{l} \text{mass } \text{CaO} \text{ in} \\ \text{product molten slag} \end{array} \right] * 1 + \left[\begin{array}{l} \text{mass } \text{SiO}_2 \text{ in} \\ \text{product molten slag} \end{array} \right] * 1.05 \quad (32.6)$$

and the amount of MgO in the slag may be described by;

$$\frac{\left[\begin{array}{l} \text{mass } \text{MgO} \text{ in} \\ \text{product molten slag} \end{array} \right]}{\left[\begin{array}{l} \text{mass } \text{SiO}_2 \text{ in} \\ \text{product molten slag} \end{array} \right]} = \frac{\left[\begin{array}{l} 10 \text{ mass\% } \text{MgO} \text{ in} \\ \text{product molten slag} \end{array} \right]}{\left[\begin{array}{l} 39 \text{ mass\% } \text{SiO}_2 \text{ in} \\ \text{product molten slag} \end{array} \right]} = 0.256$$

or

$$\left[\frac{\text{mass MgO in}}{\text{product molten slag}} \right] * 1 = 0.256 * \left[\frac{\text{mass SiO}_2 \text{ in}}{\text{product molten slag}} \right]$$

or subtracting $\left\{ \left[\frac{\text{mass MgO in}}{\text{product molten slag}} \right] * 1 \right\}$ from both sides;

$$0 = - \left[\frac{\text{mass MgO in}}{\text{product molten slag}} \right] * 1 + \left[\frac{\text{mass SiO}_2 \text{ in}}{\text{product molten slag}} \right] * 0.256 \quad (32.7)$$

or

$$0 = - \left[\frac{\text{mass Al}_2\text{O}_3 \text{ in}}{\text{descending flux}} \right] * 1 + \left[\frac{\text{mass Al}_2\text{O}_3 \text{ in}}{\text{molten slag}} \right] * 1 \quad (32.8)$$

and

$$\left[\frac{\text{mass CaO descending}}{\text{into the bottom segment}} \right] = \left[\frac{\text{mass CaO in}}{\text{molten slag}} \right]$$

or

$$0 = - \left[\frac{\text{mass CaO descending}}{\text{into the bottom segment}} \right] * 1 + \left[\frac{\text{mass CaO in}}{\text{molten slag}} \right] * 1 \quad (32.9)$$

and

$$\left[\frac{\text{mass MgO descending}}{\text{into the bottom segment}} \right] = \left[\frac{\text{mass MgO in}}{\text{molten slag}} \right]$$

or

$$0 = - \left[\frac{\text{mass MgO descending}}{\text{into the bottom segment}} \right] * 1 + \left[\frac{\text{mass MgO in}}{\text{molten slag}} \right] * 1 \quad (32.10)$$

all per 1000 kg of Fe in product molten iron.

32.7 BOTTOM-SEGMENT MASS BALANCES AND INPUT SiO_2 , Al_2O_3 , CaO , AND MgO MASSES

Bottom-segment slag forming inputs of Fig. 32.2 are;

1. solid SiO_2 from the ore charge, 930°C , and
2. solid Al_2O_3 , CaO , and MgO from fluxes, 930°C .

This is a simplification because $\text{SiO}_2(s)$ and $\text{Al}_2\text{O}_3(s)$ also enter the blast furnace in coke ash and injected coal's ash, Chapter 34, Bottom-Segment Slag Calculations—Coke Ash, and Chapter 37, Bottom-Segment Calculations With Pulverized Coal Injection. Also, a small amount of SiO_2 is reduced to $\text{Si}(l)$ -in-molten iron in the bottom segment (Chapter 35: Bottom-Segment Calculations - Reduction of SiO_2).

CaO and MgO are charged to the blast furnace as oxides and carbonates. Ultimately, they enter the bottom segment as oxides. CaCO_3 decomposes at 840°C . MgCO_3 decomposes at 780°C .

The masses of Al_2O_3 , CaO , and MgO descending into the bottom segment are given by the bottom-segment Al_2O_3 , CaO , and MgO steady-state mass balances. They are;

$$\left[\frac{\text{mass Al}_2\text{O}_3 \text{ in}}{\text{descending flux}} \right] = \left[\frac{\text{mass Al}_2\text{O}_3 \text{ in}}{\text{molten slag}} \right]$$

32.8 BOTTOM-SEGMENT ENTHALPY BALANCE EQUATION

The blast furnace bottom segment of Fig. 32.2 has four new inputs and four new outputs. Its enthalpy balance must include enthalpies for all eight of these substances.

The input enthalpies are;

$$\frac{H^\circ_{930^\circ\text{C}}}{\text{MW}_{\text{Al}_2\text{O}_3} \text{ Al}_2\text{O}_3(s, \alpha)} = -15.41 \text{ MJ/kg}$$

$$\frac{H^\circ_{930^\circ\text{C}}}{\text{MW}_{\text{CaO}} \text{ CaO}(s)} = -10.50 \text{ MJ/kg}$$

$$\frac{H^\circ_{930^\circ\text{C}}}{\text{MW}_{\text{MgO}} \text{ MgO}(s)} = -13.84 \text{ MJ/kg}$$

$$\frac{H^\circ_{\text{SiO}_2(\text{s}, \text{high cristobalite})}}{\text{MW}_{\text{SiO}_2}} = -14.13 \text{ MJ/kg}$$

in Table J.1.

The output enthalpies are described in Table J.1. They are;

$$\frac{H^\circ_{\text{Al}_2\text{O}_3(\text{in molten slag})}}{\text{MW}_{\text{Al}_2\text{O}_3}} = -13.58 \text{ MJ/kg}$$

$$\frac{H^\circ_{\text{CaO}(\text{in molten slag})}}{\text{MW}_{\text{CaO}}} = -8.495 \text{ MJ/kg}$$

$$\frac{H^\circ_{\text{MgO}(\text{in molten slag})}}{\text{MW}_{\text{MgO}}} = -11.14 \text{ MJ/kg}$$

$$\frac{H^\circ_{\text{SiO}_2(\text{in molten slag})}}{\text{MW}_{\text{SiO}_2}} = -13.28 \text{ MJ/kg.}$$

With these new enthalpies, the bottom-segment enthalpy balance Eq. (7.15) becomes;

$$\begin{aligned}
 -320 = & -[\text{mass Fe}_{0.947}\text{O into bottom segment}] * (-3.152) \\
 & -[\text{mass C in descending coke}] * 1.359 \\
 & -[\text{mass O}_2 \text{ in blast air}] * 1.239 \\
 & -[\text{mass N}_2 \text{ in blast air}] * 1.339 \\
 & -[\text{mass Al}_2\text{O}_3 \text{ descending in dissociated flux}] \\
 & * (-15.41) \\
 & -[\text{mass CaO descending in dissociated flux}] \\
 & * (-10.50) \\
 & -[\text{mass MgO descending in dissociated flux}] \\
 & * (-13.84) \\
 & -[\text{mass SiO}_2 \text{ descending in ore gangue}] * (-14.13) \\
 & +[\text{mass Fe out in molten iron}] * 1.269 \\
 & +[\text{mass C out in molten iron}] * 5 \\
 & +[\text{mass CO gas out in ascending gas}] * (-2.926) \\
 & +[\text{mass CO}_2 \text{ out in ascending gas}] * (-7.926) \\
 & +[\text{mass N}_2 \text{ out in ascending gas}] * 1.008 \\
 & +[\text{mass Al}_2\text{O}_3 \text{ out in molten slag}] * (-13.58) \\
 & +[\text{mass CaO out in molten slag}] * (-8.495) \\
 & +[\text{mass MgO out in molten slag}] * (-11.14) \\
 & +[\text{mass SiO}_2 \text{ out in molten slag}] * (-13.28)
 \end{aligned} \tag{32.11}$$

where the enthalpies are for the temperatures as in Fig. 32.2.

32.9 MATRIX AND CALCULATIONS

Table 32.1 is our matrix with SiO_2 -in-ore, Al_2O_3 , CaO , and MgO in flux and Al_2O_3 , CaO , MgO , and SiO_2 in molten slag. It is matrix Table 7.2 with these eight new variables and their equivalent eight new equations. The enthalpy equation has also been modified to include the enthalpies of all these substances.

32.10 RESULTS

Fig. 32.3 shows the effect of mass% SiO_2 in top-charged ore on bottom-segment (hence whole furnace) C-in-coke and O_2 -in-blast air requirements for steady production of:

- molten iron, 1500°C , and
- specified molten slag, 1500°C , of Section 32.1.3.

Both increase. This is because the slag components must be heated and melted in the bottom segment—requiring more combustion of C-in-coke by O_2 -in-blast air.

32.11 SUMMARY

This chapter shows how to include;

- SiO_2 in top-charged ore, and
- top-charged Al_2O_3 , CaO , and MgO fluxes in our bottom-segment matrix calculations.

Ore and molten slag compositions are specified and;

- C-in-coke,
- O_2 -in-blast,
- Al_2O_3 in slag,
- CaO in slag, and
- MgO in slag

requirements for steady production of 1500°C molten iron and 1500°C molten slag are calculated.

TABLE 32.1 Bottom-Segment Matrix of Fig. 32.2

	A	B	C	D	E	F	G	H	I	J	K
1 BOTTOM SEGMENT CALCULATIONS											
Equation	Description	Numerical term	mass Fe _{0.947} O into bottom segment	mass C in descending coke	mass O ₂ in blast air	mass N ₂ in blast air	mass Fe out in molten iron	mass C out in molten iron	mass CO out in ascending gas	mass CO ₂ out in ascending gas	
2											
3	7.7 Fe out in molten iron specification	1000	0	0	0	0	1	0	0	0	
4	32.2 SiO ₂ descending in ore	0	0	0	0	0	0.0753	0	0	0	
5	7.2 Fe mass balance	0	-0.768	0	0	0	1	0	0	0	
6	7.3 O mass balance	0	-0.232	0	-1	0	0	0	0.571	0.727	
7	7.4 C mass balance	0	0	-1	0	0	0	1	0.429	0.273	
8	32.4 SiO ₂ mass balance	0	0	0	0	0	0	0	0	0	
9	7.5 N mass balance	0	0	0	0	-1	0	0	0	0	
10	7.6 N ₂ in blast air specification	0	0	0	3.3	-1	0	0	0	0	
11	7.9 Equilibrium CO _y /CO mass ratio	0	0	0	0	0	0	0	0.694	-1	
12	7.8 C out in molten iron specification	0	0	0	0	0	0.047	-1	0	0	
13	32.5 Al ₂ O ₃ out in molten slag specification	0	0	0	0	0	0	0	0	0	
14	32.8 Al ₂ O ₃ mass balance	0	0	0	0	0	0	0	0	0	
15	32.6 CaO out in molten slag specification	0	0	0	0	0	0	0	0	0	
16	32.9 CaO mass balance	0	0	0	0	0	0	0	0	0	
17	32.7 MgO out in molten slag specification	0	0	0	0	0	0	0	0	0	
18	32.10 MgO mass balance	0	0	0	0	0	0	0	0	0	
19	32.11 Enthalpy balance	-320	3.152	-1.359	-1.239	-1.339	1.269	5	-2.926	-7.926	
20			930°C	930°C	1200°C	1200°C	1500°C	1500°C	930°C	930°C	
21											

	L	M	N	O	P	Q	R	S	T
1									
2	mass N ₂ out in ascending gas	mass SiO ₂ in descending ore	mass SiO ₂ out in molten slag	mass Al ₂ O ₃ in descending flux	mass Al ₂ O ₃ out in molten slag	mass CaO in descending flux	mass CaO out in molten slag	mass MgO in descending flux	mass MgO out in molten slag
3	0	0	0	0	0	0	0	0	0
4	0	-1	0	0	0	0	0	0	0
5	0	0	0	0	0	0	0	0	0
6	0	0	0	0	0	0	0	0	0
7	0	0	0	0	0	0	0	0	0
8	0	-1	1	0	0	0	0	0	0
9	1	0	0	0	0	0	0	0	0
10	0	0	0	0	0	0	0	0	0
11	0	0	0	0	0	0	0	0	0
12	0	0	0	0	0	0	0	0	0
13	0	0	0.256	0	-1	0	0	0	0
14	0	0	0	-1	1	0	0	0	0
15	0	0	1.05	0	0	0	-1	0	0
16	0	0	0	0	0	-1	1	0	0
17	0	0	0.256	0	0	0	0	0	-1
18	0	0	0	0	0	0	0	-1	1
19	1.008	14.13	-13.28	15.41	-13.58	10.50	-8.495	13.84	-11.14
20	930°C	930°C	1500°C	930°C	1500°C	930°C	1500°C	930°C	1500°C
21									

Table 32.1 is matrix of Table 7.2 with eight new variables and eight new equations plus a modified enthalpy balance, Eq. (32.11). The solution is given in Table 32.2. Note that the matrix is split in two—for better visibility.

TABLE 32.2 Results Calculated With Matrix of Table 32.1

	A	B	C	D	E	F	G	H
23		Bottom segment calculated values	kg per 1000 kg of Fe out in molten iron					
24		mass Fe _{0.947} O into bottom segment	1302					
25		mass C in descending coke	408	also = mass C in the furnace's coke charge, Eqn. (7.16)				
26		mass O ₂ in blast air	326					
27		mass N ₂ in blast air	1077					
28		mass Fe out in molten iron	1000					
29		mass C out in molten iron	47					
30		mass CO out in ascending gas	584					
31		mass CO ₂ out in ascending gas	405					
32		mass N ₂ out in ascending gas	1077					
33		mass SiO ₂ in descending ore	75					
34		mass SiO ₂ out in molten slag	75					
35		mass Al ₂ O ₃ in descending flux	19					
36		mass Al ₂ O ₃ out in molten slag	19					
37		mass CaO in descending flux	79					
38		mass CaO out in molten slag	79					
39		mass MgO in descending flux	19					
40		mass MgO out in molten slag	19					
41								

The C-in-coke and O₂-in-blast air requirements for steadily producing molten iron and molten slag, 1500°C, are shown to be;

- 408 kg C-in-coke, and
 - 326 kg O₂-in-blast air
- as compared to;
- 392 kg C-in-coke, and
 - 298 kg O₂-in-blast air of Table 7.2
- with no slag production.

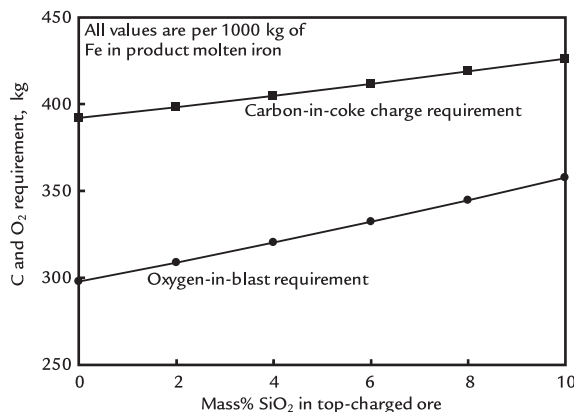


FIGURE 32.3 Effect of mass% SiO₂ in top-charged ore on C-in-coke and O₂-in-blast requirements for steadily producing (1) molten iron, 1500°C, and (2) molten slag, 1500°C, of Section 32.1.3. Both increase. The lines are not quite straight because slag mass increases nonlinearly with increasing mass% SiO₂ in top-charged ore (Fig. 32.4).

The requirements all increase with increasing mass% SiO₂ in ore.

Oxide ash in top-charged coke and tuyere-injected pulverized coal are not represented in this chapter's calculations. They are described in Chapter 34, Bottom-Segment Slag Calculations - Coke Ash, and Chapter 37, Bottom-Segment Calculations With Pulverized Coal Injection.

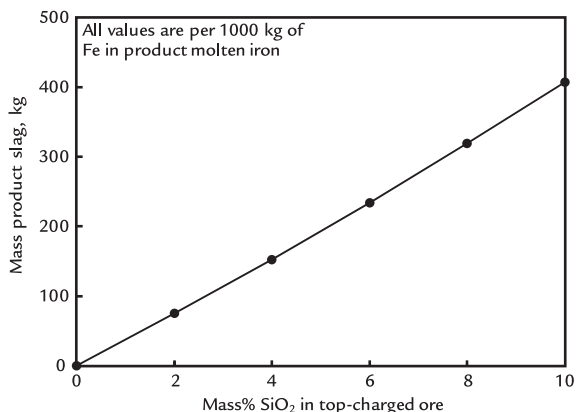


FIGURE 32.4 Slag mass as a function of mass% SiO₂ in top-charged ore where mass slag = C34 + C36 + C38 + C40 (Table 32.2). The increase is about 40 kg of slag per mass% SiO₂ in ore. It is nonlinear because the equation;

$$\begin{aligned}
 & \frac{\left[\text{mass SiO}_2 \text{ in} \right]}{\left[\text{mass Fe in} \right]} * \\
 & \frac{\left[\text{top charged ore} \right]}{\left[\text{top charged ore} \right]} \\
 & = \frac{\left[\text{mass% SiO}_2 \text{ in} \right]}{\left[\text{mass% Fe}_2\text{O}_3 \text{ in} \right] * (66.9 \text{ mass% Fe in Fe}_2\text{O}_3 / 100\%)} \\
 & = \frac{\left[\text{mass% SiO}_2 \text{ in} \right]}{\left(100\% - \left[\text{mass% SiO}_2 \text{ in} \right] \right)} \\
 & * (66.9 \text{ mass% Fe in Fe}_2\text{O}_3 / 100\%) \}
 \end{aligned}$$

is nonlinear. Industrial blast furnace slag production is typically ~280 kg/1000 kg of Fe in product molten iron.

EXERCISES

32.1. A steel company sells solid granulated slag to a cement-manufacturing company. The cement company requests that the slag composition be;

- 12 mass% Al₂O₃,
- 40 mass% CaO,
- 10 mass% MgO, and
- 38 mass% SiO₂.

By how much would this change the blast furnace of Section 32.4;

- C-in-coke requirement, and
- O₂-in-blast requirement

for steady production of molten blast furnace iron, 1500°C?

Also, by how much would it change slag mass?

Please give your results in kg per 1000 kg of Fe in product molten iron.

32.2. In Exercise 32.1, the purchasing department of the steel company has just learned that it can get a bargain on 15 mass% SiO₂, 85 mass% Fe₂O₃ ore pellets. Blast furnace management of

Fig. 32.1 asks you to determine the effects of charging this ore into its furnaces, specifically

- how much more slag will be produced?
- how much more Al_2O_3 , CaO , and MgO in flux will be required?
- how much more C-in-coke and O_2 -in-blast air would be required?
- how much more bottom-segment exit gas will be produced?

per 1000 kg of Fe in product molten iron.

Use your answer of Exercise 32.1 as the base case.

- 32.3.** Continuing with Exercise 32.2, by how much will this bargain ore decrease molten iron production, if the bottom-segment ascending gas flow

must not exceed the amount of Exercise 32.2?

- 32.4.** Ore of [Section 32.4](#) is found to contain 0.02 mass% TiO_2 . Please calculate what mass% TiO_2 -in-slag will result from this ore. Assume that all the TiO_2 -in-ore ends up as TiO_2 -in-slag. A one significant figure answer will do.

The enthalpies of 930°C $\text{TiO}_2(\text{s})$ and 1500°C TiO_2 -in-molten slag are

$$\frac{H^\circ_{930\text{ }^\circ\text{C}}}{\text{MW}_{\text{TiO}_2}} = -11.03 \text{ MJ/kg}$$

and

$$\frac{H^\circ_{1500\text{ }^\circ\text{C}}}{\text{MW}_{\text{TiO}_2}} = -9.64 \text{ MJ/kg.}$$

Bottom-Segment Slag Calculations-With Excess Al₂O₃ in Ore

OUTLINE

33.1 Understanding How to Remove Al ₂ O ₃ in Iron Ore to Slag	285	33.6 Matrix and Calculations	287
33.2 Al ₂ O ₃ -in-Ore Specification	286	33.7 Discussion	287
33.3 Masses of SiO ₂ , CaO, and MgO in Molten Slag	286	33.8 More Complex Calculations	290
33.4 Bottom-Segment Mass Balances	287	33.9 Summary	290
33.5 Bottom-Segment Enthalpy Balance	287	Exercise	290

33.1 UNDERSTANDING HOW TO REMOVE Al₂O₃ IN IRON ORE TO SLAG

Chapter 32, Bottom-Segment Slag Calculations - Ore, Fluxes, and Slag, discussed flux requirements with SiO₂ gangue in the top-charge iron ore.

Alumina (Al₂O₃) is a common impurity in Australian and Indian iron ores. The impact of alumina in ore on the bottom-segment calculations is described. We calculated the steady-state amounts of Al₂O₃, CaO, and MgO fluxes that

will steadily produce 1500°C molten iron and 1500°C molten;

- 10 mass% Al₂O₃,
- 41 mass% CaO,
- 10 mass% MgO, and
- 39 mass% SiO₂

slag.

This chapter does the same with Al₂O₃ gangue in the iron ore. In this case, we calculate the amounts of SiO₂, CaO, and MgO fluxes that will produce 1500°C molten iron and the above molten slag (Fig. 33.1).

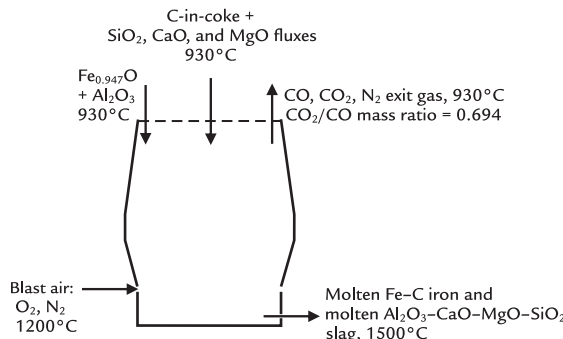


FIGURE 33.1 Blast furnace bottom segment with Al₂O₃ gangue in iron ore and CaO, MgO, and SiO₂ fluxes.

The objectives of this chapter are to;

1. show how the matrix of Table 32.1 is modified to examine SiO₂ fluxing of Al₂O₃ gangue-in-ore, and
2. indicate how multiple gangue minerals can be handled.

33.2 Al₂O₃-IN-ORE SPECIFICATION

To simplify comparisons with Chapter 32, Bottom-Segment Slag Calculations - Ore, Fluxes, and Slag, our alumina-in-ore calculations are based on;

- 95 mass% Fe₂O₃, and
- 5 mass% Al₂O₃

ore.

From Section 32.4, this is equivalent to

- 5 mass% Al₂O₃,
- 66.4 mass% Fe, and
- 28.6 mass% O (excluding the O in Al₂O₃).

As Eq. (32.1) shows, this composition is described by the following equation;

$$\left[\frac{\text{mass Al}_2\text{O}_3 \text{ in}}{\text{top charged ore}} \right] = 0.0753 * \left[\frac{\text{mass Fe in}}{\text{top charged ore}} \right] \quad (33.1)$$

which leads to;

$$\left[\frac{\text{mass Al}_2\text{O}_3 \text{ in}}{\text{descending ore}} \right] = 0.0753 * \left[\frac{\text{mass Fe in}}{\text{product molten iron}} \right]$$

or

$$0 = - \left[\frac{\text{mass Al}_2\text{O}_3 \text{ in}}{\text{descending ore}} \right] * 1 + \left[\frac{\text{mass Fe in}}{\text{product molten iron}} \right] * 0.0753 \quad (33.2)$$

33.3 MASSES OF SiO₂, CaO, AND MgO IN MOLTEN SLAG

As described above, this chapter and Chapter 32, Bottom-Segment Slag Calculations - Ore, Fluxes, and Slag, specify the same slag composition, that is;

- 10 mass% Al₂O₃,
- 41 mass% CaO,
- 10 mass% MgO, and
- 39 mass% SiO₂

as are described by the following equations:

$$0 = - \left[\frac{\text{mass Al}_2\text{O}_3 \text{ in}}{\text{molten slag}} \right] * 1 + \left[\frac{\text{mass SiO}_2 \text{ in}}{\text{molten slag}} \right] * 0.256 \quad (32.5)$$

where 0.256 = 10 mass% Al₂O₃ in slag/39 mass% SiO₂ in slag

$$0 = - \left[\frac{\text{mass MgO in}}{\text{molten slag}} \right] * 1 + \left[\frac{\text{mass SiO}_2 \text{ in}}{\text{molten slag}} \right] * 0.256 \quad (32.7)$$

where 0.256 = 10 mass% MgO in slag/39 mass% SiO₂ in slag

$$0 = - \left[\frac{\text{mass CaO in}}{\text{molten slag}} \right] * 1 + \left[\frac{\text{mass SiO}_2 \text{ in}}{\text{molten slag}} \right] * 1.05 \quad (32.6)$$

where 1.05 = 41 mass% CaO in slag/39 mass% SiO₂ in slag.

33.4 BOTTOM-SEGMENT MASS BALANCES

Mass balances of Fig. 33.1 are;

$$\left[\begin{array}{l} \text{mass Al}_2\text{O}_3 \text{ in} \\ \text{descending ore} \end{array} \right] = \left[\begin{array}{l} \text{mass Al}_2\text{O}_3 \text{ in} \\ \text{molten slag} \end{array} \right]$$

or

$$0 = - \left[\begin{array}{l} \text{mass Al}_2\text{O}_3 \text{ in} \\ \text{descending ore} \end{array} \right] * 1 + \left[\begin{array}{l} \text{mass Al}_2\text{O}_3 \text{ in} \\ \text{molten slag} \end{array} \right] * 1 \quad (33.3)$$

and

$$0 = - \left[\begin{array}{l} \text{mass SiO}_2 \text{ in} \\ \text{descending flux} \end{array} \right] * 1 + \left[\begin{array}{l} \text{mass SiO}_2 \text{ in} \\ \text{molten slag} \end{array} \right] * 1 \quad (33.4)$$

and

$$0 = - \left[\begin{array}{l} \text{mass CaO in} \\ \text{descending flux} \end{array} \right] * 1 + \left[\begin{array}{l} \text{mass CaO in} \\ \text{molten slag} \end{array} \right] * 1 \quad (32.9)$$

and

$$0 = - \left[\begin{array}{l} \text{mass MgO in} \\ \text{descending flux} \end{array} \right] * 1 + \left[\begin{array}{l} \text{mass MgO in} \\ \text{molten slag} \end{array} \right] * 1 \quad (32.10)$$

33.5 BOTTOM-SEGMENT ENTHALPY BALANCE

Bottom-segment enthalpy balance of this chapter is the same as Eq. (32.11), except that;

$$-\left[\begin{array}{l} \text{mass SiO}_2 \text{ in} \\ \text{descending ore} \end{array} \right] \text{ becomes } -\left[\begin{array}{l} \text{mass SiO}_2 \text{ in} \\ \text{descending flux} \end{array} \right]$$

and

$$-\left[\begin{array}{l} \text{mass Al}_2\text{O}_3 \text{ in} \\ \text{descending flux} \end{array} \right] \text{ becomes } -\left[\begin{array}{l} \text{mass Al}_2\text{O}_3 \text{ in} \\ \text{descending ore} \end{array} \right]$$

33.6 MATRIX AND CALCULATIONS

Tables 33.1 and 33.2 show our Al_2O_3 -in-ore matrix and its calculation results.

33.7 DISCUSSION

Note how easy it is to check the slag component masses:

1. From Eq. (33.2) mass Al_2O_3 in slag = $0.0753 * \text{mass Fe in product molten iron} = 0.0753 * 1000 \text{ kg} = 75.3 \text{ kg}$.
2. From 10 mass% Al_2O_3 and 10 mass% MgO – mass MgO in slag = $(10/10) * \text{mass Al}_2\text{O}_3 \text{ in slag} = 75.3 \text{ kg}$.
3. From 41 mass% CaO and 10 mass% Al_2O_3 in slag – mass CaO in slag = $(41/10) * \text{mass Al}_2\text{O}_3 \text{ in slag} = 4.1 * 75.3 = 309 \text{ kg}$.
4. From 39 mass% SiO_2 and 10 mass% Al_2O_3 in slag – mass SiO_2 in slag = $(39/10) * \text{mass Al}_2\text{O}_3 \text{ in slag} = 3.9 * 75.3 = 294 \text{ kg}$.

Notice how much more slag is produced with 5 mass% alumina-in-ore as compared to 5 mass% silica in ore;

- 753 kg of slag with Al_2O_3 -in-ore (Table 33.2) as compared to
- 192 kg of slag with SiO_2 in ore (Table 32.2).

This is mainly because;

$$\frac{[\text{mass CaO in slag}]}{[\text{mass Al}_2\text{O}_3 \text{ in ore}]} = \frac{[41 \text{ mass\% CaO in slag}]}{[10 \text{ mass\% Al}_2\text{O}_3 \text{ in slag}]}$$

while

$$\frac{[\text{mass CaO in slag}]}{[\text{mass SiO}_2 \text{ in ore}]} = \frac{[41 \text{ mass\% CaO in slag}]}{[39 \text{ mass\% SiO}_2 \text{ in slag}]}$$

The impact on the silica flux requirements is dramatic, see Fig. 33.2. Calculations with 3 mass% Al_2O_3 are described in the “Exercise” section of this chapter.

TABLE 33.1 Bottom-Segment Matrix With Al_2O_3 Gangue-in-Ore

A	B	C	D	E	F	G	H	I	J	K
1 BOTTOM SEGMENT CALCULATIONS										
Equation	Description	Numerical term	mass $\text{Fe}_{0.947}\text{O}$ into bottom segment	mass C in descending coke	mass O_2 in blast air	mass N_2 in blast air	mass Fe out in molten iron	mass C out in molten iron	mass CO out in ascending gas	mass CO_2 out in ascending gas
3 7.7	Fe out in molten iron specification	1000	0	0	0	0	1	0	0	0
4 33.2	Al_2O_3 descending in ore	0	0	0	0	0	0.0753	0	0	0
5 7.2	Fe mass balance	0	-0.768	0	0	0	1	0	0	0
6 7.3	O mass balance	0	-0.232	0	-1	0	0	0	0.571	0.727
7 7.4	C mass balance	0	0	-1	0	0	0	1	0.429	0.273
8 33.3	Al_2O_3 mass balance	0	0	0	0	0	0	0	0	0
9 7.5	N mass balance	0	0	0	0	-1	0	0	0	0
10 7.6	N_2 in air specification	0	0	0	3.3	-1	0	0	0	0
11 7.9	Equilibrium CO_2/CO mass ratio	0	0	0	0	0	0	0	0.694	-1
12 7.8	C in output molten iron specification	0	0	0	0	0	0.047	-1	0	0
13 32.5	SiO_2 in molten slag specification	0	0	0	0	0	0	0	0	0
14 33.4	SiO_2 mass balance	0	0	0	0	0	0	0	0	0
15 32.6	CaO in molten slag specification	0	0	0	0	0	0	0	0	0
16 32.9	CaO mass balance	0	0	0	0	0	0	0	0	0
17 32.7	MgO in molten slag specification	0	0	0	0	0	0	0	0	0
18 32.10	MgO mass balance	0	0	0	0	0	0	0	0	0
19 32.11	Enthalpy balance	-320	3.152	-1.359	-1.239	-1.339	1.269	5	-2.926	-7.926
20			930°C	930°C	1200°C	1200°C	1500°C	1500°C	930°C	930°C
21										

L	M	N	O	P	Q	R	S	T
mass N_2 out in ascending gas	mass Al_2O_3 in descending ore	mass Al_2O_3 out in molten slag	mass SiO_2 in descending flux	mass SiO_2 out in molten slag	mass CaO in descending flux	mass CaO out in molten slag	mass MgO in descending flux	mass MgO out in molten slag
3 0	0	0	0	0	0	0	0	0
4 0	-1	0	0	0	0	0	0	0
5 0	0	0	0	0	0	0	0	0
6 0	0	0	0	0	0	0	0	0
7 0	0	0	0	0	0	0	0	0
8 0	-1	1	0	0	0	0	0	0
9 1	0	0	0	0	0	0	0	0
10 0	0	0	0	0	0	0	0	0
11 0	0	0	0	0	0	0	0	0
12 0	0	0	0	0	0	0	0	0
13 0	0	-1	0	0.256	0	0	0	0
14 0	0	0	-1	1	0	0	0	0
15 0	0	0	0	1.05	0	-1	0	0
16 0	0	0	0	0	-1	1	0	0
17 0	0	0	0	0.256	0	0	0	-1
18 0	0	0	0	0	0	0	-1	1
19 1.008	15.41	-13.58	14.13	-13.28	10.50	-8.495	13.84	-11.14
20 930°C	930°C	1500°C	930°C	1500°C	930°C	1500°C	930°C	1500°C
21								

There are no tuyere injectants. The matrix is presented in two parts for clarity.

TABLE 33.2 Calculated Values From Bottom-Segment Matrix [Table 33.1](#)

	A	B	C	D	E	F	G
			kg per 1000 kg of Fe in product iron				
23		Bottom segment calculated values					
24		mass Fe _{0.947} O into bottom segment	1302				
25		mass C in descending coke	456	also = mass C in the furnace's coke charge, Eqn. (7.16)			
26		mass O ₂ in blast air	408				
27		mass N ₂ in blast air	1348				
28		mass Fe out in molten iron	1000				
29		mass C out in molten iron	47				
30		mass CO out in ascending gas	661				
31		mass CO ₂ out in ascending gas	458				
32		mass N ₂ out in ascending gas	1348				
33		mass Al ₂ O ₃ in descending ore	75				
34		mass Al ₂ O ₃ out in molten slag	75				
35		mass SiO ₂ in descending flux	294				
36		mass SiO ₂ out in molten slag	294				
37		mass CaO in descending flux	309				
38		mass CaO out in molten slag	309				
39		mass MgO in descending flux	75				
40		mass MgO out in molten slag	75				
41							

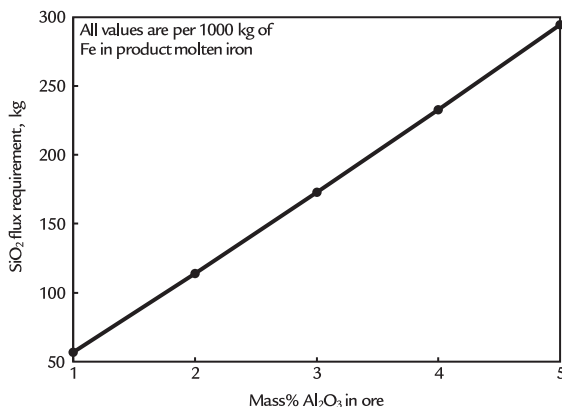


FIGURE 33.2 Amount of SiO₂ flux required to maintain the slag composition of this chapter. It increases with increasing mass % Al₂O₃ gangue in the top-charged Fe₂O₃ ore. The line is not quite straight because ratios are used in the calculations. CaO flux requirement = SiO₂ flux requirement * 41/39. MgO flux requirement = SiO₂ flux requirement * 10/39.

33.8 MORE COMPLEX CALCULATIONS

We can also consider the case where the ore contains 2.5 mass% SiO₂ and 2.5 mass% Al₂O₃. This requires that the matrices of Chapter 32, Bottom-Segment Slag Calculations - Ore, Fluxes, and Slag, and this chapter have two *descending ore* columns and a second *mass-in-ore* equation.

Interestingly, no SiO₂ flux and no Al₂O₃ flux are required when the SiO₂/Al₂O₃ mass ratio of the ore is the same as that prescribed for the slag, that is, when this chapter's:

$$\frac{[\text{mass Al}_2\text{O}_3 \text{ in ore}]}{[\text{mass SiO}_2 \text{ in ore}]} = \frac{[10 \text{ mass\% Al}_2\text{O}_3 \text{ in slag}]}{[39 \text{ mass\% SiO}_2 \text{ in slag}]}$$

A lesser [mass% Al₂O₃ in ore]/[mass% SiO₂ in ore] ratio than this requires alumina fluxing (Chapter 32: Bottom-Segment Slag Calculations - Ore, Fluxes, and Slag).

A larger [mass% Al₂O₃ in ore]/[mass% SiO₂ in ore] ratio than this requires silica fluxing (this chapter).

This knowledge can tell us which chapter's matrix should be used for our fluxing calculations.

33.9 SUMMARY

This chapter has shown how to include;

- Al₂O₃-in-ore, and
- top-charged SiO₂, CaO, and MgO fluxes

in our bottom-segment calculations. The calculations are much like those in Chapter 32, Bottom-Segment Slag Calculations - Ore, Fluxes, and Slag.

With mixed Al₂O₃-SiO₂ gangue-in-ore;

1. the matrix of Chapter 32, Bottom-Segment Slag Calculations - Ore, Fluxes, and Slag, must be used when SiO₂ is in excess in the Fe₂O₃ ore, and
2. the matrix of this chapter must be used when Al₂O₃ is in excess in the Fe₂O₃ ore.

The decision point is described in [Section 33.8](#).

As will be seen later in the book, slag calculations are complicated by ash in top-charged coke and ash in tuyere-injected coal. They are also complicated by SiO₂-Si reduction in the furnace hearth. With that said, they all follow the basic principles of these two chapters.

EXERCISE

- 33.1. A more realistic Al₂O₃ concentration in Al₂O₃ ore is 3 mass%. Please calculate the blast furnace of [Table 33.1](#);
 - a C-in-coke;
 - b O₂-in-blast air; and
 - c CaO, MgO, and SiO₂ flux requirements with this 3 mass% Al₂O₃ ore.

Bottom-Segment Slag Calculations

O U T L I N E

34.1 Coke Ash Contribution to Blast Furnace Slag	291	34.6 Altered Enthalpy Balance	294
34.2 New Variables	292	34.7 Matrix and Calculations	294
34.3 Al_2O_3 in Descending Coke Equation	292	34.8 Results	294
34.4 SiO_2 in Descending Coke Equation	293	34.9 Summary	294
34.5 Altered Bottom-Segment Al_2O_3 and SiO_2 Mass Balances	293	Exercises	297

34.1 COKE ASH CONTRIBUTION TO BLAST FURNACE SLAG

Chapter 32, Bottom-Segment Slag Calculations - Ore, Fluxes, and Slag, showed us how to include (1) iron ore's impurity oxides and (2) flux oxides in our blast furnace calculations. This chapter shows us how to include coke ash oxides, Fig. 34.1.

Top-charged coke of Fig. 34.1 contains;

- 90 mass% C,
- 7 mass% SiO_2 , and
- 3 mass% Al_2O_3 .

The matrix table in this chapter determines how the coke ash SiO_2 and Al_2O_3 affect the amounts of;

- C-in-coke and
- O_2 -in-blast

that are needed to steadily produce 1500°C molten iron and molten slag with this coke charge.

We continue with the specification of Chapter 32, Bottom-Segment Slag Calculations - Ore, Fluxes, and Slag, that the blast furnace slag must contain;

- 10 mass% Al_2O_3 ,
- 41 mass% CaO ,

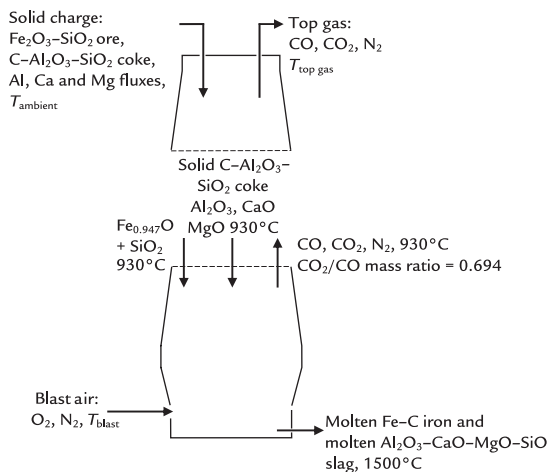


FIGURE 34.1 Blast furnace top and bottom segments including Al_2O_3 and SiO_2 in top-charged coke.

- 10 mass% MgO , and
- 39 mass% SiO_2

for it to be safely molten at 1500°C and useful when the slag solidifies.

The objectives of this chapter are to;

1. add coke ash variables and equations to the bottom-segment matrix Table 32.1;
2. calculate the amounts of
 - a. C-in-coke,
 - b. O_2 -in-blast, and
 - c. Al_2O_3 , CaO , and MgO fluxes
- that are needed to steadily produce 1500°C molten iron and slag with Al_2O_3 and SiO_2 in the top-charged coke; and
3. calculate the mass of product molten slag including coke's Al_2O_3 and SiO_2 .

34.2 NEW VARIABLES

Al_2O_3 -in-coke and SiO_2 -in-coke introduce two new variables into Table 32.1 matrix. They are:

$$\left[\begin{array}{l} \text{mass } \text{Al}_2\text{O}_3 \text{ in} \\ \text{descending coke} \end{array} \right]$$

and

$$\left[\begin{array}{l} \text{mass } \text{SiO}_2 \text{ in} \\ \text{descending coke} \end{array} \right]$$

These new variables require two additional equations in bottom-segment matrix of Table 32.1, as follows.

34.3 Al_2O_3 IN DESCENDING COKE EQUATION

Matrix Table 32.1 already includes the variable;

$$\left[\begin{array}{l} \text{mass C in} \\ \text{descending coke} \end{array} \right]$$

with our specified 90 mass% C, 3 mass% Al_2O_3 , and 7 mass% SiO_2 coke; this variable is connected to;

$$\left[\begin{array}{l} \text{mass } \text{Al}_2\text{O}_3 \text{ in} \\ \text{descending coke} \end{array} \right]$$

by the equation;

$$\frac{\left[\begin{array}{l} \text{mass } \text{Al}_2\text{O}_3 \text{ in} \\ \text{descending coke} \end{array} \right]}{\left[\begin{array}{l} \text{mass C in} \\ \text{descending coke} \end{array} \right]} = \frac{\left[\begin{array}{l} 3 \text{ mass\% } \text{Al}_2\text{O}_3 \text{ in} \\ \text{descending coke} \end{array} \right]}{\left[\begin{array}{l} 90 \text{ mass\% C in} \\ \text{descending coke} \end{array} \right]} = 0.0333 \quad (34.1)$$

or

$$\left[\begin{array}{l} \text{mass } \text{Al}_2\text{O}_3 \text{ in} \\ \text{descending coke} \end{array} \right] * 1 = \left[\begin{array}{l} \text{mass C in} \\ \text{descending coke} \end{array} \right] * 0.0333$$

or subtracting $\left\{ \left[\begin{array}{l} \text{mass } \text{Al}_2\text{O}_3 \text{ in} \\ \text{descending coke} \end{array} \right] * 1 \right\}$ from both sides;

$$0 = - \left[\begin{array}{l} \text{mass } \text{Al}_2\text{O}_3 \text{ in} \\ \text{descending coke} \end{array} \right] * 1 + \left[\begin{array}{l} \text{mass C in} \\ \text{descending coke} \end{array} \right] * 0.0333 \quad (34.2)$$

where the masses are per 1000 kg of Fe in product molten iron.

This equation requires, of course, that there is no C-in-coke oxidation in the blast furnace top segment, as specified in Section 7.12.

34.4 SiO_2 IN DESCENDING COKE EQUATION

The new SiO_2 in descending coke equation is developed exactly like the above Al_2O_3 in descending coke equation. With 7 mass% SiO_2 and 90 mass% C in the coke, the basic equation is;

$$\frac{\left[\begin{array}{l} \text{mass } \text{SiO}_2 \text{ in} \\ \text{descending coke} \end{array} \right]}{\left[\begin{array}{l} \text{mass C in} \\ \text{descending coke} \end{array} \right]} = \frac{\left[\begin{array}{l} 7 \text{ mass\% } \text{SiO}_2 \text{ in} \\ \text{descending coke} \end{array} \right]}{\left[\begin{array}{l} 90 \text{ mass\% C in} \\ \text{descending coke} \end{array} \right]} = 0.0778 \quad (34.3)$$

or

$$\left[\begin{array}{l} \text{mass } \text{SiO}_2 \text{ in} \\ \text{descending coke} \end{array} \right] * 1 = \left[\begin{array}{l} \text{mass C in} \\ \text{descending coke} \end{array} \right] * 0.0778$$

or subtracting $\left\{ \left[\begin{array}{l} \text{mass } \text{SiO}_2 \text{ in} \\ \text{descending coke} \end{array} \right] * 1 \right\}$ from both sides;

$$0 = - \left[\begin{array}{l} \text{mass } \text{SiO}_2 \text{ in} \\ \text{descending coke} \end{array} \right] * 1 + \left[\begin{array}{l} \text{mass C in} \\ \text{descending coke} \end{array} \right] * 0.0778 \quad (34.4)$$

where the masses are per 1000 kg of Fe in product molten iron.

34.5 ALTERED BOTTOM-SEGMENT Al_2O_3 AND SiO_2 MASS BALANCES

Descent of Al_2O_3 -in-coke and SiO_2 -in-coke into the bottom-segment changes both of their mass balances.

Al_2O_3 mass balance equation of Chapter 32, Bottom-Segment Slag Calculations—Ore, Fluxes, and Slag;

$$\left[\begin{array}{l} \text{mass } \text{Al}_2\text{O}_3 \text{ in} \\ \text{descending flux} \end{array} \right] = \left[\begin{array}{l} \text{mass } \text{Al}_2\text{O}_3 \text{ in} \\ \text{molten slag} \end{array} \right]$$

becomes;

$$\begin{aligned} & \left[\begin{array}{l} \text{mass } \text{Al}_2\text{O}_3 \text{ in} \\ \text{descending flux} \end{array} \right] + \left[\begin{array}{l} \text{mass } \text{Al}_2\text{O}_3 \text{ in} \\ \text{descending coke} \end{array} \right] \\ &= \left[\begin{array}{l} \text{mass } \text{Al}_2\text{O}_3 \text{ in} \\ \text{molten slag} \end{array} \right] \end{aligned} \quad (34.5)$$

or subtracting $\left\{ \left[\begin{array}{l} \text{mass } \text{Al}_2\text{O}_3 \text{ in} \\ \text{descending flux} \end{array} \right] \right\}$ from both sides;

$$\begin{aligned} 0 &= - \left[\begin{array}{l} \text{mass } \text{Al}_2\text{O}_3 \text{ in} \\ \text{descending flux} \end{array} \right] * 1 \\ &\quad - \left[\begin{array}{l} \text{mass } \text{Al}_2\text{O}_3 \text{ in} \\ \text{descending coke} \end{array} \right] * 1 \\ &\quad + \left[\begin{array}{l} \text{mass } \text{Al}_2\text{O}_3 \text{ in} \\ \text{molten slag} \end{array} \right] * 1 \end{aligned} \quad (34.6)$$

Likewise, SiO_2 mass balance equation of Chapter 32, Bottom-Segment Slag Calculations—Ore, Fluxes, and Slag;

$$\left[\begin{array}{l} \text{mass } \text{SiO}_2 \text{ in} \\ \text{descending ore} \end{array} \right] = \left[\begin{array}{l} \text{mass } \text{SiO}_2 \text{ in} \\ \text{molten slag} \end{array} \right] \quad (32.3)$$

becomes;

$$\begin{aligned} & \left[\begin{array}{l} \text{mass } \text{SiO}_2 \text{ in} \\ \text{descending ore} \end{array} \right] + \left[\begin{array}{l} \text{mass } \text{SiO}_2 \text{ in} \\ \text{descending coke} \end{array} \right] \\ &= \left[\begin{array}{l} \text{mass } \text{SiO}_2 \text{ in} \\ \text{molten slag} \end{array} \right] \end{aligned} \quad (34.7)$$

or subtracting $\left\{ \left[\begin{array}{l} \text{mass } \text{SiO}_2 \text{ in} \\ \text{descending ore} \end{array} \right] + \left[\begin{array}{l} \text{mass } \text{SiO}_2 \text{ in} \\ \text{descending coke} \end{array} \right] \right\}$ from both sides

$$\begin{aligned} 0 &= - \left[\begin{array}{l} \text{mass } \text{SiO}_2 \text{ in} \\ \text{descending ore} \end{array} \right] * 1 \\ &\quad - \left[\begin{array}{l} \text{mass } \text{SiO}_2 \text{ in} \\ \text{descending coke} \end{array} \right] * 1 \\ &\quad + \left[\begin{array}{l} \text{mass } \text{SiO}_2 \text{ in} \\ \text{molten slag} \end{array} \right] * 1 \end{aligned} \quad (34.8)$$

This equation specifies that there is no reduction of SiO_2 to Si (ℓ) in molten iron. Chapter 35, Bottom Segment Calculations - Reduction of SiO_2 , removes this restriction.

34.6 ALTERED ENTHALPY BALANCE

This chapter's two new variables;

$$\left[\begin{array}{l} \text{mass Al}_2\text{O}_3 \text{ in} \\ \text{descending coke} \end{array} \right]$$

and

$$\left[\begin{array}{l} \text{mass SiO}_2 \text{ in} \\ \text{descending coke} \end{array} \right]$$

change the bottom-segment enthalpy balance Eq. (32.11) to;

$$\begin{aligned}
 -320 = & -[\text{mass Fe}_{0.947}\text{O into bottom segment}] * (-3.152) \\
 & -[\text{mass C in descending coke}] * 1.359 \\
 & -[\text{mass O}_2 \text{ in blast air}] * 1.239 \\
 & -[\text{mass N}_2 \text{ in blast air}] * 1.339 \\
 & -[\text{mass Al}_2\text{O}_3 \text{ descending in flux}] * (-15.41) \\
 & -[\text{mass Al}_2\text{O}_3 \text{ in descending coke}] * (-15.41) \\
 & -[\text{mass CaO descending in flux}] * (-10.50) \\
 & -[\text{mass MgO descending in flux}] * (-13.84) \\
 & -[\text{mass SiO}_2 \text{ in descending ore}] * (-14.13) \\
 & -[\text{mass SiO}_2 \text{ in descending coke}] * (-14.13) \\
 & +[\text{mass Fe out in molten iron}] * 1.269 \\
 & +[\text{mass C out in molten iron}] * 5 \\
 & +[\text{mass CO gas out in ascending gas}] * (-2.926) \\
 & +[\text{mass CO}_2 \text{ out in ascending gas}] * (-7.926) \\
 & +[\text{mass N}_2 \text{ out in ascending gas}] * 1.008 \\
 & +[\text{mass Al}_2\text{O}_3 \text{ out in molten slag}] * (-13.58) \\
 & +[\text{mass CaO out in molten slag}] * (-8.495) \\
 & +[\text{mass MgO out in molten slag}] * (-11.14) \\
 & +[\text{mass SiO}_2 \text{ out in molten slag}] * (-13.28)
 \end{aligned} \tag{34.9}$$

2. new Al_2O_3 -in-coke and SiO_2 -in-coke concentration specification equations,
3. altered Al_2O_3 and SiO_2 mass balance equations, and
4. an altered enthalpy balance equation.

34.8 RESULTS

Figs. 34.2 and 34.3 show the effect of the mass $(\text{Al}_2\text{O}_3 + \text{SiO}_2)$ -in-coke on steady-state bottom segment and hence whole furnace C-in-coke and O_2 -in-blast requirements. Both increase.

This is because coke's SiO_2 and Al_2O_3 in ash must be heated and melted in the bottom segment, requiring more combustion of C-in-coke by O_2 -in-blast.

34.9 SUMMARY

This chapter shows how;

- Al_2O_3 -in-coke, and
- SiO_2 -in-coke

are included in our blast furnace calculations.

Mass% Al_2O_3 -in-coke and mass% SiO_2 -in-coke are specified, and two new variables;

$$\left[\begin{array}{l} \text{mass Al}_2\text{O}_3 \text{ in} \\ \text{descending coke} \end{array} \right]$$

and

$$\left[\begin{array}{l} \text{mass SiO}_2 \text{ in} \\ \text{descending coke} \end{array} \right]$$

are introduced then related to;

$$\left[\begin{array}{l} \text{mass C in} \\ \text{descending coke} \end{array} \right]$$

Al_2O_3 , SiO_2 , and enthalpy balances of matrix Table 32.1 are then altered to include the new variables as shown in Table 34.1.

The results show that a blast furnace's steady-state C-in-coke and O_2 -in-blast are both

34.7 MATRIX AND CALCULATIONS

Tables 34.1 and 34.2 are bottom-segment matrix Tables 32.1 and 32.2 plus;

1. new $\left[\begin{array}{l} \text{mass Al}_2\text{O}_3 \text{ in} \\ \text{descending coke} \end{array} \right]$ and $\left[\begin{array}{l} \text{mass SiO}_2 \text{ in} \\ \text{descending coke} \end{array} \right]$ variables,

TABLE 34.1 Bottom-Segment Matrix of Fig. 34.1

A	B	C	D	E	F	G	H	I	J	K	L
BOTTOM SEGMENT CALCULATIONS											
Equation	Description	Numerical term	mass Fe _{0.947} O into bottom segment	mass C in descending coke	mass O ₂ in blast air	mass N ₂ in blast air	mass Fe out in molten iron	mass C out in molten iron	mass CO out in ascending gas	mass CO ₂ out in ascending gas	mass N ₂ out in ascending gas
2	7.7 Fe out in molten iron specification	1000	0	0	0	0	1	0	0	0	0
3	32.2 SiO ₂ descending in ore	0	0	0	0	0.0753	0	0	0	0	0
4	34.4 SiO ₂ in coke specification	0	0	0.0778	0	0	0	0	0	0	0
5	7.2 Fe mass balance	0	-0.768	0	0	0	1	0	0	0	0
6	7.3 O mass balance	0	-0.232	0	-1	0	0	0	0.571	0.727	0
7	7.4 C mass balance	0	0	-1	0	0	0	1	0.429	0.273	0
8	34.8 SiO ₂ mass balance	0	0	0	0	0	0	0	0	0	0
9	7.5 N mass balance	0	0	0	0	-1	0	0	0	0	1
10	7.6 N ₂ in blast air specification	0	0	0	3.3	-1	0	0	0	0	0
11	7.9 Equilibrium CO ₂ /CO mass ratio	0	0	0	0	0	0	0	0.694	-1	0
12	7.8 C out in molten iron specification	0	0	0	0	0	0.047	-1	0	0	0
13	34.2 Al ₂ O ₃ in coke specification	0	0	0.0333	0	0	0	0	0	0	0
14	32.5 Al ₂ O ₃ out in molten slag specification	0	0	0	0	0	0	0	0	0	0
15	34.6 Al ₂ O ₃ mass balance	0	0	0	0	0	0	0	0	0	0
16	32.6 CaO out in molten slag specification	0	0	0	0	0	0	0	0	0	0
17	32.9 CaO mass balance	0	0	0	0	0	0	0	0	0	0
18	32.7 MgO out in molten slag specification	0	0	0	0	0	0	0	0	0	0
19	32.10 MgO mass balance	0	0	0	0	0	0	0	0	0	0
20	34.9 Enthalpy balance	-320	3.152	-1.359	-1.239	-1.339	1.269	5	-2.926	-7.926	1.008
21			930°C	930°C	1200°C	1200°C	1500°C	1500°C	930°C	930°C	930°C
22											

M	N	O	P	Q	R	S	T	U	V	
mass SiO ₂ in descending ore	mass SiO ₂ in descending coke	mass SiO ₂ out in molten slag	mass Al ₂ O ₃ in descending flux	mass Al ₂ O ₃ in descending coke	mass Al ₂ O ₃ out in molten slag	mass CaO in descending flux	mass CaO out in molten slag	mass MgO in descending flux	mass MgO out in molten slag	
3	0	0	0	0	0	0	0	0	0	
4	-1	0	0	0	0	0	0	0	0	
5	0	-1	0	0	0	0	0	0	0	
6	0	0	0	0	0	0	0	0	0	
7	0	0	0	0	0	0	0	0	0	
8	0	0	0	0	0	0	0	0	0	
9	-1	-1	1	0	0	0	0	0	0	
10	0	0	0	0	0	0	0	0	0	
11	0	0	0	0	0	0	0	0	0	
12	0	0	0	0	0	0	0	0	0	
13	0	0	0	0	0	0	0	0	0	
14	0	0	0	-1	0	0	0	0	0	
15	0	0	0.256	0	0	-1	0	0	0	
16	0	0	0	-1	-1	1	0	0	0	
17	0	0	1.05	0	0	0	0	-1	0	
18	0	0	0	0	0	-1	1	0	0	
19	0	0	0.256	0	0	0	0	0	-1	
20	0	0	0	0	0	0	0	-1	1	
21	14.13	14.13	-13.28	15.41	15.41	-13.58	10.50	-8.495	13.84	-11.14
22	930°C	930°C	1500°C	930°C	930°C	1500°C	930°C	1500°C	930°C	1500°C

Remember that 0.0778 in Cell E5 is $\frac{7 \text{ mass\% SiO}_2 \text{ in descending coke}}{90 \text{ mass\% C in descending coke}}$ and 0.0333 in Cell E14 is $\frac{3 \text{ mass\% Al}_2\text{O}_3 \text{ in descending coke}}{90 \text{ mass\% C in descending coke}}$.

This is Table 32.1 with two new variables (mass Al₂O₃ and SiO₂ in descending coke) and two new equations (mass Al₂O₃-in-coke and mass SiO₂-in-coke) plus modified Al₂O₃, SiO₂, and enthalpy balances. The calculated results are shown in Table 34.2.

TABLE 34.2 Solution to Matrix of Table 34.1

	A	B	C	D	E	F	G
			kg per 1000 kg of Fe out in molten iron				
23		Bottom segment calculated values					
24		mass Fe _{0.947} O into bottom segment	1302				
25		mass C in descending coke	415	also = mass C in the furnace's coke charge, Eqn. (7.16)			
26		mass O ₂ in blast air	338				
27		mass N ₂ in blast air	1117				
28		mass Fe out in molten iron	1000				
29		mass C out in molten iron	47				
30		mass CO out in ascending gas	595				
31		mass CO ₂ out in ascending gas	413				
32		mass N ₂ out in ascending gas	1117				
33		mass SiO ₂ in descending ore	75				
34		mass SiO ₂ in descending coke	32				
35		mass SiO ₂ out in molten slag	108				
36		mass Al ₂ O ₃ in descending flux	14				
37		mass Al ₂ O ₃ in descending coke	14				
38		mass Al ₂ O ₃ out in molten slag	28				
39		mass CaO in descending flux	113				
40		mass CaO out in molten slag	113				
41		mass MgO in descending flux	28				
42		mass MgO out in molten slag	28				
43							

C-in-coke and O₂-in-blast for steady production of molten iron and molten slag, 1500°C, are shown to be 415 kg C-in-coke and 338 kg O₂-in-blast; with Al₂O₃-in-coke and SiO₂-in-coke as compared to 408 kg C-in-coke and 326 kg O₂-in-blast of Table 32.1; without Al₂O₃ and SiO₂ in coke.

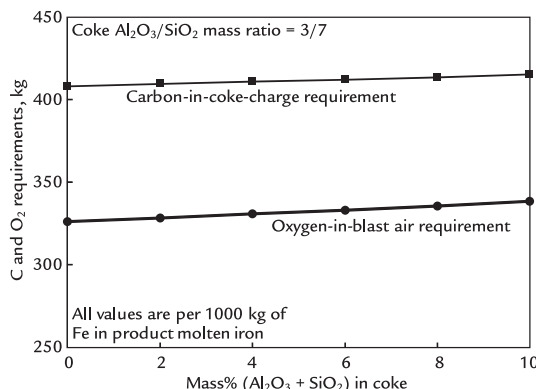


FIGURE 34.2 Effect of mass% ($\text{Al}_2\text{O}_3 + \text{SiO}_2$)-in-coke on C-in-coke and O₂-in-blast requirement for steady production of molten iron and slag, 1500°C. Both increase. The $\text{Al}_2\text{O}_3/\text{SiO}_2$ mass ratio in the coke is constant at 3/7. The lines are not straight because an increase in mass% ($\text{Al}_2\text{O}_3 + \text{SiO}_2$)-in-coke causes a commensurate decrease in mass% C-in-coke as discussed in caption of Fig. 32.4.

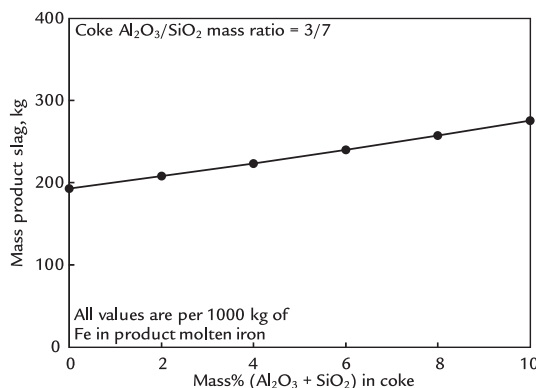


FIGURE 34.3 Slag mass as a function of mass% ($\text{Al}_2\text{O}_3 + \text{SiO}_2$) in top-charge coke. The increase is about 8 kg/mass% ($\text{Al}_2\text{O}_3 + \text{SiO}_2$)-in-coke. The line is not straight because an increase in mass% ($\text{Al}_2\text{O}_3 + \text{SiO}_2$)-in-coke causes a commensurate decrease in mass% C-in-coke (as described in the caption of Fig. 32.4).

increased by Al_2O_3 -in-coke and SiO_2 -in-coke. This is because the SiO_2 -in-coke must be heated and melted in the bottom segment, requiring more oxidation of C-in-coke by O₂-in-blast.

As expected, SiO_2 -in-coke also increases slag mass. This is the result of the coke's SiO_2 plus the increased amounts of CaO and MgO flux that are required to maintain specified slag composition of Section 32.6.

For the values used in this chapter, the coke's Al_2O_3 has a negligible effect on blast furnace requirements because it merely lowers the requirement for Al_2O_3 flux. This can change when the Al_2O_3 input from ore and coke is very high as experienced in India and China for example.

EXERCISES

All masses in this problem set are in kg per 1000 kg of Fe in product molten iron.

- 34.1.** A blast furnace company receives coking coal from a new supplier. The coke product from this new coal contains 5 mass% Al_2O_3 and 5 mass% SiO_2 , remainder carbon.

What effect will this new coke have on;

- C-in-coke,
- coke,
- O₂-in-blast,
- blast,
- Al_2O_3 flux,
- CaO flux,
- MgO flux, and
- SiO_2 flux of [Table 34.1](#)

requirements for steady production of;

- 1500°C molten iron: 4.5 mass% C, 95.5 mass% Fe, and
- 1500°C molten slag: 10 mass% Al_2O_3 , 41 mass% CaO, 10 mass% MgO, and 39 mass% SiO_2 ?

Also, what mass of slag will be produced by this operation?

- 34.2.** A cement manufacturer wishes to try slag that contains;
- 12 mass% Al_2O_3 ,
 - 40 mass% CaO,

- c. 10 mass% MgO, and
- d. 38 mass% SiO₂.

Blast furnace team of [Table 34.1](#) wishes to ascertain what flux masses will be necessary to produce this slag while steadily producing

1500°C molten iron, 4.5 mass% C and 95.5 mass% Fe.

Please determine these for them.

Notice that this slag composition is the same as that in Exercise 32.1.

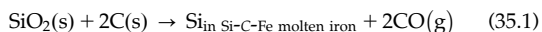
Bottom-Segment Calculations - Reduction of SiO₂

O U T L I N E

35.1 Silica Reduction	299	35.5 Bottom-Segment Oxygen Balance	302
35.2 Calculation Strategy	300	35.6 Bottom-Segment Enthalpy Equation	302
35.3 C- and Si-in-Iron Specification Equations	300	35.7 Matrix and Calculation Results	303
35.3.1 Mass Si in Product Molten Iron Equation	301	35.7.1 Flux Requirements	303
35.4 Bottom-Segment Steady-State SiO ₂ Balance Equation	301	35.8 Summary	306
		Exercises	306

35.1 SILICA REDUCTION

A small amount of SiO₂ in the coal and coke ash is inadvertently reduced to Si in the blast furnace bottom segment. Silicon in hot metal is commonly regarded as a thermal indicator of the blast furnace process. The overall reaction is;



The objectives of this chapter are to examine this SiO₂ reduction from the points of view of how it affects;

1. steady-state C-in-coke and O₂-in-blast requirements for steady production of 1500°C, 0.4 mass% Si, 4.5 mass% C, 95.1 mass% C molten iron, Fig. 35.1, and
 2. steady-state Al₂O₃, CaO, and MgO-in flux requirements to steadily produce;
 - a. 10 mass% Al₂O₃,
 - b. 41 mass% CaO,
 - c. 10 mass% MgO, and
 - d. 39 mass% SiO₂
- molten slag at 1500°C, of Chapter 32, Bottom-Segment Slag Calculations—Ore, Fluxes, and Slag.

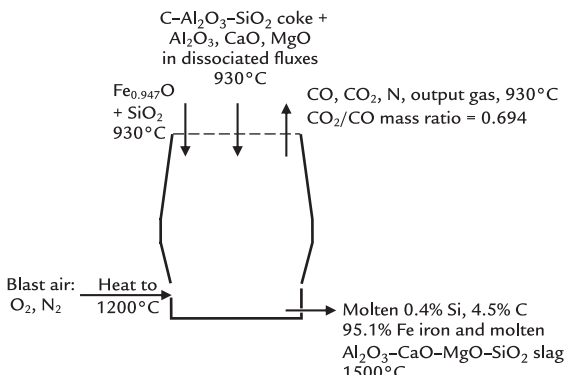


FIGURE 35.1 Blast furnace conceptual bottom segment showing that the product molten iron contains 0.4% Si. For simplicity, there are no tuyere injectants in this chapter.

Silicon transfer in the blast furnace is complex. From a mass and enthalpy balance perspective, the mass% Si in product molten iron is lowered by decreasing tuyere raceway flame temperature - which has the effect of decreasing molten iron temperature. It is raised by increasing raceway flame temperature. Si in hot metal is also impacted by blast pressure and slag chemistry, details provided in Chapter 58, Blast Furnace Slag.

Si oxidation from blast furnace iron during oxygen steelmaking serves as fuel for melting steel scrap - the larger the %Si, the larger the scrap smelting capability. This can be beneficial when scrap prices are low and scrap is readily available.

35.2 CALCULATION STRATEGY

Our calculation strategy for this chapter is to;

- specify a target molten iron composition, 0.4% Si, 4.5% C, and 95.1% Fe, [Fig. 35.1](#);
- develop equations that relate;
 - mass Si out in product molten iron, and

- b. mass C out in product molten iron to mass% Si and mass% C in product molten iron;
- 3. alter the steady state bottom segment;
 - SiO_2 ,
 - O, and
 - enthalpy balances to include $\text{SiO}_2 \rightarrow \text{Si}$ reduction; and
- 4. prepare a matrix that includes these equations and calculates C-in-coke, O₂-in-blast, and Al_2O_3 , CaO , and MgO flux requirements of the blast furnace for steady production of the above-specified molten iron and slag.

As always, all masses are per 1000 kg of Fe in product molten iron.

35.3 C- AND Si-IN-IRON SPECIFICATION EQUATIONS

Product molten iron of this chapter is specified to contain;

- 0.4% mass% Si,
- 4.5% mass% C, and
- 95.1% mass% Fe.

Its;

$$\frac{\text{mass C}}{\text{mass Fe}} \text{ ratio} = \frac{4.5 \text{ mass\% C}}{100 - 4.5 \text{ mass\% C} - 0.4 \text{ mass\% Si}} = \frac{4.5 \text{ mass\% C}}{95.1 \text{ mass\% Fe}} = 0.0473$$

which, in terms of our matrix variables, may be written as;

$$\left[\frac{\text{mass C out in product molten iron}}{\text{mass Fe out in product molten iron}} \right] = 0.0473$$

or

$$\begin{aligned} & \left[\frac{\text{mass C out in product molten iron}}{\text{mass Fe out in product molten iron}} \right] * 1 \\ &= \left[\frac{\text{mass Fe out in product molten iron}}{\text{mass C out in product molten iron}} \right] * 0.0473 \end{aligned} \quad (35.2)$$

or subtracting $\left\{ \left[\frac{\text{mass C out in}}{\text{product molten iron}} \right] * 1 \right\}$ from both sides;

$$0 = - \left[\frac{\text{mass C out in}}{\text{product molten iron}} \right] * 1 + \left[\frac{\text{mass Fe out in}}{\text{product molten iron}} \right] * 0.0473 \quad (35.3)$$

35.3.1 Mass Si in Product Molten Iron Equation

The Si/Fe mass ratio of the specified product molten iron is;

$$\begin{aligned} \frac{\text{mass Si}}{\text{mass Fe}} &= \frac{0.4 \text{ mass\% Si}}{100 - 4.5 \text{ mass\% C} - 0.4 \text{ mass\% Si}} \\ &= \frac{0.4 \text{ mass\% Si}}{95.1 \text{ mass\% Fe}} = 0.00421 \end{aligned}$$

or in matrix terms;

$$\frac{\left[\frac{\text{mass Si out in}}{\text{product molten iron}} \right]}{\left[\frac{\text{mass Fe out in}}{\text{product molten iron}} \right]} = 0.00421$$

or

$$\begin{aligned} \left[\frac{\text{mass Si out in}}{\text{product molten iron}} \right] * 1 \\ = \left[\frac{\text{mass Fe out in}}{\text{product molten iron}} \right] * 0.00421 \end{aligned} \quad (35.4)$$

or subtracting $\left\{ \left[\frac{\text{mass Si out in}}{\text{product molten iron}} \right] * 1 \right\}$ from both sides;

$$0 = - \left[\frac{\text{mass Si out in}}{\text{product molten iron}} \right] * 1 + \left[\frac{\text{mass Fe out in}}{\text{product molten iron}} \right] * 0.00421 \quad (35.5)$$

35.4 BOTTOM-SEGMENT STEADY-STATE SiO₂ BALANCE EQUATION

This section develops a new steady-state SiO₂ balance for the bottom segment. With SiO₂ → Si reduction this balance is;

$$\begin{aligned} \left[\frac{\text{mass SiO}_2 \text{ into}}{\text{bottom segment}} \right] * 1 &= \left[\frac{\text{mass SiO}_2 \text{ in}}{\text{product molten slag}} \right] * 1 \\ &\quad + \left[\frac{\text{mass SiO}_2 \text{ reduced to Si}}{\text{and O in bottom segment}} \right] * 1 \end{aligned} \quad (35.6)$$

The last term is new. It is related to $\left[\frac{\text{mass Si out in}}{\text{product molten iron}} \right]$ by the equation;

$$\begin{aligned} \left[\frac{\text{mass SiO}_2 \text{ reduced to Si}}{\text{and O in bottom segment}} \right] * 1 \\ = \left[\frac{\text{mass Si out in}}{\text{product molten iron}} \right] * \frac{\text{MW}_{\text{SiO}_2}}{\text{MW}_{\text{Si}}} \\ = \left[\frac{\text{mass Si out in}}{\text{product molten iron}} \right] * \frac{60.1}{28.1} \end{aligned}$$

(1 kg mol of Si production consumes 1 kg mol of SiO₂) or;

$$\begin{aligned} \left[\frac{\text{mass SiO}_2 \text{ reduced to Si}}{\text{and O in bottom segment}} \right] * 1 \\ = \left[\frac{\text{mass Si out in}}{\text{product molten iron}} \right] * 2.14 \end{aligned}$$

so that Eq. (32.3) becomes;

$$\begin{aligned} \left[\frac{\text{mass SiO}_2 \text{ into}}{\text{bottom segment}} \right] * 1 &= \left[\frac{\text{mass SiO}_2 \text{ in}}{\text{product molten slag}} \right] * 1 \\ &\quad + \left[\frac{\text{mass Si out in}}{\text{product molten iron}} \right] * 2.14 \end{aligned} \quad (35.7)$$

or including two sources of input SiO₂ of the bottom segment;

$$\begin{aligned} \left[\frac{\text{mass SiO}_2 \text{ in}}{\text{descending ore}} \right] * 1 + \left[\frac{\text{mass SiO}_2 \text{ in}}{\text{descending coke}} \right] * 1 \\ = \left[\frac{\text{mass SiO}_2 \text{ in}}{\text{product molten slag}} \right] * 1 \\ + \left[\frac{\text{mass Si out in}}{\text{product molten iron}} \right] * 2.14 \end{aligned} \quad (35.8)$$

or subtracting $\left\{ \left[\frac{\text{mass SiO}_2 \text{ in}}{\text{descending ore}} \right] * 1 + \left[\frac{\text{mass SiO}_2 \text{ in}}{\text{descending coke}} \right] * 1 \right\}$ from both sides;

$$0 = - \left[\begin{array}{l} \text{mass SiO}_2 \text{ in} \\ \text{descending ore} \end{array} \right] * 1 - \left[\begin{array}{l} \text{mass SiO}_2 \text{ in} \\ \text{descending coke} \end{array} \right] * 1 \\ + \left[\begin{array}{l} \text{mass SiO}_2 \text{ in} \\ \text{product molten slag} \end{array} \right] * 1 \\ + \left[\begin{array}{l} \text{mass Si out in} \\ \text{product molten iron} \end{array} \right] * 2.14 \quad (35.9)$$

or subtracting $\left\{ \begin{array}{l} \text{mass Fe}_{0.947}\text{O into} \\ \text{bottom segment} \end{array} \right\} * 0.232 + \left[\begin{array}{l} \text{mass O}_2 \\ \text{in blast air} \end{array} \right] * 1 + \left[\begin{array}{l} \text{mass Si out in} \\ \text{product molten iron} \end{array} \right] * 1.14 \right\}$ from both sides;

$$0 = - \left[\begin{array}{l} \text{mass Fe}_{0.947}\text{O into} \\ \text{bottom segment} \end{array} \right] * 0.232 - \left[\begin{array}{l} \text{mass O}_2 \\ \text{in blast air} \end{array} \right] * 1 \\ - \left[\begin{array}{l} \text{mass Si out in} \\ \text{product molten iron} \end{array} \right] * 1.14 \\ + \left[\begin{array}{l} \text{mass CO out} \\ \text{in ascending gas} \end{array} \right] * 0.571 \\ + \left[\begin{array}{l} \text{mass CO}_2 \text{ out} \\ \text{in ascending gas} \end{array} \right] * 0.727 \quad (35.12)$$

35.5 BOTTOM-SEGMENT OXYGEN BALANCE

This section develops a new steady-state bottom-segment oxygen balance equation.

The bottom-segment oxygen balance with SiO₂ → Si reduction is;

$$\left[\begin{array}{l} \text{mass O into} \\ \text{bottom segment} \end{array} \right] + \left[\begin{array}{l} \text{mass O released} \\ \text{by SiO}_2 \text{ reduction} \\ \text{in bottom segment} \end{array} \right] \quad (35.10) \\ = \left[\begin{array}{l} \text{mass O ascending out} \\ \text{of bottom segment} \end{array} \right]$$

where $\left[\begin{array}{l} \text{mass O released} \\ \text{by SiO}_2 \text{ reduction} \\ \text{in bottom segment} \end{array} \right]$ is the amount of O originally in the SiO₂ that departs the bottom segment in ascending CO(g) and CO₂(g).

The $\left[\begin{array}{l} \text{mass O released} \\ \text{by SiO}_2 \text{ reduction} \\ \text{in bottom segment} \end{array} \right]$ term is new. It is;

$$\left[\begin{array}{l} \text{mass O released} \\ \text{by SiO}_2 \text{ reduction} \end{array} \right] = \left[\begin{array}{l} \text{mass Si out in} \\ \text{product molten iron} \end{array} \right] * \frac{\text{MW}_{\text{O}_2}}{\text{MW}_{\text{Si}}} \\ = \left[\begin{array}{l} \text{mass Si out in} \\ \text{product molten iron} \end{array} \right] * \frac{32}{28} \\ = \left[\begin{array}{l} \text{mass Si out in} \\ \text{product molten iron} \end{array} \right] * 1.14$$

Including the right side of this equation, bottom-segment oxygen balance (7.3) becomes;

$$\left[\begin{array}{l} \text{mass Fe}_{0.947}\text{O into} \\ \text{bottom segment} \end{array} \right] * 0.232 + \left[\begin{array}{l} \text{mass O}_2 \\ \text{in blast air} \end{array} \right] * 1 \\ + \left[\begin{array}{l} \text{mass Si out in} \\ \text{product molten iron} \end{array} \right] * 1.14 \quad (35.11) \\ = \left[\begin{array}{l} \text{mass CO out} \\ \text{in ascending gas} \end{array} \right] * 0.571 \\ + \left[\begin{array}{l} \text{mass CO}_2 \text{ out} \\ \text{in ascending gas} \end{array} \right] * 0.727$$

Note that this balance does not include O in unreduced SiO₂ and flux oxides.

35.6 BOTTOM-SEGMENT ENTHALPY EQUATION

The bottom-segment enthalpy balance *without* SiO₂ reduction is;

$$- 320 = - [\text{mass Fe}_{0.947}\text{O into bottom segment}] * (-3.152) \\ - [\text{mass C in descending coke}] * 1.359 \\ - [\text{mass O}_2 \text{ in blast}] * 1.239 \\ - [\text{mass N}_2 \text{ in blast}] * 1.339 \\ - [\text{mass Al}_2\text{O}_3 \text{ in descending flux}] * (-15.41) \\ - [\text{mass Al}_2\text{O}_3 \text{ in descending coke}] * (-15.41) \\ - [\text{mass CaO in descending flux}] * (-10.50) \\ - [\text{mass MgO in descending flux}] * (-13.84) \\ - [\text{mass SiO}_2 \text{ in descending ore}] * (-14.13) \\ - [\text{mass SiO}_2 \text{ in descending coke}] * (-14.13) \\ + [\text{mass Fe out in molten iron}] * 1.269 \\ + [\text{mass C out in molten iron}] * 5 \\ + [\text{mass CO gas out in ascending gas}] * (-2.926) \\ + [\text{mass CO}_2 \text{ out in ascending gas}] * (-7.926) \\ + [\text{mass N}_2 \text{ out in ascending gas}] * 1.008 \\ + [\text{mass Al}_2\text{O}_3 \text{ out in molten slag}] * (-13.58) \\ + [\text{mass CaO out in molten slag}] * (-8.495) \\ + [\text{mass MgO out in molten slag}] * (-11.14) \\ + [\text{mass SiO}_2 \text{ out in molten slag}] * (-13.28)$$

With SiO_2 reduction to Si-in-molten-iron, we must add the enthalpy term;

$$\left[\frac{\text{mass Si out in}}{\text{product molten iron}} \right] * \frac{H_{1500^\circ\text{C}}}{\frac{\text{Si(dissolved)}}{\text{MW}_{\text{Si}}}}$$

Notice that the output silicon enthalpy is represented by;

$$\frac{H_{1500^\circ\text{C}}}{\frac{\text{Si(dissolved)}}{\text{MW}_{\text{Si}}}}$$

rather than

$$\frac{H_{1500^\circ\text{C}}}{\frac{\text{Si(l)}}{\text{MW}_{\text{Si}}}}$$

This is because the silicon is present in thermodynamically nonideal molten Fe–C–Si alloy.

The enthalpy of Si dissolved in Si–Fe alloy is calculated in Appendix S. It is;

$$\frac{H_{1500^\circ\text{C}}}{\frac{\text{Si(dissolved)}}{\text{MW}_{\text{Si}}}} = -2.15 \text{ MJ/kg of dissolved silicon}$$

With this value, the new enthalpy term is;

$$\left[\frac{\text{mass Si out in}}{\text{product molten iron}} \right] * (-2.15)$$

and the bottom-segment enthalpy equation becomes;

$$\begin{aligned} -320 = & -[\text{mass } \text{Fe}_{0.94}\text{O into bottom segment}] * (-3.152) \\ & -[\text{mass C in descending coke}] * 1.359 \\ & -[\text{mass O}_2 \text{ in blast}] * 1.239 \\ & -[\text{mass N}_2 \text{ in blast}] * 1.339 \\ & -[\text{mass Al}_2\text{O}_3 \text{ in descending flux}] * (-15.41) \\ & -[\text{mass Al}_2\text{O}_3 \text{ in descending coke}] * (-15.41) \\ & -[\text{mass CaO descending in flux}] * (-10.50) \\ & -[\text{mass MgO descending in flux}] * (-13.84) \\ & -[\text{mass SiO}_2 \text{ in descending ore}] * (-14.13) \\ & -[\text{mass SiO}_2 \text{ in descending coke}] * (-14.13) \\ & +[\text{mass Fe out in molten iron}] * 1.269 \\ & +[\text{mass C out in molten iron}] * 5 \\ & +[\text{mass CO gas out in ascending gas}] * (-2.926) \\ & +[\text{mass CO}_2 \text{ out in ascending gas}] * (-7.926) \\ & +[\text{mass N}_2 \text{ out in ascending gas}] * 1.008 \\ & +[\text{mass Al}_2\text{O}_3 \text{ out in molten slag}] * (-13.58) \\ & +[\text{mass CaO out in molten slag}] * (-8.495) \\ & +[\text{mass MgO out in molten slag}] * (-11.14) \\ & +[\text{mass SiO}_2 \text{ out in molten slag}] * (-13.28) \\ & +[\text{mass Si out in product molten iron}] * (-2.15) \end{aligned} \quad (35.13)$$

This and all the equations of Fig. 35.1 are now put in Excel spreadsheet as shown in Table 35.1 and solved.

35.7 MATRIX AND CALCULATION RESULTS

Tables 35.1 and 35.2 show the bottom-segment matrix and its calculated steady-state inputs and outputs with $\text{SiO}_2 \rightarrow \text{Si}$ reduction. They are for the specific case of 0.4 mass% Si, 4.5 mass% C, and 95.1 mass% Fe product molten iron. Production of this iron requires;

- 421 kg of C-in-coke (468 kg of 90% C coke), and
- 342 kg of O₂-in-blast

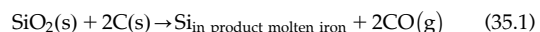
as compared to;

- 415 kg of C-in-coke (461 kg of 90% C coke), and
- 338 kg of O₂-in-blast

with no Si in product molten iron.

We now plot C-in-coke and O₂-in-blast requirements as a function of mass% Si in product molten iron, Fig. 35.2. C-in-coke and O₂-in-blast requirements both increase slightly with increasing mass% Si in iron.

These increases are the result of all of equations of Table 35.1. We may postulate that the extra C-in-coke is required to reduce SiO₂ to Si, that is, for the reaction;



and to provide heat (when combusted with air) for dissociating the SiO₂, the extra O₂-in-blast is required for additional C combustion.

35.7.1 Flux Requirements

Fig. 35.3 plots Al₂O₃, CaO, and MgO flux requirements with $\text{SiO}_2 \rightarrow \text{Si}$ reduction. They show that;

Al₂O₃, CaO, and MgO-in-flux requirements all decrease with increasing mass% Si in product molten iron.

This is because some of the input SiO₂ from ore gangue and coke ash leaves the furnace as Si in molten iron so it doesn't require fluxing.

TABLE 35.1 Bottom-Segment Matrix Including $\text{SiO}_2 \rightarrow \text{Si}$ Reduction

A	B	C	D	E	F	G	H	I	J	K	L
1	BOTTOM SEGMENT CALCULATIONS										
Equation	Description	Numerical term	mass $\text{Fe}_{0.94}\text{O}$ into bottom segment	mass C in descending coke	mass O_2 in blast	mass N_2 in blast	mass Fe out in molten iron	mass C out in molten iron	mass CO out in ascending gas	mass CO_2 out in ascending gas	mass N_2 out in ascending gas
3	7.7 Fe out in molten iron specification	1000	0	0	0	0	1	0	0	0	0
4	32.2 SiO_2 descending in ore	0	0	0	0	0.0753	0	0	0	0	0
5	34.4 SiO_2 in coke specification	0	0	0.0778	0	0	0	0	0	0	0
6	7.2 Fe mass balance	0	-0.768	0	0	0	1	0	0	0	0
7	35.12 O mass balance	0	-0.232	0	-1	0	0	0	0.571	0.727	0
8	7.4 C mass balance	0	-0.232	-1	0	0	0	1	0.429	0.273	0
9	35.9 SiO_2 mass balance	0	0	0	0	0	0	0	0	0	0
10	7.5 N mass balance	0	0	0	0	-1	0	0	0	0	1
11	7.6 N_2 in blast air specification	0	0	0	3.3	-1	0	0	0	0	0
12	7.8 Equilibrium CO/CO mass ratio	0	0	0	0	0	0	0	0.694	-1	0
13	35.2 C out in molten iron specification	0	0	0	0	0	0.0473	-1	0	0	0
14	34.2 Al_2O_3 in coke specification	0	0	0.0333	0	0	0	0	0	0	0
15	32.5 Al_2O_3 out in molten slag specification	0	0	0	0	0	0	0	0	0	0
16	34.6 Al_2O_3 mass balance	0	0	0	0	0	0	0	0	0	0
17	32.6 CaO out in molten slag specification	0	0	0	0	0	0	0	0	0	0
18	32.9 CaO mass balance	0	0	0	0	0	0	0	0	0	0
19	32.7 MgO out in molten slag specification	0	0	0	0	0	0	0	0	0	0
20	32.10 MgO mass balance	0	0	0	0	0	0	0	0	0	0
21	35.13 Enthalpy balance	-320	3.152	-1.359	-1.239	-1.339	1.269	5	2.926	-7.926	1.008
22	35.5 Si out in molten iron specification	0	0	0	0	0	0.00421	0	0	0	0

M	N	O	P	Q	R	S	T	U	V	W	
1											
2	mass SiO_2 in descending ore	mass SiO_2 in descending coke	mass SiO_2 out in molten slag	mass Al_2O_3 in descending flux	mass Al_2O_3 in descending coke	mass Al_2O_3 out in molten slag	mass CaO in descending flux	mass CaO out in molten slag	mass MgO in descending flux	mass MgO out in molten slag	
3	0	0	0	0	0	0	0	0	0	0	
4	-1	0	0	0	0	0	0	0	0	0	
5	0	-1	0	0	0	0	0	0	0	0	
6	0	0	0	0	0	0	0	0	0	0	
7	0	0	0	0	0	0	0	0	0	-1.14	
8	0	0	0	0	0	0	0	0	0	0	
9	-1	-1	1	0	0	0	0	0	0	2.14	
10	0	0	0	0	0	0	0	0	0	0	
11	0	0	0	0	0	0	0	0	0	0	
12	0	0	0	0	0	0	0	0	0	0	
13	0	0	0	0	0	0	0	0	0	0	
14	0	0	0	0	-1	0	0	0	0	0	
15	0	0	0.256	0	0	-1	0	0	0	0	
16	0	0	0	-1	-1	1	0	0	0	0	
17	0	0	1.05	0	0	0	0	-1	0	0	
18	0	0	0	0	0	0	-1	1	0	0	
19	0	0	0.256	0	0	0	0	0	0	-1	
20	0	0	0	0	0	0	0	-1	1	0	
21	14.13	14.13	-13.28	15.41	15.41	-13.58	10.50	-8.495	13.84	-11.14	-2.15
22	0	0	0	0	0	0	0	0	0	-1	

Table 35.1 is matrix Table 34.1 with 0.4 mass% Si, 4.5 mass% C, 95.1 mass% Fe product molten iron. The C-in-iron specification in Row 13 and the Si-in-iron specification equations in Row 22 are notable.

TABLE 35.2 Bottom-Segment Values Calculated by Matrix of Table 35.1

	A	B	C	D	E	F	G
23		Bottom segment calculated values	kg per 1000 kg of Fe out in molten iron				
24		mass Fe _{0.947} O into bottom segment	1302.1				
25		mass C in descending coke	421	also = mass C in the furnace's coke charge, Eqn. (7.16)			
26		mass O ₂ in blast	342				
27		mass N ₂ in blast	1129				
28		mass Fe out in molten iron	1000				
29		mass C out in molten iron	47				
30		mass CO out in ascending gas	604				
31		mass CO ₂ out in ascending gas	419				
32		mass N ₂ out in ascending gas	1129				
33		mass SiO ₂ in descending ore	75				
34		mass SiO ₂ in descending coke	33				
35		mass SiO ₂ out in molten slag	99				
36		mass Al ₂ O ₃ in descending flux	11				
37		mass Al ₂ O ₃ in descending coke	14				
38		mass Al ₂ O ₃ out in molten slag	25				
39		mass CaO in descending flux	104				
40		mass CaO out in molten slag	104				
41		mass MgO in descending flux	25				
42		mass MgO out in molten slag	25				
43		mass Si out in molten iron	4.2				
44							

Steady-state C-in-coke and O₂-in-blast requirements are plotted in Fig. 35.2. Steady-state Al₂O₃, CaO, and MgO flux requirements are plotted in Fig. 35.3.

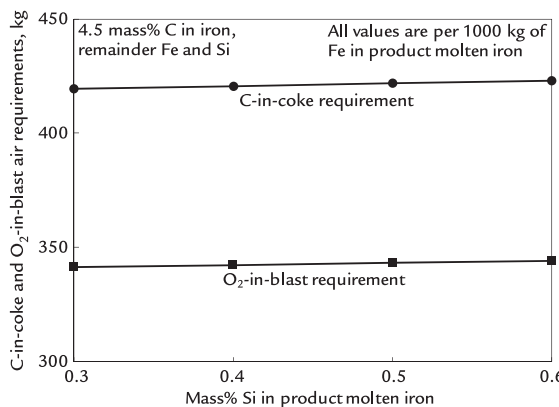


FIGURE 35.2 Steady-state blast furnace C-in-coke and O₂-in-blast requirements with some of input SiO₂ of Fig. 35.1 being reduced to Si in molten iron. C-in-coke and O₂-in-blast requirements both increase slightly with increasing mass% Si in product molten iron. The product molten iron composition is 4.5 mass% C, 95.5 mass% (Si + Fe). The coke is 90 mass% C, so coke requirement = C-in-coke requirement/0.9.

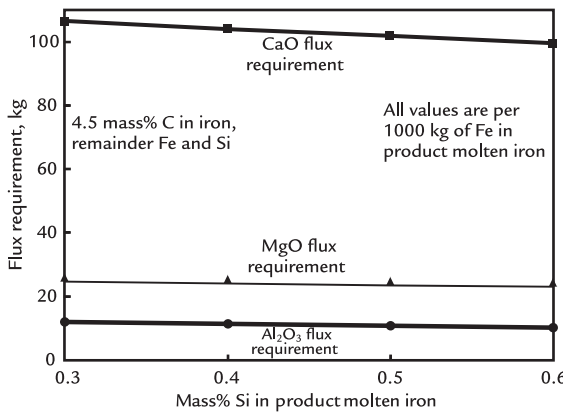


FIGURE 35.3 Steady-state Al₂O₃, CaO, and MgO from flux requirements as affected by mass% Si in product molten iron. The requirements all decrease per 1000 kg of product molten iron because a portion of the top-charged SiO₂ goes to molten iron rather than to molten slag.

35.8 SUMMARY

This chapter shows that Si_{in} product molten iron is readily represented in our matrix calculations. It requires one new equation;

1. Si/Fe mass ratio in product molten iron and four modified equations, that is, steady state bottom segment,
2. C/Fe mass ratio in product molten iron,
3. SiO₂ mass balance,
4. O mass balance, and
5. enthalpy balance.

The calculations show that per 1000 kg of Fe in product molten iron, silicon in blast furnace molten iron;

1. increases the amounts of C-in-coke and O₂-in-blast, and
2. decreases the amounts of Al₂O₃, CaO, and MgO flux

that are required for steady production of 1500°C molten iron and 1500°C molten slag.

EXERCISES

- 35.1. The steel plant that uses 0.4 mass% Si molten blast furnace iron of this chapter to make steel, asks blast furnace operators of this chapter to increase the Si content of their molten iron to 0.5 mass%.

Please;

1. tell the blast furnace operators how to do this;
2. calculate for them the amounts of extra coke and blast air that will be needed to make this higher Si molten iron; and

3. also calculate for them the amounts of Al₂O₃, CaO, and MgO fluxes that will be required to maintain steady production of;
- 10 mass% Al₂O₃,
 - 41 mass% CaO,
 - 10 mass% MgO, and
 - 39 mass% SiO₂
- molten slag.
Please give your numerical answers in kg per 1000 kg of Fe in product molten iron. Perhaps use mass M/mass Fe calculator of Appendix T.
- 35.2. Why might the steelmakers want this higher %Si-in-molten iron?

Bottom-Segment Calculations - Reduction of MnO

OUTLINE

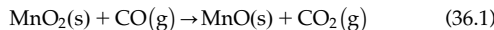
36.1 Manganese and Blast Furnace Operations	309	36.6 Bottom-Segment MnO Reduction Efficiency	312
36.2 Specifications	310	36.7 Bottom-Segment Oxygen Balance With Descending MnO	313
36.3 Calculation Strategy	310	36.8 Bottom-Segment Enthalpy Equation	314
36.4 C-in-Molten Iron Specification Equation	311	<i>36.8.1 Descending MnO Enthalpy</i>	314
<i>36.4.1 Si-in-Molten Iron Specification Equation</i>	311	<i>36.8.2 MnO-in-Product Molten Slag</i>	314
<i>36.4.2 Mn-in-Molten Iron Specification</i>	311	<i>36.8.3 Enthalpy of Dissolved Mn</i>	314
36.5 Bottom-Segment Steady-State Mn Mass Balance	312	36.9 Matrix Calculations and Results	315
		36.10 Summary	315
		Exercises	318

36.1 MANGANESE AND BLAST FURNACE OPERATIONS

Manganese is purposefully present in all molten blast furnace iron. It mostly comes from top-charged pyrolusite (MnO_2) or an iron ore that has an elevated Mn content that is deliberately added to enrich the hot

metal with a small amount of Mn. The molten iron typically contains 0.5 mass% Mn, sometimes up to 1 mass% Mn. Newer grades of sheet steel have increased Mn requirements. Mn-rich ore added at the blast furnace is a low cost option to meet the final steel Mn content.

The pyrolusite is reduced in the top segment of a blast furnace by reactions like;



The product MnO then descends into the bottom segment where it is reduced to Mn in product molten iron by the overall reaction;



Most of this manganese proceeds through steelmaking into the solid steel product where it enhances the steel's;

- hardenability and hardness,
- toughness, and
- machinability.

Mn also diminishes the deleterious effects of inadvertent sulfur-in-product-steel.

Some blast furnace operators monitor the Mn partition ratio ($\text{Mn}_{\text{slag}}/\text{Mn}_{\text{iron}}$) as a thermal control indicator. A sudden increase in this ratio can forecast a decrease in the hot metal temperature.

The objectives of this chapter are to;

1. show how MnO and Mn-in-molten iron are represented in our conceptual bottom-segment calculations, Fig. 36.1, and
2. determine how MnO and Mn affect the steady state of the blast furnace;

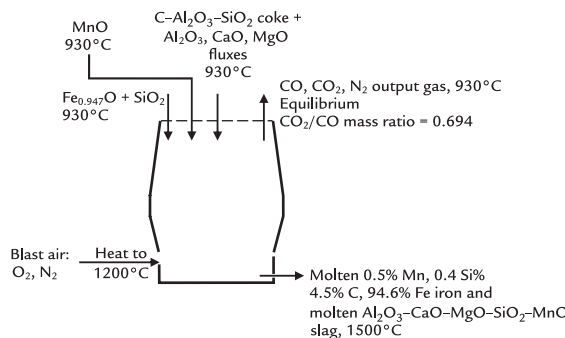


FIGURE 36.1 Conceptual blast furnace bottom segment with descending $\text{MnO}(\text{s})$, 930°C and 0.5 mass% Mn in product molten iron, 1500°C .

- a. C-in-coke,
- b. O₂-in-blast, and
- c. bottom-segment MnO

requirements for steady production of molten iron and slag, 1500°C .

36.2 SPECIFICATIONS

For simplicity, we;

1. specify that the target mass% Mn level in product molten iron is 0.5 mass%, that is, that composition of the iron is;
 - a. 4.5 mass% C,
 - b. 0.4 mass% Si,
 - c. 0.5 mass% Mn, and
 - d. 94.6 mass% Fe;
 2. slightly alter the slag composition to;
 - a. 10 mass% Al_2O_3 ,
 - b. 41 mass% CaO ,
 - c. 10 mass% MgO , and
 - d. 39 mass% SiO_2
- in the $\text{Al}_2\text{O}_3 + \text{CaO} + \text{MgO} + \text{SiO}_2$ portion of the slag + MnO ;
3. specify that manganese enters the blast furnace as pyrolusite (MnO_2) and descends into the bottom segment as MnO, Fig. 36.1; and;
 4. specify that 90% of the Mn-in-top-charge ends up as Mn in product molten iron while 10% ends up as MnO in molten slag.

36.3 CALCULATION STRATEGY

Our calculation strategy is to;

1. develop an equation that relates $\frac{\text{mass Mn in molten iron}}{\text{mass Fe in molten iron}}$ to mass% Mn in the iron;
2. alter the equations that relate;
 - a. $\frac{\text{mass C in molten iron}}{\text{mass Fe in molten iron}}$ to mass% C in the iron, and
 - b. $\frac{\text{mass Si in molten iron}}{\text{mass Fe in molten iron}}$ to mass% Si in the iron;
3. develop an equation that describes 90% reduction of MnO to Mn;

4. develop a bottom-segment steady-state Mn mass balance equation;
5. modify the bottom-segment O and enthalpy balance equations to include descending MnO(s), Mn in product molten iron and MnO in product molten slag;
6. prepare a matrix with these equations; and
7. calculate bottom-segment C-in-coke, O₂-in-blast, MnO, and flux requirements for steady production of 1500°C molten iron and molten slag.

As always, all the equations are based on 1000 kg of Fe in product molten iron.

36.4 C-IN-MOLTEN IRON SPECIFICATION EQUATION

Product molten iron of this chapter is specified to contain;

- 0.5 mass% Mn,
- 0.4 mass% Si,
- 4.5 mass% C, and
- 94.6 mass% Fe.

The molten iron's;

$$\frac{\text{mass C}}{\text{mass Fe}} \text{ ratio} = \frac{4.5 \text{ mass\% C}}{94.6 \text{ mass\% Fe}} = 0.0476$$

which, in terms of our matrix variables, may be written;

$$\frac{\left[\begin{array}{l} \text{mass C out in} \\ \text{product molten iron} \end{array} \right]}{\left[\begin{array}{l} \text{mass Fe out in} \\ \text{product molten iron} \end{array} \right]} = 0.0476$$

or

$$\begin{aligned} & \left[\begin{array}{l} \text{mass C out in} \\ \text{product molten iron} \end{array} \right] * 1 \\ &= \left[\begin{array}{l} \text{mass Fe out in} \\ \text{product molten iron} \end{array} \right] * 0.0476 \end{aligned}$$

or subtracting $\left\{ \left[\begin{array}{l} \text{mass C out in} \\ \text{product molten iron} \end{array} \right] * 1 \right\}$ from both sides;

$$0 = - \left[\begin{array}{l} \text{mass C out in} \\ \text{product molten iron} \end{array} \right] * 1 + \left[\begin{array}{l} \text{mass Fe out in} \\ \text{product molten iron} \end{array} \right] * 0.0476 \quad (36.3)$$

36.4.1 Si-in-Molten Iron Specification Equation

The above-specified 0.4% Si-in-iron concentration is described by;

$$\frac{\text{mass Si}}{\text{mass Fe}} \text{ ratio} = \frac{0.4 \text{ mass\% Si}}{94.6 \text{ mass\% Fe}} = 0.00423$$

or in matrix terms;

$$\frac{\left[\begin{array}{l} \text{mass Si out in} \\ \text{product molten iron} \end{array} \right]}{\left[\begin{array}{l} \text{mass Fe out in} \\ \text{product molten iron} \end{array} \right]} = 0.00423$$

or

$$\left[\begin{array}{l} \text{mass Si out in} \\ \text{product molten iron} \end{array} \right] * 1 = \left[\begin{array}{l} \text{mass Fe out in} \\ \text{product molten iron} \end{array} \right] * 0.00423$$

or subtracting $\left\{ \left[\begin{array}{l} \text{mass Si out in} \\ \text{product molten iron} \end{array} \right] * 1 \right\}$ from both sides;

$$0 = - \left[\begin{array}{l} \text{mass Si out in} \\ \text{product molten iron} \end{array} \right] * 1 + \left[\begin{array}{l} \text{mass Fe out in} \\ \text{product molten iron} \end{array} \right] * 0.00423 \quad (36.4)$$

36.4.2 Mn-in-Molten Iron Specification

Finally, the above-specified 0.5% Mn-in-iron concentration is described by;

$$\frac{\text{mass Mn}}{\text{mass Fe}} \text{ ratio} = \frac{0.5 \text{ mass\% Mn}}{94.6 \text{ mass\% Fe}} = 0.00529$$

or in matrix terms;

$$\frac{\left[\begin{array}{l} \text{mass Mn out in} \\ \text{product molten iron} \end{array} \right]}{\left[\begin{array}{l} \text{mass Fe out in} \\ \text{product molten iron} \end{array} \right]} = 0.00529$$

or

$$\begin{aligned} & \left[\frac{\text{mass Mn out in}}{\text{product molten iron}} \right] * 1 \\ & = \left[\frac{\text{mass Fe out in}}{\text{product molten iron}} \right] * 0.00529 \end{aligned}$$

or subtracting $\left\{ \left[\frac{\text{mass Mn out in}}{\text{product molten iron}} \right] * 1 \right\}$ from both sides;

$$\begin{aligned} 0 = & - \left[\frac{\text{mass Mn out in}}{\text{product molten iron}} \right] * 1 \\ & + \left[\frac{\text{mass Fe out in}}{\text{product molten iron}} \right] * 0.00529 \quad (36.5) \end{aligned}$$

The numerical values in Eqs. (36.3)–(36.5) with changing iron composition are readily calculated with the *C/Fe*, *Si/Fe*, and *Mn/Fe ratio calculator* of Appendix T.

or

$$\begin{aligned} & \left[\frac{\text{mass MnO descending}}{\text{into bottom segment}} \right] * 0.774 \\ & = \left[\frac{\text{mass Mn in product}}{\text{molten iron}} \right] * 1 \\ & + \left[\frac{\text{mass MnO in product}}{\text{molten slag}} \right] * 0.774 \end{aligned}$$

or subtracting $\left\{ \left[\frac{\text{mass MnO descending}}{\text{into bottom segment}} \right] * 0.774 \right\}$ from both sides;

$$\begin{aligned} 0 = & - \left[\frac{\text{mass MnO descending}}{\text{into bottom segment}} \right] * 0.774 \\ & + \left[\frac{\text{mass Mn in product}}{\text{molten iron}} \right] * 1 \\ & + \left[\frac{\text{mass MnO in product}}{\text{molten slag}} \right] * 0.774 \quad (36.7) \end{aligned}$$

36.5 BOTTOM-SEGMENT STEADY-STATE Mn MASS BALANCE

The steady-state bottom-segment Mn mass balance is;

$$\left[\frac{\text{mass Mn into}}{\text{bottom segment}} \right] = \left[\frac{\text{mass Mn out of}}{\text{bottom segment}} \right] \quad (36.6)$$

Mn enters the bottom segment in descending MnO, Fig. 36.1. It leaves the bottom segment as Mn in molten iron and MnO in molten slag. The MnO contains;

- 77.4 mass% Mn, and
- 22.6 mass% O,

As described in Appendix A. Eq. (36.6) therefore expands to;

$$\begin{aligned} & \left[\frac{\text{mass MnO descending}}{\text{into bottom segment}} \right] * \frac{77.4 \text{ mass% Mn in MnO}}{100\%} \\ & = \left[\frac{\text{mass Mn in product}}{\text{molten iron}} \right] * 1 \\ & + \left[\frac{\text{mass MnO in product}}{\text{molten slag}} \right] * \frac{77.4 \text{ mass% Mn in MnO}}{100\%} \end{aligned}$$

36.6 BOTTOM-SEGMENT MnO REDUCTION EFFICIENCY

From industrial data, we specify that;

1. 90% of the MnO entering the bottom segment leaves as Mn in the product molten iron, and
2. 10% of the MnO entering the bottom segment leaves as MnO in the product molten slag.

The latter can be expressed by

$$\begin{aligned} & \left[\frac{\text{mass MnO in product}}{\text{molten slag}} \right] \\ & = \left[\frac{\text{mass MnO descending}}{\text{into bottom segment}} \right] * \frac{10\%}{100\%} \\ & = \left[\frac{\text{mass MnO descending}}{\text{into bottom segment}} \right] * 0.1 \quad (36.8) \end{aligned}$$

or

$$\begin{aligned} & \left[\frac{\text{mass MnO descending}}{\text{into bottom segment}} \right] * 0.1 \\ & = \left[\frac{\text{mass MnO in product}}{\text{molten slag}} \right] * 1 \end{aligned}$$

or subtracting $\left\{ \left[\begin{array}{l} \text{mass MnO descending} \\ \text{into bottom segment} \end{array} \right] * 0.1 \right\}$ from both sides;

$$0 = - \left[\begin{array}{l} \text{mass MnO descending} \\ \text{into bottom segment} \end{array} \right] * 0.1 + \left[\begin{array}{l} \text{mass MnO in product} \\ \text{molten slag} \end{array} \right] * 1 \quad (36.9)$$

The $\left[\begin{array}{l} \text{mass O released} \\ \text{by MnO reduction} \\ \text{in bottom segment} \end{array} \right]$ term is new. It is related to mass Mn in product molten iron by the following equation:

$$\begin{aligned} & \left[\begin{array}{l} \text{mass O released} \\ \text{by MnO reduction} \\ \text{in bottom segment} \end{array} \right] * 1 \\ &= \left[\begin{array}{l} \text{mass Mn out in} \\ \text{product molten iron} \end{array} \right] * \frac{\text{MW}_\text{O}}{\text{MW}_\text{Mn}} \\ &= \left[\begin{array}{l} \text{mass Mn out in} \\ \text{product molten iron} \end{array} \right] * \frac{16}{54.9} \\ &= \left[\begin{array}{l} \text{mass Mn out in} \\ \text{product molten iron} \end{array} \right] * 0.291 \end{aligned}$$

36.7 BOTTOM-SEGMENT OXYGEN BALANCE WITH DESCENDING MnO

This section prepares a steady-state oxygen mass balance equation with MnO and SiO₂ reduction in the conceptual bottom segment of the blast furnace.

It expands Eq. (35.10);

$$\left[\begin{array}{l} \text{mass O into} \\ \text{bottom segment} \end{array} \right] + \left[\begin{array}{l} \text{mass O released} \\ \text{by SiO}_2 \text{ reduction} \\ \text{in bottom segment} \end{array} \right] = \left[\begin{array}{l} \text{mass O out of} \\ \text{bottom segment} \end{array} \right] \quad (35.10)$$

to

$$\begin{aligned} & \left[\begin{array}{l} \text{mass O into} \\ \text{bottom segment} \end{array} \right] + \left[\begin{array}{l} \text{mass O released} \\ \text{by SiO}_2 \text{ reduction} \\ \text{in bottom segment} \end{array} \right] \\ &+ \left[\begin{array}{l} \text{mass O released} \\ \text{by MnO reduction} \\ \text{in bottom segment} \end{array} \right] = \left[\begin{array}{l} \text{mass O out of} \\ \text{bottom segment} \end{array} \right] \quad (36.10) \end{aligned}$$

where $\left[\begin{array}{l} \text{mass O released} \\ \text{by SiO}_2 \text{ reduction} \\ \text{in bottom segment} \end{array} \right]$ and $\left[\begin{array}{l} \text{mass O released} \\ \text{by MnO reduction} \\ \text{in bottom segment} \end{array} \right]$ are the amounts of O originally in SiO₂ and MnO that ascend from the bottom segment as CO(g) and CO₂(g).

Including the right side of this equation, bottom-segment oxygen balance Eq. (35.11) becomes;

$$\begin{aligned} & \left[\begin{array}{l} \text{mass Fe}_{0.947}\text{O into} \\ \text{bottom segment} \end{array} \right] * 0.232 \\ &+ \left[\begin{array}{l} \text{mass O}_2 \\ \text{in blast air} \end{array} \right] * 1 \\ &+ \left[\begin{array}{l} \text{mass Si out in} \\ \text{product molten iron} \end{array} \right] * 1.14 \\ &+ \left[\begin{array}{l} \text{mass Mn out in} \\ \text{product molten iron} \end{array} \right] * 0.291 \\ &= \left[\begin{array}{l} \text{mass CO out} \\ \text{in ascending gas} \end{array} \right] * 0.571 \\ &+ \left[\begin{array}{l} \text{mass CO}_2 \text{ out} \\ \text{in ascending gas} \end{array} \right] * 0.727 \quad (36.11) \end{aligned}$$

or subtracting;

$$\left\{ \begin{aligned} & \left[\begin{array}{l} \text{mass Fe}_{0.947}\text{O into} \\ \text{bottom segment} \end{array} \right] * 0.232 \\ &+ \left[\begin{array}{l} \text{mass O}_2 \\ \text{in blast air} \end{array} \right] * 1 \\ &+ \left[\begin{array}{l} \text{mass Si out in} \\ \text{product molten iron} \end{array} \right] * 1.14 \\ &+ \left[\begin{array}{l} \text{mass Mn out in} \\ \text{product molten iron} \end{array} \right] * 0.291 \end{aligned} \right\}$$

from both sides;

$$\begin{aligned}
 0 = & - \left[\frac{\text{mass Fe}_{0.947}\text{O into}}{\text{bottom segment}} \right] * 0.232 \\
 & - \left[\frac{\text{mass O}_2}{\text{in blast air}} \right] * 1 - \left[\frac{\text{mass Si out in}}{\text{product molten iron}} \right] * 1.14 \\
 & - \left[\frac{\text{mass Mn out in}}{\text{product molten iron}} \right] * 0.291 \\
 & + \left[\frac{\text{mass CO out}}{\text{in ascending gas}} \right] * 0.571 \\
 & + \left[\frac{\text{mass CO}_2 \text{ out}}{\text{in ascending gas}} \right] * 0.727
 \end{aligned} \tag{36.12}$$

36.8 BOTTOM-SEGMENT ENTHALPY EQUATION

Chapter 35's bottom segment enthalpy balance *without* MnO reduction is:

$$\begin{aligned}
 -320 = & - [\text{mass Fe}_{0.947}\text{O into bottom segment}] * (-3.152) \\
 & - [\text{mass C in descending coke}] * 1.359 \\
 & - [\text{mass O}_2 \text{ in blast}] * 1.239 \\
 & - [\text{mass N}_2 \text{ in blast}] * 1.339 \\
 & - [\text{mass Al}_2\text{O}_3 \text{ in descending flux}] * (-15.41) \\
 & - [\text{mass Al}_2\text{O}_3 \text{ in descending coke}] * (-15.41) \\
 & - [\text{mass CaO in descending flux}] * (-10.50) \\
 & - [\text{mass MgO in descending flux}] * (-13.84) \\
 & - [\text{mass SiO}_2 \text{ in descending ore}] * (-14.13) \\
 & - [\text{mass SiO}_2 \text{ in descending coke}] * (-14.13) \\
 & + [\text{mass Fe out in molten iron}] * 1.269 \\
 & + [\text{mass C out in molten iron}] * 5 \\
 & + [\text{mass CO gas out in ascending gas}] * (-2.926) \\
 & + [\text{mass CO}_2 \text{ out in ascending gas}] * (-7.926) \\
 & + [\text{mass N}_2 \text{ out in ascending gas}] * 1.008 \\
 & + [\text{mass Al}_2\text{O}_3 \text{ out in molten slag}] * (-13.58) \\
 & + [\text{mass CaO out in molten slag}] * (-8.495) \\
 & + [\text{mass MgO out in molten slag}] * (-11.14) \\
 & + [\text{mass SiO}_2 \text{ out in molten slag}] * (-13.28) \\
 & + [\text{mass Si out in molten iron}] * (-2.15)
 \end{aligned} \tag{35.13}$$

With;

1. MnO(s) descending into the bottom segment,
2. MnO leaving the furnace in product molten slag, and
3. Mn leaving in product molten iron

we must add three new enthalpy terms, all of which are described in the next 3 sections.

36.8.1 Descending MnO Enthalpy

The descending MnO enthalpy term is;

$$\begin{aligned}
 & \left[\frac{\text{mass MnO descending}}{\text{into bottom segment}} \right] * \frac{H^\circ_{930^\circ\text{C}}}{\text{MnO(s)}} \\
 & = \left[\frac{\text{mass MnO descending}}{\text{into bottom segment}} \right] * (-4.770)
 \end{aligned} \tag{36.13}$$

where the $H^\circ_{930^\circ\text{C}} / \text{MW}_{\text{MnO}}$ value is from Appendix J.

36.8.2 MnO-in-Product Molten Slag

The MnO in product molten slag enthalpy is;

$$\begin{aligned}
 & \left[\frac{\text{mass MnO in product}}{\text{molten slag}} \right] \\
 & H^\circ_{1500^\circ\text{C}} \\
 & * \frac{\text{MnO(in molten slag)}}{\text{MW}_{\text{MnO}}} \\
 & \text{or since } \frac{\text{MnO(in molten slag)}}{\text{MW}_{\text{MnO}}} \\
 & = -3.530 \text{ MJ/kg of MnO in molten slag}
 \end{aligned}$$

the MnO in slag enthalpy term is:

$$\left[\frac{\text{mass MnO in product}}{\text{molten slag}} \right] * (-3.530)$$

36.8.3 Enthalpy of Dissolved Mn

The enthalpy of Mn dissolved in Fe–Mn alloy is calculated in Appendix U. It is:

$$\begin{aligned}
 & \frac{H^\circ_{1500^\circ\text{C}}}{\text{Mn(dissolved in molten Fe – Mn alloy)}} \\
 & \text{MW}_{\text{Mn}} \\
 & = 1.27 \text{ MJ/kg of Mn in product molten iron}
 \end{aligned}$$

Mn enthalpy is represented in the enthalpy Eq. (36.14) by the term mass Mn out in molten iron * 1.27 (bottom row).

With these three new enthalpy terms, enthalpy Eq. (35.13) becomes;

$$\begin{aligned}
 -320 = & -[\text{mass Fe}_{0.947}\text{O into bottom segment}] * (-3.152) \\
 & -[\text{mass C in descending coke}] * 1.359 \\
 & -[\text{mass O}_2 \text{ in blast}] * 1.239 \\
 & -[\text{mass N}_2 \text{ in blast}] * 1.339 \\
 & -[\text{mass Al}_2\text{O}_3 \text{ in descending flux}] * (-15.41) \\
 & -[\text{mass Al}_2\text{O}_3 \text{ in descending coke}] * (-15.41) \\
 & -[\text{mass CaO in descending flux}] * (-10.50) \\
 & -[\text{mass MgO in descending flux}] * (-13.84) \\
 & -[\text{mass MnO into bottom segment}] * (-4.770) \\
 & -[\text{mass SiO}_2 \text{ in descending ore}] * (-14.13) \\
 & -[\text{mass SiO}_2 \text{ in descending coke}] * (-14.13) \\
 & +[\text{mass Fe out in molten iron}] * 1.269 \\
 & +[\text{mass C out in molten iron}] * 5 \\
 & +[\text{mass CO gas out in ascending gas}] * (-2.926) \\
 & +[\text{mass CO}_2 \text{ out in ascending gas}] * (-7.926) \\
 & +[\text{mass N}_2 \text{ out in ascending gas}] * 1.008 \\
 & +[\text{mass Al}_2\text{O}_3 \text{ out in molten slag}] * (-13.58) \\
 & +[\text{mass CaO out in molten slag}] * (-8.495) \\
 & +[\text{mass MgO out in molten slag}] * (-11.14) \\
 & +[\text{mass SiO}_2 \text{ out in molten slag}] * (-13.28) \\
 & +[\text{mass MnO out in molten slag}] * (-3.530) \\
 & +[\text{mass Si out in molten iron}] * (-2.15) \\
 & +[\text{mass Mn out in molten iron}] * 1.27
 \end{aligned} \tag{36.14}$$

- 423 kg of C-in-coke, and
- 345 kg of O₂-in-blast

are required for steady production of 0.5 mass % Mn, 0.4 mass% Si, 4.5 mass% C, and 94.6 mass% Fe molten iron as compared to;

- 421 kg of C-in-coke, and
- 342 kg of O₂-in-blast

with C, Fe, and Si in the molten iron, Table 35.2.

Table 36.2 shows also that the slag contains 0.8 kg of MnO and that the total mass of slag; kg Al₂O₃ + kg CaO + kg MgO + kg MnO + kg SiO₂ = 254 kg,

equivalent to 0.3 mass% MnO in slag. This has a negligible effect on slag melting point and viscosity.

We now plot bottom-segment MnO, C-in-coke, and O₂-in-blast requirements as a function of mass% Mn in product molten iron, see **Figs. 36.2 and 36.3**. All increase.

36.10 SUMMARY

This chapter shows how steady-state production of Mn-bearing molten iron is included in our matrix calculations.

It introduces three new variables;

1. mass MnO(s) descending into the conceptual blast furnace bottom segment,
2. mass Mn in product molten iron, and
3. mass MnO in product molten slag

and develops three new steady-state equations;

1. a mass Mn in product molten iron specification equation,
2. a bottom-segment MnO → Mn reduction efficiency equation, and

36.9 MATRIX CALCULATIONS AND RESULTS

All the above new and modified equations are included in our matrix as shown in **Table 36.1**. The results are shown in **Table 36.2**.

Table 36.1 shows equations of Table 35.1 plus the new and modified equations of this chapter. There are three new manganese columns and three new manganese equations, Eqs. (36.5), (36.7), and (36.9). **Table 36.2** shows that;

TABLE 36.1 Matrix With (1) New and Modified Equations From This Chapter and (2) Unmodified Equations of Table 35.1

TABLE 36.2 Steady-State Results From Matrix Calculation of [Table 36.1](#)

	A	B	C	D	E	F	G
27		Bottom segment calculated values	kg per 1000 kg of Fe out in molten iron				
28	mass Fe _{0.947} O into bottom segment		1302				
29	mass C in descending coke		423	also = mass C in the furnace's coke charge, Eqn. (7.16)			
30	mass O ₂ in blast air		345				
31	mass N ₂ in blast air		1138				
32	mass Fe out in molten iron		1000				
33	mass C out in molten iron		48				
34	mass CO out in ascending gas		607				
35	mass CO ₂ out in ascending gas		422				
36	mass N ₂ out in ascending gas		1138				
37	mass SiO ₂ in descending ore		75				
38	mass SiO ₂ in descending coke		33				
39	mass SiO ₂ out in molten slag		99				
40	mass Al ₂ O ₃ in descending flux		11				
41	mass Al ₂ O ₃ in descending coke		14				
42	mass Al ₂ O ₃ out in molten slag		25				
43	mass CaO in descending flux		104				
44	mass CaO out in molten slag		104				
45	mass MgO in descending flux		25				
46	mass MgO out in molten slag		25				
47	mass Si out in molten iron		4.2				
48	mass descending MnO		7.6				
49	mass MnO out in molten slag		0.8				
50	mass Mn out in molten iron		5.3				

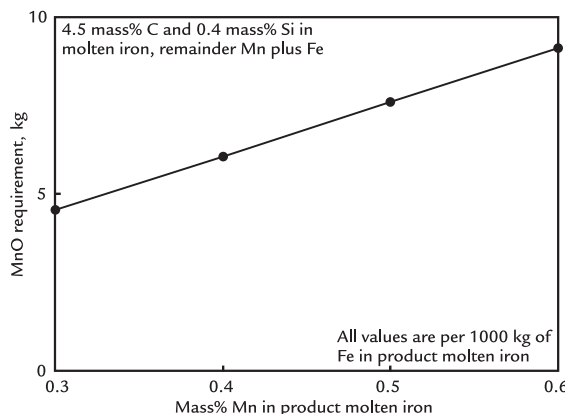


FIGURE 36.2 Bottom-segment MnO requirement for producing molten iron with increasing mass% Mn. As expected, MnO requirement increases with increasing mass% Mn in product molten iron. The equivalent top-charge MnO₂ requirement is obtained by the equation:

$$\begin{aligned} & [\text{mass top-charge MnO}_2 \text{ requirement}] \\ & = [\text{bottom segment MnO requirement}] * \frac{86.94}{70.94} \end{aligned}$$

where 86.94 is the molecular mass of MnO₂ and 70.94 is the molecular mass of MnO, kg per kg mol.

3. a steady-state bottom-segment Mn mass balance equation.

We also modified the steady-state oxygen and enthalpy balance equations of Chapter 35, Bottom-Segment Calculations—Reduction of SiO₂.

Mn in product molten iron requires;

1. steady descent of MnO into the bottom segment,
2. extra C-in-coke for (1) reducing MnO to Mn and (2) heating MnO and Mn by C combustion with O₂-in-blast, and
3. extra O₂-in-blast for this carbon combustion.

Flux requirements of the furnace are virtually unchanged by Mn in product molten iron of the blast furnace.

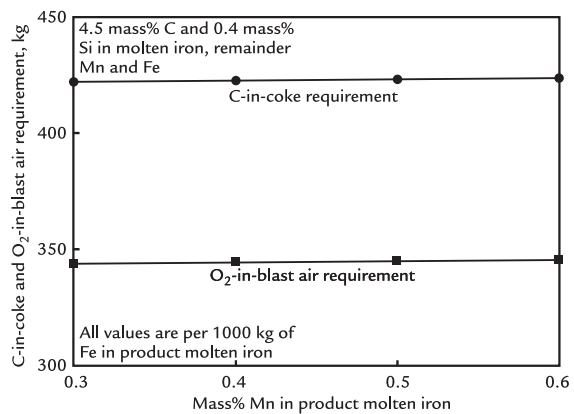


FIGURE 36.3 C-in-coke and O₂-in-blast requirements as affected by mass% Mn in product molten iron. Both increase with increasing %Mn. The increases are the result of all of equations of Table 36.1. However, we may speculate that the increased C-in-coke requirement is for (1) the reaction C + MnO → CO + Mn and for (2) heating and melting MnO and Mn (by combusting extra C with O₂-in-blast). The increased O₂-in-blast is for the extra carbon combustion.

EXERCISES

- 36.1. The steelmakers who use the molten iron of this chapter to make steel wish to raise the manganese concentration of iron to 1 mass% Mn.
 - a Why might they want to do this?
 - b How might they do this?
- 36.2. Please calculate the extra amounts of;
 - a. coke, and
 - b. blast air
 that will be needed to raise the Mn concentration from 0.5 mass% Mn (this chapter) to 1 mass% Mn. Please use two calculation methods.

Also please calculate the extra amount of MnO that must enter the bottom segment to produce 1 mass% Mn, 4.5 mass% C, 0.4 mass% Si, and 94.1 mass% Fe.

- 36.3. Many blast furnace plants judge their manganese reduction efficiency by the ratio;

$$\frac{[\text{mass Mn in product slag}]}{[\text{mass Mn in product iron}]}$$

What is this ratio with your 1 mass% Mn in iron calculated values? Does it vary with % Mn-in-iron.

- 36.4. Does increasing % Mn in molten blast furnace iron from 0.5% to 1% alter blast furnace slag composition?
- 36.5. Unfortunately, a blast furnace is producing only 0.7 mass% Mn molten iron, which is lower than the steelmakers need. Can the steelmakers compensate for this somewhere in their process? Perhaps refer to Chapter 3, Making Steel From Molten Blast Furnace Iron.

37

Bottom-Segment Calculations With Pulverized Coal Injection

O U T L I N E

37.1 Pulverized coal injection	322	37.9.1 Al_2O_3 balance	325
37.2 Coal elemental composition	322	37.9.2 SiO_2 balance	325
37.3 Coal enthalpy	323	37.10 Altered enthalpy balance	326
37.4 Calculation strategy	323	37.11 Matrix and calculations	327
37.5 Injected coal quantity specification	323	37.12 Results	327
37.6 Mass $H_2O(g)$ /Mass $H_2(g)$ Equilibrium Ratio Equilibrium Ratio	323	37.12.1 Coke and O_2 -in-blast Air requirements	327
37.7 New hydrogen balance equation	324	37.13 Flux requirements	327
37.8 Altered Bottom-Segment Steady-State C, N, O, Al_2O_3 , and SiO_2 Mass Balances	324	37.13.1 Total SiO_2 input	327
37.8.1 Carbon balance	324	37.13.2 CaO flux requirement	327
37.8.2 Oxygen balance	324	37.14 MgO and Al_2O_3 -in-flux requirements	331
37.8.3 Nitrogen balance	325	37.14.1 MnO requirement	332
37.9 Altered Al_2O_3 and SiO_2 mass balances	325	37.15 Summary	332
		Exercises	332
		Reference	333

37.1 PULVERIZED COAL INJECTION

Chapter 13, Bottom Segment With Pulverized Hydrocarbon Injection, described tuyere injection of coal hydrocarbon. This chapter expands this description to include $\text{Al}_2\text{O}_3(\text{s})$ and $\text{SiO}_2(\text{s})$ in the coal's interstitial rock particles known as coal ash, [Table 37.1](#).

This chapter starts with the ore gangue, coke ash, fluxes, slag, Si reduction, and Mn reduction calculations of Chapter 36, Bottom Segment Calculations—Reduction of MnO , and adds tuyere injection of coal of [Table 37.1](#).

The objectives of this chapter are to show how tuyere-injection of pulverized coal (PCI) is included in our matrix calculations - with specific reference to its effect on steady state;

1. coke and O_2 -in-blast requirements for producing 1500°C;
 - a. 4.5 mass% C;
 - b. 94.6 mass% Fe;
 - c. 0.5 mass% Mn; and
 - d. 0.4 mass% Si of Chapter 36, Bottom-Segment Calculations—Reduction of MnO , molten iron, and
2. Al_2O_3 , CaO , MgO , and SiO_2 in flux requirements for producing 1500°C;
 - a. 10 mass% Al_2O_3 ;
 - b. 41 mass% CaO ;
 - c. 10 mass% MgO ; and
 - d. 39 mass% SiO_2 of Chapter 32, Bottom-Segment Slag Calculations—Ore, Fluxes, and Slag molten slag, [Fig. 37.1](#).

37.2 COAL ELEMENTAL COMPOSITION

[Table 37.2](#) shows the elemental composition of the coal from [Table 37.1](#). These values are used throughout this chapter.

TABLE 37.1 Composition of Tuyere-Injected Dried Pulverized Coal of this Chapter

Substance	Mass(%)
Solid hydrocarbon	92
$\text{Al}_2\text{O}_3(\text{s})$	2.4
$\text{SiO}_2(\text{s})$	5.6

Pulverized coal also contains small quantities of potassium/sodium, phosphates and sulfates.

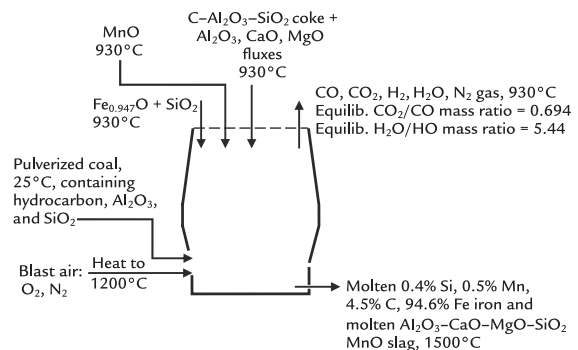


FIGURE 37.1 Conceptual blast furnace bottom segment showing steady-state inputs and outputs with pulverized coal injection. The hydrocarbon + Al_2O_3 + SiO_2 coal is new. The coal is dried during pulverization.

TABLE 37.2 Elemental Composition of the Coal from [Table 37.1](#)

Element	Mass (%)
C	81.0
H	5.5
N	0.9
O	4.6 ^a
Al_2O_3	2.4
SiO_2	5.6

^aExcluding O in Al_2O_3 and SiO_2 . This was calculated in Appendix V.

37.3 COAL ENTHALPY

Coal injection alters the conceptual bottom-segment enthalpy balance of the blast furnace. The enthalpy of the coal from Table 37.1 is given by the following equation;

$$\begin{aligned} \text{Coal enthalpy, MJ/kg of coal} \\ = & \frac{92 \text{ mass\% hydrocarbon in coal}}{100\%} * H_{\text{coal hydrocarbon}}^{25^\circ\text{C}} \\ + & \frac{2.4 \text{ mass\% Al}_2\text{O}_3 \text{ in coal}}{100\%} * \frac{H_{\text{Al}_2\text{O}_3(\text{s})}^{25^\circ\text{C}}}{\text{MW}_{\text{Al}_2\text{O}_3}} \\ + & \frac{5.6 \text{ mass\% SiO}_2 \text{ in coal}}{100\%} * \frac{H_{\text{SiO}_2(\text{s})}^{25^\circ\text{C}}}{\text{MW}_{\text{SiO}_2}} \end{aligned} \quad (37.1)$$

where;

$$H_{\text{coal hydrocarbon}}^{25^\circ\text{C}} = 0 \text{ MJ/kg, Section 13.5}$$

$$\frac{H_{\text{Al}_2\text{O}_3(\text{s})}^{25^\circ\text{C}}}{\text{MW}_{\text{Al}_2\text{O}_3}} = -16.43 \text{ MJ/kg, Table J.1}$$

$$\frac{H_{\text{SiO}_2(\text{s})}^{25^\circ\text{C}}}{\text{MW}_{\text{SiO}_2}} = -15.16 \text{ MJ/kg, Table J.1}$$

Eq. (37.1) and these enthalpy values together give;

$$\begin{aligned} \text{Coal enthalpy} &= 0.92 * 0 + 0.024 * (-16.43) \\ &\quad + 0.056 * (-15.16) \\ &= -1.2 \text{ MJ/kg of coal.} \end{aligned}$$

37.4 CALCULATION STRATEGY

This chapter uses the same strategy as shown in Chapter 13, Bottom-Segment With Pulverized Hydrocarbon Injection.

It;

1. specifies the amount of pulverized coal being injected into the blast furnace per 1000 kg of Fe in product molten iron;
2. represents hydrogen of the coal by three variables;
 - a. mass H in injected coal,
 - b. mass H₂ in bottom-segment exit gas, and
 - c. mass H₂O in bottom-segment exit gas;
3. adds three new equations to matrix Table 36.1, that is, our;
 - a. coal injection quantity specification,
 - b. hydrogen mass balance, and
 - c. 930°C equilibrium mass H₂O(g)/mass H₂(g) ratio specification;
4. modifies the blast furnace bottom-segment Al₂O₃, C, N, O, and SiO₂ mass balances to reflect their presence in the coal;
5. includes 25°C coal, 930°C H₂(g), and 930°C H₂O(g) enthalpies of Table J.1 in the bottom-segment enthalpy balance; and
6. calculates the coke, O₂-in-blast and flux requirements for steadily producing 1500°C molten Fe, C, Mn, Si iron, and molten slag.

37.5 INJECTED COAL QUANTITY SPECIFICATION

Our tuyere injected coal quantity specification is represented by the following equation:

$$60 = \left[\frac{\text{mass tuyere-}}{\text{injected coal}} \right] * 1 \quad (37.2)$$

which indicates that 60 kg of coal is being injected through tuyeres per 1000 kg of Fe in product molten iron.

37.6 MASS H₂O(g)/MASS H₂(g) EQUILIBRIUM RATIO

The 930°C equilibrium mass H₂O(g)/mass H₂(g) ratio specification used since Chapter 11, Bottom Segment with CH₄(g) Injection, is:

$$0 = - \left[\begin{array}{l} \text{mass H}_2\text{O out} \\ \text{in ascending gas} \end{array} \right] * 1 + \left[\begin{array}{l} \text{mass H}_2 \text{ out} \\ \text{in ascending gas} \end{array} \right] * 5.44 \quad (11.8)$$

It is also used for the pulverized coal analysis presented here.

37.7 NEW HYDROGEN BALANCE EQUATION

Fig. 37.1 shows that hydrogen enters the bottom segment in injected coal and leaves in ascending $\text{H}_2\text{(g)}$ and $\text{H}_2\text{O(g)}$. This is represented by the following equation;

$$\left[\begin{array}{l} \text{mass H in tuyere-} \\ \text{injected coal} \end{array} \right] = \left[\begin{array}{l} \text{mass H in} \\ \text{ascending H}_2\text{(g)} \end{array} \right] + \left[\begin{array}{l} \text{mass H in} \\ \text{ascending H}_2\text{O(g)} \end{array} \right]$$

which expands to;

$$\begin{aligned} & \left[\begin{array}{l} \text{mass tuyere-} \\ \text{injected coal} \end{array} \right] * \frac{5.5 \text{ mass\% H in the coal}}{100\%} \\ &= \left[\begin{array}{l} \text{mass H}_2 \text{ out in} \\ \text{ascending gas} \end{array} \right] * \frac{100 \text{ mass\% H in H}_2}{100\%} \\ &+ \left[\begin{array}{l} \text{mass H}_2\text{O out in} \\ \text{ascending gas} \end{array} \right] * \frac{11.2 \text{ mass\% H in H}_2\text{O}}{100\%} \end{aligned}$$

or

$$\begin{aligned} & \left[\begin{array}{l} \text{mass tuyere-} \\ \text{injected coal} \end{array} \right] * 0.055 = \left[\begin{array}{l} \text{mass H}_2 \text{ out in} \\ \text{ascending gas} \end{array} \right] * 1 \\ &+ \left[\begin{array}{l} \text{mass H}_2\text{O out in} \\ \text{ascending gas} \end{array} \right] * 0.112 \end{aligned}$$

or subtracting $\left\{ \left[\begin{array}{l} \text{mass tuyere-} \\ \text{injected coal} \end{array} \right] * 0.055 \right\}$ from both sides;

$$\begin{aligned} 0 &= - \left[\begin{array}{l} \text{mass tuyere-} \\ \text{injected coal} \end{array} \right] * 0.055 + \left[\begin{array}{l} \text{mass H}_2 \text{ out in} \\ \text{ascending gas} \end{array} \right] * 1 \\ &+ \left[\begin{array}{l} \text{mass H}_2\text{O out in} \\ \text{ascending gas} \end{array} \right] * 0.112 \end{aligned} \quad (37.3)$$

37.8 ALTERED BOTTOM-SEGMENT STEADY-STATE C, N, O, Al_2O_3 , AND SiO_2 MASS BALANCES

37.8.1 Carbon Balance

With coal injection, the bottom-segment carbon balance Eq. (7.3) becomes;

$$\begin{aligned} 0 &= - \left[\begin{array}{l} \text{mass tuyere-} \\ \text{injected coal} \end{array} \right] * 0.810 - \left[\begin{array}{l} \text{mass C in} \\ \text{descending coke} \end{array} \right] * 1 \\ &+ \left[\begin{array}{l} \text{mass CO out} \\ \text{in ascending gas} \end{array} \right] * 0.429 \\ &+ \left[\begin{array}{l} \text{mass CO}_2 \text{ out} \\ \text{in ascending gas} \end{array} \right] * 0.273 + \left[\begin{array}{l} \text{mass C out} \\ \text{in molten iron} \end{array} \right] * 1 \end{aligned} \quad (37.4)$$

where;

$0.810 = 81.0 \text{ mass\% C in the injected coal}/100\%$; Table 37.2.

37.8.2 Oxygen Balance

Likewise, the bottom-segment oxygen balance Eq. (36.12) becomes;

$$\begin{aligned} 0 &= - \left[\begin{array}{l} \text{mass tuyere-} \\ \text{injected coal} \end{array} \right] * 0.046 - \left[\begin{array}{l} \text{mass Fe}_{0.947}\text{O into} \\ \text{bottom segment} \end{array} \right] * 0.232 \\ &- \left[\begin{array}{l} \text{mass O}_2 \\ \text{in blast air} \end{array} \right] * 1 - \left[\begin{array}{l} \text{mass Si out in} \\ \text{product molten iron} \end{array} \right] * 1.14 \\ &- \left[\begin{array}{l} \text{mass Mn out in} \\ \text{product molten iron} \end{array} \right] * 0.291 \\ &+ \left[\begin{array}{l} \text{mass CO out} \\ \text{in ascending gas} \end{array} \right] * 0.571 \\ &+ \left[\begin{array}{l} \text{mass CO}_2 \text{ out} \\ \text{in ascending gas} \end{array} \right] * 0.727 \\ &+ \left[\begin{array}{l} \text{mass H}_2\text{O(g) out} \\ \text{in ascending gas} \end{array} \right] * 0.888 \end{aligned} \quad (37.5)$$

where;

$0.046 = 4.6 \text{ mass\% O in the coal}/100\%$; 1.14 for Si out in product molten iron is explained in Section 35.4, and 0.291 for Mn out in product molten iron is explained in Section 36.7.

37.8.3 Nitrogen Balance

The nitrogen balance equation becomes

$$0 = - \left[\begin{array}{l} \text{mass tuyere-} \\ \text{injected coal} \end{array} \right] * 0.009 - \left[\begin{array}{l} \text{mass N}_2 \\ \text{in blast air} \end{array} \right] * 1 + \left[\begin{array}{l} \text{mass N}_2 \text{ out} \\ \text{in ascending gas} \end{array} \right] * 1 \quad (37.6)$$

where $0.009 = 0.9$ mass% N in the coal/100%. Nitrogen used to inject the coal into the blast furnace is ignored; this value can be included if it is available.

37.9 ALTERED Al₂O₃ AND SiO₂ MASS BALANCES

This section expands Al₂O₃ and SiO₂ mass balances of Chapter 34, Bottom-Segment Slag Calculations - Coke Ash, to include Al₂O₃- and SiO₂-in-coal contents of [Table 37.2](#).

37.9.1 Al₂O₃ Balance

Eq. (34.5) of Chapter 34, Adding Coke Ash to the Bottom-Segment Slag Calculations - Coke Ash, the Al₂O₃ balance is;

$$\left[\begin{array}{l} \text{mass Al}_2\text{O}_3 \text{ in} \\ \text{descending flux} \end{array} \right] * 1 + \left[\begin{array}{l} \text{mass Al}_2\text{O}_3 \text{ in} \\ \text{descending coke} \end{array} \right] * 1 = \left[\begin{array}{l} \text{mass Al}_2\text{O}_3 \text{ in} \\ \text{molten slag} \end{array} \right] * 1 \quad (34.5)$$

With Al₂O₃ in injected coal, it becomes;

$$\left[\begin{array}{l} \text{mass Al}_2\text{O}_3 \text{ in tuyere-} \\ \text{injected coal} \end{array} \right] * 1 + \left[\begin{array}{l} \text{mass Al}_2\text{O}_3 \text{ in} \\ \text{descending flux} \end{array} \right] * 1 + \left[\begin{array}{l} \text{mass Al}_2\text{O}_3 \text{ in} \\ \text{descending coke} \end{array} \right] * 1 = \left[\begin{array}{l} \text{mass Al}_2\text{O}_3 \text{ in} \\ \text{molten slag} \end{array} \right] * 1$$

which expands to;

$$\left[\begin{array}{l} \text{mass tuyere-} \\ \text{injected coal} \end{array} \right] * \frac{2.4 \text{ mass\% Al}_2\text{O}_3 \text{ in injected coal}}{100\%} + \left[\begin{array}{l} \text{mass Al}_2\text{O}_3 \text{ in} \\ \text{descending flux} \end{array} \right] * 1 + \left[\begin{array}{l} \text{mass Al}_2\text{O}_3 \text{ in} \\ \text{descending coke} \end{array} \right] * 1 = \left[\begin{array}{l} \text{mass Al}_2\text{O}_3 \text{ in} \\ \text{molten slag} \end{array} \right] * 1$$

or

$$\left[\begin{array}{l} \text{mass tuyere-} \\ \text{injected coal} \end{array} \right] * 0.024 + \left[\begin{array}{l} \text{mass Al}_2\text{O}_3 \text{ in} \\ \text{descending flux} \end{array} \right] * 1 + \left[\begin{array}{l} \text{mass Al}_2\text{O}_3 \text{ in} \\ \text{descending coke} \end{array} \right] * 1 = \left[\begin{array}{l} \text{mass Al}_2\text{O}_3 \text{ in} \\ \text{molten slag} \end{array} \right] * 1$$

or subtracting $\left\{ \left[\begin{array}{l} \text{mass tuyere-} \\ \text{injected coal} \end{array} \right] * 0.024 + \left[\begin{array}{l} \text{mass Al}_2\text{O}_3 \text{ in} \\ \text{descending flux} \end{array} \right] * 1 + \left[\begin{array}{l} \text{mass Al}_2\text{O}_3 \text{ in} \\ \text{descending coke} \end{array} \right] * 1 \right\}$ from both sides;

$$0 = - \left[\begin{array}{l} \text{mass tuyere-} \\ \text{injected coal} \end{array} \right] * 0.024 - \left[\begin{array}{l} \text{mass Al}_2\text{O}_3 \text{ in} \\ \text{descending flux} \end{array} \right] * 1 - \left[\begin{array}{l} \text{mass Al}_2\text{O}_3 \text{ in} \\ \text{descending coke} \end{array} \right] * 1 + \left[\begin{array}{l} \text{mass Al}_2\text{O}_3 \text{ in} \\ \text{molten slag} \end{array} \right] * 1 \quad (37.7)$$

37.9.2 SiO₂ Balance

Eq. (35.8) of Chapter 35, Bottom-Segment Calculations - Reduction of SiO₂, SiO₂ mass balance is;

$$\begin{aligned} & \left[\begin{array}{l} \text{mass SiO}_2 \text{ in} \\ \text{descending ore} \end{array} \right] * 1 + \left[\begin{array}{l} \text{mass SiO}_2 \text{ in} \\ \text{descending coke} \end{array} \right] * 1 \\ &= \left[\begin{array}{l} \text{mass SiO}_2 \text{ out in} \\ \text{product molten slag} \end{array} \right] * 1 \\ &+ \left[\begin{array}{l} \text{mass Si out in} \\ \text{product molten iron} \end{array} \right] * 2.14 \end{aligned} \quad (35.8)$$

where 2.14 is from Section 35.4.

With tuyere PCI, this becomes;

$$\begin{aligned} & \left[\begin{array}{l} \text{mass SiO}_2 \text{ in} \\ \text{injected coal} \end{array} \right] * 1 + \left[\begin{array}{l} \text{mass SiO}_2 \text{ in} \\ \text{descending ore} \end{array} \right] * 1 \\ &+ \left[\begin{array}{l} \text{mass SiO}_2 \text{ in} \\ \text{descending coke} \end{array} \right] * 1 = \left[\begin{array}{l} \text{mass SiO}_2 \text{ out in} \\ \text{product molten slag} \end{array} \right] * 1 \\ &+ \left[\begin{array}{l} \text{mass Si out in} \\ \text{product molten iron} \end{array} \right] * 2.14 \end{aligned}$$

which expands to;

$$\begin{aligned} & \left[\begin{array}{l} \text{mass tuyere-} \\ \text{injected coal} \end{array} \right] * \frac{5.6 \text{ mass\% SiO}_2 \text{ in injected coal}}{100\%} \\ &+ \left[\begin{array}{l} \text{mass SiO}_2 \text{ in} \\ \text{descending ore} \end{array} \right] * 1 + \left[\begin{array}{l} \text{mass SiO}_2 \text{ in} \\ \text{descending coke} \end{array} \right] * 1 \\ &= \left[\begin{array}{l} \text{mass SiO}_2 \text{ out in} \\ \text{product molten slag} \end{array} \right] * 1 \\ &+ \left[\begin{array}{l} \text{mass Si out in} \\ \text{product molten iron} \end{array} \right] * 2.14 \end{aligned} \quad (37.8)$$

or

$$\begin{aligned} & \left[\frac{\text{mass tuyere}}{\text{injected coal}} \right] * 0.056 + \left[\frac{\text{mass SiO}_2 \text{ in}}{\text{descending ore}} \right] * 1 \\ & + \left[\frac{\text{mass SiO}_2 \text{ in}}{\text{descending coke}} \right] * 1 \\ & = \left[\frac{\text{mass SiO}_2 \text{ out in}}{\text{product molten slag}} \right] * 1 \\ & + \left[\frac{\text{mass Si out in}}{\text{product molten iron}} \right] * 2.14 \end{aligned}$$

or subtracting $\left\{ \left[\frac{\text{mass tuyere}}{\text{injected coal}} \right] * 0.056 + \left[\frac{\text{mass SiO}_2 \text{ in}}{\text{descending ore}} \right] * 1 + \left[\frac{\text{mass SiO}_2 \text{ in}}{\text{descending coke}} \right] * 1 \right\}$ from both sides;

$$\begin{aligned} 0 = & - \left[\frac{\text{mass tuyere}}{\text{injected coal}} \right] * 0.056 - \left[\frac{\text{mass SiO}_2 \text{ in}}{\text{descending ore}} \right] * 1 \\ & - \left[\frac{\text{mass SiO}_2 \text{ in}}{\text{descending coke}} \right] * 1 + \left[\frac{\text{mass SiO}_2 \text{ out in}}{\text{product molten slag}} \right] * 1 \\ & + \left[\frac{\text{mass Si out in}}{\text{product molten iron}} \right] * 2.14 \end{aligned} \quad (37.9)$$

37.10 ALTERED ENTHALPY BALANCE

Coal injection adds three more enthalpy terms to the bottom-segment enthalpy balance, that is;

$$\begin{aligned} & \left[\frac{\text{mass tuyere-}}{\text{injected coal}} \right] * [\text{coal enthalpy}] \\ & = \left[\frac{\text{mass tuyere-}}{\text{injected coal}} \right] * -1.2 \text{ MJ/kg of coal} \\ & \left[\frac{\text{mass H}_2 \text{ out in}}{\text{ascending gas}} \right] * \frac{H_{930^\circ\text{C}}}{\text{MW}_{\text{H}_2}} \\ & = \left[\frac{\text{mass H}_2 \text{ out in}}{\text{ascending gas}} \right] * 13.35 \text{ MJ/kg of H}_2 \end{aligned} \quad (37.10)$$

$$\begin{aligned} & \left[\frac{\text{mass H}_2\text{O out in}}{\text{ascending gas}} \right] * \frac{H_{930^\circ\text{C}}}{\text{MW}_{\text{H}_2\text{O}}} \\ & = \left[\frac{\text{mass H}_2\text{O out in}}{\text{ascending gas}} \right] * -11.49 \text{ MJ/kg of H}_2 \end{aligned}$$

where the coal enthalpy is from [Section 37.3](#), and the H_2 and $\text{H}_2\text{O(g)}$ enthalpies are from [Appendix J](#).

This changes bottom-segment enthalpy balance Eq. (36.14) to:

$$\begin{aligned} -320 = & -[\text{mass tuyere-injected coal}] * (-1.2) \\ & -[\text{mass Fe}_{0.947}\text{O into bottom segment}] * (-3.152) \\ & -[\text{mass C in descending coke}] * 1.359 \\ & -[\text{mass O}_2 \text{ in blast}] * 1.239 \\ & -[\text{mass N}_2 \text{ in blast}] * 1.339 \\ & -[\text{mass Al}_2\text{O}_3 \text{ descending in dissociated flux}] \\ & * (-15.41) \\ & -[\text{mass Al}_2\text{O}_3 \text{ in descending coke}] * (-15.41) \\ & -[\text{mass CaO descending in dissociated flux}] \\ & * (-10.50) \\ & -[\text{mass MgO descending in dissociated flux}] \\ & * (-13.84) \\ & -[\text{mass MnO descending into bottom segment}] \\ & * (-4.770) \\ & -[\text{mass SiO}_2 \text{ in descending ore}] * (-14.13) \\ & -[\text{mass SiO}_2 \text{ in descending coke}] * (-14.13) \\ & +[\text{mass Fe out in molten iron}] * 1.269 \\ & +[\text{mass C out in molten iron}] * 5 \\ & +[\text{mass CO gas out in ascending gas}] * (-2.926) \\ & +[\text{mass CO}_2 \text{ out in ascending gas}] * (-7.926) \\ & +[\text{mass N}_2 \text{ out in ascending gas}] * 1.008 \\ & +[\text{mass Al}_2\text{O}_3 \text{ out in molten slag}] * (-13.58) \\ & +[\text{mass CaO out in molten slag}] * (-8.495) \\ & +[\text{mass MgO out in molten slag}] * (-11.14) \\ & +[\text{mass SiO}_2 \text{ out in molten slag}] * (-13.28) \\ & +[\text{mass MnO out in molten slag}] * (-3.530) \\ & +[\text{mass Si out in molten iron}] * (-2.15) \\ & +[\text{mass Mn out in molten iron}] * 1.27 \\ & +[\text{mass H}_2 \text{ out in ascending gas}] * 13.35 \\ & +[\text{mass H}_2\text{O(g) out in ascending gas}] * (-11.49) \end{aligned} \quad (37.11)$$

37.11 MATRIX AND CALCULATIONS

Tables 37.3 and 37.4 are matrix Tables 36.1 and 36.2 with;

1. a new injected coal quantity specification;
2. new equilibrium mass H₂O(g)/mass H₂(g) and H mass balance equations;
3. modified C, N, O, Al₂O₃, and SiO₂ mass balance equations; and
4. an altered enthalpy balance equation.

37.12 RESULTS

Table 37.4 shows that production of 1500°C;

- 4.5 mass% C,
- 94.6 mass% Fe,
- 0.5 mass% Mn, and
- 0.4 mass% Si

molten iron, and

- 10 mass% Al₂O₃,
- 41 mass% CaO,
- 10 mass% MgO, and
- 39 mass% SiO₂

molten slag with 60 kg of injected coal requires;

- 347 kg of O₂ in blast air, and
- 372 kg of descending C-in-coke (equivalent to 413 kg of 90 mass% C coke).

This point and others are plotted in Fig. 37.2.

37.12.1 Coke and O₂-in-Blast Air Requirements

As expected, coke requirement decreases markedly with increasing coal injection, Fig. 37.2. One kilogram of PCI saves 0.95 kg of coke.

This trend is similar to the one seen in Fig. 8.3.

Fig. 37.2 also shows that O₂-in-blast requirement increases slightly with increasing coal injection. This trend is also similar to the one seen in Fig. 8.5.

37.13 FLUX REQUIREMENTS

This section discusses the effect of coal injection on blast furnace flux requirements. It examines the effect of coal injection on;

1. total SiO₂ input,
2. CaO, MgO flux requirements,
3. Al₂O₃ flux requirement, and
4. MnO requirement (for reduction to Mn-in-molten-iron).

37.13.1 Total SiO₂ Input

Fig. 37.3 shows the effect of coal injection on the total input of SiO₂ of Fig. 37.1 furnace in;

- ore gangue,
- top-charged coke ash, and
- injected pulverized coal ash.

SiO₂ input decreases with increasing coal injection.

This decrease is due to all of equations of Table 37.1. We may speculate that it is at least partially due to the injected coal's lower SiO₂ concentration of 5.6 mass% SiO₂ as compared to the top charged coke's 7 mass% SiO₂.

37.13.2 CaO Flux Requirement

Blast furnace slag of Chapter 32, Bottom-Segment Slag Calculations - Ore, Fluxes, and Slag, contains CaO and SiO₂ in a fixed ratio, that is:

$$[\text{mass\% CaO}]/[\text{mass\% SiO}_2] = 41/39 = 1.05 \quad (37.11)$$

This and the decreasing total SiO₂ input of Fig. 37.3 result in decreasing blast furnace CaO-in-flux requirement of Fig. 37.4.

TABLE 37.3 Bottom-Segment Matrix for Calculating the Coke, O₂-in-Blast Air and Al₂O₃, CaO, and MgO-in Flux Requirements for Steady Production of 1500°C Molten Iron and Molten Slag, With Tuyere Injection of Pulverized Coal

	L	M	N	O	P	Q	R	S	T	U	V
1	mass N ₂ out in ascending gas	mass SiO ₂ in descending ore	mass SiO ₂ in descending coke	mass SiO ₂ out in molten slag	mass Al ₂ O ₃ in descending flux	mass Al ₂ O ₃ in descending coke	mass Al ₂ O ₃ out in molten slag	mass CaO in descending flux	mass CaO out in molten slag	mass MgO in descending flux	mass MgO out in molten slag
2											
3	0	0	0	0	0	0	0	0	0	0	0
4	0	-1	0	0	0	0	0	0	0	0	0
5	0	0	-1	0	0	0	0	0	0	0	0
6	0	0	0	0	0	0	0	0	0	0	0
7	0	0	0	0	0	0	0	0	0	0	0
8	0	0	0	0	0	0	0	0	0	0	0
9	0	-1	-1	1	0	0	0	0	0	0	0
10	1	0	0	0	0	0	0	0	0	0	0
11	0	0	0	0	0	0	0	0	0	0	0
12	0	0	0	0	0	0	0	0	0	0	0
13	0	0	0	0	0	0	0	0	0	0	0
14	0	0	0	0	0	-1	0	0	0	0	0
15	0	0	0	0.256	0	0	-1	0	0	0	0
16	0	0	0	0	-1	-1	1	0	0	0	0
17	0	0	0	1.05	0	0	0	0	-1	0	0
18	0	0	0	0	0	0	0	-1	1	0	0
19	0	0	0	0.256	0	0	0	0	0	0	-1
20	0	0	0	0	0	0	0	0	0	-1	1
21	1.008	14.13	14.13	-13.28	15.41	15.41	-13.58	10.50	-8.495	13.84	-11.14
22	0	0	0	0	0	0	0	0	0	0	0
23	0	0	0	0	0	0	0	0	0	0	0
24	0	0	0	0	0	0	0	0	0	0	0
25	0	0	0	0	0	0	0	0	0	0	0
26	0	0	0	0	0	0	0	0	0	0	0
27	0	0	0	0	0	0	0	0	0	0	0
28	0	0	0	0	0	0	0	0	0	0	0
29											

	W	X	Y	Z	AA	AB	AC
1	mass Si out in molten iron	mass descending MnO	mass MnO out in molten slag	mass Mn out in molten iron	mass H ₂ out in ascending gas	mass H ₂ O out in ascending gas	mass tuyere-injected coal
2							
3	0	0	0	0	0	0	0
4	0	0	0	0	0	0	0
5	0	0	0	0	0	0	0
6	0	0	0	0	0	0	0
7	-1.14	0	0	-0.291	0	0.888	-0.046
8	0	0	0	0	0	0	-0.81
9	2.14	0	0	0	0	0	-0.056
10	0	0	0	0	0	0	-0.009
11	0	0	0	0	0	0	0
12	0	0	0	0	0	0	0
13	0	0	0	0	0	0	0
14	0	0	0	0	0	0	0
15	0	0	0	0	0	0	0
16	0	0	0	0	0	0	-0.024
17	0	0	0	0	0	0	0
18	0	0	0	0	0	0	0
19	0	0	0	0	0	0	0
20	0	0	0	0	0	0	0
21	-2.15	4.77	-3.530	1.27	13.35	-11.49	1.2
22	-1	0	0	0	0	0	0
23	0	0	0	-1	0	0	0
24	0	-0.774	0.774	1	0	0	0
25	0	-0.1	1	0	0	0	0
26	0	0	0	0	1	0.112	-0.055
27	0	0	0	0	5.44	-1	0
28	0	0	0	0	0	0	1
29							

The iron and slag compositions are those in Section 36.2. The matrix is split into sections for visibility.

TABLE 37.4 Steady-State Results From Matrix Calculations of Table 37.3, That is, With 60-kg of Injected Pulverized Coal

A	B	C	D	E	F	G
		kg per 1000 kg of Fe out in molten iron				
33	Bottom segment calculated values					
34	mass Fe _{0.947} O into bottom segment	1302				
35	mass C in descending coke	372	also = mass C in the furnace's coke charge, Eqn. (7.16)			
36	mass O ₂ in blast air	347				
37	mass N ₂ in blast air	1146				
38	mass Fe out in molten iron	1000				
39	mass C out in molten iron	48				
40	mass CO out in ascending gas	603				
41	mass CO ₂ out in ascending gas	419				
42	mass N ₂ out in ascending gas	1147				
43	mass SiO ₂ in descending ore	75				
44	mass SiO ₂ in descending coke	29				
45	mass SiO ₂ out in molten slag	99				
46	mass Al ₂ O ₃ in descending flux	11				
47	mass Al ₂ O ₃ in descending coke	12				
48	mass Al ₂ O ₃ out in molten slag	25				
49	mass CaO in descending flux	103				
50	mass CaO out in molten slag	103				
51	mass MgO in descending flux	25				
52	mass MgO out in molten slag	25				
53	mass Si out in molten iron	4.2				
54	mass descending MnO	7.6				
55	mass MnO out in molten slag	0.8				
56	mass Mn out in molten iron	5.3				
57	mass H ₂ out in ascending gas	2.1				
58	mass H ₂ O out in ascending gas	11				
59	mass tuyere-injected coal	60				
60						

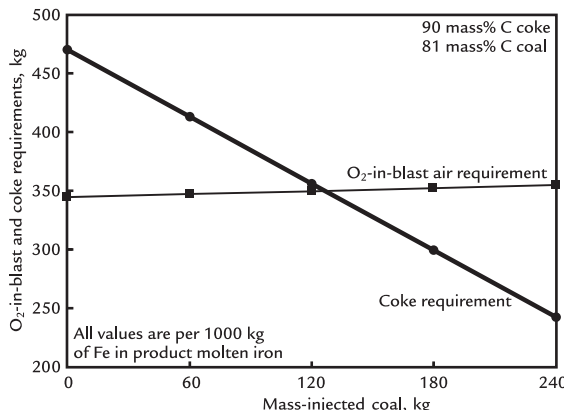


FIGURE 37.2 Coke and O₂-in-blast air requirements for steady production of molten iron and slag, 1500°C. Coke requirement decreases sharply with increasing coal injection. Oxygen requirement increases slightly. Both lines are straight.

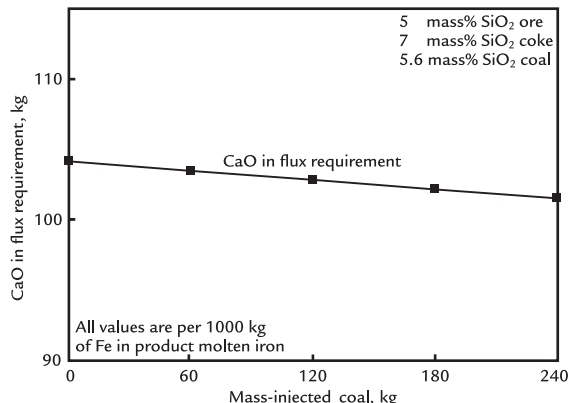


FIGURE 37.4 The effect of coal injection on CaO-in-flux requirement. The requirement decreases commensurately with decreasing total SiO₂ input of Fig. 37.3. The same is true for MgO, Fig. 37.5.

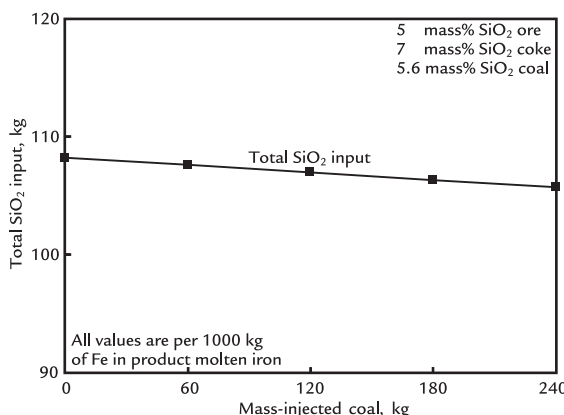


FIGURE 37.3 The effect of coal injection on the total amount of SiO₂ entering the blast furnace of Fig. 37.1. It decreases slightly with increasing pulverized coal injection. The line is straight.

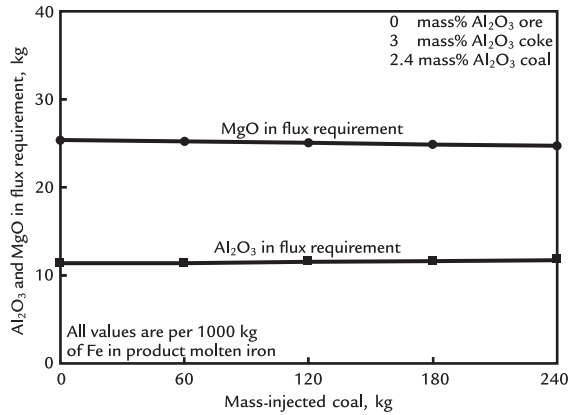


FIGURE 37.5 The effect of real coal injection on MgO- and Al₂O₃-in-flux requirements for steadily making molten 10 mass% MgO–10 mass% Al₂O₃ slag. Less Al₂O₃-in-flux is required because Al₂O₃ also enters the furnace in coke and injected coal. The lines are straight.

37.14 MgO AND Al_2O_3 -IN-FLUX REQUIREMENTS

This chapter specifies that molten slag product of Fig. 37.1 contains 10 mass% MgO and 10 mass% Al₂O₃. MgO enters the blast furnace

only in flux while Al₂O₃ enters in flux, coke, and injected coal.

A consequence of this is shown in Fig. 37.5, which shows that less Al₂O₃ flux than MgO flux is needed to achieve 10 mass% in slag.

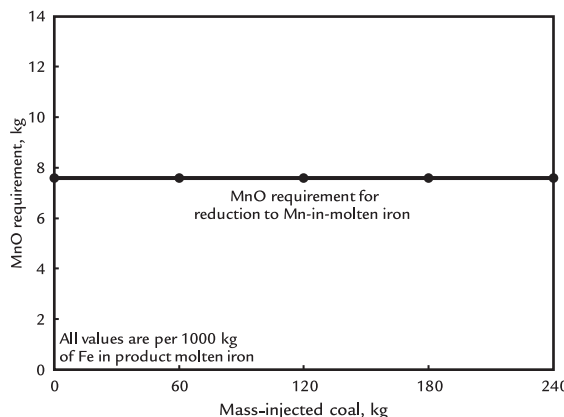


FIGURE 37.6 The effect of injected coal quantity on bottom-segment MnO requirement. As described above, coal injection has no effect.

Notice also that;

1. the MgO in flux requirement decreases slightly with increasing coal injection, just like CaO, Fig. 37.4,
- but that;
2. the Al₂O₃-in-flux requirement increases slightly with increasing coal injection, and
3. arises because coal injection replaces 3 mass % Al₂O₃ coke with 2.4 mass% Al₂O₃ coal.

37.14.1 MnO Requirement

Fig. 37.6 shows MnO requirement of the bottom segment for producing 0.5 mass% Mn in product molten iron. It is unaffected by the amount of injected coal. This is because (1) the Mn/Fe ratio in the product molten iron is specified as constant throughout this chapter, and (2) MnO is the bottom segment's only source of Mn (Fig. 37.1).

37.15 SUMMARY

This chapter shows how to include industrial coal injection in our bottom-segment calculations. It builds on;

1. coal hydrocarbon calculations of Chapter 13, Bottom-Segment With Pulverized Hydrocarbon Injection, and
2. ore gangue, coke ash, Si and Mn reduction, and flux requirement calculations of Chapter 36, Bottom-Segment Calculations—Reduction of MnO.

We pay special attention to the Al₂O₃ + SiO₂ ash in the injected coal.

Our calculations show that 1 kg of injected coal saves 0.95 kg of top charged coke, depending on their exact compositions. This savings is somewhat larger than the 0.91 kg coke saving published in Geerdes et al.¹

The chapter also shows the effect of coal injection on CaO, MgO, and Al₂O₃-in-flux requirements for steady production of molten slag. CaO and MgO requirements decrease slightly. Al₂O₃ requirement increases slightly.

MnO requirement is constant (per 1000 kg of Fe in product molten iron), determined only by the product molten iron's constant composition.

EXERCISES

- 37.1. Management of the blast furnace of Fig. 37.1 is considering buying cheap;
 - a. 88 mass% hydrocarbon
 - b. 3.6 mass% Al₂O₃
 - c. 1.0 mass% CaO
 - d. 8.4 mass% SiO₂ coal.

They wish to know how much coke will be replaced by injecting 60 kg of this coal into Fig. 37.1 furnace. Please calculate this for them.

Please also calculate;

- a. mass blast air;
- b. mass Al₂O₃ flux, mass CaO flux, and mass MgO flux;
- c. mass MnO; and
- d. mass top-charge MnO₂

that will give steady-state production of 1500°C molten products of Fig. 37.1, all per 1000 kg of Fe in product molten iron.

Perhaps use Appendix J to determine this coal's C, H, N, O, Al₂O₃, and SiO₂ composition. Use the enthalpies in Section 37.3.

- 37.2. When Exercise 37.1 coal arrives at the blast furnace plant, it is found to also contain 1 mass% CaO. By how much will this affect your Exercise 37.1 calculation results? The composition of the coal is found to be;
- a. 87 mass% hydrocarbon,
 - b. 3.6 mass% Al₂O₃,
 - c. 8.4 mass% SiO₂, and
 - d. 1 mass% CaO.

- 37.3. The blast furnace plant of Exercise 37.1 has had some more bad luck. Its CaO flux supplier has had an accident at its limestone mine so that it can only deliver 95 kg of CaO/1000 kg of Fe in product molten iron for the next month. By how much will management have to decrease molten iron production rate to compensate for this fall in CaO supply?

Reference

1. Geerdes M, Chaigneau R, Kurunov I, Lingiardi O, Ricketts J. *Modern blast furnace ironmaking (an introduction)*. 3rd ed. Amsterdam: IOS Press BV; 2015.

38

Bottom-Segment Calculations With Multiple Injectants

O U T L I N E

38.1 Using Multiple Injectants in Blast Furnace Ironmaking	336	38.4.2 H Balance	340
		38.4.3 N Balance	341
38.2 Adding Pure Oxygen Injection to Matrix	336	38.4.4 C Balance	341
38.2.1 Inserting Oxygen Quantity Specification	339	38.4.5 Enthalpy Balance	341
38.2.2 Amended Oxygen Mass Balance	339		
38.2.3 Amended Enthalpy Balance	339	38.5 Leaving Room for Other Injectants	341
38.3 Adding Through-Tuyere Input H ₂ O(g)	339	38.6 Matrix Results	341
38.3.1 O Balance	339	38.7 Discussion	343
38.3.2 H Balance	340	38.7.1 Steady-State Coke Requirement	343
38.3.3 Enthalpy Balance	340	38.7.2 Dry Air Requirement	343
38.4 Including Natural Gas Injection in Matrix	340	38.8 Summary	344
38.4.1 O Balance	340	Exercises	344
		References	344

38.1 USING MULTIPLE INJECTANTS IN BLAST FURNACE IRONMAKING

This chapter examines coal injection, as described in Chapter 37, Bottom-Segment Calculations With Pulverized Coal Injection, - plus simultaneous injection of;

- pure oxygen; and
- natural gas

and through-tuyere input of:

- $H_2O(g)$ in blast, Fig. 38.1.

Room is also left for a fifth injectant, for example, oil.

The objective of this chapter is to prepare a matrix that can determine the best (i.e., optimum) way to;

- operate a blast furnace to achieve a specified goal.

Example, goals are;

- lowest cost,
- least coke, and
- lowest carbon emission

for molten iron production.

The most obvious way to achieve these goals is to simultaneously;

1. inject various fuel/reductants and other substances through tuyeres of a blast furnace, and
2. vary their quantities according to cost and availability.

Other contributors to optimization are blast temperature and top-charged materials, discussed in Chapter 43, Top-Charged Scrap Steel.

The remainder of this chapter shows how to represent simultaneous through-tuyere input of;

- pulverized coal, pure oxygen, blast moisture, and natural gas in preparation for our optimization calculations.

All the instructions are illustrated in matrix Table 38.1.

38.2 ADDING PURE OXYGEN INJECTION TO MATRIX TABLE 37.3

Pure oxygen injection is included in the coal injection matrix, Table 37.3, by adding;

1. a new column on the right side of matrix Table 37.3 by putting the heading *mass O_2 in tuyere-injected pure oxygen* on the top of Column AD (Cell AD2),
2. a new row at the bottom of Table 37.3 by putting the label *mass O_2 in tuyere-injected pure oxygen* in Cell B29,
3. an oxygen quantity equation to the new row and by;
4. amending the oxygen and enthalpy balances of Table 37.3.

These are all shown in matrix Table 38.1.

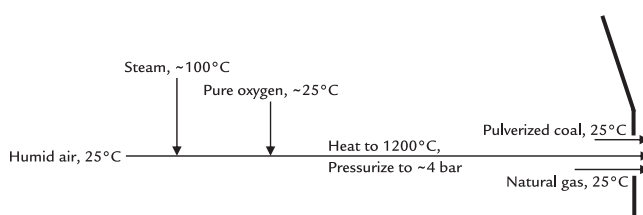


FIGURE 38.1 Schematic of pulverized coal, natural gas, pure oxygen, and $H_2O(g)$, from humid air and steam, entering a blast furnace through its tuyeres.

TABLE 38.1 Bottom-Segment Matrix With Pulverized Coal, Pure Oxygen, H₂O(g)-in-Blast, and Natural Gas Entering the Blast Furnace Through Its Tuyeres

	A	B	C	D	E	F	G	H	I	J	K
1	BOTTOM SEGMENT CALCULATIONS										
2	Equation	Description	Numerical term	mass Fe _{0.947} O into bottom segment	mass C in descending coke	mass O ₂ in blast air	mass N ₂ in blast air	mass Fe out in molten iron	mass C out in molten iron	mass CO out in ascending gas	mass CO ₂ out in ascending gas
3	7.7	Fe out in molten iron specification	1000	0	0	0	0	1	0	0	0
4	32.2	SiO ₂ descending in ore	0	0	0	0	0	0.0753	0	0	0
5	34.4	SiO ₂ in coke specification	0	0	0.0778	0	0	0	0	0	0
6	7.2	Fe mass balance	0	-0.768	0	0	0	1	0	0	0
7	0	mass balance	0	-0.232	0	-1	0	0	0	0.571	0.727
8	C mass balance	0	0	-1	0	0	0	0	1	0.429	0.273
9	37.9	SiO ₂ mass balance	0	0	0	0	0	0	0	0	0
10	N mass balance	0	0	0	0	0	-1	0	0	0	0
11	7.6	N ₂ in blast air specification	0	0	0	3.3	-1	0	0	0	0
12	7.9	Equilibrium CO ₂ /CO mass ratio	0	0	0	0	0	0	0	0.694	-1
13	36.3	C out in molten iron specification	0	0	0	0	0	0.0476	-1	0	0
14	34.2	Al ₂ O ₃ in coke specification	0	0	0.0333	0	0	0	0	0	0
15	32.5	Al ₂ O ₃ out in molten slag specification	0	0	0	0	0	0	0	0	0
16	37.7	Al ₂ O ₃ mass balance	0	0	0	0	0	0	0	0	0
17	32.6	CaO out in molten slag specification	0	0	0	0	0	0	0	0	0
18	32.9	CaO mass balance	0	0	0	0	0	0	0	0	0
19	32.7	MgO out in molten slag specification	0	0	0	0	0	0	0	0	0
20	32.1	MgO mass balance	0	0	0	0	0	0	0	0	0
21	Enthalpy balance	-320	3.152	-1.359	-1.239	-1.339	1.269	5	-2.926	-7.926	
22	36.4	Si out in molten iron specification	0	0	0	0	0	0.00423	0	0	0
23	36.5	Mn out in molten iron specification	0	0	0	0	0	0.00529	0	0	0
24	36.7	Mn mass balance	0	0	0	0	0	0	0	0	0
25	36.9	Mn reduction efficiency	0	0	0	0	0	0	0	0	0
26	H mass balance	0	0	0	0	0	0	0	0	0	0
27	11.8	Equilibrium H ₂ O/H ₂ mass ratio	0	0	0	0	0	0	0	0	0
28	37.2	Coal injection quantity	60	0	0	0	0	0	0	0	0
29	9.1	Mass O ₂ in tuyere-injected pure oxygen	30	0	0	0	0	0	0	0	0
30	12.2	Mass through-tuyere input H ₂ O(g)	0	0	0	0.0118	0.0118	0	0	0	0
31	29.1	Mass tuyere-injected natural gas	60	0	0	0	0	0	0	0	0
32	Additional injectant quantity equation	0	0	0	0	0	0	0	0	0	0

(Continued)

TABLE 38.1 (Continued)

L	M	N	O	P	Cl	K	S	T	U	V
mass N ₂ out in ascending gas	mass H ₂ out in ascending gas	mass H ₂ O out in ascending gas	mass SiO ₂ in descending ore	mass SiO ₂ in descending coke	mass SiO ₂ out in molten slag	mass Al ₂ O ₃ in descending decomposed flux	mass Al ₂ O ₃ in descending coke	mass Al ₂ O ₃ out in molten slag	mass CaO in descending decomposed flux	mass CaO out in molten slag
3 0	0	0	0	0	0	0	0	0	0	0
4 0	0	0	-1	0	0	0	0	0	0	0
5 0	0	0	0	-1	0	0	0	0	0	0
6 0	0	0	0	0	0	0	0	0	0	0
7 0	0	0	0.888	0	0	0	0	0	0	0
8 0	0	0	0	0	0	0	0	0	0	0
9 0	0	0	-1	-1	1	0	0	0	0	0
10 1	0	0	0	0	0	0	0	0	0	0
11 0	0	0	0	0	0	0	0	0	0	0
12 0	0	0	0	0	0	0	0	0	0	0
13 0	0	0	0	0	0	0	0	0	0	0
14 0	0	0	0	0	0	0	-1	0	0	0
15 0	0	0	0	0	0.256	0	0	-1	0	0
16 0	0	0	0	0	0	-1	-1	1	0	0
17 0	0	0	0	0	1.05	0	0	0	0	-1
18 0	0	0	0	0	0	0	0	0	-1	1
19 0	0	0	0	0	0.256	0	0	0	0	0
20 0	0	0	0	0	0	0	0	0	0	0
21 1.008	13.35	-11.49	14.13	14.13	-13.28	15.41	15.41	-13.58	10.50	-8.495
22 0	0	0	0	0	0	0	0	0	0	0
23 0	0	0	0	0	0	0	0	0	0	0
24 0	0	0	0	0	0	0	0	0	0	0
25 0	0	0	0	0	0	0	0	0	0	0
26 0	1	0.112	0	0	0	0	0	0	0	0
27 0	5.44	-1	0	0	0	0	0	0	0	0
28 0	0	0	0	0	0	0	0	0	0	0
29 0	0	0	0	0	0	0	0	0	0	0
30 0	0	0	0	0	0	0	0	0	0	0
31 0	0	0	0	0	0	0	0	0	0	0
32 0	0	0	0	0	0	0	0	0	0	0
W	X	Y	Z	AA	AB	AC	AD	AE	AF	AG
mass MgO in descending decomposed flux	mass MgO out in molten slag	mass Si out in molten iron	mass Mn out in molten iron	mass descending MnO	mass MnO out in molten slag	mass tuyere-injected coal	mass O ₂ in tuyere-injected pure oxygen	mass through-tuyere input H ₂ O(g)	mass tuyere-injected natural gas	mass additional tuyere injectant
3 0	0	0	0	0	0	0	0	0	0	0
4 0	0	0	0	0	0	0	0	0	0	0
5 0	0	0	0	0	0	0	0	0	0	0
6 0	0	0	0	0	0	0	0	0	0	0
7 0	0	0	-1.14	-0.291	0	0	-0.046	-1	-0.888	-0.01
8 0	0	0	0	0	0	0	-0.81	0	0	-0.734
9 0	0	0	2.14	0	0	0	-0.056	0	0	0
10 0	0	0	0	0	0	0	-0.009	0	0	0.017
11 0	0	0	0	0	0	0	0	0	0	0
12 0	0	0	0	0	0	0	0	0	0	0
13 0	0	0	0	0	0	0	0	0	0	0
14 0	0	0	0	0	0	0	0	0	0	0
15 0	0	0	0	0	0	0	0	0	0	0
16 0	0	0	0	0	0	0	0.024	0	0	0
17 0	0	0	0	0	0	0	0	0	0	0
18 0	0	0	0	0	0	0	0	0	0	0
19 0	0	-1	0	0	0	0	0	0	0	0
20 -1	1	0	0	0	0	0	0	0	0	0
21 13.84	-11.14	-2.15	1.27	4.77	-3.530	1.2	-1.239	10.81	4.52	0
22 0	0	-1	0	0	0	0	0	0	0	0
23 0	0	0	-1	0	0	0	0	0	0	0
24 0	0	0	0	1	0.774	0.774	0	0	0	0
25 0	0	0	0	0	-0.1	1	0	0	0	0
26 0	0	0	0	0	0	0	-0.056	0	-0.112	-0.240
27 0	0	0	0	0	0	0	0	0	0	0
28 0	0	0	0	0	0	0	1	0	0	0
29 0	0	0	0	0	0	0	0	1	0	0
30 0	0	0	0	0	0	0	0	0	-1	0
31 0	0	0	0	0	0	0	0	0	1	0
32 0	0	0	0	0	0	0	0	0	0	1

The table is presented in three sections for clarity.

38.2.1 Inserting Oxygen Quantity Specification Eq. (9.1)

Our chosen oxygen quantity specification equation is;

$$30 = \left[\begin{array}{l} \text{mass O}_2 \text{ in tuyere-} \\ \text{injected pure oxygen} \end{array} \right] * 1 \quad (9.1)$$

as shown in matrix [Table 38.1](#), new Row 29. The 30 in Eq. (9.1) is placed in Cell C29. The 1 is placed in Cell AD29.

38.2.2 Amended Oxygen Mass Balance

Oxygen injection also adds terms to the oxygen and enthalpy balances of Table 38.1.

As shown in Section 9.2.2, oxygen injection requires that Row 7 oxygen balance equation of Table 37.3 must contain the new term:

$$-\left[\begin{array}{l} \text{mass O}_2 \text{ in tuyere-} \\ \text{injected pure oxygen} \end{array} \right] * 1$$

This is added as **-1** in Cell AD7 of [Table 38.1](#).

38.2.3 Amended Enthalpy Balance

As shown in Section 9.2.3, oxygen injection also requires that the enthalpy balance (Row 21) of Table 37.3 contains the new term;

$$-\left[\begin{array}{l} \text{mass O}_2 \text{ in tuyere-} \\ \text{injected pure oxygen} \end{array} \right] * 1.239$$

where 1.239 is the 1200°C enthalpy of O₂, MJ per kg.

This new enthalpy term is added as **-1.239** in Cell AD21 of [Table 38.1](#).

The matrix can now be solved for simultaneous coal and oxygen injection (as in Chapter 9: Bottom-Segment With Oxygen Enrichment of Blast Air), but we postpone solving until our H₂O(g) and natural gas inputs have also been added to the matrix.

38.3 ADDING THROUGH-TUYERE INPUT H₂O(g)

Through-tuyere H₂O(g) input is added to matrix [Table 38.1](#) by;

1. adding a new column to the matrix by labeling Column AE with *mass through-tuyere input H₂O(g)* (Cell AE2),
2. adding a new row to the matrix by labeling Row 30 with *mass through-tuyere input H₂O(g)* (Cell B30), and
3. adding input H₂O(g) quantity Eq. (12.2) to the expanded matrix, that is;

$$\begin{aligned} 0 = & -\left[\begin{array}{l} \text{mass through-tuyere} \\ \text{input H}_2\text{O(g)} \end{array} \right] * 1 \\ & + \left[\begin{array}{l} \text{mass O}_2 \\ \text{in blast air} \end{array} \right] * 0.0118 \\ & + \left[\begin{array}{l} \text{mass N}_2 \\ \text{in blast air} \end{array} \right] * 0.0118 \end{aligned} \quad (12.2)$$

as detailed in Chapter 12, Bottom-Segment With Moisture in Blast Air, and Appendix O. The 0.0118 coefficient is for 15 g of H₂O(g) in blast per Nm³ of dry air in blast.

Matrix [Table 38.1](#) represents this equation by;

- inserting **0** in Cell C30,
- inserting **-1** in Cell AE30, and
- inserting **0.0118** in Cells F30 and G30.

38.3.1 O Balance

As shown in Section 12.7, through-tuyere H₂O(g) input requires that the right side of Row 7, the O balance of [Table 38.1](#), contains the new term;

$$-\left[\begin{array}{l} \text{mass through-tuyere} \\ \text{input H}_2\text{O(g)} \end{array} \right] * 0.888$$

where $0.888 = 88.8 \text{ mass\% O in H}_2\text{O}/100\%$

This is represented in matrix [Table 38.1](#) by inserting **-0.888** into Cell AE7.

38.3.2 H Balance

As shown in Section 12.5, through-tuyere $\text{H}_2\text{O(g)}$ input also requires a new term in Row 26, the H balance of [Table 38.1](#). This is;

$$-\left[\frac{\text{mass through-tuyere}}{\text{input } \text{H}_2\text{O(g)}} \right] * 0.112$$

where $0.112 = 11.2 \text{ mass\% H in } \text{H}_2\text{O}/100\%$.

This is represented by **-0.112** in Cell AE26 of [Table 38.1](#).

38.3.3 Enthalpy Balance

As shown in Section 12.8, through-tuyere $\text{H}_2\text{O(g)}$ input injection requires that Row 21, the enthalpy balance of [Table 38.1](#), contains the new term;

$$-\left[\frac{\text{mass through-tuyere}}{\text{input } \text{H}_2\text{O(g)}} \right] * (-10.81)$$

where (-10.81) is the 1200°C enthalpy of $\text{H}_2\text{O(g)}$, MJ per kg.

This new enthalpy term is represented by **10.81** in Cell AE21 of [Table 38.1](#).

The matrix can now be solved for simultaneous coal injection, oxygen injection and through-tuyere input $\text{H}_2\text{O(g)}$ - but we postpone solving until natural gas injection has been added to the matrix.

38.4 INCLUDING NATURAL GAS INJECTION IN MATRIX [TABLE 38.1](#)

Natural gas injection is now included in the pulverized coal, pure oxygen injection, $\text{H}_2\text{O(g)}$ input matrix by;

1. adding a new column to the matrix of [Section 38.3](#) by heading Column AF with *mass tuyere-injected natural gas* (Cell AF2),
2. adding a new row to the matrix of [Section 38.3](#) by labeling Row 31 with *mass tuyere-injected natural gas* in Cell B31, and

3. adding Eq. (29.1) to the expanded matrix, that is:

$$60 = \left[\frac{\text{mass tuyere-injected}}{\text{natural gas}} \right] * 1$$

Matrix [Table 38.1](#) represents this equation by;

- inserting **60** in Cell C31, and
- inserting **1** in Cell AF31

We are using the same natural gas as is used in previous chapters. It contains;

- 73.4 mass% C,
- 24.0 mass% H,
- 1.7 mass% N, and
- 1.0 mass% O

Its enthalpy is -4.52 MJ/kg of natural gas, Appendix J.

38.4.1 O Balance

As shown in Section 29.3.4, natural gas injection requires that the O balance of [Table 38.1](#) contains the new term;

$$-\left[\frac{\text{mass tuyere-injected}}{\text{natural gas}} \right] * 0.01$$

where $0.01 = 1 \text{ mass\% O in natural gas}/100\%$

This is represented by **-0.01** in new Cell AF7 of [Table 38.1](#).

38.4.2 H Balance

As shown in Section 29.3.2, natural gas also requires a new term in Row 26, the H balance of [Table 38.1](#). It is;

$$-\left[\frac{\text{mass tuyere-injected}}{\text{natural gas}} \right] * 0.24$$

where $0.240 = 24.0 \text{ mass\% H in natural gas}/100\%$.

This is represented by **-0.240** in Cell AF26 of [Table 38.1](#).

38.4.3 N Balance

As shown in Section 29.3.5, natural gas requires a new term in Row 10 N balance of [Table 38.1](#). It is;

$$-\left[\begin{array}{c} \text{mass tuyere-injected} \\ \text{natural gas} \end{array} \right] * 0.017$$

where 0.017 is 1.7 mass% N in natural gas/100%.

This is represented by **-0.017** in Cell AF10 of [Table 38.1](#).

38.4.4 C Balance

Finally, as shown in Section 29.3.6, natural gas also requires a new term in the C balance of [Table 38.1](#). It is;

$$-\left[\begin{array}{c} \text{mass tuyere-injected} \\ \text{natural gas} \end{array} \right] * 0.734$$

where 0.734 is 73.4 mass% C in natural gas/100%.

This is represented by **-0.734** in Cell AF8 of [Table 38.1](#).

38.4.5 Enthalpy Balance

As shown in Section 11.2.5, natural gas injection requires that the right side of the enthalpy balance of Table 11.1 contains the additional term;

$$-\left[\begin{array}{c} \text{mass tuyere-injected} \\ \text{natural gas} \end{array} \right] * (-4.52)$$

where **(-4.52)** is the 25°C enthalpy of our natural gas, MJ per kg.

This new enthalpy term is represented by inserting **4.52** in Cell AF21 of [Table 38.1](#).

The matrix is now solved for simultaneous coal injection, oxygen injection, through-tuyere input H₂O(g), and natural gas injection. The results are shown in [Table 38.2](#).

38.5 LEAVING ROOM FOR OTHER INJECTANTS

Room can be left for another injectant by;

1. inserting a heading in the far-right column of matrix [Table 38.1](#), for example, *mass additional tuyere injectant* in Cell AG2;
2. inserting a label into Cell B32 at the bottom of matrix [Table 38.1](#) (Cell B32), for example, *additional injectant quantity* equation; and
3. inserting **0** in Cell C32 and **1** in new Cell AG32.

The **0** in instruction (3) indicates that no *additional injectant* is being injected through the tuyeres.

These instructions can be followed multiple times.

[Table 38.1](#) collects all the above inputs and instructions. [Table 38.2](#) shows calculated values of the matrix.

38.6 MATRIX RESULTS

[Table 38.2](#) shows the C-in-coke and O₂ in dry blast air results with;

- 60 kg of tuyere-injected coal,
- 30 kg of O₂ in injected pure oxygen,
- 18 kg of H₂O(g) in input moist blast, and
- 60 kg of tuyere-injected natural gas

for the steady-state production of 1500°C molten 4.5 mass% C, 94.6 mass% Fe, 0.5 mass% Mn, and 0.4 mass% Si requires;

- 326 kg of C-in-coke (366 kg of coke because coke is 90 mass% C) and,
- 347 kg of O₂-in-blast air (1489 kg of dry air because dry air is 23.3 mass% O₂).

This and other points are shown in [Figs. 38.2 and 38.3](#).

TABLE 38.2 Results From Solving Matrix Table 38.1. They are Discussed in Sections 38.6 Onward

A	B	C	D	E	F	G
33	Bottom segment calculated values	kg per 1000 kg of Fe out in molten iron				
34	mass Fe _{0.947} O into bottom segment	1302				
35	mass C in descending coke	326	also = mass C in the furnace's coke charge, Eqn. (7.16)			
36	mass O ₂ in blast air	347				
37	mass N ₂ in blast air	1145				
38	mass Fe out in molten iron	1000				
39	mass C out in molten iron	48				
40	mass CO out in ascending gas	600				
41	mass CO ₂ out in ascending gas	416				
42	mass N ₂ out in ascending gas	1146				
43	mass H ₂ out in ascending gas	12				
44	mass H ₂ O out in ascending gas	67				
45	mass SiO ₂ in descending ore	75				
46	mass SiO ₂ in descending coke	25				
47	mass SiO ₂ out in molten slag	95				
48	mass Al ₂ O ₃ in descending decomposed flux	12				
49	mass Al ₂ O ₃ in descending coke	11				
50	mass Al ₂ O ₃ out in molten slag	24				
51	mass CaO in descending decomposed flux	100				
52	mass CaO out in molten slag	100				
53	mass MgO in descending decomposed flux	24				
54	mass MgO out in molten slag	24				
55	mass Si out in molten iron	4.2				
56	mass Mn out in molten iron	5.3				
57	mass descending MnO	7.6				
58	mass MnO out in molten slag	0.8				
59	mass tuyere-injected coal	60				
60	mass O ₂ in tuyere-injected pure oxygen	30				
61	mass through-tuyere input H ₂ O(g)	18				
62	mass tuyere-injected natural gas	60				
63	mass additional tuyere injectant	0				

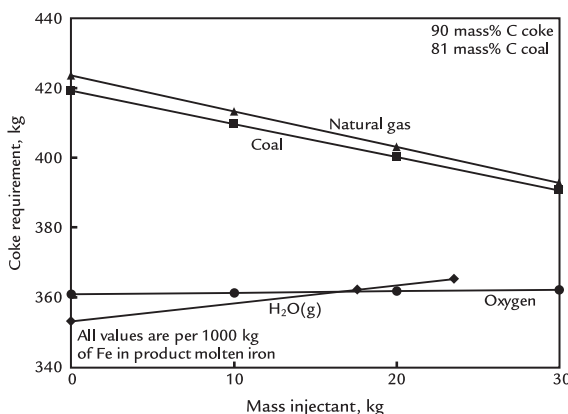


FIGURE 38.2 Effect of increasing individual tuyere input quantities on blast furnace coke requirement. Coal and natural gas decrease the requirement. Oxygen has a negligible effect. $\text{H}_2\text{O}(\text{g})$ increases the requirement. The lines are straight. All masses are per 1000 kg of Fe in product molten iron.

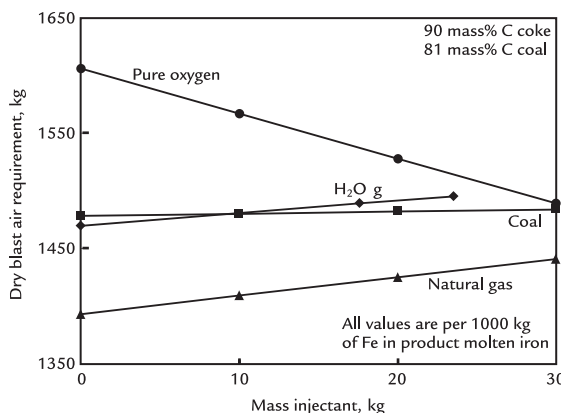


FIGURE 38.3 Effect of increasing individual tuyere input quantities on blast furnace air requirements. Oxygen decreases the air requirement. Input $\text{H}_2\text{O}(\text{g})$, natural gas, and coal all increase it, coal slightly less than the others. All masses are per 1000 kg of Fe in product molten iron.

38.7 DISCUSSION

Figs. 38.2 and 38.3 show the effects of varying the amount of one injectant while holding the others at constant values as listed in Table 38.1.

Fig. 38.2 shows the effect on the amount of coke needed for steady production of 1500°C 4.5% C, 94.6% Fe, 0.5% Mn, 0.4% Si molten iron. Fig. 38.3 shows the effect on its steady state dry air requirement.

38.7.1 Steady-State Coke Requirement

Fig. 38.2 shows that coke requirement is decreased by increasing;

- mass-injected coal, and
- mass-injected natural gas.

This is expected because they both supply carbon, lowering the steady-state C-in-coke requirement.

Injected pure oxygen has very little effect while through-tuyere input $\text{H}_2\text{O}(\text{g})$ increases the coke requirement.

The $\text{H}_2\text{O}(\text{g})$ effect is due to all of matrix equations of Table 38.1. We speculate that the increased coke requirement is due to the large negative enthalpy of $\text{H}_2\text{O}(\text{g})$, which must be overcome by burning more C-in-coke in front of the tuyeres.

38.7.2 Dry Air Requirement

Fig. 38.3 shows that the air requirement drops with increasing pure oxygen input quantity. This is because pure oxygen lowers the amount of O_2 -in-blast needed for steady state furnace operation.

Air requirement is increased by $\text{H}_2\text{O}(\text{g})$ input, pulverized coal injection and natural gas injection.

Required air increases with more $\text{H}_2\text{O}(\text{g})$ input because more C-in-coke must be burnt with O_2 in front of the tuyeres (Section 38.7.1).

The increased air requirement with increasing 25°C coal and 25°C natural gas injection is due to all of matrix equations of Table 38.1. We may postulate that more C-in-coke must

be burnt in front of the tuyeres to heat these cool injectants (and to dissociate natural gas)—requiring slightly more air.

38.8 SUMMARY

This chapter shows how to represent simultaneous input of multiple injectants in our matrices. Each injectant requires;

1. a new column on the right side of the matrix,
2. a new row at the bottom of the matrix,
3. a new injectant quantity equation, and
4. amended mass and enthalpy balance equations.

The changes are intuitive and easy to apply and read.

The results of our simultaneous coal, oxygen, $H_2O(g)$, and natural gas injection confirm that;

1. hydrocarbon injectants save considerable coke,
2. $H_2O(g)$ input increases coke requirement, and
3. oxygen injection has a negligible effect on the coke requirement.

Chapters 39, and 40; Flame Temperature and Top-Segment Calculations with Multiple Injectants, continue with these four injectants by showing how they are included in our tuyere raceway and top-segment calculations.

EXERCISES

All masses in this exercise set are kg per 1000 kg of Fe in product molten iron.

All exercises in this set include tuyere injection of 60 kg of pulverized coal, 30 kg of pure oxygen, and 60 kg of natural gas as described in [Table 38.1](#). The blast is 1200°C. It contains 15 g of $H_2O(g)$ per Nm^3 of dry blast air also as described in [Table 38.1](#).

- 38.1.** Blast furnace management of Table 31.1 is considering injecting 20 kg/1000 kg of oil of Fe in product molten iron (in addition to injectants of [Table 38.1](#)). The oil they have in mind contains;

- a. 85 mass% C,
- b. 13 mass% H,
- c. 1 mass% N, and
- d. 1 mass% O.

Its 25°C enthalpy is -1.7 MJ/kg of oil.¹

Please add this injectant to the matrix of [Table 38.1](#) and determine its effect on coke and dry blast air requirements. You may still leave room for an additional injectant or use the vacant column and vacant row in the matrix of [Table 38.1](#).

- 38.2.** Blast furnace companies have long wished to inject chopped recycle polymers into their blast furnaces. One choice is chopped polyethylene, $C_2H_4(s)$. In Exercise 38.1, management is considering replacing its 20 kg of oil injectant with 20 kg of chopped polyethylene injectant.

Please make this replacement and determine its effect on coke and dry blast air requirements of their furnace. Its 25°C enthalpy is -2.0 MJ/kg .²

- 38.3.** In Exercise 38.2, management is thinking of hydrogen as a future injectant. They wish to know how hydrogen injection will affect their coke and dry air requirements. To determine this, please replace 20 kg of polyethylene injectant of Exercise 38.2 with 20 kg of 25°C $H_2(g)$ injectant.

References

1. Peacey JG, Davenport WG. *The iron blast furnace—theory and practice*. Oxford: Elsevier; 1979. p. 211.
2. Splitstone PL, Johnson WH. The enthalpies of combustion and formation of linear polyethylene. *J Res Natl Bur Stand* 1974;78A(5):611–16 Washington.

Raceway Flame Temperature With Multiple Injectants

OUTLINE

39.1 Calculating the Raceway Flame Temperature With Tuyere Injectants	345	39.3.1 Raceway Output Enthalpy	349
		39.3.2 Flame Temperature Calculation	349
39.2 Raceway Matrix	346	39.4 Results	352
39.2.1 Mass of Al_2O_3 in Falling Coke Particles	346	39.5 List of Raceway Equations of This Chapter in Table 39.2	353
39.2.2 Mass of SiO_2 in Falling Coke Particles	349	39.6 Summary	354
39.3 Calculation of Raceway Input Enthalpy, Output Enthalpy, and Flame Temperature	349	Exercises	354
		Reference	354

39.1 CALCULATING THE RACEWAY FLAME TEMPERATURE WITH TUYERE INJECTANTS

In this chapter, we automatically calculate tuyere raceway flame temperatures with simultaneous tuyere injection of;

- pulverized coal,
- pure oxygen,

- $\text{H}_2\text{O(g)}$ -in-blast (from humidity and steam), and
- natural gas.

Fig. 39.1 shows a raceway with these injectants plus falling $\text{C}-\text{Al}_2\text{O}_3-\text{SiO}_2$ coke particles.

Raceway flame temperature must be kept within a narrow range $\sim 2000^\circ\text{C}$ to 2300°C while blast furnace's inputs are being varied to

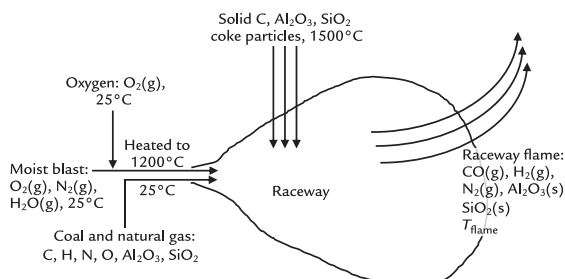


FIGURE 39.1 Sketch of blast furnace raceway with simultaneous tuyere injection of coal, oxygen, $H_2O(g)$, and natural gas. Note that the falling coke and tuyere-injected coal both contain Al_2O_3 and SiO_2 . Raceway matrix Table 39.1 and Eqs. (39.3), (39.5), and (39.6) calculate the temperature of the departing gases and solids, that is, the raceway flame temperature. Note that the raceway output gas contains only $CO(g)$ and $H_2(g)$, that is, no $CO_2(g)$ or $H_2O(g)$. This is discussed in Chapter 14, Raceway Flame Temperature.

optimize a blast furnace operation, for example, to minimize molten iron production cost.

The flame must be;

1. hot enough to ensure that the blast furnace's product iron and slag are completely molten at 1500°C, but
2. not so hot as to impact the reduction and melting behavior of the ferrous raw materials. This can lead to irregular burden descent characterized by the burden hanging and slipping.

The objectives of this chapter are to;

1. build a spreadsheet that will automatically calculate raceway flame temperatures from bottom-segment calculated inputs and outputs, with multiple injectants, and
2. plot and discuss the effect of injectant amounts on raceway flame temperature.

39.2 RACEWAY MATRIX

The bottom-segment inputs for multiple injectants are provided in Table 39.1, all values are per 1000 kg of Fe in product molten iron.

Table 39.2 (split for clarity) is the flame temperature matrix of this chapter with the bottom-segment inputs and outputs of Table 39.1. It consists of;

1. steady-state raceway input O_2 and N_2 -in-blast air masses, expressed by Eqs. (39.7) and (39.8);
2. injected coal, oxygen, $H_2O(g)$, and natural gas raceway input masses of Chapter 38, Bottom-Segment Calculations With Multiple Injectants, expressed by Eqs. (39.15)–(39.18);
3. raceway C, O, N, H, Al_2O_3 , and SiO_2 mass balance Eqs. (39.9)–(39.14); and
4. masses of Al_2O_3 -in-coke and SiO_2 -in-coke falling into raceway of Fig. 39.1, described below Eqs. (39.1)–(39.2).

39.2.1 Mass of Al_2O_3 in Falling Coke Particles

The amount of Al_2O_3 falling into the raceway is described by;

$$\left[\frac{\text{mass } Al_2O_3 \text{ in falling}}{\text{coke particles}} \right] = \left[\frac{\text{mass\% } Al_2O_3}{\text{in coke}} \right]$$

$$\left[\frac{\text{mass C in falling}}{\text{coke particles}} \right] = \left[\frac{\text{mass\% C}}{\text{in coke}} \right]$$

$$= \frac{3 \text{ mass\% } Al_2O_3 \text{ in coke}}{90 \text{ mass\% C in coke}} = 0.0333$$

or

$$\left[\frac{\text{mass } Al_2O_3 \text{ in falling}}{\text{coke particles}} \right] * 1 = \left[\frac{\text{mass C in falling}}{\text{coke particles}} \right] * 0.0333$$

or subtracting $\left\{ \left[\frac{\text{mass } Al_2O_3 \text{ in falling}}{\text{coke particles}} \right] * 1 \right\}$ from both sides;

$$0 = - \left[\frac{\text{mass } Al_2O_3 \text{ in falling}}{\text{coke particles}} \right] * 1 + \left[\frac{\text{mass C in falling}}{\text{coke particles}} \right] * 0.0333 \quad (39.1)$$

TABLE 39.1 Bottom-Segment Inputs and Outputs as Calculated by Bottom-Segment Matrix Table 38.1

A	B	C	D	E	F	G
33	Bottom segment calculated values	kg per 1000 kg of Fe out in molten iron				
34	mass Fe _{0.947} O into bottom segment	1302				
35	mass C in descending coke	326	also = mass C in the furnace's coke charge, Eqn. (7.16)			
36	mass O ₂ in blast air	347				
37	mass N ₂ in blast air	1145				
38	mass Fe out in molten iron	1000				
39	mass C out in molten iron	48				
40	mass CO out in ascending gas	600				
41	mass CO ₂ out in ascending gas	416				
42	mass N ₂ out in ascending gas	1146				
43	mass H ₂ out in ascending gas	12				
44	mass H ₂ O out in ascending gas	67				
45	mass SiO ₂ in descending ore	75				
46	mass SiO ₂ in descending coke	25				
47	mass SiO ₂ out in molten slag	95				
48	mass Al ₂ O ₃ in descending decomposed flux	12				
49	mass Al ₂ O ₃ in descending coke	11				
50	mass Al ₂ O ₃ out in molten slag	24				
51	mass CaO in descending decomposed flux	100				
52	mass CaO out in molten slag	100				
53	mass MgO in descending decomposed flux	24				
54	mass MgO out in molten slag	24				
55	mass Si out in molten iron	4.2				
56	mass Mn out in molten iron	5.3				
57	mass descending MnO	7.6				
58	mass MnO out in molten slag	0.8				
59	mass tuyere-injected coal	60				
60	mass O ₂ in tuyere-injected pure oxygen	30				
61	mass through-tuyere input H ₂ O(g)	18				
62	mass tuyere-injected natural gas	60				
63	mass additional tuyere injectant	0				

This is a copy of Table 38.2.

TABLE 39.2 Raceway Matrix With Simultaneous Tuyere Injection of Coal, Oxygen, H₂O(g), and Natural Gas (Matrix is Split for Clarity)

A	B	C	D	E	F	G	H	I	
			=C36 =C37						
RACEWAY INPUTS AND OUTPUTS CALCULATION									
Equation	Description	Numerical Term	mass O ₂ entering raceway in blast air	mass N ₂ entering raceway in blast air	mass C entering raceway in falling coke particles	mass Al ₂ O ₃ entering raceway in falling coke particles	mass SiO ₂ entering raceway in falling coke particles	mass CO in raceway output gas	
39.7	Mass O ₂ entering raceway in blast air	347	1	0	0	0	0	0	
39.8	Mass N ₂ entering raceway in blast air	1145	0	1	0	0	0	0	
39.9	Raceway oxygen balance	0	-1	0	0	0	0	0.571	
39.10	Raceway carbon balance	0	0	0	-1	0	0	0.429	
39.11	Raceway nitrogen balance	0	0	-1	0	0	0	0	
39.12	Raceway hydrogen balance	0	0	0	0	0	0	0	
39.1	Mass Al ₂ O ₃ entering raceway in falling coke	0	0	0	0.0333	-1	0	0	
39.2	Mass SiO ₂ entering raceway in falling coke	0	0	0	0.0778	0	-1	0	
39.13	Raceway Al ₂ O ₃ balance	0	0	0	0	-1	0	0	
39.14	Raceway SiO ₂ balance	0	0	0	0	0	-1	0	
39.15	Mass tuyere injected real coal	60	0	0	0	0	0	0	
39.16	Mass O ₂ in tuyere-injected oxygen	30	0	0	0	0	0	0	
39.17	Mass H ₂ O(g) entering raceway in blast	18	0	0	0	0	0	0	
39.18	Mass tuyere-injected natural gas	60	0	0	0	0	0	0	
39.19	Mass additional tuyere injectant	0	0	0	0	0	0	0	
83			1200°C	1200°C	1500°C	1500°C	1500°C	T _{flame}	
84									
85									
J	K	L	M	N	O	P	Q	R	
	mass N ₂ in raceway output gas	mass H ₂ in raceway output gas	mass Al ₂ O ₃ (s) in raceway output gas	mass SiO ₂ (s) in raceway output gas	mass tuyere-injected coal entering raceway	mass O ₂ entering raceway in tuyere-injected pure oxygen	mass through-tuyere input H ₂ O(g) entering raceway	mass tuyere-injected natural gas entering raceway	mass tuyere-injected additional injectant entering raceway
68	0	0	0	0	0	0	0	0	0
69	0	0	0	0	0	0	0	0	0
70	0	0	0	0	-0.046	-1	-0.888	-0.01	0
71	0	0	0	0	-0.810	0	0	-0.734	0
72	1	0	0	0	-0.009	0	0	-0.017	0
73	0	1	0	0	-0.055	0	-0.112	-0.24	0
74	0	0	0	0	0	0	0	0	0
75	0	0	0	0	0	0	0	0	0
76	0	0	1	0	-0.024	0	0	0	0
77	0	0	0	1	-0.056	0	0	0	0
78	0	0	0	0	1	0	0	0	0
79	0	0	0	0	0	1	0	0	0
80	0	0	0	0	0	0	1	0	0
81	0	0	0	0	0	0	0	1	0
82	0	0	0	0	0	0	0	0	1
83									
84	T _{flame}	T _{flame}	T _{flame}	T _{flame}	25°C	1200°C	1200°C	25°C	
85									

All its equations are given at the end of this chapter. Column C's numerical values are from Table 39.1. For continuity with these values: Cell C68 = C36, Cell C69 = C37, Cell C78 = C59, Cell C79 = C60, Cell C80 = C61, Cell C81 = C62, and Cell C82 = C63.

39.2.2 Mass of SiO₂ in Falling Coke Particles

Likewise, the amount of SiO₂ falling into the raceway is described by;

$$0 = - \left[\begin{array}{l} \text{mass SiO}_2 \text{ in} \\ \text{falling coke particles} \end{array} \right] * 1 + \left[\begin{array}{l} \text{mass C in falling} \\ \text{coke particles} \end{array} \right] * \frac{7 \text{ mass\% SiO}_2 \text{ in coke}}{90 \text{ mass\% C in coke}}$$

or

$$0 = - \left[\begin{array}{l} \text{mass SiO}_2 \text{ in} \\ \text{falling coke particles} \end{array} \right] * 1 + \left[\begin{array}{l} \text{mass C in falling} \\ \text{coke particles} \end{array} \right] * 0.0778 \quad (39.2)$$

The raceway matrix with these equations is shown in [Table 39.2](#). Its calculated values are shown in [Table 39.3](#).

39.3 CALCULATION OF RACEWAY INPUT ENTHALPY, OUTPUT ENTHALPY, AND FLAME TEMPERATURE

Raceway input enthalpy with coal, oxygen, H₂O(g), and natural gas injection is given by the following equation;

$$\begin{aligned} & [\text{total raceway input enthalpy}] \\ &= [\text{mass O}_2 \text{ entering raceway in blast air}] * 1.239 \\ &+ [\text{mass N}_2 \text{ entering raceway in blast air}] * 1.339 \\ &+ [\text{mass C entering raceway in falling coke particles}] \\ &\quad * 2.488 \\ &+ [\text{mass Al}_2\text{O}_3 \text{ entering raceway in falling coke particles}] \\ &\quad * -14.67 \\ &+ [\text{mass SiO}_2 \text{ entering raceway in falling coke particles}] \\ &\quad * -13.44 \\ &+ [\text{mass tuyere-injected coal entering raceway}] * -1.2 \\ &+ [\text{mass O}_2 \text{ entering raceway in tuyere-injected oxygen}] \\ &\quad * 1.239 \\ &+ [\text{mass through-tuyere H}_2\text{O}(g) \text{ entering raceway}] \\ &\quad * -10.81 \\ &+ [\text{mass injected natural gas entering raceway}] * -4.52 \\ &+ [\text{mass additional tuyere injectant}] * 0 \end{aligned} \quad (39.3)$$

where the numerical values are the enthalpies (H°/MW) of the substances at the temperatures of [Fig. 39.1](#).

[Eq. \(39.3\)](#) is given in [Table 39.4](#) as;

$$\begin{aligned} &= C95 * 1.239 + C96 * 1.339 \\ &+ C97 * 2.488 + C98 * (-14.67) \\ &+ C99 * (-13.44) + C105 * (-1.2) \\ &+ C106 * 1.239 + C107 * (-10.81) \\ &+ C108 * (-4.52) + C109 * 0 \end{aligned} \quad (39.4)$$

[Eq. \(39.4\)](#) is like [Eq. \(30.6\)](#) with additional terms for;

1. falling 1500°C Al₂O₃(s)-in-coke and SiO₂(s)-in-coke, and
2. injected coal, oxygen, and H₂O(g).

39.3.1 Raceway Output Enthalpy

Chapter 14, Raceway Flame Temperature, specifies that there is no conductive, convective, and radiative heat loss from the raceway, that is;

$$\begin{aligned} & [\text{total raceway output enthalpy}] + [\text{zero}] \\ &= [\text{total raceway input enthalpy}] \end{aligned} \quad (14.13)$$

so that;

$$\begin{aligned} & [\text{total raceway output enthalpy}] \\ &= [\text{total raceway input enthalpy}] \end{aligned} \quad (39.5)$$

as shown in [Table 39.4](#).

39.3.2 Flame Temperature Calculation

Chapter 18, Raceway Flame Temperature With CH₄(g) Tuyere Injection, shows that raceway flame temperature with H entering the blast furnace is;

TABLE 39.3 Raceway Calculated Values with Tuyere Injection of 60 kg of Coal, 30 kg of Oxygen, and 18 kg of H₂O(g), Calculated by Eq. (19.2), and 60 kg of Natural Gas

A	B	C
94	Raceway calculated values	kg per 1000 kg of Fe out in molten iron
95	mass O ₂ entering raceway in blast air	347
96	mass N ₂ entering raceway in blast air	1145
97	mass C entering raceway in falling coke particles	205
98	mass Al ₂ O ₃ entering raceway in falling coke particles	6.8
99	mass SiO ₂ entering raceway in falling coke particles	16
100	mass CO in raceway output gas	693
101	mass N ₂ in raceway output gas	1146
102	mass H ₂ in raceway output gas	20
103	mass Al ₂ O ₃ (s) in raceway output gas	8.3
104	mass SiO ₂ (s) in raceway output gas	19
105	mass tuyere-injected coal	60
106	mass tuyere-injected pure oxygen	30
107	mass tuyere-injected H ₂ O(g)	18
108	mass tuyere-injected natural gas	60
109	mass additional tuyere injectant	0
110		

Eqs. (39.4), (39.5), and (39.6) use these values to calculate raceway input enthalpy, output enthalpy, and raceway adiabatic flame temperature.

TABLE 39.4 Equations for Calculating Raceway Input Enthalpy, Output Enthalpy, and Flame Temperature

	A	B	C	D	E	F	G	H	I	J	K	L	M
FLAME ENTHALPY AND FLAME TEMPERATURE CALCULATIONS													
114													
115	39.4	Total Raceway input enthalpy =C95*1.239+C96*1.339+C97*2.488+C98*14.67+C99*-13.44+C105*-1.2+C106*1.239+C107*-10.81+C108*-4.52+C109*0 =								1662	MJ per 1000 kg of Fe in product molten iron		
116	39.5	Total Raceway output FLAME enthalpy =J115 =								1662	MJ per 1000 kg of Fe in product molten iron		
117													
118	39.6	Raceway flame temperature °C =(J116*C100*-4.183-C101*-0.2448-C102*-4.13-C103*-16.72-C104*-15.47)/(C100*0.00131+C101*0.001301+C102*0.01756+C103*0.001887+C104*0.001427)=								1923	°C		

The equations are like those in Table 30.1 but with more terms.

$$\left\{ \begin{array}{l} \text{raceway output} \\ \text{(flame) enthalpy} \end{array} \right. - \left[\begin{array}{l} \text{mass CO in raceway} \\ \text{output gas} \end{array} \right] * (-4.183) - \left[\begin{array}{l} \text{mass N}_2 \text{ in raceway} \\ \text{output gas} \end{array} \right] * (-0.2448) - \left[\begin{array}{l} \text{mass H}_2 \text{ in raceway} \\ \text{output gas} \end{array} \right] * (-4.130) \} = T_{\text{flame}} \quad (18.9)$$

$$\left\{ \begin{array}{l} \left[\begin{array}{l} \text{mass CO in raceway} \\ \text{output gas} \end{array} \right] * 0.001310 \\ + \left[\begin{array}{l} \text{mass N}_2 \text{ in raceway} \\ \text{output gas} \end{array} \right] * 0.001301 \\ + \left[\begin{array}{l} \text{mass H}_2 \text{ in raceway} \\ \text{output gas} \end{array} \right] * 0.01756 \end{array} \right\}$$

where the numerical values are from 1800°C to 2300°C enthalpy equations of Table J.4.

The flame temperature of this chapter is calculated similarly, but with additional terms for the raceway's output Al₂O₃(s) and SiO₂(s), which are;

$$- \left[\begin{array}{l} \text{mass Al}_2\text{O}_3 \text{ in raceway} \\ \text{output gas} \end{array} \right] * (-16.72)$$

and

$$- \left[\begin{array}{l} \text{mass SiO}_2 \text{ in raceway} \\ \text{output gas} \end{array} \right] * (-15.47)$$

on the top of Eq. (18.9), and;

$$\left[\begin{array}{l} \text{mass Al}_2\text{O}_3 \text{ in raceway} \\ \text{output gas} \end{array} \right] * (0.001887)$$

and

$$\left[\begin{array}{l} \text{mass SiO}_2 \text{ in raceway} \\ \text{output gas} \end{array} \right] * (0.001427)$$

on the bottom of Eq. (18.9) where the numerical values are from Appendix J.

In spreadsheet form, the equation is

$$T_{\text{flame}} = \frac{\{J116 - C100 * (-4.183) - C101 * (-0.2448) - C102 * (-4.13) - C103 * (-16.72) - C104 * (-15.47)\}}{\{C100 * 0.00131 + C101 * 0.001301 + C102 * 0.01756 + C103 * 0.001887 + C104 * 0.001427\}} \quad (39.6)$$

39.4 RESULTS

Table 39.4 shows that the raceway temperature with;

- 60 kg of injected pulverized coal,
- 30 kg of injected pure oxygen,
- 18 kg H₂O(g)-in-blast (Cell C61, **Table 39.1**), and
- 60 kg of natural gas

is 1923°C.

The flame temperatures with other combinations of injectants are shown in **Fig. 39.2**.

Our calculations confirm that;

- oxygen injection increases raceway flame temperature, but
- coal injection, H₂O(g)-in-blast, and natural gas injection decrease flame temperature.

These same conclusions are reached in;

- Chapter 17, Raceway Flame Temperature with Oxygen Enrichment;
- Chapter 16, Raceway Flame Temperature with Pulverized Carbon Injection;

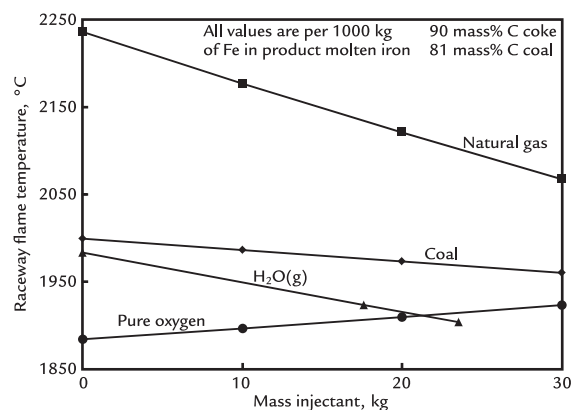


FIGURE 39.2 Effect of increasing individual tuyere input quantities on raceway flame temperature while holding the others injectants constant. Oxygen increases flame temperature. Coal, H₂O(g), and natural gas decrease flame temperature.

- Chapter 19, Raceway Flame Temperature with Moisture in Blast Air; and
- Chapter 30, Raceway Flame Temperature with Natural Gas Injection.

[Fig. 39.2](#) also shows that 25°C natural gas is more effective at lowering flame temperature than 1200°C H₂O(g).

39.5 LIST OF RACEWAY EQUATIONS OF THIS CHAPTER IN TABLE 39.2

A number of new equations were added to the raceway matrix to allow for RAFT calculation with multiple injectants. These equations are:

Row 68. O₂ entering raceway in blast air:

$$347 = \left[\begin{array}{l} \text{mass O}_2 \text{ entering raceway} \\ \text{in blast air} \end{array} \right] * 1 \quad (39.7)$$

Row 69. N₂ entering raceway in blast air:

$$1145 = \left[\begin{array}{l} \text{mass N}_2 \text{ entering raceway} \\ \text{in blast air} \end{array} \right] * 1 \quad (39.8)$$

Row 70. Raceway oxygen balance:

$$\begin{aligned} 0 = & - \left[\begin{array}{l} \text{mass O}_2 \text{ entering raceway} \\ \text{in blast air} \end{array} \right] * 1 \\ & - \left[\begin{array}{l} \text{mass tuyere-injected coal} \\ \text{entering raceway} \end{array} \right] * 0.046 \\ & - \left[\begin{array}{l} \text{mass O}_2 \text{ entering raceway} \\ \text{in tuyere-injected pure oxygen} \end{array} \right] * 1 \\ & - \left[\begin{array}{l} \text{mass through-tuyere input} \\ \text{H}_2\text{O}(g) \text{ entering raceway} \end{array} \right] * 0.888 \\ & - \left[\begin{array}{l} \text{mass tuyere-injected natural} \\ \text{gas entering raceway} \end{array} \right] * 0.01 \\ & + \left[\begin{array}{l} \text{mass CO in raceway} \\ \text{output gas} \end{array} \right] * 0.571 \end{aligned} \quad (39.9)$$

Row 71. Raceway carbon balance:

$$\begin{aligned} 0 = & - \left[\begin{array}{l} \text{mass C entering raceway} \\ \text{in falling coke particles} \end{array} \right] * 1 \\ & - \left[\begin{array}{l} \text{mass tuyere-injected coal} \\ \text{entering raceway} \end{array} \right] * 0.810 \\ & - \left[\begin{array}{l} \text{mass tuyere-injected natural} \\ \text{gas entering raceway} \end{array} \right] * 0.734 \\ & + \left[\begin{array}{l} \text{mass CO in raceway} \\ \text{output gas} \end{array} \right] * 0.429 \end{aligned} \quad (39.10)$$

Row 72. Raceway nitrogen balance:

$$\begin{aligned} 0 = & - \left[\begin{array}{l} \text{mass N}_2 \text{ entering raceway} \\ \text{in blast air} \end{array} \right] * 1 \\ & - \left[\begin{array}{l} \text{mass tuyere-injected coal} \\ \text{entering raceway} \end{array} \right] * 0.009 \\ & - \left[\begin{array}{l} \text{mass tuyere-injected natural} \\ \text{gas entering raceway} \end{array} \right] * 0.017 \\ & + \left[\begin{array}{l} \text{mass N}_2 \text{ in raceway} \\ \text{output gas} \end{array} \right] * 1 \end{aligned} \quad (39.11)$$

Row 73. Raceway hydrogen balance:

$$\begin{aligned} 0 = & - \left[\begin{array}{l} \text{mass tuyere-injected coal} \\ \text{entering raceway} \end{array} \right] * 0.055 \\ & - \left[\begin{array}{l} \text{mass through-tuyere input} \\ \text{H}_2\text{O}(g) \text{ entering raceway} \end{array} \right] * 0.112 \\ & - \left[\begin{array}{l} \text{mass tuyere-injected natural} \\ \text{gas entering raceway} \end{array} \right] * 0.240 \\ & + \left[\begin{array}{l} \text{mass H}_2 \text{ in raceway} \\ \text{output gas} \end{array} \right] * 1 \end{aligned} \quad (39.12)$$

Row 74. Al₂O₃(s) entering raceway in falling coke:

$$\begin{aligned} 0 = & - \left[\begin{array}{l} \text{mass Al}_2\text{O}_3 \text{ entering raceway} \\ \text{in falling coke particles} \end{array} \right] * 1 \\ & + \left[\begin{array}{l} \text{mass C entering raceway} \\ \text{in falling coke particles} \end{array} \right] * 0.0333 \end{aligned} \quad (39.1)$$

Row 75. SiO₂ entering raceway in falling coke:

$$\begin{aligned} 0 = & - \left[\begin{array}{l} \text{mass SiO}_2 \text{ entering raceway} \\ \text{in falling coke particles} \end{array} \right] * 1 \\ & + \left[\begin{array}{l} \text{mass C entering raceway} \\ \text{in falling coke particles} \end{array} \right] * 0.0778 \end{aligned} \quad (39.2)$$

Row 76. Raceway Al_2O_3 balance:

$$0 = - \left[\begin{array}{l} \text{mass } \text{Al}_2\text{O}_3 \text{ entering raceway} \\ \text{in falling coke particles} \end{array} \right] * 1 \\ - \left[\begin{array}{l} \text{mass tuyere-injected coal} \\ \text{entering raceway} \end{array} \right] * 0.024 \\ + \left[\begin{array}{l} \text{mass } \text{Al}_2\text{O}_3(\text{s}) \text{ in raceway} \\ \text{output gas} \end{array} \right] * 1 \quad (39.13)$$

Row 77. Raceway SiO_2 balance:

$$0 = - \left[\begin{array}{l} \text{mass } \text{SiO}_2 \text{ entering raceway} \\ \text{in falling coke particles} \end{array} \right] * 1 \\ - \left[\begin{array}{l} \text{mass tuyere-injected coal} \\ \text{entering raceway} \end{array} \right] * 0.056 \\ + \left[\begin{array}{l} \text{mass } \text{SiO}_2(\text{s}) \text{ in raceway} \\ \text{output gas} \end{array} \right] * 1 \quad (39.14)$$

Row 78. Mass tuyere-injected coal entering raceway:

$$60 = \left[\begin{array}{l} \text{mass tuyere-injected coal} \\ \text{entering raceway} \end{array} \right] * 1 \quad (39.15)$$

Row 79. Mass O_2 in tuyere-injected pure oxygen entering raceway:

$$30 = \left[\begin{array}{l} \text{mass } \text{O}_2 \text{ entering raceway} \\ \text{in tuyere-injected pure oxygen} \end{array} \right] * 1 \quad (39.16)$$

Row 80. Mass through-tuyere input $\text{H}_2\text{O(g)}$ entering raceway:

$$18 = \left[\begin{array}{l} \text{mass through-tuyere input} \\ \text{H}_2\text{O(g) entering raceway} \end{array} \right] * 1 \quad (39.17)$$

Row 81. Mass tuyere-injected natural gas entering raceway:

$$60 = \left[\begin{array}{l} \text{mass tuyere-injected natural} \\ \text{gas entering raceway} \end{array} \right] * 1 \quad (39.18)$$

Row 82. Mass additional tuyere injectant entering raceway:

$$0 = \left[\begin{array}{l} \text{mass additional tuyere} \\ \text{injectant entering raceway} \end{array} \right] * 1 \quad (39.19)$$

39.6 SUMMARY

This chapter shows how to automatically calculate tuyere raceway flame temperatures from bottom-segment calculated values with multiple injectants.

It also shows how to set up the raceway matrix and equations for additional tuyere injectants.

Matrix calculations of this chapter show that;

1. oxygen injection increases flame temperature, and
2. pulverized coal, $\text{H}_2\text{O(g)}$, and natural gas injection decrease flame temperature

as reported by Geerdes et al. (p 115).¹

Chapter 40, Top-Segment Calculations With Multiple Injectants, will show how to similarly calculate top gas temperatures.

EXERCISES

All masses in this exercise are kg per 1000 kg of Fe in product molten iron.

- 39.1. The blast furnace management team of Fig. 39.1 is planning to inject 20 kg of oil into their furnace along with all of the existing through-tuyere injectants of Table 38.2. They wish to know how this oil will affect their raceway flame temperature. Please predict the effect and then calculate it. Use the oil composition of your results in Exercise 38.1.

Reference

1. Geerdes M, Chaigneau R, Kurunov I, Lingiardi O, Ricketts J. *Modern blast furnace ironmaking (an introduction)*. 3rd ed. Amsterdam: IOS Press BV; 2015. p. 115.

40

Top-Segment Calculations With Multiple Injectants

OUTLINE

40.1 Understanding the Top Segment With Multiple Injectants	355	40.7 Results	364
40.2 Top-Segment Equations With Gangue, Ash, Fluxes, and Slag Plus Injection of Coal, Oxygen, $H_2O(g)$, and Natural Gas	356	40.8 List of Top-Segment Equations of Table 40.2	364
40.3 Top-Segment Input Enthalpy	362	40.9 Matching the model to Commercial Blast Furnace Data	366
40.4 Top-Segment Output Enthalpy	362	40.10 Summary	367
40.5 Top Gas Enthalpy	362	Exercises	368
40.6 Top Gas Temperature	363	Reference	368

40.1 UNDERSTANDING THE TOP SEGMENT WITH MULTIPLE INJECTANTS

In this chapter, we calculate top gas composition, enthalpy, and temperature with tuyere injection of;

- pulverized coal,
- pure oxygen,

- $H_2O(g)$ -in-blast (from humid air and injected steam), and
- natural gas.

It is important to understand how top gas temperature is affected by these injectants. Top gas must be warm enough to;

1. efficiently evaporate the top charge's moisture content so that iron ore reduction begins quickly,

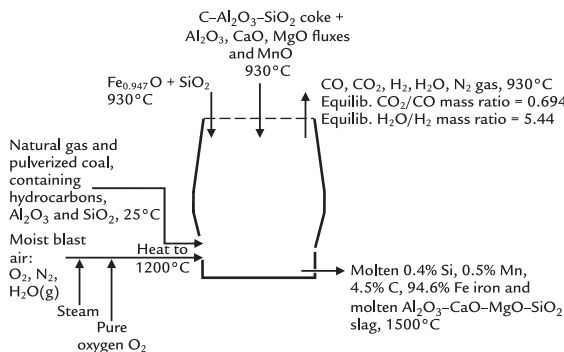


FIGURE 40.1 Conceptual bottom segment of blast furnace with moist blast air, injection of oxygen into the blast, and injection of pulverized coal and natural gas into the furnace. The flows descending from the top segment and ascending into the top segment are notable. Fig. 40.2 shows the equivalent conceptual top segment with its top-charged inputs and the same cross-segment flows.

2. avoid unwanted condensation of moisture in the charge that can move down the furnace walls and damage hearth refractory, and
3. purge undesirable minor elements, especially zinc in the burden materials but not so warm as to;
4. increase the fuel rate due to excessive energy lost to the top gas and
5. damage the top-charging equipment

110°C–140°C appears to be the optimum range.

The objectives of this chapter are to;

1. build a top-segment matrix based on bottom-segment cross-division flows of Chapter 38, Bottom-Segment Calculations with Multiple Injectants (Fig. 40.1), and top charged inputs of Fig. 40.2;
2. use the matrix to calculate top gas composition of Fig. 40.2;
3. develop equations to calculate top-segment input enthalpy, top-segment output enthalpy, and top gas enthalpy of Fig. 40.2; and;
4. develop an equation that calculates top gas temperature of Fig. 40.2 from (1)'s top gas composition and (3)'s top gas enthalpy.

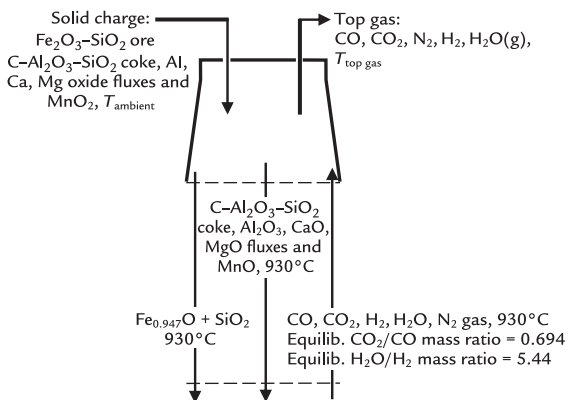


FIGURE 40.2 Conceptual blast furnace top segment and the flows between it and the bottom segment, Fig. 40.1.

These steps finish the development of our blast furnace model. When connected to the automatic flame temperature calculation and automatic inclusion of blast temperature of Chapter 39, Raceway Flame Temperature with Multiple Injectants, in the bottom-segment calculations, these calculations form the basis for our blast furnace optimization analysis.

40.2 TOP-SEGMENT EQUATIONS WITH GANGUE, ASH, FLUXES, AND SLAG PLUS INJECTION OF COAL, OXYGEN, $\text{H}_2\text{O(g)}$, AND NATURAL GAS

Fig. 40.2 shows that;

1. the top segment's top-charged inputs are;
 - a. Fe-SiO_2 ore;
 - b. $\text{Al}_2\text{O}_3\text{-C-SiO}_2$ coke;
 - c. Al_2O_3 , CaO , MgO , SiO_2 fluxes; and
 - d. MnO_2 ore, and;
2. its ascending-from-bottom-segment inputs are
 - a. CO ;
 - b. CO_2 ;
 - c. H_2 ;
 - d. $\text{H}_2\text{O(g)}$; and
 - e. N_2 .

The top-segment outputs are;

3. $\text{Fe}_{0.947}\text{O}-\text{SiO}_2$ partially reduced ore, $\text{Al}_2\text{O}_3-\text{C}-\text{SiO}_2$ coke, Al_2O_3 , CaO , MgO fluxes, and MnO (partially reduced MnO_2) descending into the bottom segment, and;
4. CO , CO_2 , H_2 , H_2O , and N_2 departing in top gas.

Notice that tuyere injectants are not part of our top-segment calculations—except as they affect the bottom segment's cross-division mass flows, [Table 40.1](#).

[Table 40.2](#) shows our top-segment matrix, based in part on Table 31.2. The relevant equations are listed at the end of the chapter.

[Table 40.3](#) shows the calculated input and output quantities. These are now used to calculate;

- top-segment input enthalpy,
- top-segment output enthalpy,
- top gas enthalpy, and
- top gas temperature ([Table 40.4](#)).

TABLE 40.1 Bottom-Segment Matrix Results With Through-Tuyere Injection of Pulverized Coal, Oxygen, $\text{H}_2\text{O}(\text{g})$, and Natural Gas

	A	B	C kg per 1000 kg of Fe out in molten iron
33	Bottom segment calculated values		
34	mass $\text{Fe}_{0.947}\text{O}$ into bottom segment		1302
35	mass C in descending coke		326
36	mass O_2 in blast air		347
37	mass N_2 in blast air		1145
38	mass Fe out in molten iron		1000
39	mass C out in molten iron		48
40	mass CO out in ascending gas		600
41	mass CO_2 out in ascending gas		416
42	mass N_2 out in ascending gas		1146
43	mass H_2 out in ascending gas		12
44	mass H_2O out in ascending gas		67
45	mass SiO_2 in descending ore		75
46	mass SiO_2 in descending coke		25
47	mass SiO_2 out in molten slag		95
48	mass Al_2O_3 in descending decomposed flux		12
49	mass Al_2O_3 in descending coke		11
50	mass Al_2O_3 out in molten slag		24
51	mass CaO in descending decomposed flux		100
52	mass CaO out in molten slag		100
53	mass MgO in descending decomposed flux		24
54	mass MgO out in molten slag		24
55	mass Si out in molten iron		4.2
56	mass Mn out in molten iron		5.3
57	mass descending MnO		7.6
58	mass MnO out in molten slag		0.8
59	mass tuyere-injected coal		60
60	mass O_2 in tuyere-injected pure oxygen		30
61	mass through-tuyere input $\text{H}_2\text{O}(\text{g})$		18
62	mass tuyere-injected natural gas		60
63	mass additional tuyere injectant		0

This is a copy of Table 38.2.

TABLE 40.2 Matrix for Top-Segment of Fig. 40.2

M	III	IV	V	VI	VII	VIII	IX	X	XI	XII
TOP SEGMENT CALCULATIONS										
Equation	Description	Numerical term	mass Fe_2O_3 in top charged ore	mass SiO_2 in top charged ore	mass C in top-charged coke	mass Al_2O_3 in top-charged coke	mass SiO_2 in top-charged coke	mass top-charged Al_2O_3 flux	mass top-charged CaO flux	mass top-charged MgO flux
3	40.8 Mass CO descending from bottom segment	600	0	0	0	0	0	0	0	0
4	40.9 Mass CO_2 ascending from bottom segment	416	0	0	0	0	0	0	0	0
5	40.10 Mass H ₂ ascending from bottom segment	12.3	0	0	0	0	0	0	0	0
6	40.11 Mass H_2O ascending from bottom segment	67	0	0	0	0	0	0	0	0
7	40.12 Mass N_2 ascending from bottom segment	1146	0	0	0	0	0	0	0	0
8	40.13 Mass Al_2O_3 -in-coke descending out of top segment	11	0	0	0	0	0	0	0	0
9	40.14 Mass Al_2O_3 flux descending out of top segment	12	0	0	0	0	0	0	0	0
10	40.15 Mass CaO -in-coke descending out of top segment	326	0	0	0	0	0	0	0	0
11	40.16 Mass CaO -flux descending out of top segment	1302	0	0	0	0	0	0	0	0
12	40.17 Mass CdO -in-coke descending out of top segment	100	0	0	0	0	0	0	0	0
13	40.18 Mass MgO flux descending out of top segment	24	0	0	0	0	0	0	0	0
14	40.19 Mass Mn descending out of top segment	7.6	0	0	0	0	0	0	0	0
15	40.20 Mass SiO_2 -in-coke descending out of top segment	25	0	0	0	0	0	0	0	0
16	40.21 Mass SiO_2 -in-ore descending out of top segment	75	0	0	0	0	0	0	0	0
17	40.22 Al_2O_3 -in-coke mass balance	0	0	0	0	-1	0	0	0	0
18	40.23 Al_2O_3 flux mass balance	0	0	0	0	0	0	-1	0	0
19	40.24 C mass balance	0	0	0	-1	0	0	0	0	0
20	40.25 Ca mass balance	0	0	0	0	0	0	0	-1	0
21	40.26 Fe mass balance	0	-0.699	0	0	0	0	0	0	0
22	40.27 H mass balance	0	0	0	0	0	0	0	0	0
23	40.28 MgO mass balance	0	0	0	0	0	0	0	0	-1
24	40.29 Mn mass balance	0	0	0	0	0	0	0	0	0
25	40.30 N mass balance	0	0	0	0	0	0	0	0	0
26	40.31 O mass balance	0	-0.301	0	0	0	0	0	0	0
27	40.32 SiO_2 -in-coke mass balance	0	0	0	0	0	-1	0	0	0
28	40.33 SiO_2 -in-ore mass balance	0	0	-1	0	0	0	0	0	0
29	40.34 No top-segment C oxidation equation	0	0	0	-1	0	0	0	0	0
30	25.13 H_2/CO relative reaction extent equation	0	0	0	0	0	0	0	0	0
31										
32										

M	III	IV	V	VI	VII	VIII	IX	X	XI	XII
TOP SEGMENT CALCULATIONS										
Equation	mass Al_2O_3 -in-coke descending out of top segment	mass Al_2O_3 flux descending out of top segment	mass CaO flux descending out of top segment	mass C-in-coke descending out of top segment	mass $\text{Fe}_{0.98}\text{O}$ flux descending out of top segment	mass MgO flux descending out of top segment	mass MnO descending out of top segment	mass SiO_2 -in-coke descending out of top segment	mass SiO_2 -in-ore descending out of top segment	mass CO ascending into top segment
3	0	0	0	0	0	0	0	0	0	1
4	0	0	0	0	0	0	0	0	0	0
5	0	0	0	0	0	0	0	0	0	0
6	0	0	0	0	0	0	0	0	0	0
7	0	0	0	0	0	0	0	0	0	0
8	0	0	1	0	0	0	0	0	0	0
9	0	0	1	0	0	0	0	0	0	0
10	0	0	0	1	0	0	0	0	0	0
11	0	0	0	0	0	1	0	0	0	0
12	0	0	0	0	0	1	0	0	0	0
13	0	0	0	0	0	0	1	0	0	0
14	0	0	0	0	0	0	0	1	0	0
15	0	0	0	0	0	0	0	0	1	0
16	0	0	0	0	0	0	0	0	0	1
17	0	1	0	0	0	0	0	0	0	0
18	0	0	1	0	0	0	0	0	0	0
19	0	0	0	1	0	0	0	0	0	0
20	0	0	0	0	1	0	0	0	0	0
21	0	0	0	0	0	0.768	0	0	0	0
22	0	0	0	0	0	0	0	0	0	0
23	0	0	0	0	0	0	1	0	0	0
24	-0.632	0	0	0	0	0	0	0.774	0	0
25	0	0	0	0	0	0	0	0	0	0
26	-0.308	0	0	0	0.232	0	0.226	0	0	0.571
27	0	0	0	0	0	0	0	1	0	0
28	0	0	0	0	0	0	0	0	1	0
29	0	0	0	1	0	0	0	0	0	0
30	0	0	0	0	0	0	0	0	0	0
31										
32										

(Continued)

TABLE 40.2 (Continued)

	BW	BX	BY	BZ	CA	CB	CC	CD	CE
1	mass CO ₂ ascending into top segment	mass H ₂ ascending into top segment	mass H ₂ O ascending into top segment	mass N ₂ ascending into top segment	mass CO departing in top gas	mass CO ₂ departing in top gas	mass H ₂ departing in top gas	mass H ₂ O departing in top gas	mass N ₂ departing in top gas
2									
3	0	0	0	0	0	0	0	0	0
4	1	0	0	0	0	0	0	0	0
5	0	1	0	0	0	0	0	0	0
6	0	0	1	0	0	0	0	0	0
7	0	0	0	1	0	0	0	0	0
8	0	0	0	0	0	0	0	0	0
9	0	0	0	0	0	0	0	0	0
10	0	0	0	0	0	0	0	0	0
11	0	0	0	0	0	0	0	0	0
12	0	0	0	0	0	0	0	0	0
13	0	0	0	0	0	0	0	0	0
14	0	0	0	0	0	0	0	0	0
15	0	0	0	0	0	0	0	0	0
16	0	0	0	0	0	0	0	0	0
17	0	0	0	0	0	0	0	0	0
18	0	0	0	0	0	0	0	0	0
19	-0.273	0	0	0	0.429	0.273	0	0	0
20	0	0	0	0	0	0	0	0	0
21	0	0	0	0	0	0	0	0	0
22	0	-1	-0.112	0	0	0	1	0.112	0
23	0	0	0	0	0	0	0	0	0
24	0	0	0	0	0	0	0	0	0
25	0	0	0	-1	0	0	0	0	1
26	-0.727	0	-0.888	0	0.571	0.727	0	0.888	0
27	0	0	0	0	0	0	0	0	0
28	0	0	0	0	0	0	0	0	0
29	0	0	0	0	0	0	0	0	0
30	-0.117	0	1	0	0	0.117	0	-1	0
31	=BC5/BC3*5.7				=BC5/BC3*5.7				
32									

The related equations are listed at the end of this chapter. Numerical values of Column BC are from Table 40.1

TABLE 40.3 Top-Segment Mass Flows Calculated From Matrix Table 40.2

	BB	BC
	Top segment calculated values	kg per 1000 kg of Fe out in molten iron
71		
72	mass Fe_2O_3 in top-charged ore	1431
73	mass SiO_2 in top-charged ore	75
74	mass C in top-charged coke	326
75	mass Al_2O_3 in top-charged coke	11
76	mass SiO_2 in top-charged coke	25
77	mass top-charged Al_2O_3 flux	12
78	mass top-charged CaO flux	100
79	mass top-charged MgO flux	24
80	mass top-charged MnO_2 ore	9.3
81	mass Al_2O_3 -in-coke descending out of top segment	11
82	mass Al_2O_3 flux descending out of top segment	12
83	mass C-in-coke descending out of top segment	326
84	mass CaO flux descending out of top segment	100
85	mass $\text{Fe}_{0.947}\text{O}$ descending out of top segment	1302
86	mass MgO flux descending out of top segment	24
87	mass MnO descending out of top segment	7.6
88	mass SiO_2 -in-coke descending out of top segment	25
89	mass SiO_2 -in-ore descending out of top segment	75
90	mass CO ascending into top segment	600
91	mass CO_2 ascending into top segment	416
92	mass H_2 ascending into top segment	12
93	mass H_2O ascending into top segment	67
94	mass N_2 ascending into top segment	1146
95	mass CO departing in top gas	422
96	mass CO_2 departing in top gas	695
97	mass H_2 departing in top gas	8.6
98	mass H_2O departing in top gas	99
99	mass N_2 departing in top gas	1146
100		

TABLE 40.4 Equations for Automatically Calculating Top-Segment Input Enthalpy, Top-Segment Output Enthalpy, Top Gas Enthalpy and Top Gas Temperature

40.3 TOP-SEGMENT INPUT ENTHALPY

Top-segment input enthalpy is calculated by the following equation;

top segment input enthalpy

$$\begin{aligned}
 &= [1431 \text{ kg of Fe}_2\text{O}_3 \text{ in top-charged ore}] * -5.169 \\
 &+ [75 \text{ kg of SiO}_2 \text{ in top-charged ore}] * -15.16 \\
 &+ [326 \text{ kg of C in top-charged coke}] * 0 \\
 &+ [11 \text{ kg of Al}_2\text{O}_3 \text{ in top-charged coke}] * -16.43 \\
 &+ [25 \text{ kg of SiO}_2 \text{ in top-charged coke}] * -15.16 \\
 &+ [12 \text{ kg of top-charge Al}_2\text{O}_3 \text{ flux}] * -16.43 \\
 &+ [100 \text{ kg of top-charged CaO flux}] * -11.32 \\
 &+ [24 \text{ kg of top-charged MgO flux}] * -14.92 \\
 &+ [9 \text{ kg of top-charge MnO}_2 \text{ ore}] * -5.98 \\
 &+ [600 \text{ kg of CO ascending into the top segment}] * -2.926 \\
 &+ [416 \text{ kg of CO}_2 \text{ ascending into the top segment}] * -7.926 \\
 &+ [12 \text{ kg of H}_2 \text{ ascending into the top segment}] * 13.35 \\
 &+ [67 \text{ kg of H}_2\text{O ascending into the top segment}] * -11.49 \\
 &+ [1146 \text{ kg of N}_2 \text{ ascending into the top segment}] * 1.008
 \end{aligned} \tag{40.1}$$

where the masses are from [Table 40.3](#) and the enthalpies (on the right) are for temperatures of [Fig. 40.2](#), Appendix J. With these values, Eq. (40.1) gives:

$$\left[\begin{array}{l} \text{top segment} \\ \text{input enthalpy} \end{array} \right] = -15,345 \text{ MJ/1000 kg of Fe in product molten iron}$$

In automatic spreadsheet form, the equation is:

$$\begin{aligned}
 &= BC72 * (-5.169) + BC73 * (-15.16) + BC74 * 0 \\
 &+ BC75 * (-16.43) + BC76 * (-15.16) + BC77 * (-16.43) \\
 &+ BC78 * (-11.32) + BC79 * (-14.92) \\
 &+ BC80 * (-5.98) + BC90 * (-2.926) + BC91 * (-7.926) \\
 &+ BC92 * 13.35 + BC93 * (-11.49) + BC94 * 1.008
 \end{aligned} \tag{40.2}$$

as shown in [Table 40.4](#).

40.4 TOP-SEGMENT OUTPUT ENTHALPY

Top-segment output enthalpy (MJ per 1000 kg of Fe in product molten iron) is calculated by Eq. (21.4);

$$\left[\begin{array}{l} \text{top segment} \\ \text{output enthalpy} \end{array} \right] = \left[\begin{array}{l} \text{top segment} \\ \text{input enthalpy} \end{array} \right] - \left[\begin{array}{l} 80 \text{ MJ conductive, convective} \\ \text{and radiative heat loss} \\ \text{from the top segment} \end{array} \right] \tag{21.4}$$

which in the present case is:

$$\left[\begin{array}{l} \text{top segment} \\ \text{output enthalpy} \end{array} \right] = -15,345 - 80 = -15,425 \text{ MJ/1000 kg of Fe in product molten iron} \tag{40.3}$$

40.5 TOP GAS ENTHALPY

Top gas enthalpy is a portion of top-segment output enthalpy of [Section 40.4](#).

The other portion is the enthalpy of the 930°C;

- Al₂O₃-in-coke,
- Al₂O₃ flux,
- C-in-coke,
- CaO flux,
- Fe_{0.947}O (partially reduced Fe₂O₃) ,
- MgO flux,
- MnO (partially reduced MnO₂) ,
- SiO₂-in-coke, and
- SiO₂-in-ore

descending out of the top segment.

In the present case, the equation is;

$$\begin{aligned}
 [\text{top gas enthalpy}] &= [\text{top-segment output enthalpy}] \\
 &\quad - [\text{mass Al}_2\text{O}_3\text{-in-coke}] * -15.41 \\
 &\quad - [\text{mass Al}_2\text{O}_3 \text{ flux}] * -15.41 \\
 &\quad - [\text{mass C-in-coke}] * 1.359 \\
 &\quad - [\text{mass CaO flux}] * -10.50 \\
 &\quad - [\text{mass Fe}_{0.947}\text{O}] * -3.152 \\
 &\quad - [\text{mass MgO flux}] * -13.84 \\
 &\quad - [\text{mass MnO}] * -4.770 \\
 &\quad - [\text{mass SiO}_2\text{-in-coke}] * -14.13 \\
 &\quad - [\text{mass SiO}_2\text{-in-ore}] * -14.13
 \end{aligned} \tag{40.4}$$

where all the enthalpies are at 930°C.

With top-segment output enthalpy of Section 40.4 and masses of Table 40.4, the equation becomes;

$$\begin{aligned}
 [\text{top gas enthalpy}] &= -15,425 \\
 &\quad - [11 \text{ kg of Al}_2\text{O}_3 \text{ in descending coke}] * -15.41 \\
 &\quad - [12 \text{ kg of descending Al}_2\text{O}_3 \text{ flux}] * -15.41 \\
 &\quad - [326 \text{ kg of C in descending coke}] * 1.359 \\
 &\quad - [100 \text{ kg of descending CaO flux}] * -10.50 \\
 &\quad - [1302 \text{ kg of descending Fe}_{0.947}\text{O}] * -3.152 \\
 &\quad - [24 \text{ kg of descending MgO flux}] * -13.84 \\
 &\quad - [7.6 \text{ kg of descending MnO}] * -4.770 \\
 &\quad - [25 \text{ kg of descending SiO}_2\text{-in-coke}] * -14.13 \\
 &\quad - [75 \text{ kg of descending SiO}_2\text{-in-ore}] * -14.13
 \end{aligned}$$

which totals to;

$$[\text{top gas enthalpy}] = -8570 \text{ MJ}/1000 \text{ kg of Fe in product molten iron.}$$

As shown in Table 40.4, the automatic spreadsheet version of Eq. (40.4) is:

$$\begin{aligned}
 [\text{top gas enthalpy}] &= BC113 - BC81 * (-15.41) - BC82 * (-15.41) \\
 &\quad - BC83 * 1.359 - BC84 * (-10.50) - BC85 * (-3.152) \\
 &\quad - BC86 * (-13.84) - BC87 * (-4.770) \\
 &\quad - BC88 * (-14.13) - BC89 * (-14.13) \\
 &= -8570 \text{ MJ}/1000 \text{ kg of Fe in product molten iron.}
 \end{aligned} \tag{40.5}$$

40.6 TOP GAS TEMPERATURE

As in Chapter 27, Top Gas Temperature with CH₄(g) Injection, we calculate our top gas temperature by the equation;

$$T_{\text{top gas}} = \frac{\left\{ \begin{array}{l} \left[\begin{array}{l} \text{top-gas} \\ \text{enthalpy} \end{array} \right] - \left[\begin{array}{l} \text{mass CO out} \\ \text{in top gas} \end{array} \right] * (-3.972) \\ - \left[\begin{array}{l} \text{mass CO}_2 \text{ out} \\ \text{in top gas} \end{array} \right] * (-8.966) \\ - \left[\begin{array}{l} \text{mass H}_2 \text{ out} \\ \text{in top gas} \end{array} \right] * (-0.3616) \\ - \left[\begin{array}{l} \text{mass H}_2\text{O out} \\ \text{in top gas} \end{array} \right] * (-13.47) \\ - \left[\begin{array}{l} \text{mass N}_2 \text{ out} \\ \text{in top gas} \end{array} \right] * (-0.02624) \end{array} \right\}}{\left\{ \begin{array}{l} \left[\begin{array}{l} \text{mass CO out} \\ \text{in top gas} \end{array} \right] * 0.001049 \\ + \left[\begin{array}{l} \text{mass CO}_2 \text{ out} \\ \text{in top gas} \end{array} \right] * 0.0009314 \\ + \left[\begin{array}{l} \text{mass H}_2 \text{ out} \\ \text{in top gas} \end{array} \right] * 0.01442 \\ + \left[\begin{array}{l} \text{mass H}_2\text{O out} \\ \text{in top gas} \end{array} \right] * 0.001902 \\ + \left[\begin{array}{l} \text{mass N}_2 \text{ out} \\ \text{in top gas} \end{array} \right] * 0.001044 \end{array} \right\}} \tag{27.2}$$

or with mass flows of Table 40.3

$$\begin{aligned}
 T_{\text{top gas}} &= \frac{\left\{ -8570 - (422 * (-3.972)) - (695 * (-8.966)) \right. \\ &\quad \left. - (8.6 * (-0.3616)) - (99 * (-13.47)) \right. \\ &\quad \left. - (1146 * (-0.02624)) \right\}}{\left\{ 422 * 0.001049 + 695 * 0.0009314 + 8.6 * 0.01442 \right. \\ &\quad \left. + 99 * 0.001902 + 1146 * 0.001044 \right\}} \\ &= 273^\circ\text{C}
 \end{aligned} \tag{40.6}$$

In automatic spreadsheet form, this equation is;

$$T_{\text{top gas}} = \frac{\left(\begin{array}{l} \text{BJ116} - \text{BC95} * (-3.972) - \text{BC96} * (-8.966) \\ - \text{BC97} * (-0.3616) - \text{BC98} * (-13.47) \\ - \text{BC99} * (-0.02624) \end{array} \right)}{\left(\begin{array}{l} \text{BC95} * 0.001049 + \text{BC96} * 0.0009314 + \text{BC97} \\ * 0.01442 + \text{BC98} * 0.001902 + \text{BC99} * 0.001044 \end{array} \right)} = 273^{\circ}\text{C}$$

(40.7)

40.7 RESULTS

The above calculations show that the top gas temperature produced with the injection of;

- 60 kg of pulverized coal,
- 30 kg of oxygen,
- 18 kg of $\text{H}_2\text{O(g)}$ in moist blast, and
- 60 kg of natural gas

is 273°C .

This temperature and others are plotted in Fig. 40.3 for the injectants shown above.

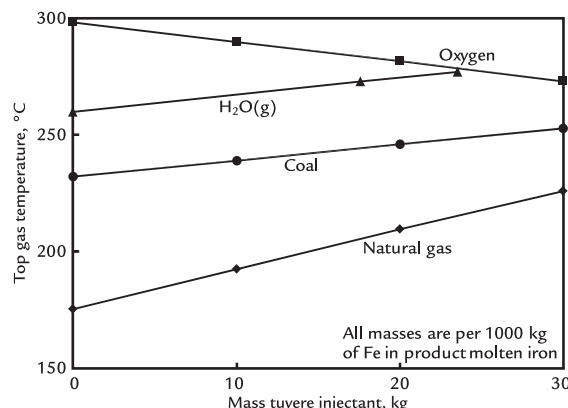


FIGURE 40.3 The effect of increasing individual tuyere input quantities, while holding all other injectants constant, on top gas temperature. Oxygen decreases top gas temperature. Coal, $\text{H}_2\text{O(g)}$, and natural gas increase top gas temperature. The trends are confirmed by Geerdes et al. (see Ref. [1], p 115).

40.8 LIST OF TOP-SEGMENT EQUATIONS OF TABLE 40.2

Mass CO ascending into top segment:

$$600 = \left[\begin{array}{l} \text{mass CO ascending} \\ \text{into top segment} \end{array} \right] * 1 \quad (40.8)$$

Mass CO_2 ascending into top segment:

$$416 = \left[\begin{array}{l} \text{mass } \text{CO}_2 \text{ ascending} \\ \text{into top segment} \end{array} \right] * 1 \quad (40.9)$$

Mass H_2 ascending into top segment:

$$12 = \left[\begin{array}{l} \text{mass } \text{H}_2 \text{ ascending} \\ \text{into top segment} \end{array} \right] * 1 \quad (40.10)$$

Mass H_2O ascending into top segment:

$$67 = \left[\begin{array}{l} \text{mass } \text{H}_2\text{O ascending} \\ \text{into top segment} \end{array} \right] * 1 \quad (40.11)$$

Mass N_2 ascending into top segment:

$$1146 = \left[\begin{array}{l} \text{mass } \text{N}_2 \text{ ascending} \\ \text{into top segment} \end{array} \right] * 1 \quad (40.12)$$

Mass Al_2O_3 -in-coke descending out of top segment:

$$11 = \left[\begin{array}{l} \text{mass } \text{Al}_2\text{O}_3\text{-in-coke} \\ \text{descending out of top segment} \end{array} \right] * 1 \quad (40.13)$$

Mass Al_2O_3 flux descending out of top segment:

$$12 = \left[\begin{array}{l} \text{mass } \text{Al}_2\text{O}_3 \text{ flux descending} \\ \text{out of top segment} \end{array} \right] * 1 \quad (40.14)$$

Mass C-in-coke descending out of top segment:

$$326 = \left[\begin{array}{l} \text{mass C-in-coke descending} \\ \text{out of top segment} \end{array} \right] * 1 \quad (40.15)$$

Mass $\text{Fe}_{0.947}\text{O}$ descending out of top segment:

$$1302 = \left[\begin{array}{l} \text{mass } \text{Fe}_{0.947}\text{O descending} \\ \text{out of top segment} \end{array} \right] * 1 \quad (40.16)$$

Mass CaO descending out of top segment:

$$100 = \left[\begin{array}{l} \text{mass } \text{CaO} \text{ descending} \\ \text{out of top segment} \end{array} \right] * 1 \quad (40.17)$$

Mass MgO descending out of top segment:

$$24 = \left[\begin{array}{l} \text{mass } \text{MgO} \text{ descending} \\ \text{out of top segment} \end{array} \right] * 1 \quad (40.18)$$

Mass MnO descending out of top segment:

$$7.6 = \left[\begin{array}{l} \text{mass MnO descending} \\ \text{out of top segment} \end{array} \right] * 1 \quad (40.19)$$

Mass SiO₂-in-coke descending out of top segment:

$$25 = \left[\begin{array}{l} \text{mass SiO}_2\text{-in-coke} \\ \text{descending out of top segment} \end{array} \right] * 1 \quad (40.20)$$

Mass SiO₂-in-reduced ore descending out of top segment:

$$75 = \left[\begin{array}{l} \text{mass SiO}_2\text{-in-reduced ore} \\ \text{descending out of top segment} \end{array} \right] * 1 \quad (40.21)$$

Al₂O₃-in-coke mass balance:

$$\begin{aligned} 0 = & - \left[\begin{array}{l} \text{mass Al}_2\text{O}_3 \text{ in top} \\ \text{charged coke} \end{array} \right] * 1 \\ & + \left[\begin{array}{l} \text{mass Al}_2\text{O}_3\text{-in-coke} \\ \text{descending out of top segment} \end{array} \right] * 1 \end{aligned} \quad (40.22)$$

Al₂O₃-in-flux mass balance:

$$\begin{aligned} 0 = & - \left[\begin{array}{l} \text{mass top charged} \\ \text{Al}_2\text{O}_3 \text{ flux} \end{array} \right] * 1 \\ & + \left[\begin{array}{l} \text{mass Al}_2\text{O}_3 \text{ flux descending} \\ \text{out of top segment} \end{array} \right] * 1 \end{aligned} \quad (40.23)$$

C mass balance:

$$\begin{aligned} 0 = & - \left[\begin{array}{l} \text{mass C in} \\ \text{top-charged coke} \end{array} \right] * 1 \\ & - \left[\begin{array}{l} \text{mass CO ascending} \\ \text{into top segment} \end{array} \right] * 0.429 \\ & - \left[\begin{array}{l} \text{mass CO}_2 \text{ ascending} \\ \text{into top segment} \end{array} \right] * 0.273 \\ & + \left[\begin{array}{l} \text{mass C-in-coke descending} \\ \text{out of top segment} \end{array} \right] * 1 \\ & + \left[\begin{array}{l} \text{mass CO departing top} \\ \text{segment in top gas} \end{array} \right] * 0.429 \\ & + \left[\begin{array}{l} \text{mass CO departing top} \\ \text{segment in top gas} \end{array} \right] * 0.273 \end{aligned} \quad (40.24)$$

CaO mass balance:

$$0 = - \left[\begin{array}{l} \text{mass top charged} \\ \text{CaO flux} \end{array} \right] * 1 + \left[\begin{array}{l} \text{mass CaO descending} \\ \text{out of top segment} \end{array} \right] * 1 \quad (40.25)$$

Fe mass balance:

$$\begin{aligned} 0 = & - \left[\begin{array}{l} \text{mass Fe}_2\text{O}_3 \text{ in} \\ \text{top-charged ore} \end{array} \right] * 0.699 \\ & + \left[\begin{array}{l} \text{mass Fe}_{0.94}\text{O descending} \\ \text{out of top segment} \end{array} \right] * 0.768 \end{aligned} \quad (40.26)$$

H mass balance:

$$\begin{aligned} 0 = & - \left[\begin{array}{l} \text{mass H}_2 \text{ ascending} \\ \text{into top segment} \end{array} \right] * 1 \\ & - \left[\begin{array}{l} \text{mass H}_2\text{O ascending} \\ \text{into top segment} \end{array} \right] * 0.112 \\ & + \left[\begin{array}{l} \text{mass H}_2 \text{ departing top} \\ \text{segment in top gas} \end{array} \right] * 1 \\ & + \left[\begin{array}{l} \text{mass H}_2\text{O departing top} \\ \text{segment in top gas} \end{array} \right] * 0.112 \end{aligned} \quad (40.27)$$

MgO mass balance:

$$0 = - \left[\begin{array}{l} \text{mass top charged} \\ \text{MgO flux} \end{array} \right] * 1 + \left[\begin{array}{l} \text{mass MgO descending} \\ \text{out of top segment} \end{array} \right] * 1 \quad (40.28)$$

Mn mass balance:

$$\begin{aligned} 0 = & - \left[\begin{array}{l} \text{mass top charged} \\ \text{MnO}_2 \text{ ore} \end{array} \right] * 0.621 \\ & + \left[\begin{array}{l} \text{mass MnO descending} \\ \text{out of top segment} \end{array} \right] * 0.774 \end{aligned} \quad (40.29)$$

N mass balance:

$$\begin{aligned} 0 = & - \left[\begin{array}{l} \text{mass N}_2 \text{ ascending} \\ \text{into top segment} \end{array} \right] * 1 \\ & + \left[\begin{array}{l} \text{mass N}_2 \text{ departing top} \\ \text{segment in top gas} \end{array} \right] * 1 \end{aligned} \quad (40.30)$$

O balance:

$$\begin{aligned}
 0 = & - \left[\begin{array}{l} \text{mass Fe}_2\text{O}_3 \text{ in} \\ \text{top-charged ore} \end{array} \right] * 0.301 \\
 & - \left[\begin{array}{l} \text{mass top-charged} \\ \text{MnO}_2 \text{ ore} \end{array} \right] * 0.368 \\
 & - \left[\begin{array}{l} \text{mass CO ascending} \\ \text{into top segment} \end{array} \right] * 0.571 \\
 & - \left[\begin{array}{l} \text{mass CO}_2 \text{ ascending} \\ \text{into top segment} \end{array} \right] * 0.727 \\
 & - \left[\begin{array}{l} \text{mass H}_2\text{O ascending} \\ \text{into top segment} \end{array} \right] * 0.888 \\
 & + \left[\begin{array}{l} \text{mass Fe}_{0.947}\text{O descending} \\ \text{into bottom segment} \end{array} \right] * 0.232 \\
 & + \left[\begin{array}{l} \text{mass MnO descending} \\ \text{into bottom segment} \end{array} \right] * 0.226 \\
 & + \left[\begin{array}{l} \text{mass CO departing top} \\ \text{segment in top gas} \end{array} \right] * 0.571 \\
 & + \left[\begin{array}{l} \text{mass CO}_2 \text{ departing top} \\ \text{segment in top gas} \end{array} \right] * 0.727 \\
 & + \left[\begin{array}{l} \text{mass H}_2\text{O departing top} \\ \text{segment in top gas} \end{array} \right] * 0.888
 \end{aligned} \tag{40.31}$$

SiO₂-in-coke mass balance:

$$\begin{aligned}
 0 = & - \left[\begin{array}{l} \text{mass SiO}_2 \text{ in top-} \\ \text{charged coke} \end{array} \right] * 1 \\
 & + \left[\begin{array}{l} \text{mass SiO}_2\text{-in-coke} \\ \text{descending out of top segment} \end{array} \right] * 1
 \end{aligned} \tag{40.32}$$

SiO₂-in-iron-ore mass balance:

$$\begin{aligned}
 0 = & \left[\begin{array}{l} \text{mass SiO}_2 \text{ in top-} \\ \text{charged iron ore} \end{array} \right] * 1 \\
 & + \left[\begin{array}{l} \text{mass SiO}_2\text{-in-reduced ore} \\ \text{descending out of top segment} \end{array} \right] * 1
 \end{aligned} \tag{40.33}$$

C oxidation in top-segment equation:

$$\begin{aligned}
 0 = & - \left[\begin{array}{l} \text{mass C in} \\ \text{top-charged coke} \end{array} \right] * 1 \\
 & + \left[\begin{array}{l} \text{mass C-in-coke descending} \\ \text{out of top segment} \end{array} \right] * 1
 \end{aligned} \tag{40.34}$$

Top-segment CO/H₂ relative reaction extent:

$$\begin{aligned}
 0 = & - \left[\begin{array}{l} \text{mass CO}_2 \text{ ascending} \\ \text{from bottom segment} \end{array} \right] * 0.117 \\
 & + \left[\begin{array}{l} \text{mass CO}_2 \text{ out} \\ \text{in top gas} \end{array} \right] * 0.117 \\
 & + \left[\begin{array}{l} \text{mass H}_2\text{O ascending} \\ \text{from bottom segment} \end{array} \right] * 1 - \left[\begin{array}{l} \text{mass H}_2\text{O out} \\ \text{in top gas} \end{array} \right] * 1
 \end{aligned} \tag{25.13}$$

where from Section 25.5

$$0.117 = \left(\frac{\left[\begin{array}{l} \text{mass H}_2 \text{ ascending} \\ \text{from bottom segment} \end{array} \right]}{\left[\begin{array}{l} \text{mass CO ascending} \\ \text{from bottom segment} \end{array} \right]} \right) * 5.7 \tag{25.12}$$

40.9 MATCHING THE MODEL TO COMMERCIAL BLAST FURNACE DATA

When the matrix model prepared in this book is used to simulate a commercial blast furnace, the user may find it challenging to get a precise match of the key operating parameters. While the model describes most aspects of the blast furnace process, some changes must be considered to match industrial data. Through experience, the authors have found that the following parameters may need adjustment:

- The model assumes that all iron ore is hematite, Fe₂O₃. Blast furnace sinter contains 5–10% FeO, this will need to be considered in the iron and oxygen balances.
- Adjust CO₂/CO equilibrium mass ratio leaving the bottom segment, which has been assumed to be 0.694, to match the observed coke rate. This may represent gas flow issues/short circuiting in the bottom segment that creates inefficiency as the reducing gases cannot react with the descending iron oxides. A blast furnace operating with a central coke chimney for permeability reasons is a good example as there is no iron ore to react with the rising CO at the center of the blast furnace.
- Adjust H₂O/H₂ equilibrium mass ratio leaving the bottom segment, which has been assumed to be 5.44, to match the observed H₂ top gas production/analysis. H₂ conversion to H₂O may be under reported due to inefficient gas flow in the bottom segment as described earlier.
- Adjust top/bottom segment heat loss rates, 320 and 80 MJ/1000 kg Fe in product

molten iron, respectively, to match top gas temperature. Actual heat losses may be understated.

When matching your model calculations to industrial data, take a note that the following measuring errors could impact your ability to make a good match:

- Accurate measurement of the blast air volume can be challenging due to the large quantity to be measured and need for a long straight pipe section between the turbo blower and blast furnace to take a precise measurement. A viable blast furnace model may not match the measured air volume, the latter of which could be in error.
- Measurement of the total carbon input can be in error. Ability to measure the coke moisture content and charge coke on a dry basis can lead to an input carbon measurement error. Injected pulverized coal can have a variable carbon content depending on quality control at the coal mine.
- Errors in top gas temperature measurement. The model calculates the top gas temperature leaving the charged burden surface. The actual measurement in the furnace uptakes is about 10 m higher, this could lead to a small difference in top gas temperature. Above burden probes or newer systems like TMT—Tapping Measuring Technologies' SOMA system provide a better indication of the top gas temperature leaving the charged burden surface. While the difference in top gas temperature may not be large, it can impact the model accuracy as a large volume of gas leaves the blast furnace.
- Not all heat losses may be measured. Some blast furnaces do not measure the heat losses to all cooling systems. The reported values may underestimate the actual cooling losses.
- Reported raceway adiabatic flame temperature may not match the matrix model calculation. Many producers use empirical equations that may be inaccurate.

The model calculated flame temperature is more comprehensive and defendable.

Armed with this knowledge, adjustments can be easily made to the matrix calculations to match the model to the available industrial data. Knowing what adjustments are needed can help identify measurement errors that may be present at the industrial blast furnace. Once the model has been calibrated to the observed measurements, the blast furnace engineer can extrapolate to future conditions/scenarios with confidence and accuracy.

40.10 SUMMARY

In this chapter, we completed our matrix development by including the effects of multiple through-tuyere inputs in our top gas calculations.

Through-tuyere inputs don't appear in our top-segment matrix because they are not present in top segment of Fig. 40.2. They do, however, influence the masses of CO, CO₂, H₂, H₂O(g), and N₂ rising into the top segment. This changes the top-segment input, output, and top gas enthalpies and hence top gas temperature, Fig. 40.3.

Our automatic top gas calculations are nearly complete. We must, however, consider the effects of moisture in the top-charged ores, coke, and fluxes. This is done in Chapter 41, Top-Segment Calculations with Raw Material Moisture, by adding top-charge moisture to matrix Table 40.2.

The top gas temperatures in Fig. 40.3 are higher than industrial top gas temperatures; 110°C–140°C. This is because in this chapter, we did not include several top-segment endothermic reactions, that is, moisture-in-top charge evaporation and carbonate flux dissociation. These are added to our calculations in Chapter 41, Top-Segment Calculations with Raw Material Moisture, and Chapter 42, Top Segment with Carbonate Fluxes.

EXERCISES

- 40.1.** Please predict for the management of Exercise 38.1 what their top gas temperature will be with 20 kg of 25°C oil injection of Exercise 38.1 (plus all the other injectants). Can you suggest a trend before you do the calculation?
- 40.2.** The blast furnace operators of Exercise 40.1 want a top gas temperature of 280°C. They wish to know how much oil

injection will give them this temperature. Please calculate this for them.

Caution: make sure that your bottom-segment calculated values transfer automatically to the top-segment matrix.

Reference

1. Geerdes M, Chaigneau R, Kurunov I, Lingiardi O, Ricketts J. *Modern blast furnace ironmaking (an introduction)*. 3rd ed IOS Press BV: Amsterdam; 2015.

Top-Segment Calculations with Raw Material Moisture

OUTLINE

41.1 Accounting for Moisture in the Charge Materials	369	41.6 Top Gas Enthalpy	371
41.2 $\text{H}_2\text{O}(\ell)$ Quantity Equation	370	41.7 Top Gas Temperature	371
41.3 Output $\text{H}_2\text{O(g)}$ Quantity Specification	370	41.7.1 Calculation Result	371
41.4 Top-Segment Input Enthalpy	371	41.8 Summary	377
41.5 Top-Segment Output Enthalpy	371	Exercises	377

41.1 ACCOUNTING FOR MOISTURE IN THE CHARGE MATERIALS

Top-charged burden of a blast furnace always contains moisture from processing and from the environment. A base load moisture content in each burden material can be further increased during periods of heavy rain as burden materials are stored outdoors. When the moisture of the burden is in excess, the start of reduction is delayed which creates a “short” furnace with inadequate time for all reduction reactions to

proceed. Productivity may have to be decreased to increase the burden’s residence and hence drying time. Typical values of burden moisture are nearly 0 to about 5 mass% H_2O .

In this chapter, we learn how to automatically quantify this temperature drop, based on Fig. 41.1

The objectives of this chapter are to show;

1. how to include top-charged $\text{H}_2\text{O}(\ell)$ in our automatic top-segment calculations, including calculation of;
 - a. top-segment input enthalpy,
 - b. top-segment output enthalpy,

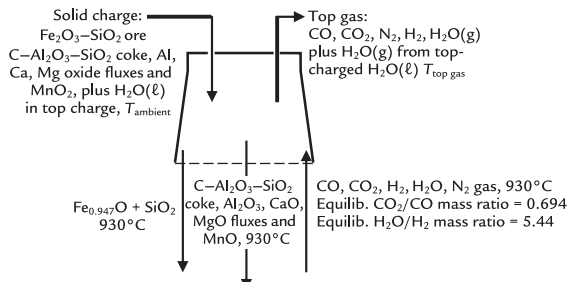


FIGURE 41.1 Sketch of conceptual blast furnace top-segment with $\text{H}_2\text{O}(\ell)$ in the furnace charge. We specify that all the top-charged $\text{H}_2\text{O}(\ell)$ leaves the furnace as H_2O (g) without reacting. In the matrix, its name is *mass $\text{H}_2\text{O}(\ell)$ departing in top gas from top-charged $\text{H}_2\text{O}(\ell)$* .

- c. top gas enthalpy, and
- d. top gas temperature, and
- 2. how top gas temperature is affected by mass $\text{H}_2\text{O}(\ell)$ in top charge.

41.2 $\text{H}_2\text{O}(\ell)$ QUANTITY EQUATION

Mass $\text{H}_2\text{O}(\ell)$ in top charge is described generally by;

$$\begin{aligned} & \left[\begin{array}{l} \text{mass } \text{H}_2\text{O}(\ell) \\ \text{in top-charged} \\ \text{ore, coke, and fluxes} \end{array} \right] \\ &= \left[\begin{array}{l} \text{mass } \text{Fe}_2\text{O}_3 \text{ in} \\ \text{top-charged ore} \end{array} \right] * [\text{mass\% } \text{H}_2\text{O}(\ell) \text{ in ore}] / 100\% \\ &+ \left[\begin{array}{l} \text{mass } \text{SiO}_2 \text{ in} \\ \text{top-charged ore} \end{array} \right] * [\text{mass\% } \text{H}_2\text{O}(\ell) \text{ in ore}] / 100\% \\ &+ \left[\begin{array}{l} \text{mass } \text{C} \text{ in} \\ \text{top-charged coke} \end{array} \right] * [\text{mass\% } \text{H}_2\text{O}(\ell) \text{ in coke}] / 100\% \\ &+ \left[\begin{array}{l} \text{mass } \text{Al}_2\text{O}_3 \text{ in} \\ \text{top-charged coke} \end{array} \right] * [\text{mass\% } \text{H}_2\text{O}(\ell) \text{ in coke}] / 100\% \\ &+ \left[\begin{array}{l} \text{mass } \text{SiO}_2 \text{ in} \\ \text{top-charged coke} \end{array} \right] * [\text{mass\% } \text{H}_2\text{O}(\ell) \text{ in coke}] / 100\% \\ &+ \left[\begin{array}{l} \text{mass top-charged} \\ \text{Al}_2\text{O}_3 \text{ flux} \end{array} \right] * [\text{mass\% } \text{H}_2\text{O}(\ell) \text{ in Al}_2\text{O}_3 \text{ flux}] / 100\% \\ &+ \left[\begin{array}{l} \text{mass top-charged} \\ \text{CaO flux} \end{array} \right] * [\text{mass\% } \text{H}_2\text{O}(\ell) \text{ in CaO flux}] / 100\% \\ &+ \left[\begin{array}{l} \text{mass top-charged} \\ \text{MgO flux} \end{array} \right] * [\text{mass\% } \text{H}_2\text{O}(\ell) \text{ in MgO flux}] / 100\% \\ &+ \left[\begin{array}{l} \text{mass top-charged} \\ \text{MnO}_2 \text{ ore} \end{array} \right] * [\text{mass\% } \text{H}_2\text{O}(\ell) \text{ in MnO}_2 \text{ ore}] / 100\% \end{aligned} \quad (41.1)$$

or subtracting $\left[\begin{array}{l} \text{mass } \text{H}_2\text{O}(\ell) \\ \text{in top-charged} \\ \text{ore, coke, and fluxes} \end{array} \right]$ from both sides and specifying an average of 5 mass% $\text{H}_2\text{O}(\ell)$ in the top-charged materials:

$$\begin{aligned} 0 = & - \left[\begin{array}{l} \text{mass } \text{H}_2\text{O}(\ell) \\ \text{in top-charged} \\ \text{ore, coke, and fluxes} \end{array} \right] * 1 \\ &+ \left[\begin{array}{l} \text{mass } \text{Fe}_2\text{O}_3 \text{ in} \\ \text{top-charged ore} \end{array} \right] * 0.05 \\ &+ \left[\begin{array}{l} \text{mass } \text{SiO}_2 \text{ in} \\ \text{top-charged ore} \end{array} \right] * 0.05 \\ &+ \left[\begin{array}{l} \text{mass } \text{C} \text{ in} \\ \text{top-charged coke} \end{array} \right] * 0.05 \\ &+ \left[\begin{array}{l} \text{mass } \text{Al}_2\text{O}_3 \text{ in} \\ \text{top-charged coke} \end{array} \right] * 0.05 \\ &+ \left[\begin{array}{l} \text{mass } \text{SiO}_2 \text{ in} \\ \text{top-charged coke} \end{array} \right] * 0.05 \\ &+ \left[\begin{array}{l} \text{mass top-charged} \\ \text{Al}_2\text{O}_3 \text{ flux} \end{array} \right] * 0.05 \\ &+ \left[\begin{array}{l} \text{mass top-charged} \\ \text{CaO flux} \end{array} \right] * 0.05 \\ &+ \left[\begin{array}{l} \text{mass top-charged} \\ \text{MgO flux} \end{array} \right] * 0.05 \\ &+ \left[\begin{array}{l} \text{mass top-charged} \\ \text{MnO}_2 \text{ ore} \end{array} \right] * 0.05 \end{aligned} \quad (41.2)$$

41.3 OUTPUT H_2O (g) QUANTITY SPECIFICATION

The simplest way to include the amount of H_2O (g) produced by evaporation of $\text{H}_2\text{O}(\ell)$ -in-top charge is by;

$$\left[\begin{array}{l} \text{mass } \text{H}_2\text{O}(g) \text{ departing} \\ \text{in top gas from} \\ \text{top-charged } \text{H}_2\text{O}(\ell) \end{array} \right] = \left[\begin{array}{l} \text{Mass } \text{H}_2\text{O}(\ell) \text{ in top-charged} \\ \text{ore, coke, and fluxes} \end{array} \right] \quad (41.3)$$

or

$$\left[\begin{array}{l} \text{mass } \text{H}_2\text{O}(\ell) \\ \text{in top-charged} \\ \text{ore, coke, and fluxes} \end{array} \right] = \left[\begin{array}{l} \text{mass } \text{H}_2\text{O}(g) \text{ departing} \\ \text{in top gas from} \\ \text{top-charged } \text{H}_2\text{O}(\ell) \end{array} \right]$$

or subtracting $\left[\begin{array}{c} \text{mass H}_2\text{O}(\ell) \\ \text{in top-charged} \\ \text{ore, coke, and fluxes} \end{array} \right]$ from both sides;

$$0 = - \left[\begin{array}{c} \text{mass H}_2\text{O}(\ell) \\ \text{in top-charged} \\ \text{ore, coke, and fluxes} \end{array} \right] * 1 + \left[\begin{array}{c} \text{mass H}_2\text{O(g)} \text{ departing} \\ \text{in top gas from} \\ \text{top-charged H}_2\text{O}(\ell) \end{array} \right] * 1 \quad (41.4)$$

Eqs. (41.2) and (41.4) and their variables are included in the top-segment matrix of Table 40.2 by adding (1) two rows and (2) two columns as shown in Table 41.1.

We also change the name of the variable of Chapter 40, Top-Segment Calculations with Multiple Injectants;

$$\left[\begin{array}{c} \text{mass H}_2\text{O(g)} \\ \text{in top gas} \end{array} \right]$$

to

$$\left[\begin{array}{c} \text{mass H}_2\text{O(g)} \text{ from} \\ \text{reactions departing} \\ \text{in top gas} \end{array} \right]$$

as also shown in Table 41.1, column CD. Table 41.1 shows the matrix coefficients. Table 41.2 shows the solution to the matrix of Table 41.1.

41.4 TOP-SEGMENT INPUT ENTHALPY

$\text{H}_2\text{O}(\ell)$ in top charge of a blast furnace adds one term to top-segment input enthalpy. It is;

$$\left[\begin{array}{c} \text{mass H}_2\text{O}(\ell) \\ \text{in top-charged} \\ \text{ore, coke, and fluxes} \end{array} \right] * \frac{H_{25^\circ\text{C}}^{\circ}}{\frac{\text{H}_2\text{O}(\ell)}{\text{MW}_{\text{H}_2\text{O}}}}$$

and numerically;

$$\left[\begin{array}{c} \text{mass H}_2\text{O}(\ell) \\ \text{in top-charged} \\ \text{ore, coke, and fluxes} \end{array} \right] * -15.87$$

as shown in Table 41.3 where Cell BC100 is $\left[\begin{array}{c} \text{mass H}_2\text{O}(\ell) \\ \text{in top-charged} \\ \text{ore, coke, and fluxes} \end{array} \right]$

41.5 TOP-SEGMENT OUTPUT ENTHALPY

Top-segment output enthalpy Eq. (40.3) is unchanged by $\text{H}_2\text{O}(\ell)$ in top-charged ore, coke, and fluxes burden.

41.6 TOP GAS ENTHALPY

Likewise, top gas enthalpy Eq. (40.5) is also unchanged by $\text{H}_2\text{O}(\ell)$ in top-charged ore, coke, and fluxes burden.

41.7 TOP GAS TEMPERATURE

Top gas temperature Eq. (40.7) contains the term;

$$\left[\begin{array}{c} \text{mass H}_2\text{O(g)} \\ \text{departing in top gas} \end{array} \right]$$

on the top and on the bottom.

In this chapter, we replace that term with;

$$\left\{ \left[\begin{array}{c} \text{mass H}_2\text{O(g)} \text{ from} \\ \text{reactions departing} \\ \text{in top gas} \end{array} \right] + \left[\begin{array}{c} \text{mass H}_2\text{O(g)} \text{ departing} \\ \text{in top gas from} \\ \text{top-charged H}_2\text{O}(\ell) \end{array} \right] \right\}$$

as shown in Table 41.3 - where it is represented by (BC98 + BC101).

41.7.1 Calculation Result

Table 41.3 shows that the top gas temperature with an average of 5 mass% $\text{H}_2\text{O}(\ell)$ in the top-charged ore, coke, and fluxes is 168°C .

This is 105°C cooler than with no $\text{H}_2\text{O(g)}$ in the furnace top charge, Section 40.6.

TABLE 41.1 Top-Segment Calculation With (1) Four Tuyere Injectants and (2) 5 mass% Moisture in All the Top-Charged Solids, Row 31

	BL	BM	BN	BO	BP	BQ	BR	BS	BT	BU	BV
1	mass top charged MnO ₂ ore	mass Al ₂ O ₃ -in-coke descending out of top segment	mass Al ₂ O ₃ flux descending out of top segment	mass C-in-coke descending out of top segment	mass CaO flux descending out of top segment	mass Fe _{0.947} O descending out of top segment	mass MgO flux descending out of top segment	mass MnO descending out of top segment	mass SiO ₂ -in-coke descending out of top segment	mass SiO ₂ -in ore descending out of top segment	mass CO ascending into top segment
2											
3	0	0	0	0	0	0	0	0	0	0	1
4	0	0	0	0	0	0	0	0	0	0	0
5	0	0	0	0	0	0	0	0	0	0	0
6	0	0	0	0	0	0	0	0	0	0	0
7	0	0	0	0	0	0	0	0	0	0	0
8	0	1	0	0	0	0	0	0	0	0	0
9	0	0	1	0	0	0	0	0	0	0	0
10	0	0	0	1	0	0	0	0	0	0	0
11	0	0	0	0	0	1	0	0	0	0	0
12	0	0	0	0	1	0	0	0	0	0	0
13	0	0	0	0	0	0	1	0	0	0	0
14	0	0	0	0	0	0	0	1	0	0	0
15	0	0	0	0	0	0	0	0	1	0	0
16	0	0	0	0	0	0	0	0	0	1	0
17	0	1	0	0	0	0	0	0	0	0	0
18	0	0	1	0	0	0	0	0	0	0	0
19	0	0	0	1	0	0	0	0	0	0	0.429
20	0	0	0	0	1	0	0	0	0	0	0
21	0	0	0	0	0	0.768	0	0	0	0	0
22	0	0	0	0	0	0	0	0	0	0	0
23	0	0	0	0	0	0	1	0	0	0	0
24	-0.632	0	0	0	0	0	0	0.774	0	0	0
25	0	0	0	0	0	0	0	0	0	0	0
26	-0.368	0	0	0	0	0.232	0	0.226	0	0	-0.571
27	0	0	0	0	0	0	0	1	0	0	0
28	0	0	0	0	0	0	0	0	1	0	0
29	0	0	0	1	0	0	0	0	0	0	0
30	0	0	0	0	0	0	0	0	0	0	0
31	0.05	0	0	0	0	0	0	0	0	0	0
32	0	0	0	0	0	0	0	0	0	0	0
33											

(Continued)

TABLE 41.1 (Continued)

	BW	BX	BY	BZ	CA	CB	CC	CD	CE	CF	CG
1	mass CO ₂ ascending into top segment	mass H ₂ ascending into top segment	mass H ₂ O(g) ascending into top segment	mass N ₂ ascending into top segment	mass CO out in top gas	mass CO ₂ out in top gas	mass H ₂ out in top gas	mass H ₂ O(g) from reactions departing in top gas	mass N ₂ out in top gas	Mass H ₂ O(l) in top-charged ore, coke and fluxes	mass H ₂ O(g) from top-charged H ₂ O(l)
2											
3	0	0	0	0	0	0	0	0	0	0	0
4	1	0	0	0	0	0	0	0	0	0	0
5	0	1	0	0	0	0	0	0	0	0	0
6	0	0	1	0	0	0	0	0	0	0	0
7	0	0	0	1	0	0	0	0	0	0	0
8	0	0	0	0	0	0	0	0	0	0	0
9	0	0	0	0	0	0	0	0	0	0	0
10	0	0	0	0	0	0	0	0	0	0	0
11	0	0	0	0	0	0	0	0	0	0	0
12	0	0	0	0	0	0	0	0	0	0	0
13	0	0	0	0	0	0	0	0	0	0	0
14	0	0	0	0	0	0	0	0	0	0	0
15	0	0	0	0	0	0	0	0	0	0	0
16	0	0	0	0	0	0	0	0	0	0	0
17	0	0	0	0	0	0	0	0	0	0	0
18	0	0	0	0	0	0	0	0	0	0	0
19	-0.273	0	0	0	0.429	0.273	0	0	0	0	0
20	0	0	0	0	0	0	0	0	0	0	0
21	0	0	0	0	0	0	0	0	0	0	0
22	0	-1	-0.112	0	0	0	1	0.112	0	0	0
23	0	0	0	0	0	0	0	0	0	0	0
24	0	0	0	0	0	0	0	0	0	0	0
25	0	0	0	-1	0	0	0	0	1	0	0
26	-0.727	0	-0.888	0	0.571	0.727	0	0.888	0	0	0
27	0	0	0	0	0	0	0	0	0	0	0
28	0	0	0	0	0	0	0	0	0	0	0
29	0	0	0	0	0	0	0	0	0	0	0
30	-0.12	0	1	0	0	0.12	0	-1	0	0	0
31	0	0	0	0	0	0	0	0	0	-1	0
32	0	0	0	0	0	0	0	0	0	-1	1
33	=BC5/BC3*5.7				=BC5/BC3*5.7						

Rows 31 and 32 and Columns CF and CG are new.

TABLE 41.2 Top-Segment Calculated Values With H₂O(l) in the Top-Charged Materials

	BB	BC
71	Top segment calculated values	kg per 1000 kg of Fe out in molten iron
72	mass Fe ₂ O ₃ in top-charged ore	1431
73	mass SiO ₂ in top-charged ore	75
74	mass C in top-charged coke	326
75	mass Al ₂ O ₃ in top-charged coke	11
76	mass SiO ₂ in top-charged coke	25
77	mass top-charged Al ₂ O ₃ flux	12
78	mass top-charged CaO flux	100
79	mass top-charged MgO flux	24
80	mass top-charged MnO ₂ ore	9.3
81	mass Al ₂ O ₃ -in-coke descending out of top segment	11
82	mass Al ₂ O ₃ flux descending out of top segment	12
83	mass C-in-coke descending out of top segment	326
84	mass CaO flux descending out of top segment	100
85	mass Fe _{0.947} O descending out of top segment	1302
86	mass MgO flux descending out of top segment	24
87	mass MnO descending out of top segment	7.6
88	mass SiO ₂ -in-coke descending out of top segment	25
89	mass SiO ₂ -in-ore descending out of top segment	75
90	mass CO ascending into top segment	600
91	mass CO ₂ ascending into top segment	416
92	mass H ₂ ascending into top segment	12
93	mass H ₂ O ascending into top segment	67
94	mass N ₂ ascending into top segment	1146
95	mass CO out in top gas	422
96	mass CO ₂ out in top gas	695
97	mass H ₂ out in top gas	8.6
98	mass H ₂ O from reactions departing in top gas	99
99	mass N ₂ out in top gas	1146
100	Mass top-charged H ₂ O(l)	101
101	Mass departing H ₂ O(g) from top-charge H ₂ O(l)	101

TABLE 41.3 Calculation of Top-Segment (1) Input and Output Enthalpies, (2) Top Gas Enthalpy, and (3) Top Gas Temperature

	BA	BB	BC	BD	BE	BF	BG	BH	BI	BJ	BK	BL	BM	BN	BO	
TOP SEGMENT INPUT AND OUTPUT ENTHALPY CALCULATIONS																
111																
112																
113	40.3	Top segment input enthalpy =	BC72* -5.169 + BC73* -15.16 + BC74* 0 + BC75* -16.43 + BC76* -15.16 + BC77* -16.43 + BC78* -11.32 + BC79* -14.92 + BC80* -5.98 + BC90* -2.926 + BC91* -7.926 + BC92* 13.35 + BC93* -11.49 + BC94* 1.009 + BC100* -15.87 =									-16943	MJ per 1000 kg of Fe in product molten iron			
114		Top segment output enthalpy =	BL112-80 =										-17023	MJ per 1000 kg of Fe in product molten iron		
TOP GAS ENTHALPY CALCULATION																
115	40.5	Top gas enthalpy =	BL113*BC81* 15.41 *BC82* 15.41 *BC83* 1.359 *BC84* 10.5 *BC85* 3.152 *BC86* 13.84 *BC87* 4.77 *BC88* 14.13 *BC89* 14.13									-10167	MJ per 1000 kg of Fe in product molten iron			
TOP-GAS TEMPERATURE CALCULATION																
116																
117																
118																
119													168			

The output and top gas enthalpy equations are not changed by $H_2O(\ell)$ in the top-charged materials.

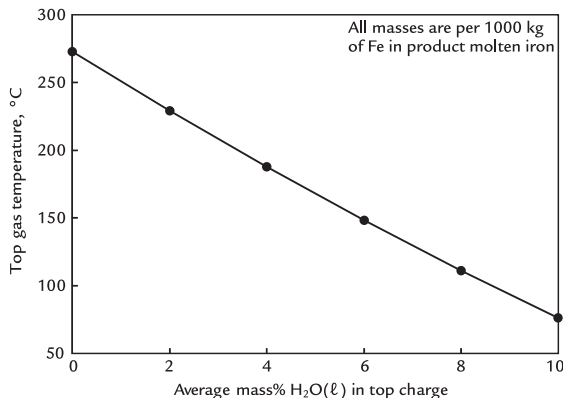


FIGURE 41.2 Effect of average mass% $\text{H}_2\text{O}(l)$ in top-charged materials on top gas temperature. The cooling effect of $\text{H}_2\text{O}(l)$ is noticeable. This is the result of heat being used to evaporate the $\text{H}_2\text{O}(l)$ rather than to heat top gas. The points are all with tuyere injection of 60 kg of coal, 30 kg of oxygen, and 60 kg of natural gas and with a blast moisture of 15 g $\text{H}_2\text{O(g)}$ /Nm³ of dry air. The line is curved because some of our equations are nonlinear. [With 5 mass% $\text{H}_2\text{O}(l)$ in top-charged ore, coke, and fluxes, Cells BD31–BL31 of Table 41.1 all contain 0.05, etc.]

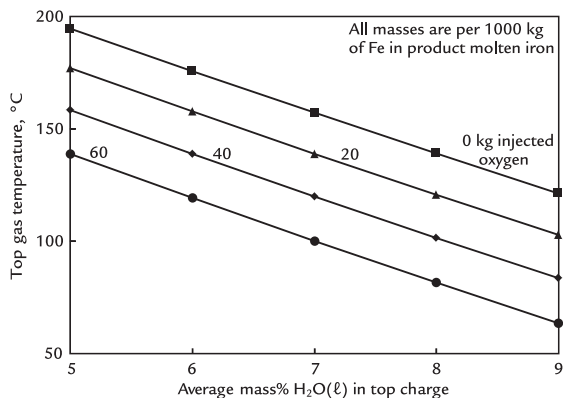


FIGURE 41.3 Effect of average mass% $\text{H}_2\text{O}(l)$ in top-charged materials on top gas temperature with differing amounts of oxygen injection. The quantities of the other injectants have been kept constant as described in Fig. 41.2. The slopes of the lines are almost the same. The lines are not exactly straight because some of our equations are nonlinear.

Additional results are shown in Fig. 41.2, which shows that a 1 mass% increase in top-charged $\text{H}_2\text{O}(l)$ lowers top gas temperature by $\sim 20^\circ\text{C}$.

Fig. 41.3 repeats some of these calculations with 0, 20, 40, and 60 kg of oxygen injection, everything else constant. It shows that the effect of $\text{H}_2\text{O}(l)$ in the top charge remains very nearly the same as that in Fig. 41.2, that is, approximately -20°C per additional mass% $\text{H}_2\text{O}(l)$ in top-charged ore, coke, and fluxes inputs.

41.8 SUMMARY

Moisture in the blast furnace top-charged materials is readily represented in our automatic top-segment (1) matrix calculation, (2) input enthalpy calculation, and (3) top gas temperature calculation. It does not change our top-segment output enthalpy and top gas enthalpy equations.

Moisture in the top charge does not affect the blast furnace's coke and air requirements. It does lower top gas temperature. This may be offset by tuyere injection of hydrocarbons which decreases the requirement for (cool) top-charged coke, hence tends to increase top gas temperature. Through-tuyere input of $\text{H}_2\text{O(g)}$ has a similar offsetting effect.

Oxygen injection has the opposite effect, mainly because it decreases the amount of hot N_2 ascending into the top segment.

EXERCISES

Unless otherwise mentioned, the bottom-segment injected masses associated with these problems are 60 kg of coal, 30 kg of pure oxygen, and 60 kg of natural gas of Chapter 38, Bottom-Segment Calculations with Multiple Injectants, with 15 g $\text{H}_2\text{O(g)}$ in 1200°C

blast/Nm³ of dry blast. All masses are per 1000 kg of Fe in product molten iron.

- 41.1.** Management of blast furnace of Fig. 41.1 now wants a top gas temperature of 100°C with 6 mass% H₂O(*l*) in all top-charged materials. How much pure oxygen injectant will be necessary to achieve this 100°C top gas target? The other tuyere inputs are as described at the top of this page.
- 41.2.** With a charge of sinter and dry quenched coke, it is possible to bring the moisture in top-charged materials of a

blast furnace down to nearly zero. Management of blast furnace of Fig. 41.1 wants to know how to achieve a 200°C top gas temperature with this completely dry charge. You suggest that this can be achieved by altering natural gas injection (Fig. 31.2). Please determine how much natural gas injectant will be needed to achieve this 200°C top gas temperature goal. The other tuyere inputs are as described at the top of this page.

- 41.3.** What advantages might a dry top charge have?

Top Segment With Carbonate Fluxes

OUTLINE

42.1 Understanding the Impact of Carbonate Fluxes on the Blast Furnace Process	379	42.5 Top-Segment Output Enthalpy With Carbonates Added	386
42.2 Amended Top-Segment Variables and Equations for Carbonates	380	42.6 Top Gas Enthalpy	386
42.3 New Variable and Its Associated Equation for Carbonates	381	42.7 Top Gas Temperature	386
42.4 Amended Top-Segment Input Enthalpy Equation With Carbonates Added	381	42.8 Results	386
		42.9 Summary	386
		Exercises	388

42.1 UNDERSTANDING THE IMPACT OF CARBONATE FLUXES ON THE BLAST FURNACE PROCESS

Previous top-segment chapters have assumed that our slag components enter the blast furnace as oxides, for example, CaO and MgO. This is the case for many industrial blast furnaces, especially those being charged with self-fluxing sinter and pellets.

Many blast furnaces charge Ca and Mg carbonate fluxes, especially those that charge

lump iron ore. Small carbonate flux additions are also used for final slag chemistry control. These carbonates decompose in the top segment to form solid oxide and CO₂ gas by reactions such as;



The product solids descend into the bottom segment, where they ultimately form molten slag (Fig. 42.1).

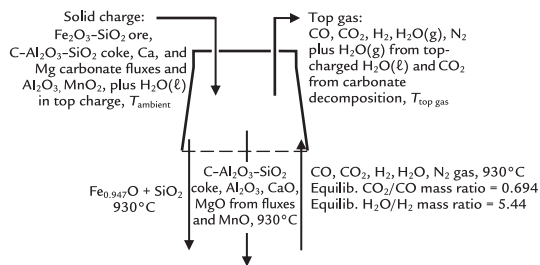


FIGURE 42.1 Conceptual blast furnace top segment with CaCO₃ and MgCO₃ fluxes (and moisture) in the top charge. We specify that all the CO₂(g) from carbonate decomposition and all the H₂O(g) from moisture evaporation leave the furnace without reacting. Notice that Ca and Mg enter the furnace in carbonates but descend out of the top segment as oxides.

The product CO₂ joins the gases that are rising through the top segment, ultimately ending up in the furnace top gas (Fig. 42.1).

Decomposition reactions (42.1) and (42.2) are endothermic. They absorb heat from the rising bottom-segment gases, ultimately resulting in top gas that is cooler than when the top-charged fluxes are oxides (Chapter 47: Bottom Segment Calculations with CO Injection).

In this chapter, we examine the effects of charging carbonate fluxes to the blast furnace, especially their effect on top gas composition, enthalpy, and temperature. Top-segment flows with carbonate fluxes [plus top-charged H₂O(l)] are shown in Fig. 42.1.

The objectives of this chapter are to;

1. calculate top gas composition, enthalpy, and temperature with top-charged carbonate fluxes, and
2. compare these calculated quantities obtained with top-charged oxide fluxes.

42.2 AMENDED TOP-SEGMENT VARIABLES AND EQUATIONS FOR CARBONATES

Replacement of oxide fluxes with carbonate fluxes changes;

$$1. \text{ the variable } \left[\frac{\text{mass top-charged}}{\text{CaO flux}} \right] \text{ to } \left[\frac{\text{mass top-charged}}{\text{CaCO}_3 \text{ flux}} \right]$$

and

$$2. \text{ the variable } \left[\frac{\text{mass top-charged}}{\text{MgO flux}} \right] \text{ to } \left[\frac{\text{mass top-charged}}{\text{MgCO}_3 \text{ flux}} \right]$$

It also changes the top-segment CaO mass balance;

$$0 = - \left[\frac{\text{mass top-charged}}{\text{CaO flux}} \right] * 1 \\ + \left[\frac{\text{mass CaO descending}}{\text{out of top segment}} \right] * 1$$

to

$$0 = - \left[\frac{\text{mass top-charged}}{\text{CaCO}_3 \text{ flux}} \right] * 0.56 \\ + \left[\frac{\text{mass CaO descending}}{\text{out of top segment}} \right] * 1 \quad (42.3)$$

where 0.56 is 56 mass% CaO in CaCO₃/100%. The top-segment MgO mass balance changes to;

$$0 = - \left[\frac{\text{mass top-charged}}{\text{MgCO}_3 \text{ flux}} \right] * 0.478 \\ + \left[\frac{\text{mass MgO descending}}{\text{out of top segment}} \right] * 1 \quad (42.4)$$

where 0.478 is 47.8 mass% MgO in MgCO₃/100%.

42.3 NEW VARIABLE AND ITS ASSOCIATED EQUATION FOR CARBONATES

Carbonate decomposition introduces one new variable to our top-segment matrix. It is;

$$\left[\begin{array}{l} \text{mass top-gas CO}_2 \text{ from} \\ \text{carbonates decomposition} \end{array} \right]$$

This variable is added to the right-most side of matrix Table 41.1 in new Column CH.

All this CO₂ comes from CaCO₃ and MgCO₃ decomposition and is best described by the following equation;

$$\begin{aligned} & \left[\begin{array}{l} \text{mass top-gas CO}_2 \text{ from} \\ \text{carbonates decomposition} \end{array} \right] \\ &= \left[\begin{array}{l} \text{mass top-charged} \\ \text{CaCO}_3 \text{ flux} \end{array} \right] * \frac{44.0 \text{ mass\% CO}_2 \text{ in CaCO}_3}{100\%} \\ &+ \left[\begin{array}{l} \text{mass top-charged} \\ \text{MgCO}_3 \text{ flux} \end{array} \right] * \frac{52.2 \text{ mass\% CO}_2 \text{ in MgCO}_3}{100\%} \\ &= \left[\begin{array}{l} \text{mass top-charged} \\ \text{CaCO}_3 \text{ flux} \end{array} \right] * 0.440 \\ &+ \left[\begin{array}{l} \text{mass top-charged} \\ \text{MgCO}_3 \text{ flux} \end{array} \right] * 0.522 \end{aligned}$$

or

$$\begin{aligned} & \left[\begin{array}{l} \text{mass top-charged} \\ \text{CaCO}_3 \text{ flux} \end{array} \right] * 0.440 \\ &+ \left[\begin{array}{l} \text{mass top-charged} \\ \text{MgCO}_3 \text{ flux} \end{array} \right] * 0.522 \\ &= \left[\begin{array}{l} \text{mass top-gas CO}_2 \text{ from} \\ \text{carbonates decomposition} \end{array} \right] * 1 \end{aligned}$$

or subtracting $\left\{ \left[\begin{array}{l} \text{mass top-charged} \\ \text{CaCO}_3 \text{ flux} \end{array} \right] * 0.440 \right. \right. \\ \left. \left. + \left[\begin{array}{l} \text{mass top-charged} \\ \text{MgCO}_3 \text{ flux} \end{array} \right] * 0.522 \right\}$ from both sides:

$$\begin{aligned} 0 = & - \left[\begin{array}{l} \text{mass top-charged} \\ \text{CaCO}_3 \text{ flux} \end{array} \right] * 0.440 \\ & - \left[\begin{array}{l} \text{mass top-charged} \\ \text{MgCO}_3 \text{ flux} \end{array} \right] * 0.522 \\ & + \left[\begin{array}{l} \text{mass top-gas CO}_2 \text{ from} \\ \text{carbonates decomposition} \end{array} \right] * 1 \end{aligned} \quad (42.5)$$

This is added to the bottom of matrix Table 41.1 in a new Row 33.

Table 42.1 shows our top-segment matrix with these changes. **Table 42.2** gives us its calculated values.

The equivalent bottom-segment matrix equations remain unchanged because all these activities take place in the top segment only.

We now calculate top-segment input enthalpy, output enthalpy, top gas enthalpy, and top gas temperature from calculated values of **Table 42.2**.

42.4 AMENDED TOP-SEGMENT INPUT ENTHALPY EQUATION WITH CARBONATES ADDED

Replacement of CaO and MgO by CaCO₃ and MgCO₃ in a furnace's top charge requires two changes to our top-segment input enthalpy equation. They are;

$$\frac{H^\circ_{25^\circ\text{C}}}{\text{MW}_{\text{CaO}}} \text{ is replaced by } \frac{H^\circ_{25^\circ\text{C}}}{\text{MW}_{\text{CaCO}_3}} = -12.06$$

$$\frac{H^\circ_{25^\circ\text{C}}}{\text{MW}_{\text{CaO}}} \text{ is replaced by } \frac{H^\circ_{25^\circ\text{C}}}{\text{MW}_{\text{MgCO}_3}} = -13.20$$

with units of, MJ/kg of substance.
This is shown by the terms;

$$\text{BC78} * (-12.06)$$

TABLE 42.1 Top-Segment Matrix With Top-Charged CaCO_3 and MgCO_3 Flux

BA	BB	BC	BD	BE	BF	BG	BH	BI	BJ	BK
TOP SEGMENT CALCULATIONS										
Equation	Description	Numerical term	mass Fe ₂ O ₃ in top-charged ore	mass SiO ₂ in top-charged ore	mass C in top-charged coke	mass Al ₂ O ₃ in top-charged coke	mass SiO ₂ in top-charged coke	mass top- charged Al ₂ O ₃ flux	mass top- charged CaCO ₃ flux	mass top- charged MgCO ₃ flux
3	40.8 Mass CO ascending from bottom segment	600	0	0	0	0	0	0	0	0
4	40.9 Mass CO ₂ ascending from bottom segment	416	0	0	0	0	0	0	0	0
5	40.10 Mass H ₂ ascending from bottom segment	12	0	0	0	0	0	0	0	0
6	40.11 Mass H ₂ O ascending from bottom segment	67	0	0	0	0	0	0	0	0
7	40.12 Mass N ₂ ascending from bottom segment	1146	0	0	0	0	0	0	0	0
8	40.13 Mass Al ₂ O ₃ -in-coke descending out of top segment	11	0	0	0	0	0	0	0	0
9	40.14 Mass Al ₂ O ₃ flux descending out of top segment	12	0	0	0	0	0	0	0	0
10	40.15 Mass C-in-coke descending out of top segment	326	0	0	0	0	0	0	0	0
11	40.16 Mass Fe _{0.947} O descending out of top segment	1302	0	0	0	0	0	0	0	0
12	40.17 Mass CaO flux descending out of top segment	99.7	0	0	0	0	0	0	0	0
13	40.18 Mass MgO flux descending out of top segment	24.3	0	0	0	0	0	0	0	0
14	40.19 Mass MnO descending out of top segment	7.6	0	0	0	0	0	0	0	0
15	40.20 Mass SiO ₂ -in-coke descending out of top segment	25	0	0	0	0	0	0	0	0
16	40.21 Mass SiO ₂ -in-ore descending out of top segment	75	0	0	0	0	0	0	0	0
17	40.22 Al ₂ O ₃ -in coke mass	0	0	0	0	-1	0	0	0	0
18	40.23 Al ₂ O ₃ flux mass balance	0	0	0	0	0	0	-1	0	0
19	40.24 C mass balance	0	0	0	-1	0	0	0	0	0
20	42.3 CaO mass balance	0	0	0	0	0	0	0	-0.560	0
21	40.26 Fe mass balance	0	-0.699	0	0	0	0	0	0	0
22	40.27 H mass balance	0	0	0	0	0	0	0	0	0
23	42.4 MgO mass balance	0	0	0	0	0	0	0	0	-0.478
24	40.29 Mn mass balance	0	0	0	0	0	0	0	0	0
25	40.30 N mass balance	0	0	0	0	0	0	0	0	0
26	40.31 O mass balance	0	-0.301	0	0	0	0	0	0	0
27	40.32 SiO ₂ -in-coke mass balance	0	0	0	0	0	-1	0	0	0
28	40.33 SiO ₂ -in-ore mass balance	0	0	-1	0	0	0	0	0	0
29	40.34 No top-segment C oxidation equation	0	0	0	-1	0	0	0	0	0
30	25.13 H ₂ /CO reaction mass ratio equation	0	0	0	0	0	0	0	0	0
31	41.2 Mass top-charged H ₂ O(l)	0	0.05	0.05	0.05	0.05	0.05	0.05	0.05	0.05
32	41.4 Mass H ₂ O(g) from top-charge H ₂ O(l)	0	0	0	0	0	0	0	0	0
33	42.5 Mass CO ₂ from top charge CaCO ₃ & MgCO ₃	0	0	0	0	0	0	0	-0.440	-0.522

	BL	BM	BN	BO	BP	BQ	BR	BS	BT	BU	BV
1	mass top charged MnO ₂ ore	mass Al ₂ O ₃ -in-coke descending out of top segment	mass Al ₂ O ₃ flux descending out of top segment	mass C-in-coke descending out of top segment	mass CaO flux descending out of top segment	mass Fe _{0.947} O descending out of top segment	mass MgO flux descending out of top segment	mass MnO descending out of top segment	mass SiO ₂ -in-ore descending out of top segment	mass SiO ₂ -in ore descending out of top segment	mass CO ascending into top segment
2											
3	0	0	0	0	0	0	0	0	0	0	1
4	0	0	0	0	0	0	0	0	0	0	0
5	0	0	0	0	0	0	0	0	0	0	0
6	0	0	0	0	0	0	0	0	0	0	0
7	0	0	0	0	0	0	0	0	0	0	0
8	0	1	0	0	0	0	0	0	0	0	0
9	0	0	1	0	0	0	0	0	0	0	0
10	0	0	0	1	0	0	0	0	0	0	0
11	0	0	0	0	0	1	0	0	0	0	0
12	0	0	0	0	1	0	0	0	0	0	0
13	0	0	0	0	0	0	1	0	0	0	0
14	0	0	0	0	0	0	0	1	0	0	0
15	0	0	0	0	0	0	0	0	1	0	0
16	0	0	0	0	0	0	0	0	0	1	0
17	0	1	0	0	0	0	0	0	0	0	0
18	0	0	1	0	0	0	0	0	0	0	0
19	0	0	0	1	0	0	0	0	0	0	-0.429
20	0	0	0	0	1	0	0	0	0	0	0
21	0	0	0	0	0	0.768	0	0	0	0	0
22	0	0	0	0	0	0	0	0	0	0	0
23	0	0	0	0	0	0	1	0	0	0	0
24	-0.632	0	0	0	0	0	0	0.774	0	0	0
25	0	0	0	0	0	0	0	0	0	0	0
26	-0.368	0	0	0	0	0.232	0	0.226	0	0	-0.571
27	0	0	0	0	0	0	0	0	1	0	0
28	0	0	0	0	0	0	0	0	0	1	0
29	0	0	0	1	0	0	0	0	0	0	0
30	0	0	0	0	0	0	0	0	0	0	0
31	0.05	0	0	0	0	0	0	0	0	0	0
32	0	0	0	0	0	0	0	0	0	0	0
33	0	0	0	0	0	0	0	0	0	0	0
34											

(Continued)

TABLE 42.1 (Continued)

	BW	BX	BY	BZ	CA	CB	CC	CD	CE	CF	CG	CH
1	mass CO ₂ ascending into top segment	mass H ₂ ascending into top segment	mass H ₂ O(g) ascending into top segment	mass N ₂ ascending into top segment	mass CO departing in top gas	mass CO ₂ departing in top gas	mass H ₂ departing in top gas	mass H ₂ O(g) departing in top gas	mass N ₂ departing in top gas	Mass H ₂ O(l) in top-charged ore	mass H ₂ O(g) from top-charged H ₂ O(l)	mass top-gas CO ₂ from carbonate dissociation
2												
3	0	0	0	0	0	0	0	0	0	0	0	0
4	1	0	0	0	0	0	0	0	0	0	0	0
5	0	1	0	0	0	0	0	0	0	0	0	0
6	0	0	1	0	0	0	0	0	0	0	0	0
7	0	0	0	1	0	0	0	0	0	0	0	0
8	0	0	0	0	0	0	0	0	0	0	0	0
9	0	0	0	0	0	0	0	0	0	0	0	0
10	0	0	0	0	0	0	0	0	0	0	0	0
11	0	0	0	0	0	0	0	0	0	0	0	0
12	0	0	0	0	0	0	0	0	0	0	0	0
13	0	0	0	0	0	0	0	0	0	0	0	0
14	0	0	0	0	0	0	0	0	0	0	0	0
15	0	0	0	0	0	0	0	0	0	0	0	0
16	0	0	0	0	0	0	0	0	0	0	0	0
17	0	0	0	0	0	0	0	0	0	0	0	0
18	0	0	0	0	0	0	0	0	0	0	0	0
19	-0.273	0	0	0.429	0.273	0	0	0	0	0	0	0
20	0	0	0	0	0	0	0	0	0	0	0	0
21	0	0	0	0	0	0	0	0	0	0	0	0
22	0	-1	-0.112	0	0	0	1	0.112	0	0	0	0
23	0	0	0	0	0	0	0	0	0	0	0	0
24	0	0	0	0	0	0	0	0	0	0	0	0
25	0	0	0	-1	0	0	0	0	1	0	0	0
26	-0.727	0	-0.888	0	0.571	0.727	0	0.888	0	0	0	0
27	0	0	0	0	0	0	0	0	0	0	0	0
28	0	0	0	0	0	0	0	0	0	0	0	0
29	0	0	0	0	0	0	0	0	0	0	0	0
30	-0.12	0	1	0	0	0.12	0	-1	0	0	0	0
31	0	0	0	0	0	0	0	0	0	-1	0	0
32	0	0	0	0	0	0	0	0	0	-1	1	0
33	0	0	0	0	0	0	0	0	0	0	0	1
34			=BC5/BC3*5.7				=BC5/BC3*5.7					

Column CH and Row 33 are new. Columns BJ and BK have changed.

TABLE 42.2 Top-Segment Matrix Table 42.1 Calculated Values

	BB	BC
71	Top segment calculated values	kg per 1000 kg of Fe out in molten iron
72	mass Fe_2O_3 in top-charged ore	1431
73	mass SiO_2 in top-charged ore	75
74	mass C in top-charged coke	326
75	mass Al_2O_3 in top-charged coke	11
76	mass SiO_2 in top-charged coke	25
77	mass top-charged Al_2O_3 flux	12
78	mass top-charged CaCO_3 flux	178.1
79	mass top-charged MgCO_3 flux	50.86
80	mass top-charged MnO_2 ore	9.3
81	mass Al_2O_3 -in-coke descending out of top segment	11
82	mass Al_2O_3 flux descending out of top segment	12
83	mass C-in-coke descending out of top segment	326
84	mass CaO flux descending out of top segment	99.7
85	mass $\text{Fe}_{0.947}\text{O}$ descending out of top segment	1302
86	mass MgO flux descending out of top segment	24.31
87	mass MnO descending out of top segment	7.6
88	mass SiO_2 -in-coke descending out of top segment	25
89	mass SiO_2 -in-ore descending out of top segment	75
90	mass CO ascending into top segment	600
91	mass CO_2 ascending into top segment	416
92	mass H_2 ascending into top segment	12
93	mass H_2O ascending into top segment	67
94	mass N_2 ascending into top segment	1146
95	mass CO out in top gas	422
96	mass CO_2 out in top gas	695
97	mass H_2 out in top gas	8.6
98	mass H_2O out in top gas	99
99	mass N_2 out in top gas	1146
100	Mass top-charged $\text{H}_2\text{O(l)}$	106
101	Mass departing $\text{H}_2\text{O(g)}$ from top-charge $\text{H}_2\text{O(l)}$	106
102	Mass CO_2 in top gas from carbonate dissociation	105

Mass CO_2 of Row 102 in top gas from carbonate decomposition is new.

and

$$\text{BC79} * (-13.20)$$

in Row 112 of [Table 42.3](#).

42.5 TOP-SEGMENT OUTPUT ENTHALPY WITH CARBONATES ADDED

Top-segment output enthalpy Eq. (40.3) is unchanged by switching to CaCO_3 and MgCO_3 fluxes.

42.6 TOP GAS ENTHALPY

Top gas enthalpy Eq. (40.5) is also unchanged by switching to CaCO_3 and MgCO_3 fluxes.

42.7 TOP GAS TEMPERATURE

Top gas temperature is not changed by CaCO_3 and MgCO_3 themselves, but it is changed by the CO_2 from their decomposition.

Top gas temperature contains the term:

$$\left[\begin{array}{l} \text{mass CO}_2 \\ \text{departing} \\ \text{in top gas} \end{array} \right]$$

In this chapter, we replace that term by:

$$\left\{ \left[\begin{array}{l} \text{mass CO}_2 \\ \text{from reactions} \\ \text{in top gas} \end{array} \right] + \left[\begin{array}{l} \text{mass top-gas CO}_2 \text{ from} \\ \text{carbonates decomposition} \end{array} \right] \right\}$$

The new term is represented in two places by;

$$(\text{BC96} + \text{BC102})$$

in Row 119 of [Table 42.3](#).

42.8 RESULTS

[Table 42.3](#) shows that top gas temperature with CaCO_3 and MgCO_3 fluxes is 24°C as compared to 168°C with CaO and MgO fluxes. This temperature (24°C) is too low for industrial blast furnace operations. In industrial practice, the operator would either need to enrich the sinter and/or pellets with CaO and MgO or increase the overall blast furnace fuel rate to achieve an acceptable top temperature. This low top gas temperature is the result of some heat in the rising gas of [Fig. 42.1](#) being used for the endothermic decomposition reactions;



and



lowering the enthalpy and temperature of the top gas.

42.9 SUMMARY

Carbonate fluxes are readily represented in our top-segment calculations. The major change is introduction of a new variable;

$$\left[\begin{array}{l} \text{mass top-gas CO}_2 \text{ from} \\ \text{carbonates decomposition} \end{array} \right]$$

and an equivalent quantity equation, (42.5), Row 33.

Also;

- CaO mass balance,
- MgO mass balance,
- top-segment input enthalpy, and
- top gas temperature

equations are slightly modified.

TABLE 42.3 Equations for Calculating Top-Segment Input Enthalpy, Output Enthalpy, Top Gas Enthalpy, and Top Gas Temperature

	BA	BB	BC	BD	BE	BF	BG	BH	BI	BJ	BK	BL	BM	BN	BO	
111	TOP SEGMENT INPUT AND OUTPUT ENTHALPY CALCULATIONS															
112																
112		Top segment input enthalpy =	BC72* .5.169+BC73* .15.16+BC74* 0+BC75* .16.43+BC76* .15.16+BC77* .16.43+BC78* .12.06+BC79* .13.2 +BC80* .5.98+BC90* .2.926+BC91* .7.926+BC92* .13.35+BC93* .11.49+BC94* .1.008+BC100* .15.87 =													
113	40.3	Top segment output enthalpy =	BN101-BO =													
114																
115	TOP GAS ENTHALPY CALCULATION															
116	40.5	Top gas enthalpy =	BJ113-BC81* .15.41+BC82* .15.41+BC83* .1.359-BC84* .10.5+BC85* .3.152+BC86* .13.84-BC87* .4.77+BC88* .14.13+BC89* .14.13													
117																
118	TOP GAS TEMPERATURE CALCULATION															
119																
119		Top gas temperature =	(BL116-BC95* .3.972-(BC96+BC102)* .8.966+BC97* .0.3616-(BC98+BC101)* .13.47+BC99* .0.02624)/(BC95* .0.001049+(BC96+BC102)* .0.0009314+BC97* .0.01442+(BC98+BC101)* .0.001902+BC99* .0.001044)									24	°C			

The input enthalpy and top gas temperature equations have been modified to represent CaCO₃, MgCO₃, and mass CO₂ in top gas from carbonate decomposition.

Replacement of CaO and MgO fluxes with CaCO_3 and MgCO_3 results in cooler top gas. This is because endothermic carbonate decomposition reactions absorb heat from the rising blast furnace gases - lowering their enthalpy and temperature.

EXERCISES

- 42.1.** The blast furnace management of matrix [Table 42.1](#) wants to charge its slag's CaO flux as $\text{CaCO}_3(\text{s})$ but its slag's MgO flux as $\text{MgO}(\text{s})$. They want to know how much this will change the furnace's top gas temperature. Please calculate this for them. Before doing so, can you make a prediction?

43

Top-Charged Scrap Steel

O U T L I N E

43.1 Adding Fe-Rich Solids to the Blast Furnace	390	43.11 Top-Segment Matrix	395
43.2 Including Top-Charged Scrap Steel in Our Calculations	390	43.12 Top-Segment Equation	400
43.3 No Oxidation of Scrap Steel in the Top Segment	390	43.13 Amended Top-Segment Fe Mass Balance	400
43.4 Bottom-Segment Scrap Steel Quantity Specification	391	43.14 Summary of Top-Segment Calculations With Scrap Steel Added	400
43.5 Scrap Steel Composition and Bottom-Segment Fe Mass Balance	391	43.15 Calculation of Top Gas Temperature	402
43.6 Amended Bottom-Segment Enthalpy Balance	394	43.15.1 Top-Segment Input Enthalpy	402
43.7 Nearly Completed Bottom-Segment Matrix	394	43.15.2 Top-Segment Output Enthalpy	402
43.8 SiO ₂ - A Minor but Important Change	394	43.15.3 Top Gas Enthalpy	402
43.9 Raceway Matrix	395	43.15.4 Top Gas Temperature	402
43.10 Top-Segment–Bottom-Segment Connection	395	43.16 Calculated Results - Coke Requirement	402
		43.17 Calculated Results: Top Gas CO ₂ Emissions	404
		43.18 Calculated Results: Blast Air Requirement	404

43.19 Calculated Results: Raceway Flame Temperature	405	43.21 Calculated Results - Top Gas Temperature	405
43.20 Calculated Results - CaO Flux Requirements	405	43.22 Summary	406
		Exercise	406

43.1 ADDING Fe-RICH SOLIDS TO THE BLAST FURNACE

Many blast furnace operators top charge recycled steel and other Fe-rich solids to their blast furnaces. The advantages are;

1. accelerated molten iron production;
2. lowered coke consumption;
3. lowered CO₂ emission;
4. lowered cost, especially if there is a glut of cheap scrap steel; and
5. in-house consumption of Fe-rich residues avoiding disposal fees.

Scrap steel charged to the blast furnace must be granular in nature and well sized to assure that it will pass through the charging system including the bell-less top. Fe-rich residues may be briquetted using a binder to increase their size so that the material is not blown out of the blast furnace. The principle alternatives to top-charged scrap steel are top-charged direct-reduced pellets or hot briquetted iron that have had ~95% of their oxygen removed by CO(g) and H₂(g) reduction in shaft furnaces.

The objectives of this chapter are to;

1. demonstrate how top-charged scrap steel is included in our automated calculation matrices, and
2. show the effect of top-charged scrap steel on coke requirement, CO₂ emissions, flame temperature, and top gas temperature.

For simplicity, we specify that the scrap is dry pure Fe. Chapter 44, Top Charged Direct Reduced Iron, examines a more complex material.

43.2 INCLUDING TOP-CHARGED SCRAP STEEL IN OUR CALCULATIONS

Readers have now realized that the sequence of our calculations is always bottom segment then top segment. That is not immediately possible with scrap steel because;

$$\begin{bmatrix} \text{mass top-charged} \\ \text{scrap steel} \end{bmatrix}$$

is specified in the top-segment matrix. Our calculations are made possible by means of an out-of-matrix precalculation, as follows.

43.3 NO OXIDATION OF SCRAP STEEL IN THE TOP SEGMENT

Conditions near the top of the blast furnace are oxidizing with respect to Fe. It is cool in this region, so we can assume that descending pieces of scrap will be oxidized slowly or not at all ([Fig. 43.1](#)).

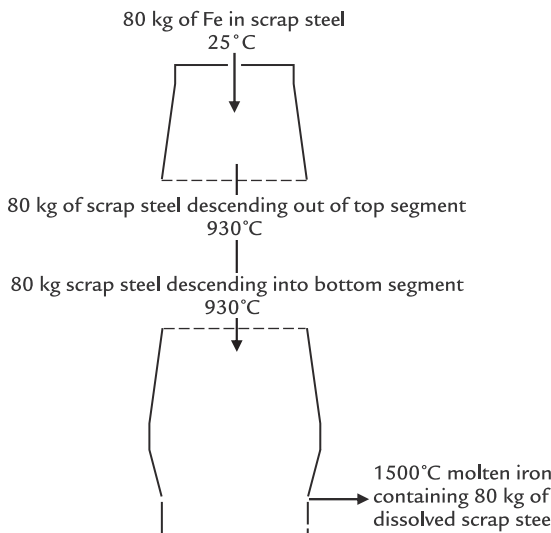


FIGURE 43.1 Sketch of 80 kg of scrap steel being charged, descending out of the top segment, descending into the bottom segment, and leaving the blast furnace dissolved in product molten iron. Its Fe is not oxidized during this journey, so each flow is 80 kg of Fe in scrap steel (per 1000 kg of Fe in product molten iron).

43.4 BOTTOM-SEGMENT SCRAP STEEL QUANTITY SPECIFICATION

We begin our bottom-segment calculations by specifying that with no oxidation in the top segment:

$$\begin{aligned} & \left[\begin{array}{l} \text{mass scrap steel descending} \\ \text{into bottom segment} \end{array} \right] \\ &= \left[\begin{array}{l} \text{mass scrap steel descending} \\ \text{out of top segment} \end{array} \right] \\ &= \left[\begin{array}{l} \text{mass top-charged} \\ \text{scrap steel} \end{array} \right] \end{aligned} \quad (43.1)$$

We now specify that 80 kg of scrap steel is being charged to the top of the furnace as described by the following equation;

$$\left[\begin{array}{l} \text{mass top-charged} \\ \text{scrap steel} \end{array} \right] = 80 \text{ kg}/1000 \text{ kg of Fe} \text{ in product molten iron} \quad (43.2)$$

and combine Eqs. (43.1) and (43.2) to give;

$$\left[\begin{array}{l} \text{mass scrap steel descending} \\ \text{into bottom segment} \end{array} \right] = 80 \quad (43.3)$$

This allows us to begin our calculations in the bottom segment. For matrix purposes, the equation is;

$$80 = \left[\begin{array}{l} \text{mass scrap steel descending} \\ \text{into bottom segment} \end{array} \right] * 1$$

where 80 is typed into Cell C33 of **Table 43.1**, and 1 is typed into Cell AH33 of **Table 43.1**.

43.5 SCRAP STEEL COMPOSITION AND BOTTOM-SEGMENT Fe MASS BALANCE

In this chapter, we specify that our scrap steel is pure Fe. This is expressed by the following equation;

$$\left[\begin{array}{l} \text{mass Fe in} \\ \text{scrap steel} \end{array} \right] = \left[\begin{array}{l} \text{mass scrap} \\ \text{steel} \end{array} \right] * \frac{100 \text{ mass\% Fe in scrap steel}}{100\%} \quad (43.4)$$

which leads to the bottom-segment Fe mass balance;

$$\begin{aligned} & \left[\begin{array}{l} \text{mass Fe}_{0.947}\text{O descending} \\ \text{into bottom segment} \end{array} \right] * \frac{76.8 \text{ mass\% Fe in Fe}_{0.947}\text{O}}{100\%} \\ &+ \left[\begin{array}{l} \text{mass scrap steel descending} \\ \text{into bottom segment} \end{array} \right] * \frac{100 \text{ mass\% Fe in scrap steel}}{100\%} \\ &= \left[\begin{array}{l} \text{mass Fe out} \\ \text{in molten iron} \end{array} \right] * 1 \end{aligned}$$

or

$$\begin{aligned} & \left[\begin{array}{l} \text{mass Fe}_{0.947}\text{O descending} \\ \text{into bottom segment} \end{array} \right] * 0.768 \\ &+ \left[\begin{array}{l} \text{mass scrap steel descending} \\ \text{into bottom segment} \end{array} \right] * 1 \\ &= \left[\begin{array}{l} \text{mass Fe out} \\ \text{in molten iron} \end{array} \right] * 1 \end{aligned}$$

TABLE 43.1 Bottom-Segment Matrix With Top-Charged Scrap Steel

	X	Y	Z	AA	AB	AC	AD	AE	AF	AG	AH
1											
2	mass MgO out in molten slag	mass Si out in molten iron	mass Mn out in molten iron	mass descending MnO	mass MnO out in molten slag	mass tuyere-injected coal	mass O ₂ in tuyere-injected pure oxygen	mass through-tuyere input H ₂ O(g)	mass tuyere-injected natural gas	mass additional tuyere injectant	mass scrap steel descending into bottom segment
3	0	0	0	0	0	0	0	0	0	0	0
4	0	0	0	0	0	0	0	0	0	0	0
5	0	0	0	0	0	0	0	0	0	0	0
6	0	0	0	0	0	0	0	0	0	0	-1
7	0	-1.14	-0.291	0	0	-0.046	-1	-0.888	-0.01	0	0
8	0	0	0	0	0	-0.81	0	0	-0.734	0	0
9	0	2.14	0	0	0	-0.056	0	0	0	0	0
10	0	0	0	0	0	-0.009	0	0	-0.017	0	0
11	0	0	0	0	0	0	0	0	0	0	0
12	0	0	0	0	0	0	0	0	0	0	0
13	0	0	0	0	0	0	0	0	0	0	0
14	0	0	0	0	0	0	0	0	0	0	0
15	0	0	0	0	0	0	0	0	0	0	0
16	0	0	0	0	0	-0.024	0	0	0	0	0
17	0	0	0	0	0	0	0	0	0	0	0
18	0	0	0	0	0	0	0	0	0	0	0
19	-1	0	0	0	0	0	0	0	0	0	0
20	1	0	0	0	0	0	0	0	0	0	0
21	-11.14	-2.15	1.27	4.77	-3.530	1.2	-1.239	10.81	4.52	0	-0.6164
22	0	-1	0	0	0	0	0	0	0	0	0
23	0	0	-1	0	0	0	0	0	0	0	0
24	0	0	1	-0.774	0.774	0	0	0	0	0	0
25	0	0	0	-0.1	1	0	0	0	0	0	0
26	0	0	0	0	0	-0.056	0	-0.112	-0.240	0	0
27	0	0	0	0	0	0	0	0	0	0	0
28	0	0	0	0	0	1	0	0	0	0	0
29	0	0	0	0	0	0	1	0	0	0	0
30	0	0	0	0	0	0	0	-1	0	0	0
31	0	0	0	0	0	0	0	0	1	0	0
32	0	0	0	0	0	0	0	0	0	1	0
33	0	0	0	0	0	0	0	0	0	0	1

The mass scrap descending into the bottom segment variable (Column AH) and quantity equation (Row 33) are notable. The amended Fe mass balance and enthalpy equations are also notable. For clarity, the matrix is presented here in three pieces. The tuyere injectants are 220 kg of pulverized coal (Cell C28), 92 kg of O₂ in pure oxygen (Cell C29), and 0 kg of natural gas (Cell C31).

or subtracting $\left\{ \begin{array}{l} \left[\text{mass Fe}_{0.947}\text{O descending} \right] * 0.768 \\ \text{into bottom segment} \end{array} \right\}$ from both sides;

$$0 = - \left[\begin{array}{l} \text{mass Fe}_{0.947}\text{O descending} \\ \text{into bottom segment} \end{array} \right] * 0.768$$

$$- \left[\begin{array}{l} \text{mass scrap steel descending} \\ \text{into bottom segment} \end{array} \right] * 1 \quad (43.5)$$

$$+ \left[\begin{array}{l} \text{mass Fe out} \\ \text{in molten iron} \end{array} \right] * 1$$

as shown in Row 6 of matrix **Table 43.1.**

43.6 AMENDED BOTTOM-SEGMENT ENTHALPY BALANCE

The descending scrap steel brings enthalpy into the bottom segment. The bottom-segment enthalpy equation must include an additional right-side term;

$$- \left[\begin{array}{l} \text{mass scrap steel descending} \\ \text{into bottom segment} \end{array} \right] * \frac{H_{930^\circ\text{C}}}{\text{scrap steel MW}_{\text{scrap steel}}}$$

which, in the case of pure Fe scrap, is;

$$- \left[\begin{array}{l} \text{mass scrap steel descending} \\ \text{into bottom segment} \end{array} \right] * \frac{H_{930^\circ\text{C}}}{\text{Fe(s) MW}_\text{Fe}}$$

where $\frac{H_{930^\circ\text{C}}}{\text{Fe(s) MW}_\text{Fe}} = 0.6164 \text{ MJ/kg of Fe}$ (Table J.1).

Together, these give the new enthalpy equation term;

$$- \left[\begin{array}{l} \text{mass scrap steel descending} \\ \text{into bottom segment} \end{array} \right] * 0.6164$$

as shown in Cell AH21 of **Table 43.1.** The enthalpy equation is renumbered to Eq. 43.6 in Row 21 of **Table 43.1.**

43.7 NEARLY COMPLETED BOTTOM-SEGMENT MATRIX

Our bottom-segment matrix is now nearly complete.

We have;

1. added one new variable, $\left[\begin{array}{l} \text{mass scrap steel descending} \\ \text{into bottom segment} \end{array} \right];$
2. added one new quantity specification equation, $80 = \left[\begin{array}{l} \text{mass scrap steel descending} \\ \text{into bottom segment} \end{array} \right] * 1;$
3. specified that the scrap steel is 100% Fe; and
4. amended the bottom-segment Fe and enthalpy balance equations to include the new variable's Fe and enthalpy contents.

43.8 SiO₂ - A MINOR BUT IMPORTANT CHANGE

Chapter 32, Bottom-Segment Slag Calculations - Ore, Fluxes, and Slag, calculates the amount of SiO₂ in descending ore by following the equation:

$$\left[\begin{array}{l} \text{mass SiO}_2 \text{ in} \\ \text{descending ore} \end{array} \right] = 0.0753 * \left[\begin{array}{l} \text{mass Fe in product} \\ \text{molten iron} \end{array} \right]$$

This is not suitable for this chapter because some of the Fe in the molten iron product comes from scrap steel.

We now use Eq. (32.2) of Chapter 32, Bottom-Segment Slag Calculations—Ore, Fluxes, and Slag, which is:

$$\left[\begin{array}{l} \text{mass SiO}_2 \text{ in} \\ \text{descending ore} \end{array} \right] = 0.0753 * \left[\begin{array}{l} \text{mass Fe in} \\ \text{descending ore} \end{array} \right] \quad (32.2)$$

To make this useful, we make the bottom-segment substitution:

$$\begin{aligned} & \left[\begin{array}{l} \text{mass Fe in} \\ \text{descending ore} \end{array} \right] \\ &= \left[\begin{array}{l} \text{mass Fe}_{0.947}\text{O into} \\ \text{bottom segment} \end{array} \right] * \frac{76.8 \text{ mass\% Fe in Fe}_{0.947}\text{O}}{100\%} \\ &= \left[\begin{array}{l} \text{mass Fe}_{0.947}\text{O into} \\ \text{bottom segment} \end{array} \right] * 0.768 \end{aligned}$$

or

$$\left[\begin{array}{l} \text{mass Fe in} \\ \text{descending ore} \end{array} \right] = \left[\begin{array}{l} \text{mass Fe}_{0.947}\text{O into} \\ \text{bottom segment} \end{array} \right] * 0.768 \quad (43.7)$$

Combining Eqs. (32.2) and (43.7) gives;

$$\begin{aligned} & \left[\begin{array}{l} \text{mass SiO}_2 \text{ in} \\ \text{descending ore} \end{array} \right] \\ &= 0.0753 * \left[\begin{array}{l} \text{mass Fe}_{0.947}\text{O into} \\ \text{bottom segment} \end{array} \right] * 0.768 \\ &= \left[\begin{array}{l} \text{mass Fe}_{0.947}\text{O into} \\ \text{bottom segment} \end{array} \right] * 0.0578 \end{aligned}$$

or

$$\begin{aligned} 0 &= - \left[\begin{array}{l} \text{mass SiO}_2 \text{ in} \\ \text{descending ore} \end{array} \right] * 1 \\ &+ \left[\begin{array}{l} \text{mass Fe}_{0.947}\text{O into} \\ \text{bottom segment} \end{array} \right] * 0.0578 \quad (43.8) \end{aligned}$$

as shown in Row 4 of bottom-segment matrix **Table 43.1**. The matrix is now solved as shown in **Tables 43.1 and 43.2**.

43.9 RACEWAY MATRIX

Scrap steel does not enter the raceway so it does not;

1. need to be included in the raceway matrix or;
2. our raceway input enthalpy, output enthalpy, or flame temperature calculations.

This does not mean that the descending scrap steel does not affect the raceway flame temperature.

In fact, it does because it affects the steady-state amounts of O₂-in-blast, N₂-in-blast, and H₂O(g)-in-blast entering the raceway, per 1000 kg of Fe in product molten iron.

43.10 TOP-SEGMENT–BOTTOM-SEGMENT CONNECTION

Bottom-segment matrix **Table 43.1** contains the equation;

$$80 = \left[\begin{array}{l} \text{mass scrap steel descending} \\ \text{into bottom segment} \end{array} \right] * 1 \quad (43.9)$$

where 80 is typed in Cell C33 and 1 is typed in Cell AH33.

We now connect this specification to the top segment by the following equation;

$$80 = \left[\begin{array}{l} \text{mass top-charged} \\ \text{scrap steel} \end{array} \right] * 1 \quad (43.10)$$

by typing = C33 in Cell BC34 and 1 in Cell CI34 of top-segment matrix **Table 43.3**.

This is consistent with **Fig. 43.1** and Eq. (43.1).

43.11 TOP-SEGMENT MATRIX

Fig. 43.1 shows that the top segment has two flows of scrap steel, that is;

- top-charged flow, and
- descent out of the top-segment flow.

They have the same mass but different temperatures, hence different enthalpies. Both flows must be represented in the top-segment matrix - requiring two new variable columns and two additional equations. The variables are;

$$\left[\begin{array}{l} \text{mass top-charged} \\ \text{scrap steel} \end{array} \right] \text{ and } \left[\begin{array}{l} \text{mass scrap steel descending} \\ \text{out of top segment} \end{array} \right]$$

TABLE 43.2 Results From Solving Table 43.1 Matrix

	B	C kg per 1000 kg of Fe in product molten iron	D	E	F
44	Bottom segment calculated values				
45	mass $Fe_{0.947}O$ into bottom segment	1198			
46	mass C in descending coke	222	also = mass C in the furnace's coke charge, Eqn. (7.16)		
47	mass O_2 in blast air	256			
48	mass N_2 in blast air	845			
49	mass Fe out in molten iron	1000			
50	mass C out in molten iron	48			
51	mass CO out in ascending gas	570			
52	mass CO_2 out in ascending gas	395			
53	mass N_2 out in ascending gas	847			
54	mass H_2 out in ascending gas	8.6			
55	mass H_2O out in ascending gas	47			
56	mass SiO_2 in descending ore	69			
57	mass SiO_2 in descending coke	17			
58	mass SiO_2 out in molten slag	90			
59	mass Al_2O_3 in descending decomposed flux	10			
60	mass Al_2O_3 in descending coke	7			
61	mass Al_2O_3 out in molten slag	23			
62	mass CaO in descending decomposed flux	94			
63	mass CaO out in molten slag	94			
64	mass MgO in descending decomposed flux	23			
65	mass MgO out in molten slag	23			
66	mass Si out in molten iron	4.2			
67	mass Mn out in molten iron	5.3			
68	mass descending MnO	7.6			
69	mass MnO out in molten slag	0.8			
70	mass tuyere-injected coal	220			
71	mass O_2 in tuyere-injected pure oxygen	92			
72	mass through-tuyere input $H_2O(g)$	13			
73	mass tuyere-injected natural gas	0			
74	mass additional tuyere injectant	0			
75	Mass scrap steel descending into bottom segment	80			

They are used in our top-segment calculations.

TABLE 43.3 Top-Segment Matrix Including Top-Charged Scrap Steel and Scrap Steel Descending Out of the Top-Segment

	BA	BB	BC	BD	BE	BF	BG	BH	BI	BJ	BK	BL
1	TOP SEGMENT CALCULATIONS											
Equation	Description		Numerical term	mass Fe ₂ O ₃ in top-charged ore	mass SiO ₂ in top-charged ore	mass C in top-charged coke	mass Al ₂ O ₃ in top-charged coke	mass SiO ₂ in top-charged coke	mass top-charged Al ₂ O ₃ flux	mass top-charged CaO flux	mass top-charged MgO flux	mass top-charged MnO ₂ ore
2												
3	40.8	Mass CO ascending from bottom segment	570	0	0	0	0	0	0	0	0	0
4	40.9	Mass CO ₂ ascending from bottom segment	395	0	0	0	0	0	0	0	0	0
5	40.10	Mass H ₂ ascending from bottom segment	9	0	0	0	0	0	0	0	0	0
6	40.11	Mass H ₂ O ascending from bottom segment	47	0	0	0	0	0	0	0	0	0
7	40.12	Mass N ₂ ascending from bottom segment	847	0	0	0	0	0	0	0	0	0
8	40.13	Mass Al ₂ O ₃ -in-coke descending out of top segment	7	0	0	0	0	0	0	0	0	0
9	40.14	Mass Al ₂ O ₃ flux descending out of top segment	10	0	0	0	0	0	0	0	0	0
10	40.15	Mass C-in-coke descending out of top segment	222	0	0	0	0	0	0	0	0	0
11	40.16	Mass Fe _{0.94} O descending out of top segment	1198	0	0	0	0	0	0	0	0	0
12	40.17	Mass CaO flux descending out of top segment	94	0	0	0	0	0	0	0	0	0
13	40.18	Mass MgO flux descending out of top segment	23	0	0	0	0	0	0	0	0	0
14	40.19	Mass MnO descending out of top segment	7.6	0	0	0	0	0	0	0	0	0
15	40.20	Mass SiO ₂ -in-coke descending out of top segment	17	0	0	0	0	0	0	0	0	0
16	40.21	Mass SiO ₂ -in-ore descending out of top segment	69	0	0	0	0	0	0	0	0	0
17	40.22	Al ₂ O ₃ in coke mass	0	0	0	0	-1	0	0	0	0	0
18	40.23	Al ₂ O ₃ flux mass balance	0	0	0	0	0	0	-1	0	0	0
19	40.24	C mass balance	0	0	0	-1	0	0	0	0	0	0
20	40.25	CaO mass balance	0	0	0	0	0	0	0	-1	0	0
21	43.13	Fe mass balance	0	-0.699	0	0	0	0	0	0	0	0
22	40.27	H mass balance	0	0	0	0	0	0	0	0	0	0
23	40.28	MgO mass balance	0	0	0	0	0	0	0	0	-1	0
24	40.29	Mn mass balance	0	0	0	0	0	0	0	0	0	-0.632
25	40.30	N mass balance	0	0	0	0	0	0	0	0	0	0
26	40.31	O mass balance	0	-0.301	0	0	0	0	0	0	0	-0.368
27	40.32	SiO ₂ -in-coke mass balance	0	0	0	0	0	-1	0	0	0	0
28	40.33	SiO ₂ -in-ore mass balance	0	0	-1	0	0	0	0	0	0	0
29	40.34	No top-segment C oxidation equation	0	0	0	-1	0	0	0	0	0	0
30	25.13	H ₂ /CO reaction mass ratio equation	0	0	0	0	0	0	0	0	0	0
31	41.2	Mass H ₂ O(l) in top-charged ore, coke and fluxes	0	0.05	0.05	0.05	0.05	0.05	0.05	0.05	0.05	0.05
32	41.4	Mass H ₂ O(g) departing in top gas from top-charge H ₂ O(l)	0	0	0	0	0	0	0	0	0	0
33	43.11	Mass scrap steel descending out of top segment	0	0	0	0	0	0	0	0	0	0
34	43.10	Mass top-charged scrap steel	=C33	80	0	0	0	0	0	0	0	0
35												

(Continued)

TABLE 43.3 (Continued)

	BY	BZ	CA	CB	CC	CD	CE	CF	CG	CH	CI
1	mass H ₂ O ascending into top segment	mass N ₂ ascending into top segment	mass CO departing in top gas	mass CO ₂ from reactions departing in top gas	mass H ₂ departing in top gas	mass H ₂ O(g) from reactions departing in top gas	mass N ₂ departing in top gas	Mass H ₂ O(l) in top-charged ore, coke and fluxes	Mass H ₂ O(g) departing in top-gas from top-charge H ₂ O(l)	Mass scrap steel descending out of top segment	Mass top-charged scrap steel
2	0	0	0	0	0	0	0	0	0	0	0
3	0	0	0	0	0	0	0	0	0	0	0
4	0	0	0	0	0	0	0	0	0	0	0
5	0	0	0	0	0	0	0	0	0	0	0
6	1	0	0	0	0	0	0	0	0	0	0
7	0	1	0	0	0	0	0	0	0	0	0
8	0	0	0	0	0	0	0	0	0	0	0
9	0	0	0	0	0	0	0	0	0	0	0
10	0	0	0	0	0	0	0	0	0	0	0
11	0	0	0	0	0	0	0	0	0	0	0
12	0	0	0	0	0	0	0	0	0	0	0
13	0	0	0	0	0	0	0	0	0	0	0
14	0	0	0	0	0	0	0	0	0	0	0
15	0	0	0	0	0	0	0	0	0	0	0
16	0	0	0	0	0	0	0	0	0	0	0
17	0	0	0	0	0	0	0	0	0	0	0
18	0	0	0	0	0	0	0	0	0	0	0
19	0	0	0.429	0.273	0	0	0	0	0	0	0
20	0	0	0	0	0	0	0	0	0	0	0
21	0	0	0	0	0	0	0	0	1	-1	
22	0.112	0	0	0	1	0.112	0	0	0	0	
23	0	0	0	0	0	0	0	0	0	0	
24	0	0	0	0	0	0	0	0	0	0	
25	0	-1	0	0	0	0	1	0	0	0	
26	0.888	0	0.571	0.727	0	0.888	0	0	0	0	
27	0	0	0	0	0	0	0	0	0	0	
28	0	0	0	0	0	0	0	0	0	0	
29	0	0	0	0	0	0	0	0	0	0	
30	1	0	0	0	0.09	-1	0	-1	0	0	
31	0	0	0	0	0	0	0	0	0	0	
32	0	0	0	0	0	0	-1	1	0	0	
33	0	0	0	0	0	0	0	0	1	-1	
34	0	0	0	0	0	0	0	0	0	1	
35						=BC5/BC3*5.7					

43.12 TOP-SEGMENT EQUATION

We begin our top-segment calculations with the equation in Fig. 43.1;

$$\begin{aligned} & \left[\begin{array}{l} \text{mass scrap steel descending} \\ \text{into bottom segment} \end{array} \right] \\ & = \left[\begin{array}{l} \text{mass scrap steel descending} \\ \text{out of top segment} \end{array} \right] \\ & = \left[\begin{array}{l} \text{mass top-charged} \\ \text{scrap steel} \end{array} \right] \end{aligned} \quad (43.1)$$

from which we now obtain the equation;

$$\left[\begin{array}{l} \text{mass top-charged} \\ \text{scrap steel} \end{array} \right] = \left[\begin{array}{l} \text{mass scrap steel descending} \\ \text{out of top segment} \end{array} \right]$$

or

$$\begin{aligned} 0 &= - \left[\begin{array}{l} \text{mass top-charged} \\ \text{scrap steel} \end{array} \right] * 1 \\ &+ \left[\begin{array}{l} \text{mass scrap steel descending} \\ \text{out of top segment} \end{array} \right] * 1 \end{aligned} \quad (43.11)$$

as shown in Row 33 of Table 43.3.

43.13 AMENDED TOP-SEGMENT Fe MASS BALANCE

Including the $\left[\begin{array}{l} \text{mass top-charged} \\ \text{scrap steel} \end{array} \right]$ and $\left[\begin{array}{l} \text{mass scrap steel descending} \\ \text{out of top segment} \end{array} \right]$ variables, the top-

segment Fe mass balance is;

$$\begin{aligned} & \left[\begin{array}{l} \text{mass Fe}_2\text{O}_3 \text{ in} \\ \text{top-charged ore} \end{array} \right] * 0.699 \\ & + \left[\begin{array}{l} \text{mass top-charged} \\ \text{scrap steel} \end{array} \right] * 1 \\ & = \left[\begin{array}{l} \text{mass Fe}_{0.947}\text{O descending} \\ \text{out of top segment} \end{array} \right] * 0.768 \\ & + \left[\begin{array}{l} \text{mass scrap steel descending} \\ \text{out of top segment} \end{array} \right] * 1 \end{aligned} \quad (43.12)$$

where the values "1" are 100 mass% Fe in scrap steel/100% as prescribed in Section 43.5.

Eq. (43.12) is put in matrix form by subtracting $\left[\begin{array}{l} \text{mass Fe}_2\text{O}_3 \text{ in} \\ \text{top-charged ore} \end{array} \right] * 0.699 + \left[\begin{array}{l} \text{mass top-charged} \\ \text{scrap steel} \end{array} \right] * 1$ from both sides, giving;

$$\begin{aligned} 0 &= - \left[\begin{array}{l} \text{mass Fe}_2\text{O}_3 \text{ in} \\ \text{top-charged ore} \end{array} \right] * 0.699 \\ &- \left[\begin{array}{l} \text{mass top-charged} \\ \text{scrap steel} \end{array} \right] * 1 \\ &+ \left[\begin{array}{l} \text{mass Fe}_{0.947}\text{O descending} \\ \text{out of top segment} \end{array} \right] * 0.768 \\ &+ \left[\begin{array}{l} \text{mass scrap steel descending} \\ \text{out of top segment} \end{array} \right] * 1 \end{aligned} \quad (43.13)$$

as shown in Row 21 of Table 43.3.

43.14 SUMMARY OF TOP-SEGMENT CALCULATIONS WITH SCRAP STEEL ADDED

Our top-segment calculations;

- introduce two new variables;

$$\left[\begin{array}{l} \text{mass top-charged} \\ \text{scrap steel} \end{array} \right]$$

and

$$\left[\begin{array}{l} \text{mass scrap steel descending} \\ \text{out of top segment} \end{array} \right];$$

- introduce two new equations, namely, a;

$$\left[\begin{array}{l} \text{mass top-charged} \\ \text{scrap steel} \end{array} \right]$$

quantity specification equation, and;

$$\left[\begin{array}{l} \text{mass scrap steel descending} \\ \text{out of top segment} \end{array} \right] = \left[\begin{array}{l} \text{mass top-charged} \\ \text{scrap steel} \end{array} \right]$$

- specify that the scrap steel is 100% Fe; and

- amend the top-segment Fe mass balance equation to include the two new variables.

Table 43.3 shows the top-segment matrix with these variables and equations. Table 43.4 shows the solution to the top segment matrix.

TABLE 43.4 Calculated Values of Matrix 43.3

	BB	BC
	kg per 1000 kg of Fe in product molten iron	
49	Top segment calculated values	
50	mass Fe_2O_3 in top-charged ore	1316
51	mass SiO_2 in top-charged ore	69
52	mass C in top-charged coke	222
53	mass Al_2O_3 in top-charged coke	7.4
54	mass SiO_2 in top-charged coke	17
55	mass top-charged Al_2O_3 flux	10
56	mass top-charged CaO flux	94
57	mass top-charged MgO flux	23
58	mass top-charged MnO_2 ore	9.3
59	mass Al_2O_3 -in-coke descending out of top segment	7.4
60	mass Al_2O_3 flux descending out of top segment	10
61	mass C-in-coke descending out of top segment	222
62	mass CaO flux descending out of top segment	94
63	mass $\text{Fe}_{0.947}\text{O}$ descending out of top segment	1198
64	mass MgO flux descending out of top segment	23
65	mass MnO descending out of top segment	7.6
66	mass SiO_2 -in-coke descending out of top segment	17
67	mass SiO_2 -in-ore descending out of top segment	69
68	mass CO ascending into top segment	570
69	mass CO_2 ascending into top segment	395
70	mass H_2 ascending into top segment	8.6
71	mass H_2O ascending into top segment	47
72	mass N_2 ascending into top segment	847
73	mass CO departing in top gas	396
74	mass CO_2 from reactions departing in top gas	668
75	mass H_2 departing in top gas	5.9
76	mass $\text{H}_2\text{O(g)}$ from reactions departing in top gas	70
77	mass N_2 departing in top gas	847
78	Mass $\text{H}_2\text{O(l)}$ in top-charged ore, coke and fluxes	88
79	Mass $\text{H}_2\text{O(g)}$ departing in top gas from top-charge $\text{H}_2\text{O(l)}$	88
80	Mass scrap steel descending out of top segment	80
81	Mass top-charged scrap steel	80

43.15 CALCULATION OF TOP GAS TEMPERATURE

The next few sections describe how to calculate top gas temperature when scrap steel is being charged to the blast furnace. It requires four calculation steps;

1. top-segment input enthalpy,
2. top-segment output enthalpy,
3. top gas enthalpy, and
4. top gas temperature

as follows.

43.15.1 Top-Segment Input Enthalpy

The top charging of scrap steel to the blast furnace requires the addition of the term;

$$-\left[\frac{\text{mass top-charged}}{\text{scrap steel}} \right] * \frac{H_{25^\circ\text{C}}}{\text{MW}_{\text{scrap steel}}}$$

to the right side of top-segment input enthalpy.

In our case of pure Fe scrap, this term is;

$$-\left[\frac{\text{mass top-charged}}{\text{scrap steel}} \right] * \frac{H_{25^\circ\text{C}}}{\text{MW}_\text{Fe}}$$

Of course, $H_{25^\circ\text{C}}/\text{MW}_\text{Fe} = 0$ as Fe is in its most common state at 25°C so the final new term is;

$$-\left[\frac{\text{mass Fe in top-charged scrap steel}}{\text{scrap steel}} \right] * 0$$

as shown by Eq. (43.14) of Table 43.5.

Top-segment input enthalpy

$$\begin{aligned} &= +\text{BC50}^* - 5.163 + \text{BC51}^* - 15.16 + \text{BC52}^*0 + \text{BC53}^* \\ &- 16.43 + \text{BC54}^* - 15.16 + \text{BC55}^* - 16.43 + \text{BC56}^* \\ &- 11.32 + \text{BC57}^* - 14.92 + \text{BC58}^* - 5.98 + \text{BC68}^* \\ &- 2.926 + \text{BC69}^* - 7.926 + \text{BC70}^* - 13.35 + \text{BC71}^* \\ &- 11.49 + \text{BC72}^* - 1.008 + \text{BC78}^* - 15^*87 + \text{BC81}^*0 \end{aligned} \quad (43.14)$$

43.15.2 Top-Segment Output Enthalpy

Top-segment output enthalpy Eq. (40.3) is unchanged by top charging of scrap steel.

43.15.3 Top Gas Enthalpy

Calculation of top gas enthalpy with top charging of scrap steel requires subtraction of the term;

$$\left[\frac{\text{mass scrap steel descending}}{\text{out of top segment}} \right] * \frac{H_{930^\circ\text{C}}}{\text{MW}_{\text{scrap steel}}}$$

or for 100% Fe scrap;

$$\begin{aligned} &\left[\frac{\text{mass scrap steel descending}}{\text{out of top segment}} \right] * \frac{H_{930^\circ\text{C}}}{\text{MW}_\text{Fe}} \\ &= \left[\frac{\text{mass scrap steel descending}}{\text{out of top segment}} \right] \\ &\quad * 0.6164 \text{ MJ/kg of Fe} \end{aligned}$$

from the right side of top gas enthalpy Eq. (40.5), where $H_{930^\circ\text{C}}/\text{MW}_\text{Fe}$
 $\text{Fe(s)} = 0.6164 \text{ MJ/kg of Fe}$. This gives Eq. (43.15) of Table 43.5.

$$\begin{aligned} \text{Top gas enthalpy} &= +\text{BL113} - \text{BC59}^* - 15.41 - \text{BC60}^* \\ &- 15.41 - \text{BC61}^*1.359 - \text{BC62}^* - 10.5 - \text{BC63}^* \\ &- 3.152 - \text{BC64}^* - 13.84 - \text{BC65}^* - 4.77 - \text{BC66}^* \\ &- 14.13 - \text{BC67}^* - 14.13 - \text{BC80}^*0.6164 \end{aligned} \quad (43.15)$$

43.15.4 Top Gas Temperature

There is no Fe in the top gas, so the top gas temperature equation is unchanged by top charging of scrap steel.

43.16 CALCULATED RESULTS - COKE REQUIREMENT

Fig. 43.2 shows the effect of top-charged scrap on the amount of coke required to steadily produce 1500°C molten iron and slag. An amount of 100 kg of Fe scrap saves ~ 35 kg of coke.

TABLE 43.5 Equations and Calculations of (1) Top-Segment Input and Output Enthalpies, (2) Top Gas Enthalpy, and (3) Top Gas Temperature With Charging of Scrap Steel

	BA	BB	BC	BD	BE	BF	BG	BH	BI	BJ	BK	BL	BM	BN	BO
TOP SEGMENT INPUT AND OUTPUT ENTHALPY CALCULATIONS															
112	43.14														
112	43.14	Top segment input enthalpy =BC50*-5.69+BC51*15.16+BC52*0+BC53*-16.43+BC54*15.16+BC55*-16.43+BC56*-11.32+BC57*-14.92+BC58*-5.98+BC59*-2.926+BC60*-7.926+BC70*-13.35+BC71*-11.49+BC72*-1.008+BC78*-15.87+BC81*0 -										-15641	MJ per 1000 kg of Fe in product molten iron		
113	40.3	Top segment output enthalpy =BL112*80 =											-15721	MJ per 1000 kg of Fe in product molten iron	
TOP GAS ENTHALPY CALCULATION															
116	43.15	Top gas enthalpy =BL113-BC59*-15.41-BC60*-15.41-BC61*1.359-BC62*-10.5-BC63*-3.152-BC64*-13.84-BC65*-4.77-BC66*-14.13-BC67*-14.13-BC80*0.6164											.9457	MJ per 1000 kg of Fe in product molten iron	
TOP-GAS TEMPERATURE CALCULATION															
119		Top gas temperature =(BL116-BC73*-3.972-BC74*-8.966-BC75*-0.3616-(BC76+BC79)*-13.47-BC77*-0.02624)/(BC73*0.001049+BC74*0.0009314+BC75*0.01442+(BC76+BC79)*0.001902+BC77*0.001044)											114	*C	

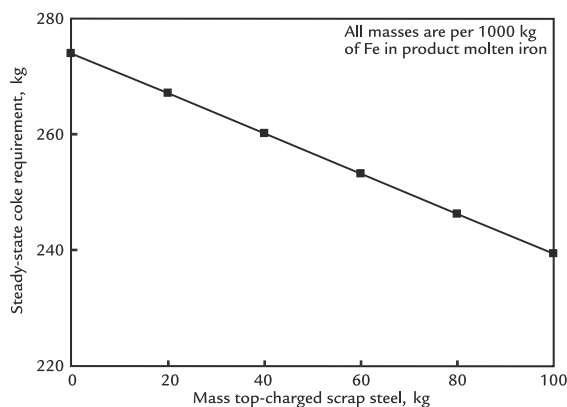


FIGURE 43.2 Effect of top-charged Fe scrap on the amount of coke needed to steadily produce molten iron and molten slag, 1500°C. One kilogram of Fe scrap saves 0.35 kg of 90% C, 3% Al₂O₃, and 7% SiO₂ coke. The line is straight.

This saving is due to the portion of Fe in the product molten iron that is produced directly from Fe scrap, that is;

- without using any carbon for iron oxide reduction.

The saving is smaller than might be expected. This is because the solid scrap must be heated and melted in the bottom segment (Fig. 43.1), that is, by combusting C-in-coke with O₂-in-blast.

43.17 CALCULATED RESULTS: TOP GAS CO₂ EMISSIONS

Fig. 43.3 shows the effect of top-charged scrap steel on the steady-state amount of CO₂ that is being emitted in a blast furnace's top gas. As expected from Fig. 43.2, scrap charging decreases C oxidation, hence CO₂(g) emissions.

CO₂(g) is a greenhouse gas contributing to global warming, so the trend of decreasing CO₂(g) emissions seen in Fig. 43.3 is valuable to the environment.

In those countries that levy a carbon tax on CO₂(g) emissions, the lower CO₂(g) emission will also have financial benefits. Such taxes are expected to increase over time.

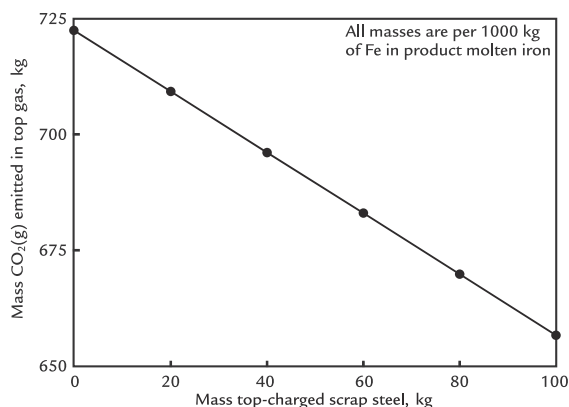


FIGURE 43.3 Effect of top-charged scrap steel on the steady-state blast furnace CO₂(g) emission from the blast furnace of Fig. 43.1. Scrap steel lowers CO₂(g) emission by ~0.66 kg/kg of top-charged scrap steel. This decrease is expected because steady-state coke requirement decreases with increasing mass scrap (Fig. 43.2). The line is straight.

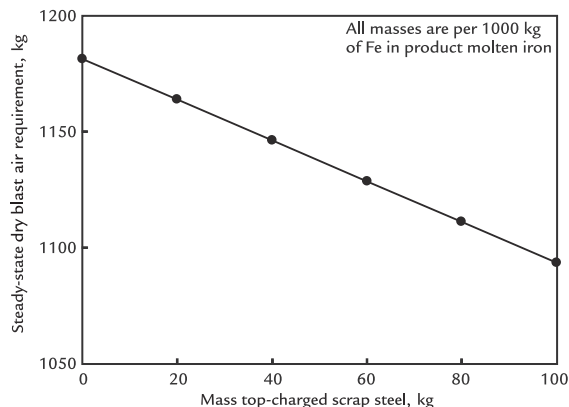


FIGURE 43.4 Effect of top-charged scrap steel on the amount of dry air required to steadily produce molten iron and molten slag, 1500°C. Blast air requirement decreases by ~1 kg/kg of top-charged scrap steel.

43.18 CALCULATED RESULTS: BLAST AIR REQUIREMENT

Fig. 43.4 shows the effect of top-charged scrap steel on the blast air requirement. It decreases the dry air requirement by ~1 kg of air/kg of scrap steel.

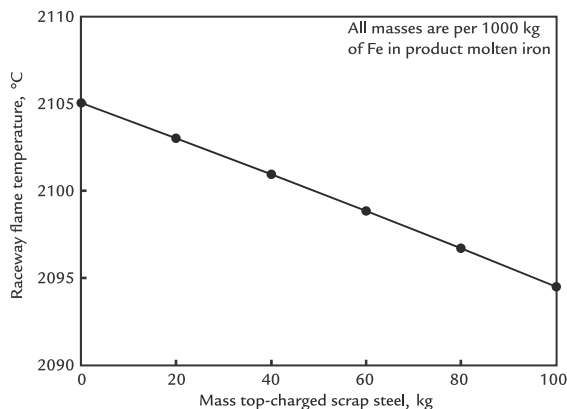


FIGURE 43.5 Effect of top-charged scrap steel on raceway flame temperature. Flame temperature drops about 12°C with 100 kg of top-charged scrap steel. This is a result of all our equations. The line is not quite straight.

This decrease is the result of all our equations. We may postulate that it is mainly due to less coke combustion in front of the tuyeres (Fig. 43.2).

43.19 CALCULATED RESULTS: RACEWAY FLAME TEMPERATURE

Fig. 43.5 shows the effect of top-charged scrap steel on tuyere raceway flame temperature. It lowers the flame temperature by about $12^{\circ}\text{C}/100 \text{ kg}$ of top-charged scrap steel.

Scrap steel does not enter the raceway, so it does not directly affect raceway flame temperature. We may speculate that it has the effect of decreasing coke combustion in front of the tuyeres, Fig. 43.2, thereby lowering flame temperature.

43.20 CALCULATED RESULTS - CaO FLUX REQUIREMENTS

Fig. 43.6 shows the effect of top-charged scrap steel on CaO flux requirement. The

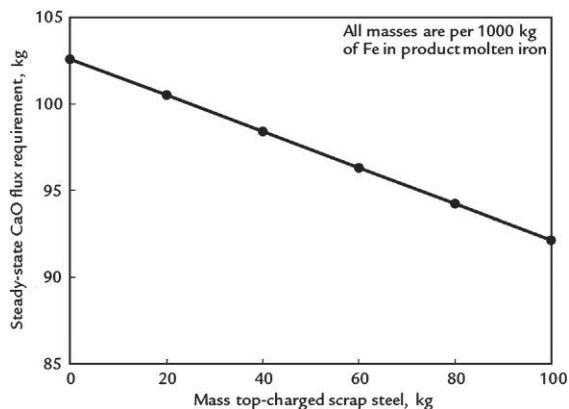


FIGURE 43.6 Effect of top-charged scrap steel on the amount of CaO flux that is required to produce 10 mass% Al_2O_3 , 41 mass% CaO, 10 mass% MgO, and 39 mass% SiO_2 molten slag, 1500°C , of Chapter 32, Bottom-Segment Slag Calculations—Ore, Fluxes, and Slag. The CaO requirement decreases with increasing scrap steel. This is because the scrap steel contains no SiO_2 while the ore contains 3–6 mass% SiO_2 – which needs fluxing with CaO. Al_2O_3 and MgO requirements correspondingly decrease.

requirement decreases with increasing mass top-charged scrap steel. This is a consequence of the scrap steel containing no SiO_2 , decreasing the need for CaO fluxing.

43.21 CALCULATED RESULTS - TOP GAS TEMPERATURE

Although there is no Fe in the blast furnace's departing top gas, the amounts of CO , CO_2 , H_2 , H_2O , and N_2 vary with the amount of scrap that is being charged to the furnace—thus changing the top gas temperature (Fig. 43.7). This is the consequence of all our equations. We may speculate that it is the result of less hot nitrogen (Fig. 43.4) rising into the top segment.

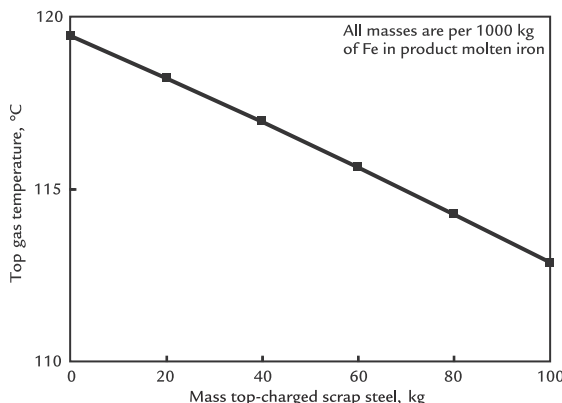


FIGURE 43.7 Effect of top-charged scrap steel on top gas temperature. The temperature falls about $7^{\circ}\text{C}/100\text{ kg}$ of scrap charge. The line is slightly curved.

43.22 SUMMARY

Scrap steel and other Fe-rich solids are often charged to the top of the blast furnace. The procedure;

1. saves coke,
2. increases molten iron production rate,
3. decreases greenhouse gas $\text{CO}_2(\text{g})$ emission, and
4. consumes Fe-rich materials that may otherwise be disposed of.

Calculations of this chapter explain and quantify these observations.

The calculations are different than our previous calculations because they rely on specifying that the top-charged scrap steel does not oxidize in the top segment of the furnace. This specification is consistent with our Chapter 2, Inside the Blast Furnace, specification that C-in-coke does not oxidize in the top segment of the furnace.

In this chapter, we show that top charging of scrap steel decreases both tuyere raceway flame temperature and top gas temperature. This is unusual because all our previous chapters have shown that if flame temperature is lowered by making a change to blast furnace operation, for example, coal injection—top gas temperature rises—and vice versa.

EXERCISE

All masses in these calculations are $\text{kg}/1000\text{ kg of Fe in product molten iron}$.

Throughout this chapter, the reference blast furnace is being injected with 220 kg of pulverized coal and 92 kg of pure oxygen. The 1200°C blast contains 15 g of $\text{H}_2\text{O}(\text{g})/\text{Nm}^3$ of dry air in blast and all the fluxes are oxides. These values are based on an industrial blast furnace. The top charge contains 5 mass% $\text{H}_2\text{O}(\ell)$, excluding the scrap, which is dry.

- 43.1. The blast furnace of Fig. 43.1 is top charging 80 kg of scrap (pure Fe) steel. However, its operators anticipate a shortage of scrap so they start lowering the scrap charge to 40 kg/1000 kg of Fe in product molten iron. They know from Fig. 43.6 that their Al_2O_3 , CaO , and MgO flux requirements will all increase (per 1000 kg of Fe in product molten iron) with this decreased scrap top charge, but not by how much.

For the operators, please calculate;

1. how much additional SiO_2 must be fluxed, and

2. how much additional Al_2O_3 , CaO , and MgO flux will be required when the scrap top charge is decreased from 80 kg of scrap steel to 40 kg of scrap steel.
- 43.2.** Luckily, more cheap scrap steel has become available, and the blast furnace operators of Exercise 43.1 now want to

increase scrap steel charging as much as possible. However, they do not want their top gas temperature to fall below 110°C. What is the upper limit of scrap steel charging that can be used without causing the top gas temperature to fall below this value?

CHAPTER

44

Top Charged Direct Reduced Iron

OUTLINE

44.1 Using Direct Reduced Iron in the Blast Furnace	410	44.10 Top-Segment Matrix	420
44.2 Calculation Description	411	44.11 Altered Top-Segment Mass Balances	420
44.3 No Reaction of DRI Pellets in the Top Segment	411	44.11.1 Fe Mass Balance	420
44.4 Bottom-Segment Specifications	411	44.11.2 C Mass Balance	420
44.5 Amended Bottom-Segment Fe Mass Balance	411	44.11.3 O Mass Balance	421
44.6 Other Bottom-Segment Mass Balances	415	44.11.4 Al_2O_3 Mass Balance	421
44.6.1 Bottom-Segment C Mass Balance	415	44.11.5 SiO_2 Mass Balance	421
44.6.2 Bottom-Segment O Mass Balance	415	44.12 Calculation of Top-Gas Temperature	421
44.6.3 Bottom-Segment Al_2O_3 Mass Balance	415	44.12.1 Top-Segment Input Enthalpy	421
44.6.4 Bottom-Segment SiO_2 Mass Balance	415	44.12.2 Top-Segment Output Enthalpy	421
44.7 Amended Bottom-Segment Enthalpy Balance	415	44.12.3 Top-Gas Enthalpy	421
44.8 Raceway Matrix	415	44.12.4 Top-Gas Temperature	422
44.9 Top-Segment–Bottom-Segment Connection	416	44.13 Calculated Results - Coke Requirement	424
		44.14 Calculated Results - Iron Ore Requirement	424
		44.15 $\text{CO}_2(\text{g})$ Emission as a Function of DRI Pellet Input	424
		44.16 Total Top-Gas Emission as a Function of DRI Pellet Input	424
		44.17 Mass $\text{N}_2(\text{g})$ in Top-Gas as a Function of DRI Pellet Input	424

44.18 Mass SiO₂ in Slag as a Function of DRI Pellet Input	424	44.22 Calculation of DRI Pellet Enthalpies, MJ per kg of DRI Pellets	427
44.19 Flame Temperature With Top-Charged DRI Pellets	426	44.23 Summary	427
44.20 Top-Gas Temperature With Top-Charged DRI Pellets	426	Exercise	428
44.21 Discussion	426	Reference	428

44.1 USING DIRECT REDUCED IRON IN THE BLAST FURNACE

Chapter 43, Top-Charged Scrap Steel, showed how to include top-charged scrap steel in our matrix calculations. This chapter shows how to include top-charged *mostly reduced* iron ore in our matrix calculations. Mostly reduced iron ore refers to pellets or briquettes that are made from iron ore pellets that have been reduced with $[CO(g) + H_2(g)]$; the $CO(g) + H_2(g)$ reductant is usually made from natural gas.] in a shaft furnace - until about 95% of the ore's oxygen has been removed. These reduced pellets/briquettes are usually charged to electric arc furnaces and converted into liquid steel, but they are also top-charged to iron blast furnaces.

Throughout this chapter, we refer to mostly reduced iron ore as direct reduced iron, *DRI*. DRI will be used interchangeably for the two principle products;

- DRI pellets, and
- Hot briquetted iron - made by pressing DRI pellets at elevated temperature.

In the blast furnace, the DRI has the same advantages as scrap steel:

1. accelerated molten iron production
2. lowered coke consumption

3. lowered CO₂(g) emission, and
4. lowered cost, especially where natural gas is inexpensive

The composition of the direct reduced pellets considered throughout the chapter is;

- 93 mass% Fe,
- 2 mass% C,
- 2 mass% O,
- 1 mass% Al₂O₃, and
- 2 mass% SiO₂

on a dry basis.

The DRI 25°C enthalpy is -0.80 MJ/kg. Its 930°C enthalpy is -0.148 MJ/kg. These values are calculated in [Section 44.22](#).

The objectives of this chapter are to;

1. demonstrate how top-charged DRI pellets are included in our automated calculation matrix spreadsheets, and
2. show the effect of top-charged DRI pellets on blast furnace;
 - a. coke requirement,
 - b. iron ore requirement,
 - c. flux requirements,
 - d. CO₂(g) emission,
 - e. total top-gas emission,
 - f. raceway flame temperature, and
 - g. top-gas temperature.

44.2 CALCULATION DESCRIPTION

Readers will remember that our calculations are almost always done in the order *bottom segment* then *top segment*. This is not possible in this chapter because our DRI pellet specification;

$$\left[\begin{array}{l} \text{mass top-charged} \\ \text{DRI pellets} \end{array} \right]$$

is a *top segment* variable.

We make it possible to include DRI by an out-of-matrix precalculation, much as in Chapter 43, Top-Charged Scrap Steel.

44.3 NO REACTION OF DRI PELLETS IN THE TOP SEGMENT

As with scrap steel top-charging described in Chapter 43, Top-Charged Scrap Steel, we specify that the 93 mass% Fe DRI pellets are not oxidized nor reduced during their descent through the top of the furnace and the chemical reserve zone. So, the DRI mass and composition entering the bottom segment are the same as its top-charge mass and composition. This allows us to specify that;

$$\begin{aligned} & \left[\begin{array}{l} \text{mass DRI pellets descending} \\ \text{into the bottom segment} \end{array} \right] \\ & = \left[\begin{array}{l} \text{mass top-charged} \\ \text{DRI pellets} \end{array} \right] = 80 \text{ kg} \end{aligned} \quad (44.1a)$$

where 80 kg is our specified charge amount of top-charged DRI pellets per 1000 kg of Fe in product molten iron.

Fig. 44.1 sketches this situation.

44.4 BOTTOM-SEGMENT SPECIFICATIONS

Our bottom-segment calculations are begun by specifying that;

$$\left[\begin{array}{l} \text{mass DRI pellets descending} \\ \text{into the bottom segment} \end{array} \right] = 80 \text{ kg} \quad (44.1b)$$

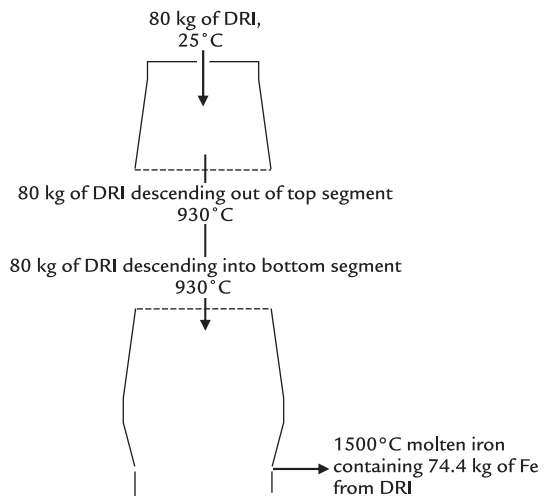


FIGURE 44.1 Sketch of top and bottom segments with DRI pellet flows in and between the segments. We specify that the DRI pellets aren't oxidized nor reduced in the top segment. The 74.4 kg of Fe from DRI pellets in the product molten iron is not 80 kg because the pellets contain only 93 mass% Fe. To be clear, of 1000 kg of Fe in the product molten iron, 74.4 kg comes from DRI pellets and 925.6 kg comes from ore.

or, in matrix form;

$$80 = \left[\begin{array}{l} \text{mass DRI pellets descending} \\ \text{into the bottom segment} \end{array} \right] * 1 \quad (44.2)$$

This equation replaces Eq. (43.9) in the bottom row of the bottom-segment matrix. For calculation purposes, its 80 is typed into Cell C33 of Table 44.1 and its 1 is typed into Cell AH33 of Table 44.1.

44.5 AMENDED BOTTOM-SEGMENT Fe MASS BALANCE

Bottom-segment Fe mass balance Eq. (43.5) of Chapter 43, Top-Charged Scrap Steel, becomes;

TABLE 44.1 Bottom-Segment Matrix With Top-Charging of DRI Pellets

	L	M	N	O	P	Q	R	S	T	U	V
1	mass N ₂ out in ascending gas	mass H ₂ out in ascending gas	mass H ₂ O out in ascending gas	mass SiO ₂ in descending ore	mass SiO ₂ in descending coke	mass SiO ₂ out in molten slag	mass Al ₂ O ₃ in descending flux	mass Al ₂ O ₃ in descending coke	mass Al ₂ O ₃ out in molten slag	mass CaO in descending flux	mass CaO out in molten slag
2											
3	0	0	0	0	0	0	0	0	0	0	0
4	0	0	0	-1	0	0	0	0	0	0	0
5	0	0	0	0	-1	0	0	0	0	0	0
6	0	0	0	0	0	0	0	0	0	0	0
7	0	0	0.888	0	0	0	0	0	0	0	0
8	0	0	0	0	0	0	0	0	0	0	0
9	0	0	0	-1	-1	1	0	0	0	0	0
10	1	0	0	0	0	0	0	0	0	0	0
11	0	0	0	0	0	0	0	0	0	0	0
12	0	0	0	0	0	0	0	0	0	0	0
13	0	0	0	0	0	0	0	0	0	0	0
14	0	0	0	0	0	0	0	-1	0	0	0
15	0	0	0	0	0	0.256	0	0	-1	0	0
16	0	0	0	0	0	0	-1	-1	1	0	0
17	0	0	0	0	0	1.05	0	0	0	0	-1
18	0	0	0	0	0	0	0	0	0	-1	1
19	0	0	0	0	0	0.256	0	0	0	0	0
20	0	0	0	0	0	0	0	0	0	0	0
21	1.008	13.35	-11.49	14.13	14.13	-13.28	15.41	15.41	-13.58	10.50	-8.495
22	0	0	0	0	0	0	0	0	0	0	0
23	0	0	0	0	0	0	0	0	0	0	0
24	0	0	0	0	0	0	0	0	0	0	0
25	0	0	0	0	0	0	0	0	0	0	0
26	0	1	0.112	0	0	0	0	0	0	0	0
27	0	5.44	-1	0	0	0	0	0	0	0	0
28	0	0	0	0	0	0	0	0	0	0	0
29	0	0	0	0	0	0	0	0	0	0	0
30	0	0	0	0	0	0	0	0	0	0	0
31	0	0	0	0	0	0	0	0	0	0	0
32	0	0	0	0	0	0	0	0	0	0	0
33	0	0	0	0	0	0	0	0	0	0	0

(Continued)

TABLE 44.1 (Continued)

	W	X	Y	Z	AA	AB	AC	AD	AE	AF	AG	AH
1	mass MgO in descending flux	mass MgO out in molten slag	mass Si out in molten iron	mass Mn out in molten iron	mass descending MnO	mass MnO out in molten slag	mass tuyere-injected coal	mass O ₂ in tuyere-injected pure oxygen	mass through-tuyere input H ₂ O(g)	mass tuyere-injected natural gas	mass additional tuyere injectant	mass DRI pellets descending into bottom segment
2												
3	0	0	0	0	0	0	0	0	0	0	0	0
4	0	0	0	0	0	0	0	0	0	0	0	0
5	0	0	0	0	0	0	0	0	0	0	0	0
6	0	0	0	0	0	0	0	0	0	0	0	-0.93
7	0	0	-1.14	-0.291	0	0	-0.046	-1	-0.888	-0.01	0	-0.02
8	0	0	0	0	0	0	-0.81	0	0	-0.734	0	-0.02
9	0	0	2.14	0	0	0	-0.056	0	0	0	0	-0.02
10	0	0	0	0	0	0	-0.009	0	0	-0.017	0	0
11	0	0	0	0	0	0	0	0	0	0	0	0
12	0	0	0	0	0	0	0	0	0	0	0	0
13	0	0	0	0	0	0	0	0	0	0	0	0
14	0	0	0	0	0	0	0	0	0	0	0	0
15	0	0	0	0	0	0	0	0	0	0	0	0
16	0	0	0	0	0	0	-0.024	0	0	0	0	-0.01
17	0	0	0	0	0	0	0	0	0	0	0	0
18	0	0	0	0	0	0	0	0	0	0	0	0
19	0	-1	0	0	0	0	0	0	0	0	0	0
20	-1	1	0	0	0	0	0	0	0	0	0	0
21	13.84	-11.14	-2.15	1.27	4.77	-3.530	1.2	-1.239	10.81	4.52	0	0.148
22	0	0	-1	0	0	0	0	0	0	0	0	0
23	0	0	0	-1	0	0	0	0	0	0	0	0
24	0	0	0	1	-0.774	0.774	0	0	0	0	0	0
25	0	0	0	0	-0.1	1	0	0	0	0	0	0
26	0	0	0	0	0	0	-0.056	0	-0.112	-0.240	0	0
27	0	0	0	0	0	0	0	0	0	0	0	0
28	0	0	0	0	0	0	1	0	0	0	0	0
29	0	0	0	0	0	0	0	1	0	0	0	0
30	0	0	0	0	0	0	0	0	-1	0	0	0
31	0	0	0	0	0	0	0	0	0	1	0	0
32	0	0	0	0	0	0	0	0	0	0	1	0
33	0	0	0	0	0	0	0	0	0	0	0	1

The pellet composition is described in Column AH. The tuyere injectants are 220 kg of pulverized coal (Cell C28), 92 kg of O₂ in pure oxygen (Cell C29), and 0 kg of natural gas (Cell C31).

$$0 = - \left[\begin{array}{l} \text{mass DRI pellets descending} \\ \text{into the bottom segment} \end{array} \right] * 0.93 \\ - \left[\begin{array}{l} \text{mass Fe}_{0.947}\text{O into} \\ \text{bottom segment} \end{array} \right] * 0.768 + \left[\begin{array}{l} \text{mass Fe out} \\ \text{in molten iron} \end{array} \right] * 1$$

where;

$0.93 = 93 \text{ mass\% Fe in DRI pellets}/100\%$ as shown in Row 6 of [Table 44.1](#), Cell AH6.

44.6 OTHER BOTTOM-SEGMENT MASS BALANCES

As well as Fe, DRI pellets also contain C, O, Al_2O_3 , and SiO_2 . Each of these substances' mass balances must include a $\left[\begin{array}{l} \text{mass DRI pellets descending} \\ \text{into the bottom segment} \end{array} \right]$ term.

44.6.1 Bottom-Segment C Mass Balance

C-in-DRI pellets is included in the bottom-segment C mass balance equation by adding the term;

$$-\left[\begin{array}{l} \text{mass DRI pellets descending} \\ \text{into the bottom segment} \end{array} \right] * \frac{2 \text{ mass\% C in DRI pellets}}{100\%}$$

or;

$$-\left[\begin{array}{l} \text{mass DRI pellets descending} \\ \text{into the bottom segment} \end{array} \right] * 0.02$$

to the bottom-segment C mass balance as shown in Row 8 of [Table 44.1](#), Cell AH8.

44.6.2 Bottom-Segment O Mass Balance

O-in-DRI pellets is included in the bottom-segment O mass balance equation by adding the term;

$$-\left[\begin{array}{l} \text{mass DRI pellets descending} \\ \text{into the bottom segment} \end{array} \right] * \frac{2 \text{ mass\% O in DRI pellets}}{100\%}$$

or;

$$-\left[\begin{array}{l} \text{mass DRI pellets descending} \\ \text{into the bottom segment} \end{array} \right] * 0.02$$

to the bottom-segment O mass balance equation as shown in Row 7 of [Table 44.1](#), Cell AH7.

44.6.3 Bottom-Segment Al_2O_3 Mass Balance

Al_2O_3 -in-DRI pellets is included in the bottom-segment Al_2O_3 mass balance equation by adding the term;

$$-\left[\begin{array}{l} \text{mass DRI pellets descending} \\ \text{into the bottom segment} \end{array} \right] * \frac{1 \text{ mass\% } \text{Al}_2\text{O}_3 \text{ in DRI pellets}}{100\%}$$

or;

$$-\left[\begin{array}{l} \text{mass DRI pellets descending} \\ \text{into the bottom segment} \end{array} \right] * 0.01$$

to the bottom-segment Al_2O_3 mass balance as shown in Row 16 of [Table 44.1](#), Cell AH16.

44.6.4 Bottom-Segment SiO_2 Mass Balance

SiO_2 -in-DRI pellets is included in the bottom-segment SiO_2 mass balance equation by adding the term;

$$-\left[\begin{array}{l} \text{mass DRI pellets descending} \\ \text{into the bottom segment} \end{array} \right] * \frac{2 \text{ mass\% } \text{SiO}_2 \text{ in DRI pellets}}{100\%}$$

or;

$$-\left[\begin{array}{l} \text{mass DRI pellets descending} \\ \text{into the bottom segment} \end{array} \right] * 0.02$$

to the bottom-segment SiO_2 mass balance as shown in Row 9 of [Table 44.1](#), Cell AH9.

44.7 AMENDED BOTTOM-SEGMENT ENTHALPY BALANCE

Section 43.6 indicates that the bottom-segment enthalpy equation with top-charged steel scrap (100% Fe) included the term:

$$-\left[\begin{array}{l} \text{mass Fe in scrap descending} \\ \text{into bottom segment} \end{array} \right] * 0.6164$$

With DRI pellets, this becomes;

$$-\left[\begin{array}{l} \text{mass DRI pellets descending} \\ \text{into the bottom segment} \end{array} \right] * -0.148$$

where -0.148 is the 930°C enthalpy of the pellets, MJ per kg of pellets, [Section 44.22](#).

This is shown in Row 21 of [Table 44.1](#), Cell AH21.

[Table 44.1](#) shows our bottom-segment matrix. [Table 44.2](#) shows its calculated results.

44.8 RACEWAY MATRIX

As with top-charged steel scrap, DRI pellets don't enter the raceway so they don't affect our raceway matrix equations, enthalpy equations, or flame temperature equation.

TABLE 44.2 Bottom-Segment Calculated Results of [Table 44.1](#)

	B	C	D	E	F
44	Bottom segment calculated values	kg per 1000 kg of Fe in product iron			
45	mass $\text{Fe}_{0.947}$ O into bottom segment	1205			
46	mass C in descending coke	224	also = mass C in the furnace's coke charge, Eqn. (7.16)		
47	mass O_2 in blast air	259			
48	mass N_2 in blast air	855			
49	mass Fe out in molten iron	1000			
50	mass C out in molten iron	48			
51	mass CO out in ascending gas	575			
52	mass CO_2 out in ascending gas	399			
53	mass N_2 out in ascending gas	857			
54	mass H_2 out in ascending gas	8.6			
55	mass H_2O out in ascending gas	47			
56	mass SiO_2 in descending ore	70			
57	mass SiO_2 in descending coke	17			
58	mass SiO_2 out in molten slag	92			
59	mass Al_2O_3 in descending decomposed flux	10			
60	mass Al_2O_3 in descending coke	7.4			
61	mass Al_2O_3 out in molten slag	24			
62	mass CaO in descending decomposed flux	97			
63	mass CaO out in molten slag	97			
64	mass MgO in descending decomposed flux	24			
65	mass MgO out in molten slag	24			
66	mass Si out in molten iron	4.2			
67	mass Mn out in molten iron	5.3			
68	mass descending MnO	7.6			
69	mass MnO out in molten slag	0.8			
70	mass tuyere-injected coal	220			
71	mass O_2 in tuyere-injected pure oxygen	92			
72	mass through-tuyere input $\text{H}_2\text{O(g)}$	13			
73	mass tuyere-injected natural gas	0			
74	mass additional tuyere injectant	0			
75	Mass DRI pellets descending into bottom segment	80			

The furnace inputs are 80 kg of dry DRI pellets, 220 kg of tuyere injected coal, 92 kg of tuyere injected oxygen, and 15 g $\text{H}_2\text{O(g)}/\text{Nm}^3$ of dry blast air.

44.9 TOP-SEGMENT–BOTTOM-SEGMENT CONNECTION

Bottom-segment matrix [Table 44.1](#) contains the following equation;

$$80 = \left[\begin{array}{l} \text{mass DRI pellets descending} \\ \text{into the bottom segment} \end{array} \right] * 1 \quad (44.2)$$

where 80 is typed in Cell C33 and 1 is typed in Cell AH33.

We now connect this specification to the top segment by;

$$80 = \left[\begin{array}{l} \text{mass top-charged} \\ \text{DRI pellets} \end{array} \right] * 1 \quad (44.3)$$

by typing = C33 in Cell BC34 and 1 in Cell CI34 of top-segment matrix [Table 44.3](#).

This is consistent with [Fig. 44.1](#) and Eqs. [\(44.1a\)](#) and [\(44.1b\)](#).

TABLE 44.3 Top-Segment Matrix With Top-Charging of DRI Pellets

	BB	BB	BC	BD	BE	BF	BG	BH	BI	BJ	BK	BL
1	TOP SEGMENT CALCULATIONS											
Equation	Description	Numerical term	mass Fe ₂ O ₃ in top-charged ore	mass SiO ₂ in top-charged ore	mass C in top-charged coke	mass Al ₂ O ₃ in top-charged coke	mass SiO ₂ in top-charged coke	mass top-charged Al ₂ O ₃ flux	mass top-charged CaO flux	mass top-charged MgO flux	mass top charged MnO ₂ ore	
2												
3	40.8 Mass CO ascending from bottom segment	575	0	0	0	0	0	0	0	0	0	0
4	40.9 Mass CO ₂ ascending from bottom segment	399	0	0	0	0	0	0	0	0	0	0
5	40.10 Mass H ₂ ascending from bottom segment	9	0	0	0	0	0	0	0	0	0	0
6	40.11 Mass H ₂ O ascending from bottom segment	47	0	0	0	0	0	0	0	0	0	0
7	40.12 Mass N ₂ ascending from bottom segment	857	0	0	0	0	0	0	0	0	0	0
8	40.13 Mass Al ₂ O ₃ -in-coke descending out of top segment	7	0	0	0	0	0	0	0	0	0	0
9	40.14 Mass Al ₂ O ₃ flux descending out of top segment	10	0	0	0	0	0	0	0	0	0	0
10	40.15 Mass C-in-coke descending out of top segment	224	0	0	0	0	0	0	0	0	0	0
11	40.16 Mass Fe _{0.94} O descending out of top segment	1205	0	0	0	0	0	0	0	0	0	0
12	40.17 Mass CaO flux descending out of top segment	97	0	0	0	0	0	0	0	0	0	0
13	40.18 Mass MgO flux descending out of top segment	24	0	0	0	0	0	0	0	0	0	0
14	40.19 Mass MnO descending out of top segment	7.6	0	0	0	0	0	0	0	0	0	0
15	40.20 Mass SiO ₂ -in-coke descending out of top segment	17	0	0	0	0	0	0	0	0	0	0
16	40.21 Mass SiO ₂ -in-ore descending out of top segment	70	0	0	0	0	0	0	0	0	0	0
17	40.22 Al ₂ O ₃ -in-coke mass	0	0	0	0	-1	0	0	0	0	0	0
18	Al ₂ O ₃ mass balance	0	0	0	0	0	0	0	-1	0	0	0
19	C mass balance	0	0	0	-1	0	0	0	0	0	0	0
20	CaO mass balance	0	0	0	0	0	0	0	0	-1	0	0
21	40.26 Fe mass balance	0	-0.699	0	0	0	0	0	0	0	0	0
22	40.27 H mass balance	0	0	0	0	0	0	0	0	0	0	0
23	40.28 MgO mass balance	0	0	0	0	0	0	0	0	0	-1	0
24	40.29 Mn mass balance	0	0	0	0	0	0	0	0	0	0	-0.632
25	40.30 N mass balance	0	0	0	0	0	0	0	0	0	0	0
26	O mass balance	0	-0.301	0	0	0	0	0	0	0	0	-0.368
27	SiO ₂ -in-coke mass balance	0	0	0	0	0	0	-1	0	0	0	0
28	SiO ₂ mass balance	0	0	-1	0	0	0	0	0	0	0	0
29	40.34 No top segment C oxidation equation	0	0	0	-1	0	0	0	0	0	0	0
30	25.13 H ₂ /CO reaction mass ratio equation	0	0	0	0	0	0	0	0	0	0	0
31	41.2 Mass H ₂ O(l) in top-charged ore, coke and fluxes	0	0.05	0.05	0.05	0.05	0.05	0.05	0.05	0.05	0.05	0.05
32	41.4 Mass H ₂ O(g) departing in top gas from top-charge H ₂ O(l)	0	0	0	0	0	0	0	0	0	0	0
33	44.5 Mass DRI pellets descending out of top segment	0	0	0	0	0	0	0	0	0	0	0
34	44.4 Mass top-charged DRI pellets	80	0	0	0	0	0	0	0	0	0	0
35			=C33									

(Continued)

TABLE 44.3 (Continued)

	BY	BZ	CA	CB	CC	CD	CE	CF	CG	CH	CI
1	mass H ₂ O(g) ascending into top segment	mass N ₂ ascending into top segment	mass CO departing in top gas	mass CO ₂ departing in top gas	mass H ₂ departing in top gas	mass H ₂ O(g) from reactions departing in top gas	mass N ₂ departing in top gas	Mass H ₂ O(l) in top- charged ore, coke and fluxes	mass H ₂ O(g) departing in top gas from top-charged H ₂ O(l)	mass DRI pellets descending out of top segment	mass top- charged DRI pellets
2											
3	0	0	0	0	0	0	0	0	0	0	0
4	0	0	0	0	0	0	0	0	0	0	0
5	0	0	0	0	0	0	0	0	0	0	0
6	1	0	0	0	0	0	0	0	0	0	0
7	0	1	0	0	0	0	0	0	0	0	0
8	0	0	0	0	0	0	0	0	0	0	0
9	0	0	0	0	0	0	0	0	0	0	0
10	0	0	0	0	0	0	0	0	0	0	0
11	0	0	0	0	0	0	0	0	0	0	0
12	0	0	0	0	0	0	0	0	0	0	0
13	0	0	0	0	0	0	0	0	0	0	0
14	0	0	0	0	0	0	0	0	0	0	0
15	0	0	0	0	0	0	0	0	0	0	0
16	0	0	0	0	0	0	0	0	0	0	0
17	0	0	0	0	0	0	0	0	0	0	0
18	0	0	0	0	0	0	0	0	0	0.01	-0.01
19	0	0	0.429	0.273	0	0	0	0	0	0.02	-0.02
20	0	0	0	0	0	0	0	0	0	0	0
21	0	0	0	0	0	0	0	0	0	0.93	-0.93
22	-0.112	0	0	0	1	0.112	0	0	0	0	0
23	0	0	0	0	0	0	0	0	0	0	0
24	0	0	0	0	0	0	0	0	0	0	0
25	0	-1	0	0	0	0	1	0	0	0	0
26	-0.888	0	0.571	0.727	0	0.888	0	0	0	0.02	-0.02
27	0	0	0	0	0	0	0	0	0	0	0
28	0	0	0	0	0	0	0	0	0	0.02	-0.02
29	0	0	0	0	0	0	0	0	0	0	0
30	1	0	0	0.08	0	-1	0	0	0	0	0
31	0	0	0	0	0	0	0	-1	0	0	0
32	0	0	0	0	0	0	0	-1	1	0	0
33	0	0	0	0	0	0	0	0	0	1	-1
34	0	0	0	0	0	0	0	0	0	0	1
35					=BC5/BC3*5.7						

The DRI pellet composition is given in Columns CH and CI.

44.10 TOP-SEGMENT MATRIX

Fig. 44.1 shows that the top segment has two flows of DRI pellets, that is;

- top-charge flow, and
- descent out of top-segment flow.

They have the same mass and composition - but different temperatures, hence different enthalpies. As with scrap steel top charging, both must be represented in our top-segment calculations. This requires two matrix columns and two equation rows.

In this case, the two columns are;

$$\begin{bmatrix} \text{mass top-charged} \\ \text{DRI pellets} \end{bmatrix}$$

and;

$$\begin{bmatrix} \text{mass DRI pellets descending} \\ \text{out of top segment} \end{bmatrix}$$

The two equations are;

$$C33 = \begin{bmatrix} \text{mass top-charged} \\ \text{DRI pellets} \end{bmatrix} * 1 \quad (44.4)$$

and;

$$0 = - \begin{bmatrix} \text{mass top-charged} \\ \text{DRI pellets} \end{bmatrix} * 1 + \begin{bmatrix} \text{mass DRI pellets descending} \\ \text{out of top segment} \end{bmatrix} * 1 \quad (44.5)$$

because the DRI pellets are not oxidized nor reduced in the top segment.

44.11 ALTERED TOP-SEGMENT MASS BALANCES

44.11.1 Fe Mass Balance

Including the $\begin{bmatrix} \text{mass top-charged} \\ \text{DRI pellets} \end{bmatrix}$ and $\begin{bmatrix} \text{mass DRI pellets descending} \\ \text{out of top segment} \end{bmatrix}$ variables, the top-
segment Fe mass balance is;

$$\begin{aligned} & \left[\begin{bmatrix} \text{mass Fe}_2\text{O}_3 \text{ in} \\ \text{top-charged ore} \end{bmatrix} * 0.699 + \begin{bmatrix} \text{mass top-charged} \\ \text{DRI pellets} \end{bmatrix} * 0.93 \right] \\ &= \left[\begin{bmatrix} \text{mass Fe}_{0.947}\text{O} \text{ descending} \\ \text{out of top segment} \end{bmatrix} * 0.768 \right. \\ &\quad \left. + \begin{bmatrix} \text{mass DRI pellets descending} \\ \text{out of top segment} \end{bmatrix} * 0.93 \right] \end{aligned} \quad (44.6)$$

where the 0.93 values are 93 mass% Fe in DRI pellet/100% as described at the beginning of the chapter.

Eq. (44.6) is put in matrix form by subtracting; $\left\{ \begin{bmatrix} \text{mass Fe}_2\text{O}_3 \text{ in} \\ \text{top-charged ore} \end{bmatrix} * 0.699 + \begin{bmatrix} \text{mass top-charged} \\ \text{DRI pellets} \end{bmatrix} * 0.93 \right\}$ from both sides, giving;

$$\begin{aligned} 0 &= - \begin{bmatrix} \text{mass Fe}_2\text{O}_3 \text{ in} \\ \text{top-charged ore} \end{bmatrix} * 0.699 \begin{bmatrix} \text{mass top-charged} \\ \text{DRI pellets} \end{bmatrix} * 0.93 \\ &\quad + \begin{bmatrix} \text{mass Fe}_{0.947}\text{O} \text{ descending} \\ \text{out of top segment} \end{bmatrix} * 0.768 \\ &\quad + \begin{bmatrix} \text{mass DRI pellets descending} \\ \text{out of top segment} \end{bmatrix} * 0.93 \end{aligned} \quad (44.7)$$

as shown in top-segment Row 21 of Table 44.3.

44.11.2 C Mass Balance

With top-charged DRI pellets, the top-segment C balance requires two additional terms;

$$\begin{aligned} & - \left[\begin{bmatrix} \text{mass top-charged} \\ \text{DRI pellets} \end{bmatrix} * \frac{2 \text{ mass\% C in DRI pellets}}{100\%} \right] \\ &= - \left[\begin{bmatrix} \text{mass top-charged} \\ \text{DRI pellets} \end{bmatrix} * 0.02 \right] \end{aligned}$$

and;

$$\begin{aligned} & + \left[\begin{bmatrix} \text{mass DRI pellets descending} \\ \text{out of top segment} \end{bmatrix} * \frac{2 \text{ mass\% C in DRI pellets}}{100\%} \right] \\ &= \left[\begin{bmatrix} \text{mass DRI pellets descending} \\ \text{out of top segment} \end{bmatrix} * 0.02 \right] \end{aligned}$$

as shown in top-segment Row 19 of Table 44.3.

44.11.3 O Mass Balance

Likewise, the top-segment O balance requires two additional terms;

$$\begin{aligned} & - \left[\frac{\text{mass top-charged}}{\text{DRI pellets}} \right] \\ & * \frac{2 \text{ mass\% O in DRI pellets}}{100\%} \\ & = - \left[\frac{\text{mass top-charged}}{\text{DRI pellets}} \right] * 0.02 \end{aligned}$$

and;

$$\begin{aligned} & + \left[\frac{\text{mass DRI pellets descending}}{\text{out of top segment}} \right] \\ & * \frac{2 \text{ mass\% O in DRI pellets}}{100\%} \\ & = \left[\frac{\text{mass DRI pellets descending}}{\text{out of top segment}} \right] * 0.02 \end{aligned}$$

as shown in top-segment Row 26.

44.11.4 Al₂O₃ Mass Balance

Also, the top-segment Al₂O₃ balance requires two additional terms;

$$\begin{aligned} & - \left[\frac{\text{mass top-charged}}{\text{DRI pellets}} \right] * \frac{1 \text{ mass\% Al}_2\text{O}_3 \text{ in DRI pellets}}{100\%} \\ & = - \left[\frac{\text{mass top-charged}}{\text{DRI pellets}} \right] * 0.01 \end{aligned}$$

and;

$$\begin{aligned} & + \left[\frac{\text{mass DRI pellets descending}}{\text{out of top segment}} \right] \\ & * \frac{1 \text{ mass\% Al}_2\text{O}_3 \text{ in DRI pellets}}{100\%} \\ & = \left[\frac{\text{mass DRI pellets descending}}{\text{out of top segment}} \right] * 0.01 \end{aligned}$$

as shown in top-segment Row 18.

44.11.5 SiO₂ Mass Balance

Also, the top-segment SiO₂ balance requires two additional terms;

$$\begin{aligned} & - \left[\frac{\text{mass top-charged}}{\text{DRI pellets}} \right] * \frac{2 \text{ mass\% SiO}_2 \text{ in DRI pellets}}{100\%} \\ & = - \left[\frac{\text{mass top-charged}}{\text{DRI pellets}} \right] * 0.02 \end{aligned}$$

and;

$$\begin{aligned} & + \left[\frac{\text{mass DRI pellets descending}}{\text{out of top segment}} \right] \\ & * \frac{2 \text{ mass\% SiO}_2 \text{ in DRI pellets}}{100\%} \\ & = \left[\frac{\text{mass DRI pellets descending}}{\text{out of top segment}} \right] * 0.02 \end{aligned}$$

as shown in top-segment Row 28.

These terms are all represented in the two right-most columns of the top-segment matrix ([Table 44.4](#)).

44.12 CALCULATION OF TOP-GAS TEMPERATURE

The next few sections describe how to calculate top-gas temperature when DRI pellets are being charged to the furnace. This requires four calculation steps;

1. top-segment input enthalpy,
2. top-segment output enthalpy,
3. top-gas enthalpy, and
4. top-gas temperature

as follows.

44.12.1 Top-Segment Input Enthalpy

The top charging of DRI pellets to the blast furnace requires addition of the term;

$$\left[\frac{\text{mass top-charged}}{\text{DRI pellets}} \right] * (-0.800)$$

to the right side of the top-segment input enthalpy equation where -0.800 is the 25°C enthalpy of the DRI pellets, MJ per kg of pellets, [Section 44.22](#). This is shown in Cell BB132 of [Table 44.5](#).

44.12.2 Top-Segment Output Enthalpy

Top-segment output enthalpy Eq. (40.3) is unchanged by DRI pellet charging.

44.12.3 Top-Gas Enthalpy

Calculation of top-gas enthalpy with DRI top-charging requires subtraction of the term;

TABLE 44.4 Top-Segment Matrix Calculated Results

	BB	BC
91	Top segment calculated values	kg per 1000 kg of Fe in product molten iron
92	mass Fe_2O_3 in top-charged ore	1324
93	mass SiO_2 in top-charged ore	70
94	mass C in top-charged coke	224
95	mass Al_2O_3 in top-charged coke	7.4
96	mass SiO_2 in top-charged coke	17
97	mass top-charged Al_2O_3 flux	10
98	mass top-charged CaO flux	97
99	mass top-charged MgO flux	24
100	mass top charged MnO_2 ore	9.3
101	mass Al_2O_3 -in-coke descending out of top segment	7.4
102	mass Al_2O_3 flux descending out of top segment	10
103	mass C-in-coke descending out of top segment	224
104	mass CaO flux descending out of top segment	97
105	mass $\text{Fe}_{0.947}\text{O}$ descending out of top segment	1205
106	mass MgO flux descending out of top segment	24
107	mass MnO descending out of top segment	7.6
108	mass SiO_2 -in-coke descending out of top segment	17
109	mass SiO_2 -in-ore descending out of top segment	70
110	mass CO ascending into top segment	575
111	mass CO_2 ascending into top segment	399
112	mass H_2 ascending into top segment	8.6
113	mass $\text{H}_2\text{O(g)}$ ascending into top segment	47
114	mass N_2 ascending into top segment	857
115	mass CO departing in top gas	401
116	mass CO_2 departing in top gas	674
117	mass H_2 departing in top gas	6.0
118	mass $\text{H}_2\text{O(g)}$ from reactions departing in top gas	70
119	mass N_2 departing in top gas	857
120	Mass $\text{H}_2\text{O(l)}$ in top-charged ore, coke and fluxes	89
121	mass $\text{H}_2\text{O(g)}$ departing in top gas from top-charged $\text{H}_2\text{O(l)}$	89
122	mass DRI pellets descending out of top segment	80
123	mass top-charged DRI pellets	80

The blast furnace inputs are 80 kg of dry DRI pellets, 220 kg of tuyere-injected coal, 92 kg of oxygen, and 15 g $\text{H}_2\text{O(g)}/\text{Nm}^3$ of dry blast air.

$$\left[\begin{array}{l} \text{mass DRI pellets descending} \\ \text{into the bottom segment} \end{array} \right] * (-0.148)$$

from the right side of the top gas enthalpy equation (cell BB136 of Table 44.5) where -0.148 is the 930°C enthalpy of DRI pellets, MJ per kg of pellets.

44.12.4 Top-Gas Temperature

Blast furnace top gas contains only gases - so top gas temperature is unchanged by top charging of DRI pellets.

TABLE 44.5 Top-Segment Input Enthalpy, Output Enthalpy, Top-Gas Enthalpy, and Top-Gas Temperature Equations

44.13 CALCULATED RESULTS - COKE REQUIREMENT

This section answers the question;

how much coke (90 mass% C) is required to steadily produce molten iron and molten slag

with top-charged DRI pellets. This is answered by Fig. 44.2.

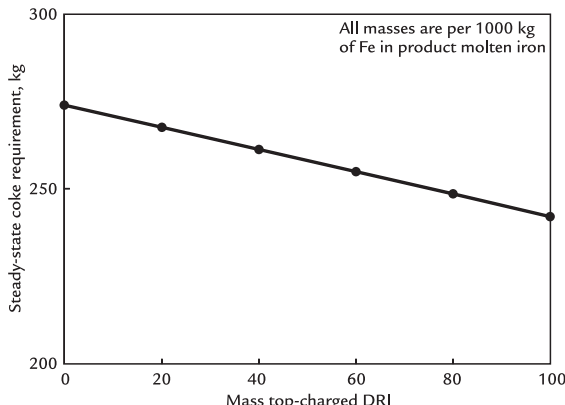


FIGURE 44.2 Effect of top-charged DRI pellets on steady-state coke requirement. As expected, coke requirement decreases with increasing DRI pellet quantity. This is because the DRI pellets contain 93 mass% Fe, so very little reduction (and very little coke) is required to reduce them to molten iron.

44.14 CALCULATED RESULTS - IRON ORE REQUIREMENT

This section answers the question;

how much iron ore (95 mass% Fe_2O_3) is required to steadily produce molten iron and molten slag

as a function of top-charged DRI pellet quantity. This is answered by Fig. 44.3.

44.15 $CO_2(g)$ EMISSION AS A FUNCTION OF DRI PELLET INPUT

Top charging of DRI pellets lowers the amount of $CO_2(g)$ that is emitted by a blast

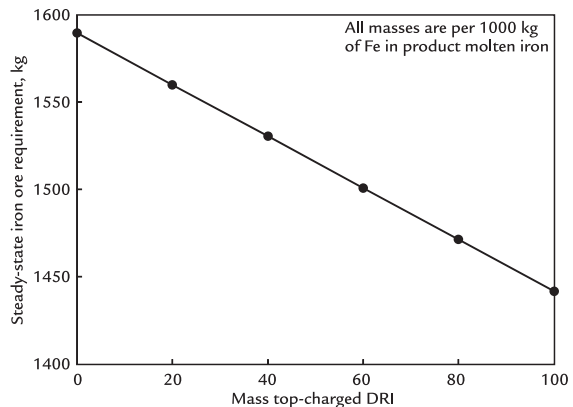


FIGURE 44.3 Effect of top-charged DRI pellets on 95 mass% Fe_2O_3 , 5 mass% SiO_2 ore requirement for producing 1500°C molten iron and 1500°C molten slag. As expected, iron ore requirement decreases with increasing DRI pellet quantity. The ore requirement decreases because the top-charged DRI pellets supply a portion of the product molten iron's Fe.

furnace, per 1000 kg of Fe in product molten iron. This is shown in Fig. 44.4.

44.16 TOTAL TOP-GAS EMISSION AS A FUNCTION OF DRI PELLET INPUT

Top charging of DRI pellets lowers total top-gas production, as shown in Fig. 44.5.

44.17 MASS $N_2(g)$ IN TOP-GAS AS A FUNCTION OF DRI PELLET INPUT

Top charging of DRI pellets lowers blast furnace $N_2(g)$ emission, as shown in Fig. 44.6.

44.18 MASS SiO_2 IN SLAG AS A FUNCTION OF DRI PELLET INPUT

Top charging of DRI pellets lowers mass SiO_2 -in-slag, Fig. 44.7.

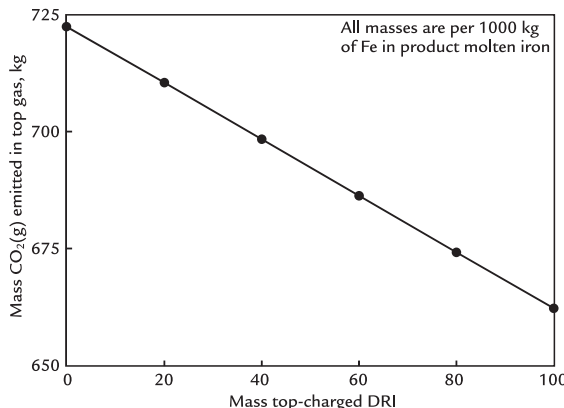


FIGURE 44.4 Effect of top-charged DRI pellets on blast furnace CO₂(g) emission. Like top-charged scrap, top-charged DRI pellets lowers CO₂(g) emission per 1000 kg of Fe in product molten iron. This is due to the metallic Fe in the top-charged pellets, which proceeds directly to the molten iron product without producing carbonaceous gases and is confirmed by the furnace's decreasing coke requirement, Fig. 44.1. *voestalpine Stahl* has started to charge DRI pellets to its blast furnaces in Linz and Donawitz, Austria, to take advantage of this CO₂(g) emission reduction benefit¹.

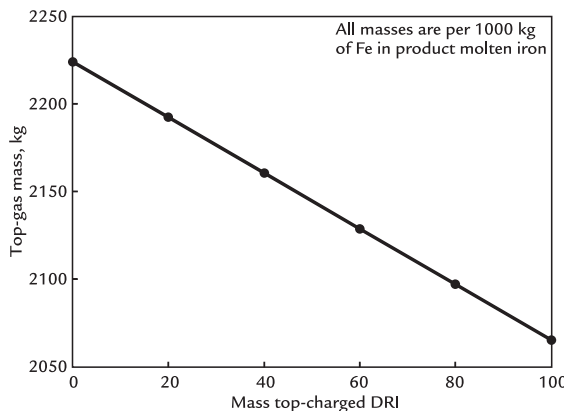


FIGURE 44.5 Blast furnace top-gas production as affected by top-charging of DRI pellets. It declines with increasing mass top-charged DRI pellets. This is due to the decreasing amount of CO₂(g) (Fig. 44.4) and N₂(g) from blast air (Fig. 44.6). The implication is that DRI pellet top charging permits faster molten iron production with no increase in upward gas flow rate and velocity. AK Steel Middletown (BF#3) has top charged DRI pellets to take advantage of this effect.

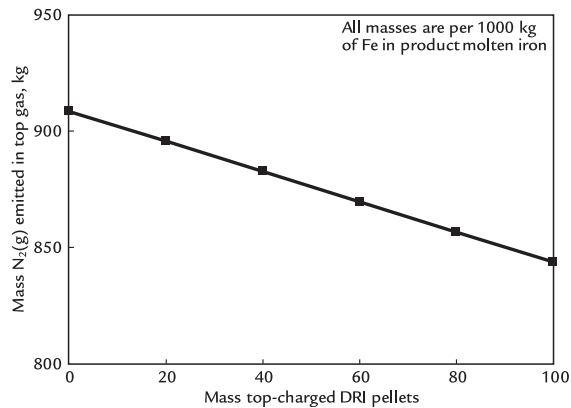


FIGURE 44.6 Effect of mass top-charged DRI pellets on mass N₂(g) from blast air in top gas. The decrease is notable. Almost all the N₂(g) enters the blast furnace in its blast air, which decreases due to less coke combustion in front of the tuyeres, Fig. 44.2.

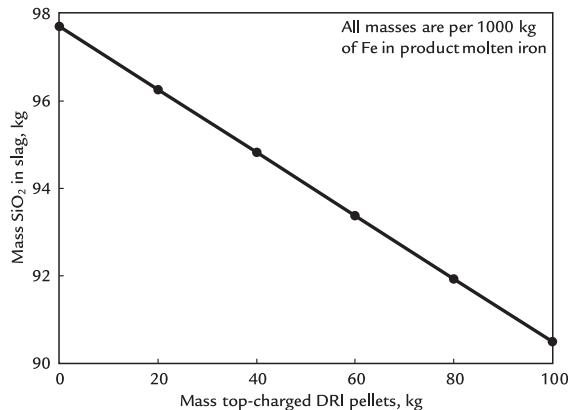


FIGURE 44.7 Effect of top-charged DRI pellets on mass SiO₂ in slag per 1000 kg of Fe in product molten iron. It decreases because 5 mass% SiO₂ ore (Chapter 32: Bottom Segment Slag Calculations - Ore, Fluxes, and Slag) is replaced by 2 mass% SiO₂ DRI pellets. Decreased coke (7 mass% SiO₂) requirement (Fig. 44.2) also contributes to this effect. The slag is specified to contain 39 mass% SiO₂ (Chapter 32: Bottom Segment Slag Calculations—Ore, Fluxes, and Slag) so that total mass slag = mass SiO₂-in-slag/0.39. The remainder of the slag is 10 mass% Al₂O₃, 41 mass% CaO, and 10 mass% MgO, mostly from fluxes.

44.19 FLAME TEMPERATURE WITH TOP-CHARGED DRI PELLETS

Fig. 44.8 shows the effect of top-charged DRI pellets on raceway flame temperature. The flame temperature drops by $10^{\circ}\text{C}/100 \text{ kg}$ of pellets.

44.20 TOP-GAS TEMPERATURE WITH TOP-CHARGED DRI PELLETS

Fig. 44.9 shows the effect of top-charged DRI pellets on blast furnace top-gas temperature. Top-gas temperature falls with increasing pellet quantity by about 14°C per 100 kg of pellets. This has been predicted to be 15°C industrially, but not confirmed.

44.21 DISCUSSION

Top charging of mostly reduced iron ore pellets is readily represented in our automated spread sheet calculations. The steps are;

1. calculation of DRI pellet enthalpies at 25°C and 930°C , the top-segment–bottom-segment division temperature;
2. specification that the DRI pellets are not oxidized nor reduced while descending through the top segment so that their mass and composition entering the bottom segment are the same as when they are top charged; and
3. replacement of $\left[\begin{matrix} \text{mass scrap steel descending} \\ \text{into the bottom segment} \end{matrix} \right]$ column of Chapter 43, Top-Charged Scrap Steel, with $\left[\begin{matrix} \text{mass DRI pellets descending} \\ \text{into the bottom segment} \end{matrix} \right]$ column as shown in Table 44.1.

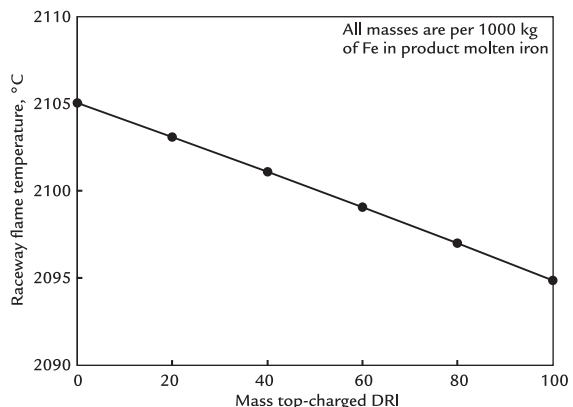


FIGURE 44.8 Effect of top-charged DRI pellet quantity on raceway flame temperature. Flame temperature falls with increasing DRI pellet quantity per 1000 kg of Fe in product molten iron. This is a consequence of all our equations but we may speculate that it is at least partially due to the smaller amount of coke that is being burnt in the raceway, Fig. 44.2.

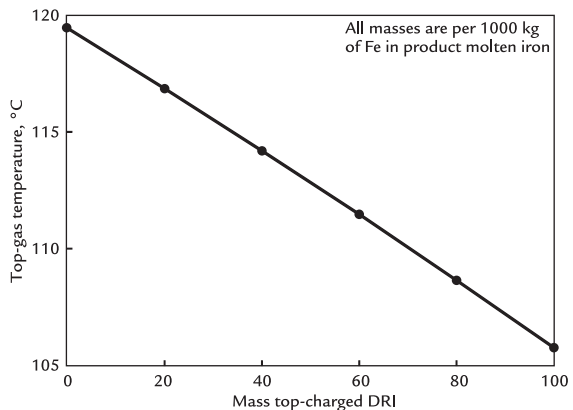


FIGURE 44.9 Effect of top-charged DRI pellet amount on blast furnace top-gas temperature. It falls with increasing pellet amount. The line is almost straight. The decreasing temperature is a consequence of all our equations but it may be the result of less carbon being combusted in the bottom segment and less hot (1) N_2 and (2) carbonaceous gases rising into the top segment.

We have used this technique to calculate;

1. coke requirement ([Fig. 44.2](#)),
2. iron ore requirement ([Fig. 44.3](#)),
3. top-gas CO₂ emission ([Fig. 44.4](#)),
4. top-gas mass ([Fig. 44.5](#)), and
5. SiO₂-in-slag mass and total slag mass all per 1000 kg of Fe in product molten iron ([Fig. 44.7](#)), and
6. flame temperature ([Fig. 44.8](#)) and top-gas temperature ([Fig. 44.9](#)) with and without charging DRI pellets.

- 0.864 kg of Fe(s),
- 0.02 kg of C(s),
- 0.086 kg of Fe_{0.947}O(s),
- 0.01 kg of Al₂O₃(s), and
- 0.02 kg of SiO₂(s)

per kg of DRI pellets.

The DRI pellet 25°C enthalpy is given by the following equation:

$$\begin{aligned} \text{25°C DRI pellet enthalpy} &= 0.864 \text{ kg of Fe(s)} * 0 \\ &+ 0.02 \text{ kg of C(s)} * 0 \\ &+ 0.086 \text{ kg of Fe}_{0.947}\text{O(s)} * -3.865 \\ &+ 0.01 \text{ kg of Al}_2\text{O}_3(\text{s}) * -16.43 \\ &+ 0.02 \text{ kg of SiO}_2(\text{s}) * -15.16 \\ &= -0.800 \text{ MJ/kg of pellets} \end{aligned}$$

44.22 CALCULATION OF DRI PELLET ENTHALPIES, MJ PER kg OF DRI PELLETS

This section calculates the enthalpies of DRI pellets at the top-charge temperature (25°C) and chemical reserve temperature (930°C).

It is based on the pellet composition:

- 93 mass% Fe
- 2 mass% C
- 2 mass% O
- 1 mass% Al₂O₃
- 2 mass% SiO₂

We assume that;

1. the Al₂O₃ and SiO₂ are present as Al₂O₃(s) and SiO₂(s),
2. the C is present as solid elemental carbon,
3. the O is present as Fe_{0.947}O(s), and
4. the Fe is present mostly as Fe(s), the remainder as Fe_{0.947}O(s).

We base our calculations on 1 kg of pellets.

Fe_{0.947}O is 23.2 mass% O so that the 0.02 mass% of O in the pellets is equivalent to 0.02 kg O/0.232 = 0.086 kg of Fe_{0.947}O which ties up (0.086 – 0.02) kg of Fe, that is, 0.066 kg of Fe.

This leaves (0.93 kg of Fe – 0.066 kg) of elemental Fe = 0.864 kg.

So, we base our DRI pellet enthalpies on;

The right-most values (e.g., 0) are enthalpies of the elements and compounds, MJ per kg (from Table J.1).

Similarly, the 930°C DRI pellet enthalpy is:

$$\begin{aligned} \text{930°C DRI pellet enthalpy} &= 0.864 \text{ kg of Fe(s)} * 0.6164 \\ &+ 0.02 \text{ kg of C(s)} * 1.359 \\ &+ 0.086 \text{ kg of Fe}_{0.947}\text{O(s)} * -3.152 \\ &+ 0.01 \text{ kg of Al}_2\text{O}_3(\text{s}) * -15.41 \\ &+ 0.02 \text{ kg of SiO}_2(\text{s}) * -14.13 \\ &= -0.148 \text{ MJ/kg of pellets} \end{aligned}$$

44.23 SUMMARY

Top charging of mostly reduced DRI pellets decreases;

1. coke and ore requirements for producing 1500°C molten iron and molten iron,
2. top-gas CO₂ emission,
3. top-gas mass, and
4. slag mass

all per 1000 kg of Fe in product molten iron.

Adding DRI pellets also decreases tuyere raceway flame and top-gas temperatures.

Less top-gas is advantageous because it allows more rapid molten iron production

without increasing blast furnace upward gas flowrate. Greater production can be achieved with the same burden permeability to gas flow and with the same pressure drop limits used with 100% oxide iron ore, sinter, and pellets.

Top-gas CO₂ emission lowering is advantageous because it decreases emission of greenhouse gas per 1000 kg of Fe in product molten iron. It may also lower carbon tax cost.

Mostly reduced iron ore pellets are used extensively in several blast furnace plants, specifically *AK Steel Middletown* in the United States to increase production and *voestalpine Stahl* in Austria to reduce CO₂ emissions¹.

EXERCISE

All masses in these calculations are kg per 1000 kg of Fe in product molten iron.

As throughout this chapter, these exercises' blast furnace is being injected with 220 kg of pulverized coal and 92 kg of pure oxygen. The 1200°C blast contains 15 g of H₂O(g)/Nm³ of dry air in blast and all the fluxes are oxides. These values are based on an industrial blast furnace. The top charge contains 5 mass% H₂O (v), excluding the DRI, which is dry.

- 44.1.** The Fig. 44.2 blast furnace operators plan to cut their *direct reduced iron* pellet input to 45 kg/1000 kg of Fe in product molten iron. They wish to know how much Al₂O₃, CaO, and MgO flux they will need to be top charging to obtain this chapter's; 10 mass% Al₂O₃, 41 mass% CaO, 10 mass% MgO, and 39 mass% SiO₂ molten slag. Please calculate these for them.
- 44.2.** Fig. 44.2 management foresees that their local government will soon mandate that their CO₂(g) emission be below 625 kg/kg of Fe in product molten iron. Please calculate for them the minimum quantity of DRI pellets that will have to be charged (per 1000 kg of Fe in product molten iron) to achieve this goal. Please use two methods of calculation.

Reference

1. Grieser A. "Use of HBI in Blast Furnace". 8th ICSTI, Vienna, 2018.

Bottom-Segment Calculations With H₂(g) Injection

O U T L I N E

45.1 Reasons for Injecting Hydrogen into the Blast Furnace	429	45.2.3 Carbon Mass Balance Equation With H ₂ (g) Injection	430
45.2 Bottom-Segment Equations With H ₂ (g) Injection	430	45.2.4 Enthalpy Equation With H ₂ (g) Injection	430
45.2.1 H ₂ (g) Injectant Quantity Specification Equation	430	45.3 Calculation Results	432
45.2.2 Bottom-Segment H Mass Balance Equation With H ₂ (g) Injection	430	45.4 Summary	432
		Exercises	433

45.1 REASONS FOR INJECTING HYDROGEN INTO THE BLAST FURNACE

As of 2019, hydrogen is *not* injected into industrial iron blast furnaces. Its use is being suggested as an alternative to natural gas - to minimize blast furnace carbon emissions and carbon tax. This chapter explores the consequences of injecting hydrogen through a blast

furnace's tuyeres. Fig. 45.1 shows bottom-segment flows with 25°C H₂(g) injection.

The objectives of this chapter are to;

1. show how H₂(g) injection is represented in our bottom-segment matrix calculations,
2. determine the effects of H₂(g) injection on the amounts of C-in-coke and O₂-in-blast that are needed for steady production of 1500°C molten iron, and

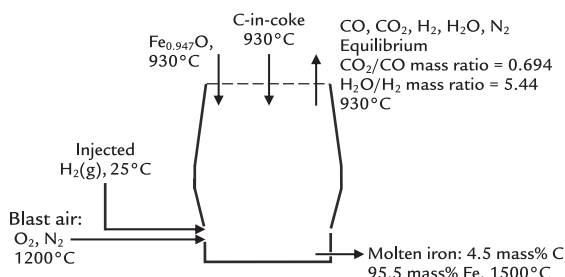


FIGURE 45.1 Conceptual blast furnace bottom segment with H₂(g) injection. 25°C H₂(g) replaces the 25°C CH₄(g) injection in Fig. 11.1. Otherwise, the flows are the same.

3. determine the effect of H₂(g) injection on the amount of N₂(g) that accompanies item 2's input O₂-in-blast air.

45.2 BOTTOM-SEGMENT EQUATIONS WITH H₂(g) INJECTION

We now develop equations to describe the flows presented in [Fig. 45.1](#).

45.2.1 H₂(g) Injectant Quantity Specification Equation

H₂ injection quantity of [Fig. 45.1](#) is represented by changing Eq. (11.1) of CH₄(g) injection to;

$$\left[\frac{\text{mass tuyere}}{\text{injected H}_2\text{(g)}} \right] = 20 \text{ kg/1000 kg of Fe in product molten iron}$$

or in matrix form;

$$20 = \left[\frac{\text{mass tuyere}}{\text{injected H}_2\text{(g)}} \right] * 1 \quad (45.1)$$

as is shown in [Table 45.1](#), Row 14.

45.2.2 Bottom-Segment H Mass Balance Equation With H₂(g) Injection

CH₄(g) is 25.1 mass% H. H₂ is 100% H. This changes CH₄(g) injection hydrogen mass balance equation (11.4) to;

$$0 = - \left[\frac{\text{mass tuyere}}{\text{injected H}_2\text{(g)}} \right] * 1 + \left[\frac{\text{mass H}_2 \text{ out}}{\text{in ascending gas}} \right] * 1 + \left[\frac{\text{mass H}_2\text{O out}}{\text{in ascending gas}} \right] * 0.112 \quad (45.2)$$

as shown in [Table 45.1](#), Row 8.

45.2.3 Carbon Mass Balance Equation With H₂(g) Injection

H₂(g) injectant contains no carbon. This simplifies bottom-segment CH₄(g) injection carbon balance equation (11.4) of Chapter 11, Bottom Segment with CH₄(g) Injection, to;

$$0 = - \left[\frac{\text{mass C in}}{\text{descending coke}} \right] * 1 + \left[\frac{\text{mass CO out}}{\text{in ascending gas}} \right] * 0.429 + \left[\frac{\text{mass CO}_2 \text{ out}}{\text{in ascending gas}} \right] * 0.273 + \left[\frac{\text{mass C out}}{\text{in molten iron}} \right] * 1 \quad (7.4)$$

as shown in [Table 45.1](#), Row 6.

45.2.4 Enthalpy Equation With H₂(g) Injection

The 25°C enthalpy of H₂(g) is zero (element in its most common state at 25°C).

TABLE 45.1 Bottom Blast Furnace Segment Matrix With H₂(g) Injection Through Its Tuyeres (Fig. 45.1)

	A	B	C	D	E	F	G	H	I	J	K	L	M	N	O
1 BOTTOM SEGMENT CALCULATIONS															
Equation	Description	Numerical term	mass Fe _{0.94} O into bottom segment	mass C in descending coke	mass O ₂ in blast air	mass N ₂ in blast air	mass Fe out in molten iron	mass C out in molten iron	mass CO out in ascending gas	mass CO ₂ out in ascending gas	mass N ₂ out in ascending gas	mass H ₂ out in ascending gas	mass H ₂ O out in ascending gas	mass tuyere-injected H ₂ (g)	
7.7	Fe out in molten iron specification	1000	0	0	0	0	1	0	0	0	0	0	0	0	0
7.2	Fe mass balance	0	-0.768	0	0	0	1	0	0	0	0	0	0	0	0
11.5	O mass balance	0	-0.232	0	-1	0	0	0	0.571	0.727	0	0	0.888	0	
7.4	C mass balance	0	0	-1	0	0	0	1	0.429	0.273	0	0	0	0	
7.5	N mass balance	0	0	0	0	-1	0	0	0	0	1	0	0	0	
45.2	H mass balance	0	0	0	0	0	0	0	0	0	0	1	0.112	-1	
7.6	N ₂ in blast air specification	0	0	0	3.3	-1	0	0	0	0	0	0	0	0	
7.9	Equilibrium CO ₂ /CO mass ratio	0	0	0	0	0	0	0	0.694	-1	0	0	0	0	
11.8	Equilibrium H ₂ O/H ₂ mass ratio	0	0	0	0	0	0	0	0	0	0	5.44	-1	0	
7.8	C out in molten iron specification	0	0	0	0	0	0.047	-1	0	0	0	0	0	0	
45.3	Enthalpy balance	-320	3.152	-1.359	-1.239	-1.339	1.269	5	-2.926	-7.926	1.008	13.35	-11.50	0	
45.1	Tuyere-injected H ₂ (g)	20	0	0	0	0	0	0	0	0	0	0	0	1	
		930°C	930°C	1200°C	1200°C	1500°C	1500°C	930°C	930°C	930°C	930°C	930°C	930°C	25°C	
Bottom segment calculated values															
	kg per 4000 kg of Fe out in molten iron														
mass Fe _{0.94} O into bottom segment	1302														
mass C in descending coke	353	also = mass C in the furnace's coke charge, Eqn. (7.16)													
mass O ₂ in blast air	289														
mass N ₂ in blast air	955														
mass Fe out in molten iron	1000														
mass C out in molten iron	47														
mass CO out in ascending gas	494														
mass CO ₂ out in ascending gas	343														
mass N ₂ out in ascending gas	955														
mass H ₂ out in ascending gas	12														
mass H ₂ O out in ascending gas	68														
mass tuyere-injected H ₂ (g)	20														

The differences between this matrix and CH₄(g) injection matrix Table 11.1 are (1) altered carbon mass balance equation, Row 6; (2) altered hydrogen mass balance equation, Row 8; (3) altered enthalpy balance equation, Row 13; and (4) new H₂ injection quantity specification, Row 14.

This changes CH₄(g)'s bottom-segment enthalpy balance equation (11.7) to;

$$\begin{aligned}
 -320 = & -[\text{mass tuyere-injected H}_2\text{(g)}] * (0) \\
 & -[\text{mass Fe}_{0.947}\text{O into bottom segment}] * (-3.152) \\
 & -[\text{mass C in descending coke}] * 1.359 \\
 & -[\text{mass O}_2\text{ in blast air}] * 1.239 \\
 & -[\text{mass N}_2\text{ in blast air}] * 1.339 \\
 & +[\text{mass Fe out in molten iron}] * 1.269 \\
 & +[\text{mass C out in molten iron}] * 5 \\
 & +[\text{mass CO gas out in ascending gas}] * (-2.926) \\
 & +[\text{mass CO}_2\text{ gas out in ascending gas}] * (-7.926) \\
 & +[\text{mass N}_2\text{ out in ascending gas}] * 1.008 \\
 & +[\text{mass H}_2\text{ gas out in ascending gas}] * 13.35 \\
 & +[\text{mass H}_2\text{O gas out in ascending gas}] * (-11.50)
 \end{aligned} \quad (45.3)$$

as shown in [Table 45.1](#), Row 13.

45.3 CALCULATION RESULTS

[Figs. 45.2–45.4](#) summarize the results of matrix [Table 45.1](#). They show that H₂(g) injection;

1. saves considerable C-in-coke,
2. decreases steady-state O₂-in-blast air requirement of the blast furnace, and
3. commensurately decreases the amount of N₂ that enters the furnace in blast air and subsequently departs the furnace in top gas.

45.4 SUMMARY

Tuyere injection of H₂(g) is readily described in matrix form by making four minor changes to the CH₄(g) injection matrix of Chapter 11, Bottom Segment with CH₄(g) Injection.

The matrix calculations show that 1 kg of H₂(g) injection saves about 2 kg of C-in-top-charged coke. This, in turn, decreases a similar amount of C emission [as CO(g) and CO₂(g)] in the blast furnace's top gas, Chapter 46, Top-Segment Calculations With H₂(g) Injection.

H₂(g) injection also lowers the amount of O₂-in-blast air that is needed to steadily

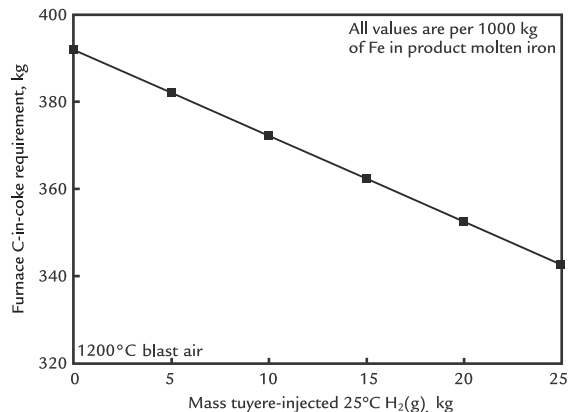


FIGURE 45.2 Effect of 25°C H₂(g) injection on the amount of C-in-coke needed to steadily produce 1500°C molten iron. The line is straight. 1 kg of 25°C H₂(g) saves about 2 kg of C-in-coke (per 1000 kg of Fe in product molten iron). The injected H₂(g) lowers C-in-coke requirement because it carries out a portion of iron oxide-to-iron reduction of the blast furnace as confirmed by the presence of H₂O(g) in top gas of the blast furnace (Chapter 46: Top-Segment Calculations With H₂(g) Injection). The decrease in C-in-coke requirement per 1000 kg of Fe in product molten iron equally decreases the emission of C in top gas.

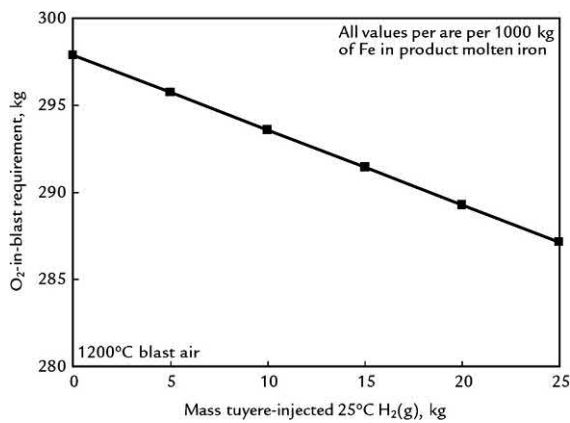


FIGURE 45.3 Graph showing that H₂(g) injection decreases the amount of O₂-in-blast air that is needed for steady production of 1500°C molten iron. The calculated values are the result of all equations of matrix [Table 45.1](#). We may speculate that it is mainly because less O₂ is required to burn carbon to CO(g) in front of the tuyeres of the blast furnace.

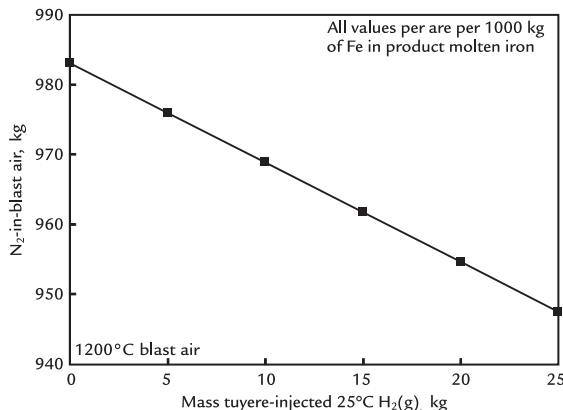


FIGURE 45.4 Mass of N_2 that accompanies O_2 -in-blast air of Fig. 45.3. The slope is 3.3 times the slope of Fig. 45.3 because the N_2/O_2 mass ratio in air is constant at 3.3.

produce $1500^\circ C$ molten iron—and the N_2 -in-blast air that accompanies it.

EXERCISES

Please express your answers in kg per 1000 kg of Fe in product molten iron.

- 45.1.** How is $H_2(g)$ made and what are its most common raw materials? Can it be produced without emitting carbon to the atmosphere? Name four techniques.

- 45.2.** Management of the blast furnace of Table 45.1 want to know the effects of raising $H_2(g)$ injection to 30 kg (per 1000 kg of Fe in product molten iron). Please quantify these for them by calculating the amounts of;

1. C-in-coke,
2. O_2 -in-blast air,
3. N_2 -in-blast air, and
4. air

that will be needed to steadily produce $1500^\circ C$ molten iron with this amount of injection.

- 45.3.** The engineering team of Table 45.1 believes that smooth operation of their furnace requires that it be charged with 250 kg or more of C-in-coke (per 1000 kg of Fe in product molten iron). They would like to know how much $H_2(g)$ can be injected without lowering the C-in-coke requirement below this 250 kg level. Please calculate this for them. Use two methods of calculation.

- 45.4.** Hydrogen reduction of iron oxides of a blast furnace will result in considerable production of $H_2O(g)$. Looking ahead, do you think that this $H_2O(g)$ might cause a problem at the top of the blast furnace? What might that problem be?

Top-Segment Calculations With H₂(g) Injection

OUTLINE

46.1 Examining the Impact of H ₂ (g) Injection on the Top-Segment Balances	435	46.4 Top Gas Temperature Results	436
46.2 Bottom-Segment Calculations With Hydrogen Injection and Dry Blast Air	436	46.5 Top Gas Carbon Emissions	436
46.3 Top-Segment Calculations	436	46.6 C-in-Top-Charged Coke	436
		46.7 Summary	439
		Exercises	440

46.1 EXAMINING THE IMPACT OF H₂(g) INJECTION ON THE TOP-SEGMENT BALANCES

The objectives of the chapter are to show;

1. how to calculate top gas masses, enthalpies, and temperature with hydrogen injection,
2. how hydrogen injection affects top gas temperature, and
3. how hydrogen injection affects top gas carbon emissions.

Fig. 46.1 shows steady-state flows across the conceptual division of a blast furnace with

hydrogen injection. Qualitatively, they are the same as with CH₄(g) injection and H₂O(g) in blast, that is;

- descending Fe_{0.947}O(s) and C(s)-in-coke, and
- ascending CO(g), CO₂(g), N₂(g), H₂(g), and H₂O(g).

We now calculate the steady-state mass flows of these substances with;

1. injection of 20 kg of 25°C H₂(g) per 1000 kg of Fe in product molten iron, and
2. 1200°C dry blast air.

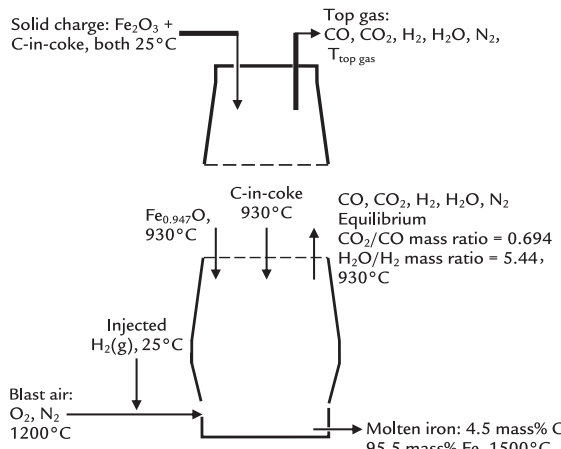


FIGURE 46.1 Conceptually divided blast furnace with tuyere-injected 25°C hydrogen and 1200°C dry blast air. Note the flows of Fe_{0.947}O(s), C(s)-in-coke, CO(g), CO₂(g), N₂(g), H₂(g), and H₂O(g) across the conceptual division. They are the same, qualitatively, as with CH₄(g) and steam injection with or without humidity in blast, Chapter 25, Top Segment Mass Balance with CH₄(g) Injection, and Chapter 28, Top Segment Calculation with Moisture in Blast Air.

46.2 BOTTOM-SEGMENT CALCULATIONS WITH HYDROGEN INJECTION AND DRY BLAST AIR

Table 46.1 shows our bottom-segment matrix with H₂(g) injection. This is a copy of Table 45.1. The solution of the equations to the bottom segment are used as inputs in the top segment matrix of **Table 46.2**.

46.3 TOP-SEGMENT CALCULATIONS

Table 46.2 is the *top segment matrix* with 20 kg of 25°C H₂(g) injection and dry blast air. Qualitatively it is the same as Table 28.2. The only inputs that change are those in Column AC3 through AC16, which come from

Table 46.1's Column C bottom segment calculated values.

46.4 TOP GAS TEMPERATURE RESULTS

Table 46.2 shows that the blast furnace top gas temperature with 20 kg of 25°C injected H₂(g) per 1000 kg of Fe in product molten iron is 227°C.

This value and others are plotted in **Fig. 46.2**.

46.5 TOP GAS CARBON EMISSIONS

Table 46.2 calculates top gas carbon emission in Cell AL25. The equation is;

$$\begin{aligned}
 & \left[\begin{array}{l} \text{total C emission} \\ \text{in top gas} \end{array} \right] \\
 &= \left[\begin{array}{l} \text{mass CO} \\ \text{in top gas} \end{array} \right] * \frac{42.9 \text{ mass\% C in CO}}{100\%} \\
 &+ \left[\begin{array}{l} \text{mass CO}_2 \\ \text{in top gas} \end{array} \right] * \frac{27.3 \text{ mass\% C in CO}_2}{(100\%)} \quad (46.3) \\
 &= \left[\begin{array}{l} \text{mass CO} \\ \text{in top gas} \end{array} \right] * 0.429 \\
 &+ \left[\begin{array}{l} \text{mass CO}_2 \\ \text{in top gas} \end{array} \right] * 0.273
 \end{aligned}$$

or in spreadsheet form;

$$= AC25 * 0.429 + AC26 * 0.273 \quad (46.4)$$

as shown to the left of Cell AL25.

Fig. 46.3 shows the results.

46.6 C-IN-TOP-CHARGED COKE

This section shows the effect of 25°C H₂(g) on top charge C-in-coke requirement for

TABLE 46.1 Bottom-Segment Matrix With H₂(g) Injection

	A	B	C	D	E	F	G	H	I	J	K	L	M	N	O	
BOTTOM SEGMENT CALCULATIONS																
Equation	Description	Numerical term	mass Fe _{0.947} O into bottom segment	mass C in descending coke	mass O ₂ in blast air	mass N ₂ in blast air	mass Fe out in molten iron	mass C out in molten iron	mass CO out in ascending gas	mass CO ₂ out in ascending gas	mass N ₂ out in ascending gas	mass H ₂ out in ascending gas	mass H ₂ O out in ascending gas	mass tuyere-injected H ₂ (g)		
7.7	Fe out in molten iron specification	1000	0	0	0	0	1	0	0	0	0	0	0	0	0	
7.2	Fe mass balance	0	-0.768	0	0	0	1	0	0	0	0	0	0	0	0	
11.5	O mass balance	0	-0.232	0	-1	0	0	0	0.571	0.727	0	0	0.888	0	0	
7.4	C mass balance	0	0	-1	0	0	0	1	0.429	0.273	0	0	0	0	0	
7.5	N mass balance	0	0	0	0	-1	0	0	0	0	1	0	0	0	0	
45.2	H mass balance	0	0	0	0	0	0	0	0	0	0	1	0.112	-1	0	
7.6	N ₂ in blast air specification	0	0	0	3.3	-1	0	0	0	0	0	0	0	0	0	
10.9	Equilibrium CO ₂ /CO mass ratio	0	0	0	0	0	0	0	0.694	-1	0	0	0	0	0	
11.8	Equilibrium H ₂ O/H ₂ mass ratio	0	0	0	0	0	0	0	0	0	5.44	-1	0	0	0	
7.8	C out in molten iron specification	0	0	0	0	0	0.047	-1	0	0	0	0	0	0	0	
45.3	Enthalpy balance	320	3.152	-1.359	1.239	-1.339	1.269	5	2.926	-7.926	1.008	13.35	-11.50	0	0	
45.1	Tuyere-injected H ₂ (g)	20	0	0	0	0	0	0	0	0	0	0	0	1	0	
		930°C	930°C	1200°C	1200°C	1500°C	1500°C	930°C	930°C	930°C	930°C	930°C	930°C	25°C		
Bottom segment calculated values																
		kg per 1000 kg of Fe out in molten iron														
14	mass Fe _{0.947} O into bottom segment	1302														
15	mass C in descending coke	353	also = mass C in the furnace's coke charge, Eqn. (7.16)													
16	mass O ₂ in blast air	289														
17	mass N ₂ in blast air	955														
18	mass Fe out in molten iron	1000														
19	mass C out in molten iron	47														
20	mass CO out in ascending gas	494														
21	mass CO ₂ out in ascending gas	343														
22	mass N ₂ out in ascending gas	955														
23	mass H ₂ out in ascending gas	12														
24	mass H ₂ O out in ascending gas	68														
25	mass tuyere-injected H ₂ (g)	20														

This is a copy of Table 45.1.

TABLE 46.2 Top-Segment Spreadsheet With 20 kg of 25°C H₂(g) Injection and Dry Blast Air

AA	AB	AC	AD	AE	AF	AG	AH	AI	AJ	AK	AM	AN	AO	AP	AQ	
TOP SEGMENT CALCULATIONS																
Equation	Description	Numerical term	mass Fe _{0.947} O ₁ in furnace charge	mass C in coke charge	mass CO ascending from bottom segment	mass CO ₂ ascending from bottom segment	mass N ₂ ascending from bottom segment	mass Fe _{0.947} O ₁ descending into bottom segment	mass C-in-coke descending into bottom segment	mass CO out in top gas	mass CO ₂ out in top gas	mass N ₂ out in top gas	mass H ₂ ascending from bottom segment	mass H ₂ O ascending from bottom segment	mass H ₂ out in top gas	mass H ₂ O out in top gas
2			0	0	0	0	0	1	0	0	0	0	0	0	0	
3	20.6 Mass Fe _{0.947} O ₁ descending into bottom segment	1302	0	0	0	0	0	0	0	0	0	0	0	0	0	
4	20.2 Fe mass balance	0	-0.699	0	0	0	0.768	0	0	0	0	0	0	0	0	
5	25.5 O mass balance	0	-0.301	0	-0.571	-0.727	0	0.232	0	0.571	0.727	0	0	-0.888	0	
6	20.4 C mass balance	0	0	-1	0.429	-0.273	0	0	1	0.429	0.273	0	0	0	0.888	
7	N mass balance	0	0	0	0	-1	0	0	0	0	0	1	0	0	0	
8	20.8 Mass CO ascending from bottom segment	494	0	0	1	0	0	0	0	0	0	0	0	0	0	
9	20.9 Mass CO ₂ ascending from bottom segment	343	0	0	0	1	0	0	0	0	0	0	0	0	0	
10	20.1 Mass N ₂ ascending from bottom segment	955	0	0	0	0	1	0	0	0	0	0	0	0	0	
11	20.7 Mass C-in-coke descending into bottom segment	353	0	0	0	0	0	0	1	0	0	0	0	0	0	
12	20.11 Unreacted C-in-coke specification	0	0	-1	0	0	0	0	1	0	0	0	0	0	0	
13	25.4 H mass balance	0	0	0	0	0	0	0	0	0	0	-1	-0.112	1	0.112	
14	25.1 Mass H ₂ ascending from bottom segment	12.4	0	0	0	0	0	0	0	0	0	1	0	0	0	
15	25.5 Mass H ₂ O ascending from bottom segment	68	0	0	0	0	0	0	0	0	0	0	1	0	0	
16	H ₂ /CO reaction ratio equation	0	0	0	0	-0.14	0	0	0	0	0.14	0	0	1	-1	
17	Top segment calculated values	kg per 1000 kg of Fe in product molten iron														
18	mass Fe _{0.947} O ₁ in furnace charge	1431														
19	mass C in coke charge	353														
20	mass CO ascending from bottom segment	494														
21	mass CO ₂ ascending from bottom segment	343														
22	mass N ₂ ascending from bottom segment	955														
23	mass Fe _{0.947} O ₁ descending into bottom segment	1302														
24	mass C-in-coke descending into bottom segment	353														
25	mass CO out in top gas	328														
26	mass CO ₂ out in top gas	604														
27	mass N ₂ out in top gas	955														
28	mass H ₂ ascending from bottom segment	12														
29	mass H ₂ O ascending from bottom segment	68														
30	mass H ₂ leaving in top gas	8.2														
31	mass H ₂ O leaving in top gas	105														
32	TOP SEGMENT INPUT AND OUTPUT ENTHALPY CALCULATIONS															
33	26.2 Top segment input enthalpy =AC18*-5.169+AC19*0+AC20*-2.926+AC21*-7.926+AC22*1.008+AC28*13.34+AC29*-11.49 =															
34	26.4 Top segment output enthalpy=AG33-80 =															
35																
36	TOP-GAS ENTHALPY CALCULATION															
37	26.5 Top-gas enthalpy =AG34 AC23*-3.152 AC24*1.359 =															
38																
39	TOP-GAS TEMPERATURE CALCULATION															
40	27.4 Top-gas temperature =(AG37-AC25*-3.972 AC26*-8.966 AC27*-0.02624 AC30*-0.3616 AC31*-13.47)/(AC25*0.001049+AC26*0.0009314+AC27*0.001044+AC30*0.01442+AC31*0.001902) =															
41																

Qualitatively, this matrix is the same as Table 28.2. The only inputs that change are those in Columns AC3–AC16, which come from Column C bottom-segment calculated values of Table 46.1. The top gas temperature under the prescribed conditions is 227°C, Cell AL40.

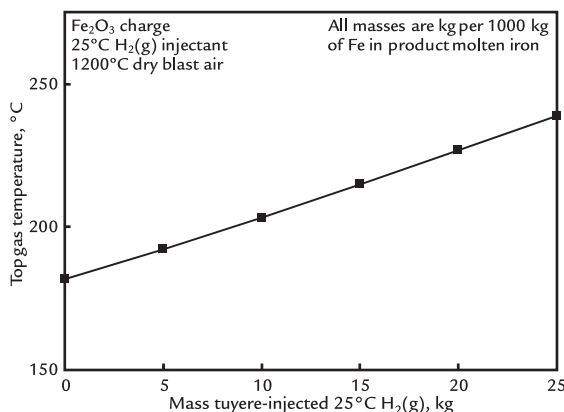


FIGURE 46.2 Effect of $\text{H}_2(\text{g})$ injection on top gas temperature. Top gas temperature increases with increasing $\text{H}_2(\text{g})$ injection quantity just as it does with all other injectants (except O_2). Our general conclusion is that, except for O_2 , all industrial injectants increase blast furnace top gas temperature. Of course, this means that top gas temperature may be controlled by simultaneous $\text{H}_2(\text{g})$ injection and $\text{O}_2(\text{g})$ injection.

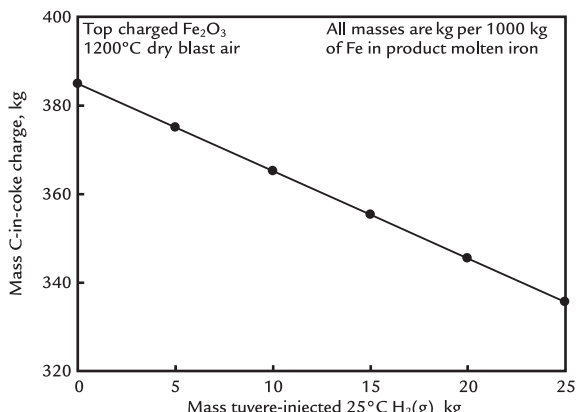


FIGURE 46.4 Steady-state mass C-in-coke charge requirement as affected by mass tuyere-injected $\text{H}_2(\text{g})$. As expected from Fig. 46.3, carbon demand decreases with increasing $\text{H}_2(\text{g})$ injection. The slope is the same as in Fig. 46.3. The charged C quantity is 47 kg more than the top gas quantity. This is because 47 kg of C leaves the blast furnace in the product molten iron as shown by in Cell 23 of Table 46.1. All quantities are per 1000 kg of Fe in product molten iron.

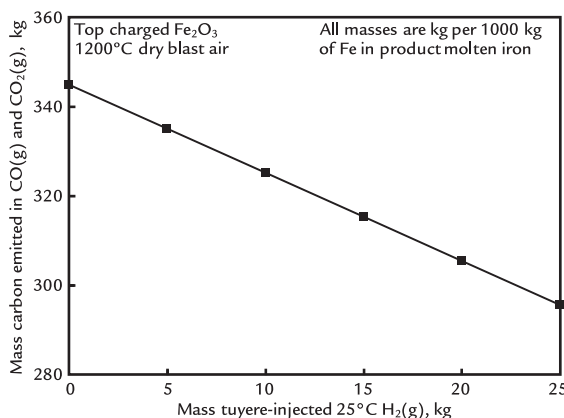


FIGURE 46.3 Effect of H_2 injection on top gas carbon emission. Carbon emission decreases by $\sim 2 \text{ kg}$ per kg of injected $\text{H}_2(\text{g})$. This indicates that injection of electrolytically produced $\text{H}_2(\text{g})$ can substantially reduce carbon emissions assuming wind, solar cell, hydroelectric, and/or nuclear electricity production are used to make the $\text{H}_2(\text{g})$.

steady-state production of 1500°C molten iron. The value with 20 kg of $\text{H}_2(\text{g})$ injection is 353 kg C-in-coke/1000 kg of Fe in product molten iron (Cell AC19).

This and other values are plotted in Fig. 46.4 which shows, as expected, that C in top-charged coke requirement decreases with increasing hydrogen injection.

46.7 SUMMARY

This chapter shows how to include 25°C $\text{H}_2(\text{g})$ tuyere injection in our top gas calculations. It requires no changes to our $\text{CH}_4(\text{g})$ -injection top gas temperature calculation spreadsheet and only three minor changes to our bottom-segment matrix.

Tuyere-injection of $\text{H}_2(\text{g})$ reduces top gas carbon emissions by $\sim 2 \text{ kg}/\text{kg}$ of injected $\text{H}_2(\text{g})$. This is because the injected hydrogen does some of the blast furnace's Fe_2O_3 to

Fe reduction, thereby lowering the need for top charged C-in-coke.

Like all injectants, except O₂, hydrogen injection increases top gas temperature. This is due to all of our equations, but we may speculate that the increase is at least partially due to decreasing (cool) C in top-charged coke requirement of Fig. 46.4.

EXERCISES

- 46.1.** Please calculate top gas temperature of [Table 46.1](#)/[Table 46.2](#) blast furnace, C in CO(g) + CO₂(g) top gas emission, and top charge C-in-coke requirement with

30 kg of 25°C H₂(g) injection. Please use two methods of calculation.

- 46.2.** The blast furnace operating team of [Table 46.1](#)/[Table 46.2](#) wants a 200°C top gas temperature. How much H₂(g) (kg per 1000 kg of Fe in product molten iron) must the team inject to obtain this temperature. Please calculate this for them using two methods of calculation.
- 46.3.** The blast furnace operating team of [Table 46.1](#)/[Table 46.2](#) wants to lower its top gas temperature - without (1) changing its H₂(g) injection quantity (20 kg) or (2) injecting any other substance. How can they do this? Please examine the specific case of 210°C top gas.

CO(g) Injection Into Bottom and Top Segments

O U T L I N E

47.1 Objectives of CO(g) Injection	442	47.4 Summary of CO(g) Injection Into the Bottom Segment	445
47.2 Bottom-Segment Equations With CO(g) Injection	442	47.5 Calculation Strategy of CO(g) Injection Into Top Segment	445
47.2.1 Bottom-Segment CO(g) Injectant Quantity Specification Equation	442	47.6 Coke Requirement With Top-Segment CO(g) Injection	446
47.2.2 Carbon Mass Balance Equation With CO(g) Injection	442	47.7 Calculation Results of CO(g) Injection Into Top Segment	450
47.2.3 Oxygen Mass Balance Equation With CO(g) Injection Into Bottom Segment	443	47.8 Discussion and Conclusion of CO(g) Injection Into Top Segment	450
47.2.4 Enthalpy Balance Equation With CO(g) Injection Into Bottom Segment	443	47.9 Summary	450
47.3 Calculation Results of CO(g) Injection Into Bottom Segment	443	Exercises	451
47.3.1 Total Carbon Input	445	Reference	451

47.1 OBJECTIVES OF CO(g) INJECTION

As of 2019, carbon monoxide was *not* being injected into industrial iron blast furnaces. Its use is being discussed to minimize carbon emissions. The first half of this chapter examines tuyere injection of 50 kg of 25°C CO(g). Our objectives for the first half of the chapter are to;

1. show how CO(g) injection is included in our bottom-segment calculations, and
2. determine the effect of CO(g) injection on the amount of C-in-coke that is needed to steadily produce 1500°C molten iron.

The objective of the second half of this chapter is to calculate the amount of C-in-coke that will be saved by injecting 80 kg of CO(g) into a blast furnace's top segment, Fig. 47.1.

As the figure shows, CO(g) is injected through a row of tuyeres just above the conceptual top-segment-bottom-segment division. This gives

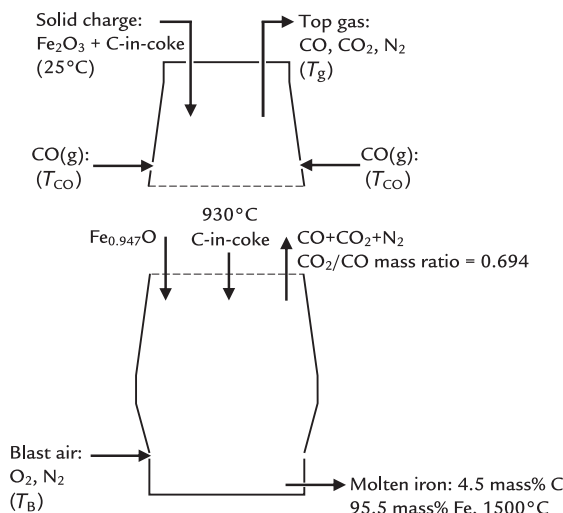


FIGURE 47.1 Sketch of conceptually divided blast furnace with top-segment CO(g) injection. There is no bottom-segment injection. We specify that none of the top-injected CO(g) eddies back into the bottom segment. The CO(g) enters the blast furnace top segment through tuyeres placed around the top-segment circumference.

the CO(g) every opportunity to ascend and react to its fullest possible extent. None of the CO(g) eddies back into the bottom segment because the strong upward gas flow drags it all upward.

47.2 BOTTOM-SEGMENT EQUATIONS WITH CO(g) INJECTION

Fig. 47.2 shows bottom-segment flows with CO(g) injection at a rate of 50 kg/1000 kg Fe in product molten iron. We now develop equations to describe these flows.

47.2.1 Bottom-Segment CO(g) Injectant Quantity Specification Equation

CO(g) injection quantity of Fig. 47.2 is represented by changing the C(s) injection Eq. (8.1) of Chapter 8, Bottom Segment with Pulverized Carbon Injection, to:

$$50 = \left[\frac{\text{mass tuyere}}{\text{injected CO(g)}} \right] * 1 \quad (47.1)$$

47.2.2 Carbon Mass Balance Equation With CO(g) Injection

With CO(g) injection instead of C(s) injection, C balance Eq. (8.3) of Chapter 8, Bottom Segment with Pulverized Carbon Injection, becomes;

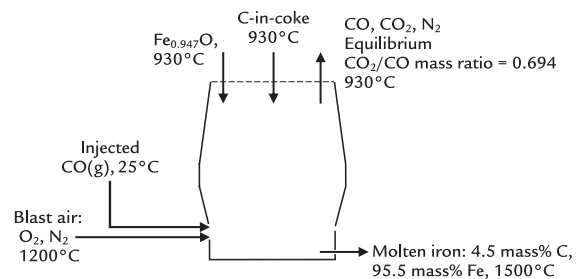


FIGURE 47.2 Conceptual blast furnace bottom segment with CO(g) injection. The blast air enters the furnace at 1200°C, the injected CO(g) at 25°C.

$$\begin{aligned}
 0 = & - \left[\begin{array}{l} \text{mass tuyere} \\ \text{injected CO(g)} \end{array} \right] * 0.429 - \left[\begin{array}{l} \text{mass C in} \\ \text{descending coke} \end{array} \right] * 1 \\
 & + \left[\begin{array}{l} \text{mass CO out} \\ \text{in ascending gas} \end{array} \right] * 0.429 \\
 & + \left[\begin{array}{l} \text{mass CO}_2 \text{ out} \\ \text{in ascending gas} \end{array} \right] * 0.273 \\
 & + \left[\begin{array}{l} \text{mass C out} \\ \text{in molten iron} \end{array} \right] * 1
 \end{aligned} \tag{47.2}$$

where $0.429 = 42.9 \text{ mass\% C in CO}/100\%$

$$\begin{aligned}
 -320 = & -[\text{mass tuyere injected CO(g)}] * (-3.946) \\
 & - [\text{mass Fe}_{0.947}\text{O into bottom segment}] * (-3.152) \\
 & - [\text{mass C in descending coke}] * 1.359 \\
 & - [\text{mass O}_2 \text{ in blast air}] * 1.239 \\
 & - [\text{mass N}_2 \text{ in blast air}] * 1.339 \\
 & + [\text{mass Fe out in molten iron}] * 1.269 \\
 & + [\text{mass C out in molten iron}] * 5 \\
 & + [\text{mass CO gas out in ascending gas}] * (-2.926) \\
 & + [\text{mass CO}_2 \text{ gas out in ascending gas}] * (-7.926) \\
 & + [\text{mass N}_2 \text{ out in ascending gas}] * 1.008
 \end{aligned} \tag{47.4}$$

where -3.946 is $H_{25^\circ\text{C}}^{\circ}/\text{MW}_{\text{CO}}$, MJ/kg of CO(g),
Table J.1.

47.2.3 Oxygen Mass Balance Equation With CO(g) Injection Into Bottom Segment

With CO(g) injection, O balance of Table 8.1, Eq. (7.3) becomes;

$$\begin{aligned}
 0 = & - \left[\begin{array}{l} \text{mass tuyere} \\ \text{injected CO(g)} \end{array} \right] * 0.571 \\
 & - \left[\begin{array}{l} \text{mass Fe}_{0.947}\text{O into} \\ \text{bottom segment} \end{array} \right] * 0.232 \\
 & - \left[\begin{array}{l} \text{mass O}_2 \\ \text{in blast air} \end{array} \right] * 1 \\
 & + \left[\begin{array}{l} \text{mass CO out} \\ \text{in ascending gas} \end{array} \right] * 0.571 \\
 & + \left[\begin{array}{l} \text{mass CO}_2 \text{ out} \\ \text{in ascending gas} \end{array} \right] * 0.727
 \end{aligned} \tag{47.3}$$

where the first term is new and where $0.571 = 57.1 \text{ mass\% O in CO}/100\%$.

47.2.4 Enthalpy Balance Equation With CO(g) Injection Into Bottom Segment

Lastly, with 25°C CO(g) injection rather than 25°C C(s) injection, the enthalpy balance Eq. (8.5) of Chapter 8, Bottom Segment with Pulverized Carbon Injection, becomes;

47.3 CALCULATION RESULTS OF CO(g) INJECTION INTO BOTTOM SEGMENT

Fig. 47.3 summarizes calculation results of Table 47.1. It shows that CO(g) injection decreases C-in-coke requirement by 0.12 kg/kg of injected CO.

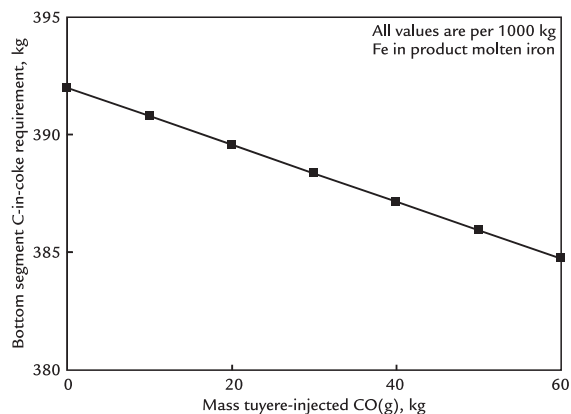


FIGURE 47.3 Effect of 25°C CO(g) injection on amount of C-in-coke required to steadily produce 1500°C molten iron. Injection of 1 kg of CO(g) saves 0.12 kg of C-in-coke. The line is straight.

TABLE 47.1 Blast Furnace Bottom-Segment Matrix With Tuyere Injection of 25°C CO(g)

	A	B	C	D	E	F	G	H	I	J	K	L	M
1	BOTTOM SEGMENT CALCULATIONS												
2	Equation	Description	Numerical term	mass Fe _{0.947} O into bottom segment	mass C in descending coke	mass O ₂ in blast air	mass N ₂ in blast air	mass Fe out in molten iron	mass C out in molten iron	mass CO out in ascending gas	mass CO ₂ out in ascending gas	mass N ₂ out in ascending gas	mass tuyere-injected CO(g)
3	7.7	Fe out in molten iron specification	1000	0	0	0	0	1	0	0	0	0	0
4	7.2	Fe mass balance	0	-0.768	0	0	0	1	0	0	0	0	0
5	47.3	O mass balance	0	-0.232	0	-1	0	0	0	0.571	0.727	0	-0.571
6	47.2	C mass balance	0	0	-1	0	0	0	1	0.429	0.273	0	-0.429
7	7.5	N mass balance	0	0	0	0	-1	0	0	0	0	1	0
8	7.6	N ₂ in air specification	0	0	0	3.3	-1	0	0	0	0	0	0
9	7.9	Equilibrium CO ₂ /CO mass ratio	0	0	0	0	0	0	0	0.694	-1	0	0
10	7.8	C in output iron specification	0	0	0	0	0	0.047	-1	0	0	0	0
11	47.4	Enthalpy balance	-320	3.152	-1.359	-1.239	-1.339	1.269	5	-2.926	-7.926	1.008	3.946
12	47.1	CO(g) injected through tuyeres	50	0	0	0	0	0	0	0	0	0	1
13				930°C	930°C	1200°C	1200°C	1500°C	1500°C	930°C	930°C	930°C	1200°C
14		Calculated values	kg per 1000 kg of Fe in product iron										
15	mass Fe _{0.947} O into bottom segment	1302											
16	mass C in descending coke	386											
17	mass O ₂ in blast air	296	also = mass C in the furnace's coke charge, Eqn. (7.16)										
18	mass N ₂ in blast air	977											
19	mass Fe out in molten iron	1000											
20	mass C out in molten iron	47											
21	mass CO out in ascending gas	583											
22	mass CO ₂ out in ascending gas	404											
23	mass N ₂ out in ascending gas	977											
24	mass tuyere-injected CO(g)	50											

The differences between this matrix and C(s) injection matrix of Table 8.1 are that Chapter 8's, Bottom Segment with Pulverized Carbon Injection; (1) C(s) quantity Eq. (8.1) has been changed to CO(g) injection quantity [Eq. \(47.1\)](#); (2) C balance Eq. (8.3) has been changed to C balance [Eq. \(47.2\)](#); (3) mass balance Eq. (7.3) has been changed to [Eq. \(47.3\)](#); and (4) enthalpy balance Eq. (8.5) has been changed to [Eq. \(47.4\)](#).

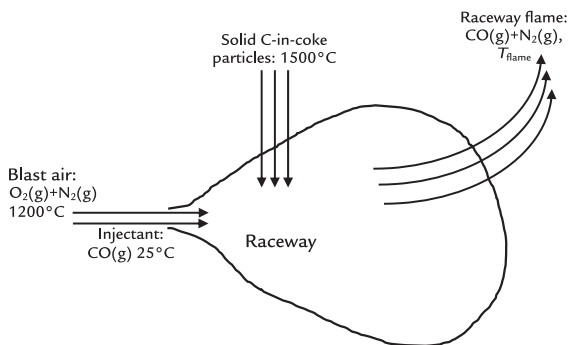


FIGURE 47.4 Tuyere raceway including 25°C CO(g) injection. When compared with Fig. 14.1, the CO(g) is a raceway coolant, which must be offset by combusting additional coke in the raceway.

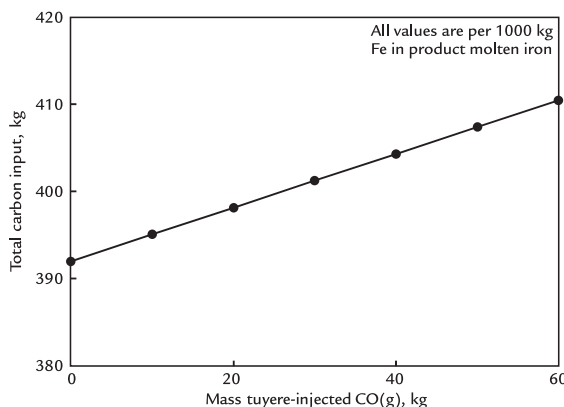


FIGURE 47.5 Total blast furnace carbon input as a function of mass injected CO(g). The increase is notable. An unfortunate consequence of this is an increase in blast furnace carbon emission with increased CO(g) injection. Total input mass C = mass C-in-coke + mass injected CO * (42.9 mass% C in CO/100%). The line is straight. Total carbon requirement increases by 0.31 kg/kg of injected CO(g). This increase could of course be lowered by preheating the tuyere-injected CO(g).

The small size of the saving is difficult to explain, except by all our matrix's equations.

We may speculate that the small coke savings arises because the injected 25°C CO(g) must be heated to the raceway's exit gas (flame) temperature, requiring considerable combustion of C-in-coke, Fig. 47.4.

47.3.1 Total Carbon Input

Fig. 47.5 shows total carbon input with CO(g) injection, that is, mass C-in-coke plus mass C in injected CO. This increases with increasing CO(g) injection. This means that CO(g) injection increases the top gas carbon emissions.

47.4 SUMMARY OF CO(g) INJECTION INTO THE BOTTOM SEGMENT

Tuyere injection of CO(g) is described in matrix form by making four minor changes to C injection matrix Table 8.1.

25°C CO(g) saves 0.12 kg of coke/kg of injected CO(g). It *increases* total carbon input and carbon emissions by 0.31 kg/kg of injected CO(g), all masses per 1000 kg of Fe in product molten iron.

47.5 CALCULATION STRATEGY OF CO(g) INJECTION INTO TOP SEGMENT

Our calculation strategy is to calculate the coke requirement with no CO(g) injection, Fig. 47.6, Tables 20.1 and 20.2.

We start our calculations with bottom- and top-segment matrix Tables 20.1 and 20.2 of Fig. 47.6. They are greatly simplified blast furnace representations with;

1. 1200°C dry blast air;
2. top charged Fe₂O₃ ore and C-in-coke;
3. 1500°C 4.5 mass% C, 95.5 mass% Fe product molten iron; and
4. no gangue, coke ash, flux, or slag.

As can be seen in the in bottom-segment calculated values list of Table 20.1, steady-state production of 1500°C product molten Fe-C iron requires 392 kg of C-in-coke per 1000 kg of Fe in product molten iron. As expected from

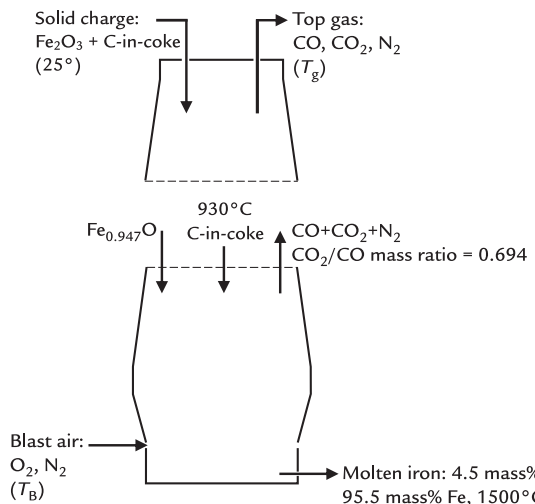


FIGURE 47.6 Fig. 47.1 without top-segment CO(g) injection. It is a combination of Figs. 20.1 and 20.2. The blast air enters the furnace through a row of tuyeres around the bottom-segment circumference.

Eq. (7.16), the top-segment calculated values list of Table 20.2 also shows that steady-state molten iron requires 392 kg of C-in-coke charge per 1000 kg of Fe in product molten iron.

47.6 COKE REQUIREMENT WITH TOP-SEGMENT CO(g) INJECTION

We start our top-segment CO(g) injection calculations with matrix Table 20.1 (Section 47.5).

We can do this because we specify that none of the top-segment-injected CO(g) eddies back into the bottom segment.

Because of this, top-segment CO(g) injection doesn't change any of the bottom-segment equations.

However, it does change the top-segment matrix, Table 47.2.

It requires;

1. a new top-segment variable,

$$\left[\begin{array}{l} \text{mass CO injected} \\ \text{into top segment} \end{array} \right]$$

2. an equivalent new top-segment input CO quantity equation;

$$80 = \left[\begin{array}{l} \text{mass CO injected} \\ \text{into top segment} \end{array} \right] * 1 \quad (47.5)$$

which specifies that 80 kg of CO is being injected into the top segment per 1000 kg of Fe in product molten iron, and

3. changes to the top-segment carbon and oxygen mass balances, which become;

carbon balance

$$0 = - \left[\begin{array}{l} \text{mass CO injected} \\ \text{into top segment} \end{array} \right] * 0.429 - \left[\begin{array}{l} \text{mass C in} \\ \text{coke charge} \end{array} \right] * 1 - \left[\begin{array}{l} \text{mass CO ascending} \\ \text{from bottom segment} \end{array} \right] * 0.429 - \left[\begin{array}{l} \text{mass CO}_2 \text{ ascending} \\ \text{from bottom segment} \end{array} \right] * 0.273 + \left[\begin{array}{l} \text{mass C-in-coke} \\ \text{descending} \end{array} \right] * 1 + \left[\begin{array}{l} \text{mass CO out} \\ \text{in top gas} \end{array} \right] * 0.429 + \left[\begin{array}{l} \text{mass CO}_2 \text{ out} \\ \text{in top gas} \end{array} \right] * 0.273 \quad (47.6)$$

oxygen balance

$$0 = - \left[\begin{array}{l} \text{mass CO injected} \\ \text{into top segment} \end{array} \right] * 0.571 - \left[\begin{array}{l} \text{mass Fe}_2\text{O}_3 \text{ in} \\ \text{furnace charge} \end{array} \right] * 0.301 - \left[\begin{array}{l} \text{mass CO ascending} \\ \text{from bottom segment} \end{array} \right] * 0.571 - \left[\begin{array}{l} \text{mass CO}_2 \text{ ascending} \\ \text{from bottom segment} \end{array} \right] * 0.727 + \left[\begin{array}{l} \text{mass Fe}_{0.947}\text{O} \text{ descending} \\ \text{into bottom segment} \end{array} \right] * 0.232 + \left[\begin{array}{l} \text{mass CO out} \\ \text{in top gas} \end{array} \right] * 0.571 + \left[\begin{array}{l} \text{mass CO}_2 \text{ out} \\ \text{in top gas} \end{array} \right] * 0.727 \quad (47.7)$$

where;

$$0.429 = \frac{42.9 \text{ mass\% C in CO}}{100\%}, \text{ Appendix A, and}$$

TABLE 20.1 Bottom-Segment Calculations With no CO(g) Injection Into Either Segment

TABLE 20.2 Top-Segment Matrix With no CO(g) Injection Into Either Segment

TABLE 47.2 Top-Segment Matrix With 80 kg of CO(g) Into the Top-Segment, Fig. 47.1

$0.571 = \frac{57.1 \text{ mass\% O in CO}}{100\%}$, Appendix A.

The first terms in Eqs. (47.6) and (47.7) are new.

Matrix Table 47.2 shows these changes, Rows 13, 6, and 5.

47.7 CALCULATION RESULTS OF CO(g) INJECTION INTO TOP SEGMENT

Interestingly, top-segment calculated values table (Table 47.2) shows that the C-in-coke requirement is unchanged by top-segment CO(g) injection. It remains as in Tables 20.1 and 20.2, that is, 392 kg of C-in-coke per 1000 kg of Fe in product molten iron.

So where does the 80 kg of injected CO go?

We can answer this by comparing Table 20.2 and Table 47.2 top-segment calculated values tables, which shows that;

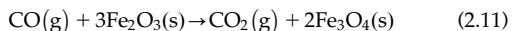
1. mass CO in top gas of Table 20.1 is 333 kg/1000 kg of Fe in product molten iron, and
2. mass CO in top gas of Table 47.2 is 413 kg/1000 kg of Fe in product molten iron.

So, we can conclude that the 80 kg of injected CO(g) rises unreacted through the top segment.

This is consistent with the unchanged C-in-coke requirement, described above, and the same mass CO₂ in top gas values in both top-segment matrix tables.

47.8 DISCUSSION AND CONCLUSION OF CO(g) INJECTION INTO TOP SEGMENT

The last iron oxide that the ascending CO(g) encounters high in the furnace is Fe₂O₃(s). The CO(g) tries to reduce this Fe₂O₃(s) to Fe₃O₄(s). The reaction is:



It takes place at $\sim 100^\circ\text{C}$, the charge level temperature.

At this temperature and in equilibrium, this reaction would go virtually to completion (Appendix W), that is, the carbonaceous portion of the top gas would be nearly 100% CO₂(g).

However, industrial top gas contains considerable CO(g), even without top-segment CO(g) injection, see Table 1.1.

We can conclude that;

1. the gas rising from the bottom segment contains more than enough CO for Fe₂O₃ reduction, and
2. any addition of more CO(g) to the top segment will just be wasted.

This is confirmed by matrix calculations of this chapter.

47.9 SUMMARY

We have shown using our model that with tuyere injection of CO(g) at 25°C ;

- the coke rate is reduced by 0.12 kg coke per kg of injected CO(g), and
- the overall carbon rate increases by 0.31 kg/kg of injected CO(g) per 1000 kg of Fe in product molten iron.

Injection of CO(g) at 25°C into the top segment had no impact on the coke rate, the CO(g) just passed through the top segment without reducing any iron ore.

To reduce the coke usage via CO(g) injection through the tuyeres, the CO(g) must be heated to the maximum temperature possible. To minimize carbon usage, the heating energy should come from a fuel source with as low as possible carbon content.

CO(g) injected into the top segment must be injected at the thermal reserve temperature,

930°C to reduce any iron oxides in the top segment. The CO(g) should also be heated using a low carbon containing fuel source.

Europe's Ultra-Low CO₂ Steelmaking Consortium (ULCOS) successfully injected CO (g) into the experimental blast furnace located in MEFOS, Sweden. Blast furnace top gas was processed in vapor pressure swing absorption plant, and CO and CO₂ rich streams were produced. The refined CO-rich gas contained a significant amount of H₂ and some N₂. This mixture was injected at both tuyere and shaft elevations at 1200°C and 900°C. Blast air was eliminated, and coal and oxygen were injected through the tuyeres at ambient temperature. The experimental blast furnace coke rate and carbon emissions were reduced.¹

Our model calculations confirm the necessity to heat the CO(g) prior to injection to have any meaningful impact on the blast furnace coke and carbon rates. The model can be adjusted to reflect the practice used by ULCOS starting with the matrices prepared in Chapters 45–47.

At the time of writing this book, ULCOS had not advanced the technology to separate CO and CO₂ in top gas and inject the CO-rich portion into the blast furnace. This was in part due to the complexity and cost of modifying the blast furnace off-gas system. Also, the CO₂-rich portion of the refined top gas must be sequestered underground to achieve the 50% CO₂ reduction that the ULCOS team proposed to achieve. Sequestering was not possible due

to excessive costs to deliver the CO₂ rich to a suitable geological area that can absorb and retain the CO₂ for an indefinite period.

EXERCISES

- 47.1. Fig. 47.1 blast furnace team wishes to increase its CO(g) injection to 70 kg/1000 kg of Fe in product molten iron.

Please predict for them the amounts of;

- C-in-coke,
- (C-in-coke + C-in-CO injectant), and
- blast air

that will be needed to steadily produce 1500°C molten iron with this amount of CO(g) injection. Please express your answers per 1000 kg of Fe in product molten iron.

- 47.2. This chapter concludes that top-segment CO(g) injection doesn't save coke. For what other ironmaking purpose could this CO(g) be used?
- 47.3. Why don't we have to specify CO(g) injection temperature in top-segment calculations of this chapter.

Reference

1. Cameron I. A., The iron blast furnace theory and practice – 35 years later. In: *53rd annual conference of metallurgists (COM 2014)*, metallurgical society of the Canadian Institute of Mining and Metallurgy. Vancouver; 2014.

Introduction to Blast Furnace Optimization

O U T L I N E

48.1 Introduction to Optimization	453	48.4 Need for Blast Furnace Optimization	457
48.2 Constraining the Optimization	454	48.5 Optimizing Operations Using the Blast Furnace Model	457
48.3 Optimization Techniques	455	48.5.1 Objective Function	458
48.3.1 Linear Optimization	455	48.5.2 Manipulated Variables	458
48.3.2 Nonlinear Optimization	456	48.5.3 Constraints	458
48.3.3 “Guess and Check” Algorithms	456	48.6 Summary	459
48.3.4 Comparison of Optimization Techniques	457	Exercises	459

48.1 INTRODUCTION TO OPTIMIZATION

Previous chapters have provided details on how to develop a heat and mass balance model of a blast furnace operation. The algebraic nature of the blast furnace model lends itself to be optimized using conventional techniques. This chapter aims to;

- introduce the concept and theory of optimization;

- explain why optimization is necessary for blast furnace operations; and
- introduce how to optimize blast furnace operations using the model developed in this book.

Most people will have an example of something they wish to improve or optimize. Perhaps there is a baking recipe where you'd like to get the best taste or shortest preparation time; or on your trip to work or school, you would like to take the fastest route possible.

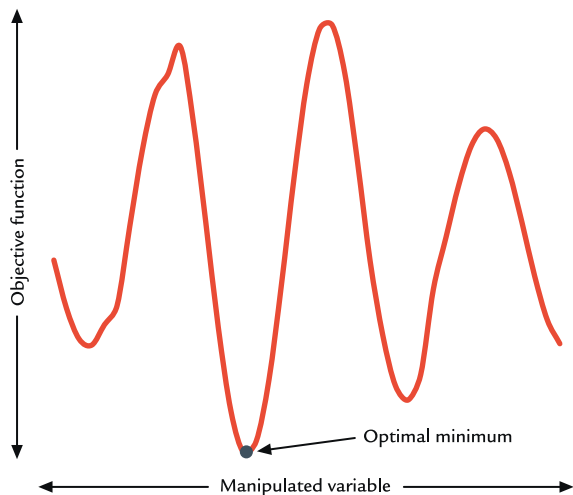


FIGURE 48.1 Example of an optimization problem highlighting the location of the optimal minimum value for a given objective function.

These are examples of optimization - getting the best possible outcome out of an operation, a situation, or a resource.

All forms of optimization have two main components:

1. Objective function—The variable that is to be optimized. In the above examples, this would be taste, preparation time, or travel time.
2. Manipulated variables—The variables that can be changed to reach the optimal point. In the above baking example, these could be things such as ingredient amount, baking time, baking temperature, etc.

The goal of every optimization exercise is to get the ideal or optimal result in the objective function by changing the manipulated variables. The optimization can be to maximize or minimize the objective function, such as maximize taste in our baking example or minimize travel time in our commuting example. An illustration of a minimization optimization problem is provided in Fig. 48.1.

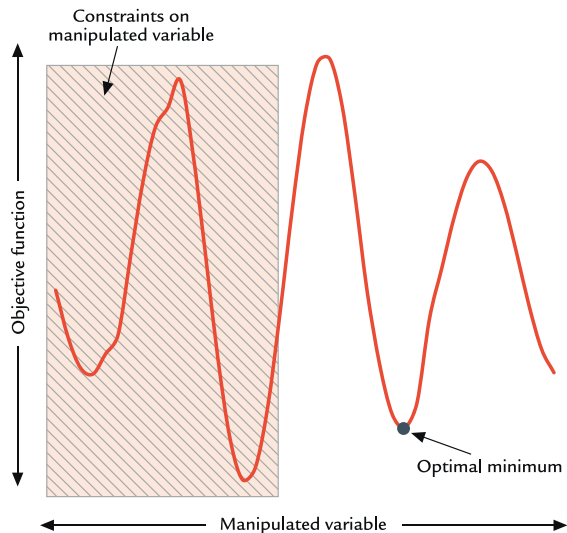


FIGURE 48.2 Example of an optimization problem with direct constraints on the manipulated variables. The location of an optimal minimum value for the constrained objective function is highlighted and differs from the true minimum of the objective function.

The objective function has a wide variety of peaks and valleys, with the lowest objective function value, the optimal minimum, located at the highlighted point.

48.2 CONSTRAINING THE OPTIMIZATION

A third component of most optimizations is constraints. In the baking example, there may be a minimum amount of flour that must be added or there may be a maximum acceptable level of sugar. These represent constraints, properties that cannot be outside of specific ranges during the optimization. The example constraints put restrictions on the acceptable range for the manipulated variables and may change the location of the acceptable optimal value. An expansion of the previous illustration highlighting the effect of manipulated variable constraints is provided in Fig. 48.2.

The previous optimal minimum lies in the constrained area of the manipulated variable. This means that a new optimal minimum must be found, one that does not violate the constraints.

Constraints do not need to be related to either the objective function or the manipulated variables - they can be variables that are measured but not directly controlled and are not the objective function. For the baking example, perhaps there is a restriction on the size of the baked good or there may be a minimum quantity that must be made, or the preparation time is fixed. These represent constraints that limit the acceptable range of the manipulated variables, but perhaps not in an obvious way. An expansion of the previous illustration highlighting the effect of constraint not directly applied to the manipulated variables is provided in Fig. 48.3.

The new constraint does not simply limit the manipulated variable to a specific range; it

restricts the acceptable area in a way that is not necessarily obvious. Once again, the new constraint makes the previous optimal minimum invalid and a new minimum is found that does not violate the constraints.

48.3 OPTIMIZATION TECHNIQUES

Mathematical optimization can be completed in a variety of ways depending on the nature of the problem. The main techniques are;

- linear optimization - for solving simple linear systems;
- nonlinear optimization - for solving relatively simple nonlinear systems; and
- “guess and check” algorithms - for solving complex systems.

The following sections provide a brief overview of each technique, its uses, and limitations.

48.3.1 Linear Optimization

As the name implies, linear optimization is employed for optimizing linear problems. For all linear systems, the global optimum, that is, the optimum solution of the whole function given the constraints, is at an “extreme point.” This is a point where one or more of the constraints is at its limit. As a result, the number of points that can be the optimum solution is dramatically limited. This allows for quick identification by evaluating all the feasible solutions. A widely used linear optimization algorithm is the simplex method; it uses a method like that described above. While linear programming can quickly identify the global optimum, it can only be applied to linear systems, that is a system entirely made of linear equations. Very few practical problems can be reduced to a simple system of linear equations, thus linear optimization is not widely used for “real-world” applications.

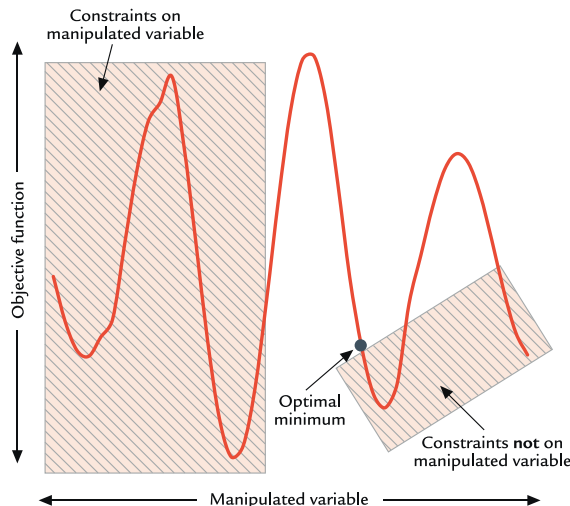


FIGURE 48.3 Example of an optimization problem with direct and indirect constraints on the manipulated variables. The location of an optimal minimum value for the constrained objective function is highlighted and is different than both the true minimum and the manipulated variable minimum constraint.

48.3.2 Nonlinear Optimization

Nonlinear optimization, as the name implies, is used for optimizing nonlinear problems. This makes up the clear majority of problems encountered when solving engineering problems. Nonlinear optimization follows the method of “steepest descent.” The algorithm will analyze the change of the objective function with respect to each manipulated variable and change the variables in the direction that increases or reduces the objective function, depending on whether one is maximizing or minimizing, as dramatically as possible. The optimization will stop when the algorithm comes to a point where either increasing or decreasing any of the manipulated variables causes a negative effect on the objective function. For example, if the objective function was to be minimized, the optimization will stop when changing any variable causes an increase in the objective function. Meanwhile if the objective function was to be maximized, the optimization will stop when changing any variable causes a decrease in the objective function.

At this point, the algorithm is at a *local* optimum and further optimization ends. Nonlinear optimization methods are not guaranteed to reach *global* optimums and are highly dependent on the starting point of the algorithm. A

mathematical equation/expression of the objective function is also required, which is not necessarily the case for empirical or “black box” systems.

48.3.3 “Guess and Check” Algorithms

The “guess and check” methods are optimization techniques that mirror the methods that most people, either intentionally or unintentionally, employ when doing daily optimizations. A variety of combinations of the manipulated variables, called points, are evaluated. Based on the objective function values of all points, slight modifications are made to the values of the manipulated variables of each point to bring it slightly closer to the location of the current optimal point. This process is repeated until all points converge to a single location, which is a *local* optimum. A depiction of the iterative process is provided in Fig. 48.4.

The benefit of the “guess and check” algorithms are that they are more likely to find the global optimum (although not guaranteed) and are less sensitive to the starting locations of the points as the wide variety of points lead to an increase in algorithm robustness. These methods do not require the objective function

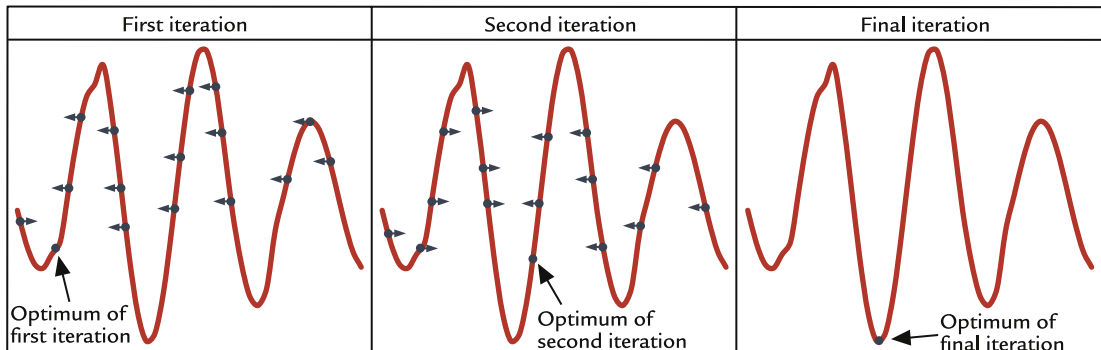


FIGURE 48.4 Depiction of how the “guess and check” algorithms converge on a local optimum location. Arrows on each point indicate the direction they move on the x -axis in order to get closer to the currently identified optimal location.

TABLE 48.1: Pros and Cons of the Most Common Optimization Techniques

	Linear Optimization	Nonlinear Optimization	"Guess and Check" Methods
Pros	<ul style="list-style-type: none"> • Quick identification of optimum • Finds the <i>global</i> optimum location 	<ul style="list-style-type: none"> • Able to handle nonlinear systems • Relatively fast for nonlinear systems 	<ul style="list-style-type: none"> • Able to handle nonlinear systems • Robust—more likely to find <i>global</i> optimum and less sensitive to starting location • Can solve “black box” systems
Cons	<ul style="list-style-type: none"> • Only valid for linear systems 	<ul style="list-style-type: none"> • Finds <i>local</i> optimum, not guaranteed to be the global optimum • Highly dependent on starting location • Requires mathematical description of the objective function 	<ul style="list-style-type: none"> • Only guaranteed to find <i>local</i> optimum • Relatively slow algorithm

to be known and can optimize “black box” systems. The downside of the “guess and check” algorithms is its considerable number of points and related iterations which require time for an optimal value to be found.

48.3.4 Comparison of Optimization Techniques

There are optimization techniques beyond these three that can be used; however, these three cover the majority of optimization solving techniques. A table comparing the pros and cons of each technique is provided in [Table 48.1](#).

might differ, the underlying need for blast furnace optimization is the same. *Blast furnace operators want to get the best possible performance given their system inputs and their operating constraints.*

Many operators find that the “best possible performance” is highly dependent on how they define “best.” Is it best to minimize coke rate, minimize cost, maximize production, or minimize CO₂(g) emissions? There is no universal answer, and blast furnaces may vary their operating point based on economic and/or market factors. In Chapter 49, we will investigate optimizing the same blast furnace with varying constraints and objective functions.

48.4 NEED FOR BLAST FURNACE OPTIMIZATION

As with all industries, blast furnace operators are constantly optimizing their performance. Operating at suboptimal conditions leads to reduced performance and always offers areas for improvement. While the parameter to be optimized for each blast furnace, or at varying times for the same furnace,

48.5 OPTIMIZING OPERATIONS USING THE BLAST FURNACE MODEL

As you have worked your way through this book, you have developed a detailed model that can predict blast furnace operations given a wide variety of inputs. The model can be used to optimize the blast furnace operation using the techniques outlined above. We will

look at each individual aspect of optimization to determine how to implement it for the blast furnace model.

Please note, as the model was developed in Excel, we have assumed that the Solver Add-In is available to perform optimization calculations. If you developed the blast furnace model in an alternative software, then you will need to determine how to optimize using that software.

The complexity of the blast furnace yields a nonlinear system; therefore, the simplex method of linear optimization cannot be used. The “Generalized Reduced Gradient (GRG) Nonlinear” optimization method available in Solver offers a method to optimize nonlinear systems that will be described in the remainder of this book.

48.5.1 Objective Function

The objective function is entirely dependent on the purpose of the optimization. It can be something calculated directly by the model, such as C-in-coke per 1000 kg Fe in product molten iron, or it can be something calculated based on the model results, such as productivity, total fuel rate, or total slag rate.

There are some circumstances where the objective function can be to optimize an input; however, this is not common. An example of this is maximizing the pulverized coal injection (PCI) rate while maintaining a variety of system constraints. Again, this is unlikely because the reason to maximize PCI rate is likely driven by something else, such as minimizing coke rate or maximizing productivity.

As previously stated, the goal of the optimization can be to maximize or minimize this objective function and should be set up accordingly.

When using the Solver Add-In in Excel, the objective function is placed in the “Set Objective” part of the interface and should refer to the cell *by name* (e.g., B3) containing the parameter to be optimized.

48.5.2 Manipulated Variables

The manipulated variables are dependent on the nature of the optimization. The one limitation is that the manipulated variables must be an input to the model rather than an output. The likely manipulated variables are injectant rates; however, one can also manipulate the desired slag chemistry, raw material properties, or any combination of the blast furnace model inputs.

When using the Solver Add-In in Excel, the manipulated variables are placed in the “By Changing Variable Cells” part of the interface. This section can refer to any number of cells and should only refer to the cells that are to be varied to optimize the objective function.

48.5.3 Constraints

Unlike the objective function and the manipulated variables, the optimization constraints are not required to be only model inputs or model outputs. The optimization can be constrained by any number and any combination of parameters. Perhaps you wish to vary the rate of natural gas injection; however, you are limited to 50 kg/1000 kg Fe in product molten iron due to supply restrictions. This represents a constraint on an input.

Top gas temperature and flame temperature are output variables that are very commonly constrained in blast furnace operations. They both have maximum and minimum values that must be maintained to protect blast furnace equipment and allow stable operations. These ranges represent constraints on a model output.

When using the Solver Add-In in Excel, the constraints are added to the “Subject to the Constraints” section of the interface. There are no limitations to the type and quantity of constraints that can be added. This book will only contain range constraints (greater than or equal to, less than or equal to, equals) and will

refrain from using binary or integer constraints. This is because the manipulated variables used are not binary (i.e., on or off) and do not need to be integer values.

In addition, the “Make Unconstrained Variables Non-Negative” box should be checked as this limits the manipulated variables to positive values. If somehow your manipulated variable can practically be negative, then this box should be unchecked; however, the nonnegative constraint is typically a physical constraint that must be met, that is, you cannot have a negative PCI rate.

48.6 SUMMARY

This chapter introduces optimization, why it is needed for blast furnace operations, and how to use the model developed in this book to complete blast furnace optimization studies.

In Chapter 49, Blast Furnace Optimization Case Studies, we will use these optimization techniques to evaluate some typical case studies and determine how blast furnace operations differ when trying to optimize different parameters.

EXERCISES

- 48.1. Suppose you are planning a business trip to multiple cities and want to minimize the amount of time you are flying in the air. You must go to five different cities (A, B, C, D, and E), but the order does not matter. In this example, what are the;
- objective function(s),
 - manipulated variable(s), and
 - constraint(s).

- 48.2. You are trying to optimize a system that is defined by the following set of equations. All of the variables (A, B, and C) must be between -10 and 10, inclusively:

$$0.5A - B = 2$$

$$A + B - C = \text{Manipulated variable}$$

$$5B + C = 4$$

$$\text{Objective function} = A + B + C$$

What optimization technique would be best for this system if you wanted to find an optimal (minimum) solution quickly? Will the solution be globally optimal or locally optimal?

BONUS What is the optimal value for the manipulated variable and objective function?

- 48.3. There is a new constraint added to Exercise 2, and it is:

$$A * B < 100$$

Does your answer from Exercise 2 change? If so, how?

- 48.4. You are a blast furnace operator, and your general manager indicates that she thinks there is room for improvement. Your coke plant is currently underperforming, so you need to reduce the coke rate as much as possible. Your general manager wants to increase pulverized coal injection (PCI) rate but is concerned that the available oxygen supply will limit the ability to increase the PCI rate as additional O₂ injection is also needed to maintain a minimum flame temperature. In this example, what are the;
- objective function(s),
 - manipulated variable(s), and
 - constraint(s).

Blast Furnace Optimization Case Studies

O U T L I N E

49.1 Case Study 1 - Minimizing Coke Rate Using Pulverized Coal Injection (PCI) and Oxygen	461	<i>49.3.2 Initial Conditions</i>	467
49.1.1 Objective Function, Constraints, and Manipulated Variables	462	49.3.3 Optimization Results and Analysis	468
49.1.2 Initial Conditions	462	49.4 Case Study 4 - Minimizing CO₂(g) Emissions Using PCI, Natural Gas, and Oxygen	469
49.1.3 Optimization Results and Analysis	462	49.4.1 Objective Function, Constraints, and Manipulated Variables	469
49.2 Case Study 2 - Minimizing Coke Rate Using Natural Gas and Oxygen	464	49.4.2 Initial Conditions	470
49.2.1 Objective Function, Constraints, and Manipulated Variables	464	49.4.3 Optimization Results and Analysis	470
49.2.2 Initial Conditions	465	49.5 Comparison of the Optimization Case Studies	471
49.2.3 Optimization Results and Analysis	465	49.6 Summary	471
49.3 Case Study 3 - Minimizing Fuel Costs Using PCI, Natural Gas, and Oxygen	467	Exercises	472
49.3.1 Objective Function, Constraints, and Manipulated Variables	467		

49.1 CASE STUDY 1 - MINIMIZING COKE RATE USING PULVERIZED COAL INJECTION (PCI) AND OXYGEN

Chapter 48, Introduction to Blast Furnace Optimization, provided a background on

optimization techniques, how it applies to blast furnace operations, and how it can be used with the model developed in this book. In this chapter, we will complete several blast furnace optimization case studies and analyze the different operating conditions that result from the optimization analysis approach.

As mentioned in Chapter 48, optimizations were all performed using Excel Solver's Add-In. The Generalized Reduced Gradient (GRG) Nonlinear setting was used due to the nonlinear nature of the blast furnace model.

Blast furnace operators typically wish to reduce coke rate as much as possible due to its excessive cost. In Chapter 37, Bottom-Segment Calculations With Pulverized Coal Injection, we learned that one method to replace coke is to inject pulverized coal (PCI) through the tuyeres. While PCI does replace coke, it also reduces flame temperature and increases top gas temperature. Both temperatures should be within specified ranges to avoid adverse effects during blast furnace operations. As a result, blast furnace operators optimize their PCI rate to reduce coke consumption as much as possible while maintaining the flame temperature and the top gas temperature within their acceptable ranges.

In this case study, the coke rate will be minimized using PCI and O₂(g) injection while the flame temperature and top gas temperature will be constrained to remain within specific ranges.

49.1.1 Objective Function, Constraints, and Manipulated Variables

The objective function will be to minimize the C-in-coke charge, which is a factor directly calculated by the blast furnace model. The

TABLE 49.1 Optimization Case Study 1 Constraints

Parameter	Unit	Minimum Value	Maximum Value
Flame temperature	°C	2100	2300
Top gas temperature	°C	110	150
PCI injection	kg/t Fe in hot metal	0	150

constraints for the optimization are provided in [Table 49.1](#).

As subsequently explained in Chapter 56, Blast Furnace Fuel Injection, the flame temperature and top gas temperature are constrained within these ranges to avoid issues with blast furnace operations and associated equipment. For this case study, the PCI is limited to a maximum value due to the capacity of the coal preparation plant.

The manipulated variables for the optimization are the injection rates of PCI and O₂(g) at the tuyere level.

49.1.2 Initial Conditions

For case study 1, the blast furnace is operating under the conditions provided in [Table 49.2](#). This table provides values for all model inputs parameters.

For these initial conditions, the resulting coke rate, flame temperature, and top gas temperature are as shown in [Table 49.3](#).

All constraints are satisfied for the nominated initial conditions. It is unlikely that this represents the minimum coke rate.

49.1.3 Optimization Results and Analysis

The coke rate minimization, subject to the constraints outlined above, yields the results shown in [Table 49.4](#).

The results of the optimization indicate that two of the constraints are at their extremes. The PCI injection is at its maximum, while the flame temperature is at its minimum. This can be explained by evaluating an “operating window” using PCI and O₂(g) (see the solid red area in [Fig. 49.1](#)) and comparing that to how the coke rate responds to changes in PCI and O₂(g) injection (see the dashed lines in [Fig. 49.1](#)).

[Fig. 49.1](#) indicates that the coke rate is at its lowest with a high PCI rate and corresponding O₂(g) injection rate to control top and flame

TABLE 49.2 Optimization Case Study 1 Initial Conditions

Parameter	Value	Unit
HEAT LOSS		
Wüstite reduction zone heat loss	320	MJ/t Fe in hot metal
Top segment heat loss	80	MJ/t Fe in hot metal
TUYERE INJECTION		
PCI injection	80	kg/t Fe in hot metal
O ₂ (g) injection	0	kg/t Fe in hot metal
H ₂ O injection	15	g/Nm ³ dry air
BLAST FURNACE TEMPERATURES		
Thermal reserve zone temperature	930	°C
Blast temperature	1200	°C
Hot metal temperature	1500	°C
Slag temperature	1500	°C
Top charge temperature	25	°C
COKE COMPOSITION		
SiO ₂ - dry basis	7	wt%
Al ₂ O ₃ - dry basis	3	wt%
C - dry basis	90	wt%
Moisture content	5	wt%
SLAG COMPOSITION		
Al ₂ O ₃	10	wt%
CaO	41	wt%
MgO	10	wt%
SiO ₂	39	wt%
PCI COMPOSITION		
Coal mass on a dry, ash-free basis (daf)	92.0	wt%
Al ₂ O ₃	2.4	wt%
SiO ₂	5.6	wt%
C	88.0	wt% daf basis%

(Continued)

TABLE 49.2 (Continued)

Parameter	Value	Unit
H	6.0	wt% daf basis %
O	5.0	wt% daf basis %
N	1.0	wt% daf basis %
HOT METAL COMPOSITION		
C	4.5	wt%
Si	0.4	wt%
Mn	0.5	wt%
Mn partition	90.0	%fed reporting to hot metal
ALL TOP CHARGE MATERIAL		
Moisture content	5.0	wt%

TABLE 49.3 Case Study 1 Key Output Initial Conditions

Parameter	Value	Unit
C-in-coke charge	363	kg/t Fe in Hot Metal
Flame temperature	2146	°C
Top gas temperature	111	°C

TABLE 49.4 Case Study 1 Outputs

Parameter	Unit	Case 1 Values	Minimum Value	Maximum Value
OBJECTIVE FUNCTION				
C-in-coke charge	kg/t Fe in hot metal	305	—	—
MANIPULATED VARIABLES				
PCI injection	kg/t Fe in hot metal	150	0	150
O ₂ (g) injection	kg/t Fe in hot metal	32.6	—	—
CONSTRAINTS				
Flame temperature	°C	2100	2100	2300
Top gas temperature	°C	129	110	150

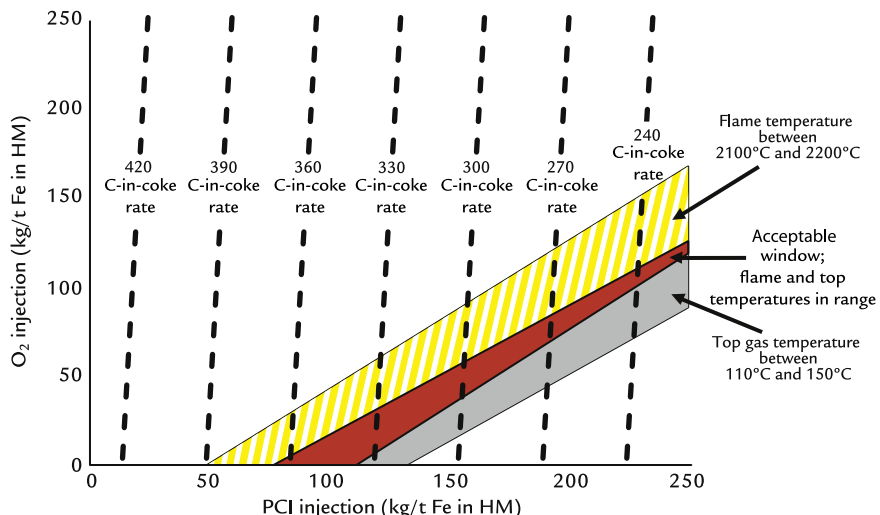


FIGURE 49.1 Blast furnace operating window for PCI and $O_2(g)$ injection.

temperatures. The figure also indicates that high PCI rates and low $O_2(g)$ rates will lead to very high top gas temperatures and, potentially, flame temperatures less than the minimum value of 2100°C . In this optimization, the lowest coke rate would therefore be with the maximum amount of PCI and the minimum amount of $O_2(g)$ required to satisfy all constraints. The major constraint is the PCI injection that is limited to $150 \text{ kg/t Fe in hot metal (HM)}$ due to equipment limitations. The $O_2(g)$ injection can be increased until the flame temperature is in the appropriate range and should not be further increased as higher $O_2(g)$ injection rates result in higher coke requirements.

49.2 CASE STUDY 2 - MINIMIZING COKE RATE USING NATURAL GAS AND OXYGEN

Case study 1 described one method to reduce coke rate using PCI; however, another method is to inject natural gas (NG) into the tuyeres instead of PCI. Much like PCI,

Chapter 29, Bottom Segment Calculations With Natural Gas Injection showed that NG injection decreases flame temperature and increases top gas temperature. One of the main differences between the injectants is that NG has a much more dramatic effect on both variables and therefore results in very different operating conditions.

In case study 2, the coke rate will be minimized using NG and $O_2(g)$ injection while the flame temperature and top gas temperature will be constrained to remain within specified ranges.

49.2.1 Objective Function, Constraints, and Manipulated Variables

Much like case study 1, the objective function will be to minimize the C-in-coke charge, which is a factor directly calculated by the blast furnace model. The constraints for the optimization are provided in [Table 49.5](#).

The manipulated variables for the optimization are the injection quantities of NG and $O_2(g)$ through the tuyeres.

TABLE 49.5 Optimization Case Study 2 Constraints

Parameter	Unit	Minimum Value	Maximum Value
Flame temperature	°C	2000	2100
Top gas temperature	°C	110	150
NG injection	kg/t Fe in hot metal	0	150

TABLE 49.6 Optimization Case Study 2 Initial Conditions

Parameter	Value	Unit
TYUERE INJECTION		
NG injection	80	kg/t Fe in hot metal
O ₂ (g) injection	0	kg/t Fe in hot metal
H ₂ O injection	15	g/Nm ³ dry air
NATURAL GAS COMPOSITION^a		
CH ₄	95.0	mol%
C ₂ H ₆	3.2	mol%
C ₃ H ₈	0.2	mol%
C ₄ H ₁₀	0.06	mol%
C ₅ H ₁₂	0.02	mol%
C ₆ H ₁₄	0.01	mol%
N ₂	1.0	mol%
CO ₂	0.5	mol%
O ₂	0.02	mol%

^aSee Table 56.9 in Chapter 56, Blast Furnace Fuel Injection, for more details.

49.2.2 Initial Conditions

For case study 2, the blast furnace is operating under the conditions provided in Table 49.6. The values not listed, such as blast temperature, are assumed to be identical to

TABLE 49.7 Case Study 2 Key Output Initial Conditions

Parameter	Value	Unit
C-in-coke charge	358	kg/t Fe in hot metal
Flame temperature	1869	°C
Top gas temperature	184	°C

those found in Table 49.2, the initial conditions of the first optimization, and were not repeated for brevity.

With these initial conditions, the coke rate, flame temperature, and top gas temperature are shown in Table 49.7.

Unlike case study 1, these initial conditions do not satisfy the constraints as the top gas temperature is too high and flame temperature is too low. This confirms that NG has a much more dramatic effect on the constrained variables and may be more limited regarding its ability to reduce coke rate.

49.2.3 Optimization Results and Analysis

The minimum coke rate, subject to the constraints outlined above, yields the results shown in Table 49.8.

Unlike the case study 1 optimization, the case study 2 does not result in the NG injection rate reaching its maximum value. Instead, the flame temperature and top gas temperature are the major limiters and are both at their minimum values. Much like case study 1, this can be explained by investigating the operating window and the effect of NG injection on coke rate (Fig. 49.2).

The operating window shown in Fig. 49.2 indicates that the coke rate is lowest with a high NG injection rate and a low O₂(g) injection rate. As with PCI, Fig. 49.2 indicates that a combination of these conditions will lead to

very low flame temperatures and very high top gas temperatures. Once again, the optimization determined that the coke rate is minimized when the NG rate is maximized and the O₂(g) rate is as low as possible to satisfy the

flame temperature and top gas temperature constraints. This did not occur when the NG injection rate is at the maximum value (150 kg/t Fe in HM); however, it occurred at a lower injection rate due to the operating temperatures becoming out of spec.

In Fig. 49.2, we can see that the valid operating window (red solid area) for NG injection is far smaller than the valid operating window for PCI injection based on a minimum flame temperature of 2000°C. Even if the minimum flame temperature constraint is lowered to 1900°C, the valid operating window only increases to include the dashed yellow area. The operating window in this situation is wider, however still is smaller as compared to the operating window using PCI.

With NG injection, the ability to reduce coke rate decreases compared to PCI and more oxygen is needed on a relative basis. As we will learn in Chapter 56, Blast Furnace Fuel Injection, blast furnaces run well with NG injection. The investment cost to implement NG injection is a fraction of the cost to implement a PCI preparation plant and injection

TABLE 49.8 Case Study 2 Outputs

Parameter	Unit	Case 2 Values	Minimum Value	Maximum Value
OBJECTIVE FUNCTION				
C-in-coke charge	kg/t Fe in hot metal	370	—	—
MANIPULATED VARIABLES				
NG injection	kg/t Fe in hot metal	68.4	0	150
O ₂ (g) injection	kg/t Fe in hot metal	58.0	—	—
CONSTRAINTS				
Flame temperature	°C	2000	2000	2100
Top gas temperature	°C	110	110	150

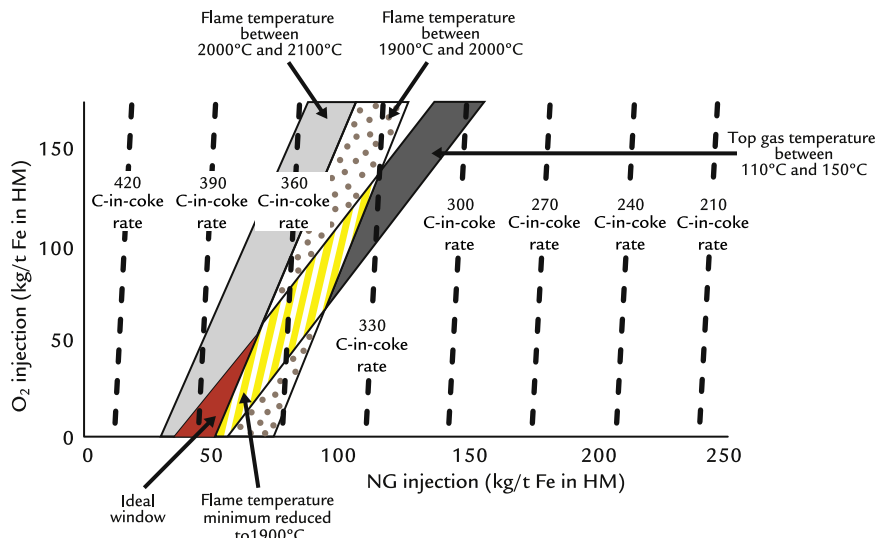


FIGURE 49.2 Blast furnace operating window using NG and O₂(g) injection. NG, Natural gas.

system. The blast furnace operator must decide on the coke rate reduction objective to decide whether NG injection or PCI will offer the needed result. Some blast furnace operators inject both fuels as we will see in case study 3.

49.3 CASE STUDY 3 - MINIMIZING FUEL COSTS USING PCI, NATURAL GAS, AND OXYGEN

The two previous case studies provided examples of how to minimize coke rate using two different injected fuels, PCI and NG. While minimizing coke rate is generally desirable, it can be difficult to assess whether it is better to replace coke with PCI, NG, or both. As with most businesses, ironmakers want to produce molten iron at the lowest operating cost. Analyzing the cost relationship between these three fuels is an activity that must be done regularly as fuel costs can, and will, change over time.

Case study 3 will minimize the cost of molten iron using a combination of coke, PCI, NG, and O₂(g). Coinjection of coal and NG is investigated to determine if there is a cost benefit to using both fuels simultaneously or if one injectant is preferable to the other on a cost basis.

49.3.1 Objective Function, Constraints, and Manipulated Variables

In case study 3, the objective function is to minimize the cost of molten iron. The unit costs of individual input materials are provided in Table 49.9. These are the same unit costs as provided in Chapter 1, The Iron Blast Furnace Process.

The constraints for the optimization are provided in Table 49.10.

The combined injection rate is limited to 200 kg/t Fe in HM to avoid having 300 kg of injected fuels. Each injectant can individually

TABLE 49.9 Unit Costs of Ironmaking Input Materials

Material	Unit Cost (USD/kg)
Coke	0.250
PCI	0.115
Natural gas	0.196
Fluxes	0.010
Oxygen	0.021
Blower air	0.0082
Ore ^a	139.6 \$/t Fe in HM
Other (electricity, labor, refractory) ^a	27.8 \$/t Fe in HM

^aNote that the ore and "other" requirements will not change when changing PCI, natural gas, or oxygen injection and therefore are a constant value and not a unit cost.

TABLE 49.10 Optimization Case Study 3 Constraints

Parameter	Unit	Minimum Value	Maximum Value
Flame temperature	°C	2000	2300
Top gas temperature	°C	110	150
PCI injection	kg/t Fe in hot metal	0	150
NG injection	kg/t Fe in hot metal	0	150
Combined injection rate (PCI and NG)	kg/t Fe in hot metal	0	200

go up to 150 kg/t Fe in HM; however, the combination of the two is limited for illustrative purposes.

The manipulated variables for the optimization are the injection rates of PCI, NG, and O₂(g) through the tuyeres.

49.3.2 Initial Conditions

For case study 3, the blast furnace is operating under the conditions minimization using

TABLE 49.11 Optimization Case Study 3 Initial Conditions

Parameter	Value	Unit
TUYERE INJECTION		
PCI injection	0	kg/t Fe in hot metal
NG injection	68.4	kg/t Fe in hot metal
O ₂ (g) injection	58.0	kg/t Fe in hot metal
H ₂ O injection	15.0	g/Nm ³ dry air
PCI COMPOSITION		
Coal mass on a dry, ash-free basis (daf)	92.0	wt%
Al ₂ O ₃	2.4	wt%
SiO ₂	5.6	wt%
C	88.0	wt% daf basis
H	6.0	wt% daf basis
O	5.0	wt% daf basis
N	1.0	wt% daf basis
NATURAL GAS COMPOSITION		
CH ₄	95.0	mol%
C ₂ H ₆	3.2	mol%
C ₃ H ₈	0.2	mol%
C ₄ H ₁₀	0.06	mol%
C ₅ H ₁₂	0.02	mol%
C ₆ H ₁₄	0.01	mol%
N ₂	1.0	mol%
CO ₂	0.5	mol%
O ₂	0.02	mol%

NG and O₂(g) injection presented in the previous sections. This base case condition was chosen as it has a relatively high operating cost due to the high cost of NG and relatively high

TABLE 49.12 Case Study 3 Key Output Initial Conditions

Parameter	Value	Unit
Ironmaking cost	298	USD/t Fe in HM
Flame temperature	2000	°C
Top gas temperature	110	°C

TABLE 49.13 Case Study 3 Initial Cost Breakdown

Material	Value	Unit
Coke	102.89	USD/t Fe in HM
PCI	0	USD/t Fe in HM
NG	13.40	USD/t Fe in HM
Fluxes	1.36	USD/t Fe in HM
Oxygen	1.22	USD/t Fe in HM
Blower air	11.29	USD/t Fe in HM
Ore	139.60	USD/t Fe in HM
Other	27.80	USD/t Fe in HM
Total	297.56	USD/t Fe in HM
		Say 298

coke rate. For reference, the provided in [Table 49.11](#).

With these initial conditions, the molten iron cost, flame temperature, and top gas temperature are as shown in [Table 49.12](#).

The breakdown of the costs is provided in [Table 49.13](#). Iron ore, coke, and NG are the main contributors to the ironmaking costs shown in [Table 49.12](#).

49.3.3 Optimization Results and Analysis

The cost minimization modeling, subject to the constraints outlined above, yields the

TABLE 49.14 Case Study 3 Outputs

Parameter	Unit	Value	Minimum Value	Maximum Value
OBJECTIVE FUNCTION				
Iron cost	USD/t Fe in hot metal	280	—	—
MANIPULATED VARIABLES				
PCI injection	kg/t Fe in hot metal	150	0	150
NG injection	kg/t Fe in hot metal	50	0	150
O ₂ (g) injection	kg/t Fe in hot metal	135	—	—
CONSTRAINTS				
Flame temperature	°C	2005	2000	2300
Top gas temperature	°C	110	110	150

TABLE 49.15 Case Study 3 Optimal Cost Breakdown

Material	Value	Unit
Coke	72.90	USD/t Fe in HM
PCI	17.25	USD/t Fe in HM
NG	9.80	USD/t Fe in HM
Fluxes	1.36	USD/t Fe in HM
Oxygen	2.83	USD/t Fe in HM
Blower air	8.83	USD/t Fe in HM
Ore	139.60	USD/t Fe in HM
Other	27.80	USD/t Fe in HM
Total	280.37	USD/t Fe in HM
Say 280		

results shown in [Table 49.14](#). The cost breakdown is provided in [Table 49.15](#).

For case study 3, the optimal cost was found when the PCI was maximized and the NG

injection rate was as high as possible considering the 200 kg coinjection limit. PCI was preferred since, on a per mass basis, it offers a lower input fuel cost and demands less oxygen injection to maintain the minimum flame temperature. The oxygen injection rate was minimized to keep the blast furnace operating within the constrained top gas temperature range. Increased oxygen injection increased coke rate and subsequently increased operating costs; therefore, oxygen added was minimized.

49.4 CASE STUDY 4 - MINIMIZING CO₂(g) EMISSIONS USING PCI, NATURAL GAS, AND OXYGEN

The global concern for climate change has resulted in a wide variety of measures to lower CO₂(g) emissions on national and international levels. The iron and steel industry are inherently a large emitter of CO₂(g) due to the size of the industry and the use of carbon as a reductant in the ironmaking process. Ironmakers have a strong interest in minimizing CO₂(g) reductions due to increasing regulatory restrictions. Case study 4 will evaluate the strategies to minimize CO₂(g) emissions using coinjection of PCI, NG, and oxygen.

49.4.1 Objective Function, Constraints, and Manipulated Variables

In case study 4, the objective function is to minimize the mass of CO₂(g) in top gas, which is a variable directly computed from the heat and mass balance model equations developed in this book. The manipulated variables will once again be the injection rates of PCI, NG, and O₂(g). The constraints will be identical to the ones in case study 3, which are presented in [Table 49.10](#).

49.4.2 Initial Conditions

In the base case, the blast furnace is operating using the optimal cost parameters calculated in case study 3. The injectant conditions are provided in [Table 49.16](#).

TABLE 49.16 Optimization Case Study 4 Initial Conditions

Parameter	Value	Unit
TUYERE INJECTION		
PCI injection	150	kg/t Fe in hot metal
NG injection	50	kg/t Fe in hot metal
O ₂ (g) injection	135	kg/t Fe in hot metal
H ₂ O injection	15	g/Nm ³ dry air
PCI COMPOSITION		
Coal mass on a dry, ash-free basis (daf)	92.0	wt%
Al ₂ O ₃	2.4	wt%
SiO ₂	5.6	wt%
C	88.0	wt% daf basis
H	6.0	wt% daf basis
O	5.0	wt% daf basis
N	1.0	wt% daf basis
NATURAL GAS COMPOSITION		
CH ₄	95.0	mol%
C ₂ H ₆	3.2	mol%
C ₃ H ₈	0.2	mol%
C ₄ H ₁₀	0.06	mol%
C ₅ H ₁₂	0.02	mol%
C ₆ H ₁₄	0.01	mol%
N ₂	1.0	mol%
CO ₂	0.5	mol%
O ₂	0.02	mol%

TABLE 49.17 Case Study 4 Key Output Initial Conditions

Parameter	Value	Unit
CO ₂ (g) in top gas	692	kg/t Fe in HM
Flame temperature	2005	°C
Top gas temperature	110	°C

TABLE 49.18 Case Study 4 Outputs

Parameter	Unit	Value	Minimum Value	Maximum Value
OBJECTIVE FUNCTION				
CO ₂ (g) in top gas	kg/t Fe in hot metal	691	—	—
MANIPULATED VARIABLES				
PCI injection	kg/t Fe in hot metal	147.8	0	150
NG injection	kg/t Fe in hot metal	52.2	0	150
O ₂ (g) injection	kg/t Fe in hot metal	137.3	—	—
CONSTRAINTS				
Flame temperature	°C	2000	2000	2300
Top gas temperature	°C	110	110	150

Using these initial conditions, the CO₂(g) in the top gas, flame temperature, and top gas temperature are as shown in [Table 49.17](#).

49.4.3 Optimization Results and Analysis

The CO₂(g) minimization, subject to the constraints outlined above, yields the results shown in [Table 49.18](#).

The optimal operating point for CO₂(g) minimization is when the maximum amount of

NG is used to replace PCI. Injected NG reduces iron ore to iron using hydrogen rather than carbon. This reduces the overall carbon requirement of the blast furnace, resulting in fewer CO₂(g) emissions. NG could not be maximized as the flame temperature would be too low; therefore, the maximum amount of NG possible was used considering the minimum flame temperature constraint. The PCI rate was increased as much as possible to be within the 200 kg coinjection limit such that the top gas temperature and flame temperature remain within the constrained ranges. The O₂(g) injection rate was minimized such that the top gas and flame temperatures are within the constrained ranges. Further, increasing O₂(g) injection would increase the total fuel rate and therefore CO₂(g) emissions.

49.5 COMPARISON OF THE OPTIMIZATION CASE STUDIES

The case studies presented offered four different scenarios that are commonly encountered within blast furnace operations and provided solutions to optimize blast furnace

performance. Interestingly, all the cases are optimal at slightly different conditions, as highlighted in Fig. 49.3.

While these case studies are all relatively simple, they do provide an introduction into the difficult nature of optimizing blast furnace operations. The nature of the optimization as well as the variables that can be changed lead to a multitude of possible operating conditions.

It is unlikely that optimizing one parameter, such as iron cost, will also optimize another parameter, such as CO₂(g) emissions. Blast furnace operators must constantly be aware of the trade-offs they are making within their plant and understand how to adjust their operations to optimize their furnace for their specific and often changing situation.

49.6 SUMMARY

Chapter 49, Blast Furnace Optimization Case Studies, presented case studies to explore the complex nature of optimizing blast furnace operations. The four case studies investigated were;

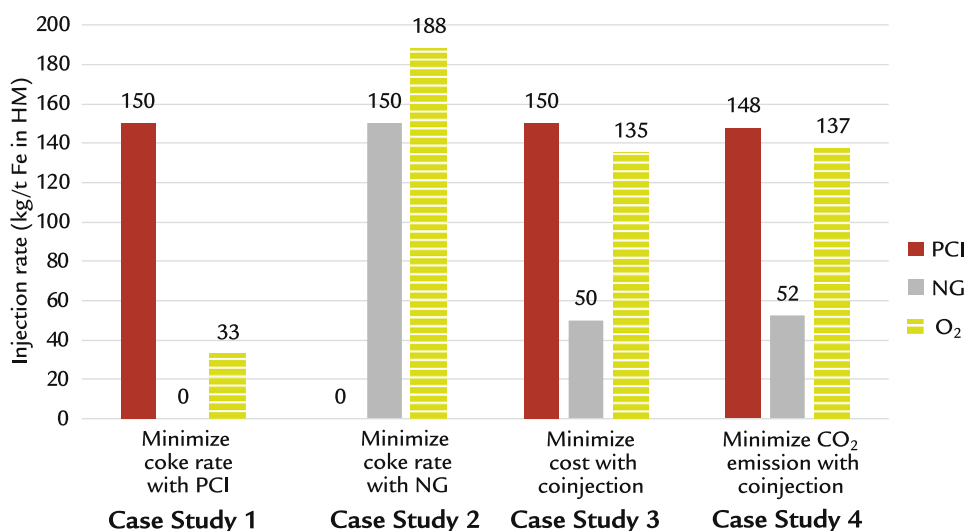


FIGURE 49.3 Comparison of optimal operating conditions for case studies 1–4.

- Case 1:** Minimizing coke rate using PCI and O₂(g) injection,
- Case 2:** Minimizing coke rate using NG and O₂(g) injection,
- Case 3:** Minimizing operating costs using PCI, NG, and O₂(g) injection, and
- Case 4:** Minimizing CO₂(g) emissions using PCI, NG, and O₂(g) injection.

All case studies were found to have slightly different operating conditions, highlighting that blast furnaces cannot simultaneously achieve all its goals.

EXERCISES

49.1. You are operating a blast furnace that recently underwent the optimization process from case study 1, that is, you are running at the minimum coke rate using PCI injection. Your general manager indicates there is an innovative technology that will allow you to run at a lower top gas temperature, allowing you to have top gas temperatures as low as 100°C! The general manager is excited and believes that you can further lower the coke rate.

- a. Prior to running the optimization, do you believe that implementing the innovative technology is a wise investment? Why?
- b. Run the optimization and indicate the new C-in-coke-charge rate, PCI injection rate, and O₂(g) injection rate.

49.2. Much like Exercise 1, you instead are operating a blast furnace that recently underwent the optimization process from case study 2, that is, you are running at a minimal coke rate using NG injection. Your general manager once again indicates there is an innovative technology that will allow you to run at a lower top gas temperature, allowing you to have top gas temperatures as low as 100°C! The general

manager is excited and believes that you can further lower the coke rate.

- a. Prior to running the optimization, do you believe this is a wise investment? Why?
- b. Run the optimization and indicate the new C-in-coke-charge rate, NG injection rate, and O₂(g) injection rate.

49.3. You are operating a blast furnace that has minimized its cost using PCI and NG injection, that is, the results of case study 3. There has been a recent shortage of coal for PCI and the price has more than tripled to \$0.35/kg.

- a. Prior to running the optimization, do you believe this will have a dramatic impact on the cost optimization strategy? Why?
- b. Your general manager foresees this price increase being a long-term issue and wishes to change the operating point to minimize operating costs. What are the PCI, NG, and O₂(g) injection rates that lead to the minimum cost, and what is that cost?

49.4. You are operating a blast furnace that has minimized its cost using PCI and NG injection, that is, the results of case study 3. Your general manager indicates there is a cheaper type of coke available that only costs \$200/t (or \$0.20/kg). Unfortunately, it is of much lower quality, with the following characteristics:

Parameter	Value	Unit
SiO ₂	15	Mass% dry
Al ₂ O ₃	10	Mass% dry
C	75	Mass% dry
Moisture content	5	%

Considering you are currently able to produce hot metal at \$280/t Fe in HM, would you recommend using this new coke in the blast furnace? Why?

Blast Furnace Rules of Thumb

O U T L I N E

50.1 Fuel Rate Adjustments	473	50.3.3 Step 3—Verifying Top and Flame Temperatures are in Range	478
50.2 Flame and Top Temperature Impacts	473	50.3.4 Step 4—Estimating the New Production Rate	480
50.3 Productivity Impact	476	50.4 Summary	480
50.3.1 Step 1—Estimating Changes in Coke Rate	477	Exercises	480
50.3.2 Step 2—Managing Short-Term Change	477	References	481

50.1 FUEL RATE ADJUSTMENTS

Throughout the long history of blast furnaces, engineers have developed “rules of thumb” to allow for planned changes to the blast furnace operation. The rules were based on experience and are useful to implement changes quickly and with confidence of a predictable outcome. Rules of thumb were developed in different countries and by individual steel plants. European (Geerdes et al.), American (Flint and Burgo), and Russian (Danshin and Chernousov) rules of thumb may be compared in Table 50.1.^{1–4}

As can be seen from Table 50.1, Flint, Burgo, and Danshin and Chernousov provided rules of thumb that cover a wider range of

operating conditions and reflect older operating practices such as low hot blast temperatures and varying blast oxygen enrichment. Generally, the coke rate adjustments agree among the three sources. Actual coke replacement values should be fine-tuned for each blast furnace operation and for the designated raw materials.

50.2 FLAME AND TOP TEMPERATURE IMPACTS

To further manage the blast furnace operation, rules of thumb regarding additional impacts on flame and top temperature for

TABLE 50.1 Comparison of Rules of Thumb from Europe, United States, and Russia^{1–4}

Item	Units	Coke Rate Impact (kg/t HM)		
		Europe Geerde et al. ¹	United States Flint ² Burgo ³	Russia
		Danshin and Chernousov ⁴		
Lump ore (size consist)		—		
2 × 4 in. (50 × 102 mm)	+50 kg/t HM		+7.5	
1 × 2 in. (25 × 50 mm)	+50 kg/t HM		+4.5	
1/2 × 1 in. (13 × 25 mm)	+50 kg/t HM		+1.5	
1/4 × 1/2 in. (6.4 × 13 mm)	+50 kg/t HM		0	
Minus 1/4 in. (−6.4 mm)	+50 kg/t HM		+4	+8
Pellet size		—		
3/8 × 5/8 in. (9.5 × 15.6 mm)	+50 kg/t HM		0	
– 1/4 in. (−6.4 mm)	+ 10% of Pellets		+20	
			–5.2% Productivity	
– 1/4 in. (−6.4 mm)	+ 20% of Pellets		+34.5	
			–6.9% Productivity	
Tumble index	Minus 1 unit <95		+10.5	
Lump ore vs. pellets	+50 kg/t HM		+2.0	
Sinter vs. acid pellets	+1% Exchange		–0.8	
Fluxed vs. acid pellets	+1% Exchange		–0.25	
Scrap	+50 kg/t HM		–16.5	
Coke		—		
ASTM stability	+1 Unit			
	Stability > 62		–1.3	
	Stability < 62		–2.5	
Ash	+1%		+15 / + 10	+6.5
Sulfur	+0.5 kg/t HM		+5.0	
Micum strength (M25)	+1%			–3.0
Micum abrasion (M10)	+1%			+14.0
Coke Reactivity Index (CRI)	+1 Unit			
	CRI > 13		+1.5	
	CRI < 13		+0.75	

(Continued)

TABLE 50.1 (Continued)

Item	Units	Coke Rate Impact (kg/t HM)		
		Europe Geerde et al. ¹	United States Flint ² Burgo ³	Russia
		Danshin and Chernousov ⁴		
<i>Blast temperature</i> (1100–1200°C)	+ 100°C	– 9.0	– 9.9 @ 1100°C	– 14 @ 21–25% O ₂
			– 9.0 @ 1200°C	– 11 @ 25–35% O ₂
				– 9 @ 35–40% O ₂
<i>Blast moisture</i>	+ 10 g/Nm ³	+ 6.0	+ 10.9 @ 1480 Nm ³ /t Blast	+ 10 @ 1550 Nm ³ /t Blast + 7.5 @ 1050 Nm ³ /t Blast
<i>Blast air oxygen enrichment</i>	+ 1%	+ 1.0	–	+ 1.0 @ 21–25% O ₂
				+ 1.5 @ 25–30% O ₂
				+ 2.0 @ 30–35% O ₂
				+ 2.5 @ 35–40% O ₂
<i>Injected natural gas</i>	+ 10 kg/t	– 10.4	– 10.0 @ 60 kg NG/t HM	– 13.0 @ 30 kg NG/tHM – 11.5 @ 75 kg NG/tHM – 9.8 @ 105 kg NG/tHM
			– 14.0	
<i>Injected oil</i>	+10 kg/t	– 11.0	– 10.0/ – 12.0	– 12.0
<i>Injected tar</i>	+10 kg/t HM		– 11.0	
<i>Injected coal</i>	+ 10 kg/t	– 9.0	– 9.0/ – 10.0	– 9.0 @ Ash < 10% – 8.0 @ Ash 10–20% – 8.0 @ High VM and ash < 10%
<i>Injected coke oven gas</i>	+ 10 kg/t	–	– 9.0 @ 50 kg/t	– 10.2 @ 45 kg/t – 9.1 @ 110 kg/t
<i>Hot metal silicon</i>	+0.1%	+ 4.0	+ 6.5/ + 5.0	+ 6.0
<i>Hot metal sulfur</i>	+0.001%	–	– 2.5 @ 0.030% S	– 5.0
<i>Hot metal Mn</i>	+0.1%	–	+ 1.25	+ 1.0
<i>Slag - coke ash</i>	+1% Coke ash	–	+ 7.6	+ 6.5
<i>Slag - limestone</i>	+10 kg/t HM	–	+ 3.0/ + 1.0	+ 2.5
<i>Slag volume</i>	+10 kg/t HM	+ 0.5	+ 2.5/ + 4.0	–
<i>Top gas utilization</i>	+1%	– 7.0	– 7.0	–
<i>Cooling losses</i>	+ 10 GJ/h	+ 1.2	+ 2.9 @ 5000 tpd	–
			+ 1.5 @ 10,000 tpd	

TABLE 50.2 Rules of Thumb - Flame and Top Temperature Impact at Constant Wind Volume

Item	Unit	Change	Flame Temperature (°C)	Top Temperature (°C)
Blast temperature	°C	+100	+55	-15
Injected coal	kg/t	+10	-13	+12
Injected natural gas	kg/t	+10	-56	+18
Injected oil	kg/t	+10	-33	+12
Oxygen enrichment	kg/t	+10	+18	-12
Blast moisture	kg/t	+10	-48	+10

selected process changes are useful and are provided in Table 50.2. These have been calculated by the authors using the model developed in this book.

This second set of rules of thumb helps the blast furnace operator maintain top temperature above 110°C to assure adequate burden drying/heating and a flame temperature above the designated minimum value. Minimum flame temperature depends on the injected fuel used. As a guideline, the following minimum flame temperatures can be considered;

- for coal injection - 2050°C minimum flame temperature,
- for natural gas injection - 1900°C minimum flame temperature, and
- for coal and natural gas together - 2000°C minimum flame temperature.

Flame temperatures should be maintained below a maximum value as well. This depends on the melting characteristics of the raw materials used, especially the ferrous burden. Acid burden or pellets with a lower melting temperature will have a lower maximum flame temperature than fluxed pellets and sinter. The

maximum flame temperature limit is not a function of the injected fuel used. The following maximum values can be considered;

- fully acid burden - 2200°C maximum flame temperature,
- mixed acid and fluxed burden - 2200°C maximum flame temperature, and
- fully fluxed burden, sinter, and/or pellets - 2300–2400°C maximum flame temperature.

Top temperature maximums are needed to protect the top charging equipment, especially the bell-less top gear box. When the top temperature exceeds a predetermined set point, top sprays are activated to cool the top gas and protect the charging equipment. The maximum top gas temperature is equipment and site dependent; typically, once top gas temperatures exceed 200–250°C, top sprays are activated.

50.3 PRODUCTIVITY IMPACT

With changes in coke rate, a change in productivity is experienced. With less coke added, and for the same blast and injected fuel rate, less coke will be burnt at the tuyeres to produce a tonne of hot metal. The production rate will increase in proportion to the coke rate decrease:

$$\text{New production (constant injectant rate, coke rate change)} = \text{Old production} * \frac{\text{Old coke rate}}{\text{New coke rate}} \quad (50.1)$$

The new productivity is estimated once all coke rate changes have been considered. The same approach is used for both a coke rate increase and decrease if the injected fuel rate remains constant.

In the case where coke rate is reduced and the injected fuel rate is increased to compensate for the reduced coke input, the production rate will change relative to the change in fuel

rate rather than coke rate. In this case, the change in the amount of coke burnt to make a tonne of hot metal will be reduced due to the added injected fuel. The extent of the change will depend on the injected fuel used and its coke replacement ratio:

$$\begin{aligned} \text{New production (change in injected fuel and coke rates)} \\ = \text{Old production} * \frac{\text{Old fuel rate}}{\text{New fuel rate}} \end{aligned} \quad (50.2)$$

As mentioned above, the same approach is used for both an increase and decrease in coke rate accompanied by an off-setting change to the injected fuel rate.

50.3.1 Step 1—Estimating Changes in Coke Rate

When considering a blast furnace process change, either real or proposed, the first step is to estimate the change in coke rate that is created. This requires an understanding of the process change's general impact to assure all the appropriate rules of thumb are considered. Rules of thumb can be added or subtracted to understand the net effect of the proposed change on the actual coke and fuel rates.

50.3.1.1 Example—Burden Distribution Change

Iron ore sinter/pellets are redirected from the wall of the blast furnace to the center using the bell-less top charging equipment. The top gas utilization (TGU) improves from 47.5 to 49.0% (an increase of 1.5%) due to better contact of the ferrous burden with the CO-rich gas in the furnace center. As this was an unanticipated result and no other process changes were made, what is the expected change to the hot metal silicon content?

50.3.1.2 Answer

An increase in top gas utilization improves the blast furnace efficiency and reduces the fuel demand. The following coke rate reduction is forecast:

$$\begin{aligned} \text{Coke rate reduction} &= -7.0 \text{ kg/tHM} \\ &\times \frac{1.5\% \text{ increase in TGU}}{1.0\% \text{ standard change in TGU}} \end{aligned} \quad (50.3)$$

$$\text{Coke rate reduction} = -10.5 \text{ kg/tHM} \quad (50.4)$$

The result of the burden distribution change is a decrease in the forecast coke rate of 10.5 kg/t HM. Since this was not anticipated nor planned for, the blast furnace will overheat and the silicon content in the hot metal will increase. Using rules of thumb in [Table 50.1](#), the Si increase can be estimated for the effective extra fuel rate that the improved gas utilization has provided:

$$\begin{aligned} \text{Silicon increase in hot metal} &= +0.1\% \\ &\times \frac{(10.5 \text{ kg/tHM effective fuel rate increase})}{4.0 \text{ kg/tHM standard change for Si}} \end{aligned} \quad (50.5)$$

$$\text{Silicon increase in hot metal} = +0.26\% \text{ Si} \quad (50.6)$$

So, without any intervention, the hot metal silicon content will increase by 0.26%. In steel-making, the increased hot metal silicon will decrease hot metal consumption per heat, increase coolant demands, and generate greater slag volumes when the basic oxygen furnace (BOF) shop converts the hot metal into liquid steel.

50.3.2 Step 2—Managing Short-Term Change

To manage known time lags in the blast furnace operation, short-term changes can be made to deal with unanticipated process conditions. For the example provided above, once the increase in gas utilization is identified and a coke rate change is implemented, it will take

7–10 hours for the burden change to descend to the blast furnace tuyeres and take effect. Operators will make tuyere level changes to adjust to the new situation and then later introduce a coke rate change in a planned manner. In this way, the changes in the hot metal chemistry can be managed to minimize the impact on the downstream steelmaking operation.

For the increase in gas utilization, two countermeasures are possible. One is to reduce the injected fuel rate by a corresponding amount to match the lower furnace conditions to the new situation of a more efficient blast furnace process. A second approach is to increase the blast moisture to place an equal heat demand to consume the extra energy that is now available. This would then later be reversed with a planned coke rate change. Let's use the rules of thumb to explore these two strategies.

50.3.2.1 Countermeasure 1 - Lower the Injected Fuel (Coal) Rate

Using the rules of thumb, the injected coal rate can be adjusted:

$$\text{New coal injection rate} = -10.0 \text{ kg coal/t HM}$$

$$* \frac{10.5 \text{ kg coke/t HM}}{9.0 \text{ kg coke/t HM}}$$
(50.7)

$$\text{New coal injection rate} = -11.7 \text{ kg coal/t HM}$$
(50.8)

By quickly reducing the coal injection rate by 11.7 kg/t hot metal, the fuel rate will be in balance with the fuel demand and the increase in hot metal silicon can be minimized. The operation can continue with this new lower coal injection rate indefinitely. Alternately, the coke rate can be reduced by 10.5 kg/t HM and once added, the coal injection rate would be increased by 11.7 kg/t HM once the new burden reached the tuyere level, usually 7–10 hours after the coke rate is changed. To make these changes, the production rate must be known so that the coal injection rate,

controlled in kg/min, is adjusted to correspond to the 11.7 kg/t HM change estimated above.

50.3.2.2 Countermeasure 2 - Increasing the Steam Addition Rate

An alternate to control silicon would be to add steam to the blast and increase the blast moisture content, in effect increasing the fuel demand to match the available excess fuel. Using Geerdes et al. rules of thumb,¹

$$\text{New blast moisture} = +10.0 \text{ g/Nm}^3$$

$$* \frac{10.5 \text{ kg coke/t HM}}{6.0 \text{ kg coke/t HM}}$$
(50.9)

$$\text{New blast moisture} = +17.5 \text{ g/Nm}^3$$
(50.10)

Increasing the blast moisture by +17.5 g/Nm³ would quickly offset the improved gas utilization and blast furnace efficiency by adding an extra heat demand. Moisture is sometimes used in this manner as it acts quickly and can reduce silicon within one cast. As this creates an unwanted inefficiency and higher fuel rate, the burden coke rate should be reduced by 10.5 kg/t HM and then as this change reaches the tuyeres in 7–10 hours, the steam injection be reduced to remove the extra 17.5 g/Nm³ of moisture added. Well timed, the increase in hot metal silicon content created by the top gas utilization can be avoided.

50.3.3 Step 3—Verifying Top and Flame Temperatures are in Range

As these countermeasures are implemented, the process engineer should verify if the top gas and flame temperature are in range. A typical target is to have the top temperature >110°C to assure burden drying and heating. The lower flame temperature limit depends on the injected fuel use, for coal injection a lower limit of 2050°C can be considered.

For a base condition where the blast furnace was operating with a top temperature of 130°C and flame temperature of 2100°C, the rules of

thumb can be used to estimate the impact of countermeasures 1 and 2 to understand their impact and determine if they are acceptable. Using the values presented in [Table 50.2](#), the changes in top and flame temperature can be estimated¹.

For countermeasure 1, a decrease of injected coal by -11.7 kg/t HM :

New flame temperature

$$= 2100^\circ\text{C} + \frac{-11.7 \text{ kg/t HM}}{10.0 \text{ kg/t HM}} * -13^\circ\text{C} \quad (50.11)$$

$$\text{New flame temperature} = 2115^\circ\text{C} \quad (50.12)$$

New top temperature

$$= 130^\circ\text{C} + \frac{-11.7 \text{ kg/t HM}}{10.0 \text{ kg/t HM}} * +12^\circ\text{C} \quad (50.13)$$

$$\text{New top temperature} = 116^\circ\text{C} \quad (50.14)$$

For countermeasure 2, an increase in blast moisture by $+17.5 \text{ g/Nm}^3$:

New flame temperature

$$= 2100^\circ\text{C} + \frac{+17.5 \text{ g/Nm}^3}{10.0 \text{ g/Nm}^3} * -48^\circ\text{C} \quad (50.15)$$

$$\text{New flame temperature} = 2016^\circ\text{C} \quad (50.16)$$

New top temperature

$$= 130^\circ\text{C} + \frac{+17.5 \text{ g/Nm}^3}{10.0 \text{ g/Nm}^3} * +10.0^\circ\text{C} \quad (50.17)$$

$$\text{New top temperature} = 148^\circ\text{C} \quad (50.18)$$

Both countermeasures 1 and 2 could be implemented to offset the increase in top gas utilization but they will have different reactions in the blast furnace. Their results can be compared in [Table 50.3](#) to choose the best strategy to implement.

The increase in the blast moisture in countermeasure 2 would have a significant impact on the flame temperature, decreasing this below the accepted minimum of 2050°C needed for good coal combustion. As a result, countermeasure 2 is not acceptable. With countermeasure 1, decreasing the coal injection rate, the flame temperature is acceptable and the top temperature is above the minimum value of 110°C . Once the new coke rate arrives at the tuyeres, the coal injection rate must be increased back to the original rate, so energy input matches energy demand.

Countermeasure 1 would be a temporary measure that would be implemented to avoid an increase in the hot metal silicon content that

TABLE 50.3 Comparing Countermeasures for Top Gas Utilization Increase of 1.5%

Change	Coke Rate Impact (kg/t HM)	Flame Temperature Impact ($^\circ\text{C}$)	Top Temperature Impact ($^\circ\text{C}$)	Comment
Top gas utilization increases by 1.5%	-10.5			Hot metal Si will increase by 0.26%
Decrease coal injection by 11.7 kg/t HM	+ 10.5	+15 Increase from 2100°C to 2115°C	-14 Decrease from 130°C to 116°C	Top gas temperature above the limit of 110°C min. Change is acceptable to implement
Increase blast moisture by 17.5 g/Nm^3	+ 10.5	-84 Decrease from 2100°C to 2016°C	+18 Increase from 130°C to 148°C	Flame temperature is below the limit of 2050°C minimum. Change is unacceptable

may be out of specification for the BOF shop. Once a change in the burden coke rate is implemented, about 7–10 hours later, counter-measure 1 must be reversed as the new burden with lower coke rate arrives at the tuyere elevation. Successfully implemented, the BOF shop would not experience increased silicon content in the hot metal. Silicon in hot metal impacts the BOF heat balance, hot metal and scrap ratio, and flux requirements. Very high levels of silicon, say above 1.3%, can lead to BOF slopping of molten slag due to a high slag volume. Production delays result as the BOF reduces its oxygen blowing rate to manage the high slag volume caused by the high hot metal silicon content.

50.3.4 Step 4—Estimating the New Production Rate

Once the new lower coke rate has been implemented in response to the increased top gas utilization, a production increase would be expected. For an initial production rate of 7000 tpd, initial coke rate of 330 kg/t HM, and coal injection rate of 170 kg/t HM, the new production rate can be estimated after implementing the new coke rate and restoring the coal injection rate back to 170 kg/t HM. Using Eq. (50.1);

New production rate

$$= 7000 \text{ tpd} * \frac{330 \text{ kg coke/t HM}}{(330 - 10.5)\text{kg coke/t HM}} \quad (50.19)$$

$$\text{New production rate} = 7230 \text{ tpd} \quad (50.20)$$

As the blast furnace stabilizes with its improved top gas utilization and the new lower coke rate is implemented, the furnace production rate will increase by 230 tpd or 3.3%.

50.4 SUMMARY

Rules of thumb offer a fast way to assess process changes and develop strategies to adjust the blast furnace operation to maintain consistent hot metal quality and planned production. The rules of thumb provide insight into process effects and related changes. They cover a wide range of experience and can be used for day-to-day control as well as longer term planning. While rules of thumb can be used to assess a range of changes, heat and mass balance models provide a more comprehensive analysis of all aspects of a process change.

EXERCISES

- 50.1. During the second year of the blast furnace campaign, the cooling losses suddenly increase from 30 to 70 GJ/h as the blow-in refractory is lost from the stave coolers. What is the required increase in the natural gas injection rate needed to offset the increased cooling losses. Assume that the blast furnace is producing 7000 tpd and injecting 70 kg of natural gas per tonne of hot metal. The furnace was operating with a flame temperature of 1950°C and top temperature of 120°C—will the new operation be sustainable with greater natural gas injection?
- 50.2. In the North America, blast furnaces that have coal injection have combined the injection of coal and natural gas to reduce costs with the introduction of low cost shale gas. Consider a blast furnace producing 5000 tpd with a coal injection rate of 150 kg/t HM, coke rate of 350 kg/t HM, flame temperature of 2100°C, blast consumption of 900 Nm³/t HM, and top

temperature of 130°C. With the plan to reduce the coke rate using 30 kg/t HM of natural gas, how much oxygen enrichment is needed? With natural gas usage, the minimum flame temperature can be reduced from 2100 to 2030°C. What is the expected cost savings considering that the blast furnace operates 350 days per year? Consider that the delivered coal cost is \$100/t, purchased coke cost is \$300/t, natural gas is \$3.00/GJ (\$0.16/kg), and oxygen is \$0.03/Nm³.

References

1. Geerdes M, et al. *Modern blast furnace ironmaking, an introduction*. 3rd ed. The Netherlands: ISO Press; 2015. p. 195.
2. Flint RV. Effect of burden materials and practices on blast furnace coke rate. *Blast Furnace Steel Plant* 1962; 50(1):47–58 74–76.
3. Burgo JA. Chapter 10—The manufacture of pig iron in the blast furnace. *The making, shaping and treating of steel—11th ed., Ironmaking Volume*. Pittsburgh, PA: The AISE Steel Foundation; 1999. p. 732.
4. Danshin V, Chernousov P. *Handbook of blast furnace worker, Metallurgiya, Chelyabinsk, (Russia)*, Table 32 [Michael Alter Trans.] ArcelorMittal Global Research; 1989. p. 190.

The Blast Furnace Plant

OUTLINE

51.1 Important Aspects of the Blast Furnace Process	483	51.5 Cold and Hot Blast Systems	487
51.2 Stockhouse	485	51.6 Blast Furnace Gas Cleaning	490
51.3 The Blast Furnace Top	485	51.7 Summary	492
51.4 Top Charging Systems	486	Exercises	492

51.1 IMPORTANT ASPECTS OF THE BLAST FURNACE PROCESS

A modern blast furnace plant is presented below in Fig. 51.1.

Important subplants must support the blast furnace operation:

- The stockhouse must receive, screen, and weigh all the burden materials charged to the top of the blast furnace. These can be delivered to the stockhouse by conveyor belt, railroad cars, and trucks.
- The raw materials are weighed as separate ore/flux and coke batches. These batches are delivered to the blast furnace using either a single charging conveyor or two skips hoisted on an incline.

- The top charging equipment is used to receive the burden materials, bring these up to the blast furnace operating pressure and charge the burden, separate coke and ore batches, onto the stockline.
- Injected fuels are piped into each of the tuyeres. Coal injection is supported by a separate preparation and injection plant. Liquid fuels such as fuel oil are stored adjacent to the blast furnace. Natural gas is delivered by pipeline. More details are provided in Chapter 56, Blast Furnace Fuel Injection.
- Ambient air is compressed and delivered to three or four hot blast stoves. The air is heated to the required temperatures using one or two of the preheated stoves. The

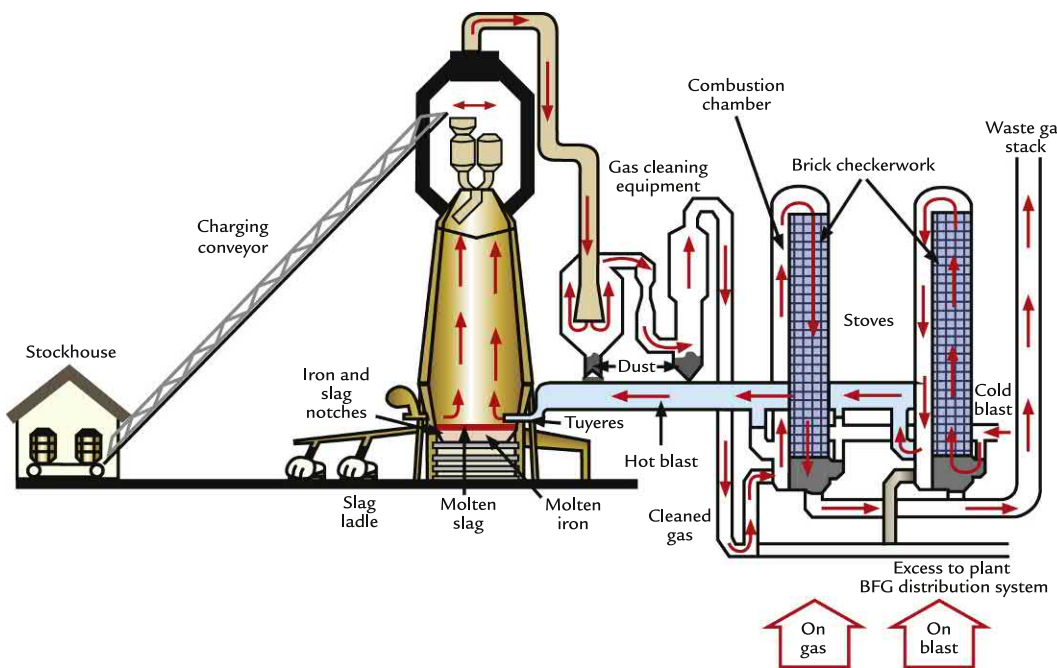


FIGURE 51.1 A modern blast furnace plant.

refractory brick in the remaining stoves is reheated to its service temperature in preparation to heat-up blast air once the stoves in use cool off. The cycle then switches, hence the regenerative nature of the hot stove system.

- Now heated, the blast air is delivered to the blast furnace via a refractory lined pipe known as the hot blast main. A mixer valve or chamber in the hot blast main adds a small amount of colder blast air from the turbo blower to control the blast air to a precise temperature. Now at the target temperature, the heated air is delivered to the round bustle pipe that equally distributes this air to the individual tuyeres.
- At each tuyere, injected fuel is added together with the blast air and injected into the blast furnace.

- The top gas exits the blast furnace through the four uptakes and then to the gas cleaning plant. The gas cleaning plant removes dust and moisture from the raw top gas. The CO and H₂ in the clean top gas are used to heat the stoves and any remaining top gas is delivered to downstream consumers such as boilers for steam generation.

- Molten iron and slag are removed from the blast furnace in the casthouse. Iron flows to ladles that are subsequently transported to the steelmaking shop for refining and casting. Slag is solidified and sold. Details of the casthouse design and operation are provided in Chapter 57, Casting the Blast Furnace.

Each of these important parts of the blast furnace plant is described in the subsequent sections.

51.2 STOCKHOUSE

Precise measurement of the iron ore, coke, fluxes, and other miscellaneous materials is needed to assure that the blast furnace operates predictably and with low operating costs. Newer furnaces feature a stockhouse located on grade, easily serviced by mobile equipment and highly automated. The charge materials are weighed and delivered by conveyor belt to the furnace top. The conveyor belt must be at a comparatively shallow angle to prevent charge materials from rolling backward down the conveyor belt. As a result, the stockhouse is located about 500–800 m from the blast furnace. Older blast furnaces feature a below grade stockhouse and skip charging system that is much closer to the furnace proper. While a smaller footprint is required, below grade stock houses are not in favor due to access challenges for mobile equipment and more complex automation demands needed to minimize staffing.

The stockhouse must have the following features:

- Receive and screen fines (<6 mm) from sinter, pellets, and lump ores. Systems to screen coke into three fractions—furnace coke (>18 mm), small coke (6 × 18 mm) also called nut coke, and coke breeze (<6 mm).
- Receive fluxes, small/nut coke, Mn ore, and other miscellaneous materials that are charged with the ferrous burden. The stockhouse should have capacity to process 6–8 fluxes/miscellaneous materials concurrently.
- Collect iron ore fines and coke breeze for reprocessing.
- Ability to weigh the charge very accurately, within 1% of the true weight.
- Measure the coke moisture using neutron-based nuclear gauges so that coke can be weighed on a dry basis. Neutrons slow as they pass through moisture present in the

coke. By counting slow neutrons, moisture can be measured.

- Measure the iron ore moisture using neutron-based gauges and with density measured by gamma radiation to improve dry charging accuracy.
- Ability to track and anticipate each material batch movement so that the stockhouse can sequence quickly through the charging recipes. Capacity to have two batches on the charge conveyor at the same time.
- Capacity to weigh complex burden recipes. Recipes can be as simple as one coke and one ore batch, but this is rarely the case. Complex recipes with 5–10 or more separate batches of ore, coke, and miscellaneous materials are common. An odd number of batches are often used to get a natural rotation between the receiving hoppers at the bell-less top and not always charge ore and coke to the same lock hoppers.
- Catch-up capacity with the ability to weigh and deliver charge materials 1.5 times faster than the maximum design hot metal production speed. Catch-up is needed when the burden level is low because of slips or sudden drops in the material level due to blast furnace process problems. Having additional stockhouse capacity has helped many blast furnaces exceed name plate capacity with low investment requirements.

A typical stockhouse arrangement is provided below in Fig. 51.2.

51.3 THE BLAST FURNACE TOP

The blast furnace top is a busy area where raw materials arrive and top gas leaves the furnace. In Fig. 51.3, the charging conveyor, top gas uptakes, and downcomer are clearly visible.

At the very top of the blast furnace, pressure relief valves, also known as bleeder valves, are located to prevent the blast furnace

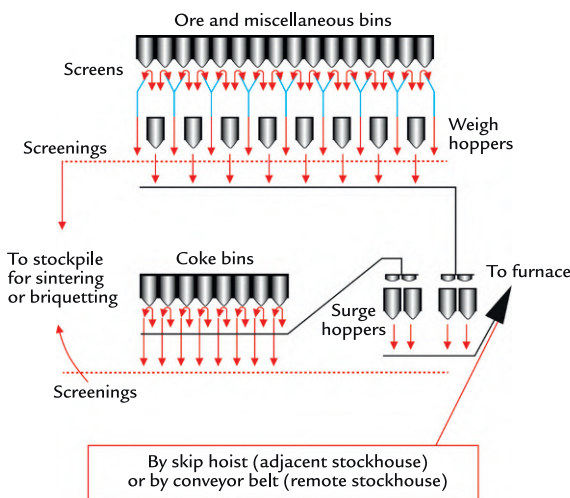


FIGURE 51.2 Typical stockhouse arrangement.



FIGURE 51.3 Blast furnace top equipment including charging conveyor on the left, three of the four top gas uptakes leading to the cross-over main, and downcomer pipe that delivers raw top gas to the gas cleaning plant.
Source: Photo courtesy: CISDI International Engineering & Consulting Co., Limited.

from being over pressured. Typically, three or four bleeder valves are used and are set at different pressure settings to protect the furnace proper. State-of-the-art blast furnaces, such as the one shown in Fig. 51.3, have a smaller pipe located on the downcomer that is used to pipe raw top gas to the gas cleaning plant when the blast furnace is brought offline for a stop and

during the subsequent restart. This is known as a semiclean bleeder and is used to minimize air emission events.

Bleeder openings occur during unstable blast furnace operations most notably slipping of the descending burden. The bleeders can open because of a widespread power outage as bleeder valves are designed to fail in the open position. Bleeder openings or pops are spectacular events where raw blast furnace gas is released under the blast furnace operating pressure to the environment. These emissions can lead to environmental complaints and possibly fines. Blast furnace operators are very focused on minimizing or eliminating bleeder openings through raw material preparation, good hot metal and slag casting practices, and prudent start-up procedures needed to establish smooth burden descent.

51.4 TOP CHARGING SYSTEMS

The top charging equipment must receive each batch of raw materials at atmospheric pressure and then bring these materials to the blast furnace top pressure. The materials are then charged on to the furnace stockline. Blast furnace engineers learned that blast furnace performance improved with specific placement of the burden materials on the stockline. Productivity advantages from increasing top pressure required effective gas sealing technologies. Engineers from Paul Wurth in Luxembourg developed a chute charging system that has dominated all new and re-built blast furnaces since 1970 with over 650 systems being sold as of 2016. Control over where the burden materials are deposited from wall-to-center led to productivity increases, reduced fuel consumption, increased fuel injection, and better control of the wall heat load. The "bell-less" or Paul Wurth top allows ultimate flexibility to place the materials anywhere on the stockline and control top pressure up to 2.5 bar. The key

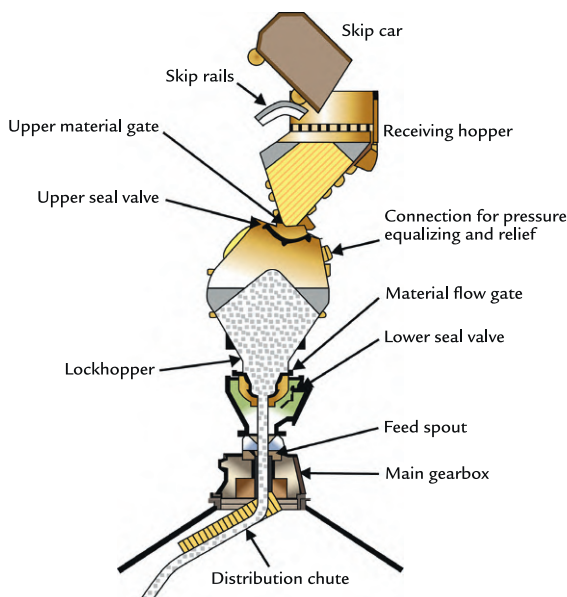


FIGURE 51.4 Single lock hopper bell-less top charging system.

features of a bell-less top are presented in Fig. 51.4; bell-less tops typically have two lockhoppers. Smaller blast furnaces can feature one lockhopper where available space is a concern. Very large blast furnaces have employed up to three lockhoppers to assure that the top can sequence quickly. More details on distributing the burden in the blast furnace are provided in Chapter 59, Burden Distribution.

After filling the lockhopper, the upper seal valve is closed and the lockhopper is pressurized to the blast furnace pressure. To discharge material, the material flow gate is set to the required position and then the lower seal valve is opened. The material flow gate controls the discharge rate for coke and ore to assure that materials are placed on the stockline at specific angles or rings. A batch is discharged in 1–2 minutes and typically 11 rings or chute positions are available for use. The burden charged to each ring can be controlled by the lockhopper weight or by ring indexing based on an estimated charging time.

51.5 COLD AND HOT BLAST SYSTEMS

The use of enormous quantities of air is an essential part of the blast furnace process. Air is first collected and then compressed in axial turbines or turbo blowers to produce cold blast that is delivered to the blast furnace stoves. Due to the heat of compression, cold blast is typically 200–300°C when it leaves the turbo blower. The axial turbines were traditionally steam powered and provided cold blast with a high degree of reliability. More recently, electrically powered blowers have been installed to reduce capital costs for the turbo blower system and generally provide for a smaller plant footprint.

Oxygen and steam are added in planned amounts and then the cold blast is delivered to the hot blast stoves where it is heated to 1200°C. An overview of the cold and hot blast systems is shown in Fig. 51.5.

The hot blast system consists of three major components:

- At least three hot blast stoves where cold blast is preheated to 1200–1300°C.
- A hot blast main that collects the preheated air and delivers this to the blast furnace.
- The bustle pipe, a large ring main that distributes the preheated air to the individual tuyeres where the hot air is injected into the blast furnace.

A typical stove arrangement is provided in Fig. 51.6.

Hot blast stoves are regenerative gas heaters where one stove is used to preheat the cold blast air while the refractory in the remaining stoves is heated using clean blast furnace gas. As the stove in use to heat blast air cools below a planned set point, cold blast air is redirected to a freshly heated stove to maintain the desired hot blast temperature. This is known as the “just-in-

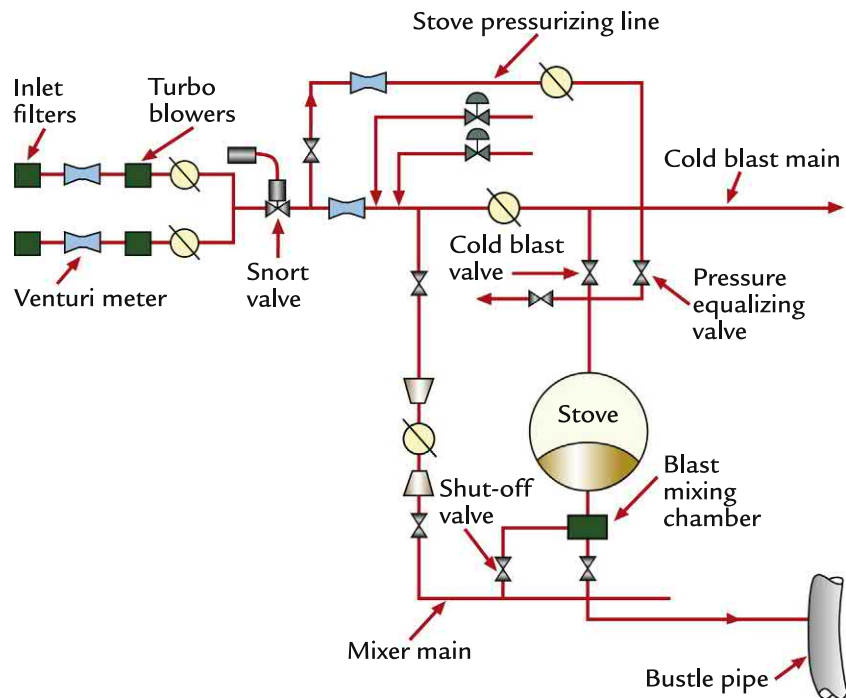


FIGURE 51.5 Cold and hot blast delivery systems with blast mixing chamber at each stove.

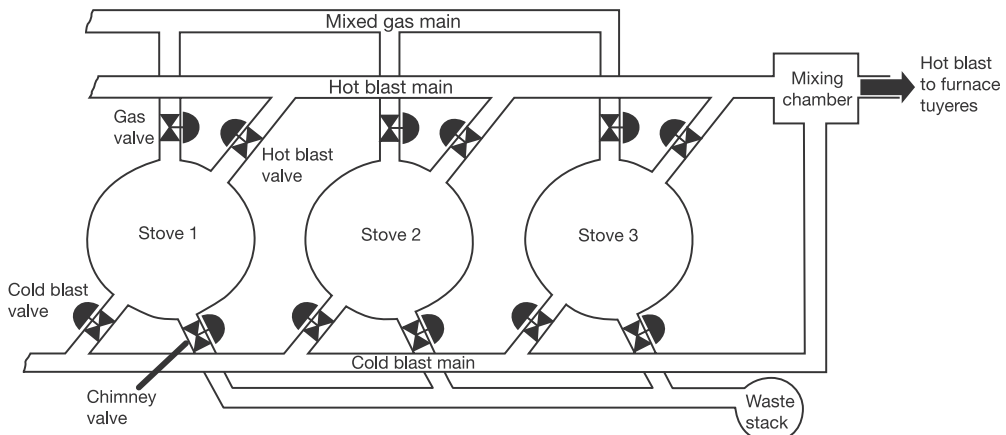


FIGURE 51.6 Typical arrangement for a three-stove hot blast system using a common mixing chamber.

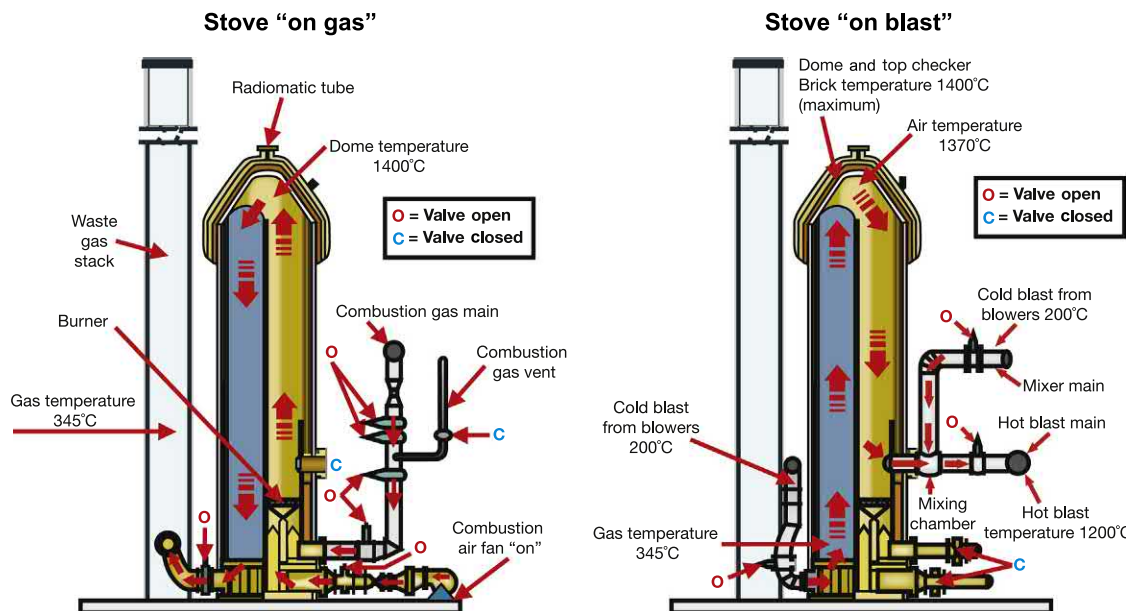


FIGURE 51.7 Internal combustion chamber hot blast stove with mixing chamber at each stove.

time” hot blast heating strategy. This is illustrated in Fig. 51.7 for an internal combustion chamber stove.

The hot blast temperature is controlled to a narrow range by adding a small amount of cold blast air into the hot blast. This cold blast air is introduced via the mixer valve. When a freshly heated stove is brought into service, the mixer valve opens and cold blast is added to reduce the hot air temperature to the target value. As the stove cools, the mixer valve gradually closes. Once the mixer valve is completely closed; a freshly heated stove is brought into service and the cold stove is put on blast furnace gas to reheat the refractory checker bricks. Mixing chambers can be located at each stove outlet. A more common arrangement is a single mixer positioned in the hot blast main that can control the hot blast temperature exiting all stoves. This can be a larger mixing chamber or more often an in-line finger mixer where cold blast is injected directly into the hot blast main through 4 or more openings.

Plants that have four stoves can use a firing strategy known as “staggered parallel.” With this approach, cold blast is preheated to the hot blast temperature using two stoves in parallel and the remaining two stoves are fired to reheat the internal refractory. As one stove cools below a planned set point, it is removed from service and a freshly heated stove is brought into service. With a staggered parallel operation, the cold blast mixer is not required as the operator can mix air from two different stoves to achieve the target hot blast temperature. A staggered parallel operation minimizes the energy losses experienced by introducing cold blast air for temperature control purposes.

Three main stove designs are used:

- The internal combustion stove is the most common where the combustion chamber and refractory column containing the checker bricks are contained in a single vessel.
- Top combustion stoves where combustion occurs above the refractory checkers. The hot

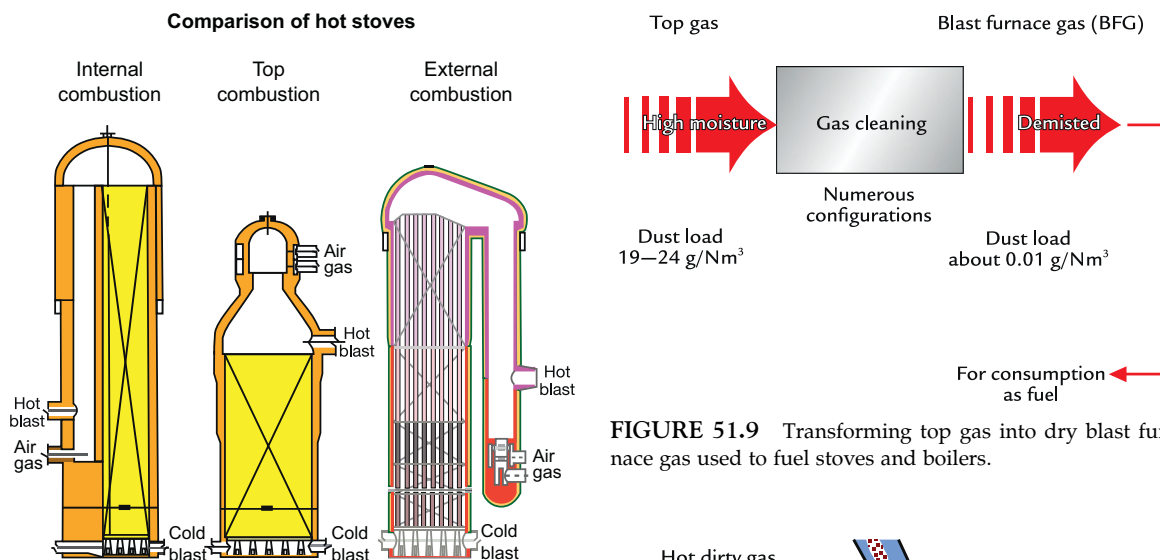


FIGURE 51.8 Comparison of internal combustion, top combustion, and external combustion stoves.

gas is drawn downward through the checkers to preheat the refractory. The process is reversed to preheat the cold blast air.

- External combustion stoves where the burner is separate from the refractory checkers and is connected by a cross-over main.

The basic arrangements and relative size of the three stove designs are shown in Fig. 51.8. Note that the hot blast exits each stove design at a different elevation. The hot blast main position must be designed to accommodate each stove design. Mixing of stove designs at a single blast furnace presents challenges due different hot blast outlet positions.

51.6 BLAST FURNACE GAS CLEANING

Due to the thermodynamics of the blast furnace process, a top gas that is rich in carbon monoxide (CO) and hydrogen (H_2) is always produced. Blast furnace gas is one

FIGURE 51.9 Transforming top gas into dry blast furnace gas used to fuel stoves and boilers.

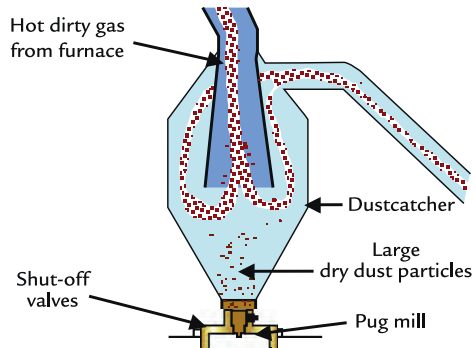


FIGURE 51.10 Dust catcher operation.

of the largest energy streams in an integrated steel works. The blast furnace top gas is first used to fire the hot blast stoves and the remaining blast furnace gas is exported for reheating purposes or to generate steam/electrical power. While blast furnace gas is plentiful, it has a low heating value, approximately 1/10th when compared to natural gas.

The raw top gas must be cleaned and dried to transform this into blast furnace gas, a fuel gas. The transformation requirement process is described in Fig. 51.9.

Upon exiting the blast furnace, larger dust particles are removed using a dust catcher.

This is a large vessel that allows the blast furnace gas to suddenly expand, reducing space velocity and enabling coarser dust to settle as shown in Fig. 51.10.

In newer blast furnaces, the dust catcher is replaced by a very large hot cyclone to enhance the rate of dust removal in this first cleaning step.

After the dust catcher/cyclone, two technologies are used to remove dust and moisture to low levels so that clean blast furnace gas can be used as a fuel. The most common is a gas washer where high pressure water jets are used to trap and collect the contained dust as thickener sludge. The cool and clean gas is then demisted to reduce its water content before being delivered to the stoves as a fuel gas. New plants are implementing dry cleaning of the blast furnace gas using bag houses designed to operate at high temperature. This allows greater electrical power generation potential.

In the gas cleaning plant, the top gas, and hence overall furnace top pressure, is regulated.

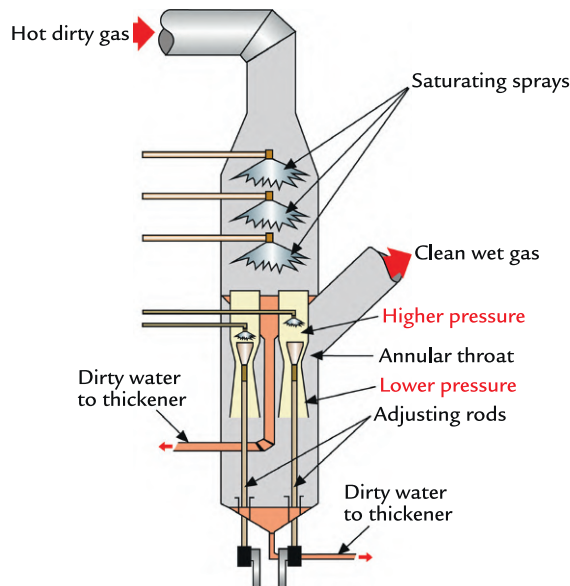


FIGURE 51.11 Annular gap gas washer.

In wet cleaning systems, one or more cones in the gas washer create an annular gap. Top gas pressure can be precisely controlled by moving the cone position and changing the size of the gap that the top gas must flow through. The gas washer is shown in Figs. 51.11 and 51.12.

The pressure contained in the top gases is an important energy source. Top pressure recovery turbines have been installed to depressurize the clean gas through an expansion turbine and generate 10–15 MW depending on the blast furnace size. With a top pressure recovery turbine, top pressure is controlled using the turbine to maximize energy recovery. Dry gas cleaning plants can generate more power as the gas is delivered to the expansion turbine at a higher pressure and temperature; both favor greater power generation. The two arrangements can be compared in Fig. 51.13.

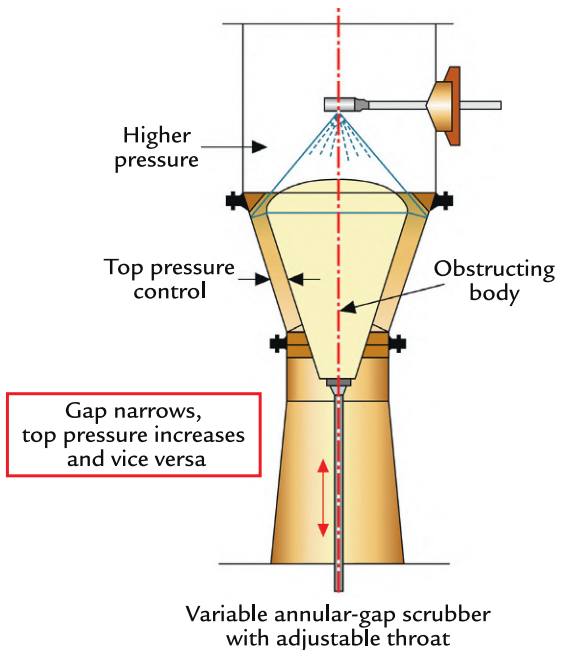


FIGURE 51.12 Top pressure control in annular gap gas washer.

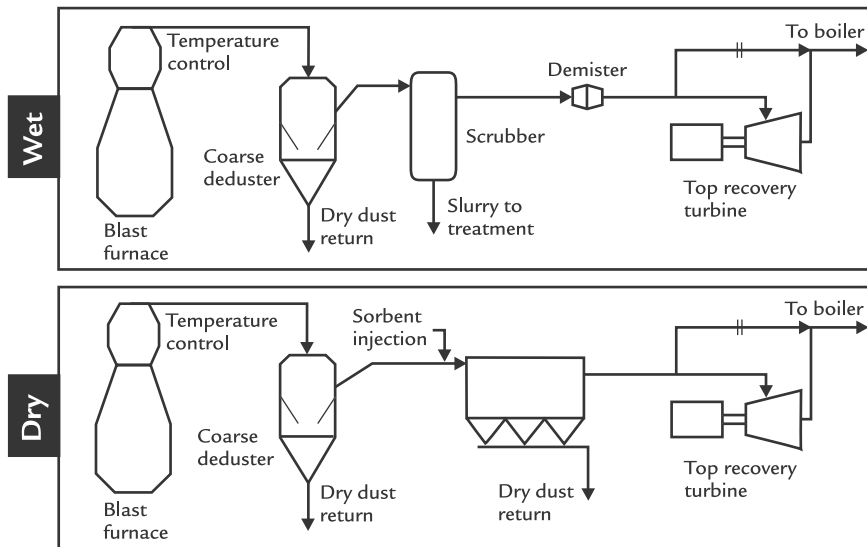


FIGURE 51.13 Wet and dry blast furnace gas cleaning arrangements. In both arrangements, top pressure is controlled with the top recovery turbine to maximize energy recovery as the top gas is depressurized.

51.7 SUMMARY

The systems required to support the blast furnace operation are in themselves complex and sophisticated. Blast furnaces operate with high availability, up to 97% for long periods of time, often for years. The supporting equipment has been engineered to provide long service life and to remain in operation for 20 years without refurbishment. As the blast furnace proper design has improved and campaign life increased, similar demands have been passed to the charging, blowing, hot blast, and gas cleaning systems.

EXERCISES

- 51.1. Straight-line aim temperature is maintained by means of (*please circle one*)
- constant air flow through the stove
 - controlling the stove burner operation
 - the correct operation of the cold air mixer

51.2. Please circle T (true) or F (false) for each of the following statements.

- | | | |
|---|---|--|
| T | F | A hot blast stove is a regenerative heat exchange system used to preheat blast air supplied to a blast furnace |
| T | F | Higher hot blast temperature requires that the stove burner be fired with blast furnace gas only |
| T | F | The top combustion chamber stove was designed to overcome hot blast temperature limitations of the internal combustion chamber stove |
| T | F | Today, all three designs of stove are technologically competitive |

51.3. Please connect, with a line, the correct ending (column 2) to the sentences begun in column 1.

- | | |
|----------------------|--|
| The stove on "blast" | is being heated |
| The stove "on gas" | has been completely heated and is on standby |
| The "bottled" stove | is heating the hot blast |

51.4. Initially, stove combustion is controlled based on (*please circle one*)

- oxygen content of the waste gas
- stove dome temperature
- stove stack temperature

51.5. Please circle T (true) or F (false) for each of the following statements.

T F A stove must be pressurized before going "on gas"

T F A stove must be depressurized before going "on gas"

T F The dome temperature limit is observed to maintain the integrity of the refractories in that area while, at the same time, maximizing the heat input to the checkers

T F The stack temperature limit is observed to maintain the integrity of the refractories in the lower stack while, at the same time, maximizing the heat input to the checkers

51.6. The top zone region is where (*please circle two*)

- the furnace gases are cleaned
- the furnace gases exit the furnace
- the furnace gases distribute the burden fines over the stockline surface
- the burden materials are distributed to form the stockline profile

51.7. The dust catcher (*please circle one*)

- is the first element in the gas cleaning system
- uses water sprays to remove the very fine dust particles
- must be emptied once a week
- is always discharged dry

51.8. The gas washer/scrubber (*please circle one*)

- is the final element in the gas *cleaning* system
- cools the blast furnace gas
- consists of a normal fixed cone to control washer efficiency
- passes blast furnace gas through to a separate demisting unit

Blast Furnace Proper

OUTLINE

52.1 Understanding the Blast Furnace as a Reactor	495	52.5.2 Protecting the Shell in the Stack, Belly, and Bosh Zones	503
52.2 The Blast Furnace Proper - Definitions and Nomenclature	496	52.6 The Tuyere Breast	506
52.3 Blast Furnace Structural Design	497	52.7 Hearth Design	508
52.4 The Basic Blast Furnace Shape	498	52.7.1 Hearth Dimensions	508
52.5 Protecting the Steel Shell - An Important Blast Furnace Design Challenge	500	52.7.2 Hearth Refractory Design	508
52.5.1 Protecting the Shell in the Furnace Throat	502	52.7.3 Hearth Cooling	509
		52.8 Summary	511
		Exercises	512
		References	513

52.1 UNDERSTANDING THE BLAST FURNACE AS A REACTOR

The blast furnace exploits the advantages of countercurrent flow, where the iron ores are dried, heated, reduced, and fused/melted by the rising hot reducing gases generated in front of each tuyere. A summary of the main process demands is provided in Fig. 52.1.

The blast furnace evolved over several centuries into a very tall shaft furnace that maximizes the benefits of countercurrent flow.

Process reactions proceed in an important sequence that maximizes heat and mass transfer efficiency. The blast furnace design accomplishes the following:

- Arranges five process steps - drying, iron ore reduction, melting, combustion, and collection of molten products - so that these processes can efficiently interact with each other.
- The blast furnace design is belly shaped to accommodate the increase in reducing gas

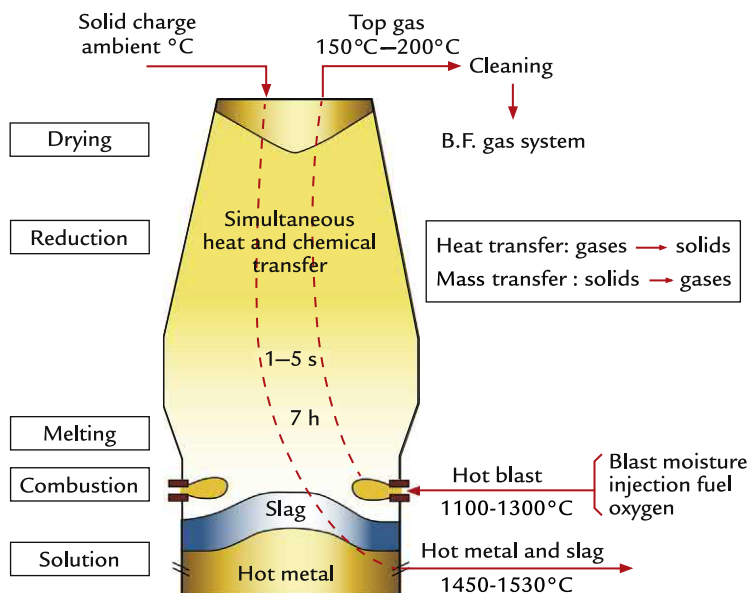


FIGURE 52.1 The blast furnace process.

volume as oxygen is removed from the iron ores. The large belly area aligns with the maximum hot gas volume. The conical stack accommodates a decrease in the reducing gas volume as these gases cool and transfer heat to the incoming charge materials.

- When the iron ores melt, an important structure called the fusion/melting/cohesive zone forms inside the furnace. The blast furnace diameter narrows below the belly to provide support for the melting zone and fix its position above the tuyeres.
- Hot blast air is injected into a coke bed via tuyeres located below the fusion zone. The tuyeres are placed at intervals of about 1.5 m around the blast furnace circumference. The highest temperature in the blast furnace is in front of the tuyeres where combustion occurs, and the flame temperature exceeds 2000°C.
- The lower blast furnace collects molten iron and slag in a refractory lined hearth. The

molten iron and slag are tapped together through a common refractory taphole. Slag and iron are subsequently separated outside of the furnace in the iron trough.

52.2 THE BLAST FURNACE PROPER - DEFINITIONS AND NOMENCLATURE

The four zones in the blast furnace are the stack, belly, bosh, and hearth. These zones are presented below along with the internal layer structure that forms in the charge materials as they descend in the furnace, Fig. 52.2.

Definitions of the various blast furnace zones and other aspects are provided in Fig. 52.3.

Blast furnace operators refer to the interior space in the furnace several separate ways:

- The *total volume* is from the hearth bottom to the top ring.

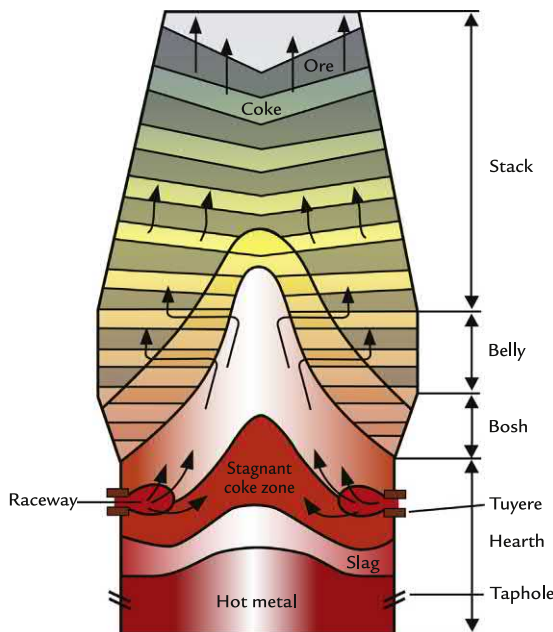


FIGURE 52.2 Positions of the stack, belly, bosh, and hearth zones in the blast furnace.

- The *inner volume* is from the iron notch/taphole elevation to the stockline level.
- The *working volume* is from the tuyere discharge to the stockline level.

The inner and working volume are frequently used when stating the daily blast furnace productivity. Asian and Russian blast furnace operators prefer to express productivity as tonne per day per m^3 inner volume where the balance of the world uses tonne per day per m^3 working volume. Increasingly, productivity is also expressed as tonne per day per m^2 of hearth area. In this case, hearth diameter is defined as the blast furnace diameter immediately below the blast furnace tuyeres.

52.3 BLAST FURNACE STRUCTURAL DESIGN

Special structural design is needed to support the blast furnace due to its great height.

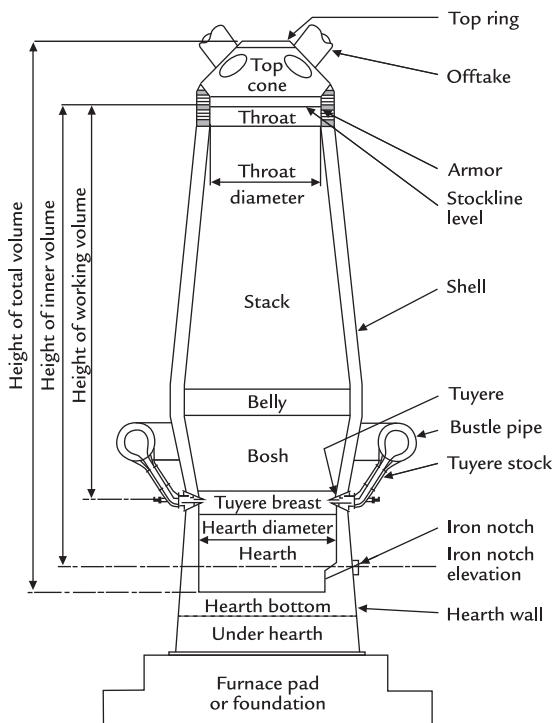


FIGURE 52.3 Complete blast furnace arrangement and nomenclature.¹

In older furnaces, built in the 1950–60s, the furnace was constructed in two sections. Large columns independently supported the upper stack and a special expansion joint was made at the mantle, located between the bosh and belly/stack of the furnace. In the 1970s, blast furnace designers built freestanding furnaces where the furnace shell was made strong enough to support the furnace and all the related equipment. Freestanding furnaces provided an interior profile that better aligned with the process conditions with a smoother transition between the belly and bosh zones. Today, freestanding furnaces are the normal design employed on any newly built blast furnaces. The mantle supported and free-standing furnaces may be compared in Fig. 52.4.

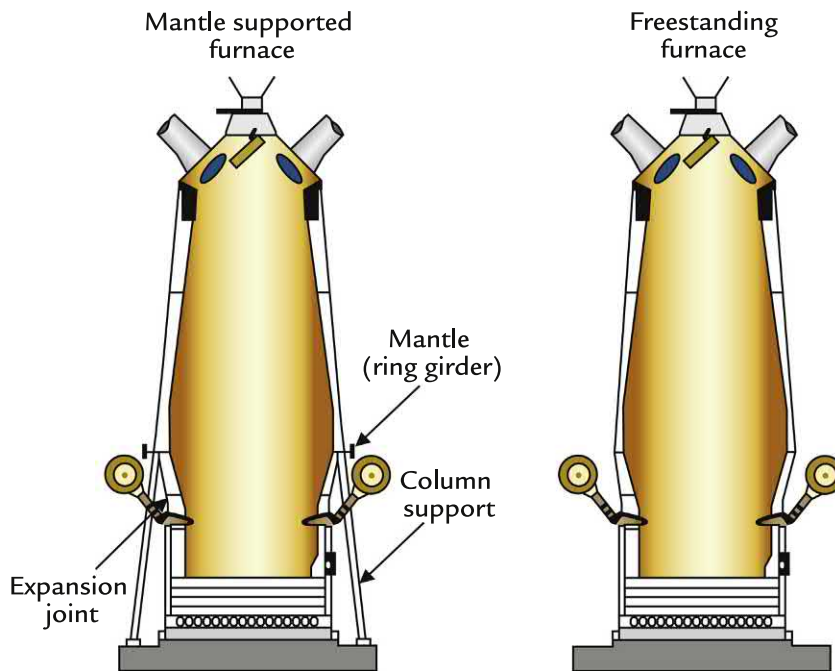


FIGURE 52.4 Mantle/column supported and free-standing blast furnace designs.

As blast furnaces were enlarged over the last 100 years, the constructors tended to reduce the blast furnace height relative to its diameter. Increasing height is expensive from a construction point of view, so designers increased the belly diameter and working volume. A comparison of working volume to the blast furnace height, from tuyeres to stockline, seen in Fig. 52.5, shows the tendency that larger blast furnaces are relatively shorter compared to smaller, and generally older, blast furnaces.

52.4 THE BASIC BLAST FURNACE SHAPE

The shape of blast furnaces evolved over time. There are specific reasons and special rules to govern the angles selected, many empirical in nature. The furnace diameter reaches its maximum when the actual volume

of hot reducing gas is greatest. The tapered shaft maintains the reducing gases' upward space velocity as the reducing gas cools and actual volume decreases. The bosh angles inward to support the fusion zone and maintain the layer structure in the upper furnace. The throat is parallel to allow consistent ore and coke layer buildup. The hearth must have enough volume to allow periodic tapping of hot metal and slag.

Nippon Steel, one of the world's leading blast furnace builders, assessed blast furnace bosh and stack dimensions using a cold model in 2006.² worldsteel published guidelines on blast furnace dimensions as part of a review of copper stave wear.³ The critical dimensions cited by these two groups are presented in Table 52.1. Specific comments on the critical dimensions are provided based on the authors' experience.

In recent years, careful focus has been made on the role bosh angle has on premature stave wear as documented by worldsteel and the

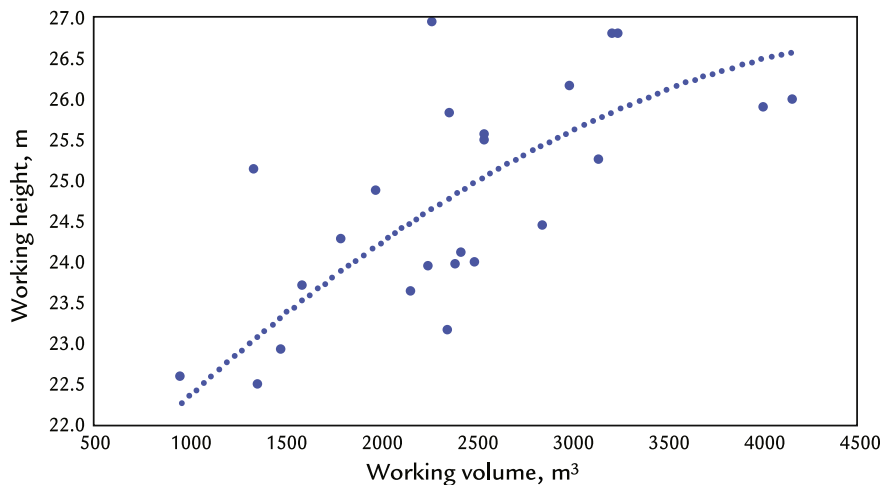


FIGURE 52.5 Trend in blast furnace height as furnace working volume increased.

TABLE 52.1 Typical Blast Furnace Dimensions and Related Criteria From Nippon Steel and Worldsteel^{2–5}

Dimension	Typical Value	Design Considerations
Throat diameter	0.75 × Hearth diameter	Sufficiently large to allow top gas to leave without fluidizing the burden
Throat height	1.5–2.0 m	Parallel to allow ore and coke layer buildup
Stack angle	80°–85°	Compensate for decreasing gas volume as gas cools. Needed to maintain ore and coke layer structure at the blast furnace wall. Shaft angle decreases with increasing working volume
Belly diameter	1.14 × Hearth diameter	Provide maximum volume at point with maximum gas volume and highest gas velocity exiting the coke slits in the fusion zone
Belly height	2.0–3.0 m	Manage the heat load from the hot gases exiting the fusion zone at high velocity
Bosh height	0.45 × Throat diameter	Supports the cohesive zone and upper furnace layer structure. Bosh height <3.5 m reduced the probability of stave wear
Bosh angle	70°–85°	Supports the fusion zone. Slightly increasing with greater working volume. Bosh angle is critical to copper stave wear; blast furnaces with a lower bosh angle (<75°) demonstrated better wear resistance
EHA	0.5–0.9	$\text{EHA} = \pi \times (\text{Hearth diameter}/2)^2 - \pi \times (\text{hearth diameter}/2 - \text{raceway depth})^2 / (\pi \times \text{hearth diameter}/2)^2$; raceway depth is typically 1.5 m Decreases with increasing inner volume

EHA, Effective hearth area.

work of Esmer.^{2–5} Subtle changes to the bosh angle can have a profound impact on blast furnace performance. When the bosh angle is high, that is a steep vertical bosh, the fusion zone position is unstable creating abrasion wear on the staves. A lower bosh angle providing a shallower transition supports the fusion zone and less stave wear was observed. Too low a bosh angle, which is $<70^\circ$, reduces hearth volume and ultimately blast furnace productivity.

Historically, bosh angle was specified using one of three rules:

- The 4-ft-by-4-ft rule from US experience; 4 ft up from the tuyere tip and then 4 ft back should intersect the refractory hot face. This results in a bosh angle of 45° .
- The 12-ft-by-5 ft rule, like above from British Steel's Scunthorpe Works. This results in a bosh angle of 67.4° .
- The 21.5° rule from Bethlehem Steel, USA, and used by the Europeans. The bosh hot face from the tuyere nose tip to the top of the bosh should be at 21.5° to minimize wear. This results in a bosh angle of 68.5° .

The 4-ft-by-4-ft rule, 12-ft-by-5-ft rule, and 21.5° rules may be compared in Fig. 52.6. All of these rules result in bosh angles $<70^\circ$. Modern blast furnaces have deployed steeper bosh angles, $75\text{--}85^\circ$ in an effort to maximize blast furnace productivity.

Recent failures of copper staves have led to new thinking about the correct bosh angles needed to reduce wear. Esmer and world-steel's investigations suggest that a lower bosh angle, $<75^\circ$, will increase copper stave life, likely by stabilizing the fusion zone position in the blast furnace.⁵

52.5 PROTECTING THE STEEL SHELL - AN IMPORTANT BLAST FURNACE DESIGN CHALLENGE

The steel shell that shapes the blast furnace must be protected from the internal process

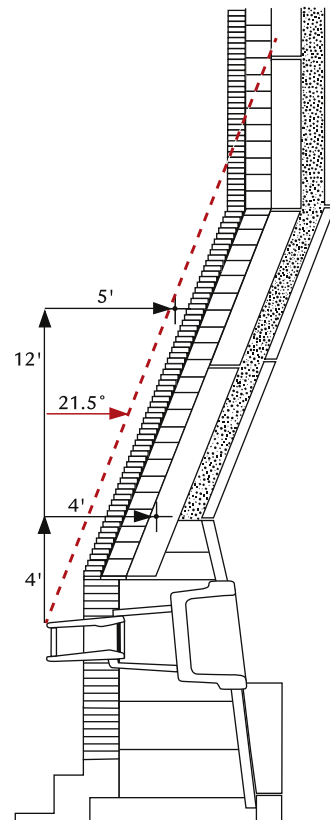


FIGURE 52.6 Comparison of bosh angle rules.

conditions. From the tuyeres to the stockline, a wide variety of wear mechanisms must be considered in designing a system to protect the steel shell. These include abrasion, elevated temperatures, and chemical attack to name a few wear mechanisms that must be considered. A summary is provided in Fig. 52.7.

Thermal attack varies with elevation, ferrous burden composition, and operating practice. These changes are illustrated in Fig. 52.8. Additional wear mechanisms including abrasion, oxidation, slag attack, and zinc and alkali attack are shown in Fig. 52.9 by blast furnace zone.

The resulting high wear areas can be seen by surveying blast furnaces at the end of their service life when the old cooling system and refractory are removed. Wear is typically the

Wear mechanism	Bosh	Belly	Lower stack	Middle stack	Upper stack
Thermal shock	Moderate-high	Extreme	Extreme	High	Low-moderate
Heat load	Moderate-high	High	Moderate	Moderate	Low-moderate
Slag attack	Extreme	Extreme	Moderate	Low	Low
Alkali/zinc attack	High	Moderate-high	High	High	Moderate-high
Oxidation	Low-moderate	Low-moderate	High	Moderate-high	Low-moderate
Abrasion	Low-moderate	Low-moderate	Moderate-high	High	High
Hot metal attack	Low-moderate	Low-moderate	Low	None	None

FIGURE 52.7 Wear considerations by blast furnace zone.

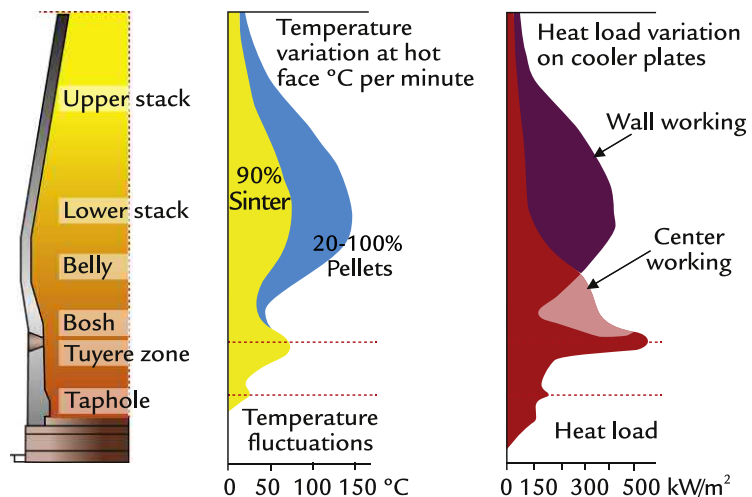


FIGURE 52.8 Impact of ferrous burden composition and operating practice on the heat loads and temperatures observed in the blast furnace cooling system.

highest in the lower stack and belly regions, Fig. 52.10.

Historically, the blast furnace was designed with a refractory lining to protect the steel

shell. Over time, the use of cooling plates and staves has greatly decreased refractory usage. Refractory and other materials used must work in harmony with the cooling system and

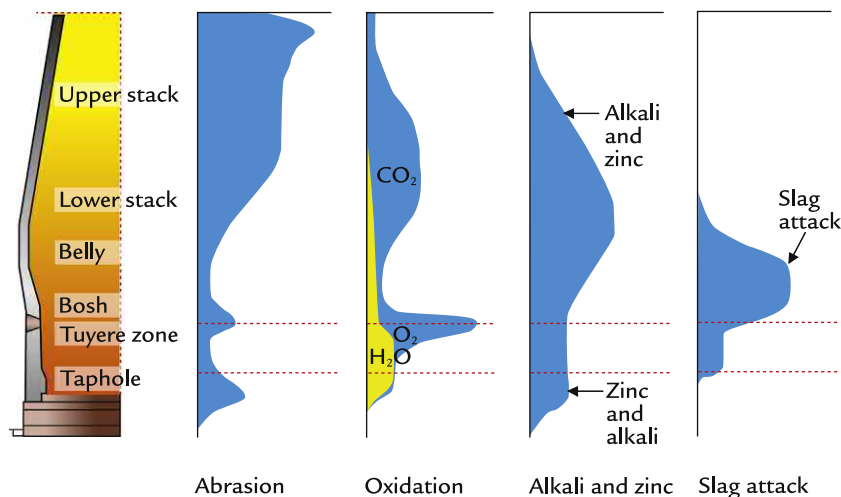


FIGURE 52.9 Lining attack mechanisms by blast furnace zone.

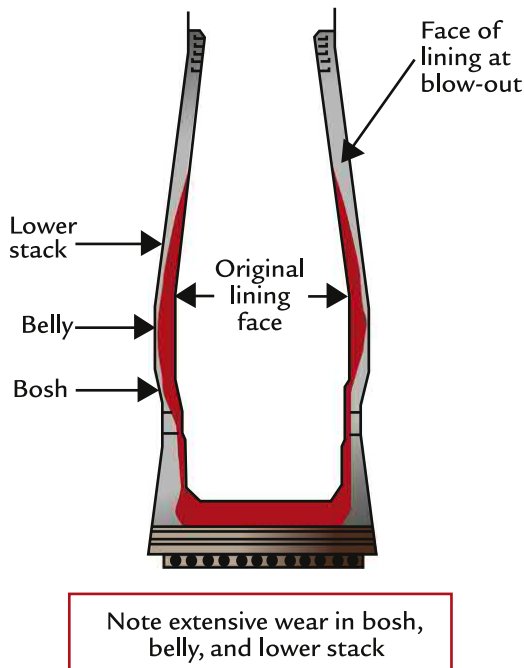


FIGURE 52.10 Typical wear profile of a blast furnace at the end of the campaign.

are selected for specific performance properties, details in the next sections.

52.5.1 Protecting the Shell in the Furnace Throat

The blast furnace throat is subject to the impact of the coke and ferrous burden during every charge. Abrasion, thermal deformation, and fatigue-related wear are the main wear threats to be considered as described by van Laar and Engel.⁶ Maintaining the parallel throat is mandatory to assure that ore and coke layers are properly created when the respective batches are charged. Throat armor design is described by van Laar and Engel⁶:

- Steel wear plates attached with a refractory backup lining.
- Cast iron staves with rib structure with embedded wear resistant refractory, such as silicon carbide, added.

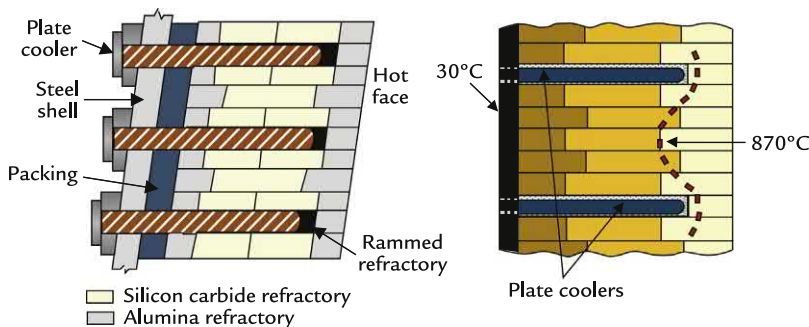


FIGURE 52.11 Basic copper cooling plate design for the upper stack.

52.5.2 Protecting the Shell in the Stack, Belly, and Bosh Zones

Finding the best technology to protect the blast furnace shell in the high wear zones in the lower stack, belly, and bosh is a continuing challenge for blast furnace designers. Two approaches have emerged to provide campaign lives of 15 years:

- Copper cooling plates inserted perpendicular to the steel shell and surrounded by refractory.
- Cooling staves, either cast iron or copper, attached parallel to the steel shell.

Both designs have matured to decrease the lining thickness and thus increasing the blast furnace working volume and production potential. Stave usage increased with the introduction of copper staves, but performance issues have provided variable success from furnace-to-furnace. Design improvements are continuing as blast furnace operators strive to consistently reach campaign lives of 20 years before a reline.

52.5.2.1 Protecting the Shell With Copper Cooling Plates

Copper cooling plates surrounded with refractory bricks have been used since the mid-1900s. The basic design is shown in Fig. 52.11.

At different elevations, the copper cooling plate design can be configured to address the predominant wear mechanism present by changing;

- the interplate spacing, both vertical and horizontal distance between plates;
- water velocity and effective cooling capacity of the copper plates employed; and
- changing the refractory material used between the plates, balancing abrasion wear resistance, thermal shock properties, chemical attack resistance, thermal conductivity, and cost.

The design approach at different stack zones is summarized in Table 52.2. Different copper cooling plate designs are provided in Fig. 52.12.

Tata Steel IJmuiden in the Netherlands has the best performance with a plate cooled stack in blast furnaces 6 and 7. Stack wear stabilized after 6–7 years and further wear has been minimal. Blast furnace 6 campaign life has exceeded 30 years and continues at the time of writing.

52.5.2.2 Protecting the Shell With Stave Coolers

Stave coolers mounted to the inside of the blast furnace shell were originally developed in the former Soviet Union in the 1960s. The first stave coolers were made of gray cast iron and featured four cooling pipes. The early designs did not use pumps to circulate the cooling

TABLE 52.2 Copper Cooling Plate Design Approaches for Various Stack Zones⁶

Zone	Copper Plate Spacing	Refractory
Upper stack	Wider spacing used due to lower heat flux from the rising reducing gas	Alumina and silicon carbide balancing cost, wear resistance, performance, and oxidation resistance
Lower stack	Close plate spacing to extract heat where process heat flux reaches maximum values	Nitride-bonded silicon carbide for abrasion resistance and increased thermal conductivity
Belly	Close plate spacing to extract heat where process heat flux reaches maximum values	Nitride-bonded silicon carbide for abrasion resistance on the hot face. Graphite around the cooling plates for high thermal conductivity and ability to cool the silicon carbide
Bosh	Close plate spacing to extract heat where process heat flux reaches maximum values	Graphite lining for high thermal conductivity and ability to sustain a frozen skull of slag and hot metal as an "in situ" wear lining
Tuyere breast	Plate coolers between the tuyeres	Graphite lining for high thermal conductivity

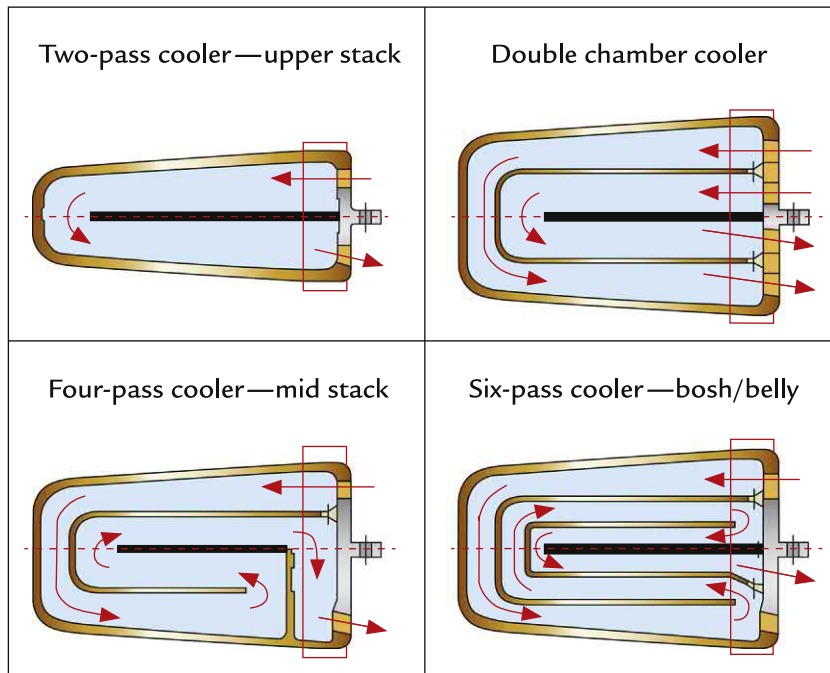


FIGURE 52.12 Various copper cooling plate water passage designs for stack usage.

water; instead the water heated within the staves, warmer water rose causing cooler water to move upward from the lower part of the cooling circuit. Steam accumulated at the top of the

stave cooling system and was released. As the stave cooling technology matured, the natural cooling system was replaced with forced circulation and heat exchangers as shown in Fig. 52.13.

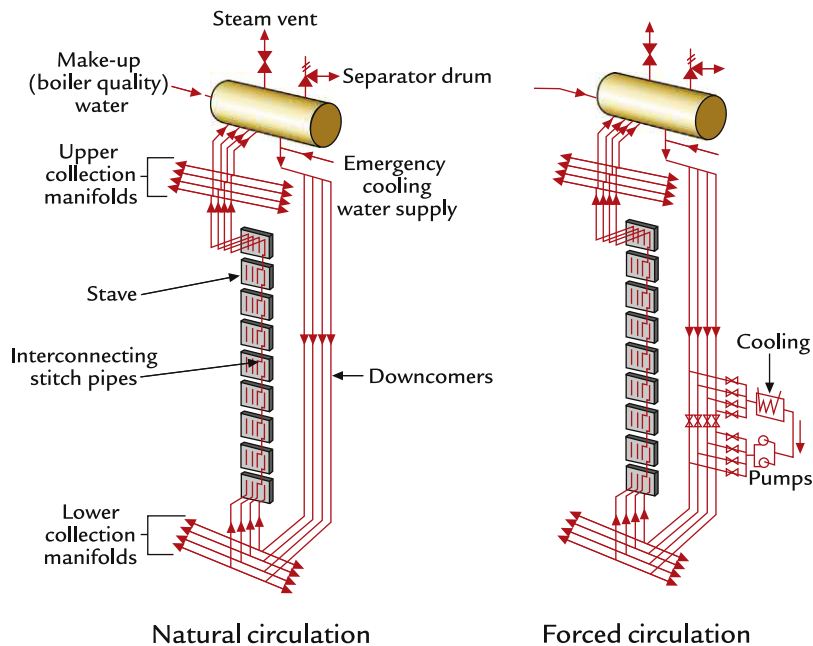


FIGURE 52.13 Stave cooling system for blast furnaces.

Cast iron staves are susceptible to cracking as the stave temperature increases and the cast iron undergoes a phase change. Stave design evolved by switching from gray to nodular cast iron and introducing increasingly intensive cast-in pipe cooling arrangements, Fig. 52.14.

In the 1990s, copper staves were developed for the high heat load areas including the bosh, belly, and lower stack. The original copper staves were machined from copper plates and then plugs inserted to form the water passages. Later, cast copper staves with a Monel or Cu–Ni pipe for the water passage were introduced as an alternative design. Copper staves were thinner than the cast iron staves they replaced providing an increase in the working volume for the same blast furnace shell design. The copper staves were implemented to freeze a process skull of slag and hot metal that in turn would protect the copper from the abrasive effects of the descending burden, Fig. 52.15.

Performance of copper staves has been variable with blast furnace operators. Early adopters had remarkable success with copper staves removed after many years in the blast furnace that look almost new. Later spectacular failures were experienced with operators having great difficulty controlling the blast furnace and major failures after 3–4 years of service. worldsteel documented this experience and identified possible failure mechanisms from both a design and operational view point.^{3,5}

Furnace designers are working to establish an improved design of copper staves to achieve the needed performance. Changes being considered are;

- alternate rib spacing and shape to create a stagnant zone at the hot face and reduce abrasion wear;⁸
- the addition of steel edges to resist abrasion;⁹ and
- implementation of wear resistant material in the copper stave hot face.¹⁰

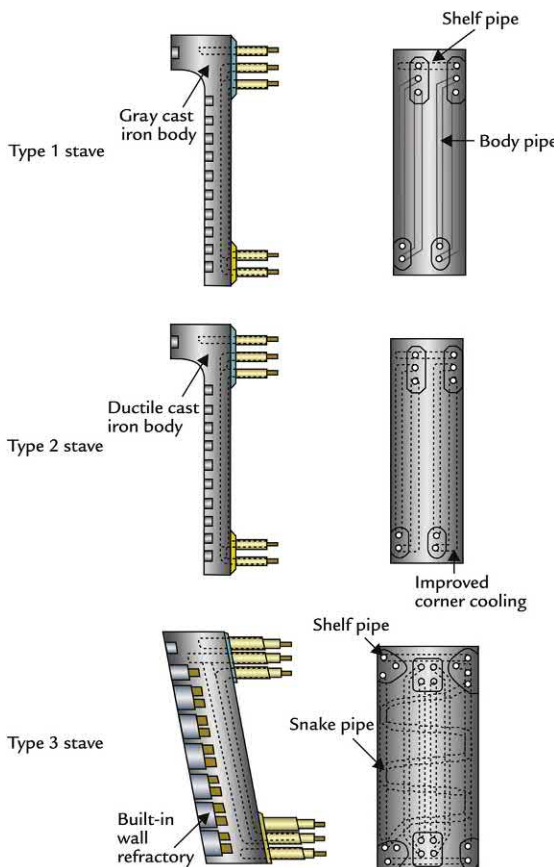


FIGURE 52.14 The evolution of cast iron staves with increased cooling and added refractory.

Copper stave cooling developments will continue to improve copper stave life due to the substantial number of global users. Some blast furnace operators have opted to convert to copper cooling plates, but such a change is expensive and time consuming as the entire blast furnace shell must be replaced to accommodate the new pattern of shell openings required for plate cooling.

52.6 THE TUYERE BREAST

The location where the blast air enters the furnace via the tuyeres is known as the tuyere



FIGURE 52.15 Copper bosh stave.⁷

breast. This area is complex; the design must hold the tuyeres in position and maintain a gas seal at the region of the blast furnace that is at the highest gas pressure. The tuyere breast construction for a stave cooled bosh is provided in Fig. 52.16.

The blast air is fed from the bustle pipe to individual tuyere stocks, through the blowpipe to the tuyere. The tuyere is held in position by a larger copper tuyere cooler. Tuyeres protrude into the blast furnace and are always angled downward.

Tuyeres operate under demanding conditions; the area of the furnace with the highest temperature and pressure, swirling hot coke, and splashing molten slag and iron. Tuyeres are intensively cooled and often feature hard or armor facing to resist abrasive wear, Fig. 52.17.

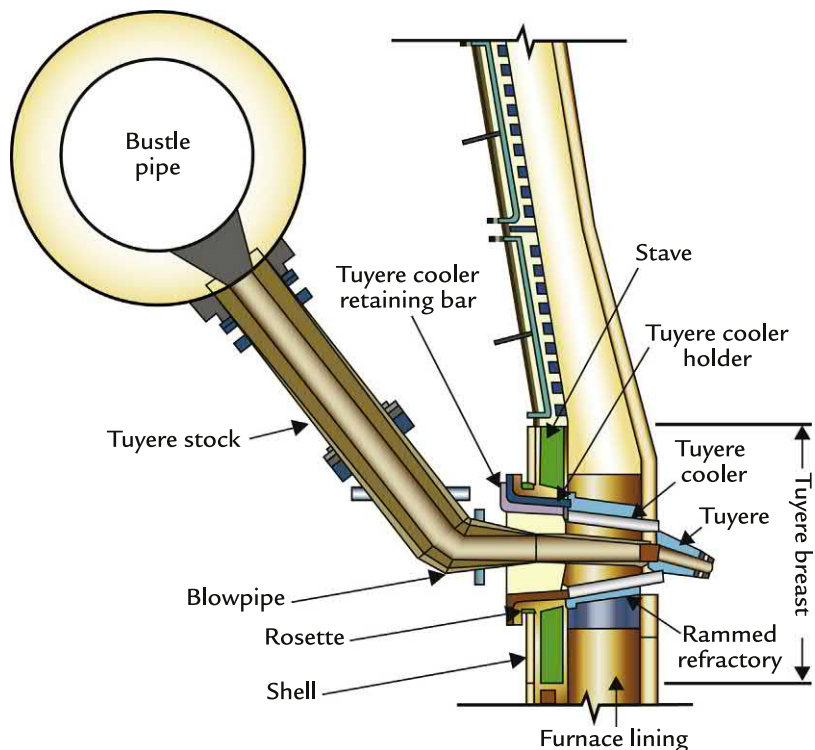


FIGURE 52.16 The tuyere breast.

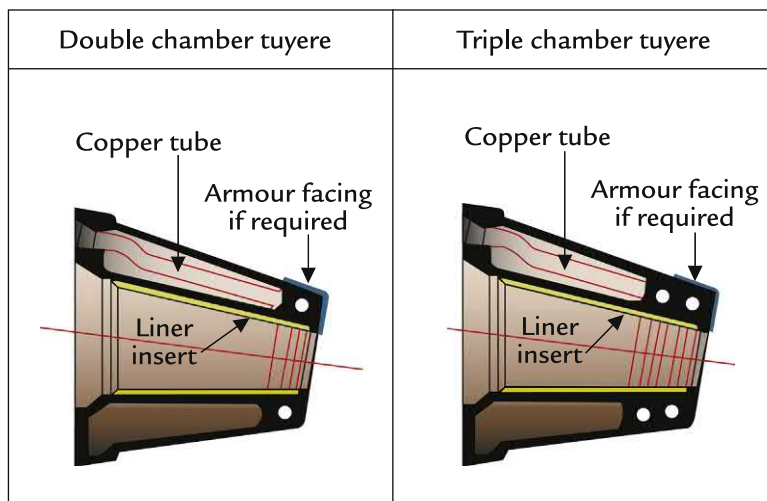


FIGURE 52.17 Selected tuyere cooling configurations.

Tuyere life is typically 1–2 years before they fail, because of abrasion or due to burns from molten iron.

52.7 HEARTH DESIGN

The hearth functions to collect the molten iron and slag and then discharge these liquids through the taphole. Basic hearth design will be covered in this section while taphole design is presented in Chapter 57, Casting the Blast Furnace.

Hearth design encompasses three main aspects:

- Hearth dimensions
- Refractory
- Hearth cooling

With the growth of injected fuel usage, especially pulverized coal injection, and the related increases in productivity, blast furnace hearth life has decreased from 10–15 years to 8–10 years. Hearth wear has been accentuated in two specific areas:

- About 2 m below the taphole and about 1.5–2.0 times the width of the taphole refractory structure
- Where the hearth bottom meets the hearth side wall—known as “elephant foot” wear, [Fig. 52.18](#)

There are many discussions in the blast furnace community regarding the best approach to hearth design. Design philosophies can be different, and a variety of solutions have emerged. A consensus hearth design has not been reached due to the long time required to prove out each design concept.

52.7.1 Hearth Dimensions

The position of the deadman has been identified as a root cause for hearth wear. As shown in [Fig. 52.18](#), a floating deadman promotes molten iron flow under the coke bed. This decreases the molten iron velocity and promotes bottom wear. A sitting deadman causes peripheral flow of molten iron and creates elephant foot wear.

Blast furnace designers have focused on increasing the hearth sump depth to assure that the deadman floats under all operating conditions. Such a change is easy for a new blast furnace but is much more challenging with an existing furnace as many working points, such as the taphole position, are expensive to change.

Blast furnace hearth walls may be vertical or can slope slightly outward. Sloped hearths increase the hearth diameter between the tuyeres and hearth bottom. This increase in diameter will promote a slower iron velocity in the hearth bottom region and reduce the elephant wear effects.

52.7.2 Hearth Refractory Design

The ideal refractory for the hearth is a carbon-based refractory as the very low

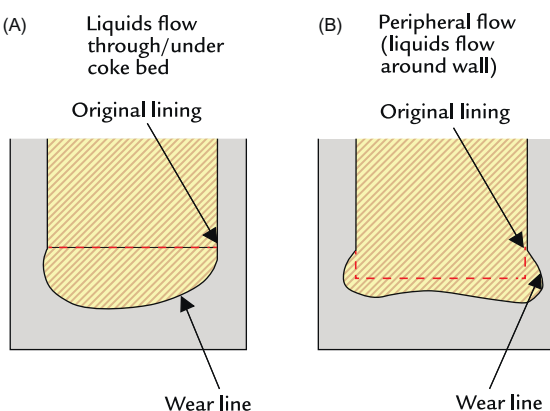


FIGURE 52.18 Hearth wear profiles. (A) Bottom wear typically with a floating deadman and (B) elephant foot wear when the deadman sits on the hearth bottom.

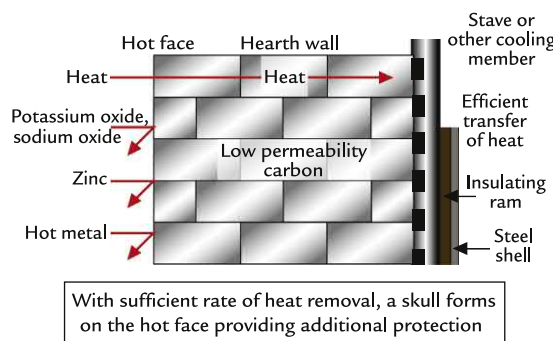


FIGURE 52.19 Key features of a hearth wall refractory construction.

oxygen pressure in the blast furnace hearth means that carbon oxidation is impossible under normal operating conditions. Carbon has valuable properties such as being nonwetting to molten iron so that it minimizes iron penetration into the refractory carbon grain structure and subsequent cracking. It also has a high thermal conductivity that enables refractory cooling to be effective.

Refractory designers have developed carbon, graphite, and semigraphite refractories for hearth applications. The focus is often to minimize pore size to prevent molten iron infiltration and provide the highest thermal conductivity. The various refractory grades are discussed by van Laar et al., additional developments are ongoing.¹¹ Low permeability of the hearth wall refractory will promote heat transfer, freeze a protective skull, and provide resistance to refractory attack, Fig. 52.19.

A major design decision is to use smaller "hot-pressed" bricks or much larger blocks. North American blast furnaces often feature the smaller bricks and have experienced good hearth wall performance. The balance of the world uses larger blocks. While many hearth designs exist, an example of a small brick design with carbon beams for the hearth bottom is provided in Fig. 52.20.

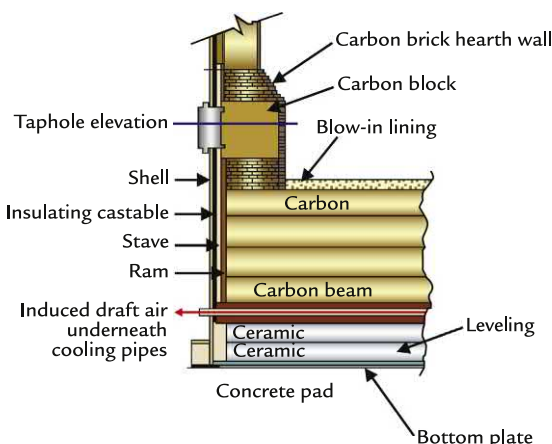


FIGURE 52.20 Heath refractory design featuring small hot-pressed bricks and carbon beam design.

The hearth wall can be a single or double ring construction. Careful design and installation of the refractory are needed to assure that the hearth bottom does not push up and compromise the hearth sidewall. Further details of this complex interaction can be found in dynamic stress analysis completed by Maleki, Chomyn, Phillips, and Ghorbani.¹² The expansion issues are created by differential expansion between the hot and cold faces of the refractory structure, Fig. 52.21.

The hearth bottom is typically constructed of several carbon beams. A top layer of chamosite or other high alumina refractory may be implemented to delay bottom wear in the initial phases of the campaign. Eventually, the ceramic layer wears away and the carbon will wear until a process skull is formed by the underhearth cooling system.

52.7.3 Hearth Cooling

Both the sides and bottom of the hearth are cooled. Side-wall cooling can be completed with cooling staves, water jacket/channel cooling, or shell sprays, Fig. 52.22.

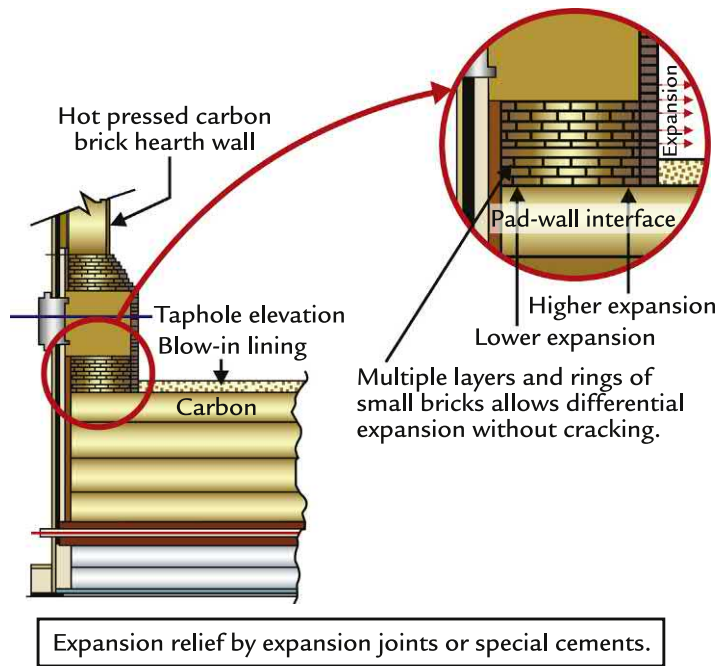


FIGURE 52.21 Expansion challenges where the hearth wall and bottom meet.

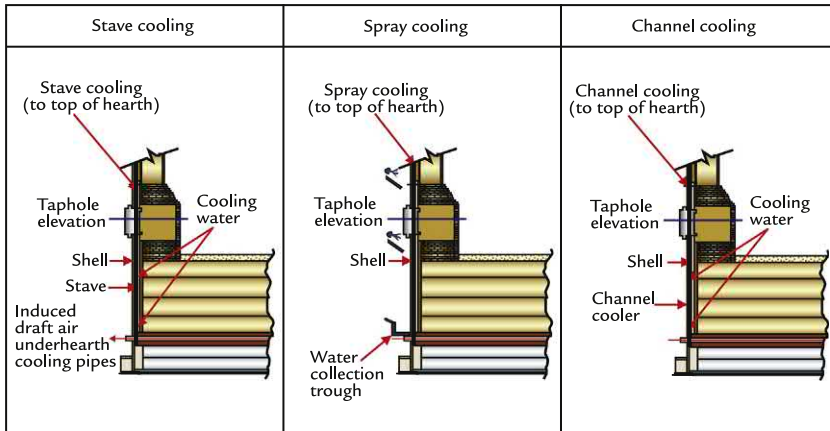


FIGURE 52.22 Hearth side-wall cooling using staves, water sprays, and channel cooling (water jackets).

The hearth bottom can be cooled using one of three methods, Fig. 52.23:

- Induced air draft, where air is sucked through channels in the hearth bottom refractory

- Water cooling using a grid of embedded pipes
- Oil cooling, like water cooling using embedded pipes.

Hearth life ultimately determines the blast furnace life as a hearth replacement forces a

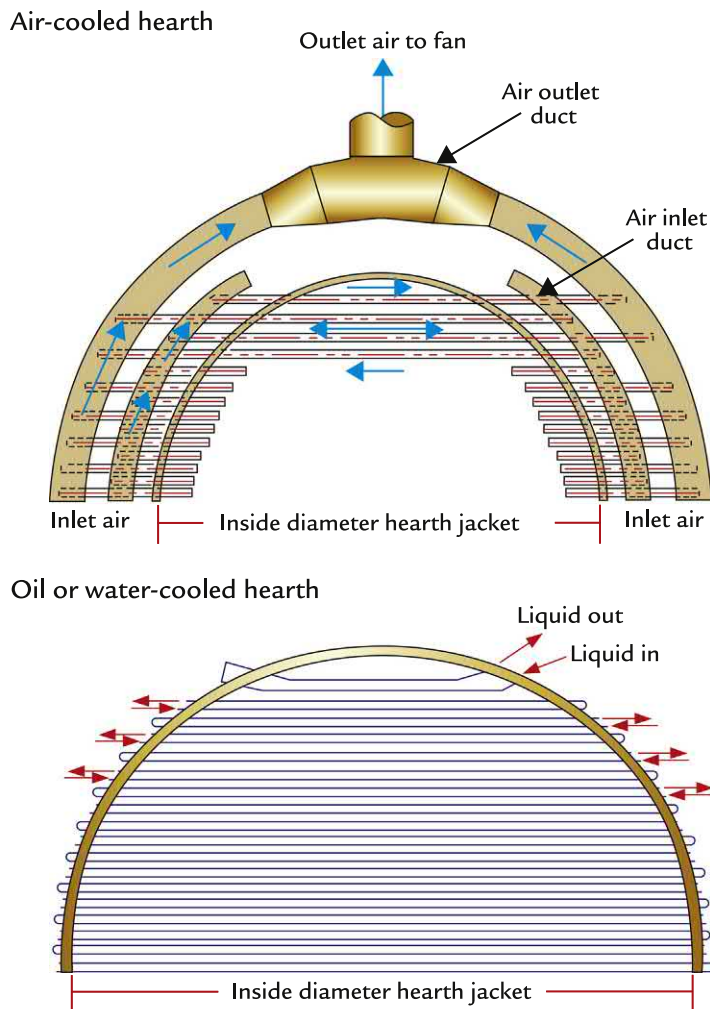


FIGURE 52.23 Air and liquid hearth bottom cooling systems.

complete blast furnace rebuild. Blast furnace designers will continue to focus on understanding hearth wear and developing technologies to provide a 20-year campaign life at high productivity rates.

52.8 SUMMARY

The blast furnace proper has been described in detail from the furnace top to the hearth

bottom. The furnace is a complex structure that incorporates decades of operational experience. Even with such history, many challenges remain to easily reach a 20-year campaign without a stop for repairs. This needs to be accomplished with increasing productivity, greater use of injected fuels, and a low coke rate. Additional blast furnace changes may emerge with future changes to reduce carbon usage such as stack injection of pre-heated process gases.

EXERCISES

52.1. Which of the following statements are true (T) and which are false (F)?

-
- | | |
|--------|--|
| T F | The ascending furnace gases drop in temperature from 1900–2200°C to 150–200°C in 5–10 s. |
| T F | The ascending gases give up oxygen to the descending iron oxide of the ore. |
| T F | All the cleaned blast furnace gas is used to heat the stoves. |
| T F | Normally, each blast furnace is equipped with three stoves. |
-

52.2. Blast furnace cooling is provided to (*please circle one*)

- cool and protect the furnace shell (refractory lined furnace)
- preserve the furnace lining (refractory lined furnace)
- provide the correct temperature for the process

52.3. Please circle T (true) or F (false) for each of the following statements.

-
- | | |
|--------|---|
| T F | Plate and stave cooling are designed to isolate the furnace shell from the cooling process. |
| T F | Shower/Spray cooling and jacket/channel cooling have the disadvantage that the shell plate acts as a cooling element. |
-

52.4. Please circle T (true) or F (false) for each of the following statements.

-
- | | |
|--------|---|
| T F | The casting operation can significantly affect stave temperature. |
| T F | Scaling of the inner wall of the stave water piping lowers the rate of heat transfer from the staves to the water. |
| T F | Since the use of untreated water in the stave systems scales up the inner wall of the water piping, its use is never justifiable. |
| T F | The water circulated in the staves is boiler quality water. |
-

52.5. Please circle T (true) or F (false) for each of the following statements.

-
- | | |
|--------|--|
| T F | The key to refractory survival in the hearth is effective, uninterrupted cooling. |
| T F | The most critical part of the refractory system is the bosh, belly, and lower stack. |
| T F | The well-designed refractory system uses only a single type of refractory in any one region of the blast furnace. |
| T F | High thermal conductivity refractories promote the formation of a protective layer (skull) on the refractory hot face. |
-

52.6. Excessive heat loading on the staves (*please circle one*)

- makes the staves more efficient
- causes protective scab to melt or peel
- increases stave resistance to abrasion
- endangers the integrity of the cast iron

52.7. Blast furnace refractories (*please circle all that apply*)

- are either carbon or ceramic
- carbon refractories are used where low heat conductivity is required
- ceramic refractories are often used a sacrificial blow-in lining
- blast furnaces use ceramic bricks to line the furnace in the upper stack

52.8. Please circle T (true) or F (false) for each of the following statements.

-
- | | |
|--------|--|
| T F | The hearth pad on most blast furnaces is constructed of carbon beams. |
| T F | The bosh, belly, and lower stack are subjected to the highest intensity of attack by the various destruction mechanisms. |
| T F | The most severe refractory wear mechanism in the hearth is slag attack. |
| T F | The most severe refractory wear mechanism in the upper stack is abrasion. |
-

References

1. Wallace JP, et al. *The blast furnace facility and equipment. Chapter 9, Ironmaking volume The making, shaping and treating of steel.* Pittsburgh, PA: The AISE Steel Foundation; 1999. p. 644.
2. Ichida M, Anan K, Kakiuchi K, Takao M, Morizane Y, Yamada I, et al. Inner profile and burden descent behavior in the blast furnace. In: *Nippon steel technical report No. 94;* 2006. <<http://www.nssmc.com/en/tech/report/nsc/pdf/n9414.pdf>> [read 20.07.18].
3. Janjua R, De Langhe Y, Esmer M, Musante R, Catalá G, Jansson B. Life extension of copper staves in blast furnaces. In: *METEC Conference Proceedings.* Dusseldorf, Germany; 2015.
4. Esmer M, Özüyük HA. A new approach for the wear failure risk of copper staves in blast furnaces. *Trans Indian Inst Met* 2017;70(8):2137–45 The Indian Institute of Metals - IIM 2017.
5. Esmer M, Özüyük HA, Janjua R, Catala G, Musantes R, Jansson B. A new practical engineering approach to improving the service reliability of copper staves in blast furnaces. In: *3rd ESTAD.* Vienna; June 2017. pp. 1798–808.
6. van Laar R and Engel E. Modern blast furnace design. In: *METEC and 2nd ESTAD.* Dusseldorf, Germany; June 2015.
7. Shaw A, Sadri A, Cameron I, Jastrzebski M, Brown R, Hyde JB. *Preserving copper staves and extending blast furnace campaign life.* Indianapolis, IN: AISTech; 2014. p. 715–22. May 2014.
8. Goto M. Long life copper stave for blast furnace developed by Nippon Steel & Sumikin Engineering. In: *7th European Coke and Ironmaking Congress—ECIC 2016.* Linz, Austria; 2016. pp. 100–8.
9. Simoes J-P, Tockert P, Goedert P, Maggioli N, de Gruiter C. The role of copper staves in achieving efficient operation and long blast furnace campaigns. In: *METEC and 2nd ESTAD.* Dusseldorf, Germany; June 2015.
10. Vickress D, Rudge D, Hyde B, Cameron I. *Technology advancements in blast furnace cooling – part 2.* Philadelphia, PA: AISTech; 2018. p. 581–7. May 2018.
11. van Laar R, van Straaten V, Wise-Alexander J. Low-cost hot metal blast furnace design In: *METEC and Inconsteel Steel Con 2011, Session 14.* Dusseldorf, Germany; June 2011.
12. Maleki M, Chomyn K, Phillips S, Ghorbani H. *Performance comparison of different blast furnace hearth designs using a novel structural refractory assessment methodology.* Nashville, TN: AISTech; 2017. p. 691–8. May 2017.

Blast Furnace Refractory Inspection Technologies*

O U T L I N E

53.1 Introduction	516	53.6.6 Acousto-Ultrasonic-Echo (AU-E)	528
53.2 Refractory Wear Mechanisms	517	53.6.7 AU-E Calibration	530
53.3 Determining the Refractory Lining Status	519	53.6.8 Thickness Measurements and Refractory Wear	530
53.4 Methods to Determine and Monitor Refractory Thickness and Condition	520	53.6.9 Detection of Anomalies	531
53.5 Offline Blast Furnace Measurement Techniques	520	53.6.10 Detection of Refractory Chemical Changes	532
53.6 Online Refractory Measurement Techniques	521	53.6.11 Metal Penetration	533
53.6.1 Refractory Thickness Estimates Based on Thermal Modeling	521	53.6.12 AU-E and Salamander Tapping	534
53.6.2 Isotopes and Radioactive Tracers	523	53.6.13 The Accuracy of AU-E Measurements	534
53.6.3 Infrared Thermography	524	53.6.14 Improvements in the AU-E Technique	535
53.6.4 Acoustic Emission	524	53.7 Summary	535
53.6.5 Ultrasonic	526	Exercises	536
		References	536
		Further Readings	538

*We thank Dr. Afshin Sadri, Global Director of Non-Destructive Testing (NDT) Group, Hatch Ltd. for his contribution to this chapter.

53.1 INTRODUCTION

Blast furnace ironmaking involves the transformation, interaction, and flow of molten liquids, solids, and gasses at elevated temperatures throughout the vessel. The steel shell is lined by carbon, graphite, and oxide refractory bricks to protect the integrity of the vessel. Water cooling elements are integrated with the shell to remove heat and keep the shell temperature low.

Carbon and graphite refractories are used for blast furnace hearth linings as the risk of oxidation in the blast furnace process is minimal. This allows the designer to take advantage of the superior thermal conductivity of carbon refractory and their ability to transfer heat to the shell and various water cooling elements. At higher elevations, oxide and silicon carbide are used for better abrasion protection. Understanding the performance of these refractory systems is essential to allow for a reliable operation and to effectively plan campaign extension strategies and ultimately reline plans and design improvements.

There are six main factors that affect the campaign life of a blast furnace:

1. Design,
2. Refractory quality and reliability,
3. Refractory lining quality and tightness,
4. Quality of the burden materials,
5. Operation consistency, and
6. Operation issues or amount of care and attention paid to maintaining the furnace lining and equipment.

Over the past two decades, significant improvements have been made to the design of blast furnaces. These improvements include increased furnace volume and operating pressure, new furnace structures and cooling designs, improved burden distribution methods, advances in monitoring instrumentation and control, and the introduction of techniques to lower energy requirements and save labor. In addition, there have been

improvements in the science and understanding of blast furnace linings. For example, the blast furnace hearth lining integrity can be maintained and its life sustained by adding various minerals that contain titania (TiO_2). Such developments have increased blast furnace campaign life and improved working conditions for operational and maintenance personnel. The typical campaign life of a modern blast furnace can range from 10-20 years, depending on the cooling and refractory design, especially for the hearth area.

Hearth repairs and relining is the costliest repair activity for blast furnaces. As a result, operators wish to extend the existing hearth life as much as possible to delay repair expenses and the related down time. Under normal operating conditions, the hearth lining deteriorates slowly/gradually throughout the life of the blast furnace. Unfortunately, many blast furnaces experience irregular refractory wear for many reasons. Excessive hearth wall wear can occur below the taphole, at the opposite side of the taphole, and at the base of the hearth wall, commonly known as the "elephant foot wear."

Recent studies show that blast furnace design, taphole position, and refractory quality have profound effects on the blast furnace hearth lining wear rate. Extended tapping time increases heat shocks/loading in the taphole region. Related refractory wear rate accelerates especially below the taphole(s). In addition to the expected lining wear, incidents such as gas and water leakage, hearth chilling, unscheduled furnace shut downs, thermal and material quality fluctuations can damage local areas of the hearth refractory. If local damage spreads, it may necessitate a refractory repair or relining. The degree of damage affects the repair costs, can reduce productivity and create safety concerns, especially hearth related damage. A reliable assessment of refractory lining status and thickness is crucial for maintaining a healthy and productive blast furnace operation and achieve a long campaign life.

53.2 REFRACTORY WEAR MECHANISMS

In a blast furnace, the refractory lining is contained by an exterior steel shell. The refractory lining and embedded cooling elements protect the steel shell from the elevated temperatures of the gasses and molten materials. The lining protects the shell from the resulting thermal stresses, chemical and mechanical attack. Depending on the brick location and the processes inside of the blast furnace, the refractory lining may either be in direct contact with the molten materials, exposed to radiation heat, exposed to fast moving hot gas, covered by build-up/accretion, or exposed to abrasion by coke and ferrous burden.

In the lower blast furnace and hearth, the dominant refractories are carbon, graphite, and semi-graphite bricks and blocks. Carbon and graphite bricks are produced with varying degrees of strength, elasticity, and porosity to serve different areas of the furnace. Around the tuyeres, castable refractory is used and in the stack, silicon carbide refractories are used to line the cast iron and copper staves. In the upper stack, abrasion resistant refractories are deployed, especially in areas without water cooling.

All castable refractory and bricks are designed to be physically and chemically stable at elevated temperatures greater than 500°C.¹ Depending on the operating environment, refractories need to be resistant to thermal shock, be chemically inert, have specific ranges of thermal conductivity and coefficient of thermal expansion. Each zone dictates the specific design of the refractories. For example, blast furnace hearths are lined with carbon and graphite refractories because of their high heat conductivity but the stack is lined with silicon carbide based refractories to resist the abrasion due to the movement of coke and pellets in that area.

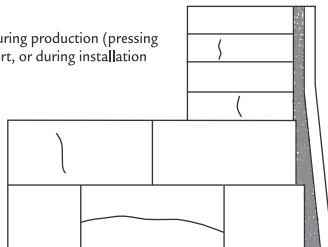
Hearth refractory wear typically follows a general wear pattern and cycle, as shown in Fig. 53.1. The formation of cracks and flaws in refractories could start from the early baking and manufacturing stage.

During the manufacturing process, and later during transportation and construction, refractory bricks experience cracks and micro-cracking. During the furnace start-up, the refractory lining undergoes rapid temperature changes resulting in thermal stresses which cause the nucleation, expansion, and growth of the existing cracks. Spalling starts at the corners and edges and then new cracks form because of thermal shocks and refractory expansions. At the areas in contact with the molten metal and slag, impregnation starts at the refractory hot face and fills the cracks and the pores. The hot face of the cracks starts to wear due to corrosion and erosion caused by the presence of molten metal. Eventually, molten metal starts to penetrate in between the brick layers through joints and cracks. On the refractory hot face, thermal cycles and stresses will cause metal impregnation into the pores and micro-cracks of the bricks, resulting in formation of an impregnated/non-impregnated boundary. After time, the existing cracks expand because of thermal cycles and eventually interconnect and form a brittle zone. At the brittle zone hot face, voids start to form and in some areas, molten metal fills the voids. Pressure and thermal stresses cause further cracking from the voids, resulting in uplifting and spalling of the damaged and brittle refractories. The impregnation and cracking cycle repeat, continuously reducing the thickness of the refractory lining and at the same time, cracks can align to form pathways for molten metal penetration.

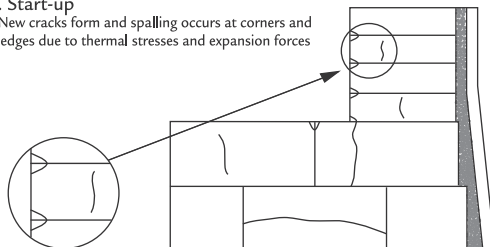
In blast furnace hearths, zinc or alkali gases can penetrate, condense, and expand into carbon refractories. Steam can oxidize carbon refractory and carbon monoxide can decompose and deposit carbon within the

1. Initial lining

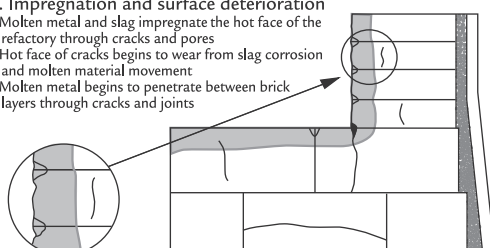
- New bricks may be cracked
- Cracks may have formed during production (pressing and firing), during transport, or during installation

**2. Start-up**

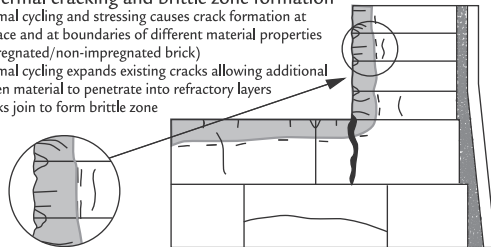
- New cracks form and spalling occurs at corners and edges due to thermal stresses and expansion forces

**3. Impregnation and surface deterioration**

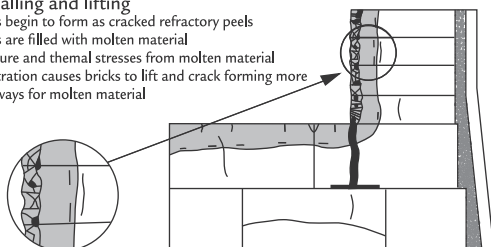
- Molten metal and slag impregnate the hot face of the refractory through cracks and pores
- Hot face of cracks begins to wear from slag corrosion and molten material movement
- Molten metal begins to penetrate between brick layers through cracks and joints

**4. Thermal cracking and brittle zone formation**

- Thermal cycling and stressing causes crack formation at hot face and at boundaries of different material properties (impregnated/non-impregnated brick)
- Thermal cycling expands existing cracks allowing additional molten material to penetrate into refractory layers
- Cracks join to form brittle zone

**5. Spalling and lifting**

- Voids begin to form as cracked refractory peels
- Voids are filled with molten material
- Pressure and thermal stresses from molten material penetration causes bricks to lift and crack forming more pathways for molten material

**6. Break-off and penetration**

- Brittle material breaks off
- Impregnation and cracking cycles repeat
- Cracks align to form pathways for molten material penetration through multiple refractory layers

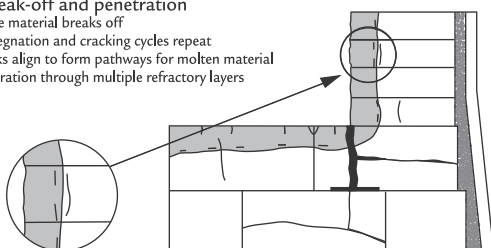


FIGURE 53.1 Distinct stages of refractory deterioration in an operating blast furnace.¹

carbon refractories, creating cracks. These events can ultimately break or oxidize the carbon, graphite, or semi-graphite refractory blocks. Once a crack exists, more gases and moisture can access the area, leaving a weak matrix of carbon particles. Interestingly, the depth and position of these chemically attacked blocks in the furnace are often uniform, which suggests that there is a specific isotherm around 800–1000 °C in the hearth wall where zinc and alkali condense within the carbon.² The temperature ranges for various modes of chemical attack on refractories are presented in Fig. 53.2.

Chemical attack can create a brittle zone where the carbon is susceptible to being dissolved into the hot metal as the hearth wall cooling is greatly reduced by the relatively insulating brittle zone. There are two requirements to make this happen. Firstly, the refractory must be in contact with hot metal (i.e. not protected by solidified material such as build-up, i.e. frozen hot metal). Secondly, the hot metal must be liquid ($T > 1150^\circ\text{C}$) to allow dissolution of the carbon refractory. In the taphole areas, casting will provide a rapid flow of the hot metal in the local area which will accelerate the carbon refractory wear especially under the tapholes where hot metal velocity is the highest.

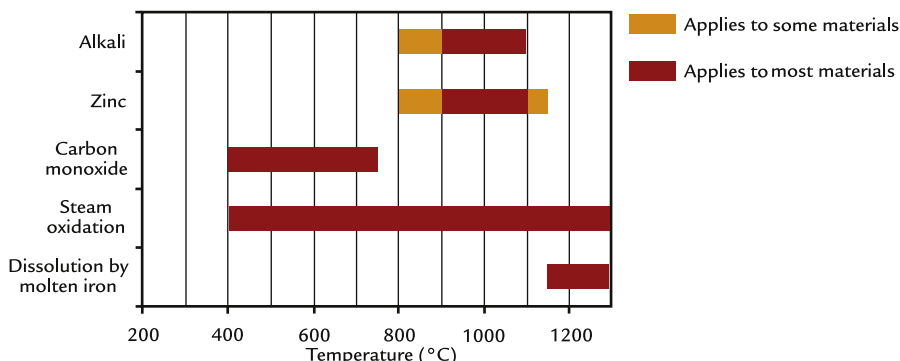


FIGURE 53.2 Temperature ranges for refractory chemical attack in blast furnace hearths.³

Water leakage and steam attack are exceptionally destructive to blast furnace refractory linings. Leakage can occur from failed tuyeres, tuyere coolers, staves, and cooling plates. In some cases, water leakage can be undetected for an extended period. Water migrates from leaking cooling members into the refractory lining, tracks along the refractory cold face, and progresses downward in the furnace, ultimately into the hearth refractory. For carbon-based hearth refractories, water can migrate to the hot face and oxidize the carbon and graphite blocks. A brittle zone, resulting from a chemical attack, can form where the water and steam have attacked the hearth blocks causing a soft and pasty residual material. This attacked refractory is sometimes called “punk carbon”.

Modern furnaces have cooling elements such as staves and plate coolers to enhance the performance of the refractory wall lining and increase the refractory lining service life. In the hearth, cooling by staves, jackets, or shell sprays pushes the freeze line further toward the hot face of the lining. This promotes the formation of accretion/buildup that protects the carbon blocks. In the lower stack, stave and plates act in an analogous way promoting an accretion that protects the wall from erosion and abrasion. In the mid and upper stack, the cooling elements, especially

cooling plates, promote refractory integrity by maintaining a lower temperature in the refractory bricks. The cooling elements create a thermal equilibrium in the multilayered wall lining that reduces thermal shocks and the possibility of chemical attacks to the refractory, which helps to maintain the refractory integrity.

53.3 DETERMINING THE REFRactory LINING STATUS

Blast furnace refractory lining failures could happen in any mode of blast furnace operation and the intensity of operation could be only one of the causes for lining failure. The lining failure could be localized, small, and manageable, which is typically called a gas or metal “leak,” shell overheating, and cracking. A hearth failure could result in a “run-out,” a larger and uncontrollable leak of molten iron and slag. A run-out causes catastrophic outcomes including unplanned shutdown and serious health and safety risks, especially explosions if the molten iron and slag contact water. The resulting unplanned downtime and emergency repairs impose considerable cost to the plant. To prevent the occurrence of an unplanned shutdown or run-out, refractory lining thickness measurements

and condition monitoring can be completed. These procedures are fundamental in understanding the health and structural integrity of a blast furnace and have become an indispensable part of furnace integrity and maintenance programs. Several methods and techniques that have been used to determine lining conditions in operating furnaces will be described in the next sections.

53.4 METHODS TO DETERMINE AND MONITOR REFRACTORY THICKNESS AND CONDITION

Refractory measurement techniques have been classified into two categories: "offline" and "online." Offline measurements refer to techniques which can only be used when the blast furnace is not operating and, in turn, online measurements refer to techniques which are used when the furnace is operational. The measurement techniques can be similarly classified as either "direct" or "indirect." Direct measurements refer to the use of physical measuring tools such as measuring tapes, drills, and rulers to measure exposed refractory bricks while the blast furnace is taken out of operation and the internal areas are accessible. All other techniques are indirect because the measurements are done when the refractory brick is not exposed and the blast furnace is in operation.

53.5 OFFLINE BLAST FURNACE MEASUREMENT TECHNIQUES

For offline furnaces, direct measurements can be done to determine refractory thickness and condition. Direct measurements yield the most accurate refractory thickness measurements. These measurements involve many phases, including efforts to investigate, study, and learn from digging out the lining, see Fig. 53.3.



FIGURE 53.3 Direct measurements of the brick thickness at the sidewall of an off-line blast furnace. Source: Photo courtesy: Dr. Afshin Sadri, Hatch Ltd.

Experience with blast furnace repair and relining is important for direct measurements. Sometimes the working lining looks perfect but it could in fact be heavily impregnated with iron, zinc, and alkali compounds. Samples must be extracted, marked, weighed, and later analyzed to understand the metal impregnation and chemical composition of the impregnated materials. Careful drilling and precise sampling of the lining is very important for learning and measuring purposes. Reference locations such as tuyere numbers and vertical elevations must apply to identify the location and position of the samples and photos.

Once inside the furnace, drilling is done on the hearth and the sidewalls to verify remaining refractory thickness and to extract samples

for laboratory studies to determine refractory compositional changes. Drilling is also done from outside during operation of the furnace for measuring thickness and quality of the refractory. A more detailed explanation will be provided in the next section.

Laser scanning allows for a three-dimensional inner volumetric measurement of the hearth and other exposed areas when the blast furnace interior is accessible. Prior to the laser scanning, the accretion/buildup must be removed so that the actual remaining lining can be determined. After the laser scan, the volumetric values can be compared to the original lining to determine the extent of refractory wear.

53.6 ONLINE REFRACTORY MEASUREMENT TECHNIQUES

Several methods are available to measure refractory lining thickness and condition while the blast furnace is in operation. These techniques are known as "indirect" methods. Different indirect techniques have measurement frequencies which can range from biaural inspections to continuous monitoring. Indirect techniques require certain assumption(s) in their calculations and measurements which can result in discrepancies and errors if the data analysis is not done correctly. In addition, the selection and implementation of the instrumentation and method must be made based on the objectives and specific area of the blast furnace.

Ideally, the blast furnace refractory lining thickness and condition must always be known to the operators. In the following sections, the history and application of various techniques to determine refractory lining thickness in blast furnaces will be presented.

53.6.1 Refractory Thickness Estimates Based on Thermal Modeling

Numerous mathematical models have been developed to determine remaining refractory thickness and to monitor deterioration and wear in a blast furnace. The base of all mathematical models is the heat transfer and conductivity of the lining. Specialized finite element analysis models based on numerical analysis and algorithms have been developed for blast furnaces considering the presence of the operational components, such as "elephant foot," "deadman," and "mushroom effects."^{3,4}

In modern blast furnaces, the walls and hearth have hundreds of embedded thermocouples to monitor the temperatures of the furnace lining. Using the temperature readings from the thermocouples, the heat fluxes in the refractory lining can be calculated. These heat flux calculations are used in the computational model(s), based on heat flow and energy conservation, to project the remaining refractory and buildup thicknesses. There are numerous types of mathematical modeling approaches and types of thermocouples that are used to make refractory wear calculations. The models are only as good as the accuracy of the assumptions and coefficients. These models rely heavily on the quantity of the installed thermocouples, the accuracy of the refractory thermal conductivity values and thermocouple distribution around the furnace.

Refractory thickness monitoring by use of thermocouples and thermal models is essential and a routine tool for the blast furnace operator for assessing hearth wear. A common approach uses duplex or triplex thermocouples, that is a single thermocouple arrangement with temperature measured at two or three depths. The one-dimensional heat transfer between the thermocouple positions can provide an indication of the heat transfer at

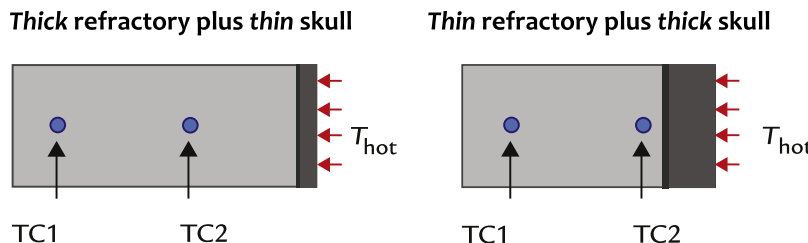


FIGURE 53.4 Two viable solutions for the same thermocouple reading.⁴

this position. Once the temperature gradient or effective thermal resistance is established, the 1150°C isotherm position can be estimated. This isotherm is generally accepted as the position of the refractory hot face.

While thermal modeling is an effective and commonly used tool, it does have notable limitations including the following:

- The heat load between thermocouple positions is unknown and must be extrapolated.
- Failure of the deepest thermocouple can reduce accuracy.
- Thermocouples, especially at the hot face, can provide suspect readings once they exceed their service temperature. A thermocouple can appear to come alive as carbon deposits at the hot junction and recreates an electrical signal and apparent temperature reading. These readings cannot be trusted.
- Without specific knowledge of the refractory thickness, extrapolation of the refractory and skull thickness can be challenging based on heat flux—see Fig. 53.4.
- The presence of a brittle zone adds an unknown thermal resistance in the heat transfer network. Skull thickness can only be estimated if an independent measurement of the refractory thickness is available—see Fig. 53.5.
- One- and two-dimensional models may not predict corner effects well such as where the hearth wall meets the hearth bottom. This is

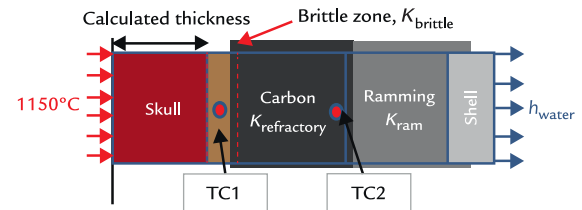


FIGURE 53.5 Estimating the skull thickness when a brittle zone is present and carbon refractory thickness is independently measured by Acousto Ultrasonic-Echo (AU-E).⁴

of concern when elephant foot wear is present.

- Thermal models are not effective in the taphole areas as the heat transfer is complex and not one-dimensional. This is of concern as refractory wear in the taphole area is a common weak point in the hearth refractory system. Three-dimensional models can provide an indication of refractory temperatures and wear.
- To be effective, thermocouple temperatures must be stored from the campaign start and in detail, that is, hourly averages for the entire campaign. This may be a 20-year period, therefore suitable computing infrastructure is needed.

Due to limitations in the effective range of the thermocouples and multivariable assumptions used in the thermal models, it is important to use other means of “nonintrusive” techniques to determine the refractory profile

in operating furnaces. In addition, refractory wear monitoring by mathematical modeling techniques is not able to distinguish between the types of various defects that are demonstrated in Fig. 53.1.

A combination of drilling and temperature calculations is also used to determine the remaining refractory thickness. This practice is common when a more accurate thickness measurement in a more focused local area is required, such as locating the salamander position prior to tapping as part of a shutdown process before relining. In this case, due to presence of molten metal, the drilling is never done completely through the lining and usually, it is always cautiously monitored by handheld thermocouples. Once the refractory temperatures reach a certain value ($\sim 500^{\circ}\text{C}$), the drilling stops and the remaining brick thickness is estimated indirectly by use of thermal calculations.

53.6.2 Isotopes and Radioactive Tracers

Isotopes and radioactive tracers have been used for determining refractory thickness in blast furnaces since the 1960s.^{5–9} This method relies on radiation from the tracer passing through the refractory and this radiation is detected by an isotope counter or Geiger counter. The higher the radiation count rate, the thinner the refractory is. The selected isotope tracer must have high energy gamma emitters for easy detection, a short half-life in the same order as the refractory lining, higher melting point than iron, and slow diffusion rate into the refractory, low vapor pressure, and low costs.

Following the selection of the radioactive tracer, the source location and isotope emissions are detected based on the following equation:

$$I = I_0 e^{-(u_1 x_1 + u_2 x_2 + \dots)} \quad (53.1)$$

where:

I = Intensity of radiation at the detector,
 I_0 = Intensity of radiation at the source,
 u_1, u_2 = Absorption coefficients of the materials between the detector and the source of radiation in centimeter,
 x_1, x_2 = Thickness of the absorbing materials, in centimeter.

Using this approach, the radioactive tracers are placed as the emission source in the refractories at different depths and elevations in the blast furnace. A baseline measurement made by an isotope counter or Geiger counter is carried out from the shell at the opposite side of each source prior to the blast furnace start-up. This is used as the reference point for each measuring station. After the blast furnace is blown-in, the refractory wear eventually reaches the tracers which will be scraped off from the walls and carried down to the hearth where eventually they dissolve into molten metal or slag and exit through the tapholes. By periodic monitoring of the measuring stations and comparing the results with the previous readings, the missing sources can be detected. This can be used to determine the refractory loss and wear rate in the blast furnace. The radioactive sources are weak enough that the slag and hot metal usage are not impacted.

There has been other experimental work, such as introducing the tracers at the top of the blast furnace contained within the iron ore pellets. As the tracer laden pellets move downward with the burden, the receiver counts the radiation that passes through the buildup, refractory, and the shell. Ideally, the quality of the refractory is the same throughout the furnace and shell thickness is uniform and so an increase in radiation counts indicates thinner and more worn refractory lining. Worn blast furnace linings are not uniform and several types of refractories with different

densities and material properties are utilized in the lining. In addition, the presence of staves and plates for cooling purposes adds to the complexity of the lining. The presence and thickness of accretion, impregnation of molten iron/slag into the refractory, and variation of refractory quality influence the radiation counts. As a result, the fluctuations in radiation counts do not necessarily indicate changes in refractory thickness.

Literature reviews on the use of radioactive tracers describe the use of ^{40}La , ^{192}Ir , and ^{60}Co isotopes for lining thickness measurements.^{6–10} In addition to measurement uncertainty, another issue with radioactive tracers is radiation exposure and their toxicity that may cause health hazards to the operators. As a result, the use of radioactive tracers has diminished.

53.6.3 Infrared Thermography

Infrared (IR) thermography is the most common nondestructive testing (NDT) technique used for determining hotspots and areas of potential concern. IR cameras provide a thermal image showing the temperature of the object on a color scale where the darker colors are cooler and the lighter areas are hot spots. Every object on earth emits IR energy. The amount of emitting energy depends on the temperature of the object and its surface emissivity. Emissivity represents a material's ability to emit thermal radiation and is an optical property of matter. Each material has different emissivity and is affected by source temperature and IR wavelength. Temperature differences on the surface may be related to differences in refractory thickness or may be a result of subsurface defects. In recent years, a large variety of systems have been commercially available with a broad range of image resolutions.

For blast furnaces with stave and plate cooling, IR cameras can only be used to

identify relative hot spots and elevated temperature areas. Many blast furnaces have water film cooling on the hearth shell where the water flows over the shell continuously for cooling and heat transfer purposes. While the water is running, IR cameras are ineffective for hearth wall temperature measurements. Sections of the film cooling can be shut off for a brief period and images are taken for evaluation purposes. Another problem related to IR thermography is that blast furnaces have a steel shell which oxidizes over time. The rusting of the steel shell affects the surface emissivity which results in inaccuracies in the IR thermography measurements.¹¹ In addition, gaps, cracks, and looseness of the refractory bonding will affect the results. Nearby heat sources and thermal reflections also affect the IR thermography data.^{11,12}

For these reasons, IR thermography is mainly used for rough estimates and the thermal images must be carefully collected under the same conditions for comparison purposes. IR thermography is effective at finding hot areas of the shell above the tuyeres, in the blast furnace bosh, belly, and stack.

53.6.4 Acoustic Emission

Acoustic emissions (AEs) are small amplitude elastic stress waves generated due to a deformation within a structure. The formation of a crack or failure of a structural component will trigger the release of AE waves which collectively are known as "acoustic events." AE transducers are attached to the blast furnace shell, with specific patterns to detect acoustic events, see Fig. 53.6.

An AE system collects data from the acoustic events and provides the location and intensity of the deformation. The ability to identify the source location gives the AE method an advantage over other monitoring

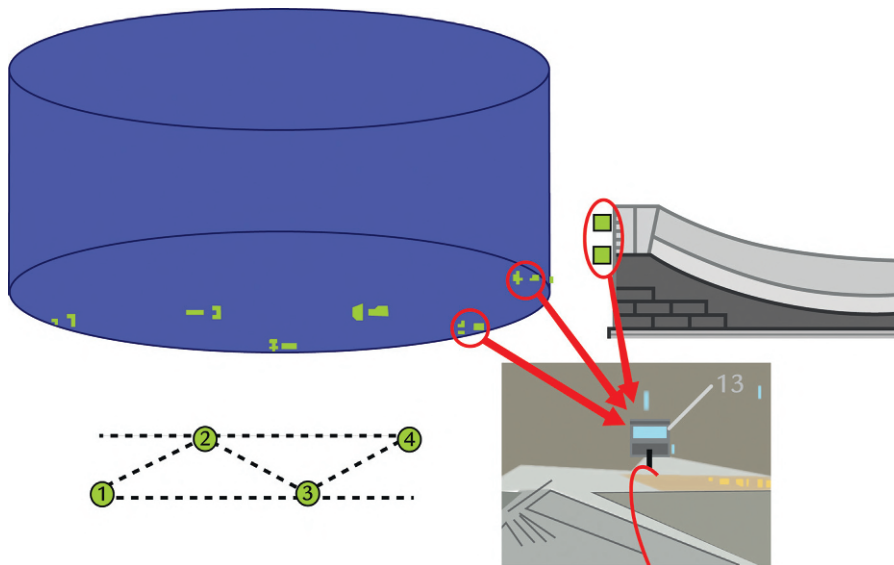


FIGURE 53.6 Acoustic emission sensors locations on the blast furnace shell.

techniques. The relative coordinates of the area of plastic deformation or microcracking across the entire furnace shell can be calculated based on the information from the AE signals.

The source location methodology originated in seismology, where the objective was to locate the epicenter of an earthquake from seismograms obtained at points distributed over the Earth's surface. Such source location was possible using an array of sensors and time of flight data, provided that the wave propagation characteristics between the source and the receivers were known. The source location solution is illustrated in Fig. 53.7.

For an array of i sensors, their coordinates are $(x_1, y_1, z_1), (x_2, y_2, z_2), \dots, (x_i, y_i, z_i)$.

Only the first breaks of the P-wave arrival times are used for the location of AE events. From the Pythagorean theorem, the i th sensor located at x_i, y_i, z_i will detect the signal when Eq. (53.2) is satisfied (t_i is the time required to reach the i th sensor, c is the wave velocity).

$$(x' - x_i)^2 + (y' - y_i)^2 + (z' - z_i)^2 = (ct_i)^2 \quad (53.2)$$

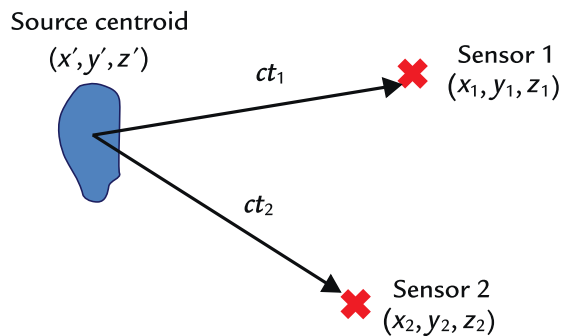


FIGURE 53.7 Source location problem.

For an array of i sensors, i unique nonlinear equations can be formed. If t_0 is the travel time required to reach the sensor closest to the source and Δt_i is the time difference between arriving at the closest sensor and arriving at the i th sensor such that $t_i = t_0 + \Delta t_i$, then the source location can be determined by solving for the four unknowns x' , y' , z' , and t_0 using four or more measured Δt_i values. In practice,

large sensor arrays are often used to allow overdetermination and enhance accuracy.

AE is a passive system and a failure or deformation must occur to trigger the system and provide information. In 1990, a study was conducted by the European Commission (EC) regarding the application of AE for detecting tuyere leakage, furnace shell cracking, and the application of "audiometry" or noise measurement of material flow over the blast furnace charging system chute.¹³ The EC study concluded that even though signal conditioning and recognition are difficult, the AE technique is a powerful technique to solve specific monitoring problems.

In 2008, a furnace integrity monitoring system (FIMS) based on application of AE was developed.¹⁴ FIMS has been utilized in operating blast furnaces to monitor furnace shell cracking and refractory wear. The FIMS technique involves filtering the surrounding noise from the signal in real-time and relating transient stress wave emissions to cracking or refractory movements and deterioration. The primary objective of FIMS is to prevent furnace leaks and run-outs and secondary objective of FIMS is to monitor refractory wear in operating blast furnaces.

53.6.5 Ultrasonic

Low-frequency "ultrasonic pulse velocity" (UPV) systems such as PUNDIT and V-Meter have been used to determine refractory quality since the mid-1980s. UPV systems involve placing a refractory with known thickness between a transmitting transducer and receiving transducer which are at opposite ends of the refractory sample. A low-frequency "ultrasonic through transmission" system with frequencies between 20 and 200 kHz is used to determine the time of flight between the transmitter and receiver. The

pulse velocity, V_p , is computed by using the following equation;

$$V_p = \frac{X}{t} \quad (53.3)$$

where X is the distance between the two transducers and t is the travel time for the pulse traveling between the transmitting transducer and the receiving transducer.

Generally, high ultrasonic wave speeds indicate low porosity, high density, and high modulus of elasticity.

"Ultrasonic pulse-echo" (UP-E) systems are required to measure refractory thickness on an operating blast furnace. UP-E systems place the transmitting and receiving transducers on the same surface such as the blast furnace shell plate. In practice, the distance between the transmitting and receiving transducers should be minimized. The thickness and position of a discontinuity are estimated based on the change in the travel time of the ultrasonic signal. Eq. (53.4) can be used to determine the refractory thickness;

$$X = \frac{V_p \cdot t}{2} \quad (53.4)$$

where V_p is ultrasonic or P-wave speed and t is the travel time.

Parker et al. demonstrated that the refractory/molten metal interface creates a distinguishable reflection surface because the acoustic impedance in liquid is typically 13–15% less than for a solid refractory or accretion material.¹⁵ As a result, at least 10% of the waves are reflected from the wall at the refractory/molten metal interface. In their study, Parker demonstrated that a large amount of ultrasonic energy attenuates within the solid refractory because of temperature and porosity. A decrease in the amplitude of reflected ultrasonic signals was noted as the sample was heated to higher temperatures. Temperature gradients also affect the travel path of ultrasonic waveforms in solid

materials.¹⁶ As the material temperature increases, the longitudinal or P-wave path widens which results in higher attenuation and a change in the reflection angle.

After years of testing, conventional ultrasound was determined to not be viable for measuring refractory thickness wear in blast furnaces. A conventional ultrasonic system uses a single frequency transducer with fixed and narrow bandwidth. Instead, an ultrasonic system with a “sweep frequency” or a “chirp” pulse generator and broadband transducers was developed by the industry to determine stave thicknesses in blast furnaces. This low-frequency pulse ultrasonic (LFPU) is a pulse-echo system that is capable of measuring stave thicknesses with a ± 2 mm precession. The multifrequency ultrasonic pulses can travel into different layers of the blast furnace wall and measure accretion and refractory thicknesses up to the tip of the stave. Even though LFPU was proven to be accurate for blast furnace stave thickness measurements,

the system has not been used on thicker furnace refractories.¹⁷ The authors believe that LFPU could be successfully implemented for refractory wall thickness measurements of up to 300 mm.

In the mid-1990s, researchers from the Magnitogorsk State Technical University in Russia attempted to utilize the “ultrasonic tomography” technique to identify blast furnace hearth refractory lining layers. Ultrasonic tomography is widely used in the medical profession and refers to imaging by sections or sectioning, using penetrating ultrasonic waves. Magnitogorsk used the “ultrasonic mirror-shadow method” to transmit and receive ultrasonic waves across sections of a blast furnace, see Fig. 53.8.

This method uses ultrasonic sensors above 20 kHz to transmit and receive the signals. The receiving transducers are placed at 0, 20, 40, 60 degree angles from the transmitting sensor across the blast furnace hearth. The measurements are repeated in three to four

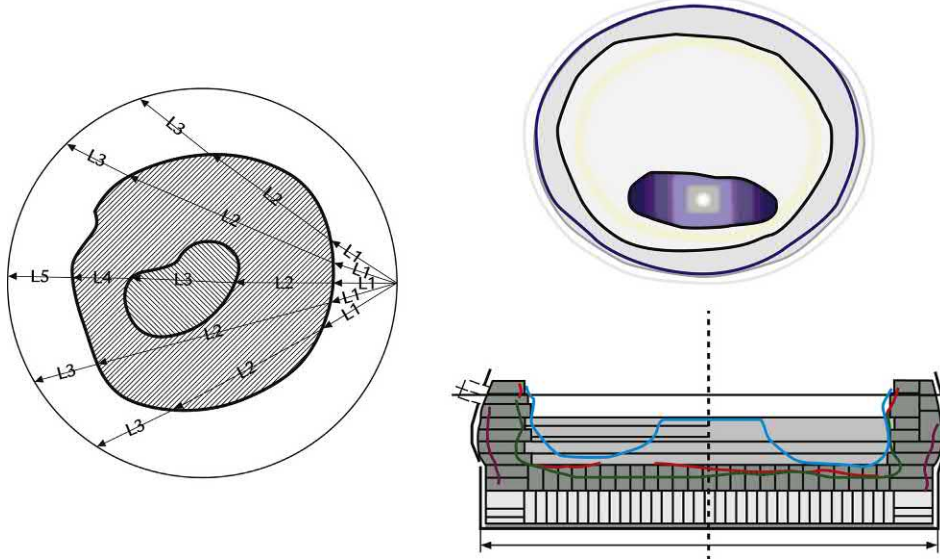


FIGURE 53.8 (left) Transmission and receiving pathways for the ultrasonic signals across the blast furnace. (right) Software for result generation.^{1,17}

various locations around the hearth diameter. Based on wave speed differences due to material changes for each layer, the measured waves are used to create an “image-shadow.” The so-called image shadow is developed based on mathematical modeling and correlations between the arriving ultrasonic waves with the blast furnace layers.¹⁸

From the published literature, the ultrasonic signals travel through the shell, ramming, thick refractory lining, molten metal, hot and porous “deadman” in the center of the hearth and again the molten metal, thick refractory lining, ramming, and finally shell before they are detected and collected on the opposite side (Fig. 53.8, see the center pathway).¹⁸ The high frequency of ultrasonic waves (above 20 kHz), high rate of signal attenuation because of temperature and material porosity, and complex signal pathway from high-to-low and low-to-high acoustic impedances are part of the challenges and concerns in conducting ultrasonic tomography on an operating blast furnace. The degree of success of the ultrasonic tomography technique to measure the internal state of an operating blast furnace is unknown.

thickness and quality evaluation in blast and non-ferrous furnaces since 1998.

AU-E is a stress wave propagation technique that uses time and frequency data analysis to determine refractory thickness and detect anomalies such as cracks, gaps, or metal penetration within the refractory lining. During the measurement, a mechanical impact on the surface of the structure (via a hammer or a mechanical impactor) generates a stress pulse, which propagates into the refractory layers. The wave is partially reflected by the change in material properties of each layer of the refractory lining. The wave also propagates through the solid refractory layers to a brick/brick or brick/gas or brick/molten metal interface. The compressive waves (or P-waves) are received by a sensor/receiver and the signals are analyzed for refractory quality and thickness assessment.

The AU-E technique uses the “apparent wave speed” in the thickness calculation, instead of the standard P-wave speed. The apparent wave speed is an average wave speed in a three-dimensional geometric space and considers the effects of numerous factors including the brick density, thermal gradients, shape factor, and elastic properties of the brick. The AU-E technique uses correction factors to account for the effects on the wave speed in each layer. The thermal correction factor, α , of a layer is calculated based on the dynamic Young's modulus of elasticity under service temperature conditions compared to the dynamic Young's modulus at room temperature [Eq. (53.5) and Fig. 53.9]. If the dynamic modulus of elasticity over a temperature gradient is given as $E_d(T)$, the temperature correction factor, α , can be calculated as;

$$\alpha = 1 + \frac{\int_{T_1}^{T_2} E_d(T) dT}{E_o} \quad (53.5)$$

where E_o is the dynamic modulus of elasticity at room temperature, $E_d(T)$ is the modulus of

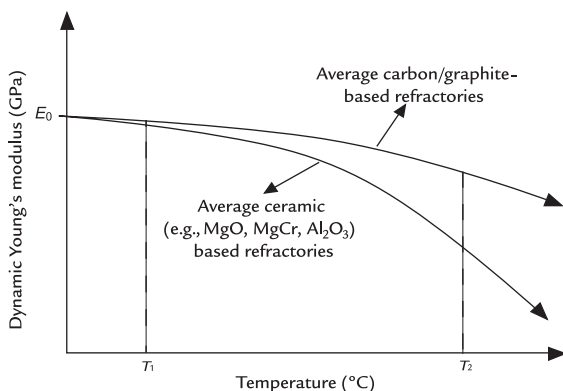


FIGURE 53.9 Effect of an increase in temperature on the dynamic Young's modulus of refractories.²²

elasticity between the temperature gradients of T_1 and T_2 , where T_2 is a higher temperature than T_1 .

In this calculation, one assumes the Young's modulus of elasticity of the refractory changes within a uniform gradient between the hot and cold face as a function of temperature. The change of the Young's modulus of elasticity as a function of temperature also depends on the type of refractory material in question. For example, the average magnesia and alumina-based refractories are more affected by temperature change than the average carbon/graphite-based refractories, see Fig. 53.9.

The shape factor β accounts for the reduction in wave speed due to the geometry of the structures through which the wave propagates. The reduction in apparent wave speed is due to excitation of the structure's natural frequencies by the impact force. The shape factor value depends on the cross-sectional dimensions of the testing area. For example, the β factor for the cross-section of a column is 0.87.¹⁹ For most blast furnaces where lateral dimensions are at least six times the thickness of the lining, the β factor is 0.96.

Considering the above factors, the governing equation for the AU-E technique is indicated by the following equation;

$$T = \frac{\alpha\beta V_p}{2f_p} \quad (53.6)$$

where T is the thickness or depth of the reflecting surface, α is the thermal correction factor [Eq. (53.5)], β is the shape factor, V_p is the propagation speed of P-wave in the material [Eq. (53.3)], and f_p is the P-wave frequency.

For a multilayered section such as a blast furnace hearth, the thickness of the final refractory layer (T_n) is calculated based on the following equation;

$$T_n = \frac{(V_p)_n \alpha_n \beta_n}{2} \left[\frac{1}{f} - \sum_{i=1}^{n-1} \frac{2 T_i}{(V_p)_i \alpha_i \beta_i} \right] \quad (53.7)$$

where f is the resonance frequency for the thickness of the n th layer.

Eq. (53.7) can be used to determine the refractory lining thickness up to the hot face, if the P-wave speed $(V_p)_i$, the thermal correction α_i , the shape correction factor β_i , and the thickness T_i of the layers prior to the inner most layer are known. Eq. (53.7) assumes that stress waves are generated by a controlled impact source and that the waves contain sufficient energy to reach the inner most layer of the lining and resonate back and forth between the two faces to create a desirable or defined P-wave thickness frequency.

In addition to understanding the mechanisms of the stress wave measurements, a key factor for successful AU-E inspections is the utilization of the right tools to complete the inspection. A broadband vertical displacement transducer of a suitable frequency range was designed with the ability to function at elevated temperatures and in wet environments. Impactors with specific spherical tip diameter, capable of generating a specific range of frequencies, were selected for stress

wave generation. A military grade data acquisition system is required that is water and dust resistant and can withstand low and elevated temperatures between 50 and 90°C.

53.6.7 AU-E Calibration

Prior to the collection of field data, the apparent P-wave speed of each brick layer is determined by calibrating representative brick samples at room temperature. The wave speed calibration measurements must be carried out on all the materials through which the wave propagates. The α factor can either be calculated experimentally, by heating brick samples and measuring the wave speeds at the desired temperatures, or it can be calculated by the brick's elastic and thermal properties. The β factor can be calculated upon measuring the dimensions of the testing area. After the calibration is done, a mathematical model is created to help the AU-E specialist customize their field data collection hardware and software settings.

53.6.8 Thickness Measurements and Refractory Wear

The field data collected in the time domain are extremely complex, containing numerous frequencies and multiple reflections, diffractions, refractions from body, and surface waves, see Fig. 53.10.

In the frequency domain, the results are better defined but still there are many different elements that can lead to misinterpretation, see Fig. 53.11.

Note that, as described by Eq. (53.7), a lower reflection frequency corresponds to a greater distance to the signal reflection interface. Fig. 53.11 demonstrates two example frequency spectra which resulted from a signal collected on a blast furnace wall with no cracks or impregnation and a signal collected across

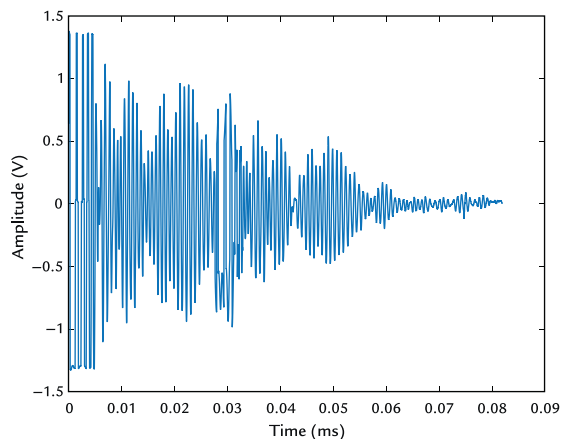


FIGURE 53.10 Typical time domain signal from a furnace wall.¹

from an opened crack across a single brick in a furnace wall, from top to bottom perpendicularly.

Refractory wear is usually thought of as the reduction of refractory thickness over time caused by the thermal and mechanical stresses in the blast furnace. When using the AU-E technique, there are a few other refractory conditions that could erroneously appear as detected remaining refractory thickness, namely, metal impregnated refractory and accretion or buildup, see Fig. 53.12. Fig. 53.13 illustrates the results of an AU-E blast furnace hearth monitoring during a certain period, demonstrating refractory wear and accretion formation.

When refractory is impregnated by metal (see Fig. 53.1 stage 3), the impregnated portion has a significant reduction in its elastic properties compared to good refractory. As a result, the AU-E signals will be reflected from the impregnation boundary, which can be mistaken for the remaining refractory thickness.

When accretion or buildup is formed on the hearth wall, the buildup/molten material interface can be misinterpreted as the remaining

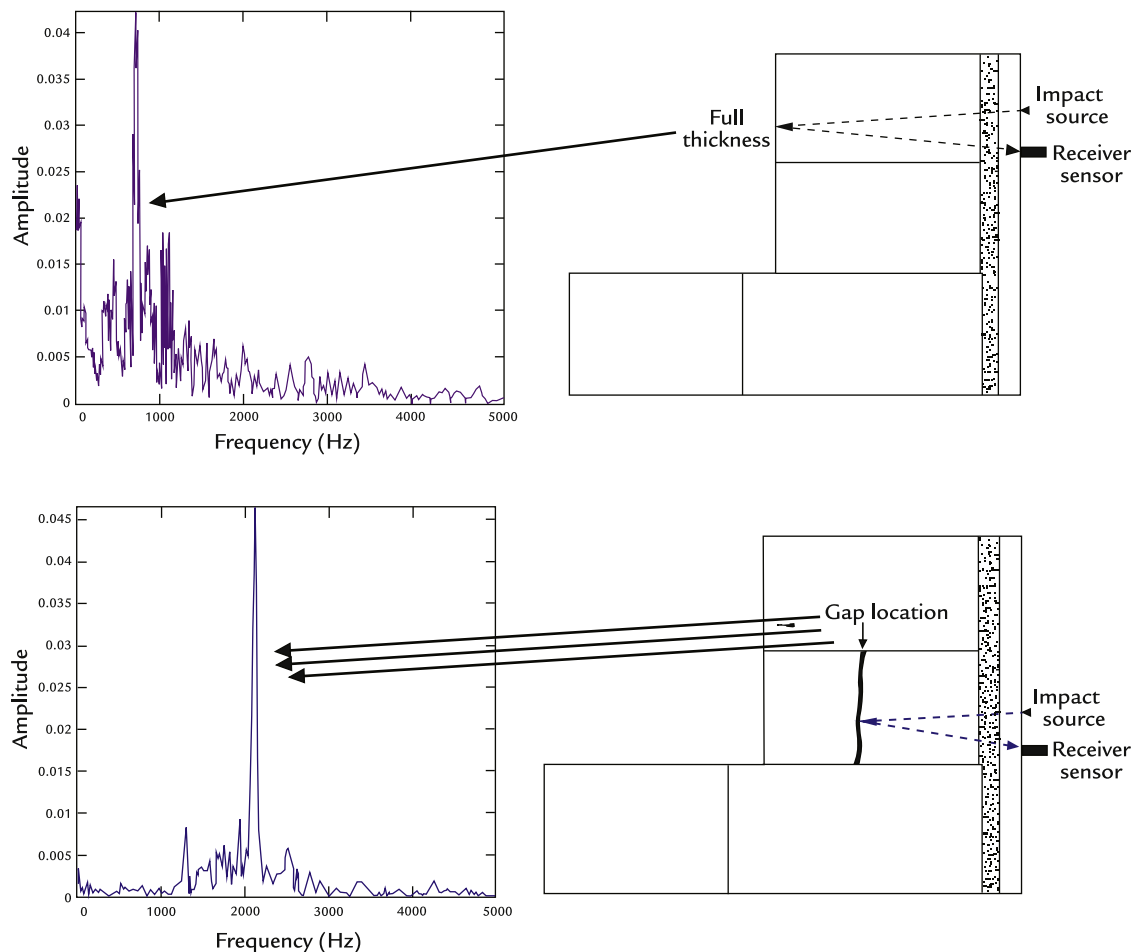


FIGURE 53.11 Hearth wall refractory top to bottom: without impregnation or buildup; refractory thickness and refractory with large opened crack.¹

refractory thickness, while the buildup/refractory interface can be misinterpreted as a crack. Proper interpretation of AU-E signals can be aided by a good understanding of the blast furnace process and operating conditions. Like other tasks that require judgment, the AU-E technique requires the experience of an AU-E specialist.

53.6.9 Detection of Anomalies

In the context of the AU-E technique, an anomaly is defined as a clear signal reflected from within the refractory lining but where the source of the reflection is unknown. Anomalies could be cracks, voids, metal penetration, oxidation, or a combination of these features.

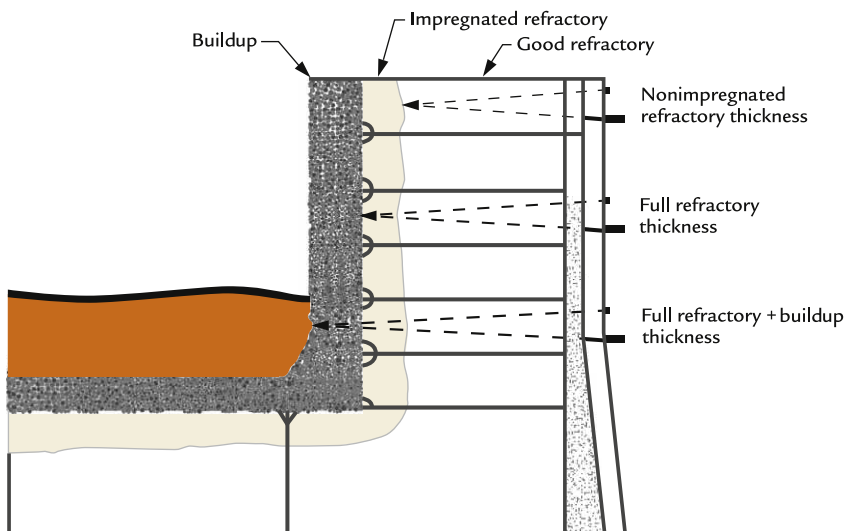


FIGURE 53.12 Hearth wall refractory lining top-to-bottom; echoes from good refractory, good refractory and impregnated refractory; good refractory, impregnated refractory and buildup.¹

When there are discontinuities, cracks, or interfaces of various materials (see Fig. 53.1), the signals often show multiple reflections and those reflections tend to be at higher frequencies compared to the low-frequency reflection for the full refractory thickness. The signal reflection frequencies are used to determine the position of the anomaly. The location of any potential cracks is important for developing mitigation measures or monitoring plans. Cracks that coalesce and propagate may cause the spalling of refractory at the hot face, which will result in a sudden reduction of refractory thickness.

When significant gaps/cracks are present in a refractory lining, impact signals may not be able to transmit through the entire thickness of the brick. They will be attenuated by the gaps and thus, signals seem to reflect from a thinner region closer to the cold face. As such, the actual remaining refractory could be thicker than detected by the signals.

53.6.10 Detection of Refractory Chemical Changes

The P-wave speed is dramatically lower in hydrated/carbonized or oxidized refractory when compared to nonaffected refractory. In such cases, greater than expected refractory thickness is typically measured in areas of hydrated/carbonized or oxidized refractory. It is important to understand that hydration, carbonization, or oxidation occur because of a chemical reaction between the refractory and oxygen or water at certain temperatures. The severity of the chemical changes to the bricks depends on the volume of the external agent (i.e., water in the case of hydration), time of exposure, temperature, and how favorable the conditions are for the chemical change. The effect on the P-wave signals depends on the severity of material changes within the lining. If the area of the chemical change is small in relation to the length and geometry

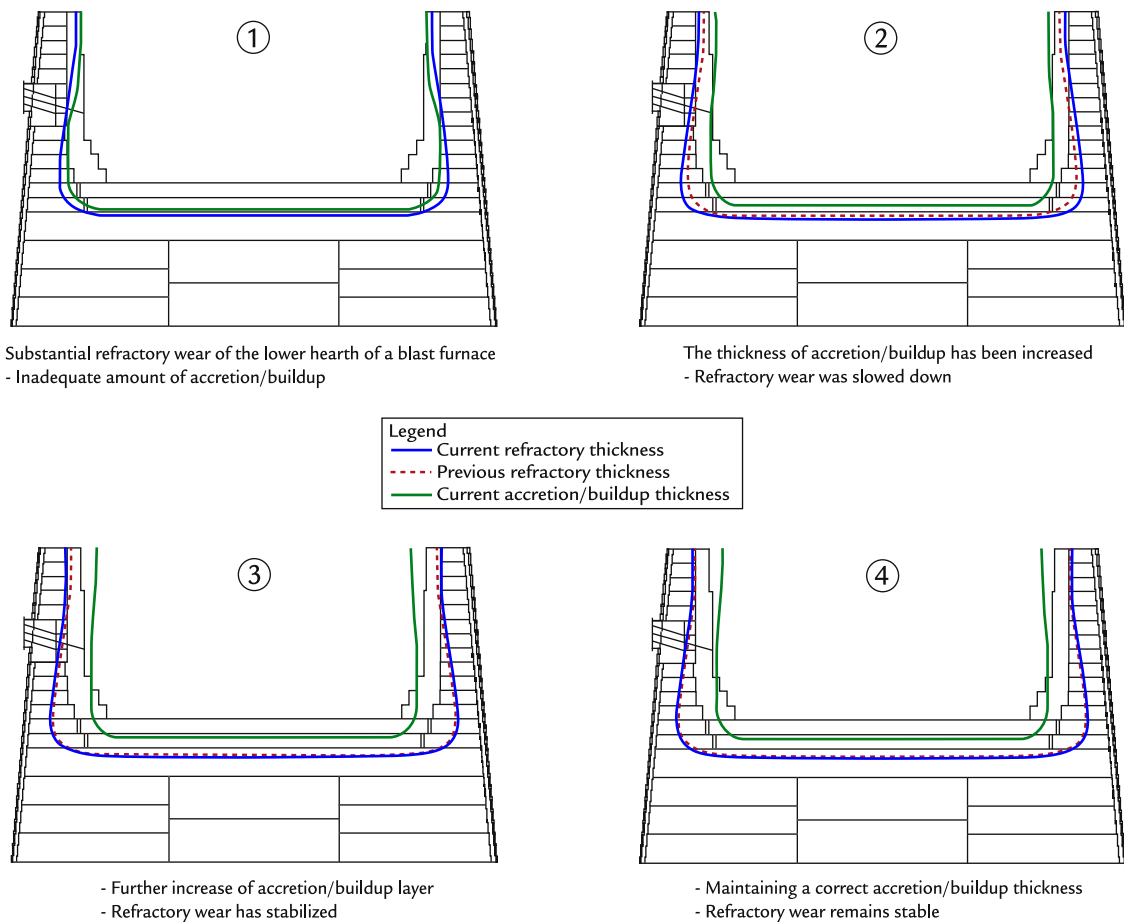


FIGURE 53.13 AU-E measurements showing progression of refractory wear and skull/accretion formation.

of the lining, the AU-E signals may not be affected and so the change in refractory quality may not be detected. On the other hand, if the chemical effects are extensive in geometry and material properties in relation to the lining, AU-E signals will readily detect the altered area. There is not enough field data to readily identify the distinct stages of chemically altered refractory using AU-E measurements.

53.6.11 Metal Penetration

Another possible explanation for “thicker than normal” lining measurements is the presence of metal penetration into the refractory. AU-E cannot identify metal penetration within the hearth wall refractory layers when the penetration is “smaller than the signal’s half wavelength” which is less than 50 mm. When metal penetration is too small for AU-E

to detect, the additional metal thickness is reported as part of the lining resulting in a “thicker than normal” reading. When using the AU-E technique in areas with both metal penetration and carbonization or oxidation, it is possible that they could be mistaken for each other.

53.6.12 AU-E and Salamander Tapping

The AU-E technique is also capable of determining the location to conduct “salamander” tapping prior to a relining or long stop. Salamander tapping is done at the salamander base, which is the bottom-most level of the liquid pool in a blast furnace hearth. A high degree of precision is required to tap the salamander base effectively and the operator has only one chance to get the drain hole implemented. Traditionally, the location the salamander base was determined by thermocouple readings and by pilot core drillings at multiple locations. These methods are typically inaccurate, expensive, and time consuming.

The AU-E technique replaces core drilling to quickly determine where the salamander base is located. The methodology is shown in Figs. 53.14 and 53.15; a vertical line of measurement points is made at a selected location on the blast furnace hearth wall.

The expected range (e.g., 1.2 m) of the salamander base is determined by thermocouple and blast furnace operator data. Over the expected range of the salamander base, tightly packed AU-E measurement points with smaller spacing are made and points to the left and right (e.g., 20 cm away) are added to confirm the measurements. The salamander base is then determined by carefully observing the signals of the tightly spaced measurement points. The AU-E technique has proven to accurately determine the salamander base in operational blast furnaces and to successfully eliminate the problems associated

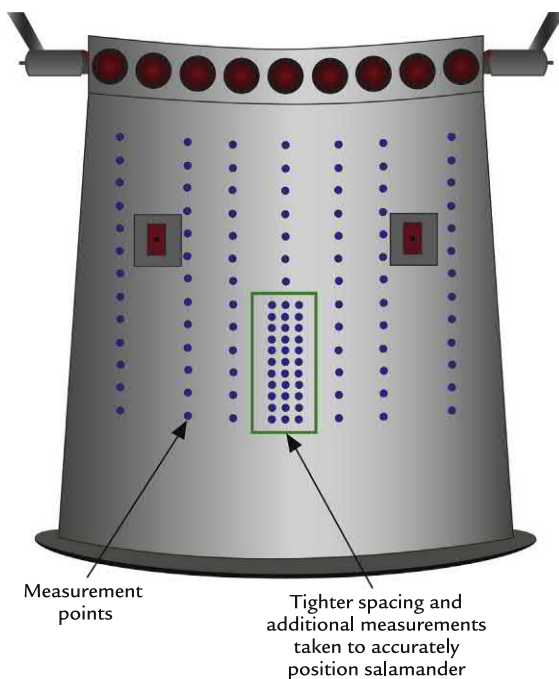


FIGURE 53.14 A plan view of tighter spacing on the shell of the blast furnace for salamander tapping location in comparison to the regular AU-E measuring stations.

with traditional methods used to drain the salamander.

53.6.13 The Accuracy of AU-E Measurements

In an article, Sadri et al. have discussed the causes of AU-E errors in detail.²⁴ In general, based on numerous verifications, the accuracy of the AU-E measurements is between 4 and 7% of the actual thicknesses or anomaly positions. Accretion or buildup thickness measurements are within 15% of physical measurements due to the greater uncertainty of the wave speed of accretion material.

Sadri et al. have written and presented numerous papers on the various aspects and applications of AU-E inspections, namely measurement principles, case studies for blast

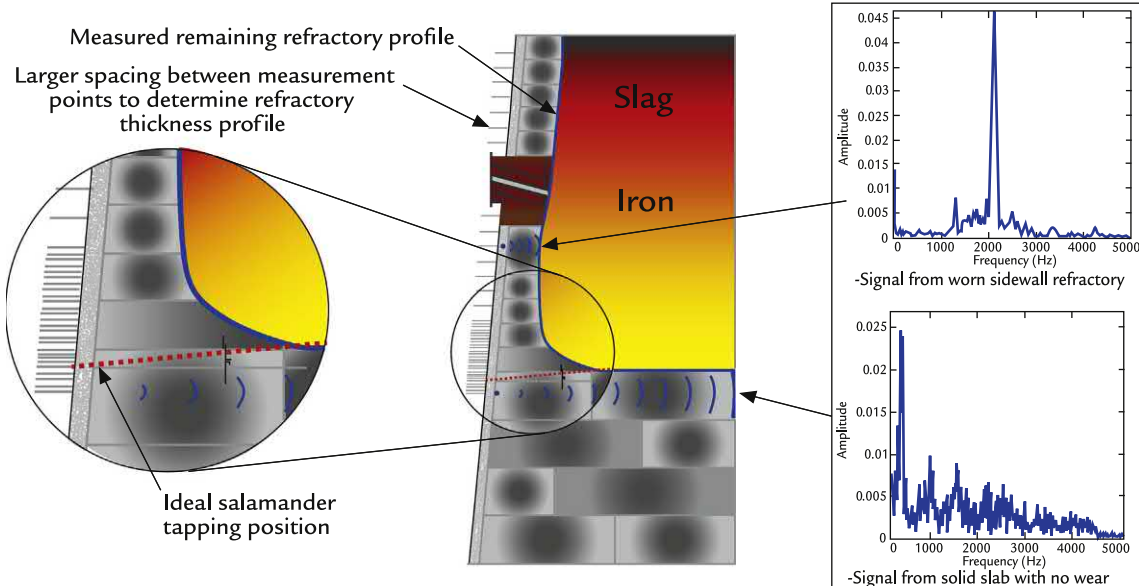


FIGURE 53.15 Methodology and results of using AU-E to determine the salamander tapping location.²³

furnaces, nonferrous furnaces and vessels, and preventing and predicting maintenance.^{22,24–35}

53.6.14 Improvements in the AU-E Technique

Since the invention of the AU-E technique in 1998, many different improvements have been introduced. Some of them can be credited to the overall rapid development and increased affordability of computers, digitizers, and software development tools. Data processing speed has increased and the results can be presented in a customized way to clearly and quickly report on the issues detected in the blast furnace lining. Greater knowledge of blast furnace operations has improved data interpretation and refractory lining thickness assessments. This is in part thanks to better cooperation with furnace operators and other technical personnel as the value of AU-E became more apparent to operating companies. Obtaining feedback from the postmortem

analysis of the linings and analyzing it in conjunction with the AU-E results have proved to add excellent value to the understanding of the refractory deterioration process.

53.7 SUMMARY

Due to the large cost to stop and reline a blast furnace, operators are always looking for knowledge to extend the blast furnace campaign in a responsible way. Hearth breakouts present a considerable safety and business risk to any steel company. Lining assessments such as those described will grow in usage and sophistication as blast furnace operators stretch the blast furnace service life as much as possible.

The “direct” use of measuring tapes on the refractory brick is a highly accurate technique; however, it can only be conducted while the blast furnace is shut down and when internal access is possible, which is a costly procedure.

The refractory thickness can be measured during blast furnace operation by a “semi-direct” method combining core drilling into the refractory and in-hole temperature measurements. The drill tip cannot go all the way to the refractory hot face as this will trigger a metal leak and run-out. To be completed safely, the drilling is interrupted and temperature readings taken at regular intervals by an accurate thermocouple. The drilling stops once the bottom of the drilled hole temperature reaches a safe temperature, for example 500°C. From that point, the thickness is calculated based on the brick thermal conductivity and drilled thickness. Due to the involved nature, only a limited number of holes can be drilled and this is a one-time measurement.

All other techniques presented in this section use “indirect” approaches because the measurements are done while the blast furnace is in operation. Each technique’s capabilities and limitations must be taken into consideration once the data are processed and assessments made. Combining techniques can increase confidence and allow for better decision making regarding the state of the blast furnace hearth.

EXERCISES

- 53.1.** What is the most common reason for termination of a blast furnace campaign life and subsequent relining?
- 53.2.** Name one NDT techniques that is capable of direct refractory measurement in operating furnaces.
- 53.3.** Why did blast furnaces stop using isotope tracers for refractory thickness measurements?
- 53.4.** While you are collecting AU-E signals on a blast furnace, the system is triggered by another signal (noise), irrelevant to the receiving signals. What could be the source of noise? How you determine the source of noise? What is a

- possible solution to prevent the sensor from being triggered by this noise?
- 53.5.** You are inspecting the hearth and sidewall of a blast furnace that was last relined 14 years ago. The operators have told you that the sidewall lining could be thin, as low as 200 mm. Should you use a small diameter sphere impactor or a large diameter sphere impactor? Why?
 - 53.6.** In an AU-E inspection, an increase in the thermal factor will have what effect on the calculated refractory thickness?
 - 53.7.** Why are regular ultrasonic systems inappropriate to measure refractory thicknesses in blast furnaces?
 - 53.8.** What could cause the temperature readings by thermocouple to drop in an operating furnace?
 - 53.9.** Why should the temperature readings on the blast furnace shell measured by a handheld thermo-gun/thermo-camera not be used in calculations to estimate the refractory thickness in the vessel?
 - 53.10.** What is the difference between stave cooling and shell cooling in a blast furnace on AU-E measurements? Why?

References

1. Sadri A, Ying W, Chataway D, Gordon Y. *Principles for blast furnace refractory lining inspection, and monitoring using acoustic and ultrasonic technologies*, AISTech 2016. Pittsburgh, PA: Association of Iron & Steel Technology (AIST); 2016. p. 681–93.
2. Sarna SK. *Refractory lining of blast furnace*. Ispat Guru; 2014. <<http://ispatguru.com/refractory-lining-of-blast-furnace/>>.
3. Chomyn K, Clement A, Ghorbani H, Busser J, Cameron I, Hyde JB. *Blast furnace hearth thermal assessment and identification of wear zones*, AISTech 2017. Nashville, TN: Association of Iron and Steel Technology (AIST); 2017. p. 853–61.
4. Chomyn K, Philips S, Ghorbani H. Blast furnace assessment by combining AU-E and thermocouple data. In: *Seventh European coke and ironmaking congress (ECIC)*, September 2016, Linz, Austria; 2016. 23–33, 978-3-200-04745-7.

5. Preuer A, Winter J, Hiebler H. Computation of the erosion in the hearth of a blast furnace. *Steel Res* 1992;63:147–51.
6. Dong H, Shaojun C. Mathematical model for fast computation of erosion profile in submerged arc furnace with freeze lining. In: *Proceedings of the thirteenth international ferroalloys congress efficient technologies in ferro-alloy industry*, June 2013. INFACON XIII, Almaty, Kazakhstan; 2013. p. 799–810.
7. Borbas JJ, Padfield RC, Moscker E. Density determination of refractories by measurement of gamma-radiation absorption. *J Am Ceram Soc* 1967;50(8):421–4.
8. Staicu L, Radu R. The use of the (γ , n) reaction to measure wear in blast furnaces and other industrial furnaces: comparison with present methods. *J Phys D: Appl Phys* 1983;16(12):2531–6.
9. Salgado J, Oliveira C, Moutinho A, Silvério C. Control of refractory lining wear by using radioisotopes. *Int J Radiat Appl Instrum, A: Appl Radiat Isot* 1988;39(12):1265–7.
10. Prasad AS, Sinha P, Qamrul M, Chatterjee A, Chakravarty PK. Some experience with radioisotopes in the study of the wear of blast furnace linings. Tata Iron and Steel Co. Ltd., Jamshedpur, India. Research and Development Division. TISCO, vol. 26, no. 3–4, p. 81–7. ISSN 0496-6536; Worldcat; 1979.
11. Bolf N. Application of infrared thermography in chemical engineering. *J Chem Chem Eng* 2004;53(12):539–55.
12. Maldaque X. Introduction to NDT by active infrared thermography. *Mater Eval* 2002;6(9):1060–73.
13. Farrington D, Stewart W, Kitson P, London M, Paddy N. *Dynamic monitoring of blast furnace plant, technical steel research*. European Commission; July 1987 to 31 December 1990. ISSN 1018-5593.
14. Gebski P, Sadri A, Ying W. Development of the system for furnace integrity monitoring based on real-time continuous acoustic emission data acquisition and analysis. In: *Conference of metallurgists (COM)*, October 2–5, 2011, Montreal, Canada; 2011.
15. Parker RL, Meanning JR, Peterson NC. Application of pulse-echo ultrasonics to locate the solid/liquid interface during solidification and melting of steel and other metals. *J Appl Phys* 1985;58(11):4150–64.
16. Sadri A, Gebski P, Ghorbani H, McGarrie G, De Vries T. Monitoring deterioration of waffle cooler thickness at Polokwane smelter. *JOM* 2009;61(10):69–73.
17. Sadri A, Ying WL. Monitoring of stave and castable refractory wear in blast furnaces. In: *Proceedings of AISTech*, May 2015, Cleveland, OH; 2015.
18. Techno-Consulting Website. <<http://www.techno-consulting.ru/en/about/index.html>> [retrieved 21.01.15].
19. Sansalone MJ, Street WB. *Impact-echo: nondestructive evaluation of concrete and masonry*. Ithaca, NY: Bullbrier Press; 1997. p. 339.
20. Sansalone MJ, Carino NJ. *Impact-echo: a method for flaw detection in concrete using transient stress waves*. National Bureau of Standards. Virginia, USA: Springfield; 1986. p. 222. USA, NBSIR 86–3452, NTIS PNB#87-104444/AS.
21. Carino NJ, Sansalone MJ. *Impact-echo: a new method for inspecting construction materials. proceedings of nondestructive testing and evaluation of materials for construction*. Urbana-Champaign, IL: University of Illinois; 1988.
22. Sadri A. An introduction to stress wave non-destructive testing and evaluation (NDT&E) of metallurgical furnaces and refractory condition monitoring. *CINDE J* 2008;29(2):7–11.
23. Sadri A, Hyde B, Ying WL, Gordon Y, Jian Lv D. *Salamander tapping position by using an acousto ultrasonic non-destructive testing (NDT) techniques*. AISTech 2017. Nashville, TN: Association of Iron & Steel Technology (AIST); 2017. p. 717–22.
24. Sadri A, Gebski P. Non-destructive testing (NDT) and inspection of the blast furnace refractory lining by stress wave propagation technique. In: *Proceedings of the 5th international congress on the science and technology of ironmaking (ICSTI'09)*, October 2009, Shanghai, China; 2009. p. 951–5.
25. Sadri A. Non-destructive determination of refractory and build-up thickness in operating furnaces using an acousto ultrasonic reflection technique. In: *Proceedings of the materials degradation: innovation, inspection, control and rehabilitation symposium*, COM2005, August 2005, Calgary, AB, Canada; 2005.
26. Sadri A, Walters G. Determination of refractory and castable quality in operating industrial furnaces, using a stress wave reflection technique. In: *Proceedings of the materials degradation: innovation, inspection, control and rehabilitation symposium*, COM2005, August 2005, Calgary, AB, Canada; 2005.
27. Sadri A, Lachemi M, Walters G. Determination of refractory lining thickness and quality in operating industrial furnaces using a stress wave reflection technique. In: *Proceedings of first CSCE specialty conference on infrastructure technologies, management and policy*, June 2005, Toronto, ON, Canada; 2005.
28. Sadri A, Timmer R. Blast furnace non-destructive testing (NDT) for defect detection and refractory thickness measurements. In: *AISTech 2006, proceedings for iron and steel technology conference, Vol. II*, May 2006, Cleveland, OH; 2006.
29. Sadri A, Gordon I, Rampersad A. Acousto ultrasonic-echo (AU-E): a non-destructive testing technique for blast furnace hearth refractory condition monitoring. In: *AdMet 2007, proceedings of international conference advances in metallurgical processes and materials*, Vol. 2, May 2007, Dnipropetrovsk, Ukraine; 2007. p. 77–85.

30. Sadri A, Marinelli P, Doro E, Gebski P, Rampersad A. Comparing the accuracy of acousto ultrasonic-echo (NDT), finite element analysis (FEA), and drilling when obtaining a blast refractory lining wear profile. In: *AISTech 2009, proceedings of iron and steel technology conference*, May 2009, St. Louis, Missouri, USA; 2009.
31. Sadri A, Gebski P, Mirkhani K, Ying WL. Monitoring refractory lining in operating furnaces by acousto ultrasonic-echo technique. In: *Proceedings of conference of metallurgists, COM 2011*, October 2011, Montreal, QC, Canada; 2011.
32. Sadri A, Gebski P, Shamel E. Refractory wear and lining profile determination in operating electric furnaces using stress wave non-destructive testing (NDT). In: *Proceedings of the twelfth international ferroalloys congress, INFACON XII*, June 2010, Helsinki, Finland; 2010. p. 881–90.
33. Sadri A, Ying WL, Gebski P. Application of specialized non-destructive testing (NDT) for operating copper process vessels. In: *Proceedings of eight international copper conference 2013, Instituto de Ingenieros de Minas de Chile (IIMCh)*, December 2013, Santiago, Chile; 2013. p. 813–33.
34. Sadri A, Gebski P, Rojas VP, Ibanez SR, Diaz CW. Inspection and evaluation of refractory lining for slag cleaning furnace and Teniente reactor at Fundición Hernán Videla Lira Empresa Nacional De Minería (ENAMI). In: Nilo E, Stegmaier R, Guzman P, editors. *Proceedings of MAPLA 2008, international conference in mine plant maintenance*, September 3–5, 2008, Santiago, Chile; 2008.
35. Sadri A, Ying WL, Dempsie B. Preventing costly smelting furnace and process vessel run-outs (both in English and Spanish versions). In: Armstrong S, Knights P, Bolaños J, Mares E, editors. *Proceedings of MAPLA 2013, 10th international conference in mining plant maintenance*, Santiago, Chile, September 2013; 2013.

Further Readings

- ASTM C71-12. *Standard terminology relating to refractories*. West Conshohocken, PA: ASTM International; 2012. <www.astm.org>.
- Perko JF, Spirko EJ. Blast furnace refractory lining wear status using radioactive sources. *Ind. Heat* 1979;42(6):74–8.
- Sadri A, Mirkhani K, Ying WL. Utilization of innovative NDT and condition monitoring techniques for improving maintenance strategies of process vessels. In: Babarovich V, Endo A, Pascual R, Stegmaier R, editors. *Proceedings of MAPLA 2012, 9th international conference in mining plant maintenance*, September 2012.

Blast Furnace Ferrous Burden Preparation*

O U T L I N E

54.1 Brief Description of Ferrous Charge Materials	539	54.4.4 Physical Properties of Blast Furnace Burden Materials	550
54.2 Types of Iron Ore Used to Produce the Ferrous Charge Materials	541	54.4.5 Metallurgical Properties of Blast Furnace Burden Materials	551
54.3 Charge Materials Production Processes	542	54.5 Impact of Ferrous Burden Materials on Blast Furnace Operations	553
54.3.1 Lump Ore Production	542	54.6 Global Ferrous Burden Material Usage	554
54.3.2 Sintering	542	54.7 Summary	555
54.3.3 Pelletizing	544	Exercises	556
54.4 Chemical, Physical, and Metallurgical Properties of Charge Materials	548	References	556
54.4.1 Iron Content	548		
54.4.2 Total Acid Gangue Content	550		
54.4.3 Binary Basicity	550		

54.1 BRIEF DESCRIPTION OF FERROUS CHARGE MATERIALS

The three principle ferrous charge materials used in the blast furnace (BF) are lump ore,

sinter, and pellets (see Fig. 54.1). These three materials account for over 95% of ferrous BF burden materials globally. Other less important burden materials such as waste oxide briquettes, made from recycled steel plant wastes,

*We thank Mr. Manuel Huerta, Senior Process Engineer, Hatch Ltd. for his contribution to this chapter.



FIGURE 54.1 Blast furnace ferrous charge materials: lump ore (left), sinter (center), and pellets (right). Source: Photo courtesy: Manuel Huerta, Hatch Ltd.

account for only a very small fraction of the ferrous burden and are thus not discussed further in this book. Chapters 43 and 44, discuss the use of ferrous scrap and direct reduced iron as ferrous charge materials.

Lump ore refers to iron ore whose as-mined physical and chemical properties make it suitable for direct charging into the BF without further beneficiation or agglomeration. Typically, the mined lump ore is simply crushed to <31.5 mm and screened to separate the -6.3 mm fraction. The resulting granular material, with a size range of +6.3, -31.5 mm, can be directly charged to the BF. The fine -6.3 mm material is used as sinter plant feed or further ground and beneficiated to become pellet plant feed.

Sinter is a clinker-type iron-bearing material that is produced when a mixture of iron ore fines, known as sinter feed, finely ground fluxes, carbon (coke breeze or anthracite), and various recycled iron-bearing materials are uniformly fired along a continuously traveling grate conveyor. This conveyor is known as a downdraft sintering machine. The sinter blend is fed onto the traveling grate and a special furnace ignites fuel present in the top of the sinter mix. The flame front is drawn down through the sinter bed by suction fans as the grate cars travel the length of the conveyor. This generates temperatures high enough for the fine particles to fuse together into a porous clinker material. The hot sinter is crushed, cooled and

subsequently sized to BF specifications. The sinter product is strong enough to be used as a BF burden material but is not sufficiently strong to withstand long distance transportation and handling. As a result, sinter plants are in close proximity to the BF; virtually all sinter plants are within an integrated BF-based steel works.

Fired iron ore pellets are hard balls that are produced to a specific size range by forming iron ore concentrate into unbaked green pellets and then heat hardening these green pellets in a dedicated induration furnace. The main feed materials are finely ground iron ore concentrate, finely ground fluxes, a binder, usually bentonite and, in the case of hematite (Fe_2O_3) ores, finely ground carbon (coke breeze or anthracite). Magnetite (Fe_3O_4) ores do not require carbon additions as the exothermic oxidation of magnetite to hematite that occurs in the induration furnace provides enough heat to sustain the pelletizing process.

The mixed materials are formed into small 8–16 mm diameter balls through the action of rotating drums or discs at a controlled moisture content. The green balls are then fired at controlled temperatures in an induration furnace which can be one of the following two types;

- a single straight grate induration furnace or;
- a train of three reactors consisting of a traveling grate, rotary kiln, and cooler, known as the grate-kiln process.

The elevated temperatures produced in either process heat harden the green pellets, producing fired pellets which are strong enough to be used as BF burden materials. Due to their higher physical strength compared to sinter, pellets can survive long distance transportation and are thus an internationally traded commodity. Depending on their final user, pellets are often categorized between BF pellets and direct reduction (DR) pellets, the latter having a higher Fe and lower gangue content consistent with the requirements of the DR process.

The BF ferrous burden can be composed of only one of the three charge materials described above, or more often a blend of two or three of these materials. The blending ratios vary widely by region and will be discussed further in [Section 54.7](#).

54.2 TYPES OF IRON ORE USED TO PRODUCE THE FERROUS CHARGE MATERIALS

The type of BF ferrous burden material produced is dictated by the available iron ore minerals. Lump ore is produced from iron ore minerals whose as-mined physical and chemical properties make them suitable for direct use at the BF without further processing other than crushing and sizing. Lump ores were once the dominant BF charge material, but high-quality reserves have been significantly depleted. The quality of the remaining lump ore deposits has decreased, forcing iron ore miners and BF operators to turn to sinter and pellets as the dominant ferrous charge materials.

Sinter, like lump ore, is produced from iron ores whose chemical properties make them suitable for BF operation without further upgrading. Sinter feed, +0.1 to -6.3 mm, is too fine for direct charging and must be agglomerated to increase its size. The sintering process evolved in the first half of the twentieth century out of the necessity to agglomerate fine -6.3 mm material that was screened out of the lump ore. If these

fines were not used in the BF, they would represent a large ferrous yield loss to the steel works. Sinter feed, and the resulting sinter, is the most widely used BF ferrous feed globally.

In the 1950s, as the quality of sinter fines in several regions declined, iron ore miners exploited lower grade resources which required fine grinding and beneficiation to upgrade their iron content to acceptable levels for BF ironmaking. Pellet feed or concentrate is a fine iron ore material, that results from the intensive upgrading and beneficiation of low-grade iron ores that are too fine for direct charging into the BF or as sinter feed. Pellet feed particle size is generally <0.15 mm.

Iron ores with Fe content as low as 25–30% are mined and finely ground to liberate the iron-bearing mineral particles from the accompanying gangue minerals (silica, alumina, titania, etc.). A variety of separation techniques are employed to remove the gangue minerals and concentrate the iron-bearing minerals. Magnetite ores normally undergo several stages of dry and/or wet magnetic separation while hematite ores are upgraded using gravity separation techniques such as spirals. For both types of iron ore, flotation of gangue materials has recently gained attention due to the increasing importance to produce concentrates with the highest degree of purity and/or to produce low gangue DR grade pellets.

While iron ores are generally hematite, magnetite or limonite ores, there are many varieties of these minerals:

- Hematite
 - Itabirite (Brazil)
 - Brockman (Australia)
 - Marra-mamba (Australia)
 - Specular hematite (Canada)
 - Marite (United States)
- Magnetite
 - Taconite (United States)
 - Titania-magnetite (Russia)

[Table 54.1](#) provides a summary of the typical chemical and sizing characteristics of iron

TABLE 54.1 Chemical and Sizing Properties of Lump Ore, Sinter Feed, and Pellet Feed

	Lump Ore (%)	Sinter Feed (%)	Pellet Feed (%)
Fe	60–64	60–66	> 65
SiO ₂ + Al ₂ O ₃	< 6	< 8	< 5
SIZING			
+6.3 mm	100	< 5	—
+1.0 mm	—	> 60	—
-0.15 mm	—	< 20	100

ores used to produce different BF ferrous burden materials.

54.3 CHARGE MATERIALS PRODUCTION PROCESSES

Having understood the types of iron ores that are used to produce the three main types of BF ferrous burden materials, the next sections describe the production processes involved.

54.3.1 Lump Ore Production

Lump ore processing is the simplest among the BF ferrous burden materials. Since lump ores are those whose as-mined properties make them suitable for BF usage, little processing is required other than crushing and screening. The crushing and screening flow sheet will vary for each individual ore deposit, but in general, a typical flow sheet will resemble the one shown in Fig. 54.2.

Typically, the run-of-mine iron ore will undergo primary crushing, which is normally carried out in jaw or gyratory crushers. Afterward, secondary crushing is done using cone crushers. Other types of crushers can be used depending on the hardness and grindability of the ore. Secondary crushing is

usually done in closed circuit with a double-deck vibrating screen to separate the +31.5 and -6.3 mm ore particles. The +31.5 mm ore is recycled back to the secondary crushing for reprocessing, and the -6.3 mm is collected as sinter feed. The remaining +6.3 to -31.5 mm ore constitutes product lump ore, which can be directly charged to the BF.

Other simple beneficiation techniques that can be performed on lump ores to increase their iron content are washing in a pugmill or heavy media separation in a ferrosilicon solution. These techniques are only effective if the silica and other gangue particles are liberated by the crushing operations described above. The operating principle for these techniques relies on the difference in density between the iron ore mineral and the liberated silica particles to efficiently separate and remove the latter.

54.3.2 Sintering

High-quality iron ores with particle sizes ranging from as fine as +0.15 mm to as coarse as -6.3 mm are collectively known as sinter feed. The Fe content of sinter feed is sufficiently high for BF ironmaking, but the material is too fine to promote the good permeability for gas flow necessary for proper BF operations. As a result, the fine particles must undergo an agglomeration process known as sintering to increase their size. Fig. 54.3 shows a schematic of the down draft sintering process.

The process begins with the preparation of sinter blend in the stockyard. Sintering blend piles are made using dedicated stackers and reclaiming machines to homogenize the main components in the sinter blend.

Properly sized sinter feed is conveyed from the storage yards into storage silos. Other feed materials, mainly flux (typically limestone) and a solid fuel (usually coke breeze or

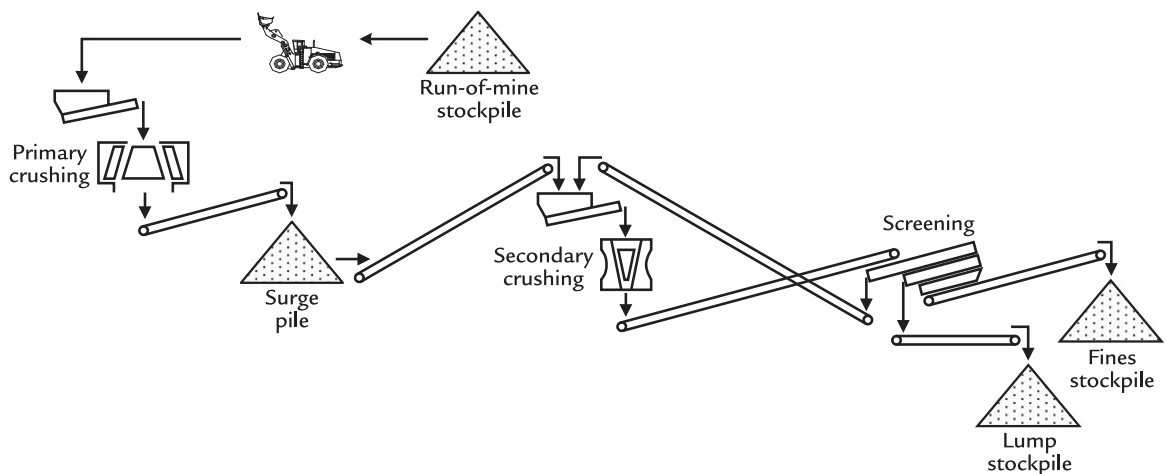


FIGURE 54.2 Schematic of a typical lump iron ore production process.

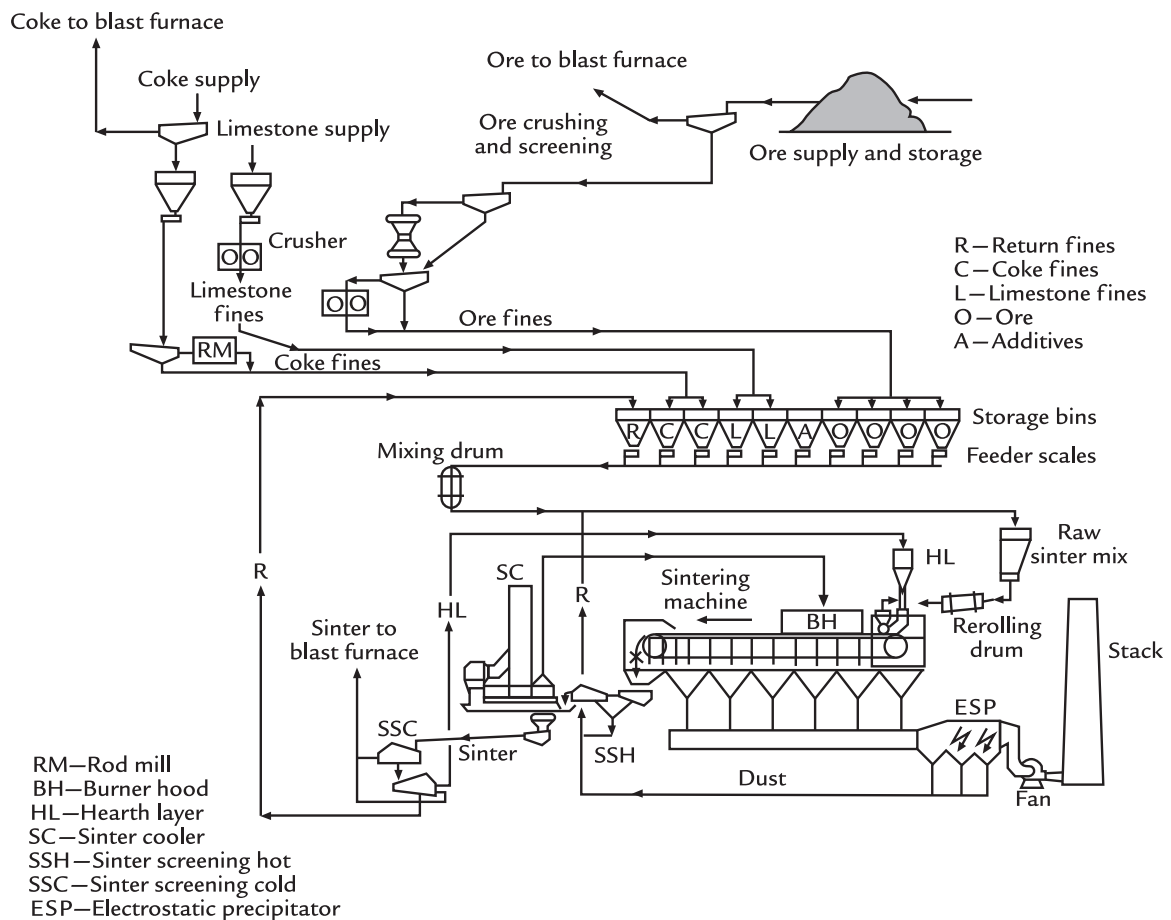


FIGURE 54.3 Schematic of the down draft iron ore sintering process.¹

anthracite), are crushed or finely ground and conveyed to storage silos. Additional storage silos for recycled screened sinter fines, as well as miscellaneous steel plant revert materials (such as BF dust and sludge, mill scale, etc.), are normally added to the sinter blend. From the storage silos, the feed materials are dosed in properly defined ratios, selected by the plant operator to attain a specific final sinter chemistry and mechanical strength.

The dosed materials travel via conveyor belt to a mixer where they are combined, and water is added for moisture adjustment. The mixer usually consists of a simple mixing drum, but modern sinter plants, and even some older plants, have incorporated high intensity mixing and granulation systems to achieve a highly homogeneous mixture. The mixed materials then travel into preagglomeration devices, which consist of either balling drums or balling discs, to produce small granules or "micropellets". These micropellets improve the permeability of the sintering bed, resulting in increased sinter strand productivity. The preagglomerated mixture is then fed to the sintering machine.

The sintering machine is an endless traveling chain of pallet or grate cars, situated over windboxes which continuously pull air down through the grate using large process fans. At the feed end, a recycled bed 25–50 mm in height of indurated sinter, known as the hearth layer, is evenly placed over the surface of the grate cars to protect the cars from excessive thermal attack. The preagglomerated feed is then carefully laid on top of the hearth layer to produce a uniform, homogeneous sintering bed. The sintering bed then passes under an ignition hood, where gas fired burners are used to ignite the solid fuel present in the sinter mixture. As the sintering bed advances over the length of the traveling grate, downdraft air is pulled by the process fans through the windboxes. This burns the solid fuel across the height of the bed. A moving burning boundary called the "combustion or

flame front" travels from the top to the bottom of the sinter bed as the grate cars pass over the windboxes. The heat generated by the solid fuel combustion elevates the sintering blend to a peak temperature of 1300–1500°C. This fuses together the sinter blend particles, in other words "sintering" the mix. The point along the length of the traveling grate where the combustion front reaches the bottom of the bed is called the "burn through point." Once this is achieved, the indurated sinter can be discharged at the end of the traveling grate where it is crushed into small chunks and fed to the hot sinter screens, where fines produced during the sintering process are removed and recycled back to the feed area of the sinter machine.

The hot sinter is then fed into the sinter cooler, which is an annular traveling grate device where atmospheric air is blown upward by the action cooling air fans to reduce the sinter temperature to below 150°C. The resulting warm air is sometimes ducted to the ignition hood to recycle its latent heat back to the process. From the sinter cooler, the sinter is discharged onto cold sinter screens where the hearth layer and fines are separated. The hearth layer is conveyed into the machine feed area to be laid on top of the grate cars while the fines are sent to a storage silo in the dosing area for recycling. The final on-size sinter is then transported directly to the BF stockhouse, or to a storage yard.

54.3.3 Pelletizing

Pelletizing is the agglomeration process applied to iron ore concentrates which were very finely ground to liberate the silica and other gangue components from the ore matrix and remove them through a mineral beneficiation technique. There are many such beneficiation techniques, but the most commonly used in the iron ore industry are fine grinding followed by magnetic separation for magnetite

ores and fine grinding followed by spirals or dense media separation for hematite ores. For both types of ores, flotation of silica has recently been used to produce ultra-low gangue concentrates, often to produce DR grade pellets. There are various flow sheet configurations for the pelletizing process, depending on the type of pellet induration technology that is employed. Each flow sheet will consider the way the iron ore concentrate is received at the plant, on-size or relatively coarse, dry or in slurry form, etc. Another factor that affects the pellet plant configuration is whether the plant

has access to a large amount of process water. If so, the raw materials preparation processes are performed on a wet basis. The following description applies for a plant configuration starting with dry coarse pellet feed undergoing a wet grinding circuit prior to balling and induration. As explained, other configurations are possible but are beyond the scope of this chapter.

Fig. 54.4 shows a schematic of a common pelletizing plant configuration.

Iron ore concentrate, also known as pellet feed, is transferred from the stockpiles to storage silos. Additives (fluxes, binders, and/or

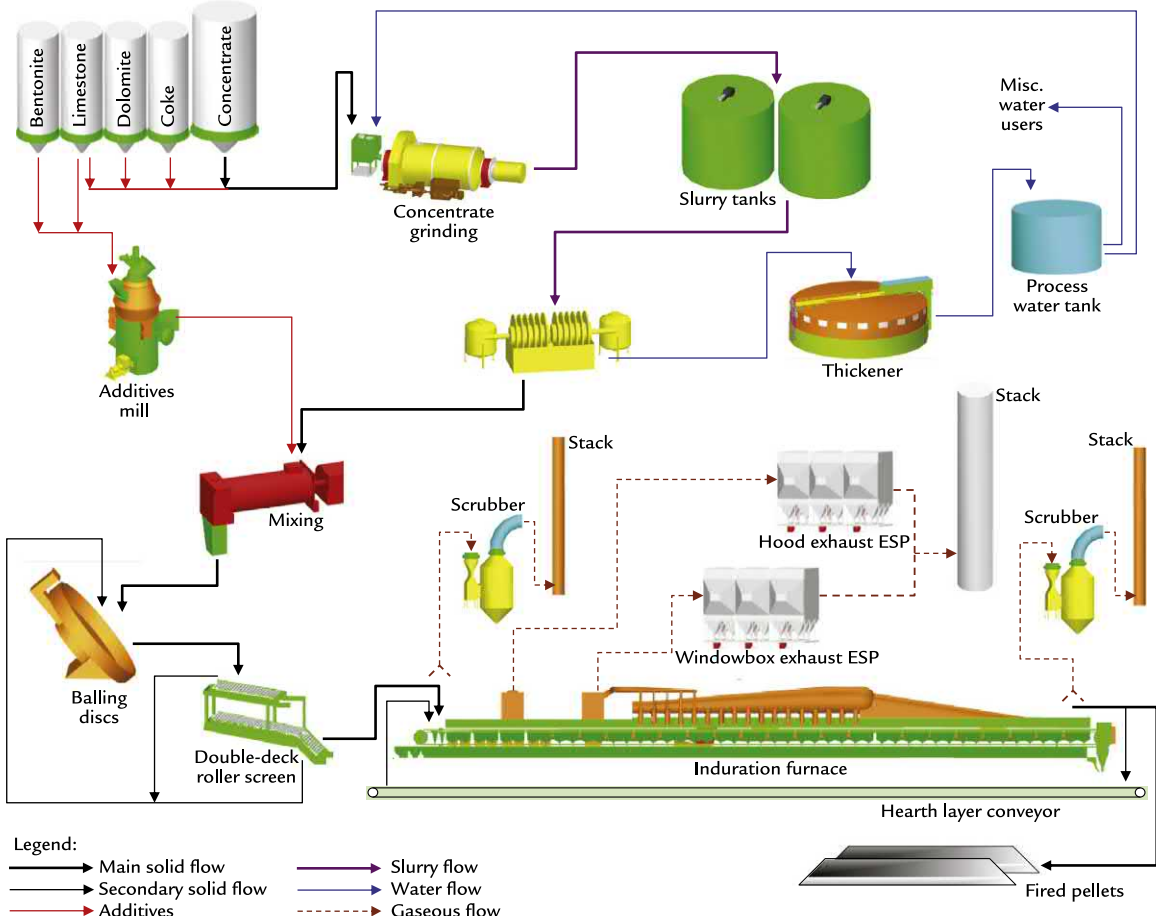


FIGURE 54.4 Schematic of the iron ore pelletizing process with a straight grate induration furnace.

solid fuel) are also transferred to separate storage silos. The additives are finely ground to 80%, $-45\text{ }\mu\text{m}$, typically in a dry vertical roller mill and then stored in aerated silos for subsequent dosing in the mixing step.

The pellet feed is fed via conveyor belts to wet ball mills, operated in open or closed circuit, to be finely ground also to 80% $-45\text{ }\mu\text{m}$. The resulting slurry of finely ground pellet feed is then pumped to storage tanks from where it is fed to a dewatering process, usually consisting of vacuum disc filters. The dewatering process is designed to produce a filter cake with 8–10% moisture which is conveyed to filter cake day bins for storage. From the day bins, the filter cake is fed to mixers together with the finely ground additives, which are dosed at precise ratios. The mixers combine the materials together, and water is added to make any necessary moisture adjustments.

The mixed filter cake and additives are transferred to the balling area, where either balling drums or balling discs are used to form small roughly spherical balls 8–16 mm in diameter known at this stage as green pellets or green balls. The green pellets go through two screening stages: first, roller screens installed at each balling drum or disc and second, through a single roller screen just before the induration furnace. Off-spec material is recycled back to the balling equipment. On-spec green balls are then conveyed to the induration process.

The objective of the induration process is to heat the green pellets to their firing temperature to agglomerate or fuse the fine particles together. Exposing the green pellets to 1250–1350°C firing temperatures ensures that the required physical and metallurgical properties are achieved. Other important processes that occur are moisture removal, magnetite oxidation, and calcination of fluxes and weathered ores. Except for magnetite oxidation which is exothermic, these processes are

endothermic. Thermal energy must be supplied to the system to meet these energy demands.

Green pellet induration is achieved through one of two technologies: the straight grate or the grate-kiln process. Both processes will be briefly described below. They can both produce superior quality BF pellets, and the choice between them depends on an array of project specific factors. Other less frequently used induration technologies include the shaft induration process and the circular pelletizing technologies. These technologies are not commonly used in the global iron ore pelletizing business and are thus not discussed further in this chapter.

Unlike sinter plants, pellet plants are usually located at the mine or shipping port. Pellets are shipped internationally using large purpose-built ships that can carry up to 300,000 t of pellets in a single cargo.

54.3.3.1 Straight Grate Pelletizing Technology

The straight or traveling grate process consists of a single furnace which encloses an endless chain of pallet or grate cars (Fig. 54.5).

At the feed end of the furnace, a small layer of indurated pellets known as the hearth layer is laid down across the width of the pallet car and against the side walls to protect the pallet cars from the high heat loads experienced during induration. The green pellets are then evenly distributed on top of the hearth layer pellets. Pellet firing is achieved by numerous burners arranged throughout the preheating and firing zones. Ambient air is blown countercurrent to the flow of pellets through the furnace cooling zones to cool and recover the latent heat in the fired pellets to the process gas. The hot process gases are then used for drying and pre-heating of the green pellets. Exhaust gases are cleaned in electrostatic precipitators and then discharged to the atmosphere through a stack.

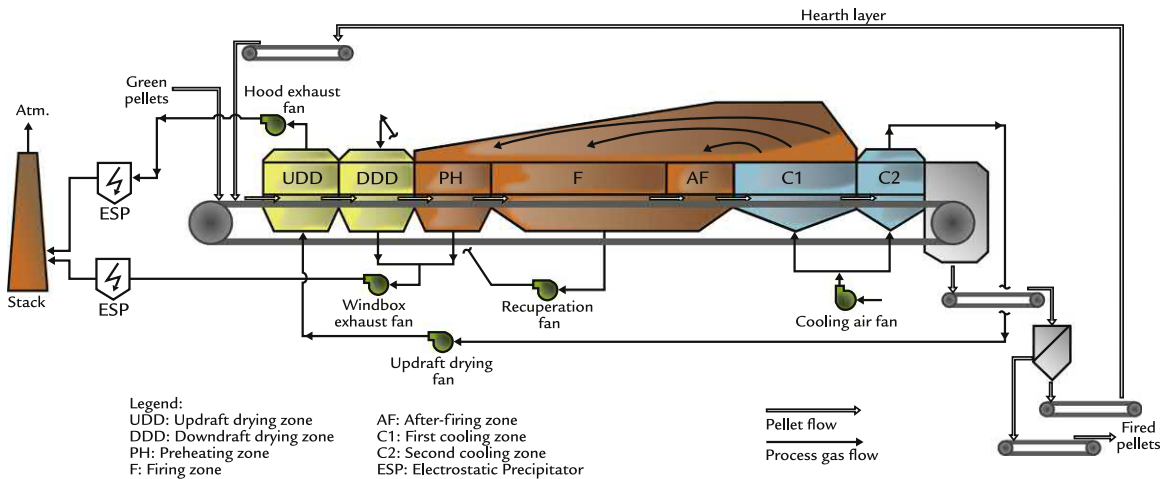


FIGURE 54.5 Schematic of the straight grate pelletizing process.²

The discharged fired pellets are conveyed to the pellet stockyard and then shipped to their final BF or DR shaft furnace client.

The straight grate technology offers the following advantages:

- High production capacity, with the newest machines rated at 8.0 Mt/year or more. In contrast, the grate-kiln system is currently limited to 6.0 Mt/year.
- Straightforward process with a single machine as opposed to three units for the grate-kiln system.
- High plant availability.
- Capable of processing both magnetite and hematite iron ores, with the option to use solid carbon fuel with hematite ores.
- Ability to use organic binders (cellulose and/or plastics) thus lowering gangue contamination in the pellet due to the bentonite addition (bentonite is a silica based clay). The use of organic binders in grate-kiln systems poses some technical challenges.

54.3.3.2 Grate-Kiln Pelletizing Technology

The grate-kiln system consists of three separate units connected in series: the traveling

grate, the rotary kiln, and the annular cooler. Green pellets are fed onto the traveling grate where they are dried and preheated before transfer to the rotary kiln. The rotation of the charge in the kiln ensures that all pellets are exposed to the same conditions and heated to the same temperature. From the rotary kiln, the hot pellets discharge into an annular cooler consisting of four cooling zones. Ambient air is blown countercurrent through the hot pellet bed to cool them for subsequent material handling. The hot process air is recycled back to the rotary kiln and various zones of the traveling grate (Fig. 54.6).

The grate-kiln technology offers the following advantages:

- Flexibility to use coal as a fuel whereas the straight grate must use oil or natural gas.
- Improved control, due to independent speed controls for preheating, induration, and cooling.
- Does not require a hearth layer of pellets, thus eliminating an important heat sink.
- Absence of a hearth layer makes it easier to change between pellet product types,

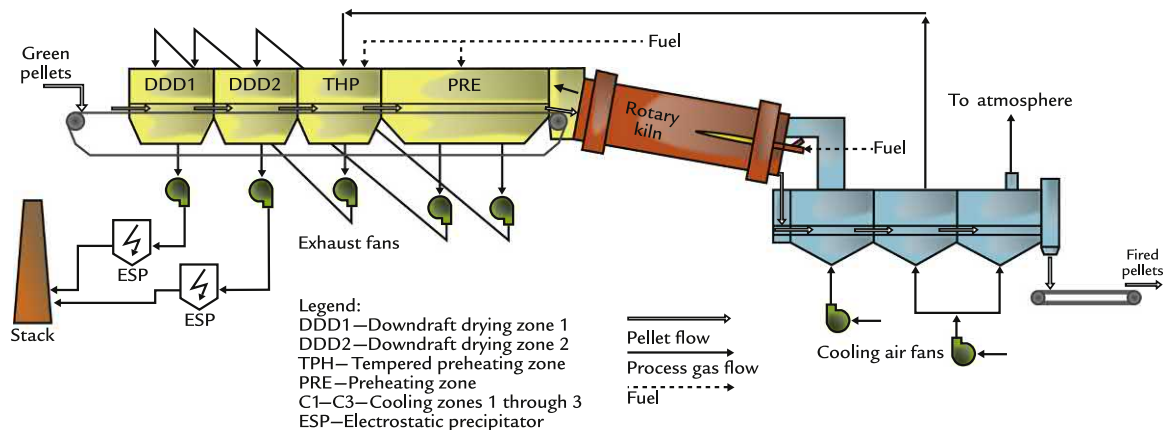


FIGURE 54.6 Schematic of grate-kiln pelletizing process (also known as the rotary kiln process).²

avoiding contamination of the new pellet grade and resulting in reduced downtime for product change overs.

- Lower bed depth, resulting in a more uniform temperature profile, reduced pressure drop, ability to use smaller process fans and thus lower power consumption.
- Mixing of the pellets in the rotary kiln produces a more homogenous product, potentially increasing BF and/or DR performance.

54.4 CHEMICAL, PHYSICAL, AND METALLURGICAL PROPERTIES OF CHARGE MATERIALS

Table 54.2 shows a list of the desirable chemical, physical, and metallurgical properties of lump ore, sinter, and pellets to ensure proper performance in the BF. The values offered in the table are typical industry values and may vary somewhat between individual BF operations, based on their specific circumstances.

From the table, it is evident that the main differences in the chemical properties between lump ore, sinter, and BF pellets are the total iron (Fe) content, the total acid gangue ($\text{SiO}_2 + \text{Al}_2\text{O}_3$) content, and the binary basicity

(CaO/SiO_2). The following subsections discuss the impacts of these differences on BF performance.

54.4.1 Iron Content

High-grade commercial lump ores can be as high as 65–68% Fe, although these are becoming increasingly scarce and expensive, hence the comparatively small use of lump ore compared to sinter and pellets.

The typical iron content of sinter is around 54–58% Fe, while BF pellets are normally 62–66% Fe. BF pellets have a higher Fe content than sinter as BF pellets are manufactured from low-grade ores that are finely ground to undergo mineral beneficiation treatments to upgrade their Fe content. Due to the requirement to use clay binders with a high SiO_2 content to form green pellets, the pelletizing process typically operate at lower basicity compared to sintering.

Acid pellets have no fluxes added, and the gangue is principally SiO_2 . BF operators learned that adding Ca and/or Mg-based fluxes to the pellet feed could greatly improve the metallurgical properties, especially reducibility, and offer higher softening and melting temperatures. Calcination of limestone and

TABLE 54.2 Desirable Chemical, Physical, and Metallurgical Properties of Lump Ore, Sinter and Blast Furnace (BF) Pellets

	Lump Ore	Sinter	BF Pellet
CHEMICAL PROPERTIES			
Fe, %	65–68	55–58	62–66
SiO ₂ , %	1–4	5–6	2–5
Al ₂ O ₃ , %	0.5–1.5	1.0–1.3	0.4–1.0
CaO, %	<0.1	9–11	1.0–4.5
MgO, %	<0.1	1.4–2.0	0.2–1.3
CaO/SiO ₂	N/A	>1.7	0.8–1.1
PHYSICAL PROPERTIES			
Size distribution	>31.5 mm: Max. 5% 6.3–31.5 mm: Min. 85% <6.3 mm: Max. 5%	>50 mm: Max. 10% <10 mm: Max. 30% <6.3 mm: Max. 5%	>16 mm: Max. 5% 8–16 mm: Min. 85% <6.3 mm: Max. 5%
Tumbler strength (ISO 3271)	>6.3 mm: Min. 95% <0.5 mm: Max. 5%	>6.3 mm: 70%–80% <0.5 mm: Max. 5%	>6.3 mm: Min. 95% <0.5 mm: Max. 5%
Cold crushing strength (ISO 4700)	N/A	N/A	Average: Min 2500 N <2000 N: Max. 10% <1500 N: Max. 5%
METALLURGICAL PROPERTIES			
Reducibility (ISO 4695)	Min. 0.8%/min	Min. 1.4–1.6%/min	Min. 0.8%/min
Low temperature reduction–disintegration, static (ISO 4696)	>6.3 mm: Min. 85% <0.5 mm: Max. 10%	<3.15 mm: Max. 35% <0.5 mm: Max. 10%	>6.3 mm: Min. 85% <0.5 mm: Max. 10%
Low temperature reduction–disintegration, dynamic (ISO 13930)	>6.3 mm: Min. 80% <0.5 mm: Max. 15%	N/A	>6.3 mm: Min. 80% <0.5 mm: Max. 15%
Reduction under load (ISO 7992)	dP80%: Max. 15 mmWC	N/A	dP80%: Max. 15 mmWC
Free swelling (ISO 4698)	N/A	N/A	Max. 20%

mmWC, mm water column.

dolomite was moved from the BF to the pellet plant. Fluxed pellets offered greater BF permeability to gas flow, faster reduction, and hence reduced coke consumption. Flux additions dilute the pellet Fe content, so it follows that

the Fe content of fluxed pellets is less than acid pellets.

The higher Fe content of lump ore and pellets increases BF productivity as more iron units are charged to the BF per unit ton of

burden material. Shipping costs are reduced as more iron units and less undesirable gangue are shipped to the final BF user.

54.4.2 Total Acid Gangue Content

The total acid gangue content, defined as $\text{SiO}_2 + \text{Al}_2\text{O}_3$, is significantly lower in lump ore and pellets compared to sinter. The main advantage of lower gangue materials is a lower BF slag rate. Since slag is composed of the gangue materials present in the ferrous burden, the ash content of coke and injected coal, and the added fluxes, it follows that less acid gangue will produce less slag per ton of hot metal. Lower slag rates directly translate into lower coke rates, as less thermal energy is required to melt the slag and calcine any free carbonates present in the fluxes. In addition to lower coke rates, another direct advantage of a lower slag rate is that a smaller volume of by-product slag must be subsequently handled.

54.4.3 Binary Basicity

The third difference in the chemistries of BF burden materials is shown by the binary basicity (B_2), defined as the ratio of CaO/SiO_2 . BF pellets have a B_2 ratio range from 0 for acid pellets to 0.8–1.1 for fluxed pellets. In sinter, the B_2 ratio is commonly set at 1.7 or more to improve sintering productivity and achieve enough sinter strength to withstand material handling operations and for satisfactory performance in the BF. For lump ore, binary basicity is not a relevant parameter since the naturally occurring amounts of CaO and MgO in lump ore are for the most part negligible.

The high basicity of sinter compared to BF pellets negatively affects the operating costs of hot metal in two ways. First, it requires a higher consumption of flux (limestone and/or dolomite) to achieve the target slag basicity. Second, it increases the slag rate, as the additional fluxes generate a higher slag volume.

Increasingly, BF operators have changed from acid to fluxed pellets. Fluxed pellets offer the following advantages:

- The BF coke requirement to reduce carbonate fluxes, principally limestone, is greatly reduced when fluxed pellets are used. The calcining reactions are moved to the pellet indurating process.
- Added limestone, when calcined, creates additional porosity in the fired pellets. This increases the pellet reducibility (i.e., speed that iron ore can be reduced by CO(g) and $\text{H}_2(\text{g})$) when fluxed pellets are charged to the BF.
- The temperature when the pellet softens and subsequently melts is increased by 100–200°C. This brings the melting characteristics of the pellet closer to the characteristics of sinter. A narrower melting zone forms in the BF and decreases the pressure drop from BF tuyeres to the stockline. The decreased pressure drop allows for smoother burden descent, and greater productivity can result. The melting zone is closer to the tuyeres and as a result, less SiO_2 is reduced to Si in the hot metal.

The blast furnace engineer must design the pellet fluxing in coordination with the sinter fluxing practice. Ideally, the B_2 of fluxed pellets and sinter should be as close as possible. Sinter strength deteriorates at B_2 from 1.2 to 1.7, this forces a typical blend of fluxed pellets with $B_2 \sim 0.8$ and sinter with $B_2 \sim 1.9$. BFs that use 100% fluxed pellets use a higher B_2 , typically ~ 1.1 . Such a B_2 is slightly higher than the hearth slag B_2 value to allow for inclusion of the SiO_2 contribution from ash in the coke and injected coal.

54.4.4 Physical Properties of Blast Furnace Burden Materials

The most important physical parameters for BF burden materials are size distribution,

tumbler strength, and cold crushing strength. The former two are relevant for all charge materials while the latter is only relevant for pellets. Desirable physical properties for typical BF lump, sinter, and pellets are presented in Table 54.2.

54.4.4.1 Size Distribution

Size distribution is measured simply by screening a sample of burden material through various sieve sizes and weighing the amount retained at each sieve size. Typical sieve sizes include 6.3, 8, 16, 22.4, and 31.5 mm, among others.

54.4.4.2 Tumbler Strength (ISO 3271)

The tumbler strength is a quality control test which is conducted on lump, sinter, and pellets to measure their resistance to degradation by impact and abrasion. The test equipment consists of a circular rotating drum with an internal diameter of 1000 mm and an internal length of 500 mm. A test sample of 15 kg of material is required. The test sample is placed in the tumble drum and rotated for 200 revolutions at 25 rpm. The material is removed from the drum, and the sample is screened. The percent weight of the fraction >6.3 mm constitutes the tumble index while the percent weight of the fraction <0.5 mm is the abrasion index.

54.4.4.3 Cold Crushing Strength (ISO 4700)

The cold crushing strength is only applicable to pellets. It measures the compressive load that must be applied to individual pellets to cause breakage. The test consists of two flat parallel plates and a device capable of setting the speed of the plates during the compression test. Each pellet sampled is first dried to constant weight at 105°C and then subjected to an applied load at a constant plate speed of 10–20 mm/min until either the load has fallen to a value of 50% or less of the maximum load, or the gap between the plates has been

reduced to 50% of their initial value. In either case, the crushing strength is the maximum load attained in the test, measured in Newtons. A sample of 60 pellets between 10 and 12.5 mm in diameter is required for the test. The cold crushing strength is the mean value obtained over the entire sample.

54.4.5 Metallurgical Properties of Blast Furnace Burden Materials

Various test methods are employed to measure the metallurgical properties of blast burden materials. These tests are performed under conditions which simulate those experienced by the burden materials as they descend through the BF shaft. Typical desirable metallurgical properties for BF burden materials are presented in Table 54.2.

54.4.5.1 Reducibility (ISO 4695)

This is a test of the susceptibility of a lump, sinter, or pellet sample to be reduced under reducing gas conditions present in the BF. A lump, sinter, or pellet sample is placed in a vertical steel tube 75 mm in diameter which is suspended inside an electrically heated test furnace. A 500 g sample with a mean size of 10–12.5 mm is first dried at 105°C and then placed inside the tube and lowered into the test furnace. The sample is first preheated with inert gas, and then hot reduction gas, at a temperature of 950°C and with a composition of 40%/60% CO/N₂, is passed through the sample at a flow rate of 50 L/min. The sample undergoes isothermal reduction until the oxygen loss reaches 65%. The reducibility index is the rate of oxygen reduction (%/minute) achieved at a 40% degree of reduction. This is calculated by measuring the time it takes to reach degrees of reduction of 30% and 60% and assumes that the rate of oxygen removal is a first-order reaction with respect to oxygen remaining in the sample.

54.4.5.2 Low-Temperature Reduction–Disintegration; Static (ISO 4696)

The degree of disintegration of the burden materials is measured in a reducing atmosphere like that in the stack of the BF. A 500 g sample of lump, sinter, or pellets measuring 10–12.5 mm is placed in a testing tube. After preheating with inert gas to the test temperature of 500°C, hot reducing gas with a composition of 20%/20%/2%/58% (CO/CO₂/H₂/N₂) passes through the sample at a flow rate of 20 L/min. After 60 minutes of reduction time, the sample is cooled below 100°C and placed in a tumbler drum to undergo 300 revolutions in total. The material is removed from the drum, and the sample is screened at 6.3, 3.15, and 0.5 mm. The weight fraction of the material retained at these sieve sizes is reported as the reduction–disintegration index.

54.4.5.3 Low-Temperature Reduction–Disintegration; Dynamic (ISO 13930)

This test is like the static test (ISO 4696 described in section 54.4.5.2) with the main difference being that the reduction of the ferrous burden material takes place in a rotating drum. Unlike the static test which is applicable to lump, sinter, and pellets, the dynamic test is only applicable to lump and pellets. The rotating drum where the reduction takes place rotates at 10 rpm for 60 minutes. The sample weight and size, test temperature, reduction gas flow rate and composition, and screen sieve sizes are the same as in the static test.

54.4.5.4 Reduction Under Load (ISO 7992)

The physical stability of a lump or pellet sample (not applicable to sinter) is evaluated under conditions resembling those of the BF. A burden sample is placed in a vertical steel tube 125 mm in diameter which is suspended inside an electrically heated furnace. A 1200 g

sample of lump or pellets with a mean size of 10–12.5 mm is first dried at 105°C and then placed inside the steel tube and lowered into the test furnace. During the entire test period, the sample is subjected to a constant load of 50 kPa.

The sample is first preheated with inert gas and then hot reduction gas at a temperature of 1050°C and with a composition of 2%/40%/58% (H₂/CO/N₂) is passed through the sample at a flow rate of 83 L/min. The sample undergoes isothermal reduction until the oxygen loss reaches 80%; the time it takes to achieve this degree of reduction is recorded. The reduction under load is reported as the pressure differential (dP_{80%}) in mm water column and the difference in height (dH_{80%}) of the test bed, both at 80% reduction.

54.4.5.5 Free Swelling Index (ISO 4698)

The free swelling test determines the volume increase of iron ore pellets during reduction. When pellets were first introduced, a swelling tendency led to damage to the BF stack, poor permeability to gas flow, and irregular burden descent. The test does not apply to lump ore or sinter.

An electrically heated furnace with a vertical reduction tube that contains a wire basket with room for 18 individual pellets is used. The pellets with sizes ranging from 10 to 12.5 mm are placed in three levels of six pellets each. The tube is 75 mm in diameter and is preheated by hot reduction gas flowing in the space between the walls. The pellets are dried at 105°C, and their volume is measured. Afterward, they are placed in the wire basket and lowered into the test furnace. The pellets are first preheated with hot inert gas to the test temperature of 900°C in a N₂ atmosphere, after which reduction gas with composition 30%/70% (CO/N₂) is introduced at a flow rate of 15 L/min. The pellets are subjected to isothermal reduction at 900°C for 60 minutes. The reduction gas is then substituted with N₂ gas

and the pellets are cooled to room temperature. The post test volume of the pellets is measured, and the free swelling index is expressed as the percent volume increase.

54.5 IMPACT OF FERROUS BURDEN MATERIALS ON BLAST FURNACE OPERATIONS

The nature of the ferrous burden has a direct impact on some key BF operating parameters, especially productivity and slag rate. Table 54.3 presents the main operating data for a small number of selected blast furnaces in North and South America, Europe, Asia, Russia, and Oceania using data from Table 1.1.

In general, the ferrous burden should have a high Fe content to minimize slag rate. This is usually achieved with a higher pellet ratio and/or with high-quality lump ore. Sinter with its heavy flux burden will increase slag volume.

From Table 54.3, BF operators could obtain low fuel rates and high productivity with a variety of sinter - pellet - lump ore ferrous burden recipes. Engineers at Tata Steel IJmuiden and NSC Nagoya achieved the lowest total fuel rate with very different burden recipes. NLMK's Rossiyanka BF achieved the highest productivity operating with a high fuel rate and slag volume. This demonstrates that a wide variety of operational outcomes can be obtained with a broad recipe of lump ore, sinter, and pellets.

TABLE 54.3 Ferrous Burden and Operating Data for Selected Blast Furnaces

Region	Unit	N. America	S. America	Europe	Asia	Russia	Oceania
Year of data		2016	2015	2015	2015	2015	2015
Company		ArcelorMittal	Ternium	Tata Steel	NSC	NLMK	BlueScope
Site		Dofasco	San Nicolas	IJmuiden	Nagoya	Lipetsk	Port Kembla
Blast furnace		4	2	6	1	Rossiyanka	5
Working volume	m ³	1609	2353	2328	4583	3361	3000
Average production	t/24 h	3435	5355	7455	10,371	11,888	6925
Productivity working volume	t/m ³ /24 h	2.1	2.4	3.2	2.3	3.5	2.3
Total metallic charge	kg/t HM	1514	1575	1529	1621	1681	1623
% Lump	%	0	40	2	15	1	14
% Sinter	%	0	30	41	77	69	84
% Pellets	%	100	30	57	8	30	2
Slag rate	kg/t HM	197	252	210	277	380	309
Coke rate	kg/t HM	326	388	281	337	405	391
PCI rate	kg/t HM	142	0	228	157	0	118
Natural gas rate	kg/t HM	33	95	0	0	99	0
Total adjusted fuel rate ^a	kg/t HM	493	502	486	478	524	497

^aTotal adjusted fuel rate = coke rate + PCI rate*0.9 + natural gas rate*1.2.

From a cost point of view, pellets and high-grade lump ores tend to be significantly costlier than sinter which brings about a tradeoff for many BF operators when selecting the appropriate ferrous burden recipe. This is especially true of market pellets that sell at a premium to sinter fines to account for extra grinding costs, yield losses during mineral processing and energy to fire the pellets.

With regards to coke rate and total fuel rate, the dependency on the type of ferrous burden is much less clear. This is because the total fuel rate depends on the overall energy balance of the BF. The latter in turn depends not only on the charge materials used but also on many other operational parameters which are beyond the scope of this chapter.

54.6 GLOBAL FERROUS BURDEN MATERIAL USAGE

As seen in [Table 54.3](#), BF operators can use a wide variety of ferrous burden mixes. The selection depends on several factors such as the raw materials available in a specific geographic region, iron ore trade agreements

between iron ore producers and steel companies, steel companies owning captive iron ore mines, and available sinter and pellet plants, among others. [Fig. 54.7](#) shows a ternary diagram of the global distribution of BF ferrous burden materials usage. Every data point is an individual BF, and the different shapes represent world regions. The data is from 2009 and excludes China and Japan.

On a global average, the BF ferrous burden is dominated by sinter usage followed by pellets and with lump ore as a distant third. The weighted average of the plotted data points provides a distribution of approximately 60% sinter, 32% pellets, and 8% lump.

Several BFs in North America, Russia (CIS region), and Europe use pellets as the principle ferrous burden because they source iron ore from mines where extensive mineral processing is needed to upgrade the Fe content of the rather poor iron ore deposits. As a result, only two sinter plants operate in North America, and they are used to recycle steel plant waste materials. The Russian blast furnaces consume a high pellet ratio burden for reasons like those in North America. At the very top of [Fig. 54.7](#), a Finnish BF that uses 100% pellets is shown. This BF is a

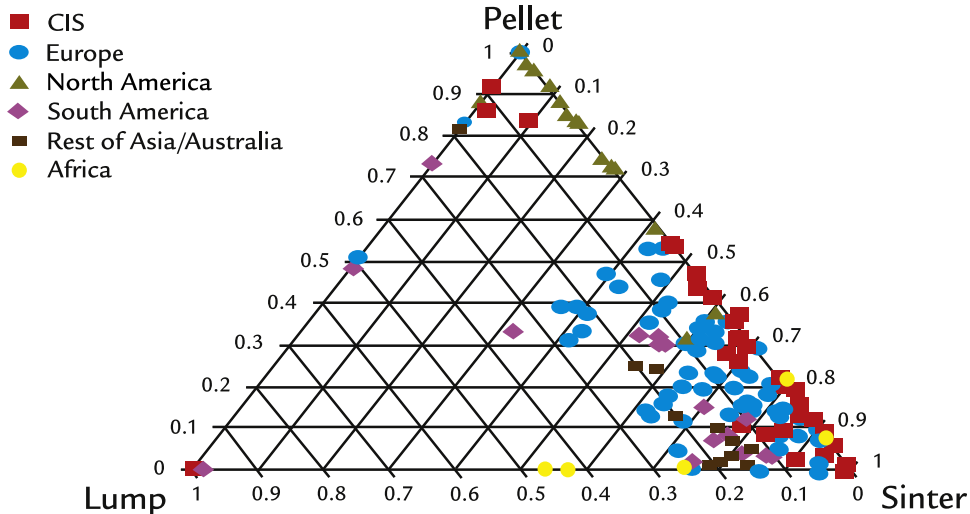


FIGURE 54.7 Global distribution of blast furnace charge materials usage (data from 2009).

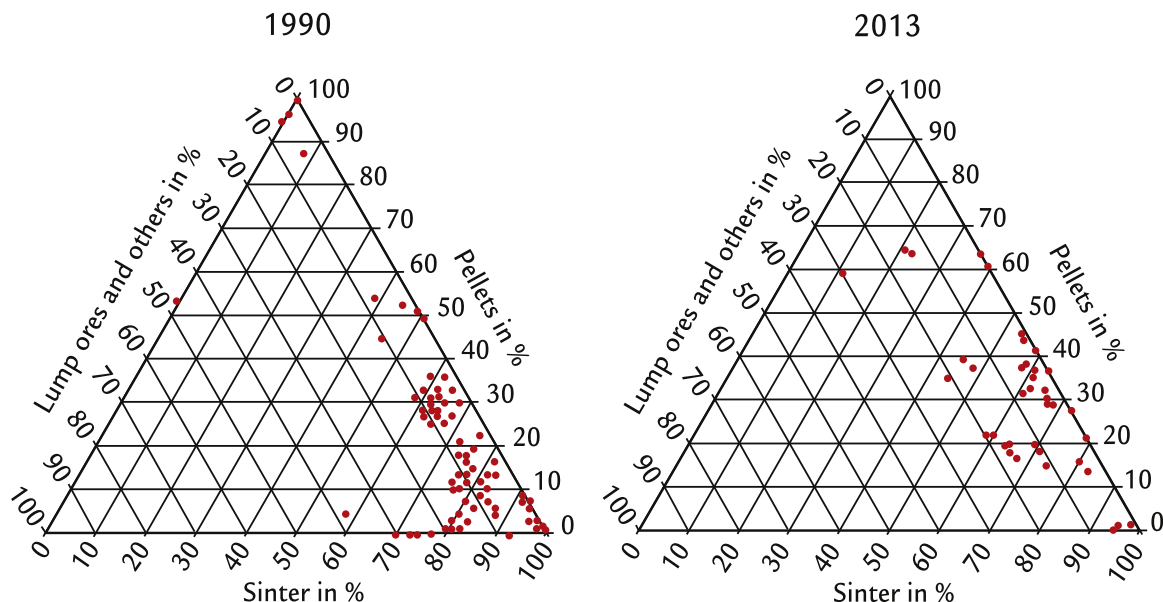


FIGURE 54.8 Trend in ferrous burden usage in Europe from 1990 to 2013.³

relatively small operation which consumes merchant pellets from Sweden.

A clear majority of the BFs use <30% of lump ore in their burden mix. The scarcity of high-quality lump ores in the global iron ore market and its comparatively high price make the use of sinter and pellets more economic. The handful of BFs that use more than 30% of lump ore in their burden mix do so mainly because they consume either captive or locally sourced high-grade lump ores.

The rest of the world relies primarily on sinter as the main BF burden constituent, complemented with pellets and, to a lesser degree, lump ore to balance the high basicity of sinter. These BFs, located in Europe, South America, Asia, and a few in Africa, normally purchase sinter feed on the global iron ore market and convert this into sinter on their own sintering machines, located adjacent to the blast furnace site. In some cases, the steel plants own captive iron ore mines to ensure a steady and consistent supply of low-cost sinter feed. The balance of pellets and/or lump ore are normally purchased from merchant

producers or in a few cases produced by the steelmakers themselves in their own pellet plants.

In Fig. 54.8, the change in ferrous burden recipe for Europe is shown comparing 1990 and 2013. A tendency to use a greater quantity of pellets is evident as European steel producers are challenged to reduce sinter production due to reduced availability of high quality sinter fines and to address environmental concerns related to the sintering process.

54.7 SUMMARY

In this chapter, we learned that three main ferrous burden materials are used in BF operation; lump ore, sinter, and pellets. The types of iron ores used to produce these three ferrous charge materials and the related production methods were described. The various analysis methods used to determine the quality of the BF charge materials were discussed, and the desirable chemical, physical, and metallurgical parameters were tabulated for reference.

Finally, the impacts of charge material usage on the blast furnace operation as well as an overview of the global distribution of charge materials usage were presented.

EXERCISES

- 54.1. A common starting material for making molten iron is hematite, Fe_2O_3 . At 100% reduction efficiency, how much pure hematite will be required to make 1000 kg (1 t) of Fe in molten iron?
- 54.2. Industrial hematite ore pellets contain 94 mass% hematite and 6 mass% SiO_2 (quartz). What is the Fe content of this ore, mass% Fe?
- 54.3. Please connect, with a line, the blast furnace zone with the pellet property which is important for good blast furnace performance.

Handling/Charging	Low swelling
Upper stack	Minimal low temperature breakdown
Lower stack	High tumbler strength
Cohesive zone	High reducibility Elevated temperature softening/meltdown

- 54.4. Fluxed pellets affect the BF operation differently from the way that acid pellets do (*please circle the effects of fluxed pellets*)
- more permeable cohesive zone
 - larger lumpy zone
 - longer dripping distance
 - thinner cohesive zone
- 54.5. The important properties of sinter parallel those of pellets in many respects; they include (*please circle*)
- high tumbler index
 - high compression strength
 - minimal low temperature degradation
 - well screened narrow size range

References

- Poveromo JJ. Iron ores. In: *The making, shaping and treating of steel*, 11th ed., Ironmaking volume; 1999, p. 607, Chapter 8.
- Huerta M, Gordon Y. *Comparison of pelletizing technologies*. Philadelphia, PA: AISTech; 2018. p. 663–72.
- Luengen HB, Peters M, Schmoele P. *Ironmaking in western Europe – status quo and future trends*. Cleveland, OH: AISTech; 2015. p. 1481–90.

Metallurgical Coke - A Key to Blast Furnace Operations

O U T L I N E

55.1 What Is Metallurgical Coke and Why Is It Required?	557	55.6.1 Chemical Composition	569
55.2 Coal Blending	558	55.6.2 Cold Strength	569
55.3 Common Coke Production Methods	559	55.6.3 Coke Size	570
55.4 By-Product Cokemaking	560	55.6.4 Properties at Elevated Temperatures	570
55.5 Heat-Recovery Cokemaking	566	55.6.5 Consistency	571
55.6 Blast Furnace Coke Quality Requirements	569	55.6.6 Coke Quality Requirements	571
		55.7 Summary	571
		Exercises	572
		References	572

55.1 WHAT IS METALLURGICAL COKE AND WHY IS IT REQUIRED?

Metallurgical coke is produced by heating and removing the volatile matter from a special mixture of coals. These coals, known as coking coals, are selected for their ability to become plastic and flow when heated and fuse into a strong carbon structure known as metallurgical coke. Macerals in the coking coal (like minerals in ores) can be grouped

into reactive, semi-inert, and inert components. Macerals identify the distinct origin of the coal when it was originally formed from decaying organic materials. Strong coke is made from an appropriate mixture of reactive and inert components. The reactive components are fluid and act as a binding agent. The inert components, either organic or inorganic, act as fillers in the ultimate coke structure. The resulting metallurgical coke is very strong and resists both crushing and



FIGURE 55.1 Metallurgical coke produced using SunCoke Energy's heat recovery coking process. *Source:* Photograph courtesy of SunCoke Energy Inc.

abrasive forces present in the blast furnace (Fig. 55.1).

Historical sources describe the production of coke in ancient China dating to the 4th century. By the 11th century, Chinese ironworkers in the Yellow River valley began to fuel their ironmaking furnaces with coke, solving their fuel problem in a tree-sparse region where charcoal production was challenging.

In 1709, Abraham Darby established a coke-fired blast furnace to produce cast iron in Great Britain. Coke's superior crushing strength allowed blast furnaces to become taller, larger, and more productive. The British iron industry requirements quickly grew from about 1 million tons a year in the early 1850s to 7 million tons in the 1880s.

In the United States, the first use of coke in an iron furnace occurred around 1817 at the Plumsock puddling furnace and rolling mill in Fayette County, West Virginia. The coal-fields of western Pennsylvania provided a rich source of raw material for cokemaking. Between 1870 and 1905, the number of beehive ovens in the United States skyrocketed from about 200 to almost 31,000, which produced nearly 18 million tons of coke in the Pittsburgh area alone. The number of beehive ovens in Pittsburgh peaked in 1910 at almost

48,000. With the introduction of by-product cokemaking in the early 20th century, beehive cokemaking quickly diminished. The benefit of producing valuable chemicals for sale from the volatile gases created during coke production provided a great financial advantage to the by-product cokemaking process which today remains the dominant cokemaking process.

Early iron foundry operators learned that the soft nature of many coals was undesirable when producing pig iron. The advent of metallurgical coke further increased performance and accelerated the development of blast furnace ironmaking. The important attributes of metallurgical coke included;

- chemical composition: coke should be low in ash, sulfur, phosphorous, and alkali (K, Na) content;
- fuel source: coke combustion generates heat and reducing gases to smelt the ferrous burden, fluxes, and slag;
- strength: strong coke supports a taller and heavier column of raw materials without being crushed. This allowed blast furnace size and productivity to increase;
- permeability: well-sized coke provides permeability essential to upward gas flow and for liquid iron and slag to drain to the blast furnace hearth; and
- elevated temperature properties: coke remains strong and granular all the way to the bottom of the blast furnace. This is important for hearth drainage and materials movement.

55.2 COAL BLENDING

Blending of coals needed to make metallurgical coke is a complex subject and will only be briefly explained in this chapter. In the 1880s, single coking coals were available that, on their own, could produce blast furnace quality coke. The famous Pittsburgh seam in

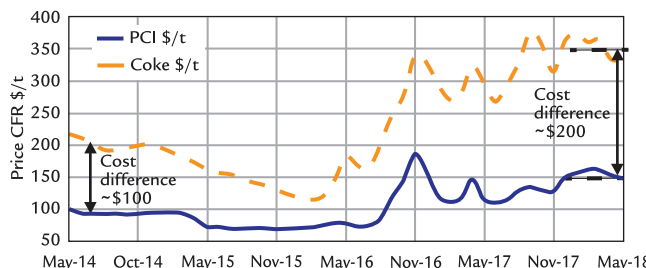


FIGURE 55.2 Delivered price premium of metallurgical coal versus pulverized injection coal from 2014 to 2018 (Price CFR - Cost and Freight (CFR) included).¹

the United States is a good example and a reason that this area became a major steelmaking region. There are similar examples in Europe, Russia, and Australia.

As these high-quality coals depleted, coking engineers learned that blending coals that, on their own were not suitable for coking, could produce high-quality blast furnace coke. Today, hard coking coal and semisoft coking coals are blended to produce all blast furnace coke.

With the advent of premature tall battery failures in the late 1970s due to oven wall pressure issues, coal blends were refined to reduce the pressure generated as the coal blend devolatilized. Blends that generated zero and near zero gas pressure were used in slot ovens over 6.0 m in height.

The introduction of high rates of coal injection increased the residence time of metallurgical coke in the blast furnace. Today's advanced blast furnaces can use injected coal to provide about 50% of the fuel requirements. The coke burning rate at the tuyeres is about half of an all-coke operation, doubling the coke residence time before it is consumed. An improvement in the elevated temperature coke properties emerged, especially the coke reactivity index (CRI) and coke strength after reaction (CSR). These properties are largely controlled by the coal blend used, specifically the ash chemistry.

A combination of the low coking pressure demands and the benefits of improved

high-temperature properties further reduced the number of coking coals that could be used to make high-quality blast furnace coke. Over time, the price premium of coking coal over injection coal increased from \$100 to \$200/t (Fig. 55.2).

Coking coal blends need to strike a balance between;

- peak coking pressure during heating, especially for slot ovens >6.0 m in height;
- coke strength
 - resistance to crushing,
 - resistance to abrasion, and
 - strength at elevated temperatures;
- coke reactivity
 - neither too reactive, nor too inert, and;
- coke size
 - 25–75 mm, with an average size of 55 mm.

The blending is complex; Fig. 55.3 is an example of blending combinations to achieve a mix of cold crushing strength, abrasion resistance, and reactivity. Additional analysis is needed to achieve the best properties at elevated temperatures.

55.3 COMMON COKE PRODUCTION METHODS

Three commercially proven processes were developed to manufacture metallurgical coke;

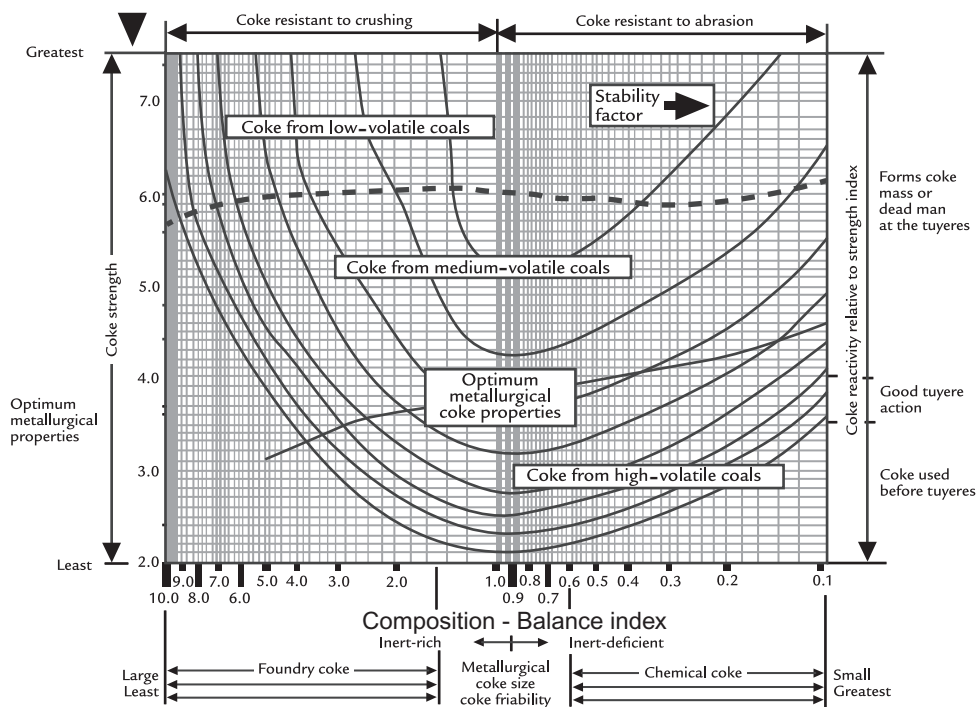


FIGURE 55.3 US Steel ASTM stability prediction model for various coal blends and coke qualities.² ASTM, American Society of Testing and Materials.

- the beehive oven process,
- the by-product process, and, more recently,
- the heat-recovery (HR) process.

The advent of by-product cokemaking and production of chemicals for sale replaced the beehive process in the first part of the 20th century. Developed in the 1960s, the HR process is a modification of the beehive process where the volatile gases are combusted and collected to produce steam and electricity. This chapter will focus on the by-product and HR technologies commonly used by the steel industry today.

Selected high quality metallurgical coals are screened, crushed to <3 mm, and blended based on their petrographic properties (ability to flow at coke oven temperatures) to produce high-quality coke while using the most cost-effective input coals. The blend is charged into the coke oven, and the volatile matter is

distilled from the coal at temperatures of 1100°C and higher. At the end of the coking cycle when 99% of the volatile matter has been released, the hot coke is pushed from the oven into a quench car. The hot coke is typically transported to the quench tower where it is doused with water to cool and stabilize the coke. While wet quenching is the most common method, coke can be dry quenched using nitrogen to produce steam and electricity. After quenching, the product coke is screened and transported to the blast furnace or stockpile. Fig. 55.4 shows a simplified coke-making flow sheet.

55.4 BY-PRODUCT COKEMAKING

Developed in the 19th century in Germany and France, by-product cokemaking involves

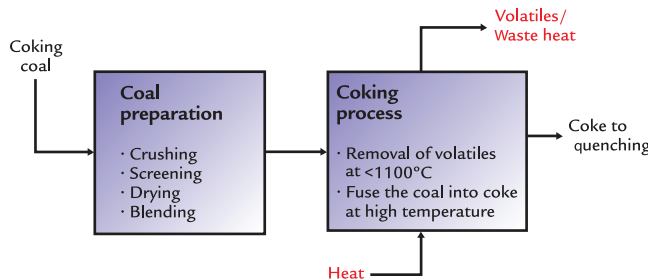


FIGURE 55.4 Conceptual cokemaking process flows.³

the collection and refining of volatile matter released during the coking process. By-product chemicals are produced on a continuous basis; volatile gases are collected from a battery of coking ovens. The coking process is performed in narrow, tall slot ovens which operate under a nonoxidizing atmosphere. A small positive pressure within the oven prevents air ingress and subsequent combustion of the volatile matter that is produced. Ovens typically range in height from 4 up to 8 m in the most modern plants. In Fig. 55.5, the horizontal cross section between two adjacent slot ovens shows the coal charge and heating flue arrangements. Note that the ovens are tapered to facilitate pushing of the coke from each oven as the heating cycle is complete.

In a by-product coke plant, the slot ovens are arranged in rows on either side of a coal storage bunker as shown in Fig. 55.6.

A symmetrical arrangement is preferred with 20–40 slot ovens on each side of a central coal bunker. Ground and blended coal is charged into the charge car, the car positions itself over the empty oven and coal is gravity fed typically through four charge holes located in the oven roof (Fig. 55.7).

After the coking cycle, typically 18–20 hours, is complete, the coke is pushed from the ovens into a quench car. The hot coke is water quenched, cooled, screened, and shipped to the blast furnace. The main steps are presented in Fig. 55.8.

The coke oven battery is a complex refractory structure with charge cars traveling on top, the slot oven itself, adjacent combustion flues, and below this a refractory regenerator where waste heat is recovered and used to preheat combustion air. The firing cycle is periodically reversed every 20–30 minutes, alternating the combustion air and fuel gas flues. This allows combustion air to be preheated by hot refractory in the refractory regenerator, and at the same time, the hot waste gas can reheat the depleted part of the regenerator. In Fig. 55.9, the complex twin flue by-product coke oven heating system construction is illustrated. This complex refractory arrangement is essential to maintain high and constant temperature profiles throughout each slot oven in the coke oven battery.

As the coke plant builders increased the slot oven height from 4 to >6 m in the 1970s, many plant failures occurred where the coke plants were damaged to the point where they were inoperable in less than 10 years. A significant factor was the wall pressure that the coal blend placed on the oven walls during coal devolatilization and its impact on the battery structure. Coke producers adopted special coal blends that produced little or no oven wall pressure. While this solved the damage with tall ovens, it further restricted the available coking coals that could be used in a coke oven blend. With the advantages that taller ovens

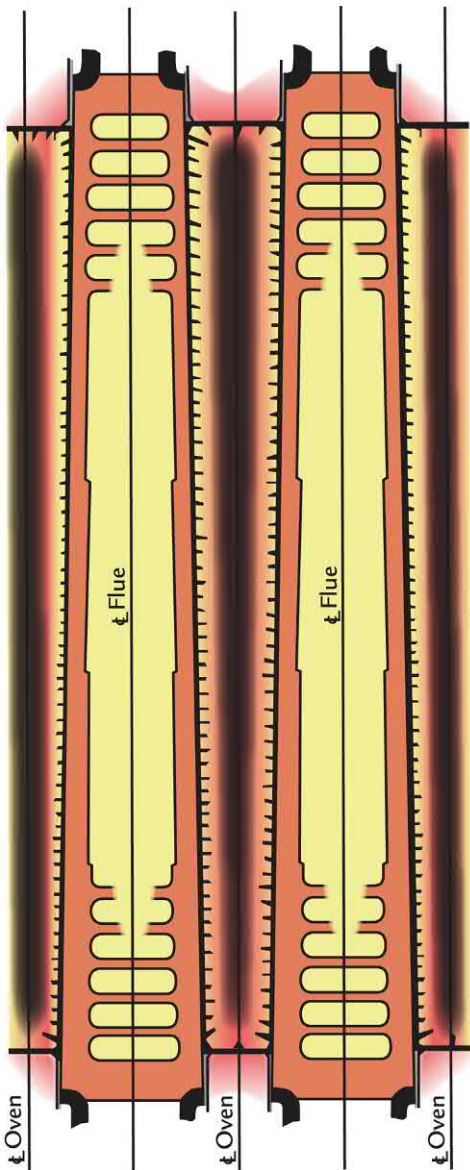


FIGURE 55.5 Horizontal cross section through a by-product slot oven.³

provide in terms of cost, productivity, and environmental performance, oven builders developed the technology to build to 7–8 m in oven chamber height in the late 1990s.

One of the main environmental concerns with by-product coke ovens is dust and gaseous emissions which occur at the coke oven closure surfaces and in the by-product plant. When coal is charged, fine coal dust can easily be released to the atmosphere depending on the available systems to mitigate coal leakage. When the oven doors are opened to push the coke, the hot coke is exposed to air and can combust and produce emissions.

Gases emitted from the ovens are known sources of carcinogenic polycyclic aromatic hydrocarbons and benzol/benzene compounds. If the coking cycle is not complete and the coke is “green,” emissions quickly increase as the volatile gases present combust with the ambient air. Taller ovens allow greater amounts of coke to be produced per oven therefore minimizing the number of charges and pushes and related emissions to make the needed tonnage.

Volatile gases evolved during the coking process flow through a refractory lined collector main and are refined in a downstream chemical plant to produce coke oven gas (COG), a valuable in-plant fuel, and other by-product chemicals. The main by-products to be removed are tar, sulfur, ammonia, and light oils (benzene, toluene, and xylene). Tar is first condensed in the primary cooler using flushing liquor, a condensate collected as the raw COG cools in the collector main. The product tar is then separated from the flushing liquor in a tar decanter, and the flushing liquor is treated in a wastewater treatment plant. The gas is further treated to remove sulfur, ammonium by-products and light oils using various unit operation arrangements as presented in Fig. 55.10.

A by-product coke plant is a key energy supplier to the balance of the integrated steel plant. The cleaned COG is boosted in pressure for use around the steel plant as a heating fuel



FIGURE 55.6 View of the pusher side of a typical 6-m by-product coke oven battery. Note that the coal storage bunker is in the background at the top of the inclined conveyor. *Source: Photograph courtesy of thyssenkrupp Industrial Solutions AG.*



FIGURE 55.7 View of the coke plant roof showing the stand pipes where gases are collected from each oven, the rail mounted charge car used to top charge coal to each oven through four charge holes. *Source: Photograph courtesy of thyssenkrupp Industrial Solutions AG.*

or for power generation. Part of the cleaned COG is returned to the coke ovens as an underfiring fuel. A gas holder can be used as a storage buffer to minimize losses of COG

when supply and demand do not match. A typical energy distribution showing the importance of COG in an integrated steel plant is provided in [Fig. 55.11](#).

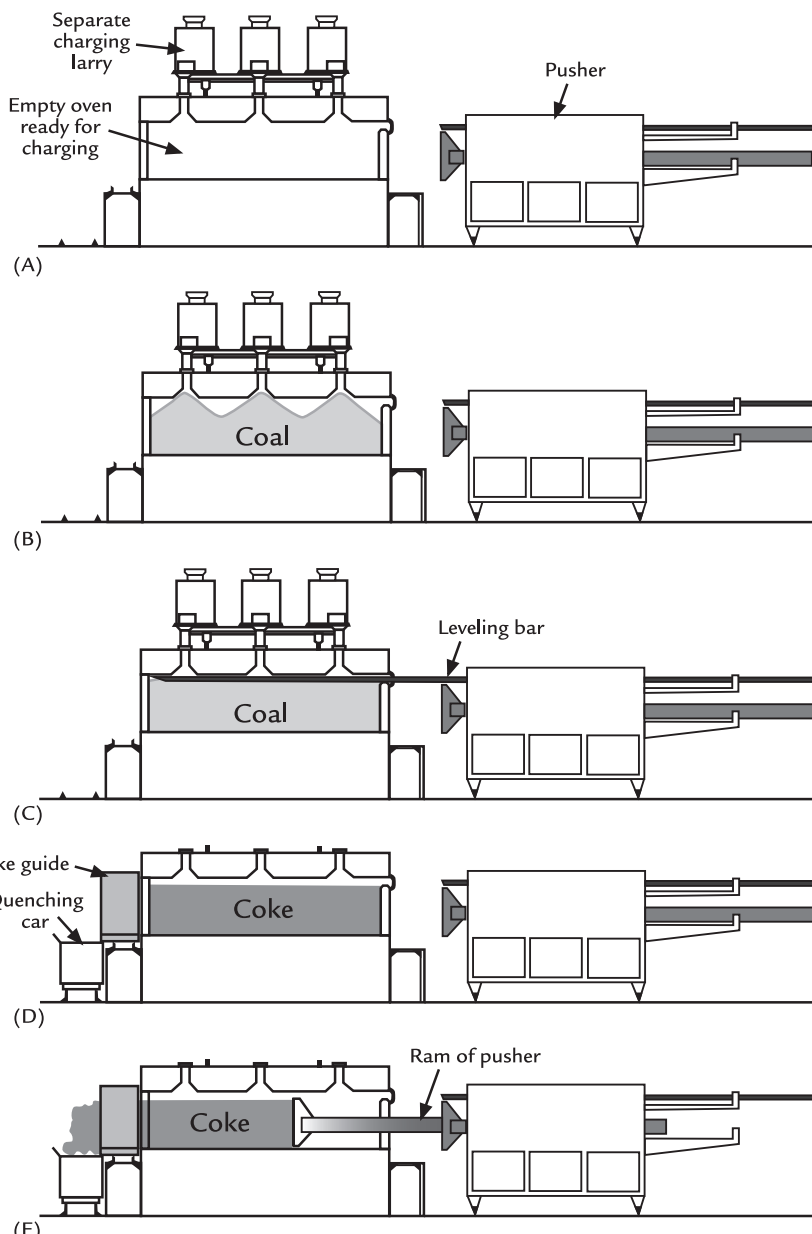


FIGURE 55.8 Sequence of operations for producing metallurgical coke in a by-product slot oven.

- (A) The charging larry car, with hoppers containing measured amounts of coal, is in position over charging holes from which covers have been removed. The pusher car is moved into position.
- (B) The coal from the larry car hoppers is dropped into the oven chamber, forming piles.
- (C) The leveling door at the top of the oven door on the pusher side is opened and the leveling bar on the pusher car is moved back and forth across the peaked coal piles to level them. The bar next is withdrawn from the oven, the leveling door and charging holes are closed, and coking cycle begins.
- (D) Coking of the coal originally charged into the oven has been completed (in about 18 h) and the oven is ready to be “pushed.” The oven doors are removed from each end, and the pusher, coke guide, and quenching car are moved into position.
- (E) The ram of the pusher car advances to push the incandescent coke out of the oven, through the coke guide and into the quenching car.²

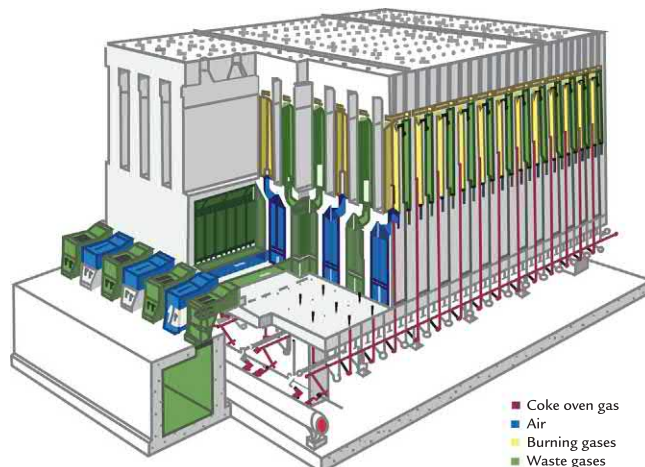


FIGURE 55.9 Cross section through a by-product coke oven battery heating system.³

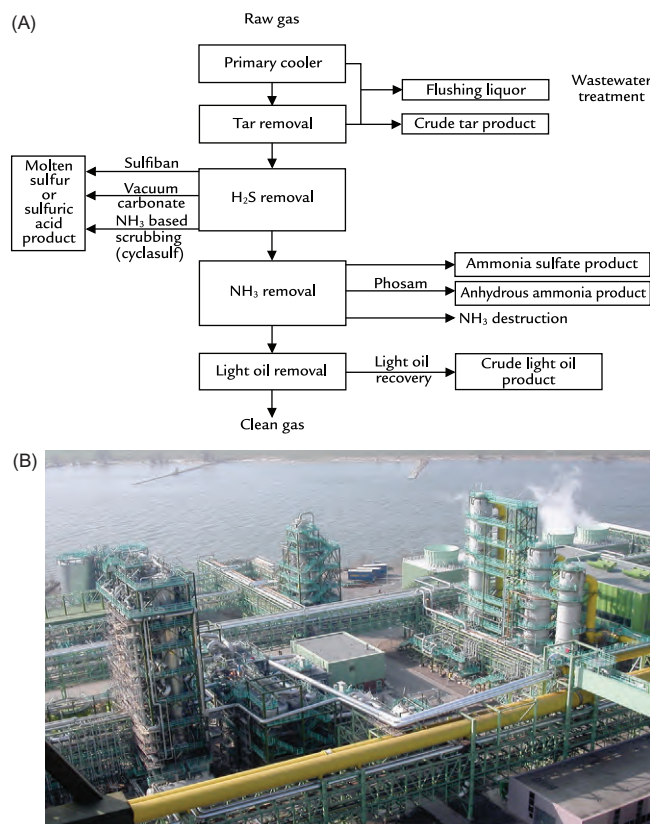


FIGURE 55.10 (A) Typical by-product plant block flow diagram. (B) Photograph of a coke oven gas cleaning plant. Source: (B) Photograph courtesy of thyssenkrupp Industrial Solutions AG.

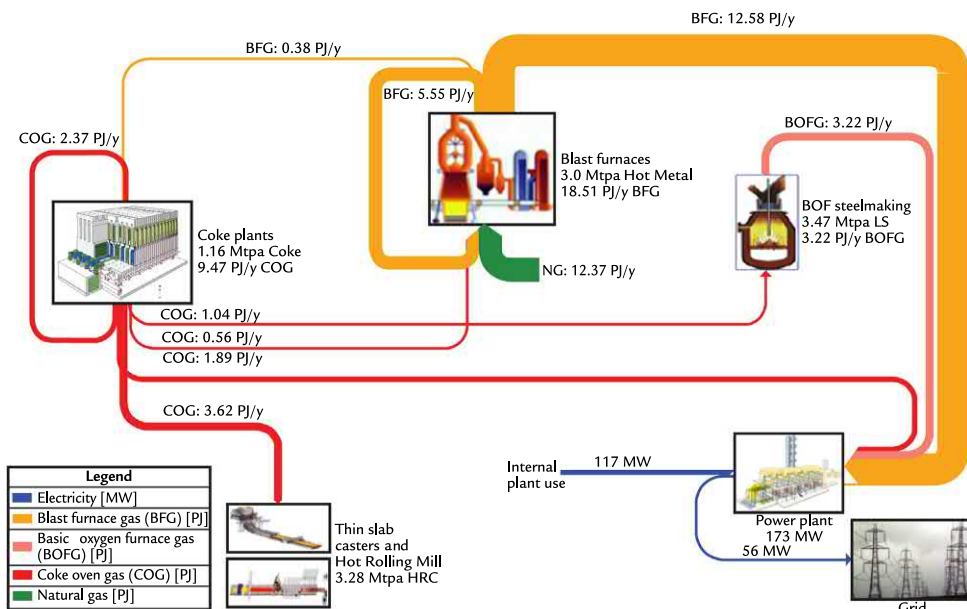


FIGURE 55.11 Energy distribution in 3.3 Mt/year steel plant (PJ/year indicates peta (10^{15}) joules per year).⁴

55.5 HEAT-RECOVERY COKEMAKING

In heat-recovery (HR) cokemaking, all the volatile matter in the charged coal is burned within each oven to provide the heat required for the cokemaking process. Excess heat is used to generate steam and electrical power. HR coke ovens are low-height, horizontal ovens operating under negative pressure. The ovens are charged by conveyor belts using a special charging machine. In some cases, the coal is mechanically stamped in a steel frame to increase coal density and then the stamped coal cake is carefully pushed into the coke oven. Stamp charging and the resulting coal densification can allow the use of marginal coking coals and still meet the quality requirements of the product coke.

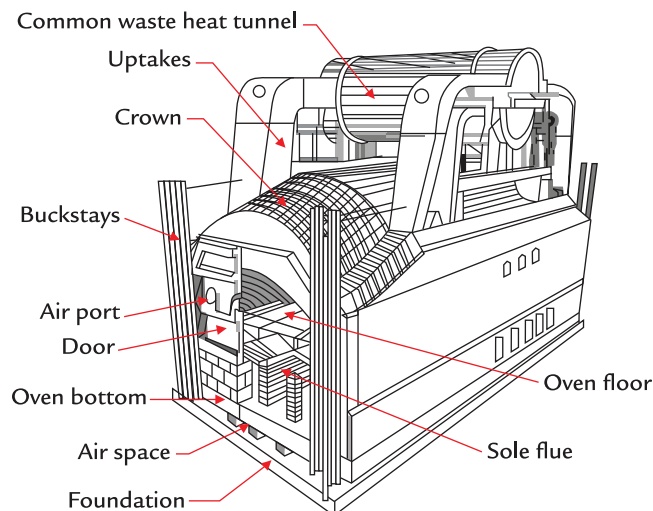
HR plants were developed by SunCoke Energy (United States), SinoSteel (China), Sesa Goa (India), and thyssenkrupp Industrial Solutions (Germany). Some coking plants build HR ovens with in-house knowledge, such as Shanxi Sanjia in China and Bla in India. The differences between the main processes is provided in Table 55.1.

All HR coke plants operate under similar principles. SunCoke Energy is the most successful developer and has six coke plants operating in the United States and Brazil. Details of the SunCoke technology are described below to illustrate the HR coke plant technology.

In the 1960s, the Jewell Coal and Coke Company, a predecessor of SunCoke Energy, developed an oven design that has matured and is deployed by SunCoke at its commercial coking plants. A schematic of a Jewell-Thompson oven is provided in Fig. 55.12.

TABLE 55.1 Comparison of the Different Heat-Recovery Technologies

Process	Charge Preparation	Charge	Refractory	Discharge	Typical Oven Dimensions (m)
SunCoke	Standard	Horizontal	Silica	Push onto wagon	3.7 × 14
SinoSteel	Stamp charged	Top		Fall into wagon	
SESA Goa	Standard	Top	Alumina	Fall into wagon	2.7 × 10.7
	Stamp charged	Horizontal			
thyssenkrupp Industrial Solutions	Stamp charged	Horizontal	Silica	Push onto wagon	3.7 × 15
Shanxi Sanjia SJ-96	Added to a cold oven	Manual	Alumina	Cool oven and manual remove	3 × 23

FIGURE 55.12 Schematic view of a Jewell-Thompson coke oven.²

The coke oven is horizontal and operates under negative pressure. Charged coal is carbonized to coke in two ways. Direct heating via the substoichiometric combustion of volatiles within the coking chamber itself and conductive heat transfer via the combustion of excess COG within sole flues arranged horizontally underneath the oven floor. Fig. 55.13 details the cross section through a HR oven and zones where primary and secondary combustion occur.

Primary combustion air is introduced through ports in the oven doors which partially combusts the volatiles in the oven chamber. Secondary air is introduced into the sole flues which run in a serpentine fashion under the coal bed. The design of the flues and the control of the air flow allow the coking rate at the top and bottom of the coal bed to be equalized. With the temperatures generated, all hydrocarbon compounds that evolve from the coal are incinerated within the oven. Hot

waste gas passes through a waste gas tunnel to HR steam generators (HRSGs). High pressure steam is produced and can be used to generate electricity, power steam-driven motors, or in some situations sold to external customers

who are close by. After the HRSGs, the cool waste gas is desulfurized and filtered prior to being discharged to atmosphere. A typical SunCoke plant arrangement is presented in Fig. 55.14.

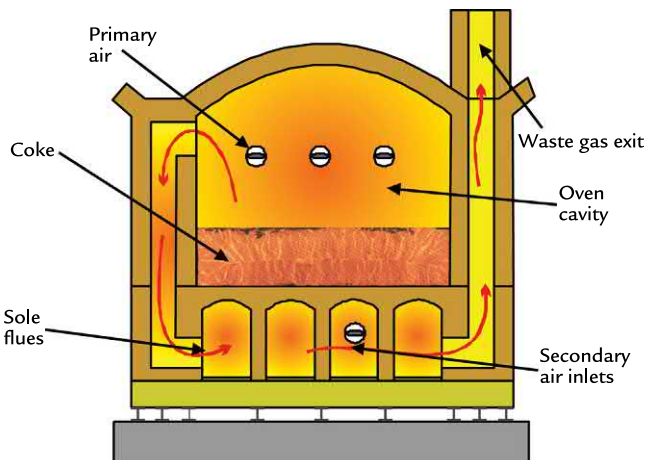


FIGURE 55.13 Cross section through a heat-recovery coke oven.³

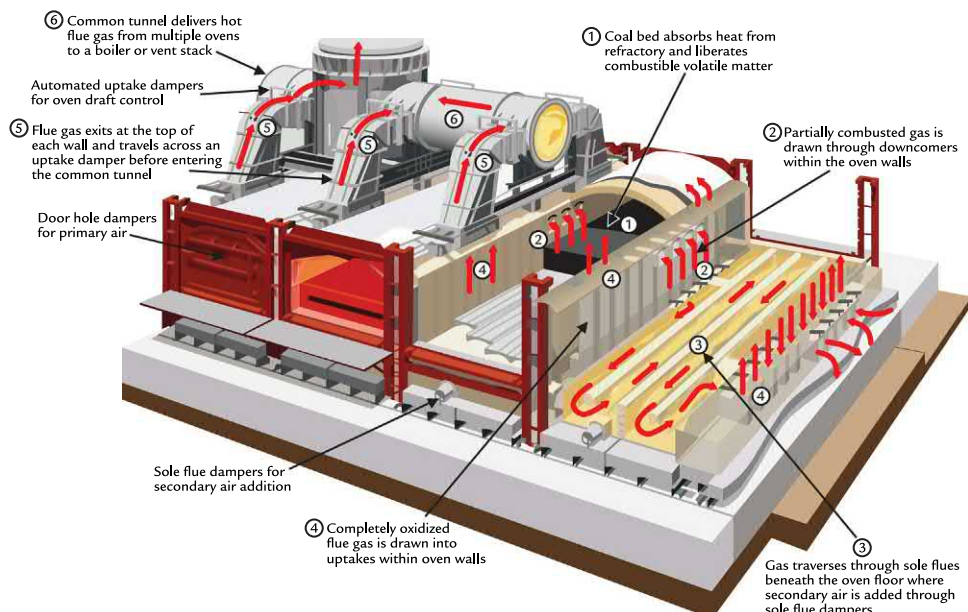


FIGURE 55.14 Schematic of SunCoke Energy heat-recovery coke oven plant. Source: Schematic courtesy of SunCoke Energy Inc.

Compared to a by-product coke plant, a HR coke plant produces better quality coke using a similar coal blend. The improved qualities include a higher CSR, higher American Society of Testing and Materials (ASTM) stability, and larger average coke size. These improvements in coke quality effectively reduce the blast furnace coke rate and total carbon consumption. In the opposite direction, the coke yield from a HR coke plant is 1.5–2.0% lower than a by-product plant due to carbon burnt within each oven. The HR coke plant can use a wider variety of coals including noncoking, semicoking coals and coal blends that develop a high coking pressure when carbonized.

HR cokemaking is a proven, mature technology able to consistently produce high-quality coke. SunCoke Energy coke plants are considered best available technology by the US Environmental Protection Agency due to negative pressure aspects of the oven operation.

55.6 BLAST FURNACE COKE QUALITY REQUIREMENTS

Blast furnace metallurgical coke has many quality requirements to maximize blast furnace performance. Quality properties have been continuously evolving as the blast furnace operators work to use decreasing amounts of coke in their fuel mix. High-quality coke provides the following essential functions in blast furnace operations.

55.6.1 Chemical Composition

Coke should be low in ash, sulfur, phosphorous, and alkali (K, Na) content. Typical limits are provided in Table 55.2.

55.6.2 Cold Strength

Strong coke is needed to support the tall and heavy column of raw materials present in

the blast furnace without being crushed. The coke must resist abrasion as well as crushing. Several cold crushing strength tests are available and are used in different regions of the world to measure the cold strength of coke. When designing a coal blend, one of the first objectives is to obtain a cold strength per the nominated measurement system as described in Table 55.3.

TABLE 55.2 Typical Metallurgical Coke Chemical Requirements

Item	Analysis (Dry Basis) (%)
Fixed carbon	86–90
Ash	8–12
Volatile matter	<0.5
Sulfur	<0.6
Alkali (K_2O and Na_2O)	<0.2
Moisture	<4

TABLE 55.3 Coke Strength Test Indices

System	Region Used	Measurement	Typical Value
ASTM	North America	ASTM stability	> 60
Micum	Germany	M10 (Hardness)	< 6
		M40 (Strength)	> 85
IRSID	France	I10 (Hardness)	< 20
		I40 (Strength)	> 50
	Japan, Korea, Taiwan, and China	JIS DI 30/15	> 90
Japanese Tumble Test (JIS)			

ASTM, American Society of Testing and Materials.

55.6.3 Coke Size

Well-sized coke provides permeability that is essential to allow gases to travel upward with minimal channeling and for liquid iron and slag to drain to the blast furnace hearth and not impede gas flow. Blast furnace coke may be screened at the coke plant and/or at the blast furnace stockhouse to generate three coke size fractions as described in **Table 55.4**.

Due to the nature of the coking process, oven produced coke has many fissures when it is formed. The coke will break along these fissures as it is handled prior to charging to the blast furnace; this process is known as stabilization. The stabilization process continues in the blast furnace stack as the coke experiences increasing forces as it descends to the tuyere and hearth zones. Comparing blast furnace performance from locally produced and purchased coke can provide different results. Local coke will appear larger based on sampling; however, the purchased coke is more stabilized and will experience less degradation and size reduction in the blast furnace stack. Blast furnace performance may be similar despite the smaller size purchased coke charged to the blast furnace top.

TABLE 55.4 Coke Size Charged to the Blast Furnace

Size Fraction	Size Requirements (mm)	Usage
Blast furnace coke	Mean size 50–60 Minimum >25	Principle coke charged to the blast furnace
Nut coke	6–25	Added with the ferrous mineral layer
Coke breeze	<6	Used as fuel in sintering or pelletizing plants

55.6.4 Properties at Elevated Temperatures

Coke remains strong and granular all the way to the bottom of the blast furnace. This is important for liquid drainage, gas flow, and burden movement. To better understand the elevated temperature performance and resistance to chemical attack by CO₂, Nippon Steel developed two important tests; the Coke Reactivity Index (CRI) and the Coke Strength after Reaction (CSR).

In the coke reactivity test, a coke sample is exposed to pure CO₂ at elevated temperature (1100°C), and the loss in mass is measured to determine the amount of coke degraded by the CO₂ and hence the CRI index. Coke loss depends on the coal blend used and ash components present. Some ash components will catalyze the CO₂ attack on the coke carbon structure and accelerate the coke degradation in the lower part of the blast furnace.

As the coke structure is attacked by CO₂, the coke is weakened and loses its mechanical strength. To measure this, following the CRI test, the coke sample is tumble tested to assess the loss in strength. This provides the CSR index based on the +10 mm fraction after 600 revolutions. The CSR index has become popular to understand the blast furnace performance especially as greater amounts of injected fuel are employed and coke residence time in the blast furnace increases significantly. A high CSR is required for very large blast furnaces with more than 3000 m³ working volume where hearth drainage concerns become more acute.

Poor CRI/CSR properties can only be significantly improved by changing the coal blend to reduce the catalytic effect of the basic oxides (Fe, Ca, Mg, K, Na) present in the coal ash. Such a change can be hard to realize, and in many cases, a substantial amount of coal, often

as much as half of the coal blend, must be replaced to eliminate the undesirable coal ash components. A large amount of imported coal may be required at great cost and expensive logistics, especially for an inland blast furnace plant.

55.6.5 Consistency

Coke present in the hearth can only leave the blast furnace through consumption at the tuyeres or by dissolving into the hot metal. Inferior quality coke can cripple a blast furnace operation and create fines that report to the center of the hearth zone, an area known as the deadman. This decreases the deadman's permeability to liquid iron and slag flow, increasing peripheral flow and related heat load on the hearth walls. When using a blend of owner produced coke and purchased coke, the blast furnace operator must apply a high standard to the purchased coke to assure a healthy hearth and permeability to liquid iron and slag flow. Variable coke supplies can lead to long-term blast furnace underperformance and remedying this is a slow process due to the long time to remove coke fines from the blast furnace hearth and deadman zones.

55.6.6 Coke Quality Requirements

Many European blast furnaces operate with very low coke rates, high injected coal rates, and high productivity. Blast furnace size ranges from medium size ($2000\text{--}3000\text{ m}^3$ working volume) to very large blast furnaces with $>4000\text{ m}^3$ working volume. The European operators have refined the coke requirements and their quality standards are provided in [Table 55.5](#).

Operators who wish to match the European blast furnace operational performance, especially coke rates $<280\text{ kg/t HM}$, are changing

TABLE 55.5 European Blast Furnace Coke Quality Standards⁵

Quality Parameter	Unit	Requirement
PHYSICAL PROPERTIES		
CSR	% > 10 mm	> 65
CRI	%	< 23
I40 (Strength)	% > 40 mm	> 57
I10 (Hardness)	% < 10 mm	< 18
CHEMICAL PROPERTIES		
Ash	mass%, dry	< 9.0
S	mass%, dry	< 0.7
P	mass%, dry	≤ 0.025
Alkalies	mass%, dry	< 0.2
Moisture	mass%	< 5.0
SIZE FRACTION		
<10 mm	%	< 3
<40 mm	%	< 18
>80 mm	%	< 10
>100 mm	%	0

CSR, Coke strength after reaction; CRI, coke reactivity index.

their coking processes to increase coke quality, especially the elevated temperature properties such as CSR. Coal selection is the most important prerequisite to achieve such quality as well as disciplined coke battery maintenance and operations.

55.7 SUMMARY

Coke is essential to blast furnace operations. When introduced in the late 1800s, blast furnace size and productivity quickly advanced. Quality coke is made from a blend of special coking coals that, when heated, will fuse to provide the strong coke quality

needed in blast furnace operations. Most global coke is produced in by-product slot ovens where the volatile hydrocarbon gases are collected and refined for sale as various chemicals. Heat recovery ovens where the hydrocarbon gases are completely combusted to produce steam and electricity are emerging due to their improved environmental performance and ability to use a greater number of metallurgical coals in the coal blend. Metallurgical coke must meet a wide range of quality specifications to assure the lowest coke rate. These quality standards, especially strength at elevated temperatures, are increasing as greater amounts of less expensive pulverized coal is injected through the blast furnace tuyeres.

EXERCISES

- 55.1.** Coke has three main roles in the blast furnace process. These are (*please circle*):
- to produce heat for the process
 - to reduce the iron oxides
 - to maintain the structural integrity of the charge column
 - to heat the charge
 - to produce reducing gas
- 55.2.** The quality of the coke can affect the coke rate. Please circle those qualities which reduce the coke rate:
- Lower ash content
 - Higher ash content
 - Lower stability
 - Higher CSR
 - Low coke moisture content
 - High coke moisture content
- 55.3.** Coke quality and coal injection. Please circle if the following statements are true or false:

T	F	With coal injection, coke is subject to a shorter residence time and increased gas attack.
T	F	Degraded, weak coke accumulates in the bird's nest in front of each tuyere.
T	F	Coke needs to be more reactive when injecting coal.
T	F	Weak, degraded hearth coke directs the liquid flow toward the furnace center, resulting in high hearth temperatures.

- 55.4.** The important characteristic that is common to all blast furnace zones is _____ and this is provided primarily by _____.

Please write in the letter of the correct answer from the following list:

- coke
- strong, large coke with minimal fines
- hot, fluid slag
- permeability
- good gas flow

References

- Steel Raw Materials Monthly, prepared from May 2014 to May 2018 monthly reports, Platts, the McGraw-Hill Companies, www.platts.com
- Sundholm JL et al., Manufacture of metallurgical coke and recovery of Coal Chemicals. In: *Chapter 7, The making, shaping and treating of steel*, 11th ed. Association of Iron and Steel Engineers; 1999. pp. 381–546.
- Towsey PS, Cameron I, Gordon Y. *Comparison of Byproduct and Heat-Recovery Cokemaking Technologies*. Pittsburgh, PA: AISTech; 2010. p. 333–43. Association of Iron & Steel Technology.
- Patel N, Cameron I, Gordon Y. *Strategies for Implementing Direct Reduction Technologies in an Integrated Steel Plant*. Cleveland, OH: AISTech; 2015. p. 345–55. Association of Iron & Steel Technology, 2015.
- Luenigen HB, Peters M, Schmoele P. *Ironmaking in Western Europe – Status Quo and Future Trends*. Cleveland, OH: AISTech; 2015. p. 1481–90. Association of Iron & Steel Technology, 2015.

Blast Furnace Fuel Injection

O U T L I N E

56.1 What is Fuel Injection and Why Is It Important?	574	56.6.1 Coal Selection and Coke Replacement	583
56.2 Principles of Fuel Injection	575	56.6.2 Coal Grinding	585
56.3 Controlling the Injected Fuel Rate	577	56.6.3 Coal Injection System Design and Equipment	587
56.3.1 Step 1—Estimate Oxygen Removed for Reduction and Slag Reactions Per Ton Hot Metal	579	56.6.4 PCI Summary	591
56.3.2 Step 2 - Calculate the Top Gas Volume and Makeup	579	56.7 Natural Gas Injection	592
56.3.3 Step 3 - Calculate the Input Oxygen from Blast	579	56.7.1 Coke Oven Gas Injection	593
56.3.4 Step 4 - Calculate the Instantaneous Production Rate	579	56.8 Coal and Natural Gas Injection	593
56.4 Using Fuel Injection to Control the Hot Metal Thermal State	580	56.9 Oil and Tar Injection	594
56.5 Coke Residence Time and Quality Requirements	581	56.10 Impact of Injected Fuels on the Blast Furnace Operation	595
56.6 Pulverized Coal Injection (PCI)	582	56.10.1 Maximizing Injected Fuel Usage	595
		56.10.2 Operating Windows to Maximize Fuel Injection	596
		56.11 Summary	597
		Exercises	598
		References	599

56.1 WHAT IS FUEL INJECTION AND WHY IS IT IMPORTANT?

As blast furnace ironmaking evolved in the 1950 and 1960s, hot blast stove technology improved and blast air temperature increased significantly during this period from about 550 to 1000°C. After this, additional stove improvements were implemented to increase blast temperature to 1100–1200°C. The newest stove designs have demonstrated performance at 1300°C.

As the blast and tuyere flame temperatures increased, blast furnace operators had operational problems related to poor melting properties of the ferrous burden materials of the day, mostly high gangue sinter and lump ores, which led to irregular burden descent, hanging, and slipping of the charge materials. The higher blast temperature allowed for steam injection to improve burden descent by increasing the bosh zone hydrogen content. A downside to this approach was an increase in coke consumption to gasify the steam into H₂ and CO gases.

Fuel injection was developed to control the tuyere flame temperature, provide additional hydrogen in the bosh zone to facilitate iron ore

reduction, and to reduce coke consumption. Systems to inject a wide variety of hydrocarbons were developed, the most popular to remain are the injection of pulverized coal and/or natural gas. Oil injection, one of the first auxiliary fuel systems to be developed into commercial practice, has largely been replaced due to the excessive cost of oil compared to the alternative fuels. The injection of other low-cost hydrocarbons continues and includes fuels such as coke oven gas, coke oven tar and tar derivatives, discard motor oil, and waste plastic. The evolution of fuel usage in Germany and implementation of important improvement technologies from 1950 to 2015 is provided in Fig. 56.1.¹

Since the 1990s, blast furnace operators have systematically increased the amount of oxygen enrichment and injected fuel to both reduce coke consumption and increase blast furnace output. Great gains have been achieved in both output and fuel rate improvements. Today's leading blast furnace operators have reduced coke consumption to about 275–290 kg/t HM.¹ In these operations, 220–230 kg/t HM of pulverized coal is injected to reach the typical fuel rate of 500 kg/t HM, representing about 45% of the fuel input. The coal injection

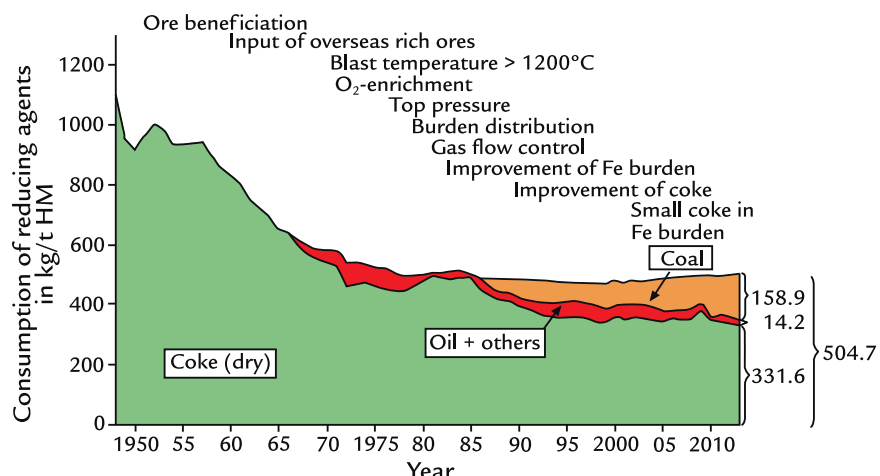


FIGURE 56.1 Reductant consumption for German blast furnaces since 1950.¹

is supported by oxygen injection rates of 30–34% O₂(g) in the blast air to sustain the raceway flame temperature.

56.2 PRINCIPLES OF FUEL INJECTION

Fuel injection was first introduced to control the raceway adiabatic flame temperature (RAFT). Blast furnace operators learned through experience that the furnace operates best in a narrow RAFT range, typically from 2000°C to 2200°C, due in-part to the smelting characteristics of the ferrous charge materials. The RAFT can be calculated by a heat balance of the tuyere conditions as presented in this book but more frequently, empirical equations are used to quickly understand the RAFT. Eq. (56.1) is the American Iron and Steel Institute RAFT formula commonly used in North America; the equation illustrates the impact of various fuels on the tuyere raceway temperature²:

$$\begin{aligned} \text{RAFT} = & 1474 + 0.82 * (\text{BT} + 17.78) + 52.8 * \text{OE} - 5.71 * \text{BM} \\ & - 4.3 * \text{Oil} - 2.8 * \text{Tar} - 2.08 * \text{Coal} \\ & - 483 * \text{HW} - 389 * \text{AS} \\ & - (37.8 + 0.507 * \text{GHV}) * \text{NG} * 100 \end{aligned} \quad (56.1)$$

where

- RAFT is the raceway adiabatic flame temperature, °C
- BT is the blast temperature, °C
- OE is the oxygen enrichment (%O₂ – 21)
- BM is the blast moisture, g/Nm³ dry blast
- Oil is the dry oil injected, g/Nm³ dry blast
- Tar is the dry tar injected, g/Nm³ dry blast
- Coal is the dry coal injected, g/Nm³ dry blast
- HW is the homogenizing water, kg/kg dry oil or kg/kg dry tar
- AS is the atomizing steam, kg/kg dry oil or kg/kg dry tar
- NG is the natural gas injected, Nm³/Nm³ dry blast

- GHV is the natural gas gross heating value in MJ/Nm³.

Eq. (56.1) can be simplified by ignoring oil and tar injection and hence atomizing steam and homogenizing water that are used to inject oil and tar. A further simplification can be made by assuming 37.3 MJ/Nm³ as a gross heating value for natural gas. Eq. (56.1) can be simplified to:

$$\begin{aligned} \text{RAFT} = & 1474 + 0.8 * (\text{BT} + 17.78) + 52.8 * \text{OE} - 5.71 * \text{BM} \\ & - 2.08 * \text{Coal} - 5671 * \text{NG} \end{aligned} \quad (56.2)$$

The commonly used hydrocarbons have a broad range of hydrogen-to-carbon ratios and related heating values as illustrated in Table 56.1.

TABLE 56.1 Hydrogen-to-Carbon Ratio and Heating Values for Blast Furnace Injected Fuels

Hydrocarbon	Ratio Carbon (C)/Hydrogen (H) by Weight	Heating Value (MJ/kg Carbon)	Dissociation Energy (MJ/kg Carbon)
Natural gas	3.2	3.0	6.2
Bunker "C" oil	8.1	8.3	0.9
Tar	12.5	8.7	0.5
Bituminous coal	15.0	8.7	0.5
Coke	450	9.2	

When injecting fuels, the energy to dissociate hydrocarbon compounds is endothermic and reduces the RAFT compared to burning metallurgical coke. To illustrate this for the commonly used fuels, in Fig. 56.2 the RAFT reduction is compared to the hydrogen-to-carbon ratio for each fuel.

Of all the injected fuels, coal provides the smallest impact on the RAFT. Natural gas provides the largest decrease in RAFT due to the large amount of energy needed to crack the

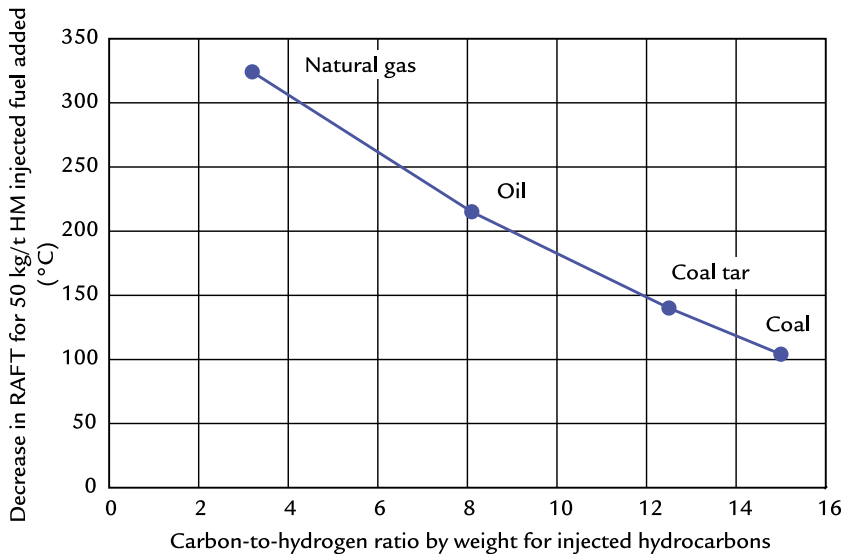


FIGURE 56.2 Impact of 50 kg/t HM injected fuel added on RAFT. RAFT, Raceway adiabatic flame temperature.

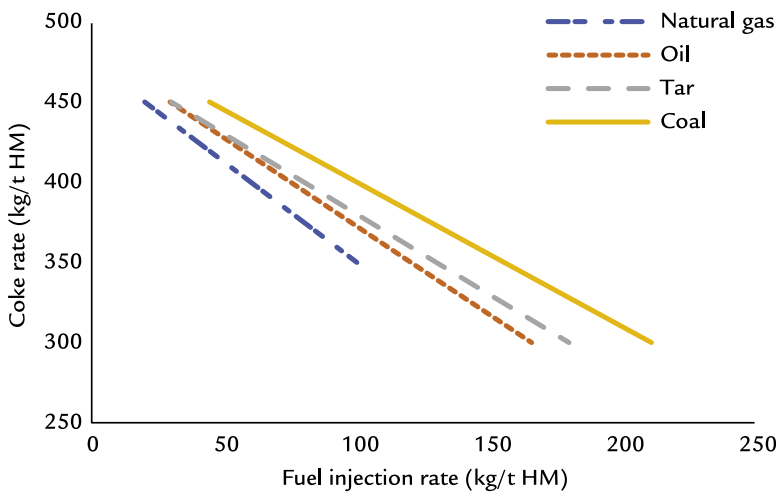


FIGURE 56.3 Typical injected fuel performance and coke rate for commonly used fuels.

methane (CH_4) bonds and reform methane into CO(g) and $\text{H}_2\text{(g)}$. In Fig. 56.3, typical injection and coke rates for the commonly used injected fuels are provided.

Blast furnace operators add oxygen to the blast air as a countermeasure to avoid a decrease of RAFT and restore RAFT to the target range of 2000–2200°C. Using Eq. (56.2), the

relative oxygen injection needed to maintain RAFT compared to coke combustion is shown in Fig. 56.4.

A large amount of oxygen enrichment is needed to support natural gas combustion compared to the other fuels. In practice, once the RAFT is controlled to the target range, injected fuel and oxygen can be increased at a

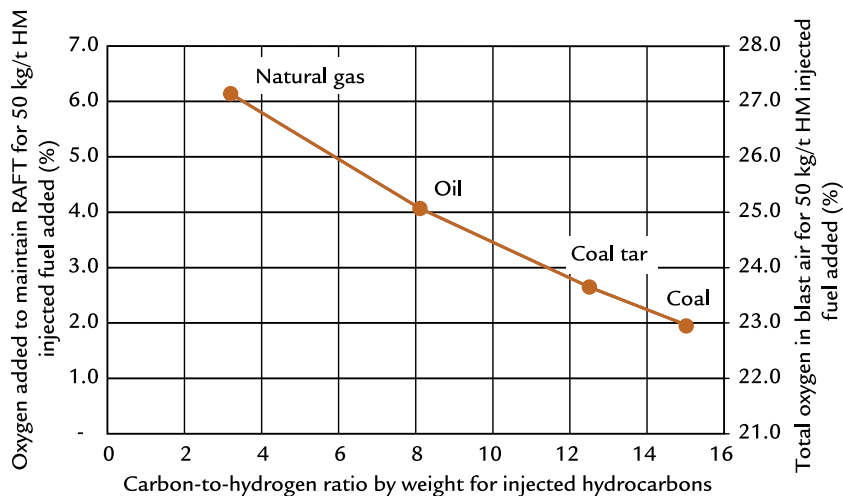


FIGURE 56.4 Relative oxygen enrichment needed to maintain RAFT for commonly injected fuels.

prescribed ratio to replace greater amounts of coke providing the top gas temperature is in an acceptable range.

Blast furnace operators that inject natural gas have historically challenged the lower limit of the acceptable RAFT range of 2000–2200°C. The additional hydrogen provided by natural gas compared to the other injectants aids in gas-based reduction of the ferrous burden. The smaller hydrogen atoms quickly diffuse into the iron ore and reduce the iron oxides to iron in the lower stack and bosh regions. More fully reduced ferrous materials are delivered to the lower regions of the furnace where the final endothermic direct reduction reactions take place.

Blast furnace operators have successfully injected natural gas with lower RAFT limits of 1850–1900°C. During the 1990s, ACME Steel in the United States successfully operated with very low flame temperatures (1600–1700°C) using substantial amounts of natural gas injection.³⁵ While the practice was not replicated, it provided confidence for blast furnace operators to challenge the previously accepted lower limit of 2000°C when injecting natural gas. A suitable lower RAFT limit must be carefully established at each blast furnace through plant trials and must consider the quality of the

ferrous burden. Adjustments to this limit may need periodic review as the ferrous charge mix is adjusted during each plant's annual procurement and material sourcing cycle.

A simple economic analysis is provided in Fig. 56.5 to illustrate the two stages of fuel injection and their economic impact.

Compared to an all coke operation, injected fuels can be added in limited amounts without oxygen enrichment before the RAFT is decreased below the minimum deemed for a safe operation. This initial stage of injection is the most cost-effective where coke consumption is decreased using the generally less expensive injected fuel. Adding oxygen extends the range of fuel injection and coke replacement but the cost benefit decreases, as seen in the inflection points of all lines in Fig. 56.5. The RAFT impact is smallest for injected coal. This allows for the greatest amount of coke replacement and supports the popularity of injected coal on a global basis.

56.3 CONTROLLING THE INJECTED FUEL RATE

A major challenge using injected fuel is to match the injected fuel rate to the fuel rate

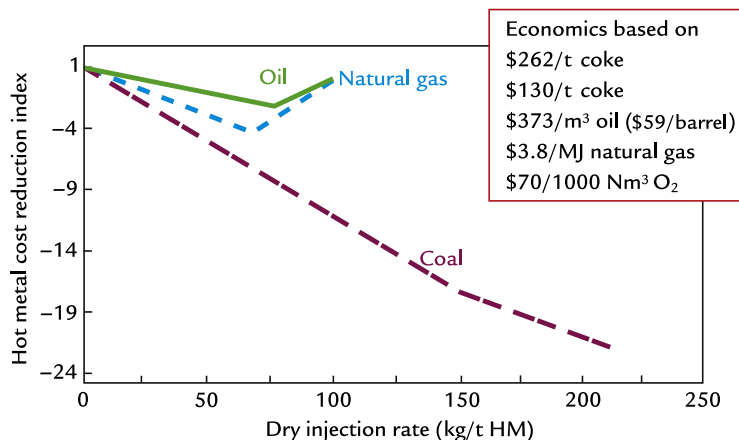


FIGURE 56.5 Cost savings using commonly injected fuels including the addition of oxygen to maintain minimum flame temperature targets for each injectant.

TABLE 56.2 Methods to Estimate Hot Metal Production Rate for Injected Fuel Rate Control

Method to Estimate Hot Metal Production Rate	Advantages	Disadvantages
From charge rate and hot metal tons per charge	<ul style="list-style-type: none"> Easy to determine charge rate 	<ul style="list-style-type: none"> Problematic when stockline is varying, for example due to slipping and hanging Does not account for changes in carbon rate due to indirect and direct reduction variations, nor changes in minor element reduction, such as %Si in hot metal
From the specific wind rate and wind volume	<ul style="list-style-type: none"> Easy to measure wind volume 	<ul style="list-style-type: none"> Specific wind rate does not reflect changes in carbon rate from changes in indirect and direct reduction, nor changes in minor element reduction, such as %Si in hot metal
Production rate estimated from the top gas analysis	<ul style="list-style-type: none"> Accurately indicates instantaneous production rate Accounts for all elements reduced and carbon/hydrogen used 	<ul style="list-style-type: none"> Requires accurate measurement of wind, injected fuel, and top gas Must be calculated by computer, too complex for a hand calculation Challenging to troubleshoot

provided from coke. The challenge is that the coke is delivered to the tuyeres on a batch basis and injected fuel on a continuous basis. To accomplish this, the production rate must be estimated and injected fuel controlled to provide the target fuel rate, expressed as kg/t HM. For the blast furnace engineer, three methods can be applied. These are compared in Table 56.2.

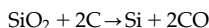
Production rate from the top gas analysis and minor element reduction is the most

complicated of methods to utilize but does allow for more rapid adjustment of the injected fuel rate to adjust to changing reduction conditions in the blast furnace. The injected fuel rate can be adjusted on shorter time intervals reflecting the actual fuel demand. The methodology to estimate the production rate from the top gas analysis is presented in the next sections.

56.3.1 Step 1—Estimate Oxygen Removed for Reduction and Slag Reactions Per Ton Hot Metal

For Si, Mn, P, and Ti present in the hot metal, oxygen removed per ton hot metal can be estimated on an atomic basis (note calculations are per tonne of hot metal, not per 1000 kg Fe in hot metal):

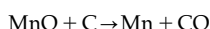
56.3.1.1 Silicon



$$\text{Kat O}_{\text{Si}} = 2 * ((\% \text{Si}/100 * 1000 \text{ kg HM/t}) / 28 \text{ kg/kmol}) \quad (56.3)$$

where Kat O_{Si} is the thousands of atoms of oxygen removed from silica (SiO₂) and %Si is the silicon content of the hot metal.

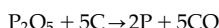
56.3.1.2 Manganese



$$\text{Kat O}_{\text{Mn}} = (\% \text{Mn}/100 * 1000 \text{ kg HM/t}) / 55 \text{ kg/kmol} \quad (56.4)$$

where Kat O_{Mn} is the thousands of atoms of oxygen removed from manganese ore (MnO) and %Mn is the manganese content of the hot metal.

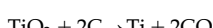
56.3.1.3 Phosphorous



$$\text{Kat O}_P = 2.5 * ((\% \text{P}/100 * 1000 \text{ kg/t HM}) / 31 \text{ kg/kmol}) \quad (56.5)$$

where Kat O_P is the thousands of atoms of oxygen removed from phosphorous in ore expressed as diphosphorus pentoxide (P₂O₅) and %P is the phosphorous content of the hot metal.

56.3.1.4 Titanium



$$\text{Kat O}_{\text{Ti}} = 2 * ((\% \text{Ti}/100 * 1000 \text{ kg/t HM}) / 48 \text{ kg/kmol}) \quad (56.6)$$

where Kat O_{Ti} is the thousands of atoms of oxygen removed from titania in ore expressed as TiO₂ and %Ti is the titanium content of the hot metal.

56.3.1.5 Iron

$$\begin{aligned} \text{Kat O}_{\text{Fe}} &= [(100 - \% \text{Si} - \% \text{Mn} - \% \text{P} - \% \text{Ti} - \% \text{C}) / 100 \\ &\quad * 1,000 \text{ kg HM/t}] * \text{O/Fe}_{\text{Charge}} / 55.8 \text{ kg/kmol} \end{aligned} \quad (56.7)$$

where:

- Kat O_{Fe} is the thousands of atoms of oxygen removed from the iron bearing minerals in the burden
- %Si is the silicon content of the hot metal
- %Mn is the manganese content of the hot metal
- %P is the phosphorous content of the hot metal
- %Ti is the titanium content of the hot metal
- %C is the carbon content of the hot metal; use either the measured value, 4.67%, or calculate %C from a thermodynamic correlation
- O/Fe_{Charge} is the charge oxygen-to-iron ratio determined for the charge materials, typically 1.49.

$$\begin{aligned} &\text{Total oxygen removed per ton hot metal} \\ &= \text{Kat O}_{\text{Si}} + \text{Kat O}_{\text{Mn}} + \text{Kat O}_P + \text{Kat O}_{\text{Ti}} + \text{Kat O}_{\text{Fe}} \end{aligned} \quad (56.8)$$

56.3.2 Step 2 - Calculate the Top Gas Volume and Makeup

The top gas volume is calculated from the blast furnace nitrogen balance, see [Tables 56.3 and 56.4](#).

56.3.3 Step 3 - Calculate the Input Oxygen from Blast

The oxygen input from blast is calculated in [Table 56.5](#).

56.3.4 Step 4 - Calculate the Instantaneous Production Rate

Calculate the oxygen removed by the blast furnace from Eq. [\(56.11\)](#) and O₂ input from above:

TABLE 56.3 Nitrogen Input Calculation

Nitrogen Input (kmol N ₂ /min)	Equation
N ₂ from blast air	= (Wind/60) *%N ₂ /100/22.4 Nm ³ /kmol = (Wind/60) *79.1/100/22.4 Nm ³ /kmol = Wind/1700
N ₂ from coal	= (Injection rate/60) *%N ₂ /100/mw N ₂ = (Injection rate/60) *%N ₂ /100/28 kg/kmol = Injection rate *%N ₂ /168,000 kg/kmol
N ₂ from injection	= (N ₂ inj. rate/60)/22.4 Nm ³ /kmol = (N ₂ inj. rate)/1344 Nm ³ /kmol
N ₂ from coke	Ignore due to small impact on calculation
N ₂ for cooling the bell-less top	= (N ₂ rate top/60)/22.4 Nm ³ /kmol = (N ₂ rate top)/1344 Nm ³ /kmol
Total N ₂ input	Sum of above

Wind is the blast rate in Nm³/h, injection rate is the coal injection rate in tonne/h, N₂ inj. rate is the nitrogen used to inject pulverized coal in Nm³/h, and N₂ rate top is the nitrogen cooling for the bell less top in Nm³/h.

$$\% \text{ Nitrogen in dry top gas} = (100 - \% \text{CO} - \% \text{CO}_2 - \% \text{H}_2) \quad (56.9)$$

$$\text{Top gas volume (TGV)} = \frac{(\text{Total N}_2 \text{ input} * 22.4 \text{ Nm}^3/\text{kmol})}{(\% \text{Nitrogen in top gas})} \quad (56.10)$$

$$\begin{aligned} &\text{Removed oxygen per minute} \\ &= \text{Total oxygen leaving in top gas} \\ &- \text{total oxygen input} \end{aligned} \quad (56.12)$$

Compare oxygen removed per minute [Eq. (56.11) and Table 56.5] to oxygen removed per ton hot metal [Eq. (56.8)].

$$\text{Production} = \frac{\text{Removed oxygen per minute}}{\text{Total oxygen removed per ton hot metal}} \quad (56.13)$$

With the instantaneous production rate in hand, the injected fuel rate can be adjusted to the aim rate expressed in kg/t HM. The injection rate can be adjusted each 15 minutes based on calculating the instantaneous production rate every 5 minutes.

56.4 USING FUEL INJECTION TO CONTROL THE HOT METAL THERMAL STATE

Fuel injection is a valuable tool to control the energy input to the blast furnace on a more rapid basis compared to ore-to-coke ratio changes. Using a combination of rules of thumb, statistical methods, and/or heat and mass balance calculations, the blast furnace engineer can estimate a fuel shortfall/surplus. Once this deviation from the set point has been estimated, the injected fuel rate can be changed to either

TABLE 56.4 Top Gas Composition

Item	Analysis (%)	Volume (Nm ³ /min)	Molar Flow (kmol/min)
H ₂	%H ₂ measured	= TGV *%H ₂ /100	KatH = 2*(TGV*%H ₂ /100/22.4 Nm ³ /kmol) As H not H ₂
Hred	Estimate of Hred to H ₂ O for production calculation		Hred = KatH *hydrogen utilization/(100 – hydrogen utilization) As H not H ₂
CO	%CO measured	= TGV *%CO/100	COmol = TGV*%CO/100/22.4 Nm ³ /kmol
CO ₂	% CO ₂ measured	= TGV *%CO ₂ /100	CO ₂ mol = TGV*%CO ₂ /100/22.4 Nm ³ /kmol
N ₂	% N ₂ calculated above	= TGV *%N ₂ /100	N ₂ mol = total N ₂ input (above)

TGV is the top gas volume, hydrogen utilization is the (hydrogen input – hydrogen in top gas)/hydrogen input*100, and KatH is the hydrogen input from blast moisture and injected fuel in atoms of H.

$$\text{Total oxygen leaving in top gas} = \text{COmol} + 2 * \text{CO}_2\text{mol} + \text{Hred}/2 \quad (56.11)$$

TABLE 56.5 Oxygen Input From Blast

Oxygen Input (Kat O per minute)	Equation (Oxygen as Kat O)
From blast air	= $2 * (\text{Wind}/60 * \% \text{O}_2/100)/22.4 \text{ Nm}^3/\text{Kat}$ = $2 * (\text{Wind}/60 * 20.9/100)/22.4 \text{ Nm}^3/\text{Kat}$ = $\text{Wind}/3215 \text{ Nm}^3/\text{Kat}$
From oxygen enrichment	= $2 * (\text{Oxygen flow}/60)/22.4 \text{ Nm}^3/\text{Kat}$ = $(\text{Oxygen flow})/672 \text{ Nm}^3/\text{Kat}$
From blast moisture	= $\text{Moisture} * (\text{wind}/60) / \text{mw H}_2\text{O}/1000 \text{ g/kg}$ = $\text{Moisture} * (\text{wind}/60) / 18,000 \text{ gr/Kat}$ = $\text{Moisture} * (\text{wind}) / 1,080,000 \text{ gr/Kat}$
From injected coal	= $(\text{Injection rate}/60) * \% \text{ O in coal}/100/16 \text{ kg/Kat}$ = $(\text{Injection rate} * \% \text{ O in coal})/96,000 \text{ kg/Kat}$
Total Oxygen input	Sum of above

Wind is the blast rate in Nm^3/h , oxygen flow is the input oxygen rate in Nm^3/h multiplied by % O_2 , moisture is the blast moisture in g/Nm^3 blast, and injection rate is the coal injection rate in t/h .

remove or add fuel to the blast furnace. The blast furnace engineer can control fuel input using hot metal temperature, silicon content, or both. Silicon control better represents the thermal state of the blast furnace, but delays getting the sampled iron information returned to the blast furnace can delay important fuel adjustment procedures.

Hot metal temperature can be measured faster and more frequently, but this temperature can be influenced by external factors such as the thermal condition of the main iron trough and the degree of slag cover during the cast. A

practice where a controlled hot metal temperature that is measured at the same point in the cast is advocated, usually at slag over or after the second torpedo ladle is filled. Using a regression analysis of hot metal temperature versus silicon, the deviation in temperature from target can be translated to an equivalent decrease/increase in hot metal silicon. Using the rule of thumb for silicon and fuel rate, an increase or decrease in fuel rate can be estimated.

Once it has been determined that an injected fuel rate change is needed, a time lag must be applied to see the impact of the change. Changes in coal injection rate impact the temperature and silicon more quickly than natural gas as coal's impact on the RAFT is much smaller. When adding natural gas to increase the fuel rate, the RAFT is reduced and with this, its related melting power. When natural gas is decreased because the hot metal is too hot, the increase in flame temperature retards the impact of the fuel reduction. In general, changes to injected natural gas can take 4–6 hours to take full effect, injected coal can work in about half this time. Both are faster than an ore-to-coke change that will take one furnace fill to implement (~7–10 hours) and a second furnace fill to reverse.

56.5 COKE RESIDENCE TIME AND QUALITY REQUIREMENTS

With increasing fuel injection, the residence time that the coke remains in the blast furnace increases. Compared to all-coke operations, modern furnaces may have 35–45% of the fuel needs supplied from injected fuel.

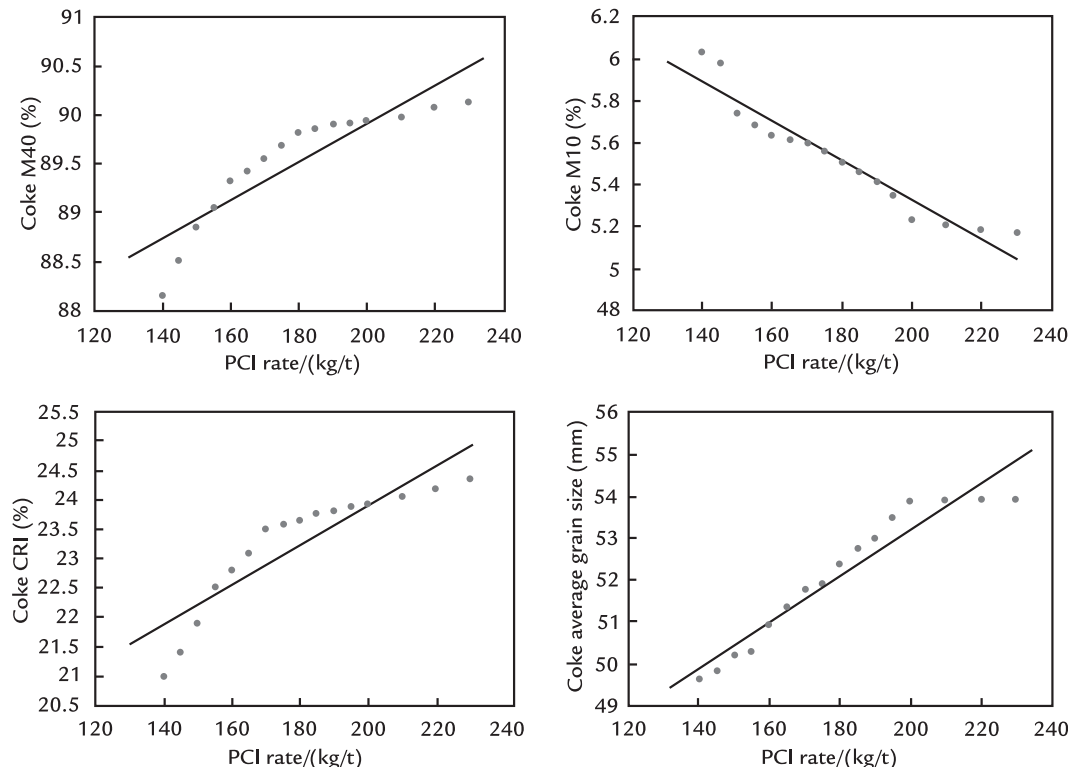


FIGURE 56.6 PCI rates and coke quality parameters reported by Shougang.⁴

The consumption of coke at the tuyeres or coke burning rate decreases proportionally - coke residence time from stockline to tuyeres increases by 1.5–1.8 times.

Blast furnace coke specifications have improved to meet the new demands. Of greatest importance are the coke size, abrasion resistance, and elevated temperature properties such as coke-strength-after-reaction (CSR). To reach coal injection rates of 200 kg/t HM, a Chinese steel producer reported the following coke quality requirements;

- average coke particle size >53 mm;
- CRI < 24 and CSR > 67;
- coke cold strength, M40 > 89; and
- coke abrasion resistance, M10 < 5.4.

Shougang's change in coke quality with PCI rate is shown in Fig. 56.6.⁴

With the likelihood that injected fuel usage will continue to increase and coke rate decrease, continuing improvement in coke quality will be needed. Quality improvements will focus on further increasing coke strength at elevated temperatures to maintain permeability in the deadman/hearth zone.

56.6 PULVERIZED COAL INJECTION (PCI)

Globally, pulverized coal is the most common injected fuel due to its low cost, wide availability, and ability to replace the greatest amount of metallurgical coke. The initial injection systems were developed in the United States by Armco in the 1960s. The technology development was accelerated in the late 1970s

and 1980s by several companies, notably in Europe. The main commercial systems are presented and issues described. While coal injection does provide the largest cost savings, the required equipment is the most expensive and complex. Nevertheless, many steel producers have invested in coal injection systems, more commonly referred to as PCI systems.

56.6.1 Coal Selection and Coke Replacement

Pulverized coal must meet a variety of specifications to assure the best replacement of coke when injected through the blast furnace tuyeres. The main chemical items specified are fixed/total carbon, volatile matter, ash, sulfur, and minor elements such as phosphorus, chlorine, potassium, sodium, and moisture. Other specifications include calorific value, hardness/grindability, and swelling characteristics. Each of these requirements will be described in the next sections.

56.6.1.1 Fixed Carbon and Volatile Matter

A wide variety of coals from semi-anthracite to low/high volatile bituminous coals have been injected into the blast furnace. Early experience was with high volatile coals ($>35\%$ VM) as the volatile matter decomposition was deemed helpful in quickly combusting the coal particles. As injection rates of high volatile coals exceeded 200 kg/t HM, operators noticed a decline in coke replacement. Further investigation into the most appropriate injection coal composition intensified.

Different coal qualities present challenges when injected into the blast furnace. The coal immediately dries and combusts in the raceway, volatile matter burns leaving coal char, CO, and H₂ gases. There is a natural tension between the benefits of a higher fixed carbon content that generates more char compared to gas generated from volatile matter

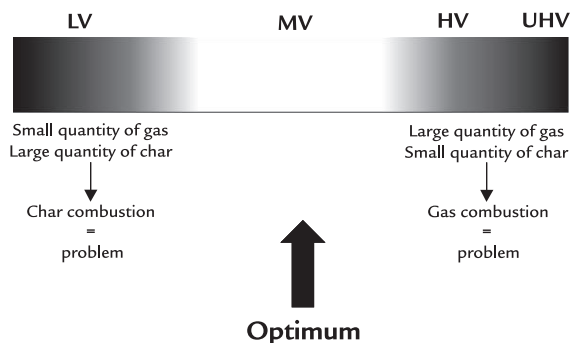


FIGURE 56.7 Process demands for pulverized coal injected into the blast furnace. Coal is designated as low volatile (LV, $<20\%$ VM), medium volatile (MV, 20–30% VM), high volatile (HV, 30–35% VM) and ultra-high volatile (UHV, $>35\%$ VM).

decomposition that assists with coal burnout/devolatilization. A balance must be achieved to get the best performance, see Fig. 56.7.

While the lower volatile matter coals provide more carbon for direct reduction and coke replacement, the lack of gas from volatile matter burnout in the raceway decreases combustion efficiency. A larger amount of char must react in the lower part of the blast furnace which can lead to a char combustion problem and produce soot (fine carbon) in the top gas. High and ultra-high volatile coals generate substantial amounts of gas in the raceway that facilitates coal combustion but burning all the volatile matter in the brief time coal is in the raceway which can lead to a gas combustion problem. As PCI usage was adapted, blast furnace operators injected increasing amount of high volatile coal but with low replacement ratios as the reducing gas was not efficiently used in the blast furnace.

Blast furnace operators searched for an injection coal that balanced demands between gas and char combustion. Medium volatile coal, say 20–30% volatile matter, meets these demands. The availability of such coals is very limited, most available coals are either $<20\%$ VM or $>30\%$ VM. In the late 1990s, blast furnace operators started to blend high and low volatile

coals to get the balance between volatile matter and fixed carbon. Binary coal blends made a significant impact on coke replacement and was a simple step to expand the number of candidate coals that could be deployed with a high coke replacement ratio. More sophisticated blending strategies will depend on the available raw material handling facilities, ability to grind a soft low volatile and hard high volatile coal concurrently, and the available coals at a low price. An arrangement where the selected coals are purchased independently and ground/blended at the blast furnace increases the range of candidate coals that can be considered.

56.6.1.2 Coal Quality Summary and Other Considerations

A summary of the injection coal quality parameters is provided in [Table 56.6](#).

Meeting these coal specifications with a single coal can be challenging. Blending even just two coals can greatly increase the number of candidate coals that can be used at the blast furnace. The injection blend can be designed to

maximize the coke replacement ratio. An example of a coal blend is provided in [Table 56.7](#).

With coal injection, blast furnace operators are injecting more than 200 kg/t HM of PCI and reducing the coke rate to <270 kg/t HM. To achieve this performance, the injection coal must be custom blended, and elevated levels of oxygen enrichment, >30%, will support the needed combustion in the raceway.

56.6.1.3 Coke Replacement Ratio

The amount of coke replaced by injected coal has been a subject of much discussion and analysis of plant data in the 1980s and 1990s. Precise relationships were hard to finalize due to variations in the plant operations and the coal itself. Street and Burgo compared various empirical equations used by blast furnace operators and identified the following⁶:

- Coke replacement ratio increased with increasing coal fixed carbon content, and this dominated all other coal properties.
- Coke replacement ratio decreased with increasing coal volatile matter.

TABLE 56.6 Pulverized Coal Quality Requirements

Quality Parameter	Typical Range	Comments
Fixed carbon	75–85%	Often need to blend two coals to reach this specification
Volatile matter	20–30%	Often need to blend two coals to reach this specification
Ash	<12%	Minimize blast furnace slag volume
Sulfur	<0.8%	Steel quality requirement, minimize sulfur removal costs
Phosphorus	<0.08%	Steel quality requirement, minimize phosphorus in hot metal
Chlorine	<0.2%	Prevent corrosion issues in blast furnace uptakes and gas cleaning plant
Sodium and potassium (Na ₂ O + K ₂ O)	<0.3%	Meet blast furnace alkali input specification
Coal-free swelling index	<8	Must be low to avoid plugging in injection lines and lances, especially as the coal heats
HGI	>50	Avoid hard coals and increased grinding power requirements (harder coals have a low HGI, softer coals a higher HGI)

HGI, Hardgrove Grinding Index.

TABLE 56.7 Typical Properties of Pulverized Injection Coal and Blast Furnace Coke⁵

Item	Pulverized Coal	Metallurgical Coke
ASSAY		
C (fixed), %	72.2	87.2
Volatile matter, %	19.5	1.0
Humidity, %	0.01	0.15 (Dry quenched)
Ash, %	8.5	11.6
SiO ₂ , %	5.7	6.5
AlO ₃ , %	2.1	3.6
MgO	0.01	0.18
CaO, %	0.30	0.47
S, %	0.39	0.65
VOLATILE MATTER, %		
C, %	68.3	74.4
N, %	4.5	8.4
H	25.2	12.6
O	2.0	4.6
PHYSICAL PROPERTIES		
Average particle size, μm	150	52,000
True density, kg/m ³	1545	1820
Particle porosity	0.70	0.45
Calorific value, kJ/kg	32,415	34,276

- The coal C/O ratio was a better predictor of coke replacement ratio compared to C/H.
- Increasing coal ash was reported to improve the coke replacement ratio due to heat balance effects.
- Most models overpredicted the coke replacement achieved in actual practice.

The key replacement ratio equations identified by Street and Burgo are provided in Table 56.8.

Ultimately, Street and Burgo advocated the benefits of controlled blast furnace trials to understand the true replacement ratio of injection coal. The empirical relationships shown in Table 56.8 can serve as a guide to anticipate actual performance and make relative comparisons between candidate injection coals. True performance can only be properly assessed on a well instrumented blast furnace operating on a stable basis for a 10–20-day period.

56.6.2 Coal Grinding

All coal must be crushed or ground to be successfully injected into the blast furnace. Coals naturally have a wide range of hardness and the resulting power needed to grind the coal can vary greatly. The power required to grind coal is expressed by the Hardgrove Grindability Index (HGI). The test is based on a reference coal with an HGI of 100 and the HGI decreases with increasing coal hardness. In the test procedure, 50 g of air dried coal with a grain size in the range between 0.6 and 1.2 mm is filled into the sample mill and a weight is put on the mill's grinding stone. After 60 rounds, the ground coal is put on a sampling sieve. The HGI index is calculated from the fraction of the coal passing through the sieve. The procedure is described by the following standards: ASTM D 409, DIN 51742, and ISO 5074.

Typical injection coals range in hardness from an HGI of 40 to 90. Modern grinding equipment can crush and grind such coals to <200 μm but complications emerge with blends. Coal blends can feature soft and hard coals, hence there is a natural tendency to overgrind the soft coal and undergrind the harder coal when both coals are ground at the same time. Blast furnace operators try to select coals with similar HGI indices but they must accept a wider size range in the ground coal size to make best use of the single grinding mill available at most PCI preparation plants.

TABLE 56.8 Coke Replacement Ratio (CRR) Equations Identified by Street and Burgo⁶

CRR Equation	Source
$CRR = -1e^{-9} \times (C/O)^6 + 2e^{-7} \times (C/O)^5 - 2e^{-5} \times (C/O)^4 + 0.006 \times (C/O)^3 - 0.013 \times (C/O)^2 + 0.1481 \times (C/O) + 0.2828$	W.P. Hutny, J.T. Price and J.F. Gransden, "Evaluation of Coals for Blast Furnace Injection using a Computer Model" Ironmaking Conf. Proc., ISS, 1990, pp. 323–330
Where C/O is the coal carbon-to-oxygen ratio	
$CRR = (0.0137 \times \text{carbon content \%}) - 0.1735$	Advanced Pulverized Coal Injection Technology and Blast Furnace Operation, K. Ishii (ed.), Pergamon, 2000
$CRR = (-118.9 + (2.3 \times C\%) + (4.5\% \times H\%) + (0.97 \times \text{ash\%})) / 100$	P. Bennett, "Using a Blast Furnace Model for the Selection of PCI Coals", 2nd Intl. Ironmaking Conf. Proc., Brazil, 2004
$CRR = (-139.44 + (2 \times C\%) + (6.2 \times H\%)) / 100$	M. Geerde, R. Chaigneau, I. Kurunov, O. Lingardi and J. Ricketts, Modern Blast Furnace Ironmaking, 3rd Edition, IOS Press, 2015

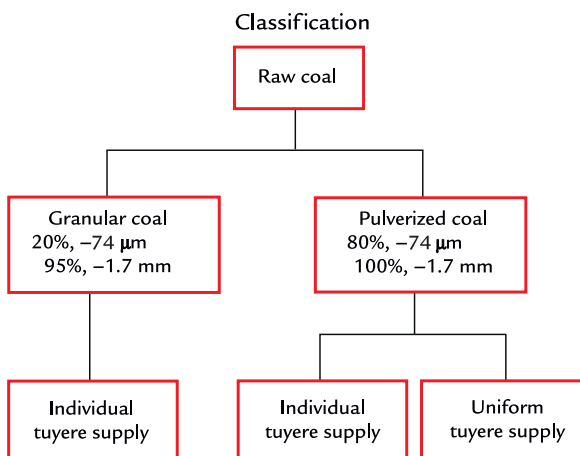


FIGURE 56.8 Commonly used blast furnace coal injection systems.

Coarse and pulverized coal injection systems emerged in the 1970s, Fig. 56.8.

The most commonly used coal injection system pulverizes coal to 80%, <200 mesh, or 74 μm. To reduce capital costs, a granular coal preparation system was also developed in the United Kingdom in the 1970s where coal was only ground to 200–300 μm. This simplified the grinding equipment where crushing could be accomplished using a hammer mill. The granular coal system had a limited implementation

rate with blast furnace operators as there was concern that the highest coal injection rates and coke replacement could not be obtained with the coarser coal particles. Today, most systems are based on pulverized coal and with uniform tuyere supply with coal being split to individual tuyeres using a distributor. Pulverized coal is most commonly ground and dried in a roller mill as shown in Fig. 56.9.

Raw coal is charged from the top onto a grinding table where hot gas (air or nitrogen) is introduced. The hot gas first dries the raw coal but also serves to transport and size the newly ground fine coal. The pulverizer has an internal size classifier so that coarse coal is separated and recycled back to the grinding table for further treatment. Once the coal meets the size requirement, it is pneumatically removed with the discharge gases and separated using a baghouse. When selecting a coal, the surface moisture and chemically entrained moisture content must be evaluated. For successful injection, the surface moisture must be reduced to less than 1.5% in the roller mill.

Roller mills are very reliable and many blast furnaces operate with a single mill and no spare. Pulverizing rates of more than 80 t/hour have been accomplished with a single mill. Initially, dry air was used to grind and dry coal

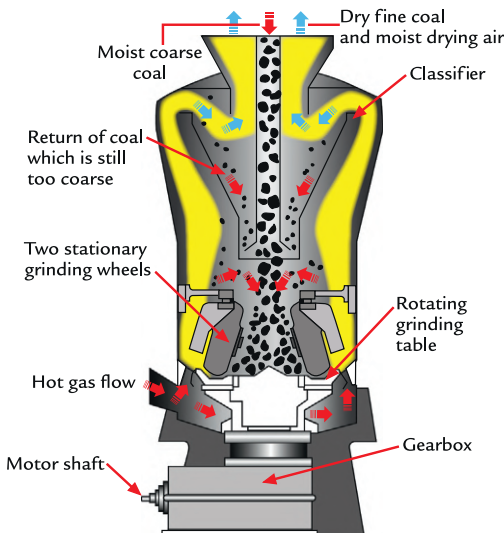


FIGURE 56.9 Principles of operation of a roller mill used to pulverize injection coal.

but an increasing number of facilities use nitrogen as it is intrinsically safer regarding coal explosion and fire potential within the roller mill and downstream process equipment, especially the baghouse used to collect the pulverized coal. Hot waste gas from stove combustion has also been used to reduce energy costs when the roller mill is located close to the blast furnace stoves.

56.6.3 Coal Injection System Design and Equipment

A typical coal preparation plant is described in Fig. 56.10.

One or more injection coals are received by bulk transportation methods, stored in open piles and reclaimed to coal storage bin(s). Coals are blended if needed and fed to the coal pulverizer, typically a roller mill that both grinds and dries the coal at the same time. Dried coal is separated from the process gas and collected in a pneumatic storage vessel ready for delivery to the blast furnace.

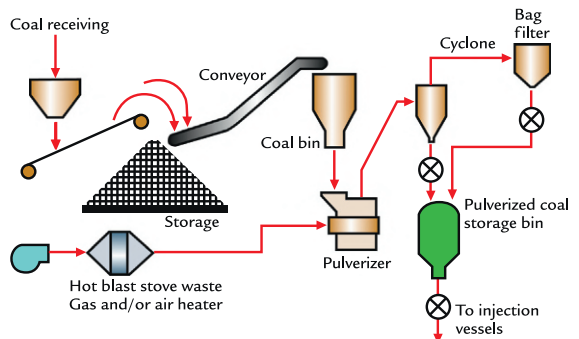


FIGURE 56.10 Typical coal injection preparation plant.



FIGURE 56.11 PCI plant in the foreground at NTMK, Russia. Source: Courtesy: Paul Wurth S.A. [Kushnarev A, Simões J-P, Mahowald P, Stamatakis G, Bermes P, Becker S, et al., First successful pulverized coal injection start-up in Russia at Evraz NTMK, AISTech 2014. Indianapolis, IN: AIST—Association of Iron & Steel Technology; 2014. p. 781–8 (see Ref. [7])]

Initially, the pneumatic bin was located close to the blast furnace but as injection skill grew, the pneumatic bin could be 1–2 km from the blast furnace. In such an arrangement, a central coal preparation plant could supply two or more blast furnaces. The PCI plant is very large and the building is tall, almost as tall as the blast furnace itself as can be seen in Fig. 56.11.

A significant engineering challenge with coal injection is to deliver the same amount of coal to each tuyere and at the correct rate to

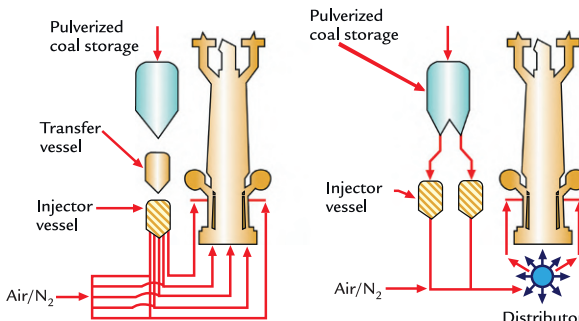


FIGURE 56.12 Injected coal supply - individual tuyere supply (left) and distributor supply (right).

meet the overall blast furnace fuel needs. Two generic systems emerged as presented in Fig. 56.12, one based on individual supply lines from the injector vessel to each tuyere and a second system where coal is transported to a distributor located at the blast furnace and then coal is evenly distributed to each tuyere.

A distributor was used in the first coal injection system developed by Armco in the United States in the 1960s. Armco originally used dry air as an injection gas but newer systems use nitrogen as it is intrinsically safer with regards to fire and safety aspects. Armco systems continue to be used and have an excellent safety record and few incidents have been reported. In many integrated steel works, nitrogen gas is available at a reasonable cost from the on-site air separation plants used to produce oxygen and argon for the steel works. For most new facilities, the owner selects nitrogen as the transport gas for coal injection.

Initially, Armco placed the distributor high in the blast furnace structure so that the length of pipe from the distributor to each tuyere was identical to provide similar resistance to flow and pressure drop. In very large furnaces, two distributors can be used injecting on alternate tuyeres, one distributor for even numbered tuyeres and a second for odd numbered tuyeres. As understanding of the

coal transport improved, the importance of keeping an identical length of pipe to each tuyere from the distributor diminished. Higher pressure and throttling discharge points on the distributor allowed for equal coal flow to each tuyere by moving the flow restriction to the distributor rather than individual pipe runs. Modern designs place the coal distributor at a lower elevation often just above the bustle pipe.

With improved knowledge on coal pneumatic conveyance, the distributor system dominates modern PCI injection systems. A fluidizing tank or chamber at the bottom of the injection tank delivers the injection coal based on a loss of weight principle measured by load cells. The inbound coal impacts a steel plate and is evenly split to the individual tuyere lines. An example of a fluidizing chamber distributor used at Shougang Steel is provided in Fig. 56.13.⁴

Initially, coal was injected in a dilute phase flow transport regime where coal particles are “uncoupled” from the transport gas, be it dry air or nitrogen. With “uncoupled” transport, the velocity of the coal particles is less than the space velocity of the pneumatic transport gas. This increased the transport gas requirements, added unnecessary nitrogen into the blast furnace, and featured high wear of the injection pipes. Most injection systems adopted dense phase injection where the coal particles are “coupled” to the transport gas and travel at a similar velocity. Dense phase injection has been widely adopted for reliability and investment cost reasons. A comparison of the two approaches can be seen in Fig. 56.14.

At each tuyere, a dedicated lance is used to inject the pulverized coal at the mouth of the blowpipe discharge positioned at the center line per Fig. 56.15.

Many different lance arrangements were developed and tested but the straight pipe arrangement generally prevailed. Combustion of the injected coal can be seen in Fig. 56.16.

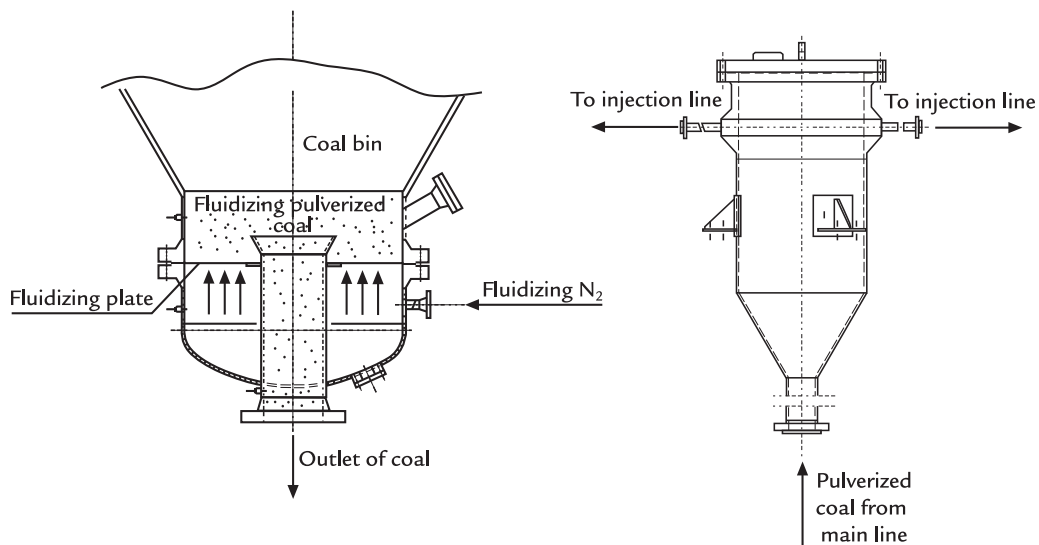


FIGURE 56.13 Injection tank fluidizing chamber and distributor used at Shougang's Qiangang (4000 m³ inner volume) blast furnace.⁴

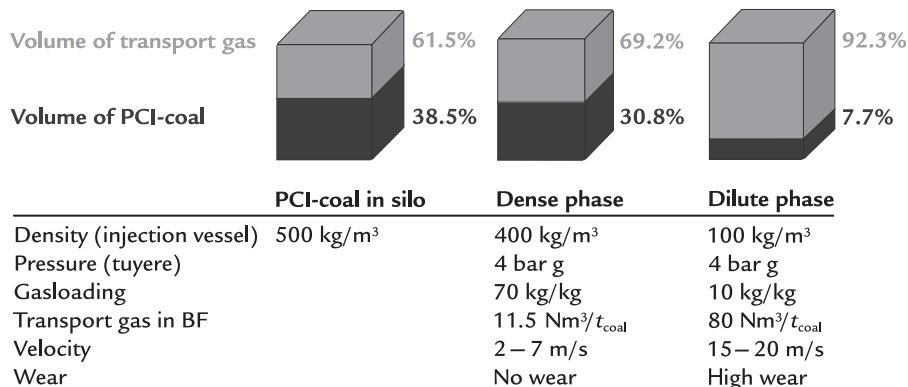


FIGURE 56.14 Comparison of dilute and dense phase coal injection.⁸

Various injection arrangements that have been evaluated including;

- swirling devices installed in the lance tip to promote coal mixing with the blast air;
- coinjection of two items in concentric pipes. These have included coal in the center pipe and either oxygen or a second fuel such as natural gas in the external pipe;

- use of two rather than one coal injection lance per tuyere to promote mixing and combustion; and
- injection of coal and natural gas simultaneously using two separate lances to minimize costs and maximize coke replacement.

Debate continues about the need to combust or gasify all coal within the tuyere itself

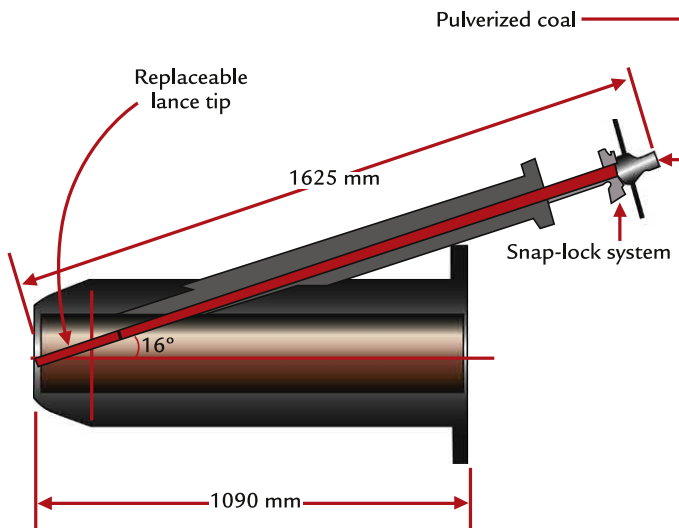


FIGURE 56.15 Typical pulverized coal injection lance with a replaceable tip positioned in the blowpipe.

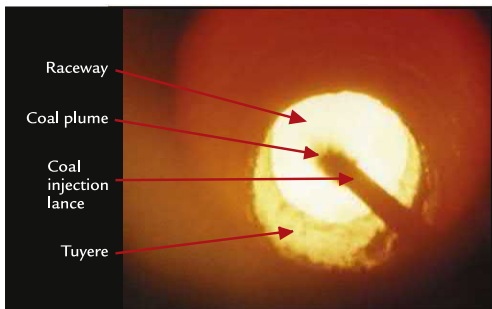


FIGURE 56.16 Coal injection conditions at a single blast furnace tuyere.⁹

compared to partial burnout and consumption of char as it ascends with the blast furnace process gases. While a case can be made for using a more sophisticated tuyere combustion arrangement, the added complexity must be rewarded by a greater coal replacement ratio. Simple single pipe equipped blast furnaces have demonstrated very high injection rates and coke replacement ratio, hence adoption of more complex arrangements has been low. Wear of the lance tip is a concern and abrasive resistant alloyed tips are employed. All injection

lances are usually changed on a planned, worn or not, basis to be assured that the best injection/combustion conditions are available.

From time to time, the blast furnace tuyere opening can become momentarily blocked by the descending burden. This stops the flow of coal into the blast furnace. This is a dangerous situation as the coal can quickly fill the tuyere stock and start a fire in the bustle pipe. Every PCI system has a safety feature to stop coal flow to an individual tuyere if there is a concern that the tuyere may be blocked. One of two systems is commonly used, measurement of the pressure drop between the bustle pipe and the individual tuyere, and the use of an optical/light detector to indicate that a tuyere is blocked. When the pressure drop between the bustle pipe and an individual tuyere decreases below a minimum setting indicating reduced blast flow to the tuyere, the coal flow is immediately stopped. The pressure drop-based system relies on reliable pressure measurements in the bustle pipe and at the tuyere as the loss of pressure drop associated with a blockage is small.

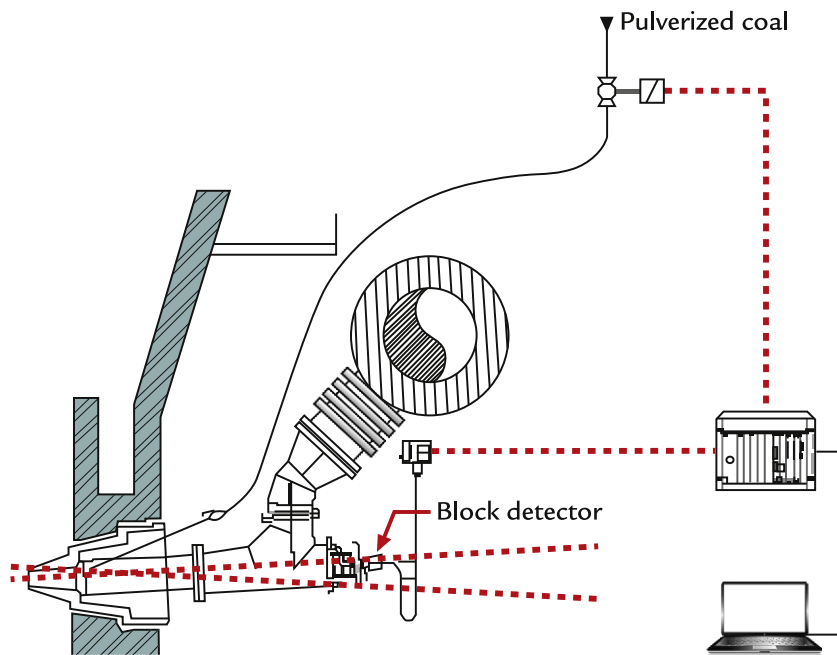


FIGURE 56.17 Detection of tuyere blockage using an optical sensor to stop PCI flow.

Many blast furnace operators use an optical detection process where a fiber optical sensor is positioned on each tuyere to observe the brightness from the raceway. If the tuyere is blocked, the tuyere would "go black" and the light emitted drops dramatically. Coal injection on the selected tuyere is stopped until the blockage disappears as the material is consumed at the tuyere tip. Details of the optical detection system are shown in Fig. 56.17.

Additional coal is injected on the remaining tuyeres until blast flow is restored to the blocked tuyere and coal injection can be restarted. The blast furnace operator may adjust the fuel rate or burden distribution to raise the melting or cohesive zone position at the wall to prevent tuyere blockages. There will be a limit to the number of blocked tuyeres that the blast furnace will allow before acting to increase the coke rate to protect the blast furnace operation. While the number of blocked tuyeres allowed depends on furnace size, typically more than

three blocked tuyeres require consideration of an increased coke rate or other actions to correct the tuyere blockage situation.

56.6.4 PCI Summary

Modern coal injection systems feature one or two roller mills to dry and pulverize the incoming raw coal. The pulverized coal will be dried to $<1.5\%$ moisture and ground to $80\% < 74 \mu\text{m}$. A pneumatic injection system will deliver the coal to each tuyere in equal amounts and at the overall prescribed mass flow rate. The pulverized coal will be injected at every tuyere via a simple injection lance pipe. Safety controls will shutoff coal injection to individual tuyeres to prevent potential fires in the bustle pipe. With the use of the right injection coal or coal blend and associated oxygen, coal rates of up to 250 kg/t HM have been achieved and metallurgical coke consumption decreased to $<270 \text{ kg/t HM}$ representing just 55–60% of the fuel input.

Further adoption of coal injection is expected due to its ability to reduce coke consumption and the widespread availability of injection coals.

56.7 NATURAL GAS INJECTION

Compared to all other injection systems, natural gas injection is the simplest and has the lowest cost to implement. Natural gas is predominately composed of methane (94% CH₄(g)

TABLE 56.9 Typical Composition of Natural Gas in North America¹⁰

Component	Typical Analysis (mole %)	Range (mole %)
Methane	93.9	87.0–97.0
Ethane	4.2	1.5–9.0
Propane	0.3	0.1–1.5
Iso-Butane	0.03	0.01–0.3
Normal-Butane	0.03	0.01–0.3
Iso-Pentane	0.01	Trace–0.04
Normal-Pentane	0.01	Trace–0.04
Hexanes plus	0.01	Trace–0.06
Nitrogen	1.0	0.2–5.5
Carbon dioxide	0.5	0.05–1.0
Oxygen	0.01	Trace–0.1
Hydrogen	trace	Trace–0.02
Specific gravity	0.59	0.57–0.62
Gross heating value (MJ/m ³), dry basis ^a	38.7	36.0–40.2
Wobbe number (MJ/m ³)	50.4	47.5–51.5

^aThe gross heating value is the total heat obtained by complete combustion at constant pressure of a unit volume of gas in air, including the heat released by condensing the water vapor in the combustion products (gas, air, and combustion products taken at standard temperature and pressure).

Courtesy: Union Gas.

on a molecular basis) with the balance being other heavier hydrocarbons. A typical natural gas composition can be seen in Table 56.9.

Natural gas requires no pretreatment other than the reduction of the supply pressure to suit the blast furnace injection conditions. A ring main is installed around the blast furnace at a designated pressure above blast pressure and individual lines supply each tuyere per Fig. 56.18.

Control of the natural gas injection rate is crucial and the use of two redundant flow meters is recommended. Tuyere blockage detectors can be employed to shut off injection at an individual tuyere but this is not commonly employed as the injected natural gas tends to find a path through a momentary blockage. Larger or small diameter injection lances may be used to provide suitable turn down ratios for various injection rates. Two lances may be employed to inject natural gas at separate positions and at a high rate. The coinjection of oxygen and natural gas has been tested to improve combustion, but this has not been widely adopted.

While overall coke replacement is less using natural gas compared to coal injection, blast furnace operation is easier with the greater

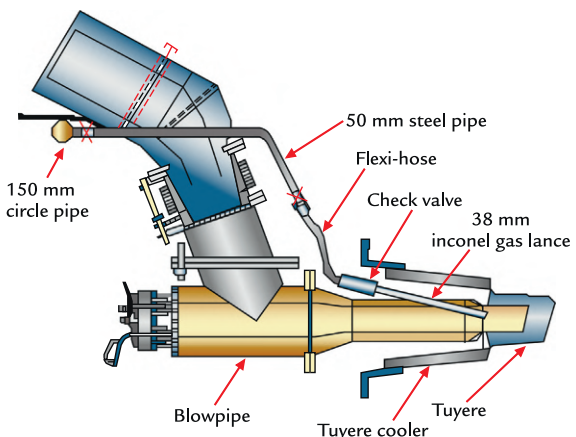


FIGURE 56.18 Typical natural gas injection system arrangement.

amount of hydrogen added. Natural gas injection is widely used in the United States, Canada, and Russia due to attractive natural gas prices and a large supply base.

56.7.1 Coke Oven Gas Injection

In a few cases, available coke oven gas has been compressed and injected into blast furnaces. The most notable facility is US Steel's

TABLE 56.10 Typical Coke Oven Gas Properties¹¹

Component	Typical Analysis (%)
CO ₂ and H ₂ S	1.3–2.4
O ₂	0.2–0.9
N ₂	2.0–9.6
CO	4.5–6.9
H ₂	46.5–57.9
CH ₄	26.7–32.1
Specific gravity	0.36–0.44
Gross heating value (MJ/m ³), dry basis	21.1–22.8
Net heating value (MJ/m ³)	18.8–20.5

Edgar Thompson Works where two blast furnaces consume the excess coke oven gas produced by the large Clairton Coke Plant located 20 km away. Coke oven gas is an attractive fuel gas as it contains a substantial amount of hydrogen, methane, and other hydrocarbons per Table 56.10.

The coke oven gas requires complete removal of condensable hydrocarbons as it must be compressed first for transportation. Upon receipt, the gas pressure is reduced and it is injected in a similar fashion as natural gas. The measurement and adjustment for changes in the heating value are needed as the coke oven gas quality can vary with the operation of the coke plant facilities.

56.8 COAL AND NATURAL GAS INJECTION

In North America, coal injection was adopted since the 1990s albeit at a slower rate than other regions. When natural gas prices dramatically decreased in 2009 due to the advent of shale-based natural gas, natural gas usage increased per Fig. 56.19.

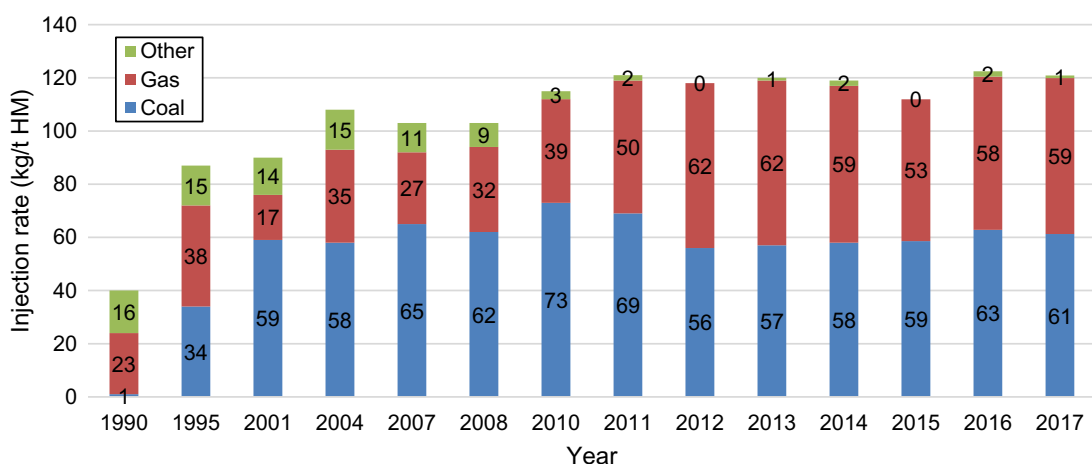


FIGURE 56.19 Fuel usage for North American blast furnace plants.^{12,13}

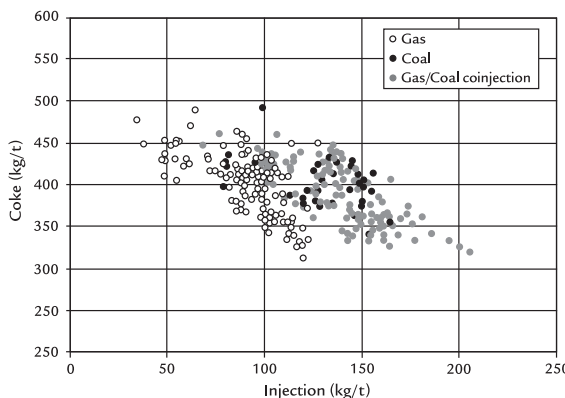


FIGURE 56.20 Monthly usage of coal, natural gas, and combined injection compared to coke rate for North American blast furnaces.¹²

Blast furnace operators with PCI systems increasingly injected both coal and natural gas concurrently to decrease operating costs. Injection was achieved largely using the available equipment and with separate lances for coal and natural gas located in each tuyere. Very high rates of combined injection have been achieved, Fig. 56.20.

Geerdes documented hidden benefits of coinjecting coal and natural gas together.¹⁴ Geerdes cited the following benefits:

- Chemical benefits due the lack of ash, sulfur, and alkali elements in natural gas.
- Natural gas increases the bosh gas hydrogen content, decreasing carbon used for direct reduction, fuel rate, and carbon footprint.
- Potential to add more energy to the lower furnace to avoid a chilled hearth event compared to using coal injection alone.

Geerdes also highlighted some concerns with coinjection including additional oxygen demands to control RAFT, concerns about controlling injection using RAFT, and process variations when operating at very low coke rates.

With natural gas remaining at a low price and considering the operational benefits of having a greater amount of hydrogen in the

blast furnace bosh zone, coinjection of natural gas and coal is expected to continue with plants that had previously made investments in PCI facilities as these operations search for the lowest fuel costs.

56.9 OIL AND TAR INJECTION

While in decline due to the inflated costs, the injection of liquid fuels, principally by-product tar, heavy oil, waste oil, and tar derivatives, is still employed by some operating blast furnaces. A typical oil injection system design for a blast furnace facility is presented in Fig. 56.21. A tar injection system is presented in Fig. 56.22.

By-product tar is one of the most difficult fuels to operate with as it must be injected hot, typically 110°C, and lances can plug should the tar overheat in the injection lances and form solid deposits in the small diameter injection lances.

Liquid fuels are often coinjected with steam or a small amount of water added to the

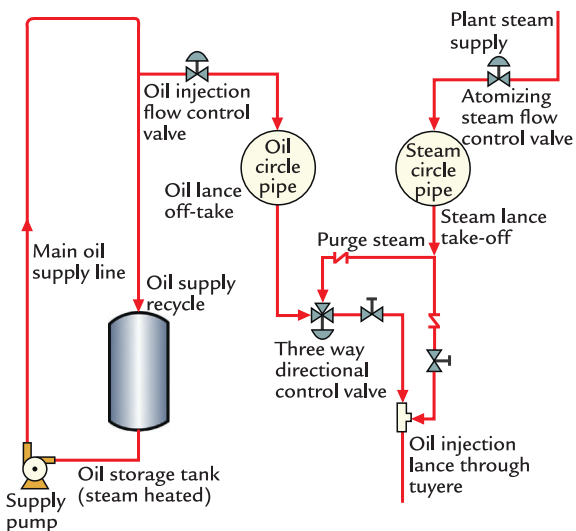


FIGURE 56.21 Typical blast furnace heavy fuel oil delivery system.

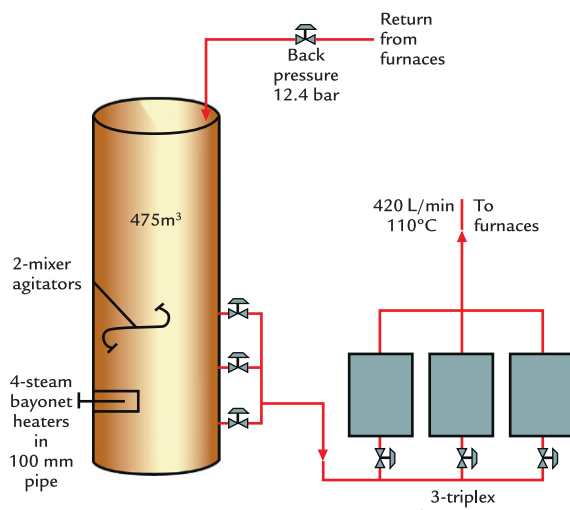


FIGURE 56.22 By-product tar injection system.

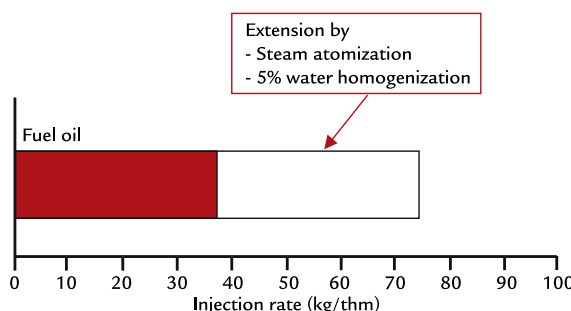


FIGURE 56.23 Increased use of fuel oil when homogenized with 5% water and assisted by steam atomization on the injection lances.

liquid fuel to facilitate the atomization and combustion of the heavy oil and tars. Reducing droplet size and dispersing the liquid fuel can virtually double consumption up to the process limits, see Fig. 56.23.

The arrangement at the blast furnace includes a ring main from which branch lines feed each tuyere. The steam is added in a small pipe in the center of the oil lance. This allows the steam and oil to interact at the point of release into the tuyere. Devices to encourage mixing between the oil and steam have been employed to reduce

steam consumption while still combusting the oil/tar as efficiently as possible.

While the use of purchased heavy fuel oil for injection has essentially stopped due to the high fuel costs, blast furnaces are still used to consume a variety of waste oils and tar derivatives such as kerosene and motor oil. Due to their relatively low volumes, the waste oil may be injected at only a single tuyere, as this is a cost-effective way to dispose of oil wastes due to the large fuel demand of the blast furnace process.

56.10 IMPACT OF INJECTED FUELS ON THE BLAST FURNACE OPERATION

Injected fuels have made an enormous impact on the technical and commercial viability of the blast furnace operation. On the technical front, injected fuels reduced coke consumption and improved the burden descent and consistency of operations. As greater and greater amounts of low and high purity oxygen became available, 90% and 99% O₂, respectively, injected fuels and oxygen were used to raise blast furnace production significantly above the name plate of many blast furnace facilities.

In this section, details on how to best use injected fuels are presented and primary and secondary impacts of the blast furnace process are described. The approach to injected fuels into the blast furnace is similar for each fuel type but their impact on the blast furnace operation differs from fuel-to-fuel.

56.10.1 Maximizing Injected Fuel Usage

When establishing the maximum injected fuel usage, the following parameters dictate the amount of injected fuel that can be added:

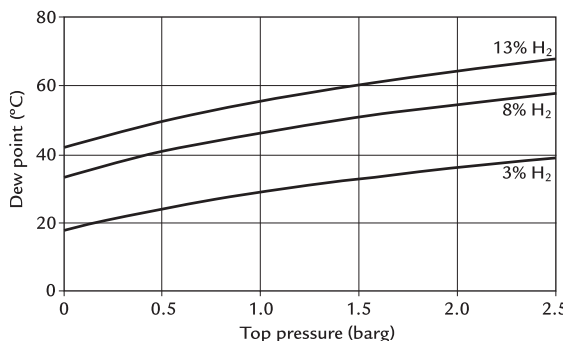


FIGURE 56.24 Dew point for various top pressure and hydrogen content in the blast furnace throat.¹⁵

- Being above a minimum RAFT defined by the raw material quality and fuel used.
- Managing the increased pressure drop when producing more gas in the lower part of the blast furnace.
- Being above a minimum top temperature and the related top gas dew point to minimize moisture condensation and maximize the opportunity to eliminate zinc included in the raw materials, Fig. 56.24.

Specific injected fuels reach different limitations and this must be recognized in the strategy to lower the coke rate:

- Natural gas strongly depresses that RAFT but industry experience shows that a blast furnace can successfully operate at a lower RAFT using natural gas, due to greater hydrogen-based reduction in the bosh region. A blast furnace injecting natural gas can successfully operate at a flame temperature as low as 1900°C, about 150–200°C lower than a similar blast furnace operation injecting pulverized coal.
- PCI injection is characterized by an increase in the resistance to gas flow as the injection rate is increased beyond 150 kg/t HM due to greater presence of gas/char in the lower furnace and decrease in available coke in the furnace for gas to pass through. Blast oxygen must increase to reduce overall bosh

gas volume. Burden distribution strategies are needed to manage the pressure drop by a careful buildup of coke and ore layers.

- Since natural gas injection is typically less than 100 kg/t HM, increased resistance to gas flow and impact on pressure drop is not experienced. More coke is available in the blast furnace for gas to pass through and the additional hydrogen reduces the bosh gas volume and related gas density.
- Increasing oxygen enrichment will reduce the specific gas volume used in the blast furnace. The top temperature will decrease and approach the top gas dew point limits, especially close to the furnace wall where the gas temperature is typically lower. A practical limit of 110–120°C is nominated to sustain a healthy operation where moisture accumulation is minimized. A peak temperature, usually in the blast furnace center, of 500–600°C is desirable to eliminate zinc that is present in the burden materials. The zinc would otherwise recirculate in the blast furnace and can damage hearth wall and shaft refractory materials.

56.10.2 Operating Windows to Maximize Fuel Injection

Industry experience indicated that coal could be injected at rates up to 100–125 kg/t HM with minimal oxygen enrichment. For many operators, PCI rates in this range are considered an initial injection rate when starting up or a minimum rate should there be any loss of available oxygen to add to the blast air.

Working within these guidelines and manipulating the production rate and oxygen added, an operating window for injected coal was defined by Geerdes et al. as illustrated in Fig. 56.25.¹⁶

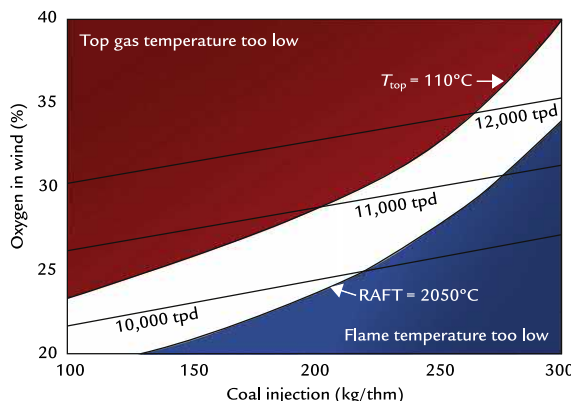


FIGURE 56.25 Blast furnace operating window shown in white for injected coal per Geerde et al.¹⁶

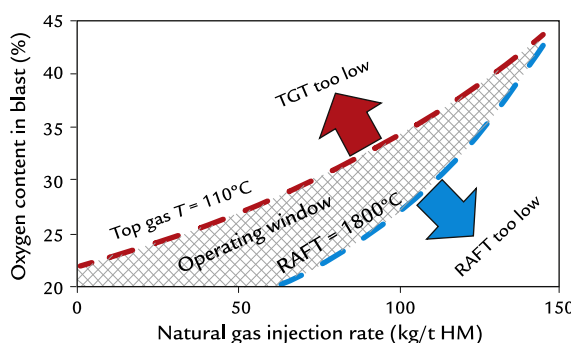


FIGURE 56.26 Operating window for natural gas injection per Gibson and Pistorius.¹⁷

As the PCI rate is increased, more oxygen is needed to combust the coal as shown in the constant production lines presented in Fig. 56.25. The oxygen added to keep production constant is insufficient to maintain the flame temperature and will eventually limit the maximum PCI injected. Adding additional oxygen and decreasing the wind rate allow the operator to continue to inject coal provided that a top temperature limit is not reached and the blast furnace is otherwise able to produce the increased hot metal needed to achieve the highest injection rates.

Injection of natural gas with its higher impact on the RAFT has a tighter and narrow

operating window as seen in Chapter 49, and as described by Gibson and Pistorius in Fig. 56.26.¹⁷

The sharp increase in oxygen demand to maintain a RAFT limits the available operating window which narrows as the natural gas injection rate increases. Gibson and Pistorius indicated a RAFT limit of 1850°C. Modern blast furnaces can inject 90–100 kg/t HM natural gas using 30% oxygen enrichment and maintaining a RAFT of 1950–2000°C. This further limits the size of the permissible operating window.

Defining the operational window and understanding the parameters that define the boundary conditions allow the blast furnace engineer to reduce the coke rate to the minimum value. Actions such as minimizing the moisture content of the charged burden can allow the blast furnace to operate at the lowest top temperature, where thermal efficiency is fully optimized.

56.11 SUMMARY

Tuyere fuel injection has allowed the blast furnace operators the opportunity to dramatically reduce coke consumption. In world class operations, almost half of the required fuel is coal injected through the tuyeres. Such practices have reduced the reliance of the blast furnace on expensive metallurgical coke. Injection practices require a thorough understanding of the impact of fuel on RAFT, the use of oxygen to support greater amounts of injected fuel, and the ability to match injected fuel added on a time basis with coke added on a batch basis. The blast furnace engineer must develop the injection practice and use of oxygen enrichment to operate between the minimum top temperature limit of 110–120°C and minimum RAFT that is a function of the injected fuel used, Table 56.11.

Injected coal is the leading fuel as coal has the smallest impact on the RAFT. In areas where

TABLE 56.11 Raceway Adiabatic Flame Temperature (RAFT) Guidelines for Various Injected Fuels

Injected Fuel	Typical RAFT (°C)
PCI	2050–2150
Natural gas	1900–2000
PCI and natural gas coinjection	2000–2150

PCI, Pulverized coal injection.

natural gas is inexpensive, gas injection has been employed due to its simplicity and low investment cost to implement. With its ability to displace expensive metallurgical coke, further improvements to increase fuel injection will be developed and world class practices adopted across the global steel industry.

EXERCISES

- 56.1.** PCI coal injection systems and transportation. Please circle if the following statements are true or false:

- T F The usual operating mode is Auto Mode. In this mode, the injection rate into the furnace is reduced when the coal supply to one of the tuyeres is shut off.
- T F Buildup of coal in the pipes leading to the furnace is reduced by increasing the amount of coal particles smaller than 10 µm.
- T F Optical tuyere block detection shuts off the coal supply to a lance in case the light intensity is too low.
- T F With dense phase injection, the gas loading volume is 90% and solids 10%

- 56.2.** Tuyere injection arrangements when looking through the tuyere peep sight. Please circle the correct option:

- A. The position of the tip of the natural gas lance is in front of the coal lance tip.

- B. The position of the tip of the natural gas lance is behind the coal lance tip.

- 56.3.** Economic justification of fuel injection. Please circle if the following statements are true or false:

- T F The replacement ratio is the amount of coal replaced by coke, expressed in kg coal/kg coke.
- T F Ash replaces carbon in injection coal. Therefore, a higher coal ash will reduce the replacement ratio and increase the amount of slag in the furnace.
- T F Natural gas has the highest replacement ratio, but coal has the highest injection capability due to its low H/C ratio.
- T F The cost advantage of natural gas injection is most significant when injecting at high rates with high levels of oxygen enrichment.

- 56.4.** Change in tuyere conditions and the impact on the flame temperature. Please indicate the expected impact of each of the following changes on the raceway adiabatic flame temperature (RAFT). Circle the correct answer:

Change in Tuyere Condition	Impact on RAFT
• Increase hot blast temperature	Increase/Decrease
• Increase blast moisture	Increase/Decrease
• Decrease oxygen enrichment	Increase/Decrease
• Decrease coal injection	Increase/Decrease

- 56.5.** The effects of injectants. Please circle if the following statements are true or false:

- T F Injectants slow down the burden descent rate by replacing coke burnt at the tuyeres.
- T F The advantage of coinjecting coal and natural gas is in the significant hydrogen

- content of coal, which stabilizes the furnace process.
- T F Injectants increase the heat load on the bosh due to the increased volume of their combustion products.
- T F Injection fuels replace moisture to control the flame temperature.
- T F The maximum amount of oxygen enrichment is restricted by top temperatures becoming too low. On the other hand, too little oxygen enrichment results in too low flame temperatures.

56.6. Coal char formation. Coal char formation can be limited by (please circle the correct options)

- A. Correct lance alignment and positioning
- B. Increasing blast moisture
- C. Increasing oxygen enrichment
- D. Dispersion of the coal plume by coinjecting natural gas
- E. Injection of a low-volatile coal

56.7. Loss of pulverized coal injection and thermal control with PCI. Please circle if the following statements are true or false:

- T F When hot metal temperatures are low, the PCI rate is decreased.
- T F High hot metal temperatures are controlled by injecting steam.
- T F In the case of loss of PCI, immediate action is required to increase the flame temperature.
- T F After a short PCI outage (less than 2 h), the lost energy input is made up for by injecting additional coal.

56.8. Fuel injection and burdening. Please circle the correct statement/statements:

A. PCI increases the ore-to-coke ratio and therefore gas flows with more difficulty.

- B. The central coke chimney is made specifically to provide an easy path for the flow of liquid metal and slag.
- C. When using coal at high injection rates, more coke must be charged to the center.

56.9. Coke quality and coal injection. Please circle if the following statements are true or false:

- T F With coal injection, coke is subject to a shorter residence time and increased gas attack (solution loss).
- T F Degraded, weak coke accumulates in the bird's nest.
- T F Coke needs to be more reactive when injecting coal.
- T F Weak, degraded hearth coke directs the liquid flow toward the furnace center, resulting in high hearth temperatures.

References

1. Lüngen H-B, Peters M, Schmoele P. *Ironmaking in western Europe—status quo and future trends*. Cleveland, OH: AISTech; 2015. 2015.
2. Busser JW. Blast furnace energy balance and optimization. In: *24th McMaster University blast furnace ironmaking course*. McMaster University; 2016, p. 12–3, Lecture #4.
3. Agarwal JC, Brown FC, Chin DL, Stevens GS, Gambol FC, Smith DM. Results of ultra-high rates of natural gas injection into the blast furnace at ACME steel company. In: *1998 ICSTI ironmaking conference proceedings*, Toronto, ON; 1998. p. 443–53.
4. Meng X, Zhang F, Li L, Cao C. *May Pulverized coal injection technology in large-sized blast furnace of Shougang*, AISTech 2017. Nashville, TN: Association of Iron & Steel Technology; 2017. p. 805–13.
5. de Castro JA, de Mattos Araújo G, da Motaa IO, Sasakib Y, Yagi J-I. Analysis of the combined injection of pulverized coal and charcoal into large blast furnaces. *J Mater Res Technol* 2013;2(4):308–14.
6. Street SJ, Burgo J. *Development of a simplified ensemble model for PCI coal selection*. Pittsburgh, PA: AISTech; 2016. p. 321–36. Proceedings.
7. Kushnarev A, Simões J-P, Mahowald P, Stamatakis G, Bermes P, Becker S, et al. *First successful pulverized coal*

- injection start-up in Russia at Evraz NTMK, AISTech 2014.* Indianapolis, IN: AIST—Association of Iron & Steel Technology; 2014. p. 781–8.
8. Schott R. *State-of-the-art PCI technology for blast furnace ensured by continuous technological and economical improvement.* Atlanta, GA: AISTech; 2012. p. 589–604. proceedings.
9. Paramanathan BK, Engel E. Pulverized coal injection optimizing the blast furnace process. In: *6th International conference on the science and technology of ironmaking (ICSTI)*, Rio de Janeiro, Brazil; 2012. p. 2455–63, ISSN 2176-3135.
10. Union Gas. <<https://www.uniongas.com/about-us/about-natural-gas/chemical-composition-of-natural-gas>>.
11. Association of Iron and Steel Technology (AIST). *Making, shaping & treating of steel.* 1999 ed. Association of Iron and Steel Technology (AIST); 1999. p. 325 [Chapter 6].
12. Lherbier, Jr. LW, Ricketts JA. Ironmaking in North America. In: *AISTech 2015 proceedings*, Cleveland, OH, Plenary Session, May 2015.
13. AIST. *AIST blast furnace round-up data for 2016, 2017 and 2018, iron and steel technology.* AIST; March 2016, March 2017 and March 2018.
14. Geerdes M. April *Co-injection of coal and gas in blast furnaces: Are there hidden benefits?* Iron and Steel Technology, AIST; 2016. p. 82–9.
15. Cegna G, Puertas G, Lingiardi O, Musante R. *Influence of process variables on blast furnace operational limits: Ternium Siderar experience.* Atlanta, GA: AISTech; 2012. p. 407–15.
16. Geerdes M, van Laar R, Vaynshteyn R. *Low-cost hot metal: the future of blast furnace ironmaking.* Pittsburgh, PA: AISTech; 2010. p. 185–92. May 2010.
17. Gibson J, Pistorius PC. *Natural gas in ironmaking: On the use of DRI and LRI in the blast furnace process.* Cleveland, OH: AISTech; 2015.

Casting the Blast Furnace*

O U T L I N E

57.1 Casting Principles	602	57.10.3 Iron Gap Time	622
57.2 Casthouse Design - The Essential Equipment	603	57.10.4 Slag Gap Time	622
57.3 Casthouse Layouts	603	57.10.5 Overlapping Casts on Multiple Taphole Blast Furnaces	623
57.4 Casthouse Emission Controls	605	57.10.6 Drill Bit Diameter	624
57.5 Drilling Open the Taphole	606	57.10.7 Measuring Hot Metal Temperature and Sampling	624
<i>57.5.1 Oxygen Lancing the Taphole</i>	<i>608</i>	<i>57.10.8 Hearth Drainage</i>	<i>625</i>
57.6 Plugging the Taphole	608	57.11 Modeling of the Hearth Liquid Level	625
57.7 Taphole Construction and the Beehive or Mushroom	610	<i>57.11.1 Filling - $m_{i,in}(t)$</i>	<i>627</i>
57.8 Taphole Clay	611	<i>57.11.2 Accumulation</i>	<i>627</i>
57.9 Trough Design and Iron-Slag Separation	613	<i>57.11.3 Draining - $m_{i,out}(t)$</i>	<i>627</i>
57.10 Casting Schedule	619	<i>57.11.4 Solving the Simplified Hearth Drainage Model</i>	<i>630</i>
<i>57.10.1 Casting Times</i>	<i>620</i>	57.12 Summary	631
<i>57.10.2 Dry Hearth Practice</i>	<i>622</i>	Exercises	632
		References	632

*We thank Mr. Luke Boivin, Process EIT, Pyrometallurgy, Hatch Ltd. for his contribution to this chapter.

57.1 CASTING PRINCIPLES

Matching the continuous nature of producing molten iron and slag to the intermittent process of casting the blast furnace has been a challenge to blast furnace designer and operators. Ideally, the rate of hot metal and slag removal would exactly match the rate at which iron and slag are smelted. The world's largest blast furnaces with four tapholes can meet this requirement by casting continuously and even with casting times greater than 24 h/day by overlapping casts - that is, two tapholes opened at the same time. Smaller blast furnaces with 1 or 2 tapholes operate as close to a 1:1 casting-to-production ratio as possible working within the limitations of the available equipment.

The blast furnace is drained by drilling the furnace open at the designate tapholes and draining the slag and iron that has accumulated in the hearth. Once the liquids are removed, gas will exit the taphole (called a gas blow) signifying that the liquid level elevation is below the taphole elevation. While this sounds obvious, as the blast furnace is under pressure, the slag and hot metal interfaces near the end of a cast are not horizontal like draining a bucket. The presence of gas pressure above the slag contorts the liquid levels, the slag curves down to the taphole, and the hot metal level curves up to the taphole (Fig. 57.1).

The degree of distortion of the slag and hot metal levels is a function of the drainage speed and blast pressure. When the operator drills a large diameter taphole or the taphole clay erodes quickly, the rapid drainage pushes the slag layer down and a gas blow is observed, signaling that the hearth is empty when in fact a significant amount of slag and

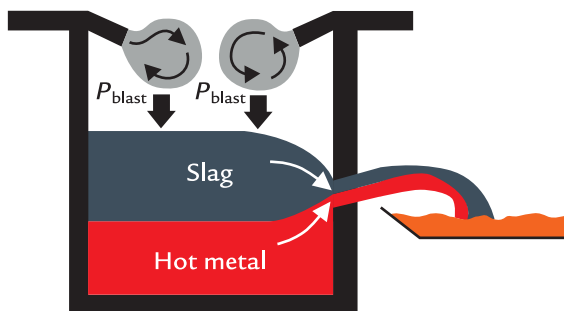


FIGURE 57.1 Iron and slag levels while casting the blast furnace.

iron remains. The best way to reduce "false blows" is to cast the blast furnace slowly and reduce the iron and slag casting rate to as close as possible to the production rate. This depends to a large degree on the taphole clay quality, the tapping schedule, and the ability to use more than one taphole while operating the blast furnace.

Understanding the nature of hearth drainage is important to keep the hearth dry and empty. The deadman present in every blast furnace hearth influences the drainage patterns. The deadman consists of fine coke created from the turbulent conditions in the raceways and solidified slag that accumulates in the center of the furnace. Due to its impermeable nature, the deadman impedes liquid flow and this can lead to channeling along the hearth walls. Repetitive channeling can place high heat loads on the blast furnace hearth walls, dissolve the protective frozen skull of iron, and wear the refractory bricks or blocks. The deadman can be floating or sitting depending on the hearth sump depth and blast furnace force balance. Whether the deadman sits, floats, or cycles between these conditions influences liquid flow patterns and hearth wear.

57.2 CASTHOUSE DESIGN - THE ESSENTIAL EQUIPMENT

The essential equipment and its function are:

- the taphole, a specially constructed opening in the hearth wall;
- the iron trough where the exiting molten stream is collected and slag and iron are separated. The trough includes an iron dam to maintain a residual amount of iron in the trough and a skimmer plate to separate lighter slag from heavier hot metal;
- iron runners to deliver the hot metal to ladles for transport to steelmaking;
- a tilting runner that can tilt to fill one of two ladles under the casting floor;
- slag runners to deliver molten slag to slag pots, open pits, or slag granulation plants;
- a drain runner to remove iron and slag from the iron trough;

- a taphole drill to open the taphole;
- a mud or clay gun to close the taphole; and
- various fume hoods connected to a baghouse to capture emissions from the casting process.

57.3 CASTHOUSE LAYOUTS

A typical casthouse arrangement for a single taphole is shown in Fig. 57.2.

As blast furnace output increased, furnace designs moved from a single taphole to multiple tapholes servicing larger furnaces. A single taphole typically limited hot metal production to ~4000 t/day. Adding a second taphole allowed operators to increase hot metal production to ~7000 t/day by shortening the time between casts to 5–10 minutes compared to 20–30 minutes for a single

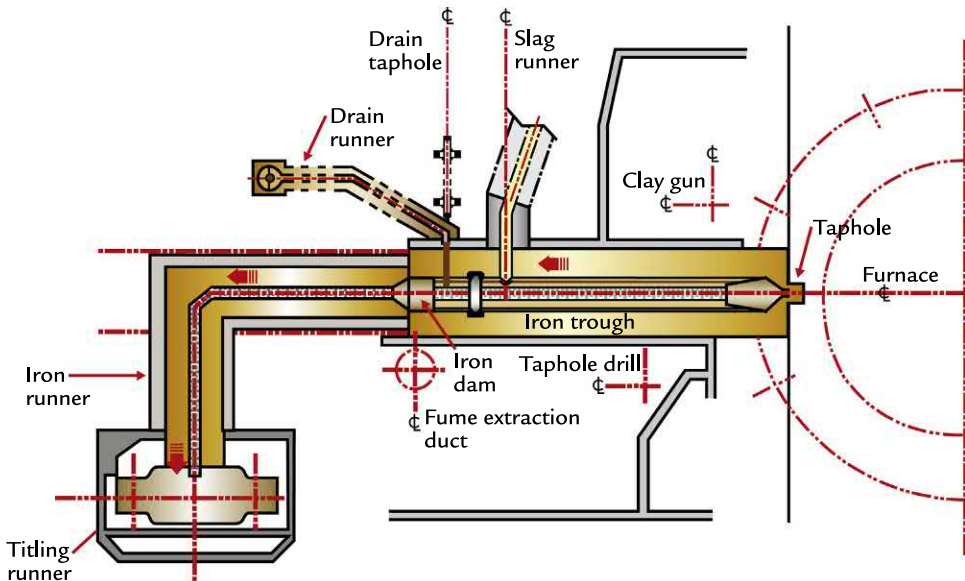


FIGURE 57.2 A typical casthouse layout, shown from the top, for a single taphole blast furnace.

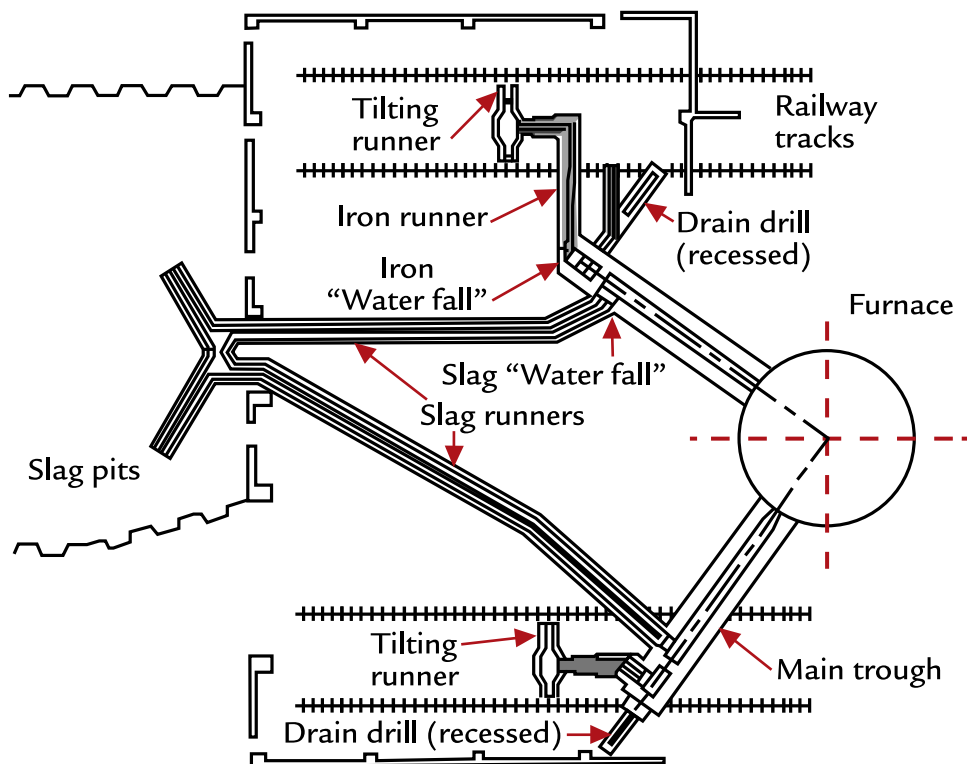


FIGURE 57.3 Blast furnace casthouse layout with two tapholes.

taphole blast furnace. A casthouse layout of two tapholes separated by 90° is provided in Fig. 57.3; casthouses with 180° layouts are also used.

To enable long casts, modern blast furnaces are equipped with tilting runners to fill the hot metal ladles. The tilting runner allows a full ladle to be replaced with an empty ladle without interrupting the casting process. A tilting runner layout is shown in Fig. 57.4.

To operate at even higher production rates, the casthouse production rate needs to match the production rate of hot metal and slag in the blast furnace proper. This could only be achieved with three or four tapholes that could be operated concurrently when need to assure that the blast furnace hearth was always completely drained.

A blast furnace with three or four tapholes requires two slag pits placed on opposite sides of the furnace to enable slag casting. The stoves and gas treatment plants need to be positioned further away from the blast furnace proper to create space around the furnace circumference. Today, the largest blast furnaces operate with four tapholes, generally two in operation, one in stand-by, and one tapping system under maintenance repairs. Blast furnaces with three tapholes are often smaller furnaces that have been enlarged and did not have the available space to install a fourth tapping system. Three taphole blast furnaces can produce at rates comparable to the largest blast furnaces with very well-planned maintenance cycles and reliable

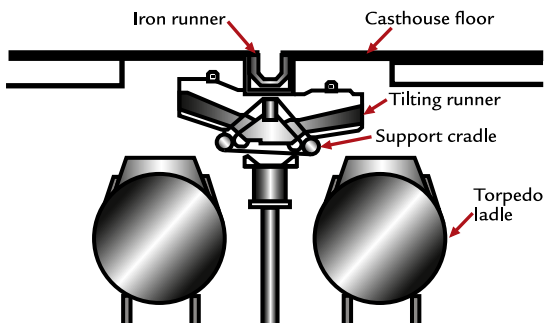


FIGURE 57.4 Tilting runner to fill hot metal ladles. The runner can tilt to the right or left as needed.

refractory performance. Three and four taphole arrangements are provided in Fig. 57.5.

Modern casthouses are designed with relatively flat floors to allow the use of mobile equipment to facilitate manual work. Implementing flat casthouse floors required many changes to provide space for the needed fume collection systems, trough and runner covers, and easy mobile equipment access. Older casthouses had sloped floors and stairs around the troughs and runners to facilitate manual cleaning. Access with mobile equipment was impossible and large crews worked hard to maintain the casting operation. Casthouses have evolved from sloped floors to flat floors as the merits of using mobile equipment became evident (Fig. 57.6).

57.4 CASTHOUSE EMISSION CONTROLS

Casthouse emissions are a major emission source that must be controlled. The emissions are event driven and require a system to collect at the most crucial point sources. A system of hoods is deployed that collects fumes, improves worker hygiene, and allows for worker access to complete necessary tasks. The hoods must be removable for maintenance

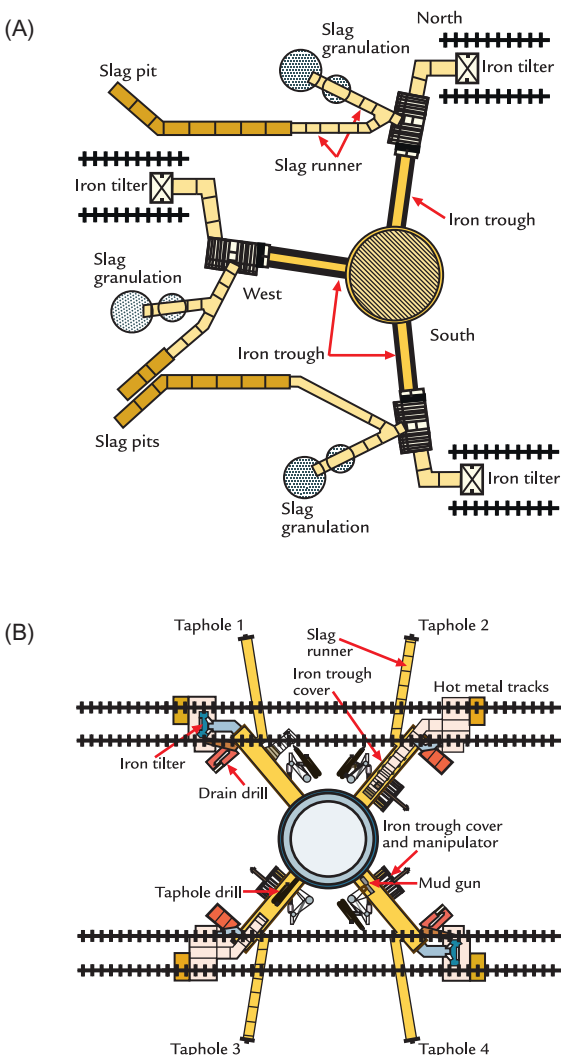


FIGURE 57.5 (A) Blast furnace with a three taphole casthouse. (B) Blast furnace with a four taphole casthouse.

tasks such as trough rebuilding. The important sources of emissions are described in Table 57.1.

A typical casthouse emission system for a single taphole is presented in Fig. 57.7.

The main area of concern is immediately above the taphole, a location where fume generation is the strongest and access from the



FIGURE 57.6 Typical flat casthouse floor. Note the hood manipulator on the right side of the photo and taphole drill and mud gun on the left side. *Source: Photo courtesy of TMT—Tapping Measuring Technology S.à r. l & G.m.b.H.*

TABLE 57.1 Casthouse Emission Sources

Area	Nature of Emission
Drilling	Taphole clay fines blown out as the taphole is drilled open
Oxygen lancing	Iron oxide fumes from lance pipe burning/burning solidified hot metal/slag
Tapping hot metal/slag stream	Iron oxide fume and carbon "kish" are generated where the tapping stream impacts the molten liquids in the main trough and other turbulent areas. Generation of sulfur fumes
Hot metal flow	Generates iron oxide and carbon "kish"
Slag stream	Generates sulfur bearing fumes
Taphole clay	Hydrocarbon fumes generated from taphole clay during plugging
Refractories	Fumes from resin and organically binders/solvents used in refractory products

taphole drill and mud gun is required. Modern casthouses have purposely designed hoods with special manipulators/cranes to facilitate access to open and close the taphole.

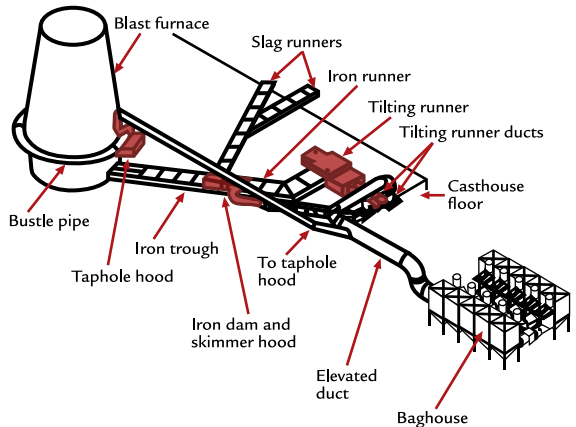


FIGURE 57.7 Typical casthouse emission system and critical hoods are shown in red.

57.5 DRILLING OPEN THE TAPHOLE

Rock mining drills were adapted to blast furnace service and are the standard method to open the taphole and drain the molten iron and slag from the blast furnace hearth. A schematic of a taphole drill is provided in Fig. 57.8.

Early taphole drills were fully pneumatic. Harder taphole clays led to the use of more powerful hydraulic drills able to drill through this clay. A mining rock bit is used to drill the taphole open, the drill rotates and hammers to increase drilling effectiveness. Nitrogen is injected through the drill shaft to clean debris from the drill bit cutting edges. Nitrogen is preferred to compressed air to minimize oxidation of the drill bit and the surrounding refractories/clay which are carbon based. A further improvement is to inject a fine water mist with the nitrogen as a cooling agent. The water mist facilitates the drilling action of the carbide tipped drill bit.

When opening the taphole, it is important to always run the drill its full stoke to be

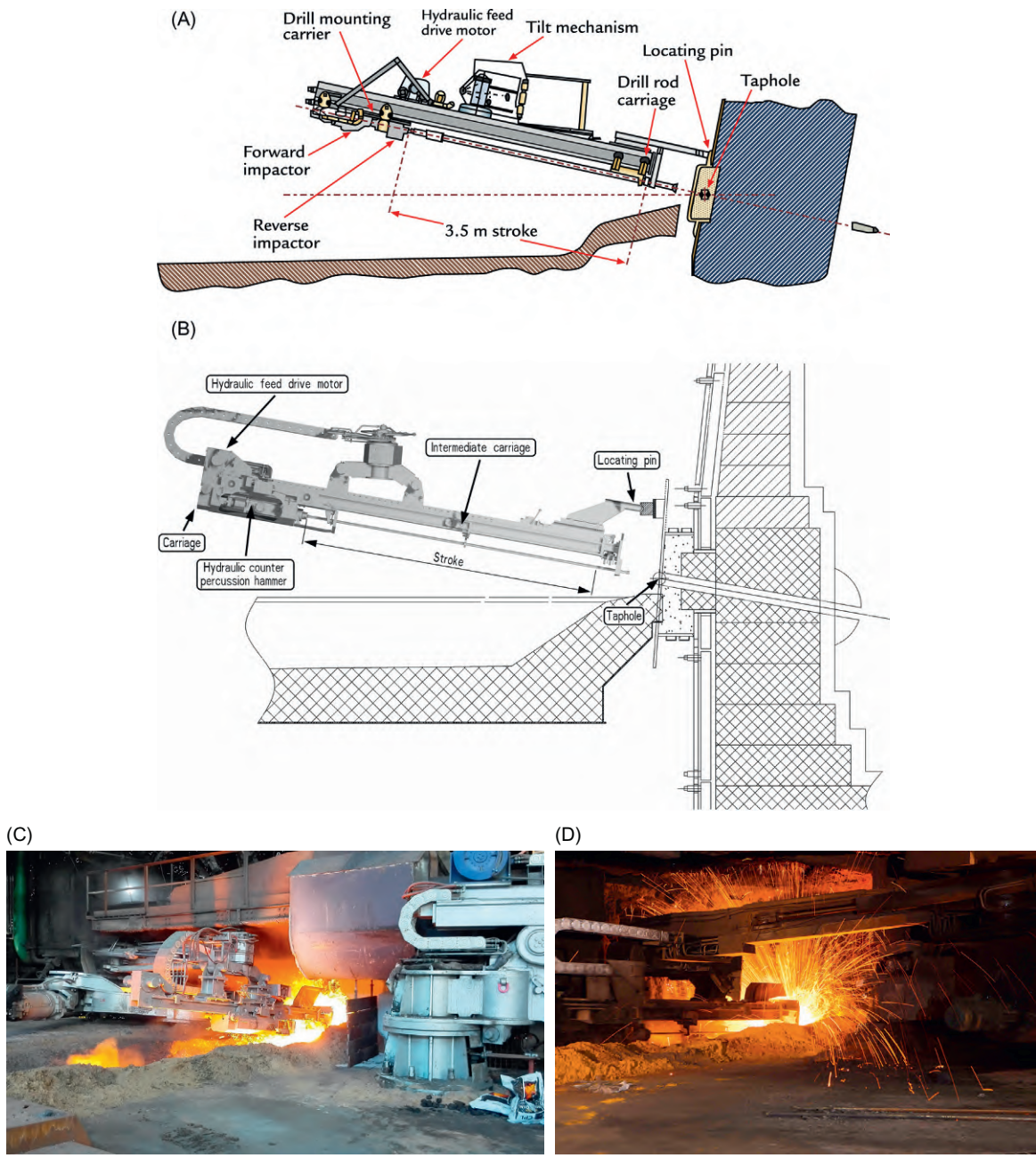


FIGURE 57.8 Blast furnace taphole drill sketches and photographs. *Source: Courtesy of TMT—Tapping Measuring Technology S.p.a r.l & G.m.b.H.*

sure that there is a clear path from the molten pool to the taphole opening. Due to the nature of the mushroom (further described in [Section 57.7](#)), a porous structure could be present near the mushroom hot face that would allow for hot metal flow but at a reduced rate. Drilling the full stroke gives the best possibility that the taphole is open to the hot metal pool.

The taphole is positioned using a locating pin and drills at a downward angle to facilitate drainage. Tapping angles were originally very steep, $15\text{--}25^\circ$, to reach the lower part of the hearth. This angle was reduced to $6\text{--}8^\circ$ as a greater understanding of hot metal and molten slag drainage indicated that a shallower angle facilitated slag removal from the furnace. The taphole is always drilled downward to delay process gases from entering the molten iron/slag stream and causing unwanted splashing too early in the cast. In situations where the blast furnace hearth is chilled, the taphole may be drilled horizontally to drain molten iron and slag from the upper regions of the hearth. Once casting is established, the angle is quickly changed to the commonly used downward angle cite above.

57.5.1 Oxygen Lancing the Taphole

In occasions when the taphole drill is unable to drill through to the molten iron pool, the taphole is manually oxygen lanced open using a mild steel pipe with oxygen injected. Burning the taphole open is both dangerous and challenging as the pipe becomes very soft as it heats up.

In situations where the hearth is frozen, larger diameter lances are used, sometimes with imbedded magnesium wires to create a hotter flame.

57.6 PLUGGING THE TAPHOLE

At the end of each cast, when gas is observed blowing from the taphole, clay is injected into the taphole using the mud gun to stop the casting process. The mud gun is a large and powerful machine that features a hydraulic piston that “extrudes” the taphole clay through a nozzle and into the tapping channel. The positioning system accurately places the mud gun at the taphole opening and has sufficient force to hold the mud gun in position as the stiff taphole clay is injected into the taphole. Taphole clay is commonly preheated prior to being charged into the mudgun. The key features of the mud gun are presented in [Fig. 57.9](#).

Gaining a tight seal is important to assure that there is no clay leakage. Operators have used a variety of ways to create the seal including fiber gaskets and even plywood rings attached to the discharge nozzle.

Once the prescribed amount of clay is added, the mud gun is held against the taphole for a brief period to allow the clay to set up and harden. The clay is “after-pressed” by advancing the piston a small amount, typically a few centimeters in one or two intervals, typically in the first 1–3 minutes after the taphole is closed and the clay is setting up. After-pressing the clay is a well-established technique to densify the taphole clay. Densifying the clay is important to seal cracks in the tapping channel and provide uniform clay performance during the cast. Cracks offer an opportunity for blast furnace gas to leak while casting causing unwanted splash. When done at the correct interval, an increase in the hydraulic cylinder pressure should be observed confirming that the clay density has increased. The after-pressing technique must be automated as the change in piston position

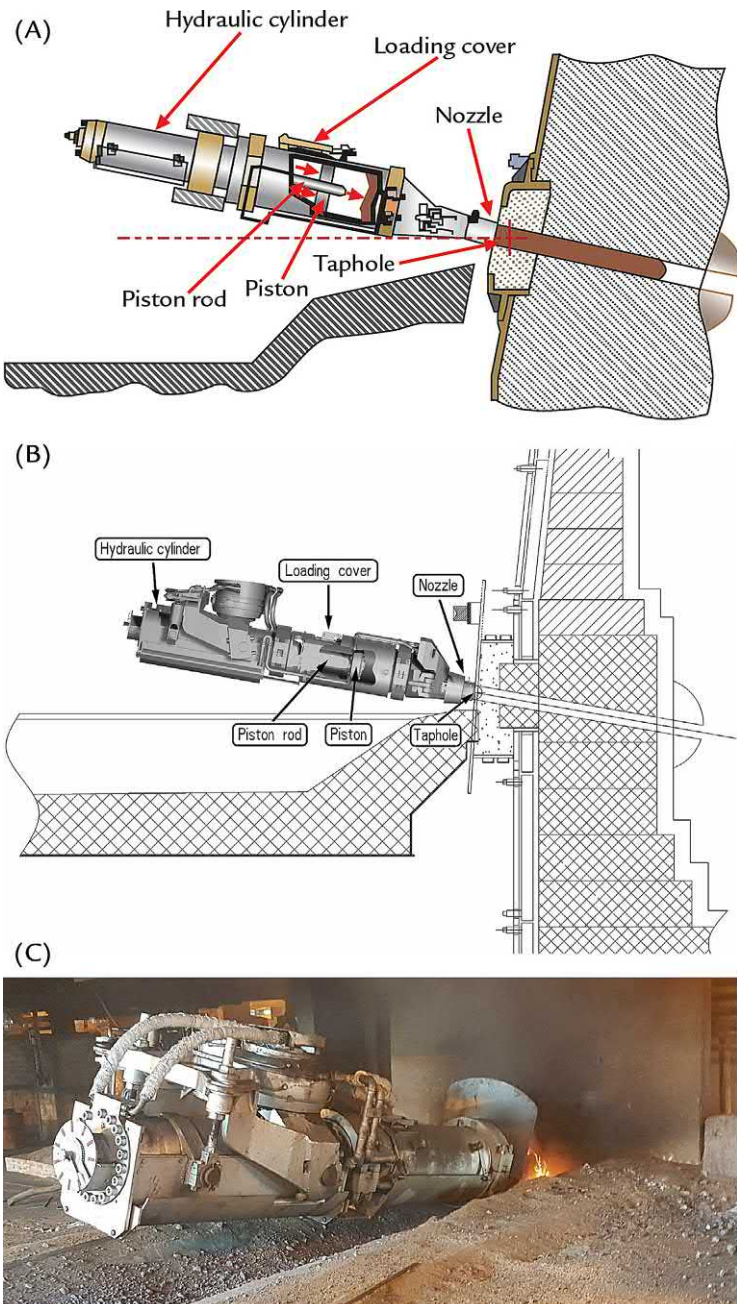


FIGURE 57.9 Blast furnace mud gun sketches and photographs. *Source: Courtesy of TMT—Tapping Measuring Technology S.à. r.l & G.m.b.H.*



FIGURE 57.10 Arrangement of mud gun and taphole drill when located on the same side of the iron trough. Source: Courtesy of TMT—Tapping Measuring Technology S.a. r.l & G.m.b.H.

is very small and difficult for operators to manually complete on a consistent basis.

Mud guns and drills can either be on the opposite or the same side of the iron trough. New plants that feature a hood manipulator as shown in Fig. 57.6 must locate the mud gun and taphole drill on the same side of the trough. This arrangement can be seen in Fig. 57.10.

57.7 TAPHOLE CONSTRUCTION AND THE BEEHIVE OR MUSHROOM

The taphole construction inside the blast furnace features a spool piece to pass through the steel shell and hearth wall cooling system followed by the carbon hearth wall. A hearth wall abutment is constructed where the hearth wall is thicker, with a size of about three tuyeres wide in the taphole area. A typical taphole construction for a stave cooled hearth wall is provided in Fig. 57.11.

The taphole face is constructed with very strong refractory material that can withstand the pushing forces from the mudgun. Due to multiple openings, the taphole face must be

periodically rebuilt to provide a flat surface for the mudgun to push against. This is also important to minimize blast furnace gas leakage through the refractory system.

Blast furnace operators measure the length of the taphole each cast by observing length drilled. Taphole length is maintained at 2.5–3.5 m by changing the amount of taphole clay added. Consistent taphole length is one of the most important parameters that the casthouse team must manage and maintain.

Closing the taphole creates a deposit of clay on the inner wall. This deposit is known as either a beehive or mushroom based on observations from hearth dissections of blown out blast furnaces. The ability to continuously replenish the mushroom allows the blast furnace taphole to have a long life and tap millions of tons of hot metal. The structure of the mushroom developed over time is shown in Fig. 57.12.

With a consistent plugging and drilling practice, the mushroom integrity can be maintained for the entire life of the blast furnace hearth. The mushroom integrity can be compromised by water leakage and poor or variable quality taphole clay.

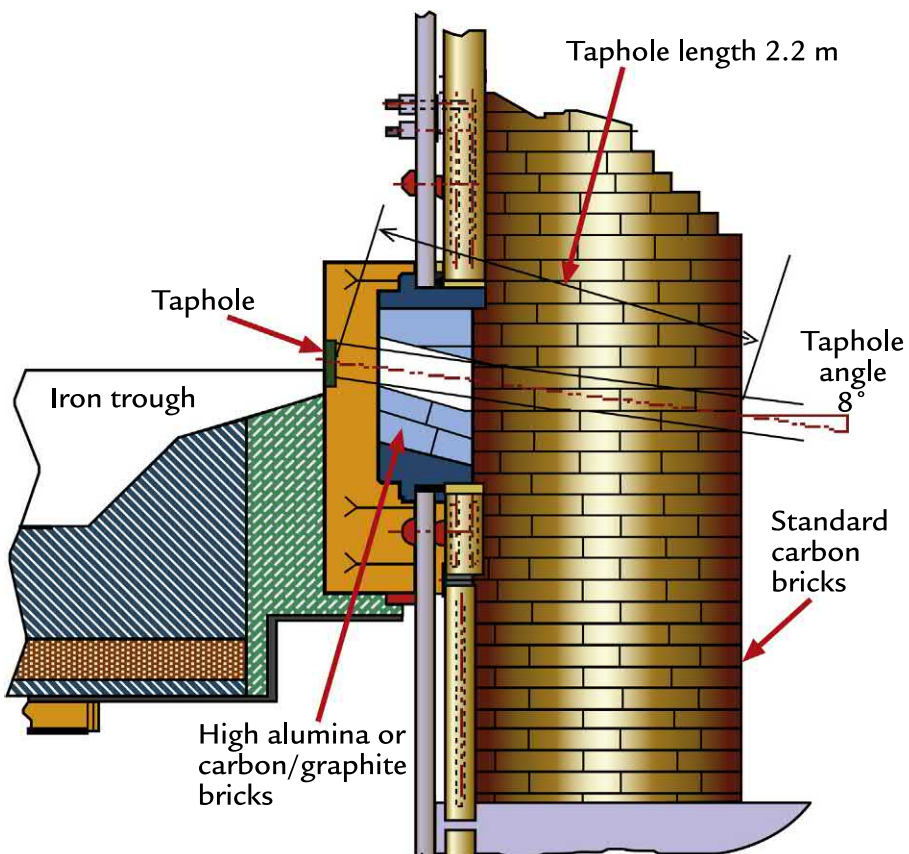


FIGURE 57.11 Blast furnace hearth wall construction at the taphole area.

57.8 TAPHOLE CLAY

Taphole clay is one of the most important consumables used at the blast furnace. Superior quality clay provides consistent removal of the liquid hot metal and slag and is mandatory for a stable blast furnace operation. Taphole clays are complex and purpose designed to meet the demands of removing molten iron and slag at 1480–1520°C for extended periods, say 1–3 hours with minimal erosion (Fig. 57.13).

A high-quality taphole clay must;

- be pliable/plastic enough so that the mudgun can push the clay into the taphole;

- set up and harden in ~15 minutes and be fully sintered before the next cast;
- be weak enough that the taphole drill can drill through the solidified clay to open the taphole;
- resist erosion from hot metal and slag for cast times from 1 to 3 hours in duration;
- resist erosion while tapping both hot metal and molten slag over the entire cast;
- sustain molten iron and slag temperatures from 1450 to 1540°C;
- sustain taphole diameter for slag superheat from 50 to 180°C; and
- meet workplace health standards for aromatic hydrocarbons and other fumes.

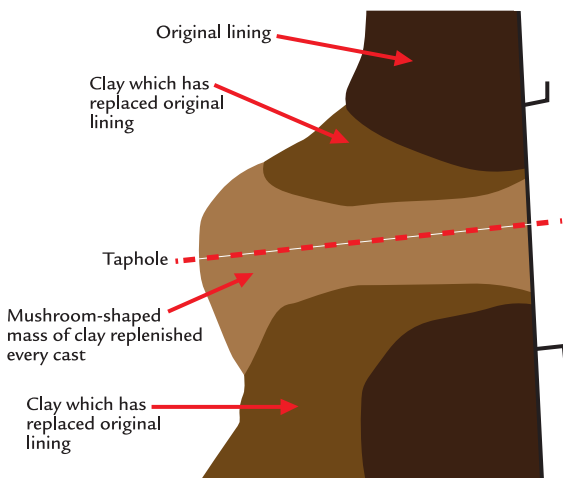


FIGURE 57.12 Elevation view of the taphole mushroom or beehive formed from taphole clay.

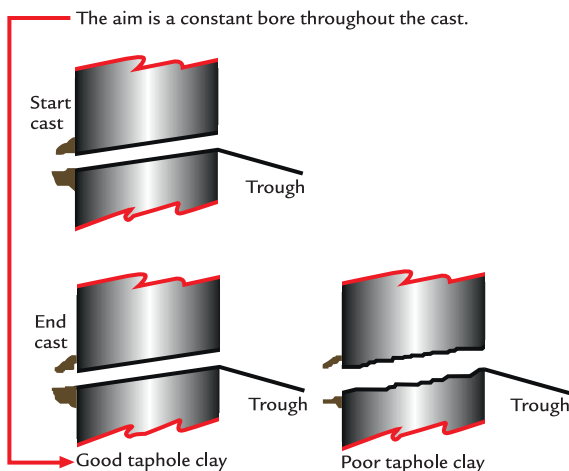


FIGURE 57.13 A good taphole clay has minimal erosion during the cast.

Early taphole clay was made of ~60% sand, ~20% metallurgical coal, and ~20% tar from the coke by-product plant. As productivity and blast pressure increased, stronger clays were developed. Sand was replaced with bauxite, and higher quality metallurgical coals

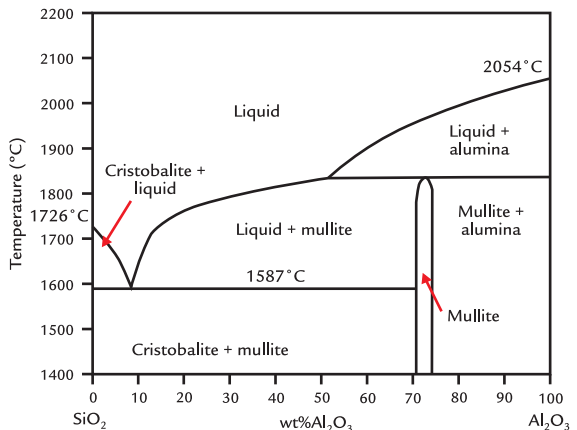


FIGURE 57.14 Alumina–silica phase diagram offers a variety of taphole clay compositions.¹

were introduced; the carbon provides slag erosion/corrosion resistance. Silicon carbide was added to protect the carbon in the clay from oxidation and enhance slag wear qualities of the taphole clay. Silicon nitride is added to improve the final clay strength and its corrosion properties as silicon nitride is not wetted by slag. Metallic silicon and aluminum can be added; these form carbides in the clay, reinforcing the clay strength at elevated temperature.

The main constituents of the taphole are alumina and silica - in solution, these minerals are solid up to 1587°C (Fig. 57.14).

Blast furnace slag, which is relatively rich in silica and has a much lower alumina content, will tend to erode alumina when the clay alumina content is low. Clays with a high alumina-to-silica ratio (> 55) will resist erosion at higher temperatures as the liquidus temperature of alumina–silica mixtures increases above 1850°C. Sintered and fused bauxite offers base materials with a high purity of alumina needed to improve slag erosion resistance. Silicon carbide improves slag corrosion properties of the taphole clay.

Tar was the preferred binder for many years but its use has diminished due to the release of carcinogenic polycyclic aromatic hydrocarbons.

Petroleum pitch has been used as a replacement binder with satisfactory results.

As an alternative to tar, phenol resin-bonded clays were developed. Resin-bonded clays cure at a much faster rate than tar-bonded clays and must be handled to avoid overheating in the mud gun before being used to close the tap-hole. Resin-bonded clays are good options for single taphole blast furnaces as the short curing time allows for the taphole to be reopened about 10 minutes after plugging rather than the 20 minutes required to fully cure tar or pitch-bonded clays. With resin-bonded clays, the after-pressing technique used to densify the tar bonded clay cannot be used as the resin-bonded clay hardens too quickly.

57.9 TROUGH DESIGN AND IRON-SLAG SEPARATION

Iron and slag are cast together through the open taphole. Initially, only iron is cast. The

proportion of slag increases during the cast and by the end, the tapping stream is predominately slag. The molten slag and iron discharge to the iron trough where the iron and slag are separated, typically by a skimmer. Some key performance objectives for the main trough are summarized in Fig. 57.15.

The iron trough was initially sloped to create a pool at the dam and skimmer to effect slag separation. This design featured high refractory wear where the molten iron and slag landed. Slag carryover to the torpedo or open ladles was also a challenge due to the strong stirring of the molten iron and slag in the trough. The blast furnace slag is very high in sulfur and this will cause quality challenges in steelmaking as most of the sulfur in the carried over slag will report to the liquid steel. This iron trough design was known as a non-pooling trough.

To improve slag–metal separation and reduce refractory wear, semipooling and pooling trough designs were developed. With a

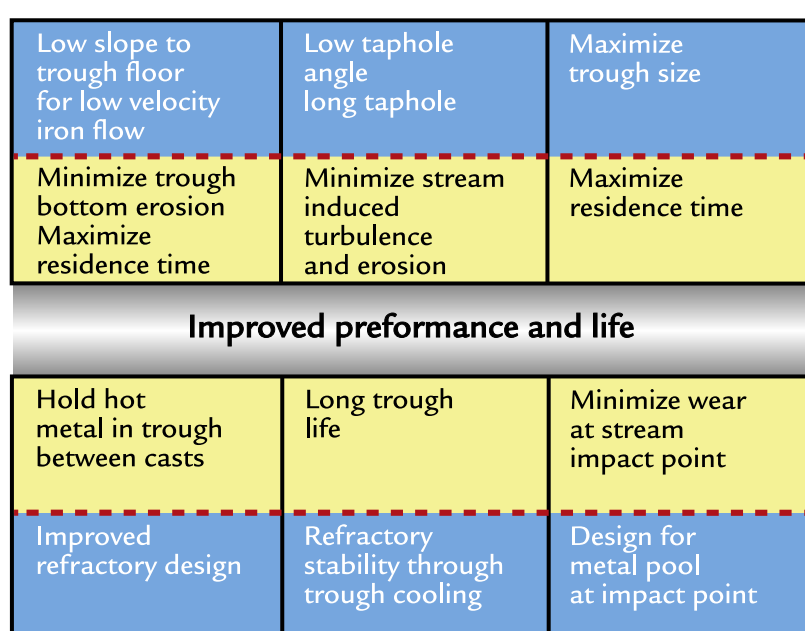


FIGURE 57.15 Key iron trough parameters to achieve iron–slag separation and long refractory life.

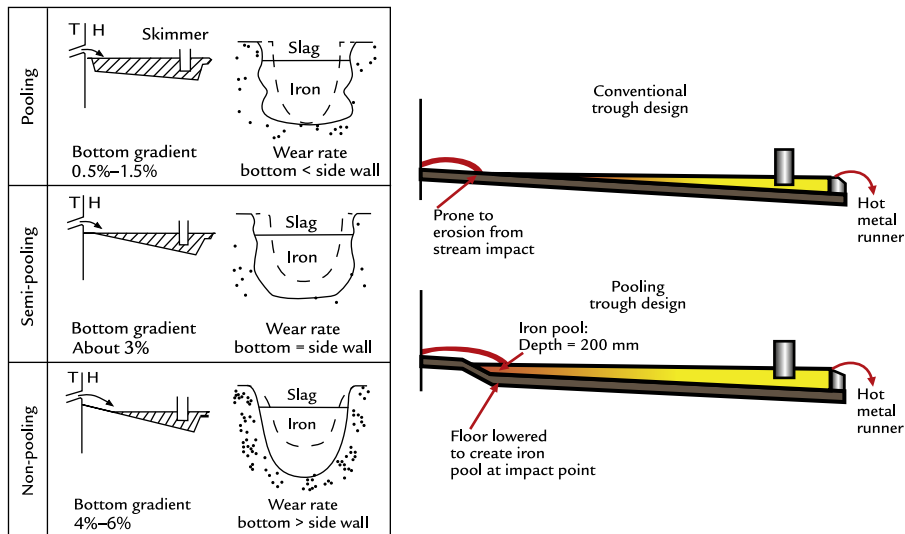


FIGURE 57.16 Profile and refractory wear of conventional, semi-pooling, and pooling trough designs.²

pooling trough, the floor slope is decreased and a liquid pool about 200 mm deep is created in the impact zone. The energy from the molten tapping stream is dissipated by the liquid pool and iron–slag separation improves. The non-pooling, semipooling, and pooling trough designs are compared in Fig. 57.16.

Cameron and Tudhope evaluated the flow patterns in the iron trough using a full-scale water model.² Using the model, they measured liquid flows and defined turbulent and quiet zones for the nonpooling and pooling trough designs, Fig. 57.17.

Variables that affect the residence time and degree of plug flow needed for slag–iron separation are the trough volume, tapping energy, and trough length. From a chemical reactor viewpoint, increasing trough volume did increase the residence time from taphole to hot metal discharge, Fig. 57.18.

Cameron and Tudhope defined the tapping energy as a measure of the kinetic energy that the tapping stream inputs into the iron trough.² The tapping stream energy considers the impact of tapping rate and taphole

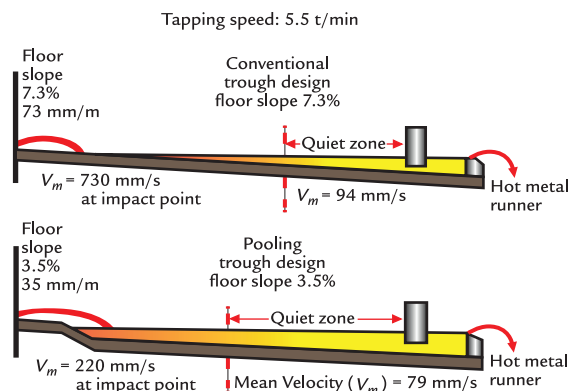


FIGURE 57.17 Comparison of nonpooling and pooling trough designs.

diameter on the stream energy as the molten hot metal leaves the taphole. Increasing the tapping stream energy reduced the degree of plug flow and hence the minimum residence time due to additional agitation, Fig. 57.19.

A larger quiet zone improved the residence time needed for iron and slag to separate before reaching the slag skimmer plate. For a

pooling trough, the quiet zone size is largely determined by the length of the trough and the degree of plug flow present. The critical dimension is the length of the trough from the beginning of the quiet zone to the face of the skimmer plate. In the quiet zone, slag particles

rise at their terminal rising velocity as defined from Stokes' Law. Increasing the quiet zone length provides additional time for slag particles to float, Fig. 57.20.

Using Stokes' Law and the measurements made on the water model, Cameron and Tudhope could characterize the performance of various iron troughs by taking a hot metal sample after the skimmer and measured the size and frequency of the slag particles present in the clean hot metal. A comparison of three different troughs is provided in Fig. 57.21; over 90% of the observed slag particles were smaller than estimated from Stokes' Law.

After collecting the data presented in Fig. 57.21, in 1993 Stelco's Blast Furnace E was relined and the trough length increased. A post evaluation showed that the new trough design decreased the amount of slag carryover to the hot metal torpedo cars. Iron samples were analyzed for slag inclusions in the same manner as the original 1987 test

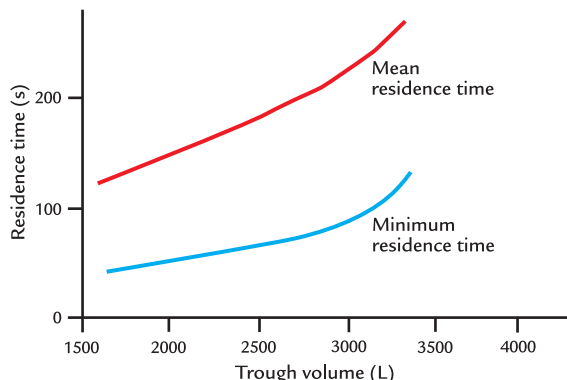


FIGURE 57.18 Impact of increasing iron trough volume on the residence time to reach hot metal discharge.

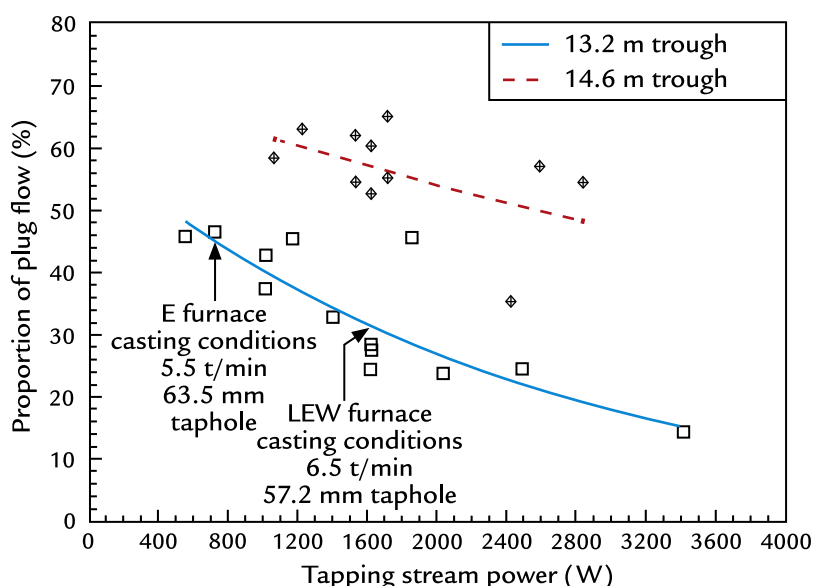


FIGURE 57.19 Impact of tapping stream power or kinetic energy on the degree of plug flow observed for the larger 14.6m trough used at Stelco Lake Erie Works (LEW) Blast Furnace No. 1 and the smaller 13.2m trough implemented at Stelco's Hamilton Works E Blast Furnace in 1993.²

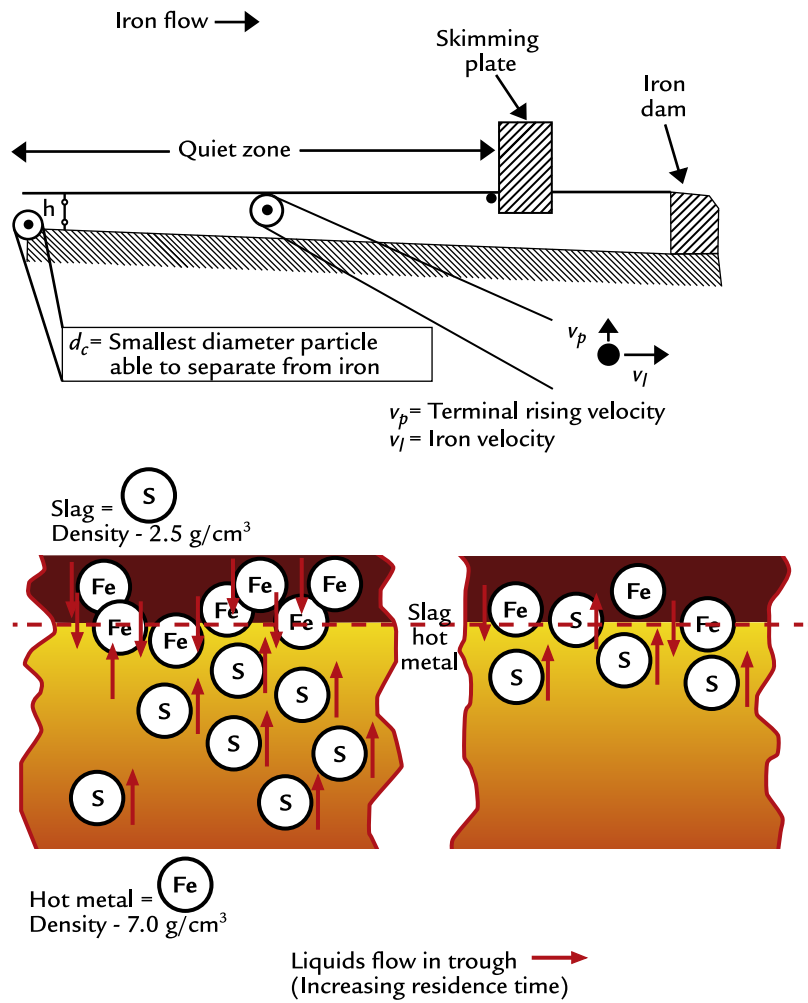


FIGURE 57.20 Iron and slag separation in the quiet zone of the iron trough.

completed prior to implementing planned trough design modifications. This comparison indicated an immense improvement in slag/iron separation as illustrated in [Table 57.2](#).

The significant improvement in slag inclusion numbers and reduction in slag inclusion size range after redesigning the E Furnace trough based on water modeling principles is shown in [Fig. 57.22](#).

Taphole angle and length can impact the trough refractory performance and slag/iron separation. Ideally, the tapping stream should have a low arch and minimal flaring or splashing as illustrated in [Fig. 57.23](#).

Typical trough slopes and dimensions are provided in [Fig. 57.24](#) for a pooling trough design. The key is to create a pool for the molten iron and slag stream to land in and to

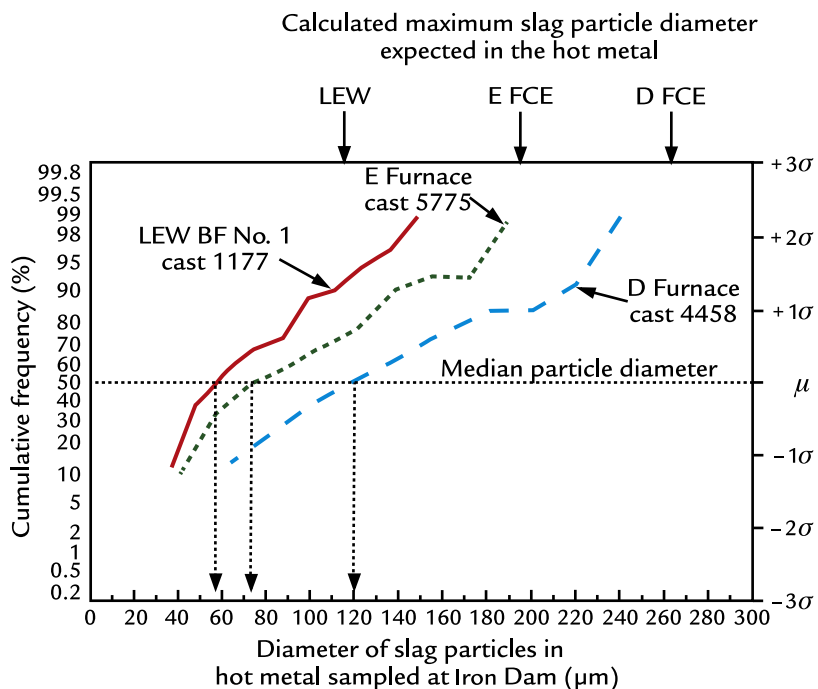


FIGURE 57.21 Slag particles in clean hot metal measured at Stelco Lake Erie Works Blast Furnace 1, Stelco Hamilton Works Blast Furnace E and Blast Furnace D.²

TABLE 57.2 Slag Inclusion Analysis for the Stelco E Blast Furnace Trough

Year	Mean Slag Particle Diameter (μm)	Slag Particle Diameter Standard Deviation (μm)	Quantity of Slag (ppm by volume)	Tonnes of Slag per Million Tonnes of Hot Metal
1987	108	43	177	67
1993	69	20	6	2

dissipate the kinetic energy associated with the tapping stream as soon as possible.

The main trough construction can include cooling ducts or pipes to help maintain the planned shape of the trough and protect

the outer trough box from heat-related distortion. When the decision is made to use cooling, the cooling elements are surrounded by heat conducting refractories. The refractory working lining must have good corrosion resistance to both hot metal and slag. The most challenging location is the slag–iron interface where the refractory must sustain conditions of both oxidation and reduction as the carbon-rich hot metal and the oxidized slag cycle over a narrow elevation of refractory materials. The hot metal–slag interface often dictates trough service life. A typical trough construction can be seen in Fig. 57.25.

Trough service life is typically 1 month between repairs. Some plants may have a series of intermediate repairs followed by a major rebuild. Intermediate repairs can take

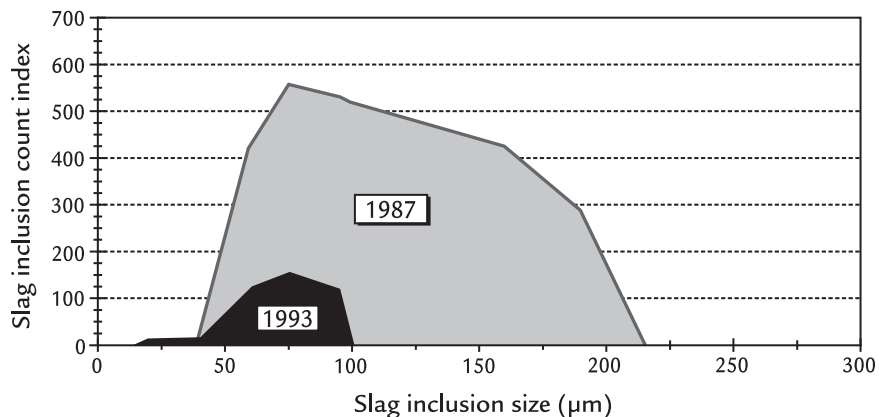


FIGURE 57.22 Slag inclusions analyses for Stelco's E Blast Furnace trough follow redesign.³

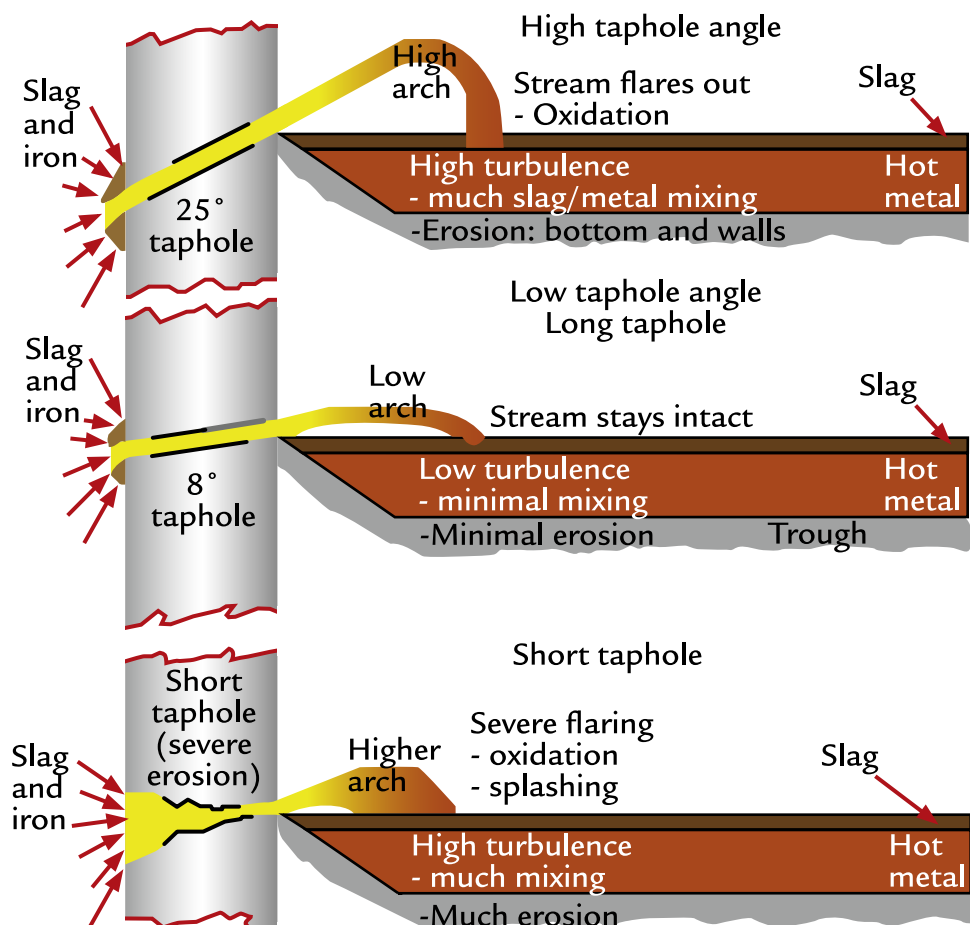


FIGURE 57.23 Impact of taphole angle and length on the tapping stream arch, refractory wear, and iron–slag separation.

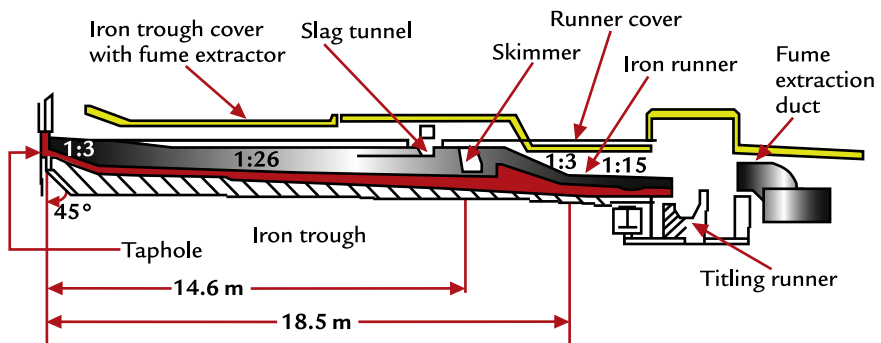


FIGURE 57.24 Typical slope and length of a pooling trough.

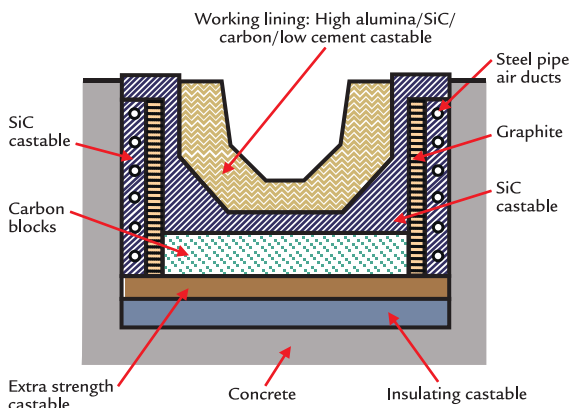


FIGURE 57.25 Typical iron trough refractory construction.

a few days while a major repair requires about a week to complete.

57.10 CASTING SCHEDULE

Ideally the casting rate of iron and slag should equal the rate at which the iron and slag are produced in the blast furnace. Under these conditions, there is no accumulation of the liquids in the blast furnace hearth. When liquids accumulate, they can exert back pressure on the tuyere raceways and distort the gas flow in the blast furnace, forcing more gas flow to the furnace

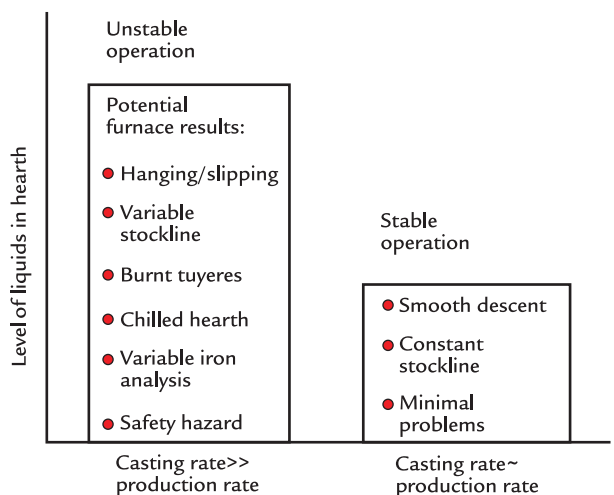


FIGURE 57.26 Impact of cycling the hearth liquid levels on the blast furnace operation.

walls. Many small casts can lead to unstable operations per Fig. 57.26.

With three and four taphole blast furnaces, tapping continues for prescribed period, about 2 hours before one taphole is closed and another opened. If the working taphole is spitting molten materials and otherwise showing that it is dry or empty, it may be closed and the second taphole opened. Periodically, say once a shift, a working taphole can be left open until a gas blow is observed to provide a reference point that the

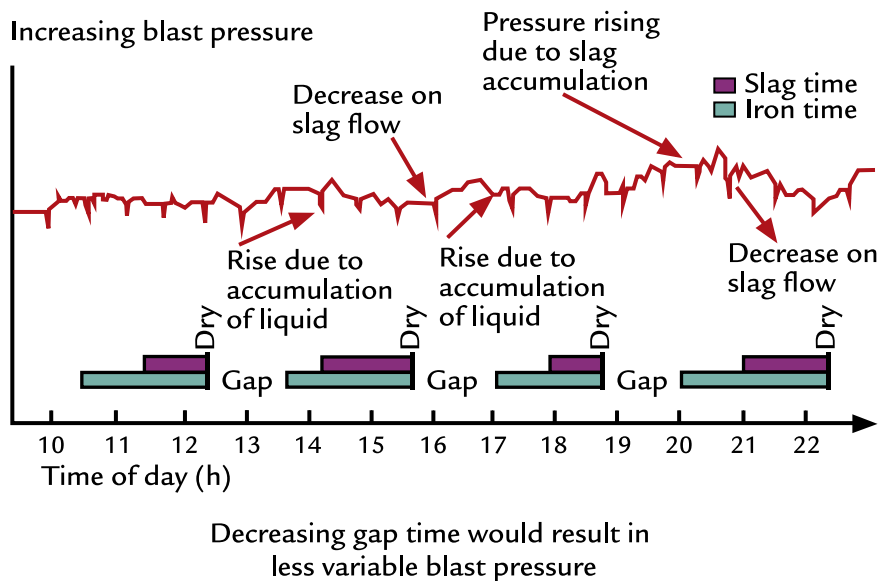


FIGURE 57.27 Impact of reduced slag time on blast pressure for a single taphole blast furnace.

hearth is dry with no residual molten iron and slag present.

Blast furnaces with two tapholes can operate on a similar basis but must reduce production when one of the iron troughs is taken out of service. During the maintenance period, a one-taphole practice must be followed.

Single taphole blast furnaces must have a delay from taphole close to taphole open to allow sufficient time for the taphole clay to cure and harden so that it is ready for the next tapping cycle. For tar-bonded taphole clay, this delay time will be about 15–20 minutes. Resin-bonded tapholes cure faster allowing the blast furnace operator to re-drill the taphole in about 8–10 minutes. A larger drill bit must be employed to assure that the tapping rate is greater than the production rate of iron and slag. Single tapholes are ideally tapped until a gas blow is observed to give confidence that the hearth is dry at the end of each cast. If there is no gas blow observed after a few casts, the production rate may

need to be reduced until such time that a gas blow is observed. An example of the impact on blast pressure for a single taphole operation is provided in Fig. 57.27.

In addition to impacting the blast pressure, accumulating and then rapidly draining the hearth can lead to slow–fast–slow charging rates and stockline movement. A major accumulation of liquid iron and slag can increase blast pressure and reduce the charging rate. In the extreme, molten slag and occasionally hot metal are at an elevation higher than the tuyeres. In this case, a sudden shutdown of the blast furnace will lead to blockage of the tuyeres and a delayed start-up to clean the tuyeres and remove the solidified slag and iron. This is a major risk that should be avoided, Fig. 57.28.

57.10.1 Casting Times

Details of the casting events must be meticulously recorded and logged for analysis and

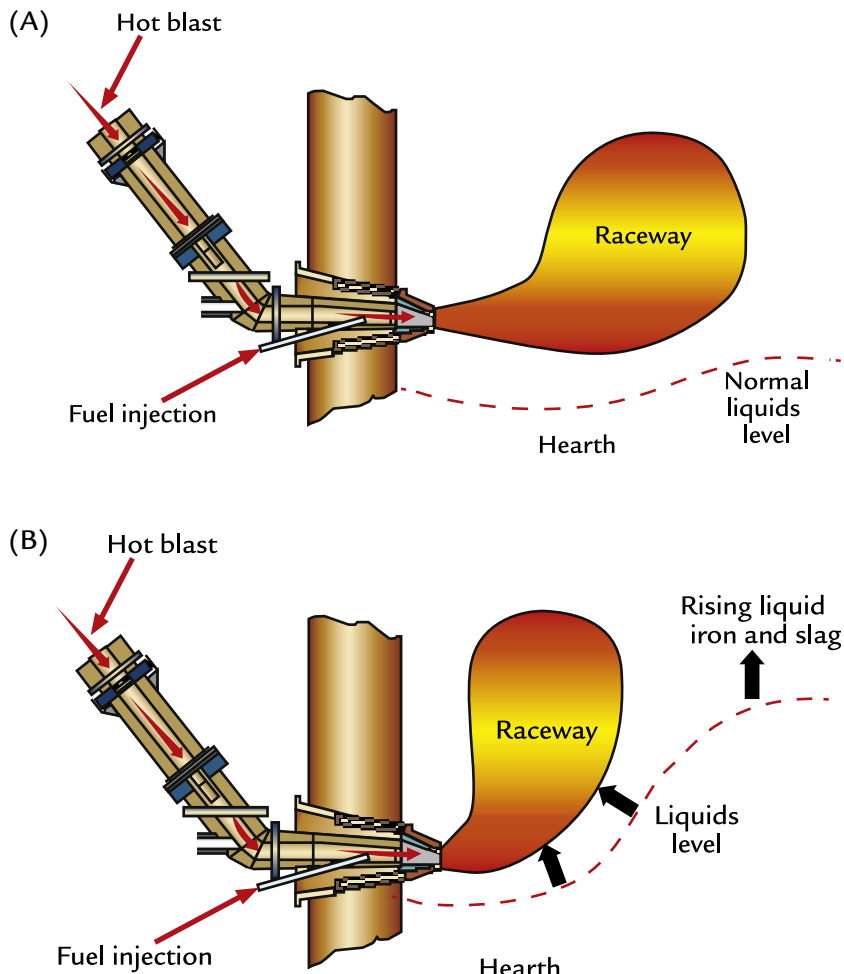


FIGURE 57.28 Raceway deformation and risk of filling tuyeres with molten iron and slag when a high liquid level is present and blast pressure is suddenly lost. (A) Normal raceway position with liquids below the tuyeres, (B) raceway pushed toward the wall as liquid levels rise above the tuyeres.

performance improvement. Important times to log include;

- time when drilling starts,
- time when drilling ends and molten iron or slag flow begins,
- time when slag flow starts from the iron trough to slag pit or granulator, and
- time that the taphole is plugged.

During casting, it is common to allow a head of slag to accumulate in the iron trough held by a simple sand dam. Once a designated amount of liquid slag has accumulated, the slag dam is broken and slag runs to the pit or granulator. Operators generally want a significant initial run of slag to be assured that the slag can flow down the slag runner without

freezing and blocking the runner. The slag time begins when the slag dam is broken.

avoid “false blows” that indicate that the hearth is drained when residual liquids remain.

57.10.2 Dry Hearth Practice

A dry hearth practice is when iron is tapped continuously and slag is tapped 95% of the time. The reduced slag time is to account for the time to accumulate slag in the iron trough before the slag dam is broken. Maintaining a dry hearth is essential for large blast furnaces with 2–4 tapholes that can sequentially cast on alternate tapholes without delays. Smaller blast furnaces that use one taphole must accumulate liquid iron and slag during the period that the taphole clay cures at the end of each cast, typically 20 minutes. This is also the case for two-taphole blast furnaces when one-taphole is out of service for repairs.

A dry hearth practices assures;

- that increasing hearth liquid levels do not impact gas flow in the blast furnace by exerting pressure on the raceway regions;
- smooth descent of the burden as iron and slag do not accumulate in the hearth; and
- allows for the blast furnace to be rapidly shutdown at any time without fear of filling the tuyeres and blow pipes with molten iron and slag. This includes emergency shutdowns.

The challenges implementing a dry hearth practice include;

- training operators to manage taphole openings/closing that keep the hearth dry;
- suitable torpedo ladle logistics to assure that ladles are always available when needed to avoid casting delays;
- consistently high coke quality so that liquid iron and slag drain easily from the hearth and deadman zones to the tapholes; and
- taphole clay that erodes at a predictable and stable rate, especially when casting slag to

57.10.3 Iron Gap Time

The iron gap time is the time between the closing of the working taphole and the subsequent opening of the next working taphole. For blast furnaces casting continuously, the iron gap time is zero. For single taphole blast furnaces, the iron gap time is 10–20 minutes depending on whether tar-bonded or faster setting resin-bonded clay is used. For two taphole blast furnaces, a small gap may be employed, say 5–10 minutes, due to torpedo ladle logistics and train movements needed between closing and opening tapholes.

57.10.4 Slag Gap Time

The time from closing the taphole until the next time that the slag dam is broken and slag is cast is known as the slag gap time. Some operations define the slag gap time as the time from taphole opening to slag casting. The authors prefer the first definition as it makes a good comparison of the slag casting-to-production ratio.

The slag gap time is critical to manage as it triggers countermeasures such as overlapping casts or a reduced production rate if slag is accumulating in the blast furnace. The percentage of time that slag is casting is an excellent measure of the blast furnace health. For large blast furnaces, a slag casting time of 95% should be maintained. For smaller single taphole blast furnaces, the typical slag time of 50–60% is experienced due to the iron gap and then time delay to cast slag from the blast furnace.

Percentage of time slag casting can be used as feedback on taphole clay quality - slag is

much more erosive to taphole clay than hot metal. Together with the slag superheat (measured slag temperature minus slag liquidus temperature), the percentage of slag time casting can indicate if the taphole clay erosion rate is consistent and low.

57.10.5 Overlapping Casts on Multiple Taphole Blast Furnaces

Multiple taphole blast furnaces will open two tapholes and have overlapping casts when too much slag has accumulated in the blast furnace. Slag delays can be related to the use of a drill bit that is too small, reduced taphole erosion when tapping slag with lower temperature/superheat, and while adjusting to changes to the production rate. Poor hearth permeability can reduce slag flow to the taphole and lead to slag delays. A slag with a composition that provides a low liquidus temperature can cause slag to accumulate in the blast furnace; this will be discussed in more detail in Chapter 58, Blast Furnace Slag.

When slag has not been cast for 15–20 minutes following the close of the working taphole, a second taphole should be opened. Ten to fifteen minutes after slag flow has started, one of the working tapholes must be closed to prepare for the next cast.

Frequently, the taphole that was opened to accelerate drainage is the taphole that is selected to be closed to provide the needed 20 minutes for the taphole clay to harden so the taphole is ready for the next cast. In some instances, the initial taphole is closed first. This is an on-the-spot judgment as to how fast the casthouse can be turned around so that a taphole is ready in a 20-minute period.

In Figs. 57.29 and 57.30, examples of overlapping casts are provided. In Fig. 57.29, taphole 3 is opened twice to accelerate drainage while also taking taphole 1 out of service and bringing taphole 2 into service.

In addition to slag delays, sometimes slag flow can stop or slow due to drainage issues in the blast furnace hearth. This can be a reason to initiate an overlap cast to be assured that the slag casting rate is greater than the production rate so the slag accumulation can be reduced or eliminated. An example of this is provided in Fig. 57.30.

A practice using overlapping casts is encouraged by creating a workable slag gap time criteria to indicate when to open a second taphole. As noted in the next section, changing the taphole diameter is harder to judge and control and may yield a less predictable acceleration of the molten iron and slag removal rates.

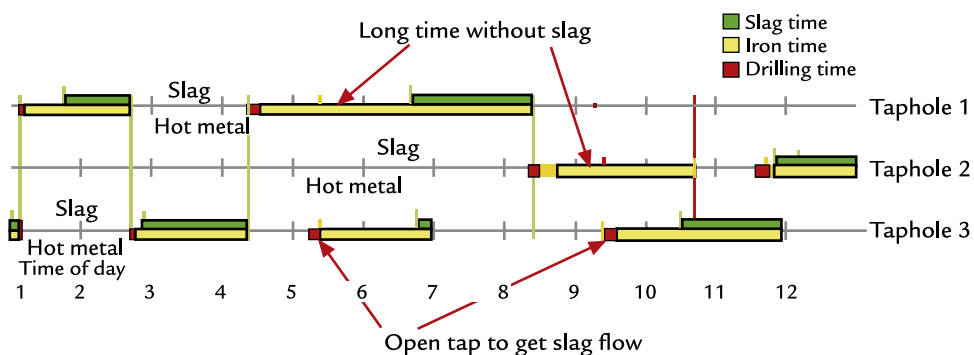


FIGURE 57.29 Overlapping casts using taphole 3 to accelerate slag drainage while bringing taphole 2 into service. Two 90-minute slag gaps can be observed.

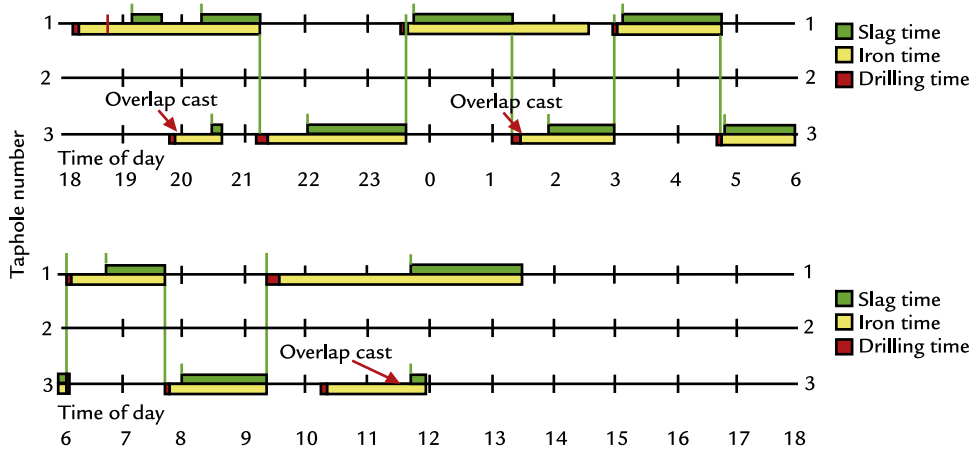


FIGURE 57.30 Use of an overlapping cast for delayed and interrupted slag flow.

57.10.6 Drill Bit Diameter

Selecting the appropriate drill bit size requires a detailed analysis of the blast furnace production rate, blast pressure, and taphole clay erosion characteristics. Limits to the range of drill bit diameters available for use must be strictly managed. Increasing the drill bit too fast as a countermeasure to a full hearth can lead to what is known as a false gas blow - this is when the liquid iron and slag cannot get to the taphole at the desired rate and blast furnace gas is prematurely released. This gives the impression that the hearth is empty when in fact there is a significant residual of molten iron and slag present.

For multiple taphole blast furnaces, a practice of limiting the available drill bits of different diameters is preferred and for the operators to use overlapping casts as the first countermeasure to drain the hearth of accumulated slag and hot metal. For a single taphole blast furnace again, the practicing of limiting the available drill bits is encouraged—should accumulating hot metal and slag be observed, the blast furnace production rate should be reduced to allow the accumulated iron and slag to drain over a few casts.

57.10.7 Measuring Hot Metal Temperature and Sampling

Spot hot metal temperatures may be measured several times during a cast using a dip thermocouple. In doing so, the operator must understand that hot metal temperature will rise during the casting process. Initially, the hot metal may be colder due to time spent in the hearth where the hot metal cools and the mixing of the tapped hot metal with the cooler hot metal present in the iron trough. Molten slag can be hotter than hot metal as slag is at a higher elevation and closer to the tuyere raceways, the hottest zone of the blast furnace. As hot metal and slag drain concurrently, the hotter slag can increase the hot metal temperature.

The hot metal temperature measured when the slag dam is broken is usually considered the most representative temperature of the hot metal and slag in the blast furnace hearth. This value is often used as the cast hot metal temperature and for fuel rate control purposes. Alternately, the temperature can be measured as each torpedo ladle is filled and averaged.

Technology to allow for continuous measurement of the hot metal temperature

upstream of the iron dam is available. A refractory tube is immersed in the hot metal pool between the slag skimmer and iron dam and the temperature of the bottom of the tube is continuously measured. This allows for rapid detection of hot metal temperature so changes to fuel rates can be implemented at the earliest opportunity.

The slag and hot metal should be sampled the moment the slag dam is broken open. This gives a repetitive event that allows for a fair comparison between casts. Many blast furnaces sample the hot metal in each torpedo ladle to facilitate downstream processing steps such as hot metal desulfurization or for weighing the appropriate amount of hot metal for basic oxygen furnace steelmaking.

57.10.8 Hearth Drainage

Understanding hearth drainage and the accumulation of iron and slag in the hearth has been an area of increasing focus. This requires an accurate measure and comparison of the rate of hot metal and slag production to the rate at which hot metal and slag are removed from the blast furnace. Hot metal and slag production are accurately measured for injected fuel rate control, so these values are generally available. The challenge is to measure the casting rates of the molten iron and slag.

Blast furnace operators have learned to measure slag casting rates from the slag granulation equipment. Two methods have been employed;

- measurement of the water temperature gain during granulation has been correlated to the casting rate of the slag entering the granulator; and
- in systems where a dewatering drum is employed, the torque of the dewatering drum as slag is lifted and water removed, has been correlated to the slag casting rate.

The hot metal casting rate has been measured by noting the amount of hot metal added to each ladle. This can be done using several techniques:

- Implementing a scale under the casthouse to weigh each ladle as it is filled.
- Using a microwave or laser level detector to measure the degree of ladle fill and correlate this to the ladle's historic carrying weight.
- Measuring the compression of the torpedo ladle springs as the torpedo ladle fills. An example of this is provided in Fig. 57.31.

57.11 MODELING OF THE HEARTH LIQUID LEVEL

Comparing the molten iron and slag production to their respective casting rates allows for estimation of the liquid level in the blast furnace hearth. With such information in place, the irregular nature of casting rates compared to production rates becomes evident. Also, the impact of liquid levels on blast pressure can be identified. With slag and iron liquid levels available, the operator can better anticipate when a suitable countermeasure should be employed, such as overlapping casts, changing drill bit diameter, or reducing the production rate.

An example of a simplified hearth liquid level management system is provided in Fig. 57.32.

The blast furnace hearth can be modeled as a control volume being continuously filled and periodically drained. Filling comes from the production of hot metal and slag as the iron ore is reduced and melts. Periodic draining results from the casting practice employed by the blast furnace operators. Knowledge of these material flow rates at a given time, as well as blast furnace geometry and material properties, allows for hearth liquid levels to be

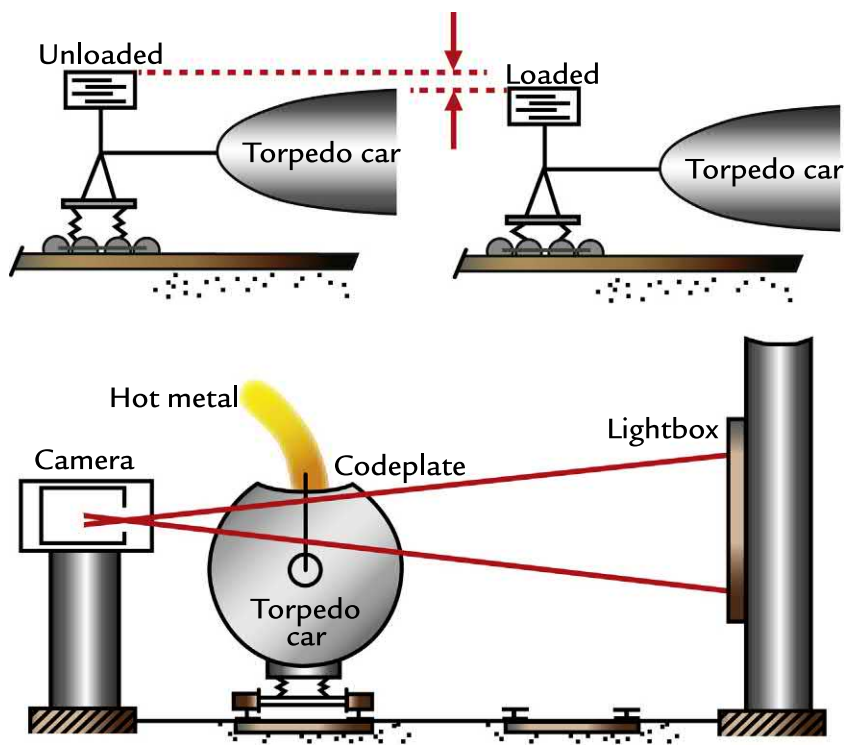


FIGURE 57.31 Measurement of hot metal casting rate based on compression of the torpedo ladle suspension.

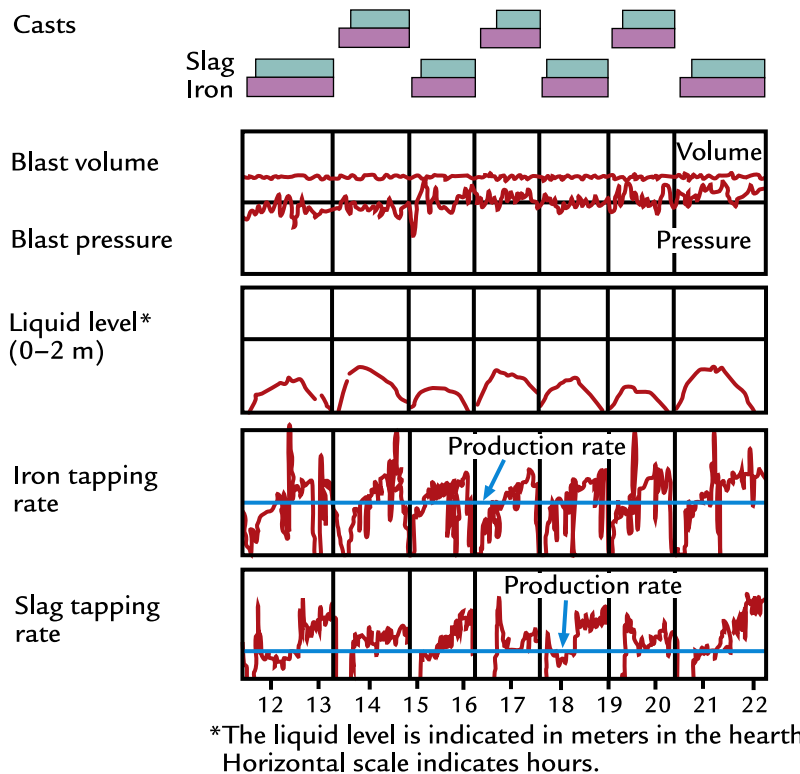


FIGURE 57.32 Comparison of slag and iron casting rates to estimated molten liquid level in the hearth.

estimated. [Table 57.3](#) summarizes the overall mass balance equation, key parameters, and calculated parameters used in a simplified hearth drainage model.

The assumptions necessary to calculate the (1) filling, (2) accumulation, and (3) draining components of the model are described in the following sections.

57.11.1 Filling - $m_{i,in}^i(t)$

Calculation of the hearth filling rate is the easiest of the three model components. Most plants estimate the instantaneous material production rates based on charging models, or analysis of the blast furnace top gas. Finding $m_{M,in}(t)$ and $m_{S,in}(t)$ can be as simple as pulling the information from the blast furnace's data historian. Hot metal and slag production rates for a large blast furnace are in the range of ~ 4.0 and ~ 1.0 t/min, respectively.

In some cases, separate production rates for the hot metal and slag may not be available. In these situations, a mass production rate of slag can be assumed to be $\sim 20\text{--}30\%$ the production rate of hot metal, depending on the charge composition/slag volume.

57.11.2 Accumulation

The mass balance for material accumulation in the hearth shown in [Table 57.3](#) is described in more detail here. The integral version of the final equation is provided in equation 57.5:

$$h_i(t) = h_{i,0} + \int_0^t \frac{m_{i,in} - m_{i,out}}{\rho_i A_h \epsilon_h} dt \quad (57.5)$$

The material flow rates $m_{i,in}$ and $m_{i,out}$ [kg/min] for both hot metal and slag are found from the (1) filling and (3) draining sections of the model. These vary with time but can be assumed constant over time intervals less than 1 minute.

The material densities ρ_i [kg/m³] are in the range of ~ 7000 kg/m³ for hot metal and ~ 2500 kg/m³ for slag. These parameters are temperature dependent; however, in this simplified model, they are assumed to be constant.

The hearth cross-sectional area A_h [m²] is typically in the range of 75–150 m² for large blast furnaces. The cross-sectional area varies as a function of hearth height due to blast furnace design and refractory wear; however, in this simplified model, a constant cross-sectional area is sufficient.

The hearth void fraction ϵ_h [%] accounts for unavailable volume due to the deadman coke resting in the hearth. Effectively, the void fraction adjusts the cross-sectional area to represent only the area available for liquid to accumulate in and drain from. Accurate estimation of this parameter is challenging as it depends on coke properties and operating practice, however it is typically in the range of $\sim 30\%$.

Material heights h_i [m] are solved using equation 57.5, and can also be used as an input or initial condition, depending on how one chooses to solve the overall model. Ideally, the hearth drainage model will be initialized at a time where material heights are known, for example, when the hearth is drained for a maintenance stop.

57.11.3 Draining - $m_{i,out}^i(t)$

Methods for measuring the casting or draining rate of material from a blast furnace were discussed in the hearth management section. Although multiple techniques exist for measuring both hot metal and slag casting rates, they are often not suitable for use in the model. The reason being that a substantial delay exists between liquids exiting the taphole, and a flow rate measurement being available. These techniques do provide a good double-check of the alternative "real-time" methods.

TABLE 57.3 Summary of Mass Balance Equation, Key Parameters, and Other Required Parameters Used in a Simplified Hearth Drainage Model



$$\text{Accumulation} = \text{Material In} - \text{Material Out} + \text{Generation}$$

$$\frac{dm_i}{dt} = \dot{m}_{i,\text{in}} - \dot{m}_{i,\text{out}} \quad (57.1)$$

$$\rho_i A_h \epsilon_h \frac{dh_i}{dt} = \dot{m}_{i,\text{in}} - \dot{m}_{i,\text{out}} \quad (57.2)$$

$$h_i(t) = h_{i,0} + \int_0^t \frac{\dot{m}_{i,\text{in}} - \dot{m}_{i,\text{out}}}{\rho_i A_h \epsilon_h} dt \quad (57.3)$$

Or, if short time interval/constant over time interval

$$h_i(t) \approx h_{i,0} + \frac{\dot{m}_{i,\text{in}} - \dot{m}_{i,\text{out}}}{\rho_i A_h \epsilon_h} \Delta t \quad (57.4)$$

where m is the mass of hot metal or slag, t is the time, i is the denotes either hot metal or slag.

(1) Hot Metal and Slag Production "Filling"	(2) Hearth Liquid Level "Accumulation"	(3) Hot Metal and Slag Casting Rate "Draining"
$\dot{m}_{M,\text{in}}(t)$	$h_M(t)$	$\dot{m}_{M,\text{out}}(t)$
$\dot{m}_{S,\text{in}}(t)$	$h_S(t)$	$\dot{m}_{S,\text{out}}(t)$
<i>Req. calculation parameters</i>	<i>Req. calculation parameters</i>	<i>Req. calculation parameters</i>
	Hot metal density	ρ_M
	Slag density	ρ_S
	Hearth area	A_h
	Hearth void fraction	ϵ_h
	Hot metal height	h_M
	Slag height	h_S
		Initial taphole diameter
		$d_{\text{TH},0}$
		Taphole wear rate
		k_{TH}
		Taphole length
		ℓ_{TH}
		Blast pressure
		P_{blast}
		Taphole pressure
		P_{TH}
		Hot metal height
		h_M
		Slag height
		h_S
		Friction factors
		λ

An alternative technique involves using a modified version of Bernoulli's equation to calculate total casting rate based on taphole geometry, blast pressure, liquid head, and friction factor assumptions. The equations and diagram describing this approach are shown in [Table 57.4](#) and [Fig. 57.33](#), respectively.

[Eq. \(57.6\)](#), a modified Bernoulli's equation, describes the relationship between the casting rates of hot metal, slag and taphole pressure. Casting rate increases with increasing taphole area [m^2], pressure [bar], and average density of liquid iron and slag in the taphole [kg/m^3]. Casting rate decreases with increasing friction [unitless] and greater taphole length [m].

[Eq. \(57.7\)](#) shows the relationship between taphole area [m^2] and taphole diameter [m].

[Eq. \(57.8\)](#) estimates the taphole diameter [m] change over the course of a cast. Taphole wear becomes substantial only after slag exits the taphole. A typical profile for taphole area over the course of a cast can be found in [Fig. 57.34](#).

Initial taphole diameters are set by the drill bit size and are in the range of ~ 50 mm. Taphole diameter wear rate depends on the clay type and is in the range of ~ 0.11 mm/min.

[Eq. \(57.9\)](#) calculates the pressure at the taphole based on blast pressure [bar] and liquid head [bar]. Due to the high density of hot metal

TABLE 57.4 Equations to Calculate Casting Rate for Hearth Drainage Model Development

Eq. (57.6)	Modified Bernoulli's equation	$m_{M,\text{out}} + m_{S,\text{out}} = A_{\text{TH}} \sqrt{\frac{2 \cdot P_{\text{TH}} \cdot \rho_{\text{avg,TH}}}{1 + ((\lambda \cdot L_{\text{TH}})/d_{\text{TH}})}}$
Eq. (57.7)	Taphole cross-sectional area	$A_{\text{TH}} = \frac{\pi \cdot (d_{\text{TH}})^2}{4}$
Eq. (57.8)	Taphole diameter wear	$d_{\text{TH}} = d_{\text{TH},0} + k_{\text{TH}}(t - t_{\text{slag start}})$
Eq. (57.9)	Taphole pressure	$P_{\text{TH}} = P_{\text{blast}} + g \cdot (\rho_M \cdot h_M + \rho_S \cdot h_S)$
Eq. (57.10)	Mass fraction of liquids exiting taphole	$x_i = \frac{\dot{m}_{i,\text{out}}}{\dot{m}_{M,\text{out}} + \dot{m}_{S,\text{out}}}$ $i = \text{"Hot Metal" or "Slag"}$
Eq. (57.11)	Average density of liquids in taphole	$\rho_{\text{avg,TH}} = \sum_i x_i \rho_i$ $i = \text{"Hot Metal" or "Slag"}$
Eq. (57.12)	Sergheide's solution to the Colebrook equation (friction)	$\frac{1}{\sqrt{\lambda}} = A - \frac{(B-A)^2}{C-2B+A}$ $A = -2\log\left(\frac{\epsilon/d_{\text{TH}}}{3.7} + \frac{12}{Re}\right)$ $B = -2\log\left(\frac{\epsilon/d_{\text{TH}}}{3.7} + \frac{2.51A}{Re}\right)$ $C = -2\log\left(\frac{\epsilon/d_{\text{TH}}}{3.7} + \frac{2.51B}{Re}\right)$ where ϵ is the taphole roughness [m]
Eq. (57.13)	Reynold's number—internal flow through cylindrical pipe	$Re = \frac{\rho_{\text{avg,TH}} \cdot v_{\text{mean}} \cdot d_{\text{TH}}}{\mu_{\text{avg,TH}}}$ $\mu_{\text{avg,TH}}$ is average dynamic viscosity [Ns/m^2]

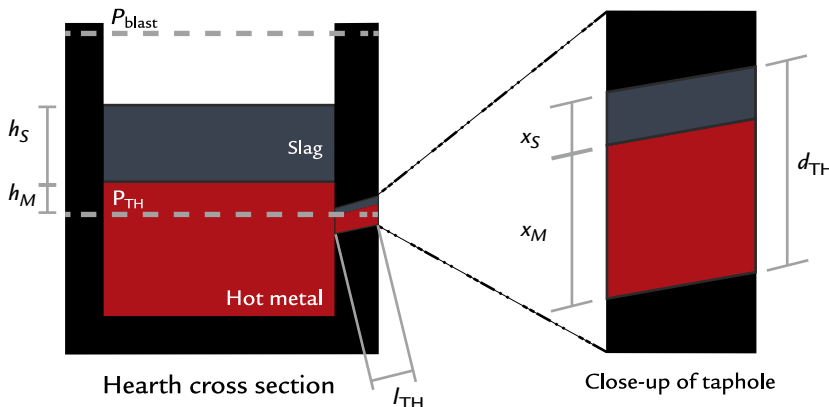


FIGURE 57.33 Hearth diagram and taphole close-up with parameter labels for hearth drainage model development.

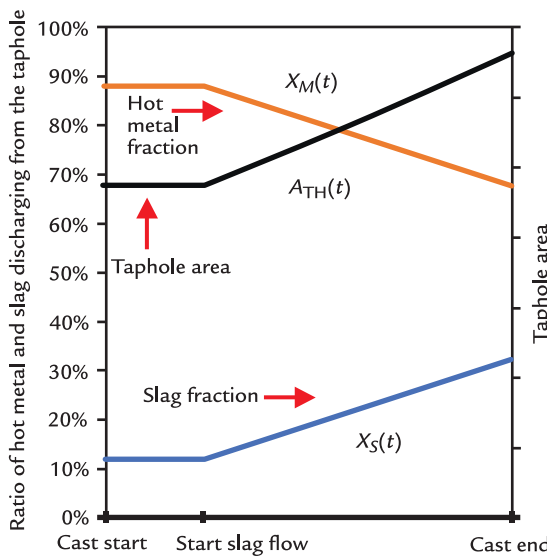


FIGURE 57.34 Assumption for taphole mass fractions of hot metal and slag over a cast.

and slag, the liquid head term can have a significant effect on the pressure at the taphole and thus the casting rate. Blast pressure is typically in the range of ~ 2.6 barg (260 kPa).

Eq. (57.10) defines a very important parameter in the hearth drainage model, the mass fractions [%] of hot metal and slag exiting the

taphole. One critical assumption is how x_M (mass fraction of hot metal) and x_S (mass fraction of slag) change throughout each cast. This assumption varies depending on the blast furnace being modeled. The simplified model assumes that once slag is observed, the x_M decreases linearly from $\sim 88\%$ at the start to $\sim 68\%$ at the end of the cast. This mass fraction profile can be observed in Fig. 57.34.

Eq. (57.11) calculates the average density [kg/m^3] of the liquids exiting the taphole based on material mass fractions [%] and densities [kg/m^3].

Eq. (57.12) estimates the friction factor using Serghides' solution of the Colebrook equation. The friction factor is typically in the range of ~ 0.038 .

Eq. (57.13) shows the definition of the dimensionless Reynold's number used in this model.

57.11.4 Solving the Simplified Hearth Drainage Model

Calculation of hearth liquid levels is done by iterating through the mass balance equations shown in Table 57.3. At every time interval, the filling ($m_{i,\text{in}}$) and draining ($m_{i,\text{out}}$)

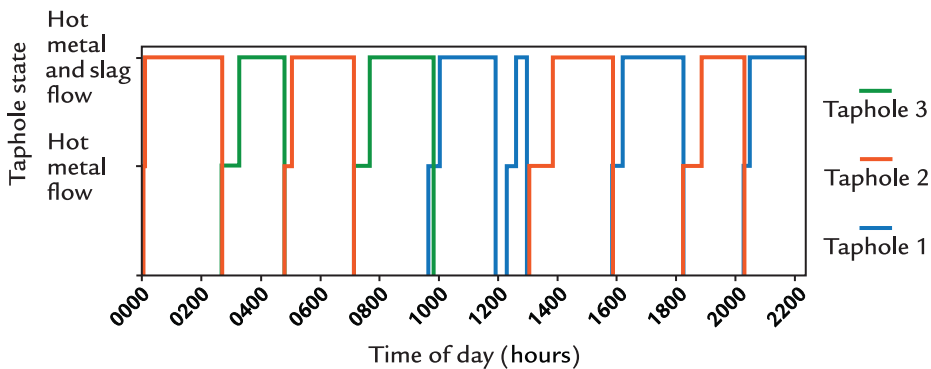


FIGURE 57.35 Taphole status for hearth drainage model scenario using real plant data. Note the iron gap at 1200 hours.

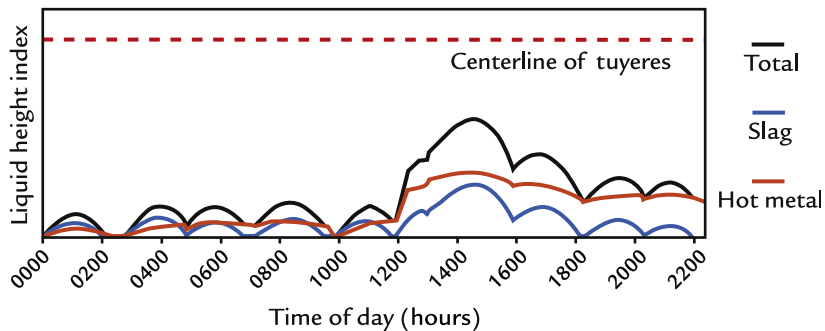


FIGURE 57.36 Hearth liquid level index generated from the hearth drainage model from commercial blast furnace data.

terms for each taphole should be calculated, and liquid level updated to serve for the following time interval's initial height condition. In the case where multiple tapholes are open at once, the draining term should be equal to the total casting from all tapholes.

Figs. 57.35 and 57.36 provide a sample output of the simplified hearth drainage model using data from a commercial blast furnace.

A 30-minute iron gap at 1200 hours causes hearth liquid levels to increase over the course of the gap. Since no corrective action was taken, the iron level remains at an elevated level for the remainder of the day. Casthouse operators could have overlapped the following two casts to drain the blast furnace quickly after realizing the 30-minute iron gap. This simple case demonstrates how a hearth drainage model can be used by blast furnace

operators to improve their casting practice and ultimately blast furnace operation.

57.12 SUMMARY

Casting the blast furnace is one of the most essential aspects to a smooth and stable blast furnace operation. When done well, the blast furnace operation is predictable, production rates are high, and costs are low. Poor casting is the most common root cause of many problems including unstable burden descent and inability to minimize coke rate by using high rates of fuel injection. The essential equipment needed to cast the blast furnace was described for single and multiple taphole blast furnaces. The importance of taphole clay and its technical qualities were presented;

consistent taphole clay quality is paramount to a good casting practice. Long pooling troughs provide the best slag–iron separation and long trough life. Understanding the casting schedule and how to use overlapping casts to avoid accumulation of iron and slag in the hearth will minimize any negative impact on the blast furnace process. The casthouse is where most of the blast furnace staff is assigned—their ability to master the casting operations is key to a successful blast furnace operation.

EXERCISES

57.1. Please circle T (true) or F (false) for each of the following statements.

- T F Good disciplined casting practice is a major key to stable blast furnace operation.
- T F An overfilled hearth has serious safety implications.
- T F Dry hearth casting practice promotes process stability.
- T F Some liquid and slag should be left in the furnace at the end of a cast to maintain heat in the hearth.

57.2. Good slag and hot metal separation in the trough is affected by (*please circle two*)

- trough design
- length of taphole
- taphole angle
- casting speed
- slag composition and temperature

57.3. Please circle T (true) or F (false) for each of the following statements.

- T F No part of the furnace deserves more care and attention than the taphole.
- T F Casting practice has no bearing on the quality of the iron sent to steelmaking.

T F The steeper the taphole angle, the emptier the hearth at end cast, so the steeper the better.

T F The clay gun has a significant role in maintaining taphole length.

57.4. The primary function of the trough is (*please circle*)

- to slow down the flow of metal to the torpedo cars
- to efficiently separate the iron and slag
- to provide a liquid pool for ease of measuring the hot metal temperature and obtaining metal and slag samples
- to hold hot metal between casts

57.5. Trough bottom slope should be (*please circle one*)

- high, to move the metal and slag quickly away from the furnace
- flat, to minimize erosion from hot metal moving over its surface
- approximately 3.5 degrees to move the iron along but with minimal turbulence and sufficient time for iron/slag separation

57.6. Good drainage of liquids from the hearth depends on (*please circle one*)

- large, fines-free coke in the hearth
- large taphole
- highly fluid iron and slag
- steep taphole

References

1. Klug FJ, Prochazka S, Doremus RH. Alumina–silica phase diagram in the mullite region. *J. Am. Ceram. Soc.* 1987;70(10):757.
2. Cameron IA, Tudhope JM. Improved trough design using water modeling. In: *Ironmaking conference proceedings, iron and steel society*, May 1988, Toronto, pp. 505–515.
3. Hyde JB. Casthouse practice and blast furnace casthouse rebuild. In: *24th McMaster University blast furnace ironmaking course, McMaster University*, 2016, Lecture 19, pp. 24–25

58

Blast Furnace Slag

O U T L I N E

58.1 Blast Furnace Slag Requirements	634	58.4 By-Product Slag Sale Requirements	641
58.2 Slag Composition and Properties	634	<i>58.4.1 Aggregate and Civil Engineering Applications</i>	641
58.2.1 Slag Fluidity	634	<i>58.4.2 Slag Cement</i>	642
58.2.2 Lookup Tables to Estimate Slag Liquidus Temperature	635	<i>58.4.3 Wet Slag Granulation</i>	642
58.2.3 Lime Content	636	<i>58.4.4 Slag Pelletizing</i>	643
58.2.4 Alumina Content	636	<i>58.4.5 Dry Granulation Using a High-Velocity Air Stream</i>	644
58.2.5 Magnesia Content	637	<i>58.4.6 Dry Granulation Using a Spinning Ceramic Cup</i>	645
58.2.6 High Alumina Slag	638		
58.2.7 Slag Volume	638	58.5 Finding a Balance Among Competing Demands	645
58.3 Hot Metal Chemistry Control	638	<i>58.5.1 Competing Demands</i>	645
58.3.1 Sulfur	638	58.6 Summary	648
58.3.2 Silicon	638	Exercises	648
58.3.3 Phosphorus	639	References	649
58.3.4 Alkali Removal	639	Further Reading	650
58.3.5 Titania in Slag	640		
58.3.6 Candidate Fluxes	641		

58.1 BLAST FURNACE SLAG REQUIREMENTS

Blast furnace slag affects hot metal quality and the process conditions inside the blast furnace. The slag composition must be selected to achieve several objectives:

- Remove gangue and ash contained in the ferrous burden, coke, and injected fuels.
- Create conditions for a smooth blast furnace operation and consistent burden descent.
- Have acceptable physical and chemical properties (viscosity and liquidus temperature) to ensure easy removal from the blast furnace.
- Provide the hot metal composition required for oxygen steelmaking.
- Remove unwanted impurities such as sulfur, sodium, and potassium in the burden materials and injected fuels.
- Meet the cement and other by-product specifications to ensure that the blast furnace slag can be sold at the highest profit margin.

Each of these aspects is discussed below to better understand how to select the optimum blast furnace slag practice.

58.2 SLAG COMPOSITION AND PROPERTIES

Most gangue minerals added to the blast furnace must be removed from the process by the blast furnace slag. The main gangue impurities are silica (SiO_2) and alumina (Al_2O_3) found in the ferrous burden, coke, and injected fuels. Fluxing materials are added to produce a slag with suitable melting or liquidus temperature. The blast furnace slag composition is typically in the merwinite, melilite, monticellite, and pyroxene phases of the $\text{CaO}-\text{SiO}_2-\text{MgO}-\text{Al}_2\text{O}_3$ slag system. Slag compositions in this area have a liquidus temperature ranging

from 1300 to 1450°C. With this composition, the slag will be molten for a range of temperatures typical of blast furnace operations. The quaternary phase diagram at the 10% Al_2O_3 plane can be seen in Fig. 58.1.

Blast furnace engineers refer to slag properties based on the slag basicity or base-to-acids ratio. Slags are polymeric in nature; basic compounds are chain builders and acid compounds are chain breakers. In blast furnace slag, CaO and MgO are considered bases; SiO_2 is acidic. Al_2O_3 is neutral to acidic in nature so it is sometimes dropped from blast furnace slag basicity indices. Three basicity indices are used; each blast furnace engineer has a preference in which one they choose to use:

- | | |
|--|---|
| <ul style="list-style-type: none"> • B2—this is a simple ratio of CaO to SiO_2 • B3—ratio of strong bases to acids • B4—major slag forming compounds included | $\text{B2} = \text{CaO}/\text{SiO}_2$ $\text{B3} = (\text{CaO} + \text{MgO})/\text{SiO}_2$ $\text{B4} = (\text{CaO} + \text{MgO})/(\text{SiO}_2 + \text{Al}_2\text{O}_3)$ |
|--|---|

58.2.1 Slag Fluidity

Blast furnace slag must be fluid at ironmaking temperatures. The primary slag is generally fluid when formed due to its relatively high FeO content. Hearth slag must be designed and fluxes added so that the slag is easily tapped from the blast furnace under a variety of conditions and temperatures. The hearth slag physical properties most discussed are the liquidus temperature and viscosity.

Increased basicity also lowers the hot metal S content. For this reason, many blast furnaces elect to work in a higher basicity range. Hearth slag can be based on the liquidus temperature only; the effects on viscosity do not usually create major operational problems except in abnormal situations. The liquidus temperature should be <1415°C, and the lower the better. The slag

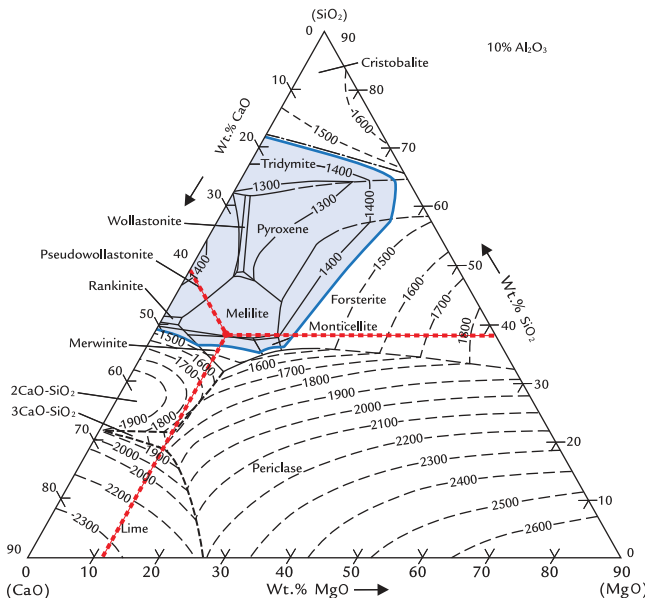


FIGURE 58.1 Ten percent Al₂O₃ plane of the CaO-SiO₂-MgO phase diagram showing a typical slag composition. The 1450°C isotherm is highlighted.¹

must be designed such that small variations in the hot metal silicon content do not lead to significant increases in slag liquidus temperature. The liquidus temperature must remain <1415°C under all anticipated scenarios.

Slag viscosity must be low to allow suitable fluidity but not too low to create aggressive slags. Normal slag has a viscosity in the range of 0.2–0.5 Pa.s (2–5 poise), with the lowest values being achieved at a neutral basicity between acidic and basic slags (Fig. 58.2).

Magnesia and alumina in slag effect slag viscosity, as indicated in Fig. 58.3.

Controlling slag MgO and Al₂O₃ contents to 10% each provides a suitably low slag liquidus temperature, low slag viscosity, and as shown below, good desulfurization performance.

58.2.2 Lookup Tables to Estimate Slag Liquidus Temperature

Since reading the slag liquidus temperature from phase diagrams can be challenging,

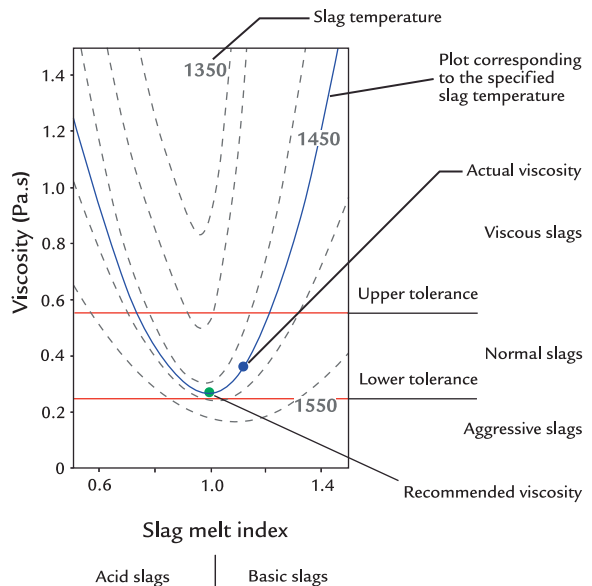


FIGURE 58.2 Blast furnace slag viscosity trends with basicity and temperature.²

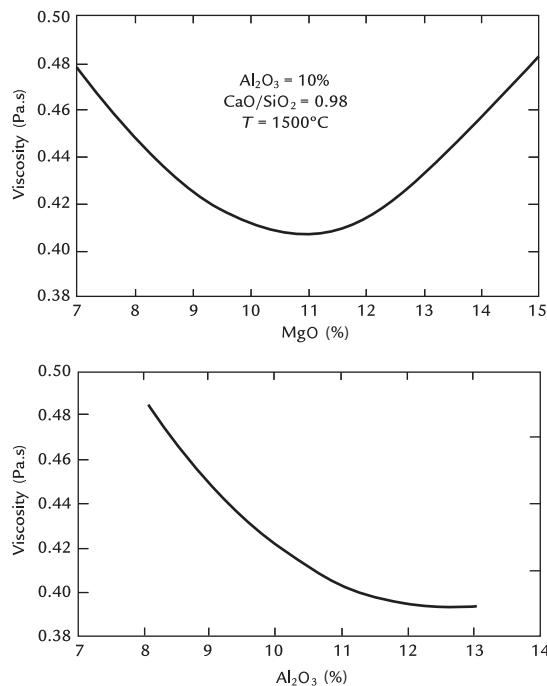


FIGURE 58.3 Impact of slag MgO and Al_2O_3 content on slag viscosity.³

lookup tables were prepared to quickly estimate this property. Liquidus temperatures were calculated using the well-known thermodynamic program FactSage. The lookup tables are included in Appendix X together with instructions on how to use these tables. Lookup tables can greatly simplify the understanding of slag properties and how to manipulate the slag chemistry to meet the blast furnace operational goals.

58.2.3 Lime Content

Lime (CaO) is the strongest fluxing compound that can lower the melting point of the gangue materials. The CaO -to- SiO_2 ratio, or B2 basicity, must be <1.2 to avoid forming dicalcium silicate (Ca_2SiO_4) which has a very high melting point, beyond the blast furnace operational temperature. A lower B2 ratio favors

removal of alkali elements (sodium and potassium), and a higher ratio yields a lower sulfur and silicon content in hot metal. Slag basicity can be adjusted; a policy in which the basicity is gradually increased tends to provide the best balance for the steel plant economics. The target for the basicity depends on the variation of silicon in the blast furnace; a low Si variation (i.e., good fuel rate control) is needed for higher basicity operations. A reasonable target for 10% Al_2O_3 and 10% MgO containing slag is about 40% CaO and 37% SiO_2 [B2 basicity $\text{CaO}/\text{SiO}_2 = 1.08$, B3 basicity $(\text{CaO} + \text{MgO})/\text{SiO}_2 = 1.35$, and B4 basicity $(\text{CaO} + \text{MgO})/(\text{SiO}_2 + \text{Al}_2\text{O}_3) = 1.06$]. Extraneous minor compounds account for the remaining 3% of the slag mass (sulfur, iron oxide, manganese oxide, etc.).

58.2.4 Alumina Content

At $<10\%$ Al_2O_3 , the liquidus temperature rises. The minimum liquidus temperature is at about 10% Al_2O_3 and the change from 10% to 12% Al_2O_3 is small; the liquidus temperature increases by just 7°C . In slags with $<10\%$ Al_2O_3 , a minor change in hot metal silicon content transfers silicon from slag to hot metal due to a hotter blast furnace thermal state. The resulting slag liquidus temperature can rise above the maximum acceptable value of 1415°C . This may result in a slag that is difficult to remove from the blast furnace, especially if the hot metal/slag temperature suddenly decreases. For example, for a B3 basicity of 1.35, the liquidus temperature for a common hot metal silicon level of 0.4% and a higher level of 0.9% silicon may be compared in Table 58.1 for slag Al_2O_3 content varying from 8 to 14%.

When silicon is unexpectedly transferred from slag to hot metal, the slag liquidus temperature increases. For the slag with 8% Al_2O_3 , the slag liquidus temperature increases to 1557°C , a temperature that is greater than the hot metal

TABLE 58.1 Impact of an Increase in Hot Metal Silicon by +0.5% Si for Various Slag Al₂O₃ Contents

Slag Al ₂ O ₃ Content	8%	→ 10%	→ 12%	→ 14%
Liquidus temperature (°C)	1414	1396	1403	1414
Liquidus temperature if hot metal Si increases by +0.5% (°C) ^a	1557	1452	1419	1430
Change (°C)	+ 143	+ 56	+ 16	+ 16
Viscosity (Pa.s)	0.22	0.23	0.24	0.25
Viscosity if hot metal Si increases by +0.5% (Pa s)	0.19	0.20	0.21	0.23

^aFor a slag volume of 250 kg/t HM.

temperature, making slag removal very difficult. For slag with 10% Al₂O₃, the liquidus temperature increases to 1452°C creating a slag that may prove challenging to remove from the furnace. The slags with 12 and 14% Al₂O₃ are closer to the maximum recommended slag liquidus temperature of 1415°C despite the transfer of silicon from the slag to the hot metal. More basic slags that result when the silicon is transferred from slag to the hot metal are less viscous but these changes are too small to significantly improve the fluidity of the slag produced. Often high silicon levels in hot metal are associated with elevated hot metal temperatures of 1500–1530°C, so slag with 10% Al₂O₃ should be molten even if the silicon in hot metal increases by +0.5%.

58.2.5 Magnesia Content

Magnesia (MgO) may or may not be present in the ironmaking raw materials. MgO will most likely be associated with the iron ore – for example some magnetite ores found in the United States have very fine MgO present that is not easily removed in mineral processing. MgO is often added as a direct charged flux, as olivine or dolomite fluxed pellets, or as part of the sinter blend to improve the desulfurization capacity of the slag. With MgO added to

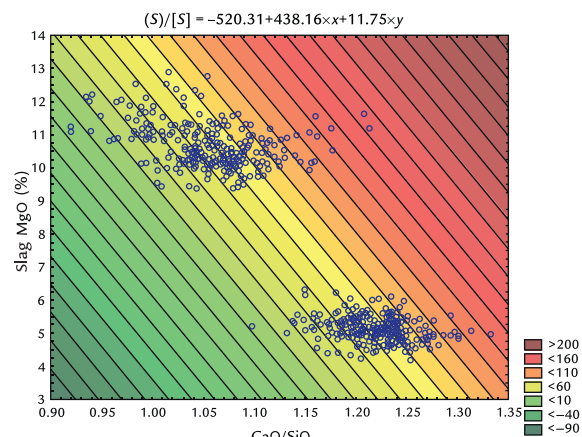


FIGURE 58.4 Comparison of slag with 5–6% MgO to slags with 10–11% MgO. Similar desulfurization can be obtained at a lower basicity when MgO is added.²

TABLE 58.2 Impact of Increasing Slag MgO Content on Slag Basicity, Liquidus Temperature and Viscosity

Slag MgO Content	8%	→ 10%	→ 12%	→ 14%
Liquidus temperature (°C)	1386	1396	1419	1432
Viscosity (Pa.s)	0.24	0.23	0.21	0.20
B3, (CaO + MgO)/SiO ₂	1.29	1.35	1.41	1.49
B4, (CaO + MgO)/(SiO ₂ + Al ₂ O ₃)	1.02	1.06	1.11	1.16

achieve 10–11% MgO in slag, greater sulfur removal can be achieved at a lower B2 basicity as illustrated in Fig. 58.4.

At 10% Al₂O₃ and high MgO levels (>12%), there is a risk of forming periclase which will quickly increase the liquidus temperature. As a result, the slag MgO content must be between 8 and 12%. The target B3 basicity should be reduced at higher MgO levels to maintain a slag liquidus temperature <1415°C as illustrated in Table 58.2.

While the increased MgO content can increase the slag liquidus temperature, the impact on the slag viscosity is very small with viscosity decreasing with increasing slag MgO content.

58.2.6 High Alumina Slag

In China, India, and other parts of Asia, the blast furnace burden often has a high alumina loading. This results from high alumina ores mined in Australia and high ash coals, especially in India. When faced with a high alumina burden, the blast furnace metallurgist must increase slag volume and basicity to dilute the alumina to a manageable concentration in the slag. This is created by adding fluxes to the sinter and decreasing its iron content and/or adding silica to the blast furnace using low-grade iron ore or silica sand. Due to the negative impact that increasing slag volume has on the blast furnace fuel rate, a blast furnace slag with a much higher basicity and alumina content is employed. The typical slag used with high alumina burdens is provided in [Table 58.3](#).

TABLE 58.3 Typical Slag Properties for Blast Furnace Slag When Operating With a High Alumina Burden

Parameter	Value
Typical high Al_2O_3 blast furnace slag assay	
SiO_2 (%)	34.5
CaO (%)	38.0
MgO (%)	11.0
Al_2O_3 (%)	14.5
$B_3 = (\text{CaO} + \text{MgO})/\text{SiO}_2$	1.42
Slag liquidus temperature (°C)	1415
Slag viscosity (Pa s)	0.23
Typical slag volume (kg/t HM)	250–300

58.2.7 Slag Volume

The lower the slag volume, the more sensitive the slag composition, and liquidus temperature is to change in hot metal silicon content. The target basicity should slightly

decrease at lower slag volumes. In contrast, the lower the slag volume, the lower the fuel rate. The slag volume and composition must be controlled at a level that optimizes both effects.

58.3 HOT METAL CHEMISTRY CONTROL

The blast furnace slag design will influence the hot metal sulfur and silicon contents. Details are provided below.

58.3.1 Sulfur

Estimations of hot metal sulfur content can be determined using the following equation⁴:

$$[\%S] = C_1 - 0.1027 \times B \quad (58.1)$$

$$B = \frac{\text{CaO}\% + 0.7 \times \text{MgO}\%}{0.94 \times \text{SiO}_2\% + 0.18 \times \text{Al}_2\text{O}_3\%} \quad (58.2)$$

where C_1 is a furnace-dependent constant that is in the order of magnitude of 0.17 and $[\%S]$ is the hot metal sulfur content in %.

This simple equation has a good correlation with blast furnace data from Dofasco, now ArcelorMittal Dofasco, before and after bauxite addition trials to increase slag Al_2O_3 content.⁴ By using a bauxite addition to increase the slag “ B ” ratio shown in Eq. (58.2), slag desulfurization was enhanced. Adding bauxite was cost-effective and reduced the external desulfurization reagent consumption and its related costs. Inland Steel, now ArcelorMittal Indiana Harbor, also reported positive benefits of adding bauxite to reduce the hot metal sulfur content.⁵

58.3.2 Silicon

Hot metal silicon is controlled by several variables including the hot metal temperature, blast pressure, cohesive zone position and

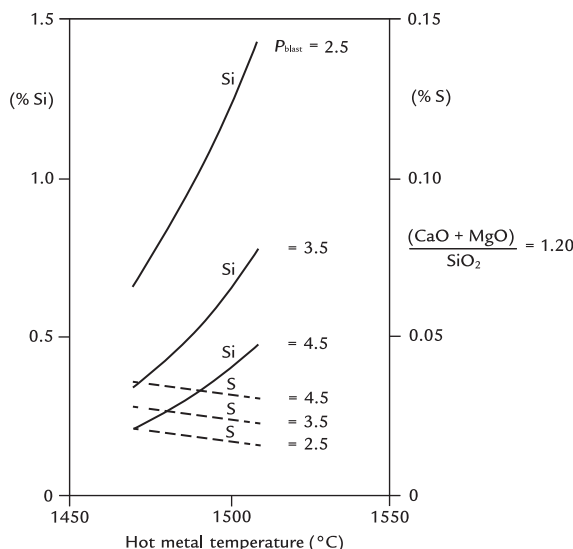


FIGURE 58.5 Impact of hot metal temperature and blast pressure on hot metal silicon and sulfur (P_{blast} is gauge pressure in bar).⁶

shape, raceway adiabatic flame temperature (RAFT), and slag basicity. Trends in silicon content for a constant basicity and RAFT are provided in Fig. 58.5.

Hot metal silicon is also affected by the slag chemistry as the hot metal and hearth slag react with each other:



The exchange reaction is, in part, driven by the activity of silica (SiO_2) in slag. When the silica activity is low, reaction (58.3) tends to the left-hand direction and hot metal silicon is reduced. A high silica activity drives reaction (58.3) to the right and increases the hot metal silicon content. Silica activity can be represented by the following equation:⁷

$$\log a_{\text{SiO}_2} = 0.036(\% \text{MgO}) + 0.061(\% \text{Al}_2\text{O}_3) + 0.123(\% \text{SiO}_2) - 0.595 \frac{\% \text{SiO}_2}{\% \text{CaO}} - 6.456 \quad (58.4)$$

Studying Eq. (58.4), we can see that increasing basicity, that is, increasing the slag CaO

content, will decrease the slag silica activity and reduce the silicon content of hot metal. While supported by theory, it is difficult to see a strong tendency of hot metal silicon with silica activity in production data due to the impact of other variables such as RAFT, blast pressure, and hot metal temperature.

The main concern with changes in hot metal silicon is the resulting effect that this can have on the slag quality and fluidity as illustrated in Table 58.1. Consistent blast furnace operation with stable raw material quality, minimum changes in blast pressure, and a well-controlled fuel rate will provide hot metal with a low silicon variation. The resulting blast furnace slag will have consistent composition and melting characteristics.

58.3.3 Phosphorus

Phosphorus is added through the raw materials as oxidized mineral compounds. Due to the strongly reducing conditions in the blast furnace, virtually all the phosphorus added with the burden is reduced to P in the hot metal.

Typically, 97% of P leaves in molten iron, 2–3% in slag, and 0–1% in blast furnace dust. Since P can enter the blast furnace via recycled basic oxygen furnace (BOF) slag or dust, the P loading must be monitored to assure that this recirculating P load does not impact steel quality. Many blast furnaces with a high loading of P from the burden materials cannot recycle BOF slag or dust.

58.3.4 Alkali Removal

Alkali elements, notably Na_2O and K_2O , must be limited due to their tendency to recirculate in the blast furnace and create accretions in the stack and bosh zones. These alkaline elements can only be removed in blast furnace slag and to a lesser extent in blast furnace dust. Na and K do not report to the hot metal in any significant quantities.

For alkali input, only K_2O is considered, as potassium is more harmful than sodium compounds regarding blast furnace operations. If the K_2O input is <2 kg/t hot metal, generally no alkali-related problems are expected. A further reduction of alkali input is worthwhile, but if the slag K concentration is <1% on a regular basis, the slag basicity does not need to be decreased for alkali removal. Elevated temperatures in the center of the furnace (i.e., >600°C) will promote alkalis removal with the top gas. For a typical K_2O input of 1.6 kg/t hot metal, about 70% of the potassium is removed with slag and 30% in the gas cleaning system (virtually no K reports to hot metal). Na behaves in a comparable manner.

Geerdes et al. established standards for slag K_2O capacity, first indicating the maximum capacity and then recommending that the blast furnace operates at about 70% of this value.⁸ The maximum K_2O slag carrying capacity as a function of slag volume and basicity is shown in Fig. 58.6.

The blast furnace slag alkali carrying capacity is also impacted by its Al_2O_3 content as illustrated by D. Papanastassiou and outlined in Fig. 58.7.⁹

When there is critical concern about alkali buildup, operating the blast furnace for 1–2

days at a low basicity can remedy the situation. Some operations will add a single low basicity charge burden 1–3 times per day to dissolve alkali buildups. This is known as a “cleaner” charge. Maintaining a good understanding of day-to-day alkali removal is paramount to prevent accretion formation and the related operational problems and refractory damage.

58.3.5 Titania in Slag

Titania (TiO_2) is occasionally added to the blast furnace in rates from 3 to 10 kg/t hot metal

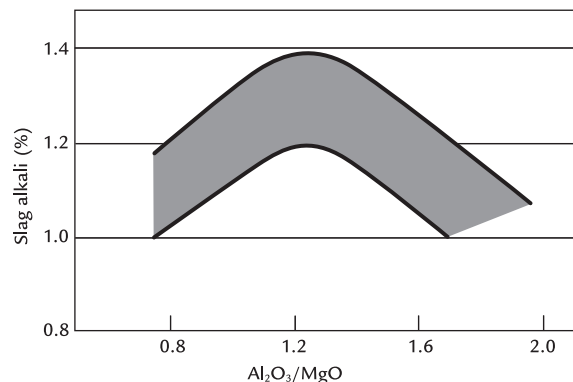


FIGURE 58.7 Impact of blast furnace slag Al_2O_3/MgO ratio on the slag alkali content for a B4 basicity of 1.1.⁹

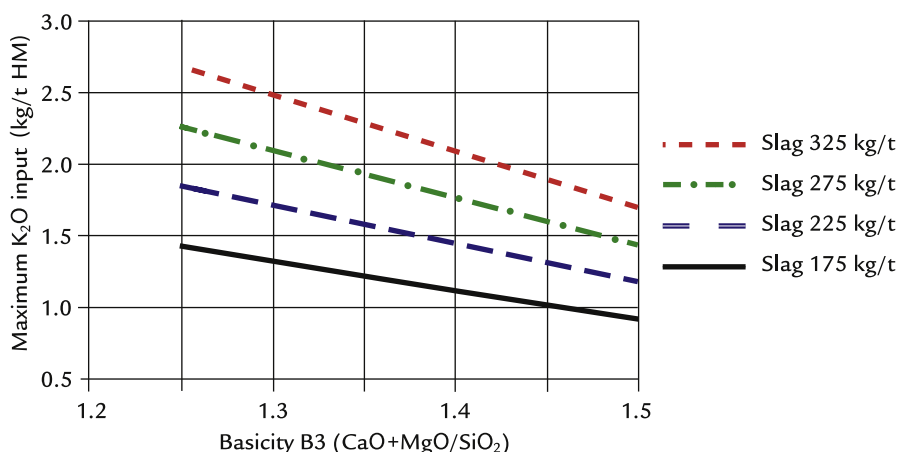


FIGURE 58.6 Maximum blast furnace slag K_2O carrying capacity per Geerdes et al.⁸

as a countermeasure to reduce elevated temperatures in the hearth walls. The added titania minerals create TiC, Ti(C, N), and TiN crystals in the slag, decreasing its liquidus temperature and increasing slag viscosity. While there are many differing views about the effectiveness of adding titania-bearing minerals and the best addition technique, the negative impact of titania on the slag liquidus temperatures is significant. A high slag titania content can also impact slag use in cement, additional discussion will follow.

58.3.6 Candidate Fluxes

To properly engineer blast furnace slag, fluxes rich in CaO, MgO, and occasionally Al₂O₃ and SiO₂ are required. Common sources of these fluxes are described in Table 58.4.

Most steelworks can access the required fluxes. Once the available fluxes are understood, the blast furnace metallurgist can design the slag to meet the many demands described in this chapter.

58.4 BY-PRODUCT SLAG SALE REQUIREMENTS

Blast furnace slag is primarily used as a cement additive or as concrete aggregate; slag also has important usage for road bases and civil engineering applications. Blast furnace slag usage in Japan is presented in Fig. 58.8.¹⁰

The environmental advantages of using blast furnace slag are significant. In 2007, 3.4 million tonnes of blast furnace slag were consumed for cement production and other applications in the United States. The following benefits were reported by the Slag Cement Association:¹¹

- An amount of 2.6 million tonnes of CO₂ emissions was avoided by eliminating limestone calcination for cement production.
- Avoided 13.7 PJ of energy.
- Conserved 4.5 million tonnes of virgin materials.

TABLE 58.4 Common Fluxes Available for Blast Furnace Slag Design

Slag Forming Compounds	Common Fluxes
CaO	Limestone
MgO	Dolomitic limestone (MgO with CaO) Olivine, dunnite, and serpentine (MgO with SiO ₂)
Al ₂ O ₃	Bauxite (Al ₂ O ₃ with iron oxide)
SiO ₂	Quartzite, silica sand (SiO ₂) Earthy, high gangue iron ores (SiO ₂ with hematite)
TiO ₂	Ilmenite and rutile (TiO ₂ rich minerals) Titania magnetite (TiO ₂ and Fe ₃ O ₄) Iron sands (Fe ₂ O ₃ with contained TiO ₂)

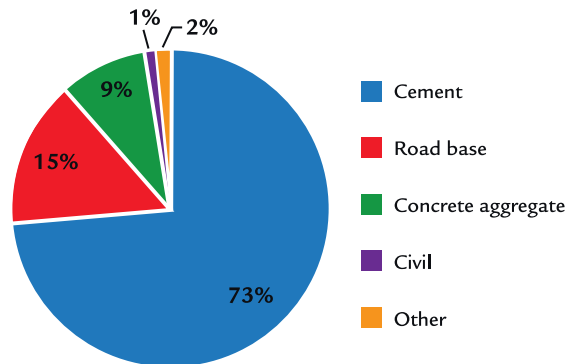


FIGURE 58.8 Use of blast furnace slag in Japan in FY2015.¹⁰

Four grades of blast furnace slag are produced; air or pit cooled, water granulated, expanded/pelletized, and dry atomized slag.

58.4.1 Aggregate and Civil Engineering Applications

The principle uses of air-cooled slag are road bases, asphalt, concrete aggregate, structural fill, railroad ballast, and mineral wool.

Other aggregate applications include roofing, sewage plant filter media, and drainage works. Blast furnace slag has several desirable characteristics for construction use including particle shape and texture that provide exceptionally high stability, nonplastic fines, volume stability under all weathering conditions, and lower weight per unit volume.¹²

58.4.2 Slag Cement

Used as a raw material in cement production, blast furnace slag can produce very high-quality cement due to the slag's latent hydraulic properties. Concrete made from slag cement mixtures with more than 60% blast furnace slag has a greater resistance to sulfate attack than concrete produced from Portland cement.¹² Blast furnace slag-based cement is preferred for sulfate and sea-water resistant structures where it performs better than Portland cement alone. Cement producers look for the following properties in blast furnace slag.^{9,12–14}

- A suitable hydraulic index expressed as:

$$F = \frac{\text{CaO} + \text{CaS} + (1/2) \times \text{MgO} + \text{Al}_2\text{O}_3}{\text{SiO}_2 + \text{MnO}} \quad (58.5)$$

- F values >1.9 provide very good hydraulic properties for the produced cement, while values <1.5 provide poor cement quality.⁹
- Other slag cement specifications are:

$$V - \text{ratio} = \frac{\text{CaO} + \text{MgO}}{\text{SiO}_2} > 1.3 \quad (58.6)$$

$$H - \text{ratio} = \frac{\text{CaO} + \text{MgO} + \text{Al}_2\text{O}_3}{\text{SiO}_2} > 1.7 \quad (58.7)$$

- Rapidly cooled slag with a glass content $>90\%$. This makes the slag more reactive, and it has better latent hydraulic properties when used in cement manufacture.
- Slag sulfide sulfur (S) to be 2.5% maximum.
- Slag color is important to cement producers; slag with a sandy color is preferred. A high SiO_2 or TiO_2 content can darken the slag to

a deep green or black color. Cold furnace conditions produce very dark slag with high SiO_2 .

- Blast furnace slag is used to prevent alkali-aggregate reactions in concrete. This occurs when siliceous aggregates react with alkaline compounds and form an expansive gel that can cause the concrete to crack. Slags with a low alkali content, expressed as $\text{Na}_2\text{O} + 0.658 \text{ K}_2\text{O} < 1.0\%$, are preferred.¹⁴
- Water granulated slag must be granulated with freshwater only, salt water is not permitted.
- Slag with alumina content 12–14% will optimize the compressive strength of the concrete produced as illustrated in Fig. 58.9.⁹

Slag cement specifications for granulated blast furnace slag are provided in Table 58.5. For slag delivered in solid form. Some companies operate granulation systems on behalf of the blast furnace operator and have a liquid slag specification.¹⁵

58.4.3 Wet Slag Granulation

Wet granulation uses enormous quantities of water to quickly quench the molten slag into sand-like granules. Typically, wet slag granulation comprises two steps. In the first step, molten slag is poured onto high pressure water jets in a water channel. The slag is rapidly

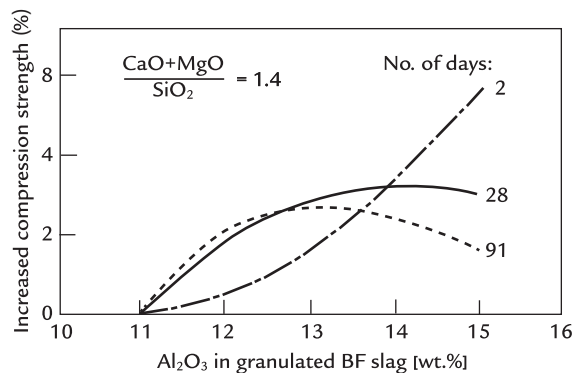


FIGURE 58.9 Impact of blast furnace slag alumina content on concrete compressive strength as the concrete cures over a 90-day period.⁹

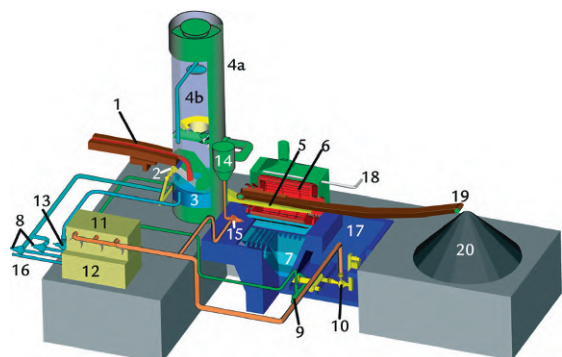
TABLE 58.5 Typical Slag Cement Specifications for Granulated (Gbfs)¹⁵

Parameter	Ranges in Practice	"Ideal Value"	Recommended
CaO/SiO ₂	0.85–1.25	~1.3	>1.0
(CaO + MgO)/SiO ₂	1.10–1.45	>1.3	>1.0
CaO (wt.%)	33.0–42.5	See CaO/SiO ₂	Maximum
MgO (wt.%)	6.5–12.0	—	<15
Al ₂ O ₃ (wt.%)	7–22	11–14	>10, ≤14.5
S (wt.%)	0.7–1.6	—	<2.0
TiO ₂ (wt.%)	0.4–2.0	0.4–0.5	Minimum
Mn ₂ O ₃ (wt.%)	0.1–1.1	Minimum	≤1.0
Fe ₂ O ₃ (wt.%) ^a	0.4–4.8	Minimum	≤2.0
Fe _{met} (wt.%) ^b	<0.1–1.0	Minimum	≤0.5
Na ₂ O _{eq} (wt.%)	0.2–1.0	—	According to application
Cl (wt.%) ^c	<0.01–0.25	According to application	According to application
Glass content (%)	65–100	~95	≥90
Bulk density (loose, dry) (kg/L)	0.60–1.30	0.8–1.1	<1.20
Moisture after storage (wt.%)	8–20	≤8	<10
Loss on ignition (wt.%)	0.2–2.6	Minimum	<1.5
Maximum grain size (mm)	3–6	—	≤6
No foreign bodies			
No dark color (indicates mainly low temperature of blast furnace slag prior to granulation)			

^aIncluding oxidic iron in glass plus metallic iron.

^bMetallic iron, separated from dry granulated blast furnace slag with laboratory magnet before chemical analysis.

^cAccording to EN 197, the limit for Cl in composite cements is 0.1%, for CEM III. Also, higher values are allowed. Cl can be subject to price negotiation.



INBA® cold water granulation system with condensation of steam

- | | |
|-----------------------------------|-----------------------------------|
| 1 Hot runner | 11 Cooling tower |
| 2 Blowing box | 12 Cold water tank |
| 3 Granulation tank | 13 Condensation water pump |
| 4a Stack | 14 Buffer tank |
| 4b Condensation tower | 15 Condensation water return pump |
| 5 Distributor and slow down boxes | 16 Make-up water |
| 6 Dewatering drum | 17 Drum cleaning water |
| 7 Hot water tank | 18 Drum cleaning air |
| 8 Granulation water pump | 19 Conveyor belt |
| 9 Recirculation pump | 20 Stock pile |
| 10 Cooling tower pump | |

FIGURE 58.10 Paul Wurth state-of-the-art cold-water granulation system with steam condensation. Source: Courtesy of Paul Wurth SA. Paul Wurth brochure. 2009. <<http://www.paulwurth.com>>.

quenched and a slurry results. In the second step, the granulated slag slurry is dewatered to a target water content that is acceptable for storage and sale. Common dewatering methods include screw classifiers, bucket excavators, and dewatering drums. Wet slag granulation is the most common technology used at blast furnace plants and can rapidly quench the slag and achieve the required high glass content. Fig. 58.10 shows Paul Wurth's state-of-the-art wet granulation system featuring cold-water granulation and steam condensation.¹⁵ This system is considered the best available technology for slag granulation by the European Union.

58.4.4 Slag Pelletizing

Slag pelletizing is accomplished by pouring the slag stream onto a rotating drum where

the slag is thrown vertically upward. The resulting slag droplets are cooled using water sprays. The pelletized product falls on the ground in a solid form and accumulates within a contained area. The wet pelletized slag is subsequently removed by a loader to a storage area. Pelletized slag is typically not dried at site but left in a pile to drain any contained moisture. An advantage of this design is the pelletizer's ability to accommodate varying slag flowrates, which permits installation of the pelletizer directly at the end of the slag runner spout. Slag pelletizing may not always provide the required glass content, and slag classification based on density is needed to meet the cement specification. There are only a few pelletizing machines in operation, and

these were designed and implemented by National Slag Limited.

58.4.5 Dry Granulation Using a High-Velocity Air Stream

In air granulation, the molten slag is poured into a high-velocity air stream where it is solidified. The air breaks up the slag stream into droplets and quenches the droplets into granules. Air granulation is a straightforward process which offers several advantages including water-free processing, potential for heat recovery, low-dust slag products, smaller footprint, and easier operations in winter climates. The granules are then sorted by size and sold. The air granulation process is shown in Fig. 58.11.

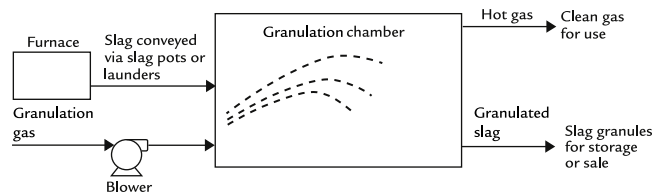


FIGURE 58.11 The air granulation process. Source: Courtesy of Hatch Ltd. (Faucher S, et al. Recent developments in commercial dry slag granulation and energy recovery. In: AISTECH 2016, association of iron and steel technology proceedings, May 2016, Pittsburgh; 2016. p. 137–44).¹⁶

While wet slag granulation dominates the blast furnace industry, dry processes such as air granulation offer lower investments costs, the elimination of water, and its related handling plus easier winter operations. Growth of dry treatment technologies is expected, especially if heat recovery systems can be implemented for preheating of stove combustion air.

58.4.6 Dry Granulation Using a Spinning Ceramic Cup

Development projects to use a spinning disk or cup have been ongoing since the 1970s to process slag on a dry basis. The target is to meet cement industry quality requirements while also recovering the heat contained in the molten slag. In 2017, Primetals implemented a 2 t/h pilot plant at voestalpine Stahl in Linz, Austria. Molten slag is poured on to a small spinning ceramic cup. The slag is spun into a free space onto water-cooled walls. The blast furnace slag solidifies either in flight or upon contacting the water-cooled walls. Cool air is passed through a bubbling fluidized slag bed where it is heated to 500°C and discharged. Air leaves the slag bed at about 560°C. Ultimately, this heated air will be cleaned in a hot cyclone and then used to produce super-heated steam at a pressure of 21 bar. The Primetals system is shown in Fig. 58.12, and more details are available in Ref. [17].

58.5 FINDING A BALANCE AMONG COMPETING DEMANDS

58.5.1 Competing Demands

Hatch assessed the conformance of the various blast furnace slags parameters with the slag cement specification, and results are shown in Fig. 58.13 and discussed in Table 58.6.

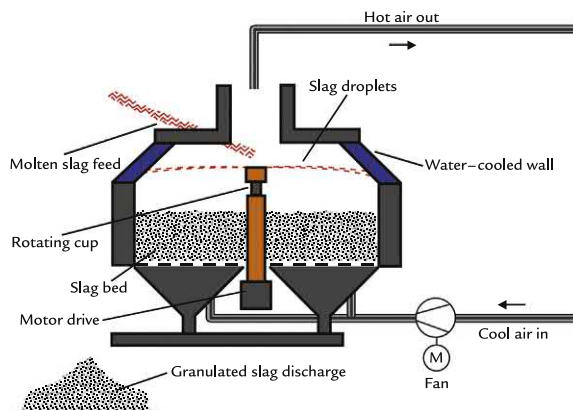


FIGURE 58.12 Spinning ceramic cup air granulation process developed by Primetals. Source: Courtesy of Primetals Technologies Austria GmbH (Fenzl T, et al. Installation of a dry slag granulation pilot plant at blast furnace A of voestalpine. Vienna: European Steel and Technology Application Days (ESTAD); 2017. p. 1763–72.).

A comparison of the slag B3 basicity or V-ratio of European and North American blast furnaces indicates that in general, the European blast furnaces operate at a higher B3 basicity than the North American operators (Fig. 58.14).

European operators have stronger motivation to sell blast furnace slag as a by-product to the cement producers to avoid high disposal costs. While North American operators do sell slag to

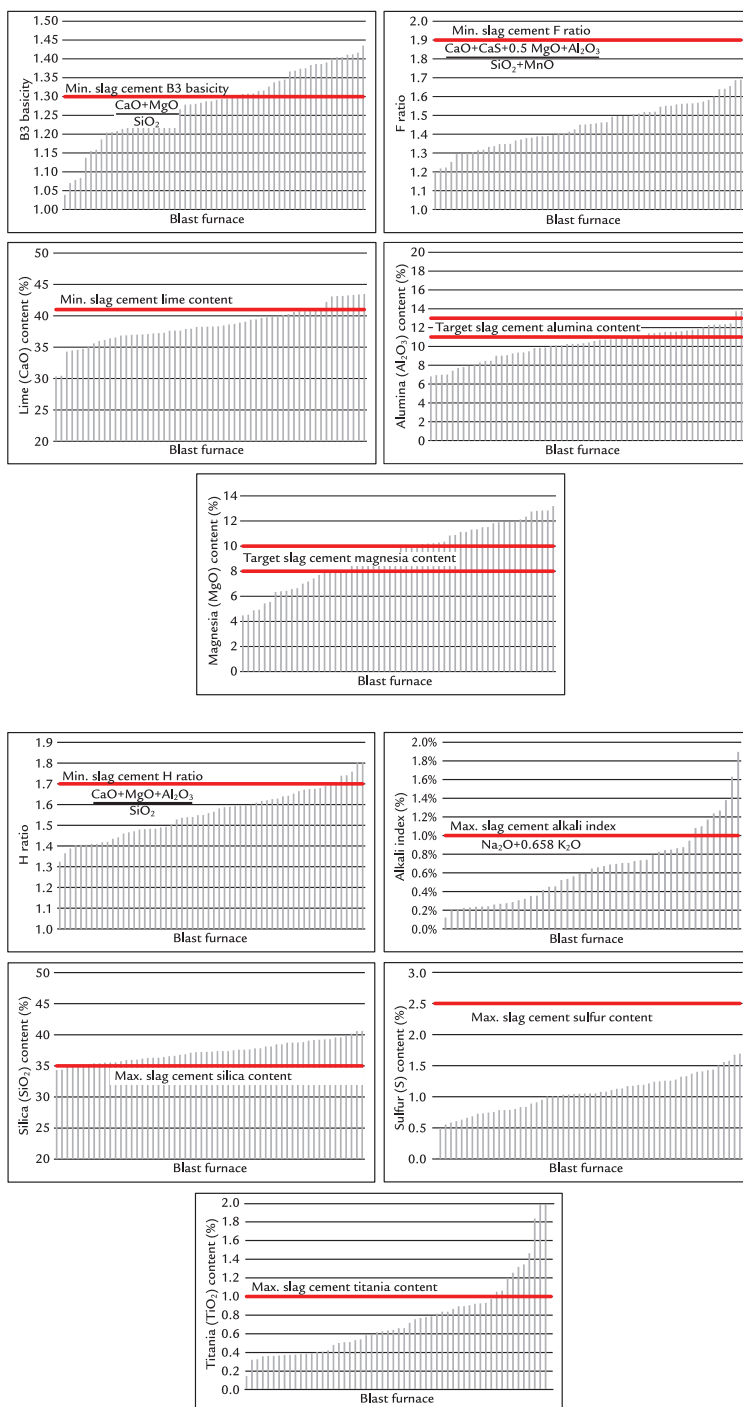
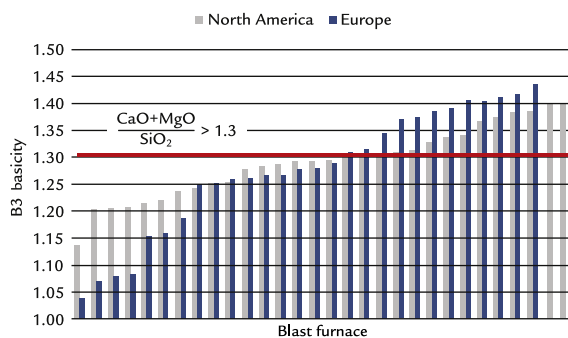


FIGURE 58.13 Comparison of blast furnace operations to the slag cement specifications.¹⁸

TABLE 58.6 Discussion of the Blast Furnace Slag Considerations for Slag Cement Sales

Slag Cement Specification	Blast Furnace Impact	Comments
High basicity B3 or V-ratio > 1.3	Challenging	Blast furnaces often operate at <1.3. A lime-rich material must be added to the cement mix to increase basicity
F-ratio >1.9 [Eq. (58.5)]	Not possible	As above—no blast furnaces operate at $F > 1.9$
H-ratio >1.7 [Eq. (58.7)]	Challenging	As above—only a few blast furnace slags have $H > 1.7$
Lime content >41%	Challenging	Blast furnaces typically operate at 35%–40% CaO to avoid the formation of dicalcium silicate. Only a few operate at >41%
Silica content <35%	Challenging	Most blast furnaces operate at >35% SiO ₂
Alumina content, >11%, <13%	Achievable	Requires an Al ₂ O ₃ rich flux to be added
Sulfur content S < 2.5	Achievable	Blast furnace sulfur input is low
Alkali content (Na ₂ O + 0.658 K ₂ O < 1.0%)	Achievable	Alkali will be low with higher basicity slag
Fe ₂ O ₃ < 2%	Achievable	Blast furnace slag has a low iron content
Magnesia content 8–10%	Achievable	Requires control of the MgO input
Titania content <1%	Achievable	Only possible without continuous titania additions for hearth temperature control
Glass content >90%	Achievable	Water or air granulation is needed to get a fast cooling rate

FIGURE 58.14 Comparison of B3 basicity or V-ratio between North American and European blast furnaces to the slag cement specified value of 1.3.¹⁸

cement producers, the by-product sales are smaller with more sales as aggregate materials.

The blast furnace operator who wants to enhance slag for sale to the cement industry

must operate as close to the slag cement specifications as possible without risking blast furnace process stability. This demands an operation with high slag basicity and the addition of alumina and magnesia-bearing fluxes to approach the slag cement specification. With a high basicity operation, the alkali input must be controlled to a lower level as the alkali removal efficiency will be reduced. Titania additions must be limited as increasing titania pushes the slag out of the cement specification. Good hot metal silicon and temperature control will allow the operator to operate with high B3 basicity and closer to the slag liquidus temperature. Such control is needed to avoid chilling and slag fluidity problems. Control strategies must be in place, such as having a high SiO₂ containing flux (i.e., low-grade iron ore) readily available to be quickly added, should a furnace chilling or irregular

operation be experienced. The high SiO_2 flux addition can be quickly reversed to minimize the amount of off-specification blast furnace slag that is produced.

58.6 SUMMARY

Blast furnace slag design is a key aspect of purifying iron ore minerals into molten pig iron/hot metal. The slag absorbs the gangue minerals in the ore and ash from the coke and injected fuels. The slag must be formulated to absorb these minerals as well as remove unwanted alkali compounds and sulfur in the charge materials and injected coal. The slag must have tolerance to routine changes in hot metal silicon content and remain at a liquidus temperature $<1415^\circ\text{C}$ and with viscosity between 0.2 and 0.5 Pa.s. The blast furnace metallurgist must have the required fluxes present, either in the charged sinter and pellets or directly charged to the blast furnace. The sale of blast furnace slag to cement producers offers an opportunity for the blast furnace operator to add value to slag and reduce the cost of the blast furnace operation. To meet cement quality specifications, hot metal silicon and temperature variations must be as low as possible to allow for a high slag basicity operation. Although demanding, the blast furnace operator will realize important slag by-product sales and savings in hot metal desulfurization costs.

Blast furnace slag usage decreases the cement producer's carbon footprint, energy use, and virgin raw materials consumption while producing cement that yields high-quality concrete with low cracking tendencies. To maximize the value of the blast furnace slag, an air or water granulation system with high availability must be implemented.

EXERCISES

58.1. The four main constituents of slag are (*please circle*)

- Hematite (Fe_2O_3)
- Alumina (Al_2O_3)
- Silica (SiO_2)
- Magnesia (MgO)
- Lime (CaO)
- Manganese oxide (MnO)
- Wustite (FeO)
- Magnetite (Fe_3O_4)

58.2. Based on the phase diagram in Fig. 58.1, why there is such a dramatic increase in the liquidus temperature of the slag when silicon is transferred from the slag to the hot metal in the 10% Al_2O_3 slag? What would be observed in the 15% Al_2O_3 plane of the same quaternary diagram?

58.3. Can any inference be made from the melting point of a component of a slag system on the effect on the liquidus temperature of increasing its fraction in the slag?

58.4. Based on slag cement specifications, why do the methods described for preparing slag for cement usage require the formation of pellets or granules during cooling?

58.5. Why is the elimination of water by use of the air granulation process beneficial?

58.6. Using Appendix X, estimate the slag liquidus temperature for the blast furnaces in Table 1.1. Which blast furnaces have a slag liquidus $<1415^\circ\text{C}$? Which slag making compound is the cause of the high slag liquidus temperatures observed? Slag composition is provided below:

Continent	Asia	Europe	Oceania	South America		North America
Country	Japan	Netherlands	Australia	Argentina	Brazil	Canada
Company	Kobe	Tata Europe	BlueScope	Siderar	CSA	ArcelorMittal
Site/Location	Kakogawa 2	IJmuiden 6	Port Kembla 5	San Nicolas 2	Santa Cruz 1/2	Dofasco 4
Slag						
Mass	kg/t	282	210	309	252	260
CaO/SiO ₂	Mass ratio	1.3	1.1	1.2	1.1	1.1
CaO	%	43.2	38.7	41.8	37.6	39.0
MgO	%	6.5	9.6	5.7	9.9	8.0
Al ₂ O ₃	%	15.2	14.6	14.3	13.2	9.0
SiO ₂	%	34.1	34.1	36.2	35.8	37.0
						35.2

References

- Verein Deutscher Eisenhuttenleute (VDEh), editor. *Slag atlas*, 2nd edition. Verlag Stahleisen; 1995. p. 156–7.
- Izumskiy N, Gordon Y. *Mathematical model and stabilization system for slag mode of blast furnace operation*. Vienna: European Steel and Technology Application Days (ESTAD); 2017. p. 1689–98.
- Papanastassiou D, et al. The effect of Al₂O₃ and MgO on the properties of blast furnace slag. *Stahl und Eisen* 2000;120(7):59–64. ©2000 Verlag Stahleisen GmbH, Düsseldorf, Germany.
- Ray JD, Schatt RR. Blast furnace slag practice at Dofasco and its influence on furnace operations. *AIME Ironmaking Proc* 1987;46, pp. 201–8.
- Chaubal PC, Ricketts J. Slag properties optimization program at inland's eight meter blast furnaces. *AIME Ironmaking Proc* 1991;50:445–55.
- Ponghis N. Recherche des Limites et des Contraintes a la Production de Fonte a Basses Teneurs en Silicium, Soufre, et Azote: Optimisation des Conditions de Marche du Haute Fourneau. In: CRM Internal report no. 7210-AA/210; 1992.
- Ohta, Suito H. Activities of SiO₂ and Al₂O₃ and activity coefficients of Fe₃O and MnO in CaO–SiO₂–Al₂O₃–MgO slags. *Metall Mater Trans B* 1998;29 (1):119–29.
- Geerdes M, et al. Standards for alkali input for blast furnaces. In: *6th International congress on the science of ironmaking (ICSTI) and 42nd ironmaking and raw material seminar*, October 2012. Rio de Janeiro, Brazil: Association of Brazilian Metallurgy (ABM), October 2012. p. 788–97.
- Papanastassiou D, Send A. Operational and environmental benefits by using bauxite in blast furnace (BF). In: *ICSTI/ironmaking conference proceedings, Iron & Steel Society ironmaking conference*, Vol. 57, Toronto, Canada; 1998. p. 1671–8.
- Nippon Slag Association. *Amounts of blast furnace slag produced and used in FY 2015*. <<http://www.slg.jp/e/statistics/index.html>>; 2016.
- Slag Cement Association web site. <<http://slagcement.org/Sustainability/Sustainability.html>>; 2016.
- ASTM Standard C989/989M-14. *Standard specification for slag cement for use in concrete and mortars*. West Conshohocken, PA: ASTM International; 2014.
- Hanson Slag Cement. GBFS specification. <www.hanson.biz> 2014.
- Lewis DW. Properties and uses of iron and steel slags. In: *Symposium on slag*. National Institute for Transport and Road Research South Africa, National Slag Association; 1992.
- Paul Wurth SA. *Paul Wurth brochure*. 2009. <www.paulwurth.com>.
- Faucher S, et al. Recent developments in commercial dry slag granulation and energy recovery. In: *AISTECH 2016, association of iron and steel technology proceedings*, May 2016, Pittsburgh; 2016. p. 137–44.
- Fenzl T, et al. *Installation of a dry slag granulation pilot plant at blast furnace A of voestalpine*. Vienna: European Steel and Technology Application Days (ESTAD); 2017. p. 1763–72.

18. Cameron I, et al. Optimum blast furnace slag composition for hot metal production, slag granulation and cement use. In: *AISTech 2017. Association of Iron and Steel Technology proceedings*, May 2017, Nashville; 2017. p. 401–12.

Further Reading

Ray HS, Sarkar SB. Correlation of sulphur in hot metal with basicity of blast furnace slags. *Trans. Indian Inst. Met.* 1990;43(4).

Burden Distribution

O U T L I N E

59.1 The Evolution of Burden Charging Systems	651	59.7.2 Ferrous Fines	665
59.2 The Two-Bell Top System	652	59.7.3 Scrap Steel and Hot Briquetted Iron	665
59.3 Bell-Less Top Charging	652	59.7.4 Fluxes	666
59.4 Size Segregation and Its Control	656	59.8 Visualizing Gas Flow Conditions in the Blast Furnace	666
59.5 Charging Practice Objectives	659	59.9 Burden Distribution Modeling	666
59.6 Charge Sequencing	660	59.10 Summary	670
59.7 Positioning Fluxes and Miscellaneous Materials	664	Exercises	672
59.7.1 Nut Coke	664	References	673

59.1 THE EVOLUTION OF BURDEN CHARGING SYSTEMS

Early blast furnace operators required a charging system that could introduce raw materials into the blast furnace at a pressure greater than atmospheric pressure. For many years, this was achieved using two-bell charging systems. In the 1970s, the two-bell systems were replaced by the bell-less top (BLT) featuring a rotating chute developed by Paul Wurth. With its improved sealing valves, the BLT

allowed the blast furnace to operate at a higher top pressure.

Blast furnace engineers knew that reducing the pressure drop as process gases traveled through the blast furnace burden materials was an opportunity to increase the blast furnace productivity. With the introduction of metallurgical coke and prepared sinter, furnace operators started to charge the coke and sinter/lump ores in separate layers. The pressure drop over the charge decreased dramatically and production rates rose. Further

improvements were achieved with the use of well-sized iron ore pellets in the 1960s.

The two-bell charging system features a chamber between the small and large bells that can be pressurized or depressurized to allow burden material to be charged at furnace pressure.

With the two-bell system, the blast furnace operators could only manipulate the ore and coke layer thickness through batch weight changes. Some control of the ore-to-coke ratio across the blast furnace diameter could be achieved through the order the charge materials were placed on the large bell. Clearly, a better technology was needed to control material position on the stockline.

With BLT charging equipment, precise charging of the raw materials was now possible. The BLT system featured a rotating charging chute that could tilt and place the raw material anywhere on the stockline. Blast operators used this innovative technology to control process gas flow and reduce blast furnace fuel rates. Strategies to increase the blast furnace service life by systematically controlling the heat load on the blast furnace walls were developed and implemented.

59.2 THE TWO-BELL TOP SYSTEM

Early blast furnaces were equipped with two charging bells to allow charging into the pressurized blast furnace. The system consisted of a small and large bell arranged in series (Fig. 59.1)

The charge materials were placed on the small bell at atmospheric pressure. The space between the large and small bell is depressurized to atmospheric pressure after which the small bell opens to release the charge materials on to the large bell. The small bell then closes, and the space between the bells is pressurized to the blast furnace top pressure. Once the burden descends to the aim stockline or charge

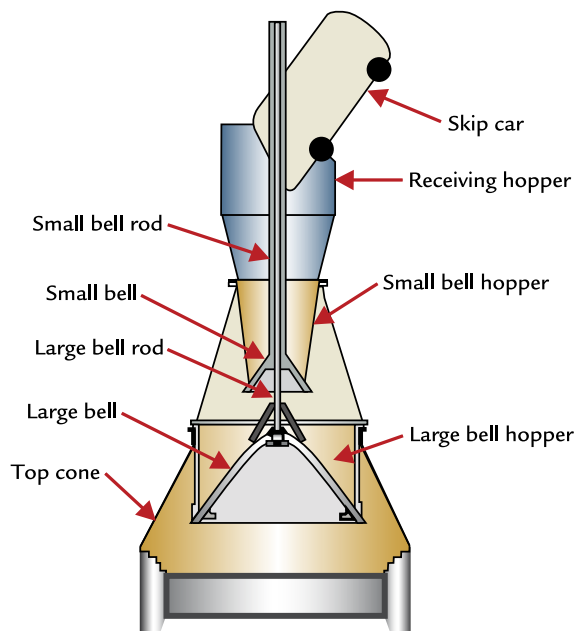


FIGURE 59.1 Two-bell charging system.

level, the large bell is lowered and the charge materials drop on to the stockline. To assure even material distribution on the large bell and hence across the blast furnace circumference, the small bell receiving hopper rotates as the skip is charged into the hopper.

59.3 BELL-LESS TOP CHARGING

In 1972, Luxembourg based Paul Wurth developed a rotating chute arrangement, or BLT, that could allow precise charging of the burden to any position on the stockline—Fig. 59.2. With the BLT, the upper seal valve opens to allow the inbound raw materials to be charged into the lockhopper. The upper seal valve is closed, and the lockhopper is pressurized to the blast furnace pressure using either nitrogen or clean blast furnace gas. Once the burden has descended to the aim charge level, the material flow gate is positioned, the

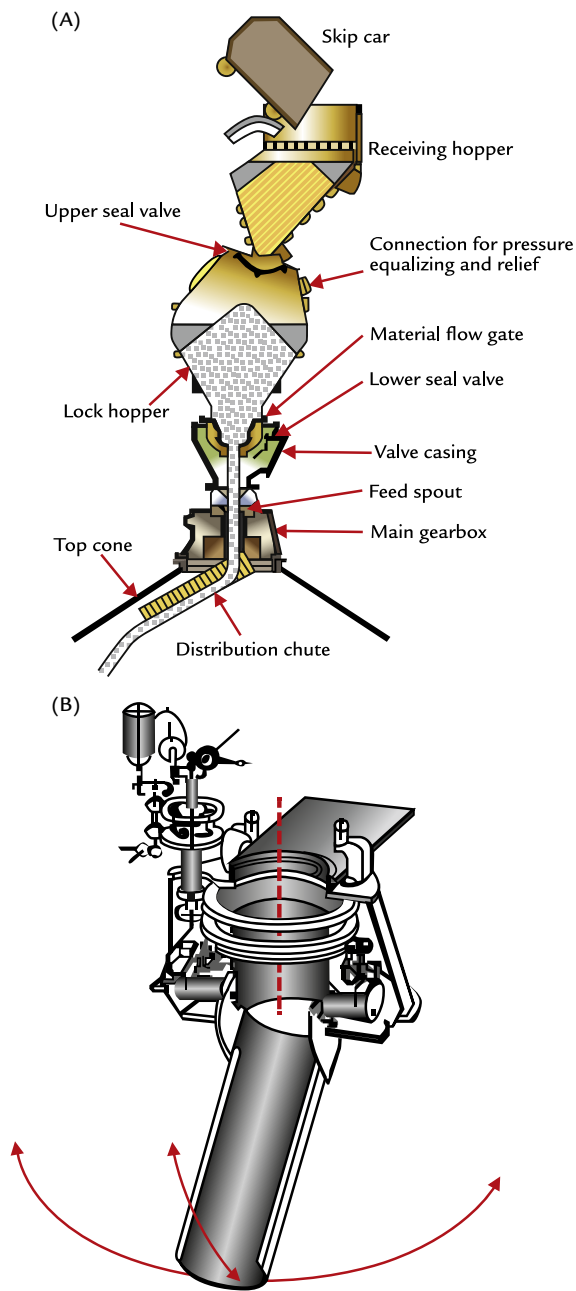


FIGURE 59.2 (A) Single lockhopper Paul Wurth bell-less top with central charging. (B) Typical drive system and chute positions.

lower seal valve opens, and the raw material descends through the feed spout/bifurcated chute onto the rotating chute. The feed spout/bifurcated chute centers the charge before it reaches the rotating chute.

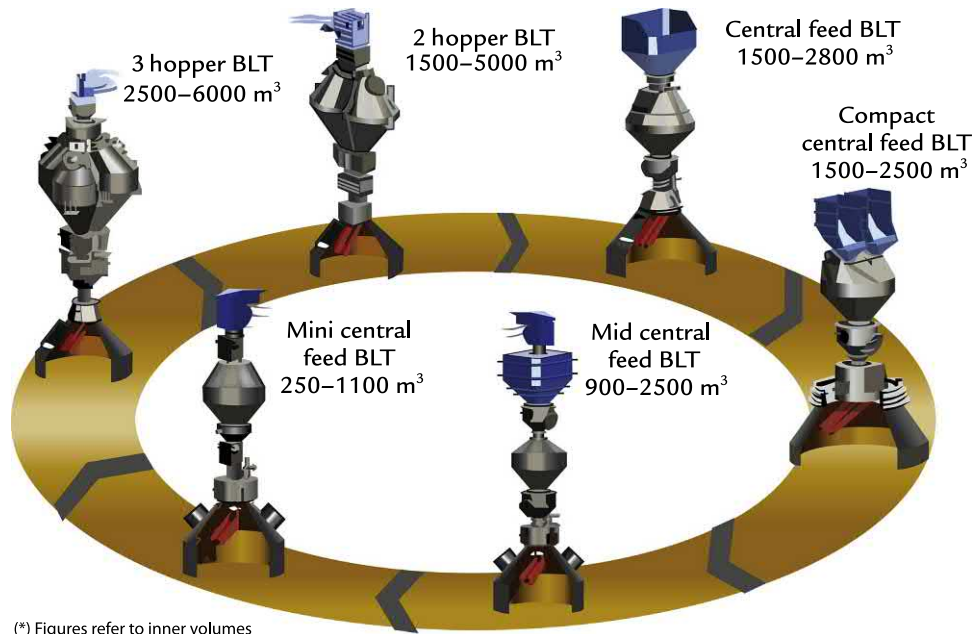
The position of the material flow gate changes for ferrous and coke charges, the gate position restricts flow to meet the planned discharge time. The discharge chute typically rotates at 8 rpm and 11 angles are available to charge the raw material onto the stockline. Discharge time is about 1–2 minutes depending on the batch size. Once the discharge is finished, the lower seal valve closes, the material flow gate returns to its home position, the lockhopper depressurizes, and the upper seal valve opens in preparation to receive the next batch of raw material in the charge sequence.

Since 1972, Paul Wurth has introduced several new BLT models. The new models are designed for a variety of blast furnace sizes, able to replace the two-bell tops on older furnaces, have more robust and better cooled gear boxes, and feature central feeding to reduce size segregation of the raw materials charged to the stockline. Six models that are commercially available are shown in Fig. 59.3.

An example of a three-lockhopper BLT for a large blast furnace is shown in Fig. 59.4.

Other equipment manufacturers have designed systems to charge the materials onto the stockline, but none have significantly displaced Paul Wurth's dominance of the marketplace. Other designs include the following:

- Similar rotating chute designs following expiration of Paul Wurth's original patents. Some have hydraulic controls versus the mechanical systems originally developed by Paul Wurth.
- Primetals developed the Gimbal top to distribute the raw materials through a rotating nozzle.³
- Russian designers developed the rotary charging unit known as the Totem top.



(*) Figures refer to inner volumes

FIGURE 59.3 Bell-less top designs available from Paul Wurth (volume figures refer to blast furnace inner volume).¹

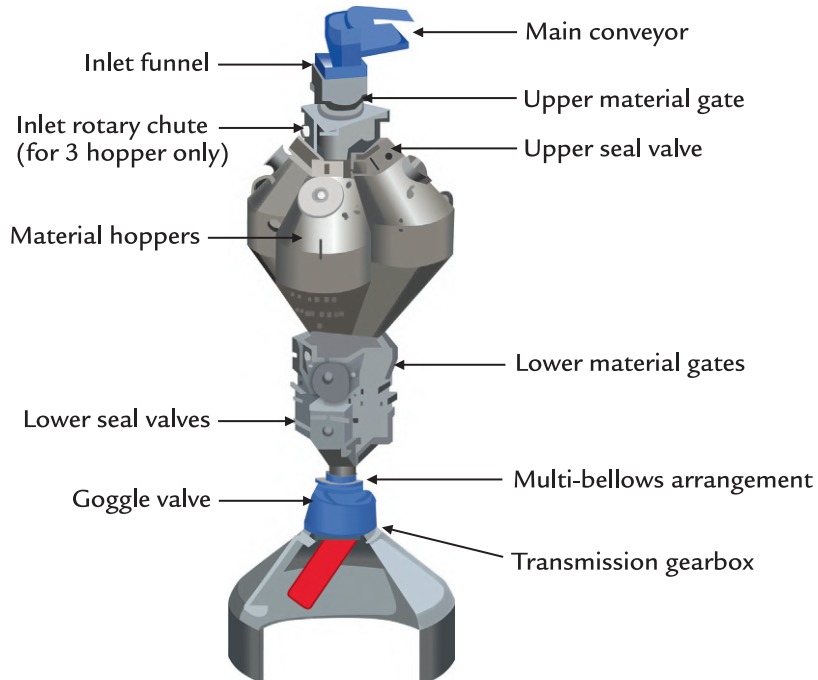


FIGURE 59.4 Paul Wurth second-generation bell-less top with three parallel lockhoppers for a large blast furnace.²

This device uses a rotating assemble to direct the falling raw materials in a precise manner to land at various points on the stockline.⁴

Due to its widespread use in blast furnace charging, the remaining discussion will focus on use of the rotating chute BLT system. The BLT technology is used to charge the burden in either a ring or spiral charging pattern as outlined in Fig. 59.5.

In spiral charging, the weight of material is designated per ring and the chute indexes inward once the designated discharge weight is reached, most likely being a partial ring. In ring charging, the chute indexes after completing a discrete number of revolutions at the designated positions. In both cases, the material flow gates regulate the material flow to allow sufficient time to discharge the material over the

selected rings. In designing a charging pattern, each batch would use only some of the available rings.

Using an infrared camera, ArcelorMittal (AM) has documented the charging behavior during blast furnace operation.⁵ AM advocated charging based on the weight of materials per ring using the lockhopper load cells, that is, spiral charging to better account for varying discharge speed as the lockhopper empties.

Blast furnace operators learned that having coke charged directly to the furnace center is important to manage the pressure drop and increase gas flow through the blast furnace. BLTs required improvements to allow precise central coke charging. These include decreasing the angle that the chute ultimately reaches and adding a plate at the end of the chute or closing the entire top to guide the coke directly

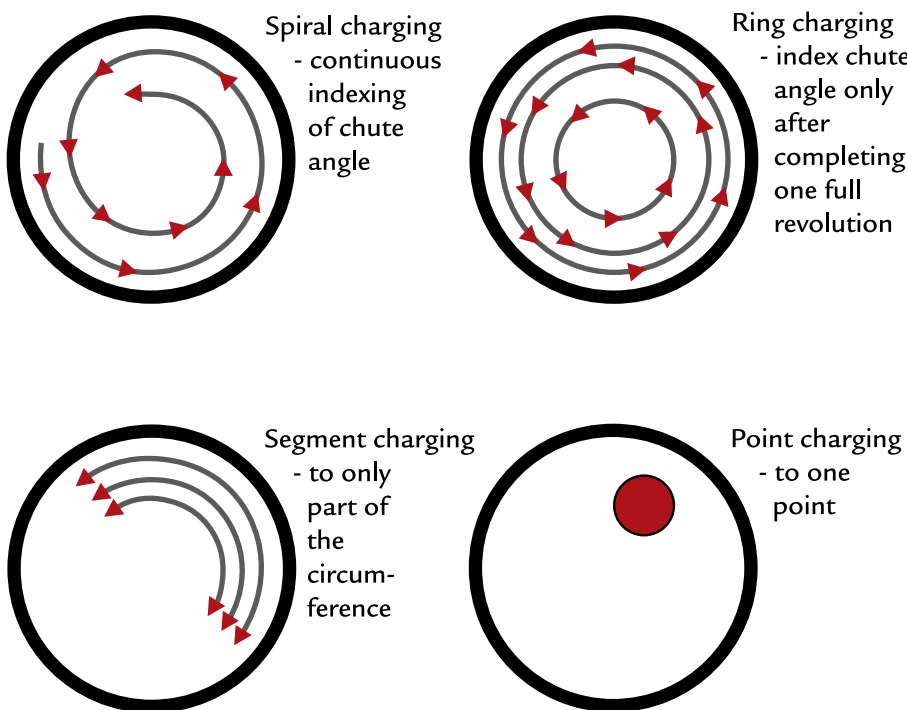


FIGURE 59.5 Burden distribution capabilities of bell-less top charging systems.

to the center. The material flow gate can close part way through the charge and retain a designated amount of coke in the lockhopper. This allows the chute to index to the center position and then the material flow gate reopens to discharge the remaining coke directly to the center ([Fig. 59.6](#)).

Sector and spot charging are used for special situations. AK Steel in Dearborn, Michigan reported point charging of ilmenite ore to reduce hearth wall temperatures over one tap-hole.⁶ Using the point charging technique, AK Steel reduced the amount of ilmenite needed by applying it only to the affected area. When blowing in a blast furnace using a limited number of tuyeres, sector charging over the active tuyeres can be used to provide coke where needed and to help maintain an even stockline. This can be especially useful when recovering a blast furnace with a chilled hearth and charging coke on a point or sector basis can speed up its delivery to the active tuyeres.

59.4 SIZE SEGREGATION AND ITS CONTROL

Size segregation can have a strong impact on burden permeability and gas flow. Resistance to gas flow is acute when small and large particles mix and the smaller particles fill the spaces between the large ones as illustrated in [Fig. 59.7](#).

As the coke, ore, and miscellaneous materials pass from the stockhouse to the BLT and eventually to the stockline, size segregation occurs. Coarser particles report to the blast furnace center as they tend to roll toward the center when a downward profile is used. Finer particles tend to remain where they are charged. The difference in particle size across the blast furnace can be significant, as shown in [Fig. 59.8](#).

Engineers have studied BLT designs to understand the causes of size segregation

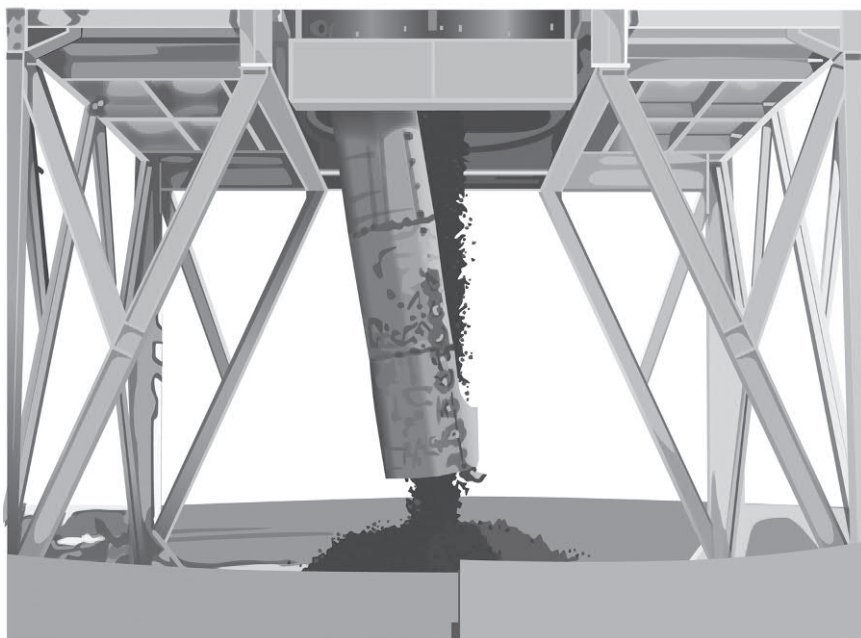


FIGURE 59.6 Charging chute modified to allow for accurate central coke charging.²

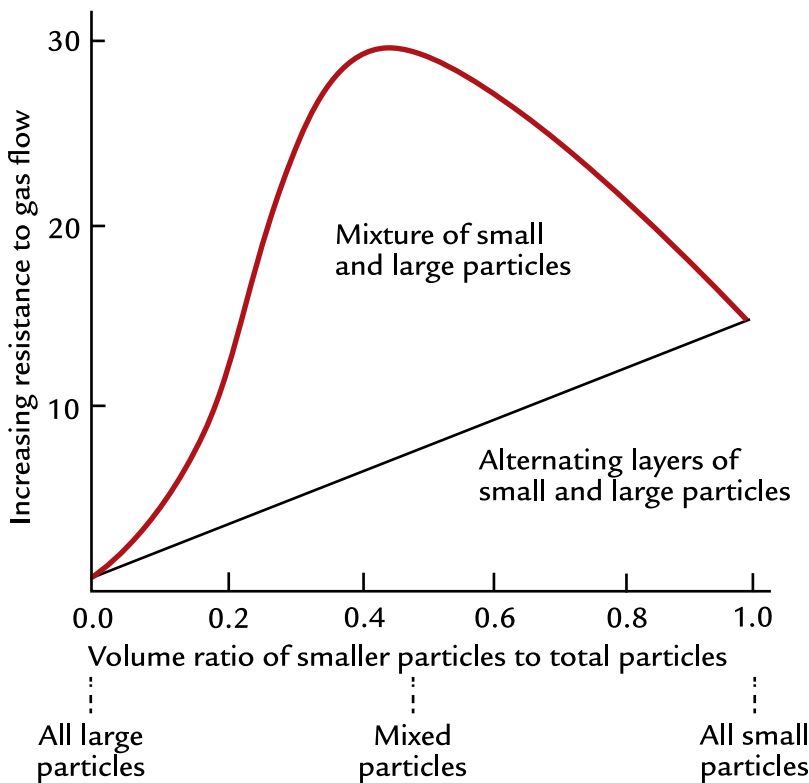


FIGURE 59.7 Impact on gas flow when mixing small and large particles.

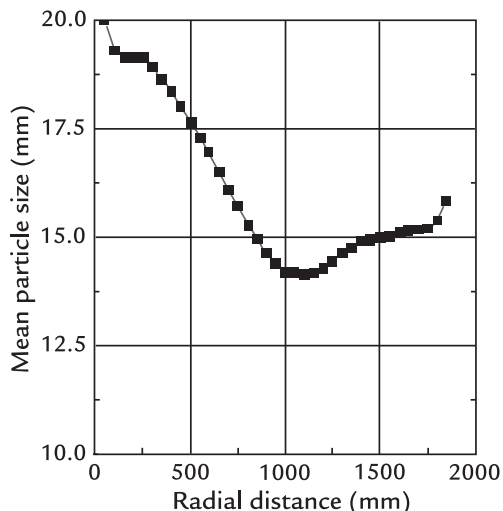


FIGURE 59.8 Difference in sinter particle size across the blast furnace throat.⁷

and how to improve the BLT design and promote an even size distribution on the stockline.

Discrete element modeling (DEM) is a powerful tool to help understand particle behavior in flowing streams. In Fig. 59.9, particle segregation can be seen in the common parallel lockhopper BLT arrangement before the lockhopper discharges the burden into the blast furnace.

Parallel lockhoppers do not discharge in a plug flow manner. As the lockhopper discharges, materials in the upper levels tend to flow downward more quickly (Fig. 59.10).

The DEM illustrates that the charge materials leave in a typical funnel flow manner where materials above the discharge point

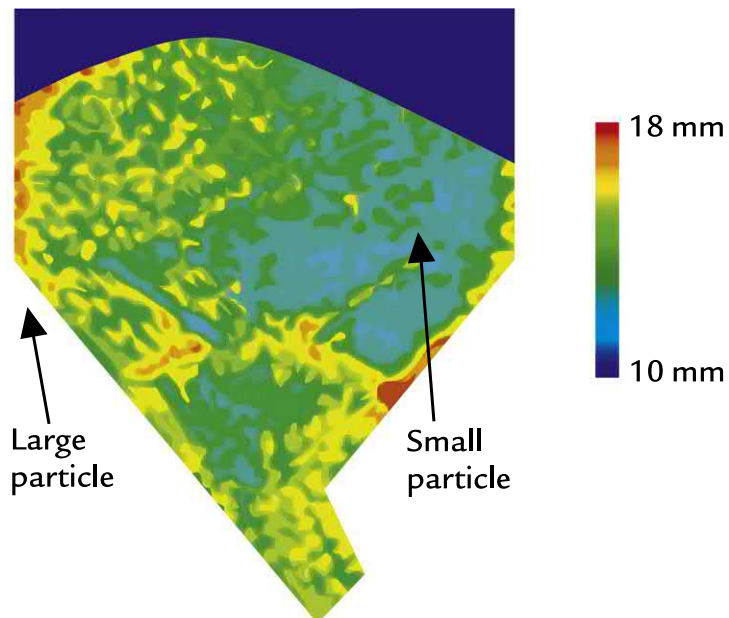


FIGURE 59.9 Sinter size segregation in BLT parallel lockhopper arrangement.⁷ BLT, Bell-less top.

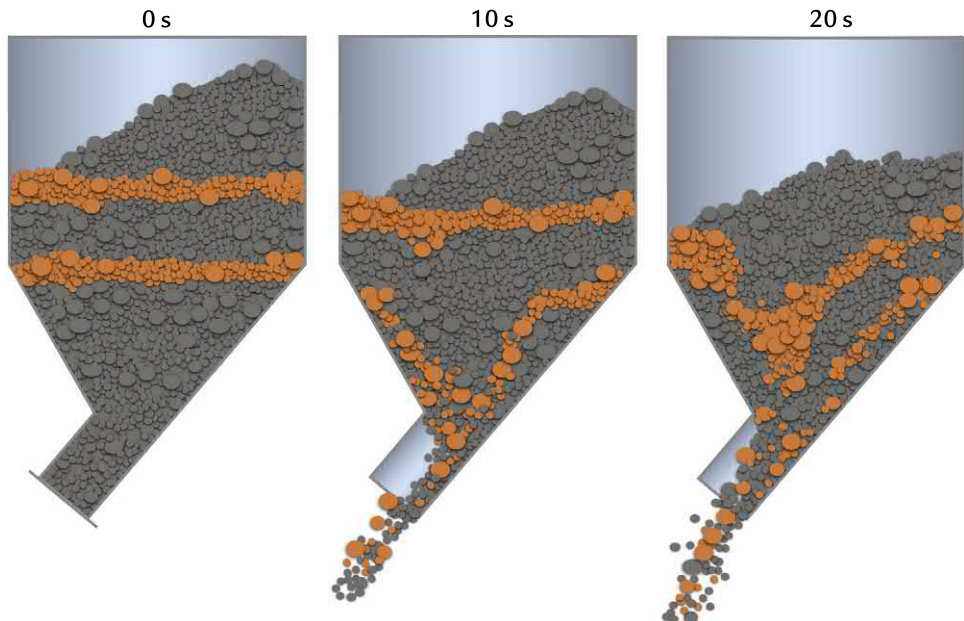


FIGURE 59.10 Discharge of BLT lockhopper showing funnel flow.⁸ BLT, Bell-less top.

and at the center flow quickly to the discharge. Knowledge of this flow behavior can be exploited when designating the loading order of nut coke, sinter fines, and fluxes into the lockhopper. Placement of these materials at the top, middle or bottom of the lockhopper can bias their flow toward the furnace center or walls. Additional segregation can occur the moment that the rotating chute aligns with the lockhopper discharge and the opposite position when the chute is 180 degrees to the lockhopper discharge position. The raw materials exit at a higher velocity when the chute and lockhopper discharge position are aligned and a slower velocity when the materials must turn almost 90 degrees. This can result in varying ore-to-coke on the plane through the lockhopper discharge locations. In some instances, the authors have witnessed a higher frequency of tuyere failures at these positions.

Several design changes have been implemented to minimize size segregation while discharging the lockhoppers. As shown in Figs. 59.2 and 59.3, on small-to-medium-sized blast furnaces, a single lockhopper can be located on the furnace center line so that the burden discharges vertically onto the rotating chute. For larger furnaces that must deploy two or three lockhoppers, the lockhopper shape was redesigned by Paul Wurth to promote central flow and reduce particle size segregation (Fig. 59.11).

As the understanding of particle size segregation improves with DEM, further improvements to the BLT design are likely to reduce particle size segregation and promote an even size distribution of coke and ferrous burden on the stockline. Understanding the nature of the segregation can be used by the blast furnace engineer to design the burden charging sequence.

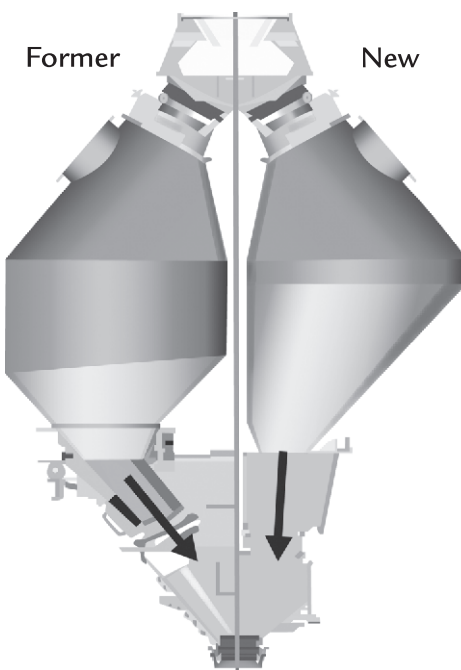


FIGURE 59.11 Changes in BLT parallel lockhopper design to promote central flow and reduce particle size segregation on the stockline.² BLT, Bell-less top.

59.5 CHARGING PRACTICE OBJECTIVES

Blast furnace instrumentation is critical to optimizing the burden distribution practice and to adapt the burden distribution for changing operational conditions. Modern blast furnaces have specialized instruments to understand gas flow in the furnace stack area as illustrated in Fig. 59.12.

The BLT charging sequence will normally have the following objectives:

- Provide the highest possible CO gas utilization.
- Assure that there is sufficient wall gas flow to dry, heat, and reduce the ferrous burden adjacent to the wall.

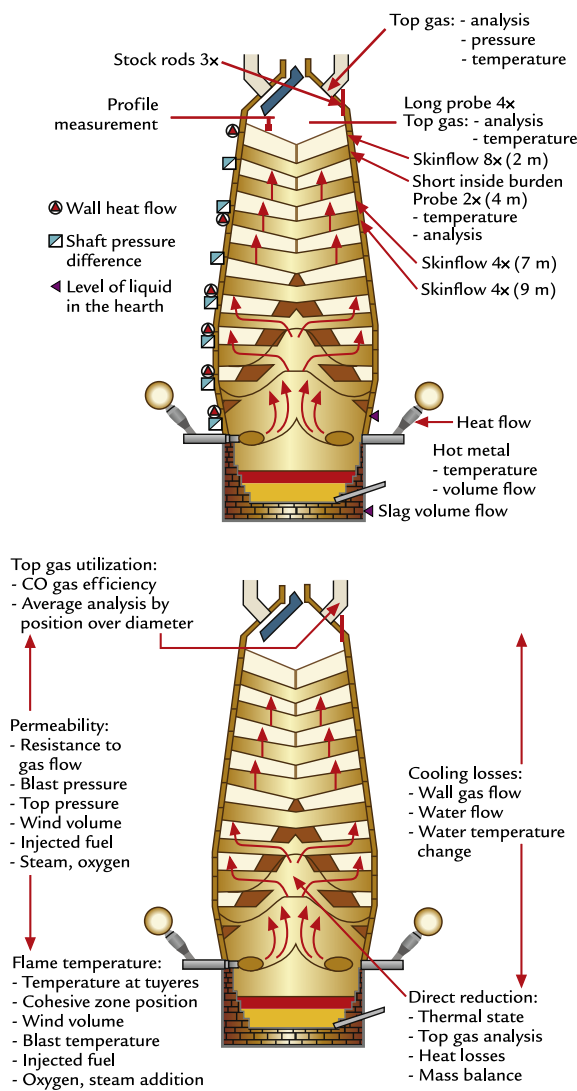


FIGURE 59.12 Instrumentation for gas flow control.

- To limit the wall gas flow to minimize wear on the stack cooling system.
- Allow sufficiently high central temperature to purge zinc contained in the burden to leave the furnace. If zinc is not adequately purged, zinc can build up within the blast

furnace and accumulate in the stack and hearth refractories, degrading their performance (refractory swelling, reduced thermal conductivity).

An idealized top temperature profile is provided in Fig. 59.13.

Interpreting the correct moment to change the charging practice is challenging and requires careful interpretation of the available instrumentation. A policy where the coke layer is first adjusted to manage the gas flow is preferred. The ore layer ultimately fuses, hence changes to the ore distribution have a stronger impact on the gas flow patterns. Coke changes are more forgiving and this reduces the risk of a blast furnace upset. As the charging practice is optimized to provide a balance of high gas utilization and low wall heat load, the blast furnace can become sensitive to relatively minor changes in the charging practice. It can be challenging to distinguish between blast furnace coke rate and gas flow distribution changes. In Fig. 59.14, a scheme to assess the blast furnace condition and decide on whether to adjust the fuel rate or the charging practice is described.

The burden distribution must be designed to assure that the root of the cohesive zone on the wall-side is high enough so that tuyere leakage or tipping problems do not occur as illustrated in Fig. 59.15.

59.6 CHARGE SEQUENCING

Ideally, the ferrous burden and coke are charged in two alternating layers. Actual charging sequences are more complex due to stockhouse arrangements, lockhopper size limitations, and burden layer thickness requirements. Alternate layering is always used, but a series of layers may be engineered to provide

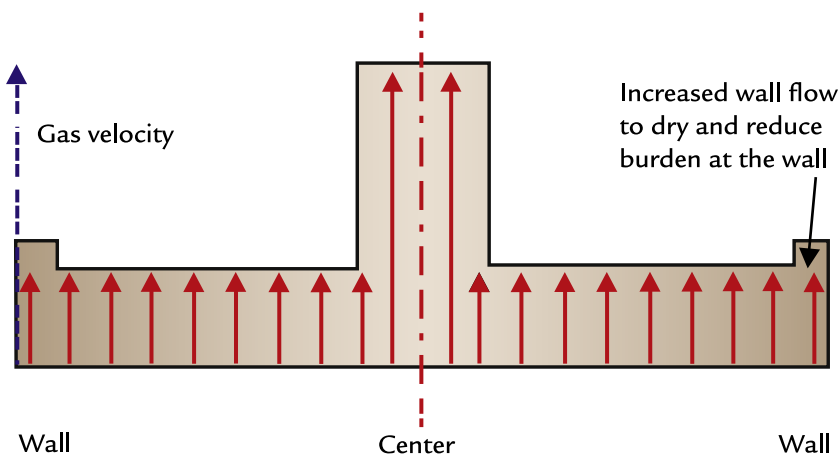


FIGURE 59.13 Idealized top temperature profile to promote gas utilization and provide sufficient wall side gas flow.

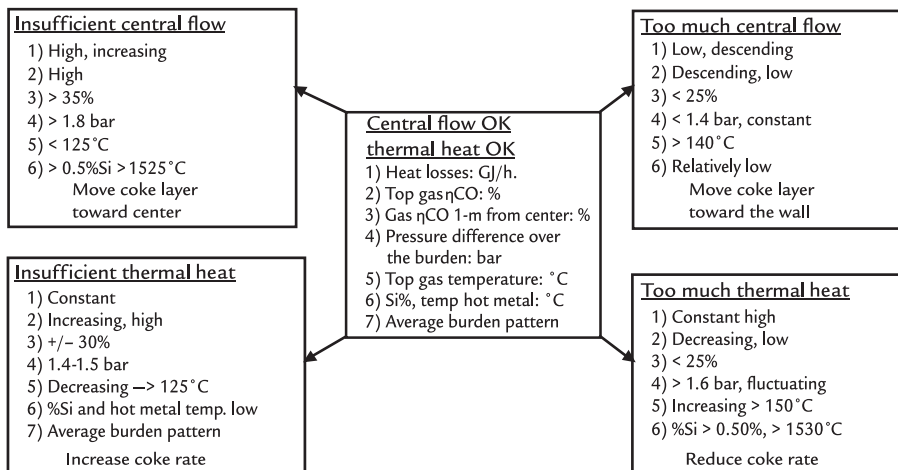


FIGURE 59.14 Interpreting blast furnace gas flow and thermal conditions.

a prescribed ore-to-coke ratio over the furnace cross section. When designing the charge, the coke batch must be large enough to provide a minimum coke layer thickness in the blast furnace belly where the cross section is the largest.

A popular sequence is a downward spiral with center coke chimney. This charging

pattern is shown in Fig. 59.16 and has the following features:

- An ore-free center is provided by a large volume of coke charged to the furnace center. This helps control the pressure drop over the burden, especially at high productivity.
- The coke at the center can block ore from moving to the center where ore can reduce

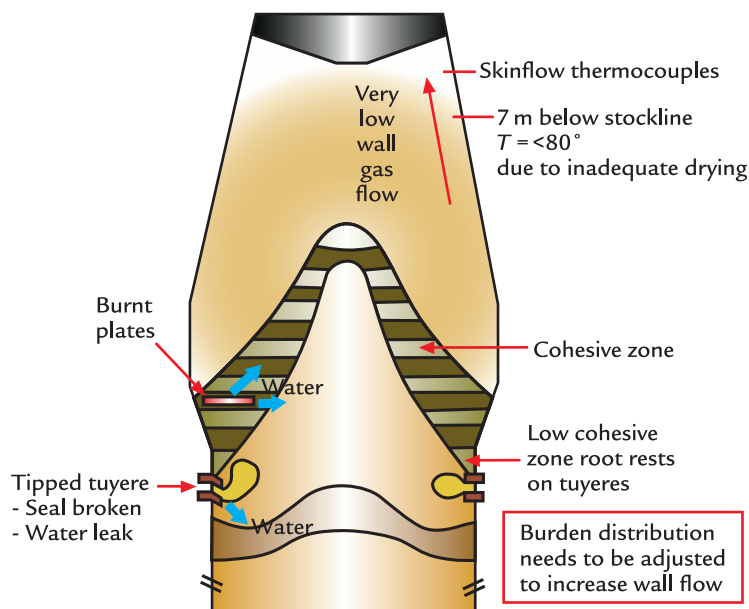


FIGURE 59.15 Blast furnace symptoms when wall gas flow is too low and the volume of coke at the wall needs to be increased.

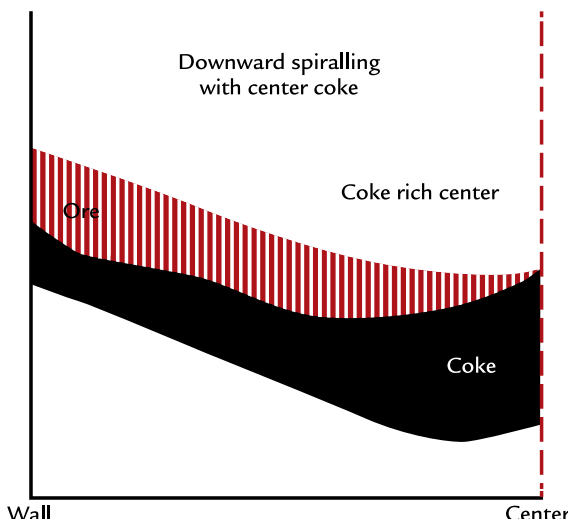


FIGURE 59.16 Coke and ore layer profile for high productivity and high gas utilization.

central gas flow, especially when the ore melts. This is important when the stockline level is below the aim position. With a low

stockline, it is harder for the materials falling from the discharge chute to reach the wall side of the furnace throat.

- The ore layer is thicker at the wall to reduce process gas flow adjacent to the wall and related wear of the refractory and cooling system.
- The ore-to-coke layer thickness is relatively even from the wall to close to the center to help improve gas utilization.

Tata Steel in The Netherlands operates with a very low coke rate, high pulverized coal injection rate, and high productivity. To achieve this, Tata Steel utilizes a flat burden profile, a nearly ore-free center, and sufficient coke at the wall to provide adequate burden drying and reduction in the upper furnace. The Tata Steel charging profile may be seen in Fig. 59.17.

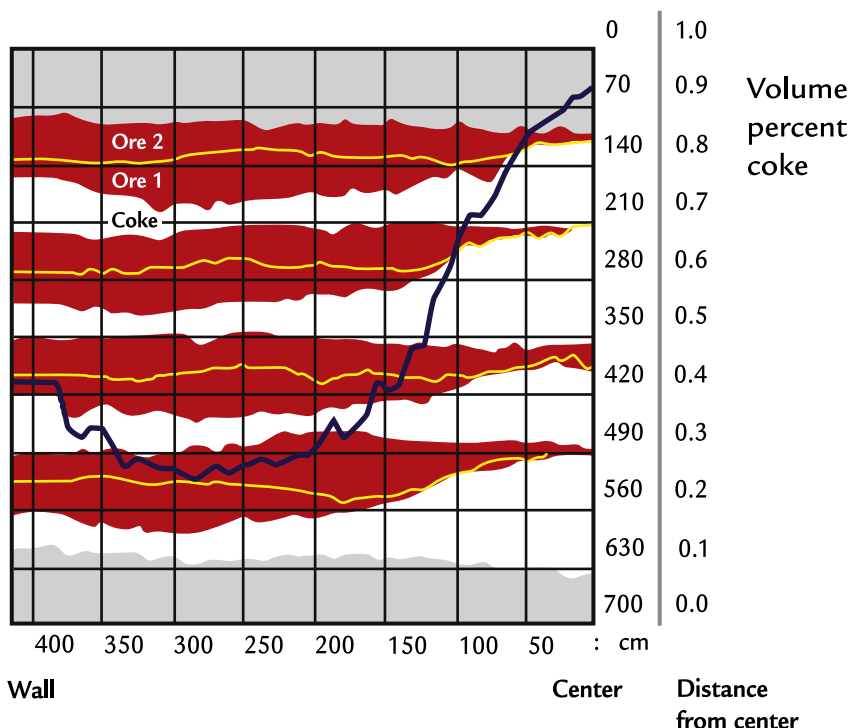


FIGURE 59.17 Burden profile for Tata Steel Blast Furnace 6 at 255 kg coke/t hot metal, as measured by a radar profile meter.⁹

From Fig. 59.17, the following can be observed:

- The burden profile is nearly flat.
- The coke layer features a large amount of coke at the furnace center to minimize rolling of the ferrous burden to the furnace center.
- Overall, the center has about 90 vol.% of coke to provide permeability for process gas flow. The small amount of ore close to the center is needed to get the highest possible CO gas utilization. Note that the alternating coke layers vary in thickness at the furnace center between ~85 and 95 vol.% to allow some ore to cover the center and improve gas utilization on alternating coke batches.

- The volume of coke at the wall side is increased to about 40 vol.% to assure that there is sufficient process gas flow at the wall. With a large volume of porous coke at the furnace center, the natural tendency is for gases to flow from wall to center to follow the path of least resistance. Increasing the volume of coke at the wall reduces this tendency by providing a porous zone for process gas to flow. This assures proper drying and reduction of the ore adjacent to the wall and positions the root of the cohesive zone in the bosh of the blast furnace. Note that the volume of coke varies on alternate layers; less coke is charged at the wall side when the center

coke is almost 100 vol.%. On the next layer, when the center coke is slightly reduced, the volume of coke at the wall side is correspondingly increased.

- Ore is charged in two batches; Ore 1 is charged on top of the coke to flatten the overall burden profile. Ore 2 is charged over the entire cross section and provides a small amount of ore in the furnace center to promote high CO gas utilization.
- Between wall and center, the volume of coke is the lowest to promote CO reduction. A smooth transition occurs from wall to center to maximize contact between reducing gases and ferrous burden in the blast furnace stack zone.
- When charging at a lower stockline position, the flat profile will provide a consistent cross-sectional ore-to-coke ratio and minimize flooding the center with ore which will increase gas flow on the wall side when the ore melts in the lower furnace.

To achieve the profile shown in Fig. 59.17, the blast furnace operator would need to use all 11 rings available in the burden distribution charging program. Special consideration will be needed to charge the center coke. For example, the chute will need to move back far enough to allow the coke to fall directly in the center. Some blast furnaces have the option to close the material flow gate based on the remaining coke in the lockhopper, index the chute to the furnace center, and then reopen the flow gate to complete the charge. This allows precise delivery of coke to the furnace center. For furnaces without this feature, the coke planned for the central rings must consider the longer chute travel time between the inner-most rings where the difference in ring angles is more significant than at the wall-side of the furnace. For example, to move from ring 11 to 10 at the wall side, the chute may only need to reduce its angle by 2–3 degrees

between rings, while in the center, the indexing between the inner-most rings may be 10–20 degrees and chute indexing speed becomes a factor in designing the charging pattern.

The positioning of sinter and pellets may vary. Pellets tend to easily roll; this increases when the pellets are in the fast-flowing gases present in the blast furnace. Sinter with its irregular shape tends not to roll as it is charged onto the stockline. When designing the charge, the engineer should anticipate the potential for pellets to roll. Pellet rolling can increase when the stockline is below the target level. The charge should be designed to avoid pellets rolling into the furnace center as the local ore-to-coke ratio could quickly increase, impacting gas flow and burden descent. A flatter profile minimizes the impact of rolling pellets. Creating a profile where pellets would roll to the mid-radius is preferred.

59.7 POSITIONING FLUXES AND MISCELLANEOUS MATERIALS

A variety of fluxes and miscellaneous materials are often part of the blast furnace charge. These can include scrap, hot briquetted iron (HBI), nut coke, sinter and pellet fines, limestone, high silica ore, quartz, bauxite, serpentine, and plant-specific mix of ferrous wastes. These materials can bring positive effects to the blast furnace operation and how they are placed in the charging sequence can maximize their impact. For discussion, these materials will be grouped as follows: nut coke, ferrous fines, scraps/HBI, and fluxes.

59.7.1 Nut Coke

Nut coke is typically metallurgical coke sized to the 5–30 mm range. When charged

with the ferrous burden, the nut coke can replace regular-sized coke on a one-to-one basis. Nut coke addition rates of 40–80 kg/t hot metal can improve performance and reduce costs.

With its high surface area, nut coke can react in the thermal reserve zone with the rising CO₂ and form CO near ore particles. Should the nut coke survive to the lower furnace, it can react directly with any wustite present and reduce it to metallic iron. In doing so, the nut coke creates porosity in the cohesive zone when the ore layer fuses and melts. Charging the nut coke as close to the wall as possible helps promote gas flow where the ore layer meets the wall, known as the root of the cohesive zone. Positioned at the wall, the nut coke raises the root of the cohesive zone above the tuyeres.

To position the nut coke against the wall, care must be taken to load the nut coke at the bottom of the lockhopper. In skip charged furnaces, the nut coke should be the last material charged into the skip so it is the first added to the lockhopper. If the lockhopper holds two skips, the nut coke should be charged entirely on the top of the first skip in the series. For conveyor belt charged furnaces, the nut coke should be the first material added to the conveyor belt to be positioned at the bottom of the lockhopper.

59.7.2 Ferrous Fines

Charging sinter and pellet fines offers a means to improve the iron recovery in the steelworks when used in small quantities. Two approaches can be considered; charge these materials mid-radius to minimize the impact on the ore layer permeability or, alternatively, charge adjacent to the blast furnace wall in the later part of the campaign to reduce gas flow/heat load on the stack and bosh cooling system.

Charging the fines at mid-radius reduces the impact that these fines can have on process gas flow by mixing the fines with the regular-sized sinter and pellets. Closer to the center, the ore layer is often thinner so the fines will have less impact on the layer permeability. This requires the fines to be charged at the top of the lockhopper to delay their consumption until the rotating chute moves away from the wall. For skip charging, ferrous fines should be charged to the bottom of the skip and preferable on the last skip filling the lockhopper. For conveyor-charged blast furnaces, the ferrous fines should be charged at the end of the ferrous materials.

When charging to the furnace wall, care must be taken not to impede the ferrous layer permeability to the point where unreduced material descends to the tuyere level and damages or tips (pushes) the tuyeres down, breaking the seal between tuyere and tuyere cooler. In practice, a balance must be made between the addition rate of the ferrous fines and the gas flow control in the blast furnace. Ultimately, only a small addition of ferrous fines can be charged into a high production blast furnace.

59.7.3 Scrap Steel and Hot Briquetted Iron

Prereduced iron-bearing materials can greatly increase the productivity of the blast furnace. Added in substantial amounts, the prereduced materials decrease the amount of process gas in the blast furnace and lower the blast furnace top temperature. This can lead to issues drying and preheating the raw materials as well as having sufficient gas temperature to remove zinc from the burden.

To minimize the cooling effect of scrap and HBI, avoid charging these materials to the wall side of the blast furnace. When the process gas flow rate decreases, the problem of low gas

flow is greatest at the wall zone. Scrap and HBI should be charged from the mid-radius towards the center. For a skip charged furnace, the scrap/HBI should be charged in the bottom half of the skip or, in a two-skip sequence, in the second skip. For conveyor-charged furnaces, the scrap and HBI should be in the second half of the ferrous charge.

59.7.4 Fluxes

Fluxes added to the blast furnace can be in three categories; acid fluxes such as high silica ore or quartz, basic fluxes such as limestone and serpentine, and neutral fluxes such as bauxite. Acid fluxes should be positioned mid-radius to react with the fluxed sinter and pellets. Basic fluxes should be charged mid-radius to the center where temperature is higher to promote early decomposition of carbonates. Neutral fluxes such as bauxite can be positioned anywhere in the charge. Charged with the limestone or lime rich sinter, the bauxite will facilitate the formation of a lower melting point primary slag as Al_2O_3 helps dissolve the CaO.

59.8 VISUALIZING GAS FLOW CONDITIONS IN THE BLAST FURNACE

A variety of sophisticated instruments are used to understand burden layer buildup, gas analysis, and gas temperature in the upper part of the blast furnace shaft. These include;

- stock rods, either mechanical or radar based, to measure the burden position;
- fixed above burden probes to measure gas temperature and analysis;
- retractable or laser-based profile meters to measure the coke and ore layer buildup;

- retractable in-burden probes that measure gas temperature and composition over the radius; and
- measurement and mapping of the surface temperature of the burden using sound waves or an infrared camera.

These probes are illustrated in Fig. 59.18.

The SONic MApping (SOMA) system developed by TMT—Tapping and Measuring Technology—uses sound waves to map the burden surface temperature, Fig. 59.19.¹⁰

The use of infrared cameras has brought great insight into the conditions present at the stockline as the burden is charged into the blast furnace. With this technology, ArcelorMittal provided evidence of the top temperature profile when pellets are charged on the coke layer—see Fig. 59.20.⁵

Events such as off-centered gas flow and wall-side gas channeling can be quickly identified with the infrared or acoustic measurement of the burden surface temperature as illustrated in Fig. 59.21.

Off-center gas flow could be related to charging systems operational issues such as material flow gate wear, short or long discharge times, lockhopper scale errors, or a worn or damaged charging chute. Plugged tuyeres could also cause a nonsymmetric gas flow pattern. Water leakage from the furnace stack cooling plates or staves may report as a cold area on the walls at the stockline. Rapid detection of these events with the advanced top temperature measurement instrumentation facilitates urgent repairs and minimizes blast furnace operational problems. Serious wall channeling events can be seen with the top surface temperature mapping.

59.9 BURDEN DISTRIBUTION MODELING

Implementing a bell-less charging program is a complex process. It begins with first

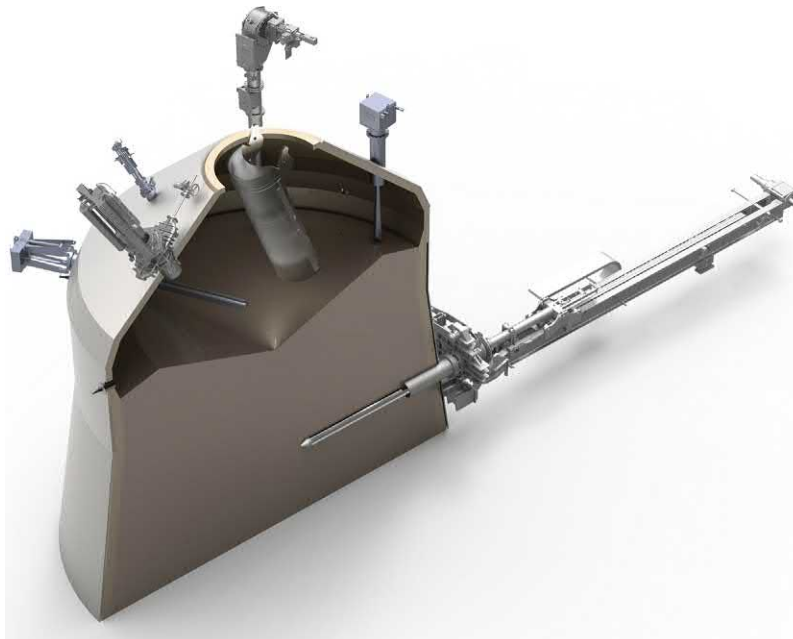


FIGURE 59.18 Typical probes used to assess burden layer buildup, gas temperature, and chemical composition and to map the burden surface temperature. *Source: Sketch courtesy: TMT—Tapping Measuring Technology S.à r. l & G.m.b.H.*

measuring the material falling curves. When the BLT was first introduced in the 1970s, operators would assemble the charging equipment in a test rig where the falling curves could be measured and material buildup assessed (see Fig. 59.6). As the industry gained experience, falling curves were measured in the blast furnace itself during the initial furnace fill prior to blow in. Falling curves can be measured by filming the material trajectories against a fixed grid made of steel or plastic. More recently, a laser net has been used to observe/film the material falling angles for each chute angle.

Tata Steel in Europe developed a special trajectory probe that can be inserted above the burden to measure the falling curves while the blast furnace is operating.⁹ The probe features a series of switches that count the particle impacts as the burden is charged into the blast

furnace. The switches with the greatest number of counts indicate where the material will be positioned on the furnace radius for a given charge angle. Tata found significant changes to the material trajectories as the charging chute wore during its service life. The trajectory probe allowed for changes to the fall curves and chute angles when a new chute is installed and as it wears. Details of the trajectory probe are provided in Fig. 59.22.

With the falling curves in-hand, the blast furnace engineer uses a layer buildup model to show the filling pattern in the furnace. Scenarios to adjust the charging practice can be assessed to improve blast furnace gas efficiency or control wall heat loads. An example of the output from burden distribution models can be seen in Fig. 59.23.

TMT developed a laser-based system to map the layer buildup in 3D. This presentation

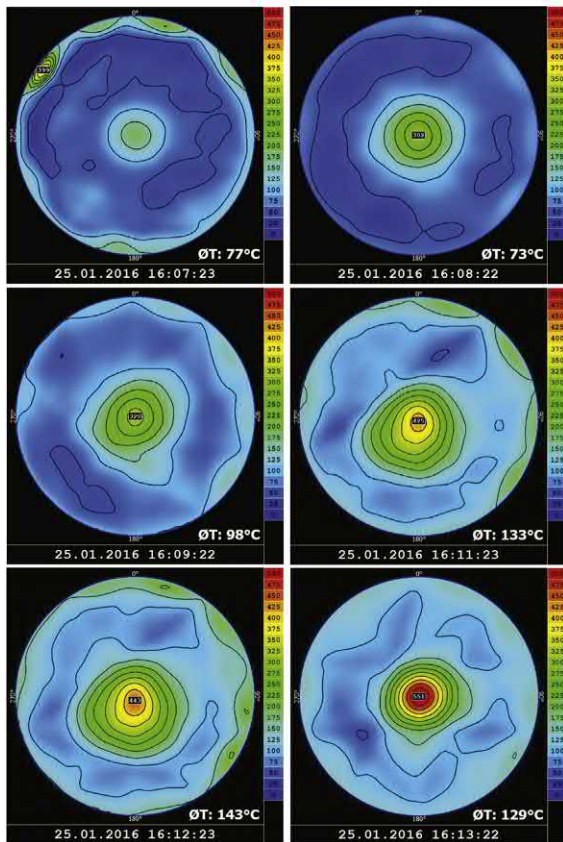


FIGURE 59.19 SOMA system of TMT maps the burden surface temperature measuring changes in the speed of sound in the space above the burden. TMT, Tapping and Measuring Technology. Source: Images courtesy: TMT—Tapping Measuring Technology S.à r.l. & G.m.b.H.

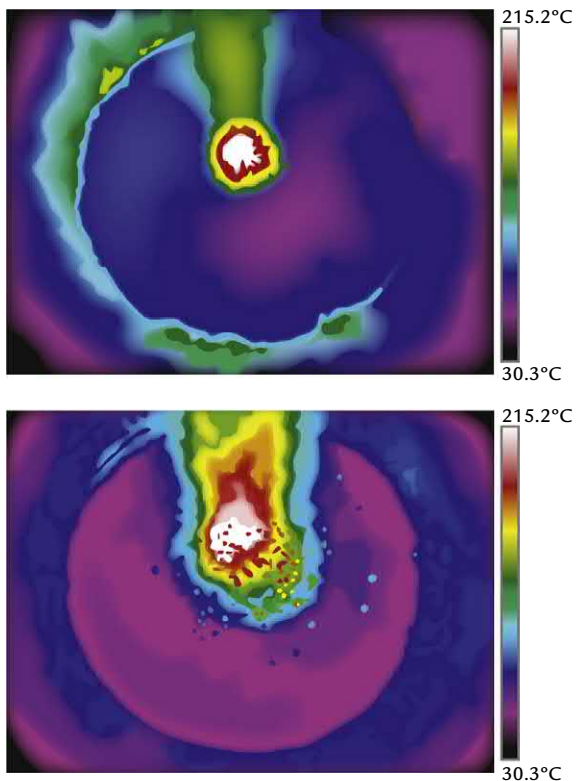


FIGURE 59.20 (Top figure) Coke layer top temperature profile prior to pellet discharge. (Bottom figure) Top temperature profile after pellet charging showing a central temperature increase and reduced temperature in the wall zone.⁵

shows variation of the layer buildup over the entire furnace throat area. Of note is the nature of the layers; they are not as repeatable as the offline material buildup models would suggest. This is a result of the dynamic nature of the blast furnace and how material buildup can be uneven because of conditions lower in the blast furnace. The 3D measurement of the layer buildup and resulting 2D volumes of ore and coke over the furnace diameter are shown in Fig. 59.24.

Burden distribution models must show the layer buildup on a ring-by-ring basis. The layer height, angle, and radial ore-to-coke ratio are necessary to design a charging

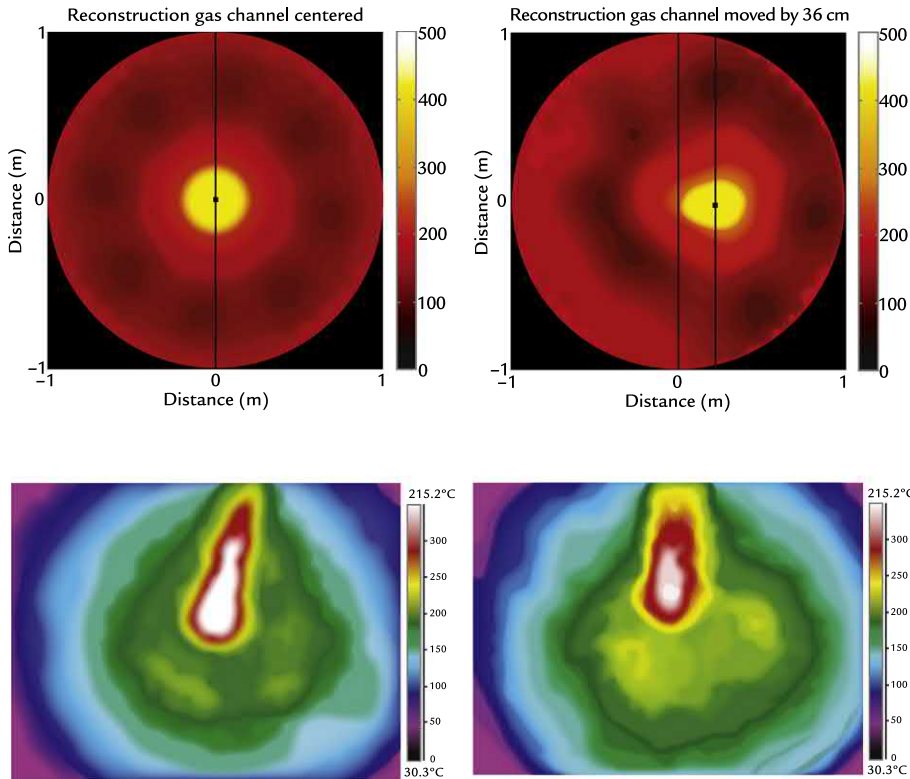


FIGURE 59.21 On the left, examples of strong gas flow at the furnace center and on the right, strong gas flow is away from the blast furnace center. Top images are measured using the SOMA acoustic system and the bottom images with an infrared camera.^{5,10}



FIGURE 59.22 Trajectory probe used at Tata Steel in Europe.⁹

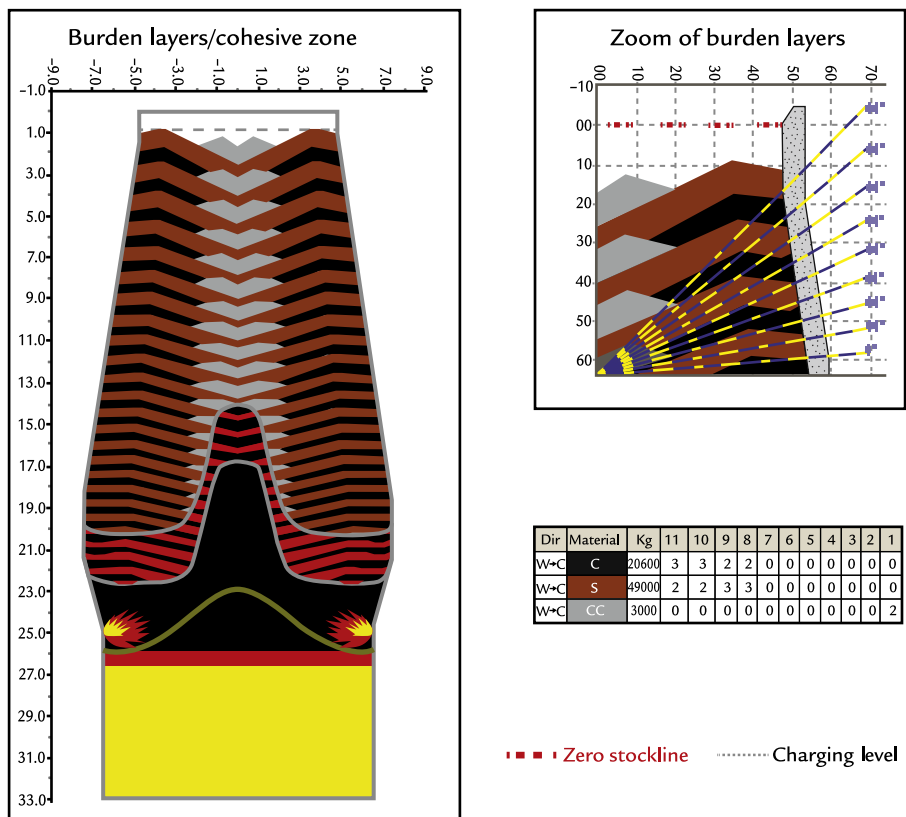


FIGURE 59.23 Burden distribution model developed by Paul Wurth for Tata Steel H Blast Furnace.¹¹

practice. Newer models use DEM to assess particle segregation. Technicians are modeling the charge from the stockhouse to lockhoppers to furnace stockline to fully understand segregation within the charge materials and its ultimate impact on gas flow in the blast furnace (Fig. 59.25).

59.10 SUMMARY

The distribution of the ore and coke layers in the blast furnace is of immense importance to optimize the blast furnace operation. The appropriate charging practice is needed to

realize the highest gas utilization, lowest wall heat load, and best transfer of heat from the process gases to the charge materials. The BLT originally developed by Paul Wurth is the charging system of choice for most blast furnace operators. Sophisticated instrumentation and models are needed to interpret the blast furnace performance and to optimize the employed charging pattern. Improved understanding of the impact of material segregation has emerged with the use of DEM where individual particle movement can be calculated. Further optimization of charging methods will emerge with the greater understanding that advanced instrumentation and DEM can provide.

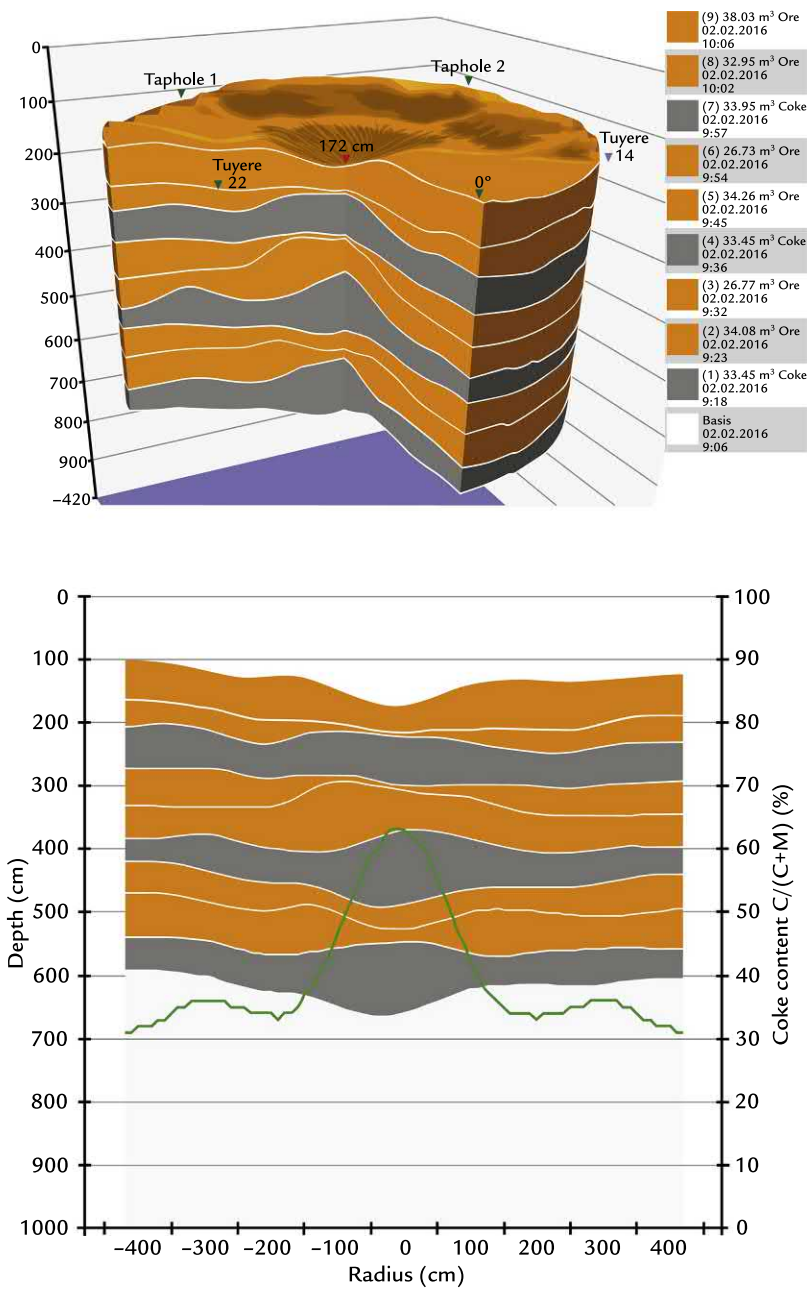


FIGURE 59.24 Layer measurements and coke volume estimate using TMT 3D TopScan System. *TMT*, Tapping and Measuring Technology. Source: Courtesy of TMT—Tapping Measuring Technology S.à r. l & G.m.b.H.

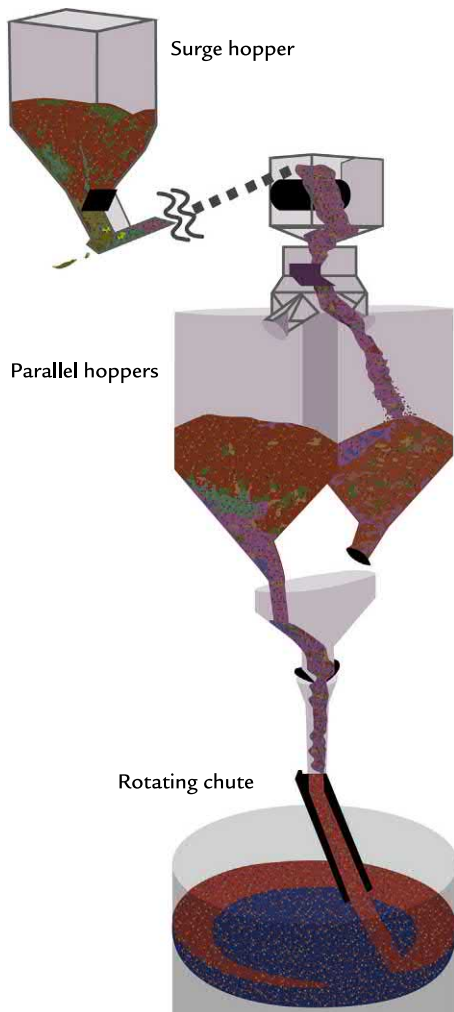


FIGURE 59.25 Nippon Steel Corporation model to simulate particle segregation in bell-less top blast furnace charging systems.⁷

EXERCISES

- 59.1.** The role of burden distribution is (*please circle one*)
- increase production
 - reduce top temperature

- allow high coal injection rates
 - control gas flow in the furnace
- 59.2.** Please circle T (true) or F (false) for each of the following statements:
- | | | |
|---|---|--|
| T | F | The bell-less top can lay down materials anywhere on the stockline. |
| T | F | Each bell-less top is purchased preprogrammed and ready to perform. |
| T | F | Probes and other instrumentation are required to track the effectiveness of the burden distribution. |
- 59.3.** Wall gas flow (not excessive) promotes (*please circle one*)
- drying of the burden and stable burden descent
 - controlled gas flow in the furnace
 - tuyere tipping
 - high gas utilization
- 59.4.** Smooth descent of the burden requires (*please circle one*)
- maintaining a pressure drop of $>160 \text{ kPa}$
 - good mixing of coke and pellets
 - maintaining the stockline
 - no overaccumulation of liquids in the hearth
 - low heat flux (low heat transfer to the staves)
- 59.5.** Uniform ore/coke ratio is desired over most of the furnace cross section because it (*please circle one*)
- lowers the coke rate
 - optimizes gas flow distribution
 - increases productivity
 - lowers hot metal silicon content
 - increases hot metal temperature
- 59.6.** Complete the sentence begun in column 1 by joining it to the appropriate ending in column 2.

Gas flow	Regions where the coke layer is relatively thick compared to the ore layer
Coke particles are larger	Takes the path of least resistance
Gas flows preferentially to	So, the coke layer is more permeable
Gas flows poorly	Since coke is solid throughout the furnace height
The coke distribution is important to manage the gas flow	Through mixed layers

59.7. The proposed ideal gas flow aims for (please circle one)

- uniform gas/solids contact over most of the furnace cross section
- a weak narrow peak of central gas flow
- a decrease in gas flow at the wall (compared to that over most of the furnace cross section)

References

1. Simoes JP, et al. BF process technology enhanced by charging control, process monitoring and mathematical models. In: *43rd Ironmaking and raw material seminar*, ABM, October 2013, Rio de Janeiro, RJ, Brazil; 2013. p. 861–70.
2. Tockert P, et al. *New developments in Bell-less Top® charging technology of blast furnaces*. St Louis, MO: Association of Iron and Steel Technology, AISTech; 2009. p. 413–21.
3. Whitfield P, et al. *The SIMETALCIS Gimbal Top® “putting it through its paces”*. St Louis, MO: Association of Iron and Steel Technology, AISTech; 2009. p. 387–96.
4. Boronbaev B, et al. On the controlled charging of blast furnaces. In: *6th International conference on the science and technology of ironmaking—ICSTI*, October 2012, Rio de Janeiro, RJ, Brazil; 2012. p. 852–9.
5. Huang D, et al. *Blast furnace above-burden infrared camera*. Pittsburgh, PA: Association of Iron and Steel Technology, AISTech; 2016. p. 493–505.
6. Street S, et al. *Curse to cure—the utilization of titanium-bearing products in blast furnace ironmaking*. Pittsburgh, PA: Association of Iron and Steel Technology, AISTech; 2013. p. 381–403.
7. Mio H, et al. Development of particle flow simulator in charging process of blast furnace by discrete element method. *Miner Eng* 2012;33:27–33.
8. Wu S, et al. DEM simulation of particle size segregation behavior during charging into and discharging from a Paul-Wurth type hopper. *Chem Eng Sci* 2013;99:314–33.
9. Bakker T, et al. *Developments of operating points of the IJmuiden blast furnaces*, METEC, June 2011, Dusseldorf, Germany, Session 13; 2011. p. 1–9.
10. Tonteling M, et al. *2D blast furnace top gas temperature measurement system—SOMA*. Pittsburgh, PA: Association of Iron and Steel Technology, AISTech; 2013. p. 2339–48.
11. Roy SK, et al. *The new TATA Steel H blast furnace: design concept, commissioning and operating results for a record time, project execution*, METEC, June 2011, Dusseldorf, Germany, 2011. p. 1–8, Session 24.

APPENDIX

A

Compound Molecular Masses and Compositions

TABLE A.1 Compound Molecular Masses and Compositions

Compound	Molecular Mass		
Al ₂ O ₃	102.0	53.0 mass% Al	47.0 mass% O
CH ₄	16.0	75.0 mass% C	25.0 mass% H
C ₂ H ₆	30.1	80.0 mass% C	20.0 mass% H
C ₃ H ₈	44.1	81.7 mass% C	18.3 mass% H
C ₄ H ₁₀	58.1	82.7 mass% C	17.3 mass% H
C ₅ H ₁₂	72.1	83.2 mass% C	16.8 mass% H
C ₆ H ₁₄	86.2	83.6 mass% C	16.4 mass% H
CO	28.0	42.9 mass% C	57.1 mass% O
CO ₂	44.0	27.3 mass% C	72.7 mass% O
CaCO ₃	100.1	56.0 mass% CaO	44.0 mass% CO ₂
CaO	56.1	71.5 mass% Ca	28.5 mass% O
CaO:SiO ₂	116.2	48.3 mass% CaO	51.7 mass% SiO ₂
(CaO) ₂ :SiO ₂	172.3	65.1 mass% CaO	34.9 mass% SiO ₂
Cr ₂ O ₃	152.0	68.4 mass% Cr	31.6 mass% O
Fe _{0.947} O	68.9	76.8 mass% Fe	23.2 mass% O
Fe ₃ O ₄	231.6	72.4 mass% Fe	27.6 mass% O

(Continued)

TABLE A.1 (Continued)

Compound	Molecular Mass		
Fe ₂ O ₃	159.7	69.9 mass% Fe	30.1 mass% O
H ₂ O	18.0	11.2 mass% H	88.8 mass% O
MgCO ₃	84.3	47.8 mass% MgO	52.2 mass% CO ₂
MgO	40.3	60.3 mass% Mg	39.7 mass% O
MnO	70.9	77.4 mass% Mn	22.6 mass% O
Mn ₃ O ₄	228.8	72.0 mass% Mn	28.0 mass% O
MnO ₂	86.9	63.2 mass% Mn	36.8 mass% O
P ₂ O ₅	141.9	43.6 mass% P	56.4 mass% O
SO ₂	64.1	50.0 mass% S	50.0 mass% O
SiO ₂	60.1	46.7 mass% Si	53.3 mass% O
CaCO ₃	100.1	56.0 mass% CaO	44.0 mass% CO ₂
		12.0 mass% C	32.0 mass% O ₂
MgCO ₃	84.3	47.8 mass% MgO	52.2 mass% CO ₂
		14.2 mass% C	38.0 mass% O ₂

B

Air Composition and Nitrogen/Oxygen Ratio Assumption

Air at ground level contains the gases given in [Table B.1](#). However, for our purposes, we treat air as 21 mol (vol.)% O₂ and 79 mol (vol.)% N₂.

TABLE B.1 Air Composition at Ground Level

Gas	Mol%
N ₂	78.084
O ₂	20.9476
Ar	0.934
CO ₂	0.0314
Ne	0.001818
CH ₄	0.0002
He	0.000524
Kr	0.000114
H ₂	0.00005
Xe	0.0000087

Values from Wikipedia Gas Composition.
Retrieved on January 1, 2018 by Googling Gas Composition.

B.1 AIR COMPOSITION, MASS%

This section calculates the composition of;

1. mass% O₂; and
2. mass% N₂

of 21 mol% O₂, 79 mol% N₂ air.

One kilogram mole of this air contains;

$$1 \text{ kg mol air} * \frac{21 \text{ mol\% O}_2}{100\%} = 0.21 \text{ kg mol O}_2$$

and

$$1 \text{ kg mol air} * \frac{79 \text{ mol\% N}_2}{100\%} = 0.79 \text{ kg mol N}_2$$

while 1 kg mol of O₂ contains 32 kg of O₂ and 1 kg mol of N₂ contains 28 kg of N₂, where 32 and 28 are the molecular masses of O₂ and N₂ respectively.

From the above four statements, 1 kg mol of air contains;

$$0.21 \text{ kg mol O}_2 * \left[\frac{32 \text{ kg O}_2}{\text{kg mol of O}_2} \right] = 6.72 \text{ kg O}_2$$

$$0.79 \text{ kg mol N}_2 * \left[\frac{28 \text{ kg N}_2}{\text{kg mol of N}_2} \right] = 22.12 \text{ kg N}_2$$

for a total mass of 28.84 kg.

These masses are equivalent to;

$$\text{mass \% O}_2 = \frac{6.72 \text{ kg O}_2}{28.84 \text{ kg air}} * 100\% = 23.3$$

$$\text{mass \% N}_2 = \frac{22.12 \text{ kg N}_2}{28.84 \text{ kg air}} * 100\% = 76.7$$

and the N₂/O₂ mass ratio of the air is:

$$\frac{\text{mass N}_2}{\text{mass O}_2} \text{ ratio} = \frac{76.7 \text{ mass\% N}_2}{23.3 \text{ mass\% O}_2} = 3.3$$

This ratio is the basis for Eq. (4.5), which is used throughout the book.

B.2 EFFECTS OF IGNORING ARGON

The chemical and thermal effects of ignoring argon are discussed in Appendix C. They are negligible.

C

Effect of Argon on Blast Furnace Calculations

Air contains ~ 1 mol (vol.)% Ar(g) (see Appendix B). We lump this Ar(g) with N₂(g) throughout our book - by designating that air contains 21 mol (vol.)% O₂(g) and 79 mol (vol.)% N₂(g).

This appendix shows that representing air's Ar(g) as N₂(g) has little effect on the results of our blast furnace calculations.

Like nitrogen, argon passes through the blast furnace without reacting. They both behave the same chemically, so they may be lumped together without misrepresenting blast furnace chemistry. Their enthalpies are slightly different, as discussed in the next section.

C.1 ENTHALPY OF 0.79 KG MOL OF N₂(g)

The enthalpy of 1 kg mol of N₂(g) at 930°C (1203.15K) from JANAF¹ is;

$$28.216 \text{ MJ}$$

and the enthalpy of 0.79 kg mol of N₂(g) at 930°C (1203.15K):

$$\begin{aligned} &= 0.79 \text{ kg mol of N}_2(\text{g}) * 28.216 \text{ MJ/kg mol of N}_2(\text{g}) \\ &= 22.291 \text{ MJ.} \end{aligned}$$

C.2 ENTHALPY OF 0.78 KG MOL OF N₂(g) + 0.01 KG MOL OF AR(g)

The enthalpy of 1 kg mol of Ar(g) at 930°C (1203.15K) is 18.811 MJ and the enthalpy of 0.78 kg mol of N₂(g) + 0.01 kg mol of Ar(g) at 1200K equals:

$$\begin{aligned} &0.78 \text{ kg mol of N}_2(\text{g}) * 28.216 \text{ MJ/kg mol of N}_2(\text{g}) \\ &+ 0.01 \text{ kg mol of Ar(g)} * 18.811 \text{ MJ/kg mol of Ar(g)} \\ &= 22.197 \text{ MJ} \end{aligned}$$

The difference is $\{(22.291 - 22.197)/22.291\} * 100\% = 0.4\%$ which will have very little effect on our matrix calculations.

Reference

1. JANAF. *NIST JANAF thermochemical tables*. Retrieved on January 1, 2016 by Googling NIST JANAF Thermochemical Tables; 2016.

D

CO Raceway Exit Gas Proof

Raceway flame temperature calculations of Chapter 14, Raceway Flame Temperature, assume that the carbonaceous portion of raceway exit gas is predominantly CO(g). The objective of this appendix is to show that this is true. Equilibrium and molar balance calculations are used.

D.1 RACEWAY INPUTS AND OUTPUTS

[Fig. D.1](#) describes inputs and outputs of our raceway, with no tuyere injectants.

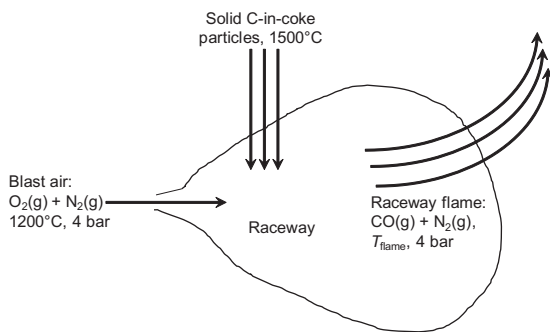
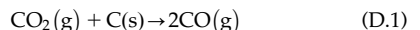


FIGURE D.1 Tuyere raceway with dry blast air (only). The inputs are 1200°C air and 1500°C falling C(s)-in-coke particles. The objective of this appendix is to show that the product carbonaceous gas is predominantly carbon monoxide.

1200°C dry air is blown into the raceway - where it reacts with falling 1500°C C(s)-in-coke particles. Reaction of these two hot inputs produces even hotter raceway exit gas ~2000°C.

First contact of the hot blast's O₂ with descending carbon particles produces CO₂(g). This CO₂(g) then reacts further with descending C-in-coke of [Fig. D.1](#) to give CO(g) by the following reaction:



We postulate that this reaction rapidly reaches equilibrium at the high temperatures in and around the raceway.

The equilibrium constant for Reaction (1) is

$$K_E^{\text{CO}_2(\text{g})+\text{C}(\text{s}) \rightarrow 2\text{CO}(\text{g})} = \frac{(a_{\text{CO}}^E)^2}{a_{\text{CO}_2}^E * a_{\text{C}}^E} \quad (\text{D.2})$$

where K_E is the equilibrium constant, unitless and a^E is the equilibrium thermodynamic activities of the reactants and product, unitless.

The equilibrium activity of C(s) is 1 because it is a pure solid.

The equilibrium activities of CO(g) and CO₂(g) are

$$a_{\text{CO}}^E = X_{\text{CO}}^E * P_t / 1$$

and

$$a_{\text{CO}_2}^E = X_{\text{CO}_2}^E * P_t / 1$$

where X_{CO}^E and $X_{CO_2}^E$ are the equilibrium mol fractions of $CO(g)$ and $CO_2(g)$ in the raceway exit gas, P_t is the absolute pressure in the raceway ~ 4 bar, and 1 is the pressure (bar) at which the thermodynamic activity of a pure ideal gas is 1.

With these substitutions, the mol fractions of $CO(g)$ and $CO_2(g)$ in the raceway exit gas are related to the equilibrium constant of Eq. (D.2) by the following equation:

$$K_E^{CO_2(g)+C(s)\rightarrow 2CO(g)} = \frac{(X_{CO}^E * (\frac{P_t}{1}))^2}{(X_{CO_2}^E * (\frac{P_t}{1})) * 1} \quad (D.3)$$

The value of this equilibrium constant at $2000^\circ C$ is 1.2×10^5 (Appendix E).

D.2 CO(g), CO₂(g), AND N₂(g) QUANTITIES AND MOL FRACTIONS IN RACEWAY EXIT GAS

This section and the next show how we calculate CO and CO₂ mol fractions of Eq. (D.1), that is, X_{CO} and X_{CO_2} .

The calculations are begun by specifying that 1 kg mol of O₂(g) enters the raceway in blast air, that is;

$$n_{O_2}^{\text{input}} = 1 \text{ kg mol} \quad (D.4)$$

All n values in this appendix are based on this 1 kg mol of O₂ in blast air.

The molar composition of dry air is ~ 79 mol% N₂ plus ~ 21 mol% O₂ (Appendix B), that is, each kg mol of air contains 0.79 kg mol of N₂ and 0.21 kg mol of O₂.

This leads to:

$$\begin{aligned} n_{N_2}^{\text{input}} &= \frac{79 \text{ mol\% } N_2}{21 \text{ mol\% } O_2} * n_{O_2}^{\text{input}} \\ &= \frac{79}{21} * 1 \text{ kg mol input } O_2 = 3.76 \text{ kg mol input } N_2 \end{aligned} \quad (D.5)$$

Furthermore, because nitrogen does not react in the raceway:

$$n_{N_2}^{\text{raceway exit gas}} = n_{N_2}^{\text{input}} = 3.76 \text{ kg mol } N_2 \text{ in raceway exit gas} \quad (D.6)$$

D.3 OXYGEN MOLAR BALANCE

We now use the raceway's steady-state oxygen molar balance to calculate kg mol of CO and CO₂ in the raceway exit gas. These are then used to determine the raceway's equilibrium exit gas CO and CO₂ mol fractions (Eq. (D.3)).

The oxygen molar balance is:

$$\begin{aligned} \left[\begin{array}{l} \text{kg mol O} \\ \text{in input } O_2 \end{array} \right] &= \left[\begin{array}{l} \text{kg mol O} \\ \text{exit gas CO} \end{array} \right] \\ &+ \left[\begin{array}{l} \text{kg mol O} \\ \text{in raceway} \end{array} \right] + \left[\begin{array}{l} \text{kg mol O} \\ \text{exit gas } CO_2 \end{array} \right] \end{aligned} \quad (D.7)$$

The equilibrium amount of O₂ in raceway exit gas is very small (Appendix F) so that Eq. (D.7) simplifies to:

$$\left[\begin{array}{l} \text{kg mol O} \\ \text{in input } O_2 \end{array} \right] = \left[\begin{array}{l} \text{kg mol O} \\ \text{exit gas CO} \end{array} \right] + \left[\begin{array}{l} \text{kg mol O} \\ \text{exit gas } CO_2 \end{array} \right] \quad (D.8)$$

One kilogram mole of O₂ contains 2 kg mol of O. One kilogram mole of CO₂ also contains 2 kg mol of O.

One kilogram mole of CO, however, contains only 1 kg mol of O so that:

$$\begin{aligned} \left[\begin{array}{l} \text{kg mol O} \\ \text{in 1 kg mol} \\ \text{of input } O_2 \end{array} \right] &= 2 * \left[\begin{array}{l} \text{kg mol } O \\ \text{input } O_2 \end{array} \right] \\ \left[\begin{array}{l} \text{kg mol O in} \\ 1 \text{ kg mol of} \\ \text{raceway exit gas CO} \end{array} \right] &= 1 * \left[\begin{array}{l} \text{kg mol CO} \\ \text{in raceway} \\ \text{exit gas} \end{array} \right] \end{aligned}$$

and

$$\left[\begin{array}{c} \text{kg mol O} \\ \text{in 1 kg mol of} \\ \text{raceway exit gas CO}_2 \end{array} \right] = 2 * \left[\begin{array}{c} \text{kg mol CO}_2 \\ \text{in raceway} \\ \text{exit gas} \end{array} \right]$$

from which Eq. (D.8) becomes;

$$2 * \left[\begin{array}{c} \text{kg mol} \\ \text{input O}_2 \end{array} \right] = 1 * \left[\begin{array}{c} \text{kg mol CO} \\ \text{in raceway} \\ \text{exit gas} \end{array} \right] + 2 * \left[\begin{array}{c} \text{kg mol CO}_2 \\ \text{in raceway} \\ \text{exit gas} \end{array} \right] \quad (\text{D.9})$$

and, because $\left[\begin{array}{c} \text{kg mol} \\ \text{input O}_2 \end{array} \right]$ is specified as 1 kg mol;

$$2 * 1 = 1 * \left[\begin{array}{c} \text{kg mol CO} \\ \text{in raceway} \\ \text{exit gas} \end{array} \right] + 2 * \left[\begin{array}{c} \text{kg mol CO}_2 \\ \text{in raceway} \\ \text{exit gas} \end{array} \right] \quad (\text{D.10})$$

which we simplify to;

$$2 = 1 * n_{\text{CO}}^{\text{raceway exit gas}} + 2 * n_{\text{CO}_2}^{\text{raceway exit gas}} \quad (\text{D.11})$$

or subtracting $\{2 * n_{\text{CO}_2}^{\text{raceway exit gas}}\}$ from both sides;

$$2 - 2 * n_{\text{CO}_2}^{\text{raceway exit gas}} = 1 * n_{\text{CO}}^{\text{raceway exit gas}}$$

or switching sides;

$$n_{\text{CO}}^{\text{raceway exit gas}} = 2 - 2 * n_{\text{CO}_2}^{\text{raceway exit gas}} \quad (\text{D.12})$$

D.4 CALCULATING CO(g) AND CO₂(g) MOL FRACTIONS FOR EQUILIBRIUM CONSTANT EQ. (D.3)

The mol fraction of CO in the raceway exit gas is;

$$X_{\text{CO}}^{\text{raceway exit gas}} = \frac{n_{\text{CO}}^{\text{raceway exit gas}}}{n_T^{\text{raceway exit gas}}}$$

where $n_T^{\text{raceway exit gas}}$ is the total mol of exit gas, that is;

$$n_T^{\text{raceway exit gas}} = n_{\text{CO}_2}^{\text{raceway exit gas}} + n_{\text{CO}}^{\text{raceway exit gas}} + n_{\text{N}_2}^{\text{raceway exit gas}} \quad (\text{D.13})$$

or because, by Equation D.12 and D.6:

$$(1) \quad n_{\text{CO}}^{\text{raceway exit gas}} = 2 - 2 * n_{\text{CO}_2}^{\text{raceway exit gas}}$$

$$(2) \quad n_{\text{N}_2}^{\text{raceway exit gas}} = 3.76$$

the total amount of raceway gas is;

$$n_T^{\text{raceway exit gas}} = n_{\text{CO}_2}^{\text{raceway exit gas}} + (2 - 2 * n_{\text{CO}_2}^{\text{raceway exit gas}}) + 3.76$$

or combining right side terms;

$$\begin{aligned} n_T^{\text{raceway exit gas}} &= 2 - n_{\text{CO}_2}^{\text{raceway exit gas}} + 3.76 \\ &= 5.76 - n_{\text{CO}_2}^{\text{raceway exit gas}} \end{aligned} \quad (\text{D.14})$$

so that;

$$X_{\text{CO}_2}^{\text{raceway exit gas}} = \frac{n_{\text{CO}_2}^{\text{raceway exit gas}}}{n_T^{\text{raceway exit gas}}} = \frac{n_{\text{CO}_2}^{\text{raceway exit gas}}}{5.76 - n_{\text{CO}_2}^{\text{raceway exit gas}}} \quad (\text{D.15})$$

Likewise;

$$X_{\text{CO}}^{\text{raceway exit gas}} = \frac{n_{\text{CO}}^{\text{raceway exit gas}}}{n_T^{\text{raceway exit gas}}} = \frac{2 - 2 * n_{\text{CO}_2}^{\text{raceway exit gas}}}{5.76 - n_{\text{CO}_2}^{\text{raceway exit gas}}} \quad (\text{D.16})$$

D.5 EQUILIBRIUM MOLE FRACTIONS

Returning to Eq. (D.3);

$$K_E^{\text{CO}_2(\text{g})+\text{C(s)} \rightarrow 2\text{CO(g)}} = \frac{\left(X_{\text{CO}}^E * \left(\frac{P_t}{1} \right) \right)^2}{\left(X_{\text{CO}_2}^E * \left(\frac{P_t}{1} \right) \right) * 1} = 1.2 \times 10^5$$

and applying Eqs. (D.15) and (D.16) gives;

$$\begin{aligned} K_E^{\text{CO}_2(\text{g})+\text{C(s)} \rightarrow 2\text{CO(g)}} &= 1.2 \times 10^5 = \frac{\left(X_{\text{CO}}^E * \frac{P_t}{1} \right)^2}{\left(X_{\text{CO}_2}^E * \frac{P_t}{1} \right) * 1} \\ &= \frac{\left(\frac{2 - 2 * n_{\text{CO}_2}^{\text{raceway exit gas}} * \frac{P_t}{1}}{5.76 - n_{\text{CO}_2}^{\text{raceway exit gas}}} \right)^2}{\left(\frac{2 - 2 * n_{\text{CO}_2}^{\text{raceway exit gas}}}{5.76 - n_{\text{CO}_2}^{\text{raceway exit gas}}} \right) * \frac{P_t}{1}} \\ &= \frac{\left(\frac{n_{\text{CO}_2}^{\text{raceway exit gas}} * \frac{P_t}{1}}{5.76 - n_{\text{CO}_2}^{\text{raceway exit gas}}} \right)^2}{\left(\frac{n_{\text{CO}_2}^{\text{raceway exit gas}}}{5.76 - n_{\text{CO}_2}^{\text{raceway exit gas}}} \right) * \frac{P_t}{1}} \end{aligned} \quad (\text{D.17})$$

from which, with 4 bar absolute pressure ($P_t = 4$) in the raceway (Section D.1):

$$n_{\text{CO}_2}^{\text{raceway exit gas}} = 2.2 * 10^{-5} \text{ kg mol CO}_2$$

and because;

$$\begin{aligned}n_{\text{CO}}^{\text{raceway exit gas}} &= 2 - 2 * n_{\text{CO}_2}^{\text{raceway exit gas}} \\&= \sim 2 \text{ kg mol CO}\end{aligned}$$

So the carbonaceous raceway exit gas is virtually all CO. Additional calculations show that this true for all temperatures above 1500°C.

Another result of the calculations is that

$$X_{\text{CO}}^E = \frac{n_{\text{CO}}^{\text{raceway exit gas}}}{n_T} = \frac{2}{2 + 3.76} = 0.35$$

This value is used in Appendix G.

E

$\text{CO}_2(\text{g}) + \text{C}(\text{s}) \rightarrow 2\text{CO}(\text{g})$ Equilibrium Constant

This appendix calculates the 2000°C equilibrium constant for the reaction:

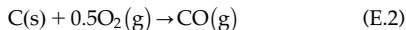


Appendix D then uses this equilibrium constant to show that tuyere raceway exit gas contains very little $\text{CO}_2(\text{g})$.

The equilibrium constant is calculated from published values of $\Delta_f G_{2000^\circ\text{C}}^{\circ}$ and $\Delta_f G_{2000^\circ\text{C}}^{\circ}$ from

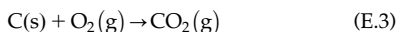
JANAF.¹

The published values are for the formation reactions:



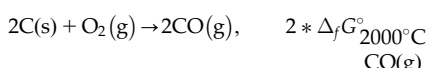
for which the Gibbs free energy of formation is; $\Delta_f G_{2000^\circ\text{C}}^{\circ} = -308.7 \text{ MJ/kg mol of CO(g)}$

and;



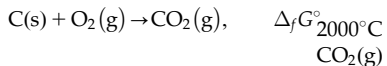
for which the Gibbs free energy of formation is; $\Delta_f G_{2000^\circ\text{C}}^{\circ} = -396.2 \text{ MJ/kg mol of CO}_2(\text{g})$.

Reaction (E.1) is made up from these formation reactions by subtracting Eq. (E.3) from $2 \times$ Eq. (E.2), that is;

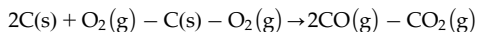


$\text{CO}(\text{g})$

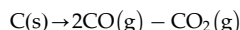
minus;



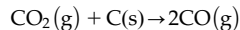
which gives;



or



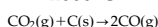
or adding $\text{CO}_2(\text{g})$ to both sides, it yields Eqn. E.1;



for which;

$$\begin{aligned} \Delta_r G_{2000^\circ\text{C}}^{\circ} &= 2 * \Delta_f G_{2000^\circ\text{C}}^{\circ} - \Delta_f G_{2000^\circ\text{C}}^{\circ} \\ \text{CO}_2(\text{g}) + \text{C}(\text{s}) \rightarrow 2\text{CO}(\text{g}) &\quad \text{CO}(\text{g}) \quad \text{CO}_2(\text{g}) \\ &= 2 * (-308.7) - (-396.2) \\ &= -221.2 \text{ MJ/kg mol of CO}_2(\text{g}) \end{aligned}$$

The equilibrium constant with this $\Delta_r G_{2000^\circ\text{C}}^{\circ}$ value is;



$$\begin{aligned} K_{E, 2000^\circ\text{C}}^{\text{CO}_2(\text{g}) + \text{C}(\text{s}) \rightarrow 2\text{CO}(\text{g})} &= e^{\left\{ \frac{-\Delta_r G_{2000^\circ\text{C}}^{\circ}}{R + T(K)} \right\}} \\ &= e^{\left\{ \frac{(-221.2)}{0.008314 + 2273.15} \right\}} = 1.2 \times 10^5 \end{aligned} \quad (\text{E.4})$$

where R is the gas constant, $0.008314 \text{ MJ/(kg mol CO}_2)/\text{K}$; $T(K)$ is the equilibrium

temperature K; and 2273.15 is the equilibrium temperature K equivalent to prescribed equilibrium temperature 2000°C.

This equilibrium constant is now used to prove that tuyere raceway gas contains very little CO₂(g), Appendix D.

We can see by inspection that Reaction (E.1) goes to near-completion. Only the details need to be worked out.

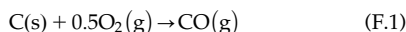
Reference

1. NIST-JANAF. *NIST-JANAF [thermochemical] tables pdf*. Gaithersburg, MD: U.S. Institute of Standards and Technology; 2016. Recovered on June 12, 2016 by Googling the title.

F

Oxygen Concentration in Blast Furnace Tuyere Raceway With CO(g) Production

This appendix calculates the O₂(g) concentration in tuyere raceway exit gas, 2000°C (2273.15K). It does so for the case where the carbonaceous product gas is all CO(g). It uses Gibbs free energy of formation data for the reaction:



at 2000°C. It also uses a raceway pressure of 4 bar absolute.

The Gibbs free energy of formation for Reaction (F.1) at 2000°C is:

$$\Delta_r G^\circ = -308.7 \text{ MJ/kg mol of C(s)} \quad (F.2)$$

This is also the Gibbs free energy of *reaction* for Reaction (F.1).

The equilibrium constant with this Gibbs free energy of reaction is:

$$K_{E,2000^\circ C}^{C(s)+0.5O_2(g) \rightarrow CO(g)} = e^{\left\{ \frac{-\Delta_r G^\circ}{R * 2273.15 \text{ K}} \right\}} = e^{\left\{ \frac{(-308.7)}{0.008314 * 2273.15(\text{K})} \right\}} = 1.24 \times 10^7 \quad (F.3)$$

where R is the gas constant, 0.008314 MJ/(kg mol of C)/K and 2273.15 is the temperature, K, that is equivalent to 2000°C.

F.1 EQUILIBRIUM CONSTANT–GAS CONCENTRATION RELATIONSHIP

Equilibrium constant of Reaction (F.1) is related to its thermodynamic activities by:

$$K_{E,2000^\circ C}^{C(s)+0.5O_2(g) \rightarrow CO(g)} = \frac{a_{CO(g)}^E}{a_{C(s)}^E * \left(a_{O_2(g)}^E \right)^{0.5}} \quad (F.4)$$

where a is the thermodynamic activities of the reactants and product (unitless).

The equilibrium thermodynamic activity of C(s) = 1, pure carbon in its most common state.

The equilibrium activities of O₂(g) and CO (g) are;

$$a_{O_2(g)}^E = X_{O_2(g)}^E * \frac{P_t}{1}$$

and

$$a_{\text{CO(g)}}^E = X_{\text{CO(g)}}^E * \frac{P_t}{1}$$

where $X_{\text{O}_2(\text{g})}^E$ and $X_{\text{CO(g)}}^E$ are the equilibrium mol fractions of $\text{O}_2(\text{g})$ and CO(g) in the raceway exit gas, P_t is the absolute pressure in the raceway ~ 4 bar, and 1 is the absolute pressure (bar) at which the thermodynamic activity of a pure ideal gas is 1.

With these substitutions, the mol fractions of $\text{O}_2(\text{g})$ and CO(g) in the raceway exit gas are related to the equilibrium constant of Eq. (F.3) by the following equation:

$$K_{E,2000^\circ\text{C}}^{\text{C(s)}+0.5\text{O}_2(\text{g}) \rightarrow \text{CO(g)}} = 1.24 \times 10^7 = \frac{X_{\text{CO(g)}}^E * (P_t/1)}{\left(X_{\text{O}_2(\text{g})}^E * (P_t/1)\right)^{0.5}} \quad (\text{F.5})$$

or because $P_t/1 = P_t$;

$$1.24 \times 10^7 = \frac{X_{\text{CO(g)}}^E * P_t}{\left(X_{\text{O}_2(\text{g})}^E\right)^{0.5} * (P_t)^{0.5}}$$

or multiplying both sides by $\left(X_{\text{O}_2(\text{g})}^E\right)^{0.5}$

$$1.24 \times 10^7 * \left(X_{\text{O}_2(\text{g})}^E\right)^{0.5} = \frac{X_{\text{CO(g)}}^E * P_t}{(P_t)^{0.5}} = X_{\text{CO(g)}}^E * (P_t)^{0.5}$$

or dividing both sides by 1.24×10^7 and inserting $P_t = 4$:

$$\begin{aligned} \left(X_{\text{O}_2(\text{g})}^E\right)^{0.5} &= \frac{X_{\text{CO(g)}}^E * (4)^{0.5}}{1.24 \times 10^7} \\ &= 8.1 \times 10^{-8} * X_{\text{CO(g)}}^E * (4)^{0.5} \\ &= 1.6 \times 10^{-7} * X_{\text{CO(g)}}^E \end{aligned}$$

Finally, squaring both sides:

$$X_{\text{O}_2(\text{g})}^E = 2.6 \times 10^{-14} * \left(X_{\text{CO(g)}}^E\right)^2$$

The maximum value that $X_{\text{CO(g)}}^E$ can have is 1; therefore $X_{\text{O}_2(\text{g})}^E$ is clearly always minuscule.

Reference

1. NIST-JANAF. *NIST-JANAF [thermochemical] tables PDF*. Gaithersburg, MD: U.S. Institute of Standards and Technology; 2016. Recovered on June 12, 2016 by Googling the title.

G

$H_2(g)$ Raceway Exit Gas Proof

Tuyere raceway calculations of Chapter 18, Raceway Flame Temperature With $CH_4(g)$ Tuyere Injection, assume that the hydrogenous portion of raceway exit gas is predominantly $H_2(g)$ -with very little $H_2O(g)$. The objective of this appendix is to show that this is true, using $CH_4(g)$ injectant as the source of the raceway's hydrogen. Equilibrium and mol fraction calculations are used.

G.1 RACEWAY INPUTS AND OUTPUTS

Fig. G.1 describes our raceway inputs and outputs with $CH_4(g)$ tuyere injection.

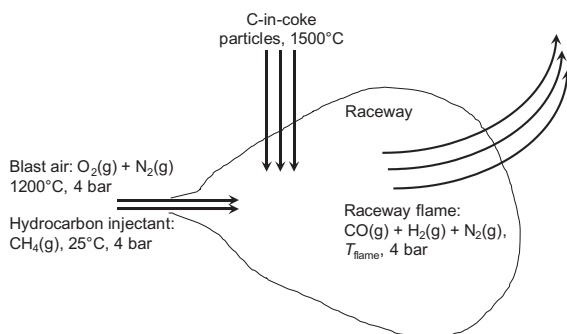
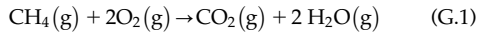


FIGURE G.1 Sketch of blast furnace raceway with $CH_4(g)$ injection.

Blast air at 1200°C and $CH_4(g)$ at 25°C are steadily blown into the raceway. Solid carbon (C-in-coke) particles at 1500°C steadily fall into the raceway.

Hot $O_2(g)$ in the blast air immediately reacts with the input $CH_4(g)$ to form hot $CO_2(g)$ and $H_2O(g)$. The reaction is:



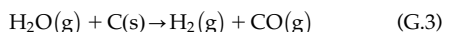
As this gas passes through the raceway, it;

1. becomes depleted in $O_2(g)$; and
2. reacts with the descending carbon to form $CO(g)$ and $H_2(g)$.

The reactions are;



and



We postulate that both of these reactions come quickly to equilibrium at the high temperature $\sim 2000^\circ\text{C}$ of the raceway exit gas.

G.2 EQUILIBRIUM RACEWAY EXIT GAS

Appendix D examines equilibrium conditions for Reaction (G.2). It shows that at

equilibrium, 2000°C, the reaction goes almost completely to CO(g).

This appendix shows that at equilibrium, 2000°C, Reaction (G.3) also goes almost to completion so that most of the hydrogenous gas is H₂(g).

Appendix H shows that the equilibrium constant for Reaction (G.3) is;

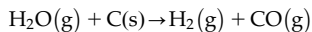
$$2.2 \times 10^4$$

which supports this idea.

The remainder of this appendix shows that the H₂O/H₂ molar ratio of the raceway exit gas is very small, that is, that most of the hydrogenous raceway exit gas is H₂(g).

G.3 H₂O(g) + C(s) → H₂(g) + CO(g) EQUILIBRIUM

The equilibrium constant for Reaction G.3;



is

$$K_E^{\text{H}_2\text{O(g)}+\text{C(s)} \rightarrow \text{H}_2\text{(g)}+\text{CO(g)}} = \frac{a_{\text{H}_2\text{(g)}}^E * a_{\text{CO(g)}}^E}{a_{\text{C(s)}}^E * a_{\text{H}_2\text{O(g)}}^E} \quad (\text{G.4})$$

where K_E is the equilibrium constant, unitless and a^E is the equilibrium thermodynamic activities of the reactants and products, unitless.

The equilibrium activity of C(s) is 1 because it is a pure solid.

The equilibrium activities of H₂(g), CO(g), and H₂O(g) are;

$$a_{\text{H}_2\text{(g)}}^E = \frac{(X_{\text{H}_2}^E * P_t)}{1}$$

$$a_{\text{CO(g)}}^E = \frac{(X_{\text{CO}}^E * P_t)}{1}$$

and

$$a_{\text{H}_2\text{O(g)}}^E = \frac{(X_{\text{H}_2\text{O}}^E * P_t)}{1}$$

where $X_{\text{H}_2}^E$, X_{CO}^E , and $X_{\text{H}_2\text{O}}^E$ are the equilibrium mole fractions of H₂(g), CO(g), and H₂O(g) in the raceway exit gas; P_t is the absolute pressure in the raceway ~4 bar; and 1 is the absolute pressure (bar) at which the thermodynamic activity of a pure ideal gas is 1.

With these substitutions, the mol fractions of H₂(g), CO(g), and H₂O(g) in the raceway exit gas are related to the equilibrium constant of Eq. (G.4) by the following equation:

$$K_E^{\text{H}_2\text{O(g)}+\text{C(s)} \rightarrow \text{H}_2\text{(g)}+\text{CO(g)}} = \frac{(X_{\text{H}_2\text{(g)}}^E * P_t/1) * (X_{\text{CO(g)}}^E * P_t/1)}{1 * (X_{\text{H}_2\text{O(g)}}^E * P_t/1)} \quad (\text{G.5})$$

or dividing the right side top and bottom by $P_t/1$:

$$\begin{aligned} K_E^{\text{H}_2\text{O(g)}+\text{C(s)} \rightarrow \text{H}_2\text{(g)}+\text{CO(g)}} &= \frac{X_{\text{H}_2\text{(g)}}^E * X_{\text{CO(g)}}^E}{X_{\text{H}_2\text{O(g)}}^E} * \frac{P_t}{1} \\ &= \frac{X_{\text{H}_2\text{(g)}}^E * X_{\text{CO(g)}}^E}{X_{\text{H}_2\text{O(g)}}^E} * P_t \end{aligned}$$

Further, multiplying both sides by $X_{\text{H}_2\text{O(g)}}^E$ then dividing both sides by $K_E^{\text{H}_2\text{O(g)}+\text{C(s)} \rightarrow \text{H}_2\text{(g)}+\text{CO(g)}}$ gives:

$$X_{\text{H}_2\text{O(g)}}^E = \frac{X_{\text{H}_2\text{(g)}}^E * X_{\text{CO(g)}}^E}{K_E^{\text{H}_2\text{O(g)}+\text{C(s)} \rightarrow \text{H}_2\text{(g)}+\text{CO(g)}}} * P_t \quad (\text{G.6})$$

Appendix H shows that $K_E^{\text{H}_2\text{O(g)}+\text{C(s)} \rightarrow \text{H}_2\text{(g)}+\text{CO(g)}} = 2.2 \times 10^4$ and P_t is typically 4 bar, which gives:

$$X_{\text{H}_2\text{O(g)}}^E = \frac{X_{\text{H}_2\text{(g)}}^E * X_{\text{CO(g)}}^E * 4}{2.2 \times 10^4} = X_{\text{H}_2\text{(g)}}^E * X_{\text{CO(g)}}^E * 1.8 \times 10^{-4}$$

Finally, Appendix D (Section D.5) shows that $X_{\text{CO(g)}}^E \approx 0.35$ so that;

$$\begin{aligned}X_{\text{H}_2\text{O(g)}}^E &= X_{\text{H}_2\text{(g)}}^E * X_{\text{CO(g)}}^E * 1.8 \times 10^{-4} \\&= X_{\text{H}_2\text{(g)}}^E * 0.35 * 1.8 \times 10^{-4} = 6.3 * 10^{-5} * X_{\text{H}_2\text{(g)}}^E\end{aligned}$$

so that;

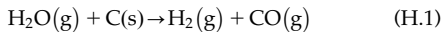
$$X_{\text{H}_2\text{O(g)}}^E < < X_{\text{H}_2\text{(g)}}^E$$

which confirms our proposition that the hydrogenous portion of raceway exit gas is predominately H₂(g).

H

$\text{H}_2\text{O(g)} + \text{C(s)} \rightarrow \text{H}_2\text{(g)} + \text{CO(g)}$ Equilibrium Constant

This appendix calculates the 2000°C equilibrium constant for the reaction:



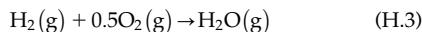
Appendix G then uses this equilibrium constant to show that raceway exit gas contains very little $\text{H}_2\text{O(g)}$.

The equilibrium constant is calculated from published values¹ of $\Delta_f G^\circ_{2000^\circ\text{C}}$ and $\Delta_f G^\circ_{2000^\circ\text{C}}$.

These published values are for the formation reactions;

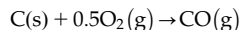


for which the standard Gibbs free energy of formation is $\Delta_f G^\circ_{2000^\circ\text{C}} = -308.7 \text{ MJ/kg mol}$ of CO(g) and;

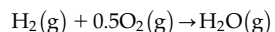


for which the standard Gibbs free energy of formation is $\Delta_f G^\circ_{2000^\circ\text{C}} = -119.6 \text{ MJ/kg mol}$ of $\text{H}_2\text{O(g)}$.

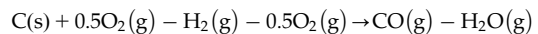
Reaction (H.1) is made up from these formation reactions by subtracting Reaction (H.3) from Reaction (H.2) that is;



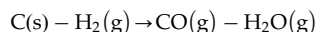
minus



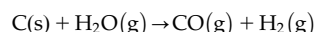
which gives;



or



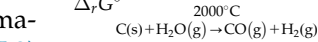
or adding $\text{H}_2\text{(g)}$ and $\text{H}_2\text{O(g)}$ to both sides;



for which;

$$\begin{aligned} \Delta_r G^\circ_{\text{C(s)} + \text{H}_2\text{O(g)} \rightarrow \text{CO(g)} + \text{H}_2\text{(g)}} &= \Delta_f G^\circ_{2000^\circ\text{C}} - \Delta_f G^\circ_{2000^\circ\text{C}} \\ &= -308.7 - (-119.6) = -189.1 \text{ MJ/kg mol of H}_2 \end{aligned} \quad (\text{H.4})$$

The equilibrium constant with this value is;



$$K_{E, 2000^\circ\text{C}}^{\text{C(s)} + \text{H}_2\text{O(g)} \rightarrow \text{CO(g)} + \text{H}_2(\text{g})} = e^{\left\{ \frac{-\left(\Delta_r G^\circ_{\text{C(s)} + \text{H}_2\text{O(g)} \rightarrow \text{CO(g)} + \text{H}_2(\text{g})} \right)}{R * 2273.15(\text{K})} \right\}}$$

$$= e^{\left\{ \frac{(-(-189.1))}{(0.008314 * 2273.15(\text{K}))} \right\}} = 2.2 \times 10^4$$

where R is the gas constant, $0.008314 \text{ MJ/(kg mol H}_2\text{)/K}$.

2273.15 is the temperature (K) that is equivalent to 2000°C .

Reference

1. NIST-JANAF. *NIST-JANAF [Thermochemical] tables PDF*. U.S. Institute of Standards and Technology, Gaithersburg, MD; 2016. Googling the title [recovered on 13.06.16].

I

Using Excel to Solve Matrices

Table 4.1 matrix is solved as follows:

1. Put Table 4.1 into an Excel spreadsheet with the top term in the numerical term column (1000) in cell C2. The matrix covers cells C2–K9. Label as shown in Table 4.1.
2. Select cells C12–C19 (by, e.g., selecting cell C12, holding down the Shift key and arrowing down to Cell C19).
3. Leave these cells selected then type $=mmult(minverse(D2:K9), C2:C9)$ then simultaneously press Ctrl + Shift + Enter.
4. Cells C12–C19 contain the solution to the matrix. An error may occur if the selected cells' range does not match the solution range. Label as show in Table 4.1.

I.1 SUBSEQUENT PROBLEMS

Subsequent problems can be solved without repeating the above steps. Section 4.7 problem is solved by putting -0.724 in cell D3 and -0.276 in cell D4 to represent magnetite (72.4 mass% Fe, 27.6 mass% O), Eqs. (4.9) and (4.10).

The new solution appears automatically in cells C12–C19. Relabel appropriately as shown in Table 4.2.

I.2 ADDITIONAL VARIABLE PROBLEMS

Additional variable problems like that in Section 4.8 can be safely started from scratch. However, they can also be prepared by;

1. deleting all the calculated value numbers (e.g., in matrix Table 4.1) simultaneously by selecting all the numbers and pressing delete;
2. adding new matrix columns, matrix rows, and calculated value rows as needed; and
3. resolving as described above.

Try it!

J

How to Compute Element and Compound Enthalpies

J.1 INTRODUCTION

The enthalpies in this book's enthalpy balance equations are obtained from the NIST–JANAF Thermochemical Tables.¹ These tables use Kelvin (K) for temperature, which we calculate with the equation:

$$T(K) = T^{\circ}\text{C} + 273.15$$

These tables;

1. define the enthalpies of elements in their most common state [e.g., C(s), O₂(g)] as zero at 25°C and 1 bar pressure;
2. give measured standard enthalpies of formation at 25°C, which we list as $\Delta_f H_{25^{\circ}\text{C}}$; and
3. give measured enthalpy versus temperature increments which we list as $H_T - H_{25^{\circ}\text{C}}$ where H_T is the enthalpy of a substance at temperature $T^{\circ}\text{C}$ and $H_{25^{\circ}\text{C}}$ is the enthalpy of the substance at 25°C.

The tables are all for pure substances in their standard states, indicated by H° . They also apply to ideal solutions, for example, air.

J.1.1 Element Enthalpies

The enthalpies of elements are calculated from the NIST–JANAF tables by following the equation;

$$H_{\text{element}}^{\circ}_T = H_{\text{element}}^{\circ}_{25^{\circ}\text{C}} + (H_T^{\circ} - H_{25^{\circ}\text{C}}^{\circ})_{\text{element}} \quad (\text{J.1})$$

where $(H_T^{\circ} - H_{25^{\circ}\text{C}}^{\circ})_{\text{element}}$ values are tabulated in NIST–JANAF.

From point (1), 25°C element enthalpies are zero, so Eq. (J.1) becomes

$$H_{\text{element}}^{\circ}_T = (H_T^{\circ} - H_{25^{\circ}\text{C}}^{\circ})_{\text{element}} \quad (\text{J.2})$$

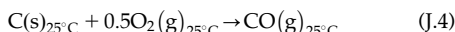
Notice that the enthalpies of elements cooler than 25°C are negative. This is a consequence of defining the enthalpy of elements in their most common state as zero at 25°C.

J.1.2 Compound Enthalpies [Using CO(g) as an Example]

$H_{25^\circ\text{C}}$ of compounds is not zero. For CO(g), it is calculated by;

$$\underset{\text{CO(g)}}{H_{25^\circ\text{C}}} = \Delta_f H_{\text{CO(g)}}^{\circ} + \underset{\text{C(s)}}{H_{25^\circ\text{C}}} + 0.5 * \underset{\text{O}_2\text{(g)}}{H_{25^\circ\text{C}}} \quad (\text{J.3})$$

where $\Delta_f H_{\text{CO(g)}}^{\circ}$ is the measured enthalpy of formation of CO(g), 25°C, from its elements at 25°C, that is:



The NIST–JANAF tables provide measured $\Delta_f H_{25^\circ\text{C}}$ values for compounds. We clarify this nomenclature slightly by attaching CO(g), for example, $\Delta_f H_{\text{CO(g)}}^{\circ}$, etc.

Further,

$H_{\text{C(s)}}^{\circ}$ and $H_{\text{O}_2\text{(g)}}^{\circ}$ are both zero because they

are elements in their most common state at 25°C, so that Eq. (J.3) becomes;

$$\underset{\text{CO(g)}}{H_{25^\circ\text{C}}} = \Delta_f H_{\text{CO(g)}}^{\circ} \quad (\text{J.5})$$

Further, by comparison with Eq. (J.1);

$$\underset{\text{CO(g)}}{H_T^{\circ}} = \underset{\text{CO(g)}}{H_{25^\circ\text{C}}} + (H_T^{\circ} - H_{25^\circ\text{C}})_{\text{CO(g)}} \quad (\text{J.6})$$

and combining Eqs. (J.5) and (J.6);

$$\underset{\text{CO(g)}}{H_T^{\circ}} = \Delta_f H_{\text{CO(g)}}^{\circ} + (H_T^{\circ} - H_{25^\circ\text{C}})_{\text{CO(g)}} \quad (\text{J.7})$$

where the measured right-hand terms are tabulated in NIST–JANAF.

J.1.3 Units

The enthalpy unit in the NIST–JANAF tables is kJ/g mol of substance. This unit converts one-for-one to MJ/kg mol, which is the unit used throughout this book.

J.1.4 Example Calculation—Enthalpy of CO at 126.85°C (400K)

NIST–JANAF (2016) lists;

$$\Delta_f H_{\text{CO(g)}}^{\circ} = -110.527 \text{ MJ/kg mol CO(g)} \quad (\text{i.e., at } 298.15 \text{ K})$$

and

$$(H_{126.85^\circ\text{C}}^{\circ} - H_{25^\circ\text{C}}^{\circ})_{\text{CO(g)}} = 2.976 \text{ MJ/kg mol CO(g)} \quad (\text{i.e., at } 400 \text{ K})$$

The enthalpy of CO(g) at 126.85°C (400K) is therefore:

$$\begin{aligned} H_{\text{CO(g)}}^{126.85^\circ\text{C}} &= \Delta_f H_{\text{CO(g)}}^{\circ} + (H_{126.85^\circ\text{C}}^{\circ} - H_{25^\circ\text{C}}^{\circ})_{\text{CO(g)}} \\ &= -110.527 + 2.976 \\ &= -107.551 \text{ MJ/kg mol of CO(g)} \end{aligned} \quad (\text{J.7})$$

The equivalent enthalpy per kg of CO is:

$$\begin{aligned} \frac{H_{\text{CO(g)}}^{126.85^\circ\text{C}}}{\text{CO molecular mass}} &= \frac{-107.551 \text{ MJ/kg mol of CO}}{28.01 \text{ kg CO/kg mol of CO}} \\ &= -3.840 \text{ MJ/kg of CO} \end{aligned} \quad (\text{J.8})$$

Notice that the enthalpies of compounds are all negative at 25°C. This is a consequence of defining the enthalpy of elements as zero at 25°C and 1 bar.

J.1.5 Significant Figures

We think that the significant figures in the NIST–JANAF tables are exaggerated. In spite of this, we use four significant figures for most of our calculations. We believe that this makes our enthalpy calculations easier to follow.

J.1.6 Impure Substance Enthalpies

This appendix shows how to calculate the enthalpies, H_T , of impure substances, Section J.4. It uses molten blast furnace iron, 4.5 mass% C, 95.5 mass% Fe as the example.

J.1.7 Independent of Pressure

Enthalpies of ideal gases are independent of pressure.²

Enthalpies of solids and liquids are virtually independent of pressure.²

J.2 USEFUL ENTHALPY TABLE

Table J.1 was prepared as a useful reference table for completing blast furnace enthalpy balances.

TABLE J.1 Useful H°_T Values of Compounds in (MJ/kg of Compound)

Temperature	Compound	H°/MW
1500°C	Al ₂ O ₃ (s)	-14.67
	Al ₂ O ₃ (oxide in molten slag)	-13.58
	C(s)	2.488
	C (dissolved in molten iron)	5
	CaO(s)	-9.925
	CaO (oxide in molten slag)	-8.495
	Fe(ℓ)	1.269
	MgO(s)	-13.08
	MgO (oxide in molten slag)	-11.14
	Mn(ℓ)	1.343
	Mn (dissolved in molten iron)	1.27
	MnO(s)	-4.300
	MnO (oxide in molten slag)	-3.530
	Si(ℓ)	3.155
	Si (dissolved in molten iron)	-2.15
	SiO ₂ (s)	-13.44
	SiO ₂ (oxide in molten slag)	-13.28
	TiO ₂ (s)	-10.48
	TiO ₂ (oxide in molten slag)	-9.64
1200°C	CO ₂ (g)	-7.573
	CO(g)	-2.591
	H ₂ O(g)	-10.81
	N ₂ (g)	1.339

TABLE J.1 (Continued)

Temperature	Compound	H°/MW
930°C	O ₂ (g)	1.239
	Al ₂ O ₃ (s)	-15.41
	C(s)	1.359
	CO(g)	-2.926
	CO ₂ (g)	-7.926
	CaO(s)	-10.50
	Fe	0.6164
	Fe _{0.947} O(s)	-3.152
	H ₂ (g)	13.35
	H ₂ O(g)	-11.49
	MgO(s)	-13.84
25°C	MnO(s)	-4.770
	N ₂ (g)	1.008
	SiO ₂ (s)	-14.13
	TiO ₂ (s)	-11.03
	Al ₂ O ₃ (s)	-16.43
	C(s)	0
	CH ₄ (g)	-4.664
	CO(g)	-3.946
	CO ₂ (g)	-8.942
	CaO(s)	-11.32
	CaCO ₃ (s)	-12.06
	Fe(s)	0
	Fe _{0.947} O	-3.865
	Fe ₂ O ₃ (s)	-5.169
	Fe ₃ O ₄ (s)	-4.841
	H ₂ (g)	0
	H ₂ O(ℓ)	-15.87
	MgO(s)	-14.92
	MgCO ₃ (s)	-13.20
	MnO ₂ (s)	-5.98
	SiO ₂ (s)	-15.16
	Coal, 25°C	-1.2
	Natural gas, 25°C	-4.52

(Continued)

TABLE J.2 Enthalpy Data From NIST–JANAF and a Simplified Enthalpy Equation of CO(g) Versus Temperature Developed

B	C	D	E	F
1	Units in first three columns: MJ/kg mol. In last column: MJ/kg.			
2	CO(g)			
3	Temperature (°C)	$\Delta_f H^\circ_{25^\circ\text{C}}$	$H^\circ_T - H^\circ_{25^\circ\text{C}}$	$H^\circ_T = \Delta_f H^\circ_{25^\circ\text{C}} + (H^\circ_T - H^\circ_{25^\circ\text{C}})$
4	25	− 110.527		H°_T / MW
5	1826.85		60.376	− 1.790
6	1926.85		64.021	− 1.660
7	2026.85		67.679	− 1.530
8	2126.85		71.348	− 1.399
9	2226.85		75.027	− 1.267
10	2326.85		78.715	− 1.136
11	$H^\circ_{\text{CO(g)}} / \text{MW} = 0.001310 \times T^\circ\text{C} - 4.183$			

J.3 ENTHALPY EQUATIONS

Section J.1 shows how to calculate enthalpy of CO(g) at 126.85°C (400K) in MJ/kg CO(g). Similarly, enthalpies at other temperatures can be calculated. This section discusses simplified equations with respect to temperature to calculate enthalpies of different compounds.

Table J.2 gives an example of how a simplified enthalpy equation of CO(g) is obtained.

The equation on the bottom row of Table J.2 is the trendline formula shown after plotting H° / MW versus temperature. With this equation, enthalpies of CO(g) in MJ/kg CO(g) can be easily calculated by plugging in temperature in Celsius.

Tables J.3–J.6 list more simplified enthalpy equations at typical blast furnace temperatures developed using the method above.

J.4 ENTHALPY OF Fe–C ALLOY FORMATION

We represent blast furnace iron as molten Fe–C alloy. It is a nonideal solution, so its

enthalpy can't be represented by H°_{Fe} and H°_{C} . We represent it by;

$$H^\circ_{\text{Fe}(l)} \text{, MJ/kg mol of Fe}$$

and

$$H^\circ_{\text{C(dissolved)}} = \left\{ H^\circ_{\text{C(s)}} + \Delta H_{\text{Fe}(l) + \text{C(s)} \rightarrow \text{(Fe-C)molten alloy}}^{1500^\circ\text{C}} \right\}, \text{ MJ/kg mol of C} \quad (\text{J.8})$$

where $\Delta H_{\text{Fe}(l) + \text{C(s)} \rightarrow \text{(Fe-C)molten alloy}}^{1500^\circ\text{C}}$ is enthalpy of reaction for producing molten Fe–C alloy, 1500°C, from pure Fe(l), 1500°C, and pure C(s), 1500°C.

This appendix calculates the value of $\Delta H_{\text{Fe}(l) + \text{C(s)} \rightarrow \text{(Fe-C)molten alloy}}^{1500^\circ\text{C}}$

J.4.1 Calculation of Alloy Mol Fractions

This appendix's calculations are all based on Hultgren's measured Fe–C enthalpy of reaction data (Hultgren et al.,³ p 484, Table J.6).

They are also all based on 4.5 mass% C and 95.5 mass% Fe alloy.

TABLE J.3 Blast Temperature $H^\circ T_{\text{blast}}/\text{MW}$,
 $T = 900^\circ\text{C} - 1400^\circ\text{C}$

$\text{N}_2(\text{g})$	$0.001237 * T_{\text{blast}}^\circ\text{C} - 0.1450$
$\text{O}_2(\text{g})$	$0.001137 * T_{\text{blast}}^\circ\text{C} - 0.1257$
$\text{H}_2\text{O}(\text{g})$	$0.002582 * T_{\text{blast}}^\circ\text{C} - 13.91$
$\text{C}(\text{s})$	$0.00197 * T_{\text{blast}}^\circ\text{C} - 0.482$

TABLE J.4 Raceway Adiabatic Flame Temperature
 $H^\circ T_{\text{flame temperature}}/\text{MW}$, $T = 1800^\circ\text{C} - 2300^\circ\text{C}$

$\text{Al}_2\text{O}_3(\text{s})$	$0.001887 * T_{\text{flame}}^\circ\text{C} - 16.72$
$\text{CO}(\text{g})$	$0.001310 * T_{\text{flame}}^\circ\text{C} - 4.183$
$\text{H}_2(\text{g})$	$0.01756 * T_{\text{flame}}^\circ\text{C} - 4.130$
$\text{N}_2(\text{g})$	$0.001301 * T_{\text{flame}}^\circ\text{C} - 0.2448$
$\text{SiO}_2(\text{s})$	$0.001427 * T_{\text{flame}}^\circ\text{C} - 15.47$

TABLE J.5 Top Gas Temperature $H^\circ T_{\text{top gas}}/\text{MW}$,
 $T = 25^\circ\text{C} - 225^\circ\text{C}$

$\text{CO}(\text{g})$	$0.001049 * T_{\text{top gas}}^\circ\text{C} - 3.972$
$\text{CO}_2(\text{g})$	$0.0009314 * T_{\text{top gas}}^\circ\text{C} - 8.966$
$\text{H}_2(\text{g})$	$0.01442 * T_{\text{top gas}}^\circ\text{C} - 0.3616$
$\text{H}_2\text{O}(\text{g})$	$0.001902 * T_{\text{top gas}}^\circ\text{C} - 13.47$
$\text{N}_2(\text{g})$	$0.001044 * T_{\text{top gas}}^\circ\text{C} - 0.02624$

TABLE J.6 Molten Iron Temperature $H^\circ T_{\text{molten iron}}/\text{MW}$,
 $T = 1400^\circ\text{C} - 1600^\circ\text{C}$

$\text{Fe}(\text{l})$	$0.0008264 * T_{\text{molten iron}}^\circ\text{C} + 0.02863$
-----------------------	--

Hultgren's enthalpy data are presented as a function of mol fraction C in Fe–C alloy. So, we start our calculations by calculating mol fraction C in 4.5 mass% C, 95.5 mass% Fe, Fe–C alloy.

We consider 100 kg of alloy. It contains 4.5 kg of C and 95.5 kg of Fe. The molecular

masses of C and Fe are 12.01 and 55.85 kg/kg mol, respectively, so that;

$$\text{kg mol C} = \frac{4.5 \text{ kg C}}{12.01 \text{ kg C/kg mol of C}} = 0.37$$

$$\text{kg mol Fe} = \frac{95.5 \text{ kg C}}{55.85 \text{ kg Fe/kg mol of Fe}} = 1.71$$

per 100 kg of alloy, which are equivalent to;

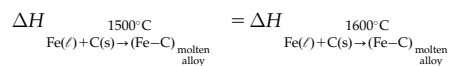
$$X_C = \frac{0.37}{(0.37 + 1.71)} = 0.18$$

$$X_{\text{Fe}} = \frac{1.71}{(0.37 + 1.71)} = 0.82$$

where X_C and X_{Fe} are mol fractions of C and Fe in 4.5 mass% C, 95.5 mass% Fe alloy.

J.4.2 Calculations: Unit Conversions

Hultgren's measured enthalpy of reaction data are for 1600°C. We make the assumption that they are nearly the same as our required 1500°C enthalpy of reaction, that is, we assume that:



Hultgren's measured $\Delta H_{\text{Fe}(\text{l}) + \text{C}(\text{s}) \xrightarrow{\text{molten alloy}} (\text{Fe}-\text{C})}^{1600^\circ\text{C}}$ value for 0.18 mol fraction C (i.e., 4.5 mass% C) molten Fe–C alloy is:

$$+1300 \text{ cal/g mol of alloy}$$

This is equivalent to:

$$+5400 \text{ J/g mol of alloy}$$

or

$$+5400 \text{ kJ/kg mol of alloy}$$

or

$$+5.4 \text{ MJ/kg mol of alloy.}$$

J.4.3 Per kg Mol of Carbon

Eq. (J.8) requires that $\Delta H_{\text{Fe}(l) + \text{C}(s) \rightarrow (\text{Fe}-\text{C})_{\text{molten alloy}}}$ ^{1500°C} be expressed per kg mol of carbon.

One kg mol of molten iron containing 0.18 mol fraction C and 0.82 mol fraction Fe contains 0.18 kg mol C.

So the 5.4 MJ value of $\Delta H_{\text{Fe}(l) + \text{C}(s) \rightarrow (\text{Fe}-\text{C})_{\text{molten alloy}}}$ ^{1500°C} per kg mol of alloy is equivalent to

$$\begin{aligned} \Delta H_{\text{Fe}(l) + \text{C}(s) \rightarrow (\text{Fe}-\text{C})_{\text{molten alloy}}}^{1500^\circ\text{C}} &= \frac{5.4 \text{ MJ/kg mol of alloy}}{0.18 \text{ kg mol of C/kg mol of alloy}} \\ &= +30 \text{ MJ/kg mole of C in alloy} \end{aligned}$$

J.4.4 Per Kg of Carbon

Chapter 5, Introduction to the Blast Furnace Enthalpy Balance, uses the enthalpy of alloy formation *per kg of carbon*. To get this, we

divide the above value by the atomic mass of carbon, that is,

$$\begin{aligned} \Delta H_{\text{Fe}(l) + \text{C}(s) \rightarrow (\text{Fe}-\text{C})_{\text{molten alloy}}}^{1500^\circ\text{C}} &= \frac{30 \text{ MJ/kg mol of C}}{12 \text{ kg/kg mol of C}} \\ &= 2.5 \text{ MJ/kg of dissolved carbon} \end{aligned}$$

This value is used in Chapter 5, Introduction to the Blast Furnace Enthalpy Balance, onward.

References

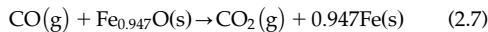
1. NIST-JANAF. *NIST-JANAF [Thermochemical] Tables PDF*. U.S. Institute of Standards and Technology, Gaithersburg, MD; 2017. Googling JANAF [recovered 15.0.18].
2. Gaskell DR. *Introduction to metallurgical thermodynamics*. 2nd ed. New York: McGraw-Hill; 1981.
3. Hultgren R, Desai PD, Hawkins DT, Gleiser M, Kelley KK. *Selected values of the thermodynamic properties of binary alloys*. Metals Park, OH: American Society for Metals; 1973. p. 484.

K

$\text{CO(g)} + \text{Fe}_{0.947}\text{O(s)} \rightarrow \text{CO}_2\text{(g)} + 0.947\text{Fe}$

Equilibrium Constants

This appendix calculates equilibrium constants for the reaction;



from tabulated values of;

$$\Delta_f G^\circ_{\text{CO}_2\text{(g)}}, \Delta_f G^\circ_{\text{CO(g)}}, \text{ and } \Delta_f G^\circ_{\text{Fe}_{0.947}\text{O(s)}}$$

where $\Delta_f G^\circ$ is Gibbs free energy of formation at any given system temperature and 1 bar pressure. Please note that $\Delta_f G^\circ$ numerical values are not affected by pressure changes (Gaskell, 1981).

We do the calculations in two steps;

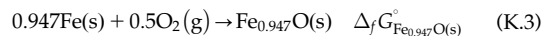
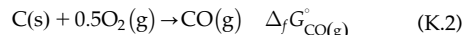
- calculation of Gibbs free energies of Reaction (2.7) $\Delta_r G^\circ_{\text{CO(g)} + \text{Fe}_{0.947}\text{O(s)} \rightarrow \text{CO}_2\text{(g)} + 0.947\text{Fe(s)}}$ from published values of;

$$\Delta_f G^\circ_{\text{CO}_2\text{(g)}}, \Delta_f G^\circ_{\text{CO(g)}}, \text{ and } \Delta_f G^\circ_{\text{Fe}_{0.947}\text{O(s)}}, \text{ and;}$$

- calculation of equilibrium constants of Reaction (2.7) from the calculated $\Delta_r G^\circ_{\text{CO(g)} + \text{Fe}_{0.947}\text{O(s)} \rightarrow \text{CO}_2\text{(g)} + 0.947\text{Fe(s)}}$ values.

K.1 GIBBS FREE ENERGY OF REACTION

The Gibbs free energies of formation that are needed to calculate $\Delta_r G^\circ_{\text{CO(g)} + \text{Fe}_{0.947}\text{O(s)} \rightarrow \text{CO}_2\text{(g)} + 0.947\text{Fe(s)}}$ are;



where the $\Delta_f G^\circ$ s are the Gibbs free energies of formation at any given system temperature and 1 bar pressure. Please note that $\Delta_f G^\circ$ numerical values are not affected by pressure changes (Gaskell, 1981).

The Gibbs free energy of reaction for Eq. (2.7) is determined by subtracting Eqs. (K.2) and (K.3) from Eq. (K.1), that is;

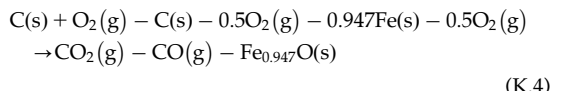


TABLE K.1 Gibbs Free Energies of Reaction and Equilibrium Constants K_E for the Reaction $\text{CO(g)} + \text{Fe}_{0.947}\text{O(s)} \rightarrow \text{CO}_2\text{(g)} + 0.947\text{Fe}$

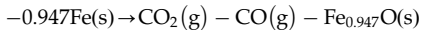
	A	B	C	D	E	F	G
1	T, K	T, °C	$\Delta_f G^\circ_{\text{CO}_2\text{(g)}}$	$\Delta_f G^\circ_{\text{CO(g)}}$	$\Delta_f G^\circ_{\text{Fe}_{0.947}\text{O(s)}}$	$\Delta_r G^\circ_{(\text{CO(g)} + \text{Fe}_{0.947}\text{O(s)} \rightarrow \text{CO}_2\text{(g)} + 0.947\text{Fe(s)})}$ $= \Delta_f G^\circ_{\text{CO}_2\text{(g)}} - \Delta_f G^\circ_{\text{CO(g)}} - \Delta_f G^\circ_{\text{Fe}_{0.947}\text{O(s)}}$	$K_E = X_{\text{CO}_2} / X_{\text{CO}}$ $= \text{EXP}(-\Delta r G^\circ / (0.008314 * T, K))$
2	900	626.85	-395.748	-191.416	-205.745	1.413	0.828
3	1000	726.85	-395.886	-200.275	-199.395	3.784	0.634
4	1100	826.85	-396.001	-209.075	-192.927	6.001	0.519
5	1200	926.85	-396.098	-217.819	-186.391	8.112	0.443
6	1203.15	930	-396.100	-218.093	-186.185	8.178	0.442
7	1300	1026.85	-396.177	-226.509	-179.840	10.172	0.390
8	1400	1126.85	-396.240	-235.149	-173.355	12.264	0.349
9	1800	1526.85	-396.353	-269.242	-147.892	20.781	0.249

Appendix L uses the 930°C equilibrium constant value of 0.442 to calculate the mass $\text{CO}_2\text{(g)}/\text{mass CO(g)}$ ratio at the blast furnace top-segment–bottom-segment division, Figs. 7.1–7.3. The Gibbs free energies of formation (columns C through E) are from NIST-JANAF. *NIST-JANAF [Thermochemical] Tables PDF*. U.S. Institute of Standards and Technology, Gaithersburg, MD; 2017. Googling JANAF [recovered 31.12.17]. The pressure is specified as 1 bar (absolute). The ΔG° units are MJ/kg mol.

and

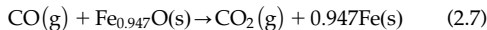
$$\begin{aligned}\Delta_r G^\circ_{\text{CO(g)} + \text{Fe}_{0.947}\text{O(s)} \rightarrow \text{CO}_2\text{(g)} + 0.947\text{Fe(s)}} \\ = \Delta_f G^\circ_{\text{CO}_2\text{(g)}} - \Delta_f G^\circ_{\text{CO(g)}} - \Delta_f G^\circ_{\text{Fe}_{0.947}\text{O(s)}}\end{aligned}$$

The C(s) and O₂(g) terms on the left-hand side of Eq. (K.4) cancel, leaving the equation;



or adding {0.947Fe(s), CO(g), and Fe_{0.947}O(s)}

to both sides;



for which the standard Gibbs free energy of reaction is:

$$\begin{aligned}\Delta_r G^\circ_{\text{CO(g)} + \text{Fe}_{0.947}\text{O(s)} \rightarrow \text{CO}_2\text{(g)} + 0.947\text{Fe(s)}} \\ = \Delta_f G^\circ_{\text{CO}_2\text{(g)}} - \Delta_f G^\circ_{\text{CO(g)}} - \Delta_f G^\circ_{\text{Fe}_{0.947}\text{O(s)}}\end{aligned} \quad (\text{K.5})$$

Table K.1 gives values for these terms and their equivalent equilibrium constants - as a function of equilibrium temperature.

K.2 CALCULATION OF EQUILIBRIUM CONSTANTS

Equilibrium constants of Reaction (2.7) are related to its Gibbs free energies of reaction by;

$$K_E^{\text{CO(g)} + \text{Fe}_{0.947}\text{O(s)} \rightarrow \text{CO}_2\text{(g)} + 0.947\text{Fe(s)}} = e^{\left\{ \frac{-\Delta_r G^\circ_{\text{CO(g)} + \text{Fe}_{0.947}\text{O(s)} \rightarrow \text{CO}_2\text{(g)} + 0.947\text{Fe(s)}}}{R \cdot T(K)} \right\}} \quad (\text{K.6})$$

where $K_E^{\text{CO(g)} + \text{Fe}_{0.947}\text{O(s)} \rightarrow \text{CO}_2\text{(g)} + 0.947\text{Fe(s)}}$ is the equilibrium constant of Reaction (2.7), unitless; $\Delta_r G^\circ_{\text{CO(g)} + \text{Fe}_{0.947}\text{O(s)} \rightarrow \text{CO}_2\text{(g)} + 0.947\text{Fe(s)}}$ is the standard Gibbs free energy of reaction for Reaction (2.7), MJ/(kg mol of Fe_{0.947}O); R is the gas constant, 0.008314 MJ/(kg mol of Fe_{0.947}O)/K; and T(K) is the temperature K, which equals (temperature, °C + 273.15).

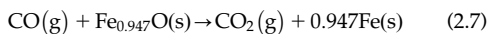
K.3 CALCULATION RESULTS

Column G in **Table K.1** gives the calculated equilibrium constant values. Note especially the value 0.442 at 930°C. Appendix L uses it to calculate the equilibrium mass CO₂/mass CO ratio at our blast furnace's bottom-segment–top-segment division.

L

Equilibrium CO₂(g)/CO(g) Mass Ratio

Chapter 7, Conceptual Division of the Blast Furnace, onward specifies that the reaction;



comes to equilibrium at the blast furnace top-segment–bottom-segment division, Fig. 7.2. Specifically, this chapter uses the mass CO₂(g)/mass CO(g) equilibrium ratio for Reaction (2.7) at 930°C, the division temperature.

This appendix now calculates this equilibrium mass CO₂(g)/mass CO(g) ratio from 930°C equilibrium constant of Appendix K

$$K_{E, 930^\circ\text{C}}^{\text{CO(g)} + \text{Fe}_{0.947}\text{O(s)} \rightarrow \text{CO}_2\text{(g)} + 0.947\text{Fe(s)}} = 0.442$$

as follows.

L.1 THERMODYNAMIC ACTIVITIES

The thermodynamic activities of reactants and products of Eq. (2.7) are related to equilibrium constant of reaction by;

$$K_{E, 930^\circ\text{C}}^{\text{CO(g)} + \text{Fe}_{0.947}\text{O(s)} \rightarrow \text{CO}_2\text{(g)} + 0.947\text{Fe(s)}} = 0.442 = \frac{a_{\text{CO}_2\text{(g)}}^E * (a_{\text{Fe(s)}}^E)^{0.947}}{a_{\text{CO(g)}}^E * a_{\text{Fe}_{0.947}\text{O(s)}}^E} \quad (\text{L.1})$$

where $K_{E, 930^\circ\text{C}}^{\text{CO(g)} + \text{Fe}_{0.947}\text{O(s)} \rightarrow \text{CO}_2\text{(g)} + 0.947\text{Fe(s)}}$ is the equilibrium constant for Reaction (2.7) at 930°C, unitless and a is the thermodynamic activities of

reactants and products of Reaction (2.7), unitless.

The thermodynamic activities of Fe_{0.947}O(s) and Fe(s) are 1 because they are pure solids.

The thermodynamic activities of CO₂(g) and CO(g) are;

$$a_{\text{CO}_2\text{(g)}}^E = \frac{X_{\text{CO}_2\text{(g)}}^E * P_t}{1} \quad (\text{L.2})$$

$$a_{\text{CO(g)}}^E = \frac{X_{\text{CO(g)}}^E * P_t}{1} \quad (\text{L.3})$$

where $X_{\text{CO}_2\text{(g)}}^E$ and $X_{\text{CO(g)}}^E$ are the equilibrium mole fractions of CO₂(g) and CO(g) at the top-segment–bottom-segment division, P_t is the absolute pressure (bar) at the top-segment–bottom-segment division, and 1 is the standard state pressure (bar) for ideal gases.

With these substitutions;

$$\begin{aligned} K_{E, 930^\circ\text{C}}^{\text{CO(g)} + \text{Fe}_{0.947}\text{O(s)} \rightarrow \text{CO}_2\text{(g)} + 0.947\text{Fe(s)}} &= 0.442 \\ &= \frac{a_{\text{CO}_2\text{(g)}}^E * (a_{\text{Fe(s)}}^E)^{0.947}}{a_{\text{CO(g)}}^E * a_{\text{Fe}_{0.947}\text{O(s)}}^E} \\ &= \frac{(X_{\text{CO}_2\text{(g)}}^E * P_t) / 1 * (1)^{0.947}}{(X_{\text{CO(g)}}^E * P_t) / 1 * 1} \\ &= \frac{X_{\text{CO}_2\text{(g)}}^E * P_t}{X_{\text{CO(g)}}^E * P_t} \end{aligned} \quad (\text{L.4})$$

and

$$K_{E, 930^\circ\text{C}}^{\text{CO(g)} + \text{Fe}_{0.947}\text{O(s)} \rightarrow \text{CO}_2(\text{g}) + 0.947\text{Fe(s)}} = 0.442 = \frac{X_{\text{CO}_2(\text{g})}^E}{X_{\text{CO(g)}}^E} \quad (\text{L.5})$$

are independent of pressure.

Furthermore;

$$n_{\text{CO}_2(\text{g})}^E = \frac{\text{mass}_{\text{CO}_2(\text{g})}^E}{44} \quad (\text{L.9})$$

and

$$n_{\text{CO(g)}}^E = \frac{\text{mass}_{\text{CO(g)}}^E}{28} \quad (\text{L.10})$$

where 44 and 28 are the molecular masses of CO₂ and CO, kg/kg mol.

Lastly;

$$\frac{n_{\text{CO}_2(\text{g})}^E}{n_{\text{CO(g)}}^E} = \frac{\text{mass}_{\text{CO}_2(\text{g})}^E / 44}{\text{mass}_{\text{CO(g)}}^E / 28} = K_{E, 930^\circ\text{C}}^{\text{CO(g)} + \text{Fe}_{0.947}\text{O(s)} \rightarrow \text{CO}_2(\text{g}) + 0.947\text{Fe(s)}} \quad (\text{L.11})$$

or inverting the divisor and multiplying;

$$\begin{aligned} \frac{n_{\text{CO}_2(\text{g})}^E}{n_{\text{CO(g)}}^E} &= \frac{\text{mass}_{\text{CO}_2(\text{g})}^E}{44} * \frac{28}{\text{mass}_{\text{CO(g)}}^E} = \frac{\text{mass}_{\text{CO}_2(\text{g})}^E}{\text{mass}_{\text{CO(g)}}^E} * \frac{28}{44} \\ &= K_{E, 930^\circ\text{C}}^{\text{CO(g)} + \text{Fe}_{0.947}\text{O(s)} \rightarrow \text{CO}_2(\text{g}) + 0.947\text{Fe(s)}} \end{aligned} \quad (\text{L.12})$$

and multiplying both sides by 44/28;

$$\begin{aligned} \frac{\text{mass}_{\text{CO}_2(\text{g})}^E}{\text{mass}_{\text{CO(g)}}^E} * 1 &= \frac{44}{28} * K_{E, 930^\circ\text{C}}^{\text{CO(g)} + \text{Fe}_{0.947}\text{O(s)} \rightarrow \text{CO}_2(\text{g}) + 0.947\text{Fe(s)}} \\ &= 1.571 * K_{E, 930^\circ\text{C}}^{\text{CO(g)} + \text{Fe}_{0.947}\text{O(s)} \rightarrow \text{CO}_2(\text{g}) + 0.947\text{Fe(s)}} \end{aligned} \quad (\text{L.13})$$

and because $K_{E, 930^\circ\text{C}}^{\text{CO(g)} + \text{Fe}_{0.947}\text{O(s)} \rightarrow \text{CO}_2(\text{g}) + 0.947\text{Fe(s)}} = 0.442$, the 930°C equilibrium mass ratio is:

$$\frac{\text{mass}_{\text{CO}_2(\text{g})}^E}{\text{mass}_{\text{CO(g)}}^E} = 1.571 * 0.442 = 0.694 \quad (\text{L.14})$$

It is used throughout our book.

$$\begin{aligned} \frac{X_{\text{CO}_2(\text{g})}^E}{X_{\text{CO(g)}}^E} &= \frac{n_{\text{CO}_2(\text{g})}^E / n_{t(\text{g})}^E}{n_{\text{CO(g)}}^E / n_{t(\text{g})}^E} = \frac{n_{\text{CO}_2(\text{g})}^E}{n_{\text{CO(g)}}^E} \\ &= K_{E, 930^\circ\text{C}}^{\text{CO(g)} + \text{Fe}_{0.947}\text{O(s)} \rightarrow \text{CO}_2(\text{g}) + 0.947\text{Fe(s)}} \end{aligned} \quad (\text{L.8})$$

and

$$X_{\text{CO}_2(\text{g})}^E = \frac{n_{\text{CO}_2(\text{g})}^E}{n_{t(\text{g})}^E} \quad (\text{L.6})$$

where $n_{\text{CO}_2(\text{g})}^E$, $n_{\text{CO(g)}}^E$, and $n_{t(\text{g})}^E$ are equilibrium kg mol of CO₂(g), CO(g), and total gas.

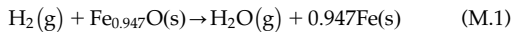
Thus;

$$\begin{aligned} \frac{X_{\text{CO}_2(\text{g})}^E}{X_{\text{CO(g)}}^E} &= \frac{n_{\text{CO}_2(\text{g})}^E / n_{t(\text{g})}^E}{n_{\text{CO(g)}}^E / n_{t(\text{g})}^E} = \frac{n_{\text{CO}_2(\text{g})}^E}{n_{\text{CO(g)}}^E} \\ &= K_{E, 930^\circ\text{C}}^{\text{CO(g)} + \text{Fe}_{0.947}\text{O(s)} \rightarrow \text{CO}_2(\text{g}) + 0.947\text{Fe(s)}} \end{aligned} \quad (\text{L.8})$$

M

Calculation of $H_2(g) + Fe_{0.947}O(s) \rightarrow H_2O(g) + 0.947Fe(s)$ Equilibrium Constants

This appendix calculates equilibrium constants for the reaction;



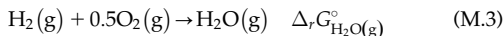
from the Gibbs free energies of reaction at 930°C and other temperatures.

The relationship is;

$$K_E^{H_2(g)+Fe_{0.947}O(s)\rightarrow H_2O(g)+0.947Fe(s)} = e^{\left\{ \frac{-\Delta_r G^\circ_{H_2(g)+Fe_{0.947}O(s)\rightarrow H_2O(g)+0.947Fe(s)}}{R*T(K)} \right\}} \quad (M.2)$$

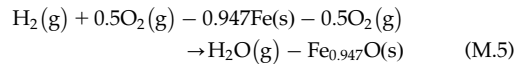
where $\Delta_r G^\circ_{H_2(g)+Fe_{0.947}O(s)\rightarrow H_2O(g)+0.947Fe(s)}$ is the standard Gibbs free energy of reaction for Reaction (M.1), MJ/kg mol of $Fe_{0.947}O$; R is the gas constant, 0.008314 MJ/(kg mol of Fe) T (K) $^{-1}$; and $T(K)$ is the temperature K, which equals (temperature, °C + 273.15).

The component Gibbs free energies of formation that are needed to calculate $\Delta_r G^\circ_{H_2(g)+Fe_{0.947}O(s)\rightarrow H_2O(g)+0.947Fe(s)}$ are;



where the $\Delta_f G^\circ$ s are Gibbs free energies of formation, MJ/kg mol of compound.

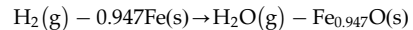
The Gibbs free energy of reaction for Eq. (M.1) is determined by subtracting Eq. (M.4) from Eq.(M.3), that is;



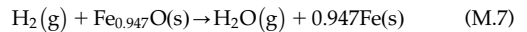
and

$$\Delta_r G^\circ_{H_2(g)+Fe_{0.947}O(s)\rightarrow H_2O(g)+0.947Fe(s)} = \Delta_r G^\circ_{H_2O(g)} - \Delta_r G^\circ_{Fe_{0.947}O(s)} \quad (M.6)$$

The O_2 terms on the left side of Eq. (M.5) cancel, leaving the equation;



or adding 0.947Fe(s) and $Fe_{0.947}O(s)$ to both sides;



for which the standard Gibbs free energy of reaction is:

$$\Delta_r G^\circ_{H_2(g)+Fe_{0.947}O(s)\rightarrow H_2O(g)+0.947Fe(s)} = \Delta_r G^\circ_{H_2O(g)} - \Delta_r G^\circ_{Fe_{0.947}O(s)} \quad (M.8)$$

Table M.1 gives values for these terms and their equivalent $K_E^{H_2(g)+Fe_{0.947}O(s)\rightarrow H_2O(g)+0.947Fe(s)}$ values as a function of temperature.

TABLE M.1 Gibbs Free Energies and Equilibrium Constants (K_E) for the Reaction $H_2(g) + Fe_{0.947}O(s) \rightarrow H_2O(g) + 0.947Fe(s)$

B	C	D	E	F	G	
14	T (K)	T (°C)	$\Delta_f G^\circ_{H_2O(g)}$	$\Delta_f G^\circ_{Fe0.947O(s)}$	$\Delta_f G^\circ_{(H_2(g) + Fe0.947O(s) \rightarrow H_2O(g) + 0.947Fe(s))}$ $= \Delta_f G^\circ_{H_2O(g)} - \Delta_f G^\circ_{Fe0.947O(s)}$	$KE = X_{H_2O}/X_{H_2}$ $= EXP(-\Delta rG^\circ/(0.008314*T, K))$
15	900	626.85	-198.083	-205.745	7.662	0.359
16	1000	726.85	-192.590	-199.395	6.805	0.441
17	1100	826.85	-187.033	-192.927	5.894	0.525
18	1200	926.85	-181.425	-186.391	4.966	0.608
19	1203.15	930	-181.247	-186.185	4.938	0.610
20	1300	1026.85	-175.774	-179.840	4.066	0.686
21	1400	1126.85	-170.089	-173.355	3.266	0.755

$H_2O(g)$ here is assumed as an ideal gas. The Gibbs free energies of formation (columns D and E) are from NIST-JANAF. The ΔG° units are MJ/kg mol of substance.

Appendix N now uses the 930°C equilibrium constant value 0.610 to calculate the equilibrium mass $H_2O(g)$ /mass $H_2(g)$ ratio at the blast furnace top-segment–bottom-segment division, Fig. 11.1.

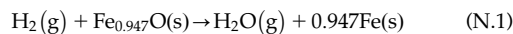
Reference

1. NIST-JANAF. *NIST-JANAF [thermochemical] tables PDF*. United States Institute of Standards and Technology, Gaithersburg, MD; 2017. Googling JANAF [recovered 31.12.17].

N

Equilibrium H₂O(g)/H₂(g) Mass Ratio

Chapter 11, Bottom Segment with CH₄(g) Injection, specifies that the reaction;



comes to equilibrium at the top-segment–bottom-segment division, Fig. 11.1. Specifically, these chapters use the mass H₂O(g)/mass H₂(g) equilibrium ratio for Reaction (N.1) at 930°C, the division temperature.

This appendix now calculates this equilibrium mass H₂O(g)/mass H₂(g) ratio from 930°C equilibrium constant;

$$K_{E, 930^\circ\text{C}}^{\text{H}_2(\text{g}) + \text{Fe}_{0.947}\text{O}(\text{s}) \rightarrow \text{H}_2\text{O}(\text{g}) + 0.947\text{Fe}(\text{s})} = 0.610 \quad (\text{N.2})$$

of Appendix M, as follows.

N.1 THERMODYNAMIC ACTIVITIES

The thermodynamic activities of components of Eq. (N.1) are related to the equilibrium constant of the reaction by the following equation:

$$K_E^{\text{H}_2(\text{g}) + \text{Fe}_{0.947}\text{O}(\text{s}) \rightarrow \text{H}_2\text{O}(\text{g}) + 0.947\text{Fe}(\text{s})} = \frac{a_{\text{H}_2\text{O}(\text{g})}^E * (a_{\text{Fe}(\text{s})}^E)^{0.947}}{a_{\text{H}_2(\text{g})}^E * a_{\text{Fe}_{0.947}\text{O}(\text{s})}^E} \quad (\text{N.3})$$

where $K_E^{\text{H}_2(\text{g}) + \text{Fe}_{0.947}\text{O}(\text{s}) \rightarrow \text{H}_2\text{O}(\text{g}) + 0.947\text{Fe}(\text{s})}$ is the equilibrium constant for Reaction (N.1) dependent only upon temperature, unitless and a is the thermodynamic activities of reactants and products of Reaction (N.1), unitless.

The thermodynamic activities of Fe_{0.947}O(s) and Fe(s) are 1 because they are pure solids.

The thermodynamic activities of H₂O(g) and H₂(g) are;

$$a_{\text{H}_2\text{O}(\text{g})}^E = \frac{X_{\text{H}_2\text{O}(\text{g})}^E * P_t}{1} \quad (\text{N.4})$$

$$a_{\text{H}_2(\text{g})}^E = \frac{X_{\text{H}_2(\text{g})}^E * P_t}{1} \quad (\text{N.5})$$

where $X_{\text{H}_2\text{O}(\text{g})}^E$ and $X_{\text{H}_2(\text{g})}^E$ are the gas's equilibrium mole fractions of H₂O(g) and H₂(g) at the bottom-segment–top-segment division, unitless; P_t is the absolute pressure at the division, bar; and 1 is the pressure (bar) at which the thermodynamic activity of a pure ideal gas is 1.

With these substitutions;

$$K_E^{\text{H}_2(\text{g}) + \text{Fe}_{0.947}\text{O}(\text{s}) \rightarrow \text{H}_2\text{O}(\text{g}) + 0.947\text{Fe}(\text{s})} = \frac{a_{\text{H}_2\text{O}(\text{g})}^E * (a_{\text{Fe}(\text{s})}^E)^{0.947}}{a_{\text{H}_2(\text{g})}^E * a_{\text{Fe}_{0.947}\text{O}(\text{s})}^E} \quad (\text{N.3})$$

$$\begin{aligned}
 &= \frac{\left(X_{\text{H}_2\text{O}(g)}^E * P_t/1 \right) * 1^{0.947}}{\left(X_{\text{H}_2(g)}^E * P_t/1 \right) * 1} \\
 &= \frac{X_{\text{H}_2\text{O}(g)}^E * P_t/1}{X_{\text{H}_2(g)}^E * P_t/1} \\
 &= \frac{X_{\text{H}_2\text{O}(g)}^E}{X_{\text{H}_2(g)}^E}
 \end{aligned} \tag{N.6}$$

is independent of pressure.

N.2 EQUILIBRIUM H₂O(g)/H₂(g) MASS RATIO

This section determines the relationship between the division's equilibrium mass H₂O(g)/mass H₂(g) ratio and $K_E^{\text{H}_2(\text{g}) + \text{Fe}_{0.947}\text{O}(\text{s}) \rightarrow \text{H}_2\text{O}(\text{g}) + 0.947\text{Fe}(\text{s})}$ as follows.

[Eq. \(N.3\)](#) shows that;

$$\frac{X_{\text{H}_2\text{O}(g)}^E}{X_{\text{H}_2(g)}^E} = K_E^{\text{H}_2(\text{g}) + \text{Fe}_{0.947}\text{O}(\text{s}) \rightarrow \text{H}_2\text{O}(\text{g}) + 0.947\text{Fe}(\text{s})}$$

also;

$$X_{\text{H}_2\text{O}(g)}^E = \frac{n_{\text{H}_2\text{O}(g)}^E}{n_{\text{t}(\text{g})}^E} \tag{N.7}$$

and

$$X_{\text{H}_2(g)}^E = \frac{n_{\text{H}_2(g)}^E}{n_{\text{t}(\text{g})}^E} \tag{N.8}$$

where $n_{\text{H}_2\text{O}(g)}^E$, $n_{\text{H}_2(g)}^E$, and $n_{\text{t}(\text{g})}^E$ are equilibrium kg mol of H₂O(g), H₂(g), and total gas so that

$$\begin{aligned}
 \frac{X_{\text{H}_2\text{O}(g)}^E}{X_{\text{H}_2(g)}^E} &= \frac{n_{\text{H}_2\text{O}(g)}^E/n_{\text{t}(\text{g})}^E}{n_{\text{H}_2(g)}^E/n_{\text{t}(\text{g})}^E} = \frac{n_{\text{H}_2\text{O}(g)}^E}{n_{\text{H}_2(g)}^E} \\
 &= K_E^{\text{H}_2(\text{g}) + \text{Fe}_{0.947}\text{O}(\text{s}) \rightarrow \text{H}_2\text{O}(\text{g}) + 0.947\text{Fe}(\text{s})}
 \end{aligned} \tag{N.9}$$

Furthermore;

$$n_{\text{H}_2\text{O}(g)}^E = \frac{\text{mass}_{\text{H}_2\text{O}(g)}^E}{18.0} \tag{N.10}$$

and

$$n_{\text{H}_2(g)}^E = \frac{\text{mass}_{\text{H}_2(g)}^E}{2.02} \tag{N.11}$$

where 18.0 and 2.02 are the molecular masses of H₂O and H₂, kg/kg mol.

Last;

$$\begin{aligned}
 \frac{n_{\text{H}_2\text{O}(g)}^E}{n_{\text{H}_2(g)}^E} &= \frac{\text{mass}_{\text{H}_2\text{O}(g)}^E/18.0}{\text{mass}_{\text{H}_2(g)}^E/2.02} = \frac{\text{mass}_{\text{H}_2\text{O}(g)}^E}{\text{mass}_{\text{H}_2(g)}^E} * \frac{2.02}{18.0} \\
 &= K_E^{\text{H}_2(\text{g}) + \text{Fe}_{0.947}\text{O}(\text{s}) \rightarrow \text{H}_2\text{O}(\text{g}) + 0.947\text{Fe}(\text{s})}
 \end{aligned} \tag{N.12}$$

and multiplying both sides by 18.0/2.02:

$$\begin{aligned}
 \frac{\text{mass H}_2\text{O(g)}}{\text{mass H}_2\text{(g)}} &= \frac{18.0}{2.02} * K_E^{\text{H}_2(\text{g}) + \text{Fe}_{0.947}\text{O}(\text{s}) \rightarrow \text{H}_2\text{O}(\text{g}) + 0.947\text{Fe}(\text{s})} \\
 &= 8.91 * K_E^{\text{H}_2(\text{g}) + \text{Fe}_{0.947}\text{O}(\text{s}) \rightarrow \text{H}_2\text{O}(\text{g}) + 0.947\text{Fe}(\text{s})}
 \end{aligned} \tag{N.13}$$

Since $K_E^{\text{H}_2(\text{g}) + \text{Fe}_{0.947}\text{O}(\text{s}) \rightarrow \text{H}_2\text{O}(\text{g}) + 0.947\text{Fe}(\text{s})} = 0.610$ at 930°C (Table M.1), the mass H₂O(g)/mass H₂(g) ratio at the bottom-segment–top-segment division is:

$$\frac{\text{mass H}_2\text{O(g)}}{\text{mass H}_2\text{(g)}} = 8.91 * 0.610 = 5.44 \tag{N.14}$$

O

Conversion of Grams H₂O(g)/Nm³ of Dry Blast Air to kg H₂O(g)/kg of Dry Blast Air

This appendix shows how to convert measured grams of H₂O(g) in blast per Nm³ of dry air in blast to kg of H₂O in blast per kg of dry air in blast.

O.1 kg mol OF IDEAL GAS PER Nm³ OF IDEAL GAS

This section calculates kg mol of ideal gas per Nm³ of ideal gas. It uses the ideal gas law equation;

$$P * V = n * R * T \quad (O.1)$$

restated as;

$$\frac{n}{V} = \frac{P}{R * T} \quad (O.2)$$

where n = kg mol of ideal gas; P = pressure, bar; V = volume of ideal gas, m³; R = gas constant = 8.314×10^{-2} (m³ bar)/(K kg mol); and T = temperature, Kelvin.

The conditions where m³ = Nm³ are;

1. 1 bar pressure, and
2. 273.15K temperature (0°C)

so that n , kg mol of ideal gas, is related to volume, Nm³ of ideal gas, by;

$$\frac{n}{V} = \frac{1}{8.314 \times 10^{-2} * 273.15} = 0.044 \text{ kg mol/Nm}^3 \quad (O.3)$$

from which we state that 1 Nm³ of ideal gas contains 0.044 kg mol of ideal gas.

O.2 kg mol O₂ AND N₂ IN 0.044 kg mol OF AIR

Air is 21 vol.% (mol)% O₂ and 79 vol.% (mol)% N₂, Appendix B. So 0.044 kg mol of air contains;

$$0.044 \text{ kg mol of air} * \frac{21 \text{ mol\% O}_2 \text{ in air}}{100\%} = 0.00924 \text{ kg mol of O}_2 \quad (O.4)$$

and

$$0.044 \text{ kg mol of air} * \frac{79 \text{ mol\% N}_2 \text{ in air}}{100\%} = 0.0348 \text{ kg mol of N}_2. \quad (O.5)$$

for a total of 0.044 kg mol of dry air.

O.3 kg OF O₂, N₂, AND AIR IN 0.044 kg mol OF DRY AIR

0.00924 kg mol of O₂ contains;

$$0.00924 \text{ kg mol O}_2 * 32 \text{ kg of O}_2/\text{kg mol O}_2 = 0.296 \text{ kg O}_2 \quad (\text{O.6})$$

and

0.0348 kg mol of N₂ contains;

$$0.0348 \text{ kg mol N}_2 * 28 \text{ kg of N}_2/\text{kg mol N}_2 = 0.974 \text{ kg N}_2 \quad (\text{O.7})$$

for a total of 1.27 kg of dry air per Nm³ of dry air (32 and 28 are the molecular masses of O₂ and N₂).

O.4 kg H₂O(g)/kg OF DRY AIR

We now specify that the H₂O(g) concentration of the blast furnace's moist blast is;

$$C_{\text{g H}_2\text{O(g)}}/\text{Nm}^3 \text{ of dry air}$$

where C is concentration.

Since, 1 Nm³ of dry air contains 1.27 kg of dry air;

$$C_{\text{g H}_2\text{O(g)}}/ \text{kg of dry air} = \frac{C_{\text{g H}_2\text{O(g)}}/\text{Nm}^3 \text{ of dry air}}{\left[\frac{1.27 \text{ kg of dry air}}{\text{Nm}^3 \text{ of dry air}} \right]}$$

or because we wish to work in kg of H₂O(g)

$$C_{\text{kg H}_2\text{O(g)}}/ \text{kg of dry air} = \frac{C_{\text{g H}_2\text{O(g)}}/\text{Nm}^3 \text{ of dry air}}{1.27 * 1000} \quad (\text{O.8})$$

O.5 MATRIX EQUATION

The value in Eq. (O.8) may be applied to the blast furnace as

$$\begin{aligned} & \left[\frac{\text{mass through-tuyere}}{\text{input H}_2\text{O(g)}} \right] * 1 \\ &= \left[\frac{\text{mass dry air}}{\text{in blast}} \right] * C_{\text{kg H}_2\text{O(g)}}/ \text{kg of dry air} \\ &= \left[\frac{\text{mass dry air}}{\text{in blast}} \right] * \frac{C_{\text{g H}_2\text{O(g)}}/\text{Nm}^3 \text{ of dry air}}{1.27 * 1000} \quad (\text{O.9}) \end{aligned}$$

which readily expands to;

$$\begin{aligned} & \left[\frac{\text{mass through-tuyere}}{\text{input H}_2\text{O(g)}} \right] * 1 \\ &= \left[\frac{\text{mass O}_2}{\text{in blast}} \right] * \frac{C_{\text{g H}_2\text{O(g)}}/\text{Nm}^3 \text{ of dry air}}{1.27 * 1000} \\ &+ \left[\frac{\text{mass N}_2}{\text{in blast}} \right] * \frac{C_{\text{g H}_2\text{O(g)}}/\text{Nm}^3 \text{ of dry air}}{1.27 * 1000} \quad (\text{O.10}) \end{aligned}$$

or subtracting $\left\{ \left[\frac{\text{mass through-tuyere}}{\text{input H}_2\text{O(g)}} \right] * 1 \right\}$ from both sides;

$$\begin{aligned} 0 &= - \left[\frac{\text{mass through-tuyere}}{\text{input H}_2\text{O(g)}} \right] * 1 \\ &+ \left[\frac{\text{mass O}_2}{\text{in blast}} \right] * \frac{C_{\text{g H}_2\text{O(g)}}/\text{Nm}^3 \text{ of dry air}}{1.27 * 10^3} \\ &+ \left[\frac{\text{mass N}_2}{\text{in blast}} \right] * \frac{C_{\text{g H}_2\text{O(g)}}/\text{Nm}^3 \text{ of dry air}}{1.27 * 10^3} \quad (\text{O.11}) \end{aligned}$$

where all masses are kg per 1000 kg of Fe in product molten iron.

We use this equation wherever the ingoing air of a blast furnace is humid and wherever steam is injected into the blast. An example moisture value is 15 g H₂O(g)/Nm³ of blast air for

$$\text{which } C_{\text{kg H}_2\text{O(g)}}/ \text{kg of dry air} = \frac{15 \text{ g of H}_2\text{O(g)}/\text{Nm}^3 \text{ of dry air}}{1.27 * 10^3} = 0.0118 \text{ kg H}_2\text{O(g)}/\text{kg of dry blast air.}$$

A P P E N D I X

P

Top Gas Mass%, Volume% Calculator

TABLE P.1 Mass% and Volume% of Top Gas Components Given Mass of Each Component

C	D	E	F	G
1 Mass%, Volume% Calculator for Section 20.6				
2 Mass CO (kg)	Mass CO ₂ (kg)	Mass N ₂ (kg)	Mass H ₂ (kg)	Mass H ₂ O (kg)
3 333	741	983	0	0
4 Mass% CO = (mass CO/total mass) × 100% etc.				
5 Mass% CO	Mass% CO ₂	Mass% N ₂	Mass% H ₂	Mass% H ₂ O
6 16.2	36.0	47.8	0.0	0.0
7				
8				
9				
10 kg mol CO = kg CO/MW _{CO} etc.				
11 kg mol CO	kg mol CO ₂	kg mol N ₂	kg mol H ₂	kg mol H ₂ O
12 11.9	16.8	35.1	0.0	0.0
13				
14 Volume% CO = mol% CO = (kg mol CO/total kg mol) × 100% etc.				
15 Mol% CO = volume% CO Mol% CO ₂ = volume% CO ₂ Mol% N ₂ = volume% N ₂ Mol% H ₂ = volume% H ₂ Mol% H ₂ O = volume% H ₂ O				
16 18.6	26.4	55.0	0.0	0.0
17				
18				
19				

(Continued)

TABLE P.1 (Continued)

	C	D	E	F	G
20 Mass%, volume% calculator with H ₂ and H ₂ O in top gas					
21	Mass CO (kg)	Mass CO ₂ (kg)	Mass N ₂ (kg)	Mass H ₂ (kg)	Mass H ₂ O (kg)
22	333	741	983	10	20
23 Mass% CO = (mass CO/total mass) × 100%, etc.					
24	Mass% CO	Mass% CO ₂	Mass% N ₂	Mass% H ₂	Mass% H ₂ O
25	16.0	35.5	47.1	0.5	1.0
26					
27					
28					
29	kg mol CO = kg CO/MW _{CO} etc.				
30	kg mol CO	kg mol CO ₂	kg mol N ₂	kg mol H ₂	kg mol H ₂ O
31	11.9	16.8	35.1	5.0	1.1
32					
33	Volume% CO = mol% CO = (kg mol CO/total kg mol) × 100% etc.				
34	Mol% CO = volume% CO	Mol% CO ₂ = volume% CO ₂	Mol% N ₂ = volume% N ₂	Mol% H ₂ = volume% H ₂	Mol% H ₂ O = volume% H ₂ O
35	17.0	24.1	50.2	7.1	1.6

Q

Calculation of Natural Gas Composition in Mass%

The mol% compound composition of the natural gas used in Chapter 29, Bottom-Segment Calculations with Natural Gas Injection, is shown in [Table Q.1](#).

This appendix converts this composition to mass% compounds, kg compound per kg of natural gas, and mass% elements, [Tables Q.2–Q.4](#).

TABLE Q.1 Composition of an Industrial Natural Gas

Compound	Mol%
CH ₄	95
C ₂ H ₆	3.2
C ₃ H ₈	0.2
C ₄ H ₁₀	0.06
C ₅ H ₁₂	0.02
C ₆ H ₁₄	0.01
N ₂	1.0
CO ₂	0.5
O ₂	0.02

Table courtesy: Union Gas.

TABLE Q.2 Composition of **Table Q.1** Natural Gas in Mass% and kg per kg of Natural Gas

	A	B	C	D	E	F	G
	Compound	mol% in natural gas	kg-mol of compound per kg-mol of natural gas	molecular mass of compound, kg per kg-mol of compound	kg of compound per kg-mol of natural gas	mass% of compound in natural gas	kg of compound per kg of natural gas
20							
21			=B22/100		=C22*D22	=E22/E\$31*100	=F22/100
22	CH ₄	95	0.950	16.0	15.2	90.4	0.904
23	C ₂ H ₆	3.2	0.032	30.1	0.96	5.7	0.057
24	C ₃ H ₈	0.2	0.002	44.1	0.09	0.5	0.005
25	C ₄ H ₁₀	0.06	0.001	58.1	0.03	0.2	0.002
26	C ₅ H ₁₂	0.02	0.0002	72.2	0.01	0.1	0.001
27	C ₆ H ₁₄	0.01	0.0001	86.2	0.01	0.1	0.001
28	N ₂	1.0	0.010	28.0	0.28	1.7	0.017
29	CO ₂	0.5	0.005	44.0	0.22	1.3	0.013
30	O ₂	0.02	0.0002	32.0	0.01	0.04	0.0004
31	Total	100	1		16.8	100	1

Row 21 shows how the values are calculated.

TABLE Q.3 Calculation of Mass% Elements in **Table Q.1** Natural Gas

	A	B	C	D	E	F	G	H	I	J	K
	Compound	kg of compound per kg of natural gas	mass% C in compound	mass% H in compound	mass% N in compound	mass% O in compound	mass C, kg per kg of natural gas	mass H, kg per kg of natural gas	mass N, kg per kg of natural gas	mass O, kg per kg of natural gas	
33											
34							=B35*C35/100	=B35*D35/100	=B35*E35/100		
35	CH ₄ (g)	0.904	74.9	25.1	0	0	0.677	0.227	0	0	
36	C ₂ H ₆ (g)	0.057	80.0	20.0	0	0	0.046	0.011	0	0	
37	C ₃ H ₈ (g)	0.005	81.8	18.2	0	0	0.004	0.010	0	0	
38	C ₄ H ₁₀ (g)	0.002	82.8	17.2	0	0	0.002	0.0036	0	0	
39	C ₅ H ₁₂ (g)	0.001	83.3	16.7	0	0	0.001	0.0014	0	0	
40	C ₆ H ₁₄ (g)	0.001	83.7	16.3	0	0	0.000	0.0008	0	0	
41	N ₂ (g)	0.017	0	0	100	0	0	0	0.017	0	
42	CO ₂ (g)	0.013	27.3	0	0	72.7	0.0036	0	0	0.0095	=B42*F42/100
43	O ₂ (g)	0.0004	0	0	0	100	0	0	0	0.0004	=B43*F43/100
44	Total	1					0.734	0.240	0.017	0.0099	=J42+J43
45											
46	Mass%						73.4	24.0	1.7	1.0	
47							=G44*100	=H44*100	=I44*100	=J44*100	

It starts with Column G of **Table Q.2**. mass% element-in-compound values of Column C–F are from Appendix A.

TABLE Q.4 Composition Summary of **Table Q.1** Natural Gas in Mass% Contained C, H, N, and O

Column G to J	Row 46
Element	Mass%
C	73.4
H	24.0
N	1.7
O	1.0

Table Q.3 now uses these values to calculate mass% elements in our natural gas.

Mass% values of **Table Q.3** are summarized in **Table Q.4**.

Mass% values of **Table Q.4** are used directly in industrial natural gas injection calculations of Chapter 29, Bottom-Segment Calculations with Natural Gas Injection.

Column G values of **Table Q.2** are used to calculate the natural gas's enthalpy, MJ/kg, Appendix R.

APPENDIX

R

Natural Gas Enthalpy

This appendix calculates the 25°C enthalpy for the industrial natural gas, MJ/kg of gas, of Appendix Q (and Chapter 29: Bottom-Segment Calculations With Natural Gas Injection). It uses;

- published enthalpy values from JANAF¹ and Wikipedia²; and

kg of compound per kg of natural gas values of Table Q.2 (Appendix Q).

The calculations are shown in [Table R.1](#).

The calculations are automated by copying Column G of Table Q.2 into Column E of [Table R.1](#).

TABLE R.1 Table for Calculating the Natural Gas's Enthalpy per kg of Natural Gas from (1) the Compound's Enthalpies (Column A) and Molecular Masses (Column B) and (2) the Natural Gas's Composition, kg of Compound per kg of Natural Gas (Column E). Note that D = Δ in Table R.1, cell B49 and D49.

	A Compound	B $D_{\text{f}}H^{\circ}_{25^\circ\text{C}}$ MJ/kg mol	C MW molecular mass of compound kg per kg mol	D $D_{\text{f}}H^{\circ}_{25^\circ\text{C}}/\text{MW}$ MJ per kg of compound	E mass of compound, kg per kg natural gas, Column G, Table Q.2	F contribution to natural gas's enthalpy, MJ/kg per kg of natural gas
49						
50				=B51/C51		=D51*E51
51	$\text{CH}_4(\text{g})$	-74.87	16.0	-4.667	0.904	-4.219
52	$\text{C}_2\text{H}_6(\text{g})$	-84.0	30.1	-2.791	0.057	-0.159
53	$\text{C}_3\text{H}_8(\text{g})$	-104.7	44.1	-2.374	0.005	-0.012
54	$\text{C}_4\text{H}_{10}(\text{g})$	-125.6	58.1	-2.162	0.002	-0.004
55	$\text{C}_6\text{H}_{12}(\text{g})$	-173.5	72.2	-2.403	0.001	-0.002
56	$\text{C}_8\text{H}_{14}(\text{g})$	-198.7	86.2	-2.305	0.001	-0.001
57	$\text{N}_2(\text{g})$	0	28.0	0.000	0.017	0.000
58	$\text{CO}_2(\text{g})$	-393.5	44.0	-8.943	0.013	-0.117
59	$\text{O}_2(\text{g})$	0	32.0	0.000	0.0004	0.000
60				Total enthalpy 25°C, MJ per kg of natural gas		-4.516

Calculation of $\text{CH}_4(\text{g})$'s enthalpy contribution is described in Row 50. The values in Column E are from Column G in Table Q.2.

R.1 COMPARISON BETWEEN CH₄(g) AND NATURAL GAS

The 25°C enthalpy of CH₄(g) is −4.667 MJ/kg.

The 25°C enthalpy of the natural gas in Appendix Q is −4.52 MJ/kg.

This decrease is due to the lower enthalpies (per kg) of the large hydrocarbon molecules.

References

1. NIST-JANAF. Retrieved by Googling JANAF then typing kinetics.nist.gov/janaf/janaf4pdf.html then typing Al for Al₂O₃ or O for O₂,Si etc.; Googled 05.2.2018.
2. Wikipedia. For example, Google Wikipedia C₂H₆(g) and record *standard enthalpy of formation* ($\Delta_fH^\circ_{298}$), which also = H°_{298} because the enthalpies of C and H are zero at 25°C (298K); Googled 05.02.2018.

S

Enthalpy of Si in Molten Iron

We represent Si-bearing molten blast furnace iron as molten Fe–Si alloy. It is a non-ideal solution, so its enthalpy can't be represented by H_{Fe}° and H_{Si}° . We represent it by;

$$H_{\text{Fe}(\ell)}^{\circ, 1500^\circ\text{C}}, \text{ MJ/kg mol of Fe}$$

and

$$H_{\text{Si(dissolved)}}^{\circ, 1500^\circ\text{C}} = \left\{ H_{\text{Si}(\ell)}^{\circ, 1500^\circ\text{C}} + \Delta H_{\text{Fe}(\ell) + \text{Si}(\ell) \rightarrow (\text{Fe-Si})_{\text{molten alloy}}}^{\circ, 1500^\circ\text{C}} \right\}, \text{ MJ/kg mol of Si}$$
(S.1)

where $\Delta H_{\text{Fe}(\ell) + \text{Si}(\ell) \rightarrow (\text{Fe-Si})_{\text{molten alloy}}}^{\circ, 1500^\circ\text{C}}$ is the enthalpy of reaction for producing molten Fe–Si alloy, 1500°C, from pure Fe(ℓ), 1500°C, and pure Si (ℓ), 1500°C, MJ/kg mole of alloy.

This appendix calculates the value of: $\Delta H_{\text{Fe}(\ell) + \text{Si}(\ell) \rightarrow (\text{Fe-Si})_{\text{molten alloy}}}^{\circ, 1500^\circ\text{C}}$

S.1 CALCULATION OF ALLOY MOL FRACTIONS

This appendix's calculations are all based on Hultgren's measured Fe–Si enthalpy of reaction data (Hultgren et al., 1973. p. 878, Table 4)¹.

They are also all based on 0.4 mass% Si, 99.6 mass% Fe, Fe–Si alloy (i.e., it ignores the presence of C in the product molten iron).

Hultgren's enthalpy data are presented as a function of mole fraction Si in Fe–Si alloy. So we start our calculations by calculating mole fraction Si in 0.4 mass% Si, 99.6 mass%, Fe–Si alloy.

We consider 100 kg of alloy. It contains 0.4 kg of Si and 99.6 kg of Fe. The molecular mass of Si and Fe are 28.09 and 55.85 kg/kg mol so that;

$$\text{kg mol Si} = \frac{0.4 \text{ kg Si}}{28.09 \text{ kg Si per kg mol of Si}} = 0.014 \quad (\text{S.2})$$

$$\text{kg mol Fe} = \frac{99.6 \text{ kg Fe}}{55.85 \text{ kg Fe per kg mol of Fe}} = 1.78 \quad (\text{S.3})$$

per 100 kg of alloy which are equivalent to;

$$X_{\text{Si}} = \frac{0.014 \text{ kg mol Si}}{(0.014 + 1.78) \text{ total kg mol}} = 0.0078 \quad (\text{S.4})$$

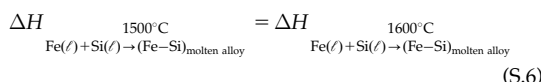
$$X_{\text{Fe}} = \frac{1.78 \text{ kg mol Fe}}{(0.014 + 1.78) \text{ total kg mol}} = 0.9922 \quad (\text{S.5})$$

where X_{Si} and X_{Fe} are the mole fractions of Si and Fe in 0.4 mass% Si and 99.6 mass% Fe alloy.

S.2 CALCULATIONS: UNIT CONVERSIONS

Hultgren's measured enthalpy of reaction data is for 1600°C. We make the assumption that they are nearly the same as our required

1500°C enthalpy of reaction, that is, we assume that:



Hultgren's measured $\Delta H_{\text{Fe}(\ell) + \text{Si}(\ell) \rightarrow (\text{Fe}-\text{Si})_{\text{molten alloy}}}^{1600^\circ\text{C}}$ value for 0.0078 mole fraction Si (i.e., 0.4 mass% Si) is -280 calories per g mol of alloy. This is equivalent to -1200 J/g mol of alloy or -1200 kJ/kg mol of alloy or -1.2 MJ/kg mol of alloy.

S.3 ENTHALPY PER kg mol OF SILICON

This section calculates:

$$\Delta H_{\text{Fe}(\ell) + \text{Si}(\ell) \rightarrow (\text{Fe}-\text{Si})_{\text{molten alloy}}}^{1500^\circ\text{C}}$$

per kg mol of Si in molten 0.4 mass% Si, 99.6 mass% Fe molten Fe-Si alloy.

From Eq. S.4, 1 kg mol of this alloy contains 0.0078 kg mol Si per kg mol of alloy, so -1.2 MJ/kg mol of molten alloy is equivalent to;

$$\frac{-1.2 \text{ MJ/kg mol of molten alloy}}{0.0078 \text{ kg mol of Si per kg mol of molten alloy}}$$

or

$$-150 \text{ MJ/kg mol of Si in alloy.}$$

S.4 PER kg OF SILICON

Chapter 35, Bottom-Segment Calculations—Reduction of SiO_2 , uses the enthalpy of alloy formation *per kg of silicon*. To get this, we divide the above value by the atomic mass of silicon, that is:

$$\frac{\Delta H_{\text{Fe}(\ell) + \text{Si}(\ell) \rightarrow (\text{Fe}-\text{Si})_{\text{molten alloy}}}^{1500^\circ\text{C}}}{\text{MW}_{\text{Si}}} = \frac{-150 \text{ MJ/kg mol of Si}}{28.09 \text{ kg/kg mol of Si}} = -5.3 \text{ MJ/kg of Si.}$$
(S.7)

We use this value in Chapter 35, Bottom-Segment Calculations—Reduction of SiO_2 , and all subsequent chapters in the book.

S.5 $H_{\text{Si(dissolved)}}^{1500^\circ\text{C}} / \text{MW}_{\text{Si}}$

The term we use in the enthalpy equation of Chapter 35, Bottom-Segment Calculations—Reduction of SiO , is $H_{\text{Si(dissolved)}}^{1500^\circ\text{C}} / \text{MW}_{\text{Si}}$.

It is calculated by the equation;

$$\frac{H_{\text{Si(dissolved)}}^{1500^\circ\text{C}}}{\text{MW}_{\text{Si}}} = \frac{H_{\text{Si}(\ell)}^{1500^\circ\text{C}}}{\text{MW}_{\text{Si}}} + \frac{\Delta H_{\text{Fe}(\ell) + \text{Si}(\ell) \rightarrow (\text{Fe}-\text{Si})_{\text{molten alloy}}}^{1500^\circ\text{C}}}{\text{MW}_{\text{Si}}}$$

where from Appendix J;

$$\frac{H_{\text{Si}(\ell)}^{1500^\circ\text{C}}}{\text{MW}_{\text{Si}}} = +3.155 \text{ MJ/kg of liquid Si}$$

and from Section S.4;

$$\frac{\Delta H_{\text{Fe}(\ell) + \text{Si}(\ell) \rightarrow (\text{Fe}-\text{Si})_{\text{molten alloy}}}^{1500^\circ\text{C}}}{\text{MW}_{\text{Si}}} = -5.3 \text{ MJ/kg of dissolved silicon}$$

giving:

$$\begin{aligned} \frac{H_{\text{Si(dissolved)}}^{1500^\circ\text{C}}}{\text{MW}_{\text{Si}}} &= \frac{H_{\text{Si}(\ell)}^{1500^\circ\text{C}}}{\text{MW}_{\text{Si}}} + \frac{\Delta H_{\text{Fe}(\ell) + \text{Si}(\ell) \rightarrow (\text{Fe}-\text{Si})_{\text{molten alloy}}}^{1500^\circ\text{C}}}{\text{MW}_{\text{Si}}} \\ &= 3.155 + (-5.3) \\ &= -2.15 \text{ MJ/kg of dissolved silicon.} \end{aligned}$$

Reference

1. Hultgren R, Desai PD, Hawkins DT, Gleiser M, Kelley KK. *Selected values of the thermodynamic properties of binary alloys*. Metals Park, OH: American Society for Metals; 1973. p. 878.

APPENDIX

T

C/Fe, Si/Fe, Mn/Fe in Molten Iron Mass Ratio Calculator

TABLE T.1 Sample Excel Calculator of C/Fe, Si/Fe, Mn/Fe in Molten Iron Mass Ratio Given Mass% of Elements

	A	B	C
3	Mass% Fe = 100 - mass% C - mass% Si - mass% Mn		
4			
5	Mass%	Input values	
6	C	4.5	
7	Si	0.4	
8	Mn	0.5	
9			
10		Calculated values	
11	Fe	94.6	=100 - B6 - B7 - B8
12			
13	Ratios		
14	C/Fe	0.0476	=B6/B\$11
15	Si/Fe	0.00423	=B7/B\$11
16	Mn/Fe	0.00529	=B8/B\$11

U

Enthalpy of Mn in Molten Iron

To determine the enthalpy of Mn-bearing blast furnace iron, we treat the iron as molten Fe–Mn alloy. It is not an ideal solution, so its enthalpy can't be represented by H_{Fe} and H_{Mn} . We represent it by;

$H_{1500^\circ\text{C}}^{\text{Fe}(\ell)}$, MJ/kg mol of Fe; and

$$H_{\text{Mn(dissolved)}}^{1500^\circ\text{C}} = \left\{ H_{\text{Mn}(\ell)}^{1500^\circ\text{C}} + \Delta H_{\text{Fe}(\ell) + \text{Mn}(\ell) \rightarrow (\text{Fe} - \text{Mn})_{\text{molten alloy}}}^{1500^\circ\text{C}} \right\}, \text{ MJ/kg mol of Mn}$$
 (U.1)

where $\Delta H_{\text{Fe}(\ell) + \text{Mn}(\ell) \rightarrow (\text{Fe} - \text{Mn})_{\text{molten alloy}}}^{1500^\circ\text{C}}$ is the enthalpy change for the $\text{Fe}(\ell) + \text{Mn}(\ell) \rightarrow (\text{Fe} - \text{Mn})_{\text{molten alloy}}$ alloy formation reaction, 1500°C .

Per kg of Mn in alloy, Eq. (U.1), becomes:

$$\frac{H_{\text{Mn(dissolved)}}^{1500^\circ\text{C}}}{\text{MW}_{\text{Mn}}} = \left\{ \frac{H_{\text{Mn}(\ell)}^{1500^\circ\text{C}}}{\text{MW}_{\text{Mn}}} + \frac{\Delta H_{\text{Fe}(\ell) + \text{Mn}(\ell) \rightarrow (\text{Fe} - \text{Mn})_{\text{molten alloy}}}^{1500^\circ\text{C}}}{\text{MW}_{\text{Mn}}} \right\}, \text{ MJ/kg of Mn}$$
 (U.2)

U.1 CALCULATION OF ALLOY MOL FRACTIONS

This appendix's calculations are based on Witusiewicz's interpolated Fe–Mn enthalpy of mixing data (Witusiewicz et al.,¹ Fig. 1, Eq. 11).

They are also all based on 0.5 mass% Mn, 99.5 mass% Fe, Fe–Mn alloy. We have to use this simplification because $\text{Fe}(\ell) + \text{Mn}(\ell) + \text{Si}(\ell) + \text{C}(s) \rightarrow \text{molten alloy}$ heats of reaction are not available.

Witusiewicz's enthalpy data are presented as a function of mol fraction Mn in Fe–Mn alloy. So we start our calculations by determining mol fraction Mn in 0.5 mass% Mn, 99.5 mass%, Fe–Mn alloy.

We consider 100 kg of alloy. It contains 0.5 kg of Mn and 99.5 kg of Fe. The molecular mass of Mn and Fe are 54.94 and 55.85 kg/kg mol so that;

$$\text{kg mol Mn} = \frac{0.5 \text{ kg Mn}}{54.94 \text{ kg Mn/kg mol of Mn}} = 0.0091$$

$$\text{kg mol Fe} = \frac{99.5 \text{ kg Fe}}{55.85 \text{ kg Fe/kg mol of Fe}} = 1.78$$

per 100 kg of alloy which are equivalent to;

$$X_{\text{Mn}} = \frac{0.0091 \text{ kg mol Mn}}{(0.0091 + 1.78) \text{ total kg mol}} = 0.0051$$

$$X_{\text{Fe}} = \frac{1.78 \text{ kg mol Fe}}{(0.0091 + 1.78) \text{ total kg mol}} = 0.9949$$

where X_{Mn} and X_{Fe} are the mol fractions of Mn and Fe in 0.5 mass% Mn, 99.5 mass% Fe alloy.

U.2 CALCULATIONS: UNIT CONVERSIONS

Witusiewicz's interpolated enthalpy of mixing data is for 1427°C. We make the assumption that they are nearly the same as our required 1500°C enthalpy of mixing, that is we assume that:

$$\Delta H_{\text{Fe}(\ell) + \text{Mn}(\ell) \rightarrow (\text{Fe}-\text{Mn})_{\text{molten alloy}}}^{1500^\circ\text{C}} = \Delta H_{\text{Fe}(\ell) + \text{Mn}(\ell) \rightarrow (\text{Fe}-\text{Mn})_{\text{molten alloy}}}^{1427^\circ\text{C}}$$

Witusiewicz's¹ interpolated
 $\Delta H_{\text{Fe}(\ell) + \text{Mn}(\ell) \rightarrow (\text{Fe}-\text{Mn})_{\text{molten alloy}}}^{1427^\circ\text{C}}$ value for 0.0091 mol

fraction Mn (i.e., 0.5 mass% Mn) is $-20 \text{ J/g mol of alloy}$ or $-20 \text{ kJ/kg mol of alloy}$ or $-0.02 \text{ MJ/kg mol of alloy}$.

U.3 ENTHALPY PER kg mol OF MANGANESE

This section calculates;

$$\Delta H_{\text{Fe}(\ell) + \text{Mn}(\ell) \rightarrow (\text{Fe}-\text{Mn})_{\text{molten alloy}}}^{1500^\circ\text{C}}$$

per kg mol of Mn in molten 0.5 mass% Mn, 99.5 mass% Fe molten Fe–Mn alloy.

As shown in Section U.1, 1 kg mol of this alloy contains 0.0051 kg mol of Mn per kg mol of molten alloy, so $-0.02 \text{ MJ/kg mol of molten alloy}$ is equivalent to;

$$\frac{-0.02 \text{ MJ/kg mol of molten alloy}}{0.0051 \text{ kg mol of Mn per kg mol of molten alloy}}$$

or $-4 \text{ MJ/kg mol of Mn in the molten alloy}$.

This value is used in Chapter 36, Bottom-Segment Calculations-Reduction of MnO, and throughout the book.

U.4 PER kg mol OF MANGANESE

Chapter 36, Bottom-Segment Calculations-Reduction of MnO, uses the enthalpy of alloy formation *per kg of manganese*. To get this, we

divide the above value by the atomic mass of manganese, that is:

$$\begin{aligned} & \frac{\Delta H_{\text{Fe}(\ell) + \text{Mn}(\ell) \rightarrow (\text{Fe}-\text{Mn})_{\text{molten alloy}}}^{1500^\circ\text{C}}}{\text{MW}_{\text{Mn}}} \\ &= \frac{-4 \text{ MJ/kg mol of Mn in the molten alloy}}{54.94 \text{ kg/kg mol of Mn}} \\ &= 0.07 \text{ MJ/kg of Mn in the molten alloy} \end{aligned}$$

U.5 $H_{\text{Mn(dissolved)}}^{1500^\circ\text{C}} / \text{MW}_{\text{Mn}}$

The term we use in enthalpy equation of Chapter 36, Bottom-Segment Calculations-Reduction of MnO, is $H_{\text{Mn(dissolved)}}^{1500^\circ\text{C}} / \text{MW}_{\text{Mn}}$.

It is calculated by the equation;

$$\frac{H_{\text{Mn(dissolved)}}^{1500^\circ\text{C}}}{\text{MW}_{\text{Mn}}} = \left\{ \frac{H_{\text{Mn}(\ell)}^{1500^\circ\text{C}}}{\text{MW}_{\text{Mn}}} + \frac{\Delta H_{\text{Fe}(\ell) + \text{Mn}(\ell) \rightarrow (\text{Fe}-\text{Mn})_{\text{molten alloy}}}^{1500^\circ\text{C}}}{\text{MW}_{\text{Mn}}} \right\},$$

MJ/kg of Mn

where from Appendix J;

$$\frac{H_{\text{Mn}(\ell)}^{1500^\circ\text{C}}}{\text{MW}_{\text{Mn}}} = 1.343 \text{ MJ/kg of Mn}$$

and from Section U.4;

$$\frac{\Delta H_{\text{Fe}(\ell) + \text{Mn}(\ell) \rightarrow (\text{Fe}-\text{Mn})_{\text{molten alloy}}}^{1500^\circ\text{C}}}{\text{MW}_{\text{Mn}}} = -0.07 \text{ MJ/kg of dissolved Mn}$$

giving:

$$\begin{aligned} \frac{H_{\text{Mn(dissolved)}}^{1500^\circ\text{C}}}{\text{MW}_{\text{Mn}}} &= \left\{ \frac{H_{\text{Mn}(\ell)}^{1500^\circ\text{C}}}{\text{MW}_{\text{Mn}}} + \frac{\Delta H_{\text{Fe}(\ell) + \text{Mn}(\ell) \rightarrow (\text{Fe}-\text{Mn})_{\text{molten alloy}}}^{1500^\circ\text{C}}}{\text{MW}_{\text{Mn}}} \right\} \\ &= 1.343 + (-0.07) \\ &= 1.27 \text{ MJ/kg of dissolved Mn.} \end{aligned}$$

Reference

- Witusiewicz VT, Sommer F, Mittemeijer EJ. Enthalpy of formation and heat capacity of Fe–Mn alloys. *Metall Mater Trans B* 2003;34B:209–23 (Equation 11, page 213).

V

Coal Elemental Composition

This appendix shows how to calculate a coal's elemental composition from its molecular make-up, [Table V.1](#), and its hydrocarbon composition, [Table V.2](#).

TABLE V.1 Composition of This Chapter's Tuyere-Injected Pulverized Coal

Substance	Mass%
Solid hydrocarbon	92.0
$\text{Al}_2\text{O}_3(\text{s})$	2.4
$\text{SiO}_2(\text{s})$	5.6

The pulverized coal also contains small amounts of potassium, sodium phosphates, and sulfates.

Table courtesy: Coal in Wikipedia, the Free Encyclopedia.¹

TABLE V.2 Elemental Composition of the Hydrocarbon Portion of a Coal

Element	Mass%
C	88
H	6
O	5
N	1

This elemental coal composition is used for all of this book's calculations.

Table courtesy: Coal in Wikipedia, the Free Encyclopedia.¹

V.1 Al_2O_3 AND SiO_2 IN COAL

From [Table V.1](#), the above coal contains 0.024 kg of Al_2O_3 and 0.056 kg of SiO_2 per kg of coal.

V.2 HYDROCARBON

One kilogram of coal contains 0.92 kg of hydrocarbon, [Table V.1](#). The masses of C, H, O, and N in this amount of hydrocarbon are:

mass C-in-coal from hydrocarbon

$$= 0.92 \text{ kg of hydrocarbon} * \frac{88 \text{ mass\% C in hydrocarbon}}{100\%}$$

$$= 0.92 \text{ kg of hydrocarbon} * 0.88$$

$$= 0.810 \text{ kg of C per kg of coal}$$

mass H-in-coal from hydrocarbon

$$= 0.92 \text{ kg of hydrocarbon} * \frac{6 \text{ mass\% H in hydrocarbon}}{100\%}$$

$$= 0.92 \text{ kg of hydrocarbon} * 0.06$$

$$= 0.055 \text{ kg H per kg of coal}$$

mass O-in-coal from hydrocarbon

$$= 0.92 \text{ kg of hydrocarbon} * \frac{5 \text{ mass\% O in hydrocarbon}}{100\%}$$

$$= 0.92 \text{ kg of hydrocarbon} * 0.05$$

$$= 0.046 \text{ kg O per kg of coal}$$

mass N-in-coal from hydrocarbon

$$= 0.92 \text{ kg of hydrocarbon} * \frac{1 \text{ mass\% N in hydrocarbon}}{100\%}$$

$$= 0.92 \text{ kg of hydrocarbon} * 0.01$$

$$= 0.009 \text{ kg N per kg of coal}$$

V.3 SUMMING UP

In summary, 1 kg of coal contains 0.024 kg of Al_2O_3 , 0.056 kg of SiO_2 , 0.810 kg of C, 0.055 kg of H, 0.046 kg of O, and 0.009 kg of N or expressed as mass% in [Table V.3](#).

This composition is used throughout our pulverized real coal injection chapters.

TABLE V.3 Elemental Composition of Coal of [Table V.1](#)

Element	Mass%
C	81.0
H	5.5
N	0.9
O	4.6 ^a
Al_2O_3	2.4
SiO_2	5.6

^aExcluding O in Al_2O_3 and SiO_2 .

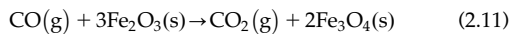
Reference

1. Wikipedia. *Coal* in Wikipedia the Free Encyclopedia; 2018 [recovered 18.03.18]. <https://en.wikipedia.org/wiki/Coal>.

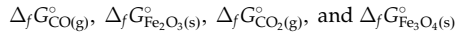
W

CO(g) + 3Fe₂O₃(s) → CO₂(g) + 2Fe₃O₄(s) Equilibrium Constant

This appendix calculates equilibrium constants and molar CO₂/CO ratios for the reaction;



from tabulated values of;



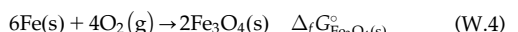
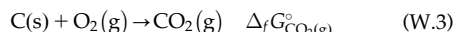
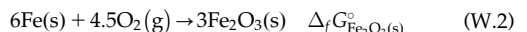
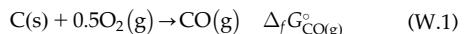
where $\Delta_f G^\circ$ is standard Gibbs-free energy of formation at any given system temperature and 1 bar pressure. Please note that $\Delta_f G^\circ$ numerical values are not affected by pressure changes.¹

We do the calculations in two steps:

- calculation of Reaction (2.11)'s standard Gibbs-free energy of reaction at 25°C and 127°C from published values of $\Delta_f G^\circ_{\text{CO}(\text{g})}, \Delta_f G^\circ_{\text{Fe}_2\text{O}_3(\text{s})}, \Delta_f G^\circ_{\text{CO}_2(\text{g})}, \text{ and } \Delta_f G^\circ_{\text{Fe}_3\text{O}_4(\text{s})}$
- calculation of equilibrium constants and molar CO₂/CO ratios of Reaction (2.11) from (1)'s calculated $\Delta_r G^\circ_{\text{CO}(\text{g})+3\text{Fe}_2\text{O}_3(\text{s}) \rightarrow \text{CO}_2(\text{g})+2\text{Fe}_3\text{O}_4(\text{s})}$ values.

W.1 STANDARD GIBBS-FREE ENERGY OF REACTION

The standard Gibbs-free energies of formation that are needed to calculate $\Delta_r G^\circ_{\text{CO}(\text{g})+3\text{Fe}_2\text{O}_3(\text{s}) \rightarrow \text{CO}_2(\text{g})+2\text{Fe}_3\text{O}_4(\text{s})}$ are;



where the $\Delta_f G^\circ$'s are the standard Gibbs-free energies of formation at our system temperatures.

The standard Gibbs-free energy of reaction for Eq. (2.11) is determined by subtracting Eq. (W.3 + W.4) from Eq. (W.1 + W.2) which gives;

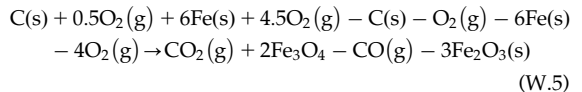


TABLE W.1 Standard Gibbs-Free Energies of Formation at 25°C (298K) and 127°C (400K)

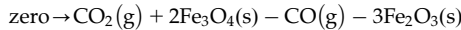
Item	298K	400K
$\Delta_f G^\circ_{\text{CO}_2(\text{g})}$	-394.4	-394.7
$\Delta_f G^\circ_{\text{Fe}_3\text{O}_4(\text{s})}$	-1017.40	-982.4
$\Delta_f G^\circ_{\text{CO}(\text{g})}$	-137.2	-146.3
$\Delta_f G^\circ_{\text{Fe}_2\text{O}_3(\text{s})}$	-743.5	-715.7

The values are from NIST/JANAF [United States Department of Commerce (public domain)].²

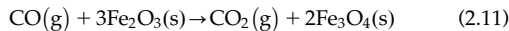
and

$$\begin{aligned}\Delta_r G^\circ_{\text{CO}(\text{g}) + 3\text{Fe}_2\text{O}_3(\text{s}) \rightarrow \text{CO}_2(\text{g}) + 2\text{Fe}_3\text{O}_4(\text{s})} &= \Delta_f G^\circ_{\text{CO}_2(\text{g})} + 2 * \Delta_f G^\circ_{\text{Fe}_3\text{O}_4(\text{s})} \\ &\quad - \Delta_f G^\circ_{\text{CO}(\text{g})} - 3 * \Delta_f G^\circ_{\text{Fe}_2\text{O}_3(\text{s})}\end{aligned}\quad (\text{W.6})$$

The C(s) and O₂(g) terms on the left side of Eq. W.5 cancel so that;



or adding [CO(g) + 3Fe₂O₃(s)] to both sides gives



for which the standard Gibbs-free energy of reaction is Eq. W.6:

$$\begin{aligned}\Delta_r G^\circ_{\text{CO}(\text{g}) + 3\text{Fe}_2\text{O}_3(\text{s}) \rightarrow \text{CO}_2(\text{g}) + 2\text{Fe}_3\text{O}_4(\text{s})} &= \Delta_f G^\circ_{\text{CO}_2(\text{g})} \\ &\quad + 2 * \Delta_f G^\circ_{\text{Fe}_3\text{O}_4(\text{s})} - \Delta_f G^\circ_{\text{CO}(\text{g})} - 3 * \Delta_f G^\circ_{\text{Fe}_2\text{O}_3(\text{s})}\end{aligned}$$

Table W.1 gives 25°C and 127°C values for the right-side terms of Eq. W.6.

They give:

$$\begin{aligned}\Delta_r G^\circ_{\text{CO}(\text{g}) + 3\text{Fe}_2\text{O}_3(\text{s}) \rightarrow \text{CO}_2(\text{g}) + 2\text{Fe}_3\text{O}_4(\text{s})} &= \Delta_f G^\circ_{298\text{K}} + 2 * \Delta_f G^\circ_{298\text{K}} - \Delta_f G^\circ_{298\text{K}} - 3 * \Delta_f G^\circ_{298\text{K}} \\ &\quad \text{CO}_2(\text{g}) \quad \text{Fe}_3\text{O}_4(\text{s}) \quad \text{CO}(\text{g}) \quad \text{Fe}_2\text{O}_3(\text{s}) \\ &= (-394.4) + 2 * (-1017.4) - (-137.2) - 3 * (-743.5) \\ &= -61.5 \text{ MJ/kg mol of CO(g)}$$

and

$$\begin{aligned}\Delta_r G^\circ_{400\text{K}} & \text{CO(g)} + 3\text{Fe}_2\text{O}_3(\text{s}) \rightarrow \text{CO}_2(\text{g}) + 2\text{Fe}_3\text{O}_4(\text{s}) \\ &= \Delta_f G^\circ_{400\text{K}} + 2 * \Delta_f G^\circ_{400\text{K}} - \Delta_f G^\circ_{400\text{K}} - 3 * \Delta_f G^\circ_{400\text{K}} \\ &\quad \text{CO}_2(\text{g}) \quad \text{Fe}_3\text{O}_4(\text{s}) \quad \text{CO(g)} \quad \text{Fe}_2\text{O}_3(\text{s}) \\ &= (-394.7) + 2 * (-982.4) - (-146.3) - 3 * (-715.7) \\ &= -66.1 \text{ MJ/kg mol of CO(g)}$$

W.2 CALCULATION OF EQUILIBRIUM CONSTANTS

Equilibrium constants of Reaction (2.11) are related to its standard Gibbs-free energies of reaction by;

$$K_E^{\text{CO}(\text{g}) + 3\text{Fe}_2\text{O}_3(\text{s}) \rightarrow \text{CO}_2(\text{g}) + 2\text{Fe}_3\text{O}_4(\text{s})} = e^{\left\{ \frac{-\Delta_r G^\circ_{\text{CO}(\text{g}) + 3\text{Fe}_2\text{O}_3(\text{s}) \rightarrow \text{CO}_2(\text{g}) + 2\text{Fe}_3\text{O}_4(\text{s})}}{R \cdot T(K)} \right\}} \quad (\text{W.7})$$

where the equilibrium constant of Reaction (2.11) is $K_E^{\text{CO}(\text{g}) + 3\text{Fe}_2\text{O}_3(\text{s}) \rightarrow \text{CO}_2(\text{g}) + 2\text{Fe}_3\text{O}_4(\text{s})}$, unitless; $\Delta_r G^\circ_{\text{CO}(\text{g}) + 3\text{Fe}_2\text{O}_3(\text{s}) \rightarrow \text{CO}_2(\text{g}) + 2\text{Fe}_3\text{O}_4(\text{s})}$ is the standard Gibbs-free energy of reaction for Reaction (2.11), MJ/(kg mol of CO); R is the gas constant, 0.008314 MJ/kg mol/K; and T(K) is the temperature K, which equals (temperature, °C + 273.15).

W.2.1 127°C (400K) and 25°C (298K) Equilibrium Constants

Chapter 47 addresses CO(g) injection into a blast furnace's top segment. The objective of that chapter is to determine if top-segment CO(g) injection lowers the blast furnace's steady-state coke requirement.

The 400K equilibrium constant is calculated by the following equation:

$$\begin{aligned}K_{E, 400\text{K}}^{\text{CO}(\text{g}) + 3\text{Fe}_2\text{O}_3(\text{s}) \rightarrow \text{CO}_2(\text{g}) + 2\text{Fe}_3\text{O}_4(\text{s})} &= e^{\left\{ \frac{-\Delta_r G^\circ_{\text{CO}(\text{g}) + 3\text{Fe}_2\text{O}_3(\text{s}) \rightarrow \text{CO}_2(\text{g}) + 2\text{Fe}_3\text{O}_4(\text{s})}}{R \cdot T(K)} \right\}} \\ &= e^{\left\{ \frac{-(-66.1)}{0.008314 \cdot 400} \right\}} = 4.1 \times 10^8\end{aligned} \quad (\text{W.8})$$

The 298K equilibrium constant is calculated by the following equation:

$$\begin{aligned} K_{E, 298K}^{\text{CO(g)} + 3\text{Fe}_2\text{O}_3(\text{s}) \rightarrow \text{CO}_2(\text{g}) + 2\text{Fe}_3\text{O}_4(\text{s})} &= e^{\left\{ \frac{-\Delta_f G^\circ}{R \times 298} \right\}} \\ &= e^{\left\{ \frac{-(-61.5)}{0.008314 \times 298} \right\}} = 6.0 \times 10^{10} \end{aligned} \quad (\text{W.9})$$

Both indicate that Eq. (2.11) goes nearly to completion close to the top of the blast furnace.

W.3 EQUILIBRIUM CO_2/CO MOLAR RATIO

In terms of reactant products of Reaction (2.11);

$$K_{E, T}^{\text{CO(g)} + 3\text{Fe}_2\text{O}_3(\text{s}) \rightarrow \text{CO}_2(\text{g}) + 2\text{Fe}_3\text{O}_4(\text{s})} = \frac{a_{\text{CO}_2(\text{g})}^E * (a_{\text{Fe}_3\text{O}_4}^E)^2}{a_{\text{CO(g)}}^E * (a_{\text{Fe}_2\text{O}_3(\text{s})}^E)^3}$$

where a is thermodynamic activity.

The thermodynamic activities of the solids are 1 (pure solid in its most common state).

The thermodynamic activities of the gases are $X_{\text{CO}} * P$ and $X_{\text{CO}_2} * P$ where X is the mol

fraction and P is the gas pressure, ~ 3 bar absolute at the top of a blast furnace (Section 1.3.1) so that:

$$K_{E, T}^{\text{CO(g)} + 3\text{Fe}_2\text{O}_3(\text{s}) \rightarrow \text{CO}_2(\text{g}) + 2\text{Fe}_3\text{O}_4(\text{s})} = \frac{X_{\text{CO}_2(\text{g})} * 3 \text{ bar} * 1^2}{X_{\text{CO(g)}} * 3 \text{ bar} * 1^3} = \frac{X_{\text{CO}_2(\text{g})}}{X_{\text{CO(g)}}} \quad (\text{W.10})$$

At 400K;

$$K_{E, 400K}^{\text{CO(g)} + 3\text{Fe}_2\text{O}_3(\text{s}) \rightarrow \text{CO}_2(\text{g}) + 2\text{Fe}_3\text{O}_4(\text{s})} = 4.1 \times 10^8 = \frac{X_{\text{CO}_2(\text{g})}}{X_{\text{CO(g)}}}$$

while at 298K;

$$K_{E, 298K}^{\text{CO(g)} + 3\text{Fe}_2\text{O}_3(\text{s}) \rightarrow \text{CO}_2(\text{g}) + 2\text{Fe}_3\text{O}_4(\text{s})} = 6.0 \times 10^{10} = \frac{X_{\text{CO}_2(\text{g})}}{X_{\text{CO(g)}}}$$

which indicates that at equilibrium, virtually all the Fe_2O_3 is reduced to Fe_3O_4 .

Reference

1. Gaskell DR. *Introduction to metallurgical thermodynamics*. 2nd ed. New York: McGraw-Hill; 1981. pp. 232, 229, 239.
2. NIST-JANAF (2017) *NIST-JANAF [Thermochemical] Tables PDF*. U.S. Institute of Standards and Technology, Gaithersburg, Maryland. Recovered on December 31, 2017 by Googling JANAF.

X

Slag Liquidus Temperature Lookup Tables

Blast furnace slag lookup tables are provided in this appendix to facilitate the assessment of the blast furnace slag liquidus temperature. The tables were calculated using FACTSage™, a well-known thermodynamic software program. Slag liquidus temperatures can be estimated for slag Al₂O₃ ranging from 5 to 18 wt.%.

To use the lookup tables, the first step is to prorate the actual slag analysis to a composition totaling 97% using the following formula:

$$\text{wt.\% of } i_{\text{Converted}} = \frac{\text{wt.\% of } i_{\text{Original}} \times 97 \text{ wt.\%}}{(\text{Al}_2\text{O}_3 \text{ wt.\%} + \text{CaO wt.\%} + \text{MgO wt.\%} + \text{SiO}_2 \text{ wt.\%})_{\text{Original}}} \quad (\text{X.1})$$

where i is Al₂O₃, CaO, or MgO.

After conversion, round each of the converted weight percentages to its nearest integer for CaO, MgO, and Al₂O₃. The weight percentage of SiO₂ will be the difference

between 97 % and the sum of the three rounded weight percentages for Al₂O₃, CaO, and MgO. Using the liquidus tables, [Table X.1](#), find the liquidus temperature for the rounded Al₂O₃ weight percentage and then the cell that corresponds to the rounded CaO and MgO weight percentage. The liquidus temperature is provided in degrees Celsius (°C). Blank cells mean that the liquidus temperature is over 1600°C and was not calculated. The recommended target for liquidus temperature is <1415°C, the lower the better. Liquidus temperatures between 1415°C and 1479°C are highlighted in yellow (light grey in print version), and liquidus temperatures greater than 1480°C are highlighted in red (dark grey in print version) and must be avoided as the slag liquidus may be higher than the hot metal temperature in some circumstances.

TABLE X.1 Blast Furnace Slag Liquidus Temperature Lookup Tables

Al_2O_3	CaO	MgO	8	9	10	11	12	13	14	15	16	17	18
5	26		1298	1310	1319	1327	1333	1336	1338	1338	1336	1331	1337
5	27		1299	1311	1320	1327	1332	1334	1335	1333	1330	1324	1338
5	28		1305	1311	1319	1325	1329	1331	1330	1328	1324	1334	1342
5	29		1321	1312	1318	1323	1326	1326	1324	1333	1343	1352	1358
5	30		1335	1324	1315	1319	1321	1326	1339	1350	1359	1366	1371
5	31		1348	1336	1322	1314	1330	1344	1356	1366	1373	1379	1381
5	32		1358	1345	1330	1331	1346	1359	1370	1379	1385	1388	1388
5	33		1367	1352	1335	1346	1361	1373	1382	1389	1393	1394	1391
5	34		1373	1356	1344	1360	1374	1385	1393	1398	1399	1397	1390
5	35		1376	1358	1358	1373	1385	1394	1400	1403	1401	1399	1422
5	36		1377	1356	1369	1383	1394	1401	1405	1405	1409	1432	1453
5	37		1375	1363	1379	1391	1400	1405	1406	1416	1440	1462	1479
5	38		1369	1373	1387	1398	1404	1407	1422	1447	1469	1487	1500
5	39		1364	1381	1393	1402	1406	1426	1452	1475	1494	1507	
5	40		1372	1387	1397	1403	1427	1454	1479	1499	1514	1592	
5	41		1377	1390	1399	1427	1455	1481	1502	1518	1533		
5	42		1382	1393	1424	1453	1480	1526	1577	1599			
5	43		1385	1418	1449	1519	1593						
5	44		1410	1484	1580								
5	45		1542										
5	46												
5	47												
5	48												
5	49												
5	50												

(Continued)

TABLE X.1 (Continued)

Al_2O_3	CaO	MgO	8	9	10	11	12	13	14	15	16	17	18
6	26		1293	1304	1312	1319	1324	1327	1327	1326	1323	1318	1342
6	27		1294	1304	1312	1318	1322	1324	1324	1321	1317	1319	1342
6	28		1294	1304	1311	1317	1319	1320	1319	1315	1322	1331	1343
6	29		1307	1303	1309	1313	1315	1315	1320	1331	1340	1347	1353
6	30		1322	1309	1306	1309	1312	1325	1337	1347	1355	1361	1365
6	31		1334	1320	1305	1315	1329	1342	1353	1362	1369	1373	1374
6	32		1344	1328	1315	1331	1345	1357	1367	1374	1379	1381	1379
6	33		1351	1334	1330	1346	1359	1370	1378	1384	1387	1386	1381
6	34		1356	1337	1344	1359	1371	1381	1387	1391	1391	1387	1394
6	35		1358	1340	1357	1371	1381	1389	1394	1395	1392	1405	1426
6	36		1357	1352	1368	1380	1390	1395	1398	1396	1415	1436	1453
6	37		1353	1363	1377	1388	1395	1399	1398	1422	1444	1463	1476
6	38		1355	1371	1384	1393	1399	1403	1428	1451	1471	1485	1583
6	39		1363	1378	1390	1397	1406	1432	1456	1477	1492	1524	
6	40		1370	1384	1393	1406	1434	1459	1481	1497	1508		
6	41		1376	1387	1404	1433	1460	1483	1501	1513			
6	42		1379	1400	1430	1458	1493	1553	1582	1588			
6	43		1392	1424	1483	1567							
6	44		1442	1550									
6	45												
6	46												
6	47												
6	48												
6	49												
6	50												

(Continued)

TABLE X.1 (Continued)

Al_2O_3	CaO	MgO	8	9	10	11	12	13	14	15	16	17	18
7	26		1287	1297	1305	1311	1315	1317	1317	1315	1311	1322	1345
7	27		1288	1297	1305	1310	1313	1314	1313	1309	1304	1322	1345
7	28		1288	1297	1303	1308	1310	1309	1307	1310	1319	1327	1345
7	29		1291	1295	1301	1304	1305	1306	1318	1328	1336	1343	1347
7	30		1305	1292	1297	1299	1312	1324	1335	1344	1351	1356	1359
7	31		1317	1301	1299	1315	1328	1340	1350	1358	1364	1367	1367
7	32		1326	1309	1315	1331	1344	1355	1363	1370	1373	1374	1371
7	33		1332	1314	1330	1345	1357	1367	1374	1379	1380	1378	1374
7	34		1336	1328	1344	1358	1369	1377	1383	1385	1384	1378	1397
7	35		1337	1340	1356	1369	1378	1385	1388	1388	1387	1408	1426
7	36		1334	1352	1366	1378	1386	1390	1391	1396	1418	1437	1451
7	37		1345	1362	1375	1385	1391	1393	1403	1426	1446	1461	1522
7	38		1355	1370	1382	1390	1394	1408	1432	1453	1469	1479	
7	39		1363	1377	1387	1393	1411	1436	1458	1475	1487		
7	40		1370	1382	1390	1412	1438	1461	1480	1493	1563		
7	41		1375	1385	1410	1438	1462	1482	1497	1505			
7	42		1379	1405	1435	1461	1521	1558	1570				
7	43		1398	1433	1531	1592							
7	44		1509	1593									
7	45												
7	46												
7	47												
7	48												
7	49												
7	50												

(Continued)

TABLE X.1 (Continued)

Al_2O_3	CaO	MgO	8	9	10	11	12	13	14	15	16	17	18
8	26		1281	1290	1297	1303	1305	1307	1306	1303	1302	1324	1346
8	27		1281	1290	1296	1301	1303	1303	1301	1297	1302	1324	1346
8	28		1280	1289	1294	1298	1299	1298	1296	1307	1316	1324	1345
8	29		1280	1287	1292	1294	1294	1305	1316	1325	1333	1339	1344
8	30		1286	1284	1288	1297	1311	1323	1333	1341	1348	1352	1353
8	31		1297	1283	1300	1314	1327	1339	1348	1355	1360	1362	1361
8	32		1306	1299	1316	1330	1342	1352	1360	1366	1369	1368	1365
8	33		1311	1314	1330	1344	1355	1364	1371	1374	1375	1372	1374
8	34		1314	1328	1343	1356	1367	1374	1379	1380	1378	1379	1398
8	35		1323	1341	1355	1367	1376	1382	1384	1383	1390	1410	1425
8	36		1335	1352	1365	1376	1383	1387	1387	1400	1420	1435	1460
8	37		1346	1362	1374	1383	1388	1389	1407	1428	1444	1456	
8	38		1355	1370	1381	1388	1391	1412	1434	1452	1464	1559	
8	39		1364	1377	1386	1391	1415	1438	1457	1471	1500		
8	40		1371	1382	1389	1416	1440	1461	1476	1486			
8	41		1376	1386	1414	1440	1462	1479	1490	1580			
8	42		1380	1409	1437	1481	1529	1549	1549				
8	43		1402	1485	1557	1599							
8	44		1552										
8	45												
8	46												
8	47												
8	48												
8	49												
8	50												

(Continued)

TABLE X.1 (Continued)

Al_2O_3	CaO	MgO	8	9	10	11	12	13	14	15	16	17	18
9	26		1275	1284	1290	1295	1297	1298	1296	1293	1305	1327	1348
9	27		1276	1284	1289	1293	1294	1294	1291	1287	1305	1327	1347
9	28		1275	1282	1287	1290	1290	1288	1296	1306	1315	1326	1346
9	29		1273	1280	1284	1285	1292	1304	1315	1324	1331	1336	1345
9	30		1271	1276	1283	1297	1310	1322	1331	1339	1345	1348	1349
9	31		1276	1284	1300	1314	1327	1337	1346	1352	1356	1358	1356
9	32		1284	1300	1316	1330	1341	1351	1358	1363	1365	1364	1360
9	33		1298	1315	1330	1344	1354	1363	1368	1371	1371	1367	1372
9	34		1312	1329	1344	1356	1365	1372	1376	1377	1374	1381	1397
9	35		1325	1342	1355	1366	1375	1380	1381	1380	1392	1409	1421
9	36		1337	1353	1365	1375	1382	1385	1384	1402	1419	1432	1559
9	37		1348	1363	1374	1382	1387	1388	1409	1427	1441	1503	
9	38		1357	1371	1381	1388	1392	1414	1434	1449	1458		
9	39		1366	1378	1387	1393	1418	1438	1454	1465	1577		
9	40		1373	1384	1393	1418	1441	1458	1470	1521			
9	41		1380	1390	1417	1441	1460	1474	1482				
9	42		1385	1412	1438	1494	1523	1529	1583				
9	43		1428	1515	1567	1593	1599	1589					
9	44		1578										
9	45												
9	46												
9	47												
9	48												
9	49												
9	50												

(Continued)

TABLE X.1 (Continued)

Al_2O_3	CaO	MgO	8	9	10	11	12	13	14	15	16	17	18
10	26		1269	1277	1283	1287	1289	1289	1287	1286	1307	1328	1348
10	27		1270	1277	1282	1285	1286	1284	1281	1286	1307	1327	1348
10	28		1269	1275	1280	1281	1281	1285	1296	1305	1313	1326	1346
10	29		1267	1273	1276	1279	1292	1304	1314	1323	1330	1334	1344
10	30		1264	1269	1284	1298	1310	1321	1330	1338	1343	1346	1347
10	31		1268	1285	1301	1315	1327	1337	1345	1351	1355	1356	1354
10	32		1285	1302	1317	1330	1341	1350	1357	1362	1363	1362	1359
10	33		1300	1317	1331	1344	1354	1362	1367	1370	1369	1365	1369
10	34		1314	1331	1345	1356	1365	1372	1375	1375	1372	1381	1395
10	35		1327	1343	1357	1367	1375	1379	1381	1378	1392	1406	1507
10	36		1340	1355	1367	1376	1382	1385	1384	1402	1417	1447	
10	37		1351	1365	1376	1384	1388	1390	1410	1425	1436	1578	
10	38		1361	1374	1384	1390	1394	1415	1432	1444	1524		
10	39		1370	1382	1390	1396	1419	1437	1450	1465			
10	40		1379	1389	1396	1420	1439	1454	1463	1582			
10	41		1386	1395	1418	1440	1456	1467	1527				
10	42		1393	1414	1452	1493	1508	1504					
10	43		1465	1529	1565	1578	1574	1576					
10	44		1590										
10	45												
10	46												
10	47												
10	48												
10	49												
10	50												

(Continued)

TABLE X.1 (Continued)

Al_2O_3	CaO	MgO	8	9	10	11	12	13	14	15	16	17	18
11	26		1264	1271	1276	1280	1281	1280	1277	1288	1308	1329	1348
11	27		1264	1271	1275	1277	1277	1275	1276	1287	1307	1328	1347
11	28		1263	1269	1272	1273	1273	1285	1296	1305	1313	1326	1345
11	29		1261	1266	1268	1280	1293	1304	1314	1323	1329	1334	1343
11	30		1258	1269	1285	1299	1311	1322	1331	1338	1343	1346	1346
11	31		1270	1287	1302	1316	1327	1337	1345	1351	1354	1355	1353
11	32		1287	1304	1318	1331	1342	1351	1358	1362	1363	1361	1379
11	33		1302	1319	1333	1346	1356	1363	1368	1370	1369	1368	1409
11	34		1317	1333	1347	1358	1367	1373	1376	1376	1372	1398	1455
11	35		1331	1346	1359	1370	1377	1381	1382	1379	1391	1425	1580
11	36		1344	1359	1370	1379	1385	1387	1385	1401	1415	1529	
11	37		1356	1370	1380	1387	1391	1391	1409	1422	1472		
11	38		1367	1379	1389	1394	1396	1414	1429	1438	1584		
11	39		1377	1388	1396	1399	1418	1434	1444	1531			
11	40		1387	1396	1401	1419	1437	1449	1474				
11	41		1395	1403	1418	1437	1451	1460	1578				
11	42		1403	1414	1458	1483	1487	1523					
11	43		1486	1532	1555	1558	1546						
11	44		1593	1588									
11	45												
11	46												
11	47												
11	48												
11	49												
11	50												

(Continued)

TABLE X.1 (Continued)

Al_2O_3	CaO	MgO	8	9	10	11	12	13	14	15	16	17	18
12	26		1259	1265	1270	1273	1273	1272	1268	1289	1309	1329	1348
12	27		1258	1265	1268	1270	1269	1267	1277	1288	1308	1327	1346
12	28		1257	1263	1265	1266	1274	1286	1297	1306	1314	1325	1344
12	29		1255	1259	1268	1282	1294	1306	1315	1324	1330	1335	1341
12	30		1255	1272	1287	1300	1313	1323	1332	1339	1344	1347	1367
12	31		1273	1290	1305	1318	1329	1339	1347	1353	1356	1356	1398
12	32		1290	1307	1321	1334	1345	1353	1360	1364	1365	1386	1426
12	33		1306	1322	1337	1349	1358	1366	1371	1372	1373	1415	1451
12	34		1321	1337	1351	1362	1371	1376	1379	1378	1403	1441	1534
12	35		1336	1351	1364	1374	1381	1385	1385	1391	1430	1480	
12	36		1349	1364	1376	1384	1389	1391	1388	1419	1452	1588	
12	37		1362	1376	1386	1393	1396	1395	1407	1442	1538		
12	38		1375	1387	1396	1400	1400	1412	1431	1483			
12	39		1386	1397	1403	1405	1416	1430	1449	1582			
12	40		1397	1405	1409	1418	1433	1442	1530				
12	41		1407	1412	1417	1434	1445	1473					
12	42		1415	1418	1455	1467	1462	1566					
12	43		1495	1527	1539	1533	1515						
12	44		1588	1599									
12	45												
12	46												
12	47												
12	48												
12	49												
12	50												

(Continued)

TABLE X.1 (Continued)

Al_2O_3	CaO	MgO	8	9	10	11	12	13	14	15	16	17	18
13	26		1254	1260	1264	1266	1266	1264	1269	1289	1309	1328	1347
13	27		1253	1259	1262	1263	1262	1267	1278	1289	1308	1327	1345
13	28		1252	1257	1259	1263	1276	1288	1299	1309	1316	1324	1358
13	29		1250	1255	1270	1284	1297	1308	1318	1326	1333	1346	1386
13	30		1258	1275	1290	1303	1316	1326	1335	1342	1347	1374	1415
13	31		1277	1293	1308	1321	1333	1343	1350	1356	1361	1403	1443
13	32		1294	1311	1325	1338	1349	1357	1364	1367	1390	1431	1468
13	33		1311	1327	1341	1353	1363	1370	1375	1377	1419	1457	1488
13	34		1327	1343	1356	1367	1376	1381	1383	1406	1445	1478	1592
13	35		1343	1358	1370	1380	1387	1390	1393	1433	1467	1544	
13	36		1357	1372	1383	1391	1396	1396	1420	1456	1492		
13	37		1371	1385	1394	1400	1402	1407	1444	1474	1587		
13	38		1385	1396	1404	1408	1406	1431	1463	1537			
13	39		1397	1407	1412	1412	1418	1451	1484				
13	40		1409	1416	1417	1416	1439	1466	1573				
13	41		1419	1422	1419	1429	1454	1521					
13	42		1426	1425	1445	1448	1465						
13	43		1496	1517	1519	1506	1550						
13	44		1577	1580	1569	1548							
13	45		1577										
13	46												
13	47												
13	48												
13	49												
13	50												

(Continued)

TABLE X.1 (Continued)

Al_2O_3	CaO	MgO	8	9	10	11	12	13	14	15	16	17	18
14	26		1255	1255	1258	1260	1259	1257	1270	1289	1309	1328	1353
14	27		1252	1254	1256	1257	1258	1270	1281	1292	1307	1341	1378
14	28		1248	1251	1253	1266	1280	1292	1303	1312	1328	1365	1405
14	29		1245	1258	1274	1288	1300	1312	1322	1330	1352	1392	1433
14	30		1262	1279	1294	1308	1320	1331	1339	1346	1379	1420	1459
14	31		1281	1298	1313	1326	1338	1348	1355	1365	1407	1447	1483
14	32		1300	1316	1331	1344	1354	1363	1369	1393	1435	1472	1503
14	33		1318	1334	1348	1360	1369	1376	1380	1421	1460	1493	1550
14	34		1335	1350	1364	1375	1383	1387	1407	1447	1482	1509	
14	35		1351	1366	1379	1388	1394	1396	1434	1470	1499	1593	
14	36		1367	1381	1392	1399	1403	1420	1457	1488	1546		
14	37		1382	1395	1404	1409	1409	1444	1476	1501			
14	38		1397	1408	1414	1415	1429	1464	1490	1580			
14	39		1410	1418	1421	1418	1450	1479	1531				
14	40		1422	1426	1425	1436	1466	1488					
14	41		1431	1431	1425	1453	1477	1559					
14	42		1437	1432	1438	1464	1506						
14	43		1491	1502	1497	1478	1581						
14	44		1562	1558	1542	1528							
14	45		1598	1574	1599								
14	46		1596										
14	47												
14	48												
14	49												
14	50												

(Continued)

TABLE X.1 (Continued)

Al_2O_3	CaO	MgO	8	9	10	11	12	13	14	15	16	17	18
15	26		1275	1269	1262	1254	1253	1250	1270	1295	1327	1361	1398
15	27		1271	1264	1256	1251	1261	1274	1286	1313	1348	1385	1423
15	28		1265	1257	1256	1271	1284	1296	1307	1334	1371	1410	1450
15	29		1258	1263	1278	1292	1305	1317	1327	1357	1397	1437	1476
15	30		1267	1284	1299	1313	1326	1336	1345	1383	1424	1463	1499
15	31		1287	1304	1319	1333	1344	1354	1368	1409	1450	1487	1518
15	32		1307	1323	1338	1351	1361	1370	1395	1436	1475	1508	1534
15	33		1326	1342	1356	1368	1377	1383	1422	1461	1496	1524	1598
15	34		1344	1360	1373	1383	1391	1406	1447	1484	1513	1553	
15	35		1362	1376	1388	1397	1402	1433	1470	1502	1526		
15	36		1379	1392	1402	1408	1417	1456	1489	1515	1588		
15	37		1395	1407	1414	1417	1441	1476	1504	1541			
15	38		1410	1419	1424	1425	1462	1491	1513				
15	39		1423	1429	1430	1446	1478	1502	1569				
15	40		1434	1436	1432	1464	1490	1519					
15	41		1442	1439	1448	1476	1496	1590					
15	42		1446	1437	1461	1483	1540						
15	43		1482	1485	1473	1487							
15	44		1545	1535	1514	1557							
15	45		1590	1570	1543								
15	46		1595	1570									
15	47												
15	48												
15	49												
15	50												

(Continued)

TABLE X.1 (Continued)

Al_2O_3	CaO	MgO	8	9	10	11	12	13	14	15	16	17	18
16	26		1293	1284	1275	1265	1254	1272	1302	1334	1367	1403	1441
16	27		1287	1277	1267	1255	1266	1287	1320	1354	1390	1428	1466
16	28		1279	1269	1261	1276	1290	1305	1339	1376	1414	1453	1491
16	29		1270	1268	1284	1299	1312	1324	1361	1400	1440	1478	1514
16	30		1274	1290	1306	1320	1333	1346	1385	1425	1465	1502	1533
16	31		1295	1312	1327	1340	1352	1369	1410	1451	1489	1522	1549
16	32		1315	1332	1347	1360	1370	1394	1436	1475	1510	1538	1560
16	33		1335	1352	1366	1377	1386	1420	1461	1497	1527	1550	
16	34		1355	1370	1383	1393	1404	1445	1483	1515	1540	1595	
16	35		1374	1388	1399	1407	1429	1468	1502	1529	1550		
16	36		1392	1405	1413	1418	1452	1488	1517	1538			
16	37		1409	1419	1425	1435	1473	1504	1527	1578			
16	38		1424	1431	1433	1457	1489	1515	1532				
16	39		1437	1440	1439	1474	1502	1521	1600				
16	40		1446	1444	1457	1487	1509	1553					
16	41		1452	1445	1471	1495	1511						
16	42		1453	1454	1481	1499	1569						
16	43		1470	1466	1485	1518							
16	44		1526	1511	1486	1582							
16	45		1566	1543	1529								
16	46		1594	1565	1591								
16	47		1579										
16	48		1597										
16	49												
16	50												

(Continued)

TABLE X.1 (Continued)

Al ₂ O ₃	CaO	MgO	8	9	10	11	12	13	14	15	16	17	18
17	26		1307	1297	1285	1273	1278	1308	1339	1373	1408	1445	1483
17	27		1300	1288	1275	1262	1293	1324	1358	1394	1431	1469	1506
17	28		1291	1278	1268	1283	1309	1343	1379	1417	1455	1493	1528
17	29		1280	1276	1291	1306	1327	1363	1401	1441	1480	1516	1548
17	30		1281	1299	1314	1329	1347	1386	1425	1465	1503	1536	1563
17	31		1304	1321	1336	1350	1369	1409	1450	1489	1523	1552	1575
17	32		1326	1342	1357	1370	1392	1434	1474	1510	1540	1564	
17	33		1347	1363	1377	1388	1417	1458	1495	1528	1554	1573	
17	34		1368	1383	1395	1403	1441	1480	1514	1542	1563		
17	35		1387	1401	1411	1423	1464	1499	1529	1552	1587		
17	36		1406	1417	1424	1446	1484	1515	1540	1557			
17	37		1423	1431	1434	1467	1500	1527	1546				
17	38		1437	1442	1448	1484	1513	1534	1564				
17	39		1449	1448	1466	1498	1521	1537					
17	40		1456	1451	1481	1507	1525	1581					
17	41		1459	1462	1491	1512	1533						
17	42		1457	1474	1497	1512	1594						
17	43		1456	1480	1498	1544							
17	44		1506	1487	1493								
17	45		1542	1516	1552								
17	46		1567	1536									
17	47		1583	1557									
17	48		1593										
17	49		1596										
17	50												

(Continued)

TABLE X.1 (Continued)

Y

Answers to Exercises

CHAPTER 1 EXERCISE ANSWERS

- 1.1.** Molten blast furnace iron is a high-carbon intermediate product that is immediately made into molten low-carbon steel, Fig. 1.6. Cast iron (~4.5 mass% C) is brittle. Low-carbon (0.1 mass% C) steel is strong and tough. It is easily made into many industrial products, for example, buildings, machinery, and vehicles.
- 1.2.** Three unusual safety problems around iron blast furnaces are:
- carbon monoxide poisoning,
 - molten iron/slag burns, and
 - water–molten iron/slag explosions.
- Carbon monoxide poisoning is avoided by wearing personal CO monitors and rigid enforced sign-in, sign-out system. Iron/slag burns are minimized by proper clothing, hats and glasses, and no-go safety zones. Water–molten iron/slag explosions are avoided by keeping hoses etc. away from tapping areas and especially away from ladles and torpedo cars.
- 1.3.** As it applies to blast furnace ironmaking, slag is a molten oxide phase composed mainly of Al_2O_3 , CaO , MgO , and SiO_2 . Its main purposes are to remove ore gangue minerals, coke and coal ash minerals, K_2O and Na_2O , and sulfur from the furnace in

a molten phase, less dense than molten iron. Its composition is adjusted by adding fluxes to the furnace, mostly CaO and MgO (sometimes provided to the furnace in the form of carbonates), also with alumina and quartz. The solidified slag is also often sold for use in cement and road aggregate.

- 1.4.** From Appendix A, Fe_2O_3 contains 69.9 mass% Fe.

So 1000 kg of Fe_2O_3 contains 699 kg of Fe. And 1431 kg of Fe_2O_3 contains 1000 kg of Fe.

Check: 1431 kg of Fe_2O_3 contains $1431^*(69.9 \text{ mass\% Fe}/100\%) = 1000 \text{ kg of Fe}$.

- 1.5.** From Appendix A, Fe_2O_3 contains 69.9 mass% Fe.

Consider 1000 kg of $\text{Fe}_2\text{O}_3-\text{SiO}_2$ ore. It contains 940 kg of Fe_2O_3 and 60 kg of SiO_2 .

940 kg of Fe_2O_3 contains $940^*(69.9 \text{ mass\% Fe in } \text{Fe}_2\text{O}_3/100\%) = 657 \text{ kg of Fe}$.

So the ore contains $(657 \text{ kg of Fe}/1000 \text{ kg of ore})*100\% = 65.7 \text{ mass\% Fe}$.

- 1.6.** A blast furnace is producing 7000 t Fe/day in 95 mass% Fe, 4.5 mass% C, 0.5 mass% Si molten iron.

Since the iron contains 95 mass% Fe,

$$\text{mass iron} = \frac{7000 \text{ kg/day of Fe}}{(95 \text{ mass\% Fe}/100\%)} = 7368 \text{ t of molten iron per day.}$$

Check: mass Fe in iron produced per day

$$= 7368 \text{ t of molten iron per day} * \left(\frac{95 \text{ mass\% Fe}}{100\%} \right) \\ = 7000 \text{ t of Fe per day.}$$

- 1.7.** 1000 kg of 23.3 mass% O₂ contains 233 kg of O₂. To get to 27 mass% O₂ in blast, we add x kg of pure O₂.

$$\% \text{O}_2 \text{ in the mixture} = 27 \text{ mass\%} = \left[\frac{(233 + x)}{(1000 + x)} \right] * 100.$$

From the above equation, one unknown gives $x = 50.7$ kg of pure O₂.

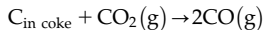
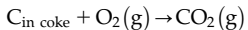
- 1.8.** With 23.3 mass% O₂ and 76.7 mass% N₂ in air, the N₂/O₂ mass ratio is 3.3, so for every kg of O₂ entering the furnace in blast, 3.3 kg of N₂ has to be heated in the furnace (by carbon oxidation).

However, with 27 mass% O₂ and 73 mass% N₂ in air, the N₂/O₂ mass ratio is 2.7 and only 2.7 kg of N₂ has to be heated by carbon oxidation.

With less N₂ to heat, the hearth temperature is higher (with the O₂-enriched blast air).

CHAPTER 2 EXERCISE ANSWERS

- 2.1.** The top-charged solids descend through the furnace under the influence of gravity;
- into the space left by gasified coke, that is, coke that is gasified by reactions like



- into space left by Fe oxides being reduced to dense Fe metal, and
 - flow of product molten iron and slag out through the tap holes
- 2.2.** On entering the furnace, the blast meets with hot coke in the raceway. The air

oxidizes the coke's carbon to form extremely hot ($\sim 2000^\circ\text{C}$) CO(g) + N₂(g) gas which is blown up the furnace by the high pressure (~ 4 bar) at the tuyere tips. In a sense, the blast blower blows the gas up the furnace. Failure of the blower would stop all of this movement through the furnace. There would be some buoyancy due to the high temperature ($\sim 2000^\circ\text{C}$) of the hot gas, but this effect would be trivial.

- 2.3.** Countercurrent heat exchangers;

- provide the hottest heat source where a high temperature is required (i.e., to melt iron and slag); and
- provide very efficient use of its heat by leaving cool out the top of the furnace (where the nearly cooled gas meets the ambient temperature solids).

- 2.4.** The advantages of hot ($\sim 1200^\circ\text{C}$) blast are;

- it produces a very high flame temperature by burning hot coke in the tuyere raceways, which ensures that its product iron and slag are molten; and fluid at the bottom of the furnace and
- its hot nitrogen heats the furnace charge as it rises up through the furnace and encourages rapid reduction reactions in the mid-section of the furnace.

- 2.5.** Adding an extra 5 m to the top of the furnace would be wasted because;

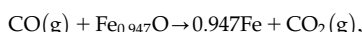
- reduction of Fe₂O₃ and Fe₃O₄ to Fe_{0.947}O requires only about 1 m at the top of the furnace; and
- reduction of 1 kg mol of Fe₂O₃ reacts to form more than 2 kg mol of Fe_{0.947}O so that the 5 m of additional height would fill with Fe_{0.947}O, that is, would increase the thickness of the chemical reserve zone. The reaction is:



- 2.6.** Less reaction hematite would increase the thickness of the Fe₂O₃ reduction zone at the top of the furnace. The extra thickness would give more time for the above

reaction to occur. As a consequence, the thickness of the chemical reserve zone would decrease. As long as the chemical reserve zone doesn't shrink to nothing, the coke utilization efficiency of the furnace won't be adversely affected.

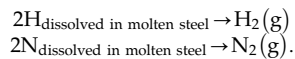
- 2.7.** The main purposes of the blast furnaces' coke are;
- provision of fuel to heat the furnace,
 - provision of reducing gas for iron oxide reduction, for example, for



- provision of slits of solid coke pieces between softening layers of iron and slag that allow gas to ascend the furnace through the fusion dome, and
 - provision of support for the furnace charge by remaining solid to the very bottom of the furnace.
- 2.8.** To prevent melting of the copper tuyere tips and furnace walls, provide them with a cooling system for passing cool water through their interiors. Passage of cool water through these interior tubes will cause heat to flow from the tips and walls to the water, cooling them and preventing them from melting.
- 2.9.** The layers would move 0.6 m.

that it must be produced at $\sim 1630^\circ\text{C}$ in order to keep it molten during subsequent processing, Fig. 3.1. Blast furnace iron has a much lower melting point ($\sim 1200^\circ\text{C}$) than steel so that 1500°C is adequate. This temperature is chosen to keep the blast furnace's byproduct slag molten and fluid (free flowing).

- 3.3.** The O-in-steel is removed from the O-rich steel by adding solid aluminum or ferrosilicon to the O-rich steel bath. The removal reactions are:
- $$2\text{Al} + 3\text{O}_{\text{dissolved in molten steel}} \rightarrow \text{Al}_2\text{O}_3\text{dissolved in molten slag}$$
- $$\text{Si} + 2\text{O}_{\text{dissolved in molten steel}} \rightarrow \text{SiO}_2\text{dissolved in molten slag}$$
- 3.4.** No heat needs to be supplied for Exercise 3.3's deoxidation. This is because both of the deoxidation reactions are exothermic.
- 3.5.** The key step to making continuous casting truly continuous is to have a constant supply of molten steel ready to descend into the caster. This constant supply is provided by a large reservoir of molten steel in a large rectangular ladle (called a tundish) above the casting machines, Fig. 3.10. In turn, this rectangular ladle is regularly supplied with steel from the degassing plant, Fig. 3.1.
- 3.6.** The chemical reactions by which dissolved H and N are removed from molten steel are:



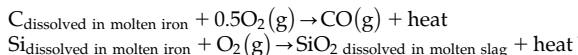
Thermodynamically, these reactions go further toward completion as the total pressure and the $\text{H}_2\text{(g)}$ and $\text{N}_2\text{(g)}$ partial pressures are drawn down to 0. This is a version of Le Chatelier's principle.

- 3.1.** You tell them that the oxygen needs to contain very little nitrogen in order to avoid nitrogen-embrittlement of the steel product. Oxygen containing 99.5% O_2 , 0.5% Ar is the normal requirement. Production of this oxygen product from air rejects most of the feed air's nitrogen to a nitrogen product stream.
- 3.2.** The carbon–iron phase diagram shows that low-carbon steel (~ 0.1 mass% C) has a melting point of $\sim 1530^\circ\text{C}$. This means

- 3.7.** The biggest difference between ironmaking slag and steelmaking slag is their Fe contents:
0.5 mass % Fe in ironmaking slag
and 17 mass% Fe mostly as FeO in steelmaking slag.

The low Fe content of ironmaking's slag is due to the strongly reducing conditions in the blast furnace. The high FeO content of steelmaking's slag is due to the strongly oxidizing conditions in the steelmaking furnace.

- 3.8.** Steel isn't made from ore in a single furnace because, under the oxidizing conditions of steelmaking, too much of the top-charged Fe-in-ore would be lost in the 17 mass% Fe in steelmaking slag.
- 3.9.** During degassing, heat flows out of the degasser's steel by conduction, convection, and radiation to and through the walls and top of the degasser. It also leaves the steel in the departing Ar, CO, H₂, and H₂ gases. All of these heat outflows cool the steel. Steel doesn't cool down during oxygen steelmaking because dissolved carbon and dissolved silicon are being exothermically oxidized by the reactions



CHAPTER 4 EXERCISE ANSWERS

4.1. Data:

The mixed ore charge contains 50 mass% Fe₂O₃, 50 mass% Fe₃O₄.

The equivalent composition is 71.1 mass% Fe, 28.9 mass% O.

Change Cell D3 of Table 4.2 to -0.711 and Cell D4 to -0.289.

Solve the matrix as described in Appendix 4.1

The top gas masses are:

$$\begin{array}{ll} 505 \text{ kg CO} & (18.0 \text{ kg mol}) \\ 671 \text{ kg CO}_2 & (15.3 \text{ kg mol}) \\ 1221 \text{ kg N}_2 & (43.6 \text{ kg mol}) \end{array}$$

which are equivalent to 21.1 mass% CO, 28.0 mass% CO₂, 50.9 mass% N₂ and 23.5 mol% CO, 19.8 mol% CO₂, 56.7 mol% N₂ and a CO₂/CO mass ratio of 1.33.

4.2. Data:

The blast contains 27 mass% O₂ and 73 mass% N₂.

The N₂/O₂ mass ratio of this gas is 2.7. Replace Cell F7 in Exercise 4.1 with 2.7. Solve the matrix.

The top gas masses are:

$$\begin{array}{l} 505 \text{ kg CO} \\ 671 \text{ kg CO}_2 \\ 999 \text{ kg N}_2 (\text{the only value that is different from Exercise 1}) \end{array}$$

which is equivalent to 23.2 mass% CO, 30.9 mass% CO₂, 45.9 mass% N₂.

4.3. Data:

The top gas masses with and without oxygen enrichment are 2175 and 2397 kg/1000 kg of Fe in product molten iron, that is, per tonne of Fe in product molten iron.

The maximum top gas flow is 400,000 kg/h.

The maximum Fe production rate with 2175 kg of top gas per tonne of Fe in product molten iron is (400,000 kg top gas/h)/(2175 kg top gas/t of Fe) = 184 t of Fe per hour.

Check: 184 t of Fe per hour*(2175 kg top gas/t of Fe) = 400,000 kg top gas/h

The maximum Fe production rate with 2397 kg of top gas per tonne of Fe in product molten iron is (400,000 kg top gas/h)/(2397 kg top gas/t of Fe) = 167 t of Fe per hour.

Check: 167 t of Fe per hour*(2397 kg top gas/t of Fe) = 400,000 kg top gas/h

4.4. Data:

The charge is 80 mass% Fe₂O₃, 20 mass% Fe.

This is equivalent to 76 mass% Fe, 24 mass% O.

Calculation: Insert -0.76 in Cell D3 and -0.24 in Cell D4 and solve.

The top gas masses with this data are 664 kg CO, 422 kg CO₂, and 1221 kg N₂ for

a total top gas mass of 2307 kg/1000 kg of Fe in product molten iron, that is, per tonne of Fe in product molten iron.

The maximum Fe production rate with 2307 kg of top gas per tonne of Fe in product molten iron is $(400,000 \text{ kg top gas/h})/(2307 \text{ kg top gas/t of Fe}) = 173 \text{ t of Fe per hour}$.

Check: $173 \text{ t of Fe per hour} * (2307 \text{ kg top gas/t of Fe}) = 400,000 \text{ kg top gas/h}$

4.5. Data:

The product molten iron consists of 5 mass% C and 95 mass% Fe, that is, its (mass C/mass Fe ratio) is 0.053.

Guess: The same amount of carbon is entering the furnace. However, more C is going to the product molten iron so less must be going to the top gas. The amount of oxygen entering the furnace remains unchanged. So with the same amount of oxygen and a smaller amount of carbon departing the furnace in top gas, the top gas CO_2/CO ratio must increase.

This problem is done by examining matrix Table 4.3. For this exercise, please replace the 0.047 in Cell H10 of Table 4.3 with 0.053.

With this change, the top gas contains 258 kg CO and 865 kg CO_2 giving a CO_2/CO ratio of 3.35—compared to 1.33 in Exercise 1.

4.6. Data:

The O_2 in blast is specified to be 370 kg in Tables 4.1–4.3.

The blast is specified to be air for which the N_2/O_2 mass ratio is always 3.3.

These specifications are true for Tables 4.1–4.3.

As a result, mass N_2 entering the furnace in blast air and leaving in top gas = $370 * 3.3$ or 1221 kg N_2 for all these tables.

4.7. a. Pure oxygen is made by (i) liquefying air then distilling gaseous nitrogen from pure liquid (99.5% O₂) oxygen. The

boiling points of oxygen and nitrogen are -183°C and -195.8°C , respectively. This is the principal method for producing the large quantities of oxygen needed by blast furnaces and other large industrial processes, for example, copper smelting. (ii) Oxygen is also made by pressure swing adsorption on then off zeolites and other adsorbants.

- b. The major cost of making pure oxygen is for the electricity that is used to liquefy the input gaseous air, that is, by refrigeration and pressurization.
- c. In the blast furnace plant, nitrogen is used to quench hot coke during coke making. Nitrogen is also used as protective gas for laser cutting of solid steel, to avoid oxidation. However, it is specifically avoided in liquid steel because it embrittles the final steel product.

CHAPTER 5 EXERCISE ANSWERS

5.1. Data: Increase the blast temperature from 1200°C to 1300°C .

From this chapter: the enthalpy of O_2 at 1200°C is 1.239 and the enthalpy of N_2 at 1200°C is 1.339 both MJ per kg. From Table J.3, the 1300°C enthalpy of O_2 is 1.352 and the 1300°C enthalpy of N_2 is 1.463, both MJ per kg.

Answer: place 1.355 in the third row of Eq. (5.7) and 1.463 in the fourth row of Eq. (5.7).

5.2. Data: Increase product molten iron temperature from 1500°C to 1550°C .

From this chapter, the enthalpy of $\text{Fe}(\ell)$ at 1500°C is 1.269 MJ/kg.

From Table J.6, the enthalpy of $\text{Fe}(\ell)$ at 1550°C is 1.310 MJ/kg.

Answer: place 1.310 in the fifth row of Eq. (5.7).

- 5.3.** The advantages of blowing hot blast into the iron blast furnace are;
- it produces a very hot flame when burning hot coke in the tuyere raceways, which ensures that the descending molten iron and slag are hot, molten, and fluid at the tapholes and in the furnace hearth; and
 - the very hot nitrogen in the flame ascends the furnace, providing heat for melting the descending charge and for the furnace's coke gasification and iron oxide reduction reactions.
- 5.4.** Enthalpy is comfortably used in our calculations because the enthalpies of ideal gases are unaffected by pressure and the enthalpies of liquids and solids are insensitive to pressure. Also, the world's literature contains enthalpy values for most of the world's substances. Further, enthalpies are based on a well-structured system of zero enthalpy for elements in their most common state at 25°C (298.15K) becoming positive with increasing temperature and becoming negative with decreasing temperature.
- Enthalpy refers to the heat content in a system. Heat refers to energy flow in a changing system, for example, heat of reaction, heat transfer.
- 5.5.** Air is an ideal solution under ironmaking conditions. For this reason, its enthalpy is 0 at 25°C and 1 bar pressure because it is made up of nitrogen and oxygen in their most common states at 25°C. Its enthalpy is also 0 at 25°C and 4 bar because the enthalpies of ideal gases are unaffected by pressure.

CHAPTER 6 EXERCISE ANSWERS

- 6.1.** Proposition: carbon charged of matrix Table 6.1 is lowered to 380 kg C/1000 kg

of Fe in product molten iron. Calculate the O₂-in-blast air and blast air requirements for steady-state operation of this furnace.

Solution: Place 380 in Cell C8 and solve.

Answers: O₂ requirement = 286 kg

Air requirement = 286 kg O₂ + 943 kg

N₂ = 1229 kg air

Both per 1000 kg of Fe in product molten iron.

- 6.2.** Proposition: the temperature of the blast furnace's blast of Table 6.1 has fallen to 1100°C. How much does this affect this furnace's steady-state O₂ and air requirements?

Data: From Table J.3, O₂'s 1100°C enthalpy is 1.125 MJ/kg and N₂'s 1000°C enthalpy is 1.216 MJ/kg.

Solution: Type -1.125 in Cell F10 of matrix Table 6.1 and -1.216 in Cell G10.

Answers: The steady-state O₂ in blast air requirement has increased from 298 to 305 kg/1000 kg of Fe in product molten iron. Likewise, the steady-state air requirement has increased from 1283 to 1312 kg/1000 kg of Fe in product molten iron.

CHAPTER 7 EXERCISE ANSWERS

- 7.1.** The blast furnace's blast temperature of Fig. 7.2 has fallen from 1200°C to 1100°C. A result of this is that the enthalpy of the blast's O₂ has fallen to 1.125 MJ/kg and the enthalpy of its N₂ has fallen to 1.216 MJ/kg, Table 7.3.

The steady-state C-in-coke requirement with 1100°C blast is calculated by inserting -1.125 in Cell F11 of Table 7.2 and -1.216 in Cell G11 of Table 7.2. The steady-state requirements with these values are;

mass C-in-coke = 401 kg

mass O₂-in-blast = 313 kg

mass N₂-in-blast = 1032 kg
 mass blast air = 1345 kg

all per 1000 kg of Fe in product molten iron. The C-in-coke requirement is 9 kg more than with 1200°C blast, Table 7.2.

- 7.2.** The 1032 kg of N₂ entering the furnace with 1100°C blast is 49 kg more than with 1200°C blast, Table 7.2 (both per 1000 kg of Fe in product molten iron).

Because N₂ doesn't react anywhere in the blast furnace, the amount of N₂ rising from the bottom segment and from the top of the furnace is exactly the same as the amount entering the furnace in the blast air, 1032 kg with 1100°C blast.

- 7.3.** C-in-coke requirement can be decreased by increasing blast temperature, Fig. 7.4. By interpolation from Fig. 7.4, a 1% decrease in C-in-coke requirement requires a 50°C increase in blast temperature.

The decrease in C-in-coke consumption decreases operating cost. However, heating the blast to a higher temperature requires extra fuel which offsets this C-in-coke cost saving.

Coke consumption can be decreased by injecting hydrocarbons through the blast furnace tuyeres. This is discussed in Chapter 8, Tuyere Injection of Pulverized Carbon, onward. Most blast furnaces do this because coke is more expensive than most hydrocarbons, for example, pulverized coal and natural gas.

- 7.4.** The CO(g) can be used for heating duties around the blast furnace plant. The top gas's 2 bar (gauge) pressure can be used to generate electricity by directing the high-pressure gas through a turbine into the atmospheric pressure pipes. Both of these are widely used in the iron and steel industry.

CO(g) is very dangerous to human health, in fact lethal. Blast furnace employees must wear a CO monitor at all times and must always check in and check out of the blast furnace plant.

CHAPTER 8 EXERCISE ANSWERS

All masses in this chapter are kg per 1000 kg of Fe in product molten iron.

- 8.1.** The main reason that pulverized coal is injected into the blast furnace is because its C is cheaper than C-in-coke.
- 8.2.** However, all the coke can't be replaced by injected coal because the coke is needed to;
- a. provide between-particle gas flow passages for gas to ascend the blast furnace, particularly locations where ore and flux are melting;
 - b. support the furnace charge by remaining solid all through the furnace, even down into the furnace hearth;
 - c. allow space for newly melted ore and flux to descend to the top-holes; and
 - d. provide hot carbon for burning the tuyere raceway, giving a very high flame temperature.
- 8.3.** The replacement rate of C-in-coke with C-in-pulverized coal is ~0.93, Fig. 8.3. This is because the C-in-coke enters the blast furnace bottom segment at 930°C while the C-in-pulverized coal enters the bottom segment at ambient temperature ~25°C.
- Section 8.7 shows that pulverized C-in-coal injection at 930°C gives a 1/1 replacement ratio. It can be concluded that pulverized C-in-coal injection at 1000°C would give a replacement ratio of ~1.01

(using 1.488 MJ/kg for C's 1000°C enthalpy, Table J.3).

- 8.4.** 120 kg of pulverized C is represented in Table 8.1 by typing 120 in Cell C12. This gives the answer that 120 kg of pulverized C-in-coal injection saves 111 kg of C-in-coke, the expected 0.93 replacement ratio.
- 8.5.** The blast furnace of Table 8.1 needs to charge not less than 250 kg of C-in-coke for successful physical operation. How much C-in-pulverized coal can be injected before the C-in-coke requirement goes below this level.

By extrapolating Fig. 8.3, up to 153 kg of C-in-pulverized coal can be injected before the C-in-coke requirement falls below 250 kg.

By Goal Seeking Cell C19 of Table 8.1 to 250 kg by changing Cell C12, up to 152.9 kg of C-in-pulverized coal can be injected before the C-in-coke requirement falls below 250 kg.

CHAPTER 9 EXERCISE ANSWERS

All masses are in kg per 1000 kg of Fe in product molten iron.

- 9.1.** Advantages of oxygen injection are;
- it decreases nitrogen flow, hence total gas flow up the furnace, making it possible to increase product molten iron production rate without increasing upward gas flow rate;
 - with less nitrogen to heat, it permits injection of inexpensive but low enthalpy pulverized coal without excessive cooling of the bottom the furnace (where hot molten iron and slag must be produced); and
 - it can be used to control the temperature of the product molten iron and slag (more oxygen, higher

temperature; less oxygen, cooler temperature).

- 9.2.** Oxygen injection costs include;
- electrical power to separate oxygen from air,
 - a physical plant including large compressors,
 - small amounts of maintenance and labor,
- all of which must be paid for.
- 9.3.** Safety issues with pure oxygen;
- increases combustion rates dramatically presenting a fire danger; and
 - causes some substances to ignite, while in air, they don't.
- 9.4.** As Table 9.1 shows, the operation of the blast furnace of Fig. 9.1 with injection of 30 kg of pure oxygen,
- the C-in-coke requirement is 394 kg, and
 - the blast air requirement is 1165 kg (including 894 kg of N₂).

With 65 kg of pure oxygen injection, we predict that much less air will be required because the additional injected oxygen will replace O₂ in blast air, total blast air and N₂ in blast air.

C-in-coke requirement is hard to guess, but with less blast air entering through the tuyeres, less hot (high enthalpy) N₂ will enter the bottom segment. This must be replaced by more 930°C (high enthalpy) carbon descending into the bottom segment as is confirmed by Fig. 9.4.

With 65 kg of pure oxygen injection,

- the C-in-coke requirement is 396 kg, and
- the blast air requirement is 1029 kg (including 790 kg of N₂).

This is calculated by replacing 30 in Cell C12 of Table 9.1 with 65 (kg of pure oxygen per 1000 kg of Fe in product molten iron).

- 9.5.** The maximum amount of N₂ entering the tuyeres and departing the top of the furnace is specified to be 700 kg/1000 kg of Fe in product molten iron. We calculate the amount of injected pure oxygen that will give this amount by two methods:

Method 1: extrapolate Fig. 9.3 to 700 kg N₂/1000 kg of Fe in product molten iron.

Answer: ~96 kg pure oxygen.

Method 2: Goal Seek Cell C21 of Table 9.1 to 700 by changing Cell C12.

Answer: 95.3 kg pure oxygen.

- 9.6.** Our guess is that more C-in-coke and O₂-in-blast air will be required with cooler blast, that is, more C-in-coke will have to be burnt with O₂-in-blast air to maintain the bottom segment's enthalpy balance. From Appendix J,

$$\text{the enthalpy of O}_2 \text{ at } 1150^\circ\text{C} = 0.001137 * 1150 - 0.1257 \\ = 1.182 \text{ MJ/kg}$$

$$\text{the enthalpy of N}_2 \text{ at } 1150^\circ\text{C} = 0.001237 * 1150 - 0.1450 \\ = 1.278 \text{ MJ/kg}$$

which are entered into Cell F11 and G11 [with minus signs because they are inputs, Eq. (9.4)] of Table 9.1.

With 30 kg of pure oxygen injection and 1200°C blast, the C-in-coke requirement is 394 kg, with 1150°C blast, 398 kg.

With 30 kg of pure oxygen injection and 1200°C blast, the blast air requirement is 1165 kg, with 1150°C blast, 1193 kg.

CHAPTER 10 EXERCISE ANSWERS

All masses in this answer set are kg per 1000 kg of Fe in product molten iron.

- 10.1.** As shown in Section 10.5, 20 mass% N₂, 80 mass% O₂ injectant, changes Eq. (10.3) to:

$$0 = -\text{mass N}_2 \text{ in injected impure oxygen} * 1 \\ + \text{mass O}_2 \text{ in injected impure oxygen} * 20/80$$

or

$$0 = -\text{mass N}_2 \text{ in injected impure oxygen} * 1 \\ + \text{mass O}_2 \text{ in injected impure oxygen} * 0.25.$$

Insert this replacement equation into Table 10.1 by replacing 0.111 in Cell M13 to 0.25.

The requirements when injection 30 kg of 20 mass% N₂, 80 mass% O₂/t of Fe in product molten iron are;

- a. 394 kg of C-in-coke,
- b. 271 kg of O₂ in blast air,
- c. 893 kg of N₂ in blast air, and
- d. 1164 kg of air.

The C-in-coke, O₂ in blast air, N₂ in blast air, and air masses are virtually the same as with 10 mass% N₂–90 mass% O₂ injectant. However, the mass of N₂ entering the furnace in the injectant increases from 3.3 to 7.5 kg/1000 kg of Fe in product molten iron.

The total amount of N₂ that will enter the furnace in blast is 901 kg (893 kg of N₂ in blast air + 7.5 kg of N₂ in injected impure oxygen). The total amount of N₂ that will leave the furnace in top gas is also 901 kg.

CHAPTER 11 EXERCISE ANSWERS

All masses in this chapter are kg per 1000 kg of Fe in product molten iron.

- 11.1.** With 120 kg of CH₄(g) injection, the requirements for steadily producing 1500°C molten iron are;

- a. C-in-coke 278 kg,
- b. O₂-in-blast air 347 kg, and
- c. blast air 1493 kg

per 1000 kg of Fe in product molten iron. These answers were automatically obtained by switching 60 in Cell C14 of Table 11.1 to 120.

- 11.2.** Calculate the maximum amount of CH₄(g) that can be injected before the steady-state C-in-coke input falls below the 250 kg minimum.

Method 1: Extrapolate Fig. 11.2 data line to 250 kg of C-in-coke

Answer: ~151 kg. More CH₄(g) than this decreases the C-in-coke below 250 kg

Method 2: Use Excel's Goal Seek tool as follows:

Goal seek Cell C19 of Table 11.1 to 250 by changing Cell C14

Answer: 150.1 kg of CH₄(g)

- 11.3.** Data: 60 kg of 600°C CH₄(g) is being injected.

The enthalpy of 600°C CH₄(g) is -2.832 MJ/kg. Insert this value [without the minus sign, Eq. (11.7)] in matrix Cell O11 of Table 11.1. The new answer automatically appears.

The C-in-coke requirement with 60 kg of 600°C CH₄(g) injectant is 329 kg. This is 6 kg less than in Table 11.1 (25°C CH₄(g) injection).

CHAPTER 12 EXERCISE ANSWERS

All masses in this chapter are per 1000 kg of Fe in product molten iron.

- 12.1.** 25 g of H₂O(g) in blast per Nm³ of dry air in blast is equivalent to;

$$\begin{aligned} &= 25 / (1.27 * 1000) \text{ kg H}_2\text{O(g)} / \text{kg of dry} \\ &\quad \text{air in blast, Eq. (O.8)} \\ &= 0.0197 \text{ kg H}_2\text{O(g)} / \text{kg of dry air in blast} \end{aligned}$$

Typing 0.0197 in Cells F14 and G14 of Table 12.1 gives the problem's answer that 404 kg of C-in-coke and 304 kg of O₂-in-blast will steadily produce 1500°C

molten iron with 25 g of H₂O(g) per Nm³ of dry air in blast.

- 12.2.** The input O₂(g), N₂(g), and H₂O(g) are all at 1300°C. From Table J.3, their 1300°C enthalpies are:

O ₂ (g)	1.352 MJ/kg
N ₂ (g)	1.463 MJ/kg
H ₂ O(g)	-10.55 MJ/kg

Insert these enthalpies in Cells F13, G13, and O13 with their signs changed, Eq. (12.7). The requirements with 1300 °C blast are:

395 kg C-in-coke
289 kg of O₂-in-blast

Both of these are considerably lower than in Exercise 12.1.

- 12.3.** The blast furnace of Table 12.1 must be run with 395 kg of C-in-coke or less. The blast temperature is 1200°C. Fig. 12.4 applies. Extrapolating the C-in-coke data line down to 395 gives:

$$\begin{aligned} &\text{maximum H}_2\text{O(g) concentration in blast} \\ &= \sim 6 \text{ g/Nm}^3 \text{ of dry air in blast} \end{aligned}$$

(We magnified Fig. 12.4 to obtain this answer.)

We can obtain a more precise answer by using Excel's Goal Seek tool.

First we must alter Table 12.1 matrix slightly. We must type:

$$= F14 \text{ in Cell G14.}$$

We then

Goal seek Cell C19 to 395 changing Cell F14

The answer is in Cell F14, 0.0051 kg H₂O(g)/kg of dry air in blast or, by Eq. (O.8);

$$\begin{aligned} &\text{kg H}_2\text{O(g) / Nm}^3 \text{ of dry air in blast} \\ &= 0.0051 * (1.27 * 1000) = 6.48 \end{aligned}$$

which confirms the above extrapolation result.

- 12.4.** 1. $15 \text{ g H}_2\text{O(g)}/\text{Nm}^3$ of dry air in blast – $10 \text{ g H}_2\text{O(g)}/\text{Nm}^3$ of dry air in humid air = $5 \text{ g steam}/\text{Nm}^3$ of dry air.
 2. $5 \text{ g steam}/\text{Nm}^3$ of dry air in blast is equivalent to 0.00394 kg of steam per kg of dry air in blast, Eq. (O.8).
 3. From Table 12.1, the furnace is using 1297 kg of dry air per 1000 kg of Fe in product molten iron from which the steam requirement per 1000 kg of Fe in product molten iron is:

$$\begin{aligned} & 1297 \text{ kg of dry air in blast} * 0.00394 \text{ kg of} \\ & \quad \text{steam per kg of dry air in blast} \\ & = 5.1 \text{ kg of steam per } 1000 \text{ kg of} \\ & \quad \text{Fe in product molten iron} \\ & = 5.1 \text{ kg of steam per tonne of} \\ & \quad \text{Fe in product molten iron.} \end{aligned}$$

- 12.5.** 400 t of 95.5 mass\% Fe molten iron per hour is equivalent to 382 t of Fe per hour. The amount of steam required per hour:

$$\begin{aligned} & = 5.1 \text{ kg of steam per tonne of Fe in product} \\ & \quad \text{molten iron} * 382 \text{ t of Fe in molten iron per hour} \\ & = 1948 \text{ kg of steam per hour.} \end{aligned}$$

CHAPTER 13 EXERCISE ANSWERS

- 13.1.** To examine the effect of increasing hydrocarbon injection of Table 13.2 to $200 \text{ kg}/1000 \text{ kg}$ of Fe in product molten iron,

type 200 in Cell C14 of Table 13.2.

The answers, all per 1000 kg of Fe in product molten iron, are;

- a. C-in-coke = 206 kg ,
- b. $\text{O}_2\text{-in-blast} = 307 \text{ kg}$,
- c. $\text{N}_2\text{-in-blast} = 1013 \text{ kg}$, and
- d. blast air = $307 + 1013 = 1320 \text{ kg}$.

- 13.2.** Data: the enthalpies of $\text{O}_2(\text{g})$ and $\text{N}_2(\text{g})$ at 1300°C are 1.352 and 1.463 MJ/kg , respectively, Table 7.3.

This exercise is solved by inserting these enthalpy values in matrix Cells F11 and G11 of Exercise 13.1 (both preceded by a minus sign, Eq. 13.6).

The matrix output shows that the 198 kg of C-in-coke is required, a savings of 8 kg of C-in-coke as compared to Exercise 13.1 1200°C blast answer (both per 1000 kg of Fe in product molten iron).

- 13.3.** This exercise is solved by Goal Seeking Cell C19 to 250 by changing Cell C14, or by trial and error. The answer is:

153 kg of coal hydrocarbon injectant per 1000 kg of Fe in product molten iron.

CHAPTER 14 EXERCISE ANSWERS

- 14.1.** The tuyere raceway exit gas must be hot enough to ensure that the blast furnace products are completely molten and fluid.
- 14.2.** The tuyere raceway exit gas must not be so hot as to soften the charge high in the furnace, which is observed to cause irregular descent of the top-charged solids.
- 14.3.** Question: flame temperature with 1250°C blast air:

Table J.3: the 1250°C enthalpy of $\text{O}_2(\text{g}) = 1.296 \text{ MJ/kg}$
 the 1250°C enthalpy of $\text{N}_2(\text{g}) = 1.401 \text{ MJ/kg}$

Solution:

- 1. Place these enthalpy values in Cells F11 and G11 of Table 14.1, with minus signs in front of them, Eq. (7.14)
- 2. Also put them in Cell E52's Eq. (14.12), in place of 1.239 and 1.339 (which are the enthalpies of O_2 and N_2 at 1200°C)

Now follow all the calculations in this chapter.

- The total C-in-coke requirement is 388 kg/1000 kg of Fe in product molten iron.
- The air requirement is 1251 kg/1000 kg of Fe in product molten iron.
- The calculated flame temperature is 2418°C.

This calculation is made simpler in Chapter 15, Automating Matrix Calculations.

- 14.4.** We can make the conclusion that raising blast temperature automatically increases raceway adiabatic flame temperature. This is because the hotter blast brings more enthalpy into the raceway, which is reflected in a higher enthalpy (i.e., higher temperature) flame.

CHAPTER 15 EXERCISE ANSWERS

- Insertion of 1250 in matrix Cell D13 of Table 15.1 gives the flame temperature answer of 2417°C. This is virtually the same value as in Exercise 14.3.
- The blast temperature required to give a 2400°C flame may be determined from Fig. 15.1 to be ~1230°C. Excel's Goal Seek tool may be used to confirm this value. In this case, the procedure is:
Goal seek Cell F55 to 2400 by changing Cell D13.
It gives the answer that 1228°C blast gives a 2400°C tuyere raceway flame.
- Raceway conditions are not adiabatic because heat is being transferred between the raceway and its 1500°C surroundings. Heat is transferred OUT of the raceway where the gas reaches its top temperature ~2000°C and above but perhaps transferred IN where 1200°C blast is entering the raceway,

whatever conditions are certainly not adiabatic.

CHAPTER 16 EXERCISE ANSWERS

- Increasing C-in-coal injection from 100 to 175 kg lowers the raceway flame temperature from 2258°C to 2173°C. This is because cold injected C-in-coal replaces descending hot C-in-coke, Fig. 16.1.
229 kg of C-in-coke will be required with 175 kg of C-in-coal injection. This amount of C in coke is probably too small for rapid gas flow up the furnace. An amount of 250 kg of C-in-coke is thought to be the industrial practical minimum.
- Interpolation of Fig. 16.1 gives the answer that ~148 kg of C-in-pulverized coal is the maximum amount of C-in-pulverized coal that can be injected without the flame temperature dropping below 2200°C.
This value may also be calculated by Excel's Goal Seek tool. In the present case, the procedure is Goal seek Cell F55 to 2200 by changing Cell C12.
The exact answer is that injection of 150.4 kg of C-in-pulverized coal is the maximum that can be injected without the flame temperature falling below 2200°C.
Injection of C-in-pulverized coal without dropping raceway flame temperature by;
 - simultaneously increasing blast temperature; and
 - simultaneously injecting oxygen through the blast furnace's tuyeres.
- Coal ash (Al_2O_3 and SiO_2) will always decrease flame temperature because it has to be heated in the raceway from its

25°C injection temperature to its ~2000°C raceway exit temperature. The more ash there is, the more the flame temperature will drop.

CHAPTER 17 EXERCISE ANSWERS

- 17.1. place 65 in Cell C12 of Table 17.1. The answer is a 2567°C flame temperature.
- 17.2. graphically locate the 2450°C point on Fig. 17.2 (answer ~26 kg O₂). Also: Goal Seek Cell F55 of Table 17.1 to 2450 by changing Cell C12, answer 26.5 kg O₂.
- 17.3. With injection of 65 kg of 90 mass% O₂, 10 mass% N₂ in place of 65 kg of pure O₂,
 - a. less O₂ will be entering the raceway, so the flame temperature will fall., Fig. 17.2, and
 - b. more inert N₂ will be entering the raceway, so the flame temperature will fall even more.

CHAPTER 18 EXERCISE ANSWERS

- 18.1. Type 65 into Cell C14 of Table 18.2. The raceway flame temperature with 120 kg of CH₄(g) injection is 1697°C, Cell G55.
- 18.2. Method 1. Interpolate Fig. 18.2. The desired 2050°C raceway flame temperature is obtained with ~47 kg of CH₄(g) injection.
Method 2. Use Excel's Goal Seek tool.
The procedure in this case is Goal Seek Cell G55 to 2050, changing Cell C14. The answer is 47.1 kg of CH₄(g).
- 18.3. The matrix Table 18.2 is set up to read the blast temperature (1300°C) in Cell E16 and to automatically calculate the 1300°C O₂-in-blast and N₂-in-blast enthalpies in Cells F14 and G14 (with a

negative sign before them, Eq. 11.7). These enthalpies are also automatically included in Eq. (18.7) of Table 18.2 as shown in Row 52.

Finally, the amount of injected CH₄(g) that will give a 2050°C raceway flame temperature with 1300°C blast is calculated as described in Exercise 18.2. It is 56.5 kg of CH₄(g) per 1000 kg of Fe in product molten iron. It is more than with 1200°C blast.

Raising blast temperature increases raceway flame temperature, Fig. 15.1. This is offset by increasing CH₄(g) injection (Fig. 18.2) to obtain the desired 2050°C raceway flame.

CHAPTER 19 EXERCISE ANSWERS

- 19.1. From Table 19.2, the raceway flame temperature with 15 g of H₂O(g) per Nm³ of dry air blast is 2290°C.
Eq. (O.8) indicates that that 25 g H₂O(g)/Nm³ of dry air blast is equivalent to 0.025 kg H₂O/Nm³ of dry air in blast/1.27 = 0.01969 kg H₂O(g)/kg of dry air in blast.
The 0.01969 value is typed into Cells F14 and G14 of Table 19.2. This causes the Table 19.2 matrix to automatically calculate a raceway temperature of 2234°C (with 25 g H₂O(g)/Nm³ of dry air blast). This decrease in flame temperature is consistent with Fig. 19.2.
- 19.2. The moist blast entering the blast furnace contains 25 g of H₂O(g) per Nm³ of dry air in blast.
 1. It is made up of 9 g H₂O(g) in humid air and 16 g of steam, both per Nm³ of dry air in blast.
From Eq. (O.8), 16 g of steam per Nm³ of dry air in blast is equivalent to

2. $0.016 \text{ kg steam}/\text{Nm}^3$ of dry air in blast/ $1.27 = 0.0126 \text{ kg}$ of steam per kg of dry air in blast.
3. With 25 g of $\text{H}_2\text{O(g)}$ per Nm^3 of dry air in blast, the steady-state input mass of dry air is $1307 \text{ kg}/1000 \text{ kg}$ of Fe in product molten iron. The amount of injected steam is therefore $1307 * 0.0126 \text{ kg}$ of steam per kg of dry air = 16.47 kg of steam per 1000 kg of Fe in product molten iron.

CHAPTER 20 EXERCISE ANSWERS

- 20.1.** Type 1250 in Cell D13 of matrix Table 20.1. This gives top gas masses in Table 20.2 as follows:

326 kg CO
736 kg CO_2
960 kg N_2

which is equivalent to;

16.1 mass% CO
36.4 mass% CO_2
47.5 mass% N_2

for a total of 100 mass%.

- 20.2.** Change column AD of Table 20.2 to Fe_3O_4 ore composition, Appendix A. This gives top gas masses as follows:

419 kg CO
605 kg CO_2
983 kg N_2

which is equivalent to;

20.9 mass% CO
30.1 mass% CO_2
49.0 mass% N_2

for a total of 100 mass%.

CHAPTER 21 EXERCISE ANSWERS

- 21.1.** Hematite ore, 1250°C blast.

You can calculate the top-segment input enthalpy with your Exercise 20.1 top-segment masses using Eq. (21.1a). It is $-11073 \text{ MJ}/1000 \text{ kg}$ of Fe in product molten iron.

The equivalent top segment output enthalpy may be calculated by Eq. (21.4). It is

$$-11077 - 80 = -11153 \text{ MJ}/1000 \text{ kg} \text{ of Fe in product molten iron.}$$

They can also be calculated automatically as shown in Table 21.2.

- 21.2. Magnetite ore, 1200°C blast.**

Remember that the 25°C enthalpy of Fe_3O_4 is -4.841 MJ/kg , Table J.1.

The top-segment input enthalpy is calculated as described above to be $-10396 \text{ MJ}/1000 \text{ g}$ of Fe in product molten iron. Likewise, the top-segment output enthalpy is $-10395 - 80 = 10476 \text{ MJ}/1000 \text{ kg}$ of Fe in product molten iron.

CHAPTER 22 EXERCISE ANSWERS

- 22.1.** First calculate top gas enthalpy from top-segment output enthalpy of Exercise 21.1. Use Eq. (22.1). With hematite ore and 1250°C blast, the top gas enthalpy is $-7576 \text{ MJ}/1000 \text{ kg}$ of Fe in product molten iron.

Now calculate the top gas temperature by Eq. (22.4). With hematite ore and 1200°C blast, the top gas temperature is 170°C . This value can also be interpolated from Fig. 22.2.

- 22.2.** Follow methods of Exercise 22.1 with magnetite ore and 1200°C blast. The top gas enthalpy is $-6905 \text{ MJ}/1000 \text{ kg}$ of Fe in product molten iron. And by Eq. (22.4), the top gas temperature is 103°C .

These can also be calculated automatically as described in Table 22.2.

CHAPTER 23 EXERCISE ANSWERS

All masses in these exercises are kg per 1000 kg of Fe in product molten iron.

- 23.1.** Requirement: exactly 200°C top gas temperature:

Adjustable variable: mass injected C-in-pulverized coal

Calculation method 1: from Fig. 23.2, ~21 kg C-in-coal will give a 200°C top gas temperature.

Calculation method 2: *Goal Seek* Cell AH 40 of Table 23.2 to 200 by *changing* Cell C12 of Table 23.1.

21.4 kg of C-in-pulverized coal will give a 200°C top gas temperature.

- 23.2.** Requirement: 200°C top gas temperature
Conditions: 1300°C blast:

Calculate the C-in-coal injectant quantity that will give a 200°C top gas temperature under these conditions.

From Table J.3: 1300°C O₂(g) enthalpy = 1.352 MJ/kg
1300°C N₂(g) enthalpy = 1.463 MJ/kg

Method: type -1.352 in Cell F11 of Table 23.1 and -1.463 in Cell G11 of Table 23.1.

Now: *Goal Seek* Cell AH40 of Table 23.2 to 200 by *changing* Cell C12 of Table 23.1.

Answer: Injection of 47.1 kg of C-in-pulverized coal gives a 200°C top gas temperature.

Conclusion: raising blast temperature increases the allowable amount of injected C-in-pulverized coal while maintaining a specified top gas temperature.

- 23.3.** The top charge almost always contains moisture, often contains carbonate fluxes,

and sometimes contains recycle steel scrap or partially reduced iron ore pellets (DRI).

CHAPTER 24 EXERCISE ANSWERS

All masses are per 1000 kg of Fe in product molten iron.

- 24.1.** Data: 60 kg of injected pure oxygen = 60 kg of injected O₂.
Method: replace 30 in Cell C12 of Table 24.1 with 60.

Answer: 104°C in Cell AH40 Table 24.2.

- 24.2.** Data: 30 kg and 60 kg of injected pure oxygen
Method: top gas mass = Cell AC25 + Cell AC26 + Cell AC27 of Table 24.2

Answers: With 30 kg of pure oxygen injection: top gas mass = 1973 kg

With 60 kg of pure oxygen injection:

top gas mass = 1887 kg

This additional 30 kg pure oxygen increase lowers top gas mass by 86 kg.

- 24.3.** Specification: Top gas temperature must be greater than 160°C.

Simultaneously, tuyere raceway flame temperature must be lower than 2400°C.

Answers: from Fig. 24.2, oxygen injection between 0 and ~18 kg gives a top gas temperature >160°C.

From Fig. 17.2, oxygen injection between 0 and ~8 kg gives a flame temperature <2400°C.

Both specifications are met between 0 and ~8 kg of pure oxygen injection.

CHAPTER 25 EXERCISE ANSWERS

All masses in the exercise answer section are kg per 1000 kg of Fe in product molten iron.

- 25.1.** Specifications: 120 kg of 25°C CH₄(g) injection, 1200°C blast

Insert 120 in Cell C14 of Table 25.1.

Matrix output data: under these conditions, top gas masses of Table 25.3 are;

CO	370 kg (Cell AC25)
CO ₂	595 kg (Cell AC26)
N ₂	1146 kg (Cell AC27)
H ₂	13 kg (Cell AC 30)
H ₂ O	150 kg (AC 31)

which, from Appendix P, are equivalent to;

16.3 mass% CO
26.2 mass% CO ₂
50.4 mass% N ₂
0.6 mass% H ₂
6.6 mass% H ₂ O

and

16.0 vol% CO
16.4 vol% CO ₂
49.4 vol% N ₂
8.2 vol% H ₂
10.1 vol% H ₂ O

- 25.2.** Specification: mass H₂O(g) in top gas must be below 55 kg.

Fig. 25.2 shows that below ~40 kg of CH₄ injection satisfies this specification.

Goal Seeking Cell C31 of Table 25.3 to 55 kg by changing Cell C14 of Table 25.1 gives the result that CH₄ injection below 40.9 kg keeps the top gas H₂O mass below 55 kg.

CHAPTER 26 EXERCISE ANSWERS

All values are per 1000 kg of Fe in product molten iron.

- 26.1.** Data:

120 kg CH₄ injection (from Exercise 25.1)

Method:

Change Cell C14 value of Table 25.1 to 120 kg (CH₄ injection)

With this new value, Cells AG33, AG34, and AG37 of Table 26.1 give:

Input enthalpy = -11539 MJ
Output enthalpy = -11619 MJ
Top gas enthalpy = -7893 MJ

- 26.2.** Data:

40.9 kg CH₄ injection (from Exercise 25.2)

Method:

Change Cell C14 value of Table 25.1 to 40.9 kg (CH₄ injection)

With this new value, Cells AG33, AG34, and AG37 of Table 26.1 give:

Input enthalpy = -11253 MJ
Output enthalpy = -11333 MJ
Top gas enthalpy = -7709 MJ

CHAPTER 27 EXERCISE ANSWERS

All values are per 1000 kg of Fe in product molten iron.

- 27.1.** Data:

120 kg of injected CH₄ (from Exercise 25.1)

Objective:

Calculate top gas temperature

Method:

Insert 120 (kg of injected CH₄) in Cell C14 of Table 25.1

Answer:

Cell AK40 of Table 27.1 automatically calculates the new top gas temperature: 374°C

- 27.2.** Data:

40.9 kg of injected CH₄ (from Exercise 25.2)

Objective:

Calculate top gas temperature

Method:

Insert 40.9 (kg of injected CH₄) in Cell C14 of Table 25.1

Answer:

Cell AK40 of Table 27.1 automatically calculates the new top gas temperature: 254°C

27.3. Data:

Top gas temperature must be 200°C or below.

Answer:

Fig. 27.2 shows that CH₄ injection must be below ~10 kg for the top gas temperature to be below 200°C.

This may also be determined by Goal Seeking Cell AK40 of Table 27.1 to 200 by changing Cell C14 of Table 25.1. This procedure confirms that a top gas temperature below 200°C requires less than 10.0 kg of CH₄ injection.

27.4. Moisture [H₂O(*l*)] in the top charge will be evaporated by the ascending warm gas. This is an endothermic reaction, which will take heat from the ascending gas, decreasing its enthalpy and temperature.

Answer:

From Fig. 28.2, ~19 g H₂O(g)/Nm³ of dry air in blast.

A more precise value, 19.3, has also been obtained by Goal Seek using the methods described in Exercise 12.3 of Chapter 12, Bottom Segment With Moisture in Blast Air.

28.3. The air entering Exercise 28.2's stoves contains 10 g H₂O(g)/Nm³ of dry air. How much steam must be added to this air to obtain Exercise 28.2's 19.3 g H₂O(g) in blast per Nm³ of dry air in blast?
Answer: 9.3 g H₂O(g)/Nm³ of dry air which is equivalent to $9.3/1270 = 0.00732$ kg of H₂O(g) per kg of dry air in blast.

You have done further calculations of this type in Exercises 12.4 and 12.5 of Chapter 12, Bottom Segment With Moisture in Blast Air.

CHAPTER 28 EXERCISE ANSWERS**28.1. Data:**

Blast of Fig. 28.1 contains 25 g H₂O(g)/Nm³ of dry air in blast.

From Exercise 12.1, this is equivalent to 0.0197 kg H₂O(g)/kg of dry air in blast.

Calculation: place 0.0197 in Cells F14 and G14 of Table 28.1.

The result is now in Cell AK40 = 205°C of Table 28.2.

28.2. Specification: Top gas temperature must be 200°C or less.

Question:

How much H₂O(g) can the blast contain before the furnace's 200°C top gas temperature upper limit is exceeded?

CHAPTER 29 EXERCISE ANSWERS**29.1. Data: 140 kg of injected natural gas.**

Objective: Calculate C-in-coke, O₂-in-blast, N₂-in-blast, and blast requirements for steady production of 1500°C product molten iron with 140 kg of injected natural gas.

Method: Insert 140 in Cell C14 of Table 29.2.

Requirements: 264 kg C-in-coke, 353 kg of O₂-in-blast, 1166 kg of N₂-in-blast (1519 kg of air).

29.2. Specification: for furnace charge support and steady gas flow, the input of C-in-coke must be 250 kg or greater.
Objective: Calculate the maximum amount of natural gas that can be injected while meeting this minimum 250 kg of C-in-coke requirement.

Method 1: Extend Fig. 29.2 to 250 kg of C-in-coke. Answer: ~155 kg of natural gas. Injection of more natural gas will lower the steady-state C-in-coke input to below 250 kg.

Method 2: Goal Seek Cell C19 of Table 29.2 to 250 by changing Cell C14. Answer: more than 155.1 kg of natural gas will lower the C-in-coke input to below 250 kg.

CHAPTER 30 EXERCISE ANSWERS

- 30.1.** Data: 45 kg of Table 29.2 natural gas injection

Objective: Calculate raceway adiabatic flame temperature with this amount of natural gas injection.

Methods:

- From Fig. 30.2, the flame temperature with 45 kg of natural gas injection is ~2075°C.
- Insert 45 into Cell C14 of Table 30.1. The answer is now in Cell G55: 2073°C

- 30.2.** Specification: 2200°C flame temperature

Objective: Calculate the amount of injected natural gas that will give the specified flame temperature.

Methods:

- Interpolate from Fig. 30.2, the answer is ~25 kg of natural gas injection will give a 2200°C flame.
- Goal Seek Cell G55 of Table 30.1 to 2200 by changing Cell C14 gives the answer: 24.6 kg natural gas injection will give a 2200°C flame.

- 30.3.** You can simultaneously inject oxygen, which increases flame temperature, Fig. 17.2.

- 30.4.** I see that the natural gas's enthalpy is less negative than CH₄'s enthalpy, which

raises raceway input enthalpy, raceway exit gas enthalpy, and flame temperature.

CHAPTER 31 EXERCISE ANSWERS

- 31.1.** Data: 45 kg of natural gas injection.

Objective: Calculate top gas temperature with this amount of natural gas injection.

Methods:

- From interpolation of Fig. 31.2, the top gas temperature is ~260°C.
- By inserting 45 in Cell C14 of Table 31.1 and Cell AK40 of Table 31.2 gives the more exact top gas temperature, 258°C.

- 31.2.** Specification: Top gas temperature must be at or below 200°C.

Objective: Calculate how much natural gas can be injected while keeping the top gas temperature at or below 200°C.

Methods:

- Interpolate from Fig. 31.2 that the maximum amount of natural gas injection that will meet the specification is ~10 kg.
- Goal Seek Cell AK40 of Table 31.2 to 200 by changing Cell C14 of Table 31.1, which gives 10.3 kg of natural gas injection. This amount of injection and less meet this problem's at-or-below 200°C top gas temperature specification.

CHAPTER 32 EXERCISE ANSWERS

- 32.1.** Data: Slag composition: 12 mass% Al₂O₃, 40 mass% CaO, 10 mass% MgO, 38 mass % SiO₂.

Objective: Calculate the amounts of C-in-coke and O₂-in-blast that will steadily produce 1500°C molten iron and 1500°C molten slag of this composition.

Description of calculation: Eq. (32.5), (32.6b), and (32.7) have to be altered to represent the above slag composition. Eq. (32.5) becomes

$$\begin{aligned} 0 &= - \left[\frac{\text{mass Al}_2\text{O}_3 \text{ on}}{\text{product molten slag}} \right] * 1 \\ &\quad + \left[\frac{\text{mass SiO}_2 \text{ in}}{\text{product molten slag}} \right] * \frac{\left[\frac{\text{mass Al}_2\text{O}_3 \text{ on}}{\text{product molten slag}} \right]}{\left[\frac{\text{mass SiO}_2 \text{ in}}{\text{product molten slag}} \right]} \\ &= - \left[\frac{\text{mass Al}_2\text{O}_3 \text{ on}}{\text{product molten slag}} \right] * 1 \\ &\quad + \left[\frac{\text{mass SiO}_2 \text{ in}}{\text{product molten slag}} \right] * \frac{12}{38} \\ &= - \left[\frac{\text{mass Al}_2\text{O}_3 \text{ on}}{\text{product molten slag}} \right] * 1 \\ &\quad + \left[\frac{\text{mass SiO}_2 \text{ in}}{\text{product molten slag}} \right] * 0.316 \end{aligned}$$

Likewise, Eq. (32.6b) becomes

$$\begin{aligned} 0 &= - \left[\frac{\text{mass CaO in}}{\text{product molten slag}} \right] * 1 \left[\frac{\text{mass SiO}_2 \text{ in}}{\text{product molten slag}} \right] * \frac{40}{38} \\ &= - \left[\frac{\text{mass CaO in}}{\text{product molten slag}} \right] * 1 \left[\frac{\text{mass SiO}_2 \text{ in}}{\text{product molten slag}} \right] * 1.053 \\ \text{and Eq. (32.7) becomes} \\ 0 &= - \left[\frac{\text{mass MgO in}}{\text{product molten slag}} \right] * 1 \left[\frac{\text{mass SiO}_2 \text{ in}}{\text{product molten slag}} \right] * \frac{10}{38} \\ &= - \left[\frac{\text{mass MgO in}}{\text{product molten slag}} \right] * 1 \left[\frac{\text{mass SiO}_2 \text{ in}}{\text{product molten slag}} \right] * 0.263 \end{aligned}$$

as can be represented in Table 32.1 by replacing Column N's 0.256 with 0.316, 1.05 with 1.053, and 0.256 with 0.263. With these new values, the C-in-coke requirement becomes 409 kg and the O₂-in-blast air becomes 327 kg as compared to 408 kg of C-in-coke and 326 kg of O₂-in-blast air of Table 32.1. Pretty small differences.

32.2. Data: Ore composition is 15 mass% SiO₂ and 85 mass% Fe₂O₃.

Slag composition is that described in Table 32.1.

Calculations:

- Calculate ore composition in mass% SiO₂, mass% Fe, and mass% O.
- Rewrite Eq. (32.2) to reflect this composition.
- Insert this new equation in Row 4 of Table 32.1.

Answers:

- Ore composition 15 mass% SiO₂, 59.4 mass% Fe, 25.6 mass% O.
- Eq. (32.2) becomes

$$\begin{aligned} 0 &= - \left[\frac{\text{mass SiO}_2 \text{ in}}{\text{descending ore}} \right] * 1 \\ &\quad + \left[\frac{\text{mass Fe in product}}{\text{molten iron}} \right] * 0.253 \end{aligned}$$

where 0.253 = 15% / 59.4%.

- This equation is placed in Row 4 of Table 32.1 by inserting 0.253 in Cell H4.
 - C-in-coke requirement = 447 kg, O₂-in-air requirement = 393 kg as compared to 408 kg of C-in-coke and 326 kg of O₂-in-blast air requirements of Table 32.1.
 - Al₂O₃ flux requirement = 65 kg, CaO flux requirement = 266 kg, MgO flux requirement = 65 kg as compared to 19 kg of Al₂O₃, 79 kg of CaO, and 19 kg of MgO of Table 32.1.
 - Total slag production = 648 kg as compared to 192 kg of Table 32.1.
 - Mass gas ascending out of bottom segment = 2392 kg as compared to 2066 kg of Table 32.1.
- Every value is larger due to the much larger concentration of SiO₂ in the cheap ore.

CHAPTER 33 EXERCISE ANSWER

33.1. Data: 3 mass% Al₂O₃, 97 mass% Fe₂O₃

Calculation: Step 1

Determine Eq. (33.2) with this ore.

We start by expanding the ore composition to;

3 mass % Al₂O₃

$$\text{mass\% Fe} = \frac{69.9 \text{ mass\% Fe in Fe}_2\text{O}_3}{100\%} * 97 \text{ mass\%}$$

Fe₂O₃ in ore = 67.8

$$\text{mass\% O} = \frac{30.1 \text{ mass\% O in Fe}_2\text{O}_3}{100\%} * 97 \text{ mass\%}$$

Fe₂O₃ in ore

= 29.2(excluding O in Al₂O₃,

which doesn't decompose)

which add to 100%.

An equation that describes this composition is;

$$\begin{bmatrix} \text{mass Al}_2\text{O}_3 \text{ in} \\ \text{top-charged ore} \end{bmatrix} = \frac{\begin{bmatrix} 3 \text{ mass\% Al}_2\text{O}_3 \text{ in} \\ \text{top-charged ore} \end{bmatrix}}{\begin{bmatrix} \text{mass Fe in} \\ \text{top-charged ore} \end{bmatrix}} = 0.0442$$

which may be restated as;

$$\begin{bmatrix} \text{mass Al}_2\text{O}_3 \text{ in} \\ \text{top-charged ore} \end{bmatrix} = 0.0442 * \begin{bmatrix} \text{mass Fe in} \\ \text{top-charged ore} \end{bmatrix}$$

This is equivalent to Eq. (32.1).

In terms of Eq. (32.2), it is:

$$0 = - \begin{bmatrix} \text{mass Al}_2\text{O}_3 \text{ in} \\ \text{descending ore} \end{bmatrix} * 1 + \begin{bmatrix} \text{mass Fe in product} \\ \text{molten iron} \end{bmatrix} * 0.0442$$

Calculation: Step 2

Calculate the C-in-coke, O₂-in-blast air, and flux requirements by inserting the above equation into Row 4 of matrix Table 33.1 (by typing 0.0442 in Cell H4). This automatically causes the matrix to give the desired answers, which are:

429 kg of C-in-coke
363 kg of O₂ in blast
181 kg of CaO flux
44 kg of MgO flux
173 kg of SiO₂ flux.

The SiO₂ flux result may be checked against Fig. 33.2. The CaO and MgO flux requirements may then be checked by means of Eqs. (32.6b) and (32.7).

CHAPTER 34 EXERCISE ANSWERS

All masses in these answers are per 1000 kg of Fe in product molten iron.

34.1. Data: Coke composition = 90 mass% C, 5 mass% Al₂O₃, 5 mass% SiO₂.

Calculation method:

These new values change Eqs.(34.2) and (34.4) to;

$$0 = - \begin{bmatrix} \text{mass Al}_2\text{O}_3 \text{ in} \\ \text{descending coke} \end{bmatrix} * 1 + \begin{bmatrix} \text{mass C in} \\ \text{descending coke} \end{bmatrix} * 0.0556$$

and

$$0 = - \begin{bmatrix} \text{mass SiO}_2 \text{ in} \\ \text{descending coke} \end{bmatrix} * 1 + \begin{bmatrix} \text{mass C in} \\ \text{descending coke} \end{bmatrix} * 0.0556$$

For this exercise,

- a. the top equation is placed in Row 14 of Table 34.1 by typing 0.0555 in Cell E14 and
- b. the bottom equation is placed in Row 5 of Table 34.1 by typing 0.0555 in Cell E5.

These replacements automatically cause the Table 34.1 matrix to calculate this exercise's results.

The furnaces's requirements are;

mass C-in-coke	413 kg
mass coke	459 kg
mass O ₂ -in-blast	335 kg
mass blast	1440 kg
mass Al ₂ O ₃ flux	2 kg
mass SiO ₂ flux	0 kg
mass CaO flux	103 kg
mass MgO flux	25 kg

and the total mass of molten product slag is 252 kg.

- 34.2.** Data: Required slag composition is 12 mass% Al₂O₃, 40 mass% CaO, 10 mass % MgO, and 38 mass% SiO₂.

Calculation:

This slag composition is the same as in Exercise 32.1. It may be represented in matrix Table 34.1 as described in that exercise. Note that the slag composition equation constants are in Column O.

The flux requirements with this new slag are;

mass Al ₂ O ₃ flux	20 kg
mass CaO flux	113 kg
mass MgO flux	28 kg
mass SiO ₂ flux	0 kg

and the total mass of product molten slag is 283 kg.

CHAPTER 35 EXERCISE ANSWERS

- 35.1. 1.** Increase mass% Si in blast furnace product iron by;

1. increasing molten iron temperature (by raising raceway flame temperature); and
2. increasing blast pressure.

Also, adjust the blast furnace slag composition so as to increase the thermodynamic activity of dissolved SiO₂.

- 2.** Data: 4.5 mass% C, 95.0 mass% Fe, 0.5 mass% Si (100 mass% total). Preliminary calculations: C/Fe mass ratio = 4.5%/95% = 0.0474, Si/Fe mass ratio = 0.5%/95% = 0.00526.

Method: Put 0.0474 in Cell H13 of Table 35.1; put 0.00526 in Cell H22 of Table 35.1.

Answers:

With 0.5 mass% Si,
C-in-coke requirement 422 kg
O₂-in-blast requirement 343 kg

Both are slightly larger than with 0.4 mass% Si (Table A35.1):

C-in-coke requirement 421 kg
O₂-in-blast requirement 342 kg

This is because silicon reduction is endothermic, which must be offset by burning more C-in-coke with O₂-in-blast.

- c.** All flux requirements are slightly lower with 0.5 mass% Si:

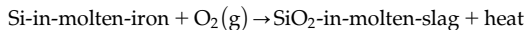
Al₂O₃ flux requirement = 10.7 kg
CaO flux requirement = 101.7 kg
MgO flux requirement = 24.8 kg

With 0.4 mass% Si:

Al₂O₃ flux requirement = 11.3 kg
CaO flux requirement = 104.0 kg
MgO flux requirement = 25.3 kg

This is because more SiO₂ is reduced with 0.5 mass% Si in molten iron, requiring less fluxing of SiO₂.

- 35.2.** Si-in-molten iron serves as a fuel in the steelmaking furnace, that is, by the reaction:



So the steelmakers can melt more solid scrap steel per 1000 kg of Fe in molten blast furnace iron. They might want to do this if scrap price falls or if blast furnace iron price rises.

CHAPTER 36 EXERCISE ANSWERS

- 36.1. a.** The steelmakers want to increase the Mn concentration in their product steel because Mn enhances a steel's; hardenability and hardness,

toughness, and machinability.

- b.** The principal way to increase % Mn in a blast furnace's product molten iron is to add more Mn-rich feed to the top of the blast furnace, mainly pyrolusite, (MnO_2) ore.

- 36.2.** Objective: Calculate a blast furnace's coke and air blast requirements when the furnace is producing 1 mass% Mn molten iron. Also calculate the amount of MnO that must enter the bottom segment of the furnace.

Data: The proposed iron composition is 4.5 mass% C, 94.1 mass% Fe, 0.4 mass% Si, and 1 mass% Mn.

As in Chapter 32, Bottom Segment Slag Calculations—Ore, Fluxes, and Slag, the slag composition is 10 mass% Al_2O_3 , 41 mass% CaO , 10 mass% MgO , and 39 mass% $\text{SiO}_2 + \text{MnO}$. Both are at 1500°C.

Preliminary calculations: C/Fe mass ratio = 0.0478; Si/Fe mass ratio = 0.00425; Mn/Fe mass ratio = 0.01063.

These numbers replace those in Column H of Table 36.1. They have been calculated by means of Appendix T. Answers: Furnace requirements to steadily produce the above described 1500°C molten iron and molten slag are:

$$\begin{aligned} \text{mass C-in-coke} &= 426 \text{ kg, mass coke (90 mass% C)} \\ &= 473 \text{ kg} \end{aligned}$$

$$\begin{aligned} \text{mass O}_2\text{-in-blast} &= 348 \text{ kg, mass air} \\ &= 1495(1147 \text{ kg N}_2 + 348 \text{ O}_2) \end{aligned}$$

$$\text{mass bottom segment input MnO} = 15 \text{ kg}$$

- 36.3.** Calculated mass Mn in product molten iron = 10.6 kg.

Calculate mass MnO in product molten slag = 1.53 kg.

The mass of Mn in the molten slag = 1.52 kg * (77.4 mass% Mn in MnO / 100%) = 1.18 kg (where the mass% Mn in MnO is from Appendix A):

The (mass Mn in product slag/mass Mn in product iron) ratio is (1.18 kg/10.6 kg) = 0.111

By comparison with the calculated values of Table 36.1, it seems to be independent of % Mn in product molten iron.

- 36.4.** Slag composition varies slightly because its MnO content increases slightly with increasing mass% Mn in product molten iron. This is because the MnO reduction efficiency is independent of % Mn in product molten iron.
- 36.5.** A steelmaker may compensate for a lower-than-expected % Mn in molten iron by adding ferromanganese or manganese to the molten steel toward the end of the steelmaking process. But this can be quite expensive.

CHAPTER 37 EXERCISE ANSWERS

All masses in this document are kg per 1000 kg of Fe in product molten iron.

- 37.1.** Data: Coal containing:

87 mass% hydrocarbon
3.6 mass% Al_2O_3
1.0 mass% CaO
8.4 mass% SiO_2

Injection amount, 60 kg/1000 kg of Fe in product molten iron.

Step 1: Calculate the coal's composition per kg of coal:

0.036 kg Al_2O_3
0.010 kg CaO
0.084 kg SiO_2

0.87 kg hydrocarbon, which, from Table 13.1, contains:

$$\begin{aligned} \text{mass C per kg of coal} &= 0.87 * \frac{88 \text{ mass% C in hydrocarbon}}{100\%} \\ &= 0.766 \text{ kg} \end{aligned}$$

$$\text{mass H per kg of coal} = 0.87 * \frac{6 \text{ mass\% H in hydrocarbon}}{100\%}$$

$$= 0.052 \text{ kg}$$

$$\text{mass N per kg of coal} = 0.87 * \frac{1 \text{ mass\% N in hydrocarbon}}{100\%}$$

$$= 0.009 \text{ kg}$$

$$\text{mass O per kg of coal} = 0.87 * \frac{5 \text{ mass\% O in hydrocarbon}}{100\%}$$

$$= 0.044 \text{ kg}$$

Step 2: Calculate the coal's 25°C enthalpy, MJ per kg of coal

Data:

$$H_{\text{coal hydrocarbon}}^{25^\circ\text{C}} = 0 \text{ (Section 13.5)}$$

$$\frac{H_{\text{Al}_2\text{O}_3(\text{s})}^{25^\circ\text{C}}}{\text{MW}_{\text{Al}_2\text{O}_3}} = -16.43 \text{ MJ/kg (Table J.1)}$$

$$\frac{H_{\text{CaO(s)}}^{25^\circ\text{C}}}{\text{MW}_{\text{CaO}}} = -11.32 \text{ MJ/kg (Table J.1)}$$

$$\frac{H_{\text{SiO}_2(\text{s})}^{25^\circ\text{C}}}{\text{MW}_{\text{SiO}_2}} = -15.16 \text{ MJ/kg (Table J.1)}$$

Enthalpy equation:

$$\begin{aligned} \left[\begin{array}{l} 25^\circ\text{C coal enthalpy} \\ \text{MJ per kg of coal} \end{array} \right] &= 0.87 \text{ kg hydrocarbon} * 0 \\ &\quad + 0.036 \text{ kg Al}_2\text{O}_3 * -16.43 \\ &\quad + 0.010 \text{ kg CaO} * -11.32 \\ &\quad + 0.084 \text{ kg SiO}_2 * -15.16 \\ &= -1.98 \text{ MJ} \end{aligned}$$

Step 3 Apply to matrix Table 37.3:

The changes are all in Column AC. All the masses are entered in their appropriate mass balance rows. All are preceded by a negative sign because of the nature of their equations, Sections 37.7–37.9. Note the new value in the CaO mass balance row.

The new enthalpy value is entered in Cell AC21, with the minus sign removed as shown in Eq. (37.11).

Answers:

Coke (90 mass% C) requirement	417 kg
Blast air requirement	1498 kg
Al ₂ O ₃ flux requirement	11 kg
CaO flux requirement	105 kg
MgO flux requirement	26 kg
MnO requirement	8 kg

much like those with coal of Table 37.1.

CHAPTER 38 EXERCISE ANSWERS

Please remember that all exercises in this set include tuyere injection of 60 kg of pulverized coal, 30 kg of pure oxygen, and 60 kg of natural gas as described in Table 38.1. The blast is 1200°C. It contains 15 g of H₂O(g) per Nm³ of dry blast air—as described in Row 30 of Table 38.1.

- 38.1. Data: 20 kg of oil injection.

Oil composition 0.85 kg of C, 0.13 kg H, 0.01 kg N, and 0.01 kg O/kg of oil

Oil enthalpy -1.7 – MJ/kg of oil

Method: Use *mass additional tuyere injectant column* and *Additional injectant quantity equation* row of Table 38.1. Insert the above values, remembering that they must be multiplied by -1 as described in Sections 37.7–37.10.

The 20 kg of oil injectant:

- a. decreases coke (90 mass% C) requirement from 362 (Table 38.2) to 341 kg; and

- b. increases the dry air requirement from 1492 (Table 38.2) to 1506 kg.

- 38.2. Data: 20 kg of polyethylene([C₂H₄(s)]) injection.

Polyethylene per mol composition:

2 kg mol C = (2*12) kg = 24 kg (where 12 is the atomic mass of C)

- 4 kg mol H = (4*1) kg = 4 kg (where 1 is the atomic mass of H)
 mass% C = $(24/(24+4))*100\% = 85.7$ mass %
 mass% H = $(4/(24+4))*100\% = 14.3$ mass % (checked to 100%)
 Polyethylene enthalpy = -2.0 MJ/kg
 Method: Repeat calculations of Exercise 38.1 with polyethylene in place of oil.
 The 20 kg of polyethylene injectant;
 a. decreases the coke (90 mass% C) requirement from 362 (Table 38.2) to 340 kg; and
 b. increases the dry air requirement from 1492 (Table 38.2) to 1509 kg.

38.3. Data: 20 kg of H₂(g) injection.

Hydrogen composition = 100 mass% H
 25°C enthalpy = 0, element in its most common state at 25°C.

Method: Repeat calculations of Exercise 38.1 with H₂(g) in place of oil.
 The 20 kg of H₂(g) injectant;
 a. decreases the coke (90 mass% C) requirement from 362 (Table 38.2) to 317 kg; and
 b. decreases the dry air requirement from 1492 (Table 38.2) to 1449 kg.

CHAPTER 39 EXERCISE ANSWER

- 39.1. Data:** 20 kg of 25°C oil is being injected into raceway of Table 39.2. The oil contains 0.85 kg of C, 0.13 kg of H, 0.01 kg of N, and 0.01 kg of O per kg of oil. Its 25°C enthalpy is -1.7 MJ/kg of oil.

The objective of this exercise is to calculate flame temperature of Fig. 39.1 with 20 kg of oil injection.

Our starting point is bottom-segment calculated values of *Exercise 38.1*.

We include the oil in raceway matrix of Table 39.1 by means of the following steps:

- Change Column R's heading to *mass tuyere-injected oil entering raceway*.
- Rename Row 82 to *mass injected oil*.
- Represent 20 kg of oil injection by typing 20 in Cell C82.
- Represent oil composition in Column R much as shown for the other injectants. Notice the minus signs (described in Sections 37.7–37.10).
- Include bottom-segment calculated values of Exercise 38.1 where needed. These steps automatically give the raceway's calculated values, much as in Table 39.3.

Only one of the equations of Table 39.4 is changed by oil injection, that is, Eq. 39.20. Its last term becomes;

$$C109 * -1.7$$

where -1.7 is the enthalpy of the oil, MJ per kg.

With 20 kg of oil injection, the raceway flame temperature drops from 1923°C (no oil injection) to 1873°C as shown in Table 39.4.

For more complex calculations (e.g., Goal Seek), the bottom-segment input values may be entered into the raceway matrix by typing in their cell name. This is described in Chapter 30, Raceway Flame Temperature With Real (Industrial) Natural Gas Injection.

CHAPTER 40 EXERCISE ANSWERS

All masses in this document are per 1000 kg of Fe in product molten iron.

- 40.1. Data:** 20 kg of oil injection.

Objective: Calculate top gas temperature with this amount of oil injection.

	B	C kg per 1000 kg of Fe in product iron
33	Bottom segment calculated values	
34	mass $\text{Fe}_{0.947}\text{O}$ into bottom segment	1302
35	mass C in descending coke	307
36	mass O_2 in air blast	350
37	mass N_2 in air blast	1156
38	mass Fe out in molten iron	1000
39	mass C out in molten iron	48
40	mass CO out in ascending gas	596
41	mass CO_2 out in ascending gas	414
42	mass N_2 out in ascending gas	1158
43	mass H_2 out in ascending gas	14
44	mass H_2O out in ascending gas	76
45	mass SiO_2 in descending ore	75
46	mass SiO_2 in descending coke	24
47	mass SiO_2 out in molten slag	93
48	mass Al_2O_3 in descending decomposed flux	12
49	mass Al_2O_3 in descending coke	10
50	mass Al_2O_3 out in molten slag	24
51	mass CaO in descending decomposed flux	98
52	mass CaO out in molten slag	98
53	mass MgO in descending decomposed flux	24
54	mass MgO out in molten slag	24
55	mass Si out in molten iron	4.2
56	mass Mn out in molten iron	5.3
57	mass descending MnO	7.6
58	mass MnO out in molten slag	0.8
59	mass tuyere-injected coal	60
60	mass O_2 in tuyere-injected pure oxygen	30
61	mass through-tuyere input $\text{H}_2\text{O(g)}$	18
62	mass tuyere-injected natural gas	60
63	mass tuyere-injected oil	20

Exercise 38.1's bottom segment calculated values.

Steps:

- Produce the equivalent of Table 40.1 with injection of 20 kg of oil.
- Transfer its values to Table 40.2. This automatically produces the following new *top-segment mass flows* table.
- These values are automatically forwarded to equations of Table 40.4, which give the result that the top gas temperature with 20 kg of oil injection

is 294°C , up 21°C from the no-oil injection value of 273°C , Table 40.4.

40.2. Data: Oil injection.

Objective: Calculate amount of oil that will give a top gas temperature of 280°C .

Caution: Make sure that your bottom-segment calculated values transfer automatically to the top-segment matrix.

Calculation: Goal Seek Cell BJ119 to 280 changing Cell C32 of Table 38.1.

Answer: 7 kg

CHAPTER 41 EXERCISE ANSWERS

Unless otherwise mentioned, the bottom-segment injected masses associated with these problems are 60 kg of coal, 30 kg of pure oxygen, and 60 kg of natural gas with 15 g H₂O(g) in 1200°C blast per Nm³ of dry air in blast of Chapter 38, Bottom-Segment Calculations With Multiple Injectants. All masses are per 1000 kg of Fe in product molten iron.

- 41.1.** Data: 6 mass% moisture in all top-charged materials.

Tuyere inputs as described above except for pure oxygen, which is our variable.

Objective: Calculate the amount of injected pure oxygen that will give 100°C top gas.

Method 1: Interpolate the answer from Fig. 41.3. Answer: ~80 kg of pure oxygen.

	B	C kg per 1000 kg of Fe in product iron
33	Bottom segment calculated values	
34	mass Fe _{0.947} O into bottom segment	1302
35	mass C in descending coke	307
36	mass O ₂ in air blast	350
37	mass N ₂ in air blast	1156
38	mass Fe out in molten iron	1000
39	mass C out in molten iron	48
40	mass CO out in ascending gas	596
41	mass CO ₂ out in ascending gas	414
42	mass N ₂ out in ascending gas	1158
43	mass H ₂ out in ascending gas	14
44	mass H ₂ O out in ascending gas	76
45	mass SiO ₂ in descending ore	75
46	mass SiO ₂ in descending coke	24
47	mass SiO ₂ out in molten slag	93
48	mass Al ₂ O ₃ in descending decomposed flux	12
49	mass Al ₂ O ₃ in descending coke	10
50	mass Al ₂ O ₃ out in molten slag	24
51	mass CaO in descending decomposed flux	98
52	mass CaO out in molten slag	98
53	mass MgO in descending decomposed flux	24
54	mass MgO out in molten slag	24
55	mass Si out in molten iron	4.2
56	mass Mn out in molten iron	5.3
57	mass descending MnO	7.6
58	mass MnO out in molten slag	0.8
59	mass tuyere-injected coal	60
60	mass O ₂ in tuyere-injected pure oxygen	30
61	mass through-tuyere input H ₂ O(g)	18
62	mass tuyere-injected natural gas	60
63	mass tuyere-injected oil	20

Bottom-segment calculated values with 20 kg of oil injection, from Exercise 38.1.

Method 2: Modify Row 31 in Table 41.1 [Eq. (41.2)]. Goal Seek Cell BL119 to 100 by changing Cell C29 of Table 38.1.

Answer: 78.6 kg of pure oxygen.

- 41.2.** Data: 0 mass% moisture in all top charge materials

Tuyere inputs as described above except for natural gas, which is our variable.

Objective: Calculate the amount of injected natural gas that will give 200°C top gas.

Method: In Table 41.1 Row 31, change all 0.05 to 0. Goal seek Cell BL119 to 200 by changing Cell C31 of Table 38.1.

Answer: 14.4 kg of natural gas.

- 41.3.** A dry top charge will;

	BB	BC
71	Top segment calculated values	kg per 1000 kg of Fe in product iron
72	mass Fe_2O_3 in top-charged ore	1431
73	mass SiO_2 in top-charged ore	75
74	mass C in top-charged coke	307
75	mass Al_2O_3 in top-charged coke	10
76	mass SiO_2 in top-charged coke	24
77	mass top-charged Al_2O_3 flux	12
78	mass top-charged CaO flux	98
79	mass top-charged MgO flux	24
80	mass top-charged MnO_2 ore	9.3
81	mass Al_2O_3 -in-coke descending out of top segment	10
82	mass Al_2O_3 flux descending out of top segment	12
83	mass C-in-coke descending out of top segment	307
84	mass CaO flux descending out of top segment	98
85	mass $\text{Fe}_{0.947}\text{O}$ descending out of top segment	1302
86	mass MgO flux descending out of top segment	24
87	mass MnO descending out of top segment	7.6
88	mass SiO_2 -in-coke descending out of top segment	24
89	mass SiO_2 -in-ore descending out of top segment	75
90	mass CO ascending into top segment	596
91	mass CO_2 ascending into top segment	414
92	mass H_2 ascending into top segment	14
93	mass H_2O ascending into top segment	76
94	mass N_2 ascending into top segment	1158
95	mass CO departing in top gas	424
96	mass CO_2 departing in top gas	684
97	mass H_2 departing in top gas	9.9
98	mass H_2O departing in top gas	111
99	mass N_2 departing in top gas	1158

- minimize $\text{H}_2\text{O}(g)$ in top gas, which will, in turn, avoid $\text{H}_2\text{O}(l)$ condensation and uneven gas flow due to top charge agglomeration near the top of the furnace;
- simplify dust collection from the top gas by avoiding moisture-caused dust particle agglomeration; and
- permit top charging of ambient temperature, low enthalpy materials (e.g., direct reduction iron pellets, scrap steel) without excessively cooling the top gas.

CHAPTER 42 EXERCISE ANSWER

- 42.1.** Data: Top-charge MgCO_3 is replaced by top-charge MgO .

From Appendix Table J.1, MgO 's 25°C enthalpy is -14.92 MJ/kg .

Objective: Calculate top gas temperature with the replacement top-charged MgO . Calculations:

Step 1: Top-segment column BK is changed to *mass top-charged MgO flux*.

Step 2: Top-segment MgO mass balance Eq. (42.4) reverts to Eq. (40.21), that is,

$$0 = - \left[\begin{array}{c} \text{mass top charge} \\ \text{MgO flux} \end{array} \right]_1 + \left[\begin{array}{c} \text{mass MgO descending} \\ \text{out of top segment} \end{array} \right] * 1$$

This changes Cell BK23 to -1 .

Step 3: Row 33 becomes *Mass CO_2 from CaCO_3* . This changes Cell BK33 to 0 .

Step 4: The MgCO_3 enthalpy term $\text{BC79}^* - 13.20$ in input enthalpy Eq. (42.6) changes to MgO enthalpy term $\text{BC79}^* - 14.92$.

Answer: Switching from MgCO_3 flux to MgO flux increases top gas temperature

from 24°C to 50°C. The increase arises because the endothermic reaction $\text{MgCO}_3 \rightarrow \text{MgO} + \text{CO}_2$ (which absorbs heat) no longer occurs in the top segment.

CHAPTER 43 EXERCISE ANSWERS

All masses are kg per 1000 kg of Fe in product molten iron.

As throughout this chapter, the reference blast furnace is being injected with 220 kg of pulverized coal and 92 kg of pure oxygen. The 1200°C blast contains 15 g of $\text{H}_2\text{O}(g)$ per Nm^3 of dry air blast and all the fluxes are oxides. These values are based on an industrial blast furnace. The top charge contains 5 mass% $\text{H}_2\text{O}(l)$, excluding the scrap, which is dry.

- 43.1.** Data: 40 kg of pure Fe scrap

Questions: As compared to 80 kg of pure Fe scrap, how much additional SiO_2 needs to be fluxed and how much Al_2O_3 , CaO , and MgO flux are required with 40 kg of pure Fe scrap?

Method: Type 40 into matrix Cell C33 of Table 43.1 and interpret the results.

Answers:

	With 80 kg of Scrap Steel	With 40 kg of Scrap Steel	Difference
SiO_2 in descending ore and coke	86	90	+ 4
Al_2O_3 flux requirement	10	11	+ 1
CaO flux requirement	94	98	+ 4
MgO flux requirement	23	24	+ 1

Explanation:

- The smaller the amount of top-charged scrap steel, the larger the requirement for (SiO_2 -bearing) ore.
- The larger the amount of (SiO_2 -bearing ore), the larger the amount of SiO_2 descending into the bottom segment.
- The larger the amount of SiO_2 descending into the bottom segment, the larger the requirements for Al_2O_3 , CaO , and MgO flux.

43.2. Data: Top gas temperature must be 110°C or higher with top-charged pure Fe scrap.

Question: What is the maximum amount of pure Fe scrap that can be added while achieving this temperature goal.

Calculation method 1: Extrapolate Fig. 43.7 to 110°C. Answer ~ 140 kg.

Calculation method 2: Goal Seek Cell BL119 of Table 43.5 to 110 by changing Cell C33 of Table 43.1. Answer 139.6 kg.

CHAPTER 44 EXERCISE ANSWERS

All masses in these calculations are kg per 1000 kg of Fe in product molten iron.

As throughout this chapter, these exercises' blast furnace is being injected with 220 kg of pulverized coal and 92 kg of pure oxygen. The 1200°C blast contains 15 g of $\text{H}_2\text{O(g)}$ per Nm^3 of dry air in blast and all the fluxes are oxides. These values are based on an industrial blast furnace. The top charge contains 5 mass% $\text{H}_2\text{O(l)}$, excluding the DRI, which is dry.

44.1. Question: steady-state Al_2O_3 , CaO , and MgO flux requirements with 45 kg of DRI pellets?

Method: Change the mass DRI pellets descending into bottom segment in Cell C33 of Table 44.1 to 45 kg.

Answers from new *Top-segment calculated values* table are

mass Al_2O_3 flux = 11 kg

mass CaO flux = 99 kg

mass MgO flux = 24 kg

(not much changed from Table 44.4).

44.2. Question: What mass of DRI pellets will drive mass $\text{CO}_2(\text{g})$ in top gas down to 625 kg?

Method 1: Extrapolate Fig. 44.4 down to 625 kg of top gas. Answer: ~ 160 kg of DRI pellets.

Method 2 Goal Seek Cell BC116 of Table 44.4 to 625 by changing Cell C33 of Table 44.1.

Answer: 161.9 kg of DRI pellets.

CHAPTER 45 EXERCISE ANSWERS

All masses in these exercises are kg per 1000 kg of Fe in product molten iron.

45.1. Hydrogen is mostly made by steam reforming of natural gas, oil, and coal. An inadvertent product of this process is $\text{CO}_2(\text{g})$. Hydrogen is also produced by electrowinning from water. This in combination with hydro-, wind-, solar panel-, and nuclear-electricity completely avoids $\text{CO}_2(\text{g})$ emission.

45.2. Data: 30 kg of 25°C $\text{H}_2(\text{g})$ injection
Method: Build matrix Table 45.1 and type 30 in Cell C14.

Answers (per 1000 kg of Fe in product molten iron):

C-in-coke requirement	= 333 kg
O_2 -in-blast-air requirement	= 285 kg
N_2 -in-blast air	= 940 kg
air requirement	= 1225 kg

- 45.3.** Data: Minimum allowable C-in-coke = 250 kg/1000 kg of Fe in product molten iron.
 Method 1: Extrapolate Fig. 45.2 until C-in-coke requirement reaches 250 kg/1000 kg of Fe in product molten iron. Answer: More than ~70 kg of H₂(g) injection will lower C-in-coke requirement below the allowable 250 kg/1000 kg of Fe in product molten iron.
 Method 2: Goal Seek Cell C19 to 250 kg C-in-coke by changing cell C14. Answer: More than 71.9 kg of H₂(g) injection will lower C-in-coke requirement below the allowable 250 kg/1000 kg of Fe in product molten iron.
- 45.4.** Hydrogen injection's large production of top gas H₂O(g) may lead to H₂O(*l*) condensation in the cool top of the blast furnace. In turn, this H₂O(*l*) may agglomerate the top charge, leading to erratic gas flow near the top of the furnace.

Insert 30 in Cell C14 of matrix Table 46.1. This gives:

Top-gas temperature	= 252°C
C-in-top gas emission	= 286 kg
Top charge C-in-coke requirement	= 333 kg

- 46.2.** Data: 200°C top gas
 Objective: Calculate how much H₂(g) injection will give this temperature.
 Calculations:
 Method 1: Graphical
 Interpolate the line in Fig. 46.2 to 200°C.
 Answer ~9 kg of H₂(g)
 Method 2: Goal Seek
Goal Seek Cell AL40 of Table 46.2 to 200, changing Cell C14 of Table 46.1. Answer: 8.5 kg.
- 46.3.** The blast furnace operating team can lower their top gas temperature by increasing blast temperature, Chapter 22, Top Gas Temperature Calculation. The blast temperature that will give 210°C top gas may be calculated by
Goal Seeking Cell AL40 of Table 46.2 to 210 by changing Cell E16 of Table 46.1. Answer: 1285°C.

CHAPTER 46 EXERCISE ANSWERS

All masses are kg per 1000 kg of Fe in product molten iron.

- 46.1.** Data: 30 kg of 25°C H₂(g) injection
 Objective: Calculate top gas temperature, C emission in CO(g) + CO₂(g) top gas, and top-charge C-in-coke requirement
 Calculations:
 Method 1:
 Extrapolate the lines in Figs. 46.2–46.4 to 30 kg of H₂(g) injection. These extrapolations give:

Top gas temperature	= ~250°C
C-in-top gas emission	= ~286 kg
Top charge C-in-coke requirement	= ~333 kg

Method 2:

CHAPTER 47 EXERCISE ANSWERS

All masses are kg per 1000 kg of Fe in product molten iron.

- 47.1** Data: 70 kg of 25°C CO(g) injectant.
 Challenge: Calculate C-in-coke requirement, air requirement, and (C-in-coke plus C-in-CO injectant) with this amount of injection.

Method 1: Extrapolate data lines of Figs. 47.2 and 47.4 to 70 kg of CO(g) injection.

Answers:

C-in-coke requirement = ~383 kg
 Total C = (C in coke plus C in CO(g) injectant) = ~414 kg

Method 2: Matrix calculation: Insert 70 in Cell C12 of Table 47.1.

Answers:

$$\begin{aligned}\text{C-in-coke requirement} &= 383.5 \text{ kg} \\ \text{Total (C-in-coke plus C-in-CO(g) injectant)} &= \text{mass C-in-coke}^*1 + \text{mass CO injectant}^* \\ (42.9 \text{ mass\% C in CO})/100\% & \\ = 383.5 + 70*0.429 &= 413.5 \text{ kg}\end{aligned}$$

Also blast air requirement = 1270 kg.

- 47.2** CO(g) can be (and is) combusted to heat blast furnace blast air.
- 47.3** We don't have to specify injection temperature because this addendum only addresses masses, not enthalpies and temperatures.

CHAPTER 48 EXERCISE ANSWERS

- 48.1.** a. The objective function is travel time in the air, that is, flying time. The optimization will seek to minimize this variable.
 b. There is only one manipulated variable, and it is the order one visits the cities. It can be A → B → C → D → E, or any combination, but this order is what is manipulated.
 c. There are no constraints explicitly stated in the problem; however, it can be assumed that one can only visit each city only once.
- 48.2.** The system is a linear system, made up entirely of linear equations, including the objective function. Therefore, the best option is to use a linear optimization technique. This would likely be the Simplex algorithm. The fact the problem says it wants to find a solution quickly is irrelevant as linear techniques will always find a globally optimal solution in a short timeframe. Since a linear

optimization technique is used, it will be a globally optimal solution, which is also a locally optimal solution.

***BONUS*:**

$$\begin{aligned}\text{Manipulated Variable} &= 22.4 \\ \text{Objective Function} &= 2.4, \\ A &= 9.6, \\ B &= 2.8, \\ C &= -10 \text{ (constrained)}\end{aligned}$$

- 48.3.** Yes, the answer changes. This constraint is nonlinear and therefore Simplex, or any linear optimization technique, cannot be used. Since the problem states that it is desired to find a solution quickly, it is best to use a "nonlinear optimization" solver rather than a "Guess and Check" method. The use of "nonlinear optimization" techniques does not guarantee a globally optimal solution; therefore, the optimization under these conditions can only be guaranteed to be locally optimal. This *may* be globally optimal as well, but there is no way to know and/or guarantee that this is the case.
- 48.4.** a. The objective function is to reduce the coke rate in the blast furnace.
 b. The general manager indicated that the PCI injection rate is the main variable to be manipulated. Oxygen injection is another variable that is manipulated to keep flame temperature above its minimum.
 c. There are two main constraints mentioned by your general manager. The first is that flame temperature must be kept above some minimum value. In addition, your general manager seemed concerned about oxygen supply, implying there is a maximum amount of oxygen that can be injected.

CHAPTER 49 EXERCISE ANSWERS

- 49.1.** a. This doesn't make sense as the optimal coke rate using PCI had a top gas temperature of 129°C. This was not at the minimum constraint; therefore, lowering the minimum constraint will not change the optimal location.
- b. As expected, the optimal operating point did not change and is still PCI at 150, O₂ at 32.6, and a C-in-coke-charge of 305.
- 49.2.** a. This has potential to further reduce coke rate as the optimal coke rate with natural gas injection was previously constrained by top gas temperature.
- b. The optimal coke rate did change, going down to the lowest possible top gas temperature of 100°C:
 C-in-coke-charge of 365 kg/t Fe in HM
 NG Injection of 74.8 kg/t Fe in HM
 O₂ Injection of 78.6 kg/t Fe in HM
- 49.3.** a. This will reduce the benefits of PCI as it now has a higher cost per kg than both natural gas and coke.
- b. PCI = 0 kg/t Fe in HM
 NG = 68.4 kg/t Fe in HM
 O₂ = 58.0 kg/t Fe in HM
 Cost = 298 kg/t Fe in HM
 This is the same operating point as minimum coke rate with natural gas injection as PCI is the most expensive fuel, while natural gas is less expensive than coke.
- 49.4.** Putting these new coke parameters and cost into the model and rerunning the optimization, the optimal cost goes to \$281/t Fe in HM. As this is higher than the current operating cost, it is not a good decision to use this new coke as it does not offer any cost savings.

CHAPTER 50 EXERCISE ANSWERS

- 50.1.** Using European rules, a + 10 GJ/h increase in cooling losses is compensated by a coke rate increase + 1.2 kg coke/t HM. Therefore a + 40 GJ/h increase in cooling losses, increases the coke rate demand by + 4.8 kg coke/t HM. To compensate the increased heat demand using natural gas rather than coke, consider that a + 10 kg NG/t HM increase in the natural gas addition, reduces coke rate by 10.4 kg coke/t HM. Therefore to increase the coke rate by + 4.8 kg coke/t, + 4.8 kg coke/t HM * (10/10.4) = + 4.6 kg of natural gas/t HM must be added. An increase of the natural gas rate by + 4.6 kg NG/t HM decreases flame temperature by (+ 4.6 / + 10) * - 56 °C = - 26 °C; therefore the new flame temperature is (1950 - 26) °C = 1924°C. This flame temperature is acceptable. Top gas temperature will increase by (+ 4.6 / + 10) * + 18 °C = + 8 °C. The new top temperature (120 + 8)°C = 128 °C is below the max threshold; therefore the change is acceptable.
 + 30 kg NG/t HM reduces flame temperature by + (30/10) * - 55 °C = - 165 °C; therefore the flame temperature will be reduced to 1935°C. This is 95 °C below the minimum flame temperature, therefore, oxygen is needed to increase flame temperature back to 2030 °C. The amount of additional oxygen enrichment is (95 °C/18 °C) * 10 kg O₂/t HM = 53 kg O₂/t HM to bring the flame temperature back to 2030 °C. The net change in top temperature is + 54 °C due to the natural gas injection and - 64 °C due to the added oxygen enrichment. Net change in top

temperature is -10°C resulting in a new top temperature of 120°C which is acceptable.

- 50.2.** $+30 \text{ kg NG/t HM}$ will reduce coke rate by $-10.4 \text{ kg coke/t HM} * (30/10) = -31.2 \text{ kg coke/t HM}$, more than the target to reduce coke rate by 25 kg/t HM . The additional oxygen will increase coke consumption. Assuming an oxygen density of 1.33 kg/Nm^3 , the increased oxygen usage will be $(53 \text{ kg/t HM}) / (1.33 \text{ kg/Nm}^3) = 39.8 \text{ Nm}^3/\text{t HM}$. The enrichment rate is $39.8/(900 + 39.8) * 100 = +4.2\%$. Using rules of thumb, the coke rate due to additional oxygen enrichment would be $+4.2\% * (1 \text{ kg coke/t HM}/1\%) = +4.2 \text{ kg coke/t HM}$. The net coke reduction would be $(-31.2 + 4.2) \text{ kg coke/t HM} = -27 \text{ kg coke/t HM}$. This reduces coke costs by $-27 \text{ kg/t HM} * 0.30 \text{ \$/kg} = -8.1 \text{ \$/t HM}$. $+30 \text{ kg/t HM}$ of natural gas costs $30 \text{ kg/t HM} * 0.16 \text{ \$/kg} = 4.8 \text{ \$/t HM}$. The additional oxygen cost is $39.8 \text{ Nm}^3/\text{t HM} * 0.03 \text{ \$/Nm}^3 = 1.2 \text{ \$/t HM}$. The overall change in hot metal cost will be; a cost savings of $8.1 \text{ \$/t HM}$ from coke reduction, less $4.8 \text{ \$/t HM}$ for additional NG and less $1.2 \text{ \$/t HM}$ for additional oxygen yielding a net cost savings of $2.1 \text{ \$/t HM}$. The production will decrease slightly due to the higher overall fuel rate. The original fuel rate was 150 kg/t HM coal + 350 kg/t HM coke for 500 kg/t HM total fuel rate. The new fuel rate is $150 \text{ kg coal/t HM} + (350 - 27) \text{ kg coke/t HM} + 30 \text{ kg NG/t HM} = 503 \text{ kg/t HM}$ total fuel rate. This is a fuel rate increase of 0.6% ; therefore, production will decrease by 0.6% to 4970 tpd. At 350 days/year, annual

production is 1.74 Mt/year hot metal. Annual savings are $1.74 \text{ Mt HM/year} * 2.1 \text{ \$/t HM} = \$3.7 \text{ million dollars per year}$ excluding any profit loss from the reduced hot metal output from the blast furnace.

CHAPTER 51 EXERCISE ANSWERS

- 51.1.** Straight line aim temperature is maintained by means of
- the correct operation of the cold air mixer

51.2.

- T A hot blast stove is a regenerative heat exchange system used to preheat blast air to a blast furnace.
- F Higher hot blast temperature requires that the stove burner be fired with blast furnace gas only. BF gas has lower calorific value and would be unable to achieve the highest blast temperatures. Natural gas or another higher calorific gas is needed to supplement the blast furnace gas.
- T The top combustion chamber stove was designed to overcome hot blast temperature limitations of the internal combustion chamber stove.
- T Today, all three designs of stove are technologically competitive. Top combustion stoves offer longer life and higher hot blast temperature.

51.3.

-
- | | |
|----------------------|-----------------------------|
| The stove on "blast" | is heating the hot blast. |
| The stove "on gas" | is being heated. |
| The "bottled" stove | has completed being heated. |
-

- 51.4.** Initially, stove combustion is controlled based on
- oxygen content of the waste gas to avoid incomplete combustion.

51.5.

- F** A stove must be pressurized before going "on gas." {The stove is removed from the higher pressure hot blast system before going 'on-gas'.}
- T** A stove must be depressurized before going "on gas."
- T** The dome temperature limit is observed to maintain the integrity of the refractories in that area while, at the same time, maximizing the heat input to the checkers.
- F** The stack temperature limit is observed to maintain the integrity of the refractories in the lower stack while, at the same time, maximizing the heat input to the checkers. {The stack temperature limit is to protect the cast iron grid that supports the checker column from damage.}

51.6. The top zone region is where

- the furnace gases exit the furnace
- the burden materials are distributed to form the stockline profile

51.7. The dust catcher

- is the first element in the gas cleaning system

51.8. The gas washer/scrubber

- cools the blast furnace gas

CHAPTER 52 EXERCISE ANSWERS**52.1.**

- F** The ascending furnace gases drop in temperature from 1900–2200°C to 150–200°C in 5–10 s. {It is shorter, see Fig. 52.1, 1–5 s.}
- F** The gases give up oxygen to the descending iron oxide of the ore. {The process gases remove oxygen from the iron ores and hence reduce the iron ore oxygen content.}
- F** All the cleaned blast furnace gas is used to heat the stoves. {Excess blast furnace gas is exported to steam boilers for power generation.}

T Normally, each blast furnace is equipped with three stoves.

52.2. Blast furnace cooling is provided to

- cool and protect the furnace shell (refractory lined furnace)

52.3.

- T** Plate and stave cooling are designed to isolate the furnace shell from the cooling process.
- T** Shower/spray cooling and jacket/channel cooling have the disadvantage that the shell plate acts as a cooling element.

52.4.

- T** The casting operation can significantly affect stave temperature.
- T** Scaling of the inner wall of the stave water piping lowers the rate of heat transfer from the staves to the water.
- T** Since the use of untreated water in the stave systems scales up the inner wall of the water piping, its use is never justifiable. {Untreated water is used but this is not considered best practice.}
- T** The water circulated in the staves is boiler quality water.

52.5.

- T** The key to refractory survival in the hearth is effective, uninterrupted cooling.
- T** The most critical part of the refractory system is the bosh, belly, and lower stack.
- F** The well-designed refractory system uses only a single type of refractory in any one region of the blast furnace.
- T** High thermal conductivity refractories promote the formation of a protective layer (skull) on the refractory hot face.

- 52.6. Excessive heat loading on the staves
- **causes protective scab to melt or peel**
- 52.7. Blast furnace refractories
- **are either carbon or ceramic**
 - **ceramic refractories are often used as a sacrificial blow-in lining**
 - **blast furnaces use ceramic bricks to line the furnace in the upper stack**

52.8.

- T The hearth pad on both most blast furnaces is constructed of carbon beams.
- T The bosh, belly, and lower stack are subjected to the highest intensity of attack by the various destruction mechanisms.
- F The most severe refractory wear mechanism in the hearth is slag attack.
- T The most severe refractory wear mechanism in the upper stack is abrasion.

CHAPTER 53 EXERCISE ANSWERS

- 53.1. The most common reason for a blast furnace relining is extensive wear in the hearth, particularly around the tapholes.
- 53.2. None. All blast furnace NDT techniques are indirect measurements. Direct measurements of a blast furnace refractory are only possible through core drilling or physical measurement following a furnace shutdown.
- 53.3. Measurement uncertainty combined with a risk of radiation exposure to operators has resulted in the diminished use of radioactive tracers for refractory thickness measurements.
- 53.4. The probable cause of the noise depends on whether it is a low frequency or high frequency. A low frequency noise on a blast furnace is most likely due to the operation of the furnace and the surrounding equipment causing low-frequency vibration.
- High-frequency noises could be due a few issues; the most common source of high-frequency noise is a damaged cable between the transducer and the data acquisition system. In highly sensitive testing equipment such as NDT systems, the cables must be shielded. Once the cable shielding is damaged, the cable may pick up noise resulting in static in the signals. The best solution is to change the cable. Another plausible reason for high-frequency noise could be lack of grounding or even a noisy plant power source. In the later case, the system needs to be powered by a DC source or a stabilizer needs to be connected between the power source and the instrument. If none of the above solutions work, the NDT operator can increase the trigger amplitude on the AU-E equipment. Since the AU-E pulses are transient and the electrical or vibration noise is continuous, data will still be collected. When viewed in the frequency spectrum, the excessive noise can be easily filtered out
- 53.5. You should use a small diameter sphere impactor since the furnace walls are assumed to be thin. The bandwidth of the impacts generated by the small diameter sphere impactor will be at a higher frequency range, hence the thinner refractory thickness can be better detected by the system. A larger sphere diameter impactor will generate a lower frequency bandwidth with wavelengths larger than the refractory thickness of 200 mm possibly resulting in false thickness computations.
- 53.6. An increase in thermal factor will result in slower effective P-wave speed and consequently a thinner calculation of the walls.

- 53.7.** Regular ultrasonic systems are designed to measure single layered isotropic and homogeneous materials such as iron, aluminum, steel, copper structures. These systems are usually low powered, single frequency instrumentations that are perfect for furnace shell and weld inspections but their signals cannot penetrate beyond the furnace shell. Even if the regular ultrasonic signals penetrate beyond the furnace shell, the heterogeneous nature of the refractory bricks makes the time domain analysis of the reflected signals very difficult.
- 53.8.** If there is a gap in the refractory lining between the tip of the thermocouple and the hot face of the refractory lining, the thermocouple readings drop. This is because the thermal conductivity of the gap is much lower than the unaltered refractory resulting in a higher thermal resistance between the thermocouple and the heat source.
- 53.9.** Handheld thermo-cameras or thermo-guns are great tools to detect hotspots or cold spots on a furnace shell. There have been successful attempts to measure refractory thicknesses for simple single and double-layered cylindrical vessels such as converters and reactors. However, for thick and complex furnaces linings such as blast furnaces with cooling systems, the accuracy of thickness calculations based on handheld thermal devices is very poor. Furthermore, thermal readings can be influenced by a variety of uncontrollable factors such as nearby heat sources, shell corrosion, and gaps and openings within the refractory lining and behind the shell. Hence, temperature readings cannot be used to reliably calculate refractory thickness.

- 53.10.** Since AU-E components are waterproof, water running on the shell (such as in shell cooling) has no impact on the signals obtained. In the case of stave cooling, the piping system has no influence on AU-E measurements because the pipes have smaller diameter than the wavelengths used by the AU-E system, hence the whole stave is treated as a lining layer with a fixed wave speed.

CHAPTER 54 EXERCISE ANSWERS

54.1. 1430 kg per 1000 kg Fe

54.2. 65.7% Fe

54.3.

Handling/ charging	high tumbler strength.
Upper stack	minimal low temperature breakdown.
Lower stack	low swelling and high reducibility.
Cohesive zone	elevated temperature softening/ meltdown.

54.4. • more permeable cohesive zone

• thinner cohesive zone

54.5. • high tumbler index

• well screened narrow size range

CHAPTER 55 EXERCISE ANSWERS

55.1. Coke has three main roles in the blast furnace process. These are:

- to produce heat for the process
- to maintain the structural integrity of the charge column
- to produce reducing gas

55.2. • lower ash content
• higher CSR

55.3.

- F With coal injection, coke is subjected to a shorter residence time and increased gas attack.
- T Degraded, weak coke accumulates in the bird's nest in front of each tuyere.
- F Coke needs to be more reactive when injecting coal.
- F Weak, degraded hearth coke directs the liquid flow toward the furnace center, resulting in high hearth temperatures.

55.4. The important characteristic that is common to all blast furnace zones is _____ and this is provided primarily by _____.

Please write in the number of the correct answer from the following list:

- coke
- strong, large coke with minimal fines
- hot, fluid slag
- permeability
- good gas flow

CHAPTER 56 EXERCISE ANSWERS

56.1.

- F The usual operating mode is Auto Mode. In this mode, the injection rate into the furnace is reduced when the coal supply to one of the tuyeres is shut off.
- F Build-up of coal in the pipes leading to the furnace is reduced by increasing the amount of coal particles smaller than 10 μm .
- T Optical tuyere block detection shuts off the coal supply to a lance in case the light intensity is too low.
- F With dense phase injection, the gas loading volume is 90% and solids 10%

56.2. The position of the tip of the natural gas lance is behind the coal lance tip.
56.3.

- F The replacement ratio is the amount of coal replaced by coke, expressed in kg coal/kg coke.
- T Ash replaces carbon in injection coal. Therefore, a higher coal ash will reduce the replacement ratio and increase the amount of slag in the furnace.
- T Natural gas has the highest replacement ratio, but coal has the highest injection capability due to its low H/C ratio.
- F The cost advantage of natural gas injection is most significant when injecting at high rates with high levels of oxygen enrichment.

56.4.

Change in Tuyere Condition	Impact on RAFT
Increase hot blast temperature	<i>Increase</i>
Increase blast moisture	<i>Decrease</i>
Decrease oxygen enrichment	<i>Decrease</i>
Decrease coal injection	<i>Increase</i>

56.5.

- T Injectants slow down the burden descent rate by replacing coke burnt at the tuyeres.
- F The advantage of coinjecting coal and natural gas is in the significant hydrogen content of coal, which stabilizes the furnace process.
- T Injectants increase the heat load on the bosh due to the increased volume of their combustion products.
- T Injection fuels replace moisture to control the flame temperature.
- T The maximum amount of oxygen enrichment is restricted by top temperatures becoming too low. On the other hand, too little oxygen enrichment results in too low flame temperatures.

56.6. A. Correct lance alignment and positioning
B. Increasing oxygen enrichment

56.7.

- F When hot metal temperatures are low, the PCI rate is decreased.
- T High hot metal temperatures are controlled by injecting steam.
- F In the case of loss of PCI, immediate action is required to increase the flame temperature.
- T After a short PCI outage (less than 2 h), the lost energy input is made up for by injecting additional coal.

56.8. A. PCI increases the ore-to-coke ratio and therefore gas flows with more difficulty.
B. When using coal at high injection rates, more coke must be charged to the center.

56.9.

- F With coal injection, coke is subject to a shorter residence time and increased gas attack (solution loss).
- F Degraded, weak coke accumulates in the bird's nest.
- F Coke needs to be more reactive when injecting coal.
- F Weak, degraded hearth coke directs the liquid flow toward the furnace center, resulting in high hearth temperatures.

CHAPTER 57 EXERCISE ANSWERS

57.1.

- T Good disciplined casting practice is a major key to stable blast furnace operation.
- T An overfilled hearth has serious safety implications.
- T Dry hearth casting practice promotes process stability.

F Some liquid and slag should be left in the furnace at the end of a cast to maintain heat in the hearth.

57.2. • trough design
• taphole angle

57.3.

- T No part of the furnace deserves more care and attention than the taphole.
- T Casting practice has no bearing on the quality of the iron sent to steelmaking.
- F The steeper the taphole angle, the emptier the hearth at end cast, so the steeper the better.
- T The clay gun has a significant role in maintaining taphole length.

57.4. The primary function of the trough is

- to efficiently separate the iron and slag

57.5. Trough bottom slope should be

- approximately 3.5 degrees to move the iron along but with minimal turbulence and sufficient time for iron/slag separation

57.6. Good drainage of liquids from the hearth depends on

- large, fines-free coke in the hearth

CHAPTER 58 EXERCISE ANSWERS

58.1. The four main constituents of slag are

Alumina (Al_2O_3)

Silica (SiO_2) Magnesia (MgO)

Lime (CaO)

58.2. Fig. 58.1 indicates that decreasing slag SiO_2 content (therefore increasing hot metal Si content) causes a phase change from melilite to merwinite and ultimately

di-calcium silicate ($2\text{CaO} \cdot \text{SiO}_2$). Hint—draw a tie line from 100% SiO_2 through the data point shown. With depleting SiO_2 , the composition moves away from pure SiO_2 and with increasing SiO_2 , the composition moves toward pure SiO_2 . Merwinite and di-calcium silicate have very high liquidus temperature ($>1500^\circ\text{C}$) with very minor changes in SiO_2 slag content.

Based on the discussion presented in Table 58.1, the liquidus temperature is much less dependent on Si content with 15% Al_2O_3 ; as the isotherms are further apart and change is more gradual.

- 58.3.** No, slag liquidus temperatures points are influenced to different degrees by the constituent components. Minor impurities like TiO_2 can have a strong impact on the slag melting temperature.
- 58.4.** The cooling method must produce solid slag that is amorphous and glassy in nature for use in cement applications. Blast furnace slag must be rapidly cooled to achieve this so that it can replace ordinary Portland cement.
- 58.5.** Dry atomization eliminates the formation of H_2S , an obnoxious gas better known as rotten egg gas. Although minimal, water usage has a cost including waste water treatment/disposal. A dry system is easier to operate in winter conditions.
- 58.6.** Slag composition is provided below:
- Siderar San Nicolas 2, TK CSA Santa Cruz 1&2 and ArcelorMittal Dofasco 4 have a slag liquidus $<1415^\circ\text{C}$
 - Low MgO and high Al_2O_3 increase the slag liquidus temperature

CHAPTER 59 EXERCISE ANSWERS

- 59.1.** The role of burden distribution is

- control gas flow in the furnace

- 59.2.** Please circle T (true) or F (false) for each of the following statements:

- T The bell-less top can lay down materials anywhere on the stockline.
- T Each bell-less top is purchased pre-programmed and ready to perform.
- T Probes and other instrumentation are required to track the effectiveness of the burden distribution.

- 59.3.** Wall gas flow (not excessive) promotes

- drying of the burden and stable burden descent

- 59.4.** Smooth descent of the burden requires
- maintaining a pressure drop of less than 160 kPa.

- 59.5.** Uniform ore/coke ratio is desired over most of the furnace cross-section because it
- lowers the coke rate

- 59.6.**

Gas flow	regions where the coke layer is relatively thick compared to the ore layer.
Coke particles are larger	takes the path of least resistance.
Gas flows preferentially to	so, the coke layer is more permeable.
Gas flows poorly	since coke is solid throughout the furnace height.
The coke distribution is important to manage the gas flow	through mixed layers.

Continent	Asia	Europe	Oceania	South America		North America
Country	Japan	Netherlands	Australia	Argentina	Brazil	Canada
Company	Kobe	Tata Europe	BlueScope	Siderar	CSA	ArcelorMittal
Site/Location	Kakogawa 2	IJmuiden 6	Port Kembla 5	San Nicolas 2	Santa Cruz 1&2	Dofasco 4
Slag						
Mass	kg/t	282	210	309	252	260
CaO/SiO ₂	mass ratio	1.3	1.1	1.2	1.1	1.1
CaO	%	43.2	38.7	41.8	37.6	39.0
MgO	%	6.5	9.6	5.7	9.9	8.0
Al ₂ O ₃	%	15.2	14.6	14.3	13.2	9.0
SiO ₂	%	34.1	34.1	36.2	35.8	37.0
Liquidus temp	°C	1446	1430	1431	1404	1380
						1415

Answers

Gas flow	takes the path of least resistance.
Coke particles are larger	so, the coke layer is more permeable.
Gas flows preferentially to	regions where the coke layer is relatively thick compared to the ore layer.
Gas flows poorly	through mixed layers.
The coke distribution is important to manage the gas flow	since coke is solid throughout the furnace height.

- 59.7. The proposed ideal gas flow aims for
- uniform gas/solids contact over most of the furnace cross-section

Epilogue

For the foreseeable future, the blast furnace will be the principle source of the world's molten iron and hence steel. No other new iron-making process can challenge the blast furnace's scale and efficiency. While electric arc furnace (EAF) steelmaking will grow, limitations in the availability of high quality scrap will ultimately place a ceiling on the amount of EAF steel that can be produced. The blast furnace will remain in the pole position.

The challenge for blast furnace engineers is to reduce carbon usage and the consumption of metallurgical coke. Blast furnace productivity and campaign life must increase to maintain the blast furnace's economies of scale. Reducing carbon usage is the greatest challenge; changing the fuel mix to use more electrical energy and hydrogen will be required in the future.

Understanding the principles presented in this book is essential to adapt and advance the blast furnace process. The authors are working

on new concepts for cooling staves to increase campaign life and the use of plasma torches to electrically heat some of the blast air and reduce coke usage. Other engineers have purified and recycled top gas, and the world's largest steel producer, ArcelorMittal, is working on reforming blast furnace top gas in a plasma fired furnace. The authors foresee that the blast furnace will continue to evolve to be the most efficient way to convert iron ore into molten iron.

Writing this book brought us immense joy and satisfaction, but we always understood that iron and steelmaking is a rather mundane subject. This changed in the summer of 2018 when the American president slapped tariffs on foreign steel and proclaimed that steel, and hence blast furnace iron, is essential to the security of the United States. This started many conversations both with our industry colleagues and our family, friends, and neighbors. Our pride increased immensely!

Index

Note: Page numbers followed by “*f*” and “*t*” refer to figures and tables, respectively.

A

- Acid pellets, 548–549
- Acoustic emissions (AEs), 524–526, 525*f*
- Acousto-Ultrasonic-Echo (AU-E), 528–530
 - calibration, 530
 - improvements in, 535
 - measurements, 533*f*, 534–535
 - and salamander tapping, 534
- After-pressing technique, 608–610, 613
- Agglomeration, 540, 542, 544–545
- Air blast composition equation, 75
- Air composition, mass%, 677–678
 - at ground level, 677*t*
- Air composition specification, 50
- Air granulation, 644–645, 644*f*
- Air–oxygen mixture, 93
- Alkali elements, 636, 639
- Alloy mol fractions, 700–701, 723
- Alumina (Al_2O_3), 635–637
 - Al_2O_3 -in-coke, 292–293
 - Al_2O_3 -in-DRI pellets, 415
 - alumina-in-ore specification, 286
 - balance, 325
 - gangue, 285, 286*f*
 - mass balance, 293, 421
 - and SiO_2 in coal, 729
- Amended top-segment variables and equations for carbonates, 380
- Annular gap gas washer, 491*f*
- Argon
 - effect on blast furnace calculations, 679
 - effects of ignoring, 678
 - stirring, 39
- Automated raceway output enthalpy, 165
- Automatic top gas calculations, 367

B

- Basic oxygen furnaces (BOFs), 34, 36*f*, 37, 38*f*
- Beehive, 558, 610
- Bell-less top (BLT) charging, 651–656, 654*f*
- Binary basicity (B2), 550
- Blast air requirement, 404–405
 - effect of blast temperature on, 66
- Blast furnace bottom-segment matrix
 - with tuyere injection, 444*f*
- Blast furnace enthalpy balance, 59–60, 702
 - conductive, convective, and radiative heat losses, 61
 - enthalpy of mixing $\text{Fe}(\ell) + \text{C}(s)$, 61
 - input and output enthalpies, 60
 - numerical values and final enthalpy equations, 61–62
- Blast furnace hearths, 517–518
- Blast furnace mass balances, 47–48
 - addition of a new variable carbon in product molten iron, 53–54
 - air composition specification, 50
 - equations for, 48–50
 - carbon balance equation, 50
 - Fe mass balance equation, 49
 - nitrogen balance equation, 50
 - oxygen balance equation, 49
 - equation shortage, 51
 - magnetite ore charge, 51–53
 - 1000 kg of Fe in product molten iron specification, 50–51
 - top gas composition, 51
- Blast furnace matrices, combining/automating, 143
- Blast furnace O₂-in-blast air requirement
 - effect of tuyere-injected CH₄(g) on, 113*f*
- Blast furnace operating window for PCI and O₂ injection, 464*f*
- Blast furnace optimization case studies, 461
 - minimizing CO₂(g) emissions using PCI, natural gas, and oxygen, 469–471
 - minimizing coke rate using natural gas and oxygen, 464–467
 - minimizing coke rate using pulverized coal injection (PCI) and oxygen, 461–464
 - minimizing fuel costs using PCI, natural gas, and oxygen, 467–469
- Blast furnace plant, 483, 484*f*
 - blast furnace top, 485–486, 486*f*
 - charging systems, 486–487
 - cold and hot blast systems, 487–490, 488*f*
 - gas cleaning, 490–491
- important aspects of blast furnace process, 483–484
- stockhouse, 485
- top combustion stoves, 489–490, 490*f*
- wet and dry blast furnace gas cleaning arrangements, 492*f*
- Blast furnace proper, 496–497
- Blast furnace refractory lining failures, 519–521
- Blast furnace slag, 633
 - by-product slag sale requirements, 641–645
 - aggregate and civil applications, 641–642
 - dry granulation using high-velocity air stream, 644–645
 - dry granulation using spinning ceramic cup, 645

- Blast furnace slag (*Continued*)
 slag cement, 642
 slag pelletizing, 643–644
 wet slag granulation, 642–643
 finding balance among competing demands, 645–648
 hot metal chemistry control, 638–641
 alkali removal, 639–640
 candidate fluxes, 641
 phosphorus, 639
 silicon, 638–639
 sulfur, 638
 titania in slag, 640–641
 slag composition and properties, 634–638, 635f
 alumina content, 636–637
 high alumina slag, 638
 lime content, 636
 lookup tables to estimate slag liquidus temperature, 635–636, 736t
 magnesia content, 637
 slag fluidity, 634–635, 635f
 slag volume, 638
- Blast furnace slag design, 648
 common fluxes available for, 641t
- Blast furnace structural design, 497–498
- Blast furnace top gas (BFG), 9–10
- Blast furnace tuyere, hydrocarbon fuel injection through, 85–86, 86f
- Blast O₂ and N₂ enthalpies, 147
- Bleeder openings, 486
- Bottom segment calculations with natural gas injection, 255–258
- Bottom segment carbon balance, 87
- Bottom segment enthalpy balance equation, 88, 95, 278–279
- Bottom segment oxygen balance equation, 102–104
- Bottom segment pure oxygen injection matrix, 96t
- Bottom segment steady-state enthalpy balance, 127
- Bottom segment steady-state mass balance, 126–127
- Bottom segment with low purity oxygen enrichment, 101
 benefits of using impure oxygen, 101
 mass N₂ in injected impure oxygen, 104
 specified mass O₂ in injected impure oxygen, 102
- Bottom segment with moisture in blast air, 115–116, 122
 importance of steam injection for blast furnace control, 116
- Bottom segment with oxygen enrichment of blast air, 93–97
- Bottom-segment calculations, 299, 300f
 bottom-segment enthalpy equation, 302–303
 bottom-segment oxygen balance, 302
 bottom-segment steady-state SiO₂ balance equation, 301–302
 C- and Si-in-iron specification equations, 300–305
 silica reduction, 299–300
- Bottom-segment calculations with multiple injectants, 335–344
- Bottom-segment carbon injection, 152
- Bottom-segment enthalpy balance, 287, 314–315, 326–327
- Bottom-segment equations with H₂(g) injection, 430–432
- Bottom-segment Fe mass balance, 391–394
- Bottom-segment H mass balance equation with H₂(g) injection, 430
- Bottom-segment H₂O(g) injection matrix, 118t
- Bottom-segment matrix, 79t, 144
 for calculating bottom-segment inputs and outputs, 215t
 for calculating bottom-segment steady-state inputs and outputs, 227t
 with through-tuyere input H₂O(g), 181t
- Bottom-segment MnO reduction efficiency, 312–313
- Bottom-segment MnO requirement effect of injected coal quantity on, 332f
- Bottom-segment oxygen balance with descending MnO, 313–314
- Bottom-segment scrap steel quantity specification, 391
- Bottom-segment slag calculations, 273–282, 285–290
 bottom-segment mass balances, 287
 and input SiO₂, Al₂O₃, CaO, and MgO masses, 278
- Bottom-segment specifications, 411
- Bottom-segment steady-state Mn mass balance, 312
- Bottom-segment tuyere injection of CH₄(g)
 top-segment matrix with, 229t
- Burden charging systems
 bell-less top (BLT) charging, 652–656
 charge sequencing, 660–664
 charging practice objectives, 659–660
 evolution of, 651–652
 gas flow control, instrumentation for, 660f
 modeling, 666–670
 positioning fluxes and miscellaneous materials, 664–666
 ferrous fines, 665
 fluxes, 666
 nut coke, 664–665
 scrap steel and hot briquetted iron, 665–666
- size segregation and control, 656–659
- trajectory probe, 669f
- two-bell charging system, 652, 652f
- visualizing gas flow conditions in blast furnace, 666
- Burden materials
 metallurgical properties of, 551–553
 physical properties of, 550–551
- By-product cokemaking, 560–565
- By-product tar, 594
- C**
- C- and Si-in-iron specification equations, 300–301
- C mass balance, 420
- C/Fe, Si/Fe, Mn/Fe in molten iron mass ratio, 725t
- Ca and Mg carbonate fluxes, 379
- CaCO₃ fluxes, 380f, 382t
- CaO flux requirements, 405
- CaO–SiO₂ flux powder, 42
- CaO–SiO₂–MgO phase diagram, 635f
- Capital costs, 15
- Carbon balance equation, 50, 256–257, 324
- Carbon emissions, 436
- Carbon injection bottom-segment matrix, 89t

- Carbon mass balance equation, 75, 194–195
with H₂(g) injection, 430
- Carbon steel, 32
- Carbonate decomposition, 381
- Carbonate fluxes
impact of, on the blast furnace process, 379–380
top segment with. *See also* Top segment with carbonate fluxes
- Carbon-in-coke gasification, 24
- Cast iron staves, 505
- Casthouse
design, 603
emission controls, 605–606
emission sources, 606*t*
layouts, 603–605, 603*f*
- Casting
principles, 602
schedule, 619–625
casting times, 620–622
drill bit diameter, 624
dry hearth practice, 622
hearth drainage, 625
iron gap time, 622
measuring hot metal temperature and sampling, 624–625
overlapping casts on multiple taphole blast furnaces, 623
slag gap time, 622–623
- CH₄(g) and real natural gas, comparison of, 256
- CH₄(g) raceway matrix adapting, to natural gas, 261–262
- CH₄(g) tuyere injection, 689
blast furnace raceway with, 689*f*
raceway flame temperature with, 169
modified raceway carbon balance equation, 173
new hydrogen balance equation, 174
raceway input CH₄(g) specification, 170
raceway input enthalpy calculation, 175
raceway matrix results and flame temperature calculation, 174
raceway N₂-in-blast air specification, 173
raceway nitrogen balance equation, 174
- raceway O₂-in-blast air input specification, 170–173
- raceway output enthalpy, 176
- raceway output gas (flame) temperature, 176–177
- raceway oxygen balance equation, 173–174
- Charge materials, accounting for moisture in, 369–370
- Charged coal, 567
- Charging methods, 6, 6*f*
- Charging sinter, 665
- Chemical reserve zone, 26, 72–73, 76, 110
- C-in-DRI pellets, 415
- C-in-molten iron specification equation, 311–312
- Mn-in-molten iron specification, 311–312
- Si-in-molten iron specification equation, 311
- C-in-top-charged coke, 436–439
- CO poisoning, 16
- CO raceway exit gas proof, 681
- CO(g), CO₂(g), and N₂(g) quantities and mol fractions in, 682–683
- equilibrium mole fractions, 683–684
- oxygen molar balance, 682–683
- raceway inputs and outputs, 681–682
- tuyere raceway, with dry blast air, 681*f*
- CO(g) injection, 441–451
- CO₂ emissions, 404, 428
- CO₂/CO mass ratio, 72–73, 80
- Coal and natural gas injection, 593–594
- Coal ash, 322
- Coal blending, 558–559
- Coal elemental composition, 729–730
- Coal hydrocarbon injected quantity specification, 126
- Coal injection, 125–126, 129, 323, 326
on total input of SiO₂, 327
- Coke ash, 6, 291
Al₂O₃ in descending coke equation, 292–293
altered bottom-segment Al₂O₃ and SiO₂ mass balances, 293
altered enthalpy balance, 294
contribution to blast furnace slag, 291–292
- SiO₂ in descending coke equation, 293
- Coke gasification, 24
kinetics of, 24–25
- Coke oven battery, 561, 563*f*
- Coke oven gas (COG), 562–563, 593
- Coke reactivity index (CRI), 559, 570–571
- Coke replacement ratio, 88–90, 473, 476–477, 586*f*
- Coke residence time and quality requirements, 581–582
- Coke strength after reaction (CSR), 559, 570–571, 582
- Coking coals, 557, 559
- Cold crushing strength, 551
- Compound enthalpies, 697–698
- Compound molecular masses and compositions, 675*t*
- Conceptual blast furnace bottom segment, 310*f*, 322*f*
- Conceptual blast furnace top segment, 356*f*, 380*f*
- Conceptual division of blast furnace, 71
additional chemical reserve gas composition specification, 76
additional specifications, 75
analysis of results, 78–80
C, 78
CO₂/CO mass ratio, 80
Fe, 78
N, 80
O, 78–79
- bottom segment enthalpy balance, 76–77
- bottom segment inputs and outputs, 73
- bottom segment matrix and results, 78
- conditions in chemical reserve, 72–73
dividing the blast furnace into two segments, 72
- Continuous casting, 41–42
copper mold, 41–42
mold powder, 42
- Copper Cooling Plate Design, 504*t*
- Copper staves, 500, 505
- D
- Degassing, 39–41
- Desulfurization reactions, 34

Direct reduced iron (DRI) in the blast furnace, 410
calculation of DRI pellet enthalpies, MJ per kg of DRI pellets, 427
 $\text{CO}_2(\text{g})$ emission as a function of DRI pellet input, 424
flame temperature with top-charged DRI pellets, 426
mass $\text{N}_2(\text{g})$ in top-gas as a function of DRI pellet input, 424
mass SiO_2 in slag as a function of DRI pellet input, 424–425
top-gas temperature with top-charged DRI pellets, 426
total top-gas emission as a function of DRI pellet input, 424

Direct reduction (DR) pellets, 541

Direct Reduction Ironmaking, 2

Discrete element modeling (DEM), 657, 670

Down-draft sintering machine, 540

Dry gas cleaning plants, 491

Dry hearth practice, 622

Dust catcher operation, 490f

E

Element enthalpies, 697

Elephant foot wear, 516

Enthalpy balance, 59–60, 104
conductive, convective, and radiative heat losses, 61
enthalpy of mixing $\text{Fe}(\ell) + \text{C}(\text{s})$, 61
input and output enthalpies, 60
numerical values and final enthalpy equations, 61–62

Enthalpy equations, 700
with $\text{H}_2(\text{g})$ injection, 430–432

Enthalpy of CO at 126.85°C (400K), 698

Enthalpy of Mn, in molten iron, 727–728

Enthalpy of Si, in molten iron, 723–724

Enthalpy table, 699

Equilibrium $\text{CO}_2(\text{g})/\text{CO}(\text{g})$ mass ratio, 708

Equilibrium CO_2/CO molar ratio, 733

Equilibrium constant, 690
calculating $\text{CO}(\text{g})$ and $\text{CO}_2(\text{g})$ mol fractions for, 683
for the reaction $\text{CO}(\text{g}) + \text{Fe}_{0.947}\text{O}(\text{s}) \rightarrow \text{CO}_2(\text{g}) + 0.947\text{Fe}$, 703, 705

for the reaction $\text{CO}(\text{g}) + 3\text{Fe}_2\text{O}_3(\text{s}) \rightarrow \text{CO}_2(\text{s}) + 2\text{Fe}_3\text{O}_4(\text{s})$, 731–733
for the reaction $\text{CO}_2(\text{g}) + \text{C}(\text{s}) \rightarrow 2\text{CO}(\text{g})$, 685–686, 732–733
for the reaction $\text{H}_2\text{O}(\text{g}) + \text{C}(\text{s}) \rightarrow \text{H}_2(\text{g}) + \text{CO}(\text{g})$, 693–694

Equilibrium constant–gas concentration relationship, 687–688

Equilibrium $\text{H}_2\text{O}(\text{g})/\text{H}_2(\text{g})$ mass ratio, 713–714

Equilibrium mole fractions, 683–684, 687–688

Equilibrium thermodynamic activity, 687, 690

F

Fe mass balance equation, 49, 74, 192

Fe–C alloy formation, 700–702

Fe–Mn alloy, 314

Fe-rich solids, 390

Ferromanganese, 37–38

Ferrous charge materials, 539–541
chemical, physical, and metallurgical properties of, 548–553
binary basicity (B_2), 550
iron content, 548–550
total acid gangue content, 550

global ferrous burden material usage, 554–555

impact of ferrous burden materials on blast furnace operations, 553–554

production processes, 542–548
lump ore production, 542
pelletizing, 544–548
sintering, 542–544

types of iron ore used to produce, 541–542

Flame temperature calculation, 174, 180

Fluxes, 6, 666

Free swelling index, 552–553

Fuel injection, 574
coal and natural gas injection, 593–594
coke residence time and quality requirements, 581–582
controlling, 577–580
impact of injected fuels on the blast furnace operation, 595–597

maximizing injected fuel usage, 595–596
operating windows to maximize fuel injection, 596–597

importance of, 574–575
natural gas injection, 592–593

coke oven gas, 593
oil and tar, 594–595
principles of, 575–577
pulverized coal injection (PCI), 582–592
coal grinding, 585–587
coal injection system design and equipment, 587–591
coal selection and coke replacement, 583–585

using fuel injection to control hot metal thermal state, 580–581

Full spreadsheet automation, 232–233

Furnace integrity monitoring system (FIMS), 526

Furnace reline, 11–13

Fusion and melting zone, 23–24

G

Gangue minerals, 634, 648

Gas cleaning plant, 491

Gibbs free energy of formation, 687, 693

Global ferrous burden material usage, 554–555

Grams $\text{H}_2\text{O}(\text{g})/\text{Nm}^3$ of dry blast air conversion to kg $\text{H}_2\text{O}(\text{g})/\text{kg}$ of dry blast air, 715–716

Green balls, 540–541

Green pellet induration, 546

Greenhouse gases, 428

“Guess and check” algorithms, 455–457, 456f

H

$\text{H}_2(\text{g}) + \text{Fe}_{0.947}\text{O}(\text{s}) \rightarrow \text{H}_2\text{O}(\text{g}) + 0.947\text{Fe}(\text{s})$

equilibrium constants, 709, 711

Gibbs free energies and equilibrium constants (KE) for, $710t$

H_2 injection, bottom-segment calculations with, 432–433

reasons for injecting hydrogen in the blast furnace, 429–430

H_2 injection, top-segment calculations with, 435–440

- examining the impact of $H_2(g)$ injection on the top-segment balances, 435
top gas carbon emissions, 436
top gas temperature results, 436
top-segment calculations, 436
- H_2 raceway exit gas proof, 689
equilibrium raceway exit gas, 689–690
raceway inputs and outputs, 689
- H_2/CO reduction ratio equation, 230–231
- $H_2O(g)$, 249, 250f
in blast, 253, 253f
through-tuyere quantity equation, 116, 116f
- $H_2O(\ell)$ quantity equation, 370
- Hardgrove Grindability Index (HGI), 585
- Hearth design, 508–511
hearth cooling, 509–511
hearth dimensions, 508
refractory design, 508–509
- Hearth drainage, 625, 629t
- Hearth liquid level, modeling of, 625–631
- Hearth reactions, 21
- Hearth refractory wear, 517
- Hearth slag, 634–635
- Heat-recovery (HR) cokemaking, 566–569, 567t, 568f
- Hematite (Fe_2O_3) reduction zone, 27–28
- Hematite iron ore pellets, 49f
- Hematite ores, 540
- Hot briquetted iron (HBI), 410, 570–571
- Hot metal silicon, 638–639
- HR steam generators (HRSGs), 567–568
- Hultgren's enthalpy data, 701, 723
- Hydraulic index, 642
- Hydrogen balance equation, 174, 256, 324
- I**
- Impure oxygen, 101, 102f
benefits of, 101
- Impure substance enthalpies, 698
- Inadvertent slag production, 274
- Industrial natural gas
composition of, 719t
top gas temperature with, 267
- Infrared (IR) thermography, 524
- Infrared cameras, 666
- Injected carbon specification, 87
- Input and output enthalpies, 60
- Input enthalpy calculation, 155
- Internal combustion chamber hot blast stove, 489f
- Investment (capital) costs, 15
- Iron blast furnace process, 1
- blast furnace raw materials, 2–7
charging methods, 6
top-charged materials, 4–6
tuyere-injected materials, 7
costs, 15–16
investment (capital) costs, 15
maintenance and relining costs, 16
operating costs, 15–16
environment, 16–17
operations, 10–15
blast furnace information, 11
campaign life, 11–15
main thermal processes, 11
principle chemical reactions, 11
production statistics, 11
products from the blast furnace, 7–10
molten iron, 7–8
molten slag, 8–9
safety, 16
- Iron gap time, 622
- Iron ore, 540
to produce the ferrous charge materials, 541–542
pellets, 37f
sinter/pellets, 477
- Iron oxides, 4–5
- Ironmaking input materials, unit costs of, 467t
- K**
- Killing steel, 37
- L**
- Ladle metallurgy furnace (LMF), 39, 40f
- Laser scanning, 521
- Lime (CaO), 636
- Linear optimization, 455
- Linear programming, 455
- Liquid steel, 37–38, 41
- Low purity oxygen enrichment, bottom segment with, 101
- Low-frequency pulse ultrasonic (LFPU), 527
- Low-temperature reduction-disintegration dynamic, 552
static, 552
- Lump ore, 540–541
production, 542
- M**
- Macerals in coking coal, 557
- Magnesia (MgO), 6, 635, 637
- Magnetite (Fe_3O_4), 540, 546
reduction to wustite, 25
- Magnetite ore charge, 51–53
- Maintenance and relining costs, 16
- Manganese, 579
enthalpy per kg mol of, 728
per kg mol of, 728
- Mass and enthalpy balance equations, combining, 65
altered enthalpy equation, 66–68
altered $O_2(g)$ and $N_2(g)$ enthalpy values, 68
effect of blast temperature on blast air requirement, 66
predictive blast furnace model, developing, 65–66
- Mass balance equations, 192–195
carbon mass balance equation, 194–195
- Fe mass balance equation, 192
nitrogen mass balance equation, 195
oxygen mass balance equation, 192–194
steady-state, 48, 74–75
- Mass of Al_2O_3 in falling coke particles, 346–348
- Mass of SiO_2 in falling coke particles equation, 349
- Mass SiO_2 in product molten slag, 277
- Mass% and volume% of top gas components, 717t
- Masses of SiO_2 , CaO , and MgO in molten slag, 286
- Matrix calculations, automating, 143
benefit, 147–150
carrying numerical values forward, 144
combining/automating blast furnace matrices, 143
equations in cells, 143–144

- Matrix calculations, automating
(Continued)
- forwarding to our flame temperature calculation, 147
 - raceway input enthalpy calculation, 144–147
 - raceway output enthalpy, 147
- Melting zone, fusion, 23–24
- Metallurgical coke, 4/*f*, 557
- by-product cokemaking, 560–565
 - coal blending, 558–559
 - heat-recovery cokemaking, 566–569
 - important attributes of, 558
 - production methods, 559–560
 - beehive oven process, 560
 - by-product process, 560
 - heat-recovery (HR) process, 560
- quality requirements, 569–571
- chemical composition, 569
 - coke size, 570
 - cold strength, 569
 - consistency, 571
 - properties at elevated temperatures, 570–571
- Methane (CH_4) injection, bottom segment with, 107
- bottom-segment $\text{CH}_4(\text{g})$ injection matrix, 112^t
- comparison of C and $\text{CH}_4(\text{g})$ injection, 111–113
- effect on bottom-segment C-in-coke requirement, 111
- effect on N_2 -in-blast air requirement, 111
- effect on O_2 -in-blast requirement, 111
- equilibrium mass (mass $\text{H}_2\text{O}(\text{g})$ /mass $\text{H}_2(\text{g})$) ratio, 110–111
- injected $\text{CH}_4(\text{g})$ quantity equation, 108
- natural gas injection, 107–108
- steady-state hydrogen balance, 108–109
- top gas temperature with, 243–246
- MgCO_3 fluxes, 380^f, 382^t
- MgO - and Al_2O_3 -in-flux requirements effect of real coal injection on, 331^f
- Micropellets, 542–544
- Minimum flame temperature, 466, 469, 476
- MnO reduction of, 309
- bottom-segment enthalpy equation, 314–315
 - descending MnO enthalpy, 314
 - dissolved Mn, enthalpy of, 314–315
 - MnO -in-product molten slag, 314
 - bottom-segment MnO reduction efficiency, 312–313
 - bottom-segment oxygen balance with descending MnO , 313–314
 - bottom-segment steady-state Mn mass balance, 312
 - C-in-molten iron specification equation, 311–312
 - Mn-in-molten iron specification, 311–312
 - Si-in-molten iron specification equation, 311
 - manganese and blast furnace operations, 309–310
- Moisture in blast air, 249
- bottom-segment results, 250
 - incorporating blast moisture into top-segment balances, 249
 - raceway flame temperature with, 179
 - top gas temperature results, 253
 - top-segment calculations, 250–253
- Moisture in top charge, 377
- Mold powder, 42
- Molecular masses and compositions, 675^t
- Molten Fe–Si alloy, 723
- Molten iron, 1–2, 7–8, 9/*f*, 309, 312
- Molten iron mass ratio calculator C/Fe, Si/Fe, Mn/Fe in, 725^t
- Molten iron temperature, 300
- Molten oxide blast furnace slag, 274–275
- inadvertent slag production, 274
 - slag functions, 274
- Molten slag, 8–9, 9/*f*, 35, 312, 331
- masses of Al_2O_3 , CaO , and MgO , 277–278
 - uses, 9
- Mudguns, 610, 610^f
- N**
- N mass balance, 174
- $\text{N}_2(\text{g})$ in-impure-oxygen, 104
- N_2 -in-blast air, 111
- Natural gas, adapting the $\text{CH}_4(\text{g})$ raceway matrix to, 261–262
- Natural gas composition, in mass%, calculation of, 719–720
- Natural gas enthalpy, 721–722
- Natural gas injection, 107–108, 255, 340, 592–593
- C-in-coke replacement by natural gas, 258
 - comparison of $\text{CH}_4(\text{g})$ and real natural gas, 256
 - equations, 256–257
 - replacing tuyere injection of $\text{CH}_4(\text{g})$ with natural gas injection, 255–256
- NG and O_2 injection
- blast furnace operating window using, 466^f
- NIST–JANAF Thermochemical Tables, 697–698
- Nitrogen balance, 50, 75, 104, 195, 257, 325
- Nondestructive testing (NDT) technique, 524
- Nonlinear optimization, 455–456
- O**
- O mass balance, 421
- bottom-segment, 415
- O_2 -in-blast air requirement, 66, 67^t, 70^f, 91^f, 299, 306^f
- Off-center gas flow, 666
- Oil and tar, 594–595
- Oil injection, 574
- Operating costs, 15–16
- Optimization, 453–457
- comparison of optimization techniques, 457
 - constraining, 454–455
 - “guess and check” algorithms, 456–457
 - linear optimization, 455
 - manipulated variables, 454, 454^f
 - mathematical optimization, 455
 - minimization optimization problem, 454
 - nonlinear optimization, 456
 - problem with direct and indirect constraints on, 455^f
 - pros and cons of, 457^t
 - using blast furnace model, 457–459
 - constraints, 458–459
 - manipulated variables, 458
 - objective function, 458

Output H₂O(g) quantity specification, 370–371
 Oxide ash in top-charged coke, 282
 Oxygen balance equation, 74, 133–135, 192–194
 Oxygen concentration in BF tuyere raceway with CO(g) production, 687–688
 Oxygen enrichment, 574–575, 596
 Oxygen injection, 98, 339 calculations, 94–95, 160 enthalpy balance with injected pure oxygen, 95 injected O₂ in oxygen mass balance, 94–95 injected oxygen quantity, 94
 Oxygen lancing, 606*t*, 608
 Oxygen molar balance, 682–683
 Oxygen quantity specification equation, 339
 Oxygen steelmaking, 34–37 molten slag, 35 nitrogen avoidance, 35 process steps, 35–37

P

Pellet feed, 541, 545–546
 Pellet fines, 664–665
 Pelletizing, 544–548 grate-kiln system, 547–548 straight grate technology, 546–547
 Pellets, 6
 Phosphorus, 38, 579
 Physical behavior blast air and gas ascend, 20–21 solids, descending, 20
 Portland cement, 9, 642
 Predictive blast furnace model, developing, 65–66
 Product molten iron, 300–301
 Pulverized carbon injection, 85, 88, 151
 blast air O₂ and N₂ requirements, 90
 carbon injection calculations, 86–88 bottom segment carbon balance, 87
 bottom segment enthalpy balance equation, 88
 injected carbon specification, 87
 C-in-coal injection, 86
 coke replacement ratio, 88–90 cross-division flows with, 214

effect of pulverized C injection on descending C-in-coke requirement, 88
 effect on raceway flame temperature, 156 impact of, 151–152 on the top segment, 213 importance of injecting hydrocarbon fuel, 85–86 input enthalpy calculation, 155 matrix with C-in-coal through tuyere injection, 88 oxygen and nitrogen balances, 154 raceway carbon balance equation with, 154 raceway flame temperature calculation, 156 raceway injectant quantity specification, 152 raceway matrix results, 155 raceway N₂-in-blast air input specification, 154 raceway O₂-in-blast air input specification, 152–154 raceway output enthalpy, 156 top-segment calculations, 214–218 total carbon requirement, 90
 Pulverized coal injection (PCI), 582–592, 596
 coal grinding, 585–587
 coal injection system design and equipment, 587–591
 coal selection and coke replacement, 583–585 rate, 458
 Pulverized coal injection, bottom-segment calculations with, 322 altered Al₂O₃ and SiO₂ mass balances, 325–326 altered enthalpy balance, 326 altered bottom-segment steady-state C, N, O, Al₂O₃, and SiO₂ mass balances, 324–325 coal elemental composition, 322 coal enthalpy, 323 coke and O₂-in-blast air requirements, 327 flux requirements, 327–330 CaO flux requirement, 327–330 total SiO₂ input, 327 injected coal quantity specification, 323

injected pulverized coal, 60 kg of, 330
 mass H₂O(g)/mass H₂(g) equilibrium ratio, 323–324
 MgO and Al₂O₃-in-flux requirements, 331–332 new hydrogen balance equation, 324 Pure oxygen injection, 95, 336–339 cross-division flows with, 219–220 bottom-segment matrix, raceway matrix, and flame temperature calculations with, 161*t* enthalpy balance with injected pure oxygen, 95 P-wave speed, 526, 530, 532–533 Pyrolusite (MnO₂), 309–310

Q

Quantity specification equations, 195–196

R

Raceway adiabatic flame temperature (RAFT), 131–133, 156, 166, 405, 575–577, 581, 594, 638–639 calculation, 133, 156 numerical calculation, 141 from total output enthalpy, 137–141 definition, 132–133 impact of natural gas injection on, 261 importance of, 131–132 with oxygen enrichment, 159 automated raceway output enthalpy, 165 benefits of oxygen enrichment and impact on, 160, 166, 166*f* raceway carbon balance, 163 raceway input enthalpy calculation, 164–165 raceway matrix results, 163 raceway N₂-in-blast air specification, 162 raceway nitrogen balance equation, 163 raceway O balance with pure oxygen injection, 162–163 raceway O₂-in-blast air input specification, 162 raceway output gas (flame) temperature, 165

Raceway adiabatic flame temperature (RAFT) (*Continued*)
 raceway pure oxygen quantity specification, 160–162
 tuyere raceways, 132, 132*f*
 Raceway carbon balance, 135, 163, 173, 262
 RAFT with moisture in blast air, 179, 187–188
 calculations results, 187
 impact on RAFT, 180
 modified raceway carbon balance equation, 184
 modified raceway hydrogen balance equation, 184–185
 modified raceway oxygen balance equation, 184
 modifying bottom segment and raceway matrices, 180–182
 raceway H₂O(g) input quantity specification, 182
 raceway input enthalpy calculation, 185–186
 raceway input N₂-in-blast air specification, 182–183
 raceway matrix results and flame temperature calculation, 185
 raceway nitrogen balance equation, 185
 raceway O₂-in-blast air input specification, 182
 raceway output enthalpy, 186
 raceway output gas (flame) temperature, 187
 RAFT with multiple injectants, 345
 calculation, 345–346
 calculation of raceway input enthalpy, output enthalpy, and flame temperature, 349–352
 raceway equations, 353–354
 raceway matrix, 346–349
 mass of Al₂O₃ in falling coke particles, 346–348
 mass of SiO₂ in falling coke particles equation, 349
 Raceway hydrogen balance, 262
 Raceway injectant quantity specification, 152
 Raceway input CH₄(g) specification, 170
 Raceway input enthalpy calculation, 135–137, 144–147, 175
 Raceway input equations, 133

Raceway mass balances, 133–135
 oxygen mass balance equation, 133–135
 raceway carbon balance equation, 135
 raceway nitrogen mass balance equation, 135
 Raceway masses, calculation of, 135
 Raceway matrix, 395, 416
 results, 174
 Raceway N₂-in-blast air input specification, 154, 173
 Raceway nitrogen balance equation, 163, 174, 185
 Raceway O₂-in-blast air input specification, 152–154, 170–173
 Raceway output enthalpy, 137, 147, 156, 176
 Raceway output gas (flame) temperature, 176–177
 Raceway oxygen balance equation, 173–174
 modified, 184
 Raceway zone, 23
 Reactions above the 930°C isotherm, 25
 Reactions above the fusion zone, 24
 Reduction under load, 552
 Reduction–disintegration index, 552
 Refractory deterioration, distinct stages of, 518*f*
 Refractory inspection technologies, 515
 determining the refractory lining status, 519–520
 methods to determine and monitor refractory thickness and condition, 520
 offline blast furnace measurement techniques, 520–521
 online refractory measurement techniques, 521–535
 accuracy of AU-E measurements, 534–535
 acoustic emission, 524–526
 Acousto-Ultrasonic-Echo (AU-E), 528–530, 534–535
 detection of anomalies, 531–532
 detection of refractory chemical changes, 532–533
 infrared thermography, 524
 isotopes and radioactive tracers, 523–524
 metal penetration, 533–534
 refractory thickness estimates based on thermal modeling, 521–523
 thickness measurements and refractory wear, 530–531
 ultrasonic, 526–528
 refractory wear mechanisms, 517–519, 519*f*
 Refractory thickness monitoring, 521–522
 Residence times, 28
 Resin-bonded clays, 613, 620
 RH steel degassing, 40
 Rolling mills, 586–587
 Rules of thumb, 473
 from Europe, United States, and Russia, comparison of, 474*t*
 flame and top temperature impacts, 473–476, 476*t*
 fuel rate adjustments, 473
 productivity impact, 476–480
 estimating changes in coke rate, 477
 estimating new production rate, 480
 managing short-term change, 477–478
 verifying top and flame temperature are in range, 478–480

S

Salamander tapping, 534, 535*f*
 Scrap steel, 390
 bottom-segment calculations, 391
 composition, and bottom-segment Fe mass balance, 391–394
 oxidation, in the top segment, 390
 top-charged, 389
 Si/Fe mass ratio, 301, 306
 Silica (SiO₂), 394–395
 balance, 325–326
 descending into the bottom segment, 276–277
 mass balance, 293, 421
 reduction, 299–300
 SiO₂-in-coke, 292–293
 SiO₂-in-DRI pellets, 415
 Silicon carbide, 516, 612
 Silicon nitride, 612
 Single lock hopper bell-less top charging system, 487*f*

Single refining process (SRP), 39f
 Sinter, 6, 540–541, 555
 Sintering, 542–544, 543f
 Slag “basicity” ratio (B4), 8
 Slag cement, 9, 642
 sales, 647t
 specifications, 642, 646f
 Slag composition, 286, 310, 634–638
 Slag functions, 274
 Slag gap time, 622–623
 Slot ovens, 560–561
 Solver Add-In in Excel, 458–459
 Spinning ceramic cup air granulation process, 645f
 Spiral charging, 655
 Spot hot metal temperatures, 624
 Stave cooling system for blast furnaces, 505f
 Steady-state bottom-segment hydrogen balance, 108
 Steady-state C-in-coke, 299
 and O₂-in-blast air requirements, 105f
 Steady-state dry air requirement, 121f
 Steady-state enthalpy balance
 equation, 59–60, 257
 Steady-state flows, 214, 219–220, 226, 249, 435
 Steady-state mass balance equations, 48–50, 74–75
 carbon mass balance equation, 75
 Fe mass balance equation, 74
 nitrogen mass balance equation, 75
 oxygen mass balance equation, 74
 Steady-state mass balances for blast furnace, 47–48
 Steady-state wustite production and consumption, 25–27
 thermal reserve zone, 26–27
 Steam injection for blast furnace control, 116
 Steel shell, protecting, 500–506
 with copper cooling plates, 503
 in the furnace throat, 502
 in the stack, belly, and bosh zones, 503–506
 with stave coolers, 503–506
 Steelmaking, 32
 Steepest descent method, 456
 Stockhouse, 483, 485, 486f
 Stokes’ Law, 614–615
 Sulfur removal, 32–34

SunCoke Energy, 566
 heat-recovery coke oven plant, 568f
 Synthetic slag, 39

T

Taphole, plugging, 608–610
 Taphole casthouse, 605f
 Taphole clay, 608, 611–613
 Taphole construction and the beehive/mushroom, 610
 Taphole drills, 606–608
 oxygen lancing, 608
 Taphole mushroom or beehive, 612f
 Tapping and Measuring Technology (TMT), 666–668, 668f, 671f
 Tapping stream energy, 614
 Thermal reserve zone, 26–27, 27f, 665
 Thermocouple reading hearth, 522f, 534
 Thermodynamic activities, 687, 707–708
 Three-stove hot blast system, 488f
 Through-tuyere H₂O(g) input quantity equation, 117
 Time domain signal, 530f
 Titania (TiO₂), 579, 640–641
 Top charged direct reduced iron, 409
 altered top-segment mass balances, 420–421
 amended bottom-segment enthalpy balance, 415–416
 amended bottom-segment Fe mass balance, 411–415
 bottom-segment mass balances, 415
 bottom-segment specifications, 411
 calculated results
 coke requirement, 424
 iron ore requirement, 424
 calculation of DRI pellet enthalpies, MJ per Kg of DRI pellets, 427
 CO₂(g) emission as a function of DRI pellet input, 424
 direct reduced iron (DRI) in the blast furnace, 410
 flame temperature with top-charged DRI pellets, 426
 mass N₂(g) in top-gas as a function of DRI pellet input, 424
 mass SiO₂ in slag as a function of DRI pellet input, 424–425
 reaction of DRI pellets in the top segment, 411

top-gas temperature, calculation of, 421–423
 top-gas temperature with top-charged DRI pellets, 426
 total top-gas emission as a function of DRI pellet input, 424
 Top gas enthalpy, 205–206, 362–363, 371, 386
 equations for automatically calculating, 361t
 Top gas mass%, volume% calculator, 717t
 Top gas temperature, 206–209, 218, 243, 363–364, 371–377, 386, 405
 calculation of, 205, 210, 243–246, 247t, 267, 371–377, 402
 top gas enthalpy, 402
 top gas temperature, 402
 with CH₄(g) injection, 243
 effect of blast temperature on, 210
 results, 246–248
 equations for automatically calculating, 361t
 Top gas volume (TGV), 594–595
 Top segment balance, 191, 196
 combining bottom and top segments of blast furnace, 191–192
 coupling top and bottom-segment calculations, 196–198
 mass balance equations, 192–195
 carbon mass balance equation, 194–195
 Fe mass balance equation, 192
 nitrogen mass balance equation, 195
 oxygen mass balance equation, 192–194
 quantity specification equations, 195–196
 top gas results, 196
 Top segment calculations with oxygen enrichment, 219
 cross-division flows with pure oxygen injection, 219–220
 impact of blast oxygen enrichment on top segment and top gas conditions, 219
 top-segment calculations, 220–223
 Top segment calculations with
 pulverized carbon injection, 213
 cross-division flows with, 214
 impact on top segment, 213

Top segment calculations with pulverized carbon injection
(Continued)
 top-segment calculations, 214–218

Top segment enthalpy balance with CH₄(g) injection, 237
 estimating top gas enthalpy with H₂(g) and H₂O(g) present, 237
 top gas enthalpy, 239–241

Top segment mass balance with CH₄(g) injection, 225
 cross-division flows, 226
 full spreadsheet automation, 232–233
 H₂/CO reduction ratio equation, 230–231
 impact of, 225
 with 60 kg of CH₄ tuyere injectant, 231
 top-segment calculations, 226–230
 top-segment matrix and calculated top gas values, 231–232

Top segment with carbonate fluxes, 379–386
 impact of carbonate fluxes on the blast furnace process, 379–380
 top gas enthalpy, 386
 top gas temperature, 386
 top-segment output enthalpy with carbonates added, 386

Top temperature maximums, 476

Top-charged coke, 97, 291

Top-charged raw materials, 4–6

Top-charged scrap steel, 389, 392*t*
 adding Fe-rich solids to the blast furnace, 390
 calculated results
 blast air requirement, 404–405
 CaO flux requirements, 405
 coke requirement, 402–404
 raceway flame temperature, 405
 top gas CO₂ emissions, 404
 top gas temperature, 405
 calculation of top gas temperature, 402
 including top-charged scrap steel in our calculations, 390–395, 400–401

scrap steel composition and bottom-segment Fe mass balance, 391–394

top-segment–bottom-segment connection, 395

Top-segment calculations with H₂ injection, 436
 with multiple injectants, 355–356 results, 364
 top-segment equations, 364–366 with natural gas injection, 267–268 natural gas, top gas temperature with, 267
 starting our top gas temperature calculations, 267
 top-segment enthalpy and top gas equations, 268

Top-segment enthalpy and top gas equations, 268

Top-segment enthalpy balance, 199
 calculated values, 203
 top-segment input enthalpy, 199–200
 top-segment output enthalpy, 200–203

Top-segment equations with gangue, ash, fluxes, and slag plus injection of coal, oxygen, H₂O(g), and natural gas, 356–361

Top-segment input enthalpy, 361*t*, 362, 371

Top-segment matrix, 196, 226, 268, 381, 390, 395–399, 420 and calculated top gas values, 231–232

Top-segment output enthalpy, 361*t*, 362, 371
 with carbonates added, 386

Torpedo ladles, 2

Total acid gangue content, 550

Trough design and iron-slag separation, 613–619

Tumbler strength, 551

Tuyere blockage detectors, 592

Tuyere breast, 506–508, 507*f*

Tuyere fuel injection, 597

Tuyere injection of CH₄(g) conceptually divided blast furnace with, 226*f*
 replacing, with natural gas injection, 255–256

Tuyere injection of H₂(g), 432

Tuyere injection of pulverized carbon, 214*f*, 217*f*
 conceptually divided blast furnace with, 214*f*

Tuyere injection of pure oxygen blast furnace raceway with, 160*f*

Tuyere raceway, 22*f*, 132

Tuyere raceway calculation matrix, 152, 160

Tuyere raceway flame temperature.
See Raceway Adiabatic Flame Temperature (RAFT)

Tuyere raceways, 132, 132*f*

Tuyere-injected carbon, effect of, 91*f*

Tuyere-injected CH₄(g), 109

Tuyere-injected dried pulverized coal, composition of, 322*t*

Tuyeres-injected materials, 7

Tuyeres, reactions in front and around, 22–23
 raceway zone, 22–23

U

Ultra-Low CO₂ Steelmaking Consortium (ULCOS), 451

Ultralow phosphorus steel, 38

Ultrasonic pulse velocity (UPV) systems, 526

Ultrasonic pulse-echo (UP-E) systems, 526

Ultrasonic system, conventional, 527

Ultrasonic tomography, 527–528

Unit conversations, 723–724

V

Vacuum degasser, 39–40, 40*f*

W

Wet quenching, 560

Wet slag granulation, 642–643, 645

Witusiewicz's enthalpy, 727

Wustite reduction, 24

Blast Furnace Ironmaking

Analysis, Control, and Optimization

- Provides sample problems, answers, and assignments for each chapter
- Explores how to optimize the blast furnace operation while maintaining the required temperatures and gas flow rates
- Describes all major blast furnace equipment and best practices
- Features blast furnace operating data from five continents

Blast Furnace Ironmaking: Analysis, Control, and Optimization uses a fundamental first principles approach to prepare a blast furnace mass and energy balance in Excel™. Robust descriptions of the main equipment and systems, process technologies, and best practices used in a modern blast furnace plant are detailed. Optimization tools are provided to help the reader to find the best blast furnace fuel mix and related costs, maximize output, or evaluate other operational strategies using the Excel™ model that the reader will develop.

The first principles blast furnace Excel™ model allows for more comprehensive process assessments than the "rules of thumb" currently being used in the industry. This book is suitable for undergraduate and postgraduate science and engineering students in the fields of chemical, mechanical, metallurgical, and materials engineering. Additionally, steel company engineers, process technologists, and management will find this book useful with its fundamental approach, best practices description, and perspective on the future.

About the Authors

Ian Cameron is the principal metallurgist ferrous at Hatch Ltd., Ontario, Canada. Ian has more than 35 years of experience including more than 20 years as a consulting engineer for Hatch and previously Corus Consulting/Hoogovens Technical Services.

Mitren Sukhram is a senior process engineer at Hatch Ltd., Ontario, Canada. He specializes in pyrometallurgical processes and works on all aspects of blast furnace ironmaking including process engineering, reline planning, techno-economic assessments, campaign life assessment/extension, and operational support for blast furnaces located around the world.

Kyle Lefebvre is a process engineer at Hatch Ltd., Ontario, Canada. His work includes pyrometallurgical process modeling and logistical simulations in the iron and steel industry. He has worked on new steel plant designs and assessed a wide range of processes in the iron and steelmaking value chain.

William Davenport is an emeritus professor, University of Arizona, United States. He has taught and consulted for more than 50 years and authored six metallurgical textbooks, most of which have been translated into multiple foreign language editions.

ISBN 978-0-12-814227-1



ELSEVIER

elsevier.com/books-and-journals



9 780128 142271